The 50th Anniversary Special Issue

Research Activities
1991–2016

RIKEN Accelerator Progress Report

2016

vol. 50

理化学研究所　仁科加速器研究センター
RIKEN Nishina Center for Accelerator-Based Science

RIKEN Accelerator Progress Report 2016

vol. **50**

理化学研究所　仁科加速器研究センター
RIKEN Nishina Center for Accelerator-Based Science
Wako, Saitama, 351-0198 JAPAN

RIKEN Accelerator Progress Report 2016 vol.50

This is an unabridged version of the 50th volume of RIKEN Accelerator Progress Report (hereinafter referred to as APR), the official annual report of the Nishina Center for Accelerator-Based Science.

A PDF version of APR can be downloaded from our website.
http://www.nishina.riken.jp/researcher/APR/index_e.html

Published by
RIKEN Nishina Center for Accelerator-Based Science
2-1 Hirosawa, Wako-shi, Saitama 351-0198 JAPAN

Director of RIKEN Nishina Center for Acclerator-Based Science
Hideto En'yo

Contact
Progress@ribf.riken.jp

RIKEN Nishina Center for Accelerator-Based Science, October 2017

PREFACE

With this volume, we celebrate the 50th anniversary of the RIKEN Accelerator Progress Report. In 1966, 50 years ago, RIKEN's 4th cyclotron was commissioned at the Wako Campus, and the first volume of the Accelerator Progress Report was issued. Now, if one were to see the Wako campus of 50 years ago, one would recognize only the administration building, main building, and our accelerator facility. That was the place and time where we restarted our scientific journey to make Yoshio Nishina's dreams come true.

On June 7, 2017, RIKEN celebrated the 50-year anniversary of the Wako Campus. At the front of the monument of the 4th cyclotron, Nishina-Tomoka, a new cherry blossom created at Nishina Center was planted, and the Nihonium Memorial Monument was unveiled. What an honor for Nishina Center! The Wako City Mayor, Matsumoto, congratulated RIKEN on the anniversary with an interesting story; this campus was initially meant to be the Athletes' Village for the Tokyo Olympics in 1966. He was happy that the campus went to Yoyogi, following which RIKEN established itself in the campus and Wako City became the birthplace of nihonium.

The year 2016 started with the news of Morita's Element 113 Research Group in RIKEN earning naming rights for element 113, which graced the front page of all major newspapers, followed by the news of nihonium (Nh) being proposed as the name and symbol for the element in June. The morning following the news report, Minister Hase of the Ministry of Education, Culture, Sports, Science and Technology (MEXT), Parliamentary Secretary Toyota for MEXT, and Wako-City Mayor Matsumoto visited Nishina Center to congratulate us and went on a tour of GARIS.

On December 1, a press conference was held in Hakata to announce that nihonium had been approved as the official name and that it will take its place at the periodic table. On January 1, 2017, we received the news that the Asahi Prize will be given to the Element 113 Research Group. Finally on March 14th, 2017, at the presence of His Imperial Highness Crown Prince, the president of the International Union of Pure and Applied Chemistry, Prof. Tarasova, declared "the 113th element is named nihonium."

In 1908, Masataka Ogawa, a professor at Tokyo Higher Normal School, discovered element 48 and named it "nipponium (Np)." Regrettably, it was later found that the element was wrongly identified and that it was, in fact, element 75, which is in the same family of elements but located one level below in the periodic table.

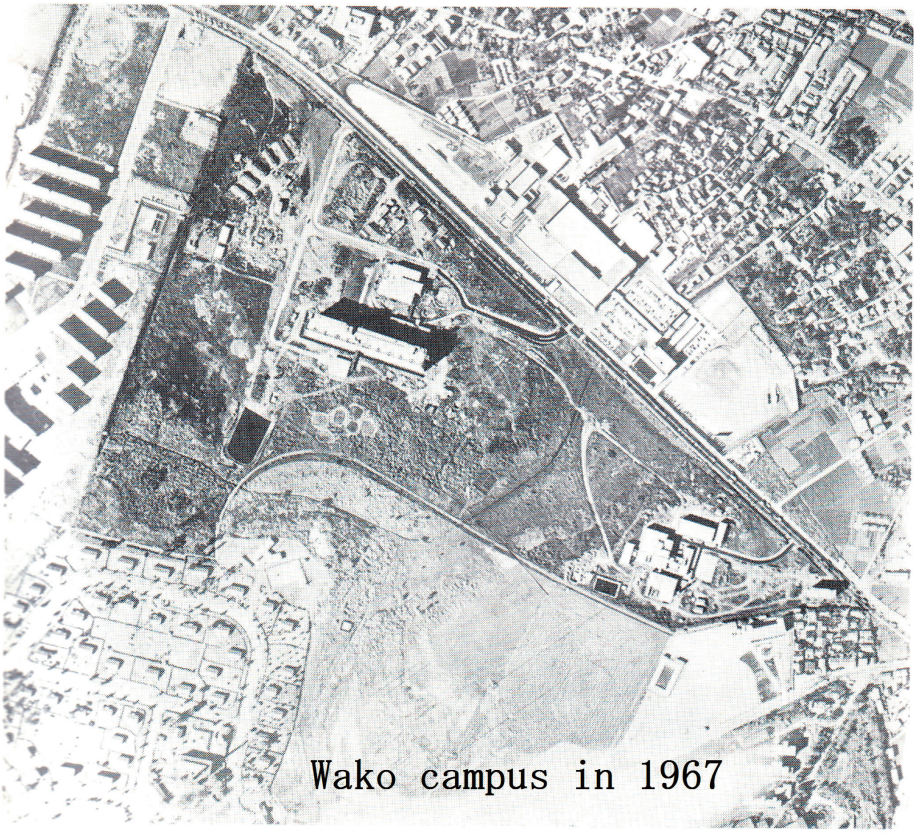

Wako campus in 1967

Eventually, elements 43 and 75 were named technetium (Tc) and rhenium (Re), respectively. It turned out that technetium was the first nuclide on the periodic table that does not have a stable isotope. In 1940, Yoshio Nishina et al. succeeded in producing element 93 but failed to identify its nuclide, and could not obtain naming rights for the element. Element 93 was later discovered by McMillan et al., who named it neptunium with the symbol Np, which had been once adopted as the symbol for nipponium.

Nishina had many seemingly impossible dreams. But now, Nishina's new element has reappeared as nihonium. Nishina's 2nd cyclotron reappeared as the RI Beam Factory, which is unparalleled in the world. Nishina's perceptions on RI applications are now our specialties. We are proud of what we have been accumulating with the 50 volumes of Accelerator Progress Reports.

In October 2016, RIKEN became a Designated National Research and Development Institute. I consider this a big chance for us to continue to move forward by going along with a positive trend that we have been blessed with in the 50 years of the Reports. With the supplementary budget of 4 billion yen for the RILAC upgrade we successfully managed to acquire, let us forge ahead toward a higher goal by advancing the RIBF upgrade project further.

Hideto En'yo
Director
RIKEN Nishina Center for Accelerator-Based Science

C O N T E N T S

Ⅰ. HIGHLIGHTS OF THE YEAR

Ⅱ. RESEARCH ACTIVITIES I (Nuclear, Particle and Astro-Physics)

1. Nuclear Physics

2. Nuclear Physics (Theory)

3. Nuclear Data

4. Hadron Physics

5. Hadron Physics (Theory)

6. Particle Physics

7. Astrophysics and Astro-Glaciology

8. Accelerator

9. Instrumentation

Ⅲ. RESEARCH ACTIVITIES II (Material Science and Biology)

1. Atomic and Solid State Physics (Ion)

2. Atomic and Solid State Physics (Muon)

3. Radiochemistry and Nuclear Chemistry

4. Radiation Chemistry and Biology

Ⅳ. OPERATION RECORDS

Ⅶ. LIST OF PREPRINTS

Ⅷ. LIST OF SYMPOSIA, WORKSHOPS & SEMINARS


The 50th Anniversary Special Issue
Research Activities
1991-2016
50

Retrospective of my 24-year "RIBF life"

Yasushige Yano*1,*2

1 Introduction

Ever since I joined RIKEN in 1979, I have devoted my efforts to the construction of the heavy-ion accelerator facility and the promotion of nuclear physics and applications of heave-ion beams. In December 1986, I completed Japan's first ring cyclotron (separate sector cyclotron) named RIKEN Ring Cyclotron (RRC) under Professor H. Kamitsubo, and in 1987, I proposed the "RI Beam Factory (RIBF)" as my dream, which eventually led to the creation of the world-class RI beam facility. Then, in 1997, the RIBF project was approved, and I undertook the construction of RIBF with the world's first superconducting ring cyclotron (SRC) as its main component. In December 2006, 20 years after the commissioning of the RRC cyclotron, I successfully led the new facility to the start of its operation. Currently, the RIBF is being utilized by the international nuclear physics community as the world's leading fast RI beam facility. In April 2006, the RIBF, the RIKEN BNL Research Center in the USA, and the RIKEN RAL Muon Facility in the UK were integrated to create the RIKEN Nishina Center for Accelerator-Based Science, and I was appointed as the first director of the Center. In September 2009, I stepped dawn, and now, I am devoted to upgrading the RIBF as the senior advisor to the Center. Here, I look back on the 24 years (from 1987 up to 2011) I devoted to the RIBF project.

2 Overview of RIBF

The RIBF[1] consists of a 22-year old facility and a new facility. These two facilities are connected to each other underground. The layout of the RIBF is shown in Fig. 1. The RIBF is now capable of providing all ions at 345 MeV/nucleon.[2] RI beams are produced via in-flight uranium fission or the projectile fragmentation of stable isotopes.

Consider uranium fission for instance. A uranium 35^+ beam obtained from the 28 GHz superconducting ECRIS[3] is pre-accelerated by the newly operational RILAC II,[4] and injected into the old RRC cyclotron. The energy of the RRC beam is boosted up to 345 MeV/nucleon by the new cyclotron cascade of fRC, IRC, and finally the superconducting ring cyclotron, SRC.[5] The 35^+ uranium ions are charge-stripped twice before and after the fRC cyclotron, from 35^+ to 71^+ at 11 MeV/nucleon and from 71^+ to 86^+ at

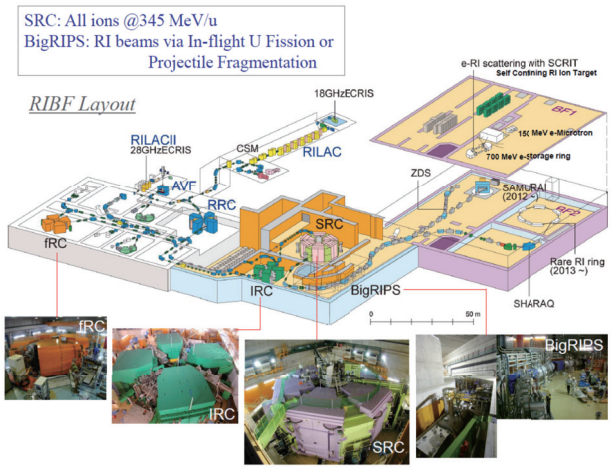

Fig. 1. Layout of the RIBF

51 MeV per nucleon. This charge stripping is now processed by an ordinary thin carbon foil (presently, the short life-time of the stripper is a serious bottle neck to increase the uranium beam intensity). The 345-MeV/nucleon uranium beam from SRC is transferred to the production target, and fission fragments are isotopically selected and collected by the large-acceptance superconducting BigRIPS.[6]

The superconducting ZeroDegree spectrometer (ZD)[6] and SHARAQ spectrometer[7] are used for the experiments, and the large-acceptance superconducting SAMURAI spectrometer[8] has been commissioned for experiments early in 2012. The unique electron-RI scattering ring with the self-confining RI ion target (SCRIT) has been completed.[9] This ring will allow the precision measurement of charge distribution, namely proton distribution inside unstable nuclei, for the first time. The construction of Rare-RI ring was completed in 2013.[10] It will allow precision mass measurements with the accuracy better than 1 p.p.m. for quite rare RIs with a productivity of 1 particle per day. The RIBF is now exhibiting its powerful potentiality to explore the nuclear world that was previously not accessible. In November 2008, 45 new radioactive isotopes were discovered in only a 4-day experimental run and with only 0.3 pnA beam intensity.[11] Among them, palladium-128 is speculated to be the origin of the second peak in the solar isotope abundance. In another two years, this uranium beam intensity will be increased by 400 times by installing a novel pressurized He-gas charge stripper having infinite lifetime. This decisive breakthrough has been devised by my younger colleague, Dr. H. Okuno.[12] RIBF will greatly expand our known nuclear world up to around pink-

*1 Director of RIKEN Nishina Center (2006–2009)
*2 Chief Scientist of Cyclotron Laboratory/Accelerator Group (1991–2008)

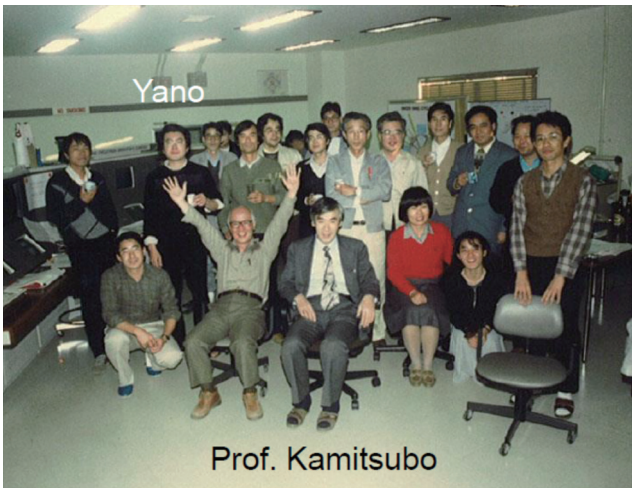

Fig. 2. Celebration of the first beam extraction from the No. 5. cyclotron (RRC) at 15:34 on Dec. 16, 1986. Twenty years later, the first beam from the No. 9 cyclotron (SRC) was produced.

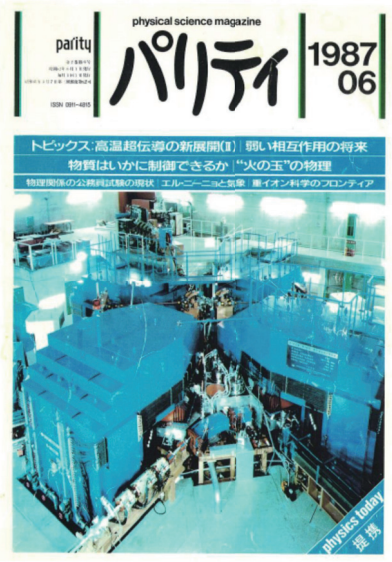

Fig. 3. Cover page of the popular Japanese science magazine "Parity" published in June, 1987.

coloured (in-flight fission) and sky-blue-coloured (projectile fragmentation) regions, which contain a hypothetical r-process pathway (green arrow) to create the uranium element at the moment of super-nova explosion, when we will achieve a primary beam intensity of 1 pμA for all ions. The RI-intensity produced at the edge of the regions is estimated by the GSI's simulation program EPAX2.[13] The significant challenge of uncovering the mystery of the element genesis has begun.

3 RARF

Let us look back on the 24 years, devoted to the RIBF project, from 1987 to date.

The RIKEN Nishina Center[14] established in 2006 is also my creation, and it is the first Japanese research center named after one of our great pioneering scientists. Dr. Nishina is called the Japanese father of nuclear science, and he mentored the first two Japanese Nobel Prize winners, Professors H. Yukawa and S. Tomonaga. Furthermore, the development of Japanese accelerators was initiated from his cyclotrons. I spent three and half years as the first director of the RIKEN Nishina Center, and now my younger colleague, Dr. H. En'yo, has succeeded me. Professor W.F. Henning, the former director of GSI, was appointed as the deputy director in charge of RIBF in 2010.

Figure 2 shows a photograph of our team celebrating the first beam extraction from the RRC cyclotron. The memorable moment occurred at 15:34 on December 16, 1986. Twenty years later, the first beam came out from the SRC cyclotron.

In 1987, Prof. M. Ishihara and I wrote a news article on the commissioning of the RIKEN Ring Cyclotron in the popular Japanese science magazine "Parity." A photo of the RRC cyclotron was shown on the cover page, as shown in Fig. 3. In the article, we wrote that our future dream is to create the world's leading "RI beam factory."

4 From RARF to RIBF

In the same year, when the discovery of high-T_C superconductivity was a hot topic, I was invited to attend a panel discussion on superconductivity and atomic energy. In this panel presentation, I presented a very conceptual drawing of the RI beam factory based on a superconducting sector-magnet cyclotron. In my scheme, I would later add an SRC and an RI beam collider downstream of the then newly operational RRC cyclotron.

In 1995, eight years after the RRC commissioning, a two-year R&D budget of nearly $2M was approved. By then, the RIBF plan consisted of a single big 150 MeV/nucleon SRC and a MUlti-use Experimental Storage rings, MUSES.[15] MUSES aimed at realizing the world's first electron-RI beam collider. However, this SRC had a serious problem in its design. In 1996, we had to conclude that the beam injection to this SRC was impossible because the central region was too narrow to set up the injection elements. This was the first hurdle we struggled to overcome.

Incidentally, the same year, I was invited over the phone by Professor B. Sinha, the then director of the VECC, in Calcutta, India to his office to take the photograph shown in Fig. 4 of us shaking hands to celebrate the conclusion of an MOU. During the flight

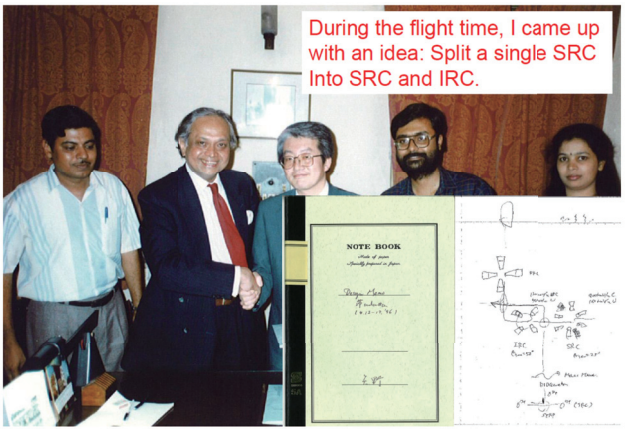

Fig. 4. VECC-RIKEN MoU conclusion meeting at Calcutta, India in 1996.

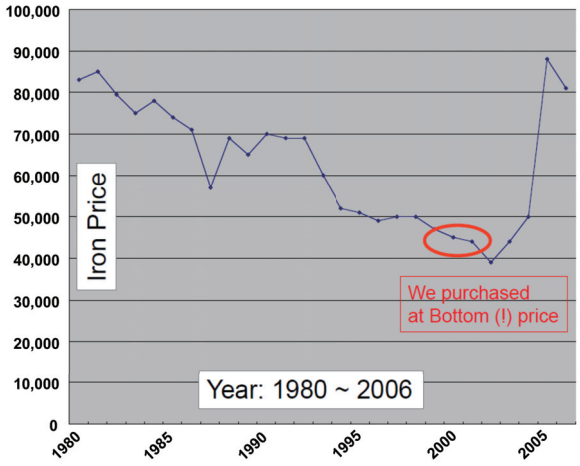

Fig. 5. Yearly trends in iron price from 1980 to 2006.

from Narita to Calcutta, I came up with an idea that the single big SRC should be split into smaller but with larger central-region SRC and an IRC cyclotron having a structure similar to the RRC.

The inset of Fig. 4, my memo in the travel note book where I jotted down this idea. In 1997, the construction budget was approved. In the figure, "SRC" and "IRC" can be seen.[16] We requested \$750M in total, but I was strongly requested by the government to reduce this cost by a significant amount. However, we still had serious problems in the SRC design. In 1998, I concluded that this SRC design included too many technical problems to be solved, and all the problems are due to the large valley-region leakage flux in the long term.

After recognizing this serious design drawback, I could not sleep well until, in 1999, I decided to cover whole valley regions with thick iron plates to absorb leakage flux. This was the simplest solution to solve all the problems.[17] The only problem was that the required mass of iron amounted to 8,000 tons, which is 1,000 tons heavier than the Eiffel Tour in Paris. Thus, the world's first, strongest, and heaviest SRC was born. This structure has self-radiation shielding capability as well. In November 2005, full excitation of the SC sector magnets was achieved.

Figure 5 shows the yearly trends of iron price from 1980 to 2006. We purchased 8,000 tons near the period when the price was minimum. In order to construct this super-facility, this stroke of luck was indispensable.

In 1999, an RIA project of the USA based on SC linacs was proposed, and the "white paper" of the project stated that the 150 MeV/nucleon uranium beam planned to be supplied through the RIBF project is insufficient to efficiently produce RI beams by in-flight fission. Instead, 400 MeV/nucleon should be achievable.[18] Then, in 2001, I decided that we add

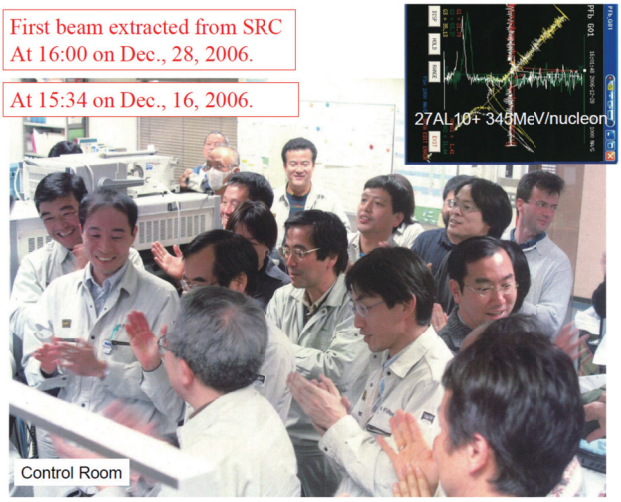

Fig. 6. A photo of the RIBF control room taken when the first beam was extracted from the SRC at 16:00 on December 28, 2006.

one more inexpensive cyclotron, fRC, to upgrade the final energy to 340 MeV/nucleon. Moreover, BigRIPS should be a large-aperture SC separator that can accept large-emittance fission fragments. These are the present design.[17]

5 The first beam and beyond

The first beam was extracted from the SRC at the moment indicated in Fig. 6, I had been declaring for years to the international accelerator community that the first beam would be extracted exactly 20 years after the first beam was extracted from the RRC cyclotron. Although the beam was slightly delayed, we almost well were successful.[19] "Science" magazine and "Nature" magazine reported the completion of RIBF.

In June 2007, the International Nuclear Physics Conference (INPC'07) was held in Tokyo, and I was given an extra session to deliver a flash report on the first outcome of RIBF: the discovery of a very neutron-rich isotope, palladium 125, by the in-flight fission of a 345-MeV/nucleon uranium beam. Incidentally palladium 112 was discovered using Dr. Nishina's cyclotron.[20] In his experiment, he discovered a much more surprising "symmetric fission" of uranium by fast neutrons, unlike the well-known "asymmetric fission" by slow neutrons. When closing my talk, I declared that a great endeavour has begun to explore areas of the nuclear world that have been inaccessible thus far. In the opening session of the conference, the Emperor delivered a very moving message to the audience about the tragedy of Japan and Japanese people caused by the atomic bombs and the role of the nuclear physics community.

Incidentally, during my directorship since 1992, I enjoyed the honour of guiding the Emperor on a tour of our cyclotron facilities twice, first in 1992 and then in 2006. I believe that now, the Japanese Emperor and Empress are the most informed royal couple in the world on cyclotrons.

How about MUSES? In 2001, the GSI reported that the luminosity obtained in MUSES is too low to create scientific impacts because the RIKEN system is based on a DC beam, rather than a pulsed beam. We absolutely agreed. Therefore, in 2003, I decided to give up the MUSES project, and instead decided to construct much better cost-effective high-performance alternatives, namely the SCRIT for precision charge-distribution measurement by electron scattering (this novel scheme was devised by my younger colleague, Dr. M. Wakasugi), and the Rare RI ring for precision mass measurement. The top of Fig. 7 shows a photograph of the completed electron-RI scattering system, and the bottom diagram shows its principle, the essence of which is that we utilize the unfavorable "ion trapping" phenomenon positively. We published two PRL papers on the experimental proof of principle.[21]

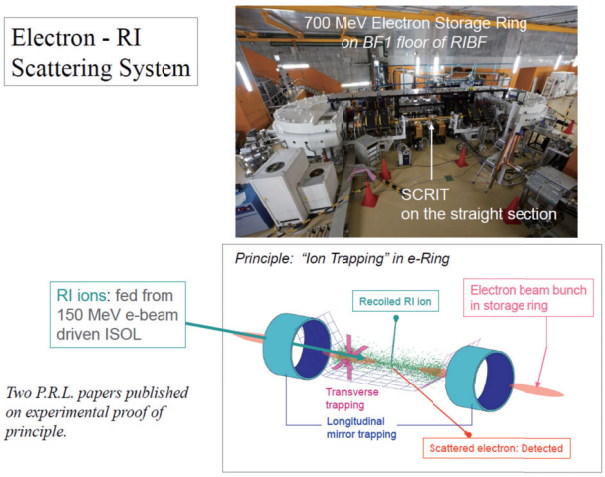

Fig. 7. Self-confining RI ion target (SCRIT) for e-RI scattering experiments.

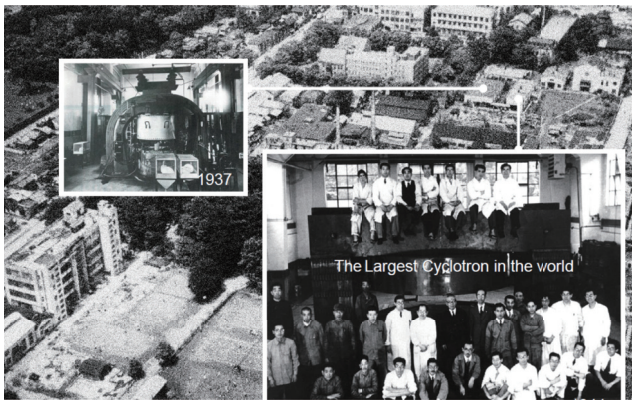

Fig. 8. Dr. Nishina's cyclotrons and the original RIKEN campus.

6 Dr. Nishina's dream

One day before the first International Particle Accelerator Conference (IPAC'10) in Kyoto, Japan, "Special lectures to commemorate the 120-th anniversary of Birth of Yoshio Nishina" was held. In this lecture meeting, distinguished Professors presented talks about Dr. Nishina and the advancement of particle accelerators and their applications in Japan. One of the lecturers, Professor M. Craddock, spoke about a very suggestive and impressive review story of Japanese cyclotrons from Dr. Nishina's pioneering work up to the present RI Beam Factory. The lecture notes can be viewed on RIKEN Nishina Center's home page.

Figure 8 shows photographs of Dr. Nishina's cyclotrons. This old aerial picture shows the original RIKEN campus, which was located near the center of Tokyo. On the top-right corner of this picture, there used to be Nishina's laboratory. The two buildings indicated in white dots housed his No. 1 and No. 2 cyclotrons. The No. 2 cyclotron, commissioned in 1944 just before the end of World War Two, was the world's largest cyclotron at that time, and was about to start experiments. However, as many of you know, these cyclotrons and at the same time Dr. Nishina's dream were killed by the War, as shown in the "Life" magazine issued in December 1945 (Fig. 9).

Since then, sixty six years have passed. I believe now that Dr. Nishina's dream has been realized. However, my dream will take a little more time to come true.

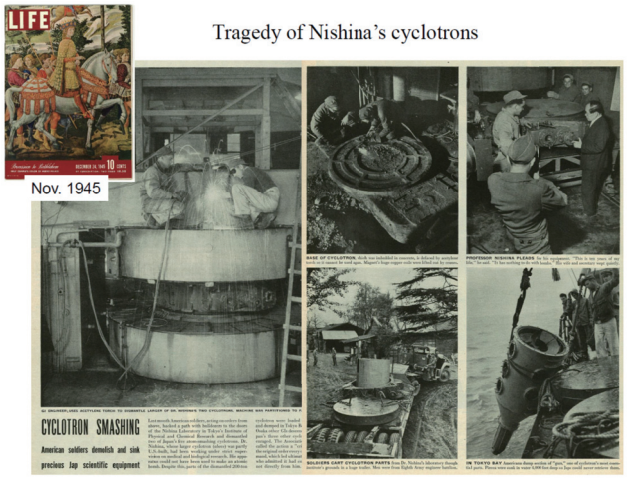

Fig. 9. Disassembling of No. 1 and No. 2 cyclotrons reported in "Life" magazine in 1945. ©1945 LIEF.

Acknowledgments

I wish to give my special thanks to many, many Japanese and foreign colleagues and collaborators and the presidents of RIKEN, especially Professor A. Arima. Without his strong support, this big project could not have started. Furthermore, I wish to express my gratitude to the International Advisory Committees (IACs) and the International Technical Advisory Committees (TACs) of the RIBF project, which have continuously led us in the right way, to the Governments that have strongly supported this project, and also to the companies that have helped us realize RIBF.

References

1) Y. Yano, Nucl. Instrum. Methods Phys. Res. B **261**, 1009 (2007).
2) O. Kamigaito et al., Proc. Cyclotrons'10.
3) Y. Higurashi et al., Proc. IPAC'10, p. 4191.
4) K. Yamada et al., Proc. IPAC'10, p. 789.
5) H. Okuno et al., IEEE Trans. Appl. Supercond. **18**, 226 (2008).
6) T. Kubo et al., IEEE Trans. Appl. Supercond. **17**, 1069 (2007).
7) S. Uesaka et al., AIP Conf. Proc. **1224**, 573 (2010).
8) Y. Shimizu et al., The International Nuclear Physics Conference 2010, INPC2010, July 5, 2010, University of British Columbia, Vancouver, Canada, J. Phys. Conf. Ser.
9) M. Wakasugi, T. Suda, Y. Yano, Nucl. Instrum. Methods Phys. Res. A **532**, 216 (2004).
10) Y. Yamaguchi et al., Nucl. Instrum. Methods Phys. Res. B **266**, 4575 (2008).
11) T. Ohnishi et al., J. Phys. Soc. Jpn. **79**, 073201 (2010).
12) H. Okuno et al., Phys. Rev. ST Accel. Beams **14**, 033503 (2011).
13) K. Suemmerer, B. Blank, Phys. Rev. C **61**, 034607 (2000).
14) `http://www.nishina.riken.jp/`.
15) Y. Yano, T. Katayama, Proc. EPAC'94, p. 515.
16) Y. Yano, A. Goto, T. Katayama, Proc. PAC'97, p. 930.
17) Y. Yano, A. Goto, M. Kase, T. Katayama, Proc. CYCLOTRON'01, p. 161.
18) *ISOL Task Force Report to NSAC*, 22 November 1999.
19) Y. Yano, Proc. PAC'07, p. 700 (2007).
20) Y. Nishina, T. Yazaki, K. Kimura, M. Ikawa, Nature, p. 660 (1939).
21) M. Wakasugi et al., Phys. Rev. Lett. **100**, 164801 (2008); T. Suda et al., Phys. Rev. Lett. **102**, 102501 (2009).

RIKEN Accelerator Research Facility (RARF) – The predecessor of Nishina Center –

M. Ishihara[*1,*2,*3]

RARF was an organization formed under the authorization of the RIKEN President to help promote scientific activities using the RIKEN facility of accelerator complex, which may be called RARF as well. The complex consisted of the central accelerator, RIKEN Ring Cyclotron (RRC), and its alternate injectors, RIKEN Linear ACcelerator (RILAC) and the AVF Cyclotron with $K = 70$ MeV. Effectively, RARF served as a research center for accelerator-driven science, and thus can be regarded as the predecessor of Nishina Center. It was organized upon the completion of RRC by the initiative of H. Kamitsubo, who was the original leader of the RRC project. It functioned from 1990 to 2001 under equal partnership among all the RIKEN Laboratories involved in the utilization of the RARF accelerators. Pursuit of a common research program entitled Multidisciplinary Researches on Heavy Ion Science was the central objective of RARF, while it also took charge of realizing the next-generation facility as it launched the RIBF project in 1995.

Naturally, the Director of RARF was elected from among the associated Chief Scientists. Thus, I served as the first Director during 1990–1997, being succeeded by I. Tanihata (1997–2001). During my term of office Y. Awaya and Y. Yano served as Deputy Directors, respectively representing the researchers other than the nuclear physicists and the accelerator staff while I represented nuclear physicists.

RARF originally involved 13 RIKEN Laboratories, of which 3 were associated with nuclear physics and 10 with other disciplines of science. Among those, the Cyclotron Laboratory led by Y. Yano played a special role by taking the full responsibility for the construction, development, and operation of the entire accelerator facility, except for the part of RILAC that was under the charge of the relevant group of the Linear Accelerator Laboratory led by M. Kase. The total beam time was shared almost evenly between nuclear physics and non-nuclear physics groups; the former primarily used RRC, while the latter also employed the injector accelerators in their stand-alone mode.

Research activities at RARF were highlighted by the following principal programs conducted with RRC. They involved 4 projects for nuclear physics; NP-1) RIPS project, NP-2) GARIS-IGISOL project, NP-3) SMART project, and NP-4) ASHURA project, and 4 projects for other scientific disciplines; OS-1) muon science project named Large Ω, Os-2) atomic physics project on multiply charged ions, OS-3) nuclear chemistry program by means of rapid chemistry, and OS-4) radiation biology program via heavy-ion irradiation.

All of these projects were approved in the mid-1980s and facilitated upon the commissioning of RRC in 1989. It is worth noting that each of these programs was proposed and conducted under the strong initiative and leadership of the respective Chief Scientists, symbolizing the spirit and principle of the traditional RIKEN system of Chief Scientists, which prevailed in the institutional operation throughout the 1990s. For some nuclear physics programs, prominent scientists from outside of RIKEN were invited to serve as Visiting Chief Scientists, and took charge of the programs of their own proposal. This arrangement was realized upon an official request by the Nuclear Physics Forum of Japan to the RIKEN President that the RRC facility be open for scientists outside of RIKEN. As it turned out, acceptance of outside researchers was very effective in enlarging the scope of scientific activities with RARF utilities. Formally, these outside users were affiliated to relevant RIKEN Laboratories, being given the status of Visitors of RIKEN. The other RIKEN systems of Special Postdoctoral Researcher and Junior Research Associate were also useful to attract young talent from universities.

It is delightful that most of the above-quoted programs were extremely successful in generating/developing novel sub-fields of atomic and subatomic science, thereby leaving a great legacy for the current research activities at Nishina Center.

Firstly, the RIPS project (NP-1) led by myself accomplished a major step forward in advancing the rising filed of RI-beam (RIB)-driven nuclear physics. The main vehicle employed was a separator called the RIKEN Projectile-fragment Separator (RIPS), which produced RIBs of epoch-making intensities. The achievements of the RIPS project were so great that they immediately triggered worldwide enthusiasm for promotion of RIB science. At RARF, the success of the RIPS project stimulated the promotion of the RIBF project to serve as the third-generation RIB facility. Thus, a variety of research fields cultivated with RIPS are now in full bloom with BigRIPS at RIBF.

Secondly, the GARIS project of NP-2) led by T. Nomura (INS, the University of Tokyo (UT)) aimed at the synthesis of super-heavy elements (SHE) by implementing a high-performance Gas-filled Recoil Ion Separator (GARIS) for the first time in the world. This was the first Japanese attempt to look for SHE with

*1 Director of RARF (1900–1997)
*2 Project Supervisor of RARF/RIBF Project Head Office (2001–2004)
*3 Chief Scientist of Radiation Laboratory (1984–2000)

contemporary accelerator facilities. While its campaign with RRC did not succeed in finding any new elements, it has left an ample set of matured expertise and advanced instrumentation. This has afforded a strong basis for a later campaign with the upgraded RILAC facility, resulting in the successful synthesis of nihonium (Nh). The Ion-Guided Isotope Separator On Line (IGISOL) project under the leadership of T. Inamura has also left a legacy in the research field with slow and stopped RIs, which is currently progressing with the SLOWRI project at RIBF.

Thirdly, the SMART project of NP-3) was initially led by H. Ohnuma (Tokyo Institute of Technology) and later by H. Sakai (UT). It addressed particle spectroscopy with intermediate-energy heavy-ion direct reactions by incorporating a magnetic analyzer named SMART. The project was drastically reinforced when a spin-polarized deuteron beam was installed through the efforts of the Sakai group. This led to the finding of a significant effect of nuclear three-body interaction, which served to invoke the currently prevalent worldwide campaign to explore the nature and influence of higher-order interactions. The current SHARAQ project under the auspice of Center for Nuclear Study (CNS), UT, is supposed to succeed this tradition of particle spectroscopy, which is to be applied to RIB-induced reactions at RIBF.

The ASHURA project led by S. Lee (Tsukuba University) aimed at the investigation of hot/dense nuclei. The destiny of this project was exceptional; it was terminated before it became ripe because of the then emerging thrust towards relativistic-energy phenomena.

The projects in the other disciplines were also rich in novelty. The Large Ω project of OS-1) led by K. Nagamine aimed at the promotion of muon-driven science by establishing a facility of strong secondary beams of muons. For that purpose, a solenoidal magnet device with a large solid angle was constructed and named as Large Ω. After the initial attempt at RRC to produce negative muons from deuteron-induced reactions, the facility site was moved to ISIS at Rutherford Appleton Laboratory (RAL), UK, as described later.

The atomic physics project of OS-2) led by Y. Awaya addressed the investigation of multiply charged ions of medium-heavy elements, which was an emerging field in those years as promoted by the advent of intermediate-energy heavy-ion beams. After initial successes with RRC, an advanced version of the ECR ion source became the major facility for this project. The low-energy beam of highly charged ions provided a unique means to analyze single and multiple electron capture processes, thereby facilitating the spectroscopy of highly excited atomic levels.

The nuclear chemistry project of OS-3) led by F. Ambe made use of the rapid transportation system of RI products from the RRC bombardment site down to the specific area for hot chemistry. This capability readily produced useful mixtures of short-lived RIs to be used to study the features of element circulation in a variety of circumstances. This novel method named "Multi-tracer method" allowed simultaneous injection of different elements into a common host sample, yielding results fairly free from the sample individualities. Thus, it was widely applied for the study of element circulation through biological bodies and in different environmental situations.

The radiation biology project led by F. Hanaoka and F. Yatagai established an irradiation system dedicated to biological samples, which allows irradiation in the air over a wide field of homogeneous dose distribution. This facility has been used for various purposes including the pilot experiment to validate the irradiation methods for heavy-ion cancer therapy to be practically used at the HIMAC facility at National Institute of Radiological Sciences (NIRS). The irradiation system was also used intensively for a project of biological transmutation promoted by S. Yoshida and T. Abe. This project is still being undertaken in full swing at RRC, as it has been so successful in generating useful variants of flowers and grains.

The research activities of RARF were also extended to programs conducted in international collaboration. Firstly, I. Tanihata launched a set of international programs on RIB physics, for which experiments were performed using the FRS facility at GSI, Germany and the RIBLL facility at IMP, China in collaboration with researchers on site. At RIPS, a Russian group from Kurchatov Institute was invited collaboratively to conduct a unique program of synthesizing super-heavy hydrogen and helium isotopes. These programs, which were significantly productive, served well to spread RIB physics worldwide.

The major undertaking of implanting a RIKEN facility at a foreign institution started when a muon facility was constructed at RAL to produce intense secondary beams of muons by incorporating high-power proton beams from the ISIS accelerator. The facility has been in operation since 1995 under the auspices of the RIKEN Facility Office at RAL, as originally directed by K. Nagamine. It is a powerful facility open for outside users, hence widely used internationally. The central activities have been on material science, where the method of muon spin rotation, relaxation, resonance (μSR) was primarily employed to investigate electron motion or spin correlation in a variety of materials. Uniquely, the facility was also committed to R&D works for the muon-catalyzed d-t fusion.

Another project in international collaboration soon followed. In 1995, the Radiation Laboratory directed by myself took the initiative to realize the Spin Physics Program to be conducted with the Relativistic Heavy-Ion Collider (RHIC) at Brookhaven National Laboratory (BNL). In starting this program, the Radia-

tion Laboratory has strongly contributed financially to the installation of Siberian snakes and spin rotators at RHIC, which are essential for the acceleration and manipulation of spin-polarized protons. It has then been committed to play a major role in the Spin Physics Program conducted in the framework of the PHENIX Collaboration. The primary aim of this program was to elucidate the so-called spin puzzle by clarifying the role of gluons in making up the nucleon spin of 1/2. Experimental runs with RHIC polarized proton beams started in 2001 when the Radiation Laboratory accepted a new Chief Scientist, H. En'yo. After several runs on double-helicity asymmetry, the integrated contribution of gluons over the accessible range of Bjorken's x was found to be compatible with the quark contribution. Thus, the quest for the remaining contributions, possibly from smaller-x gluons and/or from the parton orbital angular momenta, has provided a strong cause for proposing the next-generation US accelerator facility, Electron Ion Collider (EIC).

The RIKEN BNL Research Center (RBRC) was created in 1997 originally to support the RIKEN activities for the Spin Physics Program, while its objective was soon extended to nursing young talents of QCD theorists under the strong initiative of T. D. Lee, the first Director of RBRC.

Promotion of international cooperation on the basis of institutional agreement was another consistent policy undertaken by RARF. In this context the 1st agreement was effectively formed with Institute of Modern Physics (IMP), Lanzhou, China as early as 1979 for collaboration on accelerator issues. A series of Japan-China Joint Symposium on Accelerators for Nuclear Physics and Their Applications thus realized through 1980–1996 greatly contributed to establishing close relations between the relevant communities of the two countries. In 1988 the agreement was formalized also to cover activities on nuclear physics. Since then a couple of postdoctoral researchers from IMP were regularly invited to stay and work at RARF through 1990s. It is delightful to see that many of those colleagues are, nowadays, playing leading roles in the Chinese community of nuclear physics.

The 2nd agreement was established with a US institution, Cyclotron Laboratory, Texas A&M University (TAM) in 1982, while the collaborative experimental program using the TAM facility was already initiated in 1978. The success of this fairly early engagement stimulated later collaboration with several European institutions, including IN2P3 (France), INFN (Italy), GSI (Germany), Flerov Laboratory and Kurchatov Institute (Russia). Among those the agreement with IN2P3 started in 1985 provided a unique scheme of cooperation, essentially allowing participation of any nuclear physicists in both the countries. Indeed it has developed a blessed tradition of close partnership between the two communities, through the conduct of many collaborative works both at GANIL and RARF and of a series of Japan-France Joint Symposium (1987–1994) on Heavy-ion Science. Long-lasting collaboration with INFN has been conducted similarly since 1991.

RARF as well pursued cooperation with domestic institutions. Most importantly, intensive cooperation with CNS was started in 2000 when it moved in the Wako campus of RIKEN so that its researchers could readily join the utilization of the RARF facility. Nowadays this collaboration has grown so far as to practice joint operation of RIBF.

The research programs/projects described thus far were started before the mid-1990s. On approaching and entering the 21 century, the configuration of RARF members was considerably changed with the addition of newly assigned Chief Scientists in return for the retirement of most of the Chief Scientists originally involved. Nevertheless, most of the research enterprises mentioned above have remained to be the central involvements in the following years to come not only for RARF but also for Nishina Center.

RARF was also committed to the realization of the next-generation facility. Thus, the RIBF project was launched in 1995 under the auspices of RARF, while the construction of RIBF was performed under the leadership of Y. Yano, who led the newly organized system called Cyclotron Center. To coherently promote the construction of RIBF and the daily operation of RARF, a new organization named RARF/RIBF Project Head Office was operated through the fiscal years of 2001–2004. It effectively accommodated the entire system of the old RARF, while I. Tanihata (2001–2003) and T. Motobayashi (2003–2005) served as the Director of the Accelerator-based Research Group. It was closed in 2005 when a transient system functioning similarly to RARF was created within the framework of the RIKEN Frontier Research System. Finally, RIKEN Nishina Center for Accelerator-Based Science (RNC) was started in 2006, and Y. Yano became its first Director. Incidentally, RIBF was commissioned in the same year.

RIPS Project: Pursuit of the RIB Physics Program with RIPS

M. Ishihara[*1,*2]

The RIB Physics Program with RIPS was initiated in 1984, when I took the office of Chief Scientist of the Radiation Laboratory. The primary objective of the job was to cultivate a novel field of nuclear physics using the RIKEN Ring Cyclotron (RRC) facility,[1] which was then under construction since 1980 to be completed in 1989. RRC is an intermediate-energy heavy-ion facility, following predecessors such as NSCL, MSU at Michigan and GANIL at Caen. Since we were late comers, I was keen to select a research objective well distinguished from those of the preceding facilities, where studies of hot and/or dense nuclei were most intensively pursued. Our subject thus chosen was the study on exotic nuclei far from the line of stability by means of a radioactive ion beam (RIB), which was a research field still in its infancy in the 1980s. The major vehicle to drive our program was an in-fight projectile-fragment separator, RIKEN Projectile-fragment Separator (RIPS),[2] which emerged as the world strongest RIB deliverer, marking the advent of the second-generation RIB facility.

This program was proven to be so successful that it triggered and enhanced worldwide enthusiasm towards the promotion of RIB science. Indeed, the RIPS program has attained many of the first accomplishments in terms of identifying unique scientific agendas on exotic nuclei and of cultivating novel methods for RIB experiments. These accomplishments altogether served to constitute the universal framework for the research conduct on RIB physics through the years that followed. At RIKEN, the success of the RIPS project became the cause for promoting the project of RIKEN RI-Beam Factory (RIBF), which was commissioned in 2006 to serve as the world-leading facility for the third-generation RIB science.[3]

1 Features of RIPS

The production method of RIB by means of in-flight projectile fragments was introduced in the mid-1980s, and pioneering works with such RIBs were performed at Bevalac, LLNL to determine the radius of exotic nuclei[4] and then at LISE, GANIL mainly to synthesize new isotopes.[5] The finding of the neutron halo by the former work was particularly fascinating, as it revealed the exotic nature of nuclei very far from the line of stability. While these earlier studies were much stimulative, the fairly weak beam intensities inherent to those first-generation facilities severely hampered further extension of RIB physics. Thus, the RIPS project was aimed at drastically expanding the research territory by introducing reinforced RIB of unprecedented intensities. RIPS was also charged to facilitate the unique capability of producing spin-polarized RIB.[6]

RIPS is designed to be a separator of incoming projectile fragments, delivering the resultant RIB at the exit channel. It consists of two 45° dipoles (D1 and D2) supplemented with twelve quadrupoles and four sextupoles. The system is essentially composed of two sections in cascade with their relevant focuses. The first section with D1 gives rise to a dispersive focus at F1 and analyzes the magnetic rigidity of fragments. The second section with D2 compensates for the dispersion of the first section and gives rise to a doubly achromatic focus at F2. These two sections combined, with a wedge-shaped energy degrader placed at F1, constitute a doubly achromatic spectrometer, separating the projectile fragments with respect to their A and Z (or q).

In designing RIPS, special precautions were taken to achieve the maximum intensities for the outcoming RIB. The large angular and momentum acceptances taken as 5 msr and 6%, respectively, are essential for this purpose. Also important was the adoption of a large value of 5.76 Tm for the maximum magnetic rigidity, which well exceeds the value of 3.5 Tm of RRC. Such a large bending power allows the use of the highest possible energy of the primary beam even for the production of fragments with very large magnetic rigidity. This is useful to drastically enhance the yield of neutron drip-line nuclei like ^{11}Li, since the production rate of RIB varies with the incident energy $E_{\rm int}$ of the primary beam as $E_{\rm int}^{\alpha}$, where $\alpha \fallingdotseq 3.3$. Thus, RIPS was constructed to become an epoch-making deliverer of RIBs by affording beam intensities stronger than the preceding facilities by 3–4 orders of magnitude.

Such intensities of RIPS beams served tremendously to expand the scope of the applicable experimental methods and hence of the research subjects to be addressed. Most importantly, the RIPS beams were strong enough to easily facilitate observation of a variety of direct reactions, the cross sections of which are typically of the order of several 10 mb. As closely described later this feature greatly helped to promote in-beam studies of nuclear structure and nuclear astrophysics, thereby opening up a wide research field of RIB physics.

Moreover, the capability of RIPS was extended to deliver not only ordinary RIBs but also special types of RIBs, namely spin-polarized RIBs and RIBs of isomers. Spin-polarized fragments are produced in the course of the projectile-fragmentation process. Hence, spin polarized RIBs can be readily obtained through RIPS.[6] The spin-polarized beams thus produced provided a unique tool to determine the nuclear moments of unstable nuclei by means of an NMR method incorporating the β-decay process.

*1 Chief Scientist of Radiation Laboratory (1984–2000)
*2 Professor, the University of Tokyo (1986-2000)

2 Research goals with RIPS-RIB

In undertaking the RIPS project, we have chosen three major subjects on nuclear physics.[7] Firstly our focus was directed to reveal and explore exotic phenomena of nuclear structure, which are to be unique to unstable isotopes.[8] Thus, we placed our research emphasis on extremely neutron-rich nuclei, which are uniquely characterized by i) isospin asymmetry with a large excess of neutrons and ii) loose binding of valence neutrons. As is well recognized nowadays, the former feature gives rise to exotic bulk phenomena such as shell evolution resulting in appearance/disappearance of new/classical magic numbers, while the latter gives rise to the peripheral phenomena of neutron halo or skin. Such dilute neutron matter may enhance the cluster formation of the di-neutron. In general, decoupling of valence neutrons from the core may be another key property of extremely neutron-rich nuclei.

Direct reactions have been essential in exploring such exotic features because each variety of direct reactions will provide a sensible probe for a specific property of nuclear structure. Hence, various direct reactions at intermediate energies were combined to probe broad aspects of exotic nuclear properties. Among others, Coulomb excitation/dissociation, nuclear inelastic scattering, nucleon-removal reactions, and exchange reactions were most frequently employed.

The second primary subject concerned nuclear astrophysics. Nucleosynthesis in stellar environments often occurs via proton/neutron radiative capture processes involving targets of unstable nuclei. Hence, we focused on the determination of stellar reaction rates for those radiative processes by measuring cross sections of their effectively inverse reactions, i.e., Coulomb dissociation processes. Proton-induced radiative capture reactions occurring in the p-p chain and CNO cycle were chosen to be the primary objectives.

Finally the unique asset of RIPS, spin-polarized RIB, has facilitated the pursuit of the third primary subject; determination of nuclear moments of unstable nuclei, which are hardly accessible otherwise. The research programs and achievements on these three subjects will be separately described in Sections 4, 5, and 6, respectively.

3 Cultivation of experimental methods for RIB

Most of our experiments on the first and second subjects as defined above were conducted by observing RIB-induced direct reactions. When performing such in-beam experiment, one observes the reaction process in inversed kinematics, where the incoming projectile of RIB serves as the nucleus to be characterized while the target nucleus serves as a probing particle. One will then encounter several difficulties characteristic of RIB made of in-flight fragments: the wide energy spread and the deteriorated emittance in addition to the poor luminosity. Among others, the wide energy spread of RIB is most disturbing since in-beam spectroscopy generally requires the precise determination of excitation energy E_x of the final state of interest, while the missing mass method, which is standard with the primary beam, does not properly work with the poor energy resolution of RIB.

To manage this problem, we have developed the following two methods for the in-beam RIB experiment: one is to measure the gamma rays de-exciting the bound final states[9] and the other is to determine the invariant mass of the unbound final states via the measurement of 4 momentum vectors of all the particles emitted in the final channel.[10,11] Nowadays, these two methods have become prevalent as the standard experimental methods for RIB physics. The poor luminosity is partly overcome by the useful features of the intermediate-energy RIB, as the use of a thick target is allowed and a full solid angle can be readily covered by the detector assembly by virtue of the strong forward focusing of the outgoing particles owing to Lorenz boost.

4 Study on exotic nuclear structure of extremely neutron-rich nuclei

The experimental studies on exotic nuclear structure in the earlier stage were primarily performed in two regions of neutron-rich nuclei, one being around $N = 8$ isotones including ^{11}Li and ^{12}Be and the other around $N = 20$ isotones including ^{32}Mg. Both of the regions involve phenomena of significant shell quenching and of neutron halo as described below.

4.1 Study on halo nuclei

The neutron halo phenomenon was first indicated for ^{11}Li by the large interaction radius determined via the measurement of interaction cross section.[4] To further explore the nature of the phenomenon, we employed Coulomb dissociation as a probing reaction, as first applied to the study on ^{11}Be.[10] In this process, halo nuclei are strongly excited via the E1 transition, leading to the continuum final states at low excitation energies. This so-called soft dipole excitation turned out to be a powerful tool for characterizing the wave function of the halo nucleon, which is supposedly well decoupled from the core part of the nucleus. In fact, the decay spectrum, as observed in the single-neutron halo nucleus ^{11}Be with the invariant mass method, represents the square of Fourier transform of the wave function times radius. Hence the spectrum shape is dictated by the neutron separation energy S_n, with the peak appearing around $E_x \sim 8/5S_n$. The cross section is proportional to the square of the asymptotic normalization coefficient, which is gigantic for a halo neutron. Thus, the strength may well exceed the Weisskopf unit, yielding the cross section of several 100 mb.

This feature of huge cross sections for low excitation energies serves as a clear signature of any neutron halo nuclei. In fact, later experiments singly exploiting this feature newly identified several halo nuclei, including

^{19}C, ^{31}Ne, and ^{37}Mg. With complementary experiments, ^{19}C was ascribed to the s-wave halo like ^{11}Be, while ^{31}Ne and ^{37}Mg in the pf-shell region were ascribed to the p-wave halo. It is worth noting that the appearance of the p-wave halo is caused by deformation of those nuclei.[12)]

For the case of a two-neutron halo such as of ^{11}Li, the occurrence of a di-neutron cluster may be conceived. This phenomenon can be identified by finding an enhanced strength of soft dipole excitation, since the total strength of the E1 excitation for the case of the two-neutron halo represents the square of the radius vector of the center of gravity of the pair of neutrons. Indeed, the observed strength for ^{11}Li clearly exceeded the upper limit for the two uncorrelated neutrons, disclosing occurrence of a di-neutron cluster in the halo area of dilute density.[13)]

4.2 Disappearance of classical magic numbers as signatures of shell evolution

This quest was initially addressed to nuclei around $N = 8$ as stimulated by the notion of the $N = 7$ anomaly.[14)] As pointed out by I. Talmi et al., the supposedly higher-lying neutron level of the $2s_{1/2}{}^{+}$ orbit gradually lowers with respect to the $1p_{1/2}{}^{-}$ orbit as the neutron excess increases along $N = 7$ isotones, even crossing over at ^{11}Be. To clarify the nature of this phenomenon, we first studied the level scheme of an $N = 9$ isotone, ^{14}B, by observing the β decay of ^{14}Be.[15)] A large-acceptance detector assembly for β-γ spectroscopy was used together with a high-efficiency TOF detector array for delayed neutrons. It was confirmed that the evolution of level crossing with increasing neutron excess also occurs in $N = 9$ isotones, supporting the conjecture that $N = 8$ magicity is quenched in extremely neutron-rich isotones.

The systematic study on shell evolution was strongly activated when we introduced a novel method of in-beam γ ray spectroscopy,[9)] by which the behaviors of the first excited 2^+ state (2^+_1) and other prominent low-lying states of even-even nuclei may be easily assessed. The first experiment of this category was performed on ^{32}Mg by incorporating the intermediate-energy Coulomb excitation process (I.E. Coulex) at $E_{\rm in}/A = 49.2$ MeV. The use of Coulex at such a high energy was a challenging attempt at that time since there had prevailed a strong prejudice that the dominance of Coulex over nuclear excitation for the case of E2 transition could be only assured when the incident energy was taken well below the Coulomb barrier. As is revealed, Coulex well dominates even at intermediate energies when a target nucleus of a heavy element such as Pb is employed. Thus, the E2 strength, B(E2; $0^+_{\rm g.s.} \rightarrow 2^+_1$), and the excitation energy of the 2^+_1 state, $E_{\rm x}(2^+_1)$, were unambiguously determined for ^{32}Mg. The enhanced B(E2) and the reduced $E_{\rm x}(2^+_1)$ together provided clear evidence of enhanced collectivity, assuring the quenched magicity of $N = 20$ in this extremely neutron-rich isotope.

In-beam γ-ray spectroscopy with intermediate-energy reactions is subject to a huge Doppler effect. We thus used an array of highly segmented NaI(Tl) γ-ray detectors named DALI to facilitate the Doppler shift correction. The use of the NaI(Tl) detector was helpful to increase the photo-peak efficiency, while its relatively poor energy resolution sufficed to observe the spectrum with sparse peaks owing to the stringent selectivity inherent to intermediate-energy direct reactions. In-beam γ-ray spectroscopy with I.E. Coulex thus initiated soon became the most popular method worldwide to explore the phenomena of shell evolution.

In-beam γ-ray spectroscopy with RIB marked another big step forward when we studied ^{12}Be by incorporating the proton inelastic scattering for the first time.[16)] It was immediately recognized that the (p, p') reaction is equipped with several precious features to reinforce the method of in-beam spectroscopy. Firstly, the number of atoms per given target thickness in mg/cm^2 is huge for the proton target of $A = 1$, leading to the tremendous enhancement of event rate. Another indispensable feature of the (p, p') reaction is that it provides a different measure of transition strength, which is the deformation length δ. To make it more usable, the global optical potential is available for the proton scattering to be readily employed for DWBA analysis. The lowered $E_{\rm x}(2^+_1)$ and enhanced $\delta_2(0^+_{\rm g.s.} \rightarrow 2^+_1)$ thus obtained were clear signatures of the strong collectivity of ^{12}Be, confirming the occurrence of quenched magicity for this neutron-rich $N = 8$ isotone. For ^{12}Be, the first 1^- state[17)] and the second 0^+ state[18)] were also found close to the ground state. This implies the near degeneracy of $2s_{1/2}{}^{+}$ and $1p_{1/2}{}^{-}$ orbits, further supporting the quenched magicity.

The (p, p') reaction affords additional merits: it strongly excites the first 4^+_1 state as well as 2^+_1, in contrast to the case of I.E. Coulex, thereby providing unique information on nuclear collectivity. This feature was first exploited in the study of ^{62}Cr to assure its strong deformability.[19)] It is also worth noting that the (p, p') process occurs through nuclear interaction, while Coulex occurs through electromagnetic interaction. Accordingly, the former process is more sensitive to the neutron component of the transition matrix, while the latter to the proton component. Thus, the combination of these two reactions enables us to determine the proton and neutron matrixes separately. This feature was exploited, e.g., to clarify the nature of the strongly hindered E2 strength of ^{16}C.[20)] It was revealed that the effective charges of the valence neutrons are strongly suppressed, indicating their decoupling from the core nucleons.[21)]

Finally, the nucleon-removal reaction was introduced as the third probe reaction, as first used for the study of ^{34}Mg.[22)] It was particularly useful to broaden the accessible region of in-beam spectroscopy towards larger neutron excess. The in-RIB γ-ray spectroscopy thus developed has been intensively employed till today to explore the features of shell evolution over the broad region of the nuclear chart. So far, such endeavors worldwide

have been successful to confirm the occurrence of shell quenching at $N = 28$[23] as well $N = 8$ and 20, while such quenching only occurs in the isotones located very close to the neutron drip line. In contrast, no signature of shell quenching was found for the heavier classical magic numbers of $N = 50$ and 82, even at extremely neutron-rich isotones such as ^{78}Ni[24] and ^{128}Pd.[25] For these systematic studies on shell evolution, the 2015 Nishina Memorial Prize was awarded to T. Motobayashi and H. Sakurai on behalf of the international colleagues.

5 Study on nucleosynthesis in the cosmos: Determination of astrophysical reaction rates via RIB-induced Coulomb dissociation

Nucleosynthesis in the cosmos is supposed primarily to occur in stellar burning processes that involve very-low-energy nuclear reactions with unstable nuclei. Thus, determination of reaction rates of relevant processes should provide clues in deciding among the various possible scenarios on cosmic evolution. In this context, we set up a novel program to measure the cross section of stellar reactions of radiative capture, which is the most popular process in star burning. For this purpose, we followed the suggestion[26] by G. Baur and C. A. Bertulani that one should measure the cross sections of Coulomb dissociation with an intermediate-energy RIB, which effectively serves as the inverse reaction for the radiative capture process directly feeding the ground state of the residual nucleus. The measurement of this high-energy reaction instead of the original very-low energy reaction tremendously enhances the experimental efficiency by allowing a thicker target and a wider detection acceptance as well as affording a greatly increased cross section. These effects together contribute to increase the overall efficiency by about 6 orders of magnitude, well compensating for the disadvantage of using RIBs with much reduced intensity.

The method was first applied to determine the reaction rate of the ^{13}N(p, γ)^{14}O reaction,[11] a key reaction to ignite the hot CNO cycle of hydrogen burning in stars. The observation of Coulomb dissociation of ^{14}O by means of the invariant mass method revealed the relevant resonance of 1^- located at a decay energy of approximately 545 keV with a radiative width of $\Gamma_\gamma = 3.1 \pm 0.6$ keV. This marked the first successful experiment on the astrophysical reaction rate ever performed with RIB.

The astrophysical study with I.E. Coulex was then addressed to the ^{7}Be(p, γ)^{8}B reaction, a key process in the production of high-energy solar neutrinos by the ^{8}B β^+ decay. To determine the E1 strength free from the disturbing E2 contaminant, the first experiment using the RIPS ^{8}B beam[27] was complemented by another experiment performed using RIB of a higher incident energy at FRS-GSI.[28] The S_{17} value finally determined was $S_{17} = 20.6 \pm 1.2$ (exp.) ± 1.0 (theo.), slightly smaller than the values recently obtained directly from the low-energy bombardment of protons on a ^{7}Be target.

The Coulomb dissociation method was later applied not only to proton-capture reactions but also to a neutron-capture process, ^{14}C(n, γ)^{15}C, one of the key reactions in the Big-Bang nucleosynthesis.[29]

6 Study on nuclear moments as determined with spin-polarized RIB

Our tradition of producing spin-polarized unstable nuclei with heavy-ion reactions started as early as the mid-1970s, when we obtained spin-polarized ^{12}B isotopes via the ^{100}Mo(^{14}N, ^{12}B)X reaction at $E_{\rm in} = 90$ MeV.[30] However the polarizability could be meager in the intermediate-energy projectile fragmentation since the grazing angle of such a high-energy reaction tends to approach zero. To examine this aspect, we performed a pilot experiment at GANIL in the late 1980s to find that ^{12}B produced in ^{18}O projectile fragmentation at $E_{\rm in}/A = 60$ MeV indeed exhibited a sizable spin orientation.[31] Encouraged by this finding, a novel production scheme of spin-polarized RIB was developed.[6] RIPS was used for this purpose as well, through which the spin-polarized projectile fragments of specific nuclear species were separated and collected. To favorably collect spin-polarized fragments, two supplemental procedures were combined. One is to collect fragments emitted at angles away from zero. This was facilitated with a magnetic swinger placed upstream of the production target, which was used to tilt the direction of the incoming projectile. Secondly, the momentum bin for the in-flight fragment was selected at the intermediate dispersive focal plane so that the net polarization may be optimized. The magnitude of fragment spin polarization thus obtained is significantly large for the case of single nucleon removal, while it decreases rather rapidly as the number of removed nucleons increases.

For the measurement of g-factor, the spin-polarized β-unstable fragments were implanted into the host material, which preserves the spin orientation under an externally applied magnetic field. Meanwhile, the adiabatic fast-passage NMR method for spin reversal was applied to the implanted nucleus to find the relevant Larmor frequency and hence the g-factor of interest. The spin precession occurring across the Larmor frequency was monitored by observing asymmetric emission of β rays with respect to the spin-polarization axis. Spin-polarized unstable nuclei were also employed for the measurement of Q-moment, where a sequence of NMR procedures was applied to the fragments implanted into a host material with an adequate electric-field gradient.

Highlights in the earlier phase of the program involve firstly the determination of g-factor of ^{17}C[32] and secondly of Q-moments of ^{15,17}B isotopes.[33] The former result unambiguously confirmed the anomalous spin-parity of $3/2^+$ for this nucleus of $(d_{5/2})^3$ dominance. The latter result revealed extremely suppressed neutron effective charges of less than 0.1 as compared to the ordinary magnitude of $\sim$0.6. It was concluded that the valence neutrons of those extremely neutron-rich isotopes

are strongly decoupled from the core part of the nuclei.

The campaign of this program has been continued till today. As of 2010, g-factors and Q-moments were newly determined, respectively, for 14 and 10 unstable isotopes.

7 Collaborators

As described above, the RIPS project was carried out under the auspices of the Radiation Laboratory. On the other hand, the project has covered such a broad scope of nuclear research that a large number of collaborators from outside of the Radiation Laboratory were also involved. Among others, T. Kubo from the Linear Accelerator Laboratory should be noted as the primary contributor to the construction/operation of RIPS. Regarding the pursuit of research programs, the following three groups from outside of RIKEN played a major role in the initial stage of the project: 1) a group from the University of Tokyo (UT) led by myself and assisted by S. Shimoura, 2) a Rikkyo University group led by T. Motobayashi, 3) a group from Tokyo Institute of Technology (TIT) led by K. Asahi, and 4) a Kyushu University group led by Y. Gono. Among others, group 1) played a special role by directing the entire program jointly with the Radiation Laboratory. In the later stage, 5) a group from TIT led by T. Nakamura, 6) a group from the Science Faculty, UT, led by H. Sakurai, and 7) a group from CNS, UT, led by S. Shimoura joined to expand the scope of the program. Meanwhile, Radiation Laboratory finished its commitment to this program when I retired from the Laboratory in 2000. Instead, three RIKEN Laboratories with their respective Chief Scientists, 8) T. Motobayashi, 9) K. Asahi, and 10) H. Sakurai, were newly created to pursue RIB-related nuclear physics. The Laboratory of 9) was effectively succeeded by 11) the current Laboratory led by H. Ueno.

The research program on halo nuclei was originally implanted by group 1) and dramatically developed by the leadership of group 5) in the following stage. The program incorporating the in-RIB γ-ray spectroscopy has been most prosperous. It was originally started by groups 1) and 2) and later involved many other groups 6), 7), 8), and 10). In particular, group 2) was credited with the construction of the principal device, a γ-ray Detector Array for Low Intensity radiation (DALI). The research program on astrophysical nucleosynthesis was also initiated by groups 1) and 2), and later conducted primarily by groups 2) and 8). The research program with spin-polarized RIB was started by groups 1) and 3), and later taken over by groups 3) and 9) and finally by the current group 11). Group 4) was committed to a challenging program of developing and utilizing the so-called isomer beam. It was proven that such a beam is useful in studying, e.g., properties of excited bands built on isomeric states.[34)]

Finally, RIPS has been so useful that many research groups other than the above joined in the utilization of the facility. Among others the Linear Accelerator Laboratory group led by I. Tanihata set up a unique program on nucleosynthesis to exploit the extremely intense RIPS beam of ^{11}Li. This program, which was performed in collaboration with a group from Kurchatov Institute led by A. Korsheninnikov, has succeeded in the synthesis of e.g., "super heavy" helium isotope, ^{10}He.[35)] Another major commitment was made by a group from Osaka University led by T. Minamisono and K. Matsuta, who intensively worked on spin-dependent β-decay issues by means of spin-polarized RIB.

Altogether, the number of researchers who have participated in the RIPS-based programs is greater than 250. In particular, the participation of graduate students from various universities was significant. As of January 2008, the RIPS project resulted in the awarding of 52 Ph.D. degrees.

References

1) Y. Yano, Proc. 12th Int. Conf. on Cyclotrons and their applications, Berlin, eds. B. Martin and K. Ziegler (World Scientific, 1989) p. 13.
2) T. Kubo et al., Nucl. Instrum. Methods Phys. Res. B **70**, 309 (1992).
3) Y. Yano, Nucl. Instrum. Methods Phys. Res. B **261**, 1009 (2007).
4) I. Tanihata et al., Phys.Rev. Lett. **55**, 2676 (1985).
5) M. Langevin et al., Phys. Lett. B **150**, 21 (1985).
6) K. Asahi et al., Phys. Lett. B **251**, 488 (1990).
7) M. Ishihara, Nucl. Phys. A **538**, 309 (1992).
8) M. Ishihara, Nucl. Phys. A **583**, 747 (1995); M. Ishihara, Nucl. Phys. A **588**, 49c (1995).
9) T. Motobayashi et al., Phys. Lett. B **346**, 9 (1995).
10) T. Nakamura et al., Phys. Lett. B **331**, 296 (1994).
11) T. Motobayashi et al., Phys. Lett. B **264**, 259 (1991).
12) T. Nakamura et al., Phys. Rev. Lett. **112**, 142501 (2014).
13) T. Nakamura et al., Phys. Lett. B **331**, 296 (1994).
14) I. Talmi, I. Unna, Phys. Rev. Lett. **4**, 469 (1960).
15) N. Aoi et al., Z. Phys. A **358**, 253 (1997).
16) H. Iwasaki et al., Phys. Lett. B **481**, 7(2000).
17) H. Iwasaki et al., Phys. Lett. B **491**, 8 (2000).
18) S. Shimoura et al., Phys. Lett. B **560**, 31 (2003).
19) N. Aoi et al., Phys. Rev. Lett. **102**, 012502 (2009).
20) N. Imai et al., Phys. Rev. Lett. **92**, 062501 (2004).
21) H. J. Ong et al., Phys. Rev. C **78**, 014308 (2008).
22) K. Yoneda et al., Phys. Lett. B **499**, 233 (2001).
23) P. Doornenbal et al., Phys. Rev. Lett. **111**, 212502 (2013).
24) Z. Y. Xu et al., Phys. Rev. Lett. **112**, 132501 (2014).
25) H. Watanabe et al., Phys. Rev. Lett. **111**, 152501 (2013).
26) G. Baur, C. A. Bertulani, Nucl. Phys. A **458**, 188 (1986).
27) T. Motobayashi et al., Phys. Rev. Lett. **73**, 2680 (1994).
28) N. Iwasa et al., Phys. Rev. Lett. **83**, 2910 (1999).
29) T. Nakamura et al., Phys. Rev. C **79**, 035805 (2009).
30) M. Ishihara et al., Phys. Lett. B **73**, 281 (1978).
31) K. Asahi et al., Nucl. Phys. A **488**, 83c (1988).
32) H. Ogawa et al., Prog. Theor. Phys. Suppl. No. **146**, 607 (2002).
33) H. Ogawa et al., Phys. Rev. C **67**, 064308 (2003).
34) T. Morikawa et al., Phys. Lett. B **350**, 169 (1995).
35) A. A. Korsheninnikov et al., Phys. Lett. B **326**, 31 (1994).

Experiments at SMART and related activities

Hideyuki Sakai[*1,*2]

The E4 experimental room is now occupied with the fixed-frequency Ring Cyclotron (fRC), a part of the RIBF accelerator complex. It was once occupied by the Swinger and Magnetic Analyzer with Rotator and Twister (SMART). SMART was a versatile magnetic spectrometer primary designed for the spectroscopic study of nuclei by means of the missing-energy (mass) method induced by intermediate-energy heavy-ion beams ($A/Z \geq 2$) from the RIKEN Ring Cyclotron (RRC), and it was active during 1990–2005.

Here, some of the research programs conducted at SMART as well as related activities of the author's group are briefly described.

SMART magnetic spectrometer

The SMART magnetic spectrometer was designed and constructed by the SMART Group,[1)] led by Hajime Ohnuma of the Tokyo Institute of Technology.

SMART, shown in Fig. 1, consisted of a beam swinger and a magnetic spectrometer. To change the scattering angle of a reaction, the incident beam is swung with respect to the target, and the spectrometer stays still. The magnetic spectrometer was composed of three quadrupole magnets and two dipole magnets in the quadrupole-quadrupole-dipole-quadrupole-dipole (QQDQD) configuration.

The first three components (QQD) having the first focal plane FP1 were designed to work as a large-solid-angle (20 msr) and wide-momentum-acceptance ($\delta p/p = 40\%$) spectrometer with a momentum resolution of $p/\Delta p = 4,000$. With the full configuration (QQDQD) having the second focal plane FP2, it works as a high-momentum-resolution ($p/\Delta p = 12,000$) spectrometer with a moderate solid angle (10 msr) and momentum acceptance ($\delta p/p = 4\%$).

The construction of SMART was finished in 1990, following which commissioning works were conducted. Regrettably, SMART was decommissioned in 2005 to create space to install fRC.

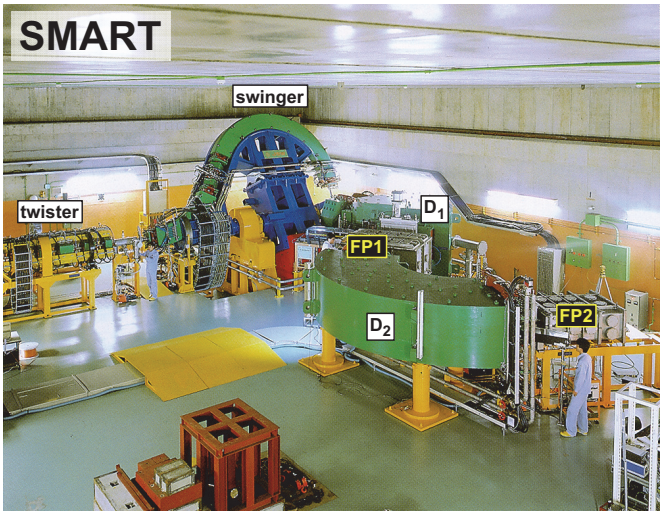

Fig. 1. Photograph of the SMART magnetic spectrometer in the E4 experimental hall.

Construction of polarized ion source

Although the deuteron beam at the RIKEN Accelerator Research Facility (RARF) with a maximum energy of 270 MeV was already unique at the time, the author's group realized that it would become truly unique if the polarization degrees of freedom are available.

We proposed the construction of an atomic-beam-type Polarized Ion Source (PIS) dedicated to the deuteron beam in 1990 (Fig. 2). It was accepted by RARF. PIS construction was finished by 1992. The beam intensity achieved was about 140 μA with 80% polarization.[2)] At the exit of PIS, a Wien filter system was equipped to rotate the deuteron polarization axis, i.e., the spin quantization axis. Owing to the single-

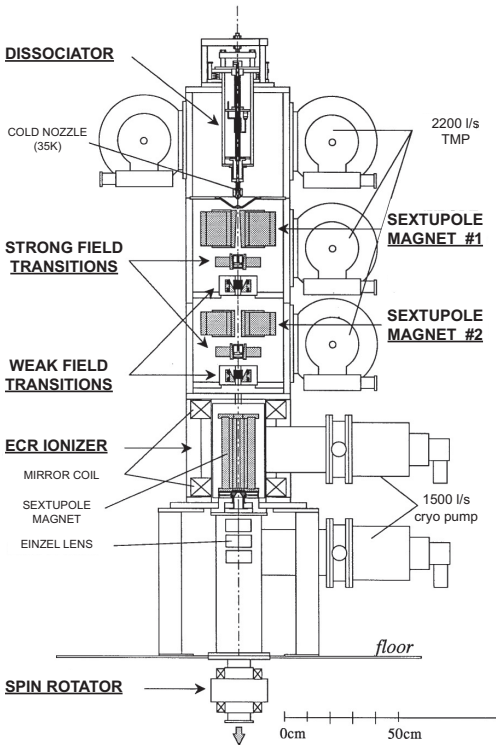

Fig. 2. Atomic-beam-type polarized ion source of RIKEN.

*1 Senior Visiting Scientist from the University of Tokyo (1993–2010)
*2 At present RIKEN Nishina Center

turn extraction for both the AVF injector cyclotron and RRC, the polarization axis is maintained during the accelerations, which allows us to control the polarization axis to any direction at the target position of SMART. This is the first facility in the world that realized this unique feature.

Polarization measurement with $d+p$ scattering

After the successful construction of PIS and subsequent acceleration of the polarized deuteron beam ($\vec{d}$) to 270 MeV, we needed to measure the absolute magnitude of the polarization. At the time, it was not known which reaction (scattering) should be chosen for polarimetry sensitive to both vector and tensor polarizations. Our first choice was the $\vec{d}+p$ scattering.

The complete analyzing powers (A_y, A_{xx}, A_{yy}, A_{xz}) for the elastic $\vec{d}+p$ scattering were successfully measured and published in Ref. [3] by using the beamline polarimeter system together with the cross sections. Since all analyzing powers showed moderate magnitudes, it was concluded that the $\vec{d}+p$ scattering could be an ideal scattering reaction for polarimetry at 270 MeV.

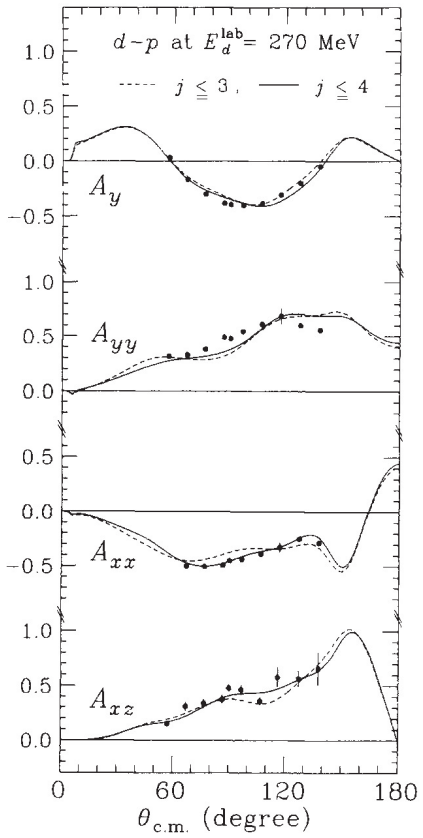

Fig. 3. Vector and tensor analyzing powers. Dashed and solid curves show the results of Faddeev calculations with the Argonne v_{14} 2NF for $j \leq 3$ and $j \leq 4$, respectively. See Ref. [3] for details.

The measured results together with Faddeev-type three-body calculations employing the modern two-nucleon force (2NF) are shown in Fig. 4. A surprisingly large discrepancy of about 30% in the cross-section-minimum region of 100°–150° was found between our measurement and the Faddeev calculations.

This discrepancy led us to get deeply involved in the study of the three-nucleon force (3NF).

Three-nucleon force study

Soon after the above study, the full Faddeev calculation with 2NF plus 3NF became available.[4] Meanwhile, we extended our $d+p$ scattering measurements to SMART, which allowed us to measure wide scattering angles $\theta_{c.m.} = 10° - 180°$. Moreover, the polarization transfer coefficients $K_{ij}^{y'}$ for the ^{1}H$(\vec{d},\vec{p})$ scattering were measured for the first time at $E_d = 270$ MeV. The scattered proton polarization was measured by the polarimeter (DPOL) set at FP2 of SMART. DPOL will be described later.

The results obtained at SMART were published in Ref. [5] together with the state-of-the-art Faddeev calculations with the modern 2NF + Tucson-Melbourne (TM) 3NF, as shown in Fig. 5 for cross sections and spin observables.

The cross-section difference is beautifully explained by the calculation, which is the first confirmation of the 3NF effects in the three-nucleon continuum (scattering) system. This was the milestone of the 3NF study. In contrast, some polarization observables were not described well with calculations, which indicates some deficiencies in the spin-dependent part of 3NF.

After this study, 3NF effects have been seriously considered not only in few-body systems but also in nuclear-structure calculations particularly for neutron-rich nuclei as well as for high-density matter such as a neutron star. For example, for the nuclear structure

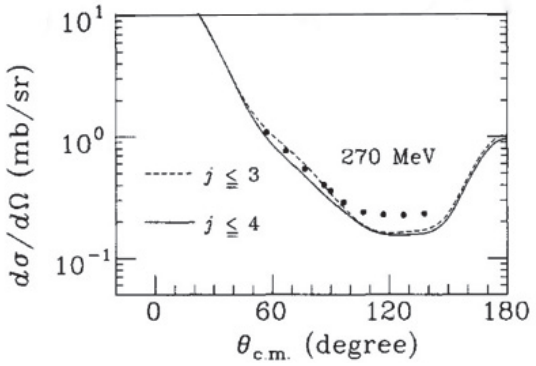

Fig. 4. Differential cross sections. The figure is taken from Ref. [3] with modification. The dashed and solid curves are the same as in Fig. 3.

calculation for neutron-rich Ca isotopes, see Ref. [6].

In SMART, measurements were extensively extended for the study of 3NF:

- Complete $d\sigma/d\Omega$, A_y^d, A_{xx}, A_{yy}, A_{xz} at $E(\vec{d}) =$ 140, 200, and 270 MeV.[7)]
- Polarization transfer $K_y^{y'}$, $K_{xx}^{y'}$, $K_{yy}^{y'}$, $K_{xz}^{y'}$, $P^{y'}$ for $\theta_{\rm c.m.} = 90°$–$180°$ at $E(\vec{d}) = 270$ MeV.[8)]
- Resolving the $d\sigma/d\Omega$ discrepancy at $E(\vec{d}) =$ 270 MeV.[9)]
- Polarization transfer for the breakup process of $\vec{d}+p \rightarrow \vec{p}+p+n$ at $E(\vec{d}) = 270$ MeV.[10)]

Now this comprehensive data-set has become a world standard for theoretical studies of 3NF effects.

The 3NF study was further extended to higher deuteron energies at the RIBF by constructing the BigDpol polarimeter:

- Complete A_y^d, A_{xx}, A_{yy}, A_{xz} at $E(\vec{d}) = 500$ and 596 MeV[11)] and at $E(\vec{d}) = 380$ MeV.[12)]

A four-body system was also studied by the ^{2}H($\vec{^2}$H, ^{3}He)n and ^{2}H($\vec{^2}$H, ^{3}H)p reactions at $E_d = 140$, 200, and 270 MeV for wide scattering angles $\theta_{\rm c.m.} = 0° - 110°$. The physics interest here was that the tensor analyzing powers A_{xx}, A_{yy}, and A_{xz} could be sensitive to the D-sate ($L = 2$) property in ^{3}He/^{3}H. Ambiguity in the reaction mechanism prevented us from drawing a clear conclusion.[13,14)]

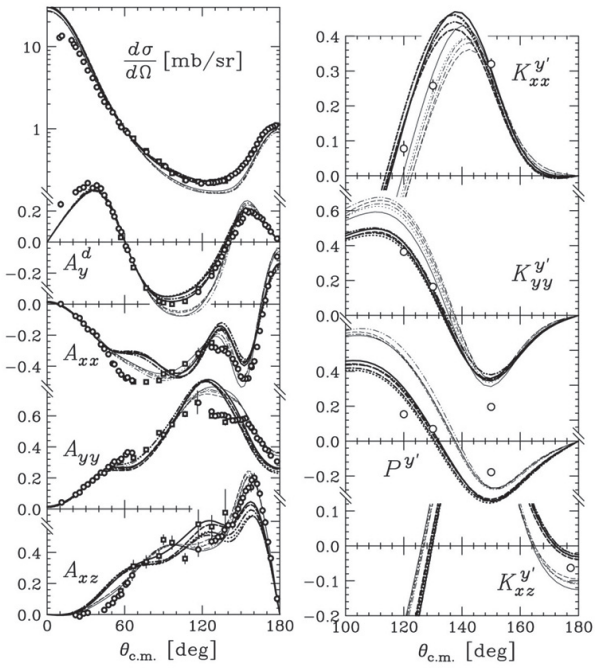

Fig. 5. Angular distributions of cross section, analyzing powers, and polarization transfer coefficients. See Ref. [5] for symbols and theoretical curves.

Spin-isospin responses with $(\vec{d}, {}^2\mathrm{He})$ reaction

The $(d, {}^2\mathrm{He})$ reaction has a very interesting quantum selection rule as a reaction probe. It excites exclusively spin-isospin flipped states $\Delta T = 1$ and $\Delta S = 1$, while the (n, p) reaction excites, in principle, $\Delta T = 1$ and $\Delta S = 1$ and 0. Thus, the $(\vec{d}, {}^2\mathrm{He})$ reaction is suited for the study of the Gamow-Teller (GT) state 1^+ as well as spin-dipole states 0^-, 1^-, and 2^- starting from a 0^+ target. Those transitions are in the β^+ direction, which plays in some cases an essential role in the evolution of star burning or supernova explosion processes. Here, ^{2}He indicates the two-proton coupling to form the spin-singlet state [^{1}S$_0$]. To ensure [^{1}S$_0$] experimentally, one needs to detect two protons in a small momentum corn ($\vec{p}_1 \simeq \vec{p}_2$), resulting in a small relative energy ($\epsilon < 1$ MeV). These conditions are not necessarily simple to satisfy by experimentally at an intermediate energy. The detection system for ^{2}He was constructed at FP1 of SMART.[15)] The first results without polarization degrees of freedom were published in Refs. [16,17] to show the usefulness of the $(d, {}^2\mathrm{He})$ reaction as a spectroscopic tool for GT transitions.

The tensor analyzing powers A_{xx} and/or A_{yy} of the

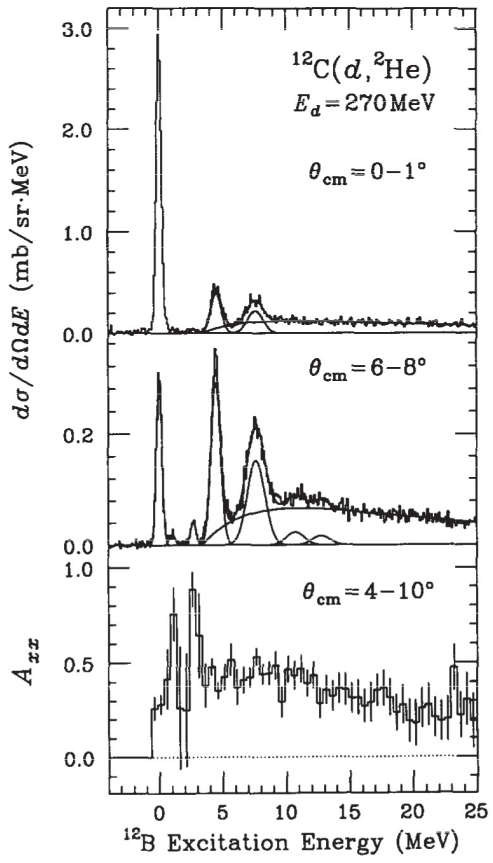

Fig. 6. Excitation energy spectra of cross section and A_{xx}. The figure is taken from Ref. [18].

$(\vec{d}, {}^2\mathrm{He})$ reaction are very useful as a spectroscopic tool in identifying the spin-parity J^π, in particular, for the spin-dipole states ($J^\pi = 0^-,\ 1^-,\ 2^-$). Finding a possible collective enhancement of 0^- states through its coupling to the pionic degrees of freedom in nuclei was of particular interest.

For natural-parity states, the tensor analyzing power predicted with PWIA tends to have an extreme value of

$$A_{xx} \sim +1 \qquad \text{for } 1^- \text{ or } 2^+,$$

while that for the unnatural-parity 0^- state is

$$\left.\begin{array}{l} A_{xx} \sim -2 \\ A_{yy} = +1 \end{array}\right\} \quad \text{for } 0^-,$$

for the scattering angles in which the cross section becomes maximum. Note that the tensor analyzing power can take a value $+1 \geq A_{ij} \geq -2$.

At $\theta = 0^\circ$, A_{zz} takes an extreme value,

$$A_{zz}(0^\circ) = +1 \quad \text{for } 1^- \text{ or } 2^+,$$
$$A_{zz}(0^\circ) = -2 \quad \text{for } 0^-.$$

Note that $A_{xx} = A_{yy}$ at $\theta = 0^\circ$ and $A_{xx} + A_{yy} + A_{zz} = 0$. It should be remarked that the result of $A_{zz}(0^\circ) = -2$ for 0^- is a model-independent one owing to the parity conservation in the spin-parity structure of $1^+ + 0^+ \to 0^+ + 0^-$.

The usefulness of the tensor analyzing powers was, for the first time, demonstrated by the $^{12}\mathrm{C}(\vec{d}, {}^2\mathrm{He})^{12}\mathrm{B}$ reaction at $E_d = 270$ MeV.[18] The result is shown in Fig. 6.

A striking feature is the conspicuously large A_{xx} observed at energies corresponding to 2^+_1 (0.95 MeV) and 1^-_1 (2.62 MeV), which agrees with the simple prediction above that A_{xx} becomes close to +1 for natural-parity states. The bump at $E_x = 7.5$ MeV in residual ^{12}B has been believed on the basis of many theoretical calculations and studies of (p,n) reactions to be dominated by 1^- states. However, the A_{xx} values corresponding to the bump are found to be almost similar to that of 2^-_2 (4.5 MeV), which clearly indicates that the bump is dominated by 2^-.

A spectroscopic study on the neutron-rich light nuclei ^{6}He, ^{9}Li, and ^{11}Be was also performed.[20,21]

A model-independent spin-parity determination of the 0^- state was applied for the first time to the $^{12}\mathrm{C}(\vec{d}, {}^2\mathrm{He})^{12}\mathrm{B}$ reaction by measuring the tensor analyzing power A_{zz} at $\theta = 0^\circ$.[19] The measurement was performed by preparing the tensor polarized deuteron beam aligned to the beam direction (p_{zz} beam), and the result is shown in Fig. 7.

It is indeed very remarkable to find that the A_{zz} of the peak at $E_x = 9.3$ MeV takes a very large negative value of ~ -1.2. Thus, it is unambiguously concluded that the bump at 9.3 MeV is dominated by 0^- states. It is noted that $A_{zz} = -2$ holds only at exactly $\theta = 0^\circ$. At $\theta \sim 5^\circ$, it takes another extreme value of $A_{zz} \sim +1$, demonstrating very strong angular dependence. The present experimental A_{zz} value of the peak at $E_x = 9.3$ MeV is an angle-integrated value over $\theta_{\mathrm{c.m.}} = 0^\circ - 1^\circ$ and, therefore, $A_{zz} \sim -1.2$ instead of -2.

$\Delta S = 1$ and 2 excitations via $(\vec{d}, \vec{d'})$ with DPOL

Isoscalar spinflip states ($T = 0$, $S = 1$) are least known because the effective interaction V_σ responsible for the excitation is weak and there is no good experimental means to isolate the state.

The deuteron inelastic scattering (d, d') is very attractive to explore the isoscalar spinflip states. Since the deuteron has an intrinsic spin of $S = 1$, the inelastic scattering could have single spinflip $\Delta S = 1$ and double spinflip $\Delta S = 2$ processes in addition to a strong non-spinflip $\Delta S = 0$ process. The $\Delta S = 1$ and $\Delta S = 2$ spinflip processes may be connected to the target spin excitations of S_1 and S_2, respectively. They are expressed in terms of polarization observables as follows:

$$S_1 = \frac{1}{9}(4 - P^{y'y'} - A_{yy} - 2K^{y'y'}_{yy}),$$
$$S_2 = \frac{1}{18}(4 + 2P^{y'y'} + 2A_{yy} - 9K^{y'}_{y} + K^{y'y'}_{yy}),$$

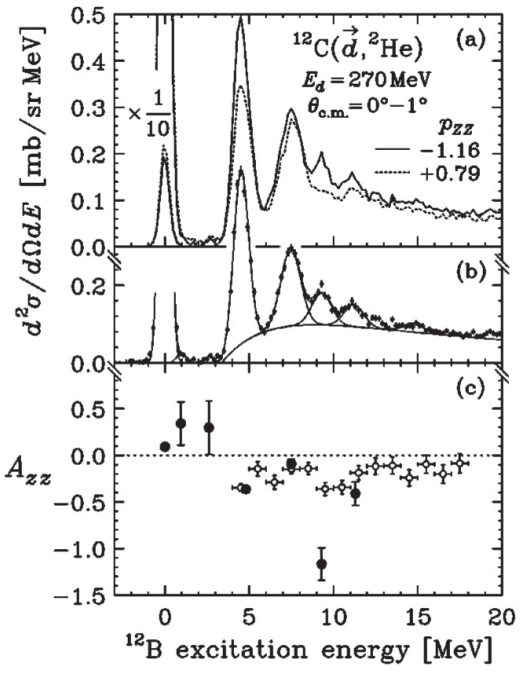

Fig. 7. (a) Double-differential cross sections at $\theta_{\mathrm{c.m.}} = 0^\circ$–$1^\circ$ as functions of ^{12}B excitation energy for $p_{zz} = -1.16$ and +0.79 polarized beams. (b) The result of peak fitting, and (c) the corresponding A_{zz} spectra. A_{zz} for each peak obtained by the fitting is shown by the closed circle, while that for the continuum binned in 1 MeV is shown by open circles. The figure is taken from Ref. [19].

where A, P, and K refer to the analyzing power, induced polarization, and polarization transfer coefficient, respectively. The vector and tensor polarizations of scattered deuterons have to be measured, which is experimentally very difficult and complicated. To measure S_1 and S_2, we constructed the Deuteron POLarimeter (DPOL) at FP2 of SMART.[22] DPOL utilizes the $\vec{d}$+C elastic scattering and the ^{1}H$(d, ^2$He) reaction for vector and tensor polarization analysis, respectively.

The ^{12}C$(\vec{d}, \vec{d'})$ reaction and ^{12}Si$(\vec{d}, \vec{d'})$ reaction were measured and S_1 and S_2 were derived for the first time.[22,23] The result is shown in Fig. 8 for the cross section and the single- and double-spinflip cross sections. The S_1 value for the 2^+ state is close to zero, while that for the well-known 1^+ state at 12.71 MeV is large. This fact clearly indicates that S_1 will be an excellent spectroscopic tool to investigate isoscalar spin excitations.

It is quite surprising to find that the S_2 values are consistent with zero over the measured excitation energy region, and no clear indication of the double spinfilp ($\Delta S = 2$) state was found.

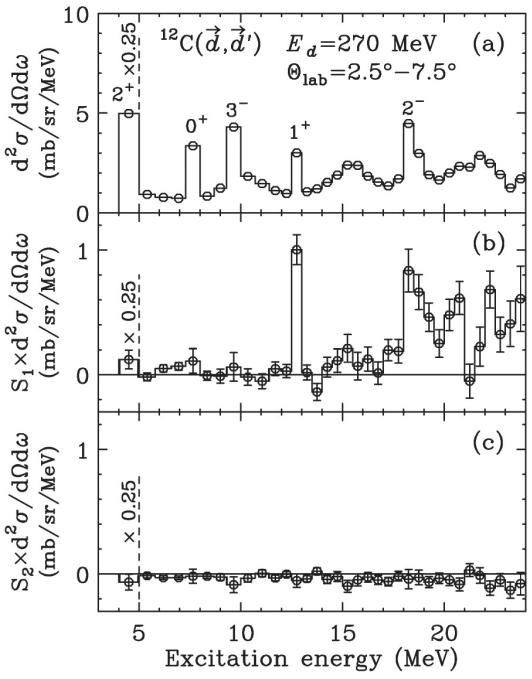

Fig. 8. Excitation energy spectra for the ^{12}C(d, d') reaction at $E_d = 270$ MeV integrated over $\theta_{\rm lab} = 2.5°$–$7.5°$. (a) An excitation energy spectrum. (b) The spectrum multiplied by S_1. (c) The spectrum multiplied by S_2. The figure is taken from Ref. [23].

HICEX reaction

Giant resonances represent major modes of collective motion of nuclei, and various multipole modes exist, reflecting isospin (T) and spin (S) degrees of freedom. Among them, an isovector non-spinflip quadrupole resonance (IVGQR), which is supposed to be a coherent state of $1p$-$1h$ excitations across two major shells ($2\hbar\omega$), was studied by the heavy-ion charge exchange reaction of ^{60}Ni(^{13}C, ^{13}N)^{60}Co at $E/A = 100$ MeV.[24] The measurement was performed at the FP2 of SMART, where a pair of the cathode readout drift chambers[25] was placed for ^{13}N detection.

Figure 9 shows typical energy spectra, which clearly display two prominent bumps at $E_x = 8.7 \pm 0.5$ MeV with $\Gamma = 2.8 \pm 0.8$ MeV and at $E_x = 20 \pm 2$ MeV with $\Gamma = 9 \pm 2$ MeV. To determine the multipolarities for those bumps, standard DWBA calculations were performed. The angular distributions of bumps were well fitted with the angular momentum transfers with $L = 1$ and $L = 2$, respectively. Based on this, it is concluded that the bump at $E_x = 8.7$ MeV is due to the well-known isovector giant dipole resonance (IVGDR) and the bump $E_x = 20$ MeV is due to IVGQR. Thus, IVGQR was unambiguously identified. It is interesting to note that an isovector giant monopole resonance (IVGMR), which is also expected at a $2\hbar\omega$ excitation energy and therefore should overlap with IVGQR, was not distinctly observed.

EPR paradox with EPOL

It is an intriguing and fascinating problem to verify the basic idea of quantum mechanics. It is well known that Einstein, Podolsky, and Rosen (EPR)[26] asserted that quantum mechanics is incomplete in terms of lo-

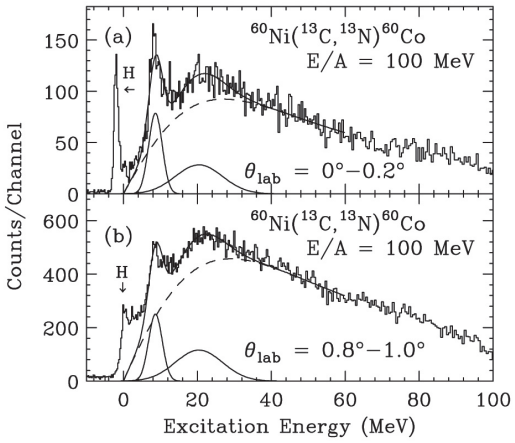

Fig. 9. Energy spectra of the ^{60}Ni(^{13}C, ^{13}N)^{60}Co reaction for the angular bins of (a) $\theta_{\rm lab} = 0° - 0.2°$ and (b) $\theta_{\rm lab} = 0.8° - 1.0°$. The figure is taken from Ref. [24].

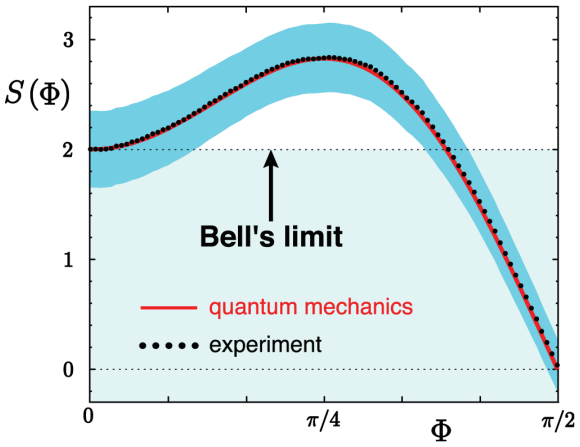

Fig. 10. Spin-correlation function $S(\Phi)$ vs Φ. The solid circles are experimental results compared with SHCH and quantum-mechanical predictions. Errors are shown by the blue band. The figure is taken from Ref. [30].

cal realism, a classical physicist's conception of nature. Bell[27] rendered this argument quantitative and amenable to experimental verification, as he showed that any local hidden variable theory will result in an inequality, which can contradict quantum mechanical predictions, i.e., Bell's inequality or equivalently the Clauser, Horne, Shimony, and Holt (CHSH) inequality.[28] The Bell-CHSH formulation concerns experiments where spin orientations have two possible outcomes (up/down). Many experiments have been performed with entangled photon pairs with great accuracy. However, there have not been any experiments with spin-$\frac{1}{2}$ particle pairs having mass with a statistically significant accuracy.

To conduct an experimental test of the Bell-CHSH inequality with massive particles, *viz.* two protons, two protons coupled to a spin singlet state [^{1}S$_0$] as the initial state must be prepared, and the spin correlation of two separated protons satisfying the locality property in the final state must be measured. The two-proton system in the spin singlet state is nothing but ^{2}He, which is very familiar to us as an ejectile of the $(d, ^2\mathrm{He})$ reaction. It should be mentioned especially that the use of ^{2}He has a huge merit. Since ^{2}He entangled by the strong interaction is an unbound two-proton system, two protons are automatically separated in a very gentle manner by the electromagnetic Coulomb force between them keeping their entanglement.

A spin polarimeter (EPOL) dedicated to measure the spins of two protons simultaneously was constructed and set up at FP2 of SMART.[29]

Entangled proton pairs were produced as a decay of ^{2}He formed in the $^1\mathrm{H}(d, ^2\mathrm{He})$ reaction at a 270 MeV deuteron beam. The experimental result is shown in Fig. 10.[29,30]

The quantum-mechanical prediction of the spin-correlation function is

$$S_{\mathrm{QM}}(\Phi) = 3\cos\Phi - \cos 3\Phi,$$

while that of Bell-CHSH states satisfied by local realistic theories is

$$S_{\mathrm{CHSH}}(\Phi) \leq 2,$$

irrespective of Φ (opening angle between spins of a proton pair). For the definition of Φ, see Refs. [29,30]. It is amazing to find that the experimental data follow the quantum-mechanical prediction faithfully for the entire angular region and exceed Bell-CHSH's limit over a wide angular range.

At $\Phi = \pi/4$, the measured value of the spin-correlation function is

$$S_{\mathrm{exp}}(\pi/4) = 2.83 \pm 0.24_{\mathrm{sta}} \pm 0.07_{\mathrm{sys}},$$

which violates Bell-CHSH inequality at the 99.3% confidence level. This is the first Bell-CHSH test using massive particles with significant accuracy. A characteristic feature of this experiment is that it is free from the loopholes of post-selection, causality (partially fulfilled), perfect detector efficiency (charged particle), and an 'event-ready' detection system.

Thus, EPR assertion does not seem to hold, and the 'Spooky action at distance,' phrased by Einstein against quantum-mechanical non-local phenomena, does exist.

Later, the Bell-CHSH inequality test was attempted with a proton-neutron pair in a singlet state via the $(d, pn[^1S_0])$ reaction. For that, a neutron polarimeter SMART-NPOL was constructed. Since the EPOL for proton and SMART-NPOL for neutron were separated by a few meters, a loophole of causality (space separation) could be overcome. Unfortunately, the statistical accuracy did not allow us to draw any conclusion.[31]

Polarized ^{3}He target and $^3\overrightarrow{\mathrm{He}}(\vec{d}, p)^4$He reaction

The ground state of deuteron is a mixture of S- and D-states with orbital angular momenta of $L = 0$ and 2, respectively. Although the D-state plays an important role in determining various properties of the deuteron, it is not well determined, in particular at the high momentum region, owing to a lack of experimental means to directly access the D-state component.

A new approach to access the D-sate component using the polarization correlation measurement by the $^3\overrightarrow{\mathrm{He}}(\vec{d}, p)^4$He reaction was proposed.[32] The polarization correlation coefficient $C_{//}$ can be defined in terms of PWBA as

$$C_{//} = \frac{9}{4}\frac{w^2(k_{pn})}{u^2(k_{pn}) + w^2(k_{pn})}, \quad (1)$$

where $u^2(k_{pn})$ and $w^2(k_{pn})$ are the S- and D-state wave

functions of deuteron in momentum space, respectively, and k_{pn} is the internal momentum. It is remarkable to see that $C_{//}$ is directly proportional to $w^2(k_{pn})$.

The $^3\vec{\mathrm{H}}\mathrm{e}(\vec{d},p)^4\mathrm{He}$ reaction was performed with the vector- and tensor-polarized deuteron beam of 270 MeV and a vector polarized ^{3}He target at $\theta_{\mathrm{lab}} = 0°$. For this purpose, a spin-exchange-type polarized ^{3}He gas target was constructed.[33] The ^{3}He nuclei were polarized via the spin-exchange reaction with the optically pumped Rb atom. The ^{3}He gas density was 2.2×10^{20} atoms/cm^3 with a polarization of 0.12. The result[32] is shown in Fig. 11. Neither DWBA nor PWBA calculations could reproduce the present result, which cast a question on the relevance of the reaction mechanism.

Polarized proton target and $^6\mathrm{He}(\vec{p},p_0)^6\mathrm{He}$ scattering

It is quite exciting if we could extend spin-observable measurements to radio-isotope (RI) beams. In the RI experiments, a high-density target is necessary to gain sufficient luminosity since the intensity of the RI beams is typically less than 10^6 particles/s. In this respect, a solid target, rather than a gas target, is desirable. For the proton, a polarized solid proton target (PSPT) is available. However, a conventional PSPT system requires a high magnetic field ($\geq$ 2.5 T) and a very low temperature ($\leq$ 1 K), which is very inconvenient for the RI beam experiments because it inevitably utilizes inverse kinematics for the scattering, i.e., it is necessary to detect very-low-energy recoiling protons. We constructed a PSPT system that overcomes such experimental difficulties.

Since the construction of the PSPT system is described in Refs. [34,35] in detail, only an outline is given below. Protons in a single crystal of naphthalene ($C_{10}H_8$) doped with pentacene ($C_{22}H_{14}$) with a size of $4\times5\times2$ mm^3 are polarized in a magnetic field of 0.3 T at 100 K by transferring a large population difference among the photo-excited triplet states of pentacene to the hydrogen nuclei. The proton polarization achieved was about 0.2.

The first RI beam experiment to measure the analyzing powers (A_y) for the $^6\mathrm{He}(\vec{p},p_{\mathrm{gnd}})^6\mathrm{He}$ scattering was conducted in inverse kinematics.[36] The ^{6}He beam with 71 MeV/nucleon was provided by the RIKEN Projectile-fragment Separator (RIPS).

Figure 12 shows the first results, in which the analyzing powers are compared with those of $^6\mathrm{Li}(\vec{p},p_0)^6\mathrm{Li}$ scattering. Although the statistics are poor, the backward angular behavior of A_y seems to be very different from each other, even though the shapes of cross sections are similar. A very simple optical model analysis indicates that the spin-orbit potential for ^{6}He is located outside by about 0.8 fm compared to that for ^{6}Li. It is noted that the present A_y behavior resembles that of the $^4\mathrm{He}(\vec{p},p_0)^4\mathrm{He}$ scattering.

Later, the $^6\mathrm{He}(\vec{p},p_0)^6\mathrm{He}$ scattering experiment was repeated with a higher proton polarization and improved detection system.[37] Further, scattering from a more exotic nucleus $^8\mathrm{He}(\vec{p},p_0)^8\mathrm{He}$, was performed.[38]

Neutron radiology study

Radiological studies such as the neutron yield induced by heavy-ions[39] or radioactive cross sections by

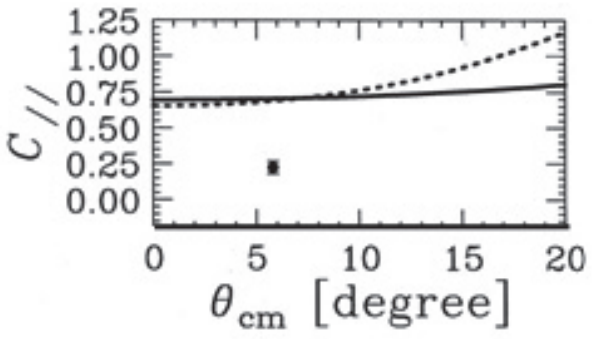

Fig. 11. Present datum in a black dot with statistical error. Solid and dashed lines are DWBA and PWBA calculations, respectively. The figure is taken from Ref. [32] with modification.

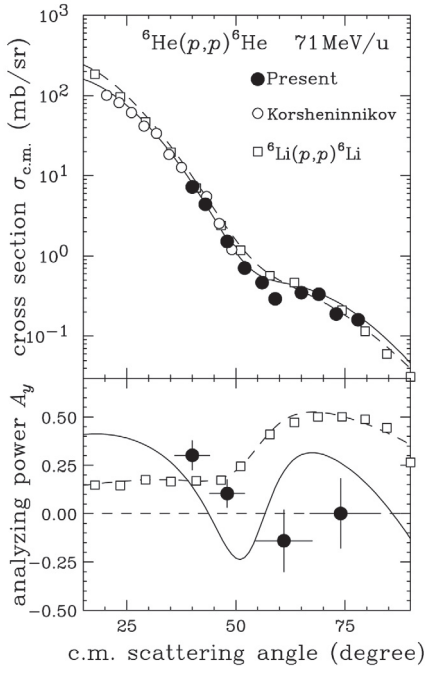

Fig. 12. Cross sections and analyzing powers. The solid and dashed lines are the results of optical model analyses fitted to the cross sections. The figure is taken from Ref. [36].

quasi-mono energetic neutrons[40,41] were conducted by Shouji Nakamura of Tohoku University and his collaborators using the swinger part of SMART. Obtained data provide very useful bases for designing radiation shields of accelerator facilities.

SHARAQ; successor of SMART

Although SMART was decommissioned and disassembled in 2005, its scientific motivation/tradition was partly succeeded by the SHARAQ project of the Center for Nuclear Study (CNS), the University of Tokyo. SHARAQ stands for Spectroscopy with High-resolution Analyzer of RadioActive Quantum beams.

The SHARAQ project was born while the author was the Director of CNS. The intention was to construct a high-resolution magnetic spectrometer dedicated to the RI beam experiments at RIBF. To achieve a high momentum resolution together with high angular resolution, SHARAQ was designed to have dispersion- and angular-matching functions utilizing the momentum dispersion of BigRIPS. The idea of 'an exothermic charge-exchange reaction with unstable RI beams to explore exotic spin-isospin responses in nuclei with a magnetic spectrometer' was approved by JSPS.[42] The construction of SHARAQ started in 2005, and its commissioning started in 2010.

It should be mentioned that the first dipole magnet of SMART was reused in SHARAQ, again as the first dipole magnet in a QQDQD configuration. Thus, SHARAQ carried forward not only the scientific motivation but also a dipole magnet of SMART.

Summary and acknowledgments

In summary, various nuclear sciences were promoted exploiting the SMART magnetic spectrometer by many users. SMART was active for 15 years. During that period, 63 peer-reviewed papers were published, and 17 graduate students earned their Ph.D degrees.

Our group consistently pursued nuclear physics utilizing spin degrees of freedom of beam, target, and scattered particles. For that aim, we constructed PIS, DPOL, EPOL, SMART-NPOL, a polarized ^{3}He target, and PSPT. Strong support by RARF is greatly appreciated, in particular on for PIS, the polarized ^{3}He target, and PSPT constructions.

I am very much indebted to many collaborators and graduate students, who were the main contributors to the works mentioned above. Without their incessant hard working efforts of day and night, nothing could have been achieved. For lack of space, I regret that the names of contributors cannot be explicitly mentioned. However, I cannot help but mention my esteemed collaborator Hiroyuki Okamura (deceased). The construction of various devices and scientific works were the result of our cooperative but critical discussions. Without him, the scientific achievements described here could not be accomplished.

References

1) H. Ohnuma et al., Proc. Second IN2P3 RIKEN Symposium on Heavy-ion Collisions, edited by B. Heusch and M. Ishihara (World Scientific, Singapore, 1990), p. 26.
2) H. Okamura et al., AIP Conf. Proc. **293**, 84 (1994).
3) N. Sakamoto et al., Phys. Lett. B **367**, 60 (1996).
4) H. Witala et al., Phys. Rev. Lett. **81**, 1183 (1998).
5) H. Sakai et al., Phys. Rev. Lett. **84**, 5288 (2000).
6) T. Otsuka et al., Phys. Rev. Lett. **105**, 032501 (2010).
7) K. Sekiguchi et al., Phys. Rev. C **65**, 034003 (2002).
8) K. Sekiguchi et al., Phys. Rev. C **70**, 014001 (2004).
9) K. Sekiguchi et al., Phys. Rev. Lett. C **95**, 162301 (2005).
10) K. Sekiguchi et al., Phys. Rev. C **79**, 054008 (2009).
11) K. Sekiguchi et al., Phys. Rev. C **89**, 064007 (2014).
12) K. Sekiguchi et al., Phys. Rev. C, to be published.
13) T. Saito et al., Mod. Rhys. Lett. A **18**, 2 (2003).
14) VP. Ladygin et al., Phys. Lett. B **598**, 47 (2004).
15) H. Okamura et al., Nucl. Instrum. Methods Phys. Res. A **406**, 78 (1998).
16) H. Ohnuma et al., Phys. Rev. C **93**, 648 (1993).
17) T. Niizeki et al., Nucl. Phys. A **577**, 37 (2009).
18) H. Okamura et al., Phys. Lett. B **345**, 1 (1995).
19) H. Okamura et al., Phys. Rev. C **66**, 054602 (2002).
20) T. Ohnishi, PhD thesis, The University of Tokyo, 2000.
21) T. Ohnishi et al., Nucl. Phys. A **687**, 38c (2001).
22) S. Ishida, PhD thesis, The University of Tokyo, 1998.
23) Y. Satou et al., Phys. Lett. B **521**, 153 (2001).
24) T. Ichihara et al., Phys. Rev. Lett. **89**, 142501 (2002).
25) M.H. Tanaka et al., Nucl. Instrum. Methods Phys. Res. A **362**, 521 (1995).
26) A. Einstein, B. Podolsky, N. Rosen, Phys. Rev. **47**, 777 (1935).
27) J. Bell, Physics **1**, 195 (1964).
28) J. F. Clauser, M. A. Horne, A. Shimony, R. A. Holt, Phys. Rev. Lett. **23**, 880 (1969).
29) T. Saito, PhD thesis, The University of Tokyo, 2005.
30) H. Sakai et al., Phys. Rev. Lett. **97**, 150405 (2006).
31) H. Kuboki, PhD thesis, The University of Tokyo, 2007.
32) T. Uesaka et al., Phys. Lett. B **467**, 199 (1999).
33) T. Uesaka et al., Nucl. Instrum. Methods Phys. Res. A **402**, 212 (1998).
34) M. Hatano, PhD thesis, The University of Tokyo, 2003.
35) T. Wakui et al., Nucl. Instrum. Methods Phys. Res. A **550**, 521 (2005).
36) M. Hatano et al., Euro. Phys. J. A **25**, 255 (2005).
37) T. Uesaka et al., Phys. Rev. C **82**, 021602(R) (2010).
38) S. Sakaguchi et al., Phys. Rev. C **87**, 021601(R) (2013).
39) H. Sato et al., Phys. Rev. C **64**, 033607 (2001).
40) N. Nakao et al., Nucl. Instrum. Methods Phys. Res. A **420**, 218 (1999).
41) E. Kim et al., Nucl. Sci. Eng. **129**, 209 (1998).
42) H. Sakai (Spokesperson), Grant-in-Aid for Specially Promoted Research 1700203.

Nuclear Chemistry Laboratory

F. Ambe*1

When the RIKEN Ring Cyclotron (RRC) was ready for utilization, I proposed two new research subjects for my nuclear chemistry group: the development of a multitracer technique and in-beam Mössbauer spectroscopy using ^{57}Mn.

The former involves the preparation of multielemental radioactive nuclides by the fragmentation of target nuclei and their application to trace the behavior of elements in various research fields. In 1990, we started a series of studies to develop radiochemical procedures for the preparation of multitracers, namely the removal of the target material from the solution of an irradiated target, leaving as much as possible of the radionuclides, and the application of the multitracers thus obtained to chemistry and other fields.[1)] More than fifty elements were studied using this technique, with twenty or more of them being traced simultaneously.

Significant features of the multitracers are as follows: (1) High efficiency: a single experiment usually yields information on twenty or more elements. (2) Accurate comparison of the behavior of a number of elements is realized under strictly identical experimental conditions. (3) Serendipity: since many elements are included in every multitracer, it is often possible to discover new important or interesting behavior of an element, which is not the main subject of the investigation. (4) All the tracers are carrier-free, that is, the multitracers contain slight amounts of stable isotopes of the tracers, which can disturb the experiment. (5) Some multitracers contain scarcely obtainable tracers such as ^{28}Mg and ^{47}Ca.

Typically, a beam of $^{12}C^{6+}$, $^{14}N^{7+}$, or $^{16}O^{8+}$ ions with an energy of 135 MeV/nucleon is used against Au, Ag, and Cu targets. The irradiated target is dissolved, and the target material is removed, leaving the radioactive nuclides in a solution. For example, in the simplest case of an Ag target, it is dissolved in nitric acid, and Ag is removed as AgCl precipitate. The measurement of the tracers is performed by means of conventional Ge detectors.

The multitracers were used for the investigation of behavior of various elements in chemistry, biochemistry, and biology in cooperation with more than 10 groups in universities and research institutes.[1,2)] The behavior of elements in rats and mice was most extensively studied by different groups. The uptake, excretion, and retention of various elements were studied in organs of Al-, Cd-, and Vitamin D-overloaded or Se-deficient rats in comparison with those of normal ones. The following studies were also made on various elements: the transportation through the blood-brain barrier and retention in different parts of the brain, labeling of immunoglobulin G, reactions with blood components and transport proteins, and in vivo and in vitro binding with liver DNA.

In the case of plants, the uptake and accumulation of elements in mushrooms, carrots, and marigolds as well as the subcellular distribution and translocation of radionuclides were studied. In chemistry, the adsorption of metal ions on α-Fe_2O_3, formation of metallofullerenes with higher-group elements, effects of model acid rain on the adsorption of trace elements upon soils, and stability constants of humate complexes with various metal ions were studied.

In this period, investigations using unstable nuclei as probes, namely Mössbauer spectroscopy and time-differential perturbed angular correlation (TDPAC) of γ rays, were continued with the use of cyclotron-produced radionuclides in cooperation with the magnetism group of RIKEN, and a project using short-lived ^{57}Mn produced by RRC was newly started.[3)] With the use of the source nuclide ^{61}Cu produced by the α-irradiation of a Ni-V alloy disk, ^{61}Ni-Mössbauer spectra of chromite spinels, $Cu_{1-x}Ni_xCr_2O_4$, were measured. Both H_{hf} and EFG were found to be well related to a lattice distortion. In $Cu_{0.9}Ni_{0.1}Cr_2O_4$, the H_{hf} was 790 kOe, which is the largest among the values for Ni^{2+} ever reported. Carrier-free ^{99}Rh produced by the proton irradiation of ^{99}Ru was chemically separated from the target and was doped in $YBa_2Cu_3O_{6.8}$ and $YBa_2Cu_3O_6$. Their Mössbauer emission spectra and TDPAC showed that ^{99}Ru ions arising from ^{99}Rh are tetravalent and occupy the Cu sites.

^{119}Sn-Mössbauer emission spectroscopy using cyclotron-produced ^{119}Sb as the source nuclide was applied to the in situ study of the chemical state of $^{119}Sb^{5+}$ adsorbed on α-Fe_2O_3. The state of $^{119}Sb^{5+}$ was shown to change depending on the pH value of the solution in contact with the powder samples on the basis of broadening of the spectra due to the magnetic interaction.

A setup for in-beam Mössbauer spectroscopy was constructed at RIPS of RRC in order to measure the spectra of ^{57}Fe with ^{57}Mn (half-life 87.2 s) produced as a beam by the projectile fragmentation of ^{59}Co. With the use of a parallel-plate avalanche counter for detection of the internal conversion electrons, we succeeded in the first observation of Mössbauer spectra of ^{57}Fe following the decay of ^{57}Mn nuclei. However, the quality of the spectra was not satisfactory because of β-rays from ^{57}Mn. Later, Dr. Y. Kobayashi and his coworkers overcame this difficulty by developing an anti-coincidence detection system and also realized time-dependent measurement with the system. Now, ^{57}Mn-Mössbauer spectroscopy is used as a unique method for atomic-scale study of reactions in solids.

References
1) F. Ambe, ed., RIKEN Rev. No. **13** (1996).
2) Y. Yano, S. Enomoto, eds., RIKEN Rev. No. **35** (2001).
3) F. Ambe, ed., RIKEN Rev. No. **16** (1997).

*1 Chief Scientist of Nuclear Chemistry Laboratory (1988–1998)

Development of atomic physics under the contribution of RIKEN Accelerator Research Facility, during 1972–1997 period

Yohko Awaya (Enomoto)*1

In this report, I will describe how the studies of atomic physics using the RIKEN Accelerator Research Facility was started and grew up, from my personal viewpoint. I will also describe a little about the "new RIKEN" started in 1958, and early days of the 160 cm Cyclotron. I suppose this may be worth to write, since people who know that time are not so many now.

When a personal name is listed, the title will be omitted and when his/her name appears in the second time, only the family name is shown. Laboratory is abbreviated as Lab. In parentheses after the laboratory, the name of its Chief Scientist is shown when it is necessary.

1 The 160 cm Cyclotron

In 1959, after half a year when RIKEN changed to a non-profit research institute sponsored by the Science and Technology Agency (STA) from a private company Kaken, I (Y. Enomoto at that time) joined the Irradiation Lab.(K. Shinohara),[a] RIKEN in Komagome, Tokyo where an electron Van de Graaff accelerator was working and was used to study the irradiation effect on polymers and so forth. Around the end of that year, I belonged to the Radiation Lab. (F. Yamasaki[b]) under the agreement between Shinohara and Yamasaki, which pleased me too. In the Radiation Lab., A. Hashizume and Y. Tendow had been mainly studying β-γ spectroscopy and K. Izumo on the theory of nuclear physics. The small cyclotron constructed in 1952 in RIKEN had been working under members of the Radiation Lab., S. Motonaga, S. Konno, M. Hemmi, and A. Shimamura. I became a member of the β-γ spectroscopy group, but also participated in experiments of direct nuclear reaction made by the group of Y. Nogami Lab., Univ. of Tokyo, using the cyclotron of the Institute for Nuclear Study (INS), Univ. of Tokyo in 1960–1961, and later in that done by K. Matsuda-group of INS.[c]

In May of 1962, the construction plan of the Cyclotron[d] including facilities was prepared and proposed to STA (representative was Yamasaki at first, but soon changed to Hiroo Kumagai). In this plan, I took responsibility for a particle analyzer and a target chamber. For the construction of the Cyclotron, M. Odera, T. Karasawa, Y. Miyazawa and T. Fujisawa joined the Radiation Lab. and soon, in June 1962, the Cyclotron Lab. (Kumagai) was founded. Four staffs mentioned above, and also Motonaga, Hemmi and Shimamura moved to this new laboratory from the Radiation Lab. Yamasaki and T. Hamada (Senior Scientist of the Radiation Lab.) supported Kumagai, who had double position of INS and RIKEN, about the construction of the Cyclotron so much. At the beginning of designing the main magnet, Tendow and I estimated the distribution of magnetic field between the pole pieces, and calculated trajectory of ion beams under Karasawa, but this job was taken over by N. Nakanishi (Cyclotron Lab.). K. Matsuda joined the Cyclotron Lab. leaving INS in 1965, and H. Kamitsubo did leaving the Institute of Solid State Physics of the Univ. Tokyo in 1966.

The Radiation Lab. got new staff members for the β-γ spectroscopy group, T. Katou in 1966 and T. Inamura, who transferred to the Cyclotron Lab. a few years later, in 1967.

The first beam of the Cyclotron was obtained in 1966. At very beginning of starting experiments of nuclear physics, three groups (headed by Odera, Matsuda, and Kamitsubo) were organized to study the elastic scattering of ^{3}He, as the acceleration of ^{3}He was one of the special features of the Cyclotron. Target elements were Al (Odera), Ca (Matsuda) and Ni (Kamitsubo). Only once, an experiment using a tritium beam was made, that was ^{100,98}Mo(t, p)^{102,100}Mo.[2,3] After that, tritium was never accelerated again because it contaminated the Cyclotron itself. Another nuclear-physics group studied in-beam spectroscopy (Hashizume-group). This mainly consisted of the β-γ spectroscopy group of the Radiation Lab. except for me. I belonged to the Matsuda-group but continued the study of β-γ spectroscopy at the Radiation Lab.

Yamasaki retired from RIKEN in 1968. Hamada became the Chief Scientist of the Radiation Lab. and after a while the Radiation Lab. moved to Yamato-machi (now, Wako-shi) from Komagome.

In March 1971, just after Matsuda was nominated for the Chief Scientist of the Cyclotron Lab., he met an accident during enjoying skiing and passed away, and Kamitsubo became the Chief Scientist of the Cyclotron Lab.

2 So-called "Atomic Physics Group"

The measurement of X rays from atoms excited by slow heavy-ions was made in 1934 by using a Van de

*1 Chief Scientist of Atomic Physics Laboratory (1990–1997)

a) Shinohara changed the name of his Lab. to the Atomic Physics Lab. in 1960. He retired from RIKEN in 1966. In these days, they call the laboratory after the Chief Scientist's name, for example, Shinohara-Lab.

b) When his family name is written by Chinese character, they usually read it as "Yamazaki." He had been a scientist of the Nishina Laboratory since old (before 1945) RIKEN and engaged in the construction of the 60" cyclotron before the War.

c) I got the degree of Dr. Sci. from Univ. of Tokyo, by one of this group's studies.[1]

d) In the documents, the expression of "160 cm Cyclotron" was not used.

Graaff accelerator, but extensive studies using heavy-ion accelerators were started in early 1960s. In these days, heavy-ion accelerators were constructed, and some of them were used for studies of beam-foil spectroscopy, which analyzed photons from fast heavy ions excited by passing through a thin foil. Heavy-ion atom collision studies were started around middle of 1960s.

Learning the worldwide trend of studies in the atomic physics and considering the ability of the Cyclotron to accelerate heavy ions, I was very interested in the studies of atomic physics by using it. In 1972, at a meeting of the Radiation Lab (T. Hamada), I proposed the study of inner-shell ionization processes in heavy-ion atom collisions by measuring X rays. The first experiment was made on October 25–26, 1972, by the group consisted of members of the Radiation Lab., Hamada, Awaya, M. Okano, Hashizume, T. Takahashi, Izumo, Tendow, Katou, Hidekazu Kumagai and M. Nishida. Kumagai took part of electronic counting systems mainly, and Nishida worked on the data handling at the computer. Experiments were made at the No. 4 beam line in the small experimental area using the target chamber for in-beam spectroscopy. A sketch of the experimental rooms with the beam lines of the Cyclotron is shown in Fig. 1 and a photograph of the control desk taken from the counting area in Fig. 2. At the beginning, we met many problems to make the experiment because of the large difference of the cross sections between the nuclear reaction and the inner-shell ionization. We needed very low-intensity beams and found that the current integrator which had been used for the nuclear reaction experiments was of no use, and thus Kumagai designed a new current integrator by using a pico-ammeter. Operators struggled to transport the beams and to make collimation at the target position because they could not detect the beams on their way. Later they made a nice devise to solve this problem. The background radiation from a collimator/slit before the target was too high to make the measurements. We paid many efforts to reduce it. Tendow designed a new small rectangular target chamber made of aluminum and we set it downstream of the in-beam target chamber in May of 1973. We bombarded ten target elements between Cr and Bi with 5 MeV/nucleon α-particles and N^{4+} ions, and measured K- and L-X rays emitted from the targets by using a Si(Li) detector. The aim of the experiment was to study the K- or L-shell ionization processes induced by α-particles and by N^{4+} ions, from the viewpoint of ${Z_1}^2$-dependence of the inner-shell ionization cross section, where Z_1 is the atomic number of the incidents ions. We also obtained the data on the K and L X-ray energies and the width of each X rays in the energy spectra.[4,5]

This group was called as X-ray group at first, but soon called as ion-atom collision group or atomic physics group. So, to avoid a confusion the name of "atomic physics group" will be used hereafter. The first RIKEN Symposium on atomic physics using accelerators, "Excitation of Inner Shell Electrons" was held in January 1974 hosted by the Radiation Lab.

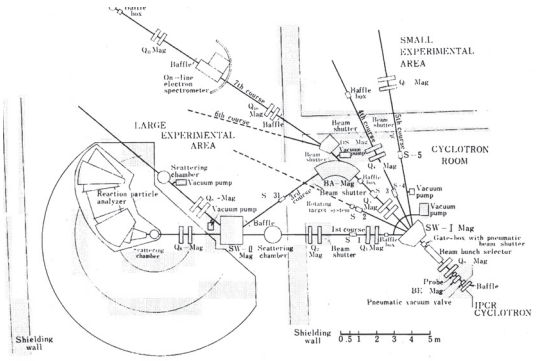

Fig. 1. Layout of the 160 cm Cyclotron beam lines.

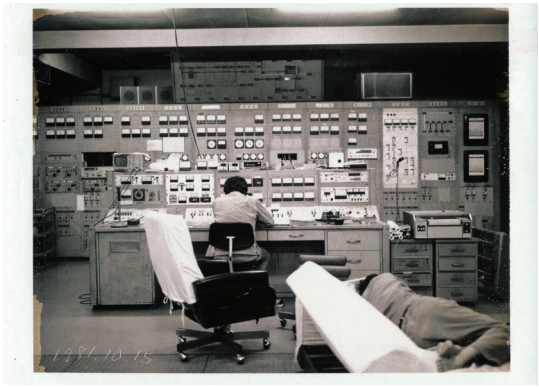

Fig. 2. A photograph of the control desk of the 160 cm Cyclotron taken from the data acquisition area.

We wanted to have a step-scanning crystal spectrometer for measuring X-ray spectra with high energy-resolution to study the multiple inner-shell ionization processes in heavy-ion atom collisions. In 1974, by getting the supplementary budget, we constructed an on-line step-scanning crystal spectrometer.[6] Kumagai designed a control system for step scanning.[7]

In 1975, M. Akiba, got the special researcher position at the Radiation Lab., and joined atomic physics group. We had a visitor, H. Tawara of Kyushu Univ. who took his gas-target system. We studied the ionization processes of Ar atoms by C^{4+}-ions impact by setting his gas-target system on the 6th beam line in the large experimental area[8] in June 1975, and in November, we installed the step-scanning X-ray spectrometer on this line.

We studied simultaneous K- and L-shell ionization processes and simultaneous L- and M-shell ones by measuring K and L X-ray spectra using the crystal spectrometer, for various combinations of target elements including gaseous elements and species of heavy ions. The incident energy of the heavy ions was also changed.[9,10] In 1975, the Linear Accelerator Lab. (M. Odera) was established and T. Tonuma, who moved from the Cyclotron

Table 1. The Budget of the 160 cm Cyclotron in 1975 (in unit of thousand yen).

Item	Budget	Working Budget
Nuclear Physics	30,110	28,900
Atomic & Molecular Physics	3,744	3,590
Nuclear Chemistry	6,770	6,500
Radiation Chemistry	1,800	1,730
Radiation Biology	1,720	1,650
Solid State Physics	3,800	3,650
Cyclotron Body	26,140	25,100
Common Facilities	20,060	19,260
Total	94,144	90,380

(The total Budget of RIKEN: 5,066 million yen.)

Lab. to this laboratory, joined the atomic physics group in 1976. He prepared the gas-target system for these experiments.[11)]

Analyzing all the data, we found the ionization probabilities of L-shell and M-shell electrons in multiple-ionization were fitted to a theoretical universal curve when we chose a proper scaling-factor.[12)] Awaya made a 30 min. oral presentation about this work at the XIth Int. Conf. on the Physics of Electronic and Atomic Collisions (ICPEAC) in Kyoto, 1979, held by Science Council of Japan and by the Society for Atomic Collision Research, and this was a good chance to debut the RIKEN atomic physics group to the worldwide community of atomic collision study.

Talking about the budget for study, the budget for Special Research "General Research using 160 cm Cyclotron" had been authorized, and we wanted to have the item concerning to atomic physics in it. In 1975, the committee of Cyclotron users agreed to add the item "studies of atomic and molecular physics" in this budget document. Table 1 shows the items in the budget document and the budget shared among them, as of 1975. Afterwards, the item concerning to study of atomic physics was included in the special budget for the accelerators, namely, "General Research using Heavy-ion Linear Accelerator" and "General Research of Heavy-ion Science."

The step-scanning crystal spectrometer had been very useful but it took a long time to get X-ray spectra as the Bragg angle had to be changed step by step. Learning that a position sensitive gas-flow proportional counter became commercially obtainable, I got an idea to make a "Broad-Range Crystal Spectrometer" by combining this counter and a flat crystal, for the first time. Considering the position resolving power of the detector, the uniformity of a flat crystal, and the size of beam spot on the target, it was concluded that this new crystal spectrometer would satisfy the aimed energy-resolving power by covering a Bragg-angle range of approximately 20° at once. We constructed this spectrometer getting the budget to Grants-in-Aid for Scientific Research.[13)] Kumagai designed the data-taking system for this spectrometer. The test of this broad-range crystal spectrometer was made in the large experimental area of the Cyclotron by setting it in the middle-size scattering chamber in 1980.[14)] Its energy-resolving power was almost equal to the step-scanning one, and its data-taking time was approximately 1/20 compared to that one. In addition to them, it was handy and easy to move to the places where experiments would be done. Figure 3 is a photograph of the broad-range crystal spectrometer and Fig. 4 shows a spectrum of Ti X rays induced by an 81 MeV N-ion bombardment measured with this spectrometer. A. Hitachi (special researcher of the Radiation Lab.) studied angular distribution of Ti K-X rays and Sn L-X rays induced by 81 MeV N-ion bombardments using the broad-range crystal spectrometer.[15)] From that time to 1997, we made many experiments using this unique and strong tool to study heavy-ion atom collisions where high-resolution spectra of K-, L-, or M-X rays emitted from either target atoms or projectile ions were requested.

T. Kambara (Linear Accelerator Lab.) joined the atomic physics group in 1979 and in next year he started

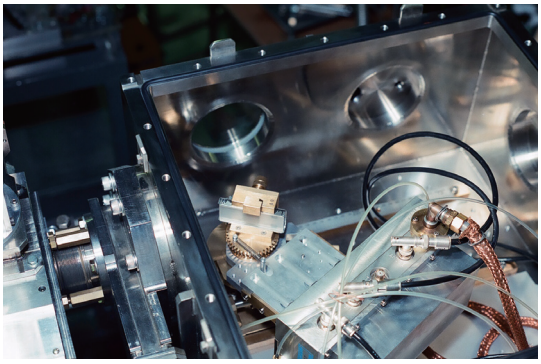

Fig. 3. Photograph of the broad-range crystal spectrometer in the chamber of (4) in Fig. 5 (shown later). This chamber was connected to the X-ray target chamber (3) with bellows.

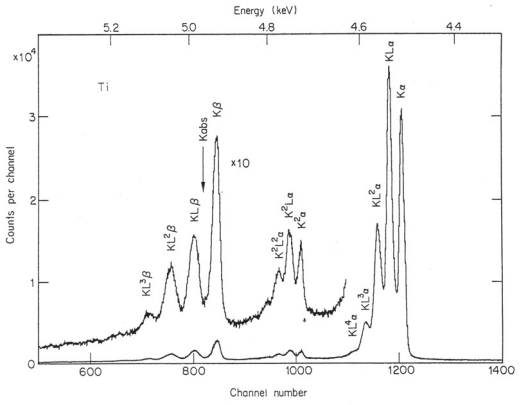

Fig. 4. Spectrum of Ti K-X rays induced by 81 MeV N ions obtained by the broad-range crystal spectrometer. The symbol K^mL^n denotes the m K-shell and n L-shell vacancies in the initial state.

to study the collisional quenching of 110 MeV Ne^{9+} ions in gaseous targets. The energy spectra of the Lyman series X rays (np→1s: $n = 2$, 3, 4 and 5) emitted by Ne^{9+} were measured by the broad-range crystal spectrometer with a crystal of RAP in this experiment.[16,e)]

Studies of radiative electron capture (REC) processes (the inverse process of photoionization) were made by measuring the REC X rays emitted from 5.5 MeV/nucleon Ne ions collided with a gaseous target.[17)] M. Kase (Linear Accelerator Lab.) and I. Kohno (Cyclotron Lab.) participated in this experiment. In 1980, Tonuma et al. made a device to analyze the recoil-ion charge states from collisions of heavy-ions and gaseous atoms. They succeeded to get charge distribution of recoil Ar^{n+} ($n = 1$–7) ions from an Ar-gas target bombarded by 84 MeV N ions[18)] and made some studies at the Cyclotron. Awaya et al. designed and constructed a target chamber for measuring angular distribution of X rays by a Si(Li) detector.[19)] J. Takahashi (special researcher of the Radiation Lab.) et al. measured the angular distribution of L-X rays from Sn bombarded by 82 MeV N ions from the Cyclotron using this chamber to study anisotropy of L X-ray emission.[20)] This chamber was moved to the experimental room of RILAC later.

From around 1980 many people became busy to prepare beam lines with experimental equipment in the experimental area of the RIKEN Heavy-ion Linear Accelerator (RILAC). This machine could accelerate ions from He to Pb, and studies using these heavy ions were very attractive for atomic physicists. Special researchers of both the Radiation Lab. and the Linear Accelerator Lab., cooperated with this preparation, too. In 1981, Kumagai and I held an additional post at the Linear Accelerator Lab. I became the Senior Scientist of the Radiation Lab. in 1982. Kumagai et al. constructed the on-line data taking system and data processing system at the counting room of RILAC.[21)]

Figure 5 shows the layout of the RILAC beam lines (as of 1993). Experimental setup installed during 1980–1984 in the experimental area of RILAC are listed below. Most of them are shown in Fig. 5, but some were prepared later. The number in parentheses after the equipment corresponds to that in Fig. 5.

⟨A1 beam line⟩

Kohno et al. designed and installed a 100 cm diameter target chamber (1) on the A1 beam line. Originally it was constructed for universal use in the nuclear scattering and reaction experiments,[22)] however, this chamber was often used for study of atomic physics.

⟨A2 beam line⟩

Tonuma et al. set the recoil-ion charge analyzer (2), which was revised frequently according to the purpose of their experiments since then.

e) By this work, Kambara got the degree of Dr. Sci from Kyoto Univ.

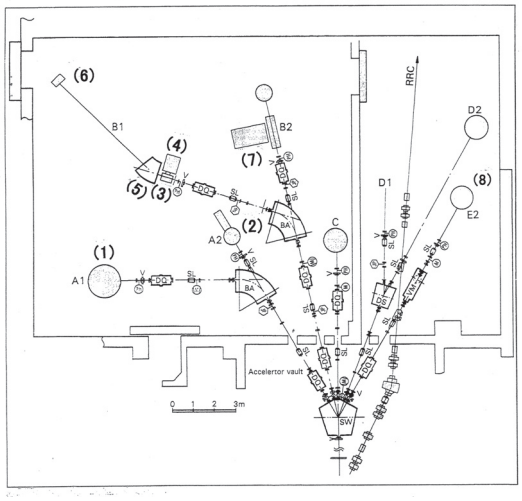

Fig. 5. Layout of the RILAC beam lines.

⟨B1 beam line⟩

An X-ray target chamber, a copy of that designed by Tendow in 1973, was installed to measure X rays with a Si(Li) detector through a thin Be window at 90° against the beam (3). A chamber for the broad-range crystal spectrometer (4) was constructed in 1981 by Awaya et al. and was connected to the X-ray target chamber at the opposite side of the Be window. The setting of B1 beam line, however, was changed very often according to the purpose of the experiments. The target chamber for measuring angular distribution of X rays by a Si(Li) detector was moved from the Cyclotron and set at downstream of (3) some time after 1984, though it is not shown in Fig. 5. The instruments (5) and (6) were installed afterwards: (5) was a broad-range charge analyzer constructed in 1986,[23)] and (6) was a two-dimensional Parallel-Plate Avalanche Counter (PPAC).

⟨B2 beam line⟩

K. Mori and K. Ando, who were members of the Thermonuclear Fusion Lab. (K. Mori), installed a beam-foil spectrometer (7), which consisted of a foil-moving system and a grazing-incident spectrometer (McPherson-247).[24)] At the downstream of (7), K. Kimura (Chemical Dynamics Lab.) installed his set-up for studies of radiation chemistry.

⟨C beam line⟩

This beam line was dedicated to a PIXE group of the Solid State Chemistry Lab.

⟨D1 and D2 beam lines⟩

These beam lines were dedicated to solid-state physics.

⟨E2 beam line⟩

A. Yagishita (Linear Accelerator Lab.) et al., installed an Auger- electron spectrometer.[25)]

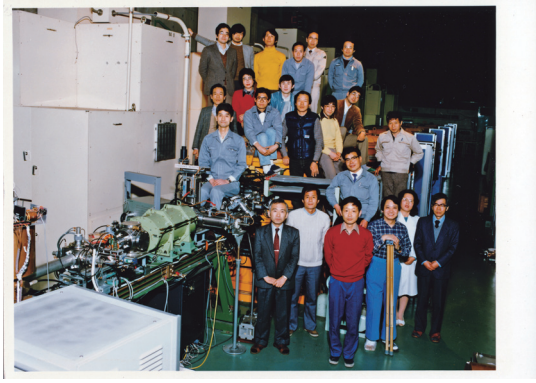

Fig. 6. Photograph of M. Odera and members of Linear Accelerator Lab. with RILAC, taken one day of March, 1985.

In February 1982, RILAC started to supply heavy-ion beams to the proposed experiments. As the basic instruments to make the experiments were ready, works were done eagerly from this time to 1997 by using beams of RILAC. Figure 6 is a photograph of Odera and the staff of the Linear Accelerator Lab. taken in March 1985 at the RILAC accelerator. The experimental works made during 1982–1997 will be introduced later.

3 Atomic Processes Laboratory

At the end of March 1982, K. Mori, Chief Scientist of the Thermonuclear Fusion Lab., retired from RIKEN. T. Watanabe (Univ. Tokyo), a theorist of atomic processes, was nominated for this position in November 1982. Among the staff of the Thermonuclear Fusion Lab., Ando and S. H. Be remained in this laboratory. Watanabe invited me to his laboratory so as to make the laboratory contribute to both the theoretical and the experimental atomic physics. So, Nishida and I moved to this new laboratory from the Radiation Lab., just after T. Hamada, Chief Scientist of the Radiation Lab., retired from RIKEN at the end of March 1983. At the same time, Katou moved to Safety Control Affairs Center. Most of other members remained in the Radiation Lab. (M. Ishihara), so the atomic physics group originated in the Radiation Lab. broke up.

Watanabe changed the name of laboratory to Atomic Processes Lab. in 1983. Tonuma and Kambara held double positions of the Linear Accelerator Lab. and the Atomic Processes Lab. Be moved to the Cyclotron Lab. The Atomic Processes Lab. got new members; in 1983, I. Shimamura, a theorist, who was promoted to the Senior Scientist in next year, and in 1985, Y. Kanai, an experimentalist. M. Odera, the Chief Scientist of the Linear Accelerator Lab., retired from RIKEN in March, 1985, and in 1986, Kambara moved to the Atomic Processes Lab., whereas Tonuma stayed at the Linear Accelerator Lab. (I. Tanihata) keeping the double position.

Watanabe managed the general administration of the laboratory and the theoretical group and I did most of the management of the experimental group consulting with him. Though the theoretical group made excellent works but I will describe here about only the experimental group except for some studies in which both group collaborated. Watanabe was eager to promote the international collaboration.

Visitors of experimentalist to the Atomic Processes Lab., were S. M. Shafroth (Univ. North Carolina), R. Schuch (Heidelberg Univ.), P. Mokler (GSI), N. Stolterfoht (Hahn-Meitner Inst.), B. Sulik (ATOMKI – Inst. Nucl. Study, Hungarian Academy of Sciences, Debrecen, Hungary), T. Papp (ATOMKI), H. Schmidt-Böcking (Frankfurt Univ.), and R. Dörner (Frankfurt Univ.). Visiting researchers whose living expenses supported by RIKEN for more than one year, were M. M. Ismail (Cairo Univ.) and G. H. Vogt (Heidelberg Univ.). The experimental group wanted to use a Semi-Classical Approximation program coded by a theorist D. Trautmann (Basel Univ., Switzerland) and invited him to the laboratory. Domestically, we had many visitors. Main visitors were: A. Danjo (Niigata Univ.), A. Hitachi (Waseda Univ.), Y. Itoh (Josai Univ.), T. Koizumi (Rikkyo Univ.), H. Shibata (Res. Cent. Nucl. Sci., Univ. Tokyo), Matsuo (Tokyo Med. Dent. Univ.), T. Mizogawa (Saitama Univ.), S. Ohtani, K. Sato and H. Tawara (Inst. Plasma Phys., Nagoya Univ.), K. Okuno (Tokyo Metropolitan Univ.), K. Shima (Tsukuba Univ.), H. Suzuki and K. Wakiya (Sophia Univ.), S. Tsurubuchi (Tokyo Univ. of Agric. Tech.), J. Urakawa (KEK), S. Takagi (Toho Univ.), Y. Yamazaki (Nucl. Reactor, Tokyo Inst. Tech.) and M. Yoshino (Shibaura Inst. Tech.).

Kambara stayed at Max-Planck Institute (MPI) for Nuclear Physics (Heidelberg) supported by Nishina Memorial Foundation for one year, and also joined experiments at MPI and UNILAC, GSI.

In 1986, we constructed a beam line for the study of atomic physics in the E2 room of the RIKEN Ring Cyclotron (RRC), as is shown in Fig. 7. We installed a target chamber to measure the angular distribution of X rays, a 100 cm-diameter target chamber for universal use, and a broad-range magnetic charge analyzer that can be rotated from 0° to 60° relative to the beam direction. In order to reduce the background radiation, there were no slits or baffles in the experimental room. A charge stripper setup was installed in the RRC vault to provide different charge-state projectile ions. The beam line was designed so as to get a vacuum better than 10^{-8} Torr.

Another facility for atomic physics was constructed in the ion source vault of the AVF cyclotron in 1988 to use low-energy highly-charged heavy ions from the ECR ion source. Schematic diagram of this beam line including a 0° electron spectrometer is shown in Fig. 8.

The Synchrotron Radiation Facility Design Group (Head: H. Kamitsubo) for the SPring-8 project was organized at RIKEN in 1988 and Watanabe chaired its user-groups in which I was included. A workshop on the

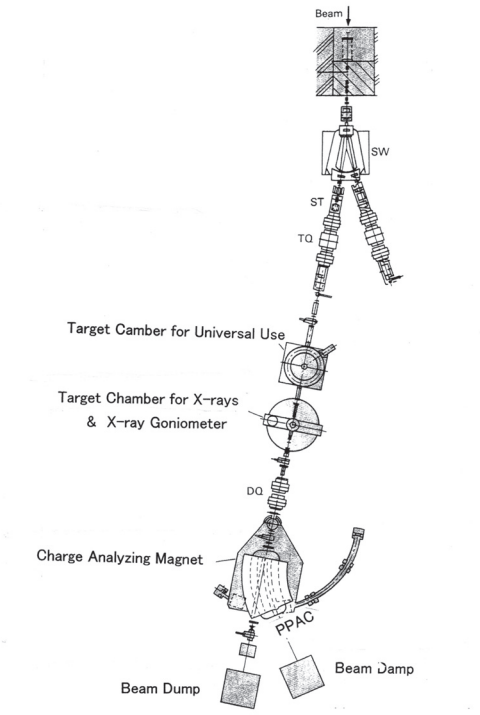

Fig. 7. Experimental setup for atomic physics in the E2-experimental room of RRC.

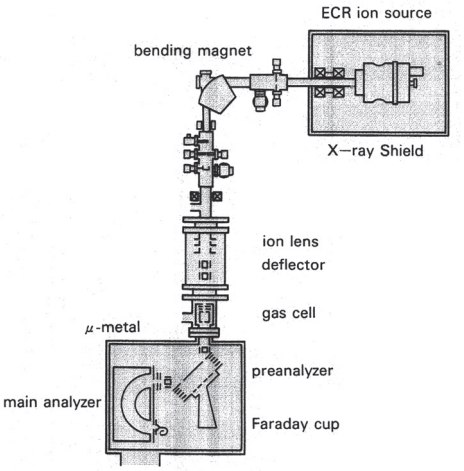

Fig. 8. Experimental setup at the AVF ECR ion source. The 0° tandem-type electron spectrometer is installed.

studies of atomic physics using this high brilliant synchrotron radiation was held among the atomic physicists of Japan in December 1988, and it was decided to organize a working group which would be managed by M. Kimura of Osaka Univ., and I. Up to the end of 1990, five meetings were held and the research and development for future studies were discussed. Some R&D plans were proposed to R&D program of the SPring-8 Project.

Fig. 9. Photograph of Atomic Physics Building (right) and Cyclotron Building (left).

Fig. 10. Photograph of members of the Atomic Physics Lab. at the entrance of the Atomic Physics Building, taken in April of 1993.

4 Atomic Physics Laboratory

In February 1990, the Atomic Processes Lab. moved from the main research building to "Cyclotron Research Building" near "Cyclotron Building." At the end of March Watanabe retired from RIKEN. I was nominated for the Chief Scientist of this laboratory taking over everything from him, except for the name of laboratory, which was changed to "Atomic Physics Laboratory." The building was renamed as "Atomic Physics Building." A photograph of Atomic Physics Building (right) and Cyclotron Building (left) located across a street each other, and that of members of the Atomic Physics Lab. taken at the entrance of Atomic Physics Building in April of 1993 are shown in Fig. 9 and Fig. 10, respectively. Both buildings were demolished to construct the RIBF Building later.

The Atomic Physics Lab. welcomed three new members for experimental studies: M. Oura in 1991, Y. Nakai in 1992 and T. Kojima in 1994. In addition to these three staff members, two special researchers of basic science program, Naoki Watanabe and M. Kitajima joined the experimental group. We had also visiting researchers, Y. Zou (Jiao Tong Univ. China), P. Bengtsson (Lund Univ.), B. Nyström (Lund Univ.), R. Hut-

ton (Lund Univ.), S. Kravis, T. Mizogawa, T. Niizeki, K. Soejima and M. Sano. Kambara became a Senior Scientist in 1993. Four special researchers of basic science program, H. Fukuda, T. Yoshida, J. Tang, and A. Igarashi, and visiting researcher, M. R. Harston joined the theoretical group. Shimamura made the management of theoretical group.

Oura moved to Synchrotron Radiation Center in 1996 keeping the position of the Atomic Physics Lab.

Collaboration with the domestic and foreign research groups were performed positively.

Agreements of collaboration on studies of atomic physics were made with Kansas State University (KSU) in 1991, Dept. of Physics, Goethe (Frankfurt) University in 1992, Lund University in around 1995 and GSI (since the Atomic Processes Lab.). There was an exchange program of scientists between Hungary and the Japan Society for the Promotion of Science, and the Atomic Physics Lab. accepted experimentalists from ATOMKI by this program. T. Papp, B. Sulik, J. Pálinkás and D. Berenyi visited RIKEN and T. Papp and B. Sulik joined the experiments.

H. Schmidt-Böcking (Frankfurt Univ.), I. Martinson (Lund Univ.), C. D. Lin (KSU, theorist) were invited to the laboratory by Eminent Scientist program of RIKEN. Every year, a post-doc of Frankfurt Univ. stayed at the laboratory for approximately two months and joined experiments. They were R. Dörner, J. Euler, S. Lencinus, L. Spielberger, O. Jagutzki, V. Mergel, M. Jeager and M. Achler. From KSU, we had five visitors, B. DePaola, C. P. Bhalla (theorist), P. Richard, L. C. Cocke and M. P. Stöckli. DePaola often visited the laboratory and joined experiments and Bhalla participated in the analysis of experimental data, calculating the fluorescence yields for the cases of multiple inner-shell vacancies existed in initial states. Visitors from Lund Univ. participated in the beam-foil experiments. They were, Martinson, S. Huldt, L. Engeström, and I. Kink. P. Spädke of GSI visited RIKEN taking his program code "AXEL," which we wanted to use to simulate the ion trajectory in the R&D research for SPring-8.

Domestically, most of the visitors at the Atomic Processes Lab. continued the collaboration with us. S. Ohtani, T. Mizogawa, and Y. Yamazaki changed their affiliations and new ones were Inst. Laser Center/Univ. Electro-Commun., Nagaoka Coll. Tech. and Coll. Arts Sci./Univ. Tokyo, respectively. Additional main visitors were T. Azuma and K. Komaki (Coll. Arts Sci., Univ. Tokyo), Keishi Ishii (Kyoto Univ.), Akio Itoh (Kyoto Univ.), K. Kuroki (Natl. Res. Inst. Police Sci.), T. Mitamura, T. Sekioka and M. Terasawa (Himeji Inst. Tech.), and T. Takayanagi (Sofia Univ.).

The Cyclotron was shut down in 1990. The RIKEN symposium "Studies using 160 cm Cyclotron – Its contribution to the accelerator science –" was held in December of that year. In this symposium two talks were given on "The sequence of events of getting the Cyclotron": one was given by T. Hamada, the former Chief Scientist of the Radiation Lab. from the viewpoint of RIKEN, and the other by K. Nagara, the former executive director, who had handled the Cyclotron budget at the STA, from the viewpoint of STA. The supplement of RIKEN Accelerator Progress Report – The 160 cm Cyclotron 1966–1990 – was published. The ceremony of demolishing of the Cyclotron was held on the 26th of February, 1999. A Photograph of that time is shown in Fig. 11.

Fig. 11. Ceremony of demolishing of the 160 cm Cyclotron was held on the 26th of February, 1999. A photograph of participants with the 160 cm Cyclotron.

In 1991, H. Kamitsubo became the director of Synchrotron Radiation Project, and Y. Yano was appointed to the Chief Scientist of the Cyclotron Lab. RIKEN Accelerator Research Facility (RARF), which included both RILAC and RRC, was organized preliminary in 1991 and next year it was established. The facility director was Ishihara and vice facility directors were Awaya (myself) and Yano. From the Atomic Physics Lab., Kambara and Kanai contributed to this facility as members of experimental support division. The chairperson of steering committee of this facility was Tanihata. Two Project Advisory Committees (PACs) were organized for RRC: a PAC for nuclear physics and that for other fields.

In September 25–28 in 1994, Advisory Meeting for the future project "RIKEN RI Beam Factory (RIBF)" was held at RIKEN. Atomic physicist, Martinson was a member of the advisory committee. At this meeting, I presented the achievements of atomic physics at RARF, and Kambara gave a talk at the session of the proposals of RIBF.

We held "The Forth RIKEN Winter School-Atomic and Molecular Processes" in January 8–12, 1995 at Tsunan, Niigata. Lecturers were T. Åberg (Helsinki Univ. Tech.), Y. Hatano (Tokyo Inst. Tech.), P. Mokler (GSI), and H. Tawara (Nat. Inst. Fusion Sci.). This winter school was hosted by RARF and held annually from 1992.

5 Experimental studies during 1982–1997

Here, I will introduce some main subjects of the experimental works at the Cyclotron, RILAC, RRC, and the

ECR ion source made during the period of the Atomic Processes Lab. and the Atomic Physics Lab., briefly. As there were so many works and space is limited, only the subjects will be mentioned in most cases and limited numbers of papers are quoted.

5.1 Studies using heavy ions from 160 cm Cyclotron

The isotope effect of REC X-ray yield

The theoretical group of the Atomic Physics Lab., K. Hino et al., had formulated the REC process and predicted so called "isotope effect" where the REC cross section depended on the mass of a target. According to isotope-effect prediction, the ratio of REC cross sections between collision systems, $Ne^{q+}+{}^3He$ and $Ne^{q+}+{}^4He$ would be close to two.[27] The experimental group checked this prediction by measuring the REC X-ray yields for 110 MeV Ne ions from the Cyclotron incident on ^{3}He and ^{4}He gas targets. Contrary to the prediction, the difference was within 7%.[28,29] Theorists reconsidered their formulation.[30]

5.2 Studies using heavy ions from RILAC

Table 2 shows the annual trend of the beam time of RILAC and how it was shared among the user's groups. As is seen in this table, approximately 1/3–1/4 of beam time were used by atomic physics.

Studies will be introduced what was done at each beam line, which is shown in Fig. 5. Names of experimental members of each study were abbreviated in most cases, but collaborated organizations are listed.

A1 and B1 beam lines

1) Studies of multiple ionization process and electronic states of target atoms or projectile heavy ions with multiple inner-shell vacancies

   The various kind of studies were made from 1982–1997, using the broad-range crystal spectrometer. Main subjects were as follows, where Z_1, q and E denote the atomic number, the charge, and the incident energy of the projectile ions, respectively. Z_2 is the atomic number of the target atoms and x is the thickness of the target foils.

   a) Systematic studies of multiple inner-shell ionization processes of the target atoms for various collision systems (Z_1, q, E, and Z_2 were changed)[31,32]

      X-ray spectra of the excited target atoms were measured in most cases, but that of the exited projectile ions were also measured if necessary.

   b) Electronic state of the projectile ions during passing through a thin foil[33]

      X rays from the projectile ions were measured by changing q, E, and x, so as to make clear how the projectile ions got equilibrium charge state, and the outer-shell vacancies contributed to the formation of the inner-shell vacancy during passing through a target foil.

   c) Studies of angular distribution of L-X rays[34]

      Measurements were made by a Si(Li) detector at first, and then by the broad-range spectrometer to resolve the L satellite lines. Studies were made for different Z_1, q, E, and Z_2. The M2/E1 mixing of L-X rays were studied.

   d) Radiative electron rearrangement transition following multiple K- and L-shell ionizations[35]

      The RER satellite lines were observed for the first time.

2) Studies on impact parameter dependence of inner-shell ionization

   This studies developed with advancement of experimental setup and technique.

   In 1985, the impact-parameter dependence of K-shell ionization of the target atoms was investigated for He^+ + Ca, Cr and Cu systems.[36] The target K-X rays were measured with a Si(Li) detector in coincidence with the scattered ions detected with a PPAC at approximately 2 m downstream of the target. The beam was collimated to 1 mm × 1 mm with a divergence of 0.02°. Later, using the same set up, target-thickness dependence of the K-vacancy production probabilities $P_K(b)$, where b was the impact parameter, and the total cross sections were studied for 40.6 MeV Ar ions + Ca and Cu systems. The obtained $P_K(b)$ for Ar ions on Ca target were compared with that of 21 MeV Cl ions on Ar target obtained at Max Planck Inst., Heidelberg, to study a solid-gas effect in the K-vacancy production in the near symmetric collision systems.[37]

   In 1986, the broad-range charge analyzer was installed (cf. Fig. 5). Charge distribution of projectile ions scattered by thin target foils, and next, by gaseous targets was measured using the two dimensional PPAC mounted at the exit of charge analyzer.[38] A four-jaw slit was set upstream of the target to make a parallel beam.

   In 1988, studies on K X-ray emission probability $P(b,\phi)$ for projectile ions with different charge states were made, where b was the impact parameter and ϕ was the angle between the scattering plane and the X-ray emission direction, using a coincidence method between signals of X-ray detector and that of the two dimensional PPAC. The b was estimated from scattering angle θ of the projectile ions.[39] The setup is shown Fig. 12. Then, studies on inner-shell ionization and transfer processes in close collisions followed, by coincidence measurements between the scattered projectiles and charge-analyzed recoil ions.

   A high-resolution recoil-ion momentum spectrometer had been developed.[40] When a very cold and localized supersonic gas jet target (internal temper-

Table 2. Beam time of RILAC and that for individual research group (in unit of day).

Year	1982	1983	1984	1985	1986	1987	1988	1989	1990	1991	1992	1993	1994	1995	1996	1997
Beam Time (days)	144	167	155	155	175	151	176	174	123	177	164	170	167	174	105	182
Atomic Physics	◎	◎	◎	66	62	36	31	41	33	63	44	41	43	60	37	45
Nuclear Physics				5	17	1	0	21	0	0	0	0	0	6	14	2
Others (*)				69	77	40	44	40	52	43	56	44	28	24	16	26
Accelerator research				15	18	11	21	5	4	7	11	16	25	6	2	16
Beam transportation to RRC				0	0	63	80	67	34	64	53	69	70	78	36	93

Others (*) is the sum of beam time for Solid state physics, Nuclear chemistry, Radiation chemistry, and Radiation biology.
◎ There are no data about the individual research group but atomic physics group used the beams in the year marked by this symbol.

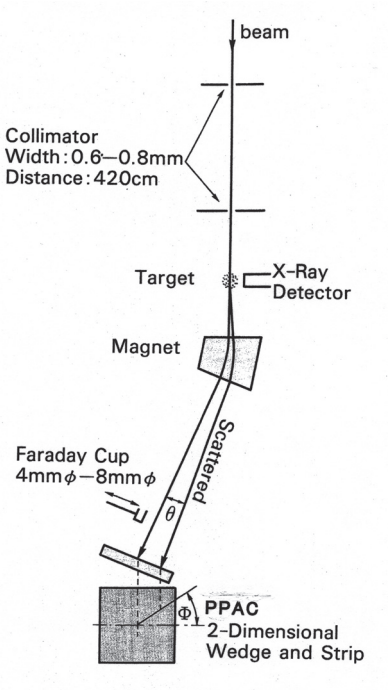

Fig. 12. Experimental setup prepared at B1 beam line for scattering angle dependent measurement.

ature as low as a few mK) and this high-resolution recoil momentum spectrometer were combined, one could obtain recoil-ion momentum with resolution of better than 0.1 au. This experimental technique was called as COLd Target Recoil Ion Momentum Spectroscopy (COLTRIMS). The detection efficiency was nearly 4π, and simultaneously the three-dimensional components of the recoil-ion momentum after a collision were obtainable. This equipment was placed at the gas-cell in Fig. 12 in 1994. Final-state selective measurements of the differential cross sections of single-electron capture and target single-ionization process were made for 8.7 MeV O^{7+}-He collisions by using this equipment under the collaboration of the Atomic Physics Lab., Frankfurt Univ. and Kansas State Univ.[41] Afterwards, some works for different collision systems were made by COLTRIMS.[42]

3) Study of the fragment-ion distribution of C_{60} in close collision with fast C ions

The experimental setting was similar to that shown in Fig. 12. A C_{60} vapor target produced by an oven was placed at the position of the target in Fig. 12. Instead of the X-ray detector, a TOF spectrometer was placed at 90° respect to the beam and analyzed the mass-to-charge ratio of the fragment ions. Close collisions were selected by the change of the projectile charge state, using the coincidence method between the signals of the TOF spectrometer and that of the PPAC.[43] This work was made in collaboration with Kyoto Univ. group.

4) Trial of studies on collisional process of electrons and heavy ions by a merged electron-ion beam method (1985–1986)

New trial of studies were started in 1985 under the collaboration with Inst. Plasma Phys./Nagoya Univ., Tokyo Metropolitan Univ., Rikkyo Univ., Josai Univ., Tokyo Univ. of Agric. Tech., Res. Center Nucl. Sci. Tech./Univ. Tokyo, and Toho Univ. An Electron Beam Ion Source (EBIS) apparatus, so-called "proto-NICE" developed at Inst. Plasma Physics/Nagoya Univ. was rebuilt in the experimental room of RILAC.[44] After testing, it was installed on the beam line (B1). A 1.24 MeV/nucleon Ar^{4+} ions entered the interaction region through an axial 2-mm-diameter hole in the cathode of the electron gun of the Proto-Nice. The electron-ion collision energy was changed by varying the electron energy, and the charge distribution of the Ar ions was measured by a magnetic charge-state analyzer and a PPAC. The data on the charge state of the Ar ions merged with the electrons (on state) and without the electrons (off state) are measured and accumulated. The observed ratio Ar^{3+}/Ar^{4+} was about 3×10^{-6} and almost same between the "on state" and "off state." Therefore it should have originated in the Ar^{4+}-residual gas (10^{-7} Torr. × 6 m) collisions. Large effort was made to reduce the amount of residual gas in the beam ducts, but finally we had to give up this trial. But as a byproduct, we experienced that the Ar-ions were focused by the electron

beam.[45)]

A2 beam line

Various kinds of experiments concerned to recoil ions (cluster ions) were made. An apparatus to measure the net ionization cross sections of rare gas targets by collisions of heavy ions was made adopting the condenser plate method in 1983.[46)] In 1987, a target gas cell and recoil ion detection system were designed and installed. The charge state of the recoil ions was analyzed by a time-of-flight spectrometer and that of the projectile ions was analyzed by an electrostatic analyzer and a PPAC Coincidence measurements between the charge-analyzed recoil ions and the projectiles were performed.[47)] The production of recoil charged ions and molecules were studied by using a molecule target.[48)] Around 1990, they started to study charged recoil ions, molecules and clusters produced when heavy ions collided with a frozen rare gas or molecule target on a thin foil at the liquid-nitrogen temperature.[49)] This work was made for various combination of target and incident heavy ions. In 1996, they planned to investigate the electron loss from H^- ions under the highly ionized MeV/nucleon ion impact and prepared a setup for it.[50)]

B2 beam line

An experiment of beam-foil spectroscopy was started in 1983. At first, the determination of the relative sensitivities of the detection system including a grazing incidence monochromator and a channel electron multiplier (Ceratron) with a secondary electron converter was made by using 14.8 MeV N ions from RILAC.[51)] Visitors from Inst. Plasma Phys./Nagoya Univ. and Tokyo Univ. Agric. Tech, and S. Kohmoto (Cyclotron Lab.) joined the experiment. During 1984–1987, beam-foil spectra of Al ions were studied. New lines of Al XII, Al XI and Al X were identified and their energies were obtained. The lifetime of $2s2p^1P$ state of Al X was determined and a transition array of Al X 2p3d-2p4d was identified.[52)] During 1988–1993, the Mg IX 3s3d-2s4f transition of beam-foil spectra was measured and analyzed. The lifetimes of the $2p^53p$ and $2p^53d$ levels in Ne-like Ti, Cr, and Fe ions were systematically studied.[53)]

During 1994–1997, following studies were made. The transition probabilities for Na-like Nb^{30+}, and Mg-like Nb^{29+} were investigated.[54)] The lifetime of the $3p\ ^2P_{3/2}$ level in Na-like Kr^{25+} were determined. The wave lengths of intercombination lines in Al- and Si-like ions from Kr to Nb and the lifetime of the intercombination transitions in Be-like and B-like Iron were studied. These works were done in collaboration with the group of Lund Univ. During the same period, beam-foil spectra of highly charged Ne ions and that of highly charged Ar ions were measured in visible regions by collaborating with the group of Kyoto Univ. Many lines were observed and identified for Ne and Ar.

E2 beam line

1) Auger electron spectroscopy (1982–1986)

Spectroscopic studies on the L-MM Auger electrons from highly ionized target Ar^{q+} (q = 7, 6 5) atoms excited by Ar ions, those from Ar excited by He, C, Ne, Al ions, and the M-NN ones from Kr bombarded by He, N, Ne and Ar ions by using Auger electron spectrometer.[55)] In 1987, N. Stolterfoht (Hahn-Meitner Inst.) visited RIKEN with a 0° electron spectrometer. K-LL Auger electrons emitted from projectile N ions were studied for collision system 1.33 MeV/nucleon N^{2+} ions on He and Ne target by using this spectrometer. Highly energy-resolved spectrum was obtained because of the emission angle of Auger electrons was 0° (without Doppler broadening). By this reason, this type of electron spectrometer was used to measure electrons hereafter.

2) Study of high charge state Rydberg ion (1990–1994)

A Rydberg-state analyzer was taken by B. DePaola (KSU) and combined with the 0° electron spectrometer of RIKEN. After 2.5 MeV/nucleon N ions colliding with a target foil, hydrogen-like N ions in Rydberg states of n∼160 were obtained. The Rydberg electrons were ionized in the electric field of the Rydberg analyzer, and were measured by the 0° electron spectrometer. A beat structure was expected in the spectra of electrons from high charge Rydberg ions. The observed period of the beats roughly agreed with that predicted by a simple model. As this study was made under collaboration with KSU, Kanai and DePaola mutually visited the partner labs.[56)] Kanai also collaborated with KSU-group, on the study of the electron capture process of multiply charged ions colliding with Rydberg state target ions.

3) Systematic studies of binary electrons (1992–1994)

Binary encounter electron peaks were measured in collision of Bi^{q+} (q = 10, 14, 16 and 32) on H_2, He, and Ar at 0° with changing the incident energy; 0.56, 0.8 and 1.2 MeV/nucleon for q = 16 and 32, and 0.8 MeV/nucleon for q = 10 and 14. The binary-encounter peak shift and the double-differential cross section were obtained as functions of the incident energy. Experimental peak shift was compared with Bohr-Lindhard model and adiabatic tunneling model.[57)]

5.3 Studies using heavy ions from RRC

1) Studies on radiative electron capture process

Immediately after the beams of RRC were available, angular distribution of K- and L-REC X rays were studied for 20.5 MeV/nucleon Ar ions on a Be target. Experimental results fit well to $\sin^2\theta$ distribution which was theoretically predicted, where θ

is the angle of the X ray relative to the beam. By analyzing the K-REC spectra, the width of K-REC peak was consistent with capture of a 2s electron of Be. This width reflected the momentum distribution of the 2s electron of Be and was compared with that obtained by Compton scattering for the first time.[58] The yields of K-REC X rays of 26 MeV/nucleon $Ar^{13,\ 18+}$ ions passing through a C foil were studied by changing the foil thickness from 10–80 $\mu g/cm^2$. It was found that single collision condition was valid even in the case of foil targets as the ion energy was high. The REC cross sections for 26 MeV/nucleon Ar^{18+} ions were obtained and compared with Bethe Salpeter theory.[59] Ratio of the REC cross section to the total electron capture cross section was studied for 77 MeV/nucleon Ar^{18+} ions in 23 and 44 $\mu g/cm^2$ carbon foils.

2) Studies of charge distribution of ions after passing through foils

Charge distribution of 26 MeV/nucleon Ar^{13+} ions after passing through a carbon foil was measured by changing the thickness of the foil (10, 20, 40, 80, 160, 200 $\mu g/cm^2$ and 4.2 mg/cm^2),[60] and that for 77 MeV/nucleon Ar^{q+} ions by changing the thickness of carbon foil (10 $\mu g/cm^2$–4.27 mg/cm^2) and the incident charge state (q = 16–18).[61] The magnetic charge analyzer and PPAC were used (cf. Fig. 7). The electron capture and loss cross sections were obtained for 77 MeV/nucleon Ar^{q+} ions. This offered also an important basic data to get heavy ions with requested charge value.

3) Systematic studies on multiple inner-shell ionization of target elements by heavy ion

Up to that time, systematic-studies were made with heavy ions from the Cyclotron and RILAC, and data at higher impact energies were desired. K_α satellite, hyper-satellite and K_β satellite X-ray spectra of target elements (Ti, Fe, Ni and Cu) excited by 26 MeV/nucleon N ions were measured, and those of target elements (Ti, V, Fe, Ni and Cu) excited by 92 MeV/nucleon Ar^{17+} were done. The broad-range crystal spectrometer was used to get spectra. All the data obtained at the Cyclotron, RILAC, and RRC were analyzed and discussed.[62]

4) Study of radiative electron rearrangement (RER) process

By using the broad-range crystal spectrometer, RER X rays from the 36.6 MeV/nucleon Ar^{14+} ions impinging on thin carbon foils were measured. The thicknesses of the foils were 10, 22, 39 and 85 $\mu g/cm^2$. At the same time, the charge distribution of the Ar ions after passing through the C-foil were measured by the magnetic charge analyzer with the PPAC.[63]

5) Studies on binary encounter electrons

Peaks of binary encounter electrons by 93 MeV/nucleon Ar^{q+} (q = 17, 18) passing through a thin carbon foil were studied by changing q and the thickness of the carbon foils (22–83 $\mu g/cm^2$) at the emission angle of 0°. Momenta of the electrons were analyzed by a magnetic electron spectrometer.[64]

6) Studies of heavy-ion irradiation effect on the superconducting materials, such as $La_{2-x}Sr_xCuO_4$

This work started in 1993 under collaboration with a group of Himeji Inst. Tech.[65] Irradiation had been made at a large target chamber shown in Fig. 7 but it took a long time to change the samples at this chamber. Kambara et al. made a setup for material irradiations on the E5A beam line of RRC in 1995.[66]

7) Collaboration to a few subjects proposed by the group of Univ. Tokyo

5.4 Studies using beams of AVF ECR Ion source

Energy levels and production mechanisms of doubly-excited states of projectile ions were studied by measuring emitted electrons with high energy resolution. A 0° Auger electron spectrometer was used. The doubly-excited states of ions were produced by double-electron capture from target gases. Study group of Sofia Univ. and visitors from Niigata Univ. and Shibaura Inst. Tech. joined this study.

1) Measurements of ejected electrons from He-like Carbon ions

$^{13}C^{6+}$ ions at 90, 66.7, 46.2 keV and $^{11}B^{5+}$ ions at 65, 50, 37.5 keV from the ECR ion source collided with a He gas target. Auger electrons from He-like states of C^{4+**} ($2lnl'$) n = 3–6 and B^{3+**} ($2lnl'$) n = 2–6 were observed. C^{4+**} ($2l2l'$) states were not produced in this experimental conditions, which could be explained by Niehaus' reaction window. Auger-electron spectra from C^{4+**} ($2l2l'$) and B^{3+**} ($2lnl'$) n = 2, 3 were measured with high energy resolution and compared with theoretical calculations.[67]

2) Studies of ejected electron spectra from O^{4+**} ($1s^2 3l3l'$)

Excited state O^{4+**} ($1s^2 3l3l'$) were produced by the double electron transfer from target gas to 60 keV O^{6+} ions. Ar, Ne, He, O_2, N_2 and H_2 were used as the target. Spectra of the ejected electrons varied depending on the targets. Production mechanisms of singlet/triplet states of the doubly-excited states were discussed.[68]

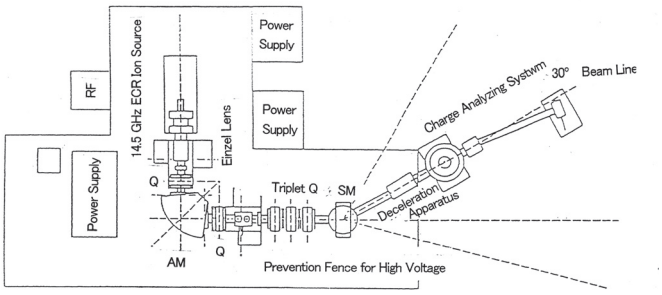

Fig. 13. Layout of the 14.5 GHz ECR ion source and setup for experiment.

6 Other studies at Atomic Physic Laboratory

1) Construction of 14.5 GHz ECR ion source

As the ECR ion source of the AVF cyclotron was an excellent facility for our studies, we desired to have one dedicated to atomic physics, and to get lower energy highly charged ions by decelerating the ions extracted from an ECR ion source. Getting the supplementary budget for construction of ion source under the name of shared-use equipment, we got a 14.5 GHz ECR ion source, Caprice, and installed it in the large experimental area of the Cyclotron.[69,70] Its beam line and instruments for studies were prepared by Special Coordination Funds for Promoting Science and Technology (representative: Awaya) since 1993 to at least 1997. Schematic Drawing of this facility, as of 1996, is shown in Fig. 13. Group of Sofia University joined the test experiments.[71]

2) R&D research works for SPring-8

As was described before, the working group of atomic physics for SPring-8 made proposals to R&D program of SPring-8 Project and got budgets for them.[72] These works were made by the members of working group, but the Atomic Physics Lab. became the base of them.

a) Development of merging beam method for photoionization of ions

T. Koizumi, Rikkyo Univ. and Y. Itoh, Josai Univ. were leading this project and many visitors from outside as well as some members of the Atomic physics Lab. joined them.

A collinear ion-photon merging-beam system was designed and constructed. The ions produced in an ion source were accelerated up to 1–2 keV and deflected by 90° through an electrostatic quadrupole ion deflector. The ions transported through a pair of orifices of 2 mm in diameter to the interaction region with photons, length of that was 15 cm. Then ion beams were analyzed by a parallel-plate ion-charge analyzer, which has a Faraday cup and two electron multipliers (Ceratron) as an ion detector. The computer code, AXCEL, developed in GSI was used to simulate the ion trajectories. The interaction region was biased to 800 V to distinguish the charged ions produced in this region from those in other regions. This equipment was completed in 1992. The use of a compact ECR ion source as the ion source was desirable, but impossible at that time. Therefore, an ion source of surface ionization type was used. In 1993, this equipment was moved to Photon Factory (PF), KEK and experiments on photoionization of ions were made. During 1993–1997, the studies on following target ions were made. Ba^+, Sr^+, Xe^+, Xe^{2+}, Xe^{3+} and Eu^+.[73–76]

b) Construction of an EBIS for use with synchrotron radiation to study the photoionization process of highly charged ions

S. Kravis, visiting researcher of the Atomic Physics Lab., was a main person of this project, and some staffs of the Atomic Physics Lab., especially N. Watanabe collaborated with him. Among the members of the working group, Okuno and Ohtani joined this work.

The highly charged ions are formed through successive ionization by electron impact while ions are trapped inside of the source by electric field. This EBIS was much smaller than typical EBIS which required liquid He for a superconducting solenoid, because of adopting the liquid nitrogen-cooled solenoid, instead of the superconducting ones. At liquid-nitrogen temperature, the resistance of copper is almost 1/10 of that at room temperature, so the power consumption was reduced. When the solenoid was cooled, the vacuum reached 10^{-10} Torr.[77] This equipment had a possibility to study the PHOBIS concept by replacing electron beams from electron gun with photon beams from SPring-8. In 1995, the test operation of this equipment was made at PF, KEK as a target of multiply charged ions and as the PHOBIS mode.[78]

3) Development of readout technique for two-dimensional position-sensitive detectors

A new technique for two-dimensional position readout from one electrode plane was proposed by T. Mizogawa.[79] This technique was applicable to a wide range of detector types, such as a gas-filled counter and a micro-channel plate This method was a combination of two one-dimensional position-readout techniques; the back-gammon method and weighted coupling capacitor method, and named as “modified backgammon method with weighted coupling capacitors (MBWC).” The patent department of RIKEN got the patent for this technique and a private com-

Fig. 14. Photograph of the opening ceremony of HCI-96.

pany "Optima" commercialized it.

At the end

In September 23–26, 1996, The 8th International Conference on the Physics of Highly Charged Ions (HCI-96) was held at Sonic City Hall in Omiya, hosted by RIKEN (Atomic Physics Lab.), and sponsored by The Japan Society for Promotion Science, Saitama Prefectural Government, Saitama Foundation for Culture and Industry and The Society of Atomic Collision Research. Akito Arima, the president of RIKEN, and Mariko Bando, the Vice Governor of Saitama Prefecture, (both the titles are of the time) gave addresses of welcome. I chaired the conference, Kanai worked as the conference secretary and Kambara was in charge of editing the proceedings of the conference, which was published by Physica Scripta.[80] A photograph of the opening ceremony is shown in Fig. 14.

This is a personal thing, but during the conference I had 60th birthday and I got an unexpected gift: in accordance with the session chairperson, HP. Winter (TU Wien), all participants sang the song "Happy Birthday" for me. In addition to this, I got another present in this year: The Physics Section, Royal Swedish Academy of Sciences and the Nobel Foundation invited me to the Nobel Prize Ceremony and Banquet, in view of my services to Swedish physics.

I retired from RIKEN in March 1997 and Y. Yamazaki took over the Atomic Physics Lab.

"There is a time for everything" is one of my favorite saying. I think that the experimental study of atomic physics using energetic highly-charged heavy ions got its time at RIKEN Accelerator Research Facility in the last quarter of the 20th century.

I am most grateful to former Chief Scientists, T. Hamada, M. Odera, T. Watanabe, and H. Kamitsubo for their understanding and support to experimental studies of Atomic Physics. I thank to the former members of RIKEN Accelerator Research Facility, especially for technical staffs, for their help to make experiments. I would like to express my gratitude to T. Kambara for his proofreading of this report and his advice. I am indebted to Y. Kanai and Y. Nakai for their comments for preparing this report.

References

1) Y. Awaya, J. Phys. Soc. Jpn. **23**, 673 (1967).
2) K. Matsuda et al., IPCR Cyclotron Progr. Rep., 5, 31 (1971).
3) S. Takeda et al., J. Phys. Soc. Jpn. **34**, 1115 (1973).
4) Y. Awaya et al., IPCR Cyclotron Progr. Rep. **7**, 87 (1973).
5) Y. Awaya et al., Phys. Rev. A **13**, 992 (1976).
6) Y. Awaya et al., IPCR Cyclotron Progr. Rep. **9**, 79 (1975).
7) K. Kumagai et al., Reports of Inst. Phys. Chem. Res. **53**, 153 (1977) (in Japanese).
8) H. Tawara et al., Phys. Lett. A **59**, 14 (1976).
9) Y. Awaya et al., IPCR Cyclotron Progr. Rep. **10**, 78 (1972); *ibid.* **11**, 91 and 93 (1973); *ibid.* **12**, 79 (1978); *ibid.* **13**, 73 and 76 (1979).
10) Y. Awaya et al., Phys. Lett. A **61**, 111 (1977).
11) T. Tonuma et al., IPCR Cyclotron Progr. Rep. **11**, 96 (1977).
12) Y. Awaya, in *Electronic and Atomic Collisions*, Eds. N. Oda, K. Takayanagi (North-Holland Pub. Co. 1980) p. 325.
13) Y. Awaya et al., RIKEN Accel. Prog. Rep. **15**, 66 (1981).
14) A. HitachiCH. Kumagai, Y. Awaya, Nucl. Instrum. Methods **195**, 631 (1982).
15) A. Hitachi et al., RIKEN Accel. Prog. Rep. **15**, 69 (1981).
16) T. Kambara, J. Phys. B: At. Mol. Phys. **17**, 1599 (1984).
17) T. Kambara et al., J. Phys. B: At. Mol. Phys. **15**, 3759 (1982).
18) T. Tonuma et al., RIKEN Accel. Prog. Rep. **15**, 70 (1981).
19) Y. Awaya et al., IPCR Cyclotron Progr. Rep. **14**, 70 (1980).
20) J. Takahashi et al., RIKEN Accel. Prog. Rep. **16**, 82 (1982).
21) H. Kumagai, T. Wada, IPCR Cyclotron Progr. Rep. **14**, 156 (1980); H. Kumagai, M. Sasagase, RIKEN Accel. Prog. Rep. **15**, 123 (1981).
22) I. Kohno et al., IPCR Cyclotron Progr. Rep. **14**, 141 (1980).
23) Y. Awaya et al., RIKEN Accel. Prog. Rep. **20**, 132 (1986).
24) K. Ando, K. Mori, IPCR Cyclotron Progr. Rep. **14**, 149 (1980); RIKEN Accel. Prog. Rep. **15**, 85 (1981).
25) A. Yagishita, T. Nakamura, IPCR Cyclotron Progr. Rep. **14**, 143 (1980).
26) Y. Awaya et al., RIKEN Accel. Prog. Rep. **22**, 149 (1988).
27) K. Hino et al., RIKEN Accel. Prog. Rep. **18**, 62 (1984).
28) T. Kambara et al., RIKEN Accel. Prog. Rep. **18**, 77 (1984).
29) T. Kambara et al., J. Phys. Soc. Jpn. **56**, 1907 (1987).
30) K. Hino, T. Watanabe, RIKEN Accel. Prog. Rep. **19**, 55 (1985).
31) Y. Awaya et al., Nucl. Instrum. Methods Phys. Res. B **10–11**, 53 (1985).
32) Y. Zou et al., Phys. Rev. A **51**, 3790 (1995).
33) T. Mizogawa et al., Phys. Rev. A **42**, 1275 (1990).

34) T. Papp et al., J. Phys. B: At. Mol. Opt. Phys. **24**, 3797 (1991).
35) M. Oura et al., VIth Int. Conf. on Phys. of Highly Charged Ions, AIP Conf. Proc. **274**, 642 (1993).
36) R. Schuch et al., Z. Phys. D: At., Mol. Clusters **4**, 339 (1987).
37) T. Kambara et al., Z. Phys. D: At., Mol. Clusters **22**, 451 (1992).
38) Y. Kanai et al., Nucl. Instrum. Methods Phys. Res. A **262**, 128 (1987).
39) T. Kambara et al., Nucl. Instrum. Methods Phys. Res. B **53**, 426 (1991).
40) O. Jagutzki et al., RIKEN Accel. Prog. Rep. **28**, 129 (1995).
41) T. Kambara et al., J. Phys. B: At. Mol. Opt. Phys. **28**, 4593 (1995).
42) T. Kambara et al., J. Phys. B: At. Mol. Opt. Phys. **30**, 1251 (1997).
43) Y. Nakai et al., J. Phys. B: At. Mol. Opt. Phys. **30**, 3049 (1997).
44) S. Ohtani et al., RIKEN Accel. Prog. Rep. **19**, 144 (1985).
45) Y. Kanai et al., RIKEN Accel. Prog. Rep. **20**, 131 (1986).
46) S. H. Be et al., J. Phys. B: At. Mol. Opt. Phys. **19**, 1771 (1986).
47) T. Tonuma et al., RIKEN Accel. Prog. Rep. **21**, 84 (1987).
48) T. Tonuma et al., Phys. Rev. A **33**, 1385 (1986).
49) H. Tawara et al., RIKEN Accel. Prog. Rep. **24**, 53 (1990).
50) H. Tawara et al., RIKEN Accel. Prog. Rep. **29**, 91 (1996).
51) K. Sato et al., RIKEN Accel. Prog. Rep. **17**, 46 (1983).
52) K. Ando et al., Nucl. Instrum. Methods Phys. Res. B **33**, 239 (1988).
53) K. Ando et al., Physica Scripta **53**, 33 (1996).
54) R. Hutton et al., Phys. Rev. A **51**, 143 (1995).
55) T. Matsuo et al., J. Phys. B: At. Mol. Opt. Phys. **21**, 1791 (1988).
56) B. D. DePaola et al., J. Phys. B: At. Mol. Opt. Phys. **29**, 1247 (1996).
57) Y. Kanai et al., VIth Int. Conf. on Phys. of Highly Charged Ions, AIP Conf. Proc. **274**, 315 (1993).
58) Y. Awaya et al., in *High-Energy Ion-Atom Collisions*, Eds. D. Berenyi, G. Hock (Springer-Verlag, 1988) p. 185.
59) Y. Awaya et al., Nucl. Instrum. Methods Phys. Res. B **53**, 375 (1991).
60) Y. Kanai et al., RIKEN Accel. Prog. Rep. **22**, 54 (1988).
61) Y. Kanai et al., RIKEN Accel. Prog. Rep. **24**, 41 (1990).
62) Y. Awaya, T. Kambara, Y. Kanai, Int. J. Mass Spectrom. **192**, 49 (1999).
63) T. Kambara et al., RIKEN Accel. Prog. Rep. **26**, 61 (1992).
64) B. D. DePaola et al., J. Phys. B: At. Mol. Opt. Phys. **28**, 4283 (1995).
65) M. Terasawa et al., Physica C **235-240**, 2805 (1994); *ibid.* **296**, 57 (1998).
66) T. Kambara et al., RIKEN Accel. Prog. Rep. **29**, 199 (1996).
67) H. A. Sakaue et al., J. Phys, B, At. Mol. Opt. Phys. **24**, 3787 (1991).
68) Y. Kanai et al., Nucl. Instrum. Methods Phys. Res. B **98**, 81 (1995).
69) Y. Kanai et al., RIKEN Accel. Prog. Rep. **29**, 208 (1996).
70) Y. Kanai et al., RIKEN Accel. Prog. Rep. **30**, 83 (1997); *ibid.* 168 (1997).
71) Y. Tamagawa et al., RIKEN Accel. Prog. Rep. **30**, 145 (1997).
72) M. Oura et al., Nucl. Instrum. Methods Phys. Res. B **86**, 190 (1994).
73) T. Koizumi et al., J. Phys. B: At. Mol. Opt. Phys. **28**, 609 (1995).
74) Y. Itoh et al., J. Phys. B: At. Mol. Opt. Phys. **28**, 4733 (1995).
75) N. Watanabe et al., J. Phys. B: At. Mol. Opt. Phys. **31**, 4137 (1998).
76) T. M. Kojima et al., J. Phys. B: At. Mol. Opt. Phys. **31**, 1463 (1998).
77) S. Kravis et al., Rev. Sci. Instr. **65**, 1066 (1994).
78) S. Kravis et al., Phys. Scr. T **71**, 121 (1997).
79) T. Mizogawa, M. Sato, Y. Awaya, Nucl. Instrum. Methods Phys. Res. A **366**, 129 (1995).
80) Proc the 8th International Conference on the Physics of Highly Charged Ions, Eds. Y. Awaya and T. Kambara), Phys. Scr. T **73**, (1997)

Ion beam breeding – An efficient synergic link between agricultural science and accelerator physics –

T. Abe[*1] and S. Yoshida[*2]

We have developed a unique technology for mutation induction using energetic heavy-ion beams at the RI Beam Factory. This development was achieved through an efficient synergic link between agricultural science and accelerator physics. At relatively low doses, ion beams induce mutations at a high rate without severely inhibiting growth. The irradiation treatment can be given to various plant materials and quick, lasting between seconds and a few minutes are enough to induce mutation. The ion beam is thus a highly efficient tool for improving crops through mutation breeding. This technology has developed in three stages.

Demonstration as a mutagen in a model plant

In 1993, we started with the seed embryos at a particular stage during fertilization in tobacco (*Nicotiana tabacum* L.) plant, which generates a large number of seeds per ovary, as a model to investigate mutagenesis by heavy-ion beams. When irradiated by heavy-ion beam immediately after fertilization, an embryo should produce a plant composed of mutant cells. The highest percentage of morphologically abnormal plants geminated seeds at 30–48 hrs of treatment stage after pollination was 18%.[1)] Morphological (e.g., variegated strains, albinos, and flower color mutants) and physiological (e.g., heavy metal, salt, and herbicide tolerance) mutants were successfully selected, suggesting the effectiveness of heavy-ion beams as a mutagen.

Fig. 1. A flower bed in front of RIBF building. These flowers were created by ion beam breeding. "Safinia Rose Veind", "Temari Sakura", and "Temari Momo" from front.

Trial use for flower plant breeding

We have collaborated with flower companies and public agricultural experiment stations since 1996 on the potential of practical breeding using heavy-ion beams. As a result, two new cultivars of plants were generated from irradiated materials in 1998. Specifically, *dahlias* "World" with large flowers and a new color was successfully generated, and have been marketed in Hiroshima City since the autumn of 2001. We successfully bred sterile *verbena* "Temari Bright Pink", which generates no seeds with a prolonged lifespan of the flower. It has been marketed since the spring of 2002. The similar successful cases were demonstrated by the new color flowers, *Petunia* "Safinia Rose Veined" (2003), "Safinia Pure White" (2012), *Torenia* "Summer Wave Pink" (2007), *Dianthous* "Olivea pure white" (2008), Cherry blossom "Nishina Zao" (2008) and many new cultivars.

Discovery of LET_{max} in a model plant

The effect of LET on mutation frequencies is important to determine the most effective irradiation condition in mutagenesis. We investigated the effect of LET on mutation induction using the model plant *Arabidopsis thaliana*. The most effective LET (LET_{max}) for mutation induction was 30 keV/μm.[2)] Subsequently, we have reported detailed analyses on the molecular nature of DNA alterations induced by heavy-ion irradiation with LET_{max} using morphological mutants. The most mutations were deletions ranging from several to several tens of bp.[3)] Irradiation at LET_{max} is effective for breeding because of its very high mutation rate. Since most mutations are small deletion, these are sufficient to disrupt a single gene.

Perspective

Recently, beneficial variants have been grown for various plant species, such as salt resistant rice, low polyphenol oxidase lettuce, low allergen peanut, high yield wakame (edible seaweed), and high oil content algae. We have found that high LET ions such as iron are effective for breeding microbes. And we worked

*1 Director of Accelerator Applications Research Group, RIKEN Nishina Center (2010–present)
*2 Chief Scientist of Plant Functions Laboratory (1994–2004)

with SAITC to create “Saitama F yeast”, that is used by 20 breweries in Saitama Pref. to ferment flavored rice wine. One brand of them is collectively known as “Nishina-Homare” (in honor of Nishina), named after Yoshio Nishina. We built a new beam line, called WACAME to increase available ion species with higher LET and longer range. The beams are accelerated by the AVF, RRC, and IRC to 160 MeV/nucleon and sent to E5 biological experiment room. We would like to contribute to advances in these fields, examine the effects of physical factors (e.g., ion species, LET, and dose) on DNA-mutated regions, and elucidate the mechanism of mutagenesis with heavy-ion beams. And the discovery of genes using the combination of mutants and genome sequencing technology may lead to new field in biology, “mutagenomics”.

References

1) T. Abe et al., Gamma Field Symposia **39**, 45 (2000).
2) Y. Kazama et al., Plant Biotech. **25**, 113 (2008).
3) Y. Kazama et al., BMC Plant Bio. **11**, 161 (2011).

Historical overview of the RIKEN-RAL Muon Facility *from catalyzed fusion to materials/life science*

K. Nagamine[*1,*2]

Introduction

Construction of the RIKEN-RAL Muon Facility was proposed by RIKEN in 1989. It had been realized as the first large-scale scientific contribution from Japan to UK. Major research outputs achieved thus far and future prospects are briefly summarized here.

Birth of RIKEN-RAL Muon Facility

At the time of the cold fusion (proposed nuclear fusion phenomena of D_2 confined in special materials such as Pd) in 1989, muon-catalyzed fusion was recognized as a real nuclear fusion process without the need for high temperature. Immediately after the cold-fusion report, RIKEN proposed the construction of a muon facility at the world's strongest pulsed proton accelerator facility, the Rutherford Appleton Laboratory in UK, and the proposal was approved by the Japanese Government in 1990.[1)] A facility composed of a superconducting pion-decay section with 4 muon extraction lines was designed, constructed, and completed in 1994, as shown in Fig. 1, and various experimental programs were started.[2)]

Muon Catalyzed Fusion (μCF)

Among the various muon sciences, μCF, which is nuclear fusion catalyzed by the muon, is the most important as a new possible energy source. Fascinating features of the μCF can be summarized as follows: a) fusion phenomena within a small muonic atom/molecule and its successive reactions, b) no need for high temperatures, c) no radioactive waste production, d) no fuel problem, e) no critical phenomena for free-running, and f) already realized in a laboratory scale and only a few efforts are required for a break-even achievement.[3)]

μCF consists of the following processes: 1) the formation of a small muonic molecule and subsequent intra-molecular fusion reaction, and 2) the mediation of a chain of fusion reactions by a single μ^- (Fig. 2), up to more than 100 cycles. The numbers such as rates are quoted from a standard textbook.

After μ^- injection and stopping in a D-T mixture, either a (dμ) or a (tμ) atom is formed. Because of the difference in the binding energies, the μ^- initially in the (dμ) undergoes a transfer reaction to the (tμ), which reacts with D_2 or DT to form a muonic molecule (dtμ) at a rate of $\lambda_{dt\mu}$, where the formation of a specific state of (dtμd2e$^-$) through a resonant molecular formation (RMF) takes place. The (dtμ) molecule, after a rapid cascade transition, causes a fusion reaction since the distance between d and t is sufficiently close to allow fusion to occur, producing a 14.1-MeV n and a 3.5-MeV α.

After the fusion inside the (dtμ) molecule, most of the μ^- is liberated to participate in the second μCF. Some small fraction is captured by the emitted α^{++} (called the initial sticking probability ω_S^0). Once the $(\alpha\mu)^+$ is formed, because of kinetic energy, the μ^- can be stripped from the $(\alpha\mu)^+$ ion and liberated again

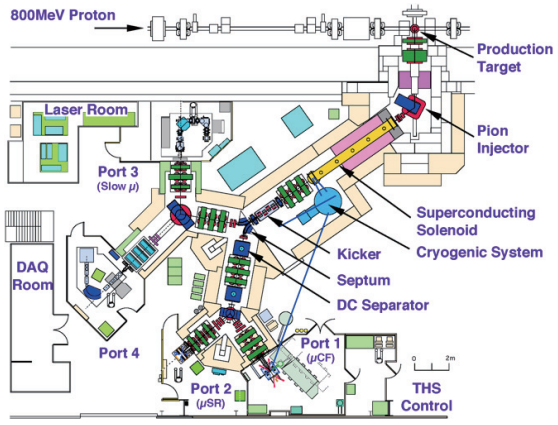

Fig. 1. Layout of the RIKEN-RAL Muon Facility in 2010.

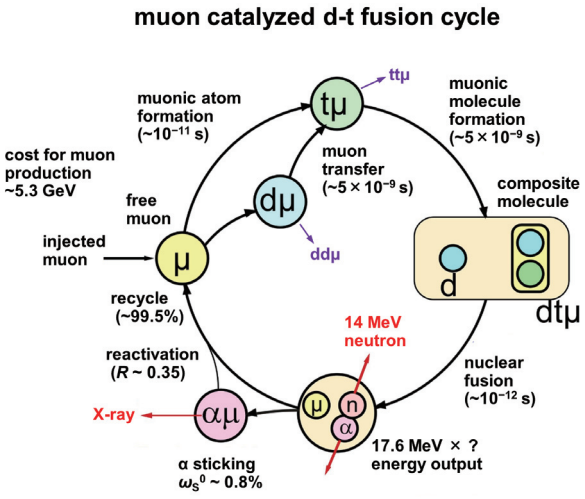

Fig. 2. Conceptual diagram of the D-T μCF cycle.

*1 Chief Scientist of Muon Science Laboratory (1984–2002)
*2 Muon Science Laboratory, IMSS, KEK

(regeneration fraction R). Thus, μ^- of either a non-stuck μ^- or a regenerated one can participate in the second μCF cycle, while the thermalized $(\alpha\mu)^+$ is left out from the μCF cycle with an effective sticking $\omega_S = (1-R)\omega_S^0$. More than 100 fusion processes are known to take place with a single μ^-.

The phenomena of sticking and regeneration were deeply investigated at RIKEN-RAL by measuring both the X-ray from stuck $(\alpha\mu)^+$ representing initial sticking and the yield of fusion neutrons representing resultant phenomena including regeneration. Here, the strong pulsed muon was essentially helpful to remove the background related to T β-decay. The temperature-dependent measurement was conducted for solid/liquid D-T.[5] Although the X-ray yield remains constant, the loss rate decreases at higher temperatures; the regeneration seems to increase in the high-temperature solid (Fig. 3).

At RIKEN-RAL, the muon molecular formation rate in D_2 μCF ($\lambda_{dd\mu}$) was investigated by controlling ortho- and para-states to study the energy matching in RMF. Contrary to theoretical expectation, the opposite tendency was discovered in solid and liquid D_2.[6,7] Although the result is preliminary, a similar opposite tendency was discovered at RIKEN-RAL for the μCF in liquid D-T by using ortho- and para-D_2 with T_2 in a non-equilibrium liquid mixture.[8] The observed ortho-para dependence of the fusion neutron yield seems to be opposite to the theoretical expectation; a greater fusion neutron yield was observed for the ortho case in experiment. All of these observations clearly demonstrate the importance of the molecular correlation effect in RMF in D_2 and D-T μCF. The molecular correlation may change the energy-level diagram in D_2 and D-T in a scale of meV at an energy spacing of the order of eV.

Based on these results, several remarks can be made on possible further increase in the energy-production capability. By using ortho-D_2 rich and high-temperature (30 K) solid D-T μCF towards economical break-even, the following can be achieved: a) ortho-para optimized D_2 can be used to increase $\lambda_{dt\mu}$ to 800 μs^{-1} b) and in order to decrease ω_S (increase R), use of high-temperature solid D-T at 30 K may cause a decrease of ω_S to 0.1% (increase of R to 0.9%). Then, the fusion neutron occurrence is $1200/\mu^-$, which corresponds to an energy production capability of 21 GeV/μ^-, well exceeding the cost of muon production of 5.0 GeV/μ^-.

Energy production in solid D-T (30 K) is not realistic. Another idea is has been proposed: strongly correlated μCF. Let us consider the spatial structure of successive D-T μCF chain, where α^{++} ions are emitted in a space of within $(120\ \mu m)^3$ from a confined spot (within $(0.2\ \mu m)^3$ towards a larger $(\alpha\mu)^+$ ion space (within $(480\ \mu m)^3$). Therefore, if we have strong pulsed muons with stopping region and μCF region overlapping each other, because of collisions between the $(\alpha\mu)^+$ ions and α^{++} ions from nearby μCF reactions, exotic regeneration of $(\alpha\mu)^+$ stripping through high-temperature plasma caused by α^{++} may occur in the high-density μCF of D-T mixtures at moderately high temperature. There, $\omega_S = 0.1\%$ can be expected, leading to the same energy production capability, which is beyond the break-even energy balance.

Condensed Matter Physics

By using the capability of long-time-range measurement of the μ^+SR time spectrum, various condensed matter studies have been proposed and conducted, mainly by external users amounting to more than 200 scientists. Topics covered a) magnetic properties of high-T_C superconductors, b) dynamic character of exotic magnetic materials, c) diffusion of μ^+ in various materials d) reactions of $\mu^+$and muonium in chemical materials, and e) light-element diffusion in battery materials. A distinguished example is presented below.

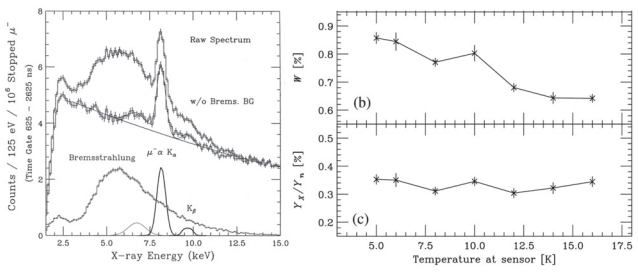

Fig. 3. Observed X-ray spectrum[4] (left) and temperature dependence of muon loss probability (ω_S), and the ratio of X-ray neutron yield for D-T μCF[5] (right).

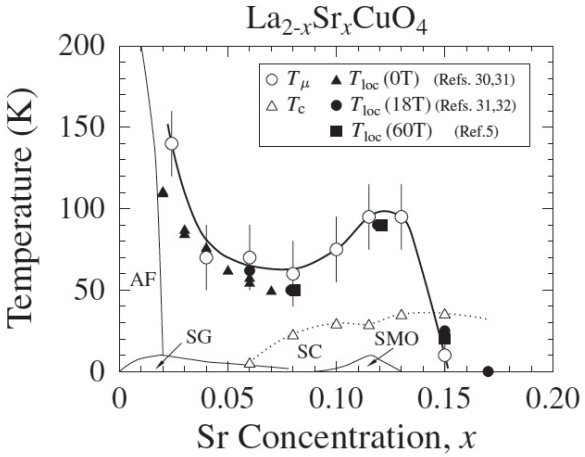

Fig. 4. Observed phase diagram of LSCO by a change of relaxation rate of muon (open circle) compared with electron resistivity (closed symbols).

Careful measurements of zero- and longitudinal-field muon-spin relaxation have been performed in order to investigate the dynamics of the electronic and magnetic states in the normal region of $La_{2-x}Sr_xCuO_4$ over a wide range of hole concentrations from 0.024 to 0.15.[9] It has been found that the dynamic depolarization rate of muon spins in zero field starts to increase monotonically from approximately 0.02 μs^{-1} with decreasing temperature at a high temperature of approximately 100 K. This effect is enhanced near a hole concentration of 1/8 per Cu, suggesting that the dynamics of fluctuating internal fields at the muon site in the normal state of $La_{2-x}Sr_xCuO_4$ changes at a high temperature of approximately 100 K and is correlated with the mobility of holes (Fig. 4). The result should be related to the origin of high T_C superconductivity.

For the μ^+SR studies of magnetism at surfaces and interfaces, the production of ultra-slow μ^+ is in high demand. By coupling pulsed lasers with pulsed muons, a production method of ultra-slow μ^+ by the laser resonant ionization of thermal muonium was developed at KEK. Advancements have been achieved at RIKEN-RAL by placing the system at the experimental port of a surface muon beam line[10] (Fig. 5). Energy was proved to be tunable from 0.1 keV to 20 keV. Space-time structure advancement was confirmed. The project is now under further development at J-PARC.

Life Sciences

By utilizing the unique and strongest pulsed muons, long-time range (more than 10 times the muon lifetime) became easily measured; consequently, the delicate muon spin response in biological environments is easily detectable.

The electron-transfer process plays highly important roles in biological activities. Two representative examples are the photosynthetic electron transfer chain and the respiratory chain in mitochondria. Most elementary molecules have been isolated, and their complicated structures have been determined one by one through crystallographic analysis. The remaining problem is the elucidation of the electron transfer mechanism.

Cytochrome *c* is a small hemoprotein and one of the members of the respiratory chain in mitochondria. It transfers an electron from protein complex III to IV, coupled with redox reactions of Fe located at the center of a porphyrin ring.

At RIKEN-RAL, μSR spectra of cytochrome *c* and myoglobin were measured.[11] μSR data were analyzed by the Risch-Kehr (R-K) theory, which was developed in order to analyze the μSR data of conducting polymers. The principle of the electron transfer in biological macromolecules studies by μSR is as follows (Fig. 6). During the slowing-down process, the injected μ^+ has a chance to pick up electron(s) to form a neutral muonium. Then, the muonium becomes thermalized, stops at an electronegative site, and forms a chemical bond to a molecule. Then, depending on the nature of the molecule, the electron brought in by the μ^+ becomes localized to form a muonic radical state and/or diffuses rapidly along either intra-molecular chains or inter-molecular paths. These behaviors of the electron caused by the μ^+ can sensitively be detected by measuring the spin-relaxation process of the μ^+ by using the μSR method. The discrimination of intra- and inter-molecular electron transfer can be discussed on the basis of the magnetic-field dependence of relaxation rates. Thus, the spin relaxation of the μ^+ due to magnetic interaction with the moving electrons near muons was derived as a characteristic function (R-K function), $G(t) = \exp(\Gamma t)\mathrm{erfc}(\Gamma t)^{1/2}$, for a rapid electron spin flip rate with the relaxation rate Γ, which

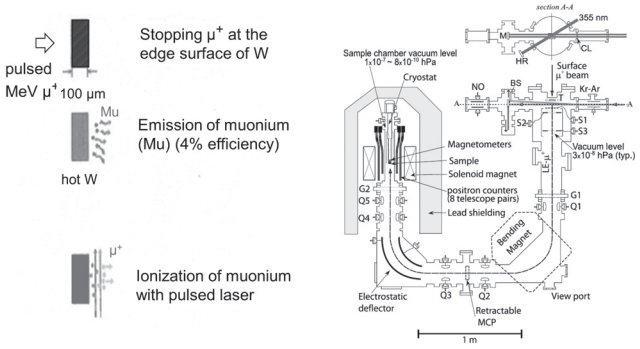

Fig. 5. Conceptual diagram showing the generation of an ultra-slow muon from an MeV muon by the laser ionization of thermal muonium (left). Layout of the dedicated experimental facility installed at port 3[10] (right).

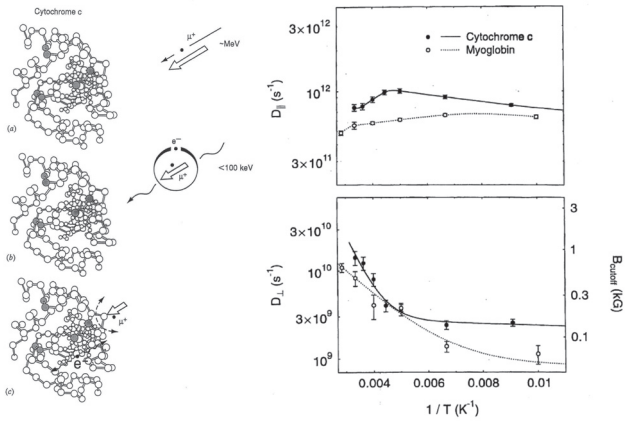

Fig. 6. Conceptual diagram showing the measurement of electron transfer in macromolecules by the μ^+SR method (left), and the measured temperature dependence of longitudinal (right-up) and transverse (right-down) diffusion rate.

has a characteristic dependence on the applied longitudinal field (B). In the case of one-dimensional intramolecular electron motion, Γ is proportional to $1/B$.

This experiment and several succeeding experiments on proteins and DNAs mainly performed at RIKEN-RAL have revealed the following facts: a) electron diffusion along the chain is temperature independent, while inter-chain diffusion has T-dependence reflecting glass transition at 100 K (Fig. 6); b) the hydration effect causes enhanced diffusion; c) the stopping position of the μ^+ in proteins seems to be away from Fe containing porphyrin but close to the part of the main poly-peptide chain.

Conclusion and future of RIKEN-RAL

As an extension of the pulsed muon facility, a facility to produce stronger pulsed muons has been constructed in Japan, the J-PARC MUSE, by KEK and JAEA. However, it is still important to keep RIKEN-RAL, since various experimental instrumentations are more easily equipped at RIKEN-RAL, promoting the increase of proposals and users. The author is grateful for the long-time collaboration of the following persons who contributed to the development of the RIKEN-RAL Muon Facility: Drs. M. Iwasaki, T. Matsuzaki, K. Ishida, I. Watanabe, R. Kadono, Y. Matsuda, S.N. Nakamura, P. Bakule, and F. Pratt.

References

1) D. Swinbanks, Nature **354**, 98 (1991).
2) T. Matsuzaki et al., Nucl. Instrum. Methods Phys. Res. A **465**, 365 (2001).
3) K. Nagamine, in *Introductory Muon Science* (Cambridge Univ. Press, Cambridge, 2003), p. 69
4) S. N. Nakamura et al., Phys. Lett. B **473**, 226 (2000).
5) N. Kawamura et al., Phys. Rev. Lett. **90**, 043401 (2003).
6) A. Toyoda et al., Phys. Rev. Lett. **90**, 243401 (2003).
7) H. Imao et al., Phys. Lett. B **632**, 192 (2006).
8) K. Ishida et al., Proc. of μCF-07 (Dubna, 2007) p. 99.
9) I. Watanabe et al., J. Phys. Soc. Jpn. **77**, 124716 (2008).
10) P. Bakule et al., Nucl. Instrum. Methods Phys. Res. B **266**, 335 (2008).
11) K. Nagamine et al., Physica B **289–290**, 631 (2000).

The RIKEN-RAL Muon Facility at the ISIS Neutron and Muon Source

P. King,[*1,*2] M. Iwasaki,[*3] K. Ishida,[*3] and I. Watanabe[*3]

The RIKEN-RAL Muon Facility is one of RIKEN's significant overseas outposts and a major collaboration between RIKEN and the UK. The Facility is part of the ISIS Neutron and Muon Source, located at the Rutherford Appleton Laboratory (RAL) in the UK. ISIS is the UK's national neutron and muon source, but it has many international partnership arrangements, and one of the largest and longest standing is the collaboration with RIKEN. The Facility performs a very wide variety of pure and applied studies using muons.

The collaboration began in the late 1980's under the leadership of Prof Kanetada Nagamine. The first agreement between RIKEN and RAL to build the Facility and collaborate in muon science was signed in 1990 for 10 years. First muons were produced in 1994 and the Facility was officially inaugurated by the then RIKEN President Prof Arima in 1995. The Facility has been performing muon science studies since then, with further agreements between RIKEN and RAL in 2000 (10 years) and 2010 (7.5 years).

In 2015 the Facility celebrated 20 years of muon production and 25 years of formal agreements between RIKEN and RAL. Over its lifetime, the Facility has been recognized in a number of ways. This includes regular presentation at meetings of the UK-Japan Joint Committee on Co-operation in Science and Technology chaired by the UK Chief Scientist, where it is used as a good example of UK-Japan science collaboration. In 2003 Prof Nagamine received the Toray Science and Engineering Prize from the Toray Science Foundation of Japan, and in 2002 Dr Paul Williams (CLRC Chief Executive) received the Minister's Commendation for Meritorious Service in the Field of International Exchange from the Japanese Minister of Education, Culture, Sports, Science and Technology.

Muons for use in the Facility are produced by the decay of pions generated by the interaction of the ISIS 800-MeV proton beam with a 1-cm thick carbon target. The Facility is able to accept "surface" muons, produced from pion decays within the carbon production target. These are positive muons with high flux and with momentum of around 30 MeV/c which are then directly transported to the experiment areas. The Facility also incorporates a decay channel, within which pions from the carbon production target are allowed to decay in-flight. This enables higher momentum (up to around 110 MeV/c) positive muons to be produced, as well as allowing negative muons to be generated. This means that the facility is very flexible, enabling both positive and negative muons with variable momenta to be generated for muon science experiments.[1)]

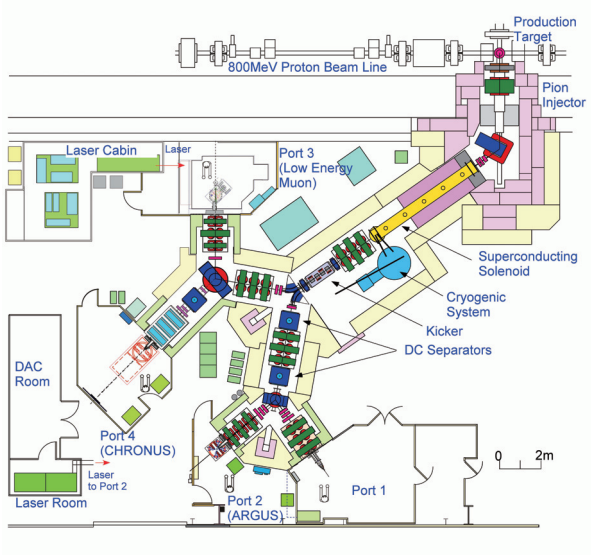

Fig. 1. The RIKEN-RAL Muon Facility at the ISIS Neutron and Muon Source, UK. Muons or pions are generated at the production target, and muons are transported to one of four experiment areas. The superconducting solenoid allows decay of pions in-flight, enabling variable momenta positive or negative muons to be produced.

The ISIS primary proton beam is pulsed at 50 Hz, meaning that the RIKEN-RAL Muon Facility is a pulsed muon source. The science that can be done at the Facility is, in many ways, complementary to that which can be done at continuous muon sources at PSI in Switzerland or TRIUMF in Canada. The RIKEN-RAL Muon Facility is the only pulsed source of decay-channel muons in Europe, and so is a unique resource for muon studies.

The science of the facility is very varied, and broadly falls into two categories: fundamental physics studies using muons, and condensed matter and molecular science employing muons as probe particles.

A key science driver for the facility when it was first established was investigation of the process of muon catalyzed fusion (μCF). μCF is a cold fusion process occurring between deuterium and tritium nuclei. A dtμ molecule is formed within a liquid or solid deuterium-tritium mixture, which enables the d and t nuclei to approach closely enough to fuse, releas-

*1 Director of RIKEN Facility Office at RAL, RIKEN Nishina Centre (2012–present)
*2 STFC ISIS Neutron and Muon Source
*3 RIKEN Nishina Centre

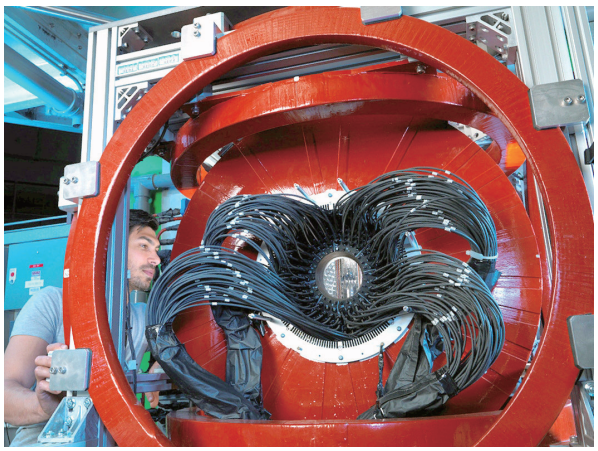

Fig. 2. Adam Berlie, joint RIKEN-RAL / ISIS appointment, with the CHRONUS spectrometer.

ing energy and characteristic reaction products. The RIKEN-RAL Muon Facility provided an ideal source of negative muons to enable this process to be studied in detail, including revealing new effects in its temperature dependence.[2] Other fundamental physics studies at the facility have included precise measurement of the muon lifetime[3] and muonic atom spectroscopy for studies of nuclei.[4]

A key application of muons is the study of atomic- and molecular-level properties of materials in condensed matter physics and chemistry. Muons produced at RIKEN-RAL are spin polarized, an effect occurring naturally from the pion decay. Positive muons maintain their polarization when implanted into materials, and observation of the time-dependence of the polarization of the muon ensemble within a sample provides information on local magnetic fields. In turn this informs on the magnetic properties of the material as well as enabling processes such as diffusion to be studied. The polarization of the implanted muons is observed by detection of the positrons emitted when the muons decay after their average lifetime of 2.2 μs. These positrons are preferentially emitted in the direction of the muon spin at time of decay, enabling the behavior of the muons with a material to be followed. The Port 2 area of the Facility has been home to the ARGUS muons spectrometer since the early days of the facility, and this was supplemented with the CHRONUS spectrometer on Port 4 which began a μSR programme in 2014.

Studies of a wide variety of magnetic and superconducting materials have been a feature of the RIKEN-RAL Muon Facility. This includes, for example, studies of critical behavior around magnetic transitions,[5] model organic systems,[6] non-Fermi liquid spin dynamics,[7] the interplay between magnetism and superconductivity,[8] spin liquid systems[9] and other frustrated systems.[10] Diffusion and charge dynamics also feature, for example in organic[11] and inorganic (battery)[12] materials.

The Facility has seen development of key techniques for condensed matter and molecular studies using muons. These include laser-stimulation of samples, allowing excited state spectroscopy,[13] and studies of materials under pressure which are enabled by the higher momentum beams available from the decay channel.

The traditional muon technique for condensed matter studies allows the bulk of the material to be probed, as muons penetrate a large fraction of a mm into a sample. In order to allow studies at much smaller depths closer to the surface, and interface studies, work has been ongoing to develop a source of low energy muons on Port 3 of the RIKEN-RAL Muon Facility. The method being used is particularly suitable to a pulsed muon facility, and involves laser ionization of muonium atoms (positive muons which have picked up an electron to form a light hydrogen atom with the muon as nucleus) to produce keV muons as opposed to the MeV muons normally used. The method has been extensively developed at RIKEN-RAL, and the characteristics of the low energy muon beam that is produced have been detailed.[14] This method is now in operation at the J-PARC muon facility following its development at RIKEN-RAL. It offers the potential for fundamental muon studies, such as muon $g-2$ measurement, as well as condensed matter investigations.

Recently, new applications of muons have been developed at the facility. This includes studies of single-event upsets in microelectronic circuits[15] and elemental analysis of materials with negative muons.[16] Novel methods are also being developed for fundamental studies of the proton radius[17] in order to resolve discrepancies between different measurements on this subject. Overall, the Facility has produced more than 400 publications since its beginning in 1994, across a very broad range of pure and applied subject areas using muons.

A particular strength of the facility has been the development of collaborations and the attraction of researchers from around the world. Over 80 separate Japanese groups have used the facility over its lifetime, and around 40 groups worldwide have collaborated on science at the facility. Particularly of note is the development of links between RIKEN and Asian universities, resulting in MoUs with five Indonesian universities (first signed in 2008 and renewed in 2011 and 2015), and an MoU with Universiti Sains Malaysia, first signed in 2012 and renewed in 2015. These Asian links have resulted in multiple workshops and meetings, a variety of publications, in, in particular, the involvement of around 10 masters and PhD students from Indonesia and Malaysia whose theses have been based on work performed at RIKEN-RAL.

References

1) T. Matsuzaki et al., Nucl. Instrum. Methods Phys. Res. A **465**, 365 (2001).
2) N. Kawamura et al., Phys. Rev. Lett. **90(4)**, 043401 (2003).
3) S.N. Nakamura et al., Nucl. Instrum. Methods Phys. Res. A **472**, 429 (2001); D. Tomono et al., J. Phys. G **29**, 2013 (2003).
4) P. Strasser et al., Nucl. Instrum. Methods Phys. Res. A **460**, 451 (2001); P. Strasser et al., J. Phys. G **29**, 2047 (2003).
5) F.L. Pratt et al., Phys. Rev. Lett. **99**, 017202 (2007).
6) F.L. Pratt et al., Phys. Rev. Lett **96**, 247302 (2006).
7) V.V. Krishnamurthy et al., Phys. Rev. Lett. **88**, 046402 (2002).
8) A.J. Drew et al., Nature Materials **8**, 310 (2009); A.J. Drew et al., Phys. Rev. Lett. **101**, 0970101 (2008).
9) F.L. Pratt et al., Nature **47**, 612 (2011).
10) T. Koyama et al., Phys. Rev. Lett. **101**, 126404 (2008).
11) F.L. Pratt et al., Phys. Rev. Lett. **79**, 2855 (1997).
12) J. Sugiyama et al., Phys. Rev. Lett. **103**, 147601 (2009).
13) P. Bakule et al., J. Phys. Chem. Lett. **3**, 2755 (2012).
14) P. Bakule et al., Nucl. Instrum. Methods Phys. Res. B **266**, 335 (2008); Y Matsuda et al., J. Phys. G **29**, 2039 (2003).
15) A. Bosser et al., Proc. RADECS, Radiation and Its Effects on Components and Systems, Sep 2016, Bremen, Germany.
16) A.D. Hillier et al., Microchemical Journal **125**, 203 (2016).
17) Y. Ma et al., Int. J. Mod. Phys. Conf. Ser. **40**, 1660046 (2016); D. Guffanti et al., J. Phys. Conf. Ser. **689**, 012018 (2016).

Pursuit of Spin Physics Program at RHIC

M. Ishihara[*1,*2]

Throughout 1990s, the Radiation Laboratory directed by M. Ishihara was engaged in two major programs: firstly the RIB Physics Program using RIPS at RARF, RIKEN and secondly the Spin Physics Program using the Relativistic Heavy-ion Collider (RHIC) at Brookhaven National Laboratory (BNL), USA. This article describes the latter engagement by emphasizing the aspects of historical evolution of the program.

Our engagement in the international collaboration program on spin physics was started in 1995, aiming at clarification of the anomalous phenomenon of proton spin crisis,[1)] which casted a fundamental question about the origin of nucleon spin. As a matter of fact, our intensive commitment served to implement this program as a flagship objective of the RHIC project, being alternate with the Heavy Ion Physics Program as originally founded. The RIKEN BNL Research Center (RBRC) was created in 1997 to support our activities on this program. The spin program has been successful in revealing the important roles of gluons and parton orbital angular momenta, and further extension of the program has motivated the proposal of the US next-generation project of Electron Ion Collider (EIC).

The Spin Physics Program is one of the two principal programs at RHIC, BNL, aiming at the determination of the polarized parton distribution function of nucleons. Our initiative to commit to this program followed a recommendation of the headquarters of RIKEN, which strongly encouraged us to set up any cutting-edge program on nuclear physics to be conducted in international collaboration. The RHIC Spin Physics Program turned to reality when the Radiation Laboratory gave its commitment to this program by bringing a sizable grant from the Science and Technology Agency (STA) to build a full set of Siberian snakes and spin rotators. Indeed, these devices were essential to facilitate the acceleration and manipulation of spin-polarized protons through the rings of RHIC. A grant was also obtained to build a single unit of muon arm for the PHENIX detector assembly. Moreover, RBRC was created in the BNL campus to support our research activities at the site of the RHIC facility.

Since we were quite new to the field of relativistic QCD physics, our major efforts in the initial stage were devoted to call for relevant international collaborators. The Japanese spin physics team was soon formed, consisting of groups from Kyoto University and Tokyo Institute of Technology as well as the RIKEN Radiation Laboratory. We also managed to establish a strong tie with the powerful spin physics group around BNL led by G. Bunce and T. Roser. Thus, these two groups from US and Japan were destined to take the leading role in promoting the RHIC Spin Physics Program. To help such practice G. Bunce was invited to serve as the Deputy Leader of the Experimental Group of RBRC while I served as the Leader. As was always the case for the RHIC project, this program was conducted under a framework of international collaboration. Between the two major collaborations formed for the RHIC project, we have chosen the PHENIX Collaboration, rather than the STAR Collaboration, since we anticipated close cooperation with a large number of Japanese researchers who had been already registered in the former Collaboration. The Radiation Laboratory group in the early stage consisted of N. Saito, Y. Goto, N. Hayashi, K. Kurita, M. Okamura, S. Yokkaichi, T. Ichihara, Y. Watanabe, A. Taketani, and J. Murata besides myself. The group was further reinforced by acquiring several fellows at RBRC, including M. G. Perdekamp, A. Deshpande, and A. Bazilevsky. They soon manifested themselves to become leading figures in the Spin Physics Program.

Throughout the 1990s, our research activities were mainly devoted to the construction of the PHENIX detector assembly and of accelerator devices required for polarized protons. Specifically, the RIKEN group was committed to the construction of one unit of muon arm, where the magnet assembly was manufactured by Mitsubishi Electric Co. under the direction of T. Ichihara while A. Taketani and K. Kurita took major roles in completing detector arrays for muon ID and J. Murata for muon tracker. The development of a laser-driven ion source was an important R&D issue to realize an intense polarized proton beam, and M. Okamura made a central contribution to its accomplishment. Another important agenda was to develop the polarimeter, which is crucial to determine the degree of spin polarization of the accelerated protons. The RIKEN group led by N. Saito and K. Kurita was successful in establishing the relevant methodology.[2)] Meanwhile, Y. Goto worked on the EM calorimeter in the central arm of the PHENIX assembly to make it useful for the Spin Physics Program. M. G. Perdekamp and A. Bazilevsky also joined in this activity. In fact the π^0 detection as described later was facilitated with this device.

At Wako a computer facility called the Computing Center in Japan for RHIC physics (CC-J) was built[3)] under the leadership of T. Ichihara. Y. Watanabe and S. Yokkaichi also made great contributions to the development and operation of the CC-J. With a computation speed equivalent to 160 high-performance CPUs and a disk capacity of about 135 TB supplemented by

*1 Chief Scientist of Radiation Laboratory (1984–2000)
*2 Group Leader of Experiment Division, RBRC (1998–2001)

tape storage capacity of 1400 TB, the CC-J immediately gained the status of the primary center for data analysis for the Spin Physics Program. It also served as a principal Asian local center for the PHENIX Collaboration by allowing Japanese and Asian colleagues to analyze the data from the Heavy-Ion Program as well. The CC-J has been in sound operation since its commissioning in 2001, being reinforced by a series of successive upgrades. It has thus far contributed to the publication of 42 papers and awarding of 42 Ph.D. degrees.

The Spin Physics Program at RHIC was originally inspired by the so-called spin puzzle that the quark contribution alone is not sufficient to account for the nucleon spin of 1/2. Hence, the extent of gluon contribution was inquired to pin down the anomalous phenomenon. In this respect, spin-polarized proton beams at RHIC were indispensable since collisions with protons well reveal various gluon-induced processes, which in turn may exhibit the polarized gluon distribution of the nucleon. Many simulation works were then performed to identify the observables most sensitive to the spin-polarized gluons. Thus, the measurement of the double-helicity asymmetry of π^0 at $\sqrt{s} = 200$ GeV was chosen to be the first experiment to be performed.

RHIC was commissioned in the year 2000, while the leadership of this program has been taken over since 2001 by H. En'yo, the newly assigned Chief Scientist of the Radiation Laboratory. The experiment on the double-helicity asymmetry of π^0 was realized in 2003[4] and several succeeding years.[5] In later years the measurement of double-helicity asymmetry was extended to other cases, such as at different energies of $\sqrt{s} = 62.4$[6] and 510 GeV[7] and with different probes like the mid-rapidity jet.[8] These data were combined to be subjected to global QCD analysis, revealing the behavior of the polarized gluon distribution over the range of Bjorken x, $0.05 < x < 0.2$. The gluon spin polarization integrated over the observed x region is reduced to 0.15 ± 0.06[9] or $0.10 + 0.06/-0.07$ in the unit of Planck constant,[10] depending on the method of global analysis. These values are roughly comparable with the known quark contribution of 20–30% of the total spin of 1/2. Consequently the combined contributions of gluons and quarks so far observed is still insufficient to account for the total spin.

Thus, missing polarized spin should be sought for over the gluons in the domain of very small x and/or in another degree of freedom, i.e., the orbital angular momenta carried by partons. In fact, several experiments performed at RHIC revealed a non-vanishing analyzing power,[11] indicating the significant roles of parton orbital angular momenta. The study of transverse components of parton spins is called for. As a matter of fact, the EIC project for the next-generation parton physics aims at the investigation of generalized (3-dimensional) parton distributions as well as of the gluon behaviors in the small x region. A. Deshpande at the Experimental Group of RBRC has been a central force to work out this proposal.

Meanwhile, the Theory Group of RBRC has developed in its own way. Since T. D. Lee took the Directorship of RBRC, he extended the center objective to serve as a world center for nursing brilliant young scientists in theoretical physics related to QCD. To enhance this activity, a novel system of joint appointment between any of the US universities and RBRC was introduced. This initiative, strongly pursued by the Director himself, resulted in great success, producing many leading nuclear theorists worldwide, such as D. E. Kharzeev, who now directs the Theory Group of RBRC.

References

1) J. Ashman et al. (EMC Collaboration), Phys. Lett. B **206**, 364 (1988).
2) J. Tojo et al., Phys. Rev. Lett. **89**, 052302 (2002).
3) T. Ichihara et al., RIKEN Accel. Prog. Rep. **35**, 236 (2002).
4) A. Adare et al. (PHENIX Collaboration), Phys. Rev. Lett. **93**, 202002 (2004).
5) e.g., A. Adare et al. (PHENIX Collaboration), Phys. Rev. Lett. **103**, 012003 (2009).
6) A. Adare et al. (PHENIX Collaboration), Phys. Rev. D **79**, 012003 (2009).
7) A. Adare et al. (PHENIX Collaboration), Phys. Rev. D **93**, 011501 (2016).
8) L. Adamczyk et al. (STAR Collaboration), Phys. Rev. Lett. **115**, 092002 (2015).
9) W. Vogelsang et al., Phys. Rev. Lett. **113**, 012001 (2014).
10) E. R. Nocera et al. (NNPDF Collaboration), Nucl. Phys. B **887**, 276 (2014).
11) e.g., J. Adams et al. (STAR Collaboration), Phys. Rev. Lett. **92**, 171801 (2004).

RBRC: A great success

Nicholas P. Samios *1

This year, 2017, marks the twentieth anniversary of the establishment of the RIKEN BNL Research Center (RBRC). It's great success is attributable to the amiable, constructive cooperation of many enlightened individuals involved in its establishment and subsequent sustainability. Equally relevant and important have been the management structures, review procedures established by RIKEN, BNL and RBRC. These involved the Management Steering Committee, Scientific Review Committee and Theory, Lattice and Experimental Advisory Committees. These were augmented by the Nishina Center and RIKEN reviews established for the consideration of the formal renewal of the RBRC, usually every five years, the fourth such successful review having taken place this year 2017. This has produced of the order of 100 outstanding fellow and post-doc graduates that now occupy leading positions at major national and international institutions.

The mission of RBRC is dedicated to the study of the strong interactions, including spin-physics, lattice QCD and RHIC (Relativistic Heavy Ion Collider). This is facilitated through the establishment of both the theoretical and experimental component, consisting of fellow and post-doctoral positions. Activities have centered around: 1) RHIC which is finishing its seventeenth year of operation having accelerated ions ranging from protons and deuterons to gold and uranium, equal and unequal species, energies from five GeV/A to 100 GeV/A and both transverse and longitudinal proton polarizations. This machine has recently attained forty times its design luminosity. 2) The Phenix Detector for which RIKEN supplied the second muon arm and has had an extraordinary enriched publication record in both QCD and Spin. 3) A series of lattice gauge computers QCDSP (1 TFLOPS), QCDOC (10 TFLOPS), QCDCQ (700 TFLOPS), the latter being a prototype for the IBM Blue Gene. These were developed by a large collaboration including Columbia U, Edinborough, RBRC and IBM and for which RIKEN made the major monetary contributions.

What has emerged has been a profusion greater than 1000 in refereed journals and conferences, a plethora of work shops greater than 100 and numerous awards for computer performance. Among the most notable findings have been 1) the discovery of the strongly interacting quark gluon plasma (sQGP) or a perfect liquid a new form of matter whose nature is being explored and deciphered, 2) dynamics of gluon saturation and the color glass condensate, 3) chiral symmetry and its implications and restoration,4) the gluon contribution to the spin of the proton where it now appears to be larger than that of the quarks, 5) lattice calculation of the CP violation in Kaon decays. RBRC has been a major contributor to all these methods.

It has been an outstanding twenty years and one is looking forward to an equally productive future.

Fig. 1. A photo taken at the signing of the memorandum of understanding in 1997 for the establishment of RBRC with (front, seated from left) Satoshi Ozaki, Head of BNL Relativistic Heavy Ion Collider Project; the author, BNL Director; T.D. Lee, RBRC Director; (back, standing from left) Henry Grahn, Associate Director for Administration; Peter Bond, Chair of BNL Physics Department; Thomas Kirk, BNL Associate Director for High-Energy & Nuclear Physics.

*1 Director of RIKEN BNL Research Center (2003–2012)

Scientific pedigree of Chief Scientists of Radiation Laboratory

Hideto En'yo[*1, *2]

Radiation Laboratory and growth of accelerator-based science

When Yoshio Nishina passed away in 1951, his laboratory was split into four laboratories. One of them, headed by Fumio Yamazaki, was soon after renamed as the Radiation Laboratory. Since then, Tastuzo Hamada, Masayasu Ishihara and Hideto En'yo have served as the Chief Scientists of the Radiation Laboratory. The first volume of APR was issued 50 years ago when Yamazaki was in charge.

Figure 1 shows the scientific pedigree of Chief Scientists who are presently engaged in Nishina Center which was inaugurated in year 2006 when the Superconducting Ring Cyclotron was commissioned. One can see the growth of accelerator-based science in RIKEN over 50 years since 1966. Apparently, the name of Radiation Laboratory has persisted for the longest time.

Radiation Laboratory and RIKEN-BNL collaboration

When the author assumed this honorable post in year 2001, the major mission of Radiation Laboratory was and still to understand how the spin of nucleon is formed with ingredients (quarks and gluons) through the RIKEN-BNL collaboration which modified Relativistic Heavy Ion Collider (RHIC) to include a capability to accelerate and collide polarized protons. M. Ishihara summarized the achievements of this project in the article "Pursuit of Spin Physics Program at RHIC" in this volume.[2)]

Besides spin physics, RHIC's original mission was to create quark gluon plasma (QGP), the state of the Universe just after the Big Bang. Y. Akiba, the associate chief scientist of Radiation Laboratory, was rewarded by the Nishina Memorial Prize in 2011 for his leading role in the measurement of thermal photons, which showed that the initial temperature reached in the central Au+Au collision at 200 GeV is approximately 350 MeV, far above the expected transition temperature $T_c \sim 170$ MeV, from hadronic phase to quark-gluon plasma.[3)] This was an important discovery that assured the creation of QGP at RHIC.

Acceleration of polarized proton at RHIC was an innovative challenge. Protons make precession in magnetic field. Once the ratio of the precession frequency to the ring-revolution frequency becomes integer, the proton spin resonates and the polarization is lost. "Siberian Snake Magnet" is a technology to overcome such resonances by flipping the spin of proton in every turn. The principle methodology is established but the reality was more difficult. The biggest problem was the depolarization that occurred in the AGS ring. M. Okamura, who once contributed to the design of the snake magnets in the RHIC main ring, solved the problem of the AGS depolarization by using a variable-pitch helical snake magnet.[4)] Okamura, J. Takano, and others in Radiation Laboratory fabricated such a novel magnet in a year by taking advantage of a special mobility of

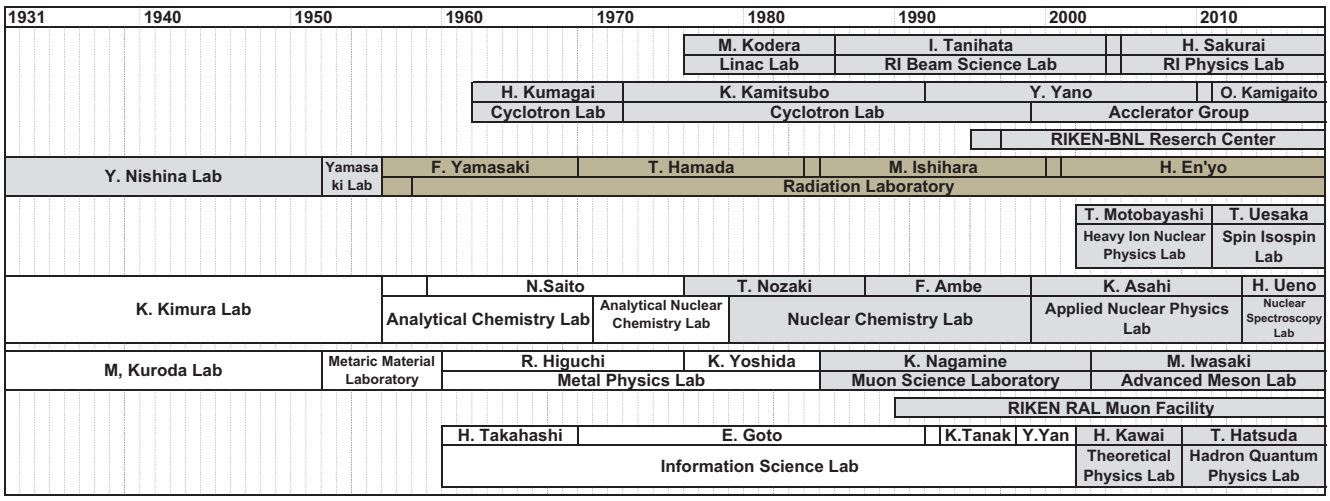

Fig. 1. History of Chief Scientists in Nishina Center. Shaded laboratories are for accelerator-based science.[1)]

*1 Chief Scientist of Radiation Laboratory (2001–present)
*2 Director of RIKEN Nishina Center (2009–present)

RIKEN.

Okamura also developed a laser ion source named Direct Plasma Injection Scheme. In this, ions are extracted, not by high voltage, but by the initial expansion of plasma diffusion. The plasma stays with neutral charge for a long time; one can get rid of the space charge effect. His ion source recorded the highest peak current many times.[5] His laser ion source technology was adopted first by the NASA Space Radiation Laboratory, and then for the RHIC injector. With those achievements, Okamura was head-hunted by BNL and is now a tenure physicist in the Collider-Accelerator Department.

Radiation Laboratory and chiral symmetry restoration

When the hadronic matter gets hotter or denser, chiral symmetry must be restored as theoretically predicted by Nambu,[6] i.e., hadrons' mass must change when they are in different vacuum. Although QGP is created at RHIC, there are no measurements so far which show a signature of restored symmetry, owing to the difficulty in performing experiments at the very high multiplicity environment of hot QGP. Complementary measurements can be done in dense but cold nuclear matter. Radiation Laboratory performed KEK E325 experiment at 12 GeV-PS and CERN NA60 experiment at SPS, and had challenged to measure mass of vector mesons when they fly in dense nuclear matter. The former used proton nuclear interaction and measured electron pairs, while the latter used indium-indium collision and measured muon pairs.

The E325 experiment produces theses by S. Yokkaichi, K. Ozawa, M. Naruki, R. Muto, F. Sakuma, and T. Tabaru. They succeeded in detecting the mass modification of ρ, ω and ϕ mesons,[7] and concluded that the measured modifications are consistent with the theoretical model by Hatsuda and Lee.[8] On the other hand, NA60 concluded that the measured spectrum modification of ρ meson is explained not by mass shift but by mass broadening.[9] The states of nuclear matter for both experiments are so different that the physics picture can be different, but it can be admitted that the two are not very consistent. To obtain the final conclusion, the E16 experiment is under preparation at J-PARC. Although the E325 experiment was only the experiment that could measure electron pair decays of ϕ mesons with high statistics. E16 is aggressively seeking to go beyond.[10]

Radiation Laboratory and neutron

From 1999 to 2005, the Radiation Laboratory hosted the Image Information Research Unit lead by H. Shimizu. This unit developed a Superconducting Tunnel Junction detector for Tera Hertz light, optical devices for neutron beams, etc. Many of the group's works have been taken over by the RIKEN Center for Advance Photonics. Especially, T. Otake and her Neutron Beam Technology Team constructed RANS, RIKEN Accelerator-driven compact Neutron Source, and developed technology "to make invisible visible." The ultimate goal is to make available a transportable non-destructive neutron inspection system for outdoor use in applications, like a bridge, tunnel, or building. This is a very active offspring from Radiation Laboratory for societal needs.[11]

Radiation Laboratory for future

RHIC was once the largest heavy-ion collider in the world. In 2010, however, the Large Hadron Collider (LHC) at CERN started lead-lead collision with energy that was 14 times higher than that at RHIC. The PHENIX detector, which the Radiation Laboratory was working on, stopped operation in 2016 to metamorphose to the upgraded sPHENIX detector, to accomplish the latest measurements, that cannot be performed by the present PHENIX.

In 2015, the Nuclear Science Advisory Committee (NSAC) was requested by the US Department of Energy (DOE) to update their long range plan; the recommendation was to construct an electron-ion collider.[12] In the past, all the NSAC recommendations were achieved in the US contradictory to recommendations by the Japan Science Council. The physics of proton structure, which was initiated by RIKEN at RHIC, will be the foundation of the future of US nuclear physics.

Selection for a new Chief Scientist in the field of hadron physics is happening currently. He/She will inaugurate a new era in the history of Radiation Laboratory that has produced streams of new scientific flow.

References

1) RIKEN's 88-year history (RIKEN 88 Nenshi), 2005.
2) M. Ishihara, RIKEN Accel. Prog. Rep. **50**, S-46 (2017).
3) A. Adare et al. (PHENIX Collaboration), Phys. Rev. Lett. **104** 132301 (2010).
4) H. Huang et al., Phys. Rev. Lett. **99**, 154801 (2007).
5) M. Okamura, Rev. Sci. Instrum. **79**, 02B314 (2008).
6) Y. Nambu, G. Jona-Lasinio, Phys. Rev. **124**, 246 (1961).
7) R. Muto et al., Phys. Rev. Lett. **98**, 042501 (2007); M. Naruki et al., Phys. Rev. Lett. **96** 092301 (2006).
8) Tetsuo Hatsuda, Su Houng Lee, Phys. Rev. C **46**, R34(R) (1992).
9) R. Arnaldi et al., Phys. Rev. Lett. **96**, 162302 (2006).
10) https://j-parc.jp/researcher/Hadron/en/pac_0606/pdf/p16-Yokkaichi_2.pdf .
11) http://www.riken.jp/en/research/labs/rap/adv_photon/neutr_beam/ .
12) https://science.energy.gov/~/media/np/nsac/pdf/2015LRP/2015_LRPNS_091815.pdf .

Advanced Meson Science Laboratory – Hadron part –

M. Iwasaki,[*1,*2,*3] H. Asano,[*2] T. Hashimoto,[*4,*2] M. Iio,[*5,*2] K. Itahashi,[*2] Y. Ma,[*2] Y. Matsuda,[*6,*2] T. Nishi,[*2] H. Ohnishi,[*7,*2] H. Outa,[*2] S. Okada,[*2] F. Sakuma,[*2] Y. Sada,[*8,*2] M. Sato,[*5,*2] and K. Tsukada[*7,*2]

The Advanced Meson Science Laboratory was launched in 2002 based on a proposal to pursue hadron physics research using the meson as a probe into nuclei to study the strong interaction. At the same time, we are requested to commit to the operation of the RIKEN-RAL branch and promotion of muon science research. The branch is in the Rutherford Appleton Laboratory (RAL) and operated under the UK-Japan scientific agreement on muon science. Thus, our Laboratory is composed of two subgroups to conduct hadron physics research using mesons and to conduct muon science studies covering fundamental particle and nuclear physics to condensed matters physics. Because the research activity in muon science is separately summarized by P. King *et al.* in this volume, let us describe hadron physics research in this article.

By embedding mesons into nuclei and studying the property change of those particles in nuclear media, one can study the physics at densities beyond standard nuclear density, e.g., in neutron star matter, as well as the origin of matter (hadron) mass, in which the standard scenario is that the hadron masses are generated by the spontaneous chiral symmetry breaking of the vacuum. For these studies, we have been conducting experiments at the world's leading accelerator facilities such as Japan Proton Accelerator Research Complex (J-PARC) for K-mesons having s-quarks, and RI Beam Factory (RIBF) for π-mesons consisting of the lightest u- and d-quarks together with their anti-quarks.

Deeply bound pionic atoms are quite interesting systems, in which the π is captured by the nucleus owing to Coulomb interaction and its wave function overlaps with that of the nucleus at the surface. Before our breakthrough experiment at GSI,[1,2] it was believed that the pionic atom cannot be realized if there exist substantial wave-function overlaps between the pion and nucleus. This misunderstanding was strengthened by the fact that the pionic-atom formation by the pion atomic capture at rest is limited up to medium-heavy nuclei, since no observation was realized in heavy nuclei previously.

In our GSI experiment, direct pion formation inside nuclei by feeding it into the atomic state was realized for the first time by introducing the (d, ^{3}He) reaction to lead target at the recoilless condition. In this neutron pickup reaction, d + "n" $\rightarrow \pi^-$ + ^{3}He, the pion can be produced almost at rest for a specific deuteron momentum (momentum transfer to the pion $q_\pi \sim 0$); therefore, it is likely to be captured, and the efficient atomic-state formation is realized.

At RIBF, we extended our research to conduct high-precision isotope-dependence studies on several Sn isotopes to acquire more quantitative information on the atomic shifts systematically. To achieve high precision, we introduced dispersion-matching optics to the BigRIPS spectrometer for the first time by taking advantage of the high-intensity beam available at RIBF. We succeed in demonstrating the outstanding performance of the dispersion-matching optics at the BigRIPS spectrometer. In fact, in the on-line monitor level, the formation of ground state of the pionic atom, together with its several exited states, has already been identified clearly.

To our surprise, a theoretically unexpected excited-state formation was also identified clearly, with the formation yield exhibiting an angular dependence. This angular dependence helps us to identify the quantum number of those excited states without ambiguity. Our analysis shows that the deduced isospin dependence of the energy shifts of the pionic-atom ground states is consistent with the standard scenario of the hadron mass-generation mechanism. We are working on publishing this result.

In the case of the π-meson, the available density range to be studied is limited to the nuclear surface density, which is well below the normal nuclear-matter density. This is because of the repulsive nature of the πN strong interaction. Pion wave functions are pushed away from nuclei, and form a hybrid state in between the atomic and nuclear bound state. Thus, it is quite interesting to know if it is possible to form a pure nuclear meson bound state deep inside nuclei.

In this context, a very interesting meson is the $\eta'(958)$-meson. It is known that its mass is very difficult to explain in a simple quark picture, and the mass deviation of this specific meson is explained by the $U_A(1)$-anomaly. We have just started a new series of experiments to study a bound system of an η' in a nucleus. The first experiment was conducted in GSI by measuring excitation spectra of carbon nuclei in ^{12}C(p, d) reactions near the η'-emission threshold. We achieved a very good resolution of $\sim$2.5 MeV (σ) and a good statistical sensitivity at a level better than 1%. The measured excitation spectra agree well with theoretical predictions but do not show distinct structures

*1 Chief Scientist of Advanced Meson Science Laboratory (2002–present)
*2 RIKEN Nishina Center
*3 Tokyo Institute of Technology
*4 JAEA
*5 KEK
*6 University of Tokyo
*7 Tohoku University
*8 Osaka University

due to formation of the η'-nucleus bound systems. The result is interpreted in terms of an interaction between an η' and a nucleus, setting stringent constraints in the optical potential for the first time.[3] Based on the results, a second experiment is being prepared in FAIR at GSI.

Another very interesting meson is the anti-kaon ($\overline{K}$) in the second-lightest K-meson group having the *strange* (s)-quark as a constituent quark, namely K^- and $\overline{K}^0$. The $\overline{K}N$ interaction was rather poorly known, in contrast to the πN interaction. The interaction seems to be strongly attractive based on the scattering data; therefore, it can form a nuclear bound state, which requires the ground state of the kaonic hydrogen atom to have a strong upward shift due to the pole below the $\overline{K}\,N$ threshold. On the other hand, previous kaonic hydrogen atom data seem to be attractive only very weakly, which is entirely inconsistent with scattering data. We played a very important role again to solve this puzzling situation.

At KEK, we conducted an x-ray measurement of the kaonic hydrogen atom to solve the $\overline{K}N$ interaction puzzle. We utilized a gaseous hydrogen target for the first time to avoid the Stark effect occurring in high-density targets, which reduces the x-ray yield substantially. To compensate for the small number of available kaons at rest in the gas, we placed multi-channel x-ray detectors directly exposed to the hydrogen gas located inside the target cell. In the experiment, we also identified two charged pions as decay products of the kaonic hydrogen atom. Using these two charged pions, we selected the fiducial volume for the target and identified background-free events by choosing the final states, in which no γ-ray can be generated because of the severe x-ray background source. Our work on kaonic hydrogen atom spectroscopy resulted in very clear spectra for the first time, and the strongly attractive interaction between a kaon and nucleon in the $I = 0$ channel is confirmed,[4,5] together with the scattering data.

This confirmation of strong attraction of the $\overline{K}N$ interaction in the $I = 0$ channel opens up another very curious question. The attraction is so strong that it is more natural to form a bound state between a kaon and proton. In fact, there is a *well-known* resonance called $\Lambda(1405)$, the mass of which is located just below the mass threshold of the kaon and proton, $M(K^-p)$; the resonance is assumed to be an exited state of a member of the Λ hyperon, i.e., it is an excited uds-quark baryon system. Thus, it is very natural to ask whether $\Lambda(1405)$ can be interpreted as a bound state of a kaon and proton due to the strong interaction, i.e., $\Lambda(1405) =$ "K^-p". If this is true, then the kaon can form a variety of nuclear bound states together with various nuclear systems. The strong $\overline{K}N$ attractive interaction might help form a high-density nuclear object beyond the standard nuclear density spontaneously. It might also help the study of the in-medium property change of mesons in nuclei.

Therefore, a variety of experimental studies have been conducted by a number of experimental groups to identify the simplest kaonic nuclear bound state, "K^-pp." The detection of the kaonic nuclear state formation is difficult from the kaon absorption at rest because the kaon mainly reacts with one of the nucleons in the mesonic channel and produces a hyperon (Λ or Y) as $K^-\,N \to \pi\,\Lambda$, without forming a kaonic nuclear state. It can also be absorbed by two nucleons simultaneously as $K^-\,N\,N \to \Lambda\,N$, and this process produces huge backgrounds. The direct kaon production channel is also attempted via the $p\,p \to K^+ +$ "K^-pp" reaction. However, this channel has large ambiguity due to the presence of $N^*(1410)$ resonance, which can decay strongly to $K^+\Lambda$. Obviously, no K^- (nor $\overline{K}$) is generated in this reaction channel, and the channel is energetically easier to be produced compared to the $K^+\,K^-$-pair production. One can easily be misled by the reaction chain of $p\,p \to N^*(1410) + p \to (K^+\Lambda) + p$ to be a "K^-pp" formation signal, if one believes the $\Lambda\,p$ in the final state (wrong pair) is the decay product of "K^-pp." There are also other experimental studies to search for the kaonic bound state, but those are limited by either null results or insufficient statistics. Therefore, there is no convincing and conclusive experimental evidence of the existence of the kaonic nuclear bound state.

We employed an entirely different approach at J-PARC K1.8BR beam-line in our experiment E15. We bombarded a K^- beam on a ^{3}He target to knockout a neutron from the target nucleus at 1 GeV/c ($\sqrt{s_{KN}} \sim$ 1.8 GeV/c^2), i.e., $K^- +^3\mathrm{He} \to K^-\,p_s\,p_s + n$ (p_s denotes spectator proton). The cross section of this reaction is rather high, because of the presence of the Y^* resonance near 1.8 GeV/c^2, which decays strongly to $\overline{K}N$. There are several key advantages in this reaction channel to search for the kaonic bound state. First, the recoil kaon momentum (or momentum transfer), q_K, is as small as $\sim$200 MeV/c ($\sim p_F$) in this reaction; therefore, one can expect very efficient nuclear formation as $K^-\,p_s\,p_s \to$ "K^-pp." Another advantage is that the presence and the commitment of K^- in this channel is secured from the beginning. Still another advantage is that the two- (or multi-) nucleon absorption reaction can be expected to have a small cross section. Finally, we can cover the target region with a cylindrical detector system (CDS) to identify the final state of "K^-pp" with sensitivity to the decay process. We also placed large-volume neutron counter arrays in the forward direction 15 m away from the target system to identify neutrons in the production channel with a high missing-mass resolution of about 10 MeV/c^2.

The pilot run of J-PARC E15 (E15^{1st}) showed quite remarkable results. The semi-inclusive forward neutron spectrum shows a large yield below the mass threshold of $M(K^-pp)$ as a long tail from the quasi-elastic kaon scattering, implying the existence of strong

$\overline{K}N$ attractive interaction.[6] An even more impressive spectrum was obtained in the Λp invariant mass spectrum of the $\Lambda p n$ final state, in which we observed an event concentration near the $M(K^- pp)$ threshold, and the centroid of the event concentration is well within the bound region.[7] Thus, we conducted a new beam time for further study, especially focusing on the $\Lambda p n$ final state (E15^{2nd}).

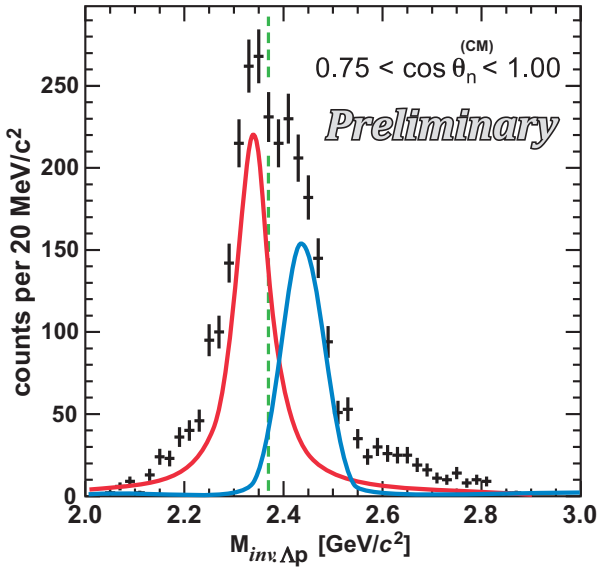

Fig. 1. A preliminary Λp invariant mass spectrum of the $\Lambda p n$ final state of the forward neutron emission ($\cos\theta_n^{\rm CM} > 0.75$) events, in which a strong event concentration is found. The spectrum is fitted by a Breit-Wigner formula for the bound region (red) and a Gaussian formula for the unbound region (blue), together with a smooth background. The dashed line indicates the mass threshold of $M(K^- pp)$.

We are still in an analysis phase, but the preliminary result is truly astonishing. As shown in Fig. 1, the event concentration near the $M(K^- pp)$ threshold is not a single peak structure, as we simply assumed in our previous publication,[7] but it has clear internal structures separated by the threshold energy indicated by the dashed line. First, the only reasonable explanation of the peak-structure formation below the $M(K^- pp)$ threshold is the kaonic nuclear bound state formation of "$K^- pp$." Events below the threshold can be generated when virtual kaons below the rest mass are produced in a quasi-elastic (QE) reaction. The peak structure can only be formed when there exists a resonance pole below the threshold, while a smooth tail is formed below the threshold if a pole does not exist. The Λp pair in the final state, together with the forward neutron, ensures that the backscattered K^- interacts with the other two spectator protons. Thus, K^-, $\overline{K}^0$, or $\Lambda(1405)$ escaping channels are naturally suppressed substantially, in contrast to the semi-inclusive missing-mass spectra of ^{3}He$(K^-, n)X$.[6] The peak centroid is located around ∼40 MeV, which is much deeper than that of the normal nuclear system about 10 MeV.

The existence of the structure above the threshold provides further confirmation that the structure below the threshold is actually the nuclear bound state of "$K^- pp$," in which the constituent particles do not lose their identity in the system. Generally, the peaks in a mass spectrum are isolated in the case of baryonic resonance. In contrast, nuclear-state formations are always associated with the *so-called* quasi-free (QF) processes in the unbound energy region, which indicate that the constituent particles can be dissolved. In this case, the structure above the threshold can be interpreted as the initial kaon backscattered at an energy above the kaon mass in the QE channel, followed by internal conversion (IC) with two spectator protons resulting in Λp in the final state. Thus, this successive reaction can be treated as a QF process of the ^{3}He$(K^-, \Lambda p)n$ reaction channel.

To finalize the present study, we are analyzing the angular distribution of the particles in the final state, to study the form factor, spin, and parity of the observed state, and to prepare an independent analysis of the data so as to reach a confirmative result on the kaonic nuclear bound state "$K^- pp$." The peak in the bound region would suggest that the ∼ on-shell K^- (or $\overline{K}$) can form a nuclear bound state (Boson & Fermion hybrid system), where u- and $\overline{u}$-quarks coexist, at-least within a time scale allowed by the width of the bound state. It is quite important and interesting to know how the hadron identity is conserved even in nuclear media.

In the future, we wish to study π, η', and K-meson bound states more precisely and to extend our study to nuclear bound states of other mesons, such as η and ϕ, for a global understanding of the hadron mass generation mechanism and the quark-confinement mechanism. We believe that the mesonic nuclear state study is a door to access the mystery of the origin of matter mass in the universe and a laboratory-based showcase to understand the physics of very-high-density matter, such as the core of a neutron star.

References

1) T. Yamazaki et al., Z. Phys. A **355**, 219 (1996).
2) H. Gilg et al., Phys. Rev. C **62**, 025201 (2000); K. Itahashi et al., *ibid.* **62**, 025202 (2000).
3) Y. K. Tanaka, K. Itahashi, H. Fujioka et al., Phys. Rev. Lett. **117**, 202501 (2016).
4) M. Iwasaki, R. S. Hayano, T. M. Ito et al., Phys. Rev. Lett. **78**, 3067 (1997).
5) T. M. Ito, R. S. Hayano, S. N. Nakamura et al., Phys. Rev. C **58**, 2366 (1998).
6) T. Hashimoto, S. Ajimura, G. Beer et al., Prog. Theor. Exp. Phys. **6**, 061D01 (2015).
7) Y. Sada, S. Ajimura, M. Bazzi et al., Prog. Theor. Exp. Phys. **5**, 051D01 (2016).

Developments of linear accelerators at RI Beam Factory

O. Kamigaito*1 for the Accelerator Group

The injection of very heavy ions such as uranium in RIBF[1] was initially performed with RILAC.[2] However, the beam current of $^{238}U^{35+}$, which was directly injected into the RRC[3] without charge stripping, was too low to meet the demand of RIBF users because of the limited performance of RILAC. In addition, a strong demand for more RILAC beam time was made by those engaged in research projects on superheavy elements (SHE) started at the RILAC facility in 2002.[4] It was obvious that such experiments conflict with the BigRIPS experiments at RIBF, as shown in Fig. 1(a). Therefore, a new injector was required to resolve these problems. By 2006, a basic design study of the new injector involving beam dynamics calculations had been conducted.[5] Fortunately, the project was approved by the supplemental budget in late FY2008, and we quickly constructed the new injector by the end of FY2009.

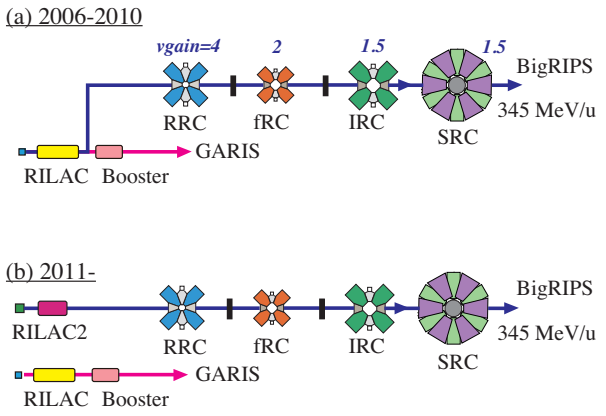

Fig. 1. Accelerator chain of RI Beam Factory. The upper panel (a) shows the uranium acceleration scheme in RIBF and metallic ion beam acceleration for the GARIS experiments until 2011. Both schemes used RILAC. The lower panel (b) shows the acceleration scheme since 2011. Now the uranium beam is injected through RILAC2, while RILAC is almost entirely dedicated to SHE experiments.

The new injector, named "RILAC2," is schematically shown in Fig. 2. It mainly consists of the 28-GHz superconducting ECR ion source,[6] a low-energy beam-transport (LEBT) line[7] including a prebuncher, an RFQ linac, and three DTL cavities. An important point in designing RILAC2 was that the required total voltage is as low as 4.6 MV, which is less than one third of that of RILAC; it is sufficient to accelerate ions with a mass-to-charge ratio of 6.8, such as $^{136}Xe^{20+}$ and $^{238}U^{35+}$, up to an energy of 670 keV/nucleon. Therefore, it was possible to reduce the total length of the linac structure to less than 8 m by choosing an rf frequency of 36.5 MHz, instead of the RILAC frequency of 18.25 MHz, whereas the prebuncher is operated at 18.25 MHz in order to match the beam bunch interval to the rf system of the RRC. We have placed the new injector in the AVF cyclotron vault, as shown in Fig. 2, which made the length of the beam transport line to RRC 36 m, less than half that of the RILAC injector. The main parameters of RILAC2 are listed in Table 1.

Table 1. Main parameters of RFQ and DTL cavities.

Resonator	RFQ	DTL1	DTL2	DTL3
Frequency (MHz)	36.5	←	←	←
Duty(%)	100	←	←	←
m/q	6.8	←	←	←
E_{in} (keV/u)	3.28	100	220	450
E_{out}(keV/u)	100	220	450	670
Length (m)	2.3	0.8	1.1	1.3
Gap number	93*	10	10	8
Gap voltage (kV)	42	110	210	260
Aperture (mm)	8**	17.5	17.5	17.5
ϕ_s(deg.)	-29.6†	-25	-25	-25
Power (kW)	18	7	13	20

* Cell number ** Mean aperture (r_0)
† Final synchronous phase

The RFQ linac used in RILAC2, which is based on a four-rod structure, is the one originally developed for use in an ion implantation device in the 1990s.[8] We modified it to yield a resonant frequency of 36.5 MHz by adding tuner blocks between the posts that support the vanes based on fine electromagnetic simulations.[9] We also diverted one of the cavities in the Charge State Multiplier[10] developed for RIBF to the last cavity of the DTLs in RILAC2.

In order to reduce the construction cost and space, we adopted a direct coupling scheme for the rf coupling between the DTL cavities and amplifiers. Since the resonators could not be designed independently from the tetrode amplifier, the frequency shift of the cavities as well as the strength of the coupling were carefully calculated based on computer simulations with the help of a lumped circuit model.[11] This calculation exhibited excellent agreement with the measured results.

The first beam test of RILAC2 was successfully conducted in December 2010, and the device was fully commissioned in October 2011 using a uranium beam. Since then, RILAC2 has provided intense uranium and xenon beams for nuclear physics experiments at RIBF very stably.[12] The completion of RILAC2 has also

*1 Director of Accelerator Group, RIKEN Nishina Center (2008–present)

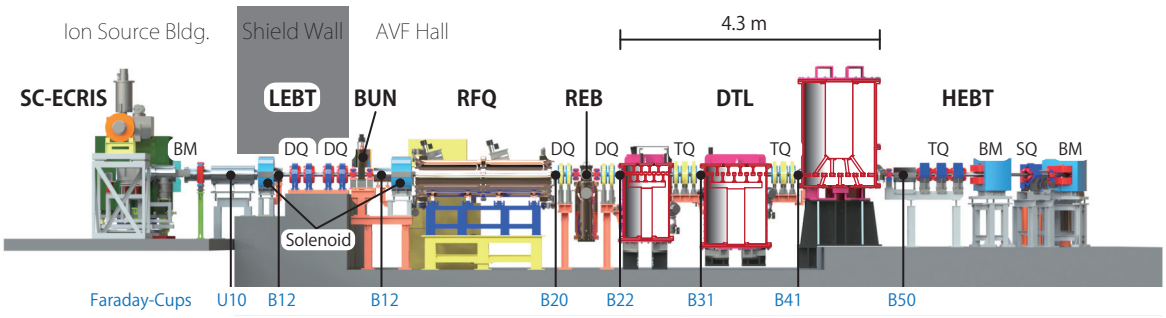

Fig. 2. Side view of the RILAC2 injector. The beam is provided with a 28-GHz ECR ion source and is accelerated through the RFQ and three DTLs. A pre-buncher and a rebuncher are implemented in the linac.

allowed us independent operation of the SHE experiments at the RILAC facility, as shown in Fig. 1 (b). We think that RILAC2 contributed to the third event of the element [113] in 2012 [13] to a certain degree.

When the name of the element [113] was proposed as "nihonium" in 2016, a supplemental budget was approved for further investigation of heavier new elements, such as [119] and [120], through a major upgrade of RILAC. The upgrade program includes the construction of a 28-GHz superconducting ECR ion source and two cryomodules that substitute the last four cavities of the RILAC booster. We expect to have very intense metallic beams of vanadium and chromium of more than 5 pμA at 6.5 MeV/nucleon. This upgrade program also aims at mass production of ^{211}At, a candidate medical isotope for radionuclide therapy in the future. For this purpose, an intense beam of ^{4}He at 29 MeV is necessary.

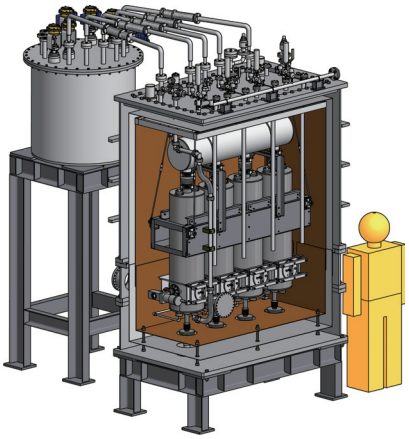

Fig. 3. Conceptual drawing of the cryomodule. Each cryomodule contains four quarter-wavelength resonators (QWRs).

Figure 3 shows a conceptual drawing of a cryomodule, which contains four quarter-wavelength resonators (QWRs). Each QWR operates at a resonant frequency of 73.0 MHz at a gap voltage of approximately 0.8 MV with a power consumption of 4.0 W. The corresponding acceleration gradient is 4.5 MV/m. The inner radius and height of the QWR are 1,090 mm and 300 mm, respectively.

We have investigated the same structure of a superconducting resonator in a proposal of an RIBF upgrade program.[14] A similar structure was also studied, constructed, and tested in the framework of the ImPACT program, [a] and we achieved a very high voltage in a vertical test.[15,16]

The construction of the new devices is in progress. We expect that the upgraded RILAC facility will start operation in FY2019. It will contribute to the intensity upgrade of RIBF in the future.

References

1) Y. Yano, Nucl. Instrum. Methods Phys. Res. B **261**, 1007 (2007).
2) M. Odera et al., Nucl. Instrum. Methods Phys. Res. B **227**, 187 (1984).
3) H. Kamitsubo, Proc. CYCLOTRONS1986 (1986), p. 17.
4) K. Morita et al., J. Phys. Soc. Jpn **73**, 1738 (2004).
5) O. Kamigaito et al., Proc. 3rd PASJ and 31st LAM (2006) p. 502.
6) T. Nakagawa et al., Proc. ECRIS2008, MOCO-B01 (2008).
7) Y. Sato et al., Proc. IPAC10, THPEB023 (2010).
8) H. Fujisawa, Nucl. Instrum. Methods Phys. Res. A **345**, 23 (1994).
9) K. Yamada et al., Proc. LINAC10, TUP070 (2010).
10) O. Kamigaito et al., Rev. Sci. Instrum. Meth **76**, 013306 (2005).
11) K. Suda et al., Nucl. Instrum. Methods Phys. Res. A **722**, 55 (2013).
12) N. Sakamoto et al., Proc. LINAC12, MO3A02 (2012).
13) K. Morita et al., J. Phys. Soc. Jpn. **81**, 103201 (2012).
14) N. Sakamoto et al., Proc. SRF2015, WEBA06 (2015).
15) K. Ozeki et al., Proc. LINAC16, TUPLR061 (2016).
16) K. Yamada et al., Proc. LINAC16, THPLR040 (2016).

[a] Impulsing PAradigm Change through disruptive Technologies Program of Council for Science, Technology and Innovation (Cabinet Office, Government of Japan)

Development of ECR ion sources at RIKEN

T. Nakagawa*1

The electron cyclotron resonance ion source (ECRIS) is one of the best choices for the RI Beam Factory (RIBF) project[1] for the production of radioisotope beams using projectile-like fragmentation and for super-heavy element search experiments.[2] Since the first beam was produced with the RIKEN 10 GHz ECRIS,[3] we have continuously improved the performance of the existing ECRIS and constructed new ECRISs to produce intense beams of highly charged heavy ions to meet the requirements of the RIKEN accelerator facility. For these purposes, we have constructed three types of high-performance ECRISs (18 GHz ECRIS, Liquid-He-free SC-ECRIS, and 28 GHz SC-ECRIS) in the last three decades. In particular, we have attempted to produce intense beams of heavy ions, such as uranium (U) ions for the RIKEN RIBF project 1) and super-heavy element search experiment 2) since the early 2000s. Figure 1 shows the time evolution of the beam intensity of highly charged heavy ions produced at RIKEN. In the last three decades, the beam intensity has been dramatically increased, as shown in the figure. For example, the beam intensity of Ar^{8+} has been increased from ∼100 μA to 2 mA. For heavier ions, the intensity of the U^{35+} ion beam increased from a few μA to ∼180 μA in the last 10 years.

The 18 GHz ECRIS,[4] which consists of two room-temperature solenoid coils and a hexapole permanent magnet to confine the plasma for producing mainly medium-charge-state heavy ions such as Ar^{8+} and Xe^{20+} and works as an external ion source of the RIKEN linear accelerator (RILAC), was constructed in 1995 and produces intense beams of various heavy ions (∼2 mA of Ar^{8+}, ∼200 μA of Xe^{20+}). To increase the variety of ion species, we adopted the various methods[5,6] to produce intense beams of metallic ions. In the early 2000s, intense beams of highly charged Zn ions were required to perform a new super-heavy element ($Z = 113$) search experiment. To meet the requirement, we adopted the insertion method and successfully produced an intense beam of highly charged Zn ions (∼2 pμA) for a long term (longer than one month) without a break.

Liquid-He-free SC-ECRIS[7] has a unique feature in that it uses a small refrigerator to achieve the superconductivity of the magnet without using liquid He. It produces a high mirror magnetic field (maximum magnetic field of ∼3 T) with low electric power consumption. It is suitable for producing higher charge states of heavy ions. For this reason, it is used as an external ion source of the AVF cyclotron, which only accepts higher-charge-state heavy ions ($A/q < 4$) for acceleration.

A fully superconducting ECRIS with 28 GHz microwaves[8] was constructed in 2007. The RIKEN SC-ECRIS can be operated at flexible axial field distributions from the so-called classical B_{min} to flat B_{min}.[9] In 2013, U^{35+} ion beams of ∼180 μA were produced at an injected RF power of several kW for a short-term test experiment using the sputtering method.[10] It produced a U^{35+} beam of ∼120 μA for the RIKEN RIBF experiment with a high-temperature oven.[11] Figure 2 shows a schematic of the ion source. Figure 3 shows the charge-state distribution of the highly charged U ion beam when tuning the ion source to produce U^{35+} ions.

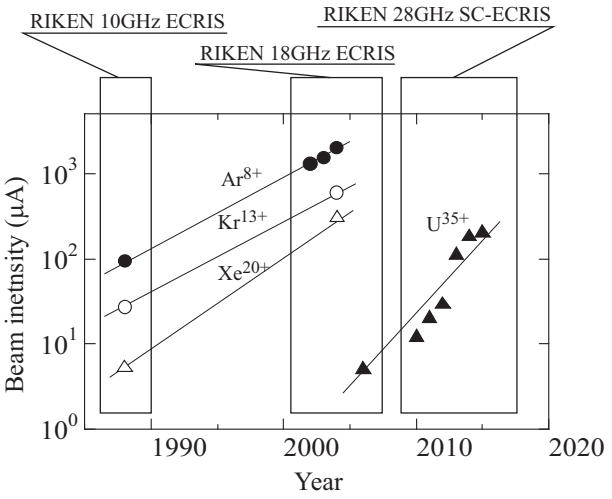

Fig. 1. Time evolution of the beam intensity of highly charged heavy ions produced at RIKEN ECRISs.

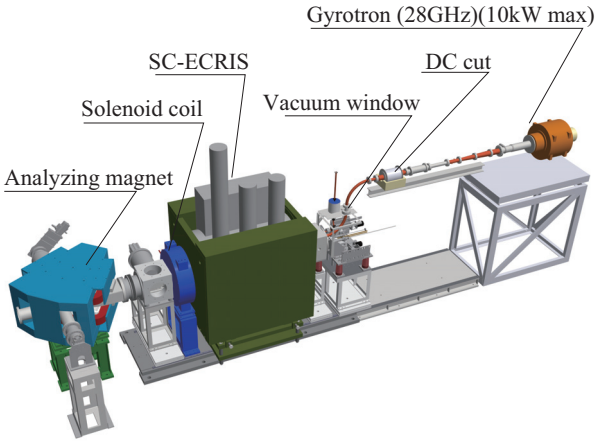

Fig. 2. Schematic drawing of the RIKEN 28 GHz SC-ECRIS.

*1 RIKEN Nishina Center

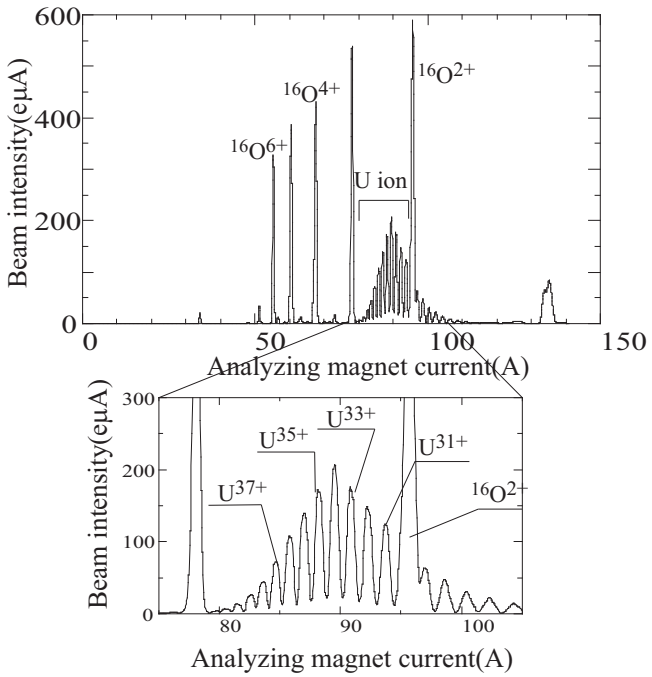

Fig. 3. Charge-state distribution of the U ion beam. The ion source was tuned to produce the U^{35+} ion beam.

For the new super-heavy element ($Z = 119$) search experiment, an intense beam of highly charged V ion beams was required. We therefore attempted to produce a highly charged V ion beam using the RIKEN 28 GHz SC-ECRIS and produced a $V^{12+,\ 13+}$ ion beam of a few hundred μA for a short-term test experiment; its intensity is almost ten times higher than that of the Zn ion beam.

References

1) Y. Yano, Nucl. Instrum. Methods Phys. Res. B **261**, 1009 (2007).
2) K. Morita et al., Nucl. Phys. A **944**, 30 (2015).
3) K. Hatanaka et al., RIKEN Accel. Prog. Rep. **22**, 219 (1988).
4) T. Nakagawa et al., Nucl. Instrum. Methods Phys. Res. B **226**, 392 (2004).
5) T. Nakagawa et al., Nucl. Instrum. Methods Phys. Res. A **396**, 9 (1997).
6) K. Ozeki et al., Rev. Sci. Instrum. **86**, 016114 (2015).
7) T. Kurita et al., Nucl. Instrum. Methods Phys. Res. B **192**, 429 (2002).
8) T. Nakagawa et al., Rev. Sci. Instrum. **81**, 02A320 (2010).
9) G. Alton, D. N. Smithe, Rev. Sci. Instrum. **65**, 775 (1994).
10) Y. Higurashi et al., Rev. Sci. Instrum. **85**, 02A953 (2014).
11) J. Ohnishi et al., Rev. Sci. Instrum. **87**, 02A709(2016).

Realization of recirculating He-gas stripper

H. Imao*1 for the Accelerator Group

The intensity upgrade of uranium beams up to our goal intensity of 1 pμA has been one of the main concerns at the RIKEN Radioactive Isotope Beam Factory (RIBF).[1] A new injector, RILAC2,[2,3] which includes a 28-GHz superconducting electron cyclotron resonance ion source (ECRIS),[4] has been successfully developed and became fully operational in fiscal year 2011. The possible output intensity of uranium beams at the RIBF at that time was mainly limited by the lifetime problem of the carbon foil strippers.[5] To further accelerate the uranium beams generated by this powerful injector, one of the highest priorities was to explore a new charge stripper for the high-power uranium beams. It has been a long-standing open problem despite extensive worldwide research efforts to find next-generation strippers involving the other huge heavy-ion projects such as the FAIR at GSI[6] and the FRIB at MSU.[7]

Our group has pursued a stripping method using gas to replace the carbon foil. The first attempt with a nitrogen (or argon)-gas stripper for uranium beams at 11 MeV/nucleon produced an equilibrium charge state up to 56+.[8] Unfortunately, the value is too low for our use because the minimum acceptable charge state is 69+ for the original fRC.

The use of a low-Z (Z; atomic number) gas (e.g., He or H_2 gas) is a possible pathway to improve the mismatch. The electron capture cross sections for low-Z gases are particularly suppressed owing to poor kinematic matching when the ion velocity significantly exceeds the velocity of the target electrons.[9] Therefore, charge strippers using a low-Z gas simultaneously provide durability, a uniform thickness, and a high charge state equilibrium.

For the first demonstration of the effect of a low-Z gas on the charge state equilibrium, the cross sections for the electron loss and electron capture for uranium in He were successfully measured with thin targets that can strip or attach only one electron at three energies of 11, 14 and 15 MeV/nucleon.[9] More directly, the charge state distribution and the energy spread after the stripper both for He and H_2 gases were measured at an injection energy of 11 MeV/nucleon by preparing the thick targets (8 m in length) required for their charge equilibrium.[10] The results of these experiments clearly indicated that the equilibrium charge states (e.g., 65+ at 11 MeV/nucleon for He) for low-Z-gas strippers are significantly higher than those for higher-Z-gas strippers (e.g., 56+ in N_2[8]). We also found that the fraction of 64+ in the charge state distribution is transiently enhanced owing to the atomic shell effect of the uranium ion. The energy spread of the beam passing through the He-gas target was suppressed to approximately one-half of that with the fixed carbon foil stripper because of the uniform thickness of the gas. We decided to adopt the He-gas stripper as a replacement for the carbon foil stripper and correspondingly modified the fRC for the acceleration of charge state 64+ (the previous acceptable charge state of the fRC is more than 69+).[11]

The major technical challenges were the windowless accumulation (more than 10-mm$^{\phi}$ beam apertures) of very thick He gas (about 1 mg/cm^2) and high-flow recirculation (300 m^3(STP)/day) of pure He gas with low gas consumption rates (less than 0.5%). It was realized by using an unprecedented scheme with a powerful multistage mechanical booster pump array. The system is designed to reduce the pressure by nine orders of magnitude from the target pressure of ~10 kPa to the beamline vacuum of 10^{-5} Pa within a length of approximately 2 m. About 300 m^3/day of He gas is recirculated by the multistage MBP array consisting of four foreline MBPs and three back MBPs with a total nominal pumping speed of 11,900 m^3/h (Fig. 1).

The system was successfully installed at the A02 site in the RRC room (Fig. 2). Since April 2012, a series of beam irradiation tests was also performed. We confirmed that there is no evidence of target impurities, and no serious problems occurred when it was used with U^{35+} beams injected at 11 MeV/nucleon with intensities up to 0.3 pμA.

After commissioning, the system was actually operated in user runs started from November 2012 with injected beams of more than 1 pμA (Fig. 2). Electron-stripped U^{64+} beams were stably delivered to subsequent accelerators without any serious deterioration in the system for six weeks.

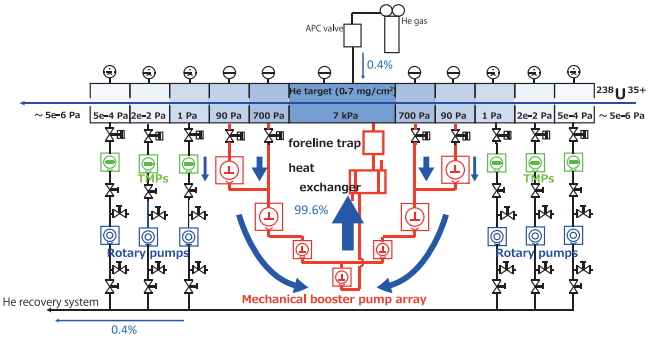

Fig. 1. Schematic of the He recirculating system. The multistage MBP array consists of seven MBPs.

*1 RIKEN Nishina Center

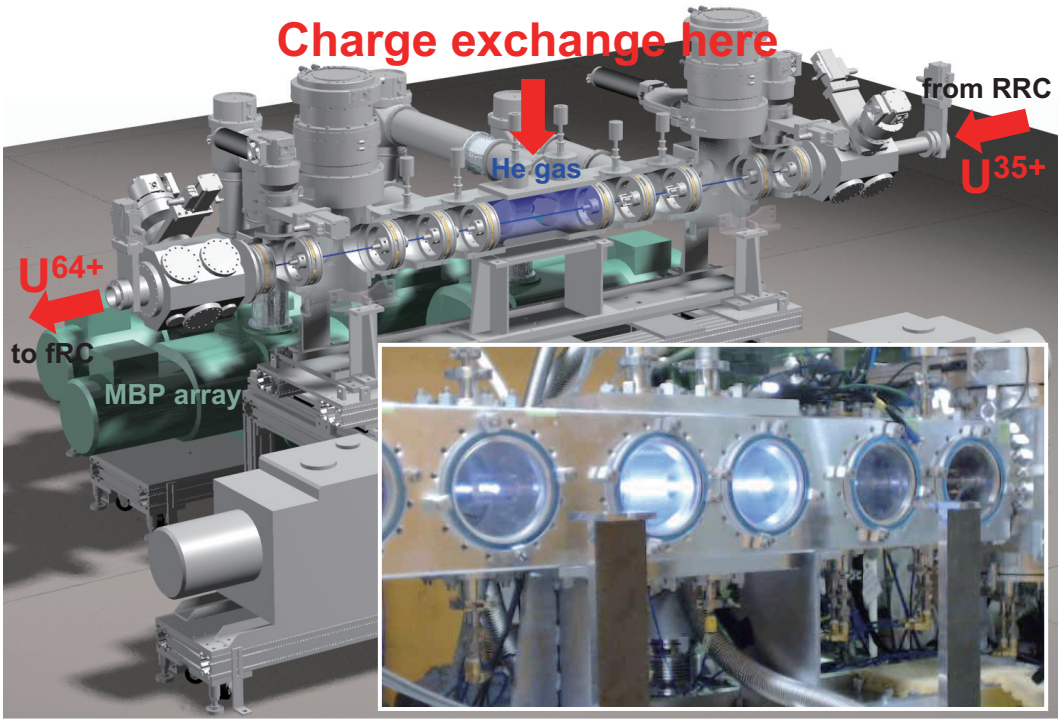

Fig. 2. Cross-sectional view of the He-gas stripper and a photograph of glowing 1-pμA uranium beams.

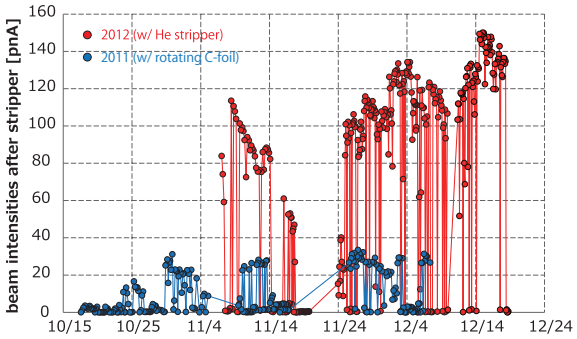

Fig. 3. Intensities of the beam through the first stripper in 2011 and 2012. The new He-gas stripper removed the primary bottleneck for high-power uranium acceleration.

The intensities of the electron-stripped beams provided from the first stripper in 2012 are drastically increased from that in 2011 (Fig. 3). The peak intensity after the SRC has reached 15 pnA, almost 10^{11} ions per second. The service rate (56.7% $\rightarrow$ 80.3%) and the mean intensity (1.6 pnA $\rightarrow$ 10.2 pnA) are also increased, primarily owing to the downtime-free stripper. The average intensity of the uranium beams provided to the user became approximately 10 times higher than it was in 2011.

The new He-gas stripper, which removed the primary bottleneck in the high-intensity uranium acceleration, and the success of some other remarkable accelerator upgrades performed in 2012 at the RIBF (e.g., ion source, high-power beam dump, K700-fRC, etc.) resulted in a tenfold increase in the average output intensity of the uranium beams from the previous year.

The realization of the new acceleration scheme of uranium beams with the He-gas stripper in 2012 has been an important breakthrough for the recent progress of the RIBF.

References

1) Y. Yano, Nucl. Instrum. Meth. Phys. Res. B **261**, 1009 (2007).
2) O. Kamigaito et al., HIAT09, (2009) MO11T.
3) K. Yamada et al., IPAC'10, Kyoto, May 2010, MOPD046; K. Yamada et al., IPAC'12, New Orleans (2012), TUOBA02.
4) Y. Higurashi et al., Rev. Sci Instrum. **83**, 02A308 (2012); Y. Higurashi et al., Rev. Sci Instrum. **83**, 02A333 (2012); Y. Higurashi et al., Cyclotrons 2013, Vancouver, Canada (2013).
5) H. Hasebe et al., Nucl. Instrum. Meth. Phys. Res. A **613**, 453 (2010); H. Hasebe et al., INTDS 2012, Mainz, Germany (2012).
6) W. Henning, Nucl. Phys. A **805**, 502c (2008).
7) FRIB, `http://frib.msu.edu/`.
8) H. Kuboki et al., Phys. Rev. ST-AB **13**, 093501 (2010); H. Kuboki et al., Phys. Rev. ST-AB **14**, 053502 (2011).
9) H. Okuno et al., Phys. Rev. ST-AB **14**, 033503 (2011).
10) H. Imao et al., Phys. Rev. ST-AB **15**, 123501 (2012).
11) N. Fukunishi et al., Cyclotrons 2013, Vancouver, Canada (2013).

Introduction of storage-ring experiments at RIBF

M. Wakasugi*1

The RI Beam Factory (RIBF) in RIKEN Nishina center is a synergetic-use facility where the world's most intense high-energy exotic nuclear beams are supplied to users worldwide mostly for nuclear physics experiments. We have introduced storage-ring-experiment capability at the RIBF in this decade by constructing both an electron storage ring and a heavy-ion storage ring. The electron storage ring facility will be used for the world's first electron scattering experiments from unstable nuclei, and the heavy-ion storage ring is used for precision mass measurements, especially for extremely exotic nuclei located on the r-process path. Both have been defined as core experimental instrumentations at RIBF.

The Self-confining RI ion target (SCRIT), which was developed for electron scattering off unstable nuclei, is a novel internal target forming technique in an electron storage ring. The construction of the SCRIT electron scattering facility[1)] was started in 2009 and almost completed in 2015. As shown in Fig. 1, it consists of an electron accelerator, RTM; an electron storage ring, SR2; an ISOL-type RI beam generator, ERIS;[2)] and a high-resolution spectrometer, WiSES, for analyzing scattered electrons. The momentum transfer distribution of elastically scattered electrons from the ^{132}Xe isotope extracted from ERIS was observed with three electron beam energies, as shown in Fig. 1, and we successfully determined the proton distribution for the first time.[3)] The luminosity reached $2 \times 10^{27}/(\mathrm{cm}^2\mathrm{s})$ with 10^8 injected target ions at an electron beam current of 200 mA − 250 mA. We evaluated the performance of the SCRIT system and demonstrated the feasibility of electron scattering off unstable nuclei. The first experiments for unstable nuclei are now under preparation.

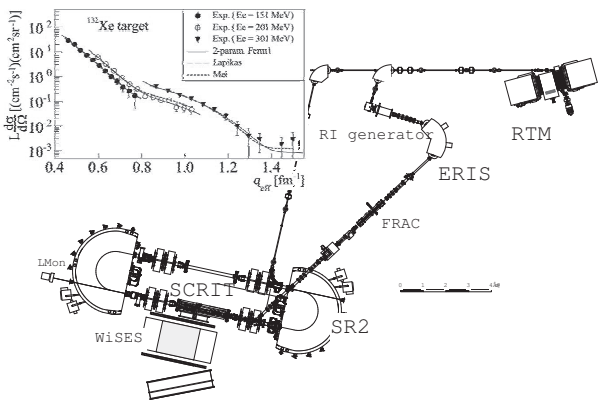

Fig. 1. Schematic view of the SCRIT electron scattering facility and the recently observed momentum transfer distribution of elastically scattered electrons from ^{132}Xe.

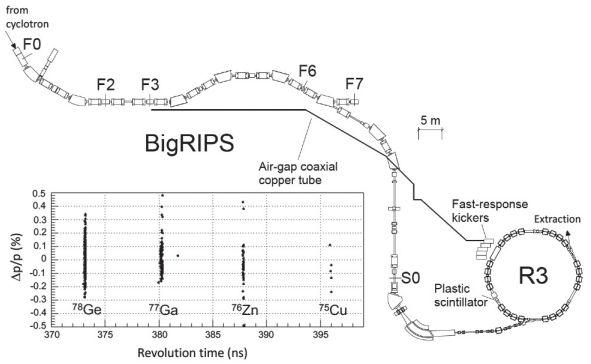

Fig. 2. Schematic view of R3 connected to BigRIPS and typical data of revolution times measured for exotic nuclei.

The heavy-ion storage ring named R3 (Rare-RI Ring)[4)] connected to BigRIPS, as shown in Fig. 2, was constructed in 2012–2014. Masses of nuclei are determined by measuring the revolution times for less than 1-ms accumulation under the isochronous condition. The magnetic structure yielding a high-precision isochronism ($\sim$ 1 ppm) is formed solely by only bending magnets equipped by trim coils. This provides not only large acceptances of $\Delta p/p \sim \pm 0.5$ % in momentum space and $\sim 150\pi$ mm mrad in transverse emittance, but also a high-precision mass-determination capability with an accuracy of the order of 1 ppm even with poor statistics. The isotope-selectable self-triggered injection (ISSI) method, which combines particle identification in the transport line and a newly developed ultrafast response kicker, was adopted in the R3 system, and it enables efficient mass measurement for rarely produced exotic nuclei. Since the injection kicker magnet is activated by a trigger signal produced by the isotope of interest at the F3 focal point, the isotope is identified with certainty and accumulated in R3 one by one. As shown in Fig. 2, revolution times for exotic nuclei measured in the commissioning are independent of their momentum spread as expected, and the mass values relative to that of the reference isotope ^{78}Ge were precisely determined. Mass measurements for $^{74-78}$Ni are now under preparation.

*1 Director of Instrumentation Development Group, RIKEN Nishina Center (2008–present)

References

1) M. Wakasugi et al., Nucl. Instrum. Methods Phys. Res. B **317**, 668 (2013).
2) T. Ohnishi et al., Nucl. Instrum. Methods Phys. Res. B **317**, 357 (2013).
3) K. Tsukada et al., Phys. Rev. Lett. **118**, 262501 (2017).
4) Y. Abe et al., Phys. Scr. T **166**, 014047 (2015).

Research activities of Research Instruments Group

Toshiyuki Kubo[*1,*2]

The Research Instruments Group, consisting of the BigRIPS team, the SAMURAI team, the GARIS team (which presently belongs to the super-heavy element group), the detector team, and the computing and network team (sometimes called data acquisition team), is the driving force for the continuous enhancement of activities and competitiveness of experimental research at RIBF. The group has been in charge of the design, development, construction, operation, and improvement of core research instruments at RIBF, such as the BigRIPS separator,[1,2] the ZeroDegree spectrometer,[2] the SAMURAI spectrometer,[3,4] and the SHARAQ spectrometer,[5,6] and also those of their related infrastructure and equipment.[7–11] Figures 1–3 show photographs of these research instruments.

Furthermore, the Research Instruments Group is in charge of the production of rare isotope (RI) beams using the BigRIPS separator and routinely delivers RI beams to every experiment performed at RIBF. The superconducting in-flight separator BigRIPS was commissioned in March 2007 and has been used to produce a variety of RI beams through the in-flight fission of a ^{238}U beam as well as projectile fragmentation of various heavy-ion beams such as ^{18}O, ^{48}Ca, ^{70}Zn, ^{78}Kr, and ^{124}Xe beams. It was designed and built as a new-generation separator, and it is characterized by three major features: large ion-optical acceptances, two-stage structure, and excellent performance in the particle identification of RI beams, which enabled very efficient production of RI beams. These advanced features of the BigRIPS separator, together with the capability and performance of the RIBF accelerators, have allowed us to greatly expand the regions of accessible exotic nuclei, compared with old-generation in-flight facilities.[12] The scope of RI-beam experiments has also been expanded, and studies of exotic nuclei at RIBF have been promoted significantly.

The research instruments group continuously performed R&D studies in order to improve the performance of the systems, which included ion-optics,[13] particle identification,[14] and beam-line detectors.[15] The group also conducted experimental studies, such as systematic measurements of production cross sections[16] and search for new isotopes[17–19] and new isomers.[20] A number of new isotopes and new isomers have been discovered using the BigRIPS separator. The production of RI beams and the discovery of new isotopes are summarized in Ref. 12.

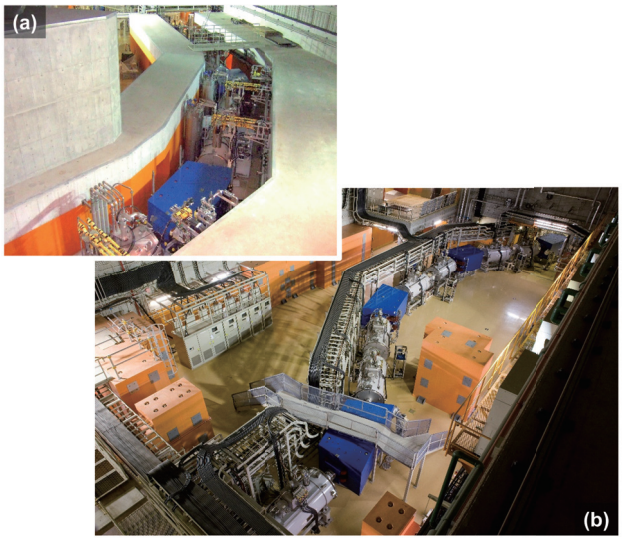

Fig. 1. Photographs of the BigRIPS separator: a) the first stage and b) the second stage.

Fig. 2. A photograph of the ZeroDegree spectrometer.

Fig. 3. A photograph of the SAMURAI spectrometer.

*1 Director of Research Instruments Group, RIKEN Nishina Center (2007–2016)
*2 Present address: FRIB/NSCL, Michigan State University

References

1) T. Kubo, Nucl. Instrum. Methods Phys. Res. B **204**, 97 (2003).
2) T. Kubo et al., Prog. Theor. Exp. Phys. **2012**, 03C003 (2012).
3) H. Sato et al., IEEE Trans. Appl. Supercond. **23**, 4500308 (2013).
4) T. Kobayashi et al., Nucl. Instrum. Methods Phys. Res. B **317**, 294 (2013).
5) T. Kawabata et al, Nucl. Instrum. Methods Phys. Res. B **266**, 4201 (2008).
6) S. Michimasa et al., Nucl. Instrum. Methods Phys. Res. B **317**, 305 (2013).
7) T. Kubo et al., IEEE Trans. Appl., Supercond. **17**, 1069 (2007).
8) A. Yoshida et al., Nucl. Instrum. Methods Phys. Res. A **655**, 10 (2011).
9) K. Yoshida et al., Nucl. Instrum. Methods Phys. Res. B **317**, 373 (2013).
10) H. Kumagai et al., Nucl. Instrum. Methods Phys. Res. B **317**, 717 (2013).
11) H. Baba et al., Nucl. Instrum. Methods Phys. Res. A **616**, (2010) 65.
12) T. Kubo, Nucl. Instrum. Methods Phys. Res. B **376**, 102 (2016).
13) H. Takeda et al., Nucl. Instrum. Methods Phys. Res. B **317**, 798 (2013).
14) N. Fukuda et al., Nucl. Instrum. Methods Phys. Res. B **317**, 323 (2013).
15) Y. Sato et al., JPS Conf. Proc. **6**, 030124 (2015).
16) H. Suzuki et al., Nucl. Instrum. Methods Phys. Res. B **317**, 756 (2013).
17) T. Ohnishi et al., J. Phys. Soc. Jpn. **77**, 083201 (2008).
18) T. Ohnishi et al., J. Phys. Soc. Jpn. **79**, 073201 (2010).
19) T. Sumikama et al., Phys. Rev. C **95**, 051601(R) (2017).
20) D. Kameda et al., Phys. Rev. C **86**, 054319 (2012).

Recent activities of the User Liaison and Industrial Cooperation

H. Sakai,[*1,*2] K. Yoneda,[*2] A. Yoshida,[*2] and Y. Watanabe[*2,*3]

The essential mission of the User Liaison and Industrial Cooperation (ULIC) Group is to maximize the research activities of RIBF by attracting users in various fields with wide scopes. The ULIC Group consists of two teams plus one sub-team. The User Support Team provides various types of support to visiting RIBF users. For this purpose, the User Office was set up in 2010. The Industrial Cooperation Team supports potential users in industries who use the heavy-ion beams for application purposes or for accelerator-related technologies other than basic research. Fee-based distribution of various radioisotopes produced by the AVF cyclotron is also one of the important missions. The produced radioisotopes are distributed to researchers in Japan for a charge through the Japan Radioisotope Association. The Public-relations and Outreach Sub-team supports various outreach activities of Nishina Center.

Fig. 1. Photograph of present ULIC members in the Cyclopedia hall.

User Liaison Team

The RIBF User Liaison Team was established in 2006, immediately before the first physics experiment with the new RIBF facility was conducted in 2007. In order to facilitate and promote efficient and fruitful use of the RIBF, the RIBF User Liaison Team takes charge of many important activities that play key roles in the facility operation. One of the important tasks is to organize international Program Advisory Committee (PAC) meetings, PAC for nuclear physics (NP-PAC) and for material and life science (ML-PAC), to review experimental proposals submitted by RIBF users. The first NP-PAC meeting was held in February 2007, and 32 proposals requesting 550 days of facility use were reviewed there. In the 10 years since then, 17 NP-PAC meetings were held, and 339 proposals requesting 3408 days of beam time were reviewed in total. These numbers clearly show the outstanding demand and importance of the facility in the science community.

Another important task is to manage the RIBF beam-time operation. Beam-time schedule planning, announcement to users and contact from users, schedule change, cancellation, collecting experiment completion reports, and so on are handled by the RIBF User Liaison Team. The Machine Time Committee Meetings are organized regularly every month, and all the important decisions and reports regarding beam-time operation are made there.

Providing support to the RIBF users is also an important task of the RIBF User Liaison Team. In 2010, the RIBF Independent User program started, which allowed a new style of participation for RIBF users in RIBF experiments. Before this program started, all users had to belong to a laboratory or a research group in RIKEN, and thus, the research outcome belonged, in principle, to RIKEN, rather than the users' institutes. But the RIBF Independent User program changed this situation; once a user becomes an RIBF Independent User, he/she can officially claim that the research outcome belongs to the home institute. However, support from the facility is limited for such users; e.g., no financial support is provided for stay. Thanks to this program, international collaborative researches at RIBF have been promoted significantly.

The RIBF Users Office (Fig. 1) was established to provide services and information required for RIBF Independent Users to take part in RIBF experiments. All procedures, such as registration as an RIBF Independent User, reservation of on-campus accommodation, issuance of a radiation badge, and initial lectures for an individual as a radiation worker and as a facility user, can be completed at the RIBF Users Office. At the end of the fiscal year 2016, 330 RIBF users, including 251 from foreign institutes, were registered as RIBF Independent Users. Now, more than half of the RIBF experiment participants are RIBF Independent Users.

Other than the functions stated above, the RIBF User Liaison Team supports the RIBF operation in many aspects, such as support for the RIBF Users Group, arrangements for the RIBF ULIC Symposia

*1 Director of User Liaison and Industrial Cooperation Group (2010–present)
*2 RIKEN Nishina Center
*3 Radiation Laboratory

and mini-Workshops, user orientation at the beginning of each fiscal year, regular summer school for international students, and facility tours of visitors. The RIBF User Liaison Team has always strived to provide support to users so that good research activities can be conducted together, and this objective will remain unchanged in the future.

Industrial Cooperation Team

The industrial cooperation team handles two fee-based non-academic activities: the utilization of heavy-ion beams by the industry and distribution of radioisotopes. The utilization of the ion beams was started in November 2009 when a new project, "Promotion of applications of high-energy heavy ions and RI beams," was approved as a grant-in-aid program of MEXT "Sharing Advanced Facilities for Common Use Program." In this project, RIKEN Nishina Center (RNC) opened a part of the RIBF facility to users including private companies. The users were to pay a beam-time fee and exclusively possess the results and intellectual properties obtained through the use of RIBF. New users with proposals intended to make novel industrial use of ion beams were able to apply for trial use with a reduced fee. A program advisory committee, industrial PAC (In-PAC), was newly set up in December 2009 to review the proposals in terms of their feasibility, possibility of contribution to the general society, and advantage of using the RIBF over other facilities. The MEXT program was terminated in 2010, but RNC continued this facility-sharing program. Thus far, the In-PAC has met six times and approved twelve proposals, four of which were trial proposals and others were fee-based utilization. They include accelerator mass spectroscopy, wear diagnostics of machine parts with implanted RI-tracer nuclei, and irradiation test of space-use semi-conductors. The team also handles fee-based distribution of radioisotopes in collaboration with the Japan Radioisotope Association (JRIA). According to a Material Transfer Agreement (MTA) between JRIA and RIKEN, JRIA mediates the transaction of the RIs and distributes them for a fixed fee to users. The project was started in October 2007 with Zn-65 and Cd-109. Y-88 was added in February 2009 and Sr-85 in April 2015. These RIs are produced by the RI Applications Team with proton and deuteron beams from the AVF cyclotron. The accumulated number of shipments and radioactivity up to March 2017 are listed in Table 1.

The team also develops technologies related to the utilization of RI beams. Under a collaboration with the University of Tokyo and private companies, we have developed a new method for real-time wear diagnostics of industrial materials using RI beams as tracers. As we can provide two intense RI beams of Be-7 and Na-22 and implant them near the surface of a metallic machine part while controlling its depth, one can distinguish the wear-loss rate of both interacting parts at the same time. Another method is the Gamma-ray Inspection of Rotating Object (GIRO), which intends to evaluate the wear-loss in a running machine with the imaging of gamma-ray source distribution.[1)] This is based on the same principle as the medical PET systems but is simpler and less expensive. Both methods led to patent applications.

Public-relations and Outreach Sub-team

This sub-team was established in 2010, to promote the publicity of RNC.

The RNC website, which introduces the organization and its research activities, was renewed in 2010 to the present form (`http://www.nishina.riken.jp`). This website also plays an important role in providing information to researchers who visit RNC to conduct his/her own research.

Various brochures introducing the organization and the studies performed at RNC have been produced. The brochures named "Your body is made of star scraps" explaining element synthesis in the universe and "Introduction of RIBF Facility" in a cartoon style for children are among them.

During the past 7 years, 23 conference/symposium posters connected with RNC were prepared on the request of organizers. For general purpose, a special poster featuring the nuclear chart has been prepared for distribution. In commemoration of the discovery of nihonium, brochures and posters dedicated to the ceremony were made. A 3D video to explain (RIBF's) accelerators and the research at RIBF won the Category Excellence Award at the 2012 Science and Technology Video Festival. Many of these can be seen on RNC website.

In April 2012, the permanent exhibition hall (RIBF Cyclopedia) located at the entrance hall of the RIBF building was set up. Explanatory illustrations on nuclear science, research at RIBF, RIBF history, a 3D nuclear chart built with LEGO blocks, and a 1/6-size GARIS model (GARIS: key apparatus for the synthesis of nihonium) are displayed to help understanding through visual means. To show an actual size of the Superconductive Ring Cyclotron (flagship accelerator), a part of the SRC magnet and liquid He vessel are drawn on the carpet of floor and on the wall, respectively. An enlarged photograph of Dr. Yoshio

Table 1. The accumulated number of shipments and radioactivity for fee-based distribution up to March 2017.

Nuclide	Zn-65	Cd-109	Y-88	Sr-85
Shipments	90	33	6	1
Activity (MBq)	496.2	204.15	5.03	1

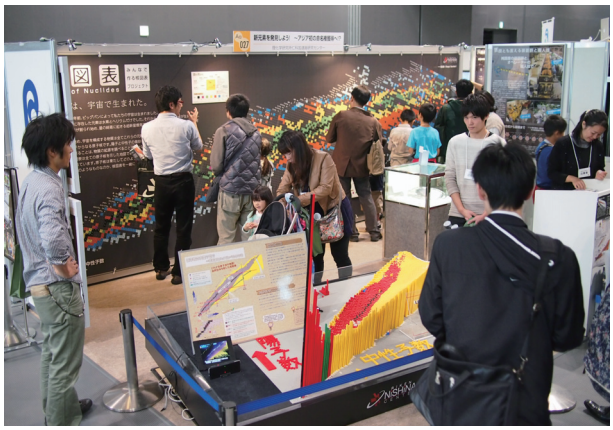

Fig. 2. RIKEN Nishina Center booth in Science Agora 2013. In front is a 3D nuclear chart built with LEGO blocks.

Nishina sitting on his second cyclotron (60-inch), taken in 1939, is also printed on the wall.

A laboratory tour for visitors guided by a researcher is organized. Typically, it takes about 40 min. The number of tours per year is about 150, and the number of visitors is about 2000.

In 2010, 2012, 2013, 2015, and 2016, the sub-team opened an exhibition booth of RNC to introduce the latest research activities on the occasion of the "Science Agora" organized by Japan Science and Technology Agency. It attracted nearly 1000 visitors and received the Science Agora Award in 2012 and 2013. Figure 2 is a snapshot taken at the booth in Science Agora 2013.

From time to time, the sub-team is invited to participate in scientific events by MEXT, Wako city, and Nissan global foundation. One attraction targeting children is the hands-on work of assembling "Iron-beads" to create a nuclear chart or a shape of nihonium. Note that most of above products, such as websites, materials, and events, are designed and/or created by Mr. Narumasa Miyauchi, a member of the sub-team.

Last but not the least, some of the above activities were carried out in collaboration with the Public Relations Office of RIKEN.

Reference

1) T. Kambara, A. Yoshida, H. Takeichi, Nucl. Instrum. Methods Phys. Res. A **797**, 1 (2015).

Safety management at Nishina Center since 1990

Y. Uwamino,[*1] N. Nakanishi,[*2] S. Fujita,[*2] S. Ito,[*3] H. Sakamoto,[*2] R. Higurashi,[*2] H. Mukai,[*2] A. Akashio,[*2] K. Tanaka,[*2] T. Okayasu,[*2] N. Fukunishi,[*2] and M. Kase[*2]

The most impressive development since 1990 has been the construction of the radioactive-isotope-beam factory (RIBF). It included the decommissioning of the old 160-cm cyclotron, safety design of the new facility, and its commissioning.

The 160-cm cyclotron was the facility built first when RIKEN moved from central Tokyo, Komagome, to the present campus. The operation started in 1966 and ended in 1990. It accelerated particles ranging from protons to Ne ions with energies of several tens of MeV. A hot laboratory was adjoined, and several points of it were contaminated since it was used for a long period. Decontamination was performed by an external company. Some parts of the accelerator were radioactivated, and the activated parts were removed and stored in the radioactive waste storehouse. The main part of the accelerator is displayed in front of the main research building of the campus, as shown in Fig. 1. However, coils and pole pieces were replaced with mock-ups since these parts were activated.

When the safety design of RIBF started, we did not have any data or computer codes for the shielding calculation. Fortunately, a similar-energy heavy-ion facility, Heavy Ion Medical Accelerator in Chiba (HIMAC), started operation. We could measure the neutron production data at a thick target bombarded by heavy ions in collaboration with Tohoku University.[1] The measured data were not only used as a source term of the high-energy neutron shielding calculation of RIBF, but they also contributed to the development of a computer code, Particle and Heavy Ion Transport Code System[2] (PHITS), which is widely used for estimations of radiation-relating affairs.

Fig. 1. The old 160-cm cyclotron displayed in front of the main research building.

Based on the measured neutron production data, shielding calculation was performed using a discrete ordinates transport code, and the shield thicknesses of the RIBF building were determined. The results were investigated by a radiation safety committee led by Dr. Kamitsubo. The committee firstly discussed the criteria of radiation levels in and around the facility. It also discussed the safety measure for induced radioactivity in accelerator components and in air and water. The committee held 6 meetings over 4 years and approved the design.

The RIBF project and its safety design[3] were explained to the mayor and the municipal government and assembly. After they acknowledged the project, we explained to the residents successfully.

The personal safety interlock system (HIS) was built several years before the installation, and its logic was tested using a simulation device. HIS was a separated system from those of Nishina and Linac buildings, and its logic was comparably simple.

During the construction of RIBF, we applied for the license of uranium acceleration at the old accelerators. On the day when we submitted the application form to the government office, a radioisotope source was illegally found outside of radiation-controlled area. We brought this accident to the notice of the same office immediately. We received a special inspection by the office and sent many documents on the facts of the accident and on measures to prevent a similar accident from occurring again. We luckily could obtain the license within a normal period.

The first beam was extracted from the superconducting cyclotron (SRC) on December 28, 2006. After the tuning of accelerators, a ^{86}Kr beam was transported to the experimental area in the very early morning on March 15, 2007, and we measured the radiation levels in and around the facility before daybreak. The government inspection of the facility was conducted on the same day in reference to our measured radiation data. The pass certificate was issued on March 22, and we could start the experiment. The accelerator staff soon succeeded in the acceleration of ^{238}U by using the fixed-frequency ring cyclotron (fRC), and we passed the government inspection for the whole facility by the end of March 2007.

*1 Director of Safety Management Group, RIKEN Nishina Center (2006–present)
*2 RIKEN Nishina Center
*3 Wako Safety Center, RIKEN

References
1) T. Kurosawa et al., J. Nucl. Sci. Technol. **36**, 41 (1999).
2) T. Sato et al., J. Nucl. Sci. Technol. **50**, 913 (2013).
3) Y. Uwamino et al., Radiat. Prot. Dosim. **115**, 279 (2005).

Superheavy element research at RIKEN Nishina Center

K. Morimoto[*1] and K. Morita[*2,*3]

The study of the heaviest nuclei (elements) by using heavy-ion beams is one of the most important research subjects. When the RIKEN Ring Cyclotron (RRC) was being constructed in 1985, Dr. Kosuke Morita designed and constructed the Gas-filled-type Recoil Ion Separator (GARIS) as the first large-scale experimental equipment in the experimental hall E1. New isotopes, ^{195}At, ^{196}Rn, ^{197}Rn, ^{199}Fr, and ^{200}Fr, were discovered using RRC and GARIS.

In 2000, the RIBF project was started, and GARIS was relocated from the E1 room to the energy-upgraded RIKEN Linear Accelerator (RILAC) facility by adding CSM accelerators in order to start a full-scale experiment to search for new elements. With the technical developments of both the accelerator/ion source and the experimental setups, the experimental system had the highest possibility in the world of providing the heaviest elements. First, follow-up experiments conducted by the preceding research group, Gesellschaft fur Schwerionenforschung (GSI), were performed. In these experiments, elements 108, 110, 111, and 112 were produced with the highest production rate to date. The experiment aimed at discovering the 113th element was started in 2003 by using the ^{209}Bi(^{70}Zn, n)^{278}113 reaction. Three decay chains originating from ^{278}113 were successfully observed in 2004,[1] 2005,[2] and 2012.[3] Furthermore, a connection to the known isotopes ^{266}Bh and ^{262}Db was established using the ^{248}Cm(^{23}Na, 5n)^{266}Bh reaction in 2009. The prolonged experimental effort for ^{278}113 was concluded in Oct. 2012. The three decay chains of ^{278}113 are presented in Fig. 1.

IUPAC finally decided to give our research group the right to name and determine the symbol for the element 113 in Dec. 2015. We proposed the name Nihonium with the symbol Nh. The name and symbol were finally accepted by IUPAC in Nov. 2016. Figure 2 shows the group members who participated in the naming meeting.

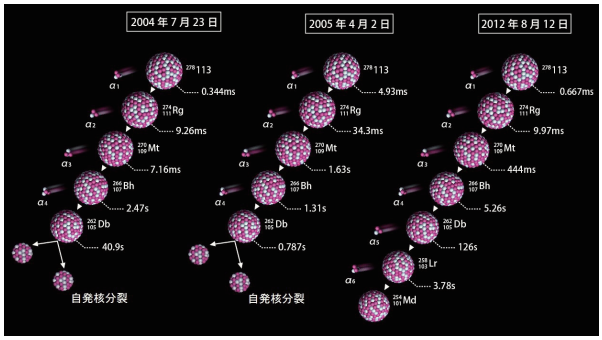

Fig. 1. Decay chains related to ^{278}113. The first two decay chains consist of four alpha decays and end with the spontaneous fission of ^{262}Db. The third decay chain consists of six alpha decays and is connected to ^{254}Md.

Fig. 2. Research group members after the conclusion of the naming meeting of the element 113.

Aiming to discover further new elements, a new Gas-filled Recoil Ion Separator (GARIS-II) for asymmetric reaction such as hot fusion reaction was developed. GARIS-II has a large angular acceptance (18.5 msr) and short path length. The transmission of GARIS-II is 1.7 times higher than that of the present GARIS. New element search using the hot fusion reaction will be started in the near future at RIKEN Nishina Center.

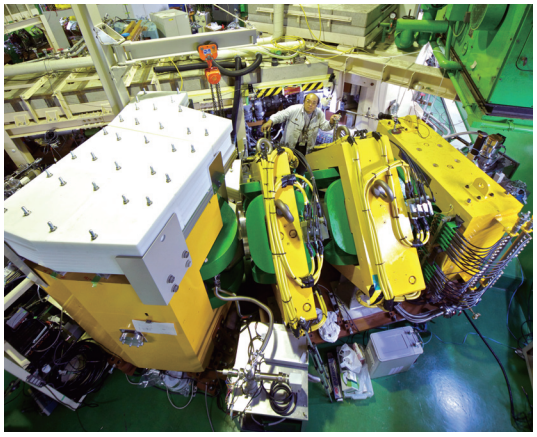

Fig. 3. Photograph of the GARIS-II separator. The separator has a Q-D-Q-Q-D configuration.

*1 RIKEN Nishina Center
*2 Director of Research Group for Superheavy Element, RIKEN Nishina Center (2013–present); Associate Chief Scientist of Superheavy Element Laboratory (2006–2013)
*3 Department of Physics, Kyusyu University

References
1) K. Morita et al., J. Phys. Soc. Jpn. **73**, 2593 (2004).
2) K. Morita et al., J. Phys. Soc. Jpn. **76**, 045001 (2007).
3) K. Morita et al., J. Phys. Soc. Jpn. **81**, 103201 (2012).

Direct reaction experiments with fast RI beams for studying properties of exotic nuclei and astrophysical nuclear processes

T. Motobayashi*1

One of the first experiments using fast radioactive isotope (RI) beams, which RIKEN started to provide in the early 1990s, was on the Coulomb dissociation of ^{14}O. The experiment was performed with ^{14}O beams and a ^{208}Pb target by a group mainly composed of researchers from Rikkyo University, ISN Grenoble, RIKEN, and University of Tokyo.[1] The ^{13}N(p, γ)^{14}O reaction in the hot CNO cycle was indirectly studied. The Grenoble team brought an array of CsI(Tl) scintillators, which was used together with a position-sensitive silicon detector array and associated electronics developed by the Rikkyo group for detecting outgoing particles in coincidence.

This study has unique properties: it is the first experiment for astrophysical reactions involving short-lived nuclei, the first Coulomb dissociation measurement for explosive nuclear burning, an international collaboration that combines experimental devices developed by respective groups, and a good example of direct reaction studies using fast (87.5 MeV/nucleon in this case) RI beams in inverse kinematics, where the nuclei in the beam are of interest and the target serves as the reaction probe.

The radiative width of the first 1^- state in ^{14}O, the key parameter for evaluating astrophysical reaction rates, was successfully extracted, and it agreed with a direct measurement at the laboratory of Louvain-la-Neuve with slow ^{13}N beams performed in a similar period. These pioneering experiments resolved a long-standing question on the ^{13}N(p, γ)^{14}O astrophysical reaction rate.

Another direct reaction experiment in inverse kinematics was on the neutron-rich $N = 20$ nucleus ^{32}Mg performed at RIKEN in 1994. The reduced transition probability B(E2 :$0^+ - 2_1^+$) was successfully determined by Coulomb excitation.[2] Again, the inverse kinematics, where fast radioactive ^{32}Mg beams were incident on a ^{208}Pb target, was employed. The population of the first 2^+ state in ^{32}Mg was identified by measuring its deexcitation γ rays, in contrast to the above-mentioned Coulomb dissociation, in which the particle decay from the unbound 1^- state in ^{14}O was measured by detecting the proton and ^{13}N in coincidence.

The extracted large B(E2) value of 454 ± 78 e^2fm^4 supports the idea of disappearance of the $N = 20$ shell closure in ^{32}Mg. This B(E2) measurement was performed for the first time long after the study determining the low 2^+ energy of 895 keV in the late 1970s.

For this type of experiments, a γ detector array, DALI, was built. It consists of ≈60 NaI(Tl) scintillators and has a large efficiency with sensitivity to the γ-ray emission angle, which is indispensable for correcting a large Doppler shift of photons from fast-moving nuclei. To adopt higher-energy beams of RIBF, a new array called DALI2 with ≈170 crystals was developed to cope with larger Doppler shifts. DALI and DALI2 have been and are still used in various experiments.[3]

The successes of these studies demonstrated the usefulness of direct reaction with fast RI beams, and triggered extensive studies of the structure of exotic nuclei and astrophysical reactions in explosive burning. They were performed at RIKEN and other facilities such as NSCL-MSU, GANIL, and GSI.

Coulomb dissociation was also applied to the ^{7}Be(p, γ)^{8}B reaction, the major process of producing high-energy neutrinos in the sun. Several experiments provided new independent results free from systematic problems caused by the radioactive ^{7}Be target used in (p, γ) measurements in normal kinematics. These studies contributed to make the ^{7}Be(p, γ)^{8}B reaction rates more reliable and, therefore, to place the discussions of the solar neutrino problem on firmer ground.[4]

In addition to the Coulomb excitation, various direct reactions have been studied. The inelastic scattering of light particles such as proton, deuteron, or α in this energy regime is dominated by the nuclear interaction and have different sensitivities to the final states. For example, for finding the 1^- state in ^{12}Be, the Coulomb excitation and proton inelastic scattering are compared, where the former is more sensitive to the $\ell = 1$ excitation.[5] We also found that the inelastic proton scattering is one of the most efficient probes to observe unknown low-lying levels. Nucleon removal reactions are commonly used, since they populate more states compared with the inelastic scattering.

Many new properties in exotic nuclei were discovered by these direct reactions in inverse kinematics. Recent examples at RIKEN are findings of a "soft" nature of ^{32}Mg by the proton inelastic scattering populating its first 4^+ state[6] and a large $N = 34$ shell gap in ^{54}Ca expected form the location of the 2^+ state populated by nucleon removal reactions.[7]

*1 Chief Scientist of Heavy Ion Nuclear Physics Laboratory (2002–2010)

References

1) T. Motobayashi et al., Phys. Lett. B **264**, 259 (1991).
2) T. Motobayashi et al., Phys. Lett. B **346**, 9 (1995).
3) S. Takeuchi et al., Nucl. Instrum. Methods Phys. Res. A **763**, 596 (2014).
4) T. Motobayashi, Nucl. Phys. A **693**, 258 (2001), and therein.
5) N. Iwasaki et al., Phys. Lett. B **491**, 8 (2000).
6) S. Takeuchi et al., Phys. Rev. C **79**, 054319 (2009).
7) D. Steppenbeck et al., Nature **502**, 207 (2013).

Radioactive Isotope Physics Laboratory

H. Sakurai*1

The Radioactive Isotope Physics Laboratory was established as one of the institutes laboratory in 2005 when Hiroyoshi Sakurai was appointed as a Chief Scientist. Since then, the Laboratory has functioned as one of the core research groups conducting programs at the world-leading heavy-ion accelerator facility, the RIKEN "RI Beam Factory (RIBF)."

The Laboratory explores exotic nuclear structures and dynamics in exotic nuclei that have never been investigated before, such as those with large imbalanced proton and neutron numbers. Our aim is to develop new experimental techniques utilizing fast radioactive isotope (RI) beams at RIBF and to discover new phenomena and properties in exotic nuclei.

Research subjects covered by the Laboratory are the shell evolution in exotic nuclei, the r-process nucleosynthesis, and the equation of state (EOS) in asymmetric nuclear matter.

The shell evolution has been investigated via in-beam gamma spectroscopy and decay spectroscopy. The two spectroscopy methods complement each other: in-beam gamma spectroscopy is a good method for finding yrast states, while decay spectroscopy gives information on non-yrast states as well. A major experimental site of in-beam gamma spectroscopy is the "ZeroDegree" spectrometer,[1] where reaction products are identified in coincidence with de-excited gamma-ray measurement at a NaI array called "DALI2."[2] The first spectroscopy at RIBF was organized as a day-one campaign in 2008 for the island-of-inversion region. The ^{48}Ca beam was utilized to produce very neutron-rich nuclei in the region. Not only the high primary beam intensity but also unexpectedly large production cross sections caused surprisingly intense secondary beams, which gave very efficient organization in managing the day-one programs. The first data on ^{32}Ne were published in PRL in 2009.[3] Since then, multitudes of programs have been conducted under the SUNFLOWER collaboration. One of the highlights is "the discovery of a new magic number 34," which was published in Nature.[4] The SEASTAR collaboration was formed as a subset of SUNFLOWER in 2014 to observe the first excited states in even-even neutron-rich isotopes, and it finished its campaign program in summer 2017. Exciting results are being published.[5]

Decay spectroscopy at RIBF was started in 2009 as a day-two campaign by utilizing a primary beam of uranium. A beta-gamma coincidence setup including four clover Ge-detectors was mounted at the end of ZeroDegree, and neutron-rich nuclei with $A \sim 110$ were implanted into active Si strip detectors "WAS3ABi." The first campaign was successfully organized for 2.5 days, and two papers on the shell evolution and the r-process path were published in PRL.[6] The first attempt made a trigger to organize the "EURICA" project, where the GSI RISING setup of Euroball-cluster Ge-detectors was coupled with RIBF. The EURICA campaign was organized from 2012 to 2016, and about 40 papers including 11 PRL papers have already been published. One of the highlights is a successful measurement of 110 half-lives of neutron-rich nuclei.[7] The measurement impacts the r-process nucleosynthesis scenario. Since 2016, the BRIKEN project of beta-delayed neutron emission probability measurement has been conducted.

The EOS in asymmetric nuclear matter at a density that of normal nuclei has been studied with heavy-ion central collisions by utilizing a large TPC, which was developed under the SπRIT collaboration.[8] In 2016, the TPC was mounted inside the SAMURAI magnet, and physics runs were organized. A huge amount of data is being analyzed to obtain $\pi^{\pm}$ yields as well as proton- and neutron-flows.

Other activities in the Laboratory were missing-mass spectroscopy with radioactive isotope beams,[9] laser spectroscopy of radioactive atoms in superfluid He, and Antarctic ice core analysis for supernova explosion events. At the occasion of a researcher leaving and new laboratories being created, their research activities were transferred to other Laboratories and other research units in Nishina Center. In 2013, a spallation reaction study with long-lived fission products was initiated by the Laboratory for the nuclear waste problem.[10] This activity was also transferred into the other group in Nishina Center in 2014.

Future projects being initiated by the Laboratory are the development of detectors such as GAGG crystals, advanced tracking Ge detectors, and silicon telescopes. Based on these detectors, new programs with decelerated radioactive isotope beams are the future research directions in the Laboratory.

*1 Chief Scientist of Radioactive Isotope Physics Laboratory (2005–present)

References

1) T. Kubo et al., Prog. Theor. Exp. Phys. **2012**, 03C003 (2012).
2) S. Takeuchi et al., Nucl. Instrum. Methods Phys. Res. A **763**, 596 (2014).
3) P. Doornenbal, H. Scheit et al., Phys. Rev. Lett. **103**, 032501 (2009).
4) D. Steppenbeck et al., Nature **502**, 207 (2013).
5) N. Paul, A. Corsi, A. Obertelli, P. Doornenbal et al., Phys. Rev. Lett. **118**, 032501 (2017)
6) S. Nishimura et al., Phys. Rev. Lett. **106**, 052502 (2011); T. Sumikama et al., Phys. Rev. Lett **106**, 202501 (2011).
7) G. Lorusso, S. Nishimura et al., Phys. Rev. Lett. **114**, 192501 (2015).
8) R. Shane, A.B. McIntosh, T. Isobe et al., Nucl. Instrum. Methods Phys. Res. A **784**, 513 (2015).
9) A. Matta, D. Beaumel, H. Otsu et al., Phys. Rev. C **92**, 041302 (2015).
10) H. Wang et al., Phys. Lett. B **754**, 104 (2016).

Spin Isospin Laboratory

Tomohiro Uesaka*1

The Spin Isospin Laboratory was started on 1st April, 2011 and, as of July 2017, consists of five staff researchers (one is concurrently appointed), nine postdoc researchers, two JRA, three IPA, four resident trainees, secretaries, and several tens of visiting researchers. The Spin Isospin Laboratory pursues research activities with a primary focus on the interplay of spin and isospin in exotic nuclei. Understanding nucleosynthesis in the universe, especially in r- and rp-processes, is another significant goal of our laboratory.

The three big pillars of our research activities are as follows: 1) direct reaction studies of nuclear matter and structure, 2) storage ring experiments for nuclear physics and nuclear astrophysics, and 3) interdisciplinary studies based on a nuclear polarization technique.

Direct reaction studies of nuclear matter and structure are being conducted mainly with the SAMURAI and SHARAQ spectrometers. We investigate spin-isospin responses in nuclei with newly developed experimental methods. Highlights from the activities are an observation of β^+-type isovector spin monopole resonances (IVSMR) in ^{208}Pb and ^{90}Zr via the $(t, {}^3\mathrm{He})$ reaction at 300 MeV/nucleon[1] and the discovery of a candidate of tetraneutron resonant state via the ^{4}He(^{8}He, ^{8}Be) reaction.[2] Another double-charge exchange reaction, (^{12}C, ^{12}Be(0_2^+)), is planned to be used to search for yet-to-be-discovered double Gamow-Teller resonances.

To investigate spin-isospin properties, the neutron-skin thickness, and the incompressibility for a single symbolic nucleus, in this case the doubly magic ^{132}Sn, we performed three experiments during 2014–2016: the (p, n) experiment to probe spin-isospin responses conducted in 2014 with the WINDS neutron detector and SAMURAI, the proton elastic scattering experiments to determine the neutron-skin thickness with the ESPRI setup, and the (d, d') experiment to extract the incompressibility performed with the CNS active target. Results from the three experiments will provide us a better understanding of isospin dependencies of nuclear-matter properties.

The laboratory hosted the MINOS setup from CEA Saclay and the NeuLAND neutron detector from GSI, and performed the SEASTAR campaigns[3] in collaboration with the RI Physics laboratory and the SAMURAI experiments to explore multi-neutron correlations in near- and beyond-dripline nuclei such as tetraneutron, ^{7}H, ^{11}Li, ^{17}B, and ^{28}O.

The second pillar consists of storage ring experiments for nuclear physics and nuclear astrophysics. In close collaboration with the Instrumentation Development Group, we have constructed a heavy-ion storage ring, the Rare RI Ring, for precise mass measurements of short-lived radioactive nuclei. Masses of the radioactive nuclei play a decisive role in the establishment of our understanding of nucleosynthesis, such as the rapid neutron capture process (r-process) and the rapid proton capture process (rp-process), in the Universe.

During 2014–2016, we accomplished two important technical achievements. One is the world's first realization of individual injection to a storage ring.[4] This technique has paved the way in the field of storage-ring science and has opened up applications in cyclotron facilities. The other is the construction of a Schottky pickup detector with the world's highest sensitivity. We have tested the newly constructed Schottky pickup detector with a ^{78}Kr beam at 168 MeV/nucleon and have confirmed that the sensitivity is twice those in other facilities. Mass measurements of radioactive nuclei will start soon.

The last pillar consists of interdisciplinary studies based on a nuclear polarization technique. We have developed a method to produce nuclear polarization using photo-excited triplet states of pentacene (*Triplet-DNP*). A distinguished feature of the Triplet-DNP technique is that it works under a low magnetic field of 0.1–0.7 T and at a high temperature of 77–300 K, in striking contrast to standard dynamic nuclear polarization (DNP) techniques working in extreme conditions of magnetic fields of several Tesla and sub-Kelvin temperatures. We have applied the technique to construct a polarized proton target system for use in RI-beam experiments and performed several experiments at RIPS and SAMURAI.

The nuclear polarization technique is now being applied to a broad field of science: a research program to apply the Triplet-DNP technique for sensitivity enhancement in the NMR spectroscopy of biomolecules started in 2016 in close collaboration with QBiC (RIKEN), Yokohama City University, the University of Tokyo, and Kansei Gakuin University. In the program, protein-protein interaction in a relatively short time scale will be investigated via two-dimensional NMR spectroscopy with sensitivity enhanced by the Triplet-DNP method. The first results will be obtained in a few years.

References

1) K. Miki et al., RIKEN Accel. Prog. Rep. **44**, iii (2011) and Phys. Rev. Lett. **108**, 262503 (2012).
2) K. Kisamori et al., RIKEN Accel. Prog. Rep. **49**, 3 (2016) and Phys. Rev. Lett. **116** 052501 (2016).
3) C. Santamaria et al., RIKEN Accel. Prog. Rep. **49**, 1 (2016) and Phys. Rev. Lett. **115** 192501 (2016).
4) Y. Yamaguchi et al., RIKEN Accel. Prog. Rep. **49**, 18 (2016).

*1 Chief Scientist of Spin Isospin Laboratory (2011–present)

Nuclear Spectroscopy Laboratory

H. Ueno*1

The Nuclear Spectroscopy Laboratory was started in 2013 in at Nishina Center. In the group, five full-time researchers are working as of 2016 together with the Chief Scientist, including three Research Scientists in the fields of nuclear physics, atomic physics, and materials science as key persons in each field of study. The group has been conducting various spectroscopic studies of radiation and fluorescence emitted from slowed-down or stopped radioactive-isotope (RI) beams produced at the RIBF facility, aiming at the measurement of electromagnetic nuclear properties such as spin, isotope shift, and electromagnetic nuclear moments. In this report, we introduce these studies by roughly categorizing them into three.

The first category comprises nuclear-structure studies utilizing spin-oriented RI beams produced in in-flight nuclear reactions. This research has been conducted successively for generations, and new techniques were developed at the accelerators in RIKEN.

A spin-polarized RI beam at RIKEN was first produced in late 1970 by the experimental group led by M. Ishihara, who was a member of the Cyclotron Laboratory at that time, based on the low-energy quasi-elastic scattering reaction of a heavy-ion beam from the 160-cm Cyclotron.[1] After the beam energy reached $E/A \sim 100$ MeV with the installation of the RIKEN Ring Cyclotron (RRC), the method was improved in early 1990 by Ishihara and K. Asahi *et al.* in the Radiation Laboratory. The method makes good use of properties of the projectile-fragmentation reaction that is dominant at this beam energy.[2,3] Here, the RIKEN projectile-fragment separator RIPS[4] played an important role. This method enabled the production of spin-polarized RI beams far from the β-decay stability line. Thus, systematic ground-state nuclear-moment measurements of light unstable nuclei were conducted from the late 1990s to the 2000s in the Applied Nuclear Physics Laboratory led by Asahi, based on the technique of fragmentation-induced spin polarization combined with the β-ray-detected NMR method. For instance, the isospin dependence of effective charges was first observed in these studies.[5] Then, the RIBF facility started operation at the end of 2006. Primary beams at RIBF are delivered typically at $E/A = 345$ MeV. At this energy, we have a great advantage in the production yield of RI beams, but we simultaneously encounter difficulties in producing spin polarization owing to the properties of the fragmentation reaction. Instead of spin polarization, we have newly developed a method to produce highly spin-aligned RI beams through the two-step nuclear reaction combined with the dispersion-matching technique[6] using the BigRIPS in-flight RI separator.[7] Isomeric-state nuclear-moment measurements are conducted by our group as its application. To extend these observations to the ground states of extremely rare RIs, we are now attempting to develop a new method and apparatus for producing spin-polarized RI beams at RIBF.

The second category comprises nuclear laser spectroscopic studies for stopped/slowed-down RI beams. We have been conducting system development for nuclear laser spectroscopy from the following two approaches in order to realize experiments for rare isotopes at RIBF. One is collinear laser spectroscopy for a large variety of elements using slowed-down RI beams produced via a projectile-fragmentation reaction, which can be achieved only by the universal low-energy RI-beam delivery system, SLOWRI. Thus far, nuclear laser spectroscopy has intensively been conducted at the CERN-ISOLDE facility, taking advantage of quite a narrow momentum spread of low-energy RI beams, although there is an element limitation. The SLOWRI facility, under installation, can deliver such high-quality low-energy RI beams without the elemental limitation because of the difference in the RI production method. We plan to start new measurements of nuclear laser spectroscopy based on this advantageous feature.

The other approach is a new method utilizing superfluid helium (He II) as a stopping medium of energetic RI beams, in which the characteristic atomic properties of ions surrounded by superfluid helium enables us to perform unique nuclear laser spectroscopy. RI ions trapped in He II are known to exhibit a characteristic excitation spectrum significantly blue-shifted compared with the emission one. Consequently, the background derived from the excitation-laser stray light, which often causes serious problems in measurements, can be drastically reduced. This enables us to measure a Zeeman or hyperfine structure splitting with a high sensitivity by applying the laser-RF/MW double resonance method to the trapped atoms.[8] These R&D studies are conducted under the supervision of Professor Y. Matsuo (Hosei Univ.), Senior Visiting Scientist of our Laboratory.

The last category comprises the application of RI and heavy-ion beams as a probe for condensed matter studies. The microscopic material dynamics and properties have been investigated through the deduced internal local fields and the spin relaxation of RI probes

*1 Chief Scientist of Nuclear Spectroscopy Laboratory (2013−present)

based on various spectroscopic studies, aiming at utilization of the RIBF facility in a wide range of research fields of, in particular, materials science. We have already conducted β-NMR/nuclear quadrupole resonance (NQR) spectroscopy, in-beam Mössbauer spectroscopy, and the γ-ray time-differential perturbed angular correlation (γ-TDPAC) spectroscopy in collaboration with Univ. of Electro-Comm., ICU, Tokyo Univ. of Sci., Osaka Univ. among the others. Among them, we note that in-beam Mössbauer spectroscopy using a ^{57}Mn RI beam was developed in the Nuclear Chemistry Laboratory led by F. Ambe.[9)]

Recently, we started studies on diamond superconductivity by high-density doping through heavy-ion implantation as well as low-density, low-field oxygen NMR/NQR studies utilizing ^{21}O as an RI probe. They are partly conducted together with several Chief-Scientist Laboratories outside the Nishina Center under the framework of a RIKEN competitive interdisciplinary-research budget program.

References

1) K. Sugimoto, N. Takahashi, A. Mizobuchi, Y. Nojiri, T. Minamisono, M. Ishihara, K. Tanaka, H. Kamitsubo, Phys. Rev. Lett. **39**, 323 (1977).
2) K. Asahi et al., Phys. Lett. B **251**, 488 (1990).
3) K. Asahi et al., Phys. Rev. C **43**, 456 (1991).
4) T. Kubo et al., Nucl. Instrum. Methods Phys. Res. B **70**, 309 (1992).
5) H. Ogawa et al., Phys. Rev. C **67**, 064308 (2003).
6) Y. Ichikawa et al., Nature Phys. **8**, 918 (2012).
7) T. Kubo et al., Nucl. Instrum. Methods Phys. Res. B **204**, 97 (2003).
8) X.F. Yang et al., Phys. Rev. A **90**, 052516 (2014).
9) M. Nakada et al., Bull. Chem. Soc. Jpn. **65**, 1 (1992).

10 years of Theoretical Physics Laboratory

H. Kawai[*1,*2]

The Theoretical Physics Laboratory was established at the dawn of the new century, in October 2001, as the first laboratory in more than 30 years that is dedicated purely to theoretical studies, since the closure of the Theoretical Physics Laboratory headed by Dr. Hideki Yukawa, Japan's first Nobel Laureate. That was the start of my days of commuting between RIKEN and my office in Kyoto University, which was previously occupied by another Japanese Nobel Laureate, Dr. Toshihide Maskawa.

Running a laboratory in RIKEN made a significant change in my research life, but RIKEN itself was also about to go through a tremendous reshaping process. One of such moves was the establishment of Nishina Center for Accelerator-based Science, under the leadership of Dr. Yasushige Yano. At that time, we were still struggling to establish the presence of theoretical studies in RIKEN. Then, Dr. Yano, who realized the immense importance of theoretical study, invited our group to form a research center together with the accelerator groups and other laboratories for nuclear physics. By securing our position in the framework of Nishina Center, we could establish our presence and also the status of theoretical studies in RIKEN. This is how we started participating in the RIKEN Accelerator Progress Report. Although our participation as the Theoretical Physics Laboratory was rather brief, I believe we were able to contribute around 47 articles to the Report.

It is my great honor, therefore, to contribute to this commemorative 50th issue of the RIKEN Accelerator Progress Report. I would like to thank the editors of the Report for kindly inviting me to write this entry. Allow me to take this opportunity to present a brief sketch of the activities that were took place at the Theoretical Physics Laboratory. First, the following list of research subjects should give a certain idea of the scope of the activities of our group:

(1) String Theory as a Fundamental Theory
- Matrix Models
- Non-commutative Geometry
- String Field Theory

(2) Application of String Theory
- Holographic QCD
- Black Hole Entropy

(3) Dynamics of Fields
- Lattice Theory
- Higher-order QED

(4) Use of Fields and Strings
- Phenomenology
- Color Superconductivity

These achievements were only possible with the help of Tsukasa Tada, Vice Chief Scientist, Makiko Nio, Nishina Center Research Scientist, and the following former members who have left RIKEN:

Masashi Hayakawa
Associate Professor at Nagoya University

Hiroshi Suzuki
Professor at Kyushu University

Koji Hashimoto
after being Associate Chief Scientist, now Professor at Osaka University

Many young researchers, all of whom I cannot name owing to the limitation of space, also contributed to the activities of our group. At one point, our Laboratory accommodated eight Special Post-Doctoral Researchers.

Furthermore, researchers from all over the world visited us for presenting seminars or for collaborations. The following list includes some of the prominent researchers who visited us:

· Harry Lipkin
· Antal Jevicki
· Yuri Makeenko
· Holger Nielsen
· Herman Verlinde
· M. Staudacher
· J. Maharana
· Robert Dijkgraaf

The following distinguished scientists also stayed at our group for a prolonged period, most of them multiple times, to conduct their research activities and collaborations:

· Toichiro Kinoshita
· Al. Zamolodchikov
· Ivan Kostov
· Amihay Hanany
· Avinash Dhar

Thus, one could say that the Theoretical Physics Laboratory at RIKEN was beginning to establish its presence in the international research community. Although the Theoretical Physics Laboratory itself ceased to exist, I hope its legacy has been passed on to the current activities for theoretical studies at RIKEN.

To conclude, I would like to thank all the former members of the Theoretical Physics Laboratory for participating in this undertaking. Special thanks go to Dr. Kanetada Nagamine, who paved the way to my position as an invited chief scientist at RIKEN. I am also grateful to all the members of Nishina Center, especially Dr. Yasushige Yano, the founding director, and Dr. Hideto En'yo, the succeeding incumbent.

*1 Chief Scientist of Theoretical Physics Laboratory (2001–2008)
*2 Present address: Department of Physics, Kyoto University

Quantum Hadron Physics Laboratory

T. Hatsuda[*1,*2]

The Quantum Hadron Physics (QHP) Laboratory[1] in RIKEN Nishina Center was established on April 1, 2011 with Tetsuo Hatsuda (Professor, Univ. Tokyo, at the time) as a concurrent Chief Scientist. On April 1, 2012, Hatsuda moved to RIKEN as a full-time Chief Scientist. He is currently a Director of RIKEN iTHES[2] (interdisciplinary Theoretical Science Research Group, FY2013–FY2017), and a Program Director of RIKEN iTHEMS[3] (interdisciplinary Theoretical and Mathematical Sciences Program, FY2016–present).

One of the most important goals of the QHP Laboratory is to attract young bright theorists to RIKEN Nishina Center and create a good atmosphere for them to interact with each other and to produce original ideas. This is exactly what Dr. Yoshio Nishina has provided to Dr. S. Tomonaga, Dr. H. Yukawa, and others at RIKEN. Here, we recapitulate an English translation of the famous saying by Nishina, "Researchers' growth depends on their environment, and a good environment depends on the researchers." To accomplish the above goal, nine core members (including T. Hatsuda) from inside and outside of RIKEN working on diverse topics in theoretical physics have been appointed, as listed below.

Particle Physics:

Dr. Tsukasa Tada (2013–)	Deputy Chief Scientist
Dr. Hiroshi Suzuki (2011–2013)	Senior Research Scientist
Dr. Makiko Nio (2011–)	Nishina Center Researcher

Hadron Physics:

Dr. Tetsuo Hatsuda (2011–)	Chief Scientist
Dr. Takumi Doi (2011–)	Senior Research Scientist
Dr. Yoshimasa Hidaka (2012–)	Senior Research Scientist

Nuclear Physics:

Dr. Haozhao Liang (2015–)	Research Scientist
Dr. Nguyen Dinh Dang (2016–)	Nishina Center Researcher

Atomic Physics:

Dr. Pascal Naidon (2012–)	Senior Research Scientist

The QHP Laboratory has also accepted a number of post-doctoral researchers and graduate students from Japan and overseas to create an active research environment. Figure 1 shows the number of QHP Laboratory members in FY2011–FY2016. The QHD Laboratory has theoreticians in particle physics, hadron physics, nuclear physics, and atomic physics (as well as broader range of researchers from iTHES/iTHEMS) in a single lab. This varied mix has generated fruitful mutual interactions among the members to venture into new directions. Furthermore, this became a source of high productivity of the QHP Laboratory, as shown in Fig. 2.

*1 Chief Scientist of Quantum Hadron Physics Laboratory (2011–present)

*2 Program Director of RIKEN iTHEMS (interdisciplinary Theoretical and Mathematical Sciences) Program (2016–present)

The scientific activities of the QHP Laboratory are highly acclaimed in the community: 7 members received 10 awards (either domestic or international) as of March, 2017. Moreover, 5 invited review articles by the QHP Laboratory members were published, and 5 highlighted works have been released in press. Outreach activities are also taken seriously in the QHP Laboratory; 11 YouTube videos have been released to explain fascinating fundamental physics to the public. Owing to the interactions with iTHES and iTHEMS, the activities of the QHP Laboratory became even broader, and collaborations among theoretical physicists, theoretical biologists, engineers, and mathematicians have started. We hope that these collaborations would spur new breakthroughs in the coming 30 years.

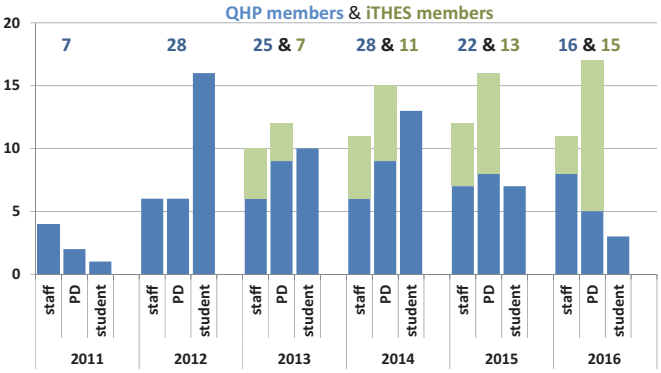

Fig. 1. Number of QHP Laboratory staff, post-doctoral researchers, students, and iTHES members in FY2011–FY2016.

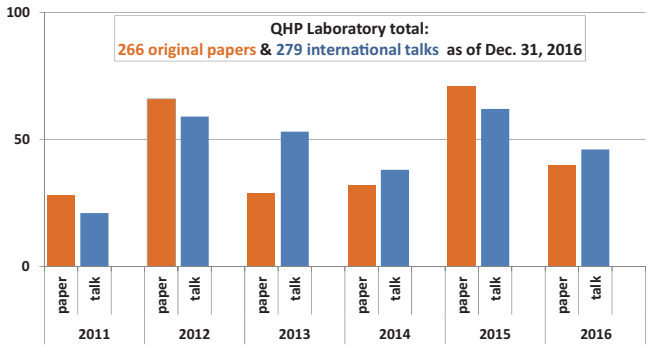

Fig. 2. Original papers and international conference talks by QHP members (as of Dec. 31, 2016).

References

1) QHP Laboratory in Nishina Center, http://ribf.riken.jp/QHP/ .
2) iTHES Research Group, http://ithes.science-server.com/ .
3) RIKEN iTHEMS Program, https://ithems.riken.jp/ .

Theoretical Nuclear Physics Laboratory

Takashi Nakatsukasa [*1,*2,*3]

The Theoretical Nuclear Physics (TNP) Laboratory started in August 2007 when I was appointed as an Associate Chief Scientist. This was the first research group in RIKEN focusing on studies of theoretical nuclear physics. Main aims of the Laboratory were to develop theories for finite quantum many-body systems and to discover/predict new concepts/phenomena in exotic nuclei. To achieve these goals, we have also developed efficient computational methodologies. Daily contacts with experimental groups provided us with stimulating environments. It was an exciting opportunity as a member of RIKEN Nishina Center, sitting inside the most powerful RI-beam facility in the world.

Soon after the TNP Laboratory was established, Dr. Kohama, who was a research staff working on the nuclear theory, moved to the TNP Laboratory from Heavy-Ion Nuclear Physics (HINP) Laboratory (Chief Sci.: Dr. Motobayashi). Thanks to many brilliant young postdoctoral fellows, we succeeded to maintain a high level of activities in our group. The number of group members changed year by year, but steadily increased up to 2010. Dr. Dinh Dang, who had been a Nishina Center Research Scientist in the HINP Laboratory, also joined the TNP Laboratory in 2010 when the HINP Laboratory was closed at the retirement of Dr. Motobayashi. We had fourteen members and several regular visitors in 2010. In 2013, I myself decided to leave RIKEN, and moved to University of Tsukuba in April 2014. Since then, the group was entering a closing stage, for which I was acting as an invited group head for two years. There were three postdocs in 2014, only one in 2015. *And Then There Were None.* The TNP Laboratory was officially closed in March 2016.

Exploring elementary modes of excitation in nuclei was one of major research subjects in the TNP Laboratory; collective motion under ultra-fast rotation, those associated with the isospin degrees of freedom, shell-structure dependence, non-adiabatic effect, strong anharmonicity in low-lying collective states, and their dissipation. The finiteness of nucleus and the nature of the strong interaction lead to unique properties of collective modes. We were interested in this uniqueness of nuclear-structure physics as a strong-coupling finite-quantum system. Currently in University of Tsukuba, I am working on somewhat continuous line of these subjects, together with graduate students.

Theoretical methodologies developed in nuclear physics have many things in common in other fields of physics. In the TNP Laboratory, there were activities in these related areas. We studied superfluidity in fermionic cold atoms, electronic dynamics in solids, photoresponse in molecules and clusters, etc., using techniques identical (similar) to nuclear physics. Quantum statistics of mesoscopic systems, dissipation in finite systems, microscopic description of macroscopic properties, etc., these are long-standing problems in the nuclear physics and important issues in the other fields of mesoscopic physics as well.

When I started the TNP Laboratory, RIKEN was in charge of constructing a peta-flops supercomputer, currently known as the "K" computer. I was involved in HPCI Strategic Program Field 5 (URL: `http://www.jicfus.jp/field5/en/`) to develop applications in nuclear physics for the K computer. This became one of major research issues in the TNP Laboratory. We made extensive effort to develop computer codes for large-scale parallel computation, based on the time-dependent density-functional approaches to collective dynamics in nuclei. Our project on the K computer produced a number of novel results in the field of nuclear physics, including photonuclear reaction, nucleus-nucleus collision, charge-exchange reaction, and neutrinoless double-beta decay.

University of Tokyo and University of Tsukuba established Joint Center for Advanced High Performance Computing (JCAHPC). JCAHPC has recently introduced a new supercomputer system "Oakforest-PACS" with 25 PFLOPS peak performance, currently the fastest in Japan. The developments done in the TNP Laboratory have produced several applications, running on the Oakforest-PACS.

I thank all the former members and visiting scientists in the TNP Laboratory. Their contributions and support were essential elements to keep the TNP Laboratory lively and active. More details about researches and history of the TNP Laboratory can be found at the following site:

`http://www.nishina.riken.jp/lab/TNP/`.

Cheers and thank you to all!

Fig. 1. Photograph on March 28, 2016, at RIBF Conf. Room.

*1 Associate Chief Scientist of Theoretical Nuclear Physics Laboratory (2007–2016)
*2 Center for Computational Sciences, University of Tsukuba
*3 iTHES Research Group, RIKEN

Gaussian Expansion Method and its application to nuclear physics with strangeness

E. Hiyama*1

In physics, there are a lot of important and interesting problems to solve the Schrödinger equation for few-body systems with high accuracy. Therefore, it is very important to develop methods for such problems. As one of the calculation methods, in the 1980s, the Gaussian Expansion Method (GEM), which is one of the ab initio variational methods for few-body systems, was proposed by Kamimura, who performed non-adiabatic three-body calculations of muonic molecules and muon-atomic collision.[1)]

This method was successfully applied to three-nucleon bound states such as the ^{3}H and ^{3}He systems, unstable nuclei, and antiprotonic helium atoms. When one proceeds to four-body systems, the calculation of the Hamiltonian matrix elements becomes rather laborious. In order to make the four-body calculation tractable even for complicated interactions, the infinitesimally shifted Gaussian lobe basis function has been proposed. GEM with the technique of infinitesimally shifted Gaussians has been applied to various three-, four-, and five-body calculations in hypernuclei; the four-nucleon systems; and ultracold-atom systems.

As shown in Fig. 1, we have been studying many subjects in various research fields of physics using the more developed GEM. The strategy for such studies is as follows. We have been applying GEM to various research fields, such as (1) hypernuclear physics, (2) ultracold-atom physics, (3) the physics of unstable nuclei, etc. and have contributed to each research field. As a feedback of the numerical efforts for the contributions, we have been able to develop the calculation method GEM further at the center and then apply the developed GEM to a new field, which has not been studied previously by the present laboratory. As a project in the laboratory, we have been repeating this type of research cycle under this strategy.

In my laboratory, we have been focusing on hypernuclear physics. Here, I mention some highlights of our studies in hypernuclear physics.

One of the main goals in hypernuclear physics is to understand the baryon-baryon interaction. The baryon-baryon interaction is fundamental and important for the study of nuclear physics.

In order to obtain information on the baryon-baryon interaction, it is important to study the structure of hypernuclei.

Since I started our laboratory in 2008, our laboratory mainly studied the charge symmetry breaking (CSB) effect between Λ and neutron, and Λ and proton by studying $A = 7$ Λ hypernuclei, $^7_\Lambda$He, $^7_\Lambda$Li($T = 1$) and $^7_\Lambda$Be.[2)] We found that, if there is a large CSB effect in s-shell Λ hypernuclei between $^4_\Lambda$H and $^4_\Lambda$He, we need an odd-state CSB effect with opposite sign with an even-state CSB for $A = 7$ hypernuclei. Another hot topic in hypernuclear physics is to obtain ΛN-ΣN coupling. For this study, in 2014, the nnΛ system was observed as a bound state at GSI.[3)] For this purpose, we studied the nnΛ system by taking ΛN-ΣN coupling explicitly to produce the binding energies of $^3_\Lambda$H, $^4_\Lambda$H, and $^4_\Lambda$He. We do not find any bound state for the nnΛ system, which contradicts the data obtained at GSI. Therefore, we need to perform a confirmation experiment at GSI. We also studied the strangeness $S = -2$ system, which is the entrance to the multi-strangeness world. Especially, the observation of the "Hida" event was reported in an emulsion experiment.[4)] We studied this event within the framework of the α+α+n+Λ+Λ five-body problem. The observed Hida event can be interpreted to be the ground state. When our calculated binding energy is compared with the experimental value of 20.83 MeV with a large uncertainty of σ = 1.27 MeV, we can say at least that our result does not contradict the data within 2σ.

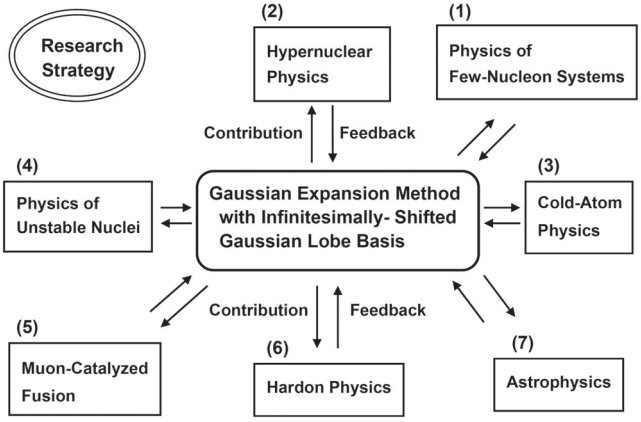

Fig. 1. Research strategy program in the strangeness nuclear physics laboratory.

References
1) E. Hiyama, Y. Kino, M. Kamimura, Prog. Part. Nucl. Phys. **51**, 223 (2003).
2) E. Hiyama, Y. Yamamoto, T. Motoba, M. Kamimura, Phys. Rev. C **80**, 054321 (2009).
3) J. K. Ahn et al., Phys. Rev. C **88**, 014003 (2013).
4) C. Rappold et al., Phys. Rev. C **88**, 041001(R) (2013).

*1 Associate Chief Scientist/Chief Scientist of Strangeness Nuclear Physics Laboratory (2008–present)

Mathematical Physics Laboratory

K. Hashimoto[*1,*2]

Mathematical Physics Laboratory, led by Associate Chief Scientist Koji Hashimoto, has been in Nishina Center for the period of April 2010–March 2015.

Here, we briefly summarize the research achievements of the laboratory.

- 74 published papers in international refereed journals, as well as 26 preprints and 9 proceedings
- 9 workshops including several workshops with more than 100 participants
- 97 lab seminars

The laboratory consists of Koji Hashimoto, the head of the lab, and 17 post-doctoral researchers in total. Among those, 4 post-doctoral researchers were promoted to permanent faculty positions in universities and research institutes.

The Mathematical Physics Laboratory was formulated such that every member can go through various subjects in theoretical physics by using the powerful force of mathematics. In particular, mathematical concepts of superstring theory have been applied to nuclear physics, elementary particle physics, condensed matter physics, and cosmology. Obviously, these fields are very different subjects from the viewpoints of energy scales, tools, objectives, and goals. However, a common mathematical structure can bridge different subjects. Our achievement is mostly on the relation between hadron physics and gravity. One of the interesting outcomes was a generalization of the Nambu-Goldstone theorem found by Dr. Hidaka, one of our members.[1)]

The idea of bridging different subjects in science, which is attempted in this laboratory, was in line with the original idea of the foundation of RIKEN. The idea was confirmed to be successful and resulted in a number of interesting research papers. It became one of the origins of the iTHES project in RIKEN, and the laboratory promoted young researchers to find novel opportunities in sciences.

Reference

1) Y. Hidaka, Phys. Rev. Lett. **110**, 9, 091601 (2013).

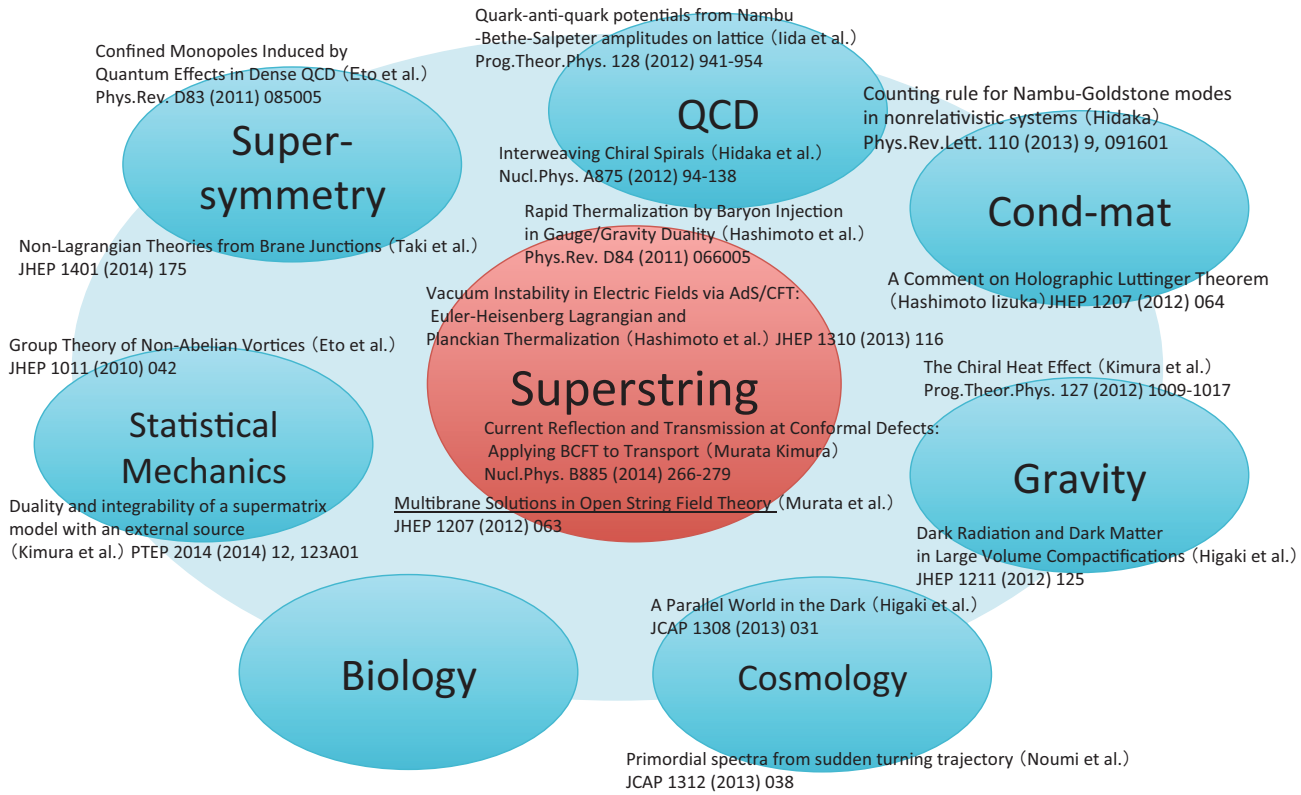

*1 Associate Chief Scientist of Mathematical Physics Laboratory (2010–2015)
*2 Present address: Department of Physics, Osaka University

A brief history of the High-Energy Astrophysics Laboratory

T. Tamagawa, *1 on behalf of the laboratory members

1 Overview

The High-Energy Astrophysics Laboratory started in April 2010. The goals of our research activities are 1) to reveal the mechanism of nucleosynthesis and the evolution of elements in our universe, 2) to study the particle acceleration mechanisms by shockwaves or electrical potential, and 3) to observe/discover exotic physical phenomena in extremely strong magnetic and/or gravitational fields. We have observed supernova remnants (SNRs), strongly magnetized neutron stars, pulsars, black holes, galaxies, and planets of the solar system with UV, X-ray, and gamma-ray astronomical satellites and/or ground-based telescopes.

At the beginning of the laboratory in 2010, we set a goal for the first five years to complete the construction of two X-ray satellite missions, ASTRO-H (spectroscopy) and PRAXyS (polarimetry). X-rays carry four independent physical quantities: position, timing, energy, and polarization. X-ray astrophysics has been advanced by observing those quantities of X-rays from high-energy astrophysical objects. However, there is significant room to improve the observational sensitivities in X-ray spectroscopy and polarimetry with current techniques. This is why we are concentrating on those two quantities to open a new window in astrophysics.

In general, the construction of satellite missions is not an easy task. Five post-doctoral fellows (A. Hayato, T. Kitaguchi, T. Enoto, W. Iwakiri, and T. Nakano) have contributed to the PRAXyS project, and five other post-doctoral fellows (T. Yuasa, H. Noda, K. Ishikawa, G. Sato, and T. Enoto) have contributed to the construction, integration, and testing of ASTRO-H.

In parallel with the contribution to those missions, we have analyzed the data of high-energy stellar objects observed by currently working satellites such as Suzaku (5th Japanese satellite launched in 2005), XMM-Newton (Europe), and Chandra (US). Some of the research highlights are the first detection of Cr and Mn in a Type-Ia SNR, the first measurement of the expansion velocity of ejecta in Tycho's SNR,[1)] and discovery of charge-exchange emission in SNRs.[2)]

2 PRAXyS and ASTRO-H missions

The polarimeter for Astrophysical X-ray Sources (PRAXyS) is one of NASA's small explorer missions and is led by the Goddard Space Flight Center (NASA/GSFC). RIKEN is a key institute of the project, providing a core device, "Gas Electron Multiplier (GEM) foil," of the X-ray polarimeter. In 2009 the project was selected by NASA for launch in 2014. However, it was cancelled in May 2012 owing to unexpected cost overrun by NASA. The joint group of NASA and RIKEN re-submitted the project proposal to NASA, which was fortunately selected for Phase-A (conceptual design) study in July 2015. We have led the Phase A study with NASA/GSFC, and our results are summarized in Iwakiri et al. (2016).[3)]

The 6th Japanese X-ray astronomical satellite ASTRO-H (named "Hitomi" after the launch), which was launched on February 17, 2016 from JAXA's Tanegashima Space Center (TNSC) by the H-IIA launch vehicle F-30. The Hitomi satellite is constructed by all the Japanese institutes related to the X-ray astrophysics including RIKEN in collaboration with US and Europe. The total mass of the satellite is 2.7 ton, and the length is 14 m after deploying the optical boom. Hitomi carries four X-ray and gamma-ray detectors covering the 0.3–600 keV energy range. Our laboratory, in collaboration with JAXA, Tokyo Metropolitan University, Kanazawa University, Saitama University, NASA/GSFC etc., contributed to the soft X-ray spectrometer (SXS), which achieved unprecedented energy resolution (∼5 eV) in the 0.3–12 keV energy band with a low-temperature micro calorimeter. Soon after the launch, SXS achieved the operation temperature and observed the Perseus galaxy cluster and some other celestial objects for verifying the detector system. Although the Hitomi satellite was lost in March 2016 owing to a tragic accident, the data obtained in the verification phase were analyzed and published in Nature.[4)] This analysis demonstrated the excellent capability of the microcalorimeter in spectroscopy. A recovery mission is planned for launch in 2021.

3 Other missions

Besides the missions described above, we are partially contributing to the following missions:

- Hisaki: The Japanese small satellite dedicated for planetary science, observing EUV photons. (Contributor: T. Kimura.) The transient brightening of Jupitar's aurora coincident with the arrival of the solar wind was discovered and published by Kimura.[5)]
- NuSTAR: NASA's small explorer mission for hard X-ray imaging in the 5–80 keV band. The world's first project with imaging capability in the hard X-ray band opened a new field in observation:

*1 Associate Chief Scientist/Chief Scientist of High Energy Astrophysics Laboratory (2010–present)

nuclear astrophysics. A major achievement is the mapping of radioactive ^{44}Ti in Cassiopeia A SNR.[6] (Contributor: T. Kitaguchi)

- NICER and MAXI: Both are X-ray observatories onboard the International Space Station (ISS). NICER is a mission of NASA/GSFC for exploring the interior of neutron stars, which was launch in June 2017. MAXI is the RIKEN-led all sky X-ray monitor mission. It is expected that alerts of transient phenomena such as outbursts of neutron star or black hole binaries detected by MAXI will trigger deeper observations by NICER. Those observations probably permit the detection of elements produced in the nuclear burning on the neutron star surface etc. (Contributors: T. Enoto, W. Iwakiri, and T. Tamagawa)
- Large Synoptic Survey Telescope (LSST): All sky survey telescope in the optical band being constructed by a US community. The telescope surveys all sky of the southern hemisphere with ∼24 mag sensitivity every three days. It is under construction and the expected first light is in 2019. This telescope has good synergy with all sky X-ray monitor missions such as MAXI in astrophysics. (Contributors: Y. Okura, T. Tamagawa through RIKEN Brookhaven Research Center) A major contribution to LSST is the evaluation of CCD systematics.[7]
- Future X-ray spectrometry missions, DIOS and Athena: DIOS is a Japanese small satellite that will explore the missing baryon in the universe in the 2020s, and Athena is the ESA's large class mission for observing the evolution of galaxies/clusters in the late 2020s. (Contributors: H. Noda, T. Tamagawa)

References

1) A. Hayato et al., Astrophys. J. **725**, 894 (2010).
2) S. Katsuda et al., The Astrophysical Journal **756**, 49 (2012).
3) W. B. Iwakiri et al., Nucl. Instrum. Meth. Phys. Res. A **838**, 89 (2016).
4) The Hitomi collaboration, Nature **535**, 117 (2016).
5) T. Kimura et al., Geophys. Res. Lett. **44**, 4523 (2017).
6) B. W. Grefenstette et al., Nature **506**, 339 (2014).
7) Y. Okura et al., Astrophys. J. **825**, 61 (2016).

Six Years of cross-disciplinary studies at the Astro-Glaciology Research Unit: Astronomical signatures in polar ice cores

Yuko Motizuki*1

Our Astro-Glaciology Research Unit (AGU), established on July 1, 2011, is the only group worldwide investigating the new cross-disciplinary research field of astro-glaciology, which combines astrophysics, climate science and solar-terrestrial physics, and glaciology, both experimentally and theoretically (Figs. 1 and 2).

Gamma rays, X-rays, and UV radiation arising from solar activity and supernova explosions in our galaxy cause changes in the chemical composition of the stratosphere (from $\sim 10 - 50$ km altitude). The effects of radiation on the stratosphere are then recorded in the chemical and isotopic composition of terrestrial ice.

An ice core is therefore a time capsule. The cylindrical ice core drilled by the Japanese Antarctic Research Expedition (JARE) at the Dome Fuji station in Antarctica is 3,035 m long and corresponds to a time period from 720,000 years ago to the present (Fig. 3). We have been studying the uppermost $\sim$100 m of an ice core that was recovered from the same hole as the deep ice core shown in Fig. 3 as well as another shallow ice core; both cases correspond to the last 2,000 years. A newly approved project to obtain an ice core corresponding to a 1,000,000 year period has already commenced.

There are significant advantages in using Dome Fuji ice cores when studying astronomical phenomena of the past, because the effects of radiation on the stratosphere recorded in ice cores in the Dome Fuji area are more pronounced than in ice cores obtained from elsewhere on the earth.

Anions and cations in our ice cores were analyzed at RIKEN using an ultra-high-sensitivity ion chromatography technique[a] (Fig. 4). The sulfate ion (SO_4^{2-}) concentration spikes indicate volcanic eruptions and can provide time markers for dating ice cores. The SO_4^{2-} spikes (Fig. 5) observed in Dome Fuji ice cores are an order of magnitude higher than those in a standard ice core drilled in West Antarctica.[b] This demonstrates an important advantage when using our cores, since high volcanic SO_4^{2-} spikes imply a high level of inclusion of stratospheric components.

Collaboration between AGU and the National Institute of Polar Research (NIPR, Tokyo) involves analyzing ionic and isotopic concentrations in Dome Fuji ice cores. Our aim is to reveal in the ice cores:

(1) signatures of past solar cycles
(2) relationships between past solar activity and climatic changes
(3) footprints of past supernova explosions in our galaxy, in order to understand better the rate of galactic supernova explosions.

Fig. 1. Our AGU group in the low temperature room (-30°C and -50°C) at NIPR (2012).

Fig. 2. Dr. Yoichi Nakai sampling an ice core in the low temperature room (-30°C) at NIPR (2012).

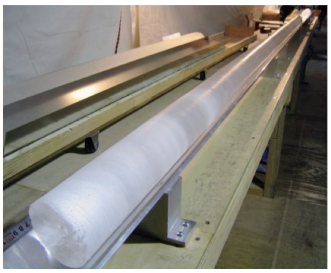

Fig. 3. A deep ice core drilled in 2007 at Dome Fuji station in inland Antarctica (photograph courtesy of NIPR).

*1 Research Unit Leader, Astro-Glaciology Research Unit, RIKEN Nishina Center (2011−present)

a) High-resolution chemical analysis of ice core samples from Dome Fuji station, Antarctica: Y. Motizuki, K. Takahashi et al.: Geochemical J. 51, 293-298 (2017) [Press-release]

b) 2000-yr record of volcanism: M. Sigl, Y. Motizuki et al.: Nature Climate Change 4, 693-697 (2014) [Press-release]

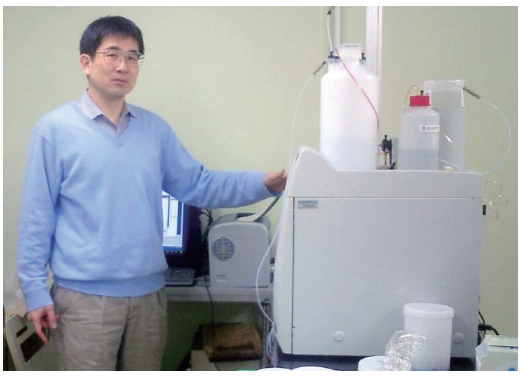

Fig. 4. Dr. Kazuya Takahashi with our first ultra-high-sensitivity anion chromatography detector (ICS2000 system) in a clean room at RIKEN (2006).

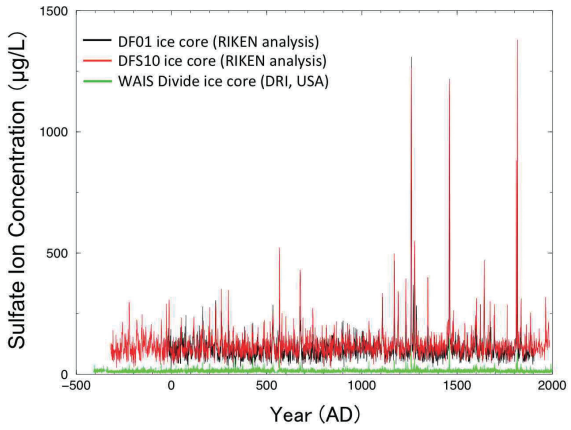

Fig. 5. SO_4^{2-} concentrations shown versus year (AD) for two Dome Fuji ice cores and a standard ice core drilled in West Antarctica (WAIS Divide, USA). The temporal resolution is ∼1 year. Spikes represent volcanic activity.

We have succeeded in extracting periodicities that correspond with solar cycles from the annually-resolved nitrate ion (NO_3^-) concentrations in a Dome Fuji ice core, and we have found candidate NO_3^- spikes that correspond with supernova explosions in our galaxy. Since the dates of several NO_3^- spikes almost match the dates of galactic supernova explosions that have occurred in the last millennium, we conjecture that yearly-scale NO_3^- concentration spikes found in Dome Fuji ice cores can be treated as a candidate proxy for supernova explosions that have occurred in our galaxy. We have also discovered a strong statistical correlation ($r = 0.84$) between variations in solar activity and variations in the temperature proxy ($^{18}O/^{16}O$) in a segment of our ice core that corresponds to a pre-industrial period.

Theoretically-based numerical simulations and experimental evidence will be combined. We have simulated chemical compositional changes in the stratosphere induced by solar proton events [SPEs: the bombardment of the atmosphere by high-energy (∼10 − 500 MeV) protons originating in solar flares], in collaboration with the National Institute of Environmental Science (Tsukuba). To do this, we developed a 1D box model, taking into account 752 reactions including ion chemistry.[1)] We are also developing a 3D chemical climate model with a view of studying changes in the chemical composition of the atmosphere and the effects on climate pertaining to past and future SPEs and supernovae in our galaxy.

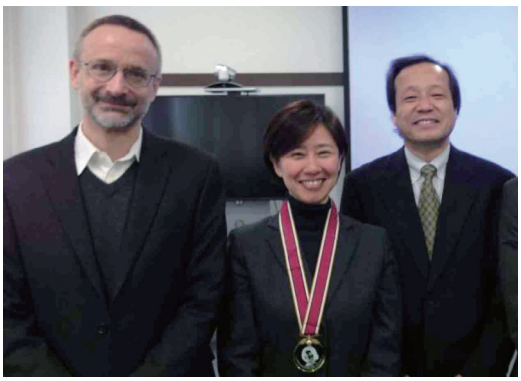

Fig. 6. Left to right: Prof. Marc Besancon (French Director, Toshiko Yuasa Laboratory (TYL)), Yuko Motizuki (AGU leader), and Prof. Junji Haba (Japanese Director, TYL) at TYL Gold Prize ceremony (Feb., 2017).

Cross-disciplinary collaboration between AGU and the RIKEN Center for Advanced Photonics has been initiated in order to develop an automated laser ice-core melting system. The system will make it possible to analyze deeper ice cores at a higher temporal resolution (∼1 month), and it will thus become possible to investigate the galactic supernova rate and solar activity of the past 1,000,000 years.

The initial 3-year research project was supported by the Funding Program for Next Generation World-Leading Researchers (NEXT Program, Grant Number GR098) of the Council for Science and Technology Policy (CSTP). The project has been awarded an S-grade by CSTP (2015) within the NEXT Program.

Our research unit leader was awarded the Toshiko Yuasa Gold Prize in 2017 (Fig. 6), the theme being "Pioneering a new interdisciplinary research field regarding Antarctic ice cores and exemplifying leadership in academia"; and our leader was also granted Nice Step Scientist Certificate by MEXT National Institute Science and Technology Policy (NISTEP) in 2015.

Two postdoctoral researchers have participated, and four undergraduates and two postgraduate students have received degrees during this research project.

Reference

1) see, e.g., Y. Nakai, Y. Motizuki et al.: in this volume.

Overview of activities of the NUSPEQ group in CNS

S. Shimoura*1

Varieties in the properties of nuclei far from stability give rich information on the nuclear structure in a wide area of the nuclear chart. Experiments using radioactive isotope (RI) beams in the last few decades have shown exotic phenomena such as neutron halos, soft collective excitations, and changes of magic numbers. We are realizing that the nuclear structure should be studied as a function of the proton and neutron numbers (Z and A) as well as of the excitation energies (E_x).

Based on this consideration, the NUSPEQ[a] group in CNS started the in-beam spectroscopy of exotic nuclei with direct reactions of RI beams at several tens of MeV per nucleon in FY2000. In FY2003, we extended the studies to approach high-spin states by using fusion reactions of RI beams at a few MeV per nucleon. Major parts of the studies before FY2006 were performed at the RIPS facility.

The firstly developed equipment was a liquid helium target,[1] which enables measurements of α-induced reactions on exotic nuclei. An array of position-sensitive Ge detectors, GRAPE, was developed for measuring in-flight γ decay with high resolution.[2] For total-energy measurements of projectile-like ejectiles, an array of NaI(Tl) detectors was also developed.

By using the developed equipments combined with invariant mass and/or in-beam γ-ray spectroscopies, the following studies were performed: (1) (α, α') reactions for studying isoscalar responses of ^{14}O[3] and cluster states in ^{12}Be.[4] (2) shell evolution in neutron-rich fluorine[5] and boron[6] by using proton-transfer reactions (α,t), and (3) electric quadrupole excitation of neutron-rich nuclei by Coulomb excitations.[7] As a by-product of the experiment using the ^{12}Be beam, the isomeric 0^+ state was discovered by analyzing cascade γ-ray decays in flight, and its lifetime was measured, which shows the disappearance of $N = 8$ magicity.[8]

For high-spin study, we developed a low-energy ^{46}Ar beam by using a set of energy degraders.[9] By using the ^{46}Ar beam and the GRAPE array, a fusion reaction ^{9}Be(^{46}Ar, 5n)^{50}Ti was measured to study high-spin states of ^{50}Ti.[10] The superdeformation in ^{40}Ar was also found for the first time by using the ^{26}Mg(^{18}O, 2p2n)^{40}Ar reaction at the JAEA tandem facility.[11]

In FY2005, CNS started the SHARAQ[b] project[12] in order to extend research opportunities in the RIBF and completed the construction of the spectrometer at the end of FY2008. The NUSPEQ group a played major role in the developments and research activities. The basic idea of the SHARAQ project is to use the RI beams as probes for the direct reactions, in which a variety of isospin (T), internal energy (mass excess), and spin (S) different from those of stable beams exist. We focused on the exothermic charge-exchange reaction of RI beams, in which the internal energy of the beam particle is used for exciting the target nucleus with a very small momentum transfer.

In the SHARAQ project, we developed tracking detectors for the high-resolution beamline[13] and the focal plane of the SHARAQ spectrometer. We also contributed to the development of the DAQ system including SHARAQ.[14]

The first result from the SHARAQ project was the isovector spin-monopole resonances in ^{90}Zr and ^{208}Pb by using the (t, ^{3}He) reaction at 300 A MeV.[15] The recent highlight is the possible candidate of the tetra-neutron resonance immediately above the 4n threshold obtained by using the ^{4}He(^{8}He, ^{8}Be) reaction at 190 A MeV[16] (Fig. 1).

Another program in the SHARAQ project is the direct measurement of the mass. In order to obtain very good timing information, we developed diamond detectors having $\sim$ 10 ps resolution.[17] The masses of nuclei around ^{54}Ca were simultaneously measured and determined with 160, 250, and 990 keV resolution for $^{55,\ 56,\ 57}$Ca to clearly demonstrate $N = 34$ magicity in the Ca isotopes.[18]

Parallel to the SHARAQ project, the NUSPEQ group joined the SEASTAR and the EURICA collaboration. Isomer spectroscopy of heavy neutron-rich nuclei was performed, several results of which have already been published.[19]

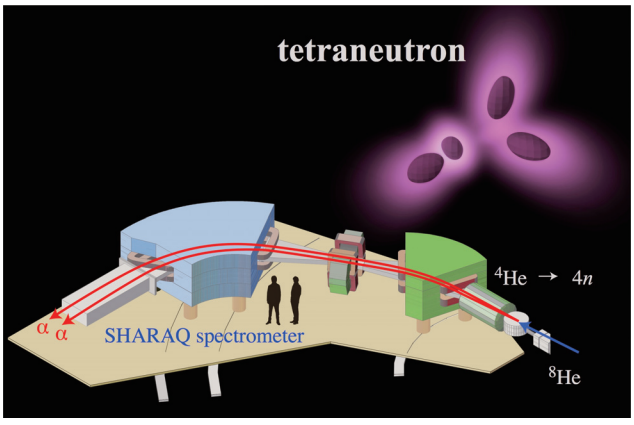

Fig. 1. Schematic image of the tetra-neutron experiment.

*1 Director of Center for Nuclear Study (CNS), the University of Tokyo (2016–present)

a) **NU**clear **SP**ectroscopy for **E**xtreme **Q**uantum system

b) **S**pectroscopy with **H**igh-resolution **A**nalyzer of **R**adio**A**ctive **Q**uantum beam

In FY2015, we have initiated the OEDO[c)] project, which aims at the deceleration of intense RI beams provided in the RIBF. Low-energy RI beams open opportunities for studying exotic nuclei by using nucleon/pair/cluster transfer, Coulomb excitation, incomplete fusion, and so on. The OEDO system consists of a mono-energetic degrader at a momentum-dispersive focus, two sets of quadrupole triplets, and an RF deflector. The RF deflector works as an optical matching element for the time-of-flight dispersion after the compression of energy spread after the degrader. The system was constructed by the end of FY2016.

The author acknowledges all the members in the NUSPEQ group over these 16 years for their excellent performance in the research activities.

References

1) H. Ryuto et al., Nucl. Instrum. Methods Phys. Res. A **555**, 1 (2005).
2) M. Kurokawa et al., IEEE Trans. Nucl. Sci. **50** 1309 (2003); S. Shimoura, Nucl. Instrum. Methods Phys. Res. A **525**, 188 (2004).
3) H. Baba et al., Nucl. Phys. A **788**, 188c (2007).
4) A. Saito et al., Nucl. Phys. A **738**, 337 (2004); A. Saito et al., Mod. Phys. Lett. A **25**, 1858 (2010).
5) S. Michimasa et al., Phys. Lett. B **638**, 146 (2006).
6) S. Ota et al., Phys. Lett. B **666**, 311 (2008).
7) H. Iwasaki et al., Phys. Lett. B **620**, 118 (2005); H. Iwasaki et al., Phys. Rev. C **78**, 021304 (2008).
8) S. Shimoura et al., Phys. Lett. B **560**, 31 (2003); S. Shimoura et al., Phys. Lett. B **654**, 87 (2007).
9) E. Ideguchi, Prog. Theor. Exp. Phys. **2012**, 03C005 (2012).
10) M. Niikura et al., Eur. Phys. J. A **42**, 471 (2009).
11) E. Ideguchi et al., Phys. Lett. B **686**, 18 (2012).
12) T. Uesaka et al., Nucl. Instrum. Methods Phys. Res. B **266**, 4218 (2008); T. Uesaka et al., Prog. Theor. Exp. Phys. **2012**, 03C007 (2012); S. Michimasa et al., Nucl. Instrum. Methods Phys. Res. B **317**, 305 (2013).
13) H. Miya et al., Nucl. Instrum. Methods Phys. Res. B **317**, 701 (2013).
14) H. Baba et al., Nucl. Instrum. Methods Phys. Res. A **616**, 65 (2010).
15) K. Miki et al., Phys. Rev. Lett **108**, 262503 (2012).
16) K. Kisamori et al., Phys. Rev. Lett. **116**, 052501 (2016).
17) S. Michimasa et al., Nucl. Instrum. Methods Phys. Res. B **317**, 710 (2013).
18) M. Kobayashi, PhD Thesis (University of Tokyo), Mar. 2017.
19) R. Yokoyama et al., Phys. Rev. C **95**, 034313 (2017); E. Ideguchi et al., Phys. Lett. B **686**, 18 (2010); E. Ideguchi et al., Phys. Rev. C **94**, 064322 (2016).

c) **O**ptimized **E**nergy **D**egrading **O**ptics for RI beam

Research activities of KEK RNB group at RIBF

H. Miyatake*1

How are gold and platinum elements synthesized in the universe? This is one of the important questions in fundamental science of the 21st century. The KISS project aims at finding the astrophysical origin of such heavy-element synthesis through the experimental nuclear physics.[1] This is a challenging and next-step project based on the scientific expertise of the Tokai Radioactive Ion Accelerator Complex (TRIAC), which was the first-generation Radioactive Nuclear Beam (RNB) facility of the post-acceleration scheme operated at the KEK Tokai campus.[2] The project was encouraged to proceed in the international review committee held in FY2009. Since then, KEK Isotope Separation System (KISS) was installed in experimental halls of the Nishina building at RIBF and has been utilized various experiments under the collaboration between RNC/RIKEN and IPNS/KEK. The first ceremonial meeting for this collaboration was held in October 2011.

According to the scenario of the rapid neutron capture (r-)process,[3] waiting nuclei as progenitors of the stable heavy elements around $A = 195$ can provide crucial information on the astrophysical circumstance through their masses, lifetimes, decay schemes, and neutron capture rates,[4] although these nuclei in the vicinity of the waiting region are still far to access.

We have proposed multi-nucleon transfer (MNT) reactions of intense neutron-rich heavy-ion beams as production tools.[5] Produced nuclei are stopped immediately in the KISS argon gas cell to be neutral atoms for further A- and Z-separation by applying the laser resonance ionization and dipole magnetic field (Fig. 1).[6] The commissioning of KISS was performed from 2011 to 2014 to confirm the A- and Z-separation of RIs reasonably extracted from the gas cell.[7] Apart from the KISS R&D, In-Gas Laser Ionization and Spectroscopy network (IGLIS-net[8]) has been launched in 2012 as an international information network of the physics subjects and techniques related to IGLIS with 15 groups and institutes worldwide. Further, the Wako Nuclear Science Center (WNSC) was established as a formal branch of IPNS, KEK at the RIKEN Wako campus in April 2015 for supporting user activities.

A new research activity on the nuclear mass measurements has been started in our group in FY2015 based on the joint R&D works with RNC of the Multi-Reflection Time-Of-Flight mass spectrograph (MRTOF).[9] The resolving power of MRTOF can reach the level of approximately 105 even for heavy-isotope measurements within a relatively short analyzing time less than 10 ms. It is a powerful tool not only for nuclear astrophysics but also for nuclear physics in a broad range of the nuclear chart.

As the first series of measurements (called the SHE-mass project), MRTOF was set at the focal plane

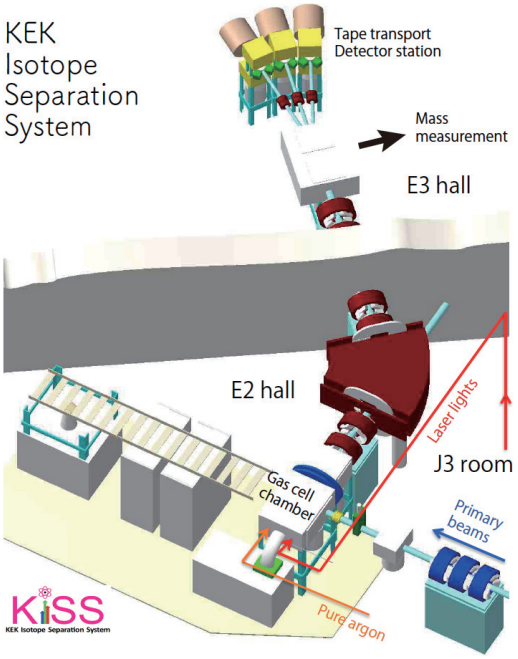

Fig. 1. Schematic drawing of KISS.

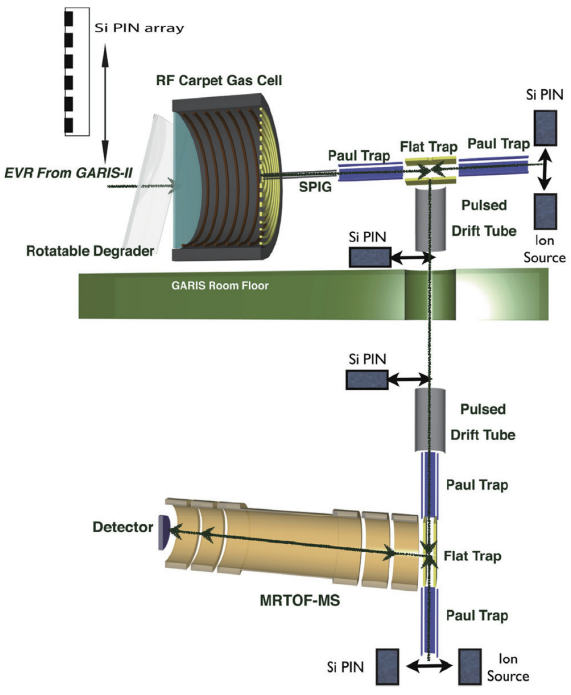

Fig. 2. Schematic drawing of the MRTOF system set at GARIS II.

*1 Head of Wako Nuclear Science Center, IPNS, KEK (2015–present).

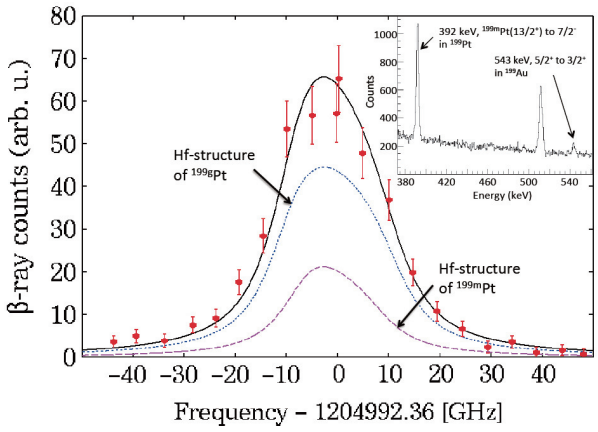

Fig. 3. Hyperfine (Hf-) structures of $^{199m,\ 199g}$Pt obtained with β-transitions of ^{199g}Pt. Short and long dotted lines indicate contributions of ^{199g}Pt and ^{199m}Pt, respectively. The Hf-structure of ^{199m}Pt is independently determined by the internal γ-transition (392 keV) from ^{199m}Pt shown in the inset.

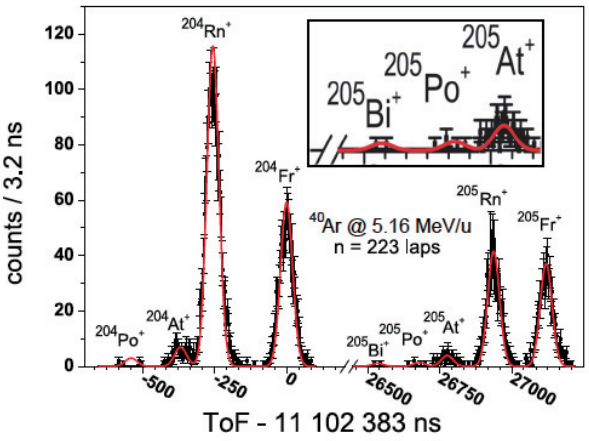

Fig. 4. Time-of-flight spectrum measured in the nuclear fusion reactions of ^{169}Tm and ^{40}Ar. Isotopes shown in the figure are clearly identified by comparison with tof-spectrum of a different number of flight laps, $n = 224$. RI of ^{205}Bi was clearly identified within an error of 1 MeV/c^2 by two detected events, as shown in the inset.

of GARIS II to determine the masses of evaporation residues in nuclear fusion reactions,[10] as shown in Fig. 2.

Thus far, a number of experimental subjects have been approved at RIBF-PAC, and their experiments have been performed with KISS and MRTOF devices. Those are RRC29, RRC37, RRC40, RRC41, RRC44, and RRC45 for the KISS experiments and LINAC07, LINAC23, and LINAC24 for the MRTOF experiments. KISS experimental subjects approved thus far include lifetime measurements of nuclei in the vicinity of the waiting region and decay- and laser-spectroscopies of isomeric and ground states in neutron-rich heavy nuclei. Subjects using MRTOF are devoted to the mass measurements of very heavy elements and proton-rich nuclei with astrophysical interests concerning X-ray bursters.

Figure 3 shows the first result of the hyperfine structures of ^{199g}Pt and ^{199m}Pt firstly measured in the recent KISS experiment (RRC41).[11] The magnetic moment and shift of the charge-radii of each state were clearly obtained. This experiment has been successfully performed under the collaboration between IBS and KEK, in which we have constructed a gamma-ray measurement system with super-clover Ge detectors from IBS and a mass measurement system with MRTOF in FY2016. The former system is already available, and the latter will be ready in FY2017 for KISS experiments and at the RAON facility[12] in future.

Figure 4 shows the first result of the SHE-mass project (LINAC07),[13] which reveals unique MRTOF characteristic as a mass spectrograph having a certain mass range with high sensitivity for a small amount of RIs. A typical mass-determination uncertainty is approximately 100 keV/c^2 for 100 detected ions in this mass region. Thus far, measurements have been performed for more than 80 isotopes, including new mass determinations of six isotopes of mendelevium ($Z = 101$) and einsteinium ($Z = 99$) elements.[14]

Based on the current research activities, WNSC has proposed an upgrade plan of the KISS project, which is KISS Stage II for a comprehensive study of element synthesis with precise nuclear spectroscopy covering the whole region of the nuclear chart.[15] It can be realized by the present KISS upgrade for accepting intense HI-beams and by installation of a pure RI spectroscopy line at the SLOWRI facility being commissioned.[16]

References

1) S. C. Jeong et al., KEK Report 2010-1 (2010).
2) H. Miyatake et al., Nucl. Instrum. Methods Phys. Res. B **204**, 746 (2003); S. C. Jeong et al., KEK Progress Report 2011-1 (2011).
3) E. M. Burbidge, G. R. Burbidge, W. A. Fowler, F. Hoyle, Rev. Mod. Phys. **29**, 547 (1957).
4) M. R. Mumpower et al., Progr. Part. Nucl. **86**, 86 (2016).
5) Y. X. Watanabe et al., Phys. Rev. Lett. **115**, 172503 (2015).
6) Y. Hirayama et al., Nucl. Instrum. Methods Phys. Res. B **376**, 52 (2016).
7) KEK RNB group, KISS_outline, (2015). `http://research.kek.jp/group/wnsc/facilities_and_devices/KISS_outline.pdf`
8) `http://research.kek.jp/group/kekrnb/iglis-net/`
9) H. Wollnik et al., Int. J. Mass Spect. **96**, 267 (1990).
10) P. Schury et al., Nucl. Instrum. Methods Phys. Res. B **376**, 425 (2016).
11) Y. Hirayama et al., accepted in Phys. Rev. C.
12) S. C. Jeong, New Physics: Sae Mulli **66** 1458 (2016).
13) P. Schury et al., Phys. Rev. C **95**, 011305(R) (2017).
14) Y. Ito et al., to be submitted.
15) H. Miyatake, at KEK-PIP Int. Rev. Comm. KEK (2016), unpublished.
16) M. Wada et al., AIP Conf. Proc. **865**, 352 (2006).

I. HIGHLIGHTS OF THE YEAR

<< Selection process of highlights >>

Highlights are selected by a two-step process. In the first step, a referee who reviews a manuscript decides whether she/he would recommend it as one of the highlights.
Members of the editorial board then make additional recommendations if they think an important contribution has not been recommended by the referee.

The second step involves the editor-in-chief proposing a list of highlights based on the recommendation given above to the editorial board. After discussing the scientific merits and uniqueness of the manuscripts from viewpoints of experts/non-experts, the editorial board makes the final decision.

Two-Proton Radioactivity of ^{67}Kr†

T. Goigoux,[*1] P. Ascher,[*1] B. Blank,[*1] M. Gerbaux,[*1] J. Giovinazzo,[*1] S. Grévy,[*1] T. Kurtukian Nieto,[*1] C. Magron,[*1] J. Agramunt,[*2] A. Algora,[*2,*3] V. Guadilla,[*2] A. Montaner-Piza,[*2] A. I. Morales,[*2] S. E. A. Orrigo,[*2] B. Rubio,[*2] D. S. Ahn,[*4] P. Doornenbal,[*4] N. Fukuda,[*4] N. Inabe,[*4] G. G. Kiss,[*4] T. Kubo,[*4] S. Kubono,[*4] S. Nishimura,[*4] H. Sakurai,[*4,*5] Y. Shimizu,[*4] C. Sidong,[*4] P.-A. Söderström,[*4] T. Sumikama,[*4] H. Suzuki,[*4] H. Takeda,[*4] P. Vi,[*4] J. Wu,[*4] Y. Fujita,[*6,*7] M. Tanaka,[*6] W. Gelletly,[*2,*8] P. Aguilera,[*9] F. Molina,[*9] F. Diel,[*10] D. Lubos,[*11] G. de Angelis,[*12] D. Napoli,[*12] C. Borcea,[*13] A. Boso,[*14] R. B. Cakirli,[*15] E. Ganioglu,[*15] J. Chiba,[*16] D. Nishimura,[*16] H. Oikawa,[*16] Y. Takei,[*16] S. Yagi,[*16] K. Wimmer,[*3] G. de France,[*17] S. Go,[*18] and B. A. Brown[*19]

β decay is the predominant decay mode in proton-rich nuclei close to stability, but further away from stability valley the binding energy of excess protons decreases and β-delayed proton emission becomes more likely. When the one or two-proton separation energies S_p and S_{2p} become negative, the dripline is reached and one- or two-proton emission from the ground state for odd- and even-Z elements, respectively, competes with β decay.

Two-proton ($2p$) radioactivity is a unique tool to study nuclear structure beyond the proton dripline. Predicted in 1960,[1] this direct emission of two protons was discovered in 2002 in the decay of ^{45}Fe.[2,3] The other known medium-mass cases ^{48}Ni [4] and ^{54}Zn [5] were discovered in the same decade.

According to mass predictions, the heavier nuclei ^{59}Ge, ^{63}Se and ^{67}Kr are candidates for $2p$ emission. They were successfully produced and identified during the ^{78}Kr beam campaign in 2015 [6] at RIBF. ^{63}Se and ^{67}Kr were observed for the first time and ^{59}Ge for the second.

The nuclei of interest [7] were implanted in WAS3ABi, a set of three DSSSDs to measure the energy of β particles and protons. The vertical and horizontal strips allowed ion-decay position correlations, greatly reducing the background in the energy spectra. WAS3ABi was surrounded by the EURICA γ-ray array.[8]

No $2p$ evidence was found for ^{59}Ge and ^{63}Se. Figure 1(a) and (c) do not show any peak without coincident β detection. However, the ^{67}Kr spectrum (e) shows a clear peak at 1690(17) keV originating from $2p$ radioactivity without any coincident β particle or 511-keV γ ray. A $2p$ branching ratio of 37(14)% and a half-life of 7.4(30) ms were found, leading to a $2p$ partial half-life of 20(11)ms, in strong disagreement with the three-body half-lives [9] for different ℓ^2 configurations.

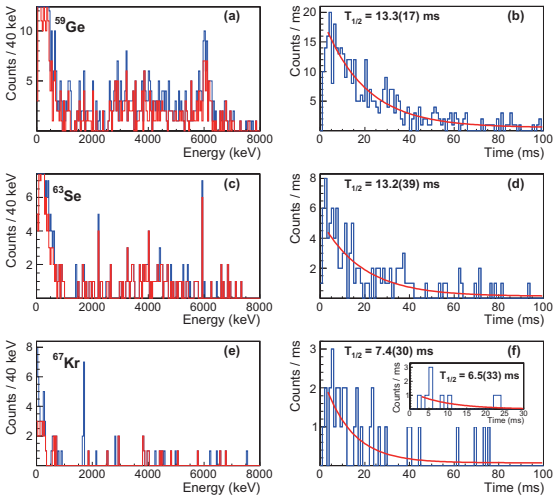

Fig. 1. Charged-particle energy spectra (left) and decay-time distributions (right) for events above 1 MeV to reject β decays without protons, for ^{59}Ge, ^{63}Se and ^{67}Kr. For the charged-particle spectra: in blue all decay events correlated within a 100 ms time window, and in red in coincidence with β particles detected in neighbouring detectors. The inset in (f) is obtained from the 1690-keV peak events of spectrum (e).[7]

References
1) V.I. Goldansky, Nucl. Phys. **19**, 482 (1960).
2) J. Giovinazzo et al., Phys.Rev. Lett. **89**, 102501 (2002).
3) M. Pfützner et al., Eur. Phys. J. A **14**, 279 (2002).
4) C. Dossat et al., Phys. Rev. C **72**, 054315 (2005).
5) B. Blank et al., Phys. Rev. Lett. **94**, 232501 (2005).
6) B. Blank et al., Phys. Rev. C **93**, 061301(R) (2016).
7) T. Goigoux et al., Phys. Rev. Lett. **117**, 162501 (2016).
8) P.-A. Söderström et al., Nucl. Instrum. Methods Phys. Res. Sect. B **317**, 649 (2013).
9) L. V. Grigorenko et al., Phys. Rev. C **68**, 054005 (2003).

† Condensed from the article in Phys. Rev. Lett. **117**, 162501 (2016)

*1 CEN Bordeaux Gradignan
*2 IFIC, CSIC-Universidad de Valencia
*3 Atomki, Debrecen
*4 RIKEN Nishina Center
*5 Department of Physics, University of Tokyo
*6 Department of Physics, Osaka University
*7 Research Center for Nuclear Physics, Osaka University
*8 Department of Physics, University of Surrey
*9 Comisíon Chilena de Energia Nuclear
*10 Institute of Nuclear Physics, University of Cologne
*11 Physik Department E12, Technische Universität München
*12 Laboratori Nazionali di Legnaro dell' INFN
*13 IFIN-HH
*14 INFN Sezione di Padova and Dipartimento di Fisica
*15 Department of Physics, Istanbul University
*16 Department of Physics, Tokyo University of Science
*17 Grand Accélérateur National d'Ions Lourds
*18 Dept. of Physics and Astronomy, University of Tennessee
*19 Department of Physics and Astronomy, and NSCL, MSU

94 β-decay half-lives of neutron-rich nuclei from $_{55}$Cs to $_{67}$Ho†

J. Wu,[*1,*2] S. Nishimura,[*2] G. Lorusso,[*2,*3,*4] P. Möller,[*5] E. Ideguchi,[*6] P.-H. Regan,[*3,*4] G.S. Simpson,[*7,*8,*9] P.-A. Söderström,[*2] P.M. Walker,[*4] H. Watanabe,[*10,*2] Z.Y. Xu,[*11,*12] D.S. Ahn,[*2] H. Baba,[*2] F. Browne,[*13,*2] R. Daido,[*14] P. Doornenbal,[*2] Y.F. Fang,[*14] N. Fukuda,[*2] G. Gey,[*7,*15,*2] N. Inabe,[*2] T. Isobe,[*2] D. Kameda,[*2] K. Korkulu,[*17] T. Kudo,[*2] P.S. Lee,[*16] J.J. Liu,[*11] Z. Li,[*1] D. Murai,[*2] Z. Patel,[*4,*2] V. Phong,[*18,*2] S. Rice,[*4,*2] H. Sakurai,[*2,*12] Y. Shimizu,[*2] L. Sinclair,[*19,*2] T. Sumikama,[*2] H. Suzuki,[*2] H. Takeda,[*2] M. Tanaka,[*6] A. Yagi,[*14] Y.L. Ye,[*1] R. Yokoyama,[*20] G.X. Zhang,[*10] on behalf of the RIBF-86 and RIBF-88 collaborations

The two most prominent features of the r-process abundances in the solar system are the large abundance of $_{52}$Te, $_{54}$Xe (mass number A∼130) and $_{78}$Pt, $_{79}$Au (A∼195), which are understood in terms of the enhanced stability of nuclei with filled major neutron shells (of neutron number N=82 and N=126). However, the production mechanism of the peak of rare-earth elements (REE) (A∼165) is still a controversial topic.[1)]

To address this problem, two β-decay spectroscopy experiments optimized for the transmission of ^{158}Nd and ^{170}Dy were performed at the Radioactive Isotope Beam Factory (RIBF) by using the in-flight fission of a 345 MeV/A ^{238}U primary beam with an average intensity of 7 and 12 pnA, respectively. The secondary beam selected and identified by BigRIPS separator was implanted to the beta-counting system of the Wide range Active Silicon-Strip Stopper Array for Beta and ion detection (WAS3ABi), which is surrounded by the high purity germanium cluster detectors of the Euroball RIken Cluster Array (EURICA). The β-decay half-life of an isotope of interest was extracted from the fit of the time distribution of electrons detected after the implantation of an ion and correlated to them in position and time[2)].

In this measurement, 57 β-decay half-lives of neutron-rich nuclei from $_{55}$Cs to $_{67}$Ho were measured for the first time with 94 half-lives measured in total. The impact of newly measured β-decay half-lives on the shape of the REE peak is illustrated in Fig. 1. The figure shows the theoretical uncertainty estimated for each model, determined by varying theoretical half-lives within a factor of two. The study indicates that the new measurements remove a significant uncertainty in the calculations associated with theoretical half-lives.

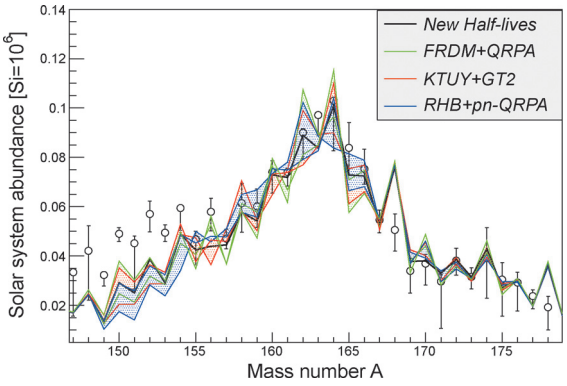

Fig. 1. (color online). The r-process abundance pattern observed in the solar system (open circles)[3)] and calculated using the experimental and theoretical half-lives. KTUY05[4)] mass and the ReaclibV1.0[5)] Database of nuclear reaction rates were employed for the baseline calculation. Experimental data and three theoretical predictions replaced the half-lives of nuclei whose values were measured for the first time.

In summary, the newly measured half-lives have a direct impact in r-process abundance calculations affecting almost all mass numbers in the range A=150−170. This is an important step towards the long-term goal of removing nuclear-physics uncertainties so that the REE peak can be used as a unique probe of the r-process freeze-out conditions and eventually reveal the currently unknown r-process site.

† Condensed from the article in J. Wu et al, Phys. Rev. Lett. 118, 072701 (2017).

*1 School of Physics, Peking University
*2 RIKEN Nishina Center
*3 National Physical Laboratory
*4 Department of Physics, University of Surrey
*5 Los Alamos National Laboratory
*6 RCNP, Osaka University
*7 LPSC, Universite Joseph Fourier Grenoble 1
*8 School of Engineering, University of the West of Scotland
*9 Physics Alliance, University of Glasgow
*10 IRCNPC, School of Physics and Nuclear Energy Engineering, Beihang University
*11 Department of Physics, the University of Hong Kong
*12 Department of Physics, University of Tokyo
*13 School of Computing Engineering and Mathematics, University of Brighton
*14 Department of Physics, Osaka University
*15 Institut Laue-Langevin
*16 Department of Physics, Chung-Ang University
*17 Hungarian Academy of Sciences
*18 Faculty of Physics, VNU Hanoi University of Science
*19 Department of Physics, University of York
*20 CNS, University of Tokyo

References

1) G.J. Mathews, J.J. Cowan, Nature **345**, 7 (1990).
2) Z.Y. Xu, PhD Thesis, University of Tokyo (2011).
3) S. Goriely, Astron. Astrophys. **342**, 881 (1999).
4) http://wwwndc.jaea.go.jp/nucldata/mass/KTUY04_E.html
5) http://groups.nscl.msu.edu/jina/reaclib/db

First Spectroscopy of ^{110}Zr

N. Paul,[*1,*2] for the SEASTAR2015 Collaboration (spokespersons: P. Doornenbal,[*1] and Alexandre Obertelli,[*1,*2]) and B. Bally,[*3] M. Bender,[*4] J.-P. Delaroche,[*5] M. Girod,[*5] P.-H. Heenen,[*6] J. Libert,[*5] T. Otsuka,[*7] T. R. Rodríguez,[*8] N. Shimizu,[*9] T. Togashi,[*9] and Y. Tsunoda,[*9]

The first spectroscopy measurement of ^{110}Zr was performed as part of the SEASTAR campaign in 2015 [1]. This nucleus has been much debated in the literature as its 40 protons and 70 neutrons correspond with magic numbers of both the harmonic oscillator and tetrahedral symmetry. Whether or not signatures of these symmetries emerge in the structure of ^{110}Zr is key information to help constrain our understanding of shell evolution far from stability. Furthermore, a stabilization effect associated with these magic numbers at ^{110}Zr has been proposed in the literature as a potential explanation of deficiencies in r-process simulations near mass 110[2].

The experiment was performed at the RIBF using a 30 pnA ^{238}U primary beam at 345 MeV/nucleon. ^{111}Nb was produced via in-flight fission on a thin Be production target at the F0 focal plane of the BigRIPS spectrometer, and focused onto a 10 cm thick liquid hydrogen target at F8 with an intensity of 20 particles per second. ^{110}Zr was produced via proton knockout in the MINOS[3] hydrogen target, emitted gamma rays were detected with the DALI2 array, and the MINOS TPC[3] tracked the outgoing protons to provide a precise doppler correction of the gamma rays. The reaction residues were identified in the ZeroDegree spectrometer.

The observed transitions in ^{110}Zr lie close in energy to the Bremsstrahlung background generated from high velocity ions colliding with electrons in the hydrogen target. This Bremsstrahlung component was measured, normalized according to the number of nuclei incident on the target, and subtracted from the gamma ray spectrum. The subtracted spectrum was fit with GEANT4 simulated DALI2 response functions, including lifetime and feeding effects. Gamma-gamma coincidences and systematics in the region were used to identify the three visible transitions as the $2_1^+ \rightarrow 0_1^+$, $4_1^+ \rightarrow 2_1^+$, and $2_2^+ \rightarrow 0_1^+$ transitions, and construct a level scheme consisting of a 2_1^+, 4_1^+, and 2_2^+ at 185(11), 565(21), and 485(11) keV, respectively .

*1 RIKEN Nishina Center
*2 SPhN, CEA Saclay
*3 ESNT, CEA Saclay
*4 IPNL Lyon
*5 Nuclear Theory Group, CEA DAM/DIF
*6 Department of Physics, University Libre of Bruxelles
*7 Department of Physics, University of Tokyo
*8 Department of Theoretical Physics, University Autonoma of Madrid
*9 Center for Nuclear Study, University of Tokyo

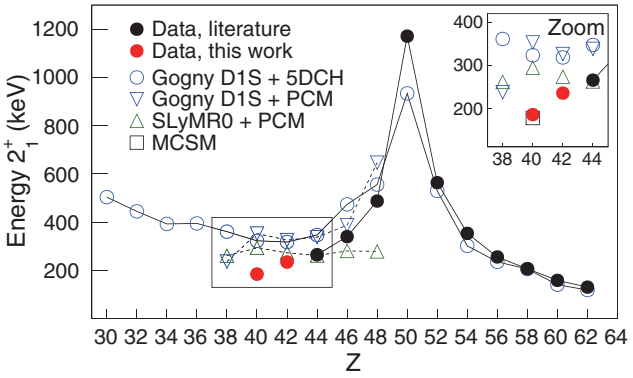

Fig. 1.: E_2^+ systematics for the N=70 isotones compared with theory: 5DCH[4] and PCM[5] with the Gogny D1S interaction, PCM with Skyrme SLyMR0[6], and MCSM calculations[7]. Experimental data are taken from Ref[8] and this work.

These results were compared with state-of-the-art beyond mean field calculations, as well as the most advanced Monte Carlo shell model (MCSM) calculations[7]. E_2^+ systematics are shown in Figure 1. We find that ^{110}Zr shows no increased E_2^+ energy that would indicate a stabilization associated with a spherical or tetrahedral symmetry, but rather it continues the sharp downward trend of E_2^+ energies going towards midshell. The $R_{42} = E_4^+/E_2^+$ ratio for this nucleus is 3.1(2), approaching the rigid rotor value of 3.33. Both these trends are even more pronounced than predicted by beyond-mean-field calculations. MCSM calculations provide the best agreement with our data. The constructed level scheme is not consistent with a tetrahedral symmetry in the ground state. Thus our data shows that ^{110}Zr is a well deformed nucleus with no indications of special stability either isotonically or isotopically associated with its 40 protons and 70 neutrons. This result also discredits a stabilized ^{110}Zr as an explanation for the r-process model deficiencies near mass 110.

References

1) condensed from N. Paul et al., Phys. Rev. Lett, 118, 032501 (2017).
2) K. L. Kratz et al., Eur. Phys. J. A 25, 633 (2005).
3) A. Obertelli et al., Eur. Phys. J. A 50, 8 (2014).
4) J. P. Delaroche et al., Phys. Rev. C 81, 014303 (2010).
5) M. Borrajo et al., Phys. Lett. B 746, 341 (2015).
6) B. Bally et al., Phys. Rev. Lett. 113, 162501 (2014).
7) T. Togashi et al., Phys. Rev. Lett. 117, 172502 (2016).
8) NNDC database, Nucl. Instrum. Methods Phys. Res., Sect. A 213 (2011).

Nucleus ^{26}O: A barely unbound system beyond the drip line†

Y. Kondo,[*1,*2] T. Nakamura,[*1,*2] R. Tanaka,[*1,*2] R. Minakata,[*1,*2] S. Ogoshi,[*1,*2] N. A. Orr,[*3] N. L. Achouri,[*3] T. Aumann,[*4,*5] H. Baba,[*2] F. Delaunay,[*3] P. Doornenbal,[*2] N. Fukuda,[*2] J. Gibelin,[*3] J. W. Hwang,[*6] N. Inabe,[*2] T. Isobe,[*2] D. Kameda,[*2] D. Kanno,[*1,*2] S. Kim,[*6] N. Kobayashi,[*1,*2] T. Kobayashi,[*7,*2] T. Kubo,[*2] S. Leblond,[*3] J. Lee,[*2] F. M. Marqués,[*3] T. Motobayashi,[*2] D. Murai,[*8] T. Murakami,[*9] K. Muto,[*7] T. Nakashima,[*1,*2] N. Nakatsuka,[*9,*2] A. Navin,[*10,*13] S. Nishi,[*1,*2] H. Otsu,[*2] H. Sato,[*2] Y. Satou,[*6] Y. Shimizu,[*2] H. Suzuki,[*2] K. Takahashi,[*7] H. Takeda,[*2] S. Takeuchi,[*2] Y. Togano,[*5,*14] A. G. Tuff,[*11] M. Vandebrouck,[*12] and K. Yoneda[*2]

The unbound nucleus ^{26}O has been investigated using invariant-mass spectroscopy following a one-proton removal reaction from a ^{27}F beam at 201 MeV/nucleon. The ground state of ^{26}O has recently been found to be barely unbound with respect to two-neutron emission – by 53 keV (1σ upper limit) in an intermediate energy reaction study[1,2] and by 120 keV (upper limit with a 95% confidence level) at high energies.[3] The 2^+_1 state has yet, however, to be located. It may be noted that Ref.[3] claimed the existence of a level at 4.2 MeV, which could be a proton-hole state, although the statistics were limited.

The ^{27}F secondary beam was produced by projectile fragmentation of ^{48}Ca (∼140 pnA) at 345 MeV/nucleon. It was purified using BigRIPS and transported to a secondary target of carbon (thickness 1.8 g/cm^2). The decay products, ^{24}O and neutron(s), were measured in coincidence using the spectrometer SAMURAI.[4] In addition to the measurements made of ^{26}O with the ^{27}F beam, data were also taken for one-proton removal from a ^{26}F beam leading to ^{25}O.

The obtained relative energy spectrum of ^{25}O was fitted with a d-wave Breit-Wigner line shape, following the prescription of Ref.[3], after taking into account the experimental response function. In practice this was done using a complete simulation of the setup based on GEANT4 and employing the QGSP_INCLXX physics model for the neutron interactions in NEBULA. A resonance energy of 749(10) keV and a width of 88(6) keV were deduced.

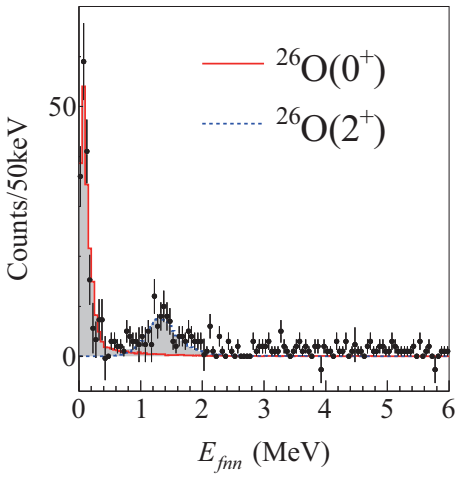

Fig. 1. Three-body decay energy spectrum of ^{26}O reconstructed from ^{24}O and two neutrons in the one-proton removal reaction from ^{27}F.

Turning now to ^{26}O, the ground-state resonance was found to lie only 18±3(stat)±4(syst) keV above the threshold (Fig. 1). In addition, a higher level, which is most likely the first 2^+ state, was observed for the first time at $1.28^{+0.11}_{-0.08}$ MeV. On the other hand, no resonance-like structure was observed at higher energies as reported in Ref.[3]. Comparison of the ^{26}O(2^+_1) energy with theory suggests that three-nucleon forces, pf-shell intruder configurations, as well as an appropriate treatment of the continuum are key elements to understanding the structure of the heaviest oxygen isotopes.

† Condensed from the article in Phys. Rev. Lett. **116**, 102503 (2016)

*1 Department of Physics, Tokyo Institute of Technology
*2 RIKEN Nishina Center
*3 LPC-Caen, ENSICAEN, Université de Caen, CNRS/IN2P3
*4 Institut für Kernphysik, Technische Universität Darmstadt
*5 ExtreMe Matter Institute (EMMI) and Research Division, GSI
*6 Department of Physics and Astronomy, Seoul National University
*7 Department of Physics, Tohoku University
*8 Departiment of Physics, Rikkyo University
*9 Department of Physics, Kyoto University
*10 GANIL, CEA/DSM-CNRS/IN2P3
*11 Department of Physics, University of York
*12 Institut de Physique Nucléaire, Université Paris-Sud,IN2P3-CNRS
*13 Present address: GANIL CEA/DRF-CNRS/IN2P3
*14 Present address: Department of Physics, Tokyo Institute of Technology

References

1) Z. Kohley et al.: Phys. Rev. C **91**, 034323 (2015).
2) E. Lunderberg et al.: Phys. Rev. Lett. **108**, 142503 (2012).
3) C. Caesar et al.: Phys. Rev. C **88**, 034313 (2013).
4) T. Kobayashi et al.: Nucl. Instrum. Methods. Phys. Res. Sect. B **317**, 294 (2013).
5) T. Nakamura, Y. Kondo et al.: Nucl. Instrum. Methods. Phys. Res. Sect. B **376**, 156 (2015).
6) C. R. Hoffman et al.: Phys. Rev. Lett. **100**, 152502 (2008).

Interaction cross section study of the two-neutron halo nucleus ^{22}C†

Y. Togano,[*1,*2] T. Nakamura,[*1,*2] Y. Kondo,[*1,*2] J. A. Tostevin,[*3] A. T. Saito,[*1,*2] J. Gibelin,[*4] N. A. Orr,[*4] N. L. Achouri,[*4] T. Aumann,[*5] H. Baba,[*2] F. Delaunay,[*4] P. Doornenbal,[*2] N. Fukuda,[*2] J. Hwang,[*6] N. Inabe,[*2] T. Isobe,[*2] D. Kameda,[*2] D. Kanno,[*1,*2] S. Kim,[*6] N. Kobayashi,[*1,*2] T. Kobayashi,[*2,*7] T. Kubo,[*2] S. Leblond,[*4] J. Lee,[*2] F. M. Marqués,[*4] R. Minakata,[*1,*2] T. Motobayashi,[*2] D. Murai,[*7] T. Murakami,[*8] K. Muto,[*6] T. Nakashima,[*1] N. Nakatsuka,[*2,*8] A. Navin,[*9] S. Nishi,[*1,*2] S. Ogoshi,[*1,*2] H. Otsu,[*2] H. Sato,[*2] Y. Satou,[*6] Y. Shimizu,[*2] H. Suzuki,[*2] K. Takahashi,[*6] H. Takeda,[*2] S. Takeuchi,[*2] R. Tanaka,[*1,*2] A. G. Tuff,[*10] M. Vandebrouck,[*11] and K. Yoneda[*2]

To obtain high precision root-mean-squared matter radius $\tilde{r}_m$ of ^{22}C, the interaction cross section σ_I has been measured with a carbon target at 235 MeV/nucleon.

Recently the most neutron-rich carbon isotope ^{22}C has attracted much attention owing to a possibly greatly extended two-neutron halo structure, as suggested by a reaction cross section (σ_R) study on a proton target at 40 MeV/nucleon.[1)] $\tilde{r}_m$ of 5.4 ± 0.9 fm was deduced from the measured $\sigma_R = 1.338 \pm 0.274$ b. These large uncertainties in σ_R and the deduced $\tilde{r}_m$ do not significantly constrain the theoretical models. A mean-field model using an adjusted Skyrme interaction yielded an $\tilde{r}_m$ of 3.89 fm.[2)] Three-body models yielded $\tilde{r}_m$ in the range of $3.5 \sim 3.7$ fm.[3,4)] Given the large uncertainty in the experimental values of Ref. 1) and that the theoretical values are within $\sim 2\sigma$ of the experimental value, more definitive conclusions require data with higher precision.

A cocktail beam of ^{19,20,22}C was produced via the projectile fragmentation of a 345 MeV/nucleon ^{48}Ca beam. The ^{19,20,22}C beams were separated and transported to SAMURAI by BigRIPS. The cocktail beam impinged on a carbon target with a thickness of 1.789 g/cm^2. The incident particles were identified event-by-event by measuring the time of flight, magnetic rigidity, and energy loss with detectors located at the upstream of the carbon target. The incident angle and position on the carbon target were measured using two multi-wire drift chambers placed just upstream of the carbon target. The reaction products from the ^{19,20,22}C + C reactions were identified using detectors located at the entrance and exit of the SAMURAI magnet. The detailed experimental setup can be found in Ref. 5).

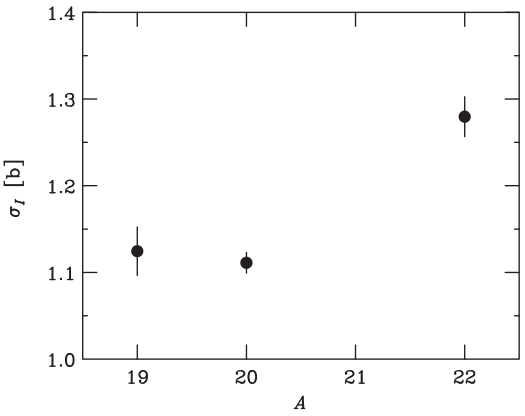

Fig. 1. Mass number dependence of the interaction cross section obtained in the present study.

The interaction cross sections σ_I obtained in the present study are shown in Fig. 1. The enhancement of σ_I for ^{22}C relative to those of ^{19,20}C is consistent with a two-neutron halo nature of ^{22}C.

The present σ_I of ^{22}C is analyzed using a four-body (three-body projectile plus target) Glauber reaction model.[4)] In the following discussion σ_I and σ_R are compared directly by assuming the inelastic scattering cross section is negligible. From the comparison with the model calculations and the present σ_I value, $\tilde{r}_m$ is deduced to be 3.44 ± 0.08 fm. This deduced $\tilde{r}_m$ is consistent with the theoretical predictions based on ^{22}C three-body model wave functions,[3,6)] while it is about 2σ smaller than the previously reported experimental value (5.4 ± 0.9 fm). More measurements, such as Coulomb dissociation, will allow for a more detailed study of the ^{22}C structure.

† Condensed from the article in Phys. Lett. B **761**, 412 (2016)
*1 Department of Physics, Tokyo Institute of Technology
*2 RIKEN Nishina Center
*3 Department of Physics, University of Surray
*4 LPC-CAEN, ENSICAEN, Université de Caen CNRS/IN2P3
*5 Institut für Kernphysik, Technische Universität Darmstadt
*6 Department of Physics and Astronomy, Seoul National University
*6 Department of Physics, Tohoku Univeristy
*7 Department of Physics, Rikkyo University
*8 Department of Physics, Kyoto University
*9 GANIL, CEA/DSM-CNRS/IN2P3
*10 Department of Physics, University of York
*11 IPN Orsay, Université Paris Sud, IN2P3-CNRS

References

1) K. Tanaka et al., Phys. Rev. Lett. **104**, 062701 (2010).
2) T. Inakura et al., Phys. Rev. C **89**, 064316 (2014).
3) W. Horiuchi, Y. Suzuki, Phys. Rev. C **74**, 034311 (2006).
4) Y. Kucuk, J. A. Tostevin, Phys. Rev. C **89**, 034607 (2014).
5) T. Kobayashi et al., Nucl. Instr. Meth. B **317**, 294 (2013).
6) S. N. Ershov et al., Phys. Rev. C **86** 034331 (2012).

Spallation reaction study for the long-lived fission product ^{107}Pd†

H. Wang,[*1] H. Otsu,[*1] H. Sakurai,[*1] D. Ahn,[*1] M. Aikawa,[*2] T. Ando,[*3] S. Araki,[*4,*1] S. Chen,[*1] N. Chiga,[*1] P. Doornenbal,[*1] N. Fukuda,[*1] T. Isobe,[*1] S. Kawakami,[*5,*1] S. Kawase,[*6,*4] T. Kin,[*4] Y. Kondo,[*7,*1] S. Koyama,[*3] S. Kubono,[*1] Y. Maeda,[*5] A. Makinaga,[*8] M. Matsushita,[*6] T. Matsuzaki,[*1] S. Michimasa,[*6] S. Momiyama,[*3] S. Nagamine,[*3] T. Nakamura,[*7,*1] K. Nakano,[*4,*1] M. Niikura,[*3] Y. Ozaki,[*7,*1] A. T. Saito,[*7,*1] T. Saito,[*3] Y. Shiga,[*1,*9] M. Shikata,[*7,*1] Y. Shimizu,[*1] S. Shimoura,[*6] T. Sumikama,[*1] P.-A. Söderström,[*1] H. Suzuki,[*1] H. Takeda,[*1] S. Takeuchi,[*7,*1] R. Taniuchi,[*1,*3] Y. Togano,[*7,*1] J. Tsubota,[*7,*1] M. Uesaka,[*1] Ya. Watanabe,[*1] Yu. Watanabe,[*4] K. Wimmer,[*3,*1] T. Yamamoto,[*5,*1] and K. Yoshida[*1]

In recent years, substantial research and development activity has been devoted to partitioning and transmutation technology for the reduction in high-level radioactive waste (HLW)[1] as well as for resource recycling from spent nuclear fuel. Fission products in HLW contain useful materials, and one promising metal is palladium. However, the palladium metal recovered from waste has a radioactive isotope, ^{107}Pd, which is a typical long-lived fission product (LLFP) with a half-life of 6.5×10^6 years[2]. In considering a possible mechanism for the reduction in the radioactivity of ^{107}Pd, we performed the studies for the proton- and deuteron-induced spallation reaction on ^{107}Pd at both 196 and 118 MeV/u using inverse kinematics technique.

A ^{238}U primary beam was accelerated to 345 MeV/u and impinged on a 1-mm thick beryllium target located at the entrance of the BigRIPS fragment separator[3]. Two settings were made in BigRIPS to make the ^{107}Pd beams with the energies of 196 and 118 MeV/u in front of the secondary targets, respectively. CH_2, CD_2[4] and ^{12}C targets were used to induce the secondary reactions. The thicknesses for CH_2 and CD_2 were 179.2 and 217.8 mg/cm^2, respectively. For the ^{12}C targets, the thicknesses were 317.2 and 226.0 mg/cm^2 for 196 and 118 MeV/u, respectively. In order to measure the background contribution, addtional data were taken by using the target holder with no target material inserted. Reaction residues were identified by the ZeroDegree spectrometer[3]. The large acceptance mode was used and five different $B\rho$ settings were applied in order to cover a broad range of fragments.

The isotopic distribution of cross sections for the different elements produced from ^{107}Pd on protons and deuterons at both 196 and 118 MeV/u were successfully obtained. It was found that the proton-induced cross sections at 196 MeV/u are similar to the deuteron-induced ones at 118 MeV/u for light products such as Ru, Tc and Mo, as shown in Fig. 1 d) - f). The production of these light products depends on the energy deposited. Because deuteron has two nucleons, the deuteron-induced reaction at 118 MeV/u dissipates an energy that is similar to that of the proton-induced reaction at 196 MeV/u in the evaporation process, resulting in a similar production. In addition, the results are discussed by comparing them with the SPACS parameterization and the PHITS calculation including both the intra-nuclear cascade and evaporation processes. Our data provide a design goal for the proton/deuteron flux for the transmutation of ^{107}Pd via spallation reactions.

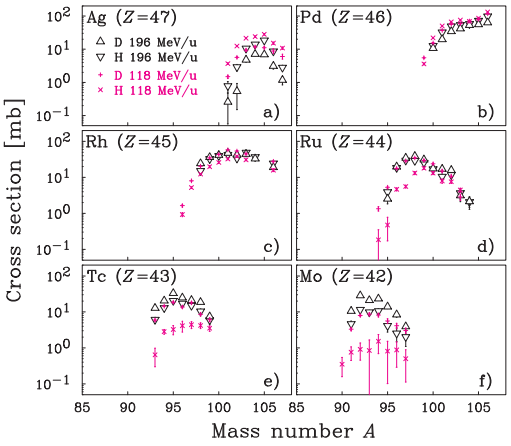

Fig. 1. Isotopic production cross sections for $42 \leq Z \leq 47$ elements produced by ^{107}Pd on protons and deuterons at different reaction energies.

This work was supported by ImPACT program of Council for Science, Technology and Innovation (Cabinet Office, Government of Japan).

References

1) IAEA Technical Reports Series No. 435 (2004).
2) W. S. Yang et al., Nucl. Sci. Eng. **146**, 291 (2004).
3) T. Kubo et al., Prog. Theor. Exp. Phys. **2012**, 03C003 (2012).
4) Y. Maeda et al., Nucl. Instr. Meth. A **490**, 518 (2002).

† Condensed from the article in Prog. Theor. Exp. Phys. 2017, 021D01 (2017)

*1 RIKEN Nishina Center
*2 Faculty of Science, Hokkaido University
*3 Department of Physics, University of Tokyo
*4 Department of Advanced Energy Engineering Science, Kyushu University
*5 Department of Applied Physics, University of Miyazaki
*6 CNS, University of Tokyo
*7 Department of Physics, Tokyo Institute of Technology
*8 JEin institute for fundamental science, NPO Einstein
*9 Department of Physics, Rikkyo University

Investigation of isoscalar and isovector dipole excitations in ^{20}O

N. Nakatsuka,[*1,*2] H. Baba,[*2,*2] N. Aoi,[*10] T. Aumann,[*3] R. Avigo,[*5,*14] S. R. Banerjee,[*12] A. Bracco,[*5,*14] C. Caesar,[*3] F. Camera,[*5,*14] S. Ceruti,[*5,*14] S. Chen,[*13,*2] V. Derya,[*4] P. Doornenbal,[*2] A. Giaz,[*5,*14] A. Horvat,[*3] K. Ieki,[*11] N. Imai,[*7] T. Kawabata,[*1] K. Yoneda,[*2] N. Kobayashi,[*8] Y. Kondo,[*9] S. Koyama,[*8] M. Kurata-Nishimura,[*2] S. Masuoka,[*7] M. Matsushita,[*7] S. Michimasa,[*7] B. Millon,[*5] T. Motobayashi,[*2] T. Murakami,[*1] T. Nakamura,[*9] T. Ohnishi,[*2] H. J. Ong,[*10] S. Ota,[*7] H. Otsu,[*2] T. Ozaki,[*9] A. T. Saito,[*9] H. Sakurai,[*2,*8] H. Scheit,[*3] F. Schindler,[*3] P. Schrock,[*3] Y. Shiga,[*11,*2] M. Shikata,[*9] S. Shimoura,[*7] D. Steppenbeck,[*2] T. Sumikama,[*6,*2] I. Syndikus,[*3] H. Takeda,[*2] S. Takeuchi,[*2] A. Tamii,[*10] R. Taniuchi,[*8] Y. Togano,[*9] J. Tscheuschner,[*3] J. Tsubota,[*9] H. Wang,[*2] O. Wieland,[*5] K. Wimmer,[*8,*2] Y. Yamaguchi,[*7] and J. Zenihiro[*2]

The electric dipole excitation is one of the most basic properties of atomic nuclei. Neutron-rich nuclei are predicted to have exotic electric dipole excitations owing to their small neutron separation energy and excess neutrons. One example of such excitations in neutron-rich nuclei is the low-energy dipole excitations found at excitation energies less than 10 MeV. Recent experimental studies on stable nuclei revealed that some low-energy dipole excitations show specific isospin character[1] called isospin splitting. In order to study the isospin properties of low-energy dipole excitations in neutron-rich oxygen isotopes, we performed an experiment at RIBF and measured the dipole resonances of the neutron-rich nucleus ^{20}O. The beam was produced via projectile fragmentation of a 345-MeV/nucleon ^{48}Ca beam on ^{9}Be target with a thickness of 2.8 g/cm^2. Two secondary targets, a 5-g/cm^2-thick gold target for coulomb excitation and a 300 mg/cm^2 thick liquid helium target for inelastic α-particle scattering, were used to obtain the isovector and isoscaler dipole strengths independently. The γ rays from the excited beam particles were detected with large volume $LaBr_3$ crystals from INFN Milano[2] in combination with DALI2[3]. A preliminary doppler-corrected γ-ray spectrum of the $\alpha(^{20}O,^{20}O\gamma)$ reaction is shown in Fig. 1 (a), and the spectrum of $Au(^{20}O,^{20}O\gamma)$ reaction is shown in Fig. 1 (b). Preliminary fits are presented by red solid lines, and two 1^- states are identified. A clear difference is observed between the two spectra. This suggests that the Coulomb excitation and inelastic α-particle scattering have different sensitivities to the isospin and are actually effective to determine the isovector and isoscalar strength. Further analysis using the distorted-wave Born approximation is in progress to determine the isovector and isoscalar strengths of the observed low-energy dipole excitations.

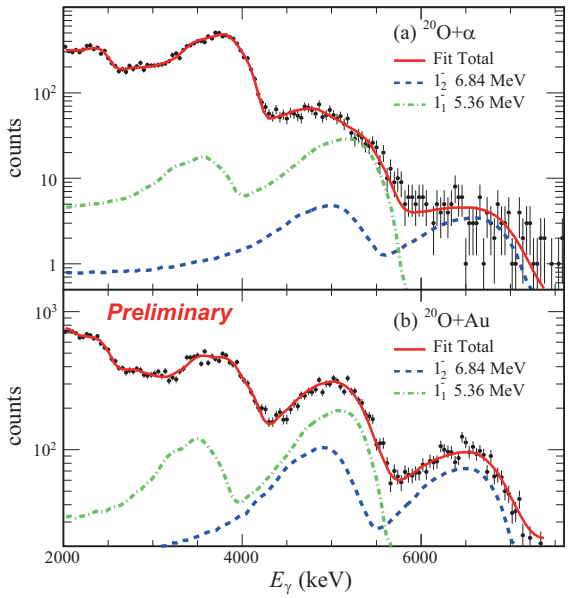

Fig. 1. Preliminary fits of Doppler-corrected γ ray spectra: ^{20}O+α (top panel) and ^{20}O+Au (bottom panel).

*1 Department of Physics, Kyoto University
*2 RIKEN Nishina Center
*3 Institut für Kernphysik, Technische Universität Darmstadt
*4 Institut für Kernphysik, Universität zu Köln
*5 Istituto Nazionale di Fisica Nucleare Milan
*6 Department of Physics, Tohoku University
*7 Center for Nuclear Study, The University of Tokyo
*8 Department of Physics, The University of Tokyo
*9 Department of Physics, Tokyo Institute of Technology
*10 Research Center for Nuclear Physics, Osaka University
*11 Department of Physics, Rikkyo University
*12 Variable Energy Cyclotron Centre, The Indian Department of Atomic Energy
*13 School of Physics, Peking University
*14 University of Milan

References

1) A. Bracco et al., Euro. Phys. J. A **51**, 99 (2015).
2) A. Giaz et al., Nucl. Instrum. Methods Phys. Res., Sec. A **729**, 910 (2013).
3) S. Takeuchi et al., Nucl. Instrum. Methods Phys. Res., Sec. A **763**, 596 (2014).

Measurement of multiple isobar chains as a first step toward SHE identification via mass spectrometry†

P. Schury,[*1] M. Wada,[*1,*2] Y. Ito,[*2] D. Kaji,[*2] A. Takamine,[*2] F. Arai,[*2,*3] H. Haba,[*2] Y. Hirayama,[*1] S. Jeong,[*7,*1] S. Kimura,[*1,*2,*3] H. Koura,[*4] M. MacCormack,[*8] H. Miyatake,[*1] J.Y. Moon,[*7,*1] K. Morimoto,[*2] K. Morita,[*2,*5] I. Murray,[*2,*8] A. Ozawa,[*2,*3] M. Reponen,[*2] M. Rosenbusch,[*2] P.-A. Söderström,[*2] T. Tanaka,[*2,*5] Y. X. Watanabe,[*1] and H. Wollnik[*6]

The SHE-mass project is a joint effort between KEK and RIKEN with a long-term goal of identifying new superheavy element (SHE) isotopes produced via hot fusion. It makes use of cryogenic-capable, high-purity helium gas cell to convert the energetic (5∼50 MeV) evaporation products of fusion reactions into thermal ions. The evaporation products are separated from projectile-like fragments by use of the GARIS-II[1] gas-filled recoil ion separator. The thermalized ions are transferred to a multi-reflection time-of-flight mass spectrograph[2] (MRTOF) which can analyze the ions with a mass resolving power of $R_m > 100\,000$. The SHE-mass system is described in some detail in Ref. 3.

We previously reported[4] initial results of the SHE-mass project, where MRTOF mass measurements were performed on ^{205,206}Fr, ^{205,206}Rn, ^{205,206}At, and ^{205}Po produced via ^{169}Tm(^{40}Ar, X) reactions at a bombarding energy of 193 MeV. In the interim, numerous upgrades were made to the apparatus, increasing the system efficiency and improving stability of operation.

In July, 2016, the ^{169}Tm(^{40}Ar, X) reaction was revisited at a bombarding energy of 207 MeV. At this higher energy, it was possible to simultaneous observe $4n$ and $5n$ evaporation channels (^{204,205}Fr$^+$), $p3n$ and $p4n$ evaporation channels (^{204,205}Rn$^+$) as well as higher-order evaporation channels (^{204,205}At$^+$, ^{204,205}Po$^+$, ^{205}Bi$^+$). The very small β-decay branching ratios of ^{204,205}Fr$^+$ (4(2)% and <1%, respectively) and the long half-lives of the lower-Z isotopes indicate that these are dominantly directly produced and not decay products.

Of particular interest for the long-term goals of the SHE-mass project, the very low-yield isotopes ^{205}Bi, ^{204,205}Po, and ^{206}Rn could be identified with very few detected ions, as shown in Figs. 1 & 2. The 3-σ deviation in the case of ^{205}Po is attributed to the admixture of a high-lying isomeric state[5]. Based on this we can confidently claim that this technique can be applied to low-yield SHE for confirmation of their identity.

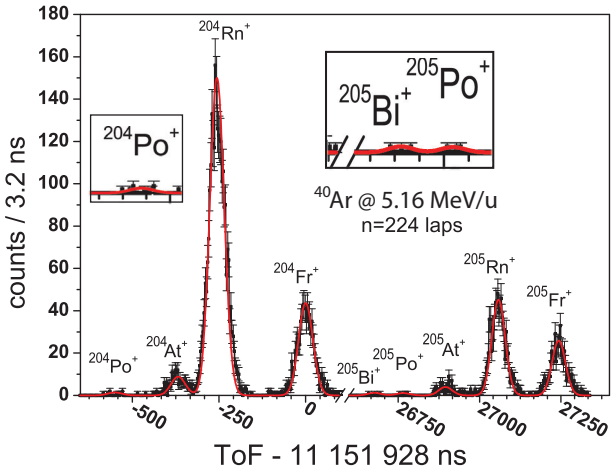

Fig. 1. Time-of-flight spectrum observed for A/q=204, 205 ions at n=224 laps.

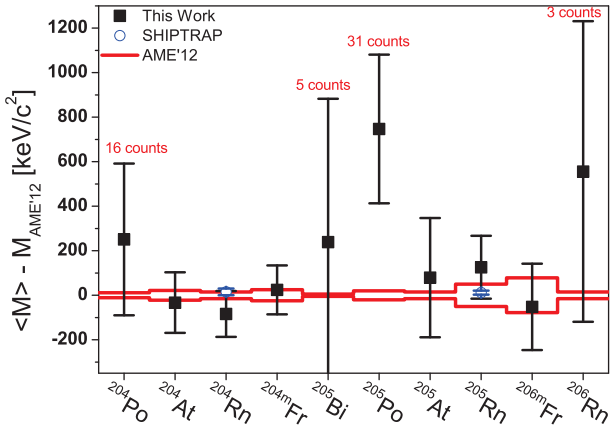

Fig. 2. Summary of the deviation of each isotopes measured mass from literature values.

† Condensed from article published in Phys. Rev. C, DOI: 10.1103/PhysRevC.95.011305

*1 KEK Wako Nuclear Science Center (WNSC)
*2 RIKEN Nishina Center
*3 Institute of Physics, University of Tsukuba
*4 Advanced Science Research Center, JAEA
*5 Dept. Physics, Kyushu University
*6 Dept. Chem. & BioChem, New Mexico State University
*7 Institute for Basic Science
*8 Institut de Physique Nucléaire, IN2P3-CNRS

References

1) D. Kaji et al., Nucl. Instrum. and Methods Phys. Res. B, 317 (2013) 311-314.
2) P. Schury et al., Nuclear Inst. and Methods in Physics Research B 335 (2014) 39-53.
3) P. Schury et al., Phys. Rev. C 95 (2017) 011305(R).
4) P. Schury et al., RIKEN Accel. Prog. Rep 49 (2017) 6.
5) F.G. Kondev, Nuclear Data Sheets 101 (2004) 521-662.

First direct mass measurements of mendelevium and einsteinium with an MRTOF mass spectrograph

Y. Ito,[*1] M. Wada,[*1,*2] P. Schury,[*2] M. Rosenbusch,[*1] D. Kaji,[*1] K. Morimoto,[*1] H. Haba,[*1] Y. Hirayama,[*2] S. Kimura,[*3] H. Koura,[*1,*4] M. MacCormick,[*5] H. Miyatake,[*2] J.Y. Moon,[*2,*6] K. Morita,[*1,*7] M. Mukai,[*3] I. Murray,[*1,*5] T. Niwase,[*7] K. Okada,[*8] A. Ozawa,[*1,*3] M. Reponen,[*1] A. Takamine,[*1] T. Tanaka,[*1,*7] H. Wollnik,[*9] S. Yamaki,[*1,*10] and Y.X. Watanabe[*2]

Precision mass measurements of trans-uranium nuclei, which provide a direct measure of the nuclear binding energy, are invaluable for nuclear structure study in heavy nuclear systems and have the potential for unique identification of atomic nuclides. Thus far, masses of only 6 nuclei of nobelium and lawrencium were directly measured with the Penning trap mass spectrometer[1,2]. Recently, we implemented a multi-reflection time-of-flight mass spectrograph (MRTOF) located after a cryogenic helium gas cell coupled with the gas-filled recoil ion separator GARIS-II[3] and performed direct mass measurements of mendelevium and einsteinium isotopes for the first time.

We produced fusion-evaporation residues (ER) of ^{254}No/$^{249-251}$Md via ^{208}Pb/^{nat}Tl(^{48}Ca, xn) reactions and ^{252}Md/^{246}Es via ^{238}U/^{232}Th(^{19}F, 5n) reactions. The ER were transported into the gas cell through GARIS-II and converted to low-energy radioactive ion (RI) beams. All isotopes were extracted as doubly charged atomic ions from the cold gas cell at 130-150 K. The extracted ions were transferred to the MRTOF, which can analyze the ions with a mass resolving power of $R_m \sim 140,000$. The MRTOF measurements were performed with a concomitant referencing method[4], wherein RI measurements and reference measurements were made sequentially in each cycle of 15 ms. The reference ions of $^{133}Cs^+$ provided from a thermal ion source were used for both time-of-flight drift compensation and mass reference. Drift-compensated spectra were fitted by an exponentially modified Gaussian function[5] (Fig. 1). Using times-of-flight for RI and reference ions, we determined the masses using a single-reference analysis method[6] and computed mass excesses and mass deviations from AME2012[7] (Fig. 2). All masses are in good agreement with AME2012 within uncertainty even for extrapolated masses. By this work, the masses of ^{246}Es and ^{249,250,252}Md were directly determined for the first time, and the uncertainties of ^{246}Es and ^{250}Md were reduced by 60%. Combining the direct masses of ^{249,250}Md with α decay Q-values of decay parents, we could determine masses of 7 heavier nuclei, up to meitnerium, for the first time.

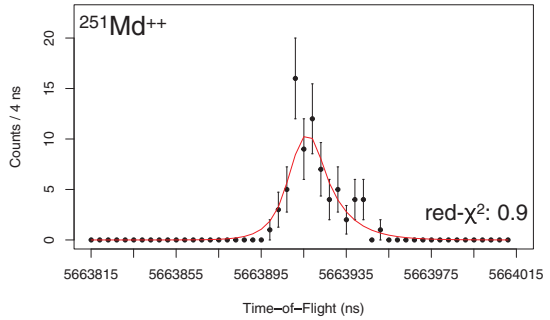

Fig. 1. Time-of-flight spectrum of $^{251}Md^{++}$ and exponentially modified Gaussian fit

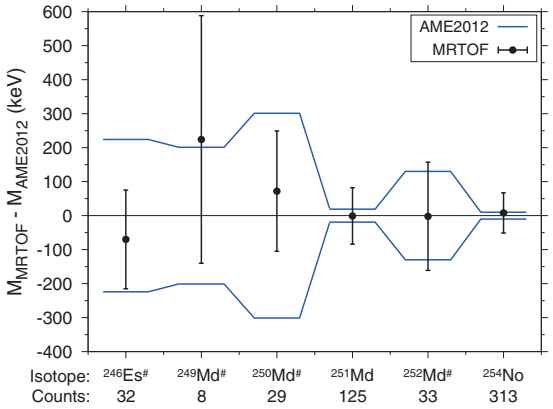

Fig. 2. Preliminary evaluation of mass deviations from the AME2012. The solid lines mark the uncertainty of the AME2012 values and # on element symbols indicate extrapolated values.

*1 RIKEN Nishina Center
*2 Wako Nuclear Science Center (WNSC), Institute of Particle and Nuclear Studies (IPNS), High Energy Accelerator Research Organization (KEK)
*3 Department of Physics, University of Tsukuba
*4 Advanced Science Research Center, Japan Atomic Energy Research Institute (JAEA)
*5 Institut de Physique Nucléaire, Orsay
*6 Institute for Basic Science
*7 Department of Physics, Kyushu University
*8 Department of Physics, Sophia University
*9 Department of Chemistry and Biochemistry, New Mexico State University
*10 Department of Physics, Saitama University

References

1) M. Block et al., Nature **463**, 785 (2010).
2) E.M. Ramirez et al., Science **337**, 1207 (2012).
3) P. Schury et al., Phys. Rev. C **95**, 011305(R) (2017).
4) M. Wada et al., Patent No. 016-037679 (29th Feb. 2016).
5) M.J. Koskelo et al., Comp. Phys. Commun. **24**, 11 (1981).
6) Y. Ito et al., Phys. Rev. C **88**, 011306 (2013).
7) G. Audi et al., Chin. Phys. C **36**, 1287 (2012).

Nuclear spectroscopy of multi-nucleon transfer reaction products in the ^{136}Xe and ^{198}Pt system

Y. Hirayama,[*1] M. Mukai,[*2,*3] Y.X. Watanabe,[*1] Y. Kakiguchi,[*1] P. Schury,[*1] M. Oyaizu,[*1] H. Miyatake,[*1] M. Wada,[*1,*2] M. Ahmed,[*1,*3] S. Kimura,[*2,*3] J.Y. Moon,[*4] J.H. Park,[*4] H. Ishiyama,[*4] S.C. Jeong,[*4] S. Kanaya,[*5] H. Muhammad,[*5] A. Odahara,[*5] T. Shimoda,[*5] S. Suzuki,[*5] and H. Tsuru[*5]

We have developed the KEK Isotope Separation System (KISS)[1] to study the β-decay properties of neutron-rich isotopes with neutron numbers around $N = 126$ for astrophysics research[2]. We extracted elastic events of ^{198}Pt and unstable nuclei of ^{199,201}Pt and ^{196,197,198}Ir produced in the ^{136}Xe beam and ^{198}Pt target system[3]. We successfully measured the lifetime of these unstable nuclei, and measured the hyperfine structure (HFS) of ^{199}Pt and ^{196,197}Ir in order to determine the magnetic dipole moment and the change in the charge radius by using the in-gas-cell laser ionization spectroscopy technique.

We performed nuclear spectroscopy using the ^{136}Xe beam with an energy of 10.75 MeV/nucleon and a maximum intensity of 100 pnA. We introduced a doughnut-shaped gas cell with the ^{198}Pt rotating target system in order to increase the extraction yield not only by increasing the ^{136}Xe primary beam intensity but also by reducing the argon-gas plasma density in the gas cell. The ^{136}Xe beam was directed onto the ^{198}Pt rotating target placed in front of the gas cell, and was stopped at a tungsten beam dump without entering the gas cell. As a result, we successfully extracted the laser ionized ^{199}Pt^{+} with a one order of magnitude higher yield than that with a primary beam intensity of 20 pnA.

Figure 1 shows a typical β-decay curve of ^{197}Ir. The half-life time was evaluated from the fit to the spectrum where the decays of the parent nucleus ^{197}Ir and daughter nucleus ^{197}Pt and a constant background were taken into account. The half-life times measured in this experiment are listed in Table 1. The measured half-life times $t_{1/2}$ were in good agreement with the reported values.

Figure 2 shows the measured HFS of ^{199}Pt obtained by detecting β-rays. We found that not only ^{199g}Pt but also ^{199m}Pt were laser-ionized, from γ-ray measurement. This indicated that the measured HFS consists of the HFS of ^{199g}Pt and ^{199m}Pt. In order to identify each HFS, we plan to measure the HFS by detecting γ-rays emitted from ^{199m}Pt, and then decompose the HFS of ^{199g}Pt. It is feasible to evaluate the magnetic dipole moment and the change in charge radius for ^{199g}Pt and ^{199m}Pt from the spectrum analysis.

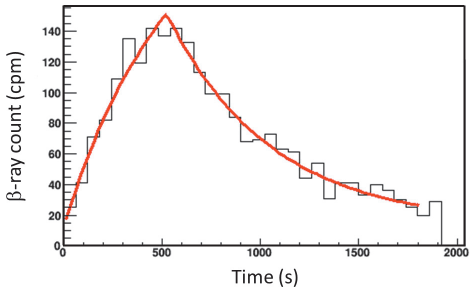

Fig. 1. Measured β-decay curve of ^{197}Ir. The red line indicates the best-fit result to evaluate the half-life time.

Table 1. Comparison between the present measured and reported half-life times of ^{199,201}Pt and ^{196,197,198}Ir.

Nuclide	Measured $t_{1/2}$	Reported $t_{1/2}$
^{199}Pt	31.3(1.5) min	30.8(2) min
^{201}Pt	1.9(5) min	2.5(1) min
^{196}Ir	52(5) s	52(1) s
^{197}Ir	6.1(4) min	5.8(5) min
^{198}Ir	10(1) s	8(1) s

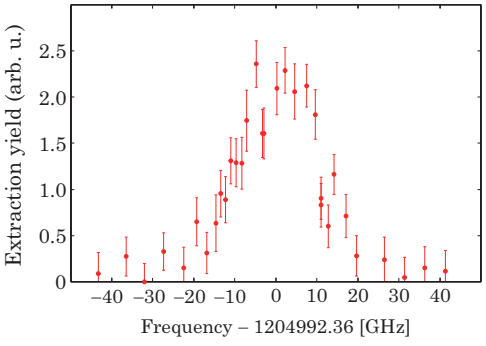

Fig. 2. Measured hyperfine structure of ^{199}Pt.

*1 Wako Nuclear Science Center (WNSC), Institute of Particle and Nuclear Studies (IPNS), High Energy Accelerator Research Organization (KEK)
*2 RIKEN Nishina Center
*3 Department of Physics, University of Tsukuba
*4 Institute for Basic Science, Rare Isotope Science Project
*5 Department of Physics, Osaka University

References

1) Y. Hirayama et al., Nucl. Instr. Meth. **B353**, 4 (2015).
2) S.C. Jeong et al.: KEK Report 2010-2.
3) Y.X. Watanabe et al., Phys. Rev. Lett. **115**, 172503 (2015).

Electron scattering off ^{208}Pb and ^{132}Xe at SCRIT electron scattering facility

K. Tsukada,[*1 *2] K. Adachi,[*3] A. Enokizono,[*1 *3] T. Fujita,[*3] M. Hori,[*2] S. Ichikawa,[*2] K. Kasama,[*1] K. Kurita,[*3] K. Namba,[*1] T. Ohnishi,[*2] S. Sasamura,[*3] T. Suda,[*1 *2] T. Tamae,[*1 *2] M. Togasaki,[*3] N. Uchida,[*3] M. Wakasugi,[*2] M. Watanabe,[*2] and K. Yamada[*3]

The SCRIT (Self-Confining Radioactive Isotope Target) electron scattering facility has been constructed at RIKEN to realize electron scattering off unstable nuclei[1]. This year, commissioning studies of the spectrometers WiSES (Window-frame Spectrometer for Electron Scattering) and LMon (Luminosity Monitor) have been performed with several stable targets. The studies of LMon are reported elsewhere.[3,4] Here, some results with WiSES for ^{208}Pb and ^{132}Xe targets are reported.

Since ^{208}Pb is one of the most extensively investigated stable nuclei and the form factor is precisely derived by electron scattering,[2] it is the best target to check the spectrometer performance. The ^{208}Pb ion was extracted from the evaporation of natural lead heated up to 300°C and transported into SCRIT by ERIS[5] and FRAC.[6] The number of ions introduced was about 10^8 particles/pulse, and the achieved lumionsity was about 10^{27} cm^{-2}s^{-1} on average. The acceptance of WiSES was evaluated by Geant4 simulation taking into account the influence of the radiation tail. Figure 1 shows the differential cross sections multiplied by luminosity for elastic electron scattering off ^{208}Pb. By changing the electron beam energy, a wide range of momentum transfer can be covered. The line represents a phase shift calculation with the nuclear charge density distribution modeled as a sum-of-Gaussian function.[2] The luminosity is considered as a fitting parameter in the present analysis because the study of the LMon to determine the absolute value of luminosity is underway. The momentum-transfer dependence is well reproduced by the calculation.

Figure 2 shows the same plots for elastic electron scattering off ^{132}Xe. The number of introduced target ions and the achieved luminosity were approximately the same as those for ^{208}Pb. The parameters of a two-parameter Fermi distribution in the elastic scattering calculation are determined to reproduce our data. The contribution of inelastic scattering[8] contaminated because of momentum resolution is negligibly small, as shown in the figure. Although ^{132}Xe is a stable nucleus and the root-mean-square radius is evaluated from the measurement of X-rays from muonic atoms,[7] electron scattering has never been performed. This work is, therefore, the first to determine the charge density distribution of ^{132}Xe. This result will be published soon.

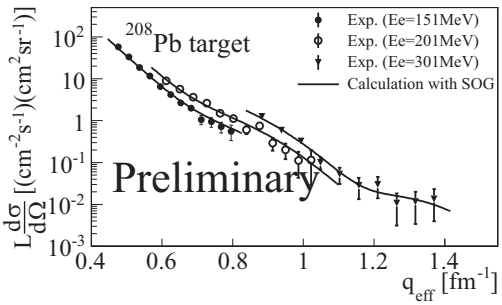

Fig. 1. Differential cross sections of ^{208}Pb(e,e) multiplied by the luminosity for the effective momentum transfer at E_e=151, 201, and 301 MeV. The line is a phase shift calculation with the nuclear charge density distribution modeled as a sum-of-Gaussian function.[2]

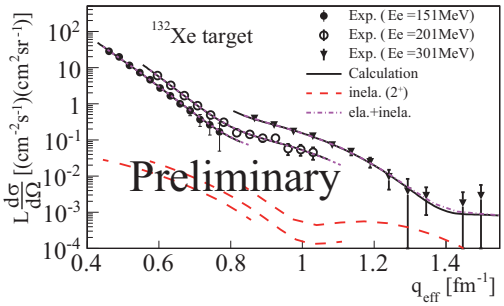

Fig. 2. Differential cross sections of ^{132}Xe(e,e) multiplied by the luminosity for the effective momentum transfer at E_e=151, 201, and 301 MeV. The lines are a phase shift calculation with the nuclear charge density distribution modeled as a two-parameter Fermi distribution (solid), contributions of inelastic scattering calculated by a beyond relativistic mean field theory[8] (dashed), and their sum (dot-dashed).

*1 RIKEN Nishina Center
*2 Research Center for Electron-Photon Science, Tohoku University
*3 Department of Physics, Rikkyo University

References
1) M. Wakasugi et al., Nucl. Instr. Meth. B**317**, 668 (2013).
2) B. Frois et al., Phys. Rev. Lett. **38**, 152 (1977).
3) T. Fujita: In this report.
4) A. Enokizono: In this report.
5) T. Ohnishi et al., Nucl. Instr. Meth. B**317**, 357 (2013).
6) M. Togasaki et al.: Proceedings of HIAT2015, WEPB25 (2015).
7) G. Fricke et al., Atomic Data and Nuclear Data Tables **60**, 177 (1995).
8) M. Hua, K. Hagino, private communication.

First direct measurement of the $^{11}C(\alpha, p)^{14}N$ stellar reaction by an extended thick-target method†

S. Hayakawa,[*1] S. Kubono,[*1,*2,*3] D. Kahl,[*4] H. Yamaguchi,[*1] D. N. Binh,[*5] T. Hashimoto,[*6] Y. Wakabayashi,[*2] J. J. He,[*3] N. Iwasa,[*2,*7] S. Kato,[*8] T. Komatsubara,[*2] Y. K. Kwon,[*6] and T. Teranishi[*9]

The $^{11}C(\alpha, p)^{14}N$ reaction is one of the important α-induced reactions competing with β-limited hydrogen-burning processes in high-temperature explosive stars.[1,2] We directly measured its reaction cross sections for the (α, p_0), (α, p_1) and (α, p_2) transitions to derive the total reaction rate at relevant stellar temperatures by an extended thick-target method featuring the time of flight of the recoil proton corresponding to each transition. This report is a condensed version of our article.[3]

The measurement was performed in inverse kinematics with ^{11}C beams at 10.12 MeV and 16.86 MeV produced at CRIB (Center for Nuclear Study Radioactive Ion Beam separator[8]). The experimental setup consisted of two beam-tracking monitors (PPAC: parallel-plate avalanche counter and MCP: microchannel plate detector), a ^4He gas target, and ΔE-E position-sensitive silicon detectors at three different angles. We carefully designed the target length (140 mm) and pressure (400 Torr). Such an extended gas target enables us to differentiate the transitions to the ground state and the excited states of ^{14}N in time of flight (TOF) between the first PPAC and the silicon telescopes. The observed TOF vs. recoil proton energy had several loci with a typical TOF difference of 5 ns so that the different excited-state transitions were identified and extracted. The present (α, p_1) and (α, p_2) cross sections are about one order of magnitude smaller than the (α, p_0) one, and those of the Hauser-Feshbach calculation[4] appear to be larger than the present experimental data.

Figure 1 shows the absolute $^{11}C(\alpha, p)^{14}N$ reaction rates of the present data and the currently available data[4–6] (upper) and their ratios to the CF88[5] data (lower). The hatched regions in the lower panel indicate the errors of the present rates. In the νp-process temperature range (T_9 = 1.5–3)[2], the present (α, p_0) reaction rate is enhanced from the CF88 rate by about 40% at most, mainly due to the resonances around 0.9 MeV and 1.35 MeV, which were not taken into account in the previous compilation works.[5,6] The contribution from the (α, p_1) and (α, p_2) reaction rate to the total reaction rate is about 20% of the (α, p_0) at most. The new total reaction rate lies between the previous (α, p_0) rate[5] and the total Hauser-Feshbach rate,[4] which supports the validity of relevant explosive hydrogen-burning process scenarios such as the νp-process that proceeds via the $^{11}C(\alpha, p)^{14}N$ reaction in addition to the triple-α process.

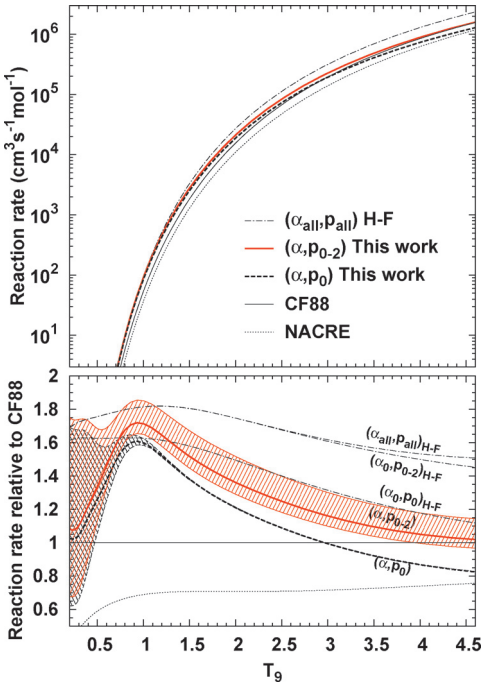

Fig. 1. Absolute $^{11}C(\alpha, p)^{14}N$ reaction rates of the present data and the currently available data[4–6] (upper) and their ratios to the CF88[5] data (lower). The uncertainties of the present (α, p_0) rate and total rate are drawn as hatches attached in the bottom panel.

References

1) M. Wiescher et al., Astrophys. J. **343**, 352 (1989).
2) S. Wanajo, H. T. Janka, S. Kubono, Astrophys. J. **729**, 46 (2011).
3) S. Hayakawa et al., Phys. Rev. C **93**, 065802 (2016).
4) P. Descouvemont, T. Rauscher, Nucl. Phys. A **777**, 137 (2006).
5) G. R. Caughlan, W. A. Fowler, At. Data Nucl. Data Tables **40**, 283 (1988).
6) C. Angulo et al., Nucl. Phys. A **656**, 3 (1999).
7) K. P. Artemov et al., Sov. J. Nucl. Phys. **52**, 408 (1990).
8) Y. Yanagisawa et al., Nucl. Instrum. Methods A **539**, 74 (2005).

† Condensed from the article in Phys. Rev. C **93**, 065802 (2016)

*1 Center for Nuclear Study, University of Tokyo
*2 RIKEN Nishina Center
*3 Institute of Modern Physics, Chinese Academy of Science
*4 School of Physics and Astronomy, University of Edinburgh
*5 Institute of Physics, Vietnamese Academy for Science and Technology
*6 Rare Isotope Science Project, Institute for Basic Science
*7 Department of Physics, Tohoku University
*8 Department of Physics, Yamagata University
*9 Department of Physics, Kyushu University

A directly measurable parameter quantifying the halo nature of one-neutron halo nuclei†

S. Watanabe,*1 M. Yahiro,*2 M. Toyokawa,*2 and T. Matsumoto*2

After the discovery of a halo nucleus ^{11}Li[1], total reaction cross sections ($\sigma_{\rm R}$) and/or interaction cross sections ($\sigma_{\rm I}$) were further measured to identify new halo nuclei[2]. For example, it was established that ^{11}Be and ^{15,19}C are one-neutron halo nuclei, and ^{6}He, ^{11}Li, ^{14}Be, and ^{22}C are two-neutron halo nuclei with Borromean structures. Nowadays, the measurements reach the pf-shell region, i.e., the vicinity of the neutron-drip line for Ne and Mg isotopes[3,4]; ^{31}Ne and ^{37}Mg are considered to be one-neutron halo nuclei[6,7]. Thus, the sudden enhancement of measured $\sigma_{\rm R}$ is a good experimental probe of halo nuclei. However, the relation between $\sigma_{\rm R}$ and the separation energies of the halo nuclei are not well understood particularly in the weak-binding limit.

In this report, we focus on the scattering of one-neutron halo nuclei (a) on a target (T) at high incident energies ($E_{\rm in} \gtrsim 240$ MeV/nucleon) where projectile-breakup effects are expected to be small. At the high incident energies, we can identify $\sigma_{\rm R}$ and $\sigma_{\rm I}$ as absorption cross sections $\sigma_{\rm abs}$. We also assume that one-neutron halo nuclei (a) are well described by the core + neutron ($c+n$) two-body model, and the scattering of a on T is well explained by the $c+n+$T three-body model. We now propose the parameter

$$\mathcal{H} = \frac{\sigma_{\rm abs}(a) - \sigma_{\rm abs}(c)}{\sigma_{\rm abs}(n)}, \qquad (1)$$

where $\sigma_{\rm abs}(x)$ is the absorption cross section of x on the same T at the same incident energy per nucleon. The parameter $\mathcal{H}$ represents an enhancement of $\sigma_{\rm abs}(a)$ from $\sigma_{\rm abs}(c)$ relative to $\sigma_{\rm abs}(n)$, and varies in a range of $0 \le \mathcal{H} \le 1$. The halo structure is most developed when $\mathcal{H} = 1$ and least developed when $\mathcal{H} = 0$[5]. Therefore, $\mathcal{H}$ is expected to quantify the degree of halo nature regardless of scattering conditions such as $E_{\rm in}$ or T.

Figure 1 shows the behavior of $\mathcal{H}$ as a function of the one-neutron separation energy S_n. Experimental data is listed in Ref.[5]. The results of the present model[5], which is based on the spherical Woods-Saxon potential and the Glauber model, are consistent with the empirical values for all halo nuclei ^{11}Be, ^{19}C, ^{31}Ne and ^{37}Mg within 1σ error bars. $\mathcal{H}$ is then extrapolated to the $S_n = 0$ limit as shown by the lines. Only for s-wave halo nuclei ^{11}Be and ^{19}C, the lines reach $\mathcal{H} = 1$ in the $S_n = 0$ limit. On the other hand, the lines saturate at about 0.55 for p-wave halo nuclei ^{31}Ne and ^{37}Mg, and at about 0.21 for a d-wave non-halo nucleus ^{17}C. As a result, the five lines are well separated into three groups of s-wave halo, p-wave halo and d-wave non-halo in the vicinity of $S_n = 0$. If s-wave halo nuclei with very small separation energy ($S_n \lesssim 0.01$ MeV) are newly discovered, they should be on or near the line. This may be also true for p-wave halo nuclei. Therefore, if $\sigma_{\rm R}(n)$, $\sigma_{\rm R}(c)$ and $\sigma_{\rm R}(a)$ are newly measured at the same incident energy per nucleon, one can derive $\mathcal{H}$ and see the halo nature of the nuclei without model calculation. $\mathcal{H}$ is thus a good indicator quantifying the halo nature of one-neutron halo nuclei.

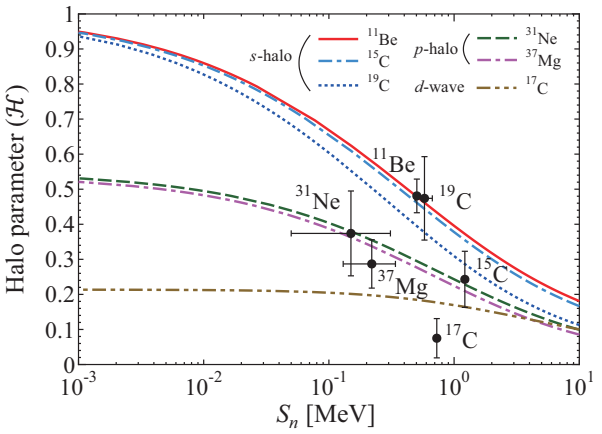

Fig. 1. Behavior of $\mathcal{H}$ as a function of S_n. The horizontal axis is in the logarithmic scale. The theoretical results are shown by the solid (dotted) line for ^{11}Be (^{19}C), the dashed (dot-dashed) line for ^{31}Ne (^{37}Mg), the dot-dot-dashed line for ^{17}C, and the dot-dashed line for ^{15}C. See Ref.[5] for the experimental data.

References
1) I. Tanihata et al., Phys. Rev. Lett. **55**, 2676 (1985); Phys. Lett. B **206**, 592 (1988).
2) A. Ozawa et al., Nucl. Phys. A **691**, 599 (2001).
3) M. Takechi et al., Phys. Lett. B **707**, 357 (2012).
4) M. Takechi et al., Phys. Rev. C **90**, 061305(R) (2014).
5) M. Yahiro et al., Phys. Rev. C **93**, 064609 (2016).
6) K. Minomo et al., Phys. Rev. Lett. **108**, 052503 (2012).
7) S. Watanabe et al., Phys. Rev. C **89**, 044610 (2014).

† Condensed from the article in Phys. Rev. C **93**, 064609 (2016)

*1 RIKEN Nishina Center
*2 Department of Physics, Kyushu University

Simultaneous microscopic description of nuclear level density and radiative strength function †

N. Quang Hung,[*1] N. Dinh Dang,[*2] and L.T. Quynh Huong[*3,*4]

According to the rules of quantum mechanics, the atomic nucleus has discrete energy levels. As the excitation energy increases, the level spacing decreases rapidly so that the levels become densely crowded. In this condition dealing with individual nuclear levels becomes impractical. Instead, it is meaningful and convenient to consider the average properties of nuclear excitations in terms of the nuclear level density (NLD) and radiative strength function (RSF). The former, introduced by Hans Bethe 80 years ago, is the number of excited levels per unit of excitation energy. The latter, proposed by Blatt and Weisskopf 64 years ago, describes the emission probability of high-energy γ-rays, which is expressed in terms of the average reduced partial radiation of γ-rays per unit energy interval.

These two quantities are indispensable ingredients in astrophysical nucleosynthesis, including the calculations of reaction rates in cosmos and production of elements, as well as in technology such as nuclear energy production and transmutation of nuclear waste. Therefore, the study of these quantities has been one of the most important topics in nuclear physics. This study has gained impetus in 2000 after the experimentalists of Oslo university proposed a method to simultaneously extract both the NLD and RSF from the primary γ-decay spectrum obtained in a single compound nuclear reaction experiment (Fig. 1). This method, however, suffers from the normalisation uncertainties.

Given the importance of the NLD and RSF, it is imperative to have a consistent theoretical basis to understand these quantities. Nonetheless, a unified theory capable of simultaneously and microscopically describing both the NLD and RSF has been absent so far.

In the present work, we propose for the very first time a microscopic approach, which is able to describe simultaneously the nuclear level density and radiative γ-ray strength function. This approach used the exact solutions of the pairing problem to construct the partition function to calculate the NLD and thermal pairing gap at finite temperature. The latter is included in the phonon damping model[1)] to calculate the RSF. The good agreement between the results obtained within this approach and the experimental data for NLD and RSF in ^{170,171,172}Yb (Fig. 1) has shown

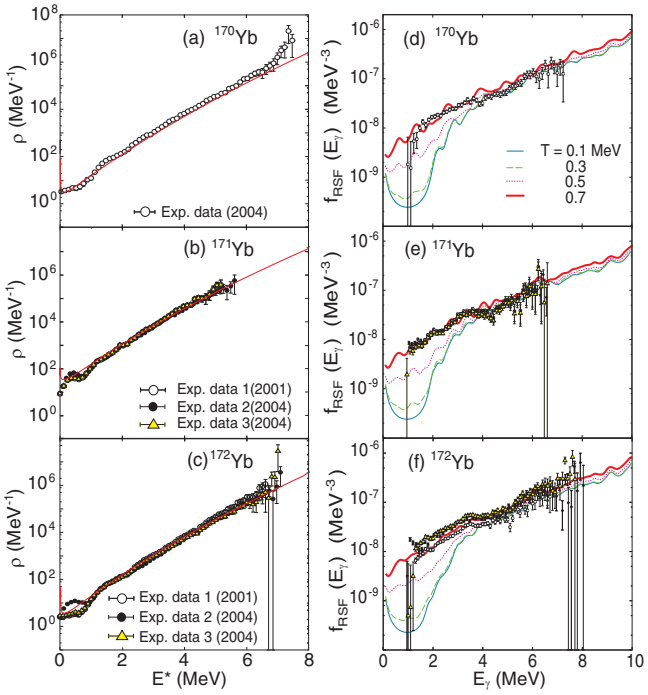

Fig. 1. NLD [(a) – (c)] as functions of excitation energy and RSF [(d) – (f)] as functions of γ-ray energy at different temperatures T, predicted by the present approach, in comparison with the experimental data for ytterbium isotopes ^{170,171,172}Yb.

that exact thermal pairing is indeed very important for the description of both NLD and RSF in the low and intermediate region of excitation and γ-ray energies. Moreover, to have a good description of the RSF the microscopic strength function with the temperature-dependent width for the giant resonances should be used instead of the Brink-Axel hypothesis. The merits of this approach are its microscopic nature and the use of only the parameters taken over from previous calculations. It does not consume much computing time either as the calculation takes less than five minutes even for a heavy nucleus, and therefore can be performed on a PC.

Reference

1) N. Dinh Dang, A. Arima, Phys. Rev. Lett. **80**, 4145 (1998); N.D. Dang, A. Arima, Nucl. Phys. A **636**, 427 (1998).

† Condensed from the article in Phys. Rev. Lett. **118**, 022502 (2017).

*1 Institute of Research and Development, Duy Tan University
*2 RIKEN Nishina Center
*3 Department of Natural Science and Technology, University of Khanh Hoa
*4 Faculty of Physics and Engineering Physics, Ho Chi Minh City University of Science

Disentangling transverse single spin asymmetries for forward neutrons in high-energy polarized-proton–nucleus collisions

G. Mitsuka*1

It is reported from the PHENIX experiment at BNL-RHIC that the transverse single spin asymmetry, denoted as $A_{\rm N}$, for forward neutrons measured in transversely polarized-proton–nucleus (pA) collisions at $\sqrt{s_{\rm NN}} = 200\,{\rm GeV}$ is far different from that in proton–proton (pp) collisions at $\sqrt{s} = 200\,{\rm GeV}$[1] (see panel (b) of Fig. 1.)

In this report, I present an important but rather unknown mechanism: ultra-peripheral pA collisions (UPCs, also known as Primakoff effects). UPCs contribute to the measured $A_{\rm N}$ modestly in pAl collisions and significantly in pAu collisions. UPCs occur when the impact parameter b is larger than the sum of the radii of each colliding particle, namely $b > R_p + R_A$ (R_p and R_A are the radius of the proton and nucleus, respectively). In UPCs, virtual photons (γ^*) emitted from the relativistic nucleus interact with the polarized protons and then produce the neutrons and other particles.

The differential cross section for single pion and neutron production, dominant among many other channels, in UPCs is given by

$$\frac{d\sigma^4_{{\rm UPC}(p{\rm A}\to\pi^+n)}}{dW\,db^2\,d\Omega_n} = \frac{d^3N_{\gamma^*}}{dW\,db^2}\frac{d\sigma_{\gamma^* p\to\pi^+n}(W)}{d\Omega_n}\overline{P_{\rm had}}(b), \quad (1)$$

where $d^3N_{\gamma^*}/d\omega^{rest}_{\gamma^*}db^2$ is the double differential photon flux due to the fast-moving nucleus, W is the $\gamma^* p$ center-of-mass energy, $d\Omega_n = \sin\Theta\, d\Theta\, d\Phi$ with the neutron scattering polar angle Θ and azimuthal angle Φ in the $\gamma^* p$ center-of-mass frame, and $\overline{P_{\rm had}}(b)$ is the probability of having no hadronic interactions in pA collisions at a given b. Single neutron and pion productions from the $\gamma^* p$ interaction are simulated following the differential cross sections predicted by the MAID 2007 model.[2] The cross section of the $\gamma^* p \to \pi^+ n$ interaction is approximated as

$$\frac{d\sigma_{\gamma^* p\to\pi^+n}}{d\Omega_\pi} \propto R_T^{00}\left(1 + \cos\Phi\frac{R_T^{0y}}{R_T^{00}}\right), \quad (2)$$

where R_T^{00} and R_T^{0y} are the response functions for pion photoproduction. $A_{\rm N}$ for forward neutrons in UPCs (hereafter $A_{\rm N}^{\rm UPC}$) inherits the target asymmetry $T(\pi - \Theta) \equiv R_T^{0y}/R_T^{00}$ in Eq. (2), which is ~ 0.7 at $W < 1.3\,{\rm GeV}$ and ~ -0.2 at $W > 1.3\,{\rm GeV}$ within the PHENIX detector acceptance. Owing to the virtual photon flux leading to low-energy photons and the pion photoproduction cross section via a $\Delta(1232)$ resonance, UPCs accordingly provide $A_{\rm N}^{\rm UPC} \sim 0.35$ for forward neutrons.

Figure 1 (a) shows the differential cross section in pAu collisions, $d\sigma/d\Phi$, as a function of Φ, for UPCs (dashed red line) and a one-pion exchange model (OPE) that represents hadronic interactions occuring at $b < R_p + R_A$ (solid black line). $A_{\rm N}$ originating in OPE well explains the PHENIX result in pp collisions but does not in pA collisions. In this study, the Glauber multiple scattering model is applied to OPE to account for nuclear effects. Here we find that UPCs have a positive and large $A_{\rm N}^{\rm UPC}$ compared with $A_{\rm N}^{\rm OPE} = -0.05$ of hadronic interactions.

In Fig. 1 (b), filled black circles indicate $A_{\rm N}$ inclusively measured by the PHENIX zero-degree calorimeter[1]. These $A_{\rm N}$ values can be compared with open red circles that correspond to the sum of UPCs and OPE MC simulations, denoted as $A_{\rm N}^{\rm UPC+OPE}$ and calculated as

$$A_{\rm N}^{\rm UPC+OPE} = \frac{\sigma_{\rm UPC}A_{\rm N}^{\rm UPC} + \sigma_{\rm OPE}A_{\rm N}^{\rm OPE}}{\sigma_{\rm UPC} + \sigma_{\rm OPE}}, \quad (3)$$

where $\sigma_{\rm UPC}$ and $\sigma_{\rm OPE}$ are the cross sections of UPCs and OPE, respectively. In pAu collisions, since $\sigma_{\rm UPC} \simeq \sigma_{\rm OPE}$, we obtain $A_{\rm N}^{\rm UPC+OPE} = 0.16$, which is consistent with the PHENIX result. Consistency between our simulation result $A_{\rm N}^{\rm UPC+OPE} = -0.02$ and the PHENIX data is also found in pAl collisions, where $\sigma_{\rm UPC}$ is 8 % of $\sigma_{\rm OPE}$.

In the MC simulations discussed in this report, electromagnetic effects (UPCs) and hadronic effects (OPE) are taken into account independently. However, the interference between these two effects, called the Coulomb-nuclear interference, would have nonzero amplitudes in the very small momentum-transfer region. The impremention of the Coulomb-nuclear interference will be a topic of future investigation.

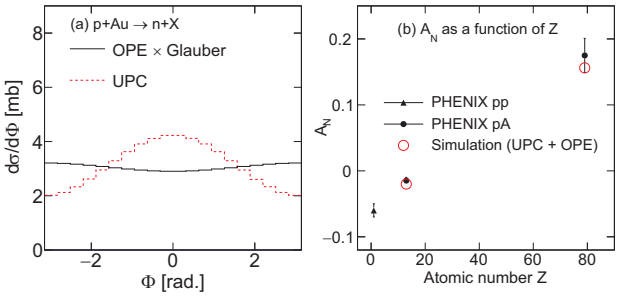

Fig. 1. Left: $d\sigma/d\Phi$ distributions for UPCs and OPE. Right: Comparison of $A_{\rm N}$ as a function of Z.

*1 RIKEN Nishina Center

References

1) I. Nakagawa et al. (PHENIX Collaboration), J. Phys. Conf. Ser. **736**, 012017 (2016).
2) D. Drechsel, S. S. Kamalov, L. Tiator, Eur. Phys. J. A **34**, 64 (2007).

Baryon interaction in lattice QCD†

T. Iritani*1 for HAL QCD Collaboration

Both Lüscher's finite volume method (direct method) and the HAL QCD method are used to study hadron interactions in lattice QCD. Theoretically, these approaches are equivalent. However, both the deuteron and dineutron are considered bound states in the direct method, while both are considered scattering states in the HAL QCD method for heavier pion mass.[2] To understand the origin of these deviations, we systematically study two-baryon systems using both the HAL QCD and finite volume methods.

In Lüscher's finite volume method, the phase shift $\delta(k)$ is obtained through

$$k \cot \delta(k) = \frac{1}{\pi L} \sum_{\vec{n} \in \mathbf{Z}^3} \frac{1}{|\vec{n}|^2 - |kL/(2\pi)|^2}, \qquad (1)$$

where k is given by the energy shift of two-baryon systems $\Delta E_{\rm BB} = 2\sqrt{m_B^2 + k^2} - 2m_B$ in the finite box L^3. In lattice simulations, $\Delta E_{\rm BB}$ is estimated from the plateau of the effective energy shift

$$\Delta E_{\rm BB}^{\rm eff}(t) \equiv -\frac{1}{a} \log \left(R_{\rm BB}(t+a)/R_{\rm BB}(t) \right), \qquad (2)$$

where $R_{\rm BB}(t) \equiv C_{\rm BB}(t)/\{C_{\rm B}(t)\}^2$ with the two-baryon propagator $C_{\rm BB}(t) \equiv \langle B(t)^2 \bar{B}(0)^2 \rangle$ and the baryon propagator $C_{\rm B}(t) \equiv \langle B(t)\bar{B}(0) \rangle$.

In lattice QCD, the signal-to-noise ratio of the multi-baryon system becomes exponentially worse for A baryons as $S(t)/N(t) \sim \exp[-A(m_B - (3/2)m_M)t]$ with the baryon number A and meson mass m_M. In addition, the energy gap of the elastic scattering states scales as $\mathcal{O}(1/L^2)$, which is about 50 MeV for a typical case. For ground-state saturation, $t \sim \mathcal{O}(10)$ fm is required.

To demonstrate the ground-state saturation problem, we consider the mock-up data as $R(t) = b_1 e^{-\Delta E_{\rm BB} t} + b_2 e^{-(\delta E_{\rm el} + \Delta E_{\rm BB})t} + c_1 e^{-(\delta E_{\rm inel} + \Delta E_{\rm BB})t}$, where $\delta E_{\rm el(inel)}$ is the gap of the (in)elastic state. Fig. 1 shows the effective energy shift of the mock-up data with typical values of the energy gaps $\delta E_{\rm el} = 50$ MeV and $\delta E_{\rm inel} = 500$ MeV. Without the elastic state $b_2/b_1 = 0$, the system converges to the ground state around $t \sim 1$ fm. However, a contamination of only 10% ($b_2/b_1 = \pm 0.1$) creates a fake plateau around $t \sim 1$ fm.

To check such fake plateaux, we study the quark source dependence of the effective energy shift. Fig. 2 shows the effective energy shift using a smeared source and wall source. Both show clear a plateau-like structure around $t \sim 15a \sim$ 1.5fm. However, their energy-shift values are different. This fake plateau problem causes serious concerns on previous studies using the direct method.[2,4]

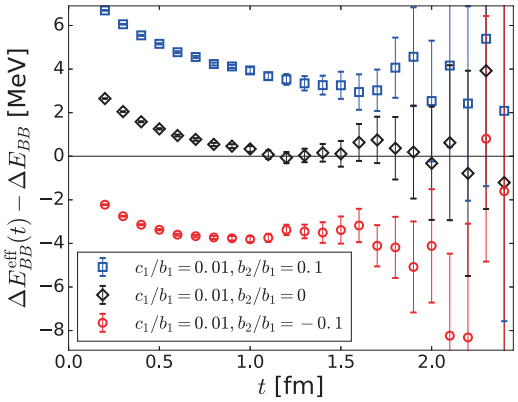

Fig. 1. Mock-up data with fluctuations.

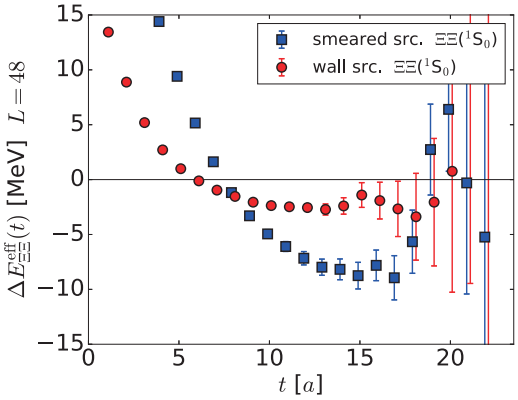

Fig. 2. Example of the effective energy shift $\Delta E^{\rm eff}(t)$.

On the other hand, in the HAL QCD method, we define the potential through the Nambu-Bethe-Salpeter function and study interactions based on this potential. In this approach, the ground-state saturation is not required, and we demonstrate the reliability of the HAL QCD method in the following papers.[3,4]

References

1) T. Iritani for HAL QCD Collaboration, J. of High Energy Phys. **1610**, 101 (2016).
2) T. Yamazaki, Proceedings of Science (LATTICE2014) 009 (2015), and references therein.
3) T. Iritani for HAL QCD Collaboration, Proceedings of Science (LATTICE2016) 107 (2016).
4) S. Aoki, T. Doi, T. Iritani, Proceedings of Science (LATTICE2016) 109 (2016).

† Condensed from the article in Journal of High Energy Physics **1610**, 101 (2016)[1]

*1 RIKEN Nishina Center

Performance of the SπRIT Time Projection Chamber

G. Cerizza,[*1,*2] J. W. Lee,[*2,*3] G. Jhang,[*2,*3] J. Barney,[*1,*2] J. Estee,[*1,*2] T. Isobe,[*2] M. Kaneko,[*2,*4] M. Kurata-Nishimura,[*2] P. Lasko,[*2,*5,*6] J. Łukasik,[*5] W.G. Lynch,[*1] A.B. McIntosh,[*7] T. Murakami,[*2,*4] P. Pawłowski,[*2,*5] K. Pelczar,[*6] H. Sakurai,[*2] C. Santamaria,[*1,*2] R. Shane,[*1] M. B. Tsang,[*1] S.J. Yennello,[*7] Y. Zhang,[*2,*8] and the SπRIT and NeuLAND collaborations

The goal of the SAMURAI Pion-Reconstruction and Ion-Tracker Time-Projection Chamber (SπRIT-TPC)[1)] project is to constrain the symmetry energy term in the nuclear-matter equation of state (EOS) at super-saturation density. We propose the comparison of π^-/π^+ production ratio among various isospin asymmetry systems through several combinations of unstable Sn beams and stable Sn targets inside the SAMURAI magnet. A commissioning run using a ^{132}Sn beam impinging on a natural tin target was performed in April 2016, immediately before the pion ratio experimental campaign of May 2016. This included four beams (^{132,124,112,108}Sn) on two different targets (^{124,112}Sn) and a cocktail beam consisting of p, d, t, ^{3}He, ^{4}He, and ^{6}Li particles used to calibrate the gain of the detector. For the commissioning experiment, the SπRIT-TPC was placed inside the SAMURAI magnet and lined up at 0° with respect to the beamline. The secondary ^{132}Sn beam impinged on a 0.5 mm natural tin foil target mounted on a ladder in front of the TPC field cage window. The complete version of the SπRITROOT analysis framework was officially deployed and tested for the first time. The three plots on the right side of Fig. 1 show the pad-plane view (with 12096 pixels) of examples of collision on target (top and middle) and active-target (bottom) events. Two spiral trajectories can be observed in the first two panels and are identifiable as rare low-energy π^- particles, which curve in the opposite direction from the positively charged ions. In the bottom panel, an active-target collision event between the ^{132}Sn beam and the gas molecules filling the volume of the TPC is shown, where the reaction vertex can be visually identified inside the TPC. In all of them, the saturation effects of the electronics caused by high-Z particles and the beam passing through the target can be observed in the center region of the pad plane (red pads). The left plot of Fig. 1 shows the particle identification spectra of particles emitted from the ^{132}Sn+^{nat}Sn collisions and detected in the TPC. The reaction vertex was extrapolated from reconstructed tracks event by event. About 30% of the events have one reconstructed vertex inside the TPC volume in active-target-like collision events. Of the remaining events, 85% have a reconstructed vertex within 5 mm from the target position along the beam axis. The average track multiplicity per event is 45 with the distribution shape affected by the multiplicity selection criteria in the multiplicity trigger arrays. Preliminary reconstruction efficiencies due to the geometry of the TPC have been estimated from Monte Carlo simulation to be above 90% for charged particles of momenta up to 2000 MeV/c in the range $[-60, 60]$ and $[-70, 70]$ degrees for polar and azimuthal angles, respectively. The expected momentum resolution is estimated to be a few percent by using GEANT4 simulation to model the TPC. The lower limit in the reconstructed pion momenta is about 30 MeV/c. With the ongoing improvement of the tracking and fitting algorithms of the SπRITROOT analysis package the final efficiencies will be determined at a later stage. The success of the first commissioning of SπRIT-TPC inside the SAMURAI magnet and the pion ratio experiments performed in May 2016 are the basis of future proposals for the physics program of constraining the symmetry energy term in the nuclear-matter equation of state (EOS) at super-saturation density.

This work is supported by the U.S. DOE under Grant Nos. DE-SC0004835, DE-SC0014530, DE-NA0002923, US NSF Grant No. PHY-1565546, the Japanese MEXT KAKENHI grant No. 24105004, and by the Polish NSC Grants UMO-2013/09/B/ST2/04064 and UMO-2013/10/M/ST2/00624.

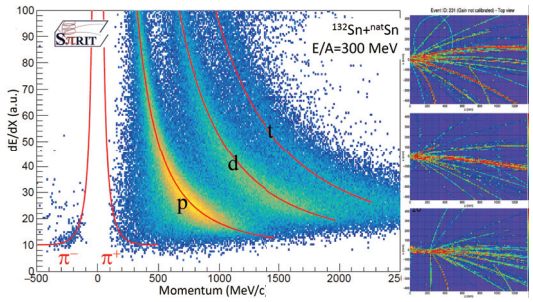

Fig. 1. Commissioning of the TPC with the ^{132}Sn radioactive beam: particle identification map (left) and pad-plane track projections for three sample events (right).

*1 NSCL and Dept. of Phys. & Ast., Michigan State University
*2 RIKEN Nishina Center
*3 Department of Physics, Korea University
*4 Department of Physics, Kyoto University
*5 IFJ PAN, Kraków
*6 Jagiellonian University, Kraków
*7 Cyclotron Institute, Texas A&M University
*8 Department of Physics, Tsinghua University

Reference
1) R. Shane et al., Nucl. Instr. Meth. A **784**, 513 (2015).

Commissioning of Rare RI Ring using exotic nuclei

D. Nagae,[*1] S. Omika,[*1,*2] Y. Abe,[*1] Y. Yamaguchi,[*1] F. Suzaki,[*1] K. Wakayama,[*2] N. Tadano,[*2] R. Igosawa,[*2] K. Inokuma,[*2] Y. Arakawa,[*2] K. Nishimuro,[*2] T. Fujii,[*2] T. Mitsui,[*2] T. Yamaguchi,[*2] T. Suzuki,[*2] S. Suzuki,[*3] T. Moriguchi,[*3] M. Amano,[*3] D. Kamioka,[*3] A. Ozawa,[*3] S. Naimi,[*1] Z. Ge,[*1,*2] Y. Yanagisawa,[*1] H. Suzuki,[*1] H. Baba,[*1] S. Michimasa,[*4] S. Ota,[*4] G. Lorusso,[*5] Yu.A. Litvinov,[*6] M. Wakasugi,[*1] T. Uesaka,[*1] and Y. Yano[*1]

The Rare RI Ring[1] is an isochronous storage ring constructed to measure the masses of short-lived rare nuclei using the time-of-flight (TOF) measurement method. We conducted two commissioning experiments[2–4] in 2015. In the first commissioning experiment, we verified the operation of each component, while in the second commissioning experiment, we made the first attempt of mass measurement using stable nuclei. This year, we have performed commissioning using exotic nuclei with well-known masses to confirm the feasibility and principle of mass determination using the following equation:

$$\frac{m_1}{q} = \frac{m_0}{q}\frac{T_1}{T_0}\sqrt{\frac{1-\beta_1^2}{1-(\frac{T_1}{T_0}\beta_1)^2}}, \quad (1)$$

where $m_{0,1}/q$ denote the mass-to-charge ratio of the reference particle and particle of interest, respectively; $T_{0,1}$ are revolution times of these particles; and β_1 is the velocity of the particle of interest. Because the isochronous condition is adjusted for the reference particle, isochronism is not fulfilled for particles of interest by the velocity measured upstream.

Exotic nuclei around ^{78}Ge were produced from the relativistic in-flight fission of a primary beam of ^{238}U at an energy of 345 MeV/nucleon on a ^{9}Be target with a thickness of 10 mm. We identified these nuclei before the F3 achromatic focus of BigRIPS. Figure 1 shows a particle identification plot. The energy loss (ΔE) was obtained using an ionization chamber located at F3, and TOF was measured between F2 and F3. Using Bρ and the measured TOF between F3 and the S0 achromatic focus of SHARAQ, the β_1 values for particles were deduced. We injected these nuclei to the ring using the individual injection method with the fast kicker system.[5] The isochronous magnetic field in the ring was adjusted for the reference particle ^{78}Ge with a precision of 5 ppm for a momentum spread of $\pm$ 0.3%.[6] We confirmed the storage of several particles by using a circulation detector[7] and a δ-ray detector.[8] These particles circulated in the ring for about 1850 turns, which corresponds to about 0.7 ms. Exotic nuclei ^{79}As, $^{77-79}$Ge, ^{76,77}Ga, ^{75,76}Zn, and ^{75}Cu were successfully extracted from the ring as indicated by the red dot in Fig. 1. $T_{0,1}$ for each nuclei are deduced from the TOF between S0 and the ring exit ELC. Figure 2 shows the TOF spectra with peak assignments. Mass accuracies are preliminary obtained for ^{79}As, ^{77}Ga, ^{76}Zn, and ^{75}Cu as 7.2×10^{-6}, 1.1×10^{-5}, 1.5×10^{-5}, and 2.1×10^{-5}, respectively. The successful individual injection, storage, extraction, and TOF measurement in the ring for exotic nuclei make the mass measurement of more neutron-rich nuclei feasible in the near future.

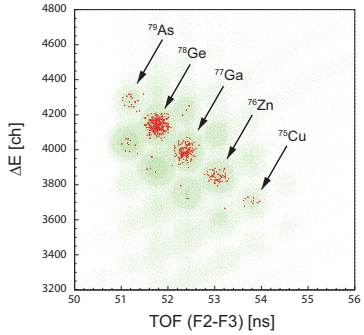

Fig. 1. Particle identification plot. Green dots indicate all events at F3, and red dots indicate extracted events.

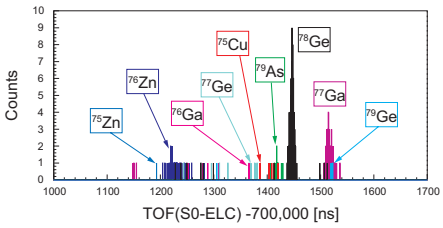

Fig. 2. TOF spectra between S0 and ELC.

*1 RIKEN Nishina Center
*2 Department of Physics, Saitama University
*3 Institute of Physics, University of Tsukuba
*4 Center for Nuclear Study, University of Tokyo
*5 Department of Physics, University of Surrey
*6 GSI Helmholtzzentrum für Schwerionenforschung

References

1) A. Ozawa et al., Prog. Theor. Exp. Phys. **2012**, 03C009 (2012).
2) Y. Yamaguchi et al., RIKEN Accel. Prog. Rep. **49**, 18 (2017).
3) Y. Abe et al., RIKEN Accel. Prog. Rep. **49**, 19 (2017).
4) F. Suzaki et al., RIKEN Accel. Prog. Rep. **49**, 179 (2017).
5) H. Miura et al., RIKEN Accel. Prog. Rep. **49**, 154 (2017).
6) Y. Yamaguchi et al., In this report.
7) D. Nagae et al., RIKEN Accel. Prog. Rep. **49**, 181 (2017).
8) S. Omika et al., In this report.

Construction status of OEDO beamline

S. Michimasa,[*1] S. Shimoura,[*1] M. Matsushita,[*1] N. Imai,[*1] K. Yako,[*1] H. Yamaguchi,[*1] S. Ota,[*1] E. Ideguchi,[*2] H. Sakurai,[*3] K. Yoshida,[*3] Y. Yanagisawa,[*3] K. Kusaka,[*3] M. Ohtake,[*3] T. Sumikama,[*3] and K. Yamada[*3]

The OEDO system is a new beamline proposed for high-quality slow-down RI beams.[1)] The OEDO is an abbreviation of **O**ptimized **E**nergy **D**egrading **O**ptics for RI beam. The idea behind it is to manipulate the timing degree of freedom in the phase space of an RI beams. To obtain a high-quality beam with a small spot size and a small energy spread, the OEDO system shifts the spreads of positions and angles to the timing spread of the beam, which corresponds to the rotation of the phase space ellipse on the position- (angle-)timing plane to obtain a small position (angle) spread. Radiofrequency (RF) electric ion-optical elements can rotate a phase space ellipse of spatial and timing components, as beams from a cyclotron have an RF bunch structure.

The main components of the OEDO system are an RF deflector[2)] synchronized with the cyclotron's RF and 2 sets of triplet quadrupole (TQ) magnets to achieve point-to-parallel/parallel-to-point ion optics. The OEDO system is to be installed downstream of a momentum-dispersive focus with a reasonable dispersion. The first TQ associates the beam energy with beam angle at the RF deflector, and the second TQ makes a small achromatic focus. This dispersion condition is fulfilled in the first half of the High-Resolution (HR) beamline.[3)] Therefore, the OEDO system will be implemented in the HR beamline by installing new electric/magnetic elements and rearranging the existing magnets.

The main part of the construction budget was funded and the OEDO project was launched in FY2014. The rearrangement from the HR beamline to the OEDO beamline will be finished in March 2017. Figure 1 shows the magnet arrangement of the OEDO beamline downstream of the FE7 focal plane, which corresponds to the FH7 focal plane of the HR beamline. The function of the OEDO system is built between the FE9 and FE11 foci. In December 2016, a superconducting triplet quadrupole (STQ) magnet was delivered. The FE12 focus is the target position of the SHARAQ spectrometer.

Figures 2 and 3 show the recent status of the delivered RF deflector and the entire OEDO system installed in the beamline leading to the SHARAQ spectrometer, respectively.

The RF deflector will be completed in March 2017 after its operation test. The commissioning run of the OEDO system is planned for the first half of FY2017.

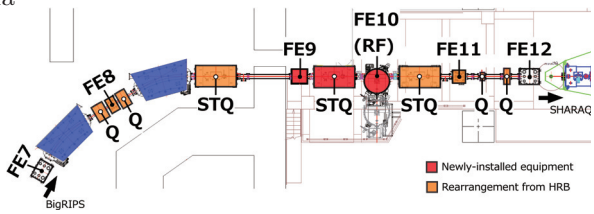

Fig. 1. Magnet configuration of the OEDO beamline

Fig. 2. A photograph of the delivered RF deflector.

Fig. 3. A photograph of the entire OEDO system.

This work was funded by ImPACT Program of Council for Science, Technology and Innovation (Cabinet Office, Government of Japan).

References

1) S. Shimoura et al., CNS Annual Report 2013, CNS-REP-93, 56 (2015).
2) K. Yamada et al., Nucl. Phys. A **746**, 156c (2004).
3) S. Michimasa et al., Nucl. Instrum. Meth. in Phys. Res. **B317**, 305 (2013).

[*1] Center for Nuclear Study, University of Tokyo
[*2] RCNP, Osaka University
[*3] RIKEN Nishina Center

Gamma-ray inspection of a rotating object

T. Kambara*1 and A. Yoshida*1

We are developing a method called gamma-ray inspection of a rotating object (GIRO) to image the spatial distribution of γ-ray sources. The setup employs two sets of collimated γ-ray detectors on the opposite sides of an object with RI sources that continuously rotates. The principle of the method and some results of test measurements have been reported.[1,2)]

We replaced the original detectors with four NaI(Tl) scintillation detectors (V51B102/2M-X from Scionix, 51 mm × 51 mm × 102 mm). Two detectors were stacked on either side of a turntable. The energy resolution of the new detectors was about 7.2 %-7.8 % full-width half maximum (fwhm) for 511-keV γ rays, which is better than the 17 %-18 % fwhm of the previous detectors.

The γ-ray collimator in the original setup was a 4-mm wide vertical aperture between two 3-cm thick lead blocks. The γ-ray photons that penetrated the edge of the block resulted in a dull collimation and caused a background near a strong source in the reconstructed image. To improve the collimation, we attached a parallel pair of wolfram plates (W-plates) to the lead blocks. The W-plates were 2-mm thick, 110-mm high, and 100-mm deep and separated by 4 mm, as shown in Fig. 1.

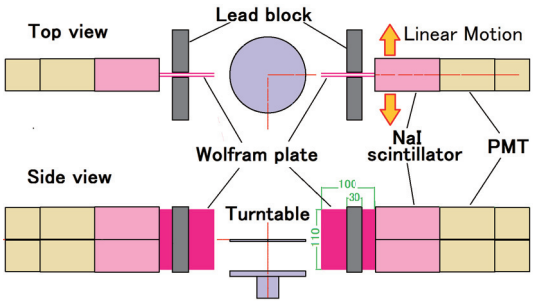

Fig. 1. GIRO detector setup with wolfram plates.

Figure 2 compares reconstructed images taken (a) without and (b) with the W-plates for three point-like ^{22}Na sources (309 kBq, 29 kBq, and 2.6 kBq) on the turntable. The turntable rotated at 150 rpm and the detectors moved by 2 mm/step and 1 step/10 s over a ±74-mm range. The measurement time was about 10.3 h without the W-plates and 20.7 h with them.

The two-dimensional image shows three spots corresponding to the sources. In the image without the W-plates, a halo-like background surrounds the spot of 309 kBq, but it disappears in the image with the W-plates. The y-axis projections of the image on the right show that the W-plates reduced the background around the highest peak.

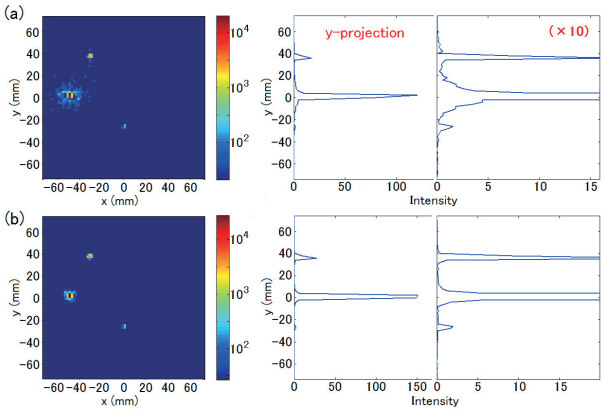

Fig. 2. Reconstructed image of three ^{22}Na sources with collimators (a) without and (b) with the W-plates. Left is the two-dimensional image, right is its projection to y-axis and its ten-fold magnification.

The measurements described above were performed in the PET mode with coincidence measurements of two 511-keV photons from the positron annihilation. GIRO also allows SPECT-mode measurements, where single γ-ray photons are detected by each detector. The SPECT mode has a lower spatial resolution for the RI distribution and higher background than the PET mode, but it is applicable to various γ-ray emitting nuclides and its measurement time is much shorter. Figure 3 shows SPECT-mode images of the same setup as shown in Fig. 2 taken by 511-keV photons. The measurement took about 27 min. The W-plates improve the resolution of the SPECT-mode image, which shows not only the 309 kBq source but also the 29 kBq source.

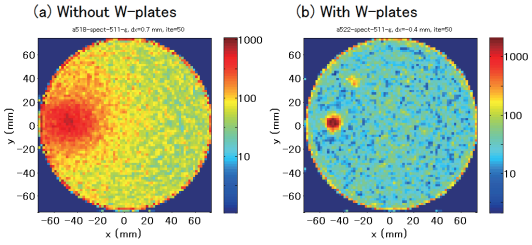

Fig. 3. SPECT-mode image of the same source shown in Fig. 2 (a) without and (b) with the W-plates.

*1 RIKEN Nishina Center

References
1) T. Kambara, A. Yoshida, and H. Takeichi: Nucl. Instr. Meth. A **797**, 1 (2015).
2) T. Kambara: Nuclear Physics News **26**, No. 4, 26 (2016).

Effects of 2.6 GeV uranium irradiation on FeSe†

Y. Sun,[*1] A. Park,[*1] S. Pyon,[*1] T. Tamegai,[*1] A. Ichinose,[*2] A. Yoshida,[*3] and T. Kambara[*3]

The introduction of nonmagnetic disorders has been proven to be an effective method to identify the gap structures of novel superconductors.[1)] For point defects introduced by light-particle irradiations, such as electrons and protons, a clear suppression of T_c was observed in both cuprates and iron pnictides, which was attributed to the sign change of the order parameter in d-wave and $s_{\pm}$ (or competition between $s_{\pm}$ and s_{++} via inter- and intra-band scatterings), respectively. In the case of correlated disorders created by heavy-ion irradiation, such as columnar defects, an obvious suppression of T_c together with the increase in the normal-state resistivity has been reported in cuprates. However, the T_c shows only a small or nondetectable change in iron pnictides. The penetration depth in Co- or K-substituted $BaFe_2As_2$ was found to change after heavy-ion irradiation, which is consistent with the $s_{\pm}$ scenario. On the other hand, the columnar defects created by heavy-ion irradiation are also strong pinning centers due to the geometrical similarity with vortices, which have already been proven to be effective for the enhancement of critical current density J_c. Their controllability is also advantageous in the study of vortex physics. Thus, studies of the effects of heavy-ion irradiation on FeSe are crucial to the understanding of its pairing mechanism and vortex physics, which is important for the application of this material.

In this report, the effects of heavy-ion irradiation on FeSe single crystals are studied in detail by irradiating 2.6-GeV uranium up to a dose-equivalent matching field of $B_\phi = 16$ T. FeSe single crystals were grown by the vapor transport method. The obtained crystals were of high quality with a sharp superconducting transition width $\Delta T_c < 0.5$ K from susceptibility measurements and a large residual resistivity ratio of ~33 as reported in our previous publications.[2–4)] Before the irradiation, single crystals were cleaved to thin plates with thickness ~20 μm along the c-axis, which is much less than the projected range of 2.6-GeV uranium for FeSe of ~60 μm, calculated by "Stopping and Range of Ions in Matter-2008 (SRIM-2008)". The 2.6 GeV uranium beam was irradiated parallel to the c-axis of the crystal at room temperature. The uranium irradiation was performed at the RI Beam Factory operated by RIKEN Nishina Center and CNS, the University of Tokyo.

The columnar defects were confirmed by high-resolution transmission electron microscopy observation, and they are almost continuous along the c-axis with a diameter of ~10 nm, which is much greater than that of 2-5 nm observed in iron pnictides. As shown in Fig. 1, the value of T_c is found to be gradually suppressed by introducing columnar defects at a rate of $dT_c/dB_\phi \sim$ -0.29 KT^{-1}, which is greater than that observed in iron pnitides.[5)] The quick suppression of T_c suggests a unique pairing mechanism of FeSe.

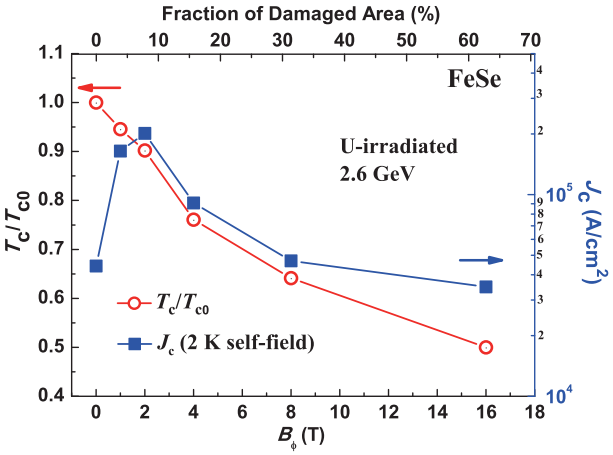

Fig. 1. Normalized T_c (T_c/T_{c0}, where T_{c0} is the value of T_c for the pristine sample) and the self-field J_c at 2 K as a function of the matching field B_ϕ (bottom axis) and damaged area (top axis) for the 2.6-GeV uranium-irradiated FeSe.

The critical current density is first dramatically enhanced with irradiation reaching a value over ~2×10^5 A/cm^2 at 2 K (self-field) for $B_\phi = 2$ T, and then gradually suppressed with further increase in B_ϕ. The evolution of T_c and J_c with irradiation dose is explained by the large diameter of columnar defects. The nature of the quick enhancement of J_c by a small dose of heavy-ion irradiation in FeSe is also advantageous for real application. In addition, vortex dynamics study shows that the δl-pinning associated with charge-carrier mean-free-path fluctuations and the δT_c-pinning associated with spatial fluctuations of the transition temperature are found to coexist in pristine FeSe, while the irradiation increases the δl-pinning and makes it dominant above $B_\phi = 4$ T.

References
1) H. Alloul et al., Phy. Mod. Rev. **81**, 45 (2009).
2) Y. Sun et al., Phy. Rev. B **92**, 144509 (2015).
3) Y. Sun et al., Phy. Rev. B **93**, 104502 (2016).
4) Y. Sun et al., Phy. Rev. B **94**, 134505 (2016).
5) F. Ohtake et al., Physica C **518**, 47 (2015).

† Condensed from Phys. Rev. B **95**, 104514 (2017)
*1 Department of Applied Physics, The University of Tokyo
*2 Central Research Institute of Electric Power Industry, Electric Power Engineering Research Laboratory
*3 RIKEN Nishina Center

Stable transmission of slow highly charged ions through tapered glass capillary with active discharging method for sub-micron sized beams†

T. Ikeda,[*1] T. M. Kojima,[*1] Y. Natsume,[*2] J. Kimura,[*2] and T. Abe[*1]

Slow (10–100 keV), highly charged ion (HCI) beams have been widely used for the processing and analysis of materials. Such ions have the advantage of being "soft" ionizers for target molecules.[1)] When a slow HCI hits a molecule, the ion captures some electrons from the target molecule, which causes the specific breaking of relatively weak bonds. The low kinetic energy of the ion limits damage to the target. In order to use the advantage in microscopic analysis and the modification of the material surface, small, simple, and stable micro-HCI beam generators are required.

In 2006, we demonstrated a simple and convenient method for producing microbeams of slow HCIs (8-keV Ar^{8+}) using a single tapered glass capillary with an outlet diameter of 24 μm.[2)] The key mechanism for beam transportation is based on self-organized charge patches on the inner surface of the capillary, which are induced by the incident beam itself. The transmitted beam had the same diameter as the capillary outlet and kept the initial charge state and energy. The intensity of the transmitted beam was several times larger than that expected from the cross-section ratio of outlet to inlet (focusing effect). Using capillaries, one can easily determine the beam position under a microscope because the beam position coincides with the capillary outlet. However, transmitted microbeams occasionally become unstable, and their transmission can be blocked[3)] or suddenly increased. These instability problems need to be solved for the use of this method in a slow micro-HCI beam generator.

The experiments were performed at the Slow Highly Charged Ion Facility in RIKEN. A large capillary made of soda lime glass, from Hamamatsu Photonics K.K., had an outer surface and the inlet and outlet surfaces which were coated with conductive material to allow operation as ring (or tube-shaped) electrodes, as indicated by 4 orange arrows in Fig. 1(a). A small capillary made of soda lime glass with D'_{out} = 0.75 μm (Figs. 1(a) and 1(b)) was used. The inlet surface of the small capillary was coated with conductive paste and placed in contact with the outlet surface of the large capillary. When the beam enters the optics, the charge on the inner surfaces near *el*-A increases. Some of the charge can flow on the inner surface and then reach the edge of the inner surface, which is the border between the inner surface and outlet surface. Once the charge reaches the outlet surface, *el*-A and the outlet surface gradually accumulate charge. To remove the excess charge from *el*-A, a mechanical relay switch was installed between *el*-A and the ground (Fig.1(c)). The relay was controlled by TTL signals with a frequency f_{TTL} = 0.1 Hz, called *active discharging*. For a 104-keV Ar^{8+} beam, Fig. 1(d) shows the number of transmitted ions per second $N_{transmit}$ (blue line). Based on the stable $I_{monitor}$ (red curve) monitored at an entrance aperture of the experimental chamber, the input current to the large capillary I_{input} was estimated to be stable. The TTL signals were sent before 3050 s and after 3350 s (light green zones). During the 300-s time without relay operation, the transmission became gradually blocked and eventually stopped. When the TTL sending restarted, the transmission also started again with almost the same $N_{transmit}$ and remained constant until the input beam stopped.

To confirm the effect of the active discharging we tested the transmission stability through the large capillary without the small capillary by measuring the transmitted beam current $I_{transmit}$ with a Faraday cup (FC). The same effect due to the active discharging was found with some density gain.

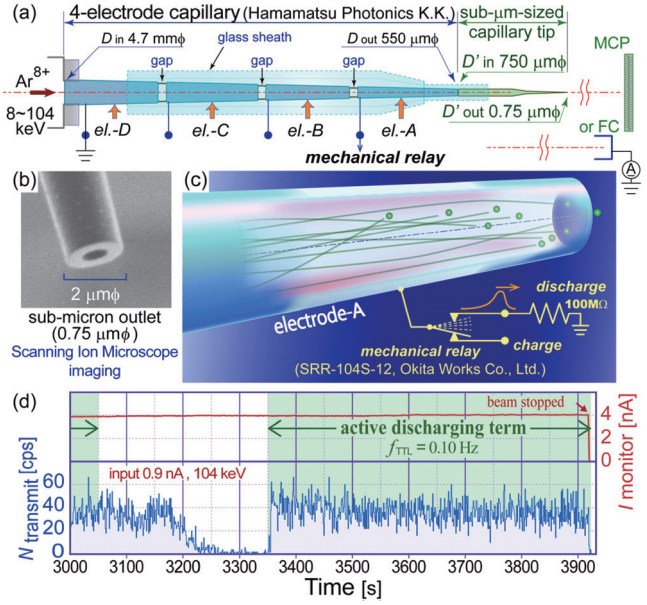

Fig. 1. (a) The glass tandem optics consisting of a 4-electrode capillary (large capillary) and a sub-μm-sized capillary tip (small capillary). (b) A magnified view of the tip outlet. (c) The active discharging maintains the charge below the level at which blocking is induced. (d) The number of transmitted ions as a function of time with or without the active discharging.

† Condensed from the article in T. Ikeda *et al.*, Appl. Phys. Lett. **109**, 133501 (2016).

*1 RIKEN Nishina Center
*2 Hamamatsu Photonics KK

References

1) S. Maclot et al., Chem. Phys. Chem. **12**, 930 (2011).
2) T. Ikeda et al., Appl. Phys. Lett. **89**, 163502 (2006).
3) N. Stolterfoht et al., Phys. Rev. A **88**, 032902 (2013).

Investigation of magnetic ordered states in the pyrochlore iridates $(Nd,Ca)_2Ir_2O_7$ probed by μSR

R. Asih,[*1,*2] D. P. Sari,[*1,*2] J. Angel,[*1,*3] K. Matsuhira,[*4] T. Nakano,[*2] Y. Nozue,[*2] and I. Watanabe[*1,*2,*3]

Pyrochlore iridates $R_2Ir_2O_7$ ($R227$, R is a lanthanide element), have attracted growing interest because of their potential for realizing new topological states in the presence of strong spin-orbit coupling (SOC) and electron correlation (U), such as the Mott insulator, Weyl semimital, and axion insulator.[1)] Interestingly, the electron correlation (U) in these compounds can be systematically tuned by changing the ionic radius of the R-ion (r). $R227$ shows systematic metal-insulator transition (MIT) at T_{MI}, which gradually decreases by increasing the ionic radius of the R^{3+} ion, and its boundary lies between R= Nd and Pr[2)]. Abundant emergent quantum states have been theoretically predicted to occur on the boundary of MIT.[1)] In order to unravel those states, it is necessary to finely tune U in this MIT-critical region. One way to do this is to substitute a nonmagnetic ion such as Ca for Nd, $(Nd_{1-x}Ca_x)_2Ir_2O_7$, which leads to the doping of holes in the Ir $5d$ band, and hence drives the transition from insulator to metal at the ground state and simultaneously suppresses magnetic orders. In this study, we systematically investigated changes in magnetic ordered states of $Nd_2Ir_2O_7$ due to hole doping by means of μSR measurements.

Pure $Nd_2Ir_2O_7$ exhibits metallic behavior and undergoes MIT at T_{MI}= 33 K.[2)] Our μSR study on $Nd_2Ir_2O_7$ showed the appearance of a long-range magnetic order of Ir^{4+} moments below T_{MI} followed by an additional magnetic order of Nd^{3+} moments below 10 K.[3)4)] In the dilute hole-doped system $x = 0.01$, this Ir ordering appears at a lower temperature of around 26 K, as displayed in Fig. 1, indicating the suppression of the onset of the magnetic ordering. The zero-field (ZF) time spectra showed spontaneous muon-spin precession below 26 K, which was then well analyzed by the following function.

$$A_{(t)} = A_r e^{-\lambda_r t} + A_\omega cos(\gamma_\mu H_{int} t + \varphi) e^{-\lambda_\omega t} \qquad (1)$$

The first component expresses the relaxing behavior with initial asymmetry A_r and relaxation rate λ_r, and the second one expresses the muon-spin precession with initial asymmetry A_ω, damping rate λ_ω and phase of the precession φ. Here γ_μ and H_{int} are the gyromagnetic ratio of the muon spin ($2\pi \times 13.55$ kHz/G) and the internal field at the muon site, respectively.

*1 RIKEN Nishina Center
*2 Department of Physics, Osaka University
*3 Department of Condense Matter Physics, Hokkaido University
*4 Graduate School of Engineering, Kyushu Institute of Technology

The temperature dependences of the parameters obtained from the analysis of the ZF-μSR data are shown in Fig. 2. The dilute hole-doping gradually suppressed the onset of magnetic ordering and the internal field coming from the Ir^{4+} ordering, while the internal field coming from the Nd^{3+} ordered moments tended to increase below 5 K. The critical slowing down in the relaxation rate (Fig. 2b) indicates that Nd^{3+} moments form a static ordering below about 10 K that does not rely on Ca concentration. Further measurements will be conducted on the intermediate and heavy Ca-doped systems to complete the magnetic phase diagram of $(Nd_{1-x}Ca_x)_2Ir_2O_7$.

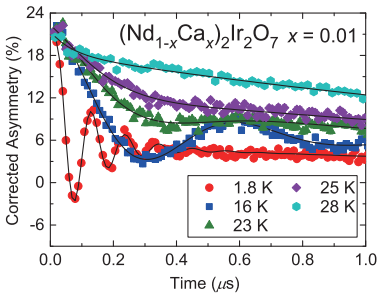

Fig. 1. Zero field time spectra of $(Nd_{1-x}Ca_x)_2Ir_2O_7$ x = 0.01 at the early time region. Solid lines show fits to the data described in the text.

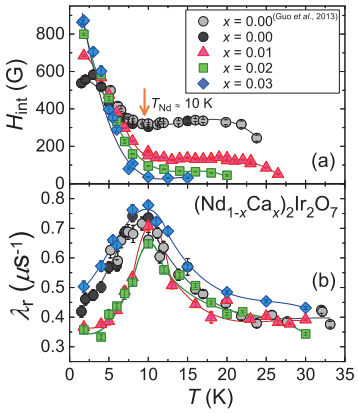

Fig. 2. Parameters derived from fitting Eq. 1 to the zero field μSR data of $(Nd_{1-x}Ca_x)_2Ir_2O_7$. (a) Internal field at muon sites H_{int} and (b) relaxation rate λ_r. Solid lines are guides for the eye.

References

1) X. Wan et al., Phys. Rev. B **83**, 205101 (2011).
2) K. Matsuhira et al., J. Phys. Soc. Jpn. **80**, 094701 (2011).
3) H. Guo et al., Phys. Rev. B **88**, 060411(R) (2013).
4) R. Asih et al., J. Phys. Soc. Jpn. **86**, 024705 (2017).

Studies of the muon transfer process in a mixture of hydrogen and higher Z gas

A. Vacchi,[*1,*2,*3] K. Ishida,[*1] E. Mocchiutti,[*3] N. Rossi,[*2] on behalf of the FAMU collaboration

The final aim of this experiment is a precision spectroscopic measurement of hyperfine splitting (hfs) in the 1S state of muonic hydrogen $\Delta E^{hfs}(\mu^- p)_{1S}$ - providing crucial information on proton structure and muon-nucleon interaction in order to provide the proton Zemach radius r_Z with higher precision than previously possible.[1)] This will allow discordant theoretical values to be disentangled and evidence any level of discrepancy that may exist between values of r_Z extracted from normal and muonic hydrogen atoms. It will also set a needed cornerstone result about not yet explained anomalies within the proton charge mean square radius r_{ch}.[2,3)] By measuring the $\Delta E^{hfs}(\mu^- p)_{1S}$ transition wavelength with an unprecedented precision of $\delta\lambda/\lambda < 10^{-5}$, the final experiment will establish new limits on the proton structure parameters and shed light on the low momentum limit of the magnetic-to-charge form factor ratio.[4)] The physical process behind this experiment is the following: muonic hydrogen atoms are formed in a gas target containing a mixture of hydrogen and a higher-Z gas. A muonic hydrogen atom in the ground state, after absorbing a photon of energy equal to the hyperfine-splitting resonance-energy $\Delta E_{hfs} \approx 0.182$ eV, is very quickly de-excited in subsequent collision with the surrounding H_2 molecules. At the exit of the collision, the muonic atom is accelerated by ~2/3 of the excitation energy ΔE_{hfs}, which is taken away as kinetic energy. The experiment will observe the products of a reaction whose rate depends on the kinetic energy of the muonic atoms. The observable is the time distribution of the characteristic X-ray emitted from the muonic atoms formed by muon transfer from hydrogen to the atom of the admixture gas $(\mu p) + Z \rightarrow (\mu Z)^* + p$ and its response to variations of the laser radiation wavelength. The $(\mu^- p)_{1S}$ hfs resonance is recognized by the maximal response to the tuned laser wavelength of the time distribution of X-ray K-lines cascade from the $(\mu Z)^*$. By means of Monte Carlo simulations based on the existing data it has been shown that the described method will provide the expected results.[5)]

During the first tests in 2014 at the beam delivery Port 4 of the RIKEN-RAL facility, the detection system and the beam condition allowed a satisfactory background situation.[6,7)] Because the efficiency of the method is bound to the collisional energy dependence of the muon transfer rate, the main focus in 2015-2016 has been a detailed experimental analysis of the muon transfer mechanism by measuring the muon transfer rate at various temperatures.

While for many gases the transfer rate at low energies is nearly constant, there is experimental evidence of a relevant energy dependence for oxygen.[7)] Our team has performed, at PORT4, the needed dedicated study of muon transfer from hydrogen to the atom of an admixture gas, and, in particular, to oxygen, at temperatures between 300 and 100 K to confirm the energy dependent muon transfer rate for oxygen and the profitability of this method (see Fig. 1). While the final data are still subject to careful verification, the presently extracted behavior of the transfer rate confirms the expectations and the proposed experimental method.

To achieve this result, great care has been put into the simulation,[8)] final design, and construction of the experimental layout with particular regard to the cryogenic high-purity gas-target able to work at temperatures below 50K and pressures up to 40 atmospheres. The tasks were the following: to minimize the material at the beam entrance window of the thermally isolated structure so as to keep a minimal induced spread of the low momentum beam, to minimize the thickness of the lateral walls so as to allow high transparency for the X-rays of the muonic cascade of interest, and finally to coat the internal vessel with thin layers of high Z material in order to promote fast nuclear muon capture for non-hydrogen muonic atoms and minimize the non-prompt noise induced by decay electrons.

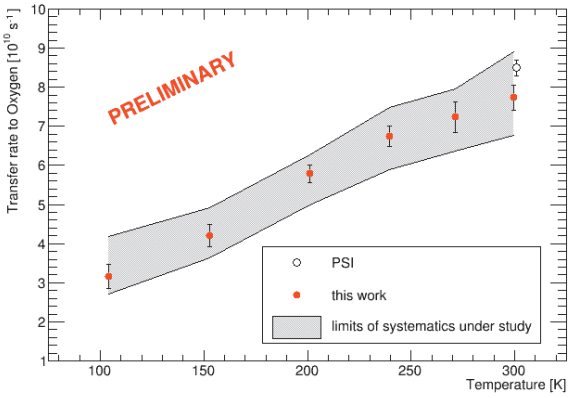

Fig. 1. Transfer rate to oxygen as function of temperature.

References
1) A. Adamczak et al., Phys. Lett. A 379 (2015).
2) R. Pohl et al., Nature 466 (2010).
3) A. Antognini et al., Science 339 (2013).
4) S.G. Karshenboim, Phys. Rev. A 91 (2014).
5) D. Bakalov et al., Can. J. Phys. 83 (2005).
6) A. Adamczak et al., J. of Inst. 11, P05007 (2016).
7) A. Vacchi et al., RIKEN Accel. Prog. Rep. 49, 230 (2016).
8) P. Danev et al., J. of Inst., 11, P03019 (2016).

*1 RIKEN Nishina Center
*2 Department Math, Info, Physics, University of Udine
*3 INFN Trieste

Gas-phase chemistry of Re carbonyl complexes with short-lived isotopes

Y. Wang,[*1] Z. Qin,[*1] F. Fan,[*1] H. Haba,[*2] Y. Komori,[*2] S. Yano,[*2] D. Kaji,[*2] K. Morimoto,[*2] and S. Cao[*1]

Since the first organometallic compound of a superheavy element, $Sg(CO)_6$, was successfully synthesized in 2014,[1] the door was opened for nuclear chemists to further study the carbonyl complexes of heavier elements such as bohrium, hassium, and even meitnerium. The next achievement was suggested to be the chemical investigation of mononuclear Bh carbonyl complexes $Bh(CO)_5$. First, however, the chemical properties of its lighter homologs $Tc(CO)_5$ and $Re(CO)_5$ required study. We previously investigated the chemical behaviours of $Tc(CO)_5$,[2] $Ru(CO)_5$, and $Rh(CO)_4$.[3] In this study, we performed a gas-phase chemical experiment on Re carbonyls with short-lived isotopes. The volatile Re carbonyls were synthesized and their adsorption enthalpies on a perfluorinated ethylene-propylene (FEP) Teflon surface were determined using low temperature isothermal chromatography (IC). Furthermore, the relative chemical yields of these Re carbonyls were obtained for the first time, which is very important for the future chemical investigation of Bh carbonyl complexes.

A $^{nat}Gd_2O_3$ target with a thickness of 340 μg/cm^2 was prepared by electrodeposition onto a 2-μm Ti foil. The $^{23}Na^{7+}$ ion beam was extracted from RILAC. The beam energy was 130.6 MeV at the middle of the target, and the typical beam intensity was 2.5 particle μA. The short-lived Re isotopes were produced in the heavy-ion reactions $^{nat}Gd(^{23}Na,xn)^{172-177}Re$.[4] GARIS was employed to preseparate the evaporation residues (ERs). For GARIS, the magnetic rigidity was 1.74 Tm and the He pressure was 33 Pa. The ERs were then guided into a recoil transfer chamber (RTC) with an inert internal surface through a 0.7-μm Mylar window that was supported by a honeycomb-hole grid with 84% transparency. In RTC, the ERs were thermalized in the mixed gas containing CO (high-purity CO/ He or high-purity CO/Ar), formed volatile carbonyl complexes *in situ*, and then were transported through a 10 m long Teflon (FEP) capillary (i.d.= 2 mm) to an IC device. The ERs could also be transported with KCl aerosols by a He gas-jet to the chemistry laboratory to evaluate relative chemical yields. The total gas flow rate was maintained at 1 L/min, and the pressure in the RTC chamber was around 80 kPa. The depths of the RTC were 7 and 100 mm for the Ar and He gas, respectively.

The gas-phase chemical behaviors of Re carbonyl complexes were systematically studied using an online low temperature IC with the Ar and CO mixture. A 5.28-m long IC column made of Teflon (i.d.= 2 mm) was used to obtain the chemical information of the high-volatile Re carbonyls.

After passing through the IC column, the surviving volatile carbonyls were collected with 800 mg of activated charcoal powders in a glass tube (4-mm i.d. × 5 cm length) facing a high-purity Ge-γ-ray detector with a relative efficiency of 20% (EG&G Ortec). By fitting the breakthrough curves of the corresponding carbonyl complexes using a Monte Carlo simulation program,[2] it was found that three short-lived $^{172m,174,176}Re$ isotopes yield the same adsorption enthalpy on the Teflon surface $\Delta H_{ads} = -43^{+2}_{-1}$ kJ mol^{-1}, which is consistent with the literature.[5]

Figure 1 shows the chemical yields of ^{172m}Re, ^{174}Re, and ^{176}Re carbonyls as a function of the CO concentration in the He gas relative to the yields obtained with the KCl aerosols in the He gas. The CO concentration was varied from 0% to 100% and all the data were normalized by the irradiation dose. The highest relative chemical yields for ^{174}Re and ^{176}Re carbonyls appeared at a 50% CO concentration with a value of around 25%. This value is the same as its lighter homolog Tc carbonyl (about 25%).[2] However, for the ^{172m}Re carbonyl complex, the highest relative chemical yield decreased to 10%, because of the shorter half-life and long transport time from the RTC to the charcoal trap. This study could help us to optimize the experimental conditions for future chemical behavior study of the Bh carbonyl complexes.

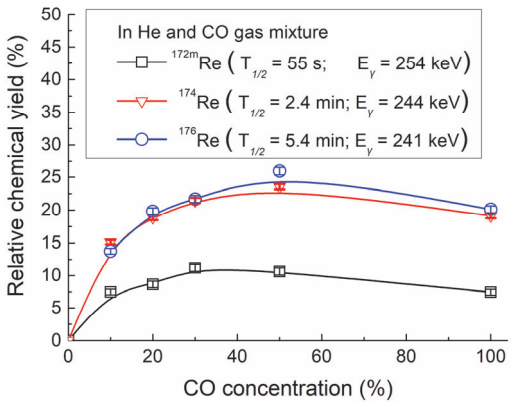

Fig. 1. Chemical yields of $^{172m,174,176}Re$ carbonyls transported with a CO and He mixed gas. The 100% value is the yield obtained with KCl aerosols in the He carrier gas.

References

1) J. Even et al., Science **345**, 1491 (2014).
2) Y. Wang et al., Phys. Chem. Chem. Phys. **17**, 13228 (2015).
3) S. Cao et al., Phys. Chem. Chem. Phys. **18**, 119 (2016).
4) H. Haba et al., RIKEN Accel. Prog. Rep. **45**, 293 (2015).
5) J. Even et al., Radiochim. Acta **102 (12)**, 1093 (2014).

[*1] Institute of Modern Physics, Chinese Academy of Sciences
[*2] RIKEN Nishina Center

Observation of the chemical reaction equilibria of element 104, rutherfordium: Solid-liquid extraction of Rf, Zr, Hf and Th with Aliquat 336 resin from HCl†

T. Yokokita,[*1] Y. Kasamatsu,[*1] A. Kino,[*1] H. Haba,[*2] Y. Shigekawa,[*1] Y. Yasuda,[*1] K. Nakamura,[*1] K. Toyomura,[*1] Y. Komori,[*2] M. Murakami,[*2] T. Yoshimura,[*3] N. Takahashi,[*1] K. Morita,[*2] and A. Shinohara[*1]

It is important to investigate the chemical properties of superheavy elements (SHEs) with an atomic number (Z) ≥ 104. Especially, in solution chemistry, we can study various non-volatile complexes. Thus far, two-phase partition methods, such as ion exchange and extraction, have been usually applied to SHEs. In these experiments, a rapid chemical separation is repeated many times by online chemical experiments using automated chemistry apparatus. The distribution coefficient (K_d) in a solid-liquid extraction or the distribution ratio (D) in a liquid-liquid extraction is often used in solution chemistry investigations for SHEs. These values are defined as the ratio of the elemental (radioactivity) concentrations of the two phases at equilibrium. However, there have been no previous experimental observations of equilibrium states for SHEs, although the experimental conditions in many previous studies were carefully adjusted based on the behaviours of homologues. To obtain the equilibrium K_d values for SHEs, we previously developed a new automated solid-liquid extraction apparatus for online use (AMBER).[1)] Herein, we applied the AMBER-based method to element 104, Rf.

In the online solid-liquid extraction of Rf and Hf, we simultaneously produced ^{261}Rf ($t_{1/2}$ = 68 s) and ^{169}Hf ($t_{1/2}$ = 3.24 min) by the bombardment of a ^{248}Cm and ^{nat}Gd mixture with ^{18}O beams delivered by the K 70 AVF cyclotron at RIKEN. The products were transported to a chemistry room by a He/KCl gas-jet system. The transported products were deposited on the collection site of AMBER's dissolution equipment for ~2 min, and were dissolved in HCl. The solution sample was injected into a chemical reaction container containing 28 wt% Aliquat 336 resin (anion exchanger). After shaking the container with a shaker for 10, 30 and 60 s, only the solution phase was discharged from the container, passing through a PTFE filter, by compressed air for 10 s. The discharged solution was collected in a Ta disk on the round table of an automated rapid α/SF detection system, and evaporated quickly to dryness using hot He gas and the halogen heat lamp. Subsequently, using the detection system's robot arm, the Ta disk was rapidly transferred into an α-particle detection chamber for α-particle measurements for ~800 s. After that, the sample was assayed by γ-ray measurement with a Ge detector for the monitor of ^{169}Hf. We also performed control experiments without the resin to determine the standard radioactivity of the solution sample. Control experiments were carried out in 7.9 M HCl with 10-s shaking and in 9.0 M HCl with 10-s and 30-s shaking. Solid-liquid extraction experiments were carried out in 7.9 M HCl with 10-, 30- and 60-s shaking and in 9.0 M HCl with 10-s shaking. The ratios of the element concentrations between the resin and solution phases (Q_d) in mL g^{-1} were determined from the radioactivities in the resin and the solution phases, the volume of the solution phase, and the mass of the dry resin.

The solid-liquid extraction of ^{89g,m}Zr and ^{173}Hf in the online experiment was performed at the Research Center for Nuclear Physics (RCNP), Osaka University in a similar way to the extraction of ^{261}Rf. The solid-liquid extraction of ^{88}Zr, ^{175}Hf and ^{234}Th in the offline experiments (usual batch method) was also performed.

In the Rf experiment, we conducted a total of 379 extraction procedure cycles, and registered 132 α events from the decay of ^{261}Rf and its daughter nuclide ^{257}No ($t_{1/2}$ = 24.5 s), including 23 time-correlated α–α correlation. The event ratios of ^{261}Rf between the resin and solution phases were estimated from these α events.

The Q_d values of Rf, Zr and Hf were constant in all the time ranges studied, indicating that equilibrium in the extraction of Rf (7.9 M HCl), as well as Zr and Hf, was accomplished within 10 s. This finding represents the first observation of the equilibrium state of the extraction reactions for SHEs on a one-atom-at-a-time basis, and the K_d value of Rf at equilibrium was obtained. Based on these results, we performed extraction experiment of Rf in 9.0 M HCl with shaking for 10 s, and obtained a lower limit for the K_d value > 1.4×10^3 mL g^{-1} (95% confidence).

For the dependence of the K_d values of Rf, Zr, Hf and Th on the HCl concentration, the K_d values of Zr and Hf in the online experiment were in good agreement with those in the offline experiment. The K_d value of Rf in 9.0 M HCl was higher than that in 7.9 M HCl, which indicates that the abundance of anionic chloride complexes of Rf increases with increasing the HCl concentration. The K_d value of Rf was close to that of Zr in 7.9 M HCl, while the value of Rf in 9.0 M HCl was clearly higher than the values of Zr and Hf by one and two orders, respectively. The significant difference in the K_d values among Rf, Zr and Hf in the HCl system was shown for the first time in this study by determining the K_d values of Rf. This result might suggest the possibility that Rf forms chloride complexes with a different configuration to its lighter homologues.

† Condensed from the article in Dalton Trans. **45**, 18827 (2016).

*1 Graduate School of Science, Osaka University
*2 RIKEN Nishina Center
*3 Radioisotope Center, Osaka University

Reference

1) Y. Kasamatsu et al.: Radiochim. Acta **103**, 513 (2015).

Optimization of mutation induction by heavy-ion beam irradiation in rice with seed water content change

Y. Hayashi,[*1] K. Ichinose,[*1] Y. Shirakawa,[*1] S. Usuda,[*1] R. Morita,[*1] H. Tokairin,[*1] T. Sato[*1,*2] and T. Abe[*1]

Radio sensitivity to X-rays and γ-rays are minimal at intermediate water contents in seeds of rice, [1), 2)] wheat and barley.[3)] It increases rapidly above and below this range. In contrast, the seed water content has little or no effect on the sensitivity to fission neutron irradiation.[2)] Our previous study revealed that the radio sensitivity to C-ion beam was affected by the water content of seeds as in the cases of X-rays and γ-rays in rice.[4)] In this report, we investigated the effect of seed water content on mutation rate by C-ion irradiation and estimated the efficient irradiation condition for optimized mutagenesis in rice.

The dry seeds of rice (*Oryza sativa* L. cv. Nipponbare) were equilibrated to 9% and 13% water contents through storage at constant humidity. Water-content-adjusted seeds were vacuum-packed in plastic bags for irradiation treatment (Fig. 1). The dose ranges of the C-ion beam were determined according to our previous study[4)] as 12.5 to 50 Gy and 100 to 200 Gy for 9% and 13% water content, respectively. The liner energy transfer (LET) values were 22.5, 30, and 50 keV/μm at each irradiation dose. M_1 plants were grown in a paddy field and M_2 seeds were obtained separately from each M_1 plant. The number of surviving M_1 plants after each treatment was counted to estimate survival rates. The spikelet fertility was evaluated using the number of fertile spikelets in the main panicle of the M_1 plant. Table 1 lists the percentage of low-fertility M_1 plants that have less than fifty fertile spikelets in a panicle. The mean value of the number of fertile spikelets per panicle in control Nipponbare was 106.2 ± 12.2. Chlorophyll-deficient mutants (CDM) were observed in two-weeks-old M_2 seedlings grown in a greenhouse. Mutation rates were calculated based on the numbers of M_1 lines, which showed CDM in M_2 generation.

Fig.1 Rice seeds set into a cassette of automatic sample changer in our irradiation system.[5)] Each bag contains three hundreds seeds of Nipponbare.

The results of survival rate, spikelet fertility, and mutation rate are listed in Table 1. In the irradiation on seeds with 9% water content, a higher frequency of CDM was obtained by high dose irradiation, which resulted in a low survival rate. In contrast, the highest frequency of CDM was obtained by the irradiation on seeds with 13% water content without the extreme reduction of both survival rate and spikelet fertility. There was no difference between seeds with 9 % and 13% water content in the responses to LET. Irradiations with 50 keV/μm were more effective than the same doses of irradiation with 22.5 or 30 keV/μm on the survival rate and spikelet fertility. As a result, we determined that the optimum condition of C-ion irradiation for mutation induction was 175 Gy (30 keV/μm) on seeds with 13% water content. In general, rice seeds are recommended to be stored under cold and dry conditions to maintain its activity. Therefore, the water content after long-term storage tends to be less than 9%. It is indispensable to measure the water content of seed before irradiation to set an appropriate condition in response to its water content. To induce mutation with high probability, we adjust the water content to 13% by keeping the seeds in a thermo-hygrostat for a week under a temperature of 22°C and humidity of 70%.

Table 1. Effect of C-ion beam irradiation on seeds with 9% and 13% water content.

Water content	LET (keV/μm)	Dose (Gy)	No. of survived M_1 plant	Survival rate (%)	Rate of low-fertility M_1 plant (%)	CDM rate (%)
9%	22.5	25	499	83.2	4.0	8.0
		50	428	71.3	11.7	8.9
	30	25	505	84.2	3.1	6.9
		50	388	64.7	18.1	9.8
	50	12.5	214	71.3	7.0	5.6
		25	151	50.3	17.2	9.9
		50	161	53.7	11.8	10.6
13%	22.5	125	99	99.0	7.2	9.09
		150	346	86.5	19.9	11.10
		175	348	87.0	24.7	14.10
		200	96	96.0	13.5	9.38
	30	125	97	97.0	3.1	8.25
		150	339	84.8	8.3	10.60
		175	325	81.2	19.7	15.10
		200	97	97.0	35.0	8.25
	50	100	94	94.0	10.6	5.32
		125	307	76.8	37.1	11.70
		150	175	43.6	48.6	11.40
		175	53	53.0	37.7	7.55

*1 RIKEN Nishina Center
*2 Graduate School of Agricultural Science, Tohoku University

References
1) C. Myttenaere et al., Radiat. Bot. **5**, 443 (1965).
2) M. J. Conatantin et al., Radiat. Bot. **10**, 539 (1970).
3) R. Biebi et al., Radiat. Bot. **5**, 1 (1965).
4) Y. Hayashi et al., RIKEN Accel. Prog. Rep. **45**, 214 (2012).
5) H. Ryuto et al., RIKEN Accel. Prog. Rep. **39**, 245 (2006).

Change in rice gene expression profile dependent on linear energy transfer after heavy-ion beam irradiation†

K. Ishii,[*1] Y. Kazama,[*1] R. Morita,[*1] T. Hirano,[*1,*2] T. Ikeda,[*1] S. Usuda,[*1] Y. Hayashi,[*1] S. Ohbu,[*1] R. Motoyama,[*3] Y. Nagamura,[*3] and T. Abe[*1]

LET is an important factor affecting several aspects of the irradiation effect, such as cell survival and mutation frequency.[1)] The effect of LET on deletion induction increases up to an LET value of approximately 100 keV/μm[2)] while the mutation frequency increases abruptly and peaks at a particular LET value.[1)] The mechanism between LET and the corresponding mutation frequency is still unknown. In this study, we focused on the effect of LET on gene expression profiles.

Oryza sativa L. cv. 'Nipponbare' seeds were imbibed for 3 days. The seeds were irradiated with 22.5 or 50 keV/μm C ions or with 63 or 80 keV/μm Ne ions at a dose of 15 Gy. Embryos were sampled 2 h after irradiation. Gene expression profiles were generated using a rice 4×44K microarray RAP-DB (Agilent Technologies, Tokyo, Japan).

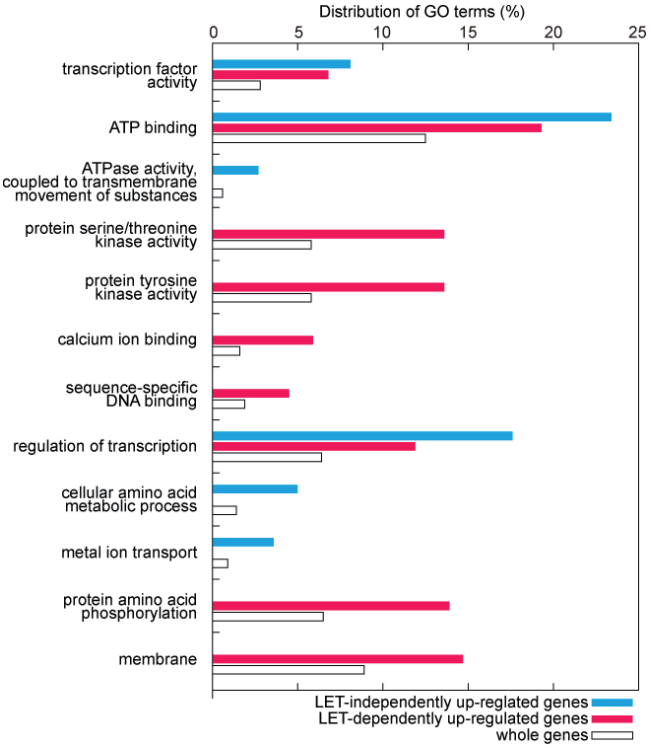

Fig 1. SEA analysis. The horizontal axis shows the distribution of the GO term, which is a percentage of genes having each GO term in the analyzed gene set. Blue, red, and white boxes indicate the distribution of LET-independent up-regulated genes, LET-dependent up-regulated genes, and whole genes (rice TIGR locus).

We defined 379 genes showing a significant change in expression level (FC > 2, and $p < 0.05$) at all four LETs as "LET-independent up-regulated genes" and 628 genes showing a significant change in expression level at an LET of 80 keV/μm, but not at 22.5 keV/μm, as "LET-dependent up-regulated genes". A singular enrichment analysis (SEA) using a gene ontology (GO) analysis toolkit agriGO revealed that GO terms significantly ($p \leq 0.01$) enriched were different in LET-dependent up-regulated genes and LET-independent up-regulated genes (Fig. 1), which implies that some specific genetic pathway is induced depending on the complexity of DNA damage.

Additionally, *OsPCNA* and *OsPARP3* were found to be LET-dependent up-regulated genes (Fig 2). Although molecular functions of rice PARP family genes are largely unknown, some of them are involved in Ku-independent non homologous end joining (A-NHEJ) with *Xrcc1* and *DNA ligase III* in animals[3)] and plants.[4)] *OsPCNA* forms a complex with *OsXRCC1* in vivo.[5)] We assume that the high expression of *OsPARP3* and *OsPCNA* is needed to repair the high-LET induced DNA lesions via Ku-independent NHEJ.

In this study, we found an LET-dependent change of gene expression profile, which is a clue to the clarification of the relationship between LET and mutation frequency.

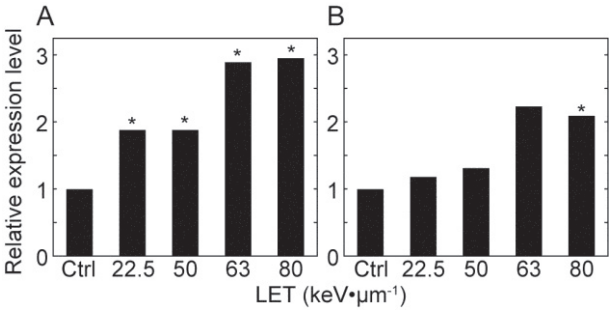

Fig 2. Response of *OsPCNA* and *OsPARP3* gene expressions to heavy-ion beam irradiation. Fold changes in expression level of *OsPCNA* (A) and *OsPARP3* (B) compared to the unirradiated control are shown. *: $p < 0.05$ (Student's t-test).

† Condensed from the article in PLoS ONE **11**(7):e0160061 (2016)

*1 RIKEN Nishina Center
*2 Faculty of Agriculture, University of Miyazaki
*3 Agrogenomics Research Center, National Institute of Agrobiological Sciences

References

1) Y. Kazama et al., Plant Biotechnol. **25**(1)113 (2008).
2) A. Ottolenghi et al., Radiat. Environ. Biophys. **34**(4)239 (1995).
3) C. Charbonnel et al., Plant J. **64**(2)280 (2010).
4) Q. Jia et al., Plant Mol. Biol. **82**(4-5)339 (2013).
5) Y. Uchiyama et al., Planta **227**(6)1233 (2008).

II. RESEARCH ACTIVITIES I
(Nuclear, Particle and Astro-Physics)

1. Nuclear Physics

μs isomers of ^{158,160}Nd†

E. Ideguchi,[*1] G.S. Simpson,[*2] R. Yokoyama,[*3] Mn. Tanaka,[*1] S. Nishimura,[*4] P. Doornenbal,[*4] G. Lorusso,[*4] P. -A. Söderström,[*4] H. Sakurai,[*4] T. Sumikama,[*4*5] J. Wu,[*4] Z. Y. Xu,[*4] and the EURICA RIBF-86 collaboration

The doubly mid-shell nuclei of the mass number $A\sim160$ region are well known for undergoing a rapid increase in the deformation of their ground states when going from the neutron number N=88 to 90[1]. From $N = 92$ onwards their quadrupole deformation is close to saturation and these nuclei possess well-deformed prolate ground-state rotational bands. Several of the $N = 98$ and 100 isotopes here are known to possess 2-qp isomeric states,[2–4], one may therefore expect similar long-lived states to exist in ^{158,160}Nd, whose level schemes are unknown. The presence of isomeric states offers the opportunity to study the structure of nuclei via the use of delayed γ-ray spectroscopy of in-flight, mass-separated beams of fission fragments. The observation of K-isomers allows the position of single-particle Nilsson states to be mapped in regions dominated by collective structures, which is useful for testing the predictions of mean-field models. In the present work we have studied excited states in the nuclei ^{158,160}Nd via delayed γ-ray spectroscopy.

In-flight fission of a 345-MeV/nucleon ^{238}U beam was performed at RIBF. Ions including ^{158,160}Nd were selected using the BigRIPS spectrometer and implanted in the WAS3ABi stopper[5], or a copper plate, situated at the F11 focal plane. The WAS3ABi stopper allowed detected β decays to be correlated with identified and implanted ions, whereas the use of a passive stopper allowed a higher ion implantation rate for isomer studies. The EURICA Ge array[5] was used to detect any γ rays emitted following ion implantation at the BigRIPS focal plane. Use of ion–γ and ion–$\gamma-\gamma$ coincidences has allowed the first level schemes to be established for the nuclei ^{158,160}Nd. More details on the experiment can be found in Ref.[6].

Delayed γ rays with energies of 151.7, 233.4 and 1197.1 keV were found to be in coincidence with ^{158}Nd ions. A delayed cascade proceeding by transitions with energies of 65.2, 149.9 and 892.8 keV was assigned to ^{160}Nd nuclei. The level schemes of ^{158,160}Nd constructed in the present work are shown in Fig. 1. The order of the decays was assigned from the level systematics in the neighboring nuclei Nd[2]. The spins and parities of the isomers were assigned from their decay patterns and half-lives, as explained in Ref.[6].

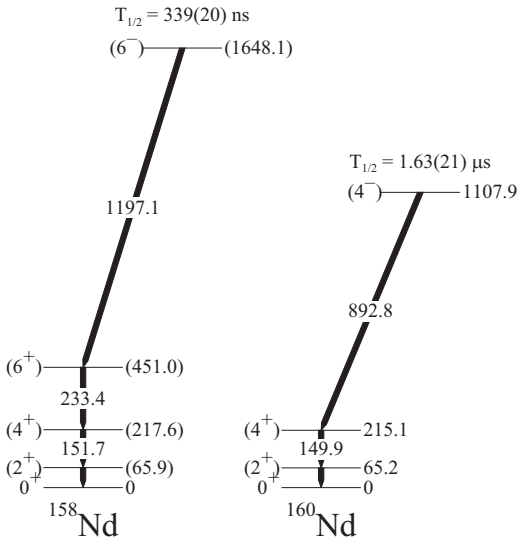

Fig. 1. Level schemes of ^{158,160}Nd obtained in the present work.

The configurations of the isomeric states of ^{158,160}Nd have been assigned with the aid of blocked-BCS (BBCS) calculations. These have allowed a $\nu5/2[523]\otimes\nu7/2[633]$ configuration to be assigned to the (6^-) isomer of ^{158}Nd and a $\nu1/2[521]\otimes\nu7/2[633]$ one to the (4^-) isomer of ^{160}Nd, the same as found in the stable ^{170}Yb[4]. It is worth noting that one experimental decay scheme is incompatible with the results of projected shell-model[7] and Hartree-Fock calculations[8].

A peak appears in the r-process abundances around mass 160 and its origin remains unclear. Measurements of β-decay half-lives performed within the EURICA campaign at RIBF have shown variations in these values in the same region, which have a nuclear structure origin[9]. Identification of further Nilsson states and analysis of the β-decay data gathered in the our experiment will help resolve these anomalies.

References
1) R. Casten *et al.*, Phys. Rev. C **33**, 1819 (1986).
2) G. Simpson *et al.*, Phys. Rev. C **80**, 024304 (2009).
3) Z. Patel *et al.*, Phys. Lett. **B 753**, 182 (2016).
4) P. Walker *et al.*, Nucl. Phys. **A 365**, 61 (1981).
5) P.A. Söderström *et al.* Nucl. Instrum. Meth. Phys. Res. **B 317**, 649 (2013).
6) E. Ideguchi *et al.*, Phys. Rev. C. **94**, 064322 (2016).
7) Y.-C. Yang *et al.*, J. Phys. G **37**, 085110 (2010).
8) S.K. Ghouri *et al.*, Int. Mod. J. Phys. **21**, 1250070 (2012).
9) J. Wu *et al.*, Phys. Rev. Lett. **118**, 072701 (2017).

† Condensed from the article in Phys. Rev. C. **94**, 064322 (2016)

*1 RCNP, Osaka University
*2 LPSC, Grenoble
*3 CNS, University of Tokyo
*4 RIKEN Nishina Center
*5 Department of Physics, Tohoku University

Long-lived K isomer and enhanced γ vibration in ^{172}Dy†

H. Watanabe*1,*2 for RIBF88 collaboration

The excitation spectrum in deformed nuclei is characterized by rotational and vibrational motion, the latter corresponding to oscillations around the equilibrium shape with a fixed orientation of the nucleus. For axially symmetric nuclei, the lowest order shape vibration is of quadrupole type (i.e., a phonon carries two units of angular momentum), which can be classified into two modes, β and γ vibrations, in terms of the component of (vibrational) angular momentum along the symmetry axis, denoted by K. The β-vibrational mode with $K^\pi = 0^+$ maintains axial symmetry, while the $K^\pi = 2^+$ γ vibration represents a dynamical distortion from axial symmetry, which may prelude the emergence of γ instability or rigid triaxial deformation approaching the transitional region where the nuclei have less-deformed quadrupole shapes.

In the present work, we have explored neutron-rich Dy isotopes ($Z = 66$) with a particular focus on the systematic behavior of the ground-state (g.s.) and γ-vibrational bands. Based on a simple assumption that the axial quadrupole deformation increases as the number of valence nucleons increases, it is conjectured that the maximum ground-state deformation occurs in the doubly mid-shell nucleus ^{170}Dy ($N = 104$). In actual nuclei, however, the stability of shape is likely to be sensitive to characteristic single-particle (Nilsson) orbitals near the Fermi surface. Experimentally, the existence of γ-vibrational levels at low excitation energy can be a signature of softening deformed shape with respect to the axially-asymmetric (γ) degree of freedom. In this report, the first spectroscopic results of the g.s. and γ bands in ^{172}Dy ($N = 106$) are presented. Its excited states have been populated through the decay from a long-lived isomeric state, which has the same configuration as the $K^\pi = 8^-$ isomers that had been identified in the $N = 106$ isotones from $Z = 68$ to 82[1]. Thus, the present work has extended a sequence of the $N = 106$ isomers to the previously inaccessible nucleus of $Z = 66$. It is notable that high-K isomers can serve as a useful probe for the underlying nuclear structure since their nature is sensitive to intrinsic orbits near the Fermi surface, pairing and other residual interactions, and the degree of axial symmetry[2].

The level structure of ^{172}Dy has been investigated by means of decay spectroscopy with the EURICA setup following in-flight fission of a ^{238}U beam. Prior to the present work, no spectroscopic information had been reported for this neutron-rich nucleus. The level scheme of ^{172}Dy established in the present work is displayed in Fig. 1. A long-lived isomeric state with

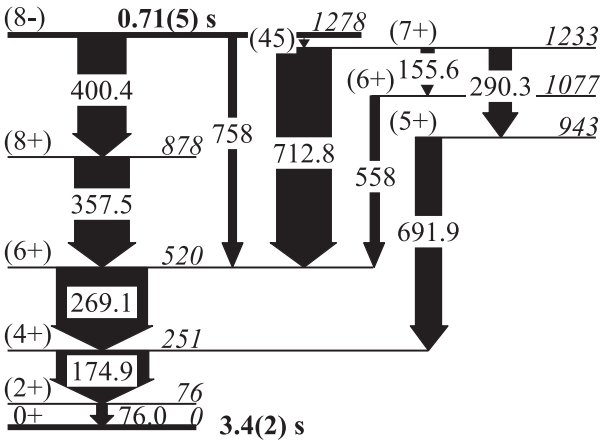

Fig. 1. Partial level scheme of ^{172}Dy constructed in the present work.

$T_{1/2} = 0.71(5)$ s and $K^\pi = 8^-$ has been identified at 1278 keV, which decays to the ground-state and γ-vibrational bands through hindered electromagnetic transitions, as well as to the daughter nucleus ^{172}Ho via allowed β decays. The robust nature of the $K^\pi = 8^-$ isomer and the ground-state rotational band reveals an axially-symmetric structure for this nucleus. Meanwhile, the γ-vibrational levels have been identified at unusually low excitation energy compared to the neighboring well-deformed nuclei, indicating the significance of the microscopic effect on the non-axial collectivity in this doubly mid-shell region.

References

1) G.D. Dracoulis *et al.*: Phys. Lett. **B 635**, 200 (2006).
2) G.D. Dracoulis: Phys. Scr. **2013**, 014015 (2013).

† Condensed from the article in Phys. Lett. **B 760**, 641 (2016)

*1 School of Physics, Beihang University
*2 RIKEN Nishina Center

K-isomer properties of the doubly mid-shell nuclide ^{170}Dy†

P.-A. Söderström,[*1] P. Walker,[*2] J. Wu,[*1,*3] H.L. Liu,[*4] P.H. Regan,[*2,*5] H. Watanabe,[*6,*7] P. Doornenbal,[*1] Z. Korkulu,[*1,*8] P. Lee,[*9] J.J. Liu,[*10] G. Lorusso,[*1,*5] V.H. Phong,[*1,*11] S. Nishimura,[*1] T. Sumikama,[*1,*12] F.R. Xu,[*3] A. Yagi,[*13] G.X. Zhang,[*7] D.S. Ahn,[*1] T. Alharbi,[*14] H. Baba,[*1] F. Browne,[*15] A.M. Bruce,[*15] R. Carroll,[*2] K.Y. Chae,[*16] Zs. Dombradi,[*8] A. Estrade,[*17] N. Fukuda,[*1] C. Griffin,[*17] E. Ideguchi,[*18] N. Inabe,[*1] T. Isobe,[*1] H. Kanaoka,[*13] S. Kanaya,[*13] I. Kojouharov,[*19] F.G. Kondev,[*20] T. Kubo,[*1] S. Kubono,[*1] N. Kurz,[*19] I. Kuti,[*8] S. Lalkovski,[*2] G.J. Lane,[*21] E.J. Lee,[*16] C.S. Lee,[*9] G. Lotay,[*2] C.-B. Moon,[*22] I. Nishizuka,[*12] C.R. Niţă,[*15,*23] A. Odahara,[*13] Z. Patel,[*2] Zs. Podolyák,[*2] O.J. Roberts,[*24] H. Sakurai,[*1,*25] H. Schaffner,[*19] C.M. Shand,[*2] H. Suzuki,[*1] H. Takeda,[*1] S. Terashima,[*7] Zs. Vajta,[*8] J.J. Valiente-Dòbon,[*26] and Z.Y. Xu[*10]

The region in the nuclear chart between $50 < Z < 82$ and $82 < N < 126$ is the largest region between traditional nuclear shells and, thus, ideal to study the evolution of collectivity and K isomerism originating from the high-j orbitals around mid-shell. The nucleus with the largest number of valence particles in this region is ^{170}Dy with proton number $Z = 66$ and neutron number $N = 104$. Accordingly it should be one of the most collective of all nuclei with $A < 208$, in its ground state[1]. One predicted property of ^{170}Dy is the long-lived $K^\pi = 6^+$ two quasi-particle isomer, where K is the total angular momentum projection on the prolate symmetry axis.

Nuclei in the ^{170}Dy region were produced by in-flight fission of a 345 MeV/u ^{238}U beam with 10 pnA intensity, incident on a Be target. The fragments were separated and identified in the BigRIPS separator and the ZeroDegree spectrometer. At the final focal plane of the beam line they were implanted in the WAS3ABi active stopper[2] and γ rays were detected in EURICA[3].

† Condensed from the article in Phys. Lett. **B762**, 404 (2016)

*1 RIKEN Nishina Center
*2 Department of Physics, University of Surrey
*3 School of Physics, Peking University
*4 School of Science, Xi'an Jiaotong University
*5 National Physical Laboratory, Teddington
*6 IRCNPC, Beihang University
*7 School of Physics and Nuclear Energy Engineering, Beihang University
*8 INR, Hungarian Academy of Sciences
*9 Department of Physics, Chung-Ang University
*10 Department of Physics, University of Hong Kong
*11 Faculty of Physics, Hanoi University of Science
*12 Department of Physics, Tohoku University
*13 Department of Physics, Osaka University
*14 Department of Physics, Almajmaah University
*15 School of Computing, Engineering and Mathematics, University of Brighton
*16 Department of Physics, Sungkyunkwan University
*17 School of Physics and Astronomy, University of Edinburgh
*18 RCNP, Osaka University
*19 GSI, Darmstadt
*20 Nuclear Engineering Division, Argonne National Laboratory
*21 Department of Nuclear Physics, Australian National University
*22 Department of Display Engineering, Hoseo University
*23 IFIN-HH, Bucharest
*24 School of Physics, University College Dublin
*25 Department of Physics, University of Tokyo
*26 INFN-LNL, Legnaro

Parts of the level scheme obtained in the current work[4] is shown in Fig. 1. The three lowest-lying excited states can be assigned as the 2^+, 4^+ and 6^+ members of the ground-state rotational band with energies closely following the expected $I(I+1)$ rotational dependence. A 1 μs isomer was assigned to 6^+ and decays into two intermediate states, assigned to spin and parity 4^+ and 5^+, respectively. This would suggest that the $6^+ \rightarrow 6^+$ transition has an energy of 1149 keV, consistent with the observation of a weak γ-ray peak at this energy.

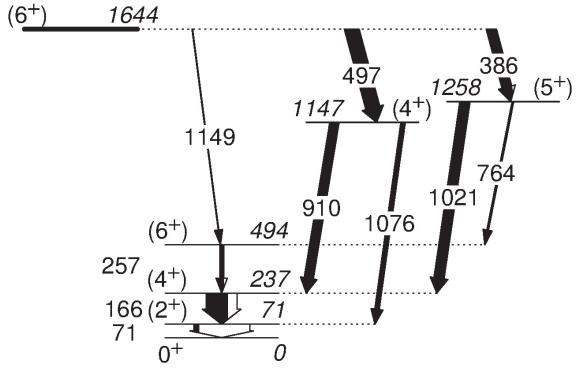

Fig. 1. Partial level scheme of ^{170}Dy from the decay of the $K^\pi = 6^+$ isomer.

Potential energy surface calculations were performed for the ground state and $K^\pi = 6^+$, $5/2^-[512] \otimes 7/2^-[514]$ two-neutron configurations, including β_6 deformation. While the deformation parameters were chosen to minimize the potential energy, the neutron-neutron pairing strength was adjusted according to systematics of similar nuclei in this region. A factor of 1.1 for the pairing strength of the entire $N = 104$ chain, gives a satisfactory reproduction of the experimental data.

References

1) P.H. Regan et al.: Phys. Rev. C **65** 037302 (2002).
2) S. Nishimura et al. RIKEN Accel. Prog. Rep. **46**, 182 (2013).
3) P.-A. Söderström et al.: Nucl. Inst. Meth. **B317**, 649 (2013).
4) P.-A. Söderström et al.: Phys. Lett. **B762**, 404 (2016).

Shape coexistence along $N = 40$ studied with isomer and beta decay

F. Recchia,[*1] S. Riccetto,[*2] K. Wimmer,[*3,*4] S.M. Lenzi,[*1] T. Davinson,[*5] A. Estrade,[*6,*4] C.J. Griffin,[*5] S. Nishimura,[*4] V. Phong,[*4] P.-A. Söderström,[*4] O. Aktas,[*7] M. Alaqueel,[*8,*9] T. Ando,[*3] H. Baba,[*4] S. Bae,[*10] S. Choi,[*10] P. Doornenbal,[*4] J. Ha,[*10,*4] L. Harkness-Brennan,[*8] T. Isobe,[*4] P. John,[*1] D. Kahl,[*5] G. Kiss,[*4] M. Labiche,[*11] K. Matsui,[*4] S. Momiyama,[*3] D. Napoli,[*12] M. Niikura,[*3] C. Nita,[*13] Y. Saito,[*4] H. Sakurai,[*4,*3] P. Schrock,[*3] T. Sumikama,[*4] C. Stahl,[*14] V. Werner,[*14] and W. Witt[*14]

In ^{68}Ni the presence of a high-lying 2^+ state with small transition probability to the ground state is a result of the N = 40 harmonic oscillator shell gap between the fp shell and the $g_{9/2}$ orbital. This shell gap is reduced as protons are removed in Fe and Cr isotopes[1]. Collective behavior is caused by quadrupole correlations which favour energetically the deformed intruder states involving the neutron $g_{9/2}$ and $d_{5/2}$ orbitals and proton excitations across the Z=28 subshell gap[2] leading to rather low-lying first 2^+ states and large B($E2$) values.

Limited experimental data is still available for the low spin states of the region of deformation that develops south of ^{68}Ni. The trend of the ratio E_{4^+}/E_{2^+} towards $N = 40$ in Cr isotopes suggests a transition from spherical (at $N = 32$) to deformed shapes, that approach better the gamma-unstable regime than the axially deformed one, while Fe isotopes lie at the O(6) limit from $N = 30$ to $N = 42$[3]. To better understand the structure of these nuclei, the knowledge of other states at low excitation energy is needed.

The large difference in angular momentum between the $p_{1/2}$, $f_{5/2}$ and $d_{5/2}$, $g_{9/2}$ orbitals around the Fermi surface in $N \approx 40$ nuclei leads to the occurrence of several isomeric states. In the Cr and Ti nuclei with $N = 39$ and $N = 41$ similar configurations should also lead to long-lived states. Observation of isomers at $N = 39$ will allow us to draw conclusions on the location and evolution of intruder orbitals towards ^{60}Ca. Theoretical and experimental investigations show that the collective behavior observed in ^{64}Cr, with its small E(2^+) energy and large B(E2) value, is restored approaching ^{60}Ca[2,4].

In this report we present some preliminary experimental results. Several new gamma transitions deexciting isomeric states, as well as states populated in the beta decay have been identified for the first time. The determination of beta decay half-lives in this region is of relevance for a better understanding of the r-process nucleosynthesis.

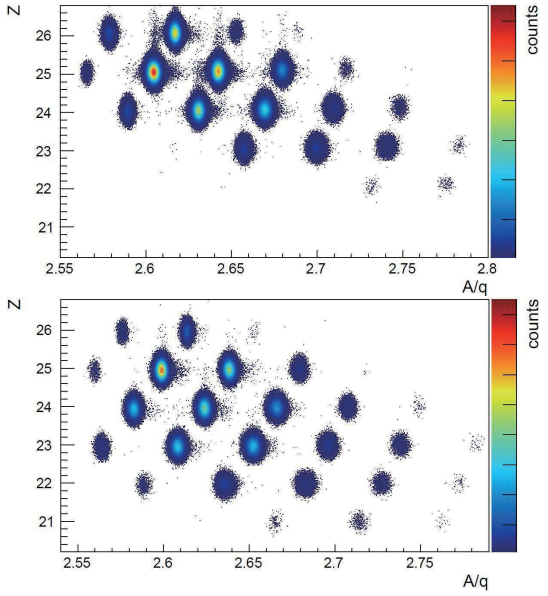

Fig. 1. Ions produced, identified and implanted into the AIDA active stopper for (top) the ^{64}Cr setting, (bottom) the ^{60}Ti setting.

A high intensity ^{238}U beam provided by the RIKEN Nishina Center Accelerator Complex impinging on a Be target was used to produce the nuclides of interest in in-flight fission. In the experiment the EURICA gamma-ray array surrounded the implantation detector AIDA into which the fragments of interest were implanted. The fragments were identified using the BigRIPS separator employing the ΔE-ToF-Bρ method. Figure 1 shows the particle identification plots of the fragments using this technique for the ^{60}Ti and the ^{64}Cr settings. The analysis of the experimental data on the β-decays in ^{64}Cr region and the isomers decay is in progress.

*1 Department of Physics and Astronomy, University and INFN Padova
*2 Department of Physics, University and INFN Perugia
*3 Department of Physics, University of Tokyo
*4 RIKEN Nishina Center
*5 School of Physics and Astronomy, University of Edinburgh
*6 Department of Physics, Central Michigan University
*7 Department of Physics, KTH Stockholm
*8 Oliver Lodge Laboratory, The University of Liverpool
*9 Imam Muhammad Ibn Saud Islamic University of Riyadh
*10 Department of Physics, Seoul National University
*11 STFC Daresbury Laboratory
*12 INFN Legnaro (Padova)
*13 IFIN Horia Hulubei Bucharest
*14 Institut für Kernphysik, Technische Universität Darmstadt

References

1) Y. Tsunoda et al. J. Phys. Conf. Ser. **445**, 012028 (2013).
2) S.M.Lenzi et al. Phys.Rev. C **82**, 054301 (2010).
3) J. Kotila and S.M. Lenzi, Phys.Rev. C **89**, 064304 (2014).
4) A. Gade et al., Phys. Rev. Lett. **112** (2014) 112503.

Beta-delayed proton spectrum from the $T_z = -2$ nucleus ^{64}Se at BigRIPS

P. Aguilera,[*1] F. Molina,[*1] B. Rubio,[*2] J. Agramunt,[*2] A. Algora,[*2] V. Guadilla,[*2] A. Montaner-Piza,[*2] A. I. Morales,[*2] S. E. A. Orrigo,[*2] B. Blank,[*3] P. Ascher,[*3] M. Gerbaux,[*3] T. Goigoux,[*3] J. Giovinazzo,[*3] S. Grévy,[*3] T. Kurtukian Nieto,[*3] C. Magron,[*3] D. Nishimura,[*4] J. Chiba,[*4] H. Oikawa,[*4] Y. Takei,[*4] S.Yagi,[*4] D. S. Ahn,[*5] P. Doornenbal,[*5] N. Fukuda,[*5] N. Inabe,[*5] G. Kiss,[*5] T. Kubo,[*5] S. Kubono,[*5] S. Nishimura,[*5] Y. Shimizu,[*5] C. Sidong,[*5] P. A. Söderström,[*5] T. Sumikama,[*5] H. Suzuki,[*5] H. Takeda,[*5] P. Vi,[*5] J. Wu,[*5] Y. Fujita,[*6] M. Tanaka,[*6] W. Gelletly,[*2,*7] F. Diel,[*8] D. Lubos,[*9] G. de Angelis,[*10] D. Napoli,[*10] C. Borcea,[*11] A. Boso,[*12] R. B. Cakirli,[*13] E. Ganioglu,[*13] G. de France,[*14] and S. Go[*15]

Spin-isospin excitations can be studied by β-decay and charge exchange reactions in mirror nuclei, shedding light on mirror symmetry. Hence we can compare our results on the β decay of proton-rich nuclei with the results of charge exchange experiments when appropriate targets for the mirror nuclei are available[1]. Accordingly we have performed experiments at GSI and GANIL to study $T_z = -1$[2] and $T_z = -2$[3,4] nuclei respectively where it became clear that the study of heavier, more exotic systems demands beam intensities available only at the RIKEN RIBF.

We have performed an experiment using the fragmentation of a 345-MeV/nucleon ^{78}Kr beam with a typical intensity of 200 pnA on a Be target. The fragments were separated in flight using the BigRIPS separator and implanted in three WAS3ABi double-sided Si strip detectors (60 mm × 40 mm × 1 mm, 60 horizontal and 40 vertical strips). The implantation setup was surrounded by the EUROBALL-RIKEN Cluster Array (EURICA). The experiment is described in detail in a previous report.[5]

Here we present the first experimental observation of the beta-delayed protons in the decay of the $T_z = -2$ ^{64}Se nucleus. The spectrum was constructed using time correlations between ^{64}Se implantations and all β signals within a single pixel, defined as the crossing of one X and one Y strip. Fig. 1 shows the β-delayed proton spectrum of ^{64}Se. The proton energies were obtained by fitting the previously known β-delayed proton response function in DSSSD detectors, detailed in Ref.[4], consisting of a Gaussian function plus an exponential tail. The WAS3ABi DSSSD detectors were calibrated using an external electron conversion in a ^{207}Bi source; thus proton energy shifts are expected. These energy shifts were compared and recalibrated using the ^{57}Zn and ^{61}Ge beta-delayed proton spectra obtained in this experiment and constructed in the same manner as the ^{64}Se beta-delayed proton spectrum. The ^{57}Zn and ^{61}Ge proton energies are taken from Ref.[6]. The uncertainties in the proton energies shown in Fig. 1 originate from the fit of the response function for each proton peak as well as the systematic shift of the proton energies compared with those reported in the literature.[6]

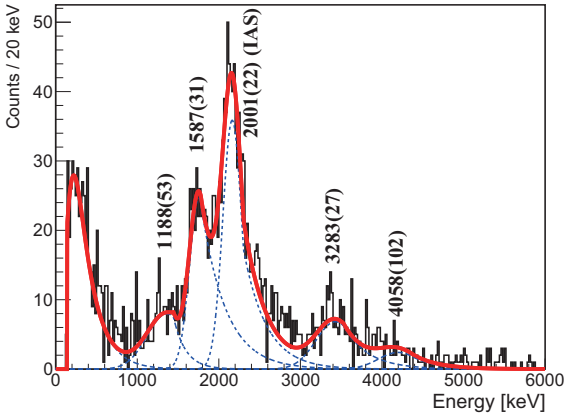

Fig. 1. β-delayed proton spectrum of ^{64}Se. The dashed blue lines represent the individual proton response functions. The numbers above the proton peaks indicate the proton energy after a shift correction has been applied (see text).

*1 Chilean Nuclear Energy Commision
*2 IFIC, CSIC-Universidad de Valencia
*3 Centre d'Etudes Nucléaires de Bordeaux-Gradignan
*4 Department of Physics, Tokyo City University
*5 RIKEN Nishina Center
*6 Department of Physics, Osaka University
*7 Department of Physics, Surrey University
*8 Institute of Nuclear Physics, Universität zu Köln
*9 Physics Department E-12, Technische Universität München
*10 Istituto Nazionale di Fisica Nucleare, Laboratorio Nazionale di Legnaro
*11 National Institute for Physics and Nuclear Engineering, IFIN-HH
*12 Istituto Nazionale di Fisica Nucleare, Sezione di Padova
*13 Department of Physics, Istanbul University
*14 Grand Accélérateur National d'Ions Lourds
*15 Department of Physics, Tennessee University

References

1) Y. Fujita, B. Rubio, W. Gelletly, Prog. Part. Nucl. Phys. **66**, 549 (2011).
2) F. Molina et al., Phys. Rev. C **91**, 014301 (2015).
3) S. E. A. Orrigo et al., Phys. Rev. Lett. **112**, 222501 (2014).
4) S. E. A. Orrigo et al., Phys. Rev. C **93**, 044336 (2016).
5) B. Rubio et al., RIKEN Accel. Prog. Rep. Vol. **49** 27 (2015).
6) B. Blank et al.: Eur. Phys. J. A **31**, 267 (2007).

Study of the beta decay of ^{70}Br

A. I. Morales,[*1] A. Algora,[*1*7] B. Rubio,[*1] J. Agramunt,[*1] V. Guadilla,[*1] A. Montaner-Piza,[*1] S. Orrigo,[*1] G. de Angelis,[*2] D. Napoli,[*2] F. Recchia,[*3] S. Lenzi,[*3] A. Boso,[*3] S. Nishimura,[*4] G. Kiss,[*4] P. Vi,[*4] J. Wu,[*4] P.-A. Söderström,[*4] T. Sumikama,[*4] H. Suzuki,[*4] H. Takeda,[*4] D. S. Ahn,[*4] H. Baba,[*4] P. Doornebal,[*4] N. Fukuda,[*4] N. Inabe,[*4] T. Isobe,[*4] T. Kubo,[*4] S. Kubono,[*4] Y. Shimizu,[*4] C. Sidong,[*4] B. Blank,[*5] P. Ascher,[*5] M. Gerbaux,[*5] T. Goigoux,[*5] J. Giovinazzo,[*5] S. Grévy,[*5] T. Kurtukian Nieto,[*5] C. Magron,[*5] W. Gelletly,[*1*6] Zs. Dombrádi,[*7] Y. Fujita,[*8] M. Tanaka,[*8] P. Aguilera,[*9] F. Molina,[*9] J. Eberth,[*10] F. Diel,[*10] D. Lubos,[*11] C. Borcea,[*12] A. Petrovici,[*12] E. Ganioglu,[*13] D. Nishimura,[*14] H. Oikawa,[*14] Y. Takei,[*14] S. Yagi,[*14] W. Korten,[*15] G. de France,[*16] and P. Davies[*17]

In this report we present some preliminary results of the analysis of the experiment NP1112-RIBF93. The main goal of the proposal is to study p-n pairing and isospin-related features in the structure of ^{70,71}Kr through the beta decay of these isotopes and through the decay of the $9/2^+$ isomer in ^{71}Kr if it is excited. In this experiment in addition to the ^{70,71}Kr nuclei, other nuclear species of interest, such as ^{70}Br and ^{68,69}Se were also produced. We have started the analysis of the experiment with the study of the beta decay of the odd-odd ^{70}Br nucleus, which is produced in two beta decaying states, namely the $T = 0$, $J^\pi = 9^+$ excited isomeric state and the $T = 1$, $J^\pi = 0^+$ ground state. The decay of the latter state is of particular relevance in the framework of superallowed transitions (see Ref. 1) for a recent review). For this kind of study inputs needed are the half-life, the Q value of the beta decay and the branching ratio of the superallowed $0^+ \rightarrow 0^+$ transition. Hence, the determination of weak Gamow-Teller transitions that compete with the superallowed one becomes essential.

To produce the nuclides of interest a high intensity ^{78}Kr beam with 345 MeV/nucleon provided by the RIBF accelerator complex was used. Neutron-deficient $A \sim 70$ nuclei were produced in in-flight fragmentation of the beam on a 7-mm thick Be target. In the study, the EURICA gamma-ray array was employed, which surrounded the implantation detector WAS3ABI. The fragments were identified using the BigRIPS separator applying the ΔE-ToF-$B\rho$ method. Figure 1 shows the identification plot of the fragments using this technique for the ^{71}Kr setting, where ^{70}Br is also seen. Figure 2 presents examples of coincidence gamma spectra associated with this setting.

Several gamma transitions deexiting states populated in the beta decay of the 9^+ isomer in ^{70}Br have been observed for the first time. A better determination of the beta-decay half-lives of the ^{70}Br 0^+ and 9^+ isomers, and in particular of the half-life of the 0^+ ground state is relevant for using this decay as an additional input to $\mathcal{F}t$ calculations of superallowed transitions.

The analysis of the experimental data on the ^{70,71}Kr beta decays and on the ^{71}Kr isomer decay is in progress.

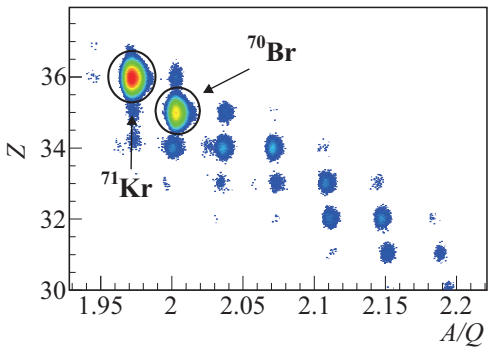

Fig. 1. Identification plot for the isotopes produced in ^{78}Kr fragmentation for the ^{71}Kr setting.

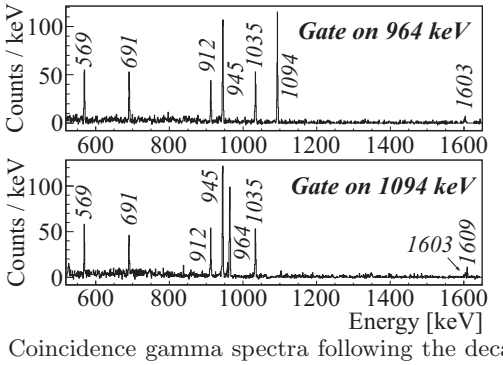

Fig. 2. Coincidence gamma spectra following the decay of the $J^\pi = 9^+$ isomer in ^{70}Br.

*1 IFIC, CSIC-Univ. Valencia
*2 INFN-Legnaro
*3 INFN-Padova
*4 RIKEN Nishina Center
*5 CEN Bordeaux-Gradignan
*6 Department of Physics, Surrey University
*7 MTA ATOMKI
*8 Osaka University
*9 CCHEN
*10 Institute of Nucl. Physics, Universität zu Köln
*11 Physik Department, Technische Universität München
*12 IFIN-HH, Bucarest
*13 Department of Physics, University of Istanbul
*14 Tokyo Univ. Sci.
*15 CEA-Saclay
*16 GANIL-Caen
*17 Department of Physics, York University

Reference

1) J. C. Hardy and I. S. Towner; Phys. Rev. C 91, 025501 (2015).

Study of β-delayed proton emitters in the region from Zn to Kr

T. Goigoux,[*1] P. Ascher,[*1] B. Blank,[*1] M. Gerbaux,[*1] J. Giovinazzo,[*1] S. Grévy,[*1] T. Kurtukian Nieto,[*1] C. Magron,[*1] J. Agramunt,[*2] A. Algora,[*2*3] V. Guadilla,[*2] A. Montaner-Piza,[*2] A. I. Morales,[*2] S. E. A. Orrigo,[*2] B. Rubio,[*2] D. S. Ahn,[*4] P. Doornenbal,[*4] N. Fukuda,[*4] N. Inabe,[*4] G. G. Kiss,[*4] T. Kubo,[*4] S. Kubono,[*4] S. Nishimura,[*4] H. Sakurai,[*4,*5] Y. Shimizu,[*4] C. Sidong,[*4] P.-A. Söderström,[*4] T. Sumikama,[*4] H. Suzuki,[*4] H. Takeda,[*4] P. Vi,[*4] J. Wu,[*4] Y. Fujita,[*6*7] M. Tanaka,[*6] W. Gelletly,[*2*8] P. Aguilera,[*9] F. Molina,[*9] F. Diel,[*10] D. Lubos,[*11] G. de Angelis,[*12] D. Napoli,[*12] C. Borcea,[*13] A. Boso,[*14] R. B. Cakirli,[*15] E. Ganioglu,[*15] J. Chiba,[*16] D. Nishimura,[*16] H. Oikawa,[*16] Y. Takei,[*16] S. Yagi,[*16] K. Wimmer,[*3] G. de France,[*17] S. Go,[*18] and B. A. Brown[*19]

Studies of nuclei far from stability can provide excellent tests of the validity of nuclear structure models. They are also of interest in relation to astrophysical processes such as the *rp*-process (rapid-proton capture) for proton-rich nuclei. They decay via direct proton, β-delayed proton (βp) or γ emission.

The production of very exotic proton-rich nuclei was achieved at RIBF by ^{78}Kr projectile fragmentation on a Be target. This reaction was used for the first time during the ^{78}Kr campaign in 2015, allowing the observation of new isotopes[1)] and 2*p* radioactivity[2)]. After selection and identification by BigRIPS and the ZD spectrometer, the nuclei were implanted in the three WAS3ABi DSSSDs to measure β particles and protons, surrounded by the EURICA γ-ray array[3)].

A DSSSD allows implantation-decay position and time correlations, strongly reducing the background in the spectra. However, a lot of random correlations remain. Background can be removed using two energy spectra: one from implantation-decay correlations in a positive time window and another in a negative one of the same width. Because the background time distribution is uniform, the background is removed when the second spectrum is subtracted from the first one. The proton branching ratios were determined comparing the number of events above 1 MeV with the number of implants happening in the same pixel. β particles have an average energy loss of 400 keV, their contribution can therefore be neglected above 1 MeV. The half-lives were determined from time spectra considering our experimental branching ratios and the β-detection efficiency for the daughter contributions. This efficiency was estimated from known β emitters.

Nucleus	Proton branching ratio (%)	Half-life (ms)
^{57}Zn	81(2)	44.8(4)
^{61}Ge	86(2)	39.1(4)
^{65}Se	88(2)	33.2(6)
^{68}Kr	90(10)	20(4)
^{69}Kr	95^{+5}_{-6}	30(2)

Table 1. Measured proton branching ratios and half-lives.

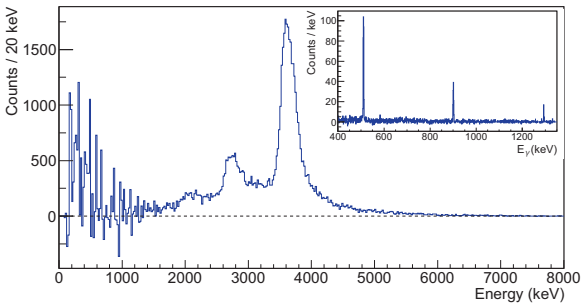

Fig. 1. Charged-particle spectrum for ^{65}Se decay after background subtraction. The inset shows the γ-ray spectrum in coincidence with the 2.6 MeV proton peak. The 901.7-keV peak confirms the feeding of the $2^+ \rightarrow 0^+$ transition in ^{64}Ge and the scheme proposed by ref.[4)].

The high statistics of the experiment gave more accurate values for βp emitters (cf. Table 1) as compared to the literature values. New measurements of ^{65}Se (see Fig. 1) and ^{69}Kr were made, relevant for the *rp*-process because of their proton-unbound β daughters ^{65}As and ^{69}Br[4)]. New values for ^{61}Ge and ^{57}Zn allow a comparison with existing ones[5)]. ^{68}Kr was measured for the first time.

*1 CEN Bordeaux Gradignan
*2 IFIC, CSIC-Universidad de Valencia
*3 Atomki, Debrecen
*4 RIKEN Nishina Center
*5 Department of Physics, University of Tokyo
*6 Department of Physics, Osaka University
*7 Research Center for Nuclear Physics, Osaka University
*8 Department of Physics, University of Surrey
*9 Comisíon Chilena de Energia Nuclear
*10 Institute of Nuclear Physics, University of Cologne
*11 Physik Department E12, Technische Universität München
*12 Laboratori Nazionali di Legnaro dell' INFN
*13 IFIN-HH
*14 INFN Sezione di Padova and Dipartimento di Fisica
*15 Department of Physics, Istanbul University
*16 Department of Physics, Tokyo University of Science
*17 Grand Accélérateur National d'Ions Lourds, Caen
*18 Dept. of Physics and Astronomy, University of Tennessee
*19 Department of Physics and Astronomy, and NSCL, MSU

References

1) B. Blank et al., Phys. Rev. C **93**, 061301(R) (2016).
2) T. Goigoux et al., Phys. Rev. Lett. **117**, 162501 (2016).
3) P.-A. Söderström et al., Nucl. Instrum. Methods Phys. Res. Sect. B **317**, 649 (2013).
4) A. M. Rogers et al., Phys. Rev. C **84**, 051306(R) (2011).
5) B. Blank et al., Eur. Phys. J. A **31**, 267 (2007).

Mass and β-decay measurement of neutron-rich nuclei around N=56

A. Estrade,[*1] D. S. Ahn,[*2] M. Amthor,[*3] O. Aktas,[*4] H. Baba,[*2] S. Bae,[*5] P. Coleman-Smith,[*6] T. Davinson,[*7] P. Doornenbal,[*2] N. Fukuda,[*2] C. Griffin,[*7] S. Gaire,[*1] Z. Ge,[*2] J. Ha,[*5] L. Harkness-Brennan,[*8] T. Isobe,[*2] N. Inabe,[*2] D. Kahl,[*7] G. G. Kiss,[*2] T. Kubo,[*2] S. Kubono,[*2] M. Labiche,[*6] G. Lorusso,[*9] G. Lotay,[*10] Y. Litvinov,[*11] C. Lizarazo,[*12] B. Moon,[*13] F. Montes,[*14] K. Matsui,[*2] S. Momiyama,[*15] S. Naimi,[*2] S. Neupane,[*1] S. Nishimura,[*2] C. Nita,[*16] V Phong,[*2] F. Recchia,[*17] S Riccetto,[*18] H. Sakurai,[*15] Y. Saito,[*15] P. Schrock,[*10] Y. Shimizu,[*2] P-A Söderström,[*2] H. Suzuki,[*2] T. Sumikama,[*2] H. Takeda,[*2] V. Werner,[*12] K. Wimmer,[*15] W. Witt,[*12] P. J. Woods[*7] and K. Yoshida[*2]

The origin of the elements around Zr (Z=40) is one of the most intriguing questions regarding nucleosynthesis of the heavy elements during the rapid neutron-capture process (r-process). In recent years, the observation of elemental abundances in a growing sample of extremely metal-poor star has shown a remarkably robust pattern of abundances in the heavier elements (beyond Te, at Z=52), in very good agreement with the r-process abundance pattern derived from the Solar System [1]. This provides evidence that the r-process is a mechanism contributing to the chemical evolution of the Galaxy from its early stages. On the other hand, the scenario for the elements in the Sr to Ag region is more complex[2]. The abundances do not show such a clear correlation with the solar r-process pattern. For example, some stars present an overabundance of A≈90 isotopes. Additional nucleosynthesis processes, such as a weak r-process acting in neutrino-driven winds of core-collapse supernovae, have been proposed as an explanation[2].

Astrophysical model calculations consistently show that the uncertainty in the available nuclear physics input contributes in a significant way to the uncertainty of their results. For some models, the region around ^{92}Se studied in our experiment, has been identified as having a high impact[3]. The region is critical to disentangle the contribution of the strong r-process from other nucleosynthesis processes. Our new data will help to address the question of what, if any, the contribution of the strong r-process to elements lighter than Ag (Z=47) is, or which alternative processes could be responsible for the synthesis of these elements.

The objective of our experiment, performed in June of 2016, is to measure for the first time the mass and β-decay half-lives of a number of neutron-rich isotopes in the Z≈34 region. The experiment combines a β-decay measurement using the Advanced Implantation Detector Array (AIDA) with a simultaneous mass measurement using the time-of-flight (TOF) technique[4]. A neutron-rich beam in the ^{92}Se region was produced by fragmentation of a 345 MeV/u primary beam of ^{238}U on a Be target. In addition to the separation of the secondary beam ions, BigRIPS was used for the TOF mass measurement. Its optics were tuned to High Resolution Mode, using a TOF flight path from the F3 to the F11 focal plane positions. The beam ions were then implanted in the double-sided silicon strip detectors of AIDA, which was placed at the focal plane of the Zero-Degree Spectrometer and surrounded by the EURICA gamma detector array.

Figure 1 shows a particle-identification plot for the experiment, with a line indicating the limit of known nuclear masses. We expect to measure new decay half-lives of 10 isotopes in the region of Ge to Kr region, and the mass for up to 10 isotopes. The data analysis for the mass and half-live measurement is in progress, as well as that for decay spectroscopy with EURICA.

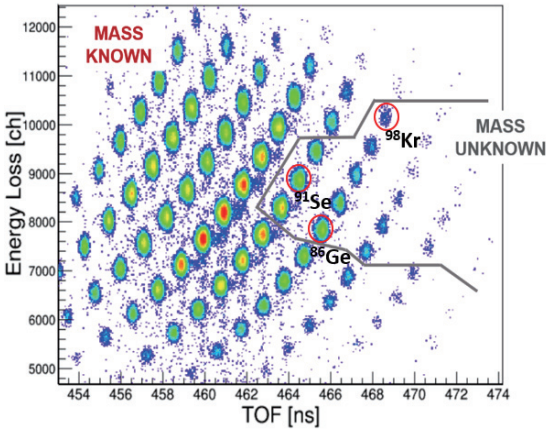

Fig. 1. Particle identification plot for secondary beam ions in the experiment, showing the limit of previously measured masses (with three isotopes labelled as reference).

[*1] Central Michigan University
[*2] RIKEN Nishina Center
[*3] Bucknell University
[*4] Middle East Technical University
[*5] Seoul National University
[*6] STFC Daresbury Laboratory
[*7] University of Edinburgh
[*8] University of Liverpool
[*8] National Physical Laboratory
[*10] University of Surrey
[*11] GSI
[*12] TU Darmstadt
[*13] Korea University
[*14] Michigan State University
[*15] University of Tokyo
[*16] IFIN Horia Hulubei Bucharest
[*17] University and INFN Padova,
[*18] University and INFN Perugia

References

1) I. U. Roederer et al.: Astrophys. J. Lett. **747**, L8 (2012).
2) C. Hansen et al: Astrophys. J. **797**, 123 (2014).
3) S. Brett et al: Eur. Phys. J. A **48**, 184 (2012).
4) M. Matos et al: Nucl. Instr. Meth. A **696**, 171 (2012).

β and β-n decay of $^{131-135}$In

G. Simpson,[*1] J. Keatings,[*2] A. Jungclaus,[*3] J. Taprogge,[*4] S. Nishimura,[*5] P. Doornenbal,[*5] G. Lorusso,[*5] P.-A. Söderström,[*5] T. Sumikama,[*5] J. Wu,[*5] Z. Y. Xu,[*5] T. Isobe,[*5] H. Sakurai,[*5] and the EURICA RIBF-85 collaboration

The shell-model is often central to our understanding of basic nuclear structure and allows many properties of nuclei in the vicinity of closed shells to be reliably described. Two ingredients are necessary for shell-model calculations; two-body matrix elements, describing the interactions between nucleons in the chosen valence space, and single-particle energies. While the former are often derived via a range of sophisticated methods the latter are taken from experimental data on single valence nucleon nuclei, if possible.

Studies of the nuclei near ^{132}Sn offer a rare opportunity to test the effective interactions used in shell-model calculations in a heavy, neutron-rich region. Nearly all single-particle energies are accurately known here, with the exception of the $\nu i_{13/2}$ and $\pi s_{1/2}$ states in ^{133}Sn and ^{133}Sb respectively. We have studied the β and β-n decays of ^{133,134}In to search for the former level in ^{133}Sn and more generally to study excited states in the semi-magic Sn nuclei. Such studies often allow the neutron-neutron part of the effective interaction to be examined, as performed recently for ^{134,136,138}Sn, using μs isomer-decay data from the present experiment[1]. New information on the β-decaying states of the parent indium nuclei has also been obtained in the present work.

The experiment was performed at the F11 focal plane of the BigRIPS spectrometer of RIBF. The in-flight fission of a 345-MeV/nucleon ^{238}U beam was used to produce $^{131-135}$In ions, along with others, with sufficient intensity for ion–$\beta-\gamma$ spectroscopy studies. The detectors of the BigRIPS spectrometer allowed these ions to be identified according to their Z and mass-to-ionic-charge ratios before they were implanted in the WAS3ABi stopper, which was situated at the F11 focal plane. The high segmentation of the WAS3ABi stopper allowed detected β decays to be correlated with identified and implanted ions. The EURICA Ge array was used to detect any γ rays emitted following the β decay of identified $^{131-135}$In ions. Use of ion–$\beta-\gamma$ and occasionally ion–$\beta-\gamma-\gamma$ coincidences allowed decay schemes, half-lives and β-delayed neutron values (P_n) to be obtained. More details on the experimental setup can be found in Ref.[2].

Excited states in the one-valence-neutron nucleus ^{133}Sn have been populated via the β and β-n decay of ^{133,134}In, respectively. This has allowed a search for the decay of the $13/2^+$ state in ^{133}Sn and for the energies of some previously reported states to be confirmed.

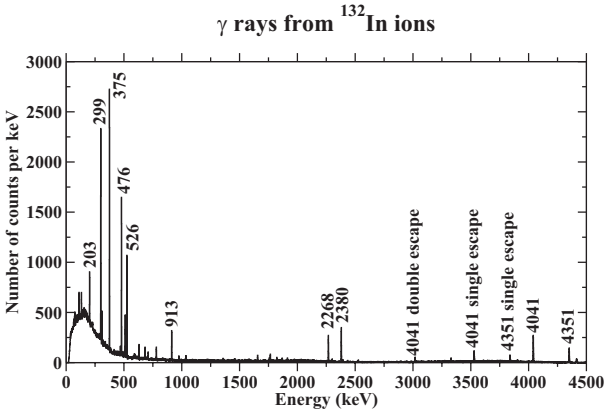

Fig. 1. Spectrum of γ rays obtained from the β decay of ^{132}In. Strong previously reported decays are present[4].

A first γ ray has been tentatively assigned to ^{135}Sn and a level scheme of ^{134}Sn has been obtained from the β decay of ^{134}In for the first time. This has allowed the limits of the ground-state spin of latter nucleus to reduced. Inconsistencies have also been found between the level schemes of two neutron-rich Sn isotopes obtained in the present work and those previously reported, raising questions about several spin/parity assignments.

The ground-state half-lives of $^{131-135}$In have been measured, along with those of any β-decaying isomers, via ion–$\beta-\gamma$ coincidences. There are some discrepancies between the half-lives measured using this technique and those obtained from only ion–β correlations [3] and values found elsewhere in the literature[4].

An examination of the γ-ray intensities in the daughter Sn and grand-daughter Sb nuclei, populated via β decay, has allowed preliminary P_n values for the indium parent and grandparent nuclei to be obtained. This includes the first P_n measurement for ^{135}In. These preliminary values still require corrections to account for reactions occurring between the last particle detector in BigRIPS and the ions being stopped in WAS3ABi.

*1 LPSC, Grenoble
*2 School of Engineering, University of the West of Scotland
*3 IEM, CSIC Madrid
*4 Fisica Teórica, Universidad Autonoma de Madrid
*5 RIKEN Nishina Center

References
1) G. Simpson *et al.*, Phys. Rev. Lett. **113**, 132502 (2014).
2) J. Taprogge *et al.*, Phys. Rev. C **91**, 054324 (2015).
3) G. Lorusso *et al.*, Phys. Rev. Lett. **114**, 192501 (2015).
4) ENSDF database, http://www.nndc.bnl.gov/ensdf

β-decay γ-ray spectroscopy of ^{140}Te : level structure of ^{140}I beyond $N = 82$

B. Moon,[*1] C.-B. Moon,[*2] A. Odahara,[*3] R. Lozeva,[*4] C. Yuan,[*5] P.-A. Söderström,[*6] F. Browne,[*6] H. S. Jung,[*7] P. Lee,[*8] C. S. Lee,[*8] A. Yagi,[*3] S. Nishimura,[*6] P. Doornenbal,[*6] G. Lorusso,[*6] H. Watanabe,[*6] I. Kojouharov,[*9] T. Sumikama,[*6] T. Isobe,[*6] H. Baba,[*6] H. Sakurai,[*6] R. Daido,[*3] Y. Fang,[*3] H. Nishibata,[*3] Z. Patel,[*10] S. Rice,[*10] L. Sinclair,[*11] J. Wu,[*6] Z. Y. Xu,[*12] R. Yokoyama,[*13] T. Kubo,[*6] N. Inabe,[*6] H. Suzuki,[*6] N. Fukuda,[*6] D. Kameda,[*6] H. Takeda,[*6] D. S. Ahn,[*6] Y. Shimizu,[*6] D. Murai,[*14] F. L. Bello Garrote,[*15] J. M. Daugas,[*6*16] F. Didierjean,[*5] E. Ideguchi,[*3] T. Ishigaki,[*3] S. Morimoto,[*3] M.Niikura,[*6] I. Nishizuka,[*17] T. Komatsubara,[*6] Y. K. Kwon,[*18] and K. Tshoo[*18]

The region beyond the doubly-magic nucleus ^{132}Sn is currently the subject of great experimental and theoretical interest in view of the shell structure evolution and rapid neutron capture processes. An accurate measurement of the β-decay of neutron-rich nuclei is crucial for the determination of the r-process path. We report the first observation of excited states of ^{140}I by the β-delayed γ-ray spectrosocopy of ^{140}Te.

The ^{140}Te nuclide was produced by the in-flight fission with a 345 MeV per nucleon ^{238}U primary beam on a ^{9}Be target by means of the BigRIPS separator. A total of 1.8×10^{6} ions of ^{140}Te was implanted during the beam time among about 10^{7} total implanted ions. After beams were implanted on the active double-side stripped silicon detector array, WAS3ABi, γ-rays following after the β-decay were detected by Euroball RIKEN HPGe Cluster Array(EURICA) surrounding WAS3ABi.[1,2)]

Total 40 γ-rays were assigned as internal transitions of ^{140}I. The level scheme of ^{140}I as shown in Fig. 1 has been built based on $\gamma\gamma$ coincidence matrices and the β-delayed γ-ray singles spectrum. The β-decay half-life of the parent ^{140}Te was obtained to be 350(5) ms by the 341-, 739-, 875-keV transitions.

Spin parity assignments of the established levels were made on the basis of the logft value argument. For instance, those with logft values of near 6 to 7, applying to the region of the first forbidden β strengths,

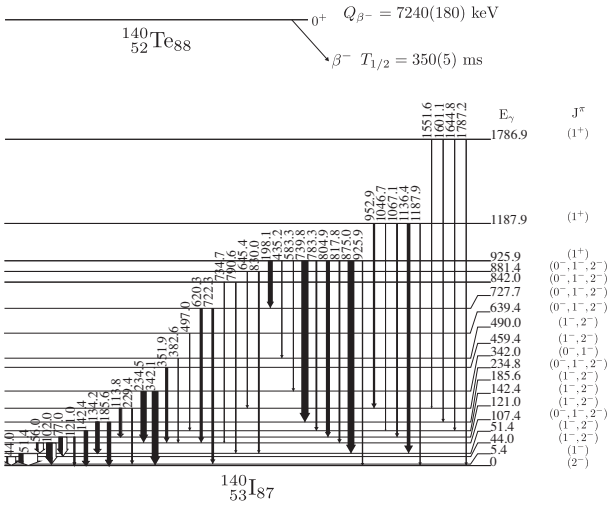

Fig. 1. The level scheme of ^{140}I. The thickness of each transition represents the relative intensity to the 44 keV transition.

are possibly 0, 1, and 2. We note that the spin-parity of the ground state should be assigned as (2^-) according to our analysis of the β-decay to ^{140}Xe. The 5.4-keV level is likely to be a (1^-) state based on the shell model calculations. Additionally, levels with a direct transition to the ground state are assigned as (1^-) or (2^-) by assuming that all transitions are M1.

The level at 926 keV is assigned as an 1^+ state with an argument based on the log ft value, 4.89. This 1^+ state is strongly related to the Gamow-Teller(G-T) transition. In this region, the only allowed β-decay transitions, G-T transitions, involves the decay of an $h_{9/2}$ neutron to an $h_{11/2}$ proton. Such a decay from an even-even nucleus gives rise to a $[\nu h_{9/2}\pi h_{11/2}]1^+$ state in the odd-odd daughter nucleus.

*1 Department of Physics, Korea University
*2 Department of Display Engineering, Hoseo University
*3 Department of Physics, Osaka University
*4 IPHC, CNRS, IN2P3 and University of Strasbourg
*5 Sino-French Institute of Nuclear Engineering and Technology, Sun Yat-Sen University
*6 RIKEN Nishina Center
*7 Agency of Defence Development
*8 Department of Physics, Chung-Ang University
*9 GSI Helmholtzzentrum für Schwerionenforschung GmbH, D-64291, Darmstadt, Germany
*10 Department of Physics, University of Surrey
*11 Department of Physics, University of York
*12 Department of Physics, University of Tokyo
*13 Center for Nuclear Study, University of Tokyo
*14 Department of Physics, Rikkyo University
*15 Department of Physics, University of Oslo
*16 CEA, DAM, DIF
*17 Department of Physics, Tohoku University
*18 Rare Isotope Science Project, Institute for Basic Science

References
1) P.-A. Söderström et al. Nucl. Instrum. Methods Phys. Res., Sect. B 317, 649 (2013).
2) S. Nishimura, Prog. Theor. Exp. Phys. 2012, 03C006 (2012).

β decay of ^{140}Sb : level scheme of ^{140}Te†

B. Moon,[*1] C.-B. Moon,[*2] P.-A.Söderström,[*3] A. Odahara,[*4] R. Lozeva,[*5] B. Hong,[*1] F. Browne,[*3] H. S. Jung,[*6] P. Lee,[*6] C. S. Lee,[*6] A. Yagi,[*4] C. Yuan,[*7] S. Nishimura,[*3] P. Doornenbal,[*3] G. Lorusso,[*3] H. Watanabe,[*3] I. Kojouharov,[*8] T. Sumikama,[*3] T. Isobe,[*3] H. Baba,[*3] H. Sakurai,[*3] R. Daido,[*4] Y. Fang,[*4] H. Nishibata,[*4] Z. Patel,[*9] S. Rice,[*9] L. Sinclair,[*10] J. Wu,[*3] Z. Y. Xu,[*11] R. Yokoyama,[*12] T. Kubo,[*3] N. Inabe,[*3] H. Suzuki,[*3] N. Fukuda,[*3] D. Kameda,[*3] H. Takeda,[*3] D. S. Ahn,[*3] Y. Shimizu,[*3] D. Murai,[*13] F. L. Bello Garrote,[*14] J. M. Daugas,[*3,*15] F. Didierjean,[*5] E. Ideguchi,[*4] T. Ishigaki,[*4] S. Morimoto,[*4] M. Niikura,[*3] I. Nishizuka,[*16] T. Komatsubara,[*3] Y. K. Kwon,[*17] and K. Tshoo[*17]

We report the first observation of the level structure of ^{140}Te through the β-delayed γ-ray spectroscopy of ^{140}Sb. The structure of Te with $N > 82$, two protons beyond $Z = 50$, is expected to provide a wealth of information on the shell evolution in extreme proton-neutron imbalanced environments. Besides, the present work provides valuable inputs for modelling the nucleosynthesis since the ^{140}Sb decay process is one of important paths along the rapid neutron capture process.

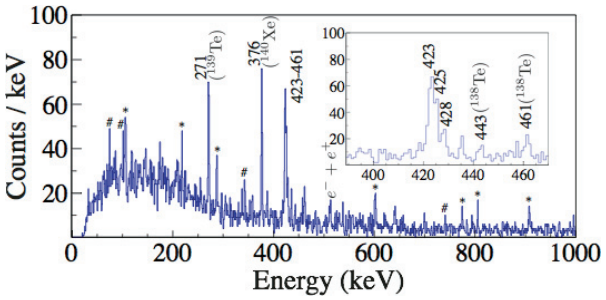

Fig. 1. Singles γ-ray spectrum associated with the β decay of ^{140}Sb obtained in 2000 ms time interval after ions are implanted on the active target. The inset is a zoomed spectrum in representing the 380 to 470 keV region. Peaks with an asterisk are room- and beam-induced backgrounds from random coincidence with β events. Peaks with a # mark represent unassigned γ rays after decays of Te nuclides.

The parent ^{140}Sb nuclides were produced by the in-flight fission of a 345 MeV per nucleon ^{238}U beam on a ^{9}Be target and selected by the first stage of the BigRIPS separator. During the beam time, a total of 7.8×10^3 ions for ^{140}Sb were collected among about 10^7 total ions. Emitted γ rays, following the β decay of ^{140}Sb were collected by EURICA, the HPGe array, surrounding the active double-side stripped Si stopper array WAS3ABi[1]. Figure 1 shows the β-delayed γ-ray spectrum of ^{140}Sb. The broad peaks around 425 keV are composed of triple photo-peak as shown in the inset of Fig. 1; 423, 425, and 428 keV. On the basis of the γγ coincidence data and γ-ray intensities in the singles spectrum, we propose that the 423- and 425-keV peaks should be assigned as γ-ray transitions in ^{140}Te.

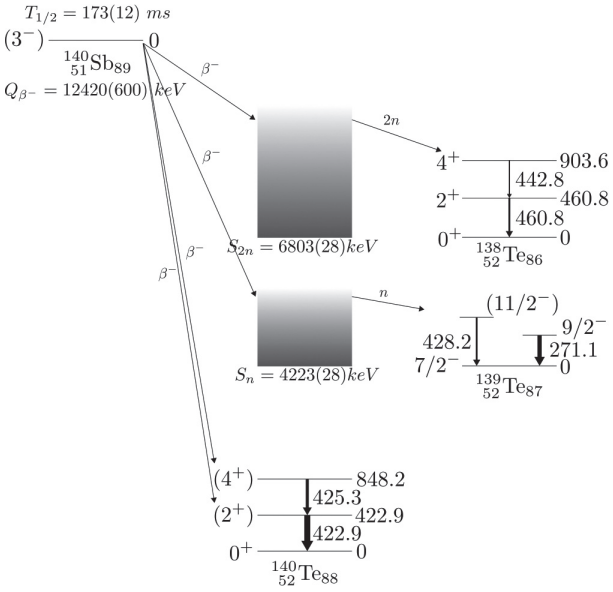

Fig. 2. The β-decay scheme of ^{140}Sb deduced from the present work. The thicknesses of each transition represent the relative intensities to the 423 keV transition.

As shown in Fig. 2, we successfully identified β-decay scheme, β-delayed one-neutron emission, and β-delayed two-neutron emission channels from the decay of ^{140}Sb.

† Condensed from the article in Phys. Rev. C. **95**, 044322 (2017)
*1 Department of Physics, Korea University
*2 Department of Display Engineering, Hoseo University
*3 RIKEN Nishina Center
*4 Department of Physics, Osaka University
*5 IPHC, CNRS, IN2P3 and University of Strasbourg
*6 Department of Physics, Chung-Ang University
*7 Sino-French Institute of Nuclear Engineering and Technology, Sun Yat-Sen University
*8 GSI Helmholtzzentrum für Schwerionenforschung GmbH
*9 Department of Physics, University of Surrey
*10 Department of Physics, University of York
*11 Department of Physics, University of Tokyo
*12 Center for Nuclear Study, University of Tokyo
*13 Department of Physics, Rikkyo University
*14 Department of Physics, University of Oslo
*15 CEA, DAM, DIF
*16 Department of Physics, Tohoku University
*17 Rare Isotope Science Project, Institute for Basic Science

Reference

1) P.-A. Söderström et al. Nucl. Instrum. Methods Phys. Res. B **317**, 649 (2013).

β-delayed γ-ray spectroscopy of ^{168}Dy

G. X. Zhang,[*1,*2] H. Watanabe,[*1,*2,*3] P. M. Walker,[*4] J. J. Liu,[*5] J. Wu,[*6] P. H. Regan,[*4,*7] P-A. Söderström,[*3] H. Kanaoka,[*8] Z. Korkulu,[*9] P. S. Lee,[*10] S. Nishimura,[*3] A. Yagi,[*8] and EURICA 2014 collaboration

Atomic nuclei tend to be deformed when moving away from shell closures, giving rise to rotational motion. In well-deformed nuclei, characteristic rotational bands can be built on intrinsic states, including not only the ground state, but also any kinds of vibrational states and other quasiparticle configurations. These intrinsic excitations play an important role in stabilizing the nuclear shape. Recent spectroscopic studies on ^{170}Dy[1] and ^{172}Dy[2] using the EUROBALL-RIKEN Cluster Array (EURICA) setup[3] revealed that the γ-vibrational levels emerge at unusually low excitation energy compared to the adjacent even-even nuclei. This result indicates an enhancement of the γ-vibrational mode in this doubly mid-shell region, leading presumably to an excursion from axial symmetry.

This report presents a preliminary result of γ-ray spectroscopy of ^{168}Dy following the β decay from ^{168}Tb. The same decay channel has been studied before in Ref. [4], where only three γ rays at 75, 173, and 227 keV were assigned for the excited states in ^{168}Dy. The former two γ rays have been confirmed as the $2^+ \rightarrow 0^+$ and $4^+ \rightarrow 2^+$ transitions in the ground-state rotational band, respectively, by means of multi-nucleon transfer reactions[5]. In the present work, we explore the level structure of ^{168}Dy with higher statistics than Ref. [4] with a particular focus on the non-yrast states being characteristic of γ- and octupole-vibrational modes.

The decay spectroscopy experiment for neutron-rich Dy isotopes has been performed at RIBF at the RIKEN Nishina Center. The nuclei of interest were produced by the in-flight fission of a ^{238}U primary beam at 345 MeV/u incident on a Be target with an average intensity of 12 pnA. About 1.2×10^4 ^{168}Tb^{65+} ions were transported through the BigRIPS-ZeroDegree spectrometers and finally implanted into the WAS3ABi[6] active stopper system comprised of two double-sided silicon-strip detectors (DSSSD). Each DSSSD has a thickness of 1 mm and an active area of 60×40 mm^2 with 1 mm pitch. The DSSSDs recorded events of heavy-ion implantation and subsequent decay

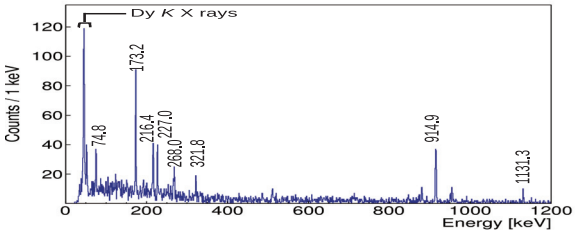

Fig. 1. Gamma-ray spectrum following implantation of ^{168}Tb within 20 s.

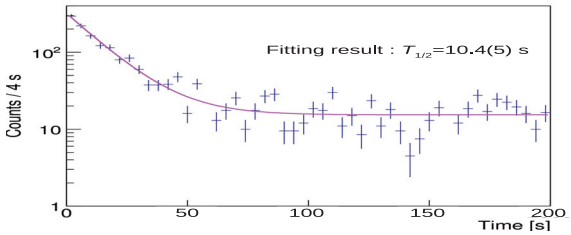

Fig. 2. Electron time distribution after implantation of ^{168}Tb measured with a sum of gates on the γ-ray peaks labeled in Fig. 1 except for the 75-keV line and X rays. An exponential function with a constant background was used for fitting.

electrons (both β rays and internal conversion electrons). Gamma rays were detected by EURICA with a full energy-peak efficiency of about 10 % for 1 MeV γ rays. Figure 1 shows the β-delayed γ-ray spectrum measured within 20 s after the implantation of ^{168}Tb. In addition to the transitions reported previously,[4,5] several new γ rays are clearly visible at 216, 322, 915 and 1131 keV. A fit of the electron time distribution measured in coincidence with these γ rays yields a half life of 10.4(5) s (see Fig. 2), which is consistent with the value obtained independently from the analysis of β-decay half lives[7]. The detailed level scheme of ^{168}Dy including these new transitions is still under consideration.

*1 IRCNPC, Beihang University
*2 School of Physics and Nuclear Energy Engineering, Beihang University
*3 RIKEN Nishina Center
*4 Department of Physics, University of Surrey
*5 Department of physics, Hong Kong University
*6 School of Physics, Peking University
*7 National Physical Laboratory, Teddington
*8 Department of Physics, Osaka University
*9 INR, Hungarian Academy of Sciences
*10 Department of Physics, Chung-Ang University

References

1) P-A. Söderström et al., Phys. Lett. B **762**, 404 (2016).
2) H. Watanabe et al., Phys. Lett. B **760**, 641 (2016).
3) P-A. Söderström et al., Nucl. Instr. Meth. B **317**, 649 (2016).
4) M. Asai et al., Phys. Rev. C **59**, 3060 (1999).
5) P-A. Söderström et al., Phys. Rev. C **81**, 034310 (2010).
6) S. Nishimura, Prog. Theor. Exp. Phys. 03C006 (2012).
7) J. Wu et al., Phys. Rev. Lett. **118**, 072701 (2017).

Measurement of $\vec{p}$–^{6}He elastic scattering at 200 A MeV

S. Sakaguchi, [*1,*2] S. Chebotaryov, [*2,*3] T. Uesaka, [*2] T. Akieda, [*4] Y. Ando, [*3] M. Assie, [*5] D. Beaumel, [*2,*5] N. Chiga, [*2] M. Dozono, [*6] A. Galindo-Uribarri, [*7] B. Heffron, [*7] A. Hirayama, [*8] T. Isobe, [*2] S. Kawase, [*1] W. Kim, [*3] T. Kobayashi, [*4] H. Kon, [*4] Y. Kondo, [*8] Y. Kubota, [*2] S. Leblond, [*9] H. Lee, [*9] T. Lokotko, [*9] Y. Maeda, [10] Y. Matsuda, [11] K. Miki, [*4] E. Milman, [*2,*3] T. Motobayashi, [*2] T. Mukai, [*4] S. Nakai, [*4] T. Nakamura, [*8] A. Ni, [*3] T. Noro, [*1] S. Ota, [*6] H. Otsu, [*2] T. Ozaki, [*8] V. Panin, [*2] S. Park, [*3] A. Saito, [*8] H. Sakaguchi, [*12] H. Sakai, [*2] M. Sasano, [*2] H. Sato, [*2] K. Sekiguchi, [*2,*4] Y. Shimizu, [*2] I. Stefan, [*5] L. Stuhl, [*6] M. Takaki, [*6] K. Taniue, [*10] K. Tateishi, [*2] S. Terashima, [*13] Y. Togano, [*8] T. Tomai, [*8] Y. Wada, [*4] T. Wakasa, [*1] T. Wakui, [*2,*14] A. Watanabe, [*4] H. Yamada, [*8] Z. Yang, [*2] M. Yasuda, [*8] J. Yasuda, [*1] K. Yoneda [*2] and J. Zenihiro [*2]

We measured the vector analyzing power for p–^{6}He elastic scattering at 200 A MeV using a spin-polarized solid proton target and the SAMURAI spectrometer with the aim of investigating spin-orbit interaction between proton and ^{6}He (SAMURAI13 experiment). The experimental setup is described in this article.

A ^{6}He beam was produced from an ^{18}O beam with 230 A MeV using a 15 mm^t Be target and an 8 mm^t F1 degrader. Triton contamination was suppressed to 25% of the total beam intensity with an F2 collimator and was further reduced to 6% by closing the F2 slit to 2 × 2 mm^2. The experimental setup around the target is schematically shown in Fig. 1. Special care was taken to reduce the size of the beam spot at F13. STQ25 was moved 1 m closer to the target for better focusing. A veto scintillator (SBV) with an ϕ18 mm hole was installed in front of the target. The beam intensity was kept at approximately 0.6 MHz. The typical transmission ratio of the beam through SBV was 78%. The beam-spot size on the target was 5 mm in sigma. The polarized proton target was placed 4 m from the SAMURAI magnet center. The target material was naphthalene ($C_{10}H_8$) with a size of ϕ24 mm × 2.5 mm^t (285 mg/cm^2). Two lasers with wavelengths of 556 nm and 545 nm and average powers of 3 W and 0.75 W, respectively, were installed near STQ25. Pulsed laser light with a repetition rate of 3 kHz was delivered to the target. Recoil protons were detected at both the left and right sides of the beamline with ESPRI-RPS[1]. Each system consists of a drift chamber, an energy absorber, one plastic scintillator and seven NaI(Tl) scintillators. For the detection of scattered particles, FDC0 was placed 400 mm away from the target. It is expected to have good high-rate tolerance because of its small cell size of 5 mm. FDC0 was operated with a position resolution of 130 μm in sigma and a tracking efficiency of >98% even for a 1 MHz beam. Two S1-MWDCs from SHARAQ Gr. were placed behind FDC0. Scattered particles were analyzed using the SAMURAI spectrometer with a magnetic field of 2.0 T. The effect of the stray field on the performance of PMTs, polarized target and oxygen monitors was not observed. 95% of the volume of the gap chamber was replaced with helium gas to maximize the acceptance of SAMURAI without severely degrading the $B\rho$ resolution. The FDC1 chamber was slightly over-pressurized (+0.35 kPa) compared to the pressure in the gap chamber to avoid reverse force on its window film. The obtained $B\rho$ resolution was about 1/300, which is one third of the typical value. This is primarily because of the multiple scattering in helium gas and secondarily because of a low magnetic field of 2.0 T. 2.9 T is ideal for ^{6}He at 200 A MeV. The beam propagating through SAMURAI was stopped by a lead block with a size of 10×10×40 cm^3 for protecting FDC2. FDC2 and HODF24 were placed parallel to SAMURAI to cover both ^{6}He and ^{4}He trajectories. Measurements of $\vec{p}$–^{6}He (physics run) and $\vec{p}$–^{4}He scattering (polarization calibration) were performed for 3 days and 1 day, respectively. The polarization axis was reversed once in each run. The carbon target and empty target data were also taken. The current status of the data analysis is described in another article[2].

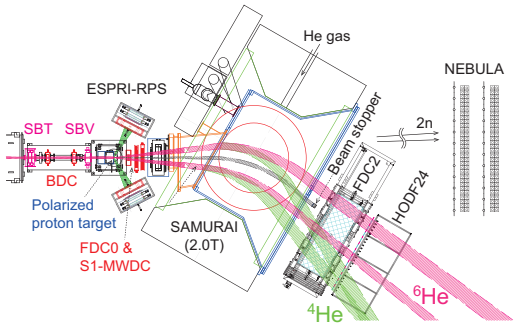

Fig. 1. Setup for SAMURAI13 experiment.

*1 Department of Physics, Kyushu University
*2 RIKEN Nishina Center
*3 Department of Physics, Kyungpook National University
*4 Department of Physics, Tohoku University
*5 IPN Orsay
*6 CNS University of Tokyo
*7 Oak Ridge National Laboratory
*8 Department of Physics, Tokyo Institute of Technology
*9 Department of Physics, University of Hong Kong
*10 Department of Physics, Miyazaki University
*11 CYRIC Tohoku University
*12 RCNP Osaka University
*13 Department of Physics, Beihang University
*14 National Institute of Radiological Sciences

References

1) Y. Matsuda et al., Phys. Rev. C **87**, 034614 (2013).
2) S. Chebotaryov et al., in this report.

Present status of data analysis of $\vec{p}-{}^{6}$He elastic scattering

S. Chebotaryov,[*1,*2] S. Sakaguchi,[*1,*3] T. Uesaka,[*1] T. Akieda,[*4] Y. Ando,[*2] M. Assie,[*5] D. Beaumel,[*1,*5] N. Chiga,[*1] M. Dozono,[*6] A. Galindo-Uribarri,[*7] B. Heffron,[*7] A. Hirayama,[*8] T. Isobe,[*1] S. Kawase,[*3] W. Kim,[*2] T. Kobayashi,[*1,*4] H. Kon,[*4] Y. Kondo,[*8] Y. Kubota,[*1] S. Leblond,[*9] H. Lee,[*9] T. Lokotko,[*9] Y. Maeda,[*10] Y. Matsuda,[*1,*11] K. Miki,[*1,*4] E. Milman,[*1,*2] T. Motobayashi,[*1] T. Mukai,[*4] S. Nakai,[*4] T. Nakamura,[*8] A. Ni,[*2] T. Noro,[*3] S. Ota,[*6] H. Otsu,[*1] T. Ozaki,[*8] V. Panin,[*1] S. Park,[*2] A. Saito,[*8] H. Sakaguchi,[*12] H. Sakai,[*1] M. Sasano,[*1] H. Sato,[*1] K. Sekiguchi,[*1,*4] Y. Shimizu,[*1] I. Stefan,[*5] L. Stuhl,[*6] M. Takaki,[*6] K. Taniue,[*10] K. Tateishi,[*1] S. Terashima,[*13] Y. Togano,[*1,*8] T. Tomai,[*1,*8] Y. Wada,[*4] T. Wakasa,[*3] T. Wakui,[*1,*14] A. Watanabe,[*4] H. Yamada,[*8] Z. Yang,[*1] M. Yasuda,[*8] J. Yasuda,[*3] K. Yoneda[*1] and J. Zenihiro[*1]

In the summer of 2016, we conducted an experiment at the RIKEN RI-beam factory (RIBF) on the elastic scattering of spin-polarized protons from unstable ^{6}He nuclei at 200A MeV to probe its spin-orbit potential. The experiment was performed at the BigRIPS beamline using the SAMURAI spectrometer and a spin-polarized proton target system.[1] Data obtained from this experiment should help us understand how an exotic structure of neutron-rich nuclei affects spin-orbit coupling owing to its extended neutron density distribution. Details of the experimental setup are presented in another report.[2] The current status of the data analysis will be presented here.

To cleanly select p-^{6}He elastic scattering events, mainly two contributions should be discriminated: inelastic channels, where incident ^{6}He breaks up into ^{4}He + 2n, and quasi-free scattering (QFS) of a proton from carbon nuclei contained in the target material ($C_{10}H_8$). For the first part, the SAMURAI spectrometer was used as it can easily discriminate ^{4}He and ^{6}He particles by Bρ analysis. Figure 1(a) shows the distribution of events at a plastic scintillator hodoscope, where ^{4}He and ^{6}He are clearly separated.

Figure 1(b) shows a PID spectrum from proton detectors. The solid line shows the simulated ΔE-E curve for a proton, which corresponds suitably well with the obtained data. On this spectrum, a separate locus of deuteron particles can also be observed, and it can be discriminated with ΔE-E cut on proton events.

Figure 1(c) shows the polar-angle correlation of recoil and scattered particles for the cases of polarized proton (upper panel) and carbon target runs (lower panel). In the upper panel, one can find a locus along the solid line that represents the kinematical correlation of elastic scattering. It overlaps with a thinner locus in the smaller $\theta_{^{6}\mathrm{He}}$ region, which corresponds to QFS from carbon, as can be seen in the lower panel. Figure 1(d) shows the projection of Fig. 1(c) along the solid line. The QFS contribution is normalized with the target thickness. It is found that the QFS contribution is as small as 10% of the elastic scattering and can be adequately subtracted.

After the event selection and background subtraction, the elastic scattering yield can be obtained with a high S/N ratio. At present, the analysis is ongoing to deduce p-^{6}He cross section and analyzing power.

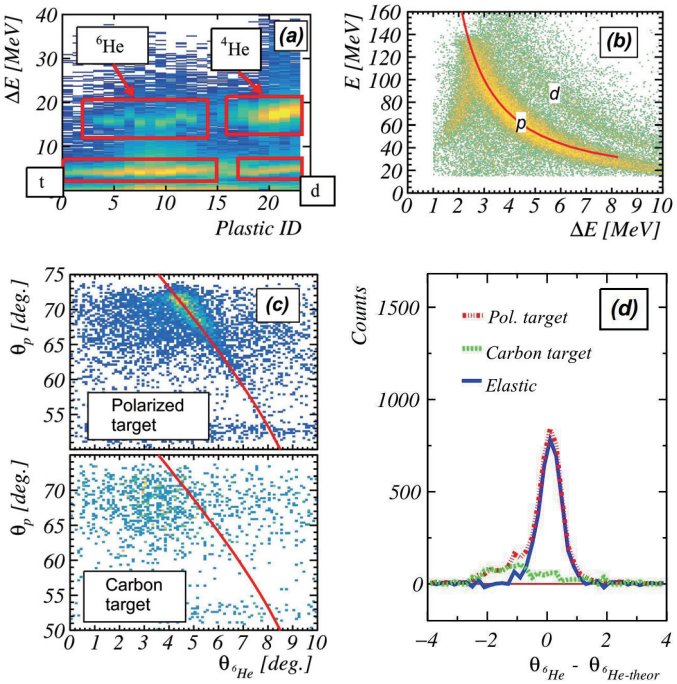

Fig. 1.: Plots showing the PID of (a) scattered and (b) recoil particles. (c) Polar-angle correlations. (d) Carbon background subtraction.

*1 RIKEN Nishina Center
*2 Department of Physics, Kyungpook National University
*3 Department of Physics, Kyushu University
*4 Department of Physics, Tohoku University
*5 IPN Orsay
*6 CNS University of Tokyo
*7 Oak Ridge National Laboratory
*8 Department of Physics, Tokyo Institute of Technology
*9 Department of Physics, University of Hong Kong
*10 Department of Physics, Miyazaki University
*11 CYRIC Tohoku University
*12 RCNP Osaka University
*13 Department of Physics, Beihang University
*14 National Institute of Radiological Sciences

References

1) T. Wakui et al.: Nucl. Instr. Meth. Phys. Res. A **550**, 521 (2005).
2) S. Sakaguchi et al.: In this report.

Study of neutron-neutron correlation in Borromean nuclei via the (p, pn) reaction with the SAMURAI spectrometer

Y. Kubota,[*1,*2] A. Corsi,[*3] G. Authelet,[*3] H. Baba,[*2] C. Caesar,[*4] D. Calvet,[*3] A. Delbart,[*3] M. Dozono,[*1] J. Feng,[*5] F. Flavigny,[*6] J.-M. Gheller,[*3] J. Gibelin,[*7] A. Giganon,[*3] A. Gillibert,[*3] K. Hasegawa,[*8] T. Isobe,[*2] Y. Kanaya,[*9] S. Kawakami,[*9] D. Kim,[*10] Y. Kiyokawa,[*1] M. Kobayashi,[*1] N. Kobayashi,[*11] T. Kobayashi,[*8] Y. Kondo,[*12] Z. Korkulu,[*13,*2] S. Koyama,[*11] V. Lapoux,[*3,*2] Y. Maeda,[*9] F. M. Marqués,[*7] T. Motobayashi,[*2] T. Miyazaki,[*11] T. Nakamura,[*12] N. Nakatsuka,[*14,*2] Y. Nishio,[*15] A. Obertelli,[*3,*2] A. Ohkura,[*15] N. A. Orr,[*7] S. Ota,[*1] H. Otsu,[*2] T. Ozaki,[*12] V. Panin,[*2] S. Paschalis,[*4] E. C. Pollacco,[*3] S. Reichert,[*16] J.-Y. Roussé,[*3] A. T. Saito,[*12] S. Sakaguchi,[*15] M. Sako,[*2] C. Santamaria,[*3,*2] M. Sasano,[*2] H. Sato,[*2] M. Shikata,[*12] Y. Shimizu,[*2] Y. Shindo,[*15] L. Stuhl,[*2] T. Sumikama,[*8,*2] M. Tabata,[*15] Y. Togano,[*12] J. Tsubota,[*12] T. Uesaka,[*2] Z. H. Yang,[*2] J. Yasuda,[*15] K. Yoneda,[*2] and J. Zenihiro[*2]

Dineutron correlation is one of the phenomena expected to appear in neutron-drip-line nuclei. It has long been presumed that the dineutron correlation is a key ingredient to understand the binding mechanism and exotic structures of these nuclei. $E1$ strengths often deduced in previous Coulomb breakup studies have been used by employing the $E1$ cluster sum rule to characterize their correlation.[1)] However, the model dependence was not negligible owing to the ^{9}Li core excitation and the final state interactions.[2)] The kinematically complete measurement of the quasi-free (p, pn) reaction was thus performed with Borromean nuclei ^{11}Li, ^{14}Be, and ^{17,19}B at the RIBF so as to determine the neutron momentum distributions that help characterize the correlation.[3)] The opening angle between the two neutrons was reconstructed from the measured momentum vectors of all the particles.

The experiment was conducted using the SAMURAI spectrometer[4)] and the liquid hydrogen target system MINOS.[5)] The beam momentum was determined from the time of flight (TOF) between focal planes F7 and F13. The trajectory was measured by beam drift chambers (BDCs). The momentum vectors of the neutron knocked out from ^{11}Li, another emitted from the resulting ^{10}Li residue, and the recoil proton were determined from the TOF and position measured by neutron telescopes WINDS and NEBULA, and a recoil proton detector (RPD), respectively. The position and angle of ^{9}Li at the entrance and exit of the SAMURAI spectrometer were measured by forward drift chambers (FDCs). The magnetic rigidity was determined from the tracking information thus obtained. The magnetic field of the spectrometer was calculated and taken into account. The relative energy $E_{\rm rel}$ of the reaction residue ^{10}Li, the missing momentum of the knocked-out neutron in the ground-state ^{11}Li, and the opening angle $\cos\theta_Y$ of two valence neutrons in ^{11}Li were reconstructed from the obtained momentum vectors.

Figure 1 shows the $\cos\theta_Y$ dependence of $E_{\rm rel}$. Smaller $\cos\theta_Y$ values are highly favored as $E_{\rm rel}$ decreases, while the yields are evenly distributed over $\cos\theta_Y$ at a higher $E_{\rm rel}$. Because the small $E_{\rm rel}$ value corresponds to the surface region of the nucleus,[6)] this result suggests that the dineutron correlation is much more developed in the surface region. This is qualitatively consistent with the theoretical prediction.[7)]

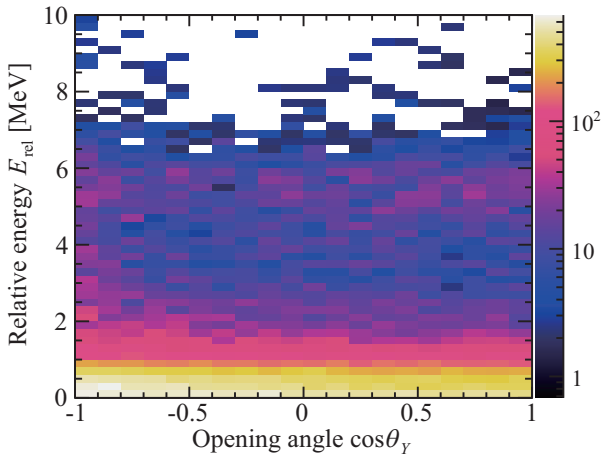

Fig. 1. $E_{\rm rel}$ vs. $\cos\theta_Y$ plot for the ^{11}Li$(p, pn)^{9}$Li $+ n$ reaction.

*1 Center for Nuclear Study, University of Tokyo
*2 RIKEN Nishina Center
*3 CEA, Saclay
*4 Department of Physics, Technische Universität Darmstadt
*5 Department of Physics, Peking University
*6 IPN Orsay
*7 LPC Caen
*8 Department of Physics, Tohoku University
*9 Department of Applied Physics, University of Miyazaki
*10 Department of Physics, Ehwa Womans University
*11 Department of Physics, University of Tokyo
*12 Department of Physics, Tokyo Institute of Technology
*13 MTA Atomki
*14 Department of Physics, Kyoto University
*15 Department of Physics, Kyushu University
*16 Department of Physics, Technische Universität München

References

1) T. Nakamura et al., Phys. Rev. Lett. **96**, 252502 (2006).
2) Y. Kikuchi et al., Phys. Rev. C **87**, 034606 (2013).
3) Y. Kubota et al., RIKEN Accel. Prog. Rep. **48**, 52 (2015).
4) T. Kobayashi et al., Nucl. Instr. Meth. B**317**, 294 (2013).
5) A. Obertelli et al., Eur. Phys. Jour. A**50**, 8 (2014).
6) Y. Kikuchi et al., Prog. Theor. Exp. Phys. **2016**, 103D03 (2016).
7) A. B. Migdal, Soviet J. Nucl. Phys. **16**, 238 (1973).

Exploring the N=16 sub-shell closure: level structure of ^{22}C and search for ^{21}B

N. Orr for the SAMURAI36 and R3B-NeuLAND Collaborations

The investigation of the most neutron-rich dripline nuclei is one of the principal themes of nuclear structure physics. These studies have, however, been limited for the most part to the He, Li and Be isotopes owing to the difficulty in producing beams of heavier nuclei at the dripline. With the advent of the RIBF and the coupling of the BigRIPS separator to intense ^{48}Ca beams, the path has been opened to exploring structure at and beyond the neutron dripline up to Z≈12. In the present work, measurements aimed at elucidating the evolution of shell structure in the most neutron-rich isotopes of B and C were undertaken. These measurements are a natural extension of the NP1106–SAMURAI04 experiment which explored ^{16,18}B and ^{21}C[1] and observed unbound ^{20}B[2] for the first time, and took advantage of recent developments in the ^{48}Ca primary beam intensity and the enhanced neutron detection capabities offered by the coupling of the large-area fast neutron arrays NeuLAND[3] and NEBULA[4].

The principal goal of the NP1512–SAMURAI36 experiment was to investigate the level structure of ^{22}C and, in particular, locate the first 2^+ state. In parallel, an attempt was made to extend our recent observation of ^{20}B to search for ^{21}B. The nuclei in question are located in a region of considerable interest in terms of the evolution of shell-structure far from stability. Specifically, they lie at the N=16 sub-shell closure below doubly-magic ^{24}O. In terms of the evolution of the single-particle orbits, the O isotopes exhibit magicity at N=14 and 16. When protons are removed, the N=14 gap is predicted to disappear and the neutron $s_{1/2}$ and $d_{5/2}$ single-particle orbitals become degenerate[5]. Such behaviour is expected to be at the origin of the formation of the *s*-wave halo neutron configuration in ^{22}C[6], rather than the naive shell model *d*-wave valence neutron occupation. Moreover, spectroscopy of ^{21}C, performed within the context of SAMURAI04, indicates that the physical $5/2^+$ and $1/2^+$ levels are inverted[1].

The measurements were accomplished using the SAMURAI facility[7], which comprised the superconducting 7 Tm spectrometer coupled to the neutron array NEBULA, which was complemented by elements of NeuLAND (four so-called "double-planes" each composed of two crossed layers of 250 cm long 5×5 cm^2 scintillator modules). In addition, the newly completed CATANA CsI(Na) γ-ray multi-detector[8] was mounted around the secondary target position. The setup was identical to that employed in the SAMURAI27 experiment[9] which was run in tandem with the present measurements. It is worthwhile noting that this experiment represented the beam commissioning of CATANA and the on-line analysis of well-know γ-rays, such as the 1.6 MeV line arising from the decay of the ^{18}C 2^+_1 state, indicated that the detector and electronics performed as expected.

Primary beam intensities as high as some 800 pnA were provided and allowed secondary beam rates of up to ∼700 pps of ^{23}N (over an order of magnitude higher than available during SAMURAI04) at ∼270 MeV/nucleon to be delivered by the RIBF. Single and two-proton removal reactions on the 2 g/cm^2 secondary carbon target will be analysed in order to establish the level structure of ^{22}C and search for ^{21}B. As ^{22}C was also present in the secondary beam (∼35 pps), efforts will be also made to investigate the population of the excited states via inelastic scattering. In the case of both the ^{22}C exited states and ^{21}B, beam velocity "core" fragments (^{20}C and ^{19}B) plus two-neutron events will be employed to reconstruct the corresponding invariant mass spectra from the measured momenta.

References

1) S. Leblond, PhD Thesis, Université de Caen (2015); https://tel.achives-ouvertes.fr/tel-01289381.
2) F.Miguel Marqués *et al.*: JPS Conf. Proc. **6**, 020002 (2015).
3) http://www.fair-center.de/fileadmin/fair/experiments/NUSTAR/Pdf/TDRs/NeuLAND-TDR-Web.pdf
4) T. Nakamura, Y. Kondo: Nucl. Instr. Meth. **B376** 1 (2015).
5) M. Stanoiu *et al.*: Phys. Rev. **C78**, 034315 (2010).
6) Y. Togano *et al.*: Phys. Lett. **B761** 412 (2016).
7) T. Kobayashi *et al.*: Nucl. Instr. Meth. **B317**, 294 (2013).
8) Y. Togano *et al.*: RIKEN Accel. Prog. Rep. **48**, 207 (2015).
9) T. Tomai *et al.*: in this report.

Measurement of the neutron-decay lifetime of the ^{26}O ground state at the SAMURAI setup at RIBF

C. Caesar,[*1,*2] J. Kahlbow,[*3,*2] V. Panin,[*2] D. S. Ahn,[*2] L. Atar,[*3,*2] T. Aumann,[*3] H. Baba,[*2] K. Boretzky,[*1,*2] H. Chae,[*4] N. Chiga,[*2] S. Choi,[*4] M. L. Cortes Sua,[*2] D. Cortina-Gil,[*5] Q. Deshayes,[*6] P. Doornenbal,[*2] Z. Elekes,[*2,*7] N. Fukuda,[*2] I. Gašparić,[*8,*2] K. I. Hahn,[*9] Z. Halász,[*7] A. Hirayama,[*11] J. Hwang,[*4] N. Inabe,[*2] T. Isobe,[*2] S. Kim,[*4] T. Kobayashi,[*10,*2] D. Körper,[*1] Y. Kondo,[*11,*2] Y. Kubota,[*2] I. Kuti,[*7] C. Lehr,[*3,*2] S. Lindberg,[*12,*2] M. Marques,[*6] M. Matsumoto,[*11] T. Murakami,[*13,*2] I. Murray,[*2] T. Nakamura,[*11,*2] T. Nilsson,[*12] H. Otsu,[*2] S. Paschalis,[*14] M. Parlog,[*6] M. Petri,[*14] D. Rossi,[*3] A. Saito,[*11] M. Sasano,[*2] H. Scheit,[*3] P. Schrock,[*15] Y. Shimizu,[*2] H. Simon,[*1] D. Sohler,[*7] S. Storck,[*3,*2] L. Stuhl,[*15] H. Suzuki,[*2] I. Syndikus,[*3] H. Takeda,[*2] H. Törnqvist,[*3,*2] T. Togano,[*11,*2] T. Tomai,[*11] T. Uesaka,[*2] H. Yamada,[*11] Z. Yang,[*2] M. Yasuda,[*11] K. I. Yoneda,[*2] for the SAMURAI20 Collaboration

In December 2016, the NP1306-SAMURAI20 experiment was conducted. A new technique to measure lifetimes of possible neutron-radioactive nuclei[1] was applied for the first time to study ^{26}O. The technique is based on the production of the neutron-unbound nucleus of interest in a target with large Z and high density that slows down the produced nucleus and the residual nucleus after (multi-) neutron emission. The spectrum of the velocity difference between neutron(s) and the residual nucleus has a characteristic shape that allows to extract the lifetime.

The experiment was carried out at the SAMURAI[2] setup with an invariant-mass configuration together with an experiment specific target region. Secondary beams of ^{27}F and ^{26}F were produced in BigRIPS by projectile fragmentation of a ^{48}Ca primary beam at 345 MeV/nucleon on a 20 mm thick beryllium production target. The combination of the incoming energy of the secondary beam and the reaction-target thickness is crucial for the sensitivity to a specific lifetime region. For this reason, the beam energy was reduced with degraders. At the first (second) momentum dispersive focal plane F1 (F5) of BigRIPS, a 15 mm (10 mm) thick aluminum wedge was installed. In addition, a ^{24}O beam with a very narrow energy spread has been used for calibration purposes to emulate the fragments of interest in the analysis.

At the SAMURAI setup, incoming beam particles were identified by two 1 mm thick plastic scintillators (SBTs), two drift chambers (BDC1 and BDC2), and one ionization chamber (ICB). In addition, one silicon pin diode was mounted in front of the target stack and two behind it for energy loss measurements.

Unbound ^{26}O was produced by proton removal from the ^{27}F beam in a target stack consisting of 6 foils separated by 0.8 mm, with decreasing thickness in the beam direction. The foils of thickness 2.04 mm, 1.59 mm, 1.35 mm, and 1.06 mm were made of tungsten. The two foils of lower thickness were platinum foils of thickness 0.77 mm and 0.61 mm. The total area density of the target amounted to 14.6 g/cm^2. The heavy target material causes a broad neutron-fragment velocity-difference distribution for prompt decays, due to the large energy loss of the fragments. In contrast, a sharp peak will be observed for out-of target decays, which allows to distinguish between these two types of events.

The decay products ^{24}O and the two neutrons were separated by the SAMURAI dipole magnet. Multi-wire drift chambers (FDC1 and FDC2) in front of the magnet and behind it and the plastic scintillator hodoscope (HODF24) were used for the detection and tracking of charged fragments. For neutron detection, the NeuLAND demonstrator in conjunction with NEBULA was used. The energy loss measurements in the silicon pin diodes can be used to select events with Z=9 (8) directly in front (behind) the target to exclude possible background contributions. The remaining 'background' was estimated in a 'null' measurement. For this purpose, the one-neutron decay of ^{25}O produced by proton removal from ^{26}F as a reference was measured. The ground state resonance of ^{25}O has a width of around 88 keV[3] corresponding to an extremely short lifetime. The analysis of the SAMURAI20 data is currently in progress.

*1 GSI Helmholtzzentrum für Schwerionenforschung, Darmstadt
*2 RIKEN Nishina Center
*3 Institut für Kernphysik, TU Darmstadt
*4 Department of Physics, Seoul National University
*5 Departamento de Fìsica de Partìculas, Universidade de Santiago de Compostela
*6 LPC, Caen
*7 ATOMKI, Debrecen
*8 Ruđer Bošković Institute, Zagreb
*9 Department of Physics, Ewha Womens University
*10 Department of Physics, Tohoku University
*11 Department of Physics, Tokyo Institute of Technology
*12 Department of Physics, Chalmers University of Technology
*13 Department of Physics, Kyoto University
*14 Department of Physics, University of York
*15 Center for Nuclear Studies (CNS), University of Tokyo

References

1) J. Kahlbow *et al.*, Nucl. Instrum. Methods, (DOI:10.1016/j.nima.2017.06.002).
2) T. Kobayashi *et al.*, Nucl. Instrum. Methods Phys. Res., Sect. B **317**, 294 (2013).
3) Y. Kondo *et al.*, Phys. Rev. Lett. **116**, 102503 (2016).

Search for unbound excited states of deformed halo nucleus ^{31}Ne using breakup reactions

T. Tomai,[*1,*2] T. Nakamura,[*1,*2] Y. Togano,[*1,*2] Y. Kondo,[*1,*2] S. Takeuchi,[*1,*2] N. Kobayashi,[*3] A. Hirayama,[*1,*2] M. Matsumoto,[*1,*2] T. Ozaki,[*1,*2] A. T. Saito,[*1,*2] H. Yamada,[*1,*2] M. Yasuda,[*1,*2] for SAMURAI27 collaboration

The neutron-rich odd nucleus ^{31}Ne, which is located in the "island of inversion," has drawn much attention owing to its halo properties. Because this nucleus has been found to have a p-wave $1n$ halo structure, it is likely to be strongly deformed.[1] So far its deformation properties have not been experimentally studied with direct methods. No excited states in ^{31}Ne, which are expected to be located in the unbound region because of its small separation energy ($S_n = 0.15^{+0.16}_{-0.10}$ MeV),[1] have been studied. This experiment thus aims at studying the excited states which should reflect the rotational band caused by the deformation. In the present study, we applied the invariant mass method to study the unbound states of ^{31}Ne in the inelastic scattering reaction C(^{31}Ne, ^{30}Ne$+n$) and one neutron removal reaction C(^{32}Ne, ^{30}Ne$+n$) to produce such excited states. In addition, we performed the Coulomb breakup reaction Pb(^{31}Ne, ^{30}Ne$+n$) to obtain further properties of the ground state.

In November 2016, we performed the SAMURAI27 experiment. A ^{48}Ca primary beam with a high intensity of approximately 400 particle nA was directed to a Be target. Secondary beams of ^{31}Ne and ^{32}Ne were produced and separated by BigRIPS. In this experiment, we used two different settings of the BigRIPS for ^{31}Ne and ^{32}Ne. The BigRIPS is settings are listed shown in Table 1.

Particle identification (PID) of the secondary beam was performed by the ΔE-TOF-$B\rho$ method. The energy loss ΔE was determined using an ionization chamber at F13 (ICB). The time of flight TOF was measured using a 3-mm-thick plastic scintillator at F7 and two 0.5-mm-thick plastic scintillators at F13 (SBT). The magnetic rigidity $B\rho$ was calculated from the horizontal position of 3-mm-thick plastic scintillator at F5. Figure 1 shows a resulting PID plot for the ^{31}Ne beam. The intensity and the purity of the beams are summarized is shown in Table 1.

The secondary beam was transported to the SAMURAI experimental area and impinged on secondary targets at a bombarding energy of 230 MeV/nucleon. We used a 2.15-g/cm^2-thick C target for the ^{31}Ne and ^{32}Ne beams, and a 2.76-g/cm^2-thick Pb target for the ^{31}Ne beam. Charged particles and neutrons generated by the breakup reactions were analyzed by the SAMURAI spectrometer.[2] The charged particles were detected by the standard drift chambers of SAMURAI (FDC1 and FDC2) and hodoscope (HODF24). Outgoing neutrons were detected by NeuLAND[3] and NEBULA, which provide a high neutron efficiency of about 50%. Additionally, CATANA,[4] a new γ-ray detector array, was placed around the secondary target. The data analysis is in progress.

Table 1. BigRIPS settings for the ^{31}Ne and ^{31}Ne beams and the resultant intensity and purity.

	^{31}Ne	^{32}Ne
Primary Be target (mm)	15	15
F1 slit (mm)	±120	±100
F1 Al wedge (mm)	8	10
F5 slit (mm)	±110	±50
F5 Al wedge (mm)	8	8
Total intensity (cps)	∼ 1500	∼ 100
Purity (%)	3	20

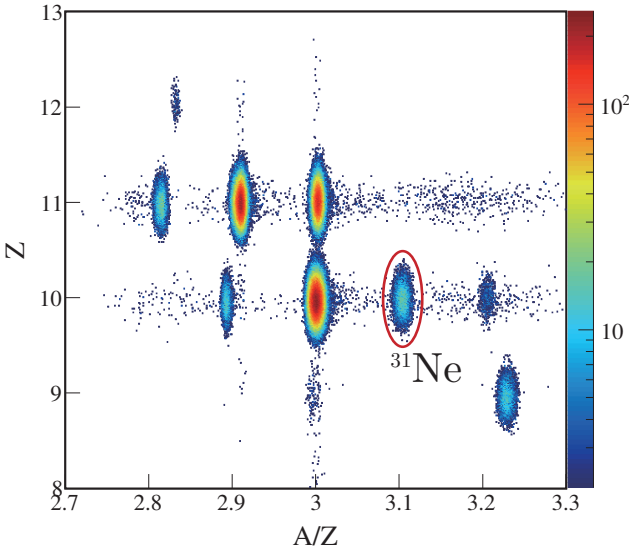

Fig. 1. PID plot for the ^{31}Ne beam setting. The horizontal axis is mass-to-charge ratio A/Z and the vertical axis is atomic number Z.

*1 Department of Physics, Tokyo Institute of Technology
*2 RIKEN Nishina Center
*3 RCNP, Osaka University

References
1) T. Nakamura et al., Phys. Rev. Lett. **112**, 142501 (2014).
2) T. Kobayashi et al., Nucl. Instrum. Methods Phys. Res. B **317**, 294 (2013).
3) http://www.fair-center.de/fileadmin/fair/experiments/NUSTAR/Pdf/TDRs/NeuLAND-TDR-Web.pdf.
4) Y. Togano et al., RIKEN Accel. Prog. Rep. **48**, 207 (2015).

Progress report of Gamow–Teller giant resonance studies at RIBF

M. Sasano,[*1] J. Yasuda,[*2] L. Stuhl,[*1,6] R.G.T. Zegers,[*3] H. Baba,[*1] W. Chao,[*1] M. Dozono,[*1] N. Fukuda,[*1] N. Inabe,[*1] T. Isobe,[*1] G. Jhang,[*1,13] D. Kamaeda,[*1] T. Kubo,[*1] M. Kurata-Nishimura,[*1] E. Milman,[*1] T. Motobayashi,[*1] H. Otsu,[*1] V. Panin, [*1] W. Powell, [*1] M. Sako, [*1] H. Sato,[*1] Y. Shimizu,[*1] H. Suzuki,[*1] T. Suwat, [*1] H. Takeda,[*1] T. Uesaka,[*1] K. Yoneda,[*1] J. Zenihiro,[*1] T. Kobayashi,[*1,4] T. Sumikama,[*1,4] T. Tako,[*4] T. Nakamura,[*5] Y. Kondo,[*5] Y. Togano,[*5] M. Shikata,[*5] J. Tsubota,[*5] K. Yako,[*6] S. Shimoura,[*6] S. Ota,[*6] S. Kawase,[*6] Y. Kubota,[*6] M. Takaki,[*6] S. Michimasa,[*6] K. Kisamori,[*6] C.S. Lee,[*6] H. Tokieda,[*6] M. Kobayashi,[*6] S. Koyama,[*7] N. Kobayashi, [*7] H. Sakai,[*1] T. Wakasa,[*2] S. Sakaguchi,[*2] A. Krasznahorkay,[*8] T. Murakami, [*9] N. Nakatsuka, [*9] M. Kaneko, [*9] Y. Matsuda, [*10] D. Mucher, [*11] S. Reichert, [*11] D. Bazin,[*3] and J.W. Lee[*12]

Among the collective modes[1], the Gamow–Teller (GT) giant resonance is an interesting excitation mode. It is a $0\hbar\omega$ excitation characterized by the quantum-number changes in orbital angular momentum ($\Delta L = 0$), spin ($\Delta S = 1$), and isospin ($\Delta T = 1$), and it is induced by the transition operator $\sigma\tau$. In the stable nuclei in medium or heavier mass regions ($A > 50$), the collectivity in this mode exhibits the GT giant resonance (GTGR), which provides information that is critically important for understanding the isovector part of the effective nucleon-nucleon interaction[2] and the symmetry potential of the equation of state[3].

We have been rapidly expanding the domain of GTGR studies at RIBF in the nuclear chart, since our development of a new method to study GT transitions on unstable nuclei via the charge-exchange (CE) (p, n) reaction with RI beams[4,5]. An experiment at RIBF was performed in March 2014 to extract the GT and spin-dipole (SD) transition strengths over a wide excitation energy range covering their giant resonances on the key doubly magic nucleus ^{132}Sn[6]. This is an essential step toward establishing comprehensive theoretical models for nuclei located between ^{78}Ni and ^{208}Pb. The data analysis of this experiment has been finalized and we are preparing a draft for publication. In 2016, the experimental program for ^{48}Cr and ^{64}Ge was reevaluated and approved by the NP-PAC meeting. A study on these nuclei will provide a unique opportunity to elucidate the role of isoscalar pairing in nuclei along the N=Z line.

From an experimental point of view, we employ a low-energy neutron detection system, WINDS[7], to detect recoil neutrons produced via the (p, n) reaction in inverse kinematics, in combination with a magnetic spectrometer such as SAMURAI[8]. Since last year, we have been working on the upgrade of WINDS to reduce background events in the detectors. The primary goal of the upgrade plan is to eliminate background events due to gamma rays arising from the environment by the so-called neutron-gamma discrimination method. Such gamma rays are considered not to be synchronized with the reaction timing, and therefore they have a flat distribution in time. The contribution of such gamma rays is enhanced in the region of forward scattering angles in the center-of-mass system, because a wide TOF range having background events uniformly distributed in time is compressed to a narrow phase space in that region. The method is being tested using a prototype low-energy neutron detector made from a novel plastic scintillator material for application of the neutron-gamma method. Details of the test are also given in Ref.[9].

*1 RIKEN Nishina Center
*2 Department of Physics,Kyushu University
*3 NSCL, Michigan State University
*4 Department of Physics, Tohoku University
*5 Department of Physics, Tokyo Institute of Technology
*6 CNS, University of Tokyo
*7 Department of Physics, University of Tokyo
*8 MTA, Atomki
*9 Department of Physics, Kyoto University
*10 Department of Physics, Konan University
*11 Department of Physics, Technical University Munich
*12 Department of Physics, Korea University

References

1) M. N. Harakeh and A. M. van der Woude: Giant Resonances (Oxford University Press, Oxford, 2001).
2) S. Fracasso and G. Colo, Phys. Rev. C**72**, 064310 (2005).
3) P. Danielewicz, Nucl. Phys. A **727**, 233 (2003).
4) M. Sasano et al., Phys. Rev. Lett. **107**, 202501 (2011).
5) M. Sasano et al., Phys. Rev. C **86**, 034324 (2012).
6) J. Yasuda et al., in this report.
7) K. Yako et al., RIKEN Accel. Prog. Rep. **45** (2012).
8) T. Kobayashi et al., Nucl. Inst. Meth. B **317**, 294-304 (2013).
9) L. Stuhl et al., in this report.

(γ,n) and (γ,2n) cross sections in Coulomb breakup reactions of ^{79}Se,^{80}Se at 200 MeV/nucleon

A. Hirayama,[*1,*2] S. Takeuchi,[*1*2] T. Nakamura,[*1*2] Y. Kondo,[*1*2] Y. Togano,[*1*2] M. Shikata,[*1*2] J. Tsubota,[*1*2] T. Ozaki,[*1*2] A. T. Saito,[*1*2] T. Tomai,[*1*2] H. Wang,[*2] H. Otsu,[*2] H. Sakurai,[*2] S. Kawase,[*3] N. Watanabe,[*3] and the ImPACT collaboration

High-level radioactive wast, generated at nuclear power plants contain long lived fission products (LLFPs). Dumping LLFPs is still difficult because of their long lifetime. One way to reduce or reuse the LLFPs is the transmutation of the LLFPs into a short-lived or stable nucleus using nuclear reactions. For this transmutation, basic nuclear reaction data on LLFPs are important. Therefore, we performed nuclear reaction experiments using the LLFPs produced as secondary beams. In this report, we focus on the (γ,n) and (n,γ) reactions for the LLFPs and ^{79,80}Se. The ^{79}Se nucleus is an LLFP with a lifetime of 0.3M years. The (n,γ) reaction of LLFPs is important for transmutation ; however, experiments on the (n,γ) reaction have several difficulties. Therefore, we have measured the (γ,n) reaction as an alternative way to deduce the (n,γ) reaction cross section by introducing the Coulomb breakup reactions of ^{79,80}Se in inverse kinematics.

The experiment was performed using the SAMURAI spectrometer[1)] at the RIKEN Nishina Center. Secondary beams of ^{79,80}Se with an energy of 200 MeV/nucleon were produced by the in-flight fission of a ^{238}U primary beam with 345 MeV/nucleon on a ^{9}Be production target. Particle identification of the secondary beams was performed using BigRIPS. The momentum slit at the F1 focus was set to 0.1%, and the ΔE-TOF method using F7 and F13 plastic scintillators and the ionization chamber (ICB) at F13 was enough to identify secondary beams without Brho reconstruction. Figure 1 shows the particle identification of the secondary beams for the ^{79}Se setting. The secondary beam intensities are 2,700 and 2,500 cps at F13, beam energies were 216 and 218 MeV/nucleon, and beam purities were 54 % and 49 % for ^{79}Se and ^{80}Se, respectively. Beam directions and positions were measured by BDC (MWDC), which was placed upstream of the secondary target. Secondary targets of Pb and C with thickness of 0.54 g/cm^2 and 0.26 g/cm^2, respectively, were placed at the F13 focus and surrounded by DALI2 to detect de-excitation γ rays for reaction identification. Neutrons decaying from the excited states were detected by NeuLAND[2)] and NEBULA.[3)] Charged fragments produced in the breakup reactions were analyzed by the SAMURAI spectrometer. FDC1 (MWDC) was placed at the entrance of the SAMURAI magnet to measure the scattering angle of charged particles. At the exit of the magnet, FDC2 (MWDC) was installed to measure the bending angles and trajectories of the charged fragments. A plastic hodoscope was placed behind the FDC2 to measure ΔE and timing information. The hodoscope consists of seven slats of plastic scintillators with a thicknesses of 5 mm.

An analysis for charged particles is now ongoing. Identification of the atomic number was performed using the plastic hodoscope. By correcting the x- and y-position dependence of the light output in the scintillator, 4σ separation for atomic number has been achieved. To obtain mass-to-charge ratio, magnetic rigidities will be deduced by tracking information from the FDC1 and FDC2. Further analysis is in progress to deduce the inclusive and exclusive cross sections of the Coulomb breakup reactions.

This research was funded by ImPACT Program of Council for Science, Technology and Innovation (Cabinet Office, Government of Japan).

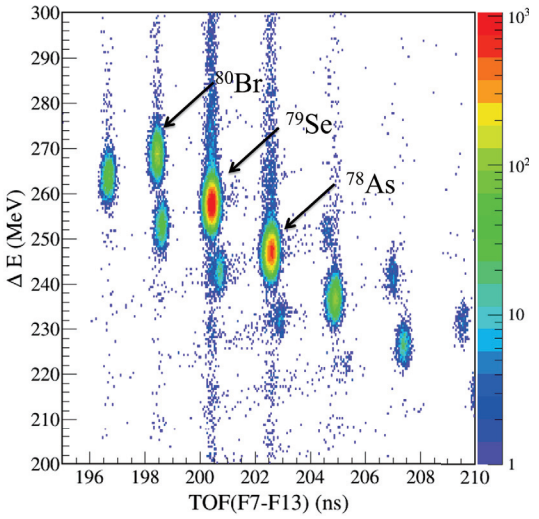

Fig. 1. Particle idetification of the secondary beam (for the ^{79}Se setup)

*1 Department of Physics, Tokyo Institute of Technology
*2 RIKEN Nishina Center
*3 Faculty of Engineering and Science, Kyushu University

References

1) T. Kobayashi et al. , Nucl. Instrum. Methods Phys. Res. Sect. B317, 294 (2013).
2) https://www.gsi.de/work/fairgsi/rareisotopebeams/r3b/neuland.htm
3) T. Nakamura et al. , Nucl. Instrum. Methods Phys. Res. Sect. B376, 156 (2016)

Measurement of Pion Multiplicities in Asymmetric Sn Reactions Using the SπRIT Time Projection Chamber

J. Barney,[*1,*2] G. Cerizza,[*1,*2] J. Estee,[*1,*2] B. Hong,[*3] T. Isobe,[*2] G. Jhang,[*3,*2] M. Kaneko,[*2,*4] M. Kurata-Nishimura,[*2] P. Lasko,[*5,*6,*2] H. S. Lee,[*7] J. W. Lee,[*3,*2] J. Łukasik,[*5] W.G. Lynch,[*1] A.B. McIntosh,[*8] T. Murakami,[*4,*2] P. Pawłowski,[*5,*2] K. Pelczar,[*6] H. Sakurai,[*2] C. Santamaria,[*1,*2] R. Shane,[*1] D. Suzuki,[*2] M. B. Tsang,[*1] S.J. Yennello,[*8] Z.G. Xiao,[*9,*2] Y. Zhang,[*9,*2] and the SπRIT and NeuLAND collaborations

Determination of the nuclear Equation of State (EOS) is of fundamental importance in nuclear physics. To constrain the symmetry energy term of the EOS at supra-saturation density, a series of measurements were proposed with neutron rich and neutron deficient Sn isotopes at about 300 MeV/U. Experimental observables include pion production, n vs. p emission and differential flow, and t and ^{3}He emission. An international collaboration initially started and funded by the groups from Michigan State University, Kyoto University, and RIKEN, which was later joined by collaborators from Korea, Poland, and China, completed the construction of the SπRIT Time Projection Chamber (TPC)[1], designed to measure pions as well as light charge particles emitted in heavy ion collisions.

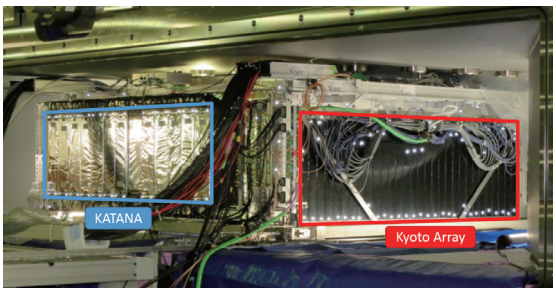

Fig. 1. The SπRIT TPC inside the SAMURAI magnet with ancillary detectors outlined.

Figure 1 shows the experimental set up, including some ancillary devices. The Kyoto Array, consisting of two arrays of 30 scintillators each, are positioned on the beam left and beam right sides of the TPC, while the Krakow Array for Triggering with Amplitude discrimiNAtion (KATANA)[2], consisting of 12 thick scintillators and three veto paddles, is positioned on the downstream side. Three KATANA beam veto scintillator paddles are used to reject unreacted beam particles. A veto collimator with 2x2 scintillators (not shown) is positioned 22 cm upstream of the target to reject beam particles which do not hit the target. The trigger condition requires a multiplicity of 4 or greater in the Kyoto Array, enhancing central collision events. The NeuLAND neutron detection system (not shown) is used to measure neutrons emitted in the reactions.

The 2016 run of the SπRIT TPC is shown in Tab. 1. A commissioning run was performed in April 2016 with the TPC inside the SAMURAI spectrometer at the 0° configuration, set to 0.5 T. A ^{132}Sn secondary beam was impinged on a 0.5 mm thick natural Sn target. The dedicated commissioning run inside the SAMURAI magnet allowed particle identification with the complete version of the SπRITROOT analysis framework. The first experiment consisted of neutron deficient ^{108}Sn and stable ^{112}Sn secondary beams impinging on 0.836 mm thick ^{112}Sn and 0.828 mm thick ^{124}Sn targets, respectively. The second experiment consisted of neutron rich ^{132}Sn and stable ^{124}Sn secondary beams impinging on 0.828 mm thick ^{124}Sn and 0.836 mm thick ^{112}Sn targets, respectively. Additionally, a cocktail beam of charge $Z = 1-3$ was produced at 100 and 300 MeV/U, providing reference points to calibrate the energy loss measurements with the TPC.

Table 1. Spring Campaign with the SπRIT TPC

Beam	Reaction Target	Triggered Events
^{132}Sn	^{nat}Sn	$\sim 2.0 \times 10^6$
^{108}Sn	^{112}Sn	$\sim 1.0 \times 10^7$
^{112}Sn	^{124}Sn	$\sim 5.9 \times 10^6$
^{124}Sn	^{112}Sn	$\sim 5.3 \times 10^6$
^{132}Sn	^{124}Sn	$\sim 1.0 \times 10^7$
Z=1-3 cocktail	No Target	$\sim 6.8 \times 10^5$

Over 250 TB of data were collected in the 2016 experimental campaign, and analysis of this data is ongoing. The experiment represents a new measurement to constrain the symmetry energy term of the EOS.

This work is supported by the U.S. DOE under Grant Nos. DE-SC0004835, DE-SC0014530, DE-NA0002923, US NSF Grant No. PHY-1565546, the Japanese MEXT KAKENHI grant No. 24105004 and by the Polish National Science Center (NCN), under contract Nos. UMO-2013/09/B/ST2/04064 and UMO-2013/10/M/ST2/00624.

*1 NSCL and Dept. of Phys. & Ast., Michigan State University
*2 RIKEN Nishina Center
*3 Department of Physics, Korea University
*4 Department of Physics, Kyoto University
*5 IFJ PAN, Kraków
*6 Jagiellonian University, Kraków
*7 Rare Isotope Science Project, Institute for Basic Science
*8 Cyclotron Institute, Texas A&M University
*9 Department of Physics, Tsinghua University

References

1) R. Shane et al., Nucl. Instr. Meth. A **784**, 513 (2015).
2) P. Lasko et al., arXiv:1610.06682 (2016).

Search for PYGMY states in ^{70}Ni†

R. Avigo,[*1,*2] O. Wieland,[*1] A. Bracco,[*1,*2] F. Camera,[*1,*2] H. Baba,[*3] N. Nakatsuka,[*3,*4] P. Doornenbal,[*3] Y. Togano,[*3] J. Tscheuschner,[*6] T. Aumann,[*6] G. Benzoni,[*1] N. Blasi,[*1] K. Boretzky,[*7] S. Brambilla,[*1] S. Ceruti,[*1,*2] S. Chen,[*8] F.C.L. Crespi,[*1,*2] N. Fukuda,[*3] A. Giaz,[*1,*2] K. Ieki,[*9] N. Kobayashi,[*10] Y. Kondo,[*3] S. Koyama,[*10] T. Kubo,[*3] S. Leoni,[*1,*2] M. Matsushita,[*11] B. Million,[*1] A.I. Morales,[*1,*2] T. Motobayashi,[*3] T. Nakamura,[*3] M. Nishimura,[*3] H. Otsu,[*3] T. Ozaki,[*3] L. Pellegri,[*1,*2,*5] A. T. Saito,[*3] H. Sakurai,[*3] H. Scheit,[*6] P. Schrock,[*6] Y. Shiga,[*3] M. Shikata,[*3] D. Steppenbeck,[*3] T. Sumikama,[*3,*12] S. Takeuchi,[*3] R. Taniuchi,[*10] J. Tsubota,[*3] H. Wang,[*3] and K. Yoneda[*3]

The search for E1 strength in neutron-rich ^{68}Ni, located around the one particle separation energy was the object of a large effort[1,2] (and references therein). Concentration of the E1 strength were measured in a variety of nuclei along the entire valley of stability, but very few data for exotic nuclei are available. Commonly they are called pygmy dipole resonance (PDR) as they lie at energies below the giant dipole resonance (GDR) and have lesser strength. As their strength is related to the excess of neutrons the strength may be connected to the neutron skin thickness[3], the symmetry energy term of the nuclear equation of state. They influence significantly the scenario within explosive nucleosynthesis.

In order to understand better the characteristics of this PDR strength it is important to study an isotopic chain of a nucleus with increasing neutron number an experiment with high intensity beam and high efficiency and resolution on ^{70}Ni at RIKEN Radioactive Isotope Beam Factory (RIBF) was performed and analyzed. A primary beam of ^{238}U was accelerated up to 345 *A*MeV and made to impinge on a 1 g/cm^2 thick Be production target. In BigRIPS[4] the Bρ-ΔE-Bρ method was applied in order to select a secondary beam of ^{70}Ni (30 kcps with 40% purity at a beam energy of 260 *A*MeV). The ^{70}Ni isotope was incident on a 2 g/cm^2 thick gold secondary reaction target. Reaction products from this target were identified using the ZeroDegree Spectrometer in the large acceptance mode, while the scattering angles were determined using parallel plate avalanche counters. In this way pure relativistic coulomb excitation[1] events could be selected. The reaction target was surrounded by a combination of eight large-volume 3.5'' x 8'' LaBr3:Ce detectors[5] mounted at 30° in the forward direction and of the DALI2 array[6] (consisting of 96 NaI(TI) crystals) at different angles in a way to detect the emitted γ rays from the reaction.

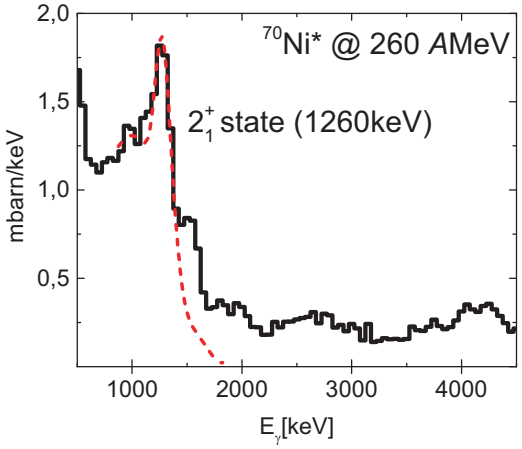

Fig. 1. Gamma-ray spectrum for the strength of the $2^+ \rightarrow 0^+_{gs}$ E2 transition cross section in ^{70}Ni together with Geant Monte Carlo simulation of the transition.

In order to determine the B(E1) values distribution in ^{70}Ni an absolute efficiency measurement of the detectors at NewSUBARU was done in 2016. Together with the measured gamma ray spectrum we determined the B(E2) strength as can be seen in Figure 1. The spectrum shows the target contribution subtracted $2^+ \rightarrow 0^+_{gs}$ transition corrected for detector response and virtual photon flux[1]. In order to extrapolate the target contribution to the spectra a statistical model simulation for the target was compared with a measurement with ^{24}O beam (no bound states are present) and the original gold-target under the same experimental conditions. This reaction gives practically only gamma emission from the target deexcitation. A good agreement has been obtained which will help for future analysis of the B(E2) strength. The future analysis of the E1 strength in the experiment will give a relation between the strength and the neutron skin in ^{70}Ni. Together with the data of the measured ^{68}Ni this will provide an important contribution to the understanding of the features of E1 strength around the particle separation energy.

† Experiment NP1306 -RIBF51R1, November 2014

*1 INFN sezione di Milano
*2 Dipartimento di fisica, Università degli studi of Milano
*3 RIKEN Nishina Center
*4 Department of Physics, University of Kyoto
*5 iThemba LABS
*6 Institut fuer Kernphysik, TU Darmstadt
*7 GSI Helmholtzzentrum Darmstadt
*8 School of Physics and State Key Laboratory, Peking University
*9 Department of Physics, Rikkyo University
*10 Department of Physics, University of Tokyo
*11 Center for Nuclear Study, University of Tokyo
*12 Department of Physics, Tohoku University

References

1) O. Wieland et al. PRL **102,** 092502 (2009).
2) D. Rossi et al. PRL **111**, 242503 (2013).
3) A. Carbone et al. Phys. Rev. C **81,** 041301(R) (2010).
4) T. Kubo et al. Prog. Theor. Exp. Phys. 03C003 (2012).
5) A. Giaz et al. NIM A**729,** 910 (2013).
6) S. Takeuchi et al. NIM A**763**, 596 (2014).

Structure of Borromean nuclei around N=16 and 20 shells

R. Kanungo,[*1] S. Bagchi,[*1,*2,*3] Y. Tanaka,[*2,*3] H. Geissel,[*2,*3] D. Ahn,[*4] H. Baba,[*4] K. Behr,[*2] F. Browne,[*5] S. Chen,[*5] M. L. Cortés,[*5] P. Doornenbal,[*5] A. Estrade,[*4,*6] N. Fukuda,[*4] E. Haettner,[*2], M. Holl,[*1,*7] K. Itahashi,[*8] N. Iwasa,[*4,*9] S. Kaur,[*1,*10], S. Matsumoto,[*11] S. Momiyama,[*12] I. Murray,[*5,*13] T. Nakamura,[*14] H.J. Ong,[*15] S. Paschalis,[*16] A. Prochazka,[*2] C. Scheidenberger,[*2,*3] P. Schrock,[*17] Y. Shimizu,[*4] D. Steppenbeck,[*4,*17] D. Suzuki,[*5] H. Suzuki,[*4] S. Takeuchi,[*14] M. Takechi,[*18] H. Takeda,[*4] R. Taniuchi,[*12] K. Wimmer,[*12] and K. Yoshida[*4]

Nuclei near the neutron drip line provide the opportunity to investigate unusual properties that depend on isospin. The emergence of nuclear halos[1),2)] and changes of nuclear shell structure[3)-6)] are some of the dramatic unexpected effects resulting from the large neutron/proton asymmetry. Nuclear halos arise from the one- or two-outermost neutrons forming a low-density extended neutron surface. Identifying and characterizing the neutron halos require knowledge of their matter and proton radii. Information on occupancy of nuclear orbitals sheds light on the evolution of nuclear shells. Two-neutron halos in Borromean nuclei have been identified in the *p-sd* shell in ^{6}He, ^{11}Li, ^{14}Be, ^{17,19}B and ^{22}C but its occurrence in the conventional *pf*-shell is still unknown. The breakdown of the N=20 shell closure has been observed in Mg-Ne isotopes, and one-neutron halo formation was found in ^{31}Ne.[7)]

In a recent experiment performed at the BigRIPS[8)] and ZeroDegree Spectrometer (ZDS) facilities at the RIKEN RI Beam Factory we aimed to investigate the structure of the Borromean N=20 drip line nucleus, ^{29}F. ^{29}F nuclei were produced via the fragmentation of a ^{48}Ca primary beam with a Be production target. The BigRIPS fragment separator and particle detectors were used to separate ^{29}F from the contaminants. The energy loss in the ionization chamber placed at the F7 achromatic focus provided Z identification. Time of flight was measured with scintillator detectors placed at F3 and F7 foci. Position sensitive PPAC detectors were used to determine the magnetic rigidity. This information led to an event by event identification of ^{29}F as shown in Fig. 1. A carbon reaction target placed at the F8 focus was surrounded by the DALI2 gamma detector array.[9)] Gamma rays from the de-excitation of the two-neutron removal fragment were detected in coincidence with ^{27}F.

The ZDS was used to transport and identify the fragments or the beam at the final achromatic focus, F11. The time of flight with scintillators placed at F11 and F8 together with position information is used to determine the momentum distribution from the two-neutron removal process. At F11 a second carbon reaction target was placed for measuring the charge changing cross section using multi sampling ionization chambers[10)] placed before and after this second reaction target. The measured interaction cross section is expected provide the matter radius of ^{29}F while the charge-changing cross section will yield a measure of its proton radius. Charge-changing cross sections were measured for the drip-line C and B isotopes as well.

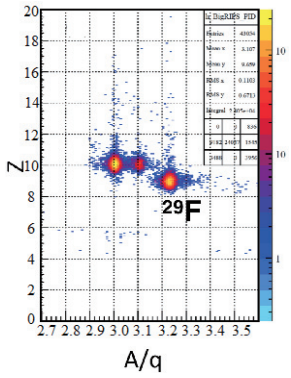

Fig. 1. Particle identification spectrum for detection of ^{29}F.

*1 Astronomy and Physics Department, Saint Mary's University
*2 GSI Helmholtz Center
*3 Physics Department, Justus-Liebig University
*4 Research Instruments Group, RIKEN
*5 Radioactive Isotope Physics Laboratory, RIKEN
*6 Central Michigan University
*7 TRIUMF
*8 Advanced Meson Science Laboratory, RIKEN
*9 Physics Department, Tohoku University
*10 Physics Department, Dalhousie University
*11 Physics Department, Kyoto University
*12 Physics Department, University of Tokyo
*13 IPN, Université Paris-Sud, Université Paris-Saclay
*14 Physics Department, Tokyo Institute of Technology
*15 Research Center for Nuclear Physics
*16 Physics Department, University of York
*17 Center for Nuclear Study
*18 Physics Department, Niigata University

References

1) I. Tanihata et al., Phys. Rev. Lett. **55**, 2676 (1985).
2) P. G. Hansen, B. Jonson, Euro. Phys. Lett. **4**, 409 (1987).
3) T. Motobayashi et al., Phys. Lett. **B 346**, 9 (1995).
4) R. Kanungo, Phys. Scr., **T152**, 014002 (2013).
5) O. Sorlin, M. –G. Porquet, Phys. Scr. **T152**, 014003 (2013).
6) D. Steppenbeck et al., Nature **502**, 207 (2013).
7) T. Nakamura et al., Phys. Rev. Lett. **103**, 262501 (2009).
8) T. Kubo et al.: Nucl. Instrm. Meth. **B 204**, 97 (2003).
9) S. Takeuchi et al., Nucl. Instrum. & Meth. **A 763**, 596 (2014).
10) A. Stolz et al., Phys. Rev. C **65**, 064603 (2002).

Study of the pygmy dipole resonance of ^{132}Sn and ^{128}Sn in inelastic α-scattering

J. Tscheuschner,[*1,*2] T. Aumann,[*1] D. S. Ahn,[*2] R. Avigo,[*3,*4] H. Baba,[*2] K. Boretzky,[*5] A. Bracco,[*3,*4] C. Caesar,[*5] A. Camera,[*3,*4] S. Chen,[*2,*6] V. Derya,[*7] P. Doornenbal,[*2] J. Endres,[*7] N. Fukuda,[*2] U. Garg,[*8] A. Giaz,[*3,*4] M. N. Harakeh,[*9] M. Heil,[*5] A. Horvat,[*1] K. Ieki,[*10] N. Imai,[*11] N. Inabe,[*2] N. Kalantar-Nayestanaki,[*9] N. Kobayashi,[*11] Y. Kondo,[*12] S. Koyama,[*11] T. Kubo,[*2] I. Martel,[*13] M. Matsushita,[*14] B. Million,[*15] T. Motobayashi,[*2] T. Nakamura,[*12] N. Nakatsuka,[*2,*16] M. Nishimura,[*2] S. Nishimura,[*2] S. Ota,[*14] H. Otsu,[*2] T. Ozaki,[*12] M. Petri,[*1] R. Reifarth,[*17] D. Rossi,[*1] A. T. Saito,[*12] H. Sakurai,[*2,*11] D. Savran,[*5] H. Scheit,[*1] F. Schindler,[*1] P. Schrock,[*1] D. Semmler,[*1] Y. Shiga,[*2,*10] M. Shikata,[*12] Y. Shimizu,[*2] H. Simon,[*5] D. Steppenbeck,[*2] H. Suzuki,[*2] T. Sumikama,[*18] D. Symochko,[*1] I. Syndikus,[*1] H. Takeda,[*2] S. Takeuchi,[*2] R. Taniuchi,[*11] Y. Togano,[*12] J. Tsubota,[*12] H. Wang,[*2] O. Wieland,[*3] K. Yoneda,[*2] J. Zenihiro,[*2] and A. Zilges[*7]

The pygmy dipole resonance in neutron-rich isotopes can be pictured as a vibration of the excess neutrons against an isospin symmetric core in the nucleus. This vibration corresponds to a dipole mode. Due to the nature of the resonance, the phenomenon should be a function of the neutron-skin thickness and also of the neutron excess. The resonance has an isoscalar and an isovector part. To distinguish between both of them experimentally one can use two different probes. The α-particle is isoscalar and will excite exclusively the isoscalar part in contrast to photon-excitation, which excites mainly the isovector part of the resonance. As the experimental data for this dipole mode is rare, even for stable nuclei[1)], interesting open questions remain. One of them is the isospin character and strength of the low-lying dipole mode. In an experiment with the stable ^{124}Sn[2)], it has been observed that a large fraction of the pygmy strength is of isoscalar character, however significant differences in the strength distribution with photo-excitation have been observed.

In October 2014, an experiment to investigate further the isoscalar character of the pygmy dipole resonance in ^{128}Sn, and ^{132}Sn was performed with inelastic α-scattering in inverse kinematics at RIKEN. The isotopes were produced with a high-intensity primary ^{238}U beam impinging with 345 MeV/u on a beryllium target. The secondary beam with approximately 220 MeV/u was transported towards the liquid-helium target, with a thickness of approximately 320 mg/cm^2. At the target position, emitted γ-rays were measured by 8 large-volume 3.5" $\times$ 8"$LaBr_3$:Ce crystals from Hector-array at INFN Milano[3)] and 95 large-volume NaI DALI2[4)] crystals. The 8 $LaBr_3$:Ce crystals were placed at an angle θ of 30° and the DALI2 crystals covered a range in θ from about 45° to about 150°. Both detector types are distributed over 360° in ϕ. The registered hits in the γ-array are selected within a coincidence time-window with the beam to suppress background stemming from the intrinsic radiation of the 8 $LaBr_3$:Ce crystals, and other random background.

The particle identification and separation was done using BigRIPS and the ZeroDegree spectrometer. Those devices are using a combination of energy loss, magnetic rigidity, and time-of-flight measurements[5)]. The purity of the secondary ^{132}Sn-beam was about 28% with about 41 million registered events.

With further investigation of the γ-spectra, the strength of the (isoscalar) pygmy dipole resonances can be determined. In addition, the obtained information will allow the isovector and isoscalar parts of the pygmy dipole resonance to be separated in comparison with data of experiments already performed at GSI Darmstadt with the R^{3}B setup, as in those experiments the isovector part is predominantly excited by relativistic coulomb excitation.

The authors acknowledge the german support by the Deutsche Forschungsgesellschaft (DFG), the grant SFB 1245.

*1 Institut für Kernphysik, TU Darmstadt
*2 RIKEN Nishina Center
*3 INFN sezione di Milano
*4 Dipartimento di Fisica, Universita degli studi di Milano
*5 GSI Helmholtzzentrum Darmstadt
*6 School of Physics, Peking University
*7 Institute für Kernphysik, Universität zu Köln
*8 Department of Physics, University of Notre Dame
*9 KVI-CART Groningen
*10 Department of Physics, Rikkyo University
*11 Department of Physics, University of Tokyo
*12 Department of Physics, Tokyo Institute of Technoloy
*13 Departamento de Fisica Aplicada, Universidad de Huelva
*14 Center for Nuclear Study, University of Tokyo
*15 VECC India
*16 Department of Physics, Kyoto University
*17 Institut für Kernphysik, Goethe Universität Frankfurt
*18 Department of Physics, Tohoku University

References

1) D. Savran et al.: Prog. Part. Nucl. Phys. **70**, p.210 (2013).
2) J. Endres et al.: Phys. Rev. Lett. **105**, 212503 (2010).
3) A. Giaz et al.: NIM A**729**, 910 (2013).
4) S. Takeuchi et al.: NIM A **763**, 596 (2014).
5) T. Kubo et al.: Prog. Theor. Exp. Phys. 03C003 (2012).

Intermediate-energy Coulomb excitation of ^{136}Te

V. Vaquero,[*1] A. Jungclaus,[*1] P. Doornenbal,[*2] K. Wimmer,[*2,*3] S. Chen,[*2,*4] E. Sahin,[*5] Y. Shiga,[*6] D. Steppenbeck,[*2] R. Taniuchi,[*2,*3] Z.Y. Xu,[*7] and the NP1306-RIBF98R1 collaboration

Based on the experience from the first intermediate-energy Coulomb excitation experiment performed at RIKEN with a heavy (A>100) ion beam, namely ^{104}Sn[1)], a similar experiment was realized in 2015 to study the nucleus ^{136}Te. The main objectives have been i) to determine a reliable value of the reduced transition probability, $B(E2)$, to the first excited 2^+ state based on the measurement of differential cross sections as a function of the scattering angle with both gold and carbon targets, ii) to search for discrete feeding transitions from higher-lying excited states and to study the influence of the feeding on the γ-ray angular correlation, and finally to search for a second 2^+ state, one with mixed-symmetry character.

A primary beam of ^{238}U at 345 MeV/u with an average intensity of 15 pnA bombarded a 4-mm thick beryllium production target located at the F0 focus of the BigRIPS fragment separator. The fission products around ^{136}Te were selected and purified by employing two wedge-shaped aluminium degraders. The secondary beam was identified event by event using the ΔE-TOF-B_ρ method, where the energy loss ΔE was measured by an ionization chamber located at the focal plane F7, B_ρ was determined from position measurements using PPACs and the TOF was measured with two plastic scintillators located at the focal points F3 and F7[2)]. After the selection and identification, the

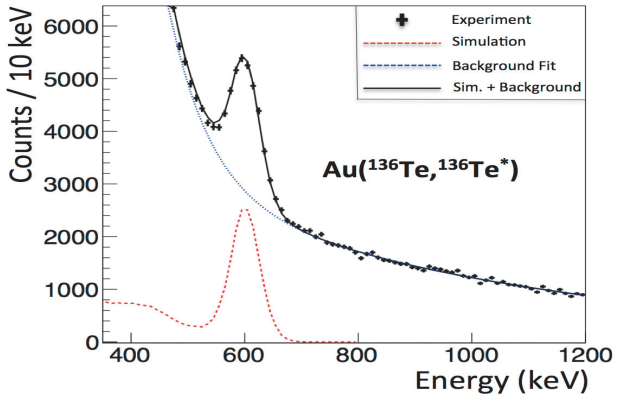

Fig. 1. Doppler-corrected γ-ray spectrum following Coulomb excitation of ^{136}Te. The observed line corresponds to the 606 keV, $2_1^+ \rightarrow 0_{gs}^+$ transition.

*1 Instituto de Estructura de la Materia, CSIC, Madrid
*2 RIKEN Nishina Center
*3 Department of Physics, University of Tokyo
*4 State Key Laboratory of Nuclear Physics and Technology, Peking University
*5 Department of Physics, University of Oslo
*6 Department of Physics, Rikkyo University
*7 Department of Physics, University of Hong Kong

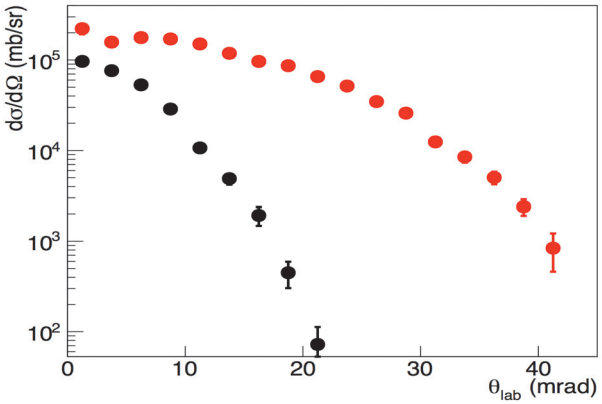

Fig. 2. The experimental differential cross sections as function of the scattering angle for inelastic excitation of the 2_1^+ state in ^{136}Te on a gold (red) and on a carbon (black) target.

secondary beams were transported to the focal point F8 where they impinged on a 950 mg/cm^2 gold target with energies around 165 MeV/u. To detect the γ radiation emitted in the decay of the excited states, the reaction target was surrounded by the DALI2 spectrometer. The reaction products left the target with energies around 110 MeV/u and were identified by the ZeroDegree spectrometer using again the previously described ΔE-TOF-B_ρ method.

The Doppler-corrected γ-ray spectrum, after selection on ^{136}Te ions in BigRIPS and ZD, is shown in Fig. 1. The fit to the experimental spectrum is shown by the thick black line which is composed of a two-exponential function describing the background (blue dotted line) and individual simulated responses (red dashed line). The line visible in the spectrum corresponds to the 606 keV, $2_1^+ \rightarrow 0_{gs}^+$ transition in ^{136}Te. The high statistics accumulated in this experiment is needed to study in detail the systematic uncertainties inherent in the determination of $B(E2)$ values using Coulomb excitation at relativistic energies. The differential cross sections measured for both the gold and the carbon target are shown in Fig. 2. The latter is used to determine the nuclear contribution to the cross section measured with the gold target. The data analysis is ongoing and the results will be presented soon.

References

1) P. Doornenbal et al.: Phys. Rev. C. **90**, 061302(R) (2014).
2) N. Fukuda et al.: Nuc. Instrum. Methods Phys. Res. Sect B **317**, 323 (2013).

Measurement of proton elastic scattering from ^{132}Sn in inverse kinematics

J. Zenihiro,[*1] S. Terashima,[*1,*2] Y. Matsuda,[*1,*3] S. Ota,[*4] S. Chebotaryov,[*1] M. Dozono,[*4] T. Harada,[*1,*10] C. Iwamoto,[*4] M. Kobayashi,[*4] A. Krasznahorkay,[*1,*11] S. Leblond,[*7] T. Lokotko,[*7] Y. Maeda,[*8] S. Masuoka,[*4] M. Matsushita,[*4] S. Michimasa,[*4] E. Milman,[*1] T. Murakami,[*1,*6] H. Nasu,[*1,*3] J. Okamoto,[*1,*3] H. Sakaguchi,[*1,*5] S. Sakaguchi,[*1,*9] M. Takaki,[*4] K. Taniue,[*1,*8] H. Tokieda,[*4] M. Tsumura,[*1,*6] T. Uesaka,[*1] O. Wieland,[*12] Z.H. Yang,[*1] Y. Yamaguchi,[*4] and R. Yokoyama[*4]

The neutron skin thicknesses of medium and heavy nuclei such as ^{208}Pb are now known to be strongly correlated with the nuclear matter equation of state (EOS), especially because of the density dependence of the isospin-asymmetric term of the EOS, so-called the symmetry energy. The symmetry energy plays an essential role in the understanding of astorphysical phenomena such as neutron star structures and supernova explosions. Precise measurements of the neutron skin thicknesses are very important to constrain the symmetry energy, but are very difficult owing to the model dependences.

Proton elastic scattering is a powerful tool to study the ground-state properties of nuclei such as proton and neutron densities, radii, and neutron skin thicknesses. For stable nuclei, thus far, we succeeded in extracting the model-independent neutron density distributions and neutron skin thicknesses from proton elastic scattering at 300 MeV.[1)] For the systematic study of neutron skin thicknesses with large isospin asymmetry, the measurements of proton elastic scattering from unstable nuclei as well as stable ones are necessary. For this purpose we launched a new experimental project to measure the elastic scattering of protons with RI beams (ESPRI) based on the missing mass technique. To measure recoil protons scattered by unstable nuclei with a wide range of momentum transfers ($1 \sim 3$ fm^{-1}), we developed a new device, recoil proton spectrometer (RPS), which consists of a 1-mm-thick solid hydrogen target (SHT),[2)] two multi-wire drift chambers (MWDC), two plastic scintillators, and fourteen rods of NaI(Tl) calorimeters, which cover an angular range from 65° to 85° in the laboratory system. At two heavy-ion facilities, GSI and HIMAC, we have already tested the performance of RPS and successfully performed ESPRI measurements for several unstable nuclei such as ^{9}C, ^{20}O, and ^{66,70}Ni. An excitation energy resolution of $\sim$ 500 keV (σ) was achieved.[3)]

In May 2016, we have performed an ESPRI measurement for ^{132}Sn (NP1512-RIBF79R1). The ^{132}Sn nucleus is a flag-ship doubly magic nucleus which has a larger isospin assymmetry than that of ^{208}Pb. The secondary beam including ^{132}Sn at 200 MeV/u was produced by a ^{238}U beam at 345 MeV/u. The intensity of the cocktail beam was very high, typically 500 kcps at F3 and 200 kcps at F7. The purity of ^{132}Sn was approximately 25%. Owing to the radiation damage and the high-rate detections with a heavy and intense RI beam, we used MWDCs and diamond detectors instead of the conventional PPACs, plastic scintillators and ion chambers. We employed a new PI technique of the TOF-$B\rho$-$B\rho$ method which was recently developed.[4)]

After the BigRIPS seperater the secondary beam was transported to F8 and finally to the SHT at F12, where the ESPRI detectors were installed. Another experimental setup of NP1312-RIBF113 using a CNS active target (CAT) was also intalled at F8.[5)] Since both the RIBF79 and RIBF113 experiments required a high-intensity ^{132}Sn beam, the same configuration of the BigRIPS detectors was used. A newly designed DAQ system was also introduced to achieve a high live-time ratio even under such a high-intensity beam condition.[6)]

Since ^{132}Sn is known to have an isomeric state of ^{132}Sn (8^+) with a half life of 2 μs, this state is a possible background of this measurement. Four LaBr(Ce) detectors were installed around a beam stopper to investigate the isomer tagging system by measuring γ rays emitted from the isomeric state.[7)]

The experiment has been successfully performed. Analysis to deduce the excitation energy spectrum and the angular distribution of cross sections is now in progress.

*1 RIKEN Nishina Center
*2 Beihang University
*3 CYRIC, Tohoku University
*4 Center for Nuclear Study, University of Tokyo
*5 RCNP, Osaka University
*6 Department of Physics, Kyoto University
*7 Department of Physics, University of Hong Kong
*8 Department of Applied Physics, University of Miyazaki
*9 Department of Physics, Kyushu University
*10 Department of Physics, Toho University
*11 MTA ATOMKI, Debrecen
*12 Istituto Nazionale di Fisica Nucleare sezione di Milano

References

1) S. Terashima et al., Phys. Rev. C **77**, 024317 (2008); J. Zenihiro et al., Phys. Rev. C **82**, 044611 (2010).
2) Y. Matsuda et al., Nucl. Instr. Meth. Phys. Res. A **643**, 6 (2011).
3) Y. Matsuda et al., Phys. Rev. C **87**, 034614 (2013).
4) S. Ota et al., RIKEN Accel. Prog. Rep. **49**, 15 (2016).
5) S. Ota et al., In this report.
6) H. Baba et al., In this report.
7) S. Terashima et al., In this report.

Measurement of isoscalar giant monopole resonance in ^{132}Sn using CNS active target

S. Ota,[*1] H. Tokieda,[*1] C. Iwamoto,[*1] M. Dozono,[*1] U. Garg,[*2] S. Hayakawa,[*1] K. Kawata,[*1] N. Kitamura,[*1] M. Kobayashi,[*1] S. Masuoka,[*1] S. Michimasa,[*1] A. Obertelli,[*3,*4] D. Suzuki,[*4] R. Yokoyama,[*1] J. Zenihiro,[*4] H. Baba,[*4] O. Beliuskina,[*1] S. Chebotaryov,[*4] P. Egelhof,[*5] T. Harada,[*6] M.N. Harakeh,[*7] K. Howard[*2] N. Imai,[*1] M. Itoh,[*8] Y. Kiyokawa,[*1] C.S. Lee,[*1] Y. Maeda,[*9] Y. Matsuda,[*8] E. Milman,[*4] V. Panin,[*4] H. Sakaguchi,[*10] P. Schrock,[*1] S. Shimoura,[*1] L. Stuhl,[*4] M. Takaki,[*1] K. Taniue,[*9] S. Terashima,[*11] T. Uesaka,[*4] Y.N. Watanabe,[*12] K. Wimmer,[*1,*4,*12] K. Yako,[*1] Y. Yamaguchi,[*1] Z. Yang,[*4] and K. Yoneda[*4]

The equation of state (EoS) of nuclear matter not only governs the femto-scale quantum many-body system, namely nuclei, but also plays an important role in the structure of neutron stars and in supernova phenomena. In particular, the EoS of isospin asymmetric nuclear matter attracts much interest from the view point of the existence of heavy neutron stars. The asymmetric term of incompressibility, K_τ, can be a benchmark for various EoSs because it can be directly deduced from the the energies of the isoscalar giant monopole resonance (ISGMR) measured along an isotopic chain, such as tin isotopes.[1] The present value of K_τ is -550±100 MeV and its error is relatively larger than those of other parameters of the EoS. In order to improve the K_τ value, the measurement on the isotopic chain should be extended to unstable nuclei. A doubly magic tin isotope, ^{132}Sn, has been chosen as a flagship for the measurements of unstable tin isotopes because of its large isospin asymmetry and double magic nature.

The excitation energy and scattering angle in the center-of-mass frame are extracted by means of missing-mass spectroscopy, where the low-energy recoil deuteron has to be measured. In order to measure such low-energy recoils, a gaseous active target system, CNS active target (CAT), has been employed. The CAT consists of a time-projection chamber (TPC) and an array of silicon detectors on both sides of TPC. A stack of thick gas electron multipliers (THGEM) is used for electron multiplication in the TPC. The THGEM has three-fold segmented electrodes. The center electrode is used for measuring the beam particles and the side electrodes are used for measuring the recoil particles. The multiplication factors at the beam and recoil region can be controlled independently, which enables us to operate the CAT with a beam of high intensity such as 10^6 particles per second.[2]

The experiment was performed at RIBF at RIKEN. A secondary ^{132}Sn beam was produced as a fission fragment of a ^{238}U beam impinging on the primary beryllium target. The maximum intensity of the primary beam was 37 pnA. The typical intensities of the secondary beam at F3 and F7 were 8.5×10^5 and 3.2×10^5 particles per second, respectively. In order to identify the particles in such a high-intensity beam on an event-by-event basis, a new method called TOF-$B\rho$-$B\rho$[3] was introduced. The TOF was measured by 200-μm-thick diamond detectors located at F3 and F7. Bρ was determined using the positions and angles measured by low-pressure multi-wire drift chambers at F3, F5, and F7. The main components of the secondary beam were ^{132}Sn, ^{133}Sb, and ^{134}Te with the purities of 21%, 46%, and 25% at F7, respectively. The data from the beamline detectors at each focus are taken using MOCO[4]. The CAT was placed at F8 with a collimator in front of it. The CAT was operated with deuterium gas at 0.4 atm and a stack of three THGEMs. The signals from the CAT were digitized using the V1740 modules (CAEN) and digitized samples were transfered through optical links to two computers. The physics trigger for the data acquisition was made using the trigger out from V1740 and HIMP, which is the readout system used for the silicon detectors. The ESPRI system was placed at F12[5] to measure the deuteron elastic scattering off ^{132}Sn for large scattering angles to determine the optical potential parameters.

The excitation-energy resolution for the ground state, determined from the analysis of recoil particles stopped in TPC, is 1 MeV in one standard deviation. The energy of ISGMR will be deduced from the multipole-decomposition analysis of double-differential cross sections. The analysis is in progress.

*1 Center for Nuclear Study, the University of Tokyo
*2 Department of Physics, University of Notre Dame
*3 Le Centre CEA de Saclay
*4 RIKEN Nishina Center
*5 GSI Helmholtzzentrum für Schwerionenforschung GmbH
*6 Department of Physics, Toho University
*7 KVI, Center for Advanced Radiation Technology
*8 Cyclotron and Radio Isotope Center, Tohoku University
*9 Department of Applied Physics, University of Miyazaki
*10 Research Center for Nuclear Physics, Osaka University
*11 Beihang University
*12 Department of Physics, the Univerisity of Tokyo

References

1) T. Li et al., Phys. Rev. Lett. **99**, 162503 (2007).
2) S. Ota et al., J. Radioanal. Nucl. Chem. **305**, 907-911 (2015).
3) S. Ota et al., RIKEN Accel. Prog. Rep. **49** 15 (2017).
4) H. Baba et al., in this report.
5) J. Zenihiro et al.: in this report.

Measurement of ^{4}He(^{8}He,^{8}Be) reaction for verifying tetra-neutron resonance

S. Masuoka,[*1] S. Shimoura,[*1] M. Takaki,[*1] D. S. Ahn,[*2] H. Baba,[*2] M. Dozono,[*1] N. Fukuda,[*2] T. Harada,[*3] E. Ideguchi,[*4] N. Imai,[*1] N. Inabe,[*2] C. Iwamoto,[*1] K. Kawata,[*1] N. Kitamura,[*1] M. Kobayashi,[*1] Y. Kondo,[*5] T. Kubo,[*2] Y. Maeda,[*6] F. M. Marqués,[*7] M. Matsushita,[*1] S. Michimasa,[*1] R. Nakajima,[*1] T. Nakamura,[*5] N. Orr,[*7] S. Ota,[*1] H. Sakai,[*2] H. Sato,[*2] P. Schrock,[*1] L. Stuhl,[*1,*2] T. Sumikama,[*2] H. Suzuki,[*2] H. Takeda,[*2] K. Taniue,[*6] H. Tokieda,[*1] T. Uesaka,[*2] K. Wimmer,[*8] K. Yako,[*1] Y. Yamaguchi,[*1] Y. Yanagisawa,[*2] R. Yokoyama,[*1] K. Yoshida,[*2] and J. Zenihiro[*2]

The existence of nuclei composed only of neutrons has been discussed for over half a century, but it has not been confirmed yet. In 2002, a candidate bound state of the tetra-neutron, which consists of four neutrons, was reported.[1] An *ab-initio* calculation suggested that there might be a tetra-neutron ($4n$) resonance, but a bound $4n$ was not reproduced.[2] An experimental search for the $4n$ resonance state conducted using the exothermic double charge exchange (DCX) ^{4}He(^{8}He,^{8}Be)$4n$ reaction was performed at the SHARAQ spectrometer in RIBF[3]. As a result, four candidate events were found with a 4.9σ significance level, and the energy of the $4n$ resonance was determined as $E_{4n} = 0.83 \pm 0.65(\text{stat.}) \pm 1.25(\text{syst.})$ MeV. To confirm the existence of $4n$ resonance, we performed a new measurement with higher statistics and with smaller energy uncertainty.

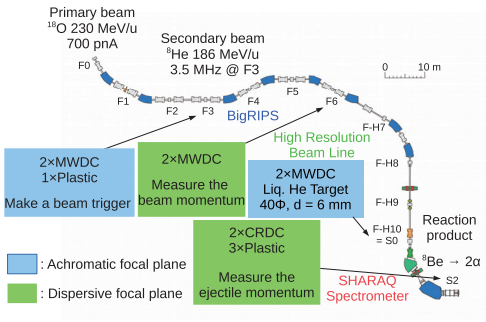

Fig. 1. Detector setup of BigRIPS/SHARAQ beam line.

Figure 1 shows a schematic view of the setup for this experiment. A primary ^{18}O beam was accelerated to about 230 MeV/nucleon by AVF+RRC+SRC. The intensity of the primary beam was about 700 particle nA. The energy of the secondary ^{8}He beam was about 186 MeV/nucleon. The beam intensity was increased from that in the previous experiment. The rate of the secondary beam at F3 was increased from about 2.0 MHz to 3.5 MHz. Six low-pressure multi-wire drift chambers (LP-MWDCs) were installed for tracking the beam. "F6" was set as a dispersive focal plane, so that the momentum of the beam could be measured by the focus position. At "S0," a liquid He target system (CRYPTA) was installed. At the final focal plane, "S2," 2 α particles from the decay of outgoing ^{8}Be were detected using 2 cathode readout drift chambers (CRDCs).

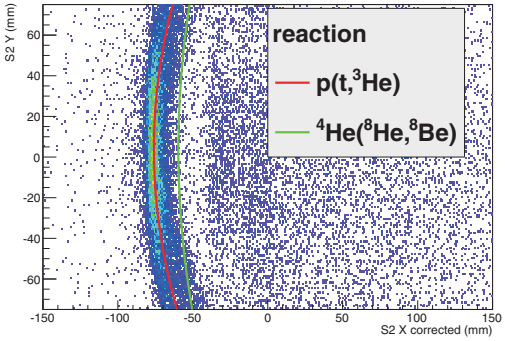

Fig. 2. A preliminary hit pattern of the ^{1}H(t,^{3}He) reaction at S2 for the energy calibration with a reaction kinematics curve. The X and Y axes represent the missing momentum and the vertical scattering angle, respectively.

In the present experiment, the method of missing-momentum calibration was changed to reduce the systematic error of the $4n$ energy. As a reference for the energy, the ^{1}H(t,^{3}He) reaction was measured with a triton beam that has the same magnetic rigidity as the ^{8}He beam (8.3 Tm). The energy can be calibrated without changing the magnetic settings. Figure 2 shows an S2 image of outgoing ^{3}He particles from the ^{1}H(t,^{3}He) reaction. The red line indicates the fitted kinematics curve of the reaction. The threshold energy of the $4n$ state can be determined from the curve. Further analysis is now in progress.

*1 Center for Nuclear Study, the University of Tokyo
*2 RIKEN Nishina Center
*3 Department of Physics, Toho University
*4 Research Center for Nuclear Physics, Osaka University
*5 Department of Physics, Tokyo Institute of Technology
*6 Faculty of Engineering, Univ. of Miyazaki
*7 Laboratorie de Physique Corpusculaire, IN2P3-CNRS, ENSICAEN et Université de Caen
*8 Department of Physics, the University of Tokyo

References

1) F.M. Marqués et. al., Phys. Rev. C **65**, 044006 (2002).
2) S.C. Pieper, Phys. Rev. Lett. **90**, 252501 (2003).
3) K. Kisamori et al., Phys. Rev. Lett. **116**, 052501 (2016).

Parity-transfer (^{16}O, ^{16}F(0$^-$)) reaction to study spin-dipole 0$^-$ states

M. Dozono,[*1] T. Uesaka,[*2] N. Fukuda,[*2] M. Ichimura,[*2] N. Inabe,[*2] S. Kawase,[*1] K. Kisamori,[*1] Y. Kiyokawa,[*1] K. Kobayashi,[*3] M. Kobayashi,[*1] T. Kubo,[*2] Y. Kubota,[*1] C. S. Lee,[*1] M. Matsushita,[*1] S. Michimasa,[*1] H. Miya,[*1] A. Ohkura,[*4] S. Ota,[*1] H. Sagawa,[*2,*5] S. Sakaguchi,[*4] H. Sakai,[*2] M. Sasano,[*2] S. Shimoura,[*1] Y. Shindo,[*4] L. Stuhl,[*2] H. Suzuki,[*2] H. Tabata,[*4] M. Takaki,[*1] H. Takeda,[*2] H. Tokieda,[*1] T. Wakasa,[*4] K. Yako,[*1] Y. Yanagisawa,[*2] J. Yasuda,[*4] R. Yokoyama,[*1] K. Yoshida,[*2] and J. Zenihiro[*2]

We proposed a new reaction probe, *parity-transfer* (^{16}O, ^{16}F(0$^-$, g.s.)) reaction, as a powerful tool to study spin-dipole (SD) 0$^-$ states in nuclei[1]. This reaction has a unique selectivity to unnatural-parity states, which is an advantage over the other reactions used thus far. As the first measurement, the ^{12}C(^{16}O, ^{16}F(0$^-$)) reaction at 247 MeV/u was studied in the SHARAQ08 experiment at RIBF. A known 0$^-$ state at $E_x = 9.3$ MeV in ^{12}B[2] serves as a benchmark to verify the effectiveness of this reaction. The details of the experimental setup and method can be found in Ref.[3].

The results of the present study are currently being prepared for publication. In this report, we discuss the selectivity of the parity-transfer reaction to 0$^-$ states by comparing our data with that previously obtained by the ^{12}C(d, ^{2}He) reaction at 270 MeV[4]. Figures 1(a) and 1(b) show excitation energy (E_x) spectra for the ^{12}C(^{16}O, ^{16}F(0$^-$)) reaction at $\theta_{\rm lab} = 0^\circ - 0.25^\circ$ and $0.25^\circ - 0.45^\circ$, respectively. The energy resolution is 2.6 MeV in FWHM. Note that the events at $E_x \sim -10$ MeV are due to hydrogens in the target. The ^{12}C(d, ^{2}He) spectra at $\theta_{\rm cm} = 0^\circ - 1^\circ$ and $6^\circ - 8^\circ$ are shown as dashed curves in Figs. 1(a) and 1(b), respectively. Here, the momentum transfer is comparable to that of our data in each figure. (Their values are $q \sim 0.3$ and 0.5 fm^{-1} in Figs. 1(a) and 1(b), respectively). Solid curves represent the (d, ^{2}He) cross sections after smearing with an energy resolution of the present experiment. The (d, ^{2}He) spectra have been arbitrarily normalized to the (^{16}O, ^{16}F(0$^-$)) cross sections for the 1$^+$ g.s.

The excitation of the 1$^+$ g.s. and the 2$^-$ state at $E_x = 4.4$ MeV can be seen in both reaction data, while the structures at $E_x \gtrsim 6$ MeV are largely different. A bump structure at $E_x = 7.5$ MeV ("A" in Fig. 1(b)) seen in the (d, ^{2}He) reaction is missing in the (^{16}O, ^{16}F(0$^-$)) spectra. This is because natural-parity states are not populated with the parity transfer reaction. Another striking difference is a peak at $E_x \sim 9$ MeV observed in Fig. 1(a); a clear enhancement appears in the (^{16}O, ^{16}F(0$^-$)) data but vanishes in the (d, ^{2}He) data. This enhancement is due to the known 0$^-$ state at $E_x = 9.3$ MeV. These differences in Fig. 1 indicate that the parity-transfer reaction has a high selectivity to 0$^-$ states. The feature will be confirmed by further discussions including angular distributions and DWBA calculations in our future publication.

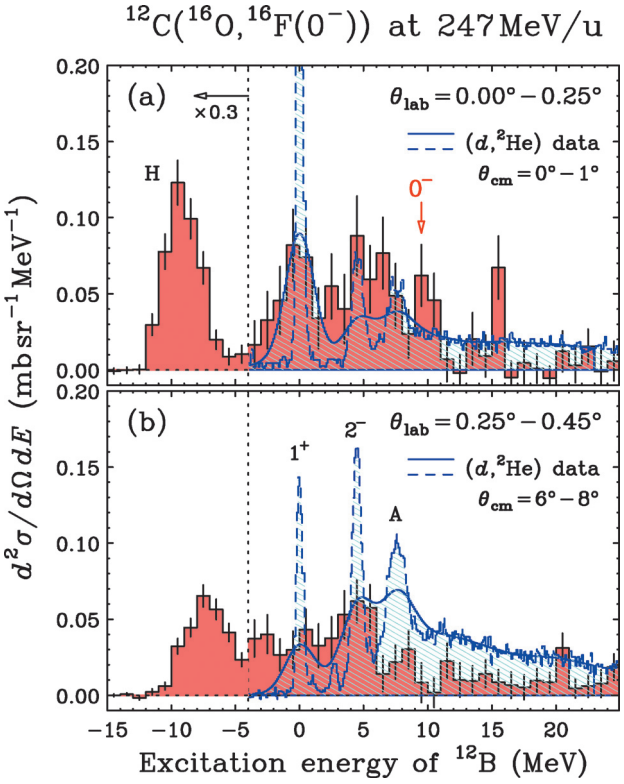

Fig. 1. Excitation energy spectra for the ^{12}C(^{16}O, ^{16}F(0$^-$)) reaction. The dashed and solid curves represent the experimental data for the ^{12}C(d, ^{2}He) reaction[4].

*1 Center for Nuclear Study, University of Tokyo
*2 RIKEN Nishina Center
*3 Department of Physics, Rikkyo University
*4 Department of Physics, Kyushu University
*5 Center for Mathematics and Physics, University of Aizu

References
1) M. Dozono et al., RIKEN Accel. Prog. Rep. **45**, 10 (2012).
2) H. Okamura et al., Phys. Rev. C **66**, 054602 (2002).
3) M. Dozono et al., Nucl. Instrum. Meth. A **830**, 233 (2016).
4) H. Okamura et al., Phys. Lett. B **345**, 1 (1995).

Neutron shell structure of ^{23,25}F and oxygen neutron dripline anomaly

T. L. Tang,[*1] S. Kawase,[*1] T. Uesaka,[*2] D. Beaumel,[*2,*3] M. Dozono,[*2] T. Fujii,[*1,*2] N. Fukuda,[*2] T. Fukunaga,[*2,*4] A. Galindo-Uribarri,[*5] S. H. Hwang,[*6] N. Inabe,[*2] D Kameda,[*2] T. Kawahara,[*2,*7] W. Y. Kim,[*6] K. Kisamori,[*1,*2] M. Kobayashi,[*1] T. Kubo,[*2] Y. Kubota,[*1,*2] K. Kusaka,[*2] C. S. Lee,[*1] Y. Maeda,[*8] H. Matsubara,[*2] S. Michimasa,[*1] H. Miya,[*1,*2] T. Noro,[*2,*4] A. Obertelli,[*9] K. Ogata,[*12] S. Ota,[*1] E. Padilla-Rodal,[*10] S. Sakaguchi,[*2,*4] H. Sakai,[*2] M. Sasano,[*2] S. Shimoura,[*1] S. S. Stepanyan,[*6] H. Suzuki,[*2] M. Takaki,[*1,*2] H. Takeda,[*2] H. Tokieda,[*1] T. Wakasa,[*2,*4] T. Wakui,[*2,*11] K. Yako,[*1] Y. Yanagisawa,[*2] J. Yasuda,[*2,*4] R. Yokoyama,[*1,*2], K. Yoshida,[*2] K. Yoshida,[*12] and J. Zenihiro,[*2] for SHARAQ04 collaboration

The nuclear shell model proposed by Mayer[1] is a cornerstone for understanding the nuclear structure. The model assumes that each nucleon moves independently and uncorrelated, and is described by a single-particle state (SPS) in a mean field. Nuclei with a doubly magic core plus a single nucleon should be well described using SPS, so that the spectroscopic factor (SF) of the single nucleon is almost unity; for example, the SFs of the valance protons in ^{17}F, ^{41}Sc, ^{49}Sc, and ^{209}Bi are 0.8 ~ 1.1.[2-6]

A decade ago, ^{24}O was found to be doubly magic[7], and the oxygen neutron dripline stops at N = 16. In contrast, the neutron dripline of fluorine was extended to N = 22, into the pf-shell, with only one proton on the sd-shell. Therefore, it is worthy to study the single-particle properties of ^{25}F because of the oxygen neutron dripline anomaly[8].

The one proton quasi-free knockout reactions on ^{23,25}F were studied in the SHARAQ04 experiment at RIBF, RIKEN. [9] The experimental result was reported in Ref. 10 and is showed in Fig. 1. We found that the ground state to ground state SFs of ^{25}F(p,2p) and ^{23}F(p,2p) reactions are ~ 0.4, which is much less than unity. At first glance, this may indicate that the 0d$_{5/2}$ proton is not in an SPS. However, the total single-particle strength (sum of SFs) of the valance proton is close to unity for ^{25}F (and most probably for ^{23}F). This means that the 0d$_{5/2}$ proton is in an SPS, and the single-particle strength of the 0d$_{5/2}$ proton is fragmented.

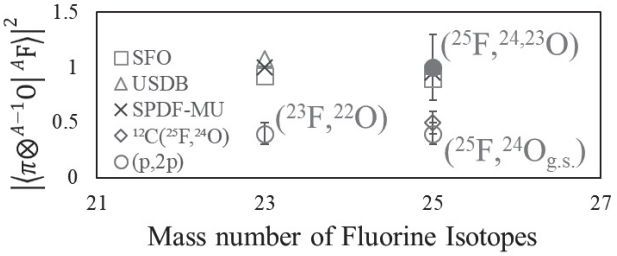

Fig. 1 Experimental and theoretical spectroscopic factors of ^{23}F and ^{25}F. The solid circle is the total strength of the (^{25}F,^{24,23}O) reaction. The result for ^{12}C(^{25}F,^{24}O) is taken from Ref. 15.

*1 Center of Nuclear Study (CNS), University of Tokyo
*2 RIKEN Nishina Center
*3 Institut de Physique Nucléaire d'Orsay
*4 Department of Physics, Kyushu University
*5 Oak Ridge National Laboratory
*6 Department of Physics, Kyungpook National University
*7 Department of Physics, Toho University
*8 Department of Applied Physics, University of Miyazaki
*9 CEA Saclay
*10 Instituto de Ciencias Nucleares, UNAM
*11 CYRIC, Tohoku University
*12 RCNP, Osaka University

We propose the wavefunction of ^{23,25}F to be

$$|\,^{A}F\rangle = |\pi\rangle\otimes\left(\beta_0|^{A-1}O_{g.s.}\rangle + \sum_i \beta_i|^{A-1}O^i\rangle\right),$$

where A is the mass number, β_j is the square root of the SF, $|\pi\rangle$ is the wavefunction of the 0d$_{5/2}$ proton, $|^{A-1}O_{g.s.}\rangle$ is the wavefunction of the ground-state oxygen core, $|^{A-1}O^i\rangle$ is the wavefunction of the oxygen core in the i-th excited state, and the symbol $\otimes$ represents the angular and isospin coupling and anti-symmetry operator. The wavefunction of the 0d$_{5/2}$ proton is factored out and represents an SPS. The ground state of fluorine has many components of the excited oxygen core, and the neutron-shell structure of fluorine is different from that of oxygen.

The mechanism of change of the neutron shell structure could be due to the tensor force between the 0d$_{5/2}$ proton and the sd-shell neutrons.[11] The proton lowers the 0d$_{3/2}$ neutron orbit and then increases the neutron configuration mixing, which creates many components of the excited oxygen core.

The result was compared with shell model calculation using the psd (SFO[12]), sd (USD-B[13]), and sd-pf (SDPF-MU[14]) model space. All interactions above predict the SF to be close to unity without fragmentation (Fig. 1). This is because the neutron shell is rigid. The experimental result suggests that the tensor force could be larger near the dripline.

In conclusion, the SPS of the valance protons of ^{23,25}F were studied. The result shows that the proton is in an SPS and the neutron-shell structure is modified significantly. The experimental result may provide a new insight into the oxygen dripline anomaly.

References

1) M. G. Mayer, Phys. Rev. **78,** 16 (1950).
2) C. J. Oliver *et al.*, Prog. Part. Nucl. Phys. **61**, 602 (2008).
3) H. G. Leighton *et al.*, Nucl. Phys. A **109**, 218-230 (1968).
4) J. J. Schwartz *et al.*, Phys. Rev. **153**, 1248 (1967).
5) B. Berthier *et al.*, Phys. Lett. B **182**, 15 (1986).
6) D. Branford *et al.*, Phys. Rev. C **63**, 014310 (2000).
7) R. V. F. Janssens, Nature **459**, 1069 (2009).
8) T. Otsuka, Phys. Scripta. **2013**, 014007 (2013).
9) S. Kawase *et al.*, CNS annual report 2012, 13 (2013).
10) T. L. Tang *et al.*, In this report.
11) T. Otsuka *et al.*, Phys. Rev. Lett. **95**, 232502 (2005).
12) T. Suzuki *et al.*, Phys. Rev. C **67**, 044302 (2003).
13) B. A. Brown *et al.*, Phys. Rev. C **74**, 034315 (2006).
14) Y. A. Utsuno *et al.*, Phys. Rev. C **86**, 051301 (2012).
15) M. Thoennessen *et al.*, Phys. Rev. C **68**, 044318 (2003).

Mass measurements of neutron-rich isotopes in the vicinity of ^{54}Ca using the TOF–$B\rho$ technique

M. Kobayashi,[*1] S. Michimasa,[*1] Y. Kiyokawa,[*1] H. Baba,[*2] G. P. A. Berg,[*3] M. Dozono,[*1] N. Fukuda,[*2] T. Furuno,[*4] E. Ideguchi,[*5] N. Inabe,[*2] T. Kawabata,[*4] S. Kawase,[*1] K. Kisamori,[*1,*2] K. Kobayashi,[*6] T. Kubo,[*2] Y. Kubota,[*1,*2] C. S. Lee,[*1,*2] M. Matsushita,[*1] H. Miya,[*1] A. Mizukami,[*7] H. Nagakura,[*6] D. Nishimura,[*7] H. Oikawa,[*7] S. Ota,[*1] H. Sakai,[*2] S. Shimoura,[*1] A. Stolz,[*8] H. Suzuki,[*2] M. Takaki,[*1] H. Takeda,[*2] S. Takeuchi,[*2] H. Tokieda,[*1] T. Uesaka,[*2] K. Yako,[*1] Y. Yamaguchi,[*6] Y. Yanagisawa,[*2] R. Yokoyama,[*1] and K. Yoshida[*2]

The mass of an atomic nucleus is a fundamental quantity because it reflects the sum of all interactions within the nucleus. Mass measurements can directly probe changes in the shell structure in nuclei far from stability, which is called "shell evolution." The presence of subshell gaps at $N = 32$ and 34 around calcium isotopes has attracted much attention over recent years (for example, see Refs. 1–3). To investigate the shell evolution at $N = 32$ and 34, mass measurements of neutron-rich nuclei in the vicinity of ^{54}Ca were performed at the RIKEN RI Beam Factory.

The masses were measured using the TOF–$B\rho$ technique. The time-of-flight (TOF) of an ion was measured by a pair of diamond detectors with extremely high time resolutions. The dispersion-matched operation of the High-Resolution Beam Line and the SHARAQ spectrometer allowed high-precision measurements of the beam momenta. Details of the experimental setup are described in Ref. 4.

The reference nuclei with known masses used for mass calibration were $^{52-54}$Ca, $^{49,51-53}$K, $^{46-48}$Ar, $^{43-46}$Cl, ^{41,42}S, $^{38-42}$P, and $^{36-40}$Si. These nuclides have mass precisions in the literature of < 320 keV and do not have known long-lived ($T_{1/2} > 100$ ns) isomeric states. Masses were deduced by fitting with a fourth-order calibration function in TOF, the positions and angles at the focal planes F3 and S2, and the horizontal position at the dispersive focus S0, which is related to $B\rho$. Figure 1 shows the differences between the deduced m/q values and the values reported in the literature for the reference nuclei. Using the standard deviation of the data points, the systematic error in the mass determination was estimated to be 6.1 keV/q.

The deduced A/Q spectrum is presented in Fig. 2. In the present experiment, the achieved mass resolution was typically $\sim 1.0 \times 10^{-4}$ (σ). We measured 21 nuclides with unknown masses: $^{62-64}$V, $^{58-62}$Ti, $^{58-60}$Sc, $^{55-57}$Ca, ^{54}K, $^{50-52}$Ar, ^{48,49}Cl, and ^{46}S. The mass precisions for ^{55,56}Ca were evaluated to be less than 300 keV. Discussion regarding the deduced mass values is in progress.

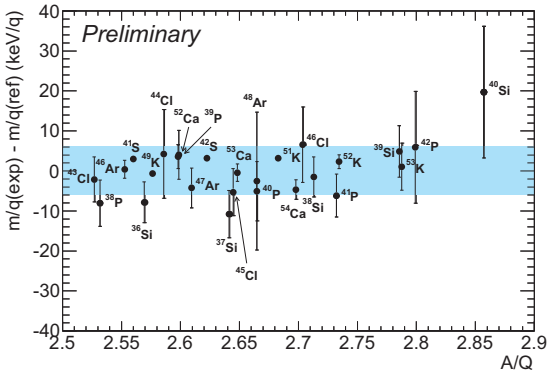

Fig. 1. Differences between the deduced and reference m/q values as a function of A/Q. The blue band indicates the region within the systematic error. Error bars represent the uncertainties in the reference values.

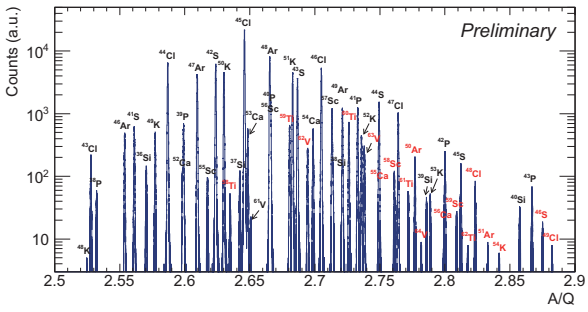

Fig. 2. A/Q spectrum deduced from the present experiment. Nuclides whose masses have not been measured previously are indicated with red letters.

*1 Center for Nuclear Study, University of Tokyo
*2 RIKEN Nishina Center
*3 JINA-CEE and Department of Physics, University of Notre Dame
*4 Department of Physics, Kyoto University
*5 Research Center for Nuclear Physics, Osaka University
*6 Department of Physics, Rikkyo University
*7 Department of Physics, Tokyo University of Science
*8 National Superconducting Cyclotron Laboratory, Michigan State University

References

1) T. Otsuka et al.: Phys. Rev. Lett. **87**, 082502 (2001).
2) F. Wienholtz et al.: Nature **498**, 349 (2013).
3) D. Steppenbeck et al.: Nature **502**, 207 (2013).
4) M. Kobayashi et al.: RIKEN Accel. Prog. Rep. **48**, 59 (2015).

Competition between shape and shell in ^{75}Cu clarified by the novel magnetic moment measurement

Y. Ichikawa,[*1] H. Nishibata,[*1,*2] A. Takamine,[*1] K. Imamura,[*1,*3] T. Fujita,[*1,*2] T. Sato,[*1,*4] S. Momiyama,[*5] Y. Shimizu,[*1] D. S. Ahn,[*1] K. Asahi,[*1,*4] H. Baba,[*1] D. L. Balabanski,[*1,*6] F. Boulay,[*1,*7,*8] J. M. Daugas,[*1,*8] T. Egami,[*9] N. Fukuda,[*1] C. Funayama,[*4] T. Furukawa,[*10] G. Georgiev,[*11] A. Gladkov,[*1,*12] N. Inabe,[*1] Y. Ishibashi,[*1,*13] T. Kawaguchi,[*9] T. Kawamura,[*2] Y. Kobayashi,[*1,*14] S. Kojima,[*4] A. Kusoglu,[*6,*11,*15] I. Mukul,[*16] M. Niikura,[*5] T. Nishizaka,[*9] A. Odahara,[*2] Y. Ohtomo,[*1,*4] T. Otsuka,[*5] D. Ralet,[*11] G. S. Simpson,[*17] T. Sumikama,[*1] H. Suzuki,[*1] H. Takeda,[*1] L. C. Tao,[*1,*18] Y. Togano,[*4] D. Tominaga,[*9] Y. Tsunoda,[*19] H. Ueno,[*1] H. Yamazaki,[*1] and X. F. Yang[*20]

The structure of a nucleus is a result of competition between the shell evolution and the shape effects, such as surface vibration and deformation. In this study, we demonstrate the precision analysis of the competition by focusing on an isomeric state of a neutron-rich ^{75}Cu nucleus[1,2], where an intriguing shell evolution along the Cu isotopic chain has been reported[3–6], through its nuclear magnetic moment.

The experiment of the magnetic moment measurement was conducted at the BigRIPS at RIBF, taking advantage of a spin-aligned RI beam obtained in a scheme of two-step projectile fragmentation with a technique of momentum-dispersion matching, recently established[7]. The ^{75}Cu beam with spin alignment reaching 30% was produced from a primary beam of ^{238}U via an intermediate product ^{76}Zn. For the measurement of the magnetic moment, a method of time-differential perturbed angular distribution (TDPAD) was employed. Owing to the high spin alignment realized with the two-step scheme, the oscillation in the $R(t)$ ratio which represents the change of anisotropy of γ-ray emission synchronized with the Larmor precession was observed for 66.2-keV γ rays with significance larger than 5σ, as shown in Fig. 1. The spin-parity of the 66.2-keV level was firmly fixed to be $3/2^-$. The magnetic moment of the 66.2-keV isomer was determined for the first time to be $\mu = 1.40(6)\mu_N$.

The magnetic moment thus obtained shows a considerable deviation from the Schmidt value, $\mu = 3.05\mu_N$, for the $p_{3/2}$ orbital. The analysis of the magnetic moment with a help of state-of-the-art shell-model calculations[8] reveals that this state contains a considerable fraction of the mixed $f_{5/2}$ configuration in addition to the primary $p_{3/2}$ configuration. The same holds true for the $5/2^-$ ground state, except that the roles played by the two orbitals are interchanged. Through the decomposition of the total angular momentum into the spins and the orbital angular momenta of the proton and the neutron, the admixing configuration is found to be brought to this state by a neutron quadrupole excitation in the $g_{9/2}$ orbital which may also play an essential role in the emergence of exotic phenomena in this extremely neutron-rich region.

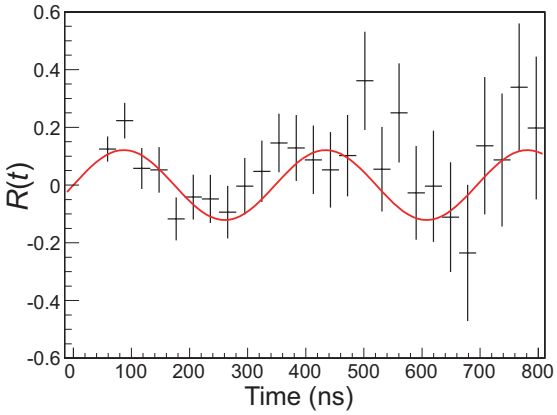

Fig. 1. $R(t)$ ratio for the 66.2-keV γ ray observed in the TDPAD measurement. The solid line represents the theoretical $R(t)$ after fitting to the experimental $R(t)$.

*1 RIKEN Nishina Center
*2 Department of Physics, Osaka University
*3 Department of Physics, Meiji University
*4 Department of Physics, Tokyo Institute of Technology
*5 Department of Physics, University of Tokyo
*6 ELI-NP, IFIN-HH
*7 GANIL, CEA/DSM-CNRS/IN2P3
*8 CEA, DAM, DIF
*9 Department of Advanced Sciences, Hosei University
*10 Department of Physics, Tokyo Metropolitan University
*11 CSNSM, CNRS/IN2P3, Université Pris-Sud
*12 Department of Physics, Kyungpook National University
*13 Department of Physics, University of Tsukuba
*14 Department of Informatics and Engineering, University of Electro-Communications
*15 Department of Physics, Istanbul University
*16 Department of Particle Physics, Weizmann Institute
*17 LPSC, Université Joseph Fourier Grenoble 1, CNRS/IN2P3
*18 School of Physics, Peking University
*19 Center for Nuclear Study, University of Tokyo
*20 Intsituut voor Kern-en Srralingsfysica, K. U. Leuven

References

1) J. M. Daugas et al.: Phys. Rev. C **81**, 034304 (2010).
2) C. Petrone et al.: Phys. Rev. C **94**, 024319 (2016).
3) S. Franchoo et al.: Phys. Rev. Lett. **81**, 3100 (1998).
4) K. T. Flanagan et al.: Phys. Rev. Lett. **103**, 142501 (2009).
5) T. Otsuka et al.: Phys. Rev. Lett. **95**, 232502 (2005).
6) M. Honma et al.: Phys. Rev. C **80**, 064323 (2009).
7) Y. Ichikawa et al.: Nature Phys. **8**, 918 (2012).
8) Y. Tsunoda et al.: Phys. Rev. C **89**, 031301(R) (2014).

Determination of neutron skin thickness via measurements of σ_{I} and σ_{CC} of Ni isotopes

M. Takechi,[*1] M. Tanaka,[*2] A. Homma,[*1] Y. Tanaka,[*2] T. Suzuki,[*3] M. Fukuda,[*2] D. Nishimura,[*4] T. Moriguchi,[*5] D. S. Ahn,[*6] A. S. Aimaganbetov,[*7,*8] M. Amano,[*5] H. Arakawa,[*3] S. Bagchi,[*9] K.-H. Behr,[*9] N. Burtebayev,[*7] K. Chikaato,[*1] H. Du,[*2] T. Fujii,[*3] N. Fukuda,[*6] H. Geissel,[*9] T. Hori,[*2] S. Hoshino,[*1] R. Igosawa,[*3] A. Ikeda,[*1] N. Inabe,[*6] K. Inomata,[*3] K. Itahashi,[*6] T. Izumikawa,[*10] D. Kamioka,[*5] N. Kanda,[*1] I. Kato,[*3] I. Kenzhina,[*11] Z. Korkulu,[*6] Ye. Kuk,[*7,*8] K. Kusaka,[*6] K. Matsuta,[*2] M. Mihara,[*2] E. Miyata,[*1] D. Nagae,[*6] S. Nakamura,[*1] M. Nassurlla,[*7] K. Nishimuro,[*3] K. Nishizuka,[*1] S. Ohmika,[*3] K. Ohnishi,[*2] M. Ohtake,[*6] T. Ohtsubo,[*1] H. J. Ong,[*12] A. Ozawa,[*5] A. Prochazka,[*9] H. Sakurai,[*6] C. Scheidenberger,[*9] Y. Shimizu,[*6] T. Sugihara,[*2] T. Sumikama,[*6] S. Suzuki,[*5] H. Suzuki,[*6] H. Takeda,[*6] Y. K. Tanaka,[*9] T. K. Zholdybayev,[*7] T. Wada,[*1] K. Wakayama,[*3] S. Yagi,[*2] T. Yamaguchi,[*3] R. Yanagihara,[*2] Y. Yanagisawa,[*6] and K. Yoshida[*3]

The exploration of the equation of state (EOS) of nuclear matter forms one of the most intriguing topics in nuclear physics, wherein the investigation of the basic properties of atomic nuclei plays a key role in the understanding of its parameters. Thus far, our abundant knowledge of stable nuclei has suitably constrained the parameters of the EOS for symmetric nuclear matter[1]. However, the behavior of nuclear matter as a function of the difference of neutron and proton numbers, which is quite important to understand extremely asymmetric nuclear matter such as neutron stars and the cores of supernovae, is unfortunately more elusive. In order to obtain a better understanding of the EOS of asymmetric matter, it is essential to study the symmetry term of the EOS. Previous theoretical studies have indicated that the determination of neutron skin thickness ΔR as a function of the asymmetry parameter $\delta(\equiv (N-Z)/A)$ yields crucial information to constrain the symmetry energy coefficient of the EOS[2]. In this regards, extensive studies have been carried out on stable nuclei thus far to determine ΔR[3], and a number of data sets have been obtained in the range of δ from 0 to 0.23; however, the data in the wider range of δ are desirable to set a narrower constraint. In this study, we measured the interaction cross sections σ_{I} and charge-changing cross sections σ_{CC} for $^{58-78}$Ni at the RIBF. The matter radii of Ni isotopes can be deduced from σ_{I} with the use of Glauber model[4] and point-proton radii can be deduced from σ_{CC}[5]; consequently, the neutron skin thickness of unstable nuclei can be obtained from our measurements in this study.

The experiments were performed at the RIBF facility operated by the RIKEN Nishina Center and the Center for Nuclear study, University of Tokyo. A primary beam of ^{238}U (maximum intensity of around 30 pnA) with incident beam energy of 345A MeV and Be production targets were utilized to produce $^{58-78}$Ni secondary beams with energies around 260A MeV. The σ_{I} values were measured by means of the transmission method[6] and the BigRIPS fragment separator[7] was used as a spectrometer to identify the incoming and outgoing particles of those nuclides that remained unchanged from the original incident beam. The schematic of the experimental setup is shown in Fig. 1. The particle identifications for the analysis of cross sections are based on the $\Delta E - TOF - B\rho$ method. In order to measure σ_{CC}, the large acceptance ion chamber was set at F5 to identify the particles that did not show change in the proton number compared with that of the incident beam. Additional reaction targets and MUlti Sampling Ion Chambers (MUSICs)[8] were set at F11, which enabled us to deduce the σ_{CC} value of the beam transported through zero-degree pectrometer (ZDS). Data analyses for σ_{I} and σ_{CC} are in progress.

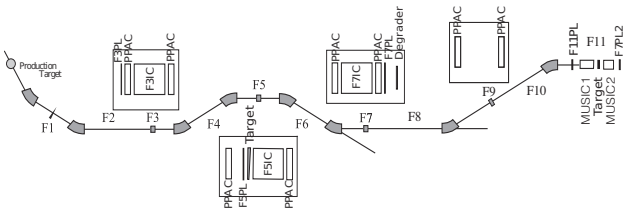

Fig. 1. Schematic of experimental setup.

*1 Department of Physics, Niigata University
*2 Department of Physics, Osaka University
*3 Department of Physics, Saitama University
*4 Department of Physics, Tokyo University of Science
*5 Institute of Physics, University of Tsukuba
*6 RIKEN Nishina Center
*7 The Institute of Nuclear Physics Kazakhstan
*8 L. N. Gumilyov Eurasian National University
*9 GSI Helmholtzzentrum für Schwerionenforschung
*10 Radioactive Isotope Center, Niigata University
*11 Al-Farabi Kazakh National University
*12 Research Center for Nuclear Physics, Osaka University

References

1) J. Piekarewicz, Phys. Rev. C **76**, 031301(R) (2007), and references therein.
2) M. Centelles et al. PRL **102**, 122502 (2009).
3) L. Cao et al. Proceedings of the 14th National Conference on Nuclear Structure in China, p. 32.
4) I. Tanihata et al., Phys. Lett. **B 287**, 307 (1992).
5) T. Yamaguchi et al., PRL **107**, 032502 (2011).
6) M. Takechi et al., Phys. Rev. C**91**, 014614(R) (2014).
7) T. Ohnishi et al., J. Phys. Soc. Jpn. 77, 083201 (2008).
8) A. Stolz et al., Phys. Rev. C **65**, 064603 (2002).

Deuteron analyzing powers for *d*-*p* elastic scattering at 186.6 MeV/nucleon

K. Sekiguchi,[*1,*2] T. Akieda,[*1] Y. Wada,[*1] D. Eto,[*1] A. Watanabe,[*1] H. Kon,[*1] N. Sakamoto,[*2] H. Sakai,[*2] M. Sasano,[*2] H. Suzuki,[*2] T. Uesaka,[*2] Y. Yanagisawa,[*2] M. Dozono,[*3] Y. Kubota,[*3] K. Yako,[*3] Y. Maeda,[*4] S. Kawakami,[*4] T. Yamamoto,[*4] S. Sakaguchi,[*5] T. Wakasa,[*5] J. Yasuda,[*5] A. Ohkura,[*5] Y. Shindo,[*5] M. Tabata,[*5] E. Milman,[*2,*6] and S. Chebotaryov[*2,*6]

The study of three nucleon forces (3NFs) is essentially important for clarifying nuclear phenomena. 3NFs arise naturally in the standard meson exchange picture[1] as well as in the framework of the chiral effective field theory (χEFT) which has a link to QCD.[2,3] Three-nucleon scattering at intermediate energies ($E/A \sim 200$ MeV) is one attractive approach to investigate the dynamical aspects of 3NFs, such as momentum and/or spin dependences. Here we report the measurement of all deuteron analyzing powers (iT_{11}, T_{20}, T_{21}, and T_{22}) in deuteron–proton (d–p) elastic scattering at 186.6 MeV/nucleon (MeV/N) performed in May 2015.

A schematic diagram of the experimental setup has been provided in Ref. (4). Vector- and tensor-polarized deuteron beams were accelerated by the injector cyclotrons AVF and RRC up to 70 MeV/N; subsequently, they were accelerated up to 186.6 MeV/N by SRC. The measurement for d–p elastic scattering was performed using a detector system, BigDpol, which was installed at the extraction beam line of SRC. Polyethylene with a thickness of 330 mg/cm^2 was used as the hydrogen target. In BigDpol, four pairs of plastic scintillators coupled with photo-multiplier tubes were placed symmetrically in the directions of azimuthal angles to the left, right, up and down. Scattered deuterons and recoil protons were detected in the kinematical coincidence condition by each pair of detectors. The angles ($\theta_{\mathrm{c.m.}}$) measured in the center-of-mass system are in the range of 39°–165°. In the experiment, the deuteron beams were stopped in a Faraday cup installed at the focal plane F0 of the BigRIPS spectrometer. The beam polarizations were monitored continuously with a beam line polarimeter Dpol prior to acceleration by SRC using the reaction of elastic d–p scattering at 70 MeV/N. At RIBF, single-turn extractions were available for all the cyclotrons used for the experiments. Therefore, depolarizations were expected to be small during beam acceleration. In the measurement typical values of the beam polarizations were 80% of the theoretical maximum values.

Results of the deuteron analyzing powers iT_{11} and T_{22} are shown with solid circles in Fig. 1. Only the statistical uncertainties are shown. It is interesting to see the potential of χEFT to describe deuteron analyzing powers for d–p elastic scattering. In Fig. 1, the data are compared with the calculations based on the χEFT N4LO NN potentials.[5] Gnerally good agreements are obtained for the vector analyzing power iT_{11}, while large discrepancies are found for the tensor analyzing power T_{22}. In order to examine how χEFT 3NFs describe the data, theoretical treatments are now in progress[6].

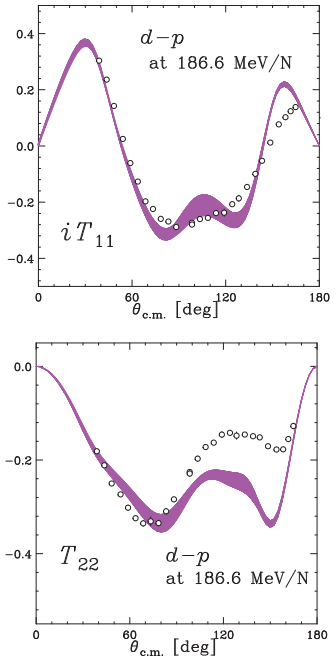

Fig. 1. Results of deuteron analyzing powers iT_{11} and T_{22} for d-p elastic scattering at 186.6 MeV/N.

*1 Department of Physics, Tohoku University
*2 RIKEN Nishina Center
*3 CNS, University of Tokyo
*4 Faculty of Engineering, University of Miyazaki
*5 Department of Physics, Kyushu University
*6 Department of Physics, Kyungpook National University

References

1) J. Fujita, H. Miyazawa, Prog. Theor. Phys. **17**, 360 (1957).
2) U. van Kolck, Phys. Rev. C **49**, 2932 (1994).
3) E. Epelbaum, H.-W. Hammer, U.-G. Meißner, Rev. Mod. Phys. **81**, 1773 (2009).
4) K. Sekiguchi et al., Phys. Rev. C **89**, 064007 (2014).
5) S. Binder et al., Phys. Rev. C **93**, 044002 (2016).
6) E. Epelbaum, private communications.

Commissioning the BRIKEN array in parasitic mode using exotic Ni-Ga secondary beam

G. G. Kiss,[*1] S. Nishimura,[*1] J. Agramunt,[*2] D. S. Ahn,[*1] A. Algora,[*2,*3] H. Baba,[*1] S. Bae,[*4] N. T. Brewer,[*5] R. Caballero Folch,[*6] T. Davinson,[*7] I. Dillmann,[*6] A. Estrade,[*8] N. Fukuda,[*1] S. Go,[*9] C. J. Griffin,[*7] R. K. Grzywacz,[*9] J. Ha,[*4] O. Hall,[*7] D. Kahl,[*7] M. Labiche,[*10] J. Liu,[*11] K. Matsui,[*1] B. Moon,[*4] N. Nepal,[*8] B. C. Rasco,[*5] K. P. Rykaczewski,[*5] H. Sakurai,[*1] Y. Shimizu,[*1] P.-A. Söderström,[*1] T. Sumikama,[*1] H. Suzuki,[*1] J. L. Tain,[*2] M. Takechi[*12] H. Takeda,[*1] A. Tarifeno-Saldivia,[*13] A. Tolosa,[*2] and P. Vi[*1]

Very neutron-rich nuclei can emit neutrons after β^--decay when the decay Q-value is larger than the (one/two/three…) neutron separation energy of the daughter nucleus ($Q_\beta > S_{xn}$). For neutron-rich nuclei away from the valley of stability, β-delayed one/two/three-… neutron emission is the dominant decay process. These β-delayed neutrons play a key role in the formation of heavy elements in the so-called astrophysical r process[1,2]. Furthermore, the emission probability (P_n) provides information about the distribution of the nuclear levels above the separation energy populated in the β^--decay. A common approach to measure P_n values is to implant the isotope of interest into a silicon detector, register its β-decay and count the delayed neutrons using a neutron detector in coincidence with the β^--decay events.

In the last year, the largest and most efficient neutron counter has been built at the RIKEN Nishina Center[3]. The neutron detector, surrounding the AIDA silicon implantation array[4], has a flexible design. The so-called compact BRIKEN array consists of 166 ^{3}He gas-filled proportional counters, embedded into a 90 cm x 90 cm x 75 cm high density polyethylene neutron moderator. The hybrid BRIKEN detector configuration contains 148 proportional counters and two Eurisol-type clover HPGe detectors. Figure 1 shows the schematic view of the experimental setup.

The detection system was commissioned in November 2016 in parasitic mode during the NP1412-RIBF123R1 main experiment. A high intensity ^{238}U beam was accelerated up to an energy of 345 MeV/nucleon at the RIKEN cyclotron accelerator complex before hitting a 5000 micron thick beryllium target to produce secondary beams by in-flight fission.

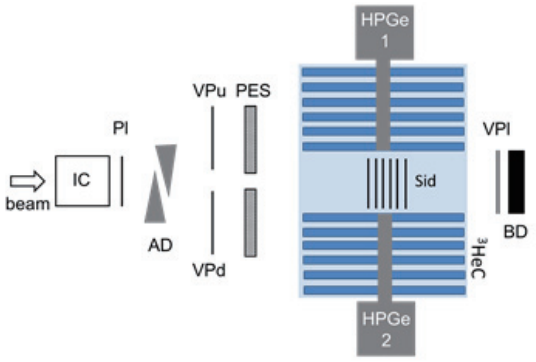

Fig. 1.: Schematic view of the experimental setup. Particle identification was carried out using the ionization chamber (IC) and the plastic scintillator (Pl) located at F11. The energy of the isotopes of interest was reduced using the adjustable degrader (AD) and then they were implanted into the silicon detectors (Sid) and their decay was measured using 166 ^{3}He counters (^{3}HeC) and the clover type HPGe detectors (HPGe1 and 2). In order to reduce the neutron background the BRIKEN array is shielded by a polyethylene wall (PES) equipped with active veto detectors (VPu and VPd). Furthermore, at the rear side of the array, a veto detector (VPl) and a beamdump (BD) are located.

The secondary radioactive beam was filtered through the BigRIPS and ZeroDregree spectrometer and implanted in the AIDA array containing 6 layers of highly segmented silicon detectors. The emitted neutrons and γ-rays following the β-decay were recorded by the BRIKEN array configured in hybrid geometry. Some of the implanted isotopes are identified as β-delayed neutron emitters with well-known P_n values, which allowed us to determine the efficiency of the array and compare it with the results of the Monte-Carlo simulations[3] and a good agreement was found. In the latter phase of the analysis, new P_n values will be obtained for isotopes with scarce or uncertain from previous experiments.

*1 RIKEN Nishina Center
*2 Instituto de Física Corpuscular
*3 Institute for Nuclear Research (Atomki)
*4 Department of Physics, Seoul National University
*5 Oak Ridge National Laboratory
*6 TRIUMF
*7 School of Physics and Astronomy, University of Edinburgh
*8 College of Science and Engineering, Central Michigan University
*9 Department of Physics and Astronomy, University of Tennessee
*10 STFC Daresbury Laboratory
*11 Department of Physics, University of Hong Kong
*12 Graduate School of Science and Technology, Niigata University
*13 Universitat Politècnica de Catalunya (UPC)

References

1) R. M. Mumpower, R. Surman, G. C. McLaughlin, A. Aprahamian, Prog. Part. Nucl. Phys. **86**, 86 (2016).
2) A. Arcones and G. Martinez Pinedo, Phys. Rev. C **83**, 045809 (2011).
3) A. Tarifeno-Saldivia et al., Jour. of Instr. **12**, P04006 (2016).
4) C. Griffin et al., POS (NIC-XIII) 097 (2014).

Search for β-delayed two and three-neutron emitters in the vicinity of N=28 using the BRIKEN array

V. H. Phong,[*1,*2] S. Nishimura,[*1] J. Agramunt,[*3] D. S. Ahn,[*1] A. Algora,[*3] H. Baba,[*1] S. Bae,[*4] N. T. Bewer,[*5] R. Caballero-Folch,[*6] T. Davinson,[*7] I. Dillmann,[*6] A. Estrade,[*1,*8] S. Go,[*9] C. J. Griffin,[*7] R. Grzywacz,[*5,*9] J. Ha,[*1,*4] O. Hall,[*7] D. Kahl,[*7] G. Kiss,[*1] M. Labiche,[*10] J. Liu,[*11] K. Matsui,[*1] B. Moon,[*12] N. Nepal,[*8] H. Sakurai,[*1] Y. Shimizu,[*1] P.-A. Söderström,[*1] H. Suzuki,[*1] B.C. Rasco,[*5] K. P. Rykaczewski,[*5] H. Takeda,[*1] J. L. Tain,[*3] A. Tarifeño-Saldivia,[*13] and A. Tolosa[*3]

The measurement of β-delayed multi-neutron emission probability (P_{2n}, P_{3n}, and so on) is an experimental challenge. Most of the existing P_{2n} values are for isotopes with masses below A=100, while only four P_{3n} values were reported so far[1]: ^{11}Li, ^{17}B and the upper limits for ^{19}B and ^{23}N. The BRIKEN project (beta-delayed neutron emission measurement at RIKEN) offers a unique opportunity to measure this rare decay mode. The BRIKEN setup, illustrated in Fig. 1, consists of an array of ^{3}He detectors embedded in a high-density polyethylene matrix as moderator,[3] surrounding a stack of silicon detectors called AIDA (Advanced Implantation Detector Array).[2] The ^{3}He array serves as an efficient neutron counter, which detects the delayed neutrons following the β decay of neutron-rich nuclei implanted in AIDA. In addition, two clover-type HPGe detectors placed close to the implantation point are employed to identify the daughter nuclei by the detection of delayed γ rays.

For the purpose of commissioning of the BRIKEN detection system for the β-delayed multi-neutron emission measurement and evaluation of the statistical errors, neutron background conditions and β-delayed γ identification, an experiment has been performed in the parasitic mode with the in-beam gamma ray experiment,[4] targeting the neutron-rich nuclei around N=28.

The secondary beam, produced by the reaction of a 345-MeV/nucleon ^{48}Ca beam on a rotating Be target, was impinged on a fixed target at the F8 focal plane surrounded by the DALI2 gamma ray detector. The reaction products and unreacted beam were transported through the ZeroDegree spectrometer and eventually reached the BRIKEN setup at the F11 focal plane.

*1 RIKEN Nishina Center
*2 Faculty of Physics, VNU Hanoi University of Science
*3 IFIC (CSIC-University of Valencia)
*4 Department of Physics, Seoul National University
*5 Oak Ridge National Laboratory
*6 TRIUMF
*7 School of Physics and Astronomy, University of Edinburgh
*8 College of Science and Engineering, Central Michigan University
*9 Department of Physics and Astronomy, University of Tennessee
*10 STFC Daresbury Laboratory
*11 Department of Physics, University of Hong Kong
*12 Department of Physics, Korea University
*13 Secció d'Enginyeria Nuclear,Universitat Politecnica de Catalunya (UPC)

Figure 2 shows a preliminary particle identification plot of RI in the ZeroDegree spectrometer, which is assumed to be implanted into the AIDA detector. In this region, the β-delayed multi-neutron emission of $^{41-43}$Si, $^{38-42}$Al and $^{35-40}$Mg predicted by Ref.[5] are expected to be measured for the first time. Moreover, the effect of the degrader setting on the neutron background can be clarified, providing useful information to optimize the background condition for the main BRIKEN experiments.

The data are currently being analyzed.

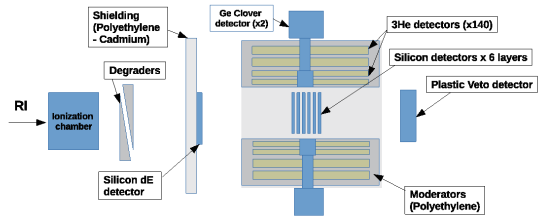

Fig. 1. A schematic view of the experimental setup.

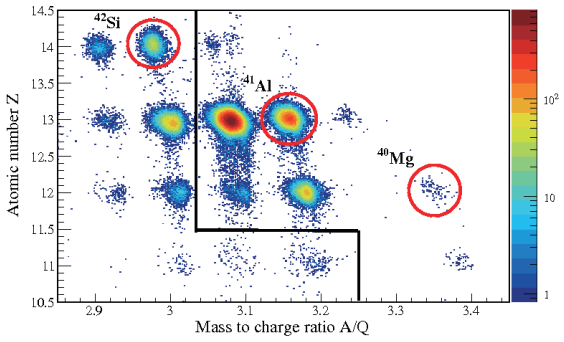

Fig. 2. A preliminary particle identification spectrum of the RI identified by the ZeroDegree spectrometer. The RI with known half lives are on the left side of the black solid line. The N=28 isotopes are tagged by red circles.

References

1) M. Birch et al., Nucl. Data Sheet **128**, 131 (2015).
2) C. J. Griffin et al.; Proc. XIII Nuclei in the Cosmos, Vol.**1** (2014), p. 97.
3) A. Tarifeño-Saldivia et al., arXiv:1606.05544.
4) NP1312-RIBF03R1
5) P. Moller et al., Phys. Rev. C **67.5**, 055802 (2013).

Initial effort to resolve isomers in MRTOF-MS via in-trap decay

P. Schury,[*1] M. Wada,[*1,*2] Y. Ito,[*2] D. Kaji,[*2] A. Takamine,[*2] H. Haba,[*2] Y. Hirayama,[*1] S. Kimura,[*1,*2,*3] H. Koura,[*2,*4] H. Miyatake,[*1] J.Y. Moon,[*7,*1] K. Morimoto,[*2] K. Morita,[*2,*5] A. Ozawa,[*2,*3] M. Reponen,[*2] T. Tanaka,[*2,*5] Y. X. Watanabe,[*1] and H. Wollnik*6

The SHE-mass project is a joint effort between KEK and RIKEN with a long-term goal of identifying new superheavy element (SHE) isotopes produced via hot fusion. It makes use of cryogenic-capable, high-purity helium gas cell to convert the energetic (5∼50 MeV) evaporation products of fusion reactions into thermal ions. The evaporation products are separated from projectile-like fragments by use of the gas-filled recoil ion separator GARIS-II[1]. The thermalized ions are transferred to a multi-reflection time-of-flight mass spectrograph[2] (MRTOF-MS) which can analyze the ions with a mass resolving power of $R_{\rm m} > 100\,000$. The SHE-mass system is described in some detail in[3].

In addition to SHE studies, it has been foreseen to use the system to study neutron-deficient isotopes from Po through Pa, where the N=126 shell-closure approaches the proton drip-line . Investigations of these nuclei have mostly been limited to α-decay studies up to now. However, the vast amount of *known* isomeric states among nuclei in this region casts some doubt on the veracity of α-decay studies and indicates a need for direct mass measurements.

Most isomeric states in this region have half-lives shorter than 1 ms, significantly shorter than the measurement cycle for MRTOF-MS. Unfortunately, many known isomers in this region have sufficiently long half-lives as to impact MRTOF-MS. Additionally, distinguishing most of these isomers from their ground states requires higher mass resolving power than is currently available from MRTOF-MS.

In the majority of cases, however, the ground state and/or the isomeric state(s) exhibit $T_{1/2} \ll 10$ s. Thus, by storing the ions in the preparation trap for an extended period before analysis in the MRTOF-MS, the isomer can decay away. We have developed a mathematical framework to use mass measurements at multiple storage times to determine the isomeric ratio and allow for precise determination of ground state masses.

As a first test of this, we used the ^{165}Ho(^{48}Ca, 7n) to produce $^{206}Fr^{2+}$ ions[4]. The duration of accumulation in the preparation trap was then varied up to 2.64 s prior to mass analysis. Unfortunately, the charge-exchange lifetime of the Fr^{2+} was short compared to the ground state decay lifetime (see Fig. 1), resulting in a complicated and ongoing analysis to determine the isomeric ratio.

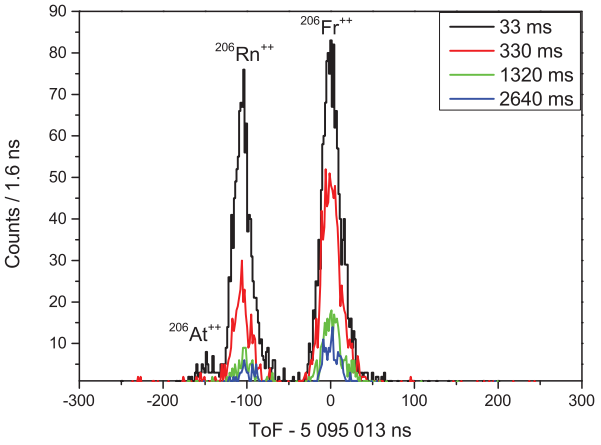

Fig. 1. ToF spectra observed for A/q=103 ions for various accumulation durations. Reductions are presumed to be caused by charge-exchange in the preparation trap.

We can use the relative intensities of observed ions as a function of accumulation time to estimate the charge exchange lifetimes in the preparation trap for doubly-charged ions of a variety of elements, listed in Table 1. The short lifetimes can be expected, as the trap is not UHV clean and operates at room temperature. In the future, we will try to repeat such studies with the traps being cryogenically cooled.

Table 1. Loss half-lives in the preparation trap. IP1 and IP2 are the first and second ionization potentials.

Ion	IP1 [eV]	IP2 [eV]	$T_{1/2}^{decay}$	$T_{1/2}^{loss}$
$^{211}Ra^{2+}$	5.3	10.14	13.2 s	>2 s
$^{206}Fr^{2+}$	4.1	22.4	16 s	422(16) ms
$^{207}Fr^{2+}$	4.1	22.4	14.8 s	414(58) ms
$^{206}Rn^{2+}$	10.7	21.4	5.67 m	183(14) ms
$^{207}Rn^{2+}$	10.7	21.4	9.25 m	216(16) ms
$^{206}At^{2+}$	9.3	17.9	30.6 m	134(32) ms
$^{207}At^{2+}$	9.3	17.9	1.81 h	157(16) ms

*1 KEK Wako Nuclear Science Center (WNSC)
*2 RIKEN Nishina Center
*3 Institute of Physics, University of Tsukuba
*4 Advanced Science Research Center, JAEA
*5 Dept. Physics, Kyushu University
*6 Dept. Chem. & BioChem., New Mexico State University
*7 Institute for Basic Science

References

1) D. Kaji et al., Nucl. Instrum. and Methods Phys. Res. B, 317 (2013) 311-314.
2) P. Schury et al., Nuclear Inst. and Methods in Physics Research B 335 (2014) 39-53.
3) P. Schury et al., Phys. Rev. C 95 (2017) 011305(R).
4) "Observation of the extraction of Fr^{2+} from a cryogenic gas cell", this volume.

Direct high-precision mass measurements of octupole-deformed nuclei with an MRTOF mass spectrograph

Y. Ito,[*1] M. Wada,[*1,*2] P. Schury,[*2] M. Rosenbusch,[*1] D. Kaji,[*1] K. Morimoto,[*1] H. Haba,[*1] Y. Hirayama,[*2] S. Kimura,[*3] H. Koura,[*1,*4] M. MacCormick,[*5] H. Miyatake,[*2] J.Y. Moon,[*2,*6] K. Morita,[*1,*7] M. Mukai,[*3] I. Murray,[*1,*5] T. Niwase,[*7] K. Okada,[*8] A. Ozawa,[*1,*3] M. Reponen,[*1] A. Takamine,[*1] T. Tanaka,[*1,*7] H. Wollnik,[*9] S. Yamaki,[*1,*10] and Y.X. Watanabe[*2]

Atomic mass is a global property that reflects the net result of all interactions in the atom. Information concerning nuclear structure can be derived by examining the binding energies and is particularly important for nuclear structure studies. The evolution as a function of proton or neutron number, often used the trend of two neutron separation energy (S_{2n}), provides information about even microscopic effects such as nuclear deformation. Theoretically, Möller et al.[1] showed that octupole contributions to the binding energy and region of octupole deformation in heavy nuclei are distributed around $Z = 85$–94 and $N = 130$–137.

We recently performed direct mass measurements of ^{223,224}Th and ^{224}Pa, which are located in the region. The radioactive ions (RI) were produced via a fusion-evaporation reaction of ^{208}Pb/^{209}Bi(^{18}O, xn) at a bombarding energy of $E_{\rm lab}^{\rm target} = 86$ MeV and transported by the gas-filled recoil ion separator GARIS-II. The RI were then transported to a multi-reflection time-of-flight mass spectrograph (MRTOF) after being thermalized in a cryogenic helium gas cell at 90 K. The MRTOF measurements were performed with a concomitant referencing method[2] and the reference ions of ^{133}Cs^{+} were used for both time-of-flight drift compensation and mass reference. By cooling the gas cell at 90 K, contaminant molecular ions were greatly suppressed; therefore, we could obtain quite a clean spectrum with ^{223,224}Th^{16}O^{++} and ^{224}Pa^{16}O^{++} (Fig. 1). Using times-of-flight for the RI and reference ions, we determined the masses using a single-reference analysis method[3] and computed mass excesses and mass deviations from AME2012.[4] The mass deviations were computed to be $\Delta m(^{223}\mathrm{Th}) = $ -124(24) keV/c^2, $\Delta m(^{224}\mathrm{Th}) = $ -130(100) keV/c^2, and $\Delta m(^{224}\mathrm{Pa}) = $ -36(35) keV/c^2, respectively. We found a significantly large deviation for ^{223}Th. The mass of ^{223}Th was evaluated by α decay Q-values along the fast multiple α decay to ^{207}Pb. We guess that some α decay goes through an unknown excited state or mis-identification of α peak. Using the measured masses, the S_{2n} for ^{223,224}Th become larger than AME2012 and enhanced a kink at $N = 133$ (Fig. 2). This may indicate an enhancement of octupole deformation in this region.

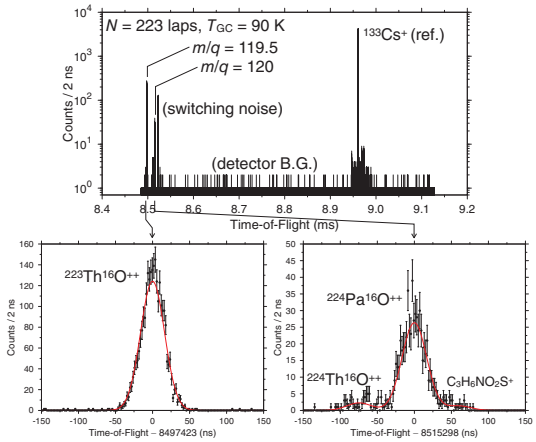

Fig. 1. (top) Full-range time-of-flight spectrum at 223 laps. RI and reference peaks are only seen on a low-rate detector background. (bottom) Enlarged spectra in the $m/q = 119.5$ and 120 regions with a Gaussian fit.

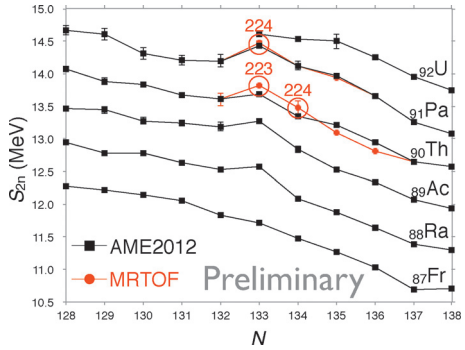

Fig. 2. S_{2n} plot in the region of this work. Black squares show AME2012 and red circles show MRTOF data.

*1 RIKEN Nishina Center
*2 Wako Nuclear Science Center (WNSC), Institute of Particle and Nuclear Studies (IPNS), High Energy Accelerator Research Organization (KEK)
*3 Department of Physics, University of Tsukuba
*4 Advanced Science Research Center, Japan Atomic Energy Research Institute (JAEA)
*5 Institut de Physique Nucléaire, Orsay
*6 Institute for Basic Science
*7 Department of Physics, Kyushu University
*8 Department of Physics, Sophia University
*9 Department of Chemistry and Biochemistry, New Mexico State University
*10 Department of Physics, Saitama University

References

1) P. Moller et al., Atom. Data Nucl. Data Tab. **109**, 1 (2016).
2) M. Wada, P. Schury, Y. Ito, and H. Wollnik, Japanese Patent No. 2016-037679 (29th February 2016).
3) Y. Ito et al., Phys. Rev. C **88**, 011306 (2013).
4) G. Audi et al., Chin. Phys. C **36**, 1287 (2012).

Precision mass measurements of proton-rich nuclei in A ∼ 60−80 region with the multireflection time-of-flight mass spectrograph

S. Kimura,[*1,*2] Y. Ito,[*2] D. Kaji,[*2] P. H. Schury,[*3] M. Wada,[*3,*2]
H. Haba,[*2] T. Hashimoto,[*4] Y. Hirayama,[*3] M. MacCormick,[*5] H. Miyatake,[*3] J. Y. Moon,[*4]
K. Morimoto,[*2] M. Mukai,[*1,*2] I. Murray,[*5,*2] A. Ozawa,[*1,*2] M. Rosenbusch,[*2] H. Schatz,[*6]
A. Takamine,[*2] T. Tanaka,[*7,*2] Y. X. Watanabe,[*3] H. Wollnik,[*8] and S. Yamaki[*9,*2]

Nuclear masses of nuclei near the proton drip line up to ^{100}Sn are crucial in determining the *rp*-process pathway which drives explosive astronomical phenomena called type I X-ray bursts (XRB). In order to compare different XRB models meaningfully, the relative mass uncertainties must be improved. Precisions of the order of $\delta m/m \lesssim 10^{-7}$ are necessary for current *rp*-process calculations[1]. Half lives of the key nuclei in the *rp*-process are of the order of several tens to several hundreds of milliseconds. The multireflection time-of-flight mass spectrograph (MRTOF) satisfies the experimental requirements for these conditions[2].

We performed mass measurements of the proton-rich nuclei in the A ∼ 60−80 region by utilizing the MRTOF combined with a gas-filled recoil ion separator GARIS-II[3] via a gas-cell and an ion transport system. To produce the proton-rich nuclei the fusion-evaporation reaction ^{nat}S(^{36}Ar,X) was used. In this reaction, it was expected that the inadequate separation in GARIS-II between the evaporation residues and the primary beam would lead to breakage of the gas cell and the GARIS-II bulkhead thin mylar windows due to irradiation damage. Therefore, we installed two independent beam stoppers[4]. We also installed a double-layered plastic scintillator combined with copper energy degraders to suppress the low energy β-rays ($E_\beta \lesssim 4$ MeV) at the GARIS-II focal plane for the β-activity search. The energy and maximum intensity of the $^{36}Ar^{10+}$ beam were 3.30 MeV/nucleon and 3 particle μA, respectively. The average target thickness of $^{nat}S_2Mo$ on Ti backing was 1.9 mg/cm^2.

Figure 1 shows the intensity distribution of β-activities as a function of magnetic rigidity. Mass measurements were performed with two different GARIS-II settings, $B\rho = 0.86$ Tm and $B\rho = 1.01$ Tm. The settings corresponded, respectively, to the sulfur reaction products and unexpected reaction products on the titanium backing. We found two dozen isotopes in the time-of-flight spectra of the MRTOF with clear peaks. The nuclear masses were determined by the single-reference method; thus, in each isobaric series, we utilized an isotope as a mass reference. The summary of the preliminary results is shown in Fig. 2.

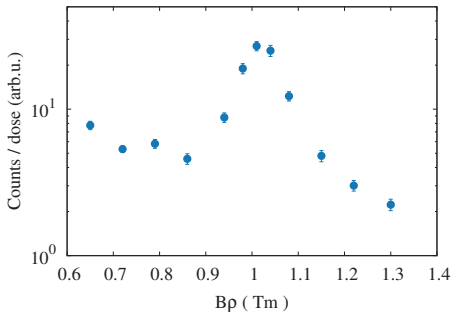

Fig. 1. Intensity distribution of β-activities as a function of magnetic rigidity.

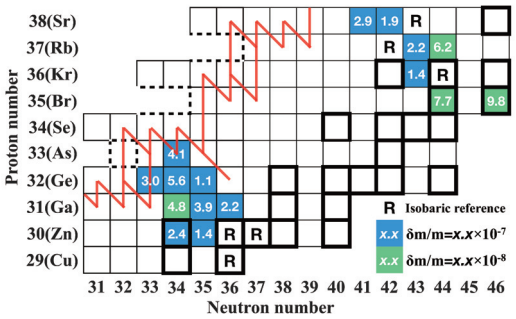

Fig. 2. Summary of the mass measurements. The bold-line boxes indicate the stable isotopes. The dashed lines indicate the proton drip line. The color-coded boxes indicate the mass precision of measurements: a precision of 10^{-7} is indicated by blue and a precision of 10^{-8} is indicated by green. The isotopes labeled "R" are used as isobaric references. The red line represents the *rp*-process pathway, which has a mass fraction greater than 10%[5].

We successfully measured nuclear masses with the required precision under the worse separation condition in GARIS-II. We must now proceed to the more proton-rich side to improve the understanding of the *rp*-process in XRBs.

*1 Institute of Physics, University of Tsukuba
*2 RIKEN Nishina Center
*3 Wako Nuclear Science Center (WNSC), Institute of Particle and Nuclear Studies (IPNS), High Energy Accelerator Research Organization (KEK)
*4 Institute for Basic Science
*5 Institut de Physique Nucléaire, Orsay
*6 Department of Physics and Astronomy and National Superconducting Cyclotron Laboratory, Michigan State University
*7 Department of Physics, Kyushu University
*8 New Mexico State University
*9 Department of Physics, Saitama University

References

1) H. Schatz, IJMS **349-350**, 181 (2013).
2) P. H. Schury et. al., NIM B **335**, 39 (2014).
3) D. Kaji et. al., NIM B **317**, 311 (2013).
4) S. Kimura et. al., in this report.
5) H. Schatz et. al., PRL **86**, 3471 (2001).

Study of barrier distribution in the reaction ^{48}Ca,^{50}Ti+^{208}Pb and ^{48}Ca+^{248}Cm at RIKEN-GARIS

T. Tanaka,[*1,*2] Y. Narikiyo,[*1,*2] K. Morita,[*1,*2] K. Fujita,[*1,*2] D. Kaji,[*1] K. Morimoto,[*1] S. Yamaki,[*1,*3] Y. Wakabayashi,[*1] K. Tanaka,[*1,*4] M. Takeyama,[*1,*5] A. Yoneda,[*1] H. Haba,[*1] K. Komori,[*1] S. Yanou,[*1] B. JP. Gall,[*1,*6] Z. Asfari,[*1,*6] H. Faure,[*1,*6] H. Hasebe,[*1] M. Huang,[*1] J. Kanaya,[*1] M. Murakami,[*1,*7] A. Yoshida,[*1] T. Yamaguchi,[*3] F. Tokanai,[*1,*5] T. Yoshida,[*1,*5] S. Yamamoto,[*1,*2] Y. Yamano,[*1,*2] K. Watanabe,[*1,*2] S. Ishizawa,[*1,*5] M. Asai,[*8] R. Aono,[*7] S. Goto,[*7] K. Katori,[*1] and K. Hagino[*9]

In order to study the nucleus-nucleus interaction for the synthesis of superheavy elements,[1] we measured excitation functions for the quasielastic scattering of ^{48}Ca,^{50}Ti+^{208}Pb and ^{48}Ca+^{248}Cm. The quasielastic scattering events were clearly separated from background events by using the gas-fillled recoil ion separator GARIS and guided to focal-plane detectors.

The barrier distributions were derived by taking the first energy derivative of the excitation function. The experimental results were well reproduced by coupled-channel calculations[2] taking account of vibrational and/or rotational excitations of nuclei and neutron transfer before the capture process (Figs. 1 and 2).

The centroids of the barrier distributions are shown to coincide with the peak of evaporation residue cross sections for the reaction ^{48}Ca,^{50}Ti+^{208}Pb.[3–6] This implies that, for these Pb-based cold fusion reactions, the peak of the cross section is in good agreement with that of the barrier distributions after one takes into account several experimental conditions such as measured energy step, which is typically 2.0 MeV, and energy coverage region, which is typically 1.0 MeV, of the target thickness.

In contrast, for the hot fusion reaction ^{48}Ca+^{248}Cm, the peak of the cross section[7,8] is shifted to the above barrier region. The barrier distribution of the above barrier region corresponds to side-by-side collision. In the compound nucleus (CN) formation process, the probability of CN formation is increased by side-by-side collision because the probability depends on the distance to the center of nuclei. It is therefore important to combine the barrier distribution study with studies on quasi-fission and evaporation processes in order to predict the optimum incident energy for a search of undiscovered superheavy elements by the hot fusion reaction.

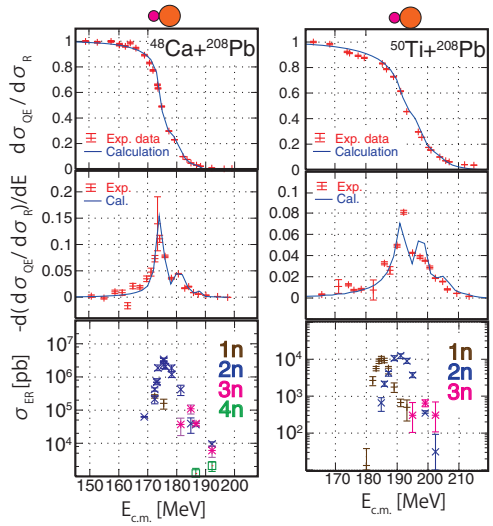

Fig. 1. Measured excitation functions of quasielastic scattering cross section relative to Rutherford cross section (upper panels) and the barrier distributions (middle panels). The lower panels show the evaporation residue cross sections for these reactions.

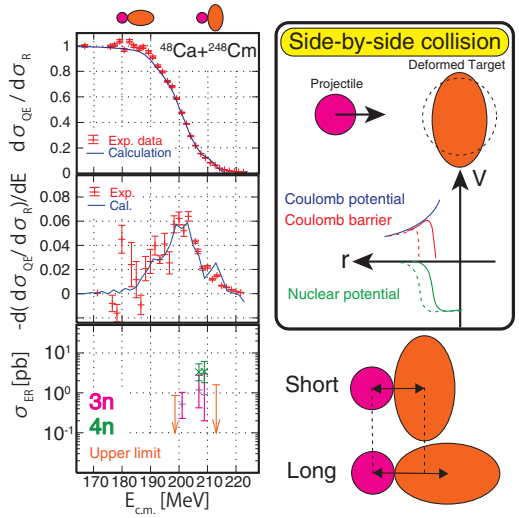

Fig. 2. Left side panels show same as Fig. 1. Right side panels show the explanation of Side-by-side collision.

*1 RIKEN Nishina Center
*2 Kyushu University
*3 Saitama University
*4 Tokyo University of Science
*5 Yamagata University
*6 IPHC-DRS/Université de Strasbourg
*7 Niigata University
*8 Advanced Science Research Center, JAEA
*9 Tohoku University

References
1) S. Mitsuoka et al., Phys. Rev. Lett. **99**, 182701 (2007).
2) K. Hagino et al., Comput. Phys. Commun. **123**, 143 (1999).
3) A. V. Belozerov et al., Eur. Phys. J. A **16**, 447 (2003).
4) H. W. Gaggeler et al., Nucl. Phys. A **502c**, 561 (1989).
5) Yu. Ts. Oganessian et al., Phys. Rev. C **64**, 054606 (2001).
6) F. P. Heßberger et al., Eur. Phys. J. A **16**, 57 (2001).
7) S. Hofmann et al., Eur. Phys. J. A **48**, 62 (2012).
8) Yu. Ts. Oganessian et al., Phys. Rev. C **70**, 064609 (2004).

Measurement of barrier distribution for ^{50}Ti,^{51}V+^{248}Cm, and ^{51}V+^{208}Pb reactions

T. Niwase,[*1,*2] Y. Yamano,[*1,*2] K. Watanabe,[*1,*2] K. Morita,[*1,*2] K. Fujita,[*1,*2] T. Hirano,[*1,*2] S. Mitsuoka,[*1,*2] K. Morimoto,[*1] D. Kaji,[*1] and H. Haba[*1]

Barrier distribution[1–3] in a heavy-ion induced fusion reaction yields information about the nucleus-nucleus interaction for the synthesis of heavy-nuclides, especially the capture process. Comprehensive studies on the barrier distribution, which is derived from taking the first derivative of the quasi elastic(QE) cross-section relative to the Rutherford scattering cross section, have always been performed for several heavier reactions.[4,5] Toward future research for new superheavy elements, in this work, the QE cross-section in reactions of ^{50}Ti, ^{51}V+^{248}Cm and ^{51}V+^{208}Pb were investigated to understand these fusion mechanisms.

The projectiles of ^{50}Ti with a charge state of 11^+ and ^{51}V charge state of 11^+ were supplied by the RILAC. These ions were extracted from the 18-GHz ECR ion source. A $^{248}Cm_2O_3$ target with a thickness of 210 μg/cm^2 was prepared by electrodeposition onto a titanium backing foil of 0.9 mg/cm^2. A ^{208}Pb target of 400 μg/cm^2 was prepared by vacuum evaporation on a 60 μg/cm^2 carbon foil. The beam energies for the ^{50}Ti+^{248}Cm, ^{51}V+^{248}Cm and ^{51}V+^{208}Pb measurements were 193 to 241 MeV, 194 to 247 MeV, and 176 to 224 MeV, respectively. The energy loss of the beam in the target was about 1 MeV. The excitation functions were obtained for steps of 2 MeV in the center-of-mass energy. The beam dose was monitored by measuring the Rutherford scattered projectiles using a Si detector mounted at 45° with respect to the beam axis. Target nuclides, which were recoiled out of the target by the backward scattering (s-wave scattering), were separated in-flight from projectiles and other charged-particles using a gas-filled recoil ion separator GARIS and guided to a focal plane detection system.[6] Then, the target nuclides were clearly identified by measuring the time-of-flight and kinetic energy of the recoils.

The normalized QE cross sections for the ^{51}V+^{208}Pb reaction were obtained by assuming the ratio of the differential cross section of the QE to the Rutherford scattering cross section $((d\sigma/d\Omega)_{QE}/(d\sigma/d\Omega)_R)$ to be one at sufficiently low energy, which is shown in Fig. 1(a). The barrier distribution obtained by differentiating with respect to energy is shown in Fig. 1(b). Comparison of the measured data with an optical potential calculation only (dashed lines) and a coupled channel calculation (solid lines) using CCFULL software[7] are shown in both figures. It was found that the data points are well reproduced when the coupling effects of the first and second excited state of ^{208}Pb and the second excited state of ^{51}V are considered in the calculation, so excited states contributed to these reactions.

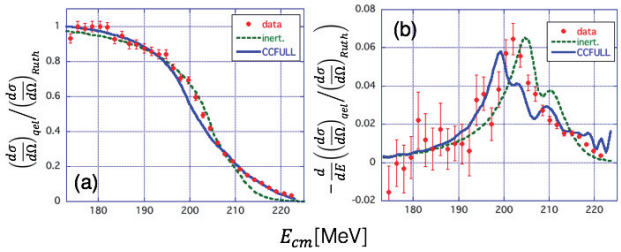

Fig. 1. Normalized quasi-elastic cross section and barrier distribution of the ^{51}V+^{208}Pb reaction.

The QE cross sections of the ^{50}Ti+^{248}Cm and ^{51}V+^{248}Cm reactions are shown in Figs. 2(a) and (b), respectively. Unfortunately, we could not measure the data in energy higher than 5.8 MeV/nucleon because of the lack of acceleration voltage of RILAC. In both figures, the calculations of the optical model and the coupled channel including the coupling effects of the excited state of the target and projectiles are also given as dashed and solid lines, respectively. However, we cannot yet discuss the channel effect as nuclear deformation and excitation. Data with higher beam energies are necessary for further discussion.

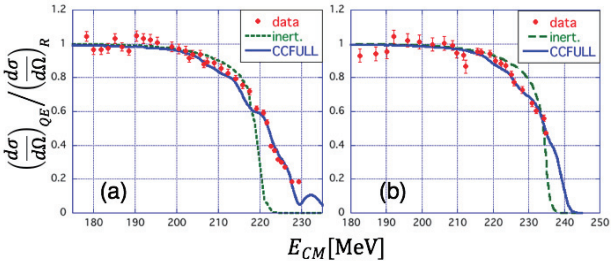

Fig. 2. Normalized quasi-elastic cross section of the ^{50}Ti+^{248}Cm (a) and ^{51}V+^{248}Cm (b) reactions.

*1 RIKEN Nishina Center
*2 Department of Physics, Kyushu University

References
1) M. V. Andres et al., Phys. Lett. B **202**, 292 (1988).
2) J. R. Leigh et al., Phys. Rev. C **52**, 3151 (1995).
3) H. Timmers et al., Nucl. Phys. A **584**, 190 (1995).
4) S. Mitsuoka et al., Phys. Rev. Lett. **99**, 182701 (2007).
5) T. Tanaka et al., RIKEN Accel. Prog. Rep. 50 (2016).
6) K. Morita et al., Eur. Phys. J. A **21**, 257 (2004).
7) K. Hagino et al., Comput. Phys. Commun.**123**, 143 (1999).

Yield development of KEK isotope separation system

Y.X. Watanabe,[*1] Y. Hirayama,[*1] M. Mukai,[*2,*3] Y. Kakiguchi,[*1] P. Schury,[*1] M. Oyaizu,[*1] H. Miyatake,[*1] M. Wada,[*1,*2] M. Ahmed,[*1,*3] S. Kimura,[*2,*3] J.Y. Moon,[*4] J.H. Park,[*4] H. Ishiyama,[*4] S.C. Jeong,[*4] and A. Taniguchi[*5]

We have been developing KEK isotope separation system (KISS)[1] for lifetime measurements of neutron-rich nuclei around $N = 126$, relevant to r-process nucleosynthesis.[2] The multinucleon transfer (MNT) reaction between the ^{136}Xe beam and ^{198}Pt target was used at KISS, and it is one of the promising candidates to efficiently produce those neutron-rich nuclei.[3] The target was located in a gas cell, and the reaction products were stopped and neutralized in the argon gas filled in the gas cell. They were transported to the exit of the gas cell by laminar gas flow, where they were irradiated by the lasers to be ionized for a specific element by laser resonance ionization technique. Those extracted ions were mass-separated and transported to the measurement area for β-decay spectroscopy.

So far, we have successfully extracted radioactive isotopes (RIs) of ^{199}Pt and ^{196,197,198}Ir.[4] The accessible isotopes were limited to the vicinity of the ^{198}Pt target because of the low extraction efficiency ($\sim 1\times10^{-4}$) and limited beam intensity ($\sim$20 pnA) to prevent heat damage at the target. The low extraction efficiency might be due to the re-neutralization of the laser-ionized isotopes caused by the radiation from the dense plasma in the argon gas, which is induced by the primary beam.[5] We have developed a doughnut-shaped gas cell and a rotating target to accept a more intense beam without injecting it into the gas cell.

In parallel, we have started to investigate other possible reaction pairs to achieve more efficient production of the desired isotopes. GRAZING calculations[6] indicate larger cross sections using the ^{238}U beam as compared with the ^{136}Xe beam. The first attempt to extract RIs produced in the MNT reactions between the ^{238}U beam and the ^{198}Pt target at KISS is reported here.

The well-studied fixed-target gas cell was used in this measurement for comparison with ^{136}Xe beam data. A ^{198}Pt target with a thickness of 11 mg/cm^2 in the gas cell was bombarded by the ^{238}U beam accelerated up to 10.75 MeV/nucleon by RRC. The beam energy on the target was tuned by energy degraders to approximately 8.5 MeV/nucleon, which is the optimal value from the GRAZING calculations. Three plastic scintillator telescopes were used to detect β-rays by measuring the extracted RIs, which were implanted into aluminized Mylar tape at the detection area to identify them by measuring their lifetimes.

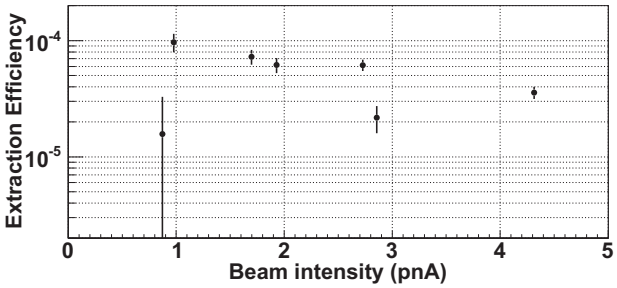

Fig. 1. Beam intensity dependence of extraction efficiency measured for ^{199}Pt.

Only one species of isotopes, ^{199}Pt, was identified in this measurement because of the low extraction efficiency and limited beam intensity. To investigate the intensity limitation, the beam intensity dependence of the extraction efficiency was measured. Figure 1 shows the result. The extraction efficiency was defined as the ratio the between number of extracted ions in the measurements and the number of ions ejected from the target in the calculations. The extraction efficiency was 1×10^{-4} at a beam intensity of approximately 1 pnA, and it decreased as the beam intensity increased. The absolute extraction efficiency and its beam-intensity dependence are similar to those in the case with the ^{136}Xe beam. Because the beam intensity was limited up to 5 pnA by the heat damage of the energy degrader foils and the target foil, the extraction efficiency was not available for higher beam intensity. In the next experiment, we will measure the extraction rates at higher intensities using rotating degraders and target with the doughnut-shaped gas cell for ^{199}Pt and other RIs.

*1 Wako Nuclear Science Center (WNSC), Institute of Particle and Nuclear Studies (IPNS), High Energy Accelerator Research Organization (KEK)
*2 RIKEN Nishina Center
*3 Department of Physics, University of Tsukuba
*4 Institute for Basic Science (IBS)
*5 Research Reactor Institute, Kyoto University

References

1) Y. Hirayama et al., Nucl. Instr. Meth. B **353**, 4 (2015).
2) S. C. Jeong et al., KEK Report 2010-2 (2010).
3) Y. X. Watanabe et al., Phys. Rev. Lett. **115**, 172503 (2015).
4) Y. Hirayama et al., RIKEN Accel. Prog. Rep. **49**, 148 (2016).
5) M. Huyse et al., Nucl. Instrum. Methods Phys. Res. Sect. B **187**, 535 (2002).
6) A. Winther, Nucl. Phys. A **572**, 191 (1994); Nucl. Phys. A **594**, 203 (1995); Program GRAZING, http://www.to.infn.in/ nanni/grazing/

Proton-proton correlations in distinguishing the two-proton emission mechanism of ^{23}Al and ^{22}Mg†

D. Q. Fang,[*1] Y. G. Ma,[*1] X. Sun,[*1] P. Zhou,[*1] Y. Togano,[*2] N. Aoi,[*2] H. Baba,[*2] X. Z. Cai,[*1] X. G. Cao,[*1] J. G. Chen,[*1] Y. Fu,[*1] W. Guo,[*1] Y. Hara,[*3] T. Honda,[*3] Z. Hu,[*4] K. Ieki,[*3] Y. Ishibashi,[*2*5] Y. Ito,[*5] N. Iwasa,[*2*6] S. Kanno,[*2] T. Kawabata,[*7] H. Kimura,[*8] Y. Kondo,[*2] K. Kurita,[*3] M. Kurokawa,[*2] T. Moriguchi,[*5] H. Murakami,[*2] H. Ooishi,[*5] K. Okada,[*3] S. Ota,[*7] A. Ozawa,[*5] H. Sakurai,[*2] S. Shimoura,[*7] R. Shioda,[*3] E. Takeshita,[*2] S. Takeuchi,[*2] W. Tian,[*1] H. Wang,[*1] J. Wang,[*4] M. Wang,[*4] K. Yamada,[*2] Y. Yamada,[*3] Y. Yasuda,[*5] K. Yoneda,[*2] G. Q. Zhang,[*1] and T. Motobayashi[*2]

Two-proton emission is a very interesting but complicated process occurring in nuclei close to the proton drip line. However, it is difficult to distinguish between the two-body sequential and three-body simultaneous emission mechanism in two-proton emission processes.[1)] In these two mechanisms, the emission time of the two protons is quite different. For the three-body simultaneous emission, the two protons are emitted almost simultaneously, while the two protons are emitted one by one in sequential emission. In heavy-ion collisions, two-particle interferometry is a well-recognized and powerful method to extract the source size and particle emission time and to probe and disentangle different reaction mechanisms.

An experiment was performed to study the proton-proton momentum correlation function for the three-body decay channels $^{23}\mathrm{Al} \rightarrow \mathrm{p} + \mathrm{p} + {}^{21}\mathrm{Na}$ and $^{22}\mathrm{Mg} \rightarrow \mathrm{p} + \mathrm{p} + {}^{20}\mathrm{Ne}$ using the RIPS beamline at the RI Beam Factory (RIBF) operated by RIKEN Nishina Center and Center for Nuclear Study, the University of Tokyo.

The proton-proton momentum correlation function (C_{pp}) was obtained by the event-mixing method with an iterative calculation. The source size and proton emission time information was extracted by comparing the CRAB calculation with the experimental C_{pp} data.[2)] In the calculation, the space and time profile of the source was assumed to be a Gaussian as $S(r,t) \sim \exp(-r^2/2r_0^2 - t/\tau)$, with r_0 referring to the source size and τ referring to the emission-time difference between the protons. As shown in Fig. 1, the source sizes were approximately $2 \sim 3$ fm for both ^{23}Al and ^{22}Mg based on the minimun reduced chi-square. However, the parameter τ is quite different for these two nuclei. For the reaction channel $^{23}\mathrm{Al} \rightarrow \mathrm{p} + \mathrm{p} + {}^{21}\mathrm{Na}$, as shown in Fig. 1(a), τ is very large (> 600 fm/c), while for the reaction channel $^{22}\mathrm{Mg} \rightarrow \mathrm{p} + \mathrm{p} + {}^{20}\mathrm{Ne}$, as shown in Fig. 1(b), τ is very small

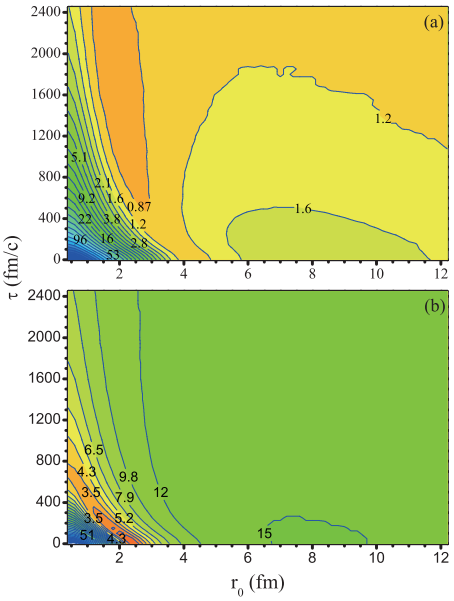

Fig. 1. Contour plot of the reduced chi-square (χ^2/ν, where ν is the number of degrees of freedom) obtained from fitting the experimental C_{pp} data by the CRAB calculation for the reaction channel of $^{23}\mathrm{Al} \rightarrow \mathrm{p} + \mathrm{p} + {}^{21}\mathrm{Na}$ (a) and $^{22}\mathrm{Mg} \rightarrow \mathrm{p} + \mathrm{p} + {}^{20}\mathrm{Ne}$ (b).

(< 50 fm/c). This implies that the emission-time difference between two protons for ^{23}Al and ^{22}Mg was quite different. For ^{23}Al, the two protons were emitted at very different times, i.e., the mechanism is sequential emission. For ^{22}Mg, the two protons were emitted almost simultaneously, i.e., the mechanism was essentially simultaneous. Based on the previous results[1)] and this work, it is possible to distinguish clearly the mechanism of two-proton emission by investigating on the proton-proton momentum correlation function, the two-proton relative momentum, and opening-angle distributions. The method presented in this work was applied for the first time to two-proton emitters, and was shown to provide new and valuable information on the mechanism of two-proton emission.

References
1) Y. G. Ma et al., Phys. Lett. B **743**, 306 (2015).
2) S. Pratt et al., Nucl. Phys. A **566**, 103c (1994).

† Condensed from the article in Phys. Rev. C **94**, 044621 (2016)

*1 Shanghai Institute of Applied Physics, CAS
*2 RIKEN Nishina Center
*3 Department of Physics, Rikkyo University
*4 Institute of Modern Physics, CAS
*5 Institute of Physics, University of Tsukuba
*6 Department of Physics, Tohoku University
*7 Center for Nuclear Study (CNS), University of Tokyo
*8 Department of Physics, University of Tokyo

Magnetic moment of the $13/2^+$ isomeric state in ^{69}Cu: Spin alignment in a single-nucleon removal reaction†

A. Kusoglu,[*1,*2,*3] G. Georgiev,[*1] C. Sotty,[*1,*4] D. L. Balabanski,[*3] A. Goasduff,[*1,*5] Y. Ishii,[*6] Y. Abe,[*7,*8] K. Asahi,[*6] M. Bostan,[*2] R. Chevrier,[*9] M. Chikamori,[*6] J. M. Daugas,[*9] T. Furukawa,[*7,*10] H. Nishibata,[*11] Y. Ichikawa,[*6,*7] Y. Ishibashi,[*7,*8] R. Lozeva,[*12] H. Miyatake,[*6] D. Nagae,[*7,*8] T. Nanao,[*6] M. Niikura,[*13,*14] T. Niwa,[*8] S. Okada,[*8] A. Ozawa,[*8] Y.Saito,[*8] H. Shirai,[*6,*7] H. Ueno,[*7] D.T. Yordanov,[*14,*15] and N. Yoshida[*6,*7]

The ^{69}Cu nucleus, having one proton outside the ^{68}Ni core, is a good probe for both the robustness of the $Z = 28$ shell closure and a possible enhancement of the $N = 40$ sub-shell gap. In order to provide direct information on the composition of the wave function of the $(13/2^+)$ isomeric state in ^{69}Cu and to compare it to large-scale shell-model calculations, the g factor of the state of interest was measured.

The experiment was performed at RIKEN with the RIPS fragment separator. A ^{70}Zn primary beam at 63.13 MeV/u was incident on a 101.46 mg/cm^2 ^{9}Be target at the entrance of the RIPS separator to produce the nuclei of interest. An Al achromatic wedge-shaped degrader of 84.99 mg/cm^2 was placed at the F1 focal plane of RIPS in order to select the fragments of interest. The purity of the secondary beam was adjusted by specific slit openings at the F2 and F3 focal planes.

The ^{69}Cu nuclei, produced by single-proton removal from the primary beam, were implanted in an annealed 1 mm thick Cu foil, positioned at the center of the setup between the poles of an electromagnet. An external magnetic field of 0.50(1) T was applied to induce Larmor precession of the nuclei. Four coaxial HPGe γ-ray detectors were placed in a horizontal plane at polar angles $\theta = \pm 135°$ and $\theta = \pm 45°$ with respect to the beam axis in order to detect the intensity variation of the γ-rays as a function of time. A plastic-scintillator detector was used to provide the start $t = 0$ signal for the isomeric lifetime measurement.

The time-dependent perturbed angular distribution (TDPAD) method was used to extract the magnetic moment of the $(13/2^+)$ state in ^{69}Cu. Its g factor was obtained by fitting the sum of the 189.7-keV and 1710.6-keV $E2$ transitions (see Fig. 1(a)) with a standard $R(t)$ function. As a result, a more precise value for $g(13/2^+) = +0.248(9)$ was deduced in the present measurement compared to a previous study.[1)] The $R(t)$ function for the sum of the 470.2-keV, 485.7-keV, 657.6-keV, and 1212.6-keV $M1$ transitions, which have an opposite sign compared to the $E2$ transitions, is also shown in Fig. 1(b). The experimentally observed degree of spin alignment for the state of interest was obtained as $A = -3.3(9)\%$ in single-nucleon removal reactions even for multi-quasiparticle states. ANTOINE[2)] shell-model calculations performed using the JUN45 and jj44b interactions both fall close to the measured g factor, indicating a mixed configuration with significant contributions from particle-hole excitations across the $N = 40$ sub-shell gap.

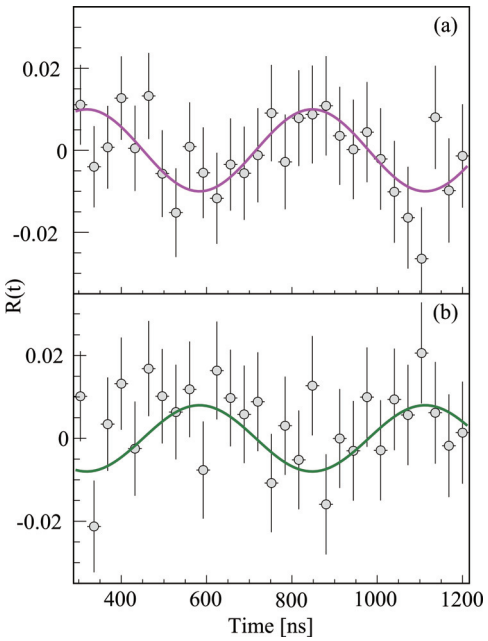

Fig. 1. $R(t)$ functions for (a) the sum of the $E2$ transitions and (b) the sum of $M1$ transitions following the decay of the $(13/2^+)$ isomer in ^{69}Cu for $\theta = \pm 135°$ detector combination.

† Condensed from the article in Phys. Rev. C **93**, 054313 (2016)

*1 CSNSM, CNRS/IN2P3, Univ. Paris-Sud
*2 Department of Physics, Istanbul University
*3 ELI-NP, IFIN-HH
*4 DFN, IFIN-HH
*5 INFN, LNL
*6 Department of Physics, Tokyo Institute of Technology
*7 RIKEN Nishina Center
*8 Department of Physics, University of Tsukuba
*9 CEA, DAM, DIF
*10 Department of Physics, Tokyo Metropolitan University
*11 Department of Physics, Osaka University
*12 IPHC, Université de Strasbourg
*13 Department of Physics, University of Tokyo
*14 IPN, CNRS-IN2P3, Univ. Paris-Sud
*15 MPIK

References

1) G. Georgiev et al., J. Phys. G **28**, 2993 (2002).
2) E. Caurier et al., Rev. Mod. Phys. **77**, 427 (2005).

Search for low-lying resonances in ^{10}N structure with proton resonant scattering

E. Milman,[*1,*2] T. Teranishi,[*3] S. Sakaguchi,[*1,*3] K. Abe,[*4] Y. Akiyama,[*1,*3] D. Beaumel,[*1,*5] S. Chebotaryov,[*1,*2] T. Fukuta,[*1,*3] A. Galindo-Uribarri,[*6] S. Hayakawa,[*4] S. Hwang,[*7] Y. Ichikawa,[*1] N. Imai,[*4] D. Kahl,[*4] R. Kaku,[*1,*3] T. Kaneko,[*1,*8] D. Kim,[*1,*9] W. Kim,[*3] N. Kitamura,[*4] Y. Norimatsu,[*1,*3] E. Romero-Romero,[*6] D. Sakae,[*1,*3] Y. Sakaguchi,[*4] M. Sasano,[*1] K. Tateishi,[*1] T. Uesaka,[*1] K. Yamada,[*1,*8] and H. Yamaguchi[*4]

Theoretically, four low-lying ^{10}N levels are expected as broad and overlapping resonances[1,2]. The level structure of ^{10}N is very important to understand the structure of its mirror nuclei,^{10}Li. The information of ^{10}Li levels can be used to constrain the ^{9}Li+n potential, which is required for constructing the three-body model of the borromean nucleus ^{11}Li.

We proposed the measurement of the excitation function of the (differential) cross section and vector analyzing power (A_y) for the ^{9}C+p resonant scattering reaction to determine these broad resonances[3].

In September 2015, a test ^{9}C+p resonant scattering experiment was conducted at RIPS[4], where the production of a low-energy ^{9}C beam was tested and the excitation function was measured. The production of the 4.17 MeV/nucleon ^{9}C beam is described in Ref.[5].

The thick-target method in inverse kinematics[6] was used for the measurement, where the excitation function of the cross section is scanned with a single beam energy utilizing the energy loss of the beam particle in the target. The range of center-of-mass energy is set to 1−5 MeV to cover the theoretically expected ground state of ^{10}N and several excited states.

A 14.85 mg/cm^2 polyethylene film with a size of 50×50 mm^2 was used as the secondary target. An 18.78 mg/cm^2 thick carbon film was used as well to evaluate the number of background events produced in the interaction of ^{9}C with carbon in the polyethylene target. The outgoing particles were detected by two telescopes placed at 22.5° and −16°. The distances between the target and telescopes were 18 cm and 24 cm for the 22.5° telescope (Tel.1) and −16° telescope (Tel.2) respectively. Each telescope consisted of three layers of silicon semiconductor detectors (SSDs). The respective thicknesses of SSDs were 46 μm, 1.5 mm, and 1.5 mm for Tel.1 and 57 μm, 1.5 mm, and 1.5 mm for Tel.2. The sensitive area of each SSD was 48 × 48 mm^2 which covered ±6.2° and ±4.8° in the laboratory frame for Tel.1 and Tel.2, respectively. Double-sided strip silicon detectors were used as the first layer of the SSDs in the telescopes to determine the scattering angle of the particles. The particles were identified by the ΔE – E method. The protons with energy below 2.2 MeV were identified by the TOF – E method using the timing information of the event.

Center-of-mass energy spectra were deduced from the measured proton energy and the scattering angle on an event-by-event basis by assuming the kinematics of elastic scattering and by considering the energy losses of both the incident heavy ion and the outgoing proton in the target. The energy resolution in the center-of-mass frame was estimated to be 150 keV in sigma.

The main background sources in the experiment were reactions of beam particles with carbon in the target and beta-delayed protons from the decay of ^{9}C ions stopped in the target. The latter contribution was evaluated by selecting events with a shifted timing, since the coincidence rate for a beam particle and a beta-delayed proton has an accidental character. The excitation spectrum (Fig. 1) of the ^{9}C+p resonant scattering was obtained by subtracting the carbon contribution and the "beta-delayed" background from the spectrum measured on the polyethylene target.

Resonance parameters will be extracted by an R-matrix analysis of the spectra.

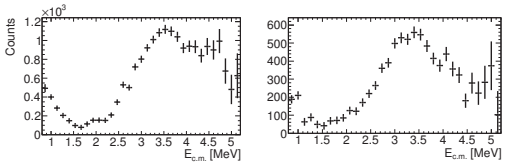

Fig. 1. Preliminary excitation spectra of the ^{9}C+p resonant scattering measured by Tel.1 (left) and Tel.2 (right).

*1 RIKEN Nishina Center
*2 Department of Physics, Kyungpook National University
*3 Department of Physics, Kyushu University
*4 CNS, The University of Tokyo
*5 IPN Orsay
*6 Oak Ridge National Laboratory
*7 JAEA
*8 Department of Physics, Toho University
*9 Department of Physics, Ewha Womans University

References

1) S. Aoyama, K. Kato, K. Ikeda, Phys. Lett. B **414**, 13 (1997).
2) E. Caurier et al., Phys. Rev. C **66**, 024314 (2002).
3) T. Teranishi et al., AIP Conf. Proc. **1525**, 552 (2013).
4) T. Kubo et al., Nucl. Instr. Meth. B **70**, 309 (1992).
5) E. Milman et al., RIKEN Accel. Prog. Rep. **49**, 160 (2015).
6) K.P. Artemov et al., Sov. J. Nucl. Phys. **52**, 408 (1990).

β-NMR measurements of ^{21}O

A. Gladkov,[*1,*2] Y. Ishibashi,[*1,*3] H. Yamazaki,[*1] Y. Ichikawa,[*1] A. Takamine,[*1] H. Nishibata,[*1] K. Asahi,[*1] T. Sato,[*1] W. Y. Kim,[*2] T. Fujita,[*1,*4] L. C. Tao,[*1,*5] T. Egami,[*1,*6] D. Tominaga,[*1,*6] T. Kawaguchi,[*1,*6] M. Sanjo,[*1,*6] W. Kobayashi,[*1,*6] K. Imamura,[*1,*7] Y. Nakamura,[*1,*7] G. Georgiev,[*8] J. M. Daugas,[*1,*9] and H. Ueno[*1]

Oxygen nuclear magnetic resonance (NMR) serves as a powerful tool to realize the atomic-scale properties of a vast variety of oxygen-containing materials. Such studies, however, have been so far complicated by different objective limitations such as low natural abundance of the NMR-active ^{17}O isotope, and difficulties and costliness of the isotopic enrichment. Alternatively, the ^{13}O and ^{19}O isotopes with known values of nuclear moments would seem appropriate to be used in β-ray-detected nuclear magnetic resonance (β-NMR) studies. However, the use of these isotopes also has strong disadvantages such as low beam purity in case of proton-rich ^{13}O and relatively long lifetime of ^{19}O($T_{1/2}$ = 26.5 s) leading to the insufficient NMR-signal intensity. All these aspects make ^{21}O a good candidate to be used as a probe to investigate the structure and properties of oxide-based systems. As a first step for such studies, the electromagnetic moments of this isotope must be determined.

In the present research, we measured the ground-state magnetic dipole moment and electric quadrupole moment of the ^{21}O isotope. The experiment was carried out using the projectile-fragment separator RIPS at the RIBF facility. A secondary beam of ^{21}O was produced in the projectile fragmentation reaction involving one neutron pick-up reaction of a ^{22}Ne beam at 69A MeV on a 1.0-mm-thick Be target. The two-stage isotope separation through the momentum and momentum-loss analyses by RIPS was applied to purify the ^{21}O beam. The momentum window and emission angle of the primary beam were selected to be $p_F = p_0 \times (0.97 \pm 0.03)$ and $\theta_F > 2.1°$, respectively.

Electromagnetic moments were measured by means of the β-NMR/NQR method in combination with the adiabatic fast passage (AFP) technique[1]. In the g-factor measurements the beam was implanted into the 0.5-mm-thick CaO stopper placed at the center of the dipole magnet of the β-NMR system that provided a static magnetic field of ∼500 mT. Some of the obtained NMR spectra are presented in Fig. 1. The NQR measurements, in turn, require the presence of the electric field gradient (EFG) in the medium.

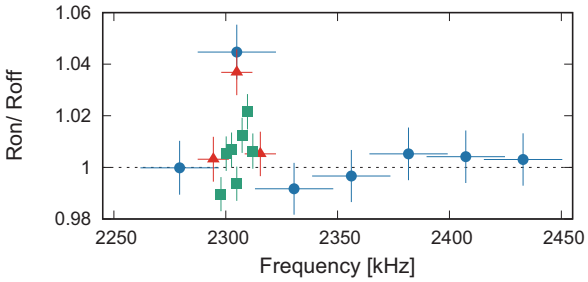

Fig. 1. β-NMR spectra of ^{21}O in a CaO crystal. Frequency sweeps with the widths of 35 kHz, 14 kHz and 3 kHz are plotted with blue circles, red triangles and green squares, respectively. During the experiment the total frequency range from 1956 kHz to 2445 kHz was scanned.

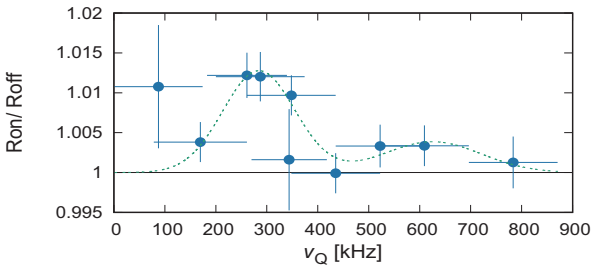

Fig. 2. β-NQR spectrum of ^{21}O in the TiO_2 single crystal. The dashed curve is a guide to the eye representing the expected fitting curve shape. The actual fitting analysis is work-in-progress. For the definition of ν_Q, see Ref. 2.

For this purpose the 0.5-mm-thick TiO_2 single crystal with a known value of EFG was used as a stopper and placed in the same magnetic field of ∼500 mT. The obtained NQR spectrum is shown in Fig. 2. R_{on} and R_{off} in Figs. 1 and 2 represent the U/D ratios between the counts of upper and lower plastic scintillators with and without the application of oscillating magnetic field, respectively.

The analysis of the obtained NMR/NQR spectra is in progress.

*1 RIKEN Nishina Center
*2 Department of Physics, Kyungpook National University
*3 Cyclotron and Radioisotope Center, Tohoku University
*4 Department of Physics, Osaka University
*5 School of Physics, Peking University
*6 Department of Physics, Hosei University
*7 Department of Physics, Meiji University
*8 CSNSM, CNRS/IN2P3, Université Paris-Sud
*9 CEA, DAM, DIF

References

1) A. Abragam: The Principles of Nuclear Magnetism (Springer, Oxford, 1961).
2) H. Izumi et al., Hyperfine Int. 97/98, 509 (1996).

New measurement of the ^{34}Si(p,p) reaction

N. Kitamura,[*1] N. Imai,[*1] S. Shimoura,[*1] K. Wimmer,[*2*3] S. Michimasa,[*1] S. Ota,[*1] O. Beliuskina,[*1] P. Schrock,[*1] M. Kobayashi,[*1] Y. Kiyokawa,[*1] Y. Yamaguchi,[*1] S. Masuoka,[*1] H. Ueno,[*3] K. Yoneda,[*3] Y. Ichikawa,[*3] T. Teranishi,[*4] N. Shimizu,[*1] and Y. Utsuno[*5]

The evolution of shell structure as a function of the proton and neutron number has been observed throughout the nuclear chart. Although this evolution is visualized as shifts in the single-particle energies, the mechanism that changes the single-particle structures in the vicinity of the so-called island of inversion has not yet been fully revealed.

The most straightforward way to explore the single-particle structure is (d,p) one-neutron transfer reactions. In inverse kinematics, (d,p) experiments suffer from low statistics and/or poor resolution because there are two conflicting requirements; on the one hand, the thickness of the target needs to be limited to minimize the energy straggling, and on the other hand, thick targets increase the luminosity. The equivalent spectroscopic information is obtained by means of isobaric analog resonances (IARs) through proton resonant elastic scattering because IARs have the same configuration as the parent states except for the isospin part. This method is powerful, especially for investigations using RI beams in combination with the thick target inverse kinematics, and its effectiveness has been proven[1,2].

This method has already been applied to the ^{35}Si nucleus located just outside the island of inversion. Six IARs were observed by measuring the proton elastic scattering on ^{34}Si[3] and spectroscopic information was deduced for each resonance by R-matrix analysis[4]. More recently, a measurement of the ^{34}Si(d,p) reaction was reported by Burgunder et al.[5], and the resulting spectroscopic factors are in disagreement with the IAR results. This motivated us to perform a new measurement with a modified experimental setup.

The experiment was performed at the RIKEN Projectile fragment Separator (RIPS) facility. To gain more statistics than in the previous measurement, the primary beam species was changed from ^{40}Ar to ^{48}Ca. The primary beam at an energy of 63 MeV/nucleon impinged on a 1.25-mm beryllium production target. A secondary ^{34}Si beam was produced with a typical purity of 30 % and an intensity of 40 kpps. Note that the EPAX 2.15 parameterization[6] overpredicted the intensity by an order of magnitude. The beam particles were identified event-by-event by the TOF-ΔE method. The beam was slowed down to 6 MeV/nucleon using a carbon rotatable degrader and irradiated a proton target. The protons were detected downstream of the target in a stack of silicon detectors, 0.1, 1.0, 1.5, and 1.5 mm thick. In order to increase the excitation energy window, the configuration was optimized with respect to the original experiment.

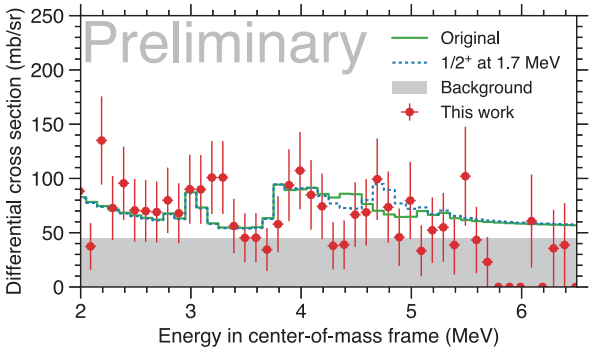

Fig. 1. Measured cross sections for ^{34}Si(p,p) (circles). The background contribution is assumed to be constant. The solid line is the R-matrix calculation from the original measurement[3]. A calculation assuming the $1/2^+$ state in ^{35}Si at 1.7 MeV is also shown (dotted).

The experimental excitation function is shown in Fig. 1, together with the R-matrix calculation. Although the statistics were very limited, the R-matrix curve reproduced our present result except for the strucuture around 4.5 MeV. In our previous measurement, a detector dead-layer could be present around this region, which potentially caused the distortion of the resonances. A peak at 4.7 MeV has been observed for the first time in this experiment, and this could correspond to the IAR of a $1/2^+$ state in ^{35}Si at 1.7 MeV, considering its shape. The energy is in good agreement with the 1688-keV $1/2^+$ state that was recently observed by an experiment of the one-neutron knockout from ^{36}Si[7].

*1 Center for Nuclear Study, University of Tokyo
*2 Department of Physics, Univeristy of Tokyo
*3 RIKEN Nishina Center
*4 Department of Physics, Kyushu University
*5 Advanced Science Research Center, Japan Atomic Energy Agency

References

1) G. V. Rogachev et al., Phys. Rev. C **67**, 041603(R) (2003).
2) N. Imai et al., Phys. Rev. C **90**, 011302 (2014).
3) N. Imai et al., Phys. Rev. C **85**, 034313 (2012).
4) W. J. Thompson et al., Phys. Rev. **173**, 975 (1968).
5) G. Burgunder et al., Phys. Rev. Lett. **112**, 042502 (2014).
6) K. Sümmerer and B. Blank, Phys. Rev. C **61**, 034607 (2000).
7) S. R. Stroberg et al., Phys. Rev. C **90** 034301 (2014).

Study on the β decay of ^{39}S

L. C. Tao,[*1,*2] Y. Ichikawa,[*1] Y. Ishibashi,[*1,*3] A. Takamine,[*1] A. Gladkov,[*1,*4] T. Fujita,[*1,*6] K. Asahi,[*1,*7] T. Egami,[*1,*8] C. Funayama,[*1,*7] K. Imamura,[*1,*5] T. Kawaguchi,[*1,*8] S. Kojima,[*1,*7] T. Nishizaka,[*8] T. Sato,[*1,*7] D. Tominaga,[*8] H. Yamazaki,[*1] and H. Ueno[*1]

We performed β-decay spectroscopy on the neutron-rich nucleus ^{39}S. The neutron-odd S isotopes with neutron numbers larger than 20 have negative-parity ground states, which decay into highly excited states with negative-parity in the Cl isotopes via allowed transitions. The investigations on the level structure of ^{39}Cl including both spin parities are necessary for understanding the nuclear structure in this mass region.

The experiment was carried out with the fragment separator RIPS in December 2015 together with the β-NMR measurement of ^{39}S[2]. A secondary beam of ^{39}S was obtained from the projectile fragmentation reaction of a ^{48}Ca projectile at an energy of 63 A MeV on a ^{9}Be target with a thickness of 0.5 mm. The beam was pulsed with the duration of the beam-on and off periods, 16 s and 16 s, respectively. The ^{39}S beam was implanted into a 0.5-mm-thick CaS stopper which was tilted at an angle of 45 degrees with respect to the beam axis. Two plastic scintillators with thicknesses of 0.5 mm and 1 mm were placed upstream and downstream of the stopper, respectively, in order to count the beam particles implanted into the stopper. The β-delayed γ rays of ^{39}S were detected using two high-purity Ge detectors that were diagonally placed at distances of 30 cm from the stopper.

In this measurement, three γ rays with energies of 1210.3(2) keV, 2571.9(4) keV and 3377.4(5) keV were newly identified to originate from ^{39}S, because their half-lives, 11.6(5) s, 11.5(5) s and 11.2(6) s, respectively, are in a good agreement with the known half-life of ^{39}S, 11.5(5) s[1]. As a result of the γ-γ coincidence analysis, the 1210-keV γ ray was found to have significant coincidence with the 485-keV one, as shown in Fig. 1. This γ ray was assigned to be a de-excitation from a new level at 2995 keV, as shown in Fig. 2. The 2572-keV γ ray was assigned to decay to the ground state directly because its energy is consistent with the known level energy[1]. On the other hand, the 3377-keV γ ray has not been assigned to the decay scheme, although its source is confirmed to be ^{39}S. The deduction of the branching ratio and the log ft values reflecting the new assignments are in progress.

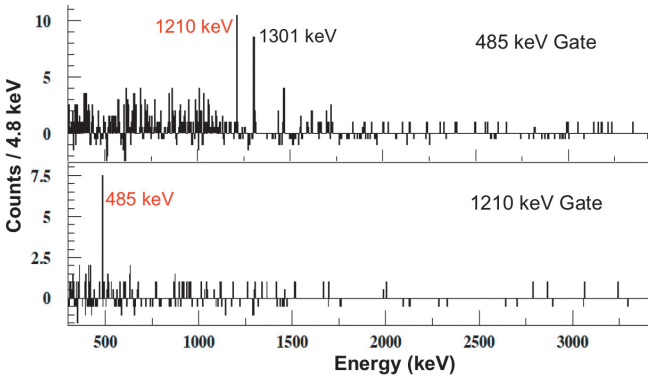

Fig. 1. γ-γ coincidence between the 1210-keV γ ray and the 485-keV γ ray.

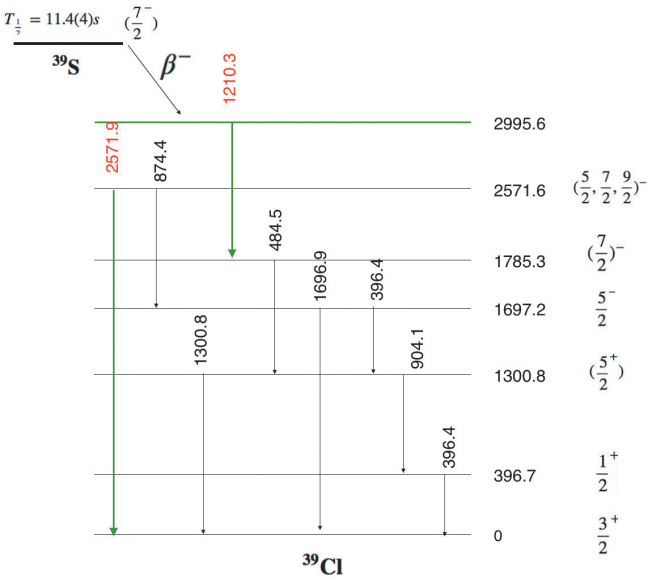

Fig. 2. β decay scheme of ^{39}S. Two γ rays of 1210 keV and 2571 keV newly identified in this work are assigned. Spin-parity values are taken from the compilation[3].

*1 RIKEN Nishina Center
*2 School of Physics and State Key Laboratory of Nuclear Physics and Technology, Peking University
*3 Department of Physics, University of Tsukuba
*4 Department of Physics, Kyungpook National University
*5 Department of Physics, Meiji University
*6 Department of Physics, Osaka University
*7 Department of Physics, Tokyo Institute of Technology
*8 Department of Physics, Hosei University

References

1) J. C. Hill, R. F. Petry, K. H. Wang: Phys. Rev. C **21**, 384 (1980).
2) Y. Ishibashi et al.: RIKEN Accel. Prog. Rep. **49**, 57 (2015).
3) B. Singh and J. Cameron, Nuclear Data Sheets **107**, 225 (2006).

Production of a ^{7}Be implanted target

A. Inoue,[*1] A. Tamii,[*1,*7] H. Yamaguchi,[*2] K. Abe,[*2] S. Adachi[*1] N. Aoi,[*1,*7] M. Asai,[*3] M. Fukuda,[*4] G. Gay,[*1] T. Hashimoto,[*5] S. Hayakawa,[*2] E. Ideguchi,[*1] N. Kobayashi,[*1] Y. Maeda,[*6] H. Makii,[*3] K. Matsuta,[*4,*7] M. Mihara,[*4] M. Miura,[*1] T. Shima,[*1] H. Shimizu,[*2] R. Tang,[*1] T. D. Trong,[*1] and L. Yang[*2]

The beam system for reaction of isotope of long-life with light-ions applying normal kinematics and implanted target (BRILLIANT) is a project to realize light-ion reaction with implanted targets. The first application is for ^{7}Be to measure the ^{7}Be(d, p) reaction for studying the primordial ^{7}Li production in Big-Bang nucleosynthesis (BBN).

The overestimation of primordial ^{7}Li abundance in the standard BBN model is one of the known and unresolved problems in nuclear astrophysics. The latest theoretical BBN model prediction of the primordial ^{7}Li abundance is still 3 times higher than the recent precise observation.[1] A key to solve the discrepancy is the destruction of ^{7}Be, for which the ^{7}Be(d, p)^{8}Be and ^{7}Be(n, α)^{4}He reactions are two promising processes. It is suggested that the contribution from ^{7}Be(d, p)^{8}Be is larger than that from ^{7}Be(n, α)^{4}He.[2,3] We focus on the ^{7}Be(d, p)^{8}Be reaction. Present available data are insufficient in terms of the accuracy or energy range.[4,5] We develop an unstable ^{7}Be target for a high-resolution measurement of the ^{7}Be(d, p)^{8}Be reaction in normal kinematics, which is a great technical challenge. We call the technique "implantation method." The ^{7}Be particles are implanted in a host material. Our goal is to implant 1×10^{12} ^{7}Be /mm^{2} in 29 h.[6,7]

We performed an experiment in June 2016 to create the ^{7}Be target at CRIB. The primary beam was ^{7}Li^{2+}, and the secondary beam was produced by the ^{1}H(^{7}Li, ^{7}Be) reaction. The ^{7}Be beam energy was 4.0 MeV/nucleon. We used a 10-μm-thick Au foil as the host material after a 15-μm-thick Au foil as an energy degrader and a 2-mmφ collimator (Fig. 1).

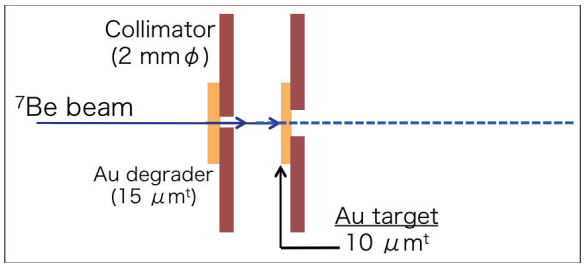

Fig. 1. Set up in the CRIB F2 chamber.

We checked the beam focus and position with the F2 PPAC detector when the beam intensity was about 10^{4} pps at F2. The beam diameter at F2 was 10 mm. We implanted ^{7}Be for 19 h after increasing the beam intensity to 1.1 eμA.

The amount of implanted ^{7}Be was measured by detecting the 477-keV γ-rays from the electron-capture decay of ^{7}Be using a $LaBr_3$ detector. Thus, we could achieve the implantation of 4×10^{10} ^{7}Be/mm^{2} in the first experiment.

The number is still smaller than the goal. We suspect that the beam-spot size and the beam position at F2 were not fully optimized for the high-intensity beam and not maintained well during the long irradiation time.

As a next step, we plan to have a development beam time to satisfy those conditions for producing a high-intensity ^{7}Be beam at CRIB.

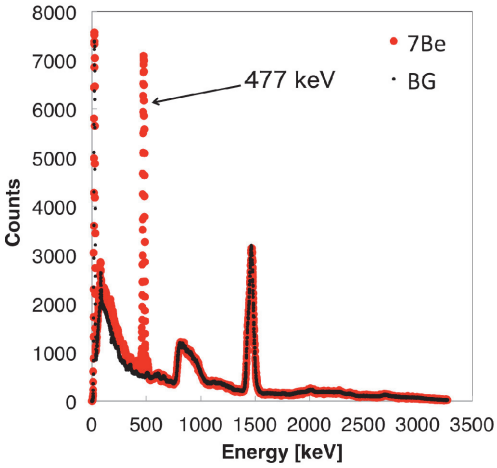

Fig. 2. Comparison between the γ-ray measurement of the implanted target and the background. An obvious 477-keV peak appeared after the irradiation.

*1 Research Center for Nuclear Physics, Osaka University
*2 Center for Nuclear Study, University of Tokyo
*3 Japan Atomic Energy Agency
*4 Department of Physics, Osaka University
*5 Rare Isotope Science Project, Institute for Basic Science
*6 Department of Applied Physics, Faculty of Engineering, University of Miyazaki
*7 RIKEN Nishina Center

References

1) R. H. Cyburt et al., J. Cosmol. Astropart. Phys. **11**, 012 (2008).
2) S. Q. Hou et al., Phys. Rev. C **91**, 055802 (2015).
3) T. Kawabata et al., Phys. Rev. Lett. **118**, 052701 (2017).
4) R. W. Kavanagh et al., Nucl. Phys. **18**, 493 (1960).
5) C. Angulo et al., Astrophys. J. **630**, L 105 (2005).
6) H. Yamaguchi et al., Nucl. Instr. Meth. A **589**, 150 (2008).
7) G. Amadio et al., Nucl. Instr. Meth. A **590**, 191 (2008).

Experimental investigation of a linear-chain structure in ^{14}C †

H. Yamaguchi,[*1] D. Kahl,[*1] S. Hayakawa,[*1] Y. Sakaguchi,[*1] and K. Abe,[*1] for CRIB collaboration

In 1956, Morinaga[1] came up with the novel idea of a particular cluster state: the linear-chain cluster state (LCCS). Now the LCCS is commonly considered as extreme and exotic, due to its presumed propensity to exhibit bending configurations. A theoretical prediction of LCCS in ^{14}C was made by Suhara and En'yo[2,3] with an antisymmetrized molecular dynamics (AMD) calculation, yielding a prolate band ($J^\pi = 0^+, 2^+, 4^+$) that has a configuration of an LCCS at a few MeV or more above the ^{10}Be+α threshold. In the present work we applied the ^{10}Be+α resonant scattering method[4–7] in inverse kinematics to identify the predicted LCCS band in ^{14}C.

The present measurement was performed at the low-energy radioactive isotope beam separator CRIB. The ^{10}Be beam had a typical intensity of 2×10^4 particles per second, and the beam purity was better than 95%. The ^{10}Be beam at 25.8 MeV impinged on the gas target, which was a chamber filled with helium gas at 700 Torr (930 mbar) and covered with a 20-μm-thick Mylar film as the beam entrance window. The measured ^{10}Be beam energy at the entrance of the helium gas target, after the Mylar film, was 24.9±0.3 MeV. α particles recoiling to the forward angles were detected by ΔE-E detector telescopes.

Finally we obtained the excitation function of the ^{10}Be+α resonant elastic scattering for 13.8–19.1 MeV, where events with $\theta_{\rm lab} = 0$–8° ($\theta_{\rm cm}$= 164–180°) were selected. We performed an R-matrix calculation to deduce the resonance parameters. The best fit parameters obtained from the analysis are summarized in Table 1. Although the analysis was performed without any assumption from the theoretical calculation, we identified three resonances perfectly corresponded to the predicted LCCS band; J^π are identical, and their energies and spacings are consistent with the theoretical prediction. We claim this as the strongest indication of the LCCS ever found. It can be also shown that both sets of level energies can be plotted almost on a line, $E_J = E_0 + \hbar^2/2\Im(J(J+1))$, where $\Im$ is the moment of inertia of the nucleus. The linearity allows us to interpret the levels as a rotational band, and the low $\hbar^2/2\Im = 0.19$ MeV implies the nucleus could be strongly deformed, consistent with the interpretation of an LCCS. The experimental Γ_α of these resonances are also compared with the theoretical predictions in terms of the dimensionless partial width θ_α^2 in Table 1, although the precision of both is quite limited. The calculation qualitatively reproduces the feature that the experimental θ_α^2 is anti-correlated with J.

Table 1. The resonance parameters in ^{14}C determined by the present work, compared with the AMD calculation[2]. Parameters in bold letters are for LCCS predicted in the calculation, and corresponding experimental resonances.

Present Work			
$E_{\rm ex}$ (MeV)	J^π	Γ_α (keV)	θ_α^2
14.21	(2^+)	17(5)	3.5%
14.50	1^-	45(14)	4.5%
15.07	**0^+**	**760(250)**	**34(12)%**
16.22	**2^+**	**190(55)**	**9.1(27)%**
16.37	(4^+)	15(4)	3.0%
16.93	(2^+)	270(85)	10.3%
17.25	(1^-)	190(45)	5.5%
18.02	(3^-)	31(19)	1.3%
18.63	5^-	72(48)	9.4%
18.87	**4^+**	**45(18)**	**2.4(9)%**

Suhara & En'yo[2]		
$E_{\rm ex}$ (MeV)	J^π	θ_α^2
15.1	**0^+**	**16%**
16.0	**2^+**	**15%**
19.2	**4^+**	**9%**

As investigated in the theoretical calculation of the ^{14}C system, the orthogonality between different quantum mechanical states is considered to play a key role in stabilizing the LCCS. Further studies may reveal whether this mechanism is universal in nuclear systems or particular to ^{14}C.

References
1) H. Morinaga, Phys. Rev. **101**, 254 (1956).
2) T. Suhara and Y. Kanada-En'yo: Phys. Rev. C **82**, 044301 (2010).
3) T. Suhara and Y. Kanada-En'yo: Phys. Rev. C **84**, 024328 (2011).
4) K. P. Artemov et al.: Sov. J. Nucl. Phys **52**, 408 (1990).
5) H. Yamaguchi et al.: Phys. Rev. C **87**, 034303 (2013).
6) M. Freer et al.: Phys. Rev. C **90**, 054324 (2014).
7) A. Fritsch et al.: Phys. Rev. C **93**, 014321 (2016).

† Condensed from the article in Phys. Lett. B **766**, 11 (2017)
*1 Center for Nuclear Study, University of Tokyo

^{7}Be$(n,p)^7$Li and ^{7}Be$(n,\alpha)^4$He reaction measurements at CRIB using the Trojan Horse method

S. Hayakawa,[*1] K. Abe,[*1] O. Beliuskina,[*1] S. M. Cha,[*2] K. Y. Chae,[*2] S. Cherubini,[*3,*4] P. Figuera,[*3,*4] Z. Ge,[*5] M. Gulino,[*3,*6] J. Hu,[*7] A. Inoue,[*8] N. Iwasa,[*5,*9] D. Kahl,[*10] A. Kim,[*11] D. H. Kim,[*11] G. Kiss,[*5] S. Kubono,[*1,*5,*7] M. La Cognata,[*3] M. La Commara,[*12,*13] L. Lamia,[*4] M. Lattuada,[*3,*4] E. J. Lee,[*2] J. Y. Moon,[*14] S. Palmerini,[*15,*16] C. Parascandolo,[*13] S. Y. Park,[*11] D. Pierroutsakou,[*13] R. G. Pizzone,[*3,*4] G. G. Rapisarda,[*3] S. Romano,[*3,*4] H. Shimizu,[*1] C. Spitaleri,[*3,*4] X. D. Tang,[*7] O. Trippella,[*15,*16] A. Tumino,[*3,*6] P. Vi,[*5] H. Yamaguchi,[*1] L. Yang,[*1] and N. T. Zhang[*7]

It has been known that the primordial ^{7}Li abundance predicted by the standard Big-Bang Nucleosynthesis (BBN) model[1] is about three times larger than the observation, which is the cosmological ^{7}Li problem. The ^{7}Be$(n,p)^7$Li reaction is considered as the main process to destruct ^{7}Be during the BBN, which is also crucial in determining the ^{7}Li abundance. The resonance structure of the ^{7}Be$(n,p)^7$Li reaction was well investigated by the R-matrix analysis[2] on several experimental data. However, the contribution of the transition to the first excited state of ^{7}Li at the BBN energies ($\sim$ 25 keV–1 MeV) has never been discussed. The other interesting reaction channel of the neutron induced reaction, ^{7}Be$(n,\alpha)^4$He, has not been investigated until recently[3,4] in terms of the relevance to the BBN scenario. Note that the new measurement[4] was limited and carried out at very low energies, which thus lacks the information on the total ^{7}Be$(n,\alpha)^4$He cross section in the BBN energy region.

We performed indirect measurements of the ^{7}Be$(n,p)^7$Li and ^{7}Be$(n,\alpha)^4$He reactions simultaneously by the Trojan horse method (THM)[5] at the Center for Nuclear Study Radioactive Ion Beam (CRIB) separator[6]. The THM is an indirect technique that allows us to approach a two-body reaction at astrophysical energies via a three-body reaction by selecting the quasi-free (QF) kinematics. Moreover, the THM is useful as a "virtual neutron source" for neutron-induced reactions by using a deuteron target[7]. Similar to the first application of THM to the RI+n reaction[8], which was performed in collaboration with our group, we used a ^{7}Be beam and a deuteron target

*1 Center for Nuclear Study, University of Tokyo
*2 Department of Physics, Sungkyunkwan University
*3 Istituto Nazionale di Fisica Nucleare - Laboratori Nazionali del Sud
*4 Department of Physics and Astronomy, Univ. of Catania
*5 RIKEN Nishina Center
*6 Faculty of Engineering and Architecture, Kore Univ. of Enna
*7 Institute of Modern Physics, Chinese Academy of Sciences
*8 Research Center for Nuclear Physics, Osaka University
*9 Department of Physics, Tohoku University
*10 School of Physics and Astronomy, University of Edinburgh
*11 Department of Physics, Ewha Womans University
*12 Depart. of Phys. 'E. Pancini', Univ. of Naples Federico II
*13 Istituto Nazionale di Fisica Nucleare - Section of Naples
*14 High Energy Accelerator Research Organization (KEK)
*15 Istituto Nazionale di Fisica Nucleare - Section of Perugia
*16 Department of Physics and Geology, University of Perugia

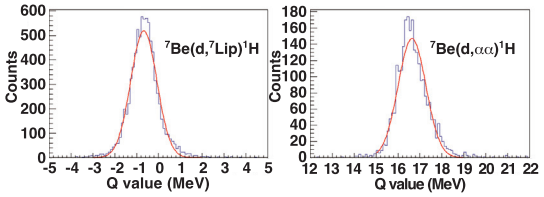

Fig. 1. Q-value spectra of the ^{7}Be$(d,^7$Li$p)^1$H (left) and the ^{7}Be$(d,\alpha\alpha)^1$H (right) reactions.

that induce the ^{7}Be$(d,^7$Li$p)^1$H and ^{7}Be$(d,\alpha\alpha)^1$H reactions in inverse kinematics to study the ^{7}Be$(n,p)^7$Li and ^{7}Be$(n,\alpha)^4$He reactions, respectively. We produced a ^{7}Be beam at 22.1±0.14 MeV with an intensity of 1×10^6 pps on target. The experimental setup consisted of two parallel-plate avalanche counters (PPACs) for beam tracking, a CD_2 target, and six ΔE-E position-sensitive silicon-detector telescopes at ±12°, ±34° and ±56°. The thickness of the CD_2 target was 64 μg/cm^2. A use of such a thin target allows reducing the energy spread to about 120 keV. This helps to identify the first excited state of ^{7}Li (478 keV) in the reconstructed Q-value spectrum. We observed p-^{7}Li and α-α coincidental events, and confirmed that they were kinematically correct as the expected three-body exit channels. Figure 1 shows three-body Q-value spectra of those channels. The peaks are fitted by Gaussian functions with mean values of -0.67 MeV and 16.64 MeV, respectively, which are consistent with the known Q values of -0.580 MeV and 16.766 MeV within the resolution of about 600 keV (rms). This resolution is expected to be improved to 150–200 keV with more precise energy and angular calibrations and further corrections. Accordingly, one can resolve both the ground and the first excited state of ^{7}Li. By selecting the corresponding kinematic region, we estimate about 3000 QF events for the ^{7}Be$(n,p)^7$Li channel in total.

References

1) A. Coc et al., J. Cosm. and Astropart. Phys. **40**, 050 (2014).
2) A. Adahchour and P. Descouvemont, J. Phys. G **29**, 395 (2003).
3) S. Q. Hou et al., Phys. Rev. C **91**, 055802 (2015).
4) M. Barbagallo et al., Phys. Rev. Lett. **117**, 152701 (2016).
5) C. Spitaleri et al., Phys. Atom. Nucl. **74**, 1725 (2011).
6) Y. Yanagisawa et al., Nucl. Instrum. and Meth. A **539**, 74 (2005).
7) M. Gulino et al., Phys. Rev. C **87**, 012801 (2013).
8) L. Lamia et al., Proc. 14th International Symposium on Nuclei in the Cosmos, JPS Conf. Proc., in publication.

Study of α-cluster structure in ^{22}Mg

K.Y. Chae,[*1] S.M. Cha,[*1] K. Abe,[*2] S.H. Bae,[*3] D.N. Binh,[*4] S.H. Choi,[*3] N.N. Duy,[*5] K.I. Hahn,[*6] S. Hayakawa,[*2] B. Hong,[*7] N. Iwasa,[*8,*9] D. Kahl,[*10] L.H. Khiem,[*11,*12] A. Kim,[*13] D.H. Kim,[*13] E.J. Kim,[*14] G.W. Kim,[*13] M.J. Kim,[*1] K. Kwak,[*15] M.S. Kwag,[*1] E.J. Lee,[*1] S.I. Lim,[*13] B. Moon,[*7] J.Y. Moon,[*16] S.Y. Park,[*13] V.H. Phong,[*9] H. Shimizu,[*2] H.Yamaguchi,[*2] L. Yang,[*2] and Z. Ge[*9]

The study of the α-cluster structure in a nucleus is one of the most important subjects in nuclear physics. In the case of self-conjugate $4N$ nuclei, it is well known that the energy levels with large α-reduced widths form the rotational bands, which indicates the molecular-like cluster structures of the nuclei. The α-cluster structure of rare isotopes is, however, still poorly understood especially for $N < Z$ proton-rich nuclei.

As pointed out by Dufour and Descouvemont,[1] the proton-rich radionuclide ^{22}Mg is expected to show an α-cluster structure. The ^{22}Mg nucleus (^{18}Ne + α system) was investigated using the generator coordinate method (GCM), which obtained results indicating the expected doubling cluster states with $J^\pi = 1^-$ and 3^- at the energy range of $12 < E_x < 13$ MeV. However, the energy levels were not clearly observed in the follow-up experiment performed by Goldberg et al.[2]

The elastic scattering of ^{18}Ne$(\alpha,\alpha)^{18}$Ne was measured in the inverse kinematics at the Center for Nuclear Study Radioactive Ion Beam Separator (CRIB) of the RIKEN Nishina Center in September 2016 for 10 days. A thick target method was adopted so that a wide energy range of ^{22}Mg nuclei could be scanned. A beam of rare isotope ^{18}Ne was produced by the ^{3}He(^{16}O, ^{18}Ne)n reaction using the primary ^{16}O beam from the AVF cyclotron ($E_{beam} = 8.0$ MeV/u). The ^{3}He gas target density was 1.54 mg/cm^2. The typical secondary beam intensity was about 3×10^5 particles per second during the runs. The ^{18}Ne with a beam energy of ~ 50 MeV impinged on the 470 Torr of the ^{4}He gas target at the final focal plane. The energy levels of ^{22}Mg up to $E_x \sim 18$ MeV were observed.

Recoiling α particles were measured by two ΔE-E silicon detector telescopes located 430 mm downstream from the target entrance window, which enabled α-particle identification using the standard energy loss technique. No significant contamination from other light charged particles was found. A background run with an 87-Torr Ar gas target was performed to see if the observed α particles originated from the desired reactions. Figure 1 shows a typical α energy spectrum. The black and red lines indicate the α energy spectra for the ^{4}He and Ar gas targets, respectively. Relative counts are shown in the figure for comparison.

A detailed calibration and energy reconstruction will be performed to determine the precise α energy spectrum. The experimental excitation function of the ^{18}Ne + α system will be extracted and compared with the theoretical R-matrix calculation.[3] The properties of populated energy levels such as excitation energies, spins, parities, and the α-reduced widths will be constrained for the α cluster structure information.

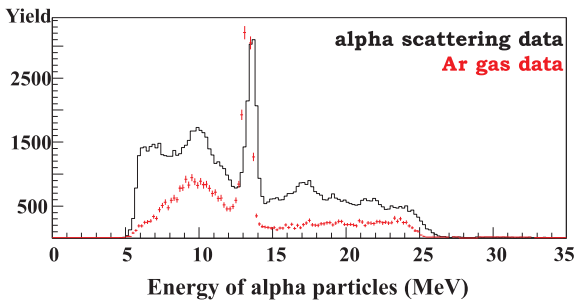

Fig. 1. Typical α spectrum. The black (red) line indicates the ^{4}He (Ar) gas run. All data were normalized by beam intensity. The strong peak near 13 MeV represents leaky α particles that originated at the production target chamber.

*1 Department of Physics, Sungkyunkwan University
*2 Center for Nuclear Study, University of Tokyo
*3 Department of Physics and Astronomy, Seoul National University
*4 30 MeV Cyclotron Center, Tran Hung Dao Hospital
*5 Department of Physics, Dong Nai University
*6 Department of Science Education, Ewha Womans University
*7 Department of Physics, Korea University
*8 Department of Physics, Tohoku University
*9 RIKEN Nishina Center
*10 School of Physics and Astronomy, University of Edinburgh
*11 Institute of Physics, Vietnam Academy of Science and Technology
*12 Graduate University, Vietnam Academy of Science and Technology
*13 Department of Physics, Ewha Womans University
*14 Division of Science Education, Chonbuk National University
*15 Department of Physics, School of Natural Science, Ulsan National Institute of Science and Technology (UNIST)
*16 Institute for Basic Science

References

1) M. Dufour and P. Descouvemont, Nucl. Phys. A **726**, 53 (2003).
2) V. Z. Goldberg et al., Phys. Rev. C **69**, 024602 (2004).
3) A. M. Lane and R. G. Thomas, Rev. Mod. Phys. **30**, 257 (1958).

^{26m}Al beam production with CRIB

D. Kahl,[*1] H. Yamaguchi,[*2] H. Shimizu,[*2] K. Abe,[*2] O. Beliuskina,[*2] S. M. Cha,[*3] K. Y. Chae,[*3] Z. Ge,[*4] S. Hayakawa,[*2] M. S. Kwag,[*3] D. H. Kim,[*5] J. Y. Moon,[*6] S. Y. Park,[*5] and L. Yang[*2]

The γ-ray emission associated with the radioactive decay of ^{26}Al is one of the key pieces of evidence indicating stellar nucleosynthesis is an ongoing process in our Galaxy. Its ground state ^{26g}Al has a half-life of 7×10^5 yr owing to its high spin $J^\pi = 5^+$, and it predominately decays to the first excited state in ^{26}Mg, which promptly de-excites by emitting a characteristic 1.809 MeV γ-ray. The situation is complicated by a low-lying isomeric state ^{26m}Al at 228 keV; this $J^\pi = 0^+$ isomer decays with a half-life of 6.3 s directly to the ground-state of ^{26}Mg.

Little is known about the ^{26m}Al(p,γ) reaction rate, and in a sensitivity study on ^{26}Al yields from massive stars, the (p,γ) rate on the isomeric state was assumed to be the same as for the ground state[1)], despite the large spin-parity difference. At present, there is only limited information on J^π and no proton partial widths Γ_p are known for low-spin resonances above the proton threshold in ^{27}Si.

In preparation for a measurement of proton elastic scattering, we undertook a two-day machine test to check the production yield, purity, and phase-space parameters of ^{26m}Al at the Center for Nuclear Study low-energy RIB separator (CRIB)[2)]. A primary beam of ^{26}Mg^{8+} was accelerated to 6.77 MeV/u and impinged on the CRIB cryogenic production target[3)], which was filled with 260 Torr of H_2 gas at 90 K (0.7 mg·cm^{-2}) and sealed with 2.5 μm Havar foils, producing the RIB of interest via the ^{1}H(^{26}Mg, ^{26}Al)n reaction. These conditions were chosen to optimize production of ^{26m}Al over ^{26g}Al based on the literature cross-sectional data[4)]. A sample particle identification plot at the achromatic focal plane F2 is shown in Fig. 1. ^{26}Al^{13+} production yield was optimized at 119.6 ± 1.5 MeV. After passing through a Wien filter, the ^{26}Al purity was 80–90% at the experimental focal plane F3, with ^{23}Na as the main contaminant. The typical intensity of ^{26}Al was 1×10^5 pps (at 25 pnA). The setup at the experimental focal plane consisted of two parallel plate avalanche counters (PPACs), a 7.5 mg·cm^{-2} CH_2 target, and a silicon telescope (SSDs).

A key purpose of the machine test was to determine the isomeric purity ^{26m}Al/^{26}Al in the cocktail beam. Although CRIB does not have the capability to distinguish between ^{26g,m}Al for individual ions, a previous measurement of ^{26g}Al(p,p) showed no resonant

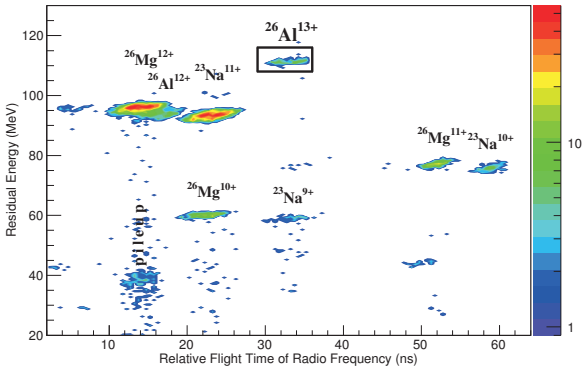

Fig. 1. Particle identification of the beam at the focal plane F2. The abscissa shows relative flight time and the ordinate shows the residual ion energy. The optical settings used to produce the histogram are not optimized for ^{26}Al but are useful for illustrative purposes.

structure[5)]. The previous work reduces our inability to uniquely identify the state of ^{26}Al event-by-event to background subtraction, provided we have a reliable determination of the isomeric purity.

To determine the isomeric purity, we performed a decay study by pulsing the primary beam in an on/off mode with a duty cycle of 12 s. When the beam was on it was implanted into the CH_2 target, and when the beam was off, we measured β^+ particles with the SSDs. Considering the long half-life of ^{26g}Al and that ^{23}Na is stable, it is reasonable to assume that all β^+ particles emitted from the target when the beam was off can be associated with the decay of ^{26m}Al (which does not decay by electron capture). Our preliminary measured half-life for the decay associated with these particles is 6.1 s; this value is close to the known ^{26m}Al half-life of 6.3 seconds considering we have yet to evaluate our error. The shape of our preliminary β^+-decay spectrum was also consistent with the expectation for ^{26m}Al. We tentatively calculate an isomeric purity of $\approx 40\%$ from the test run data. We anticipate that the developed ^{26m}Al beam is satisfactory to observe low-ℓ proton resonances with large widths in the future.

*1 School of Physics and Astronomy, University of Edinburgh
*2 Center for Nuclear Study, University of Tokyo
*3 Department of Physics, Sungkyunkwan University
*4 RIKEN Nishina Center
*5 Department of Physics, Ewha Womans University
*6 Institute for Basic Science and Wako Nuclear Science Center

References

1) C. Iliadis et al., Astrophys. J. Supp **193**, 16 (2011).
2) Y. Yanagisawa et al., Nucl. Instrum. Methods in Phys. Res., Sect. A **539**, 74 (2005).
3) H. Yamaguchi et al., Nucl. Instrum. Methods in Phys. Res., Sect. A **589**, 150 (2008).
4) R.T. Skelton et al., Phys. Rev. C **35**, 45 (1987).
5) S.T. Pittman et al., Phys. Rev. C **85**, 065804 (2012).

Shape coexistence in the N=19 neutron-rich nucleus ^{31}Mg explored by β-γ spectroscopy of spin-polarized ^{31}Na†

H. Nishibata,[*1,*2] T. Shimoda,[*1] A. Odahara,[*1] S. Morimoto,[*1] S. Kanaya,[*1] A. Yagi,[*1] H. Kanaoka,[*1] M. R. Pearson,[*3] C. D. P. Levy,[*3] and M. Kimura[*4]

One of the highlights of the recent nuclear physics is the shape coexistence of nuclei located far from the β-stability line. In particular, neutron-rich nuclei with neutron numbers close to the neutron magic number N = 20, so-called the "island of inversion"[1], have been intensively studied. However, the structures are still not clear because there exists few information on excited states, such as spin-parity, for most of the island-of-inversion nuclei.

We study the neutron-rich nucleus ^{31}Mg which is located around the "island of inversion" region. The level structure of odd-mass ^{31}Mg is one of the most sensitive probes of shape coexistence because the last neutron orbit, which governs the spin-parity of the level, is strongly affected by the nuclear structure. In the present work, detailed data are presented for the excited states of ^{31}Mg, obtained through a unique and extremely promising method[2] to measure spin-parity based on the β-decay spectroscopy of spin-polarized ^{31}Na.

Our method uses an asymmetric β decay of the polarized nucleus in the allowed transition. The angular distribution is expressed as $W(\theta) \simeq 1 + AP\cos\theta$, where A, P, and θ are the asymmetry parameter for each β transition, the spin polarization, and the emission angle of the β rays with respect to the polarization direction, respectively. The essential point is that the asymmetry parameter takes three different values depending on the spins of the parent and daughter states. In the case of the β decay of ^{31}Na ($I^\pi = 3/2^+$), the asymmetry parameter is either -1.0, -0.4, or $+0.6$ for the possible daughter state with a spin-parity of $1/2^+$, $3/2^+$, or $5/2^+$, respectively. Therefore, from the experimental asymmetry value, the spin-parity can be unambiguously assigned. Further information on this method can be found in Ref.[2]

The experiment was performed at the Isotope Separator and Accelerator (ISAC) facility in TRIUMF, where a highly polarized Na beam was achieved by simultaneously pumping both atomic ground-state levels with two laser frequencies. The β-rays and γ-rays associated with ^{31}Na β decay were measured at the end of the Osaka beam line (for detailed information on the experimental setup, see the original Letter†).

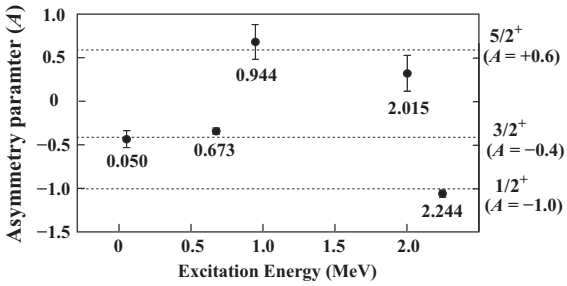

Fig. 1. Experimental asymmetry parameters for the levels at 0.050, 0.673, 0.944, 2.015, and 2.244 MeV.

Figure 1 shows the experimental asymmetry parameters. It is clearly seen that the experimental values are consistent with one of the expected values. Hence the spins and parities are firmly assigned as $1/2^+$ for the 2.244-MeV level, $3/2^+$ for the 0.050- and 0.673-MeV levels, and $5/2^+$ for the 0.944- and 2.015-MeV levels. The spins of negative-parity levels are also limited based on transition intensities from the levels with spin-parity assigned in the present work. Furthermore, 11 γ rays and 2 levels are newly found by analyzing the γ-γ coincidence data.

From the obtained spins and energies of the levels in ^{31}Mg, we propose that the positive-parity levels [$1/2^+$ 0 MeV, $3/2^+$ 0.050, $5/2^+$ 0.944, $(7/2^+)$ 1.155] and negative-parity levels [$(3/2^-)$ 0.221, $(7/2^-)$ 0.461, $(1/2^-)$ 1.029, $(11/2^-)$ 1.390] are members of the $K^\pi = 1/2^+$ and $1/2^-$ rotational bands, respectively. Through a level-by-level comparison between the experimental results and theoretical calculations of the AMD+GCM,[3] it is found that the levels at 0.673 [$3/2^+$] and 2.015 MeV [$5/2^+$] show good correspondence with spherical levels predicted at 0.81 and 1.85 MeV. Furthermore, the experimental level at 0.942 MeV [$(1/2^-$ or $3/2^-)$] is probably the $3/2^-$ level of the band-head of $K^\pi = 3/2^-$ rotational bands in the AMD+GCM calculations. However, the 2.244-MeV $1/2^+$ level cannot be explained by any theories at present. These results show clear evidence for shape coexistence in a low excitation energy region of ^{31}Mg.

† Condensed from the article in H. Nishibata *et al.*, Phys. Lett. B 767, (2017).

*1 Department of Physics, Osaka University, Osaka 560-0043, Japan
*2 RIKEN, Wako, Saitama 351-0198, Japan
*3 TRIUMF, 4004 Wesbrook Mall, Vancouver, BC V6T 2A3, Canada
*4 Department of Physics, Hokkaido University, Sapporo 060-0810, Japan

References

1) E. K. Warburton et al., Phys. Rev. C **41**, 1147 (1990).
2) K. Kura et al., Phys. Rev. C **85**, 034310 (2012).
3) M. Kimura, Phys. Rev. C **75**, 041302(R) (2007).

RI beam production at BigRIPS in 2016

H. Takeda,[*1] N. Fukuda,[*1] Y. Shimizu,[*1] H. Suzuki,[*1] D. S. Ahn,[*1] T. Sumikama,[*1] D. Murai,[*1,*2] J. Amano,[*1,*2] N. Inabe,[*1] K. Kusaka,[*1] M. Ohtake,[*1] Y. Yanagisawa,[*1] T. Komatsubara,[*1] H. Sato,[*1] and K. Yoshida[*1]

The radioactive isotope (RI) beam production at the BigRIPS fragment separator[1] in 2016 is presented here. Table 1 summarizes the experimental programs that involved the use of the BigRIPS separator in this period and the RI beams produced for the programs.

The spring beam time started with a ^{238}U primary beam in April. A machine study of the SAMURAI-TPC and the measurement of the giant monopole resonance were performed with the ^{132}Sn beam produced by the in-flight fission of ^{238}U.

Subsequently, a ^{124}Xe primary beam was used to produce $^{108, 112}$Sn for symmetry-energy studies. The production yields and the production cross sections of neutron-deficient isotopes for the Br − Cd region[2] were measured during the BigRIPS tuning for the ^{124}Xe beam.

Five experiments were conducted in the second ^{238}U beam campaign started in May. The ^{132}Sn and ^{48}Ca beams were produced for the ESPRI experiment. The $^{132, 124}$Sn and Z = 1−3 beams were delivered to the SAMURAI spectrometer for symmetry-energy studies. The ImPACT program was performed using the ^{93}Zr beam with energies of 200, 100, 50, and 20 MeV/nucleon. The ^{87}Zn setting was provided for measurements of masses and beta-decay properties of r-process nuclei around N = 56. ^{60}Ti and ^{64}V were produced to study the shape coexistence along N = 40.

The spring beam time ended with an ^{18}O beam campaign, in which two experiments were performed. First, ^{3}H and $^{4, 8}$He beams were produced for the confirmation of tetra-neutron resonance. Subsequently, $^{4, 6}$He beams were delivered for the measurement of vector analyzing powers.

Table 1. List of experimental programs and RI beams produced at the BigRIPS separator in 2016.

Primary beam (Period)	Proposal No.	Spokesperson	Course	RI beams
^{238}U 345 MeV/nucleon (Apr. 6 – Apr. 22)	MS-EXP16-01	T. Isobe	SAMURAI	^{132}Sn
	NP1312-RIBF113-01	S. Ota	ZeroDegree	^{132}Sn
^{124}Xe 345 MeV/nucleon (Apr. 29 – May 6)	NP1312-SAMURAI22-01	T. Murakami	SAMURAI	$^{108, 112}$Sn
^{238}U 345 MeV/nucleon (May 14 – Jun. 13)	NP1512-RIBF79R1-01	J. Zenihiro	F12	^{132}Sn, ^{48}Ca
	NP1312-SAMURAI15-01	W. Lynch	SAMURAI	$^{132, 124}$Sn, ^{2}H/^{4}He/^{6}Li
	IMPACT16-01	H. Sakurai	ZeroDegree	^{93}Zr
	NP1306-RIBF106-01	A. Estrade	EURICA	^{87}Zn
	NP1512-RIBF140-01	F. Recchia	EURICA	^{60}Ti, ^{64}V
^{18}O 230 MeV/nucleon (Jun. 16 – Jun. 30)	NP1512-SHARAQ10-01	S. Shimoura	SHARAQ	^{3}H, $^{4, 8}$He
	NP1206-SAMURAI13-01	S. Sakaguchi	SAMURAI	$^{4, 6}$He
^{238}U 345 MeV/nucleon (Oct. 19 – Nov. 12)	IMPACT16-02	H. Sakurai	ZeroDegree	$^{126, 127}$Sn, ^{93}Zr, ^{107}Pd
	MS-EXP16-05	T. Sonoda	PALIS	^{116}Pd
	MS-EXP16-10	Y. Yamaguchi	Rare-RI Ring	^{76}Zn
	NP1412-RIBF123R1-01	M. Takechi	BigRIPS	$^{59-78}$Ni, $^{45-50}$Ca
	PE16-03	T. Sonoda	PALIS	
	PE16-01	S. Nishimura	ZeroDegree	
^{48}Ca 345 MeV/nucleon (Nov. 15 – Dec. 6)	NP1512-SAMURAI36-01	N. Orr	SAMURAI	^{20}C, ^{22}C/^{23}N
	NP1406-SAMURAI27-01	N. Kobayashi	SAMURAI	^{22}Ne, $^{30, 31}$Ne, ^{32}Ne/^{34}Na
	NP1412-RIBF132-01	R. Kanungo	ZeroDegree	$^{27, 29}$F, $^{20, 22}$C, ^{19}B
	NP1312-RIBF03R1-02	P. Fallon	ZeroDegree	^{41}Al
	PE16-02	S. Nishimura	ZeroDegree	
	NP1306-SAMURAI20-01	C. Caesar	SAMURAI	$^{26, 27}$F, ^{24}O

*1 RIKEN Nishina Center
*2 Department of Physics, Rikkyo University

In the autumn beam time, ^{238}U and ^{48}Ca primary beams were used. The ^{238}U beam campaign started in October with the ImPACT program and the PALIS machine study. The Sn, Zr, and Pd isotope beams were provided. A machine study of the Rare-RI Ring was conducted with the ^{76}Zn beam. A large variety of Ni and Ca isotope beams were produced for the determination of neutron skin thickness.

After switching to the ^{48}Ca primary beam, the production cross sections of Ne isotopes were measured[3] during the BigRIPS tuning of the ^{48}Ca beam. C – Na isotope beams were produced for two SAMURAI experiments. Proton and matter radii were measured with $^{27, 29}$F, $^{20, 22}$C, and ^{19}B beams to study the evolution of halo structure of the Borromean nuclei. The ^{41}Al beam was produced for the study of ^{40}Mg spectroscopy. The $^{26, 27}$F and ^{24}O beams were used to measure the lifetime of the ^{26}O ground state. At the end of the ^{48}Ca beam campaign, searches for a new isotope ^{39}Na and the neutron drip line were scheduled but postponed because of a problem in the refrigerator of superconducting magnets of the BigRIPS separator.

The number of experiments using the RI beams at the BigRIPS separator is summarized in Table 2 for various primary beams in each year. A total of 137 experiments have been performed so far. Figure 1 shows the RI beams produced at the BigRIPS separator from March 2007 to December 2016 on the chart of nuclides. The number of RI beams produced at the BigRIPS separator is approximately 440. The number of new isotopes is approximately 150. Production yields for more than 1500 RI beams have been measured.

References

1) T. Kubo, Nucl. Instr. Meth. Phys. Res. B **204**, 97 (2003).
2) H. Suzuki et al.: In this report.
3) D. S. Ahn et al.: In this report.

Table 2. Number of experiments performed using RI beams in each year.

Year	^{238}U	^{124}Xe	^{86}Kr	^{78}Kr	^{70}Zn	^{48}Ca	^{18}O	^{16}O	^{14}N	^{4}He	^{2}H	Yearly total
2007	4		1									5
2008	2					4						6
2009	3					3			3	1		10
2010						10	1		2		1	14
2011	4	2					2					8
2012	6	3			1	4	6					20
2013	4	2					3					9
2014	11				1	3		1			1	17
2015	15			6		4					1	26
2016	13	1				6	2					22
Total	62	8	1	6	2	34	14	1	5	1	3	137

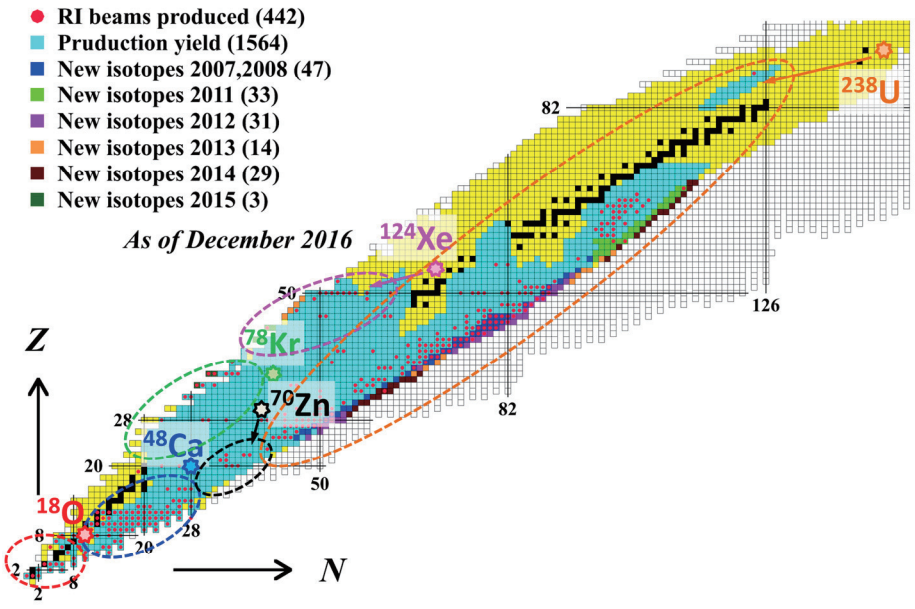

Fig. 1. RI beams produced at the BigRIPS separator from March 2007 to December 2016.

Production cross section measurements of Ne isotopes with a ^{48}Ca beam

D. S. Ahn,[*1] N. Fukuda,[*1] H. Suzuki,[*1] Y. Shimizu,[*1] H. Takeda,[*1] T. Sumikama,[*1] D. Murai,[*1,*2] J. Amano,[*1,*2] N. Inabe,[*1] K. Yoshida,[*1] Y. Yanagisawa,[*1] K. Kusaka,[*1] M . Ohtake,[*1] T. Komatsubara,[*1] H. Sato,[*1] H. Ueno,[*1] and T. Kubo[*1,*3]

The systematic trends of production cross sections are necessary to predict the production rates of rare isotopes, and important to search for new isotopes and the neutron drip line. Comparison of expected and measured yields is important to ascertain whether bound states exist in isotopes such as ^{39}Na. Expected yields for ^{39}Na (Z = 11) can be estimated from the neighboring isotopes. We measured the production cross sections of very neutron-rich Ne (Z = 10) isotopes. In the previous experiment,[1] the cross sections for many Ne isotopes were obtained with low transmission (2~5% in the worst cases). In this experiment, the production cross sections of neutron-rich $^{29\text{-}34}$Ne isotopes were measured with optimized settings for each isotope. As each isotope passed through a central orbit, a high transmission was achieved.

Ne isotopes were produced by the projectile fragmentation of a ^{48}Ca beam at an energy of 345 MeV/nucleon using the BigRIPS separator[2] of RIKEN RIBF. The same target (Be: 20 mm) and the same thickness degraders were used for both F1 (Al: 15 mm) and F5 (Al: 8 mm). The F5 degrader was used to reject contaminants in the form of light particles. A thick collimator installed before the F2 slits was developed as shown in Fig. 1. The collimator was made of an SUS material with a 50-cm thickness to block most contaminants, including tritons and other light particles. The aperture of the collimator was designed with horizontal and vertical angular acceptances of ± 20 mrad and ± 30 mrad, respectively, which correspond to ±7.5 mm in the horizontal direction at the F2 focal plane. Additional iron blocks were also installed to cover both sides of the collimator.

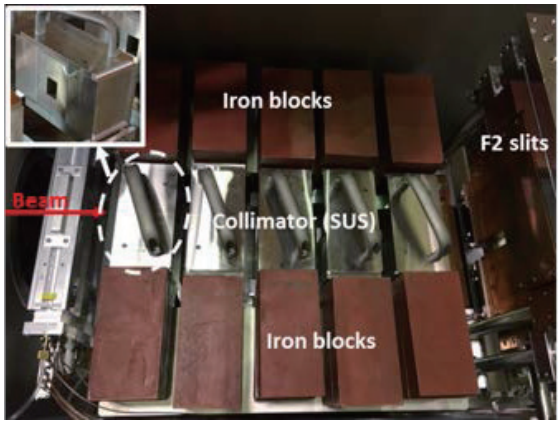

Fig 1. Schematic view of collimator and iron blocks at F2.

*1 RIKEN Nishina Center
*2 Department of Physics, Rikkyo University
*3 FRIB/NSCL, Michigan State University

Particle identification was performed using the TOF-$B\rho$-ΔE method.[3] Fig. 2 shows the production cross sections of neutron-rich Ne isotopes. The experimental results obtained in the 2008-2010[1] and 2014 experiments are also shown in Fig. 2. Different collimators were used in the previous experiments as follows: SUS material with 30-cm thickness for the 2008-2010[1] experiment and 45-cm-thick iron blocks with a large aperture for the 2014 experiment. The black line represents an empirical formula of the EPAX 2.15[4] parameterizations in the LISE^{++} calculation.[5] The present results are in good agreement with both the previous experimental results and the predictions. However, the measured production cross sections of the ^{31,34}Ne isotopes are slightly underestimated.

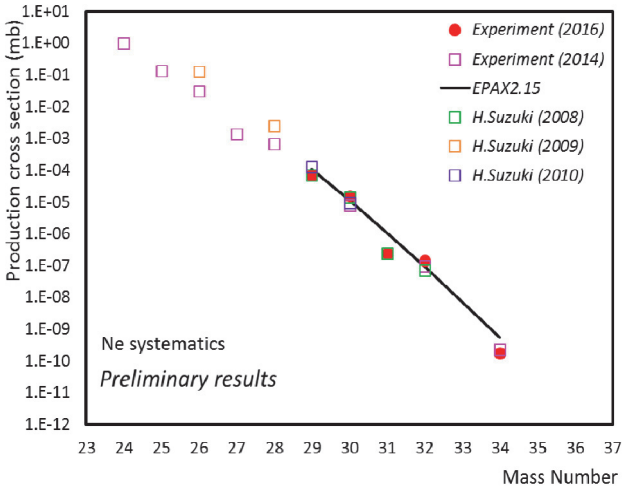

Fig. 2. Preliminary results of production cross sections of very neutron-rich Ne isotopes up to the heaviest known isotope, ^{34}Ne. The filled red circles represent the experimental results obtained from the 2016 experiment. The green, orange, violet, and pink rectangles represent the experimental results obtained from the 2008,[1] 2009,[1] 2010,[1] and 2014 experiments, respectively. The experimental measurements are compared with the EPAX 2.15 parameterizations indicated by the black line.

References

1) H. Suzuki et al., Nucl. Instrum. Meth. Phys. Res. **B317**, 756 (2013).
2) T. Kubo et al., Nucl. Instrum. Meth. Phys. Res. **B204**, 97 (2003).
3) N. Fukuda et al., Nucl. Instrum. Meth. Phys. Res. **B317**, 323 (2013).
4) K. Sümmer, B. Blank, Phys. Rev. **C 61**, 034607 (2000).
5) O. B. Tarasov, D. Bazin, Nucl. Instrum. Meth. Phys. Res. **B266**, 4657 (2008).

Production cross sections of neutron-rich nuclei in the region around $Z = 33$ using the in-flight fission of a ^{238}U beam at the 345 MeV/nucleon

Y. Shimizu,[*1] T. Kubo,[*1] N. Inabe,[*1] D.S. Ahn,[*1] N. Fukuda,[*1] K. Kusaka,[*1] D. Murai,[*1,*2] M. Ohtake,[*1] H. Suzuki,[*1] H. Takeda,[*1] Y. Yanagisawa,[*1] K. Yoshida,[*1] Y. Hirayama,[*3] Y. Ichikawa,[*1] N. Imai,[*4] T. Isobe,[*1] N. Iwasa,[*1,*5] S.C. Jeong[*3] D. Kim,[*6] E.H. Kim,[*6] S. Kimura,[*3] H. Miyatake,[*3] M. Mukai,[*3] H. Otsu,[*1] H. Sato,[*1] T. Sonoda,[*1] and A. Yagi[*7]

A new isotope search experiment in the neutron-rich region around $Z = 33$ was performed in November 2014, aiming to expand the frontier of accessible neutron-rich exotic nuclei.[1] Here, we report on the production cross sections of neutron-rich nuclei measured in this experiment.

Figure 1 shows the measured production cross sections as a function of mass number. The measured production cross sections were derived from the measured production rates and transmission efficiency in the BigRIPS separator, which was based on the LISE^{++} simulations.[2] The determination of the beam intensity was expected to cause a systematic error of 30%. An additional uncertainty of 40% was estimated to be caused by the evaluation of the transmission efficiency. The total systematic error was thus estimated to be 50%. Because the evaluation of transmission efficiency was not reliable, we did not derive the cross sections for the isotopes whose mean positions at the F2 focus were located outside the slit opening. The natural decrease of the measured cross sections with mass number seems to show a reasonable behavior.

The blue solid lines in Fig. 1 show the predictions from the LISE^{++} simulations, in which the LISE^{++} abrasion fission model is employed to calculated the cross sections of fission fragments from the ^{238}U+Be reaction. The simulations were carried out in the Monte Carlo mode. We used LISE^{++} version 8.4.1 and the standard abrasion fission model parameters.[3] The production cross sections are reproduced fairly well by the LISE^{++} predictions.

The black squares in Fig. 1 show the production cross sections obtained from previous measurement.[4] We can see that the present results are in good agreement with previous data. These results strongly support the validity and consistency of our measurement.

In this experiment, some candidates for new isotopes were found.[1] Their production cross sections will be derived using the same analysis. Detailed analysis is currently in progress.

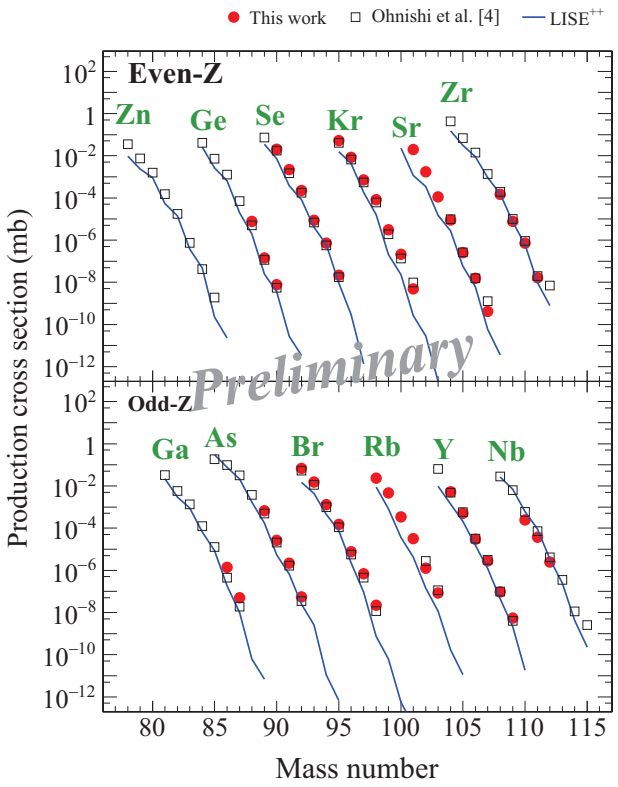

Fig. 1. Production cross section. The red circles and black squares represent those measured in this and previous work, respectively. The errors shown are statistical only. The blue solid lines show the LISE^{++} predictions.

*1 RIKEN Nishina Center
*2 Department of Physics, Rikkyo University
*3 High Energy Accelerator Research Organization (KEK)
*4 Center for Nuclear Study (CNS), University of Tokyo
*5 Department of Physics, Tohoku University
*6 Institute for Basic Science (IBS)
*7 Department of Physics, Osaka University

References

1) Y. Shimizu et al., RIKEN Accel. Prog. Rep. **48**, 71 (2015).
2) O.B. Tarasov and D. Bazin, Nucl. Instr. Meth. B **266**, 4657 (2008) and references therein.
3) H. Suzuki et al., Nucl. Instr. Meth. B **317**, 756 (2013).
4) T. Ohnishi et al., J. Phys. Soc. Jpn. **79**, 073201 (2010).

Production cross-section measurement for radioactive isotopes produced from ^{124}Xe beam at 345 MeV/nucleon by BigRIPS separator

H. Suzuki,[*1] N. Fukuda,[*1] H. Takeda,[*1] Y. Shimizu,[*1] D.S. Ahn,[*1] T. Sumikama,[*1] D. Murai,[*1,*2] J. Amano,[*1,*2] N. Inabe,[*1] K. Yoshida,[*1] K. Kusaka,[*1] Y. Yanagisawa,[*1] M. Ohtake,[*1] Z. Korkulu,[*1] T. Komatsubara,[*1] H. Sato,[*1] and T. Kubo[*1]

We have measured the production yields and the production cross-sections for a variety of proton-rich radioactive isotopes (RIs) produced from a 345-MeV/nucleon ^{124}Xe beam using the BigRIPS separator.[1] The RI beams were produced by projectile fragmentation of the ^{124}Xe beam on a 4-mm Be target. Two BigRIPS settings were conducted in this work. One was the ^{91}Rh setting, in which the $B\rho$ setting is optimized for ^{91}Rh, for producing RIs with atomic numbers $Z = 41-48$, and the other was the ^{80}Y setting for $Z = 35-42$. The particle identification of the RIs was based on the TOF-$B\rho$-ΔE method in the second stage of the BigRIPS.[2]

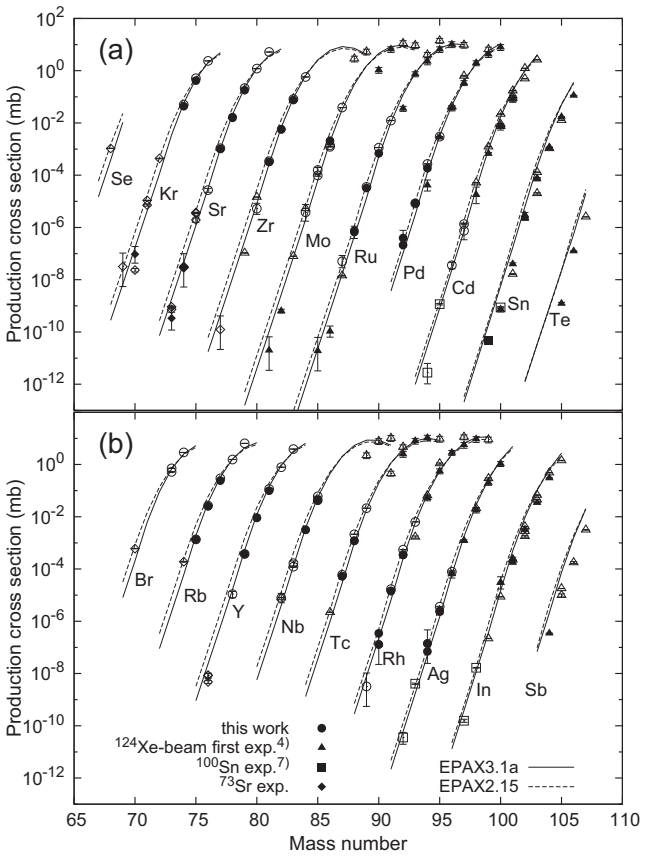

Fig. 1. Production cross-sections of RIs produced in the ^{124}Xe + Be reaction at 345 MeV/nucleon with predictions of EPAX parametrizations. (a) Results for even-Z isotopes. (b) Results for odd-Z isotopes. The filled and open symbols indicate that the distribution peaks of RIs were located inside the slit opening at each focus and outside at some foci, respectively. Solid and dashed lines show the values predicted using EPAX3.1a[5] and EPAX2.15[6] formulas, respectively.

The production cross-sections were deduced from the measured production rates and the transmission efficiency in the separator, which was simulated with the calculation code LISE^{++}.[3] In the simulation, exponential tails of the momentum distribution of the RIs in the low-momentum regions fell off slower than the momentum distribution observed in the experiment; therefore, we adjusted the parameter "coef", which controls the slope of the distribution tail. In the ^{91}Rh setting, "coef" was set to 1.9, which was obtained from the momentum distribution of ^{99}Rh in our first ^{124}Xe-beam experiment.[4] In the ^{80}Y setting, "coef" = 2.4 reproduced the distribution of RIs fairly well. The parameter "coef" may depend on the region of the RI beams. The parameters for the angular distribution were not changed from the original values in the code.

The measured production cross-sections of the RIs are shown in Fig. 1. In these figures, the solid and dashed lines show the cross sections predicted from the empirical formulas EPAX3.1a[5] and EPAX2.15,[6] respectively. EPAX3.1a reproduces the measured cross sections with a wide range of Z better than EPAX2.15; however, some isotopes show systematic discrepancies around the very proton-rich region and the high-Z region. These discrepancies are also observed in the proton-rich RIs produced from the 345-MeV/nucleon ^{78}Kr beam.[8]

*1 RIKEN Nishina Center
*2 Department of Physics, Rikkyo University

References

1) T. Kubo, Nucl. Instrum. Meth. Phys. Res. **B 204**, 97 (2003).
2) N. Fukuda et al., Nucl. Instrum. Meth. Phys. Res. **B 317**, 323 (2013).
3) O. B. Tarasov and D. Bazin: LISE^{++} site, http://lise.nscl.msu.edu, Michigan State University.
4) H. Suzuki et al., Nucl. Instrum. Meth. Phys. Res. **B 317**, 756 (2013).
5) K. Sümmer, Phys. Rev. C **86**, 014601 (2012).
6) K. Sümmer and B. Blank, Phys. Rev. C **61**, 034607 (2000).
7) I. Celikovic et al., Phys. Rev. Lett. **116**, 162501 (2016).
8) H. Suzuki et al., RIKEN Accel. Prog. Rep. **49**, 68 (2017).

2. Nuclear Physics (Theory)

Sum rule study for Double Gamow-Teller state†

H.Sagawa*1,*2 and T. Uesaka*1

Double charge exchange excitations (DCX) induced by heavy ion beams at intermediate energies[1,2] attract a lot of interest with respect to new collective excitations such as the double Gamow-Teller giant resonance (DGTR) and double beta decay matrix elements. A new research program based on a new DCX reaction (^{12}C, ^{12}Be(0_2^+)) is planned at the RIKEN RIBF facility with high intensity heavy ion beams at the optimal energy of E_{lab} =250MeV/u to excite the spin-isospin response. One notable advantage of this reaction is based on the fact that it is a $(2p, 2n)$ type DCX reaction, and one can use a neutron-rich target to excite DGT strength. Although many theoretical efforts have been made to study double beta decays, DGT strengths corresponding to the double beta decays are still too small to be identified in the reaction experiments. Minimum-biased theoretical prediction based on sum rules will provide a robust and global view of the DGTR and can be a good guideline for future experimental studies. In this paper, we present useful formulas for analyzing DGT strength using several sum rules for the double spin-isospin operator $(\sigma t_-)^2$. We also study DIAS excited through the double Fermi transition operator $(t_-)^2$ and double GT operator $(\sigma t_-)^2$.

The sum rule for the single GT transitions is well known and proportional to the neutron excess,

$$\begin{aligned} & S_- - S_+ \\ &= \sum_f |\langle f|\hat{O}_-(\mathrm{GT})|i\rangle|^2 - \sum_f |\langle f|\hat{O}_+(\mathrm{GT})|i\rangle|^2, \\ &= 3(N-Z), \end{aligned} \tag{1}$$

where the GT transition operators read

$$\hat{O}_\pm(\mathrm{GT}) = \sum_\alpha \sigma(\alpha)\mathrm{t}_\pm(\alpha). \tag{2}$$

The DGT transition operator $\hat{O}_\pm(\mathrm{GT})^2$ can be projected to good multipole states to be

$$[\hat{O}_\pm(\mathrm{GT}) \times \hat{O}_\pm(\mathrm{GT})]^J_\mu, J = 0, 2. \tag{3}$$

The sum rule strength is expressed by the reduced matrix element

$$D^J_\pm = \frac{1}{2J_i+1} \sum_{J_f} |\langle J_f||[\hat{O}_\pm \times \hat{O}_\pm]^J||J_i\rangle|^2, \tag{4}$$

where J_i and J_f are the angular momenta of the initial and final states, respectively. Hereafter, we denote the initial state $|J_iM_i\rangle$ by the simple notation $|i\rangle$. The sum rule value for $J = 0$ excitations is evaluated as

$$\begin{aligned} & D_-^{(J=0)} - D_+^{(J=0)} \\ &= \langle i| \left[[\hat{O}_+ \times \hat{O}_+]^{(J=0)}, [\hat{O}_- \times \hat{O}_-]^{(J=0)} \right] |i\rangle, \\ &= 2(N-Z)(N-Z+1) \\ &+ \frac{4}{3} \left[(N-Z)S_+ - \langle i|[i\hat{\Sigma} \cdot (\hat{O}_- \times \hat{O}_+) + \hat{\Sigma} \cdot \hat{\Sigma}]|i\rangle \right], \end{aligned} \tag{5}$$

where $\hat{\Sigma} = \sum_\alpha \sigma(\alpha)$ and $(\hat{O}_- \times \hat{O}_+)$ is the vector product of two operators. The sum rule for the $J^\pi = 2^+$ final states can be obtained in a similar way to that for the $J = 0$ states:

$$\begin{aligned} & D_-^{(J=2)} - D_+^{(J=2)} = 10(N-Z)(N-Z-2) \\ &+ \frac{10}{3} \left[2(N-Z)S_+ + \langle i|[i\hat{\Sigma} \cdot (\hat{O}_- \times \hat{O}_+) + \hat{\Sigma} \cdot \hat{\Sigma}]|i\rangle \right]. \end{aligned} \tag{6}$$

Sum rule values for DGT transitions to $J^\pi = 0^+$ and 2^+ in Eqs. (5) and (6) are calculated for 10 nuclei, ^{6}He, ^{8}He, ^{14}C, ^{18}O , ^{20}O, ^{42}Ca, ^{44}Ca, ^{46}Ca, ^{48}Ca, and ^{90}Zr, together with those for the DIAS states by the Fermi and GT operators. In $N >> Z$ nuclei, the sum rule values of DGT transitions are approximately proportional to a factor (2J+1), i.e., the value for $J = 2$ is five times larger than that for $J = 0$ in the same nucleus. However, this proportionality is significantly modified in $N \sim Z$ nuclei. In the extreme, the sum rule for $J = 2$ transitions is smaller than that for $J = 0$ in the nuclei ^{6}He, ^{14}C, and ^{18}O with $N = Z + 2$, and the two values are almost equal in ^{42}Ca. In nuclei $N > Z+2$, the $J^\pi = 2^+$ excitations dominate the DGT strength because of the multipole factor $(2J+1)$, more than 0^+ excitations. However, in nuclei with $N \sim Z$, the 0^+ excitations become substantially strong, even larger than 2^+ excitations in light nuclei with $T = 1$ such as ^{14}C and ^{18}O. The excitation to DIAS is also studied through $(\sigma t_-)^2$ and t_-^2 operators to investigate the possibility of extracting the unit cross sections for DGT strength. We point out that the strength of DIAS excitations by the $(\sigma t_-)^2$ operator is competitive with the DGT strength in the light $T = 1$ nuclei. This characteristic feature may give a good opportunity to extract the unit cross section for DGT strength.

† Condensed from the article in Phys. Rev. C **94**, 064325(2016)

*1 RIKEN Nishina Center
*2 Center for Mathematics and Physics, University of Aizu

References

1) M. Takaki et al.: Proposal for experiment at RCNP, "Search for double Gamow Teller giant resonances in ^{48}Ti via the heavy-ion double charge exchange ^{48}Ca(^{12}C, ^{12}Be(0_2^+)) reaction" (2015).
2) F. Cappuzzello et al., Journal of Physics: Conference Series **630**, 012018 (2015).

Effect of isoscalar spin-triplet pairings on spin-isospin responses†

H. Sagawa,[*1,*2] T. Suzuki,[*3] and M. Sasano[*1]

The spin-isospin response is a fundamental process in nuclear physics and astrophysics. The Gamow-Teller (GT) transition induced by $\vec{\sigma}t_{\pm}$ and, in a no-charge-exchange channel, magnetic dipole (M1) transitions are extensively observed in a broad region of the mass table. Recent high-resolution proton inelastic scattering measurements at $E_p = 295$ MeV have revealed that the isoscalar (IS) quenching is substantially smaller than the isovector (IV) quenching in the spin M1 excitations for several $N = Z$ *sd*-shell nuclei.[1)] In this paper, we study the effect of IS spin-triplet pairing correlations on the IS and IV spin M1 responses based on modern shell model effective interactions for the same set of $N = Z$ nuclei as those in Ref. 1.

We consider the IS and IV spin M1 operators, which are given as $\hat{O}_{\rm IS} = \sum_i \vec{\sigma}(i)$ and $\hat{O}_{\rm IV} = \sum_i \vec{\sigma}(i)\tau_z(i)$, respectively. The proton-neutron spin-spin correlation is defined as

$$\begin{aligned}\Delta_{\rm S} &= \frac{1}{16}\left(S(\vec{\sigma}) - S(\vec{\sigma}\tau_z)\right)\\ &= \sum_f \langle i|\sum_i \frac{\vec{\sigma}_n(i)+\vec{\sigma}_p(i)}{4}|f\rangle\langle f|\sum_i \frac{\vec{\sigma}_n(i)+\vec{\sigma}_p(i)}{4}|i\rangle\\ &- \sum_f \langle i|\sum_i \frac{\vec{\sigma}_n(i)-\vec{\sigma}_p(i)}{4}|f\rangle\langle f|\sum_i \frac{\vec{\sigma}_n(i)-\vec{\sigma}_p(i)}{4}|i\rangle\\ &= \langle i|\vec{S}_p\cdot\vec{S}_n|i\rangle, \qquad (1)\end{aligned}$$

where $\vec{S}_p = \sum_{i\in p}\vec{s}_p(i)$ and $\vec{S}_n = \sum_{i\in n}\vec{s}_n(i)$. The correlation value is 0.25 and -0.75 for a proton-neutron pair with a pure spin triplet and a spin singlet, respectively. The former corresponds to the ferromagnet limit of the spin alignment, while the latter is the antiferromagnetic one.

Shell model calculations are performed in the full *sd*-shell model space with a USDB effective interaction. In the results of USDB*, the IS spin-triplet interactions are enhanced by multiplying the relevant matrix elements by a factor of 1.2 compared to the original USDB interaction. For the results of the IV spin-M1 transitions, a quenching factor $q = 0.9$ is used for USDB**. The calculations for ^{28}Si reproduce quite well the experimental IS 1^+ state with a strong spin transition at $E_{\rm x} = 9.50$ MeV. The enhanced IS pairing has a quenching effect of approximately 20% on the transition strength [i.e., $B(\sigma) = 6.82(5.63)$ in USDB(USDB*)], but the excitation energies are less affected within a few hundred keV change. Two IV 1^+ states with strong spin strengths of $B(\sigma\tau) = 2.05$ and 0.92 are reported at $E_{\rm x} = 11.45$ and 14.01 MeV, respectively. The shell model gives strong IV M1 states at similar excitation energies. The enhanced IS pairing reduces the IV spin transition strength, corresponding to a renormalization factor of $g_s^{\rm eff}({\rm IV})/g_s({\rm IV}) = 0.87$.

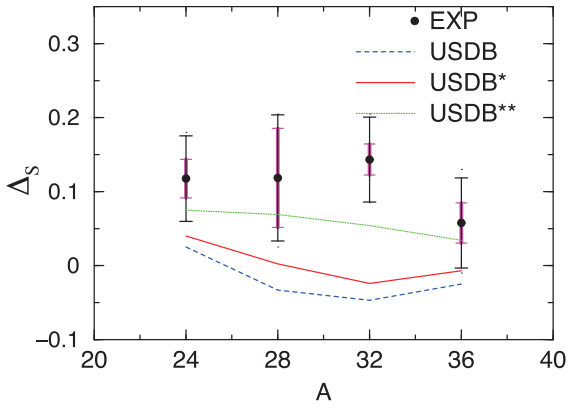

Fig. 1. (Color online) Experimental and calculated proton-neutron spin-spin correlation $\Delta_{\rm S}$. See the text for details. Experimental data are taken from Ref. 1. See Ref. 1 for a description of the experimental error bars.

Figure 1 shows the experimental and calculated proton-neutron spin-spin correlations (1). The results calculated with the USDB interaction show poor agreement with the experimental data. The results with an enhanced IS spin-triplet pairing improve the agreement to some extent. A quenching factor close to unity, $q = 0.9$, for only the IV matrix elements, results eventually in a fine agreement with the experimental values. The positive value of the correlation indicates that the population of spin triplet pairs in the ground state is larger than that of the spin singlet pairs.

In summary, we studied the IS and IV spin M1 transitions in even-even $N = Z$ *sd*-shell nuclei using shell model calculations with USDB interactions in full *sd*-shell model space. The quenching effects on the spin M1 transition matrices are larger in the IV case than in the IS case. Positive contributions for the spin-spin correlations are obtained via an enhanced isoscalar spin-triplet pairing interaction. The effect of the Δ-hole coupling is also examined on the IV spin transition, and the empirical spin-spin correlations in the ground states are reproduced well by a combined effect of the IS pairing and a quenching factor of $q = 0.9$ on the IV spin transition matrix elements.

† Condensed from the article in Phys. Rev. C **94**, 041303(R) (2016)
*1 RIKEN Nishina Center
*2 Center for Mathematics and Physics, University of Aizu
*3 Department of Physics, Nihon Univerity

Reference

1) H. Matsubara et al., Phys. Rev. Lett. **115**, 102501 (2015).

Decay dynamics of the unbound ^{25}O and ^{26}O nuclei†

K. Hagino*1 and H. Sagawa*2,*3

We study the ground and excited resonance states in ^{26}O with a three-body model by taking into account the coupling to the continuum. The main aim of our study is to extract the di-neutron correlations and the halo nature of the ground state of ^{26}O from the two-neutron decay spectrum with updated empirical inputs for the model Hamiltonian. In the present ^{24}O $+n+n$ three-body model, the neutron-core potential as well as the strength of the pairing interaction between the valence neutrons is calibrated using new experimental data from Ref. 1 and the calculations performed in Refs. 2 are refined. With the same model input, we also discuss the structure of the excited 2^+ resonance state.

We discuss the first 2^+ state in ^{26}O. One of the most important findings in the recent experiment reported in Ref. 1 is a clear second peak at $E = 1.28^{+0.11}_{-0.08}$ MeV, which is likely attributed to the 2^+ state. Because of the pairing interaction between the valence neutrons, the energy of the 2^+ state is slightly shifted towards lower energies from the unperturbed energy, whereas the energy shift is much larger for the 0^+ state due to the larger overlap between the wave functions of the two neutrons in the three-body model. The 2^+ peak appears at 1.282 MeV, which agrees perfectly with the experimental data, as shown in Table 1.

While we achieve an excellent agreement with the experimental data for the energy of the 2^+ state, it is striking that most theoretical calculations performed so far overestimate the energy. We summarize other results in Table I together with the energy of the $3/2^+$ state in ^{25}O for each calculation. The 2^+ state should certainly appear at an energy slightly lower than the unperturbed state, as long as the three-body structure is reasonable. In this sense, the ab-initio calculation with chiral NN and $3N$ interactions shows the opposite trend, and the shell model (SM) calculations, except for the continuum SM calculations of Ref. 4 and Ref. 5, seem to overestimate the correlation.

We next discuss the angular correlation of the emitted neutrons from the ground state of ^{26}O. Figure 1 shows the angular distributions thus obtained. In the absence of the correlation between the valence neutrons, the angular distribution is symmetric with respect to $\theta_{12} = \pi/2$ (see the dotted line). On the other hand, in the presence of the interaction between the valence neutrons, the angular distribution becomes highly asymmetric, with an enhancement of the back-to-back emission,[2,7] as shown by the solid line. This is a natural consequence of the dineutron correlation in the momentum space, which has an opposite trend to the correlation in the coordinate space; the di-neutron correlation has a strong peak at the small correlation angle in the coordinate space and Heisenberg's uncertainty principle converts the backward correlations in the momentum space.

Table 1. Comparison of the energies of the $3/2^+$ state of ^{25}O and the 2^+ state of ^{26}O obtained with several methods. These values, given in units of MeV, are measured from the thresholds.

Method	^{25}O ($3/2^+$)	^{26}O (2^+)	Ref.
Shell model (USDA)	1.301	1.9	3)
Shell model (USDB)	1.303	2.1	3)
chiral NN + 3N	0.742	1.64	3)
continuum SM	1.002	1.8	4)
continuum-coupled SM	0.86	1.66	5)
3-body model	?	1.6	6)
3-body model	0.749 (input)	1.282	this work
Experiment	0.749 (10)	$1.28^{+0.11}_{-0.08}$	1)

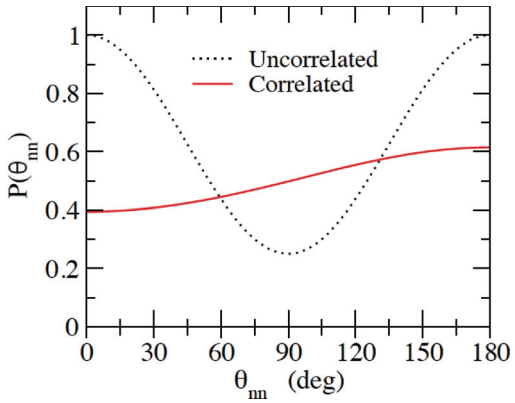

Fig. 1. (Color online) Angular correlations between the emitted neutrons from the two-neutron decay of ^{26}O. The solid and dotted lines show the correlated and uncorrelated distributions, respectively.

References
1) Y. Kondo et al., Phys. Rev. Lett.116, 102503 (2016).
2) K. Hagino and H. Sagawa, Phys. Rev. C**89**, 014331 (2014) ; Phys. Rev. C**90**, 027303 (2014).
3) C. Caesar et al., Phys. Rev. C**88**, 034313 (2013).
4) A. Volya, V. Zelevinsky, Phys. Rev. C**74**, 064314 (2006).
5) K. Tsukiyama, T. Otsuka, R. Fujimoto, Prog. Theor. Exp. Phys. **2015**, 093D01 (2015).
6) L.V. Grigorenko, M.V. Zhukov, Phys. Rev. C**91**, 064617 (2015).
7) L.V. Grigorenko, I.G. Mukha, M.V. Zhukov, Phys. Rev. Lett. **111**, 042501 (2013).

† Condensed from the article in Phys. Rev. C **93**, 034330 (2016)

*1 Department of Physics, Tohoku University
*2 RIKEN Nishina Center
*3 Center for Physics and Mathematics, University of Aizu

QRPA calculations with Skyrme energy density functional for rotating unstable nuclei

M. Yamagami[*1] and K. Matsuyanagi[*2,*3]

The energy density functional (EDF) theory is the only tractable microscopic theory that can be applied across the entire table of nuclides. The EDF has been optimized using the basic nuclear properties, and the extension to various collective dynamics in unstable nuclei is a current hot issue.

We have developed a new computer code for the quasiparticle random phase approximation (QRPA) calculations. As an input, we adopt the Skyrme EDF.

At first, we solve the Hartree-Fock-Bogoliubov (HFB) equation in the matrix form

$$\begin{pmatrix} h'-\lambda & \Delta \\ -\Delta^* & -h'+\lambda \end{pmatrix} \begin{pmatrix} U_k \\ V_k \end{pmatrix} = E_k \begin{pmatrix} U_k \\ V_k \end{pmatrix}. \quad (1)$$

The single-particle Hamiltonian $h' = h - \omega_{rot} j_x$ describes the independent-particle motion in the triaxially deformed potential that is uniformly rotating with the rotational frequency ω_{rot} about the x-axis. The Skyrme SkM* parametrization and the mixed-type density-dependent zero-range pairing force are employed. The Fourier-series expansion method is used to efficiently represent wave functions (WFs) of unbound and weakly bound states[1].

We solve the QRPA equation in the matrix form with WFs obtained by the HFB calculation. The particle–hole residual interaction is derived from the Skyrme force through the Landau–Migdal approximation, while the pairing residual interaction is selfconsistently treated.

As a first application, we studied the rotational effect on the $K^\pi = 0^+$ isoscalar quadrupole excitations in neutron-rich nuclei, ^{34}Mg and ^{36}Mg. Figure 1 shows the strength function at $\omega_{rot} = 0$ in ^{34}Mg. Here, the ground state has a prolate deformation $\beta_2 = 0.22$. We obtained a collective state at the vibrational energy $E_{vib} = 3.31$ MeV with the transition strength $B(IS2) = 11.4$ w.u.

In Fig. 1, the result without the residual pairing interaction ($\delta\Delta = 0$) is also shown. Without the fluctuation of the pairing field, this excited state can not emerge. As a main configuration, the fluctuation of the neutron-pair occupation between the oblate-type [202]3/2 orbit and the prolate-type [321]3/2 one across the $N = 22$ shell gap induces vibration of the particle-number density.

In Fig. 2, the $B(IS2)$ value of the lowest collective states in ^{34}Mg is shown as a function of ω_{rot}. We found that the $B(IS2)$ value decreases with small ω_{rot}. This is because the $K^\pi = 0^+$ excitation strongly depends on the pairing properties, while pairing is sensitive to breaking of time-reversal symmetry. Here, the neutron pairing gap is $\Delta_n = 2.2$ MeV at $\omega_{rot} = 0$, and 1.4 MeV at $\omega_{rot} = 0.6$ MeV/$\hbar$ corresponding to the total angular momentum $J_z = 2.6\hbar$. We also found the same results for ^{36}Mg, as shown in Fig. 2.

In conclusion, we developed a new computer code for the QRPA calculations with Skyrme EDF. By using this code, we emphasized the role of pairing and collective rotation for $K^\pi = 0^+$ quadrupole excitations in ^{34}Mg and ^{36}Mg. This is a unique phenomenon that can emerge only in atomic nuclei as finite quantum systems.

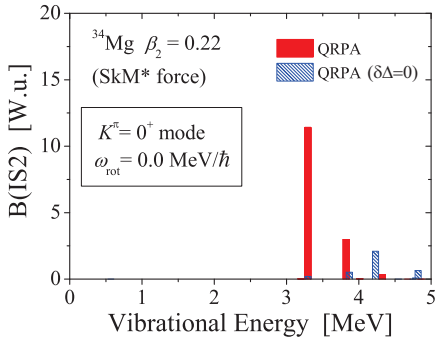

Fig. 1. Strength function of $K^\pi = 0^+$ isoscalar quadrupole excitation at $\omega_{rot} = 0$ in ^{34}Mg. The resut of QRPA calculation without the residual pairing interaction ($\delta\Delta = 0$) is also shown.

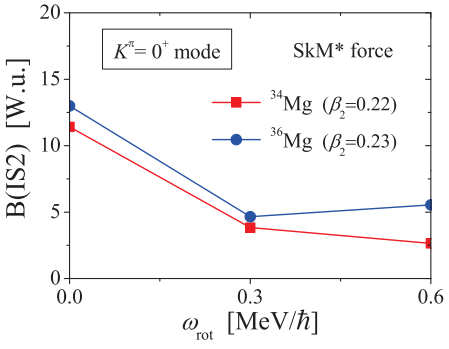

Fig. 2. $B(IS2)$ values of the lowest $K^\pi = 0^+$ excitations in ^{34}Mg and ^{36}Mg as a function of ω_{rot}.

*1 Department of Computer Science and Engineering, University of Aizu
*2 RIKEN Nishina Center
*3 Yukawa Institute for Theoretical Physics, Kyoto University

References

1) M. Yamagami et al., JPS Conf. Proc. **6**, 030051 (2015).
2) K. Yoshida et al., Phys. Rev. C **77**, 044312 (2008).

Improved treatment of blocking effect at finite temperature†

N. Quang Hung,*1 N. Dinh Dang,*2 and L. T. Quynh Huong*3

In odd nuclei with odd numbers of nucleon (neutron or proton), due to the Pauli principle, the odd particle at zero temperature ($T = 0$) completely blocks the level k which it occupies. Consequently, this level k remains unpaired with the occupation number equal to 1. Within the approximation such as the BCS theory, this level is excluded from the BCS equation for the pairing gap, whereas the particle-number equation is solved only for the even core. The resulting approximation is called the "blocked BCS"[1]. At finite temperature $T \neq 0$, the odd particle has the probabilities of occupying all the levels above the Fermi surface. As the result, any observable is then obtained by taking the average of all the above probabilities over the statistical ensembles such as the grand canonical ensemble (GCE) or canonical ensemble (CE). Several approximations have been proposed to describe the properties of odd nuclei at $T \neq 0$. One of the approximations, which is a direct extension of the blocked BCS and is widely used in nuclear physics, was proposed by Maino *et al.*[2]. This approach assumes that at $T \neq 0$, the odd particle can occupy the level k with the unity occupation number ($q_k = 1$) as at $T = 0$, but k can be any level above the Fermi surface, not only $k = k_0$ with k_0 being the lowest level located just above the Fermi level. The approach, called "Maino's" hereafter, then takes the average of any observable as the sum of all its average values taken for each blocked level k with the statistical weight as the ratio of the grand partition function for the blocked level k to the total grand partition function. The assumption of the unity occupation probability of the odd level in the Maino's approach means that temperatures have no effect on it, whereas the occupation numbers of all the levels in the pairing core are obtained by averaging over the GCE, and, they are therefore temperature-dependent. An obvious inconsistency of such assumption is that it fails to reproduce the zero-pairing limit of the equation for the particle number at finite temperature, where all the single particle occupation numbers should follow the Fermi-Dirac distribution of noninteracting fermions.

Present paper proposes an improved treatment of the blocking effect in odd nuclear systems interacting via the constant pairing force. Based on the analysis of the exact solutions of the doubly-degenerate equidistant multilevel pairing model for $N = 9$ particles and $\Omega = 10$, 14, and 20 levels whose the single-particle energies are $\epsilon_k = k$ ($k = 1, 2, ..., \Omega$), we show that the exact occupation number of the blocked level occupied by the odd particle is equal to 1 at $T = 0$ and then decreases with increasing T (See e.g., thick solid lines in Fig. 1). As the result, the conventional assumption of the unity occupation number for this blocked level is no longer valid at $T \neq 0$. Instead, we introduce the temperature-dependent occupation number q_k for the blocked level, which is directly derived from the standard equation for the particle number within the standard finite-temperature BCS [Eqs. (13), (23), and (24) of Ref.[3]]. We also construct the average q_k-blocked BCS [Eqs. (13), (23), and (25) of Ref.[3]], which follows Maino's idea and the results obtained agree well with those obtained within the Mainos approach. However, again by using the exact solutions of the pairing Hamiltonian, we demonstrate that the average procedure over all the levels above the Fermi surface as proposed in the Mainos approach does not correspond to the real situation observed in the exact solutions, where the odd particle actually always remains on the top level $k = k_0$. Based on the analysis of the results obtained in the present paper, we believe that, in the study of the odd systems with pairing, such as atomic nuclei, at finite temperature, if the BCS approach with blocking is ever applied, the q_k-blocked BCS with $k = k_0$ proposed here should be used instead of the blocked BCS, whereas neither the Maino's approach nor the average q_k-blocked BCS is necessary.

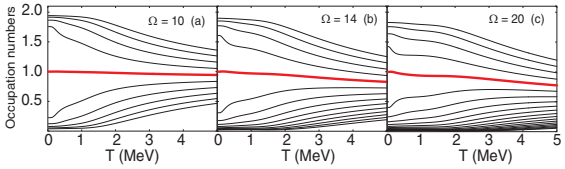

Fig. 1. Exact occupation numbers of the levels as functions of T obtained within the doubly-degenerate equidistant multilevel pairing model for $N = 9$ particles and $\Omega = 10$ (a), 14 (b), and 20 (c) levels. In each panel, the higher-located line is the occupation number of the lower-located level. The thick line, which starts from 1 at $T = 0$, is the occupation number of the level occupied by the odd particle.

† Condensed from the article in Phys. Rev. C 94, 024341 (2016)

*1 Institute of Research and Development, Duy Tan University
*2 RIKEN Nishina Center
*3 Department of Natural Science and Technology, University of Khanh Hoa

References

1) P. Ring and P. Schuck, *The Nuclear Many-Problem* (Springer, Berlin, 2004).
2) G. Maino, E. Menapace, and A. Ventura, Il Nuovo Cimento A **57**, 427 (1980).
3) N. Quang Hung, N. Dinh Dang, and L. T. Quynh Huong, Phys. Rev. C **94**, 024341 (2016).

Effective restoration of dipole sum rules within the renormalized random-phase approximation†

N. Quang Hung,[*1] N. Dinh Dang,[*2] T. V. Nhan Hao,[*1,*3] and L. Tan Phuc[*1]

The random-phase approximation (RPA) is one of the simple theoretical methods, which is widely used to describe the vibrational collective excitations of the nucleus. The RPA is derived basically based on the quasiboson approximation (QBA), which assumes that the operators of the particle-hole (ph) pairs have structure like ideal bosons, leading to the violation of the Pauli principle owing to their fermion structure. The application of the RPA to the light nuclear systems, where the concepts of the mean field and the QBA do not properly work well, is therefore questionable. One of the typical methods to preserve the Pauli principle between the RPA ph pairs is the renormalized RPA (phRRPA)[1]. The latter includes the so-called ground-state correlation (GSC) factor $D_{ph} \equiv \sqrt{f_h - f_p}$ with f_p and f_h being occupation numbers of the particles and the holes, respectively. Within the RPA, D_{ph} is equal to 1, whereas within the phRRPA it is proportional to the RPA backward-going amplitudes $(Y_{ph})^2$ and is therefore always less than or equal to 1. However, the application of the phRRPA using this GSC factor has been limited so far to the energy and $B(E3)$ value of the lowest 3^-_1 state in ^{146}Gd and ^{208}Pb only[2]. For the dipole excitation 1^-, whose first moment m_1 known as the energy-weighted sum rule (EWSR) is the most important, no investigation was carried out. The RPA fulfills this EWSR sum rule. However, within the phRRPA, the matrix elements of the ph interactions are reduced by the factor D_{ph}, leading to the decrease of the $B(E1)$ values and therefore causing the violation of the EWSR. The goal of the present paper is to restore the EWSR violated within the conventional phRRPA in an approximate and effective way.

To restore the EWSR, we propose a simple RRPA calculations taking into account, in addition to the ph excitations, the contribution of the pp and hh excitations in a perturbative way. The total isovector (IV) and isoscalar (IS) (compressional) dipole transition probabilities are then given as $B(E1) = B^{ph}(E1) + B^{pp'}(E1) + B^{hh'}(E1)$, where $B^{ss'}(E1)$ are the transition probabilities of the ss' ($ss' = ph$ or pp' or hh') transitions. The numerical calculations are carried out using the self-consistent RPA code with Skyrme SLy5 interaction[3] for IV and IS dipole strength distributions in ^{48,52,58}Ca (Fig. 1) and ^{90,96,110}Zr isotopes. The results obtained show that the GSC beyond

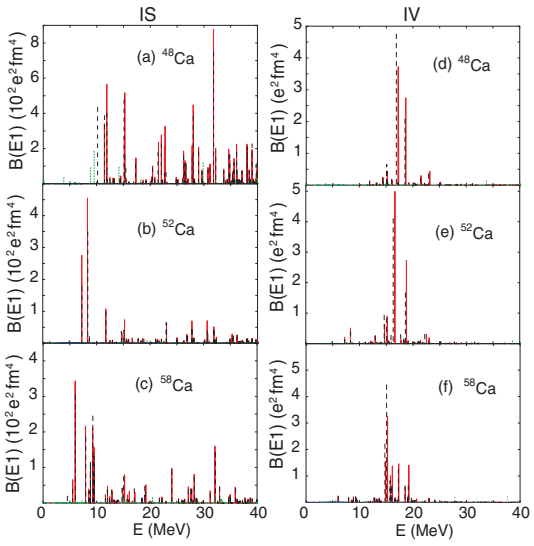

Fig. 1. Distributions of the IS and IV reduced transition probabilities $B(E1)$ for calcium obtained within the RPA, phRRPA, and RRPA. The solid and dashed vertical bars denote the $B(E1)$ values obtained within the RPA and phRRPA, respectively. The dotted vertical bars stand for the $B^{pp'}(E1)$.

the RPA reduce the IS transition strengths, whereas it slightly increases the total strength on the low-energy region (the pygmy dipole resonance – PDR) region and decreases the strength on the other side (the GDR region), leading to a significant decrease of the EWSRs for both IS and IV modes obtained within the phRRPA. This violation of the EWSR is then fully recovered by taking into account the contribution of pp and hh excitations within the RRPA. This result reveals the reason why all the RPA extensions that do not take into account the pp and hh excitations violate the EWSRs. Consequently, the ratio of the energy-weighted sum of strengths of the PDR to that of the GDR, which is almost zero in stable nuclei, increases with the neutron number. As compared to the RPA case, this ratio is in general significantly larger within the RRPA.

† Condensed from the article in Phys. Rev. C 94, 064312 (2016)

*1 Institute of Research and Development, Duy Tan University
*2 RIKEN Nishina Center
*3 Texas A&M University-Commerce

References

1) K. Hara, Prog. Theor. Phys. **32**, 88 (1964); K. Ikeda, T. Udagawa, and H. Yamaura, *ibid.* **33**, 22 (1965); J. Dukelsky and P. Schuck, Phys. Lett. B **464**, 164 (1999).
2) F. Catara, N. Dinh Dang, and M. Sambataro, Nucl. Phys. A **579**, 1 (1994).
3) G. Colo, L. Cao, N. Van Giai, and L. Capelli, Comput. Phys. Commun. **184**, 142 (2013).

Giant dipole resonance in hot rotating nuclei†

D.R. Chakrabarty,*1 N. Dinh Dang,*2 and V.M. Datar*3

Experimental observations on the dependence of the width of giant dipole resonance (GDR) on temperature (T) and angular momentum (J), covering a wide range of T, J and nuclear systems, can be summarized as follows. The GDR width is rather insensitive to the change of T up to $\sim$ 1 MeV and increases rapidly up to a moderate T of $\sim$ 2.5 MeV. At higher T, there are claims of observing a saturation of the GDR width. This observation has, however, been questioned in some works which have emphasized the need for a better characterization of the excitation energy E_X (i.e. T and J) of the source in the data analysis. The reanalysis of the data after taking into account the pre-equilibrium (PEQ) effects in the mass asymmetric channel, has shown a monotonic increase of the width at least up to $T \sim 3.5$ MeV.

On the other hand a recent experiment in a mass symmetric channel, which shows negligible PEQ effects, has suggested the GDR width saturation at $T \sim$ 3 MeV. This highlights the need to resolve this important issue in future experiments. At still higher T, the other observed phenomenon is the quenching of the GDR strength. In this regime again, various authors use a saturated GDR width in the data analysis. The GDR quenching has been related to the competition between the equilibration time for the excitation of GDR and the lifetime of the nucleus or the transition of the hot nucleus to a chaotic regime. In this regard, an interesting suggestion has been made on the relation of the vanishing of the collective vibration and the liquid to gas phase transition in nuclear systems. As for the J-dependence the GDR width, the disentangling of the J-effect from the T-effect is made mostly in the moderate T-regime. The GDR width weakly depends on J up to a certain value and increases at higher J. This value of J depends on the nuclear mass number, being, for example, $J \sim 30\hbar$ for A $\sim$ 110. In heavier nuclei (A $\sim$ 180) the width is roughly constant up to the highest measured $J \sim 50\hbar$.

Among several theoretical approaches to calculating the GDR strength function, the microscopic-macroscopic thermal-shape fluctuation model (TSFM) has been most widely employed in comparisons with experimental data. The J-dependence of the width is reasonably well explained by the model. Here the contribution to the width at low J comes from thermal shape fluctuations. The T dependence of the width is not very well reproduced by this model, particularly at low T. An improvement in this model, by including pairing fluctuations, is able to describe the GDR width at low T. The macroscopic collisional damping model (CDM) predicts a monotonic increase of width with T but does not address the J-dependence. The experimental data at high T do not agree with the CDM predictions.

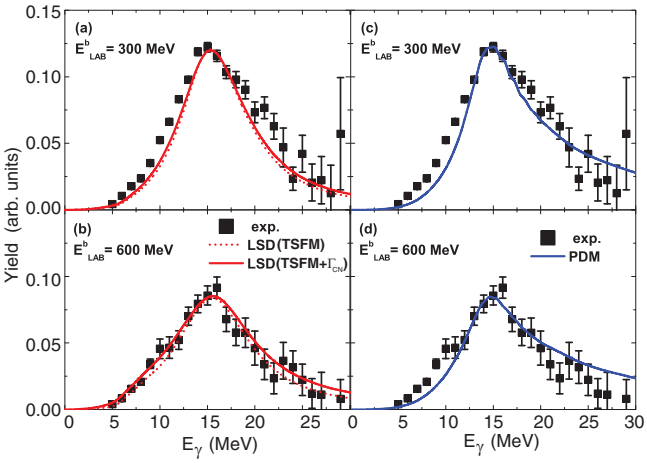

Fig. 1. Experimental and theoretical GDR strength functions in ^{88}Mo at beam energies of 300 MeV (E_X = 123.8 MeV) [(a) and (c)] and 600 MeV (E_X = 260.7 MeV) [(b) and (d)]. Results of Lublin-Strasbourg Drop model (LSD) based on TSFM (including the contribution of the evaporation width Γ_{CN}) and PDM calculations are shown by continuous lines. Dashed lines are LSD results without Γ_{CN} contribution.

The microscopic models, which go beyond the finite-temperature random-phase approximation (FT-RPA), have shown that the GDR spreading width $\Gamma^{\downarrow}$, which arises because of coupling to 2 particle - 2 hole configurations, is almost temperature-independent. Among the various microscopic models the phonon-damping model (PDM)[1] is the most successful one [Figs. 1 (c) and 1 (d), where E_x in (c) corresponds to the mean temperature T_{ev} = 2 MeV of nuclei in the evaporation process after the emission of GDR γ-ray, whereas T_{ev} = 3.1 MeV in (d)]. The results of the PDM calculations including pairing fluctuations agree with the T-dependence of the observed widths at low and moderate T. It predicts the width's saturation as well as the quenching of the GDR γ-ray yield at very high T.

† Condensed from the article in Eur. Phys. J. A **52**, 143 (2016)

*1 Nuclear Physics Division, Bhabha Atomic Research Centre
*2 RIKEN Nishina Center
*3 INO Cell, Tata Institute of Fundamental Research

Reference
1) N. Dinh Dang, A. Arima, Phys. Rev. Lett. **80**, 4145 (1998); N.D. Dang, A. Arima, Nucl. Phys. A **636**, 427 (1998).

Enhanced collectivity of γ vibration in the neutron-rich Dy isotopes around $N = 108$ †

K. Yoshida*1 and H. Watanabe*2

The γ vibrational mode of excitation is an acknowledged collective mode in deformed nuclei. Quite recently, a sudden decrease in the excitation energy of the γ vibration was observed at RIKEN for the neutron-rich Dy ($Z = 66$) isotopes at $N = 106$[1]. In the present report, by systematically studying the microscopic structure of the γ vibration in the neutron-rich Dy isotopes with $N = 98 - 114$, we try to understand the mechanism of the observed softening. The low-frequency modes of excitation in the neutron-rich rare-earth nuclei are described on the basis of nuclear density-functional theory.

Atomic nuclei reveal spontaneous breaking of rotational symmetry in both real space and gauge space in stepping away from magic numbers. Most of the deformed nuclei still retain the axial symmetry. In axially deformed nuclei, a low-frequency quadrupole mode of excitation, known as the γ vibration, emerges. The γ vibrational mode of excitation is regarded as a precursory soft mode of the permanent non-axial deformation. It would be interesting to investigate the possibility of occurrence of the γ vibration in exotic nuclei, and to achieve a deep understanding of the microscopic mechanism for the generation of collective vibrations in atomic nuclei.

Figure 1 shows the excitation energy of the γ vibration in the neutron-rich Dy isotopes. Here, we employ the Skyrme energy-density functionals (EDF's) in the Hartree-Fock-Bogoliubov calculation for the ground states and in the Quasiparticle Random-Phase Approximation (QRPA) for the excitations. The results of the calculation are compared with experimental data[1–3]. Both the SkM* and SLy4 functionals reproduce the isotopic trend in energy well; lowering when N increases from 104 to 106.

Based on the analysis of the wave functions, we found that the coherent contribution of the $\nu[512]3/2 \otimes \nu[510]1/2$, $\nu[510]1/2 \otimes \nu[512]5/2$, and $\nu[512]3/2 \otimes \nu[514]7/2$ excitations satisfying the selection rule of the non-axial quadrupole matrix element,

$$\Delta N = 0 \text{ or } 2, \Delta n_3 = 0, \Delta\Lambda = \Delta\Omega = \pm 2, \qquad (1)$$

plays a major role in generating the collectivity, *i.e.* lowering of the frequency and enhancement in the transition strength.

One can see in Fig. 1 that the excitation energy of

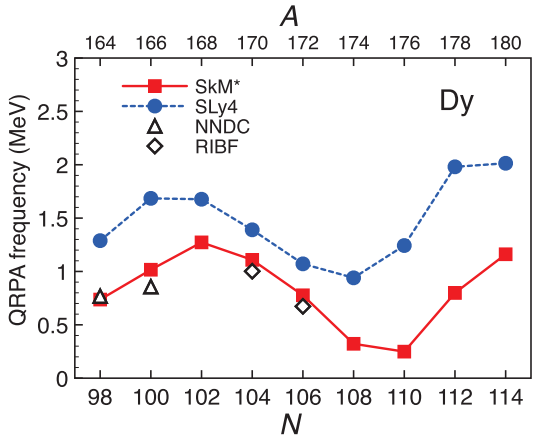

Fig. 1. QRPA frequency of γ vibration obtained by using SkM* and SLy4 EDF's. Also shown are the experimental data[1–3].

the γ vibration decreases toward $N = 110(108)$ in the case of the calculation employing the SkM* (SLy4) functional. This is because the Fermi level of neutrons lies among the orbitals that play an important role in generating the collectivity around $N = 106$.

We found a similar isotopic dependence of the excitation energy in the neutron-rich Er ($Z = 68$) and Yb ($Z = 70$) isotopes. We can thus conclude that the microscopic mechanism governing the enhanced collectivity around $N = 108$ in the Dy isotopes is robust in the neighboring nuclei. Note that we obtained the strongest collectivity for $Z = 66$ because the 2qp excitations of $\pi[411]1/2 \otimes \pi[411]3/2$ and $\pi[411]1/2 \otimes \pi[413]5/2$, located around the Fermi level of protons and satisfying the selection rule (1), make a coherent contribution to generation of the γ vibration together with the excitation of neutrons.

The numerical calculations were performed on SR16000 and CRAY XC40 at the Yukawa Institute for Theoretical Physics, Kyoto University, and on COMA (PACS-IX) at the Center for Computational Sciences, University of Tsukuba.

References

1) H. Watanabe et al: Phys. Lett. **B760**, 641 (2016).
2) National Nuclear Data Center. "Evaluated Nuclear Structure Data File", http://www.nndc.bnl.gov/ensdf.
3) P.-A. Söderström et al: Phys. Lett. **B762**, 404 (2016).

† Condensed from the article in Prog. Theor. Exp. Phys. **(2016)**, 123D02 (2016)

*1 Graduate School of Science and Technology, Niigata University
*2 School of Physics and Nuclear Energy Engineering, Beihang University

Three-body model for IS spin-triplet neutron-proton pair in ^{102}Sb†

Y. Tanimura*1 and H. Sagawa*2,*3

As the progress of radio-isotope beam facilities allows to access nuclei near the $N = Z$ line, the neutron-proton pairing has been attracting more interest than before. In general, a condition expected to maximize the chance for valence nucleons to form $T = 0$ pairs is that they lie in the orbitals on top of a $N = Z$ closed-shell core, and that both $j_>$ and $j_<$ orbitals with low l are vacant in the valence space. In addition, a large nuclear mass is favorable because the effect of the spin-orbit field at the surface becomes relatively weak. In the present study, we focus on the ^{102}Sb = ^{100}Sn+p+n system, the core of which, ^{100}Sn, is the largest $N = Z$ doubly-magic nucleus located immediately below the proton drip line. In this system, the valence nucleons can occupy d-wave states as in the ^{18}F nucleus, in which the strong effect of the $(S, T) = (1, 0)$ coupling channel is observed as an implementation of the good SU(4) symmetry.[1)]

In the present study where we have ^{100}Sn as the core, we take a self-consistent mean-field Hamiltonian for the single-particle part, $H = h_{\rm HF}(p) + h_{\rm HF}(n) + V_{\rm res}(p, n)$, where $h_{\rm HF}$ is the single-particle Hartree-Fock Hamiltonian. For the residual interaction $V_{\rm res}$, we take density-dependent zero-range pairing interactions which have both spin-singlet and spin-triplet channels.

We calculate the neutron single-particle energies in the ^{100}Sn nucleus with three non-relativistic (SLy4, SkM*, and SIII) and three relativistic point-coupling (PC-F1, PC-PK1, and PC-LA) EDFs. In particular, we found that, with the relativistic interactions, the $1g_{7/2}$ level is nearly degenerate with the $2d_{5/2}$ level. In contrast, with the Skyrme functionals except for SIII, the $1g_{7/2}$ level is located well above the $2d_{5/2}$ state and close to the $2d_{3/2}$ level. This difference may induce a substantial effect on the structure of the system as well as the $(T = 0, S = 1)$ pair coupling because it prevents the valence nucleons from efficiently gaining the pairing energy in $(d)^2$ configurations. This near degeneracy with the relativistic EDFs is due to the pseudo-spin symmetry which originates from the cancellation of large scalar and vector fields. Note that a γ ray of 172 keV between the first-excited and the ground states of ^{101}Sn has been measured in Refs.[2,3)] and interpreted as a single-neutron transition between the $d_{5/2}$ and $g_{7/2}$ levels.

We have applied a new three-body model based on self-consistent HF fields to the ^{102}Sb = ^{100}Sn + p + n nucleus. The low-lying 0^+ and 1^+ states are discussed in terms of the relation between their excitation energies and the coupling between the two valence nucleons in the $T = 0$ channel. The $T = 1$ interaction strength is fixed by the empirical neutron pairing gap, and the $T = 0$ strength is estimated from the 1^+_1 and 0^+_1 energy differences in known $N = Z$ odd-odd nuclei.

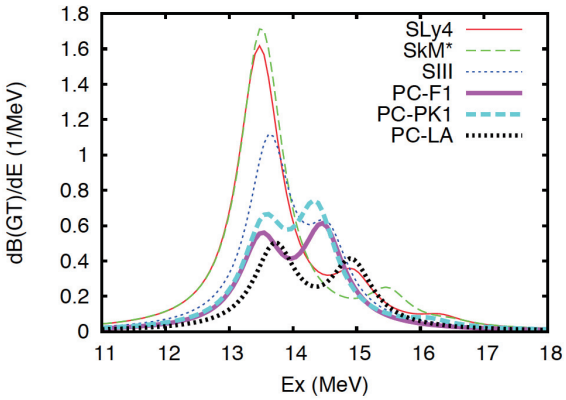

Fig. 1. (Color online) Gamow-Teller strength distributions as a function of the excitation energy from the ground state of ^{102}Sn. The ratio between IS and IV pairing strength is taken as $f = 1.5$.

We show in Fig. 1 the B(GT) distribution as a function of the excitation energy with respect to the 0^+_1 state of ^{102}Sn. A clear difference between non-relativistic and relativistic cases is observed while the low-lying 0^+ and 1^+ energy spectra are similar to each other, i.e., the strength distribution is concentrated at the first peak for SLy4 and SkM*, whereas it is fragmented into the first and second peaks for PC-F1, PC-PK1, and PC-LA. SIII shows a characteristic in between those of the two types of EDFs. By analyzing the compositions of wave functions, we observe that the enhanced occupation of the $g_{7/2}$ orbital in the relativistic model breaks the $(L, S, T) = (0, 1, 0)$ coupling scheme of the two valence nucleons, and it results in the substantial difference in the low-lying Gamow-Teller strength distributions.

In conclusion, it is expect that the coupling in the $(L, S, T) = (0, 1, 0)$ channel is strongly suppressed in the ^{100}Sn + p + n nucleus owing to the $g_{7/2}$ orbital, which is nearly degenerate with the $d_{5/2}$ orbital. The effect appears clearly in the low-lying B(GT$_-$) distribution rather than in the energy difference between 1^+_1 and 0^+_1 states.

† Condensed from the article in Phys. Rev. C**93**, 064319 (2017)
*1 Institut de Physique Nucléaire, Université Paris-Sud
*2 RIKEN Nishina Center
*3 Center for Mathematics and Physics, University of Aizu

References

1) Y. Tanimura, H. Sagawa, K. Hagino, Prog. Theor. Exp. Phys. 2014, 053D02(2014).
2) D. Seweryniak et al., Phys. Rev. Lett. **99**, 022504(2007).
3) I. G. Darby et al., Phys. Rev. Lett. **105**, 162502(2010).

Quasi-particle random phase approximation (QRPA) with quasi-particle-vibration coupling (QPVC): application to the Gamow-Teller response of a superfluid nucleus ^{120}Sn†

Y. F. Niu,[*1,*2] G. Colò,[*3,*1] E. Vigezzi,[*1] C. L. Bai,[*4] and H. Sagawa[*5,*6]

The RPA+PVC approach is obviously limited to the case of magic nuclei. In this paper we propose the QRPA+QPVA formalism for spherical superfluid nuclei, describing the nuclear ground state within the Hartree-Fock-Bogoliubov (HFB) approximation, and the collective excitations of the system within QRPA. We consider the Gamow-Teller transitions in a well bound super-fluid nucleus ^{120}Sn in this study. As a unique feature in GT transitions of superfluid nuclei, both isovector (IV) and isoscalar (IS) pairing are expected to play a relevant role. While the usual IV pairing determines the ground-state structure, the IS pairing is present in the QRPA residual interaction for Gamow-Teller transitions.

The GT strength associated with QRPA+QPVC, is given by

$$S(E) = \frac{1}{\pi}\mathrm{Im}\sum_{\nu}\langle\nu|\hat{O}_{\mathrm{GT}^{\pm}}|0\rangle^2\frac{1}{E-\Omega_\nu+i(\frac{\Gamma_\nu}{2}+\Delta)}, \quad (1)$$

where the GT operator is $\hat{O}_{\mathrm{GT}^{\pm}} = \sum_{i=1}^{A}\sigma(i)t_{\pm}(i)$ and Δ is a smearing parameter. In our calculation, we will only focus on the GT$^-$ excitations. $|\nu\rangle$ denotes the eigenstates associated with the complex eigenvalues $\Omega_\nu - i\frac{\Gamma_\nu}{2}$ obtained by diagonalizing the energy-dependent complex QRPA matrix.

The four theoretical strength functions are compared with experimental results in Fig. 1. We use a smearing parameter $\Delta = 0.5$ MeV in the QRPA and QRPA+QPVC calculation. In Fig. 1, the (^{3}He, t) experimental low-energy strength distribution is well reproduced by including isoscalar pairing, while the (p,n) data are better reproduced without it. The spreading width and lineshape of the giant resonance region are very well reproduced by the inclusion of the QPVC effect.

HFB+QRPA is an appropriate tool for neutron-rich and neutron-deficient, nuclei, especially for weakly bound nuclei. The QRPA+PVC calculation in these cases is a new research line which is still in its infancy. Improving the theoretical predictive power of such calculations is not only beneficial for our progress in understanding nuclear structure, but also of essential interest understanding weak-interaction processes in particle physics and astrophysics. Accordingly, we envisage the study of weak-interaction processes of astrophysical interest in our future research of the QRPA+QPVC model.

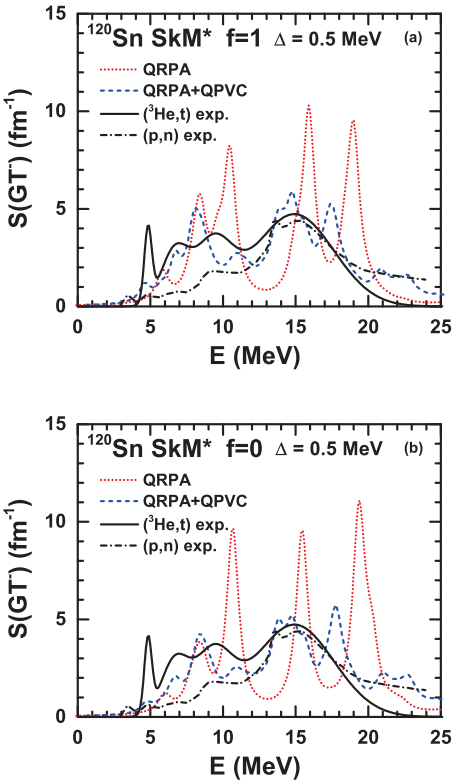

Fig. 1. (Color online) Gamow-Teller strength distributions for ^{120}Sn calculated by QRPA and QRPA+QPVC models, with [panel (a)] and without [panel (b)] isoscalar pairing, using the Skyrme interaction SkM*. The excitation energy is with respect to the ground state of ^{120}Sn. The smearing parameter $\Delta = 0.5$ MeV is used. The experimental results from (^{3}He, t) and (p,n) reactions are shown for comparison. The cross section from the (^{3}He, t) experiment is scaled by a factor of 1.6 so that the main GTR strength exhausts 65% of the Ikeda sum rule[1]. The cross section from the (p,n) reaction is normalized by the unit cross section[2]

† Condensed from the article in Phys. Rev. C 94, 064328 (2016)

*1 Istituto Nazionale di Fisica Nucleare (INFN)
*2 ELI-NP, "Horia Hulubei" National Institute for Physics and Nuclear Engineering, Bucharest-Magurele
*3 Dipartimento di Fisica, Università degli Studi di Milano
*4 School of Physical Science and Technology, Sichuan University, Chengdu
*5 RIKEN Nishina Center
*6 Center for Mathematics and Physics, University of Aizu

References
1) K. Pham et al., Phys. Rev. C**51**, 526 (1995).
2) M. Sasano et al., Phys. Rev. C**79**, 024602 (2009).

Shell-model evaluation of beta-decay half-lives for $N = 50$ neutron deficient nuclei

M. Honma,[*1] T. Otsuka,[*2,*3,*4] T. Mizusaki,[*5] Y. Utsuno,[*6,*3] N. Shimizu,[*3] and M. Hjorth-Jensen[*4,*7,*8]

An accurate description of the structure of unstable nuclei has been one of the most challenging goals in theoretical nuclear physics. A precise prediction of various properties such as binding energies and transition strengths is important as an input of astrophysical simulations especially for nuclei that are beyond the current experimental reach. The doubly-magic nucleus ^{100}Sn is one of the key nuclei for exploring the proton-rich extreme, and various theoretical as well as experimental approaches have been made. In the previous report[1] we presented the results of shell-model calculations for the Gamow-Teller transition strength distribution from ^{100}Sn. In this report, using the same framework, the β-decay half-lives are evaluated for several proton-rich N=50 nuclei.

As described in,[2] the adopted model space consists of four single-particle orbits $1p_{1/2}$, $0g_{9/2}$, $1d_{5/2}$ and $0g_{7/2}$ for both protons and neutrons. Because of the computational limitations, we need to employ a suitable truncation scheme. In the present calculation, at most five particles are allowed to excite across the N or Z=50 shell gap relative to the naive filling configurations. The effective interaction was determined in a semi-empirical way. The starting Hamiltonian is derived microscopically[3] based on the realistic N^{3}LO interaction,[4] and it is modified by iterative fits to the experimental energy data. For the purpose of the lifetime evaluation, we need to know the Q-value, but it is not necessarily known experimentally. To test the reliability of the present scheme, the Q-values are also evaluated theoretically. The β^+-decay + electron capture processes through the Gamow-Teller transitions are taken into account. The standard quenching factor 0.74 is used for the transition operator.

As shown in Fig.1, the shell-model results basically follow the trends of the available experimental data for both Q-values and the half-lives. However, a systematic deviation can be seen. The half-life is underestimated for $Z \leq 47$ and overestimated for $Z \geq 48$. A part of this deviation is due to the inaccurate estimation of the Q-values, but even if the experimental values are used, there still remain some discrepancies. Probably this problem can be attributed to the insufficiency of the model space. In the present calculations, the possibly dominating transition $\pi g_{9/2} \rightarrow \nu g_{7/2}$ is fully taken into account, but some components such as $\pi d_{5/2} \rightarrow \nu d_{3/2}$ are excluded, that are anticipated to contribute to the states with higher excitation energies. The more proton-rich, the larger the Q-value window, and such components may have larger contribution. More extensive calculation is necessary to confirm this interpretation and improve the description.

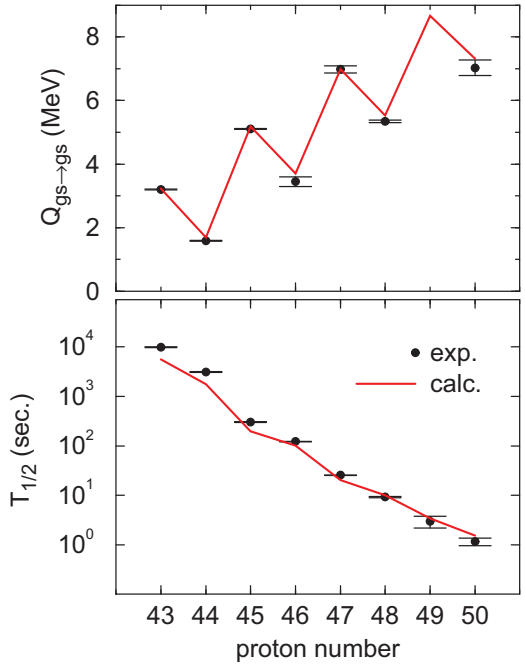

Fig. 1. Comparison of (upper panel) Q-values ($Q_{gs\rightarrow gs}$) and (lower panel) half-lives ($T_{1/2}$) between the experimental data (symbols) and the shell-model results (lines) for $N = 50$ nuclei with $43 \leq Z \leq 50$. Experimental data are taken from Ref.[5] The shell-model results are obtained by using the efficient shell-model code MSHELL64.[6]

*1 Center for Mathematical Sciences, University of Aizu
*2 Department of Physics, University of Tokyo
*3 Center for Nuclear Study, University of Tokyo
*4 National Superconducting Cyclotron Laboratory, Michigan State University
*5 Institute of Natural Sciences, Senshu University
*6 Advanced Science Research Center, Japan Atomic Energy Agency
*7 Department of Physics and Astronomy, Michigan State University
*8 Department of Physics, University of Oslo

References

1) M. Honma *et al.*, RIKEN Accel. Prog. Rep. **48**, 89 (2015).
2) M. Honma *et al.*, RIKEN Accel. Prog. Rep. **47**, 64 (2014).
3) M. Hjorth-Jensen *et al.*, Phys. Rep. **261**, 125 (1995).
4) D. R. Entem *et al.*, Phys. Rev. C **68**, 041001(R) (2003).
5) Data extracted using the NNDC WorldWideWeb site from the ENSDF database.
6) T. Mizusaki *et al.*, MSHELL64 code (unpublished).

Application of top-on-top model to $11/2^-$ band in ^{135}Pr†

K. Sugawara-Tanabe*1,*2 and K. Tanabe*3

We have proved that a transverse wobbling mode does not exist in the particle-rotor model with hydrodynamical moment of inertia (MoI).[1] Consequently, stable rotation around the middle MoI does not exist in the particle-rotor model as well as in the pure rotor case. Then, a question arises as to how the experimental data of the $11/2^-$ band in ^{135}Pr[2] can be explained. This yrast $11/2^-$ band starts near the ground state and shows backbending thrice,[3] and the levels discussed in Ref. 2 are concerned with those before the first backbending. Thus, the pairing effect is essentially important in such low-excitation states. We have proposed an analytic formula for the angular-momentum (I) dependence of MoI originating from the Coriolis antipairing effect (CAP).[4] This formula is derived from the second-order perturbation to the Coriolis term in the self-consistent HFB equation under I and nucleon-number constraints. The I dependence of the MoI is related to the rigid MoI with a functional dependence of the pairing gap together with the blocking effect. We have also achieved good success with the top-on-top model, i.e., the particle-rotor model with the I-dependent rigid MoI, for the high spin and highly excited levels in Lu isotopes in describing not only the energy scheme but also the electromagnetic transitions $B(E2)$ and $B(M1)$.[5–7] Similarly, we apply the top-on-top model for the $11/2^-$ band in ^{135}Pr. In reference to the I-dependence curve as displayed in Fig. 9 in Ref. 4, we assume a simplified functional form for the I dependence of MoI for those low-excitation levels,

$$\frac{\mathcal{J}_0}{1+\exp(-(I-b)/a)}. \qquad (1)$$

We choose two parameters $a = 7.5$ and $b = 15.5$. The asymptotic value of the MoI in the limit of $I \to \infty$ is assumed to be $\mathcal{J}_0$ =25 MeV^{-1}, and the deformation parameters $\beta_2 = 0.18$ and $\gamma = 18°$.

In Fig. 1, we compare $E(I) - 0.02I(I+1)$ as functions of I between theoretical values and experimental ones[2]. The theoretical value is normalized at $I = 11/2$ in Band 1 where $I - j$ is even, while Bands 2 and 4 have odd values of $I - j$. For the backbending curve of Band 1, we choose a larger $\mathcal{J}_0 = 35$ MeV^{-1}, which reproduces the experimental data from I=35/2 up to 57/2, indicating the CAP effect is well simulated by two common parameters a and b. The energies of $E(I) - 0.02I(I+1)$ are not sensitive to γ, but $\gamma = 18°$

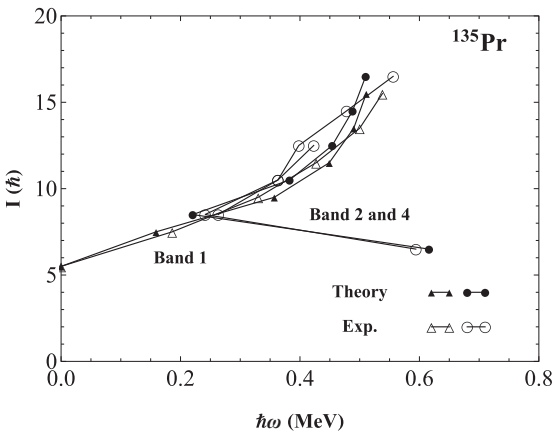

Fig. 1. Comparison of $E(I) - 0.02I(I+1)$ between theoretical results and experimental data in Ref.[2]. Theoretical values are shown by filled triangles for Band 1 and filled circles for Bands 2 and 4, while experimental data are shown for Band 1 by open triangles and for Bands 2 and 4 by open circles. Band 2 is from I=13/2 to 25/2, while Band 4 is from I=17/2 to 33/2.

seems to be favorable mainly from the electromagnetic transitions. It also gives good fit to the experimental data[2] not only in the electomagnetic transition rates but also in the mixing ratio δ.

In conclusion, the experimental data of the $11/2^-$ band in ^{135}Pr[2] is interpreted as the normal wobbling band influenced by the CAP effect, rather than the transverse wobbling mode. We point out a possibility of the violation of Bohr symmetry to a small extent, which explains the existence of Band 2, i.e., the signature partner band.

References
1) K. Tanabe, K. Sugawara-Tanabe, Phys. Rev. C **95**, 064315 (2017).
2) J. T. Matta et al., Phys. Rev. Lett. **114**, 082501 (2015).
3) E. S. Paul et al., Phys. Rev. C **84**, 047302 (2011).
4) K. Tanabe, K. Sugawara-Tanabe, Phys. Rev. C **91**, 034328 (2015).
5) K. Tanabe, K. Sugawara-Tanabe, Phys. Rev. C **73**, 034305 (2008); Phys. Rev. C **77**, 064318 (2008);
6) K. Sugawara-Tanabe, K. Tanabe, Phys. Rev. C **82**, 051303(R) (2010).
7) K. Sugawara-Tanabe, K. Tanabe, N. Yoshinaga, Prog. Theor. Exp. Phys. **2014**, 063D01 (2014).

† Condensed from the article in Phys. Rev. C, Vol.95, 064315 (2017)

*1 RIKEN Nishina Center
*2 Department of Information Design, Otsuma Women's University
*3 Department of Physics, Saitama University

Fully self-consistent study of charge-exchange resonances and their impact on the symmetry energy parameters†

X. Roca-Maza,[*1,*2] Li-Gang Cao,[*3] G. Colò,[*1,*2] and H. Sagawa[*4,*5]

A comprehensive effort is currently being devoted to the determination of the nuclear symmetry energy, particularly concerning its density dependence. The symmetry energy is defined starting from the nuclear matter equation of state. The energy per particle in a uniform system characterized by a density ρ and a relative neutron-proton asymmetry $\beta \equiv (\rho_n - \rho_p)/\rho$ can be estimated by expanding up to second order in β as

$$\frac{E}{A}(\rho,\beta) = \frac{E}{A}(\rho,\beta=0) + S(\rho)\beta^2. \quad (1)$$

This truncation has been found to be accurate for densities up to $2\rho_0$, where ρ_0 is the saturation density.

In this work, the basic idea is to use nuclear energy density functionals (EDFs) that provide different values for J, L and the neutron skin, and calculate the energy difference between the anti-analog giant dipole resonance (AGDR) and isobaric analog state (IAS), $E_{\rm AGDR} - E_{\rm IAS}$ in ^{208}Pb. After checking the existence of the above mentioned linear correlations, one can employ the experimental value for the energy difference $E_{\rm AGDR} - E_{\rm IAS}$ and deduce the corresponding values of J, L and the neutron skin. Here, we have achieved three improvements with our self-consistent model and its analysis: (i) the two-body spin-orbit interaction had not been taken into account in Ref. 1, while we adopt its exact form in the present study; (ii) we have checked the effect of implementing the exact Coulomb exchange; and (iii) we have checked the extraction method of the energy centroid of AGDR from the charge-exchange random phase approximation (RPA) calculations.

Table 1. Allowed range for J, L and the neutron skin when experimental data from both Refs. 2 and 3 are considered. The estimates from the previous calculations of Ref. 1 and from the current work are compared.

	Ref. 1	Present work
J	30.7 – 37.7 MeV	31.2 – 35.4 MeV
L	72.7 – 144.3 MeV	75.2 – 122.4 MeV
$\Delta R_{\rm np}$	0.192 – 0.316 fm	0.201 – 0.277 fm

We calculate the energy difference between AGDR and IAS energies and the impact on the symmetry energy and neutron skin in the fully self-consistent theory. The calculated results are shown in Fig. 1 together with the experimental results and the theoretical results obtained by means of relativistic mean field (RMF) calculations with the DD-ME effective Lagrangian introduced in Ref. 3. We obtained the neutron skin from the correlation plot in Fig. 1 as 0.239 ± 0.038 fm from experimental data of J. Yasuda *et al.*[2)] and 0.216 ± 0.010 fm from experimental data of A. Krasznahorkay *et al.*[3)]. These values give the symmetry energy coefficients J and L as listed in Table 1. The final results for the symmetry energy parameters J and L are changed by 10% at most compared with the previous analysis and tend to be slightly closer to the empirical values obtained in other analyses in the literature. There are still open problems, such as obtaining a better agreement with the experimental energy of IAS in ^{208}Pb and the strong correlation of the IAS energy with the neutron skin, in which the variation of the IAS energy is larger than expected from the change of the charge radii within the family.

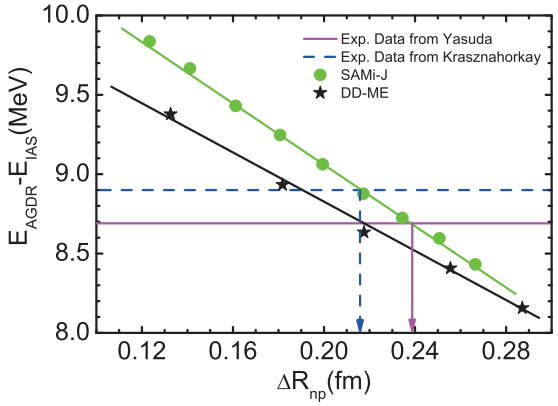

Fig. 1. (Color online) Energy difference $E_{\rm AGDR} - E_{\rm IAS}$ of AGDR and IAS as a function of the neutron-skin thickness, obtained by using the SAMi-J family of Skyrme functionals. The calculated values are presented as solid circles. Two different experimental data[2,3)] are also shown as solid (magenta) and dashed (blue) lines, respectively. The arrows indicate the neutron skin constrained by these experimental data. We also display results obtained with the covariant DD-ME Lagrangians of Ref. 3.

† Condensed from the article in Phys. Rev. C94, 044313 (2016)

*1 Dipartimento di Fisica, Università degli Studi di Milano
*2 Istituto Nazionale di Fisica Nucleare (INFN), Milano
*3 School of Mathematics and Physics, North China Electric Power University, Beijing
*4 RIKEN Nishina Center
*5 Center for Mathematics and Physics, University of Aizu

References

1) L. G. Cao, X. Roca-Moza, G. Colò, H. Sagawa, Phys. Rev. C**92**, 034308 (2015).
2) J. Yasuda et al., Prog. Theor. Exp. Phys. **2013**, 063D02 (2013).
3) A. Krasznahorkay et al., Phys. Lett. B**720**, 428 (2013); arXiv: 1311.1456 (2013).

Liquid-Gas Phase Transitions in Quantum Field Theories†

H. Nishimura,*1 M. Ogilvie,*2 and K. Pangeni*2

We address the generic problem of liquid-gas phase transitions from a field theory perspective. The general class of field theories we will study is the class of $\mathcal{CK}$-symmetric models obtained from dimensional reduction of a four-dimensional field theory at finite temperature and density. The fermions with mass m of the underlying theory are integrated out, and after dimensional reduction and redefinition of fields, we obtain a Lagrangian of the general form

$$L_{3d} = \frac{1}{2}(\nabla\phi_1)^2 + \frac{1}{2}m_1^2\phi_1^2 + \frac{1}{2}(\nabla\phi_2)^2 + \frac{1}{2}m_2^2\phi_2^2 - F(\phi_1,\phi_2)$$

where ϕ_1 is associated with the attractive force, and ϕ_2 with the repulsive force. Although charge conjugation $\mathcal{C}$ is broken at finite density, there remains a symmetry under $\mathcal{CK}$, where $\mathcal{K}$ is complex conjugation[1]. We consider four models: relativistic fermions, nonrelativistic fermions, static fermions and classical particles, corresponding to four different choices for the function $F(\phi_1,\phi_2)$. For example, F for the static fermions is given as

$$F = \frac{1}{v}\log\left[1 + e^{-\beta m+\beta\mu+\beta^{1/2}g\phi_1+i\beta^{1/2}e\phi_2}\right]$$

where β is the inverse temperature and v is a parameter with dimensions of volume, which we set it to be one. The coupling constants g and e determine the strength of the attractive and repulsive forces respectively. The thermodynamic behavior is extracted from $\mathcal{CK}$-symmetric complex saddle points of the effective field theory at tree level. The relativistic and static fermions show a liquid-gas transition, manifesting as a first-order line at low temperature and high density, terminated by a critical end point as shown in Fig. 1 and Fig. 2. In the cases of nonrelativistic fermions and classical particles, we find no first-order liquid-gas transitions at tree level.

The mass matrix controlling the behavior of correlation functions is obtained from fluctuations around the saddle points. Due to the $\mathcal{CK}$ symmetry of the models, the eigenvalues of the mass matrix can be complex[2]. This leads to the existence of disorder lines, which mark the boundaries where the eigenvalues go from purely real to complex. The regions where the mass matrix eigenvalues are complex are associated with the critical line. In the case of static fermions, a powerful duality between particles and holes allows for the analytic determination of both the critical line and the disorder lines as shown in Fig. 2. Depending on the values of the parameters, either zero, one or two disorder lines are found. Numerical results for relativistic fermions give a similar picture as shown in Fig. 1.

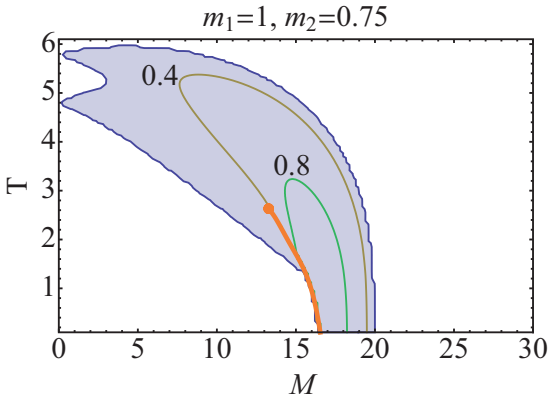

Fig. 1. Phase diagram for relativistic fermions for $m = 20$, $m_1 = 1$, $m_2 = 0.75$ with $g_1 = 1$ and $e = 0.3$. The shaded region indicates where the mass matrix eigenvalues form complex conjugate pairs, and the contour lines refer to the imaginary parts of the mass matrix eigenvalues. The thick line shows a first-order line.

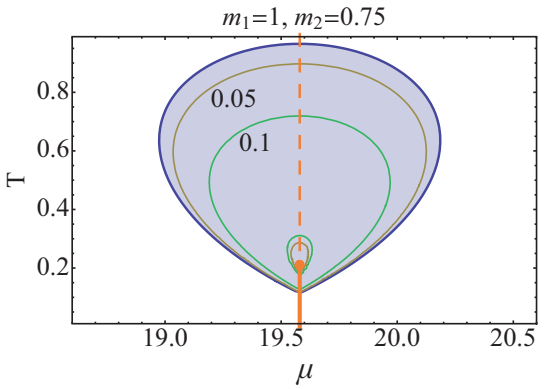

Fig. 2. Phase diagram for static fermions with the same parameter set as the relativistic fermions. The dashed vertical line emerging from the critical end point is the line of particle-hole duality.

References

1) H. Nishimura, M. C. Ogilvie and K. Pangeni, Phys. Rev. D **90**, no. 4, 045039 (2014).
2) H. Nishimura, M. C. Ogilvie and K. Pangeni, Phys. Rev. D **91**, no. 5, 054004 (2015).

† Condensed from the article in arXiv:1612.09575

*1 RIKEN Nishina Center
*2 Department of Physics, Washington University

Joint project for large-scale nuclear structure calculations in 2016

N. Shimizu,[*1] N. Tsunoda,[*1] T. Miyagi,[*2] S. Yoshida,[*2] T. Abe,[*2] T. Otsuka[*2,*1] and Y. Utsuno[*3,*1]

A joint project for large-scale nuclear structure calculations has been promoted since 2002 based on a collaboration agreement between the RIKEN Accelerator Research Facility (currently RIKEN Nishina Center) and the Center for Nuclear Study, the University of Tokyo. Currently, we maintain 16 PC servers with Intel CPUs for large-scale nuclear shell-model calculations. Based on this project, we performed shell-model calculations of the various nuclides that have been measured or are proposed to be measured at the RIKEN RI Beam Factory and other facilities, such as ^{38,40}P ^{48}Ca, ^{55}Ca, ^{128}Cd, ^{130}Sn, and ^{132}Sn, under various collaborations with many experimentalists.[1)] In parallel, we have performed several theoretical studies for understanding nuclear structure. Among them, we briefly show three theoretical achievements: the sophisticated perturbation theory for constructing shell-model interaction[2,3)] shell-model study of the beta decay of neutron-rich $13 \leq Z \leq 18$ nuclei,[4)] and the development of the unitary-model-operator approach (UMOA).[5)]

We have developed a novel many-body perturbation method to derive the effective interaction for shell model calculations. Our new theory (extended Kuo-Krenciglowa method) can handle an arbitrary model space, such as two major shells,[2)] unlike conventional standard theory (KK method). Then, we derived a new effective interaction for the $sd+pf$ shell, starting from the nuclear force based on chiral effective field theory and Fujita-Miyazawa three-body force. With this interaction, we succeeded in describing the nuclear shell structure around the region so-called "island of inversion," where the breaking of the $N = 20$ shell gap is important. In this year, we further investigated the physics around the "island of inversion" and clarified the long-standing problem of how the sd-to-pf excitations occur in Mg isotopes with distinct differences from conventional approaches. As an example, Fig. 1 shows the low-lying states of ^{31}Mg, where energy levels of positive and negative parity states are quite near and configuration mixing related to the $N = 20$ gap is important. We can see that experimental values are reproduced better than in other shell model studies.[3)] Using the EKK method, we have also started investigating nuclei in other regions.

In order to discuss the systematic properties of beta decay of neutron-rich nuclei, we performed large-scale shell-model calculations and obtained the Gamow-Teller transition for the 78 nuclei with $13 \leq Z \leq 18$ and $22 \leq N \leq 34$.[1,4)] In this calculation, the SDPF-MU interaction was adopted.[6)] Shell-model results of the beta-decay half lives and delayed neutron emission rates remarkably agree with experimental data. This indicates the validity of large-scale shell-model calculations for nuclei in the neutron rich region.

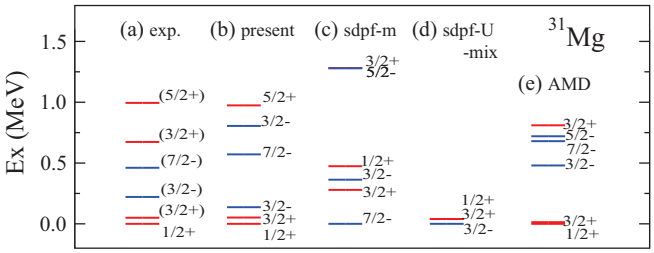

Fig. 1. Energy levels of ^{31}Mg, (a) experimental values, (b) present work, (c) sdpf-m, (d) sdpf-U-mix and (e) AMD+GCM calculation.

The UMOA was developed and extended in order to investigate the medium- and heavy-mass nuclei based on the underlying nuclear interactions.[5)] In the UMOA, we construct the effective Hamiltonian which does not induce the 1-particle-1-hole and 2-particle-2-hole excitations. We have calculated the ground-state energies and radii with the similarity-renormalization-group transformed nucleon-nucleon (NN) interactions[7)] for the closed-shell nuclei across the nuclear chart up to lead region. The converged results can be obtained when we take 15 major shells as a model space. Our resulting energies and radii are unrealistically overbound and smaller than the experimental data, respectively. We have found that the neutron-skin thicknesses are insensitive to the choice of resolution scale for the NN interaction and can be determined uniquely. For a quantitative understanding, it is necessary to include the three-nucleon-force effect which cannot be treated in the current UMOA framework. In such a situation, we are extending the UMOA framework and are carrying out benchmark calculations for light nuclei.

*1 Center for Nuclear Study, the University of Tokyo
*2 Department of Physics, the University of Tokyo
*3 Japan Atomic Energy Agency

References

1) V. Tripathi et al., Phys. Rev. C **95**, 024308 (2017).
2) N. Tsunoda et al., Phys. Rev. C **89**, 024313 (2014).
3) N. Tsunoda, T. Otsuka, N. Shimizu, M. H.-Jensen, K. Takayanagi, T. Suzuki, Phys. Rev. C **95**, 021304(R) (2017).
4) S. Yoshida, oral presentation, CNS summer school 2016 (2016).
5) T. Miyagi, T. Abe, R. Okamoto, T. Otsuka, Prog. Theor. Exp. Phys. **2015** 041D01 (2015).
6) Y. Utsuno et al., Phys. Rev. C **86**, 051301(R) (2012).
7) S. K. Bogner et al., Phys. Rev. C **75**, 061001 (2007).

3. Nuclear Data

Thick-target transmission method for excitation functions of interaction cross sections†

M. Aikawa,[*1,*2] S. Ebata,[*1] and S. Imai[*3]

Nuclear transmutation is one of the promising technologies to dispose of nuclear waste with high-level radioactivity, such as long-lived fission products (LLFP). Although the nuclear data of transmutation reactions for LLFP are essential to develop the technology, the data are scarce in the present database because the experiments are restricted by the radioactivity and chemical instability of LLFP. To avoid these restrictions experiments in inverse kinematics are available for charged-particle-induced data. Indeed, the cross section data of nuclear waste composed of ^{90}Sr and ^{137}Cs have recently been measured at RIBF.[1)]

The excitation function of the interaction cross sections $\sigma_{\rm I}$, leads to the thick-target yields of LLFP transmutation. To measure $\sigma_{\rm I}(\varepsilon)$, we propose the thick-target transmission (T3) method, which extends the conventional transmission method to that with a thick target. In the T3 method, the target also plays the role of energy moderator and its thickness corresponds to the energy degradation $I(0)$ decreases to $I(x)$ after passing through a target with the thickness x. By using the attenuation ratios $I(x)/I(0)$ and $I'(x+\Delta x)/I'(0)$ of different runs, the $\sigma_{\rm I}(x)$ is derived as

$$\sigma_{\rm I}(x) = -\frac{1}{n_T \Delta x} \ln \left[\frac{I'(x+\Delta x)}{I'(0)} \frac{I(0)}{I(x)} \right], \qquad (1)$$

where n_T is the number density of target (cm^{-3}). When the LLFP beam is applied in the T3 method, $\sigma_{\rm I}(x)$ is the transmutation cross section.

To obtain $\sigma_{\rm I}(\varepsilon)$ by the conventional transmission method, it is necessary to change the beam energy for each cross section $\sigma_{\rm I}(\varepsilon)$. The T3 method is likely applicable with less efforts to stack a foil on the target than to change the beam energy.

To test the usefulness of the T3 method, we performed a simulation on the interaction cross sections for the ^{12}C-induced reaction on ^{27}Al with the Monte Carlo simulation code PHITS.[2)] In the simulation, the incident energy of the ^{12}C beam is set to 100 MeV/nucleon, which is stopped at approximately 1.23 cm from the surface of an Al target. The target of the maximum thickness consists of 21 foils with a thickness of 0.1 cm from 0.0 cm up to 1.0 cm and of 0.02 cm from 1.0 cm up to 1.22 cm. A beam intensity of 1000 pps and an irradiation time of 100 s are assumed and correspond to a trial number of 10^5 in the PHITS simulation.

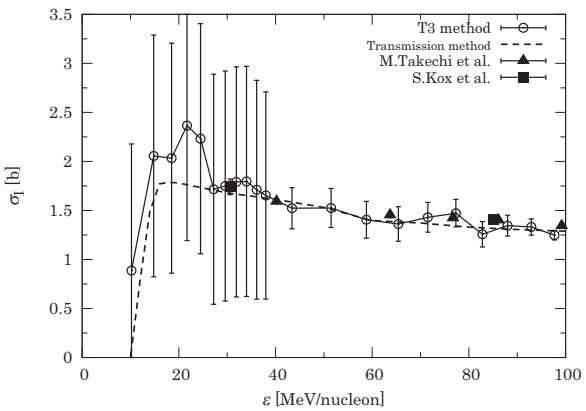

Fig. 1. Interaction cross section $\sigma_{\rm I}(\varepsilon)$ obtained from the T3 method (circles), conventional transmission method (dashed line), and experimental data (triangles and squares).[3,4)]

The results estimated by the T3 method are shown in Fig. 1 by circles. The dashed line is also obtained by the simulation but with the conventional transmission method. The filled symbols indicate the experimental data (triangles and squares).[3,4)] Our results well reproduce the tendency of experimental data, although they have large error bars owing to the low statistics at thin target foils and propagation of statistical uncertainties of $I'(x+dx)$ and $I(x)$. Thus, in spite of the small number of incident particles, such as 10^5, the interaction cross sections can be obtained. We emphasize that the experiments using the T3 method avoid the beam-energy re-adjustments, and time savings might be expected with these experiments.

The T3 method can derive the interaction cross sections through the iterative measurements of the beam attenuation ratio $I(x)/I(0)$. The energy dependence of $\sigma_{\rm I}$ is deduced by changing the target thickness. Our results calculated using PHITS simulation well reproduce the experimental data of the ^{12}C+^{27}Al reaction. The T3 method will contribute to accumulate fundamental data of the transmutation reaction for radiative targets including rare isotopes.

This work was funded by the ImPACT Program of the Council for Science, Technology and Innovation (Cabinet Office, Government of Japan).

References

1) H. Wang et al., Phys. Lett. B **754**, 104 (2016).
2) T. Sato et al., J. Nucl. Sci. Technol. **50**, 913 (2013).
3) S. Kox et al., Phys. Lett. B **159**, 15 (1985).
4) M. Takechi et al., Phys. Rev. C **79**, 061601(2009).

† Condensed from the article in Nucl. Instr. Meth. **B**383,156(2016)

*1 Faculty of Science, Hokkaido University
*2 RIKEN Nishina Center
*3 Institute for the Advancement of Higher Education, Hokkaido University

Report on EXFOR Compilation 2016 from the RIBF

D. Ichinkhorloo,[*1] M. Aikawa,[*1,*2] S. Ebata,[*1] S. Jagjit,[*1] M. Kimura,[*1] N. Otuka,[*2,*3] and A. Sarsembayeva[*1]

Nuclear reaction data are used in various fields (nuclear physics, engineering research, medical, etc.) and can be accessed through the Internet from a nuclear database when a computer is connected. The database is constructed in a special format called EXFOR (EXchange FORmat for experimental nuclear reaction data)[1] which is designed to accommodate experimental data with corresponding bibliographies and experimental descriptions including error analysis for proper interpretation of the stored experimental data.

EXFOR is maintained by the International Atomic Energy Agency (IAEA)[2] and the International Network of Nuclear Reaction Data Centres (NRDC). The NRDC collaborates in the compilation of experimental data and development of related software for compilation and dissemination. The Hokkaido University Nuclear Reaction Data Centre (JCPRG)[3] is a member of NRDC and has contributed about 10% of the charged-particle nuclear reaction data in the EXFOR library. JCPRG provides the compiled nuclear reaction data in both the international (EXFOR) and domestic (NRDF)[4] formats through an online search system.

Under collaboration with the NRDC network, experimental data published in scientific journals are continuously surveyed. Among the data obtained, the data on charged-particle and photon induced reactions obtained from the facilities in Japan should be compiled by JCPRG. We assign new papers for the compiler and check all papers finalized for compilation by the JCPRG members. For improving the quality of contents, we contact authors to provide the original numerical data plotted in each figure to ensure the accuracy of data compiled in the NRDF and the EXFOR library. If the original data cannot be obtained from the corresponding author, we digitize numerical data from the plotted figures with the digitization software GSYS[5].

We have also cooperated with the RIKEN Nishina Center for compilation since 2010. The purpose of the cooperation is to increase the availability of the nuclear reaction data produced at the RIBF. The compiled files of nuclear data produced at the RIBF are translated into the EXFOR format for the benefit of nuclear data users. In this article, we report our activities in 2016, especially the compilation of experimental nuclear reaction data from the RIBF.

In 2016, we compiled 37 new papers reporting experiments performed in Japan. Among them 15 papers were based on RIBF data and those data satisfy the compilation scope of the EXFOR library. All data are accessible by the entry numbers listed in Table 1.

We have established an effective procedure to compile all of the new publications during the last six-year collaboration with the RIKEN Nishina Center. Therefore, most of the recent experimental nuclear reaction data are provided by the authors but we digitized numerical data of E2487[9] and E2488[10] entries using the digitization software GSYS. Such additional information is also available with a list of compiled RIBF data on the JCPRG website[6].

Table 1. Entry numbers with references compiled from RIBF data in 2016

Entries	E2483[7]	E2485[8]	E2487[9]
	E2488[10]	E2592[11]	E2493[12]
	E2495[13]	E2500[14]	E2504[15]
	E2506[16]	E2507[17]	E2511[18]
	E2515[19]	E2516[20]	E2522[21]
Total		15	

References
1) http://www.jcprg.org/exfor/
2) http://www-nds.iaea.org/
3) http://www.jcprg.org/
4) http://www.jcprg.org/nrdf/
5) http://www.jcprg.org/gsys/
6) http://jcprg.org/riken/ribf-data/
7) K. Li et al., Phys. Rev. C **92**, 014608 (2015).
8) M. U. Khandaker et al., Nucl. Instrum. Meth. Phys. Res. B **362**, 151 (2015).
9) A. Kim et al., Phys. Rev. C **92**, 035801 (2015).
10) A. Matta et al., Phys. Rev. C **92**, 041302(R) (2015).
11) A. R. Usman et al., Nucl. Instrum. Meth. Phys. Res. B **368**, 112 (2016).
12) H. Wang et al., Phys. Lett. B **754**, 104 (2016).
13) N. Kobayashi et al., Phys. Rev. C **93**, 014613 (2016).
14) K. Kisamori et al., Phys. Rev. Lett. **116**, 052501 (2016).
15) P. Doornenbal et al., Phys. Rev. C **93**, 044306 (2016).
16) S. Cherubini et al., Phys. Rev. C **92**, 015805 (2015).
17) I. Celikovic et al., Phys. Lett. B **116**, 162501 (2016).
18) A. R. Usman et al., Appl. Radiat. Isot. **114**, 104 (2016).
19) B. Blank et al., Phys. Rev. C **93**, 061301(R) (2016).
20) S. Hayakawa et al., Phys. Rev. C **93**, 065802 (2016).
21) Y. Togano et al., Phys. Lett. B **761**, 412 (2014).

*1 Faculty of Science, Hokkaido University
*2 RIKEN Nishina Center
*3 NDS, IAEA

4. Hadron Physics

Charged background study for A_N of forward neutron production in $\sqrt{s}$=200 GeV polarized proton-proton collisions in PHENIX experiment

M. Kim[*1,*2] for the PHENIX collaboration

Single transverse spin asymmetry A_N is defined as

$$A_N = \frac{\sigma^{\uparrow} - \sigma^{\downarrow}}{\sigma^{\uparrow} + \sigma^{\downarrow}} \tag{1}$$

where $\uparrow$ and $\downarrow$ indicate the spin up and down of the incident beam, respectively. In 2015, A_N of forward ($6.8 < \eta < 8.8$) neutron production in p+p, p+Al and p+Au collisions at $\sqrt{s_{NN}} = 200$ GeV was measured at PHENIX using the Zero-Degree Calorimeter (ZDC) and a position-sensitive Shower Max Detector (SMD). Unexpectedly, a strong A dependence in A_N was found, which is not explained by the current theoretical framework for $p+p$ collisions[1]. In order to obtain information about the associated mechanisms, the Beam-Beam counter (BBC) correlated A_N was measured for "BBC tag" samples and "BBC veto" samples. A strong correlation with the BBC hit was observed[2].

In the previous result, one of the main systematic uncertainties of $p + p$ data comes from the proton backgrounds. In 2008, in order to reduce the charged backgrounds in the detector acceptance, a charge veto counter (CV), a plastic pad scintillator in front of the ZDC, was operated. To reduce the background uncertainty, the data taken in 2008 were analyzed. Figure 1 shows the charge distribution in the CV versus the particles x position measured by the SMD.

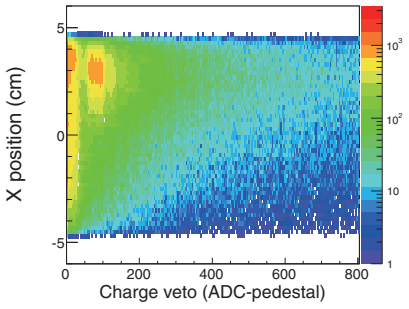

Fig. 1. The charge distribution in the CV vs the x position measured by the SMD for $p + p$ from 2008 data. One MIP peak around the 100 ADC value in the positive x region, where the proton beam bending direction, is shown.

Experimentally the asymmetry is measured by using the square-root formula as shown by Eq. (2) where $N^{\uparrow(\downarrow)}_{\phi(\phi+\pi)}$ is the number of neutrons detected at azimuthal angle ϕ ($\phi + \pi$) when the beam polarization direction is up (down).

$$A_N^{\rm fit} = \frac{1}{P}\frac{\sqrt{N^{\uparrow}_{\phi}N^{\downarrow}_{\phi+\pi}} - \sqrt{N^{\uparrow}_{\phi+\pi}N^{\downarrow}_{\phi}}}{\sqrt{N^{\uparrow}_{\phi}N^{\downarrow}_{\phi+\pi}} + \sqrt{N^{\uparrow}_{\phi+\pi}N^{\downarrow}_{\phi}}} \tag{2}$$

$$= (1-r)A_N^S + rA_N^{bg} \tag{3}$$

The signal asymmetry A_N^S and the background asymmetry A_N^B follow Eq. (3) where r is the fraction of backgrounds.

The main backgrounds are protons, generated by elastic, diffractive and hard processes. Protons from elastic and diffractive processes nearly follow the beam line, and are swept by the beam bending dipole magnet to the right side of the detectors, and a small fraction of those protons hit the right side ($x > 0$ in Fig. 1) of the detector. This background fraction is sensitive to the detector alignment, hence both the 2008 and 2015 data were measured by using the left-right asymmetry of the x distribution of particles.

Protons from hard processes are estimated by the PYTHIA event generator and GEANT Monte Carlo simulations. These protons result in even x distributions in the detector, and the same values are applied for both for the 2008 and 2015 data.

To solve Eq. (3) for two unknowns, A_N^S and A_N^B, $A_N^{\rm fit}$ and r are measured for two 2008 data samples: one from the "charge vetoed" sample, which requires a charge veto counter energy lower than half of the MIP peak, and another from the "charge not vetoed" sample, which does not require a charge veto cut. A_N^B of all BBC correlation samples is zero within statistical uncertainties. With A_N^B obtained from the 2008 data, A_N^S of 2015 data is calculated and found to be consistent with that of the 2008 data.

The resulting uncertainties on the asymmetries from the charged background are 13% for the ZDC inclusive sample, 14% for the "BBC tag" sample, and 55% for the "BBC veto" sample. The comparably large uncertainty for the "BBC veto" sample comes from the statistics and the small $A_N^{\rm fit}$. With this study, we can reduce uncertainties for ZDC inclusive and "BBC tag" samples.

*1 RIKEN Nishina Center
*2 Department of Physics and Astronomy, Seoul National University

References

1) B. Z. Kopeliovich, I. K. Potashnikova, I. Schmidt, J. Soffer : Phys. Rev. D 84, 114012 (2011).
2) M. Kim *et al.*, Accel. Prog. Rep. 49, 10 (2017).

Spin Physics in RHICf Experiment

J.S. Park[*1,*2] for RHICf collaboration

Transverse single spin asymmetry (A_N) is defined as

$$A_N = \frac{\sigma^{\uparrow} - \sigma^{\downarrow}}{\sigma^{\uparrow} + \sigma^{\downarrow}} \quad (1)$$

where $\uparrow$ and $\downarrow$ denote up and down spins, respectively, of the incident beam. Since the discovery of an unexpectdly large A_N in 1991 from the E704 experiment.[1] A_N values measured from subsequent experiments[2–4] have provided important information to expand QCD application. When we categorize QCD into perturbative QCD (pQCD) and non-perturbative QCD (non-pQCD) according to Q^2, the A_N in the pQCD region can be explained by two kinds of theoretical framworks: twist-3 perturbative QCD and the transverse-momentum-dependent parton distribution function. On the other hand, no general physical framework to calculate A_N in the region of non-pQCD exists. In the case of the inclusive neutron production process, however, A_N can be calculated by the spin-flip one pion exchange (OPE) model and spin-non-flip Reggeon exchange model.[5]

At the Relativistic Heavy Ion Collider (RHIC), the first polarized proton-proton collider, A_N measurement with forward neutrons($8.8 > \eta > 6.9$) at $\sqrt{s}$ =62 GeV, 200 GeV and 500 GeV has been performed.[6,7] These data have played an important role in testing the explanation based on the OPE model and Regge theory. Nevertheless, more A_N measurements of neutrons with high pseudorapidity and with higher pT are needed for a better understanding of the mechanism in inclusive neutron production and clarification of the relation among A_N, P_T and $\sqrt{s}$.

In the RHICf experiment, we will measure very forward neutral particles ($\eta > 6.9$) by using STAR ZDC and the RHICf detector. ZDC is a sampling type hadron calorimeter that has an energy resolution of 20% for 100 GeV neutrons with a position resolution of 1 cm. The RHICf detector is a sampling type EM calorimeter that has an energy resolution of 40% for 350GeV neutrons with a position resolution of 1 mm.[8]

In addition to the improvement of the position resolution of ZDC and the RHICf detector, we are planning to manipulate the position of the RHICf detector vertically as shown Fig. 1 and use a radial polarized beam during the dedicated beam time for the RHICf experiment.[9] These works will allow more precise measurement and higher p_T (up to 1.5 GeV/C) data. Another challenge in the RHICf experiment is the measurement of A_N with forward π^0; the RHICf detector consists of 2 towers for reconstruction from the detection of 2γ.

*1 Department of Physics and Astronomy, Seoul National University
*2 RIKEN Nishina Center

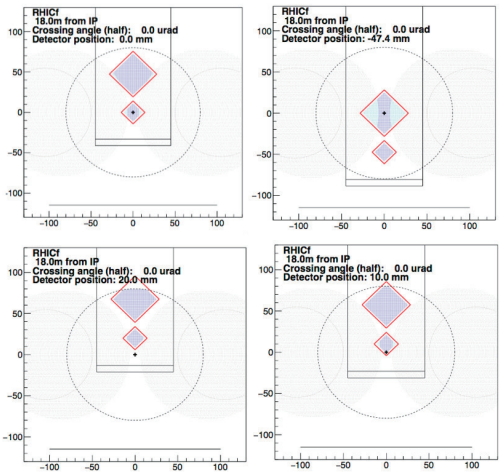

Fig. 1. Various positions of the RHICf detector. The black cross indicates the beam center.

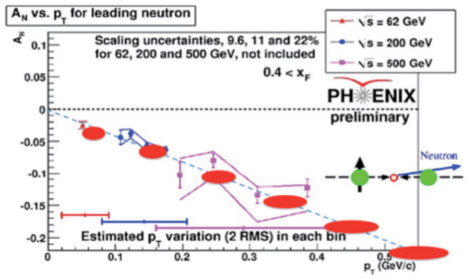

Fig. 2. Relationship between A_N of forward neutrons and pT at various collision energies. Red eclipses show the results expected from RHICf experiment.

References

1) D. L. Adams, et al., Fermilab E704 Collaboration, Nucl. Phys. B **510** 3 (1998).
2) S. S. Adler, et al., PHENIX Collaboration, Phys. Rev. Lett. **95** 202001 (2005).
3) A. Airapetian, et al., HERMES Collaboration, Phys. Rev. D **64** 097101 (2001).
4) V. Y. Alexakhin, et al., COMPASS Collaboration, Phys. Rev. Lett. **94** 202002 (2005).
5) B. Kopeliovich, et al., Physical Review D **84** 114012 (2011).
6) Y. Fukao et al., Phys. Lett. B **650**, 325 (2007).
7) A. Adare et al., PHENIX Collaboration, Physical Review D **88** 032006 (2013).
8) M. H. Kim for the RHICf Collaboration: In this report.
9) Y. Goto for the RHICf Collaboration. RIKEN Accel. Prog. Rep. **48**. (2015).

DAQ system in RHICf experiment

H. Menjo,[*1,*2] Q. Zhou,[*2,*3] K. Sato[*2,*3] for the RHICf collaboration

The data acquisition (DAQ) system of the RHICf experiment[1], which measures very forward neutral particles at RHIC, was set up in 2016, and it has been readied for data acquisition in an operation scheduled for June 2017[2]. The RHICf uses one of the LHCf detectors[3], which has 2 independent calorimeter towers composed of tungsten plates, 16 layers of GSO scintillators and 4 X-Y hodoscopes of GSO bar bundles. Figure 1 shows the schematic of the detector. The RHICf detector is located 18 m away from the STAR interaction point, which is immediately in the front of the STAR zero-degree calorimeter (ZDC). The RHICf DAQ uses read-out electronics, power supplies, and also the trigger system of the LHCf experiment. These are installed in a rack located in the STAR experimental cabin to avoid the effect of high radiation near the detector. The PMT analog signals from the sampling layers are transmitted from the detector to the rack via coaxial cables, and they are distributed over two analog-to-digital conversion (ADC) modules, CAEN V965, for charge measurement and two discriminator modules, CAEN V814B, for the trigger system via analog fanout modules. The AD conversion of signals from MAPMTs connected to the 480 GSO bars is performed in a radiation-hard front-end circuit located inside the detector. A VME board receives the digital data and stores it. The total data size per event is about 2.7 KB.

The trigger logic was designed for detecting events with electromagnetic and hadronic showers induced by incident photons and neutrons. A trigger is issued when any three successive layers have an energy deposit over a certain threshold. This type of trigger is called as a shower trigger. The logic was implemented on a field-programable gate array (FPGA) board with inputs from the discriminator boards. It was originally designed for the LHCf DAQ and optimized for the RHICf DAQ to work under the beam configuration of RHIC. Assuming discriminator threshold of 30 MeV energy-deposit equivalent signals, we estimated the trigger efficiencies of 100% for photons with energies over 30 GeV and about 70% for neutrons with energies over 50 GeV. In addition to the shower trigger, another trigger mode, the so-called π^0 trigger, was implemented. We note that π^0 particles generated in p-p collisions decay to photon pairs immediately. A π^0 trigger is issued when both the towers detect electromagnetic showers upon the condition that shower triggers are initiated in the first seven layers of each tower. The expected shower trigger rate is 18 kHz while the π^0 trigger rate is only about 60 Hz.[4] To enrich recoded π^0 trigger events within the readout rate of 1 kHz, the shower trigger rate is pre-scaled down to 0.8 kHz.

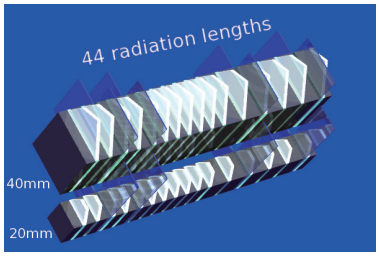

Fig. 1. Schematic view of the RHICf detector.

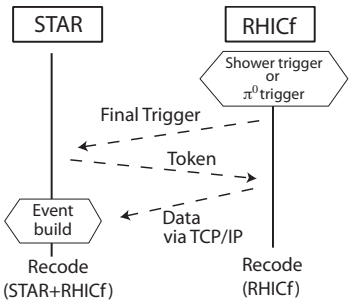

Fig. 2. Common-DAQ scheme of STAR and RHICf.

A common operation with the STAR experiment is performed. The RHICf final trigger signals are sent to the STAR trigger system to trigger the STAR DAQ. In the common operation, the RHICf works as a sub-detector of STAR. Figure 2 illustrates this common-DAQ scheme. STAR issues an event ID token for each triggered event and distributes it to all sub-detectors. The RHICf receives the token and sends RHICf data together with token via the network. The STAR DAQ combines all data from the sub-detectors and dumps it into a disk. This common operation increases the physics potential of the RHICf experiment, for example, the energy resolution for neutrons is improved upon combining the RHICf and STAR-ZDC data.[5]

*1 Graduate School of Science, Nagoya University
*2 RIKEN Nishina Center
*3 Institute for Space-Earth Environmental Research, Nagoya University

References
1) RHICf Collaboration: LOI, arXiv:1401.1004; RHICf proposal: arXiv:1409.4860.
2) T. Sako, et al.,: RIKEN Accel. Prog. Rep. 50, in press.
3) LHCf Collaboration: TDR, CERN-LHCC-2006- 004.
4) RHICf Collaboration: BUR 2017.
5) M. H. Kim for the RHICf Collaboration: RIKEN Accel. Prog. Rep. 50, in press.

Measurement of double-helicity asymmetries in inclusive J/ψ production in longitudinally polarized $p + p$ collisions at $\sqrt{s} = 510$ GeV†

Y. Goto*1 for the PHENIX Collaboration

We present a measurement of the double-helicity asymmetry, $A_{LL}^{J/\psi}$, in inclusive J/ψ production in $\sqrt{s}$ = 510 GeV longitudinally polarized $p + p$ collisions at the Relativistic Heavy Ion Collider (RHIC). The data used for the study were collected in the PHENIX experiment during the 2013 run; the sampled integrated luminosity was about 150 pb^{-1} for this analysis. We measured $A_{LL}^{J/\psi}$ by detecting the decay daughter muon pairs $\mu^+\mu^-$ within the PHENIX muon spectrometers in the rapidity range $1.2 < |y| < 2.2$. In $p + p$ collisions at RHIC energies, J/ψ particles are predominantly produced via gluon-gluon scatterings[1]. Due to the large charm quark mass, perturbative QCD is expected to work for calculations of the J/ψ and other charmonia production cross sections in high energy deep inelastic scattering and $p + p$ collisions.

By detecting the J/ψ at forward rapidity, we sample participating gluons from two distinct ranges of Bjorken x. The $A_{LL}^{J/\psi}$ can be expressed to be proportional to the product of the gluon polarization distributions at two distinct ranges of x. Quantitatively, we used a PYTHIA[2] (PYTHIA 6.4 tuned for RHIC energies) simulation at leading order to estimate the gluon x-distribution sampled in J/ψ production within the PHENIX muon arm acceptance. The simulation illustrates that for the $g + g \rightarrow J/\psi + X$ process in the forward rapidity of the PHENIX muon arm acceptance, the two gluons come from two very distinct x regions, with one gluon in the intermediate x region $x \sim 5 \times 10^{-2}$ where recent data of jet[3] and π^0[4] double helicity spin asymmetries have shown evidence of significant gluon polarization, and the other gluon covering the poorly known small-x region $x \sim 2 \times 10^{-3}$. Thus our new results could be used to further constrain the gluon polarization (ΔG) for $x < 5 \times 10^{-2}$. The $A_{LL}^{J/\psi}$ measurements offer a new way to access ΔG via heavy-quark production in $p + p$ collisions. They also serve as an important test of the universality of the helicity-dependent parton densities and QCD factorizations.

The final results for $A_{LL}^{J/\psi}$ as a function of transverse momentum p_T and rapidity $|y|$ are summarized in Fig. 1. The average $A_{LL}^{J/\psi}$ measured is 0.012 ± 0.010 (stat) ± 0.003 (syst). The black error bars show the statistical uncertainty. The red boxes show only the uncorrelated point-to-point systematic uncertainties for each p_T or $|y|$ bin. Additionally, there is a 4×10^{-4} global systematic uncertainty from the relative luminosity determination and a 6.5% global scaling systematic uncertainty from the polarization magnitude determination for all p_T or $|y|$ bins. To compare our results with the current understanding of the gluon polarization, we have calculated the $A_{LL}^{J/\psi}$ in our kinematic range using a PYTHIA simulation with NNPDFpol1.1[5] as the polarized PDF. To separate the uncertainty from the J/ψ production mechanism, we assumed $\hat{a}_{LL}^{gg\rightarrow J/\psi+X} = 1$, which is the leading order partonic asymmetry for open heavy quarks in the heavy mass limit at RHIC energies[1]. The blue curve with the shaded band is our $A_{LL}^{J/\psi}$ estimation. The solid blue curve is the central value and the blue shaded band is the $\pm 2\sigma$ range.

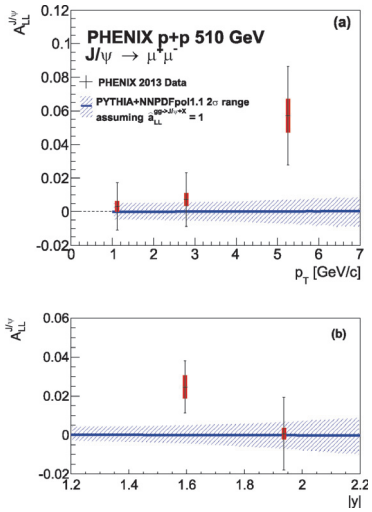

Fig. 1. $A_{LL}^{J/\psi}$ as a function of p_T (top panel) and $|y|$ (bottom panel).

References
1) S. Gupta and P. Mathews: Phys. Rev. D **56**, 7341 (1997).
2) T. Sjostrand, S. Mrenna, P. Z. Skands: JHEP **0605**, 026 (2006).
3) L. Adamczyk *et al.* [STAR Collaboration]: Phys. Rev. Lett. **115**, no. 9, 092002 (2015).
4) A. Adare *et al.* [PHENIX Collaboration]: Phys. Rev. D **90**, no. 1, 012007 (2014).
5) E. R. Nocera *et al.* [NNPDF Collaboration]: Nucl. Phys. B **887**, 276 (2014).

† Condensed from the article in Phys. Rev. D **94**, 112008 (2016)

*1 RIKEN Nishina Center

Status of double helicity asymmetries (A_{LL}) in $\pi^{\pm}$ production at mid-rapidity in longitudinally polarized p + p collisions with PHENIX experiment

T. Moon[*1,*2] for the PHENIX collaboration

The spin of the proton, $\frac{1}{2}\hbar$, is explained by the angular momentum sum rule in terms of quark and gluon components. The result of EMC experiment and others suggested that the spin of the quarks and anti-quarks only contributes about 30% of the proton spin.[1] This intrigued us to explore how much of the rest of the proton spin originates from the gluons and the orbital angular momenta of quarks and gluons.

The Relativistic Heavy Ion Collider (RHIC) provides polarized proton beams to determine the gluon helicity contribution to the proton spin as one of the main goals of the RHIC spin program.

In perturbative quantum chromodynamics (pQCD), pion and high p_T jet productions are sensitive to the gluon helicity distribution (Δg) in the proton where their production is dominated by gluon-related interactions, for example, q-g and g-g scatterings.

The RHIC double helicity asymmetries (A_{LL}) result in inclusive π^0 production at $\sqrt{s} = 510$ GeV with the RHIC 2012 and 2013 data sets extending the x range down to x $\sim$ 0.01 and confirming non-zero ΔG.[2]

For complementary information, the ordering of the asymmetries among three π meson species, π^0 and $\pi^{\pm}$, can directly reveal the sign of the gluon spin contribution to the proton spin.

The A_{LL} in $\pi^{\pm}$ production in longitudinally polarized p+p collisions can access the gluon helicity distribution (Δg) and is defined as

$$A_{LL} = \frac{\sigma_{++} - \sigma_{+-}}{\sigma_{++} + \sigma_{+-}}, \tag{1}$$

where, $\sigma_{++}(\sigma_{+-})$ denotes the $\pi^{\pm}$ cross section from a collision with the same (opposite) helicity.

At $\sqrt{s} = 510$ GeV in 2013, PHENIX recorded a total integrated luminosity of 108 pb^{-1} within a 30 cm vertex region and average polarization $P_B(P_Y) = 0.55 \pm 0.02$ (0.56 ± 0.02), where $P_B(P_Y)$ is the polarization of RHIC's blue (yellow) beam.

$\pi^{\pm}$ are reconstructed with the PHENIX tracking detectors, the drift chamber (DC) and pad chambers (PC), covering the pseudo-rapidity range $|\eta| < 0.35$ and the azimuthal angle $\Delta\phi = \pi$, and are separated from backgrounds, electrons, kaons, protons and so on by using a ring-imaging Cherenkov detector (RICH) and electromagnetic calorimeter (EMCal)

Experimentally, A_{LL} can be measured as

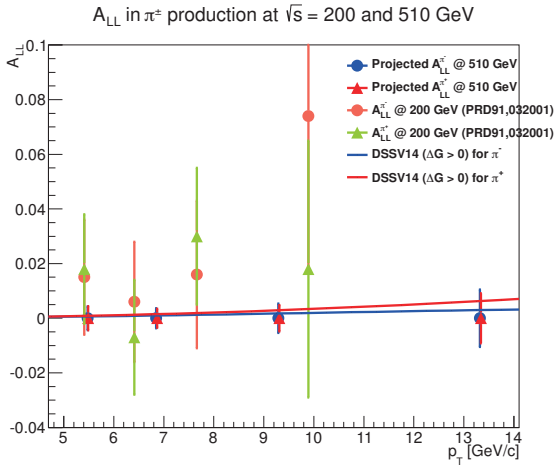

Fig. 1. Projected A_{LL} in $\pi^{\pm}$ production at $\sqrt{s} = 510$ GeV and published A_{LL} at $\sqrt{s} = 200$ GeV along with DSSV14 curve.

$$A_{LL} = \frac{1}{P_B P_Y} \frac{N_{++} - RN_{+-}}{N_{++} + RN_{+-}}, \tag{2}$$

where $N_{++}(N_{+-})$ denotes the yield of $\pi^{\pm}$ candidates from the collisions in the same (opposite) helicity. R is the relative luminosity between colliding bunches with different spin configurations:

$$R = \frac{L_{++}}{L+-}. \tag{3}$$

Figure 1 shows the comparison of projected A_{LL} in $\pi^{\pm}$ production at $\sqrt{s} = 510$ GeV and published A_{LL} at $\sqrt{s} = 200$ GeV along with the DSSV14 curve with positive gluon polarization. The uncertainty of charged pions at 510 GeV was significantly improved compared to that at 200 GeV. As a complementary probe, charged pions might help in directly inferring the sign of the gluon polarization.

In summary, charged pion analysis as a complementary probe is ongoing with improved statistics and is expected to double-check the sign of the gluon polarization.

References

1) J. Ashman et al. (EMC Collaboration), Nucl. Phys. B**328**, 167 1 (1989).
2) A. Adare et al. (PHENIX Collaboration), Phys. Rev. D**93**, 011501 (2016), 1510.02317.

*1 RIKEN Nishina Center
*2 Department of Physics, Yonsei University

Single transverse spin asymmetry (A_N) via charged pion production in polarized p + Au collisions at $\sqrt{s}$ = 200 GeV

J.H. Yoo[*1,*2] for the PHENIX collaboration

A proton is basically composed of many sea quarks and gluons in addition to the three valence quarks. According to the early EMC (European Muon Collaboration) data in the 80s, the contribution of the quarks and antiquarks to the entire proton's spin value (1/2) is less than 30%. As a result, the rest should come from the gluon spin and the orbital motions of quarks, antiquarks and gluons. The detailed spin structure of the proton can be revealed by investigating the longitudinal and transverse components. In particular, the transverse spin structure of the proton can provide some insight into the angular momentum component of the partons in the proton.

Transverse single spin asymmetries ($\mathbf{A_N}$) are relevant to the transverse spin structure of the proton. Initially, $\mathbf{A_N}$ of hadrons produced in the transversely polarized pp collision was expected to be small, but experiments instead measured large asymmetries of up to $\mathbf{A_N} \approx 40\%$. To better describe the large $\mathbf{A_N}$ measurements, the theoretical framework has been extended to include transverse momentum dependent (TMD) distributions and multiparton dynamics (higher twist effects).[1)] At least two TMD effects have been proposed to explain the observed nonzero asymmetries. The first of these, known as the Sivers effect, correlates the proton spin with the partonic transverse momentum $\mathbf{k_T}$.[1, 2)] The second TMD effect, known as the Collins effect, describes the coupling of a transverse quark polarization (transversity) and a transverse spin dependent fragmentation from a struck quark into a hadron.[1, 3)]

On the other hand, a pA collision gives a parton distribution and transverse momentum distribution in the nucleus by comparing the nucleon PDF. The generally accepted cold nuclear matter (CNM) effects are "Nuclear shadowing," "Gluon saturation," "Radiative energy loss," and the "Cronin effect." Nuclear shadowing means modification of the parton distribution functions within a nucleus. Gluon saturation signifies saturation of the gluon distribution function. Radiative energy loss means modification of the momentum fraction of partons due to multiple soft scattering. Finally, the Cronin effect implies broadening of the transverse momentum distribution due to multiple scattering of incident partons. Until recently, the transverse spin structure and CNM had been studied separately. The RHIC Run15 experiment was the first high-energy polarized proton and nuclear collision in the world. This unique collision experiment allows us to explore the spin degree of freedom in CNM effects.

$\mathbf{A_N}$ of neutral pions and inclusive charged hadrons have previously been measured with the PHENIX midrapidity spectrometer. These asymmetries have been found to be consistent with zero.[4)] These precise results are all consistent with zero over the observed $\mathbf{p_T}$ range,[1)] as shown in Fig. 1. In addition to a pp collision, $\mathbf{A_N}$ of neutral pions in a pA collision has already been analyzed. The analysis of $\mathbf{A_N}$ of charged pions using central arm detectors in the midrapidity region in a polarized pA collision is in progress. Wide **A** (nucleon number) coverage of $\mathbf{A_N}$ measurements from a polarized pp to pA collision will allow us to study the **A** dependence of $\mathbf{A_N}$ and the CNM effects in the system of transverse polarized protons colliding with nuclei.

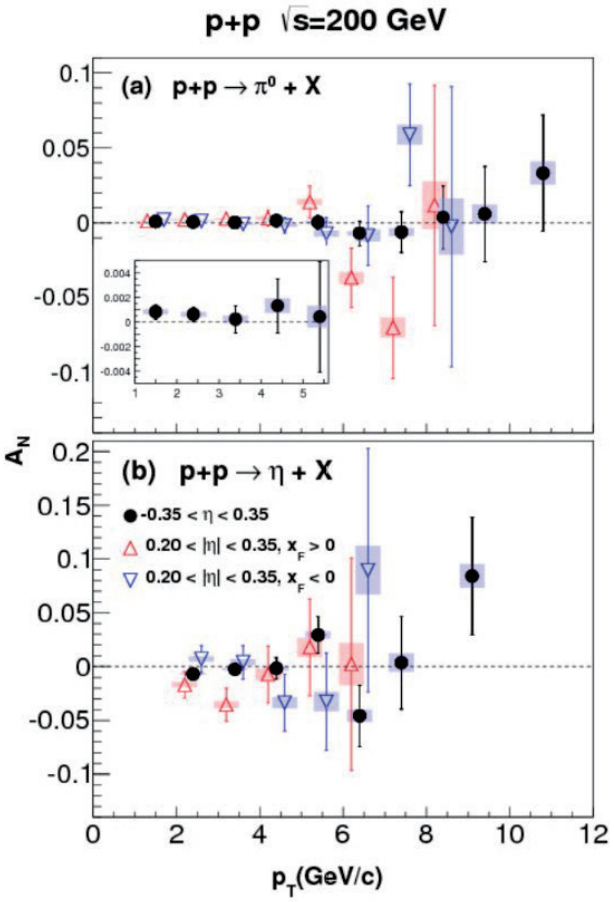

Fig. 1. $\mathbf{A_N}$ measured at midrapidity ($|\eta| < 0.35$) as a function of $\mathbf{p_T}$ for (a) π_0 and (b) η mesons.[1)]

References

1) A. Adare *et al*. (PHENIX Collaboration): Phys. Rev. D **90**, 012006 (2014).
2) D. W. Sivers: Phys. Rev. D **41**, 83 (1990).
3) J. C. Collins: Nucl. Phys. **B396**, 161 (1993).
4) N. Novitzky, SPIN 2016.

*1 RIKEN Nishina Center
*2 Department of Physics, Korea University

Nuclear modification factors of semi-leptonic charm and bottom decay electrons in central Au+Au collisions at $\sqrt{s_{NN}} = 200$ GeV

K. Nagashima[*1,*2] for the PHENIX collaboration

The PHENIX collaboration at the Relativistic Heavy Ion Collider has measured the strong suppression of electrons from heavy flavor hadron decays in quark-gluon plasma (QGP).[1] The energy loss of heavy quark provides important information on the properties of QGP. Since the bottom and charm masses are greater than Λ_{QCD} and the QGP temperature, they are produced by hard scattering in the earliest stages of a heavy-ion collisions and they experience the time evolution of QGP. The quark mass dependence of the energy loss compared with perturbative NLO calculations provide information on the QGP properties: the gluon density and diffusion coefficient. Therefore the separated measurement of charm and bottom quark suppression in QGP is very important.

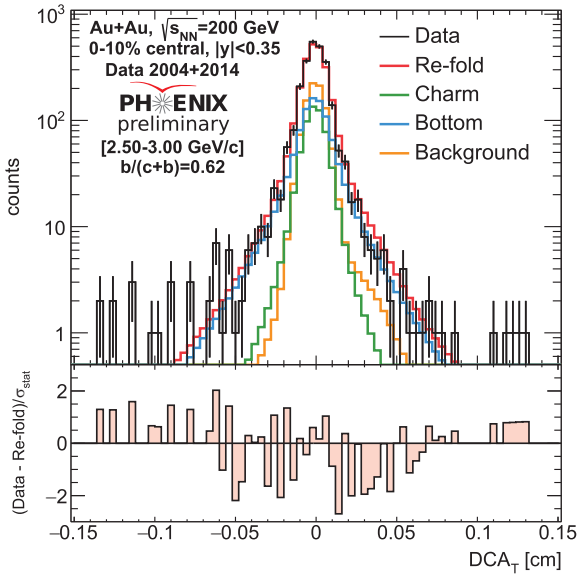

Fig. 1. DCA_T distribution for measured electrons compared with unfolded charm and bottom contributions.

The silicon vertex detector is installed at PHENIX to measure precisely displaced vertices, which allows the separation of the electron spectrum from charm and bottom semi-leptonic decays. The distribution of the distance of closest approach (DCA) of the track to the primary vertex for electrons from bottom hadron decays will be broader than that from charm hadron decays because the life time of bottom hadrons ($c\tau_{B^0}$ = 455 μm) is longer than that of charm hadrons ($c\tau_{D^0}$ = 123 μm) and they have different decay kinematics. PHENIX has published the first measurement of separated charm and bottom decay electron invariant yields and nuclear modification factor R_{AA} in 2011 for Au+Au at $\sqrt{s_{NN}}$ = 200 GeV by using Bayesian unfolding techniques applied simultaneously to the yield and DCA distributions.[2]

In 2014-2016, PHENIX collected 20 billion events in Au+Au at $\sqrt{s_{NN}}$ = 200 GeV, which is are 20 times larger than the 2011 dataset. This dataset allows the measurement of centrality dependence of R_{AA} of electrons from charm and bottom hadron decays and impose a strong constraint on theory. In this analysis, we apply Bayesian unfolding techniques and obtain the electron yields from charm and bottom hadrons separately for each $p_{\rm T}$ bin as shown in Fig. 1 and measure the R_{AA} as shown in Fig. 2 for 0-10% Au+Au collisions. We find that electrons from bottom hadron decays are less suppressed than those from charm hadron decays in 3.0-5.0 GeV/c in 0-10% central Au+Au collisions.

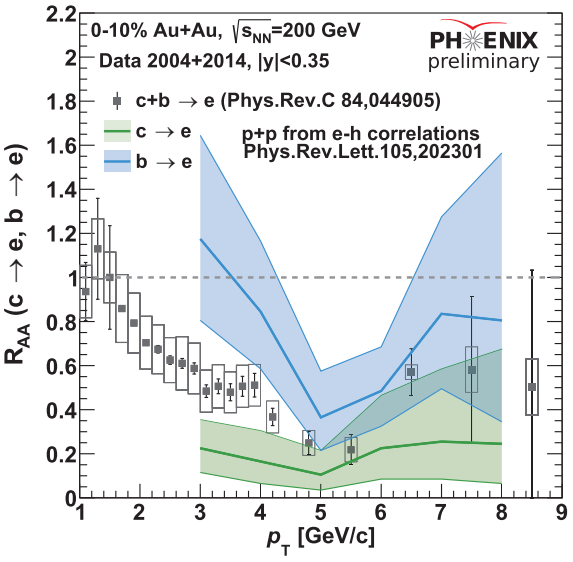

Fig. 2. Nuclear modification factor of electrons from charm and bottom in 0-10% central Au+Au collisions.

*1 Department of Physics, Hiroshima University
*2 RIKEN Nishina Center

References
1) A. Adare et al., Phys. Rev. C **84**, 044905 (2011).
2) A. Adare et al., Phys. Rev. C **93**, 034904 (2016).

Measurements of J/ψ mesons from B meson decays with the PHENIX-VTX detector

T. Hachiya [*1] for the PHENIX collaboration

Heavy quarks, bottoms and charms, are a useful probe to study the properties of quark gluon plasma (QGP) created in high-energy heavy-ion collisions. Due to their large masses ($M_b \approx 4.2$ GeV/c^2 and $M_c \approx 1.3$ GeV/c^2), heavy quarks are dominantly produced via initial hard scattering between partons in the incoming nuclei. Since none of the heavy quarks can be created during space-time evolution of the QGP, the number of heavy quarks is fixed at the beginning of the collisions. However, the final state interactions of heavy quarks in the QGP such as energy loss and collective flow can modify the momentum and angular distribution of the heavy quarks.

The PHENIX experiment recently measured single electron yields from bottom and charm quark decays separately in Au+Au collisions at $\sqrt{s_{NN}} = 200$ GeV[1)] using the silicon vertex detector (VTX). VTX consists of four layers of silicon sensors covering $|\eta| < 1.2$ and almost 2π in azimuth. VTX provides a precise displaced tracking to measure the decay length of heavy flavor hadrons. We observed that bottom quarks were less suppressed than charm quarks at $3 < p_T < 4$ GeV/c and were similarly suppressed at high p_T.

J/ψ produced from B meson decay is a direct channel to measure the bottom production, and it is especially good for low p_T. All J/ψ are promptly produced at the collision vertex except for J/ψ from B decay, called non-prompt J/ψ, because of the decay length ($c\tau_{B^0} \approx 455\mu m$). Therefore, we can separate non-prompt and prompt J/ψ by measuring their decay lengths.

The analysis is performed using data from $p+p$ and Au+Au collisions at $\sqrt{s_{NN}} = 200$ GeV recorded in 2015 and 2014. J/ψ is reconstructed by an unlike-sign di-electron pair. Electrons are identified using the ring-imaging Čerenkov detector and energy-momentum matching, where the energies and momenta are measured by the electromegnetic calorimeter and the drift chamber at the PHENIX central arm spectrometer, respectively. Electron tracks are associated with hits in VTX to remove the background tracks caused by photon conversions and Kaon decays. Figure 1 shows the invariant mass distributions of electron pairs in $p+p$ collisions. The red and blue histograms correspond to the unlike- and like-sign pairs, respectively. The like-sign distribution represents the combinatorial background qualitatively. In the distribution, the J/ψ signal is clearly seen and there is almost no background around the J/ψ mass region.

We then reconstruct the secondary vertex position of electron pair from the J/ψ decay and the collision vertex point using VTX. To identify non-prompt J/ψ, we calculate the pseudo proper time, X, which is defined as follows:

$$X = \frac{L_{xy} \cdot M_{J/\psi}}{p_{TJ/\psi}}. \quad (1)$$

Here, L_{xy} is the length between the secondary vertex and the collision vertex projected in the direction of the momentum vector of J/ψ, and $M_{J/\psi}$ and $p_{TJ/\psi}$ are the measured mass and p_T of the electron pairs, respectively. The kinematic relation of these variables is described in Fig. 2 (left). The pseudo proper time of J/ψ is an approximation of the decay length, $c\tau$, of B meson since the mass of J/ψ is close to that of the B meson. Figure 2 (right) shows the pseudo proper time distributions of simulated non-prompt and prompt J/ψ samples using PYTHIA and PHENIX detector simulation. These distributions are normalized to match their peaks in order to demonstrate the difference in the shape between non-prompt and prompt J/ψ. The non-prompt J/ψ has a longer tail on the positive side, which represents B meson decays far from the collision vertex, while the prompt J/ψ shows the symmetric shape caused by the detector resolution.

We are measuring the pseudo proper time of J/ψ using data from both $p+p$ and Au+Au collisions. These results will be published soon.

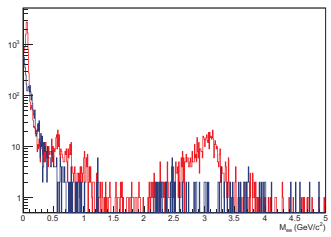

Fig. 1. Invariant mass of unlike sign(red) and like sign(blue) electron pairs.

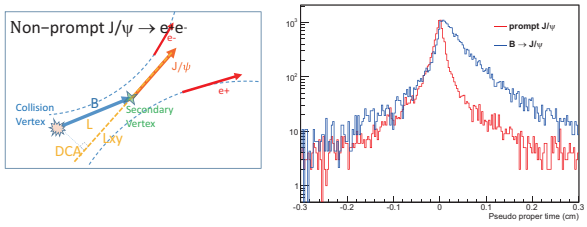

Fig. 2. (Left) Decay kinematics of non-prompt J/ψ. (Right) Pseudo proper time distribution of simulated non-prompt (blue) and prompt(red) J/ψ.

Reference
1) A. Adare *et al.*, Phys. Rev. C **93**, 034904 (2016).

*1 RIKEN Nishina Center

Improvement in the track reconstruction efficiency with VTX in the PHENIX experiment

Y. Ueda[*1*2] for the PHENIX Collaboration

Heavy quarks (charm and bottom quarks) with large masses ($M_c \approx 1$ GeV/c^2 and $M_b \approx 4$ GeV/c^2) are a good probe to study the quark gluon plasma (QGP). They are mainly produced by hard scattering in heavy-ion collisions and interact with soft partons in the QGP. The momentum and angular distributions of heavy quarks reveal the properties of the QGP.

For the measurement of heavy quarks, the Silicon Vertex Tracker (VTX) consisting of four layers of silicon detectors was installed in the PHENIX experiment. It reconstructs charged particle trajectories and their distances of closest approach (DCAs) to the primary collision vertex precisely. Since the DCA is related to the lifetime and mass of the particle, we can statistically separate electrons from semileptonic decays of the charm and bottom quarks using the DCA.

In 2014, PHENIX collected about 15 billion minimum bias Au+Au events. We measure the centrality dependence of the nuclear modification factors[1)] and the azimuthal anisotropies of the charm and bottom quarks over a wide range of values of p_T.

The track reconstruction is important for this measurement. The method of track reconstruction with VTX is as follows. First, a line from the primary vertex to a hit point on the 1st VTX layer is defined as a basic track. Then, it is propagated to the 2nd layer. If a hit point on the 2nd layer is found within certain windows in both the ϕ and z directions, called the DPHI and DZ windows, from the propagated track, the track is refitted, including the new hit. The same steps are repeated for 3rd and/or 4th layer.

The window sizes of the 2nd, 3rd and 4th layers are named DPHI0/DZ0, DPHI1/DZ1, and DPHI2/DZ2, respectively. They are changed with the multiplicity because the track density is different.

Precise determination of the primary vertex is necessary to measure the DCA precisely. However, the measurement is difficult in low multiplicity events. Furthermore, the original window sizes used in the peripheral Au+Au collisions were too tight, and a significant fraction of the track was lost. I have optimized the DPHI/DZ window sizes for low multiplicity events to improve the efficiency of track reconstruction, keeping the number of fake tracks as small as possible. Here, the fake track rate is estimated by a simulation.

In low multiplicity events (50–100% centrality), DZ0 is no longer used for the new track reconstruction. DZ1 and 2 are 1.5 times larger than the original window sizes for low multiplicity events, while the sizes for DPHI are decreased by a factor of 10. This is because an increase in only the window sizes of DZ, especially DZ0, is more effective for improving the efficiency without increasing the number of fake tracks.

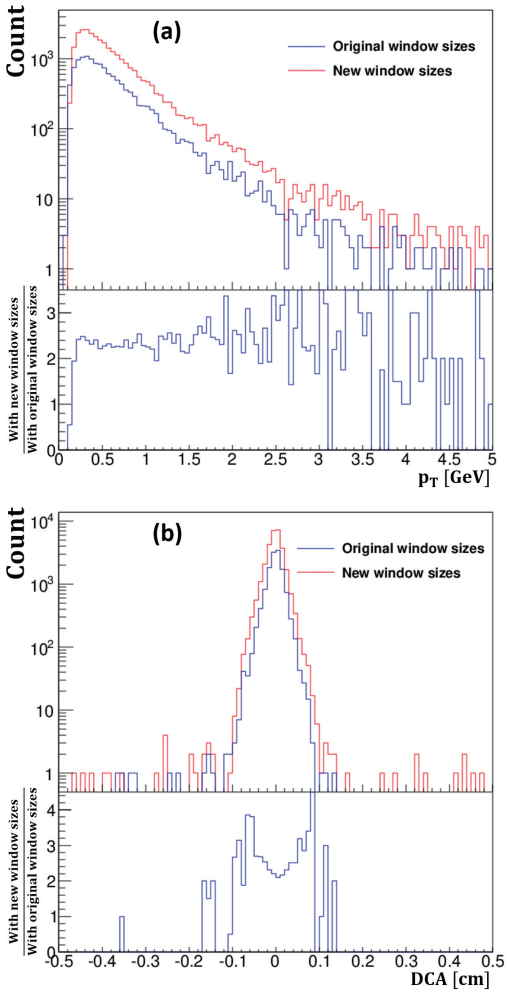

Fig. 1. (a) p_T and (b) DCA distributions in low multiplicity events with the original and new window sizes. Blue and red lines are with the original and new window sizes, respectively.

The number of tracks in low multiplicity events is increased by a factor of 2.5 using the new window sizes over the p_T range and around the DCA peak (Fig. 1). In addition, the DCA tail part around |0.1| cm is increased only by a factor of four. The fake track rate increases only by a small amount. Therefore, we will apply the new window sizes for the reconstruction of the VTX data.

*1 RIKEN Nishina Center
*2 Department of Physics, Hiroshima University

Reference
1) K. Nagashima et al.: In this report.

Development of a prototype silicon tracking detector for the sPHENIX experiment

Y. Yamaguchi,[*1] Y. Akiba,[*1] T. Hachiya,[*1] Y. Kawashima,[*1,*2] E. Mannel,[*3] H. Masuda,[*1,*2] G. Mitsuka,[*1] I. Nakagawa,[*1] D. Nemoto,[*1,*2] and R. Nouicer[*3]

Quark Gluon Plasma (QGP) is an extreme hot and dense QCD matter where quarks and gluons are released from confinement inside hadrons and it is believed to have existed in the early universe. The study of QGP gives a rich knowledge on not only how our universe has been formed but fundamental features of QCD in a high dense and high temperature environment.

The sPHENIX experiment is scheduled to start data taking from 2021 at the Relativistic Heavy Ion Collider (RHIC) to reveal the medium properties of QGP, and the tracking system of the sPHENIX detector consists of the monolithic active pixel sensors (MAPS), the intermediate silicon tracking detector (INTT), and the time projection chamber (TPC) from the inside to the outside. We have a responsibility for construction of INTT which has an important role to realize good capabilities on:

- track reconstruction by association of MAPS and TPC hit information
- single collision vertex finding with a high collision rate

We have inherited the readout system and basic idea of the module structure for the forward vertex detector (FVTX)[1] as a subsystem of the PHENIX detector to minimize R&D efforts of INTT so that INTT construction can be completed in time for start-up of the sPHENIX experiment. Therefore, we need to understand how a whole readout system of INTT including the inherited devices works using a prototype module. In this report, the current status of development of a prototype module is reported.

The first prototype modules of INTT have been assembled at BNL. Si sensors[2] with thickness of 240 and 320 μm from HAMAMATSU Photonics K.K. are used for the prototype modules. Figure 1 shows the prototype module with 320 μm-thick Si sensors. High density interconnect circuits (HDIs) are connected on either side of the Si sensors and 10 FPHX chips are mounted on each HDI. The FPHX chip is originally designed as a pre-amplifier for FVTX and contains 128 channels. The Si sensors are mechanically separated at the middle and the FPHX chips are wire-bonded to the Si sensors.

Tests of the prototype modules have been made using calibration pulses. The test result for a single

Fig. 1. A prototype module of INTT with 320 μm-thick Si sensors.

FVTX chip on the HDI is shown in Fig. 2. A clear correlation between calibration pulse amplitude and ADC values can be seen and all channels look working. It has been confirmed that the Si sensors and FPHX

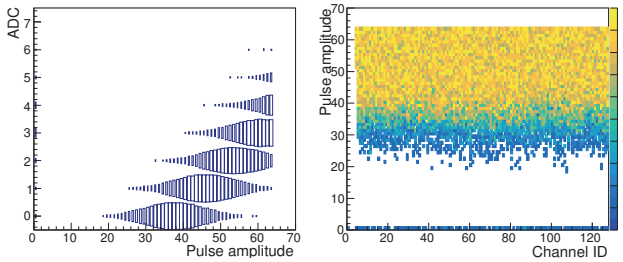

Fig. 2. The correlation between calibration pulse amplitude and ADC values (Left) and reactions with the calibration pulses for all channels on a chip (Right).

chips can be assembled successfully on a HDI and a whole readout system works well with the prototype modules.

New HDIs will be produced with an improved design to match an updated detector position configuration soon and further tests with prototype modules are scheduled including cosmic ray measurements.

References

1) C. Aidala *et al.*, NIM A **755**, 44-61 (2014).
2) Y. Akiba *et al.*, in this report.

*1 RIKEN Nishina Center
*2 Department of Physics, Rikkyo University
*3 Brookhaven National Laboratory

Fragmentation function measurements in Belle

R. Seidl,[*1] F. Giordano,[*2] A. Vossen,[*3] H. Li,[*3] W. W. Jacobs,[*3] M. Grosse-Perdekamp,[*2] C. Van Hulse[*4] and G. Schnell[*4,*5]

The fragmentation from asymptotically free partons into confined hadrons is described by fragmentation functions (FF). Since FFs are nonperturbative objects they cannot be calculated from first principles in QCD and need to be measured experimentally. Especially the electron-positron annihilation process such as studied at the Belle experiment on the KEKB accelerator is well suited for such measurements since no hadrons exist in the initial state. Once fragmentation functions are extracted universality and factorization allow its application to other processes such as semi-inclusive deep-inelastic scattering or hadron collisions in order to gain flavor as well as spin information in parton distribution functions. The transversity distribution function, for example, can be accessed using spin dependent di-hadron FFs, also called interference FFs.

Belle has obtained those previously[1)] but the unpolarized baseline is still missing. In this analysis we extract di-hadron cross sections for various pion, kaon and charge combinations differential in their fractional energy $z = 2E_{hh}/\sqrt{s}$ relative to the initial parton energy and the invariant mass of the pair. Unlike the previous publication[2)], this analysis concentrates on two hadrons from the same hemisphere in order to increase the likelihood of both emerging from the same initial parton. The various corrections reported previously have been adapted to this analysis and results are already in the Belle-internal refereeing process and are expected to be published soon.

Figure 1 displays the expected sensitivities for dipions as a function of invariant mass and in bins of fractional energy. In the opposite-sign pion pairs one clearly can identify various resonances such as the K^0_S and ρ mesons as well as the Cabbibo-suppressed decay of the D^0 meson. The same-sign pion pair cross sections display a more continuous mass distribution. All other pion, kaon and charge combinations are similarly prepared.

Other ongoing measurements include the surprising discovery of a nonzero Λ baryon polarization originating from an unpolarized parton when correlating it with the transverse momentum the Λ carries with respect to the thrust axis[3)]. Preliminary results have been shown and the results are currently being finalized.

Also other explicitly transverse momentum dependent fragmentation functions are currently being extracted. Two teams extract different types of such. One analysis concentrates on measuring the transverse momentum between two nearly back-to-back hadrons relative to one hadron's momentum direction while the other analysis studies single hadrons' transverse momenta relative to the thrust axis. While the first method is experimentally straightforward, convolutions of the intrinsic transverse momenta of both hadrons complicate the extraction of the intrinsic transverse momentum dependence. The single hadron method extracts directly the transverse momentum but the thrust axis is only approximating the initial parton's axis. Both types of analysis are progressing and are expected to be ready for publication soon.

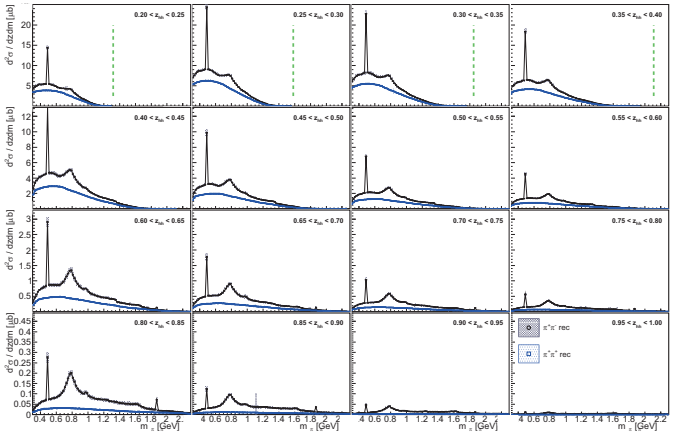

Fig. 1. Expected di-pion cross sections as a function of $m_{\pi\pi}$ in bins of z as expected by fully tracked and reconstructed Belle MC. Same sign pion pairs are displayed by blue squares while opposite-sign pion pairs are displayed by black circles.The green vertical lines represent the kinematic mass boundaries for each z bin.

References

1) A. Vossen *et al.* [Belle Collaboration], Phys. Rev. Lett. **107**, 072004 (2011).
2) R. Seidl *et al.* [Belle Collaboration], Phys. Rev. **D92**, 092007 (2015).
3) A. Abdesselam *et al.* [Belle Collaboration], e-Print: arXiv:1611.06648.

*1 RIKEN Nishina Center
*2 Physics department, University of Illinois
*3 Physics department, Indiana University
*4 Department of Theoretical Physics, University of the Basque Country
*5 Ikerbasque

Measurement of anti-quark flavor asymmetry in the proton at SeaQuest

K. Nakano,[*1,*2] Y. Goto,[*2] Y. Kunisada[*1] Y. Miyachi,[*3] S. Miyasaka,[*1] K. Nagai,[*1,*2] S. Sawada,[*2,*4] T.-A. Shibata,[*1,*2] S. Tamamushi[*1] for the E906/SeaQuest Collaboration

The distributions of light anti-quarks ($\bar{u}$ and $\bar{d}$) in the proton had been assumed to be flavor symmetric, i.e., $\bar{d}(x) = \bar{u}(x)$, because they should be created via gluon splitting ($g \to q\bar{q}$) with the same probability because of their almost equal mass and flavor independence. However, a large asymmetry has been observed by the NMC, NA51, and E866/NuSea experiments[1]. Various theoretical models are being examined to understand the origin of this flavor asymmetry.[2] The SeaQuest experiment at Fermilab aims to measure the asymmetry $\bar{d}/\bar{u}$ at high x, up to 0.45, to reveal the x dependence of $\bar{d}/\bar{u}$.

SeaQuest utilizes a 120-GeV proton beam from the Fermilab Main Injector ($\sqrt{s} = 15$ GeV). It employs liquid-hydrogen (LH_2) and liquid-deuterium (LD_2) targets to measure the Drell-Yan process in $p+p$ and $p+d$ reactions. In the Drell-Yan process, a quark in one hadron and an anti-quark in the other hadron annihilate into a virtual photon and then decay into a lepton pair: $q + \bar{q} \to \gamma^* \to l^+ + l^-$. At the forward rapidity ($x_F \gg 0$) and under p-n isospin symmetry, the ratio of $p+p$ and $p+d$ cross-sections relates to the anti-quark flavor asymmetry as

$$\frac{\sigma_{p+d}(x_2)}{2\sigma_{p+p}(x_2)} \approx \frac{1}{2}\left(1 + \frac{\bar{d}(x_2)}{\bar{u}(x_2)}\right), \quad (1)$$

where x_2 denotes the Bjorken x of partons in the target-side hadron. Most systematic errors in the measurement cancel out in this ratio.

The SeaQuest spectrometer detects the final-state muon pair of the Drell-Yan process. Details and the recent status of SeaQuest were reported last year.[3] SeaQuest has been acquiring physics data since November 2013 and had recorded 1.1×10^{18} beam protons on targets as of summer 2016. About 50% of the recorded data were analyzed.

The cross-section ratio $\sigma_{pd}/2\sigma_{pp}$ was derived from dimuon yields measured on the LH_2 and LD_2 targets. We selected dimuons with an invariant mass larger than 4.2 GeV, where the Drell-Yan events are dominant. The yields have been corrected for track-reconstruction efficiency and background dimuons. Figure 1 shows a preliminary result for $\sigma_{pd}/2\sigma_{pp}$ measured by SeaQuest. The systematic uncertainty arises from the impurity of the LD_2 target and the inaccuracy of the dimuon-yield corrections.

*1 School of Science, Tokyo Institute of Technology
*2 RIKEN Nishina Center
*3 Faculty of Science, Yamagata University
*4 Institute of Particle and Nuclear Studies, KEK

The anti-quark flavor asymmetry $\bar{d}/\bar{u}$ was extracted from $\sigma_{pd}/2\sigma_{pp}$. The cross section was computed at the leading order in α_s without nuclear correction for deuterium. Figure 2 shows a preliminary result for $\bar{d}/\bar{u}$ obtained by SeaQuest. It reveals $\bar{d}/\bar{u}$ with the best ever precision at $0.20 < x_2 < 0.58$. The systematic uncertainty includes the uncertainty of the parton distribution function (PDF) used in this extraction (CT10LO[4]). Very interestingly, it suggests $\bar{d}/\bar{u} > 1$ at high x, despite the E866 result.[1] Further analyses are being made to improve the measurement accuracy and investigate the difference with respect to E866.

Physics data are being acquired in fiscal year 2017. We expect to record about 4×10^{17} beam protons on targets. We have upgraded the spectrometer, namely achieving a wider acceptance and a faster DAQ. The statistics with the full dataset will be four times better at high x than the preliminary result.

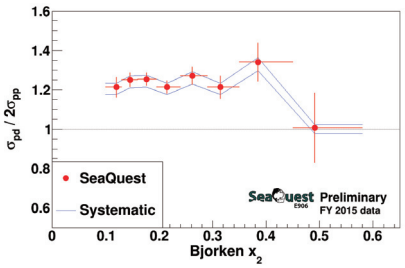

Fig. 1. Ratio of $p+p$ and $p+d$ Drell-Yan cross sections versus Bjorken x of target-side partons (x_2).

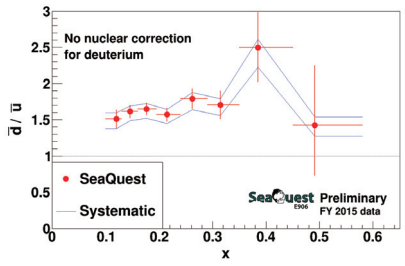

Fig. 2. Anti-quark flavor asymmetry ($\bar{d}/\bar{u}$) versus x.

References

1) R. S. Towell et al., Phys. Rev. D **64**, 052002 (2001).
2) W. C. Chang et al., Prog. Part. Nucl. Phys. **79**, 95 (2014).
3) K. Nagai et al., RIKEN Accel. Prog. Rep., **49**, 114 (2016).
4) H. L. Lai et al., Phys. Rev. D **82**, 074024 (2010).

Search for $\bar{K}NN$ bound state at J-PARC

F. Sakuma,[*1] T. Hashimoto,[*1] K. Itahashi,[*1] M. Iwasaki,[*1] Y. Ma,[*1] H. Ohnishi,[*1] S. Okada,[*2] H. Outa,[*1] M. Sato[*3] for the J-PARC E15 Collaboration

The possible existence of strongly bound $\bar{K}$ nuclear states has been widely discussed as a consequence of the strongly attractive $\bar{K}N$ interaction in the $I = 0$ channels.[1] The investigation of those exotic states will provide unique information of the $\bar{K}N$ interaction below the threshold, which is still not fully understood. Among the $\bar{K}$ nuclear-states, the simplest $\bar{K}$-nuclear cluster $\bar{K}NN$, is of special interest because it is the lightest $S = -1$ $\bar{K}$ nucleus. Many theoretical calculations based on the $\bar{K}NN - \pi\Sigma N - \pi\Lambda N$ coupled channels have predicted the existence of the bound state.[2] However, the calculated properties of the bound state, such as the binding energy (B.E.) and decay width (Γ), strongly depend on $\bar{K}N$ interaction models.

Experimentally, there are several reports on the observation of peak structure with a B.E. of $\sim$ 100 MeV.[3–5] In contrast, null results were also reported by several experiments,[6,7] and therefore the existence of the $\bar{K}NN$ bound state has remained controversial. The J-PARC E15 experiment was performed at the K1.8BR beam line using the K^- + ^{3}He reaction at p_{K^-} = 1.0 GeV/c.[8] The first physics run of the E15 experiment was conducted in May 2013 with 5.3 $\times$ 10^9 kaons incident on ^{3}He. The results of a semi-inclusive ^{3}He$(K^-, n)X$ measurement can be found in Ref[9]. To measure an expected decay mode of $\bar{K}NN \to \Lambda p$, an exclusive ^{3}He$(K^-, \Lambda p)n$ measurement was also performed by identifying two protons and one negative pion in a cylindrical detector system (CDS) surrounding a liquid ^{3}He target system.[10] The $p\pi^-$ pair associated with a specific Λ decay in the $pp\pi^-$ event was reconstructed with a log-likelihood method, and a missing neutron was identified kinematically.

The distribution of the Λp invariant mass and the neutron emission angle of the obtained Λpn final state are shown in Fig. 1 (b) and (c), respectively, and a scatter plot of the two is given in Fig. 1 (a). A bump structure is observed at the mass threshold of $K^- + p + p$ in the Λp invariant mass spectrum, which is not reproduced by a global fit based on multi-nucleon absorption processes of K^-. To explain the excess, a simple S-wave Breit-Wigner structure over the three-body phase space of the K^- ^{3}He $\to \Lambda pn$ reaction is assumed. A χ^2 test was performed between the experimental data and the simulated pole together with the multi-nucleon absorption processes, and the minimum χ^2 point was obtained with $M_X = 2355^{+6}_{-8}(stat.) \pm 12(syst.)$ MeV/c^2, $\Gamma_X = 110^{+19}_{-17}(stat.) \pm 27(syst.)$ MeV/c^2.

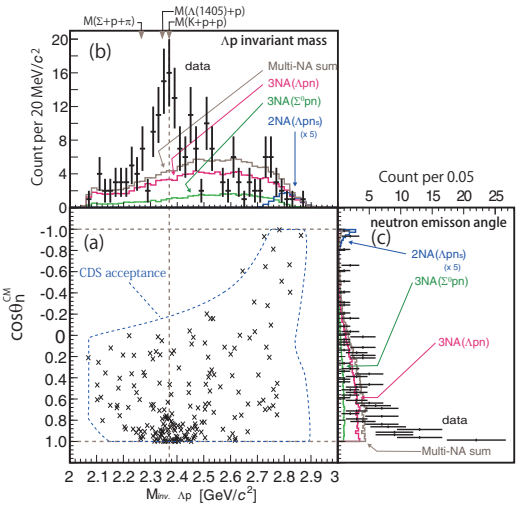

Fig. 1. (a) Distribution of the Λ invariant mass and the emission angle of the missing neutron, (b) Λ invariant mass with simulated spectra obtained by the global fit, and (c) angular distribution of the missing neutron.[10]

A naive interpretation of the structure would be the $\bar{K}NN$ bound state, since the pole position is located below the mass threshold of $K^- + p + p$ (2370 MeV/c^2). It could also be a shallow bound or unbound resonance of the $\Lambda(1405)p$ system followed by Λp conversion, the threshold of which is located at 2343 MeV/c^2 if the mass of $\Lambda(1405)$ is assumed to be 1405 MeV/c^2. To explore whether or not the observed structure is the $\bar{K}NN$ bound state in more detail, the second run was carried out in 2015 with the accumulation of 30 times more data on the Λpn final state and the analysis is in progress.

*1 RIKEN Nishina Center
*2 AMO Physics Laboratory, RIKEN
*3 Condensed Molecular Materials Laboratory, RIKEN

References

1) Y. Akaishi and T. Yamazaki, Phys. Rev. C **65**, 044005 (2002).
2) A. Dote, T. Inoue, and T. Myo, Prog. Theor. Exp. Phys. **2015** 043D02 (2015).
3) M. Agnello et al., Phys. Rev. Lett. **94**, 212303 (2005).
4) T. Yamazaki et al., Phys. Rev. Lett. **104**, 132502 (2010).
5) Y. Ichikawa et al., Prog. Theor. Exp. Phys. **2015** 021D01 (2015).
6) G. Agakishiev et al., Phys. Lett. B **742**, 242 (2015).
7) A. O. Tokiyasu et al., Phys. Lett. B **728**, 616 (2014).
8) K. Agari et al., Prog. Theor. Exp. Phys. **2012** 02B011 (2012).
9) T. Hashimoto et al., Prog. Theor. Exp. Phys. **2015** 061D01 (2015).
10) Y. Sada et al., Prog. Theor. Exp. Phys. **2016** 051D01 (2016).

Energy calibration using the $p(d,{}^3\mathrm{He})\pi^0$ reaction in pionic atom spectroscopy at BigRIPS

T. Nishi,[*1] D.S. Ahn,[*1] G.P.A. Berg,[*1,*2] M. Dozono,[*1] D. Etoh,[*1,*3] H. Fujioka,[*1,*4] N. Fukuda,[*1] N. Fukunishi,[*1] H. Geissel,[*1,*5] E. Haettner,[*1,*5] T. Hashimoto,[*1] R.S. Hayano,[*6] S. Hirenzaki,[*1,*7] H. Horii,[*1,*6] N. Ikeno,[*8] N. Inabe,[*1] K. Itahashi,[*1] M. Iwasaki,[*1] D. Kameda,[*1] S. Kawase,[*9] K. Kisamori,[*1,*9] Y. Kiyokawa,[*9] T. Kubo,[*1] K. Kusaka,[*1] M. Matsushita,[*9] S. Michimasa,[*9] G. Mishima,[*1,*6] H. Miya,[*1] D. Murai,[*1] H. Nagahiro,[*7] M. Niikura,[*1,*6] S. Ota,[*9] N. Sakamoto,[*1] K. Sekiguchi,[*1,*3] H. Suzuki,[*1] K. Suzuki,[*1,*10] M. Takaki,[*9] H. Takeda,[*1] Y.K. Tanaka,[*1,*5] T. Uesaka,[*1] Y. Wada,[*1,*3] Y.N. Watanabe,[*1,*6] H. Weick,[*1,*5] H. Yamakami,[*1,*4] Y. Yanagisawa,[*1] and K. Yoshida[*1]

In June 2014, we performed a missing-mass spectroscopy experiment on the ^{122,117}Sn(d,^{3}He) reaction to measure the binding energies and widths of deeply bound pionic states[1]. In the experiment, excitation spectra of ^{121,116}Sn near the π^- emission threshold were obtained from the measurement of ^{3}He momenta, which were magnetically analyzed using BigRIPS as a spectrometer. The momenta are determined from two types of information: the central momentum and its deviation. The former is calibrated using the two-body reaction $p(d,{}^3\mathrm{He})\pi^0$ with a polyethylene target. The latter is determined precisely by position measurements at a dispersive focal plane. In this report, the details of the calibration are explained.

To precisely calibrate the central momentum in BigRIPS, we performed Monte-Carlo simulations and compared them with experimentally obtained ^{3}He momenta and reaction angles. In the simulation, momenta and angles were obtained using the following three steps.

(a) Emittance of the primary beam

The position, angle, and momentum spread of the primary deuteron beam were taken into account. The measured emittance was 0.2 ×2.0π mm·mrad (horizontal/RMS) and 0.03% (RMS)[3]. The momentum spread is one of the main sources for the missing mass resolution.

(b) Two-body reaction at the target

The distribution of reaction angles of ^{3}He from the $d(p,{}^3\mathrm{He})\pi^0$ reaction was taken from previous experimental data[2] where the energy in the center-of-mass frame was the same as in our experiment. The corresponding momenta are obtained from two-body kinematical calculation.

(c) Analysis with a transfer matrix

The momenta and reaction angles produced in steps (a) and (b) were converted to the positions and angles at the focal plane using an experimentally measured transfer matrix. In the conversion, the effects of multiple scattering inside the target and in a 50 μm-thick stainless steel window located upstream of the focal plane were also considered. The obtained positions and angles are converted to the momenta and reaction angles using the transfer matrix, as done for the experimental data. The obtained momentum deviations (represented as δ) and reaction angles in the simulation were compared with those in the experiment. The simulation result reproduces the experimental data well, as shown in Fig. 1. In the comparison, we calculated χ^2 between two 2D histograms and determined the central momentum of BigRIPS by minimizing the χ^2.

As a result, we succeeded in suppressing the contribution from the energy calibration on the missing mass precision within 10 keV, which is negligibly small compared with other contributions such as the ambiguity of the primary beam energy. Thus, we established the energy calibration method using the $d(p,{}^3\mathrm{He})\pi^0$ reaction, which will improve the determination accuracy of the binding energy of the pionic atoms. The analysis is ongoing.

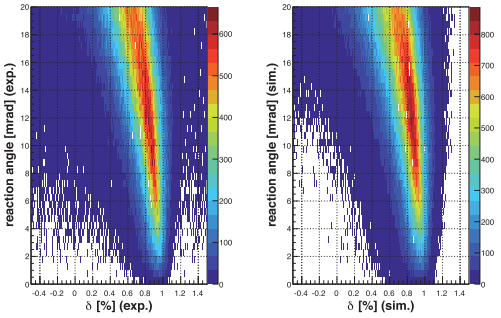

Fig. 1. δ - reaction angle plot from the $p(d,{}^3\mathrm{He})\pi^0$ reaction. (Left) Experimental data. (Right) Simulation result.

*1 RIKEN, Nishina Center
*2 JINA-CEE and Department of Physics, University of Notre Dame
*3 Department of Physics, Tohoku University
*4 Department of Physics, Kyoto University
*5 GSI Helmholtzzentrum für Schwerionenforschung GmbH
*6 Department of Physics, University of Tokyo
*7 Department of Physics, Nara Women's University
*8 Department of Regional Environment, Tottori University
*9 CNS, University of Tokyo
*10 Stefan Meyer Institute, Austrian Academy of Sciences

References

1) K. Itahashi et al., RIBF Proposal **054R1** (2013).
2) M. Betigeri et al., Nucl. Phys. A **690** 473 (2001).
3) T. Nishi et al., RIKEN Accel. Prog. Rep. **48**, 235 (2015).

Clear indication of a strong I=0 $\bar{K}N$ attraction in the $\Lambda(1405)$ region from the CLAS photo-production data

M. Hassanvand,[*1,*2] Y. Akaishi,[*2] and T. Yamazaki[*2,*3]

The possible existence of deeply bound kaonic nuclear systems was proposed[1] more than a decade ago, based on an ansatz that $\Lambda^* \equiv \Lambda(1405)$ mass is 1405 MeV/c^2, where Λ^* is a $\bar{K}N$ quasi-bound state decaying to $\Sigma\pi$. Recently, a large number of data on the photo-production of $\Lambda(1405)$ in the $\gamma p \to K^+\pi^{0\pm}\Sigma^{0\mp}$ reaction were provided by the CLAS collaboration[2], and the double-pole structure of Λ^* has been intensively discussed by chiral dynamics analyses[3–5].

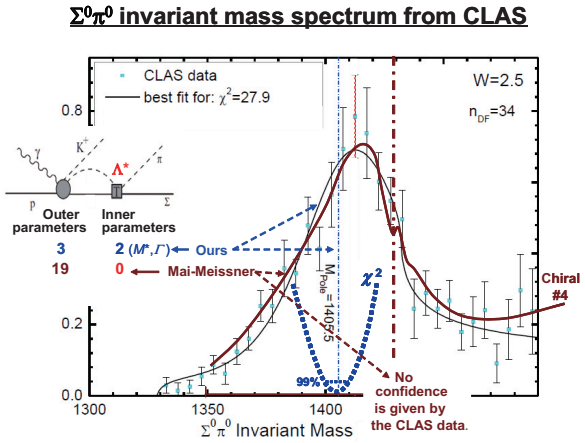

Fig. 1. Analyses of a $\Sigma^0\pi^0$ invariant mass spectrum from CLAS. Mai-Meissner's analysis (brown) with chiral theory and Hassanvand-Akaishi-Yamazaki's analysis (black and blue) are compared.

We have analyzed the CLAS data. Figure 1 compares two CLAS-data analyses. The most essential question is what the pole position of Λ^* extracted from the CLAS data themselves is. To answer it, we classified χ^2 fitting parameters into "inner" and "outer" ones, where the "inner" indicates the parameters appearing inside the T-matrix which can vary the pole position and width of Λ^*. The double pole positions recommended in Ref.[5] are cases selected using only "outer" parameters, holding the pole position unchanged in χ^2 fitting processes. Therefore, the chiral pole position in Ref.[4], for example, gets no confidence from the CLAS data. On the other hand, we used the Λ^* pole position and width as fitting parameters and found the χ^2 minimum at 1405.5 MeV/c^2, rejecting the chiral result with more than 99% statistical significance.

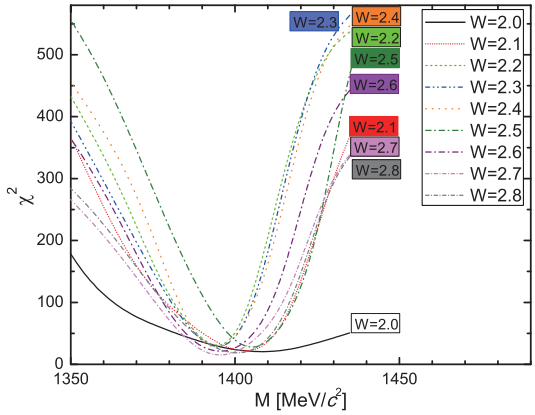

Fig. 2. Variation of χ^2 values with respect to Λ^* pole position parameter M for the $\Sigma^0\pi^0$ invariant mass spectra at γp total energies, $W = 2.0 - 2.8$ GeV, from CLAS. The χ^2 minimum appears around 1400 MeV/c^2.

Figure 2 shows the variation of χ^2 values with respect to the Λ^* pole position for all the $\Sigma^0\pi^0$ invariant mass data from CLAS. The χ^2 minimum $\chi^2_{\rm min}(M = M_{\rm pole})$ appears around $M_{\rm pole} = 1400$ MeV/c^2 in all cases. Statistical confidence of the Λ^* pole position $M_{\rm pole}$ can be obtained incrementing $\Delta\chi^2(M) \equiv \chi^2(M) - \chi^2_{\rm min}(M_{\rm pole})$: $\Delta\chi^2 = 2.36, 4.74, 9.23$, corresponding to confidence levels of 68.3%, 95% and 99.9%, respectively. Thus, the confidence of the Λ^* pole position, that is of our main concern, was obtained through the "inner" fitting parameters. It is again stressed that the "outer" parameters used in Ref.[4] (see also Table in Ref.[5]) cannot get any *quantitative* confidence about the Λ^* pole position, in spite of the seemingly beautiful reproduction of all the global neutral and charged spectra of CLAS.

In summary, the pole position for $\Lambda(1405)$ extracted from the CLAS photo-production is not shallow-$\bar{K}N$-binding ones, 1421 $\sim$ 1434 MeV/c^2 [5], but is consistent with the deep-$\bar{K}N$-binding PDG value $1405.1^{+1.3}_{-1.0}$ MeV/c^2.

*1 Department of Physics, Isfahan University of Technology
*2 RIKEN, Nishina Center
*3 Department of Physics, University of Tokyo

References
1) Y. Akaishi, T. Yamazaki, Phys. Rev. C **65** (2002) 044005.
2) K. Moriya *et al.*, Phys. Rev. C **87** (2013) 035206.
3) L. Roca, E. Oset, Phys. Rev. C **87** (2013) 055201.
4) M. Mai, U.-G. Meissner, Eur. Phys. J. A **51** (2015) 30.
5) U.-G. Meissner, T. Hyodo, Chin. Phys. C **38** (2014) 090001 and 2015 update.

5. Hadron Physics (Theory)

Transport coefficients of quark-gluon plasma in strong magnetic field

H. -U. Yee[*1,*2]

The quark-gluon plasma (QGP) created in relativistic heavy-ion collisions is subject to a strong magnetic field produced by heavily charged projectiles, whose scale is comparable to the temperature of the plasma. The question whether the magnetic field stays long enough to be able to induce interesting effects, such as chiral magnetic effect, on the plasma observables can be answered by realistic simulations of magneto hydrodynamics (MHD) that are planned, for example, in the Beam Energy Scan Theory collaboration (BEST). One of the key parameters in MHD simulations is electric conductivity, that should be rotationally asymmetric due to the magnetic field. Other key transport coefficients of the magnetized QGP that affect high energy probes such as jets and heavy quarks include jet quenching parameter $\hat{q}$ and heavy quark momentum diffusion constant κ. We report our attempts on computing them in complete leading order of perturbative QCD[1–3], and for some cases, also in strong coupling by AdS/CFT correspondence[2].

We work in the perturbative regime of $\alpha_s eB \ll T^2 \ll eB$, where the first inequality turns out to be essential to have a consistent Hard Thermal Loop (HTL) power counting scheme, and the second inequality brings us a simplification of working in the lowest Landau level (LLL) approximation for the quarks[1]. The LLL quarks are effectively 1+1 dimensional and carry only longitudinal currents flowing along the magnetic field direction. Their thermal density is $\sim (eB) \times T$, a product of transverse and longitudinal density of states, that dominates over the thermal density of hard gluons $\sim T^3$. This implies that the dominant HTL self-energy for gluons comes from the 1-loop LLL hard quark contribution that is of order $\Sigma \sim \alpha_s eB$, which sets a scale of dynamical screening $m_D^2 \sim \alpha_s eB$. Since $m_D^2 \ll T^2$ due to our assumption, hard particles of typical momentum T keep their free dispersion relation at leading order, while the soft gluons that are exchanged in infrared-sensitive scattering processes should include re-summation of HTL self-energy Σ: this gives us a consistent HTL power counting scheme we use for our leading order computations[1].

Electric conductivity in a magnetized plasma is asymmetric, with longitudinal conductivity being dominant over transverse one due to 1+1 dimensional nature of LLL states. Since the transverse dynamics is intrinsically quantum, we can use a semi-classical picture of kinetic theory of LLL quarks valid in leading order computation for only longitudinal conductivity[3]. In a massless quark limit, neglecting higher order effects from QCD sphalerons, the chiral anomaly dictates that a parallel electric and magnetic field imply a diverging longitudinal electric current, and hence an infinite longitudinal conductivity. The key dynamics taming this is the axial charge relaxation with the rate $\gamma_A \sim \alpha_s m_q^2/T$, and the longitudinal conductivity is parametrically given as $\sigma_L \sim e^2(eB)^2/(\chi\gamma_A)$ where χ is the charge susceptibility which grows linearly in B in LLL approximation $\chi \sim (eB)$, giving us an estimate[3] $\sigma_L \sim e^2(eB)T/(\alpha_s m_q^2)$. Our detailed computation reveals that the leading process in the collision term in the effective kinetic theory is 1-to-2 gluon decay into quark-antiquark pair and vice versa: $g \leftrightarrow q+\bar{q}$, which results in $\sigma_L \sim e^2(eB)T/(\alpha_s m_q^2 \log(T/m_q))$ in $m_q/T \ll 1$ limit.

For the heavy quark momentum diusion constant[1] and the jet quenching parameter[2], we compute them for both transverse and longitudinal directions with respect to magnetic field: $\kappa_{\perp,\parallel}$ and $\hat{q}_{\perp,\parallel}$. The leading order process is the t-channel 2-to-2 scatterings of heavy quark/energetic jet with hard LLL quarks via soft gluon exchange, that are enhanced by infrared divergence tamed by the HTL self-energy Σ. This is true for $\kappa_\perp$ and $\hat{q}_{\perp,\parallel}$, giving us the results of $\kappa_\perp \sim \alpha_s^2(eB)T\log(1/\alpha_s)$, $\hat{q}_\perp \sim \alpha_s^2(eB)^{\frac{3}{2}} + \alpha_s^2(eB)T\log(T^2/\alpha_s eB)$ and $\hat{q}_\parallel \sim \alpha_s^2(eB)T\log(1/\alpha_s)$, respectively. It should be noted that $\hat{q}_\perp$ does not vanish even at zero temperature: this is because a QCD gluon field from a jet can create a LLL quark-antiquark pair from the vacuum, which is consistent with 1+1 dimensional kinematics of LLL states[2]. The physics is similar to the Schwinger mechanism of pair creation.

However, the longitudinal momentum diffusion $\kappa_\parallel$ turns out to vanish at this order in massless quark limit due to 1+1 dimensional kinematics of LLL states[1]: only a light-like, longitudinal exchanged momentum is possible, $q^0 = \pm q^3$, and since κ is proportional to the static gluon spectral density at $q^0 = 0$, a longitudinal momentum transfer vanishes. The first non-vanishing contribution comes either from the t-channel scatterings with hard gluons or the effect of a finite quark mass m_q, the former being $\kappa_\parallel \sim \alpha_s^2 T^3 \log(1/\alpha_s)$ and the latter $\kappa_\parallel \sim \alpha_s(\alpha_s eB)^{\frac{1}{2}} m_q^2$, respectively[1].

References
1) K. Fukushima, K. Hattori, H. U. Yee and Y. Yin, Phys. Rev. D **93**, no. 7, 074028 (2016).
2) S. Li, K. A. Mamo and H. U. Yee, Phys. Rev. D **94**, no. 8, 085016 (2016).
3) K. Hattori, S. Li, D. Satow and H. U. Yee, Phys. Rev. D **95**, no. 7, 076008 (2017).

*1 Department of Physics, University of Illinois
*2 RIKEN Nishina Center

Renormalization in the quasi parton distribution functions†

T. Ishikawa*1,*2

In the study of high energy scattering processes, such as deep inelastic scattering (DIS) and the Drell-Yan process, one of the key concepts is "QCD collinear factorization," used to separate the perturbative and nonperturbative parts. The scattering cross sections are written as a convolution of the perturbative hard part and nonperturbative parton distribution functions (PDFs), which absorb all collinear divergences of the partonic scattering. PDFs are universal functions and thus are used to predict the cross sections of various hadronic scattering processes.

Direct calculation of the PDF by lattice QCD could give us information complementary to global QCD analyses. However, calculation of the light-cone distributions on the Euclidean lattice is difficult because of its time-dependence. Ji recently proposed the quasi-PDF approach to solve this problem.[1] The quasi-PDFs are defined with fields correlated completely along the spatial direction; for example,

$$\tilde{q}(\tilde{x},\mu,P_z) = \int \frac{d\delta z}{4\pi} e^{-i\delta z\tilde{x}P_z} \times\langle P_z|\overline{\psi}(\delta z)\gamma^3 \exp\left(-ig\int_0^{\delta z} dz' A_3(z')\right)\psi(0)|P_z\rangle \quad (1)$$

for the quasi-quark distribution, where the hadron state has a large momentum in z-direction P_z. Because of the time-independence, the quantity in Eq. (1) is calculable on the Euclidean lattice. The quasi-distributions are matched with usual light-cone distributions through the large momentum effective theory (LaMET).[2] After the quasi-distribution approach was introduced, several lattice QCD calculations of quasi-quark distributions have been carried out. These studies are still exploratory, and thus there are many uncertainties. Among the uncertainties, we address power divergences and the matching between the continuum and lattice in this article.

Unlike the original light-cone PDFs, quasi-distributions are known to have power divergences that originate from a Wilson line in the operator definition. The power divergences must be taken into account in the matching procedure. The renormalization of the non-local quark bilinears of the hadronic matrix element in the r.h.s. of Eq. (1), called $O(\delta z)$, is assumed to be[3]

$$O(\delta z) = Ze^{\delta m|\delta z|}O^{\rm ren}(\delta z), \quad (2)$$

where a superscript "ren" indicates that the operator is renormalized, Z contains logarithmic divergences, and δm denotes the mass renormalization of a test particle moving along the straight line connecting the two quark fields. Moreover, δm in the exponential factor takes care of all the power divergence, which is valid nonperturbatively. However, the multiplicative renormalizability of the logarithmic divergence is proven only up to the two-loop level.[4] While the all-order proof of the multiplicative renormalizability is important to give a solid validation to the renormalization in the quasi-distribution approach,[5] we assume the form in Eq. (2) for now. Knowing the renormalization in Eq. (2), the power divergence subtraction can be performed by defining a modified non-local operator for Eq. (1):[6]

$$O^{\rm subt}(\delta z) = e^{-\delta m|\delta z|}O(\delta z), \quad (3)$$

where the superscript "subt" indicates that this is a power divergence subtracted operator. The mass renormalization δm now needs to be fixed by imposing a renormalization condition. For this fixing, we can use static potential $V(R)$ and set $V(R_0) = V_0$ as the condition, leading to $2\delta m = V_0 - V(R_0)$.

By removing the power divergence, we can perform continuum-lattice matching. We demonstrate the one-loop matching using the lattice perturbation theory with a naive fermion and plaquette gluon. The one-loop matching factor is expressed as

$$Z_{\rm cont-latt}(\delta z) = 1 + \frac{g^2}{(4\pi)^2}C_F c(\delta z). \quad (4)$$

In the continuum, we introduce a UV cutoff scale and set to the lattice cutoff $\mu = a^{-1}$. As an example, we show the tadpole diagram contribution in Fig. 1 with and without Wilson line smearing. The smearing helps to reduce the difference between the continuum and lattice caused by the power divergence before the subtraction. Further study on the matching using the nonperturbative method is underway.

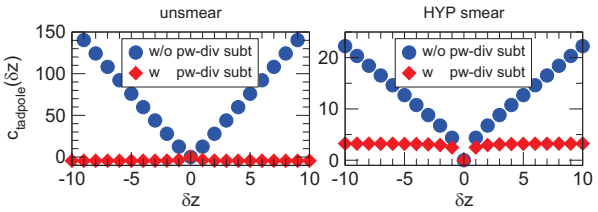

Fig. 1. Tadpole diagram contribution of the matching factor to the one-loop coefficient.

References
1) X. Ji, Phys. Rev. Lett. **110**, 262002 (2013).
2) X. Ji, Sci. China Phys. Mech. Astron. **57**, 1407 (2014).
3) H. Dorn, Fortsch. Phys. **34**, 11 (1986).
4) X. Ji et al., Phys. Rev. D **92**, 034006 (2015).
5) T. Ishikawa et al., in preparation.
6) T. Ishikawa et al., arXiv:1609.02018 [hep-lat].

† Condensed from the article in arXiv:1609.02018 [hep-lat]

*1 RIKEN Nishina Center
*2 T. D. Lee Institute, Shanghai Jiao Tong University

Coulomb sum rule in a covariant effective quark theory†

I. C. Cloët,[*1] W. Bentz,[*2,*3] and A.W. Thomas[*4]

Important information on QCD effects in nuclei came from quasielastic electron scattering on nuclear targets, where a significant quenching of the Coulomb sum rule (CSR)

$$S_L(|\mathbf{q}|) = \int_{\omega^+}^{|\mathbf{q}|} \mathrm{d}\omega \frac{R_L(\omega, |\mathbf{q}|)}{Z\, G_{Ep}^2(Q^2) + N\, G_{En}^2(Q^2)} ,$$

compared to the non-relativistic expectation ($S_L(|\mathbf{q}|) = 1$ for $|\mathbf{q}|$ much greater than the Fermi momentum), was observed[1]; on the proviso that the nucleon form factors are not modified by the nuclear medium. (In the above expression, $R_L(\omega, |\mathbf{q}|)$ is the longitudinal response function, G_{Ep} and G_{En} are the free nucleon Sachs form factors, $Q^2 = \omega^2 + \mathbf{q}^2$ is the 4-momentum transfer, and ω^+ excludes the elastic peak.)

In this work we extend our description of the free nucleon form factors[2], which were obtained by using the Nambu-Jona-Lasinio (NJL) model as an effective quark theory of QCD, to the in-medium case, including the self consistent scalar and vector potentials in the nucleon propagators. As a result, we find that at nuclear matter saturation density the proton Dirac and charge radii each increase by about 8%. Using these in-medium nucleon form factors and propagators obtained in the effective quark theory, we calculate the quasi-elastic longitudinal response function in nuclear matter by solving the Dyson equation for the polarization propagator in the relativistic random phase approximation (RPA)[3] on the level of nucleons. For the nucleon-nucleon interaction we take into account the exchange of σ, ω and ρ mesons, described in the framework of the NJL model.

Our Hartree and RPA results for the longitudinal response function are shown in Fig. 1 for $|\mathbf{q}| = 0.5$ and 0.8 GeV. We find that the longitudinal response function determined with in-medium nucleon form factors is quenched relative to the result obtained using the free form factors. In our calculation, this quenching is directly associated with a softer proton Dirac form factor (F_{1p}) in the medium. We observe a qualitative agreement with the ^{208}Pb data of Ref. 1.

Results for the CSR, using the nucleon form factors evaluated at three baryon densities ($\rho_B = 0,\ 0.1,\ 0.16\,\mathrm{fm}^{-3}$) are presented in Fig.2. At $|\mathbf{q}| \simeq 1$ GeV we find relativistic corrections of about 20% (relative to the nonrelativistic value $S_L = 1$), and an additional 30% reduction by the nuclear medium for the case $\rho_B = 0.16\,\mathrm{fm}^{-3}$. We observe a qualitative agreement with the ^{208}Pb data, but not with the state-of-the-art Green function Monte Carlo (GFMC) result for ^{12}C from Ref. 4. The ^{12}C data from Ref. 5 shown in the figure still cannot distinguish between our and the GFMC results.

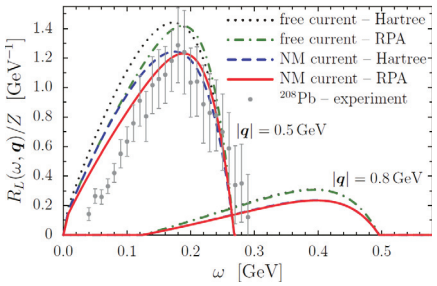

Fig. 1. Hartree and RPA results for the longitudinal response function in symmetric nuclear matter. Results labeled *free current* are obtained using the free nucleon form factors, whereas the *NM current* results use the in-medium form factors. The ^{208}Pb data at $|\mathbf{q}| = 0.5$ GeV are also shown for comparison.

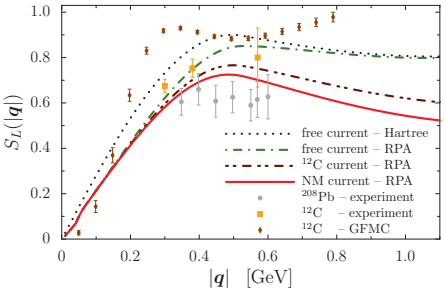

Fig. 2. CSR determined using the nucleon form factors at baryon density $\rho_B = 0$ (*free current*), $\rho_B = 0.1\,\mathrm{fm}^{-3}$ (typical of ^{12}C), and $\rho_B = 0.16\,\mathrm{fm}^{-3}$ (*NM current*). The ^{208}Pb and ^{12}C data as well as the Green Function Monte Carlo (GFMC) results from Ref. 4 are also shown for comparison.

This work was supported by the Japanese Ministry of Education, Culture, Sports, Science and Technology (Kakenhi Grant No. 25400270).

References

1) J. Morgenstern and Z. Meziani, Phys. Lett. **B 515**, 269 (2001).
2) I.C. Cloët, W. Bentz and A.W. Thomas, Phys. Rev. **C90**, 045202 (2014).
3) K. Wehrberger, Phys. Rept. **225**, 273 (1993).
4) A. Lovato et al., Phys. Rev. Lett. **111**, 092501 (2013).
5) P. Barreau et al., Nucl. Phys. **A 402**, 515 (1983).

† Condensed from an article by I. C. Cloët et al., Phys. Rev. Lett. **116**, 032701 (2016)

*1 Physics Division, Argonne National Laboratory
*2 Radiation Laboratory, RIKEN
*3 Department of Physics, Tokai University
*4 Department of Physics, University of Adelaide

Canonical approach to finite density QCD with multiple precision computation†

R. Fukuda,[*1,*2,*3] A. Nakamura,[*1,*4,*5] and S. Oka[*6]

Although QCD has a rich phase structure at a finite temperature and density,[1] investigations based on first–principles calculations are limited in small density regions. This is because the action with a finite real quark chemical potential μ_q is complex in general and the Monte Carlo method with the complex action does not work. This problem is called the sign problem.[2] In this work, the canonical approach[3] as a method for finite density QCD is studied. In the canonical approach, the grand canonical partition function $Z_{GC}(\mu_q)$ at a finite real quark chemical potential is represented as the fugacity expansion with the canonical partition function Z_n as follows:

$$Z_{GC}(\mu_q) = \sum_{n=-\infty}^{\infty} Z_n e^{n\mu_q/T}. \tag{1}$$

The canonical partition function is given by the Fourier transformation of the grand canonical partition function calculated at a purely imaginary chemical potential as follows:

$$Z_n = \frac{1}{2\pi}\int_0^{2\pi} d\left(\frac{\mu_I}{T}\right) Z_{GC}(i\mu_I)e^{-in\mu_I/T}, \tag{2}$$

where μ_I is a real number. This procedure to obtain the canonical partition functions does not suffer from the sign problem because the action with purely imaginary chemical potential is real and the Monte Carlo method works. This is a strong advantage of the canonical approach. However, we encounter some difficulties as follows. In the calculation to obtain the canonical partition function at a large baryon number, the Fourier transformation becomes a highly oscillating integral. Thus, it is difficult to numerically compute the integral because of cancellation of significant digits in the Fourier transformation. To avoid this problem, the multiple precision computation[4] is adopted in this work. Another problem is the numerical cost for the calculation of the grand canonical partition function at a purely imaginary chemical potential. To perform the Fourier transformation of the grand canonical partition function, we need the fermion determinants at many different values of the purely imaginary chemical potential. To reduce this numerical cost, the winding number expansion based on the hopping parameter expansion for the Wilson fermion formalism is developed in this work. In this method, we can expand the fermion determinant $\det D(\mu)$ with the complex coefficients $\{W_n\}$ as follows:

$$\log\det D(\mu) = \sum_{n=-\infty}^{\infty} W_n e^{n\mu/T}, \tag{3}$$

where μ is a complex number. Therefore, if we calculate the coefficients at some quark chemical potential once, we can obtain the fermion determinant at any quark chemical potential.

Figure 1 shows the baryon chemical potential μ_B dependence of the pressure evaluated by the canonical approach and the direct method. We directly use the winding number expansion of Eq. 3 for the calculation of the pressure at a real baryon chemical potential in the direct method. The upper bounds in this figure correspond to the validity range of these methods. Therefore, we can conclude that the validity range of the canonical approach is wider than that of the direct method.

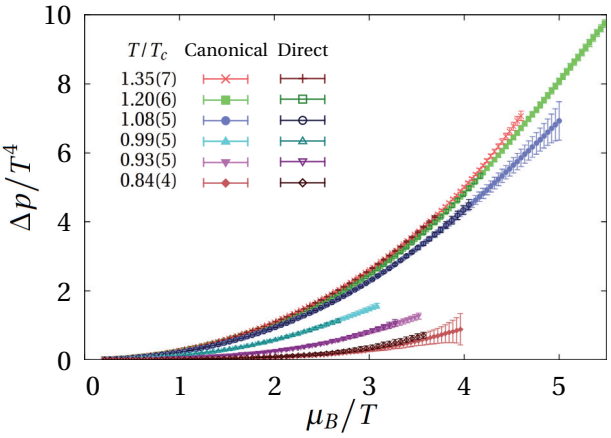

Fig. 1. The baryon chemical potential μ_B dependence of the pressure evaluated by the canonical approach and the direct method: Δp is defined as $\Delta p = p(\mu_B/T) - p(0)$.

References
1) K. Fukushima and T. Hatsuda, Rept. Prog. Phys. **74**, 014001 (2011).
2) Ph. de Forcrand, PoS (LAT2009)010 (2009).
3) A. Hasenfratz and D. Toussaint, Nucl. Phys. B **371** (1992), 539.
4) S. Oka for Z_n–Collaboration, PoS (LAT2015)166 (2015).

† Condensed from the article in Phys. Rev. D. **93**, 094508 (2016)

*1 RIKEN Nishina Center
*2 RIKEN BNL Research Center
*3 Department of Physics, the University of Tokyo
*4 Research Center for Nuclear Physics, Osaka University
*5 School of Biomedicine, Far Eastern Federal University
*6 Department of Physics, Rikkyo University

Chiral magnetic superconductivity†

D.E. Kharzeev*1*2*3

Materials with charged chiral quasiparticles in external parallel electric and magnetic fields can support an electric current that grows linearly in time, corresponding to diverging DC conductivity. From experimental viewpoint, this "Chiral Magnetic Superconductivity" (CMS) is thus analogous to conventional superconductivity. However the underlying physics is entirely different – the CMS does not require a condensate of Cooper pairs breaking the gauge degeneracy, and is thus not accompanied by Meissner effect. Instead, it owes its existence to the (temperature-independent) quantum chiral anomaly and the conservation of chirality. As a result, this phenomenon can be expected to survive to much higher temperatures. Even though the chirality of quasiparticles is not strictly conserved in real materials, the chiral magnetic superconductivity should still exhibit itself in AC measurements at frequencies larger than the chirality-flipping rate, and in microstructures of Dirac and Weyl semimetals with thickness below the mean chirality-flipping length that is about $1-100$ μm. In nuclear physics, the CMS should contribute to the charge-dependent elliptic flow in heavy ion collisions.

Let us start with a brief recap of "conventional" superconductivity. Instead of microscopic BCS theory introducing the condensate of Cooper pairs, we will base our discussion on the approach proposed in 1935 by Fritz and Heinz London. The London equations describe electromagnetic response of a superconductor and can be derived from the following bold assumption about the proportionality between the electric current $\mathbf{J}$ and the vector gauge potential $\mathbf{A}$:

$$\mathbf{J} = -\mu^2 \mathbf{A}, \tag{1}$$

where a phenomenological constant μ is related to the density of superconducting carriers n_s, electron mass m and electric charge e by $\mu = (e^2\ n_s/m)^{1/2}$.

In Coulomb gauge, the electric field is $\mathbf{E} = -\dot{\mathbf{A}}$ and the magnetic field is $\mathbf{B} = \nabla \times \mathbf{A}$; therefore, the assumption (1) yields the following two equations of superconductor electrodynamics:

$$\dot{\mathbf{J}} = \mu^2\ \mathbf{E}, \tag{2}$$

and

$$\nabla \times \mathbf{J} = -\mu^2\ \mathbf{B}. \tag{3}$$

The first of these equations (2) tells us that a constant external electric field $\mathbf{E}$ generates inside a superconductor a transient state with an electric current that grows linearly in time. Once the electric field is turned off (or screened away), Eq. (2) tells us that the current $\mathbf{J}$ is not allowed to decay and should persist – this is superconductivity.

To make an analogy with superconductivity, let us consider a chiral material (i.e. a material that hosts massless charged chiral fermions, such as a Dirac or Weyl semimetal, or a quark-gluon plasma) in external parallel magnetic and electric fields. First, let us assume that the chirality of fermions is strictly conserved. The chiral anomaly of quantum electrodynamics then dictates that the electric and magnetic fields generate the chiral charge density ρ_5 with the rate given by

$$\frac{d\rho_5}{dt} = \frac{e^2}{4\pi^2\hbar^2 c}\mathbf{E}\cdot\mathbf{B}, \tag{4}$$

and the chiral charge density grows linearly in time:

$$\rho_5 = \frac{e^2}{4\pi^2\hbar^2 c}\mathbf{E}\cdot\mathbf{B}\ t. \tag{5}$$

Let us now relate the density of the chiral charge ρ_5 and the chiral chemical potential μ_5 by introducing $\chi \equiv \partial\rho_5/\partial\mu_5$, so that $\rho_5 = \chi\mu_5 + ...$ and $\mu_5 \simeq \chi^{-1}\rho_5$ for small μ_5; note that at late times when μ_5 grows larger than other scales in the system, this relation will eventually be violated.

For $\mathbf{E}||\mathbf{B}$ we now get

$$\mathbf{J} = \frac{e^2}{2\pi^2}\ \mu_5\ \mathbf{B} = \frac{e^4}{8\pi^4\hbar^2 c}\ \chi^{-1}\mathrm{B}^2\ \mathbf{E}\ t \equiv \mu_{\mathrm{CME}}^2\ \mathbf{E}\ t. \tag{6}$$

Taking the time derivative on both sides, we get

$$\dot{\mathbf{J}} = \mu_{\mathrm{CME}}^2\ \mathbf{E}, \tag{7}$$

which is completely analogous to the corresponding expression for superconductivity (2)! We thus see that the CME[1,2] in an ideal chiral material can be viewed as a new type of superconductivity – we will call it Chiral Magnetic Superconductivity (CMS). In particular, if the electric field is switched off, the CME current according to (7) persists. In real experiments, the current will eventually decay, but on a time scale set by the chirality-flipping transitions that is much longer than a typical transport time.

† Condensed from the article in arXiv:1612.05677

*1 RIKEN Nishina Center
*2 Department of Physics and Astronomy, Stony Brook University, Stony Brook
*3 Department of Physics, Brookhaven National Laboratory, Upton

References

1) K. Fukushima, D. E. Kharzeev and H. J. Warringa, Phys. Rev. D **78**, 074033 (2008) [arXiv:0808.3382 [hep-ph]].
2) D. E. Kharzeev, Prog. Part. Nucl. Phys. **75**, 133 (2014) [arXiv:1312.3348 [hep-ph]].

Volume dependence of baryon number cumulants and their ratios†

V. Skokov*1

Experiments with ultrarelativistic heavy-ion collisions at RHIC and LHC explore the phase structure of Quantum ChromoDynamics (QCD) at nonzero temperature and density, and so probe the phase transitions associated with deconfinement and the restoration of chiral symmetry. Two of the most promising observables are the fluctuations of the net baryon number and electric charge. The cumulants and related quantities of these fluctuations may provide experimental evidence for a chiral critical endpoint or chirally inhomogenous phases.

However, there are many other effects besides the critical dynamics which might be important in the interpretation of the data. Those include the conservation of baryon number, corrections for efficiency in the detectors, hadronic rescattering, non-equilibrium effects, and finally volume fluctuations. The latter are important due to a finite size of a domain passing through the critical region during the evolution of the fireball. Usually one tries to minimize the effects of fluctuations in the volume by considering the ratios of cumulants. As we describe in the main text, in such ratios the explicit dependence on the volume cancels out, making the analysis of volume fluctuations trivial. However, we show that the implicit dependence on the volume might be very strong if the characteristic system size is below 5 fm.

In this study we use the quark-meson model as a realization of the chiral symmetry in QCD at low energies. The quark-meson (QM) model consists of a $O(4)$ multiplet of mesons, $\phi = (\sigma, \vec{\pi})$, coupled to quark fields through a Yukawa-type coupling.

In order to formulate a non-perturbative thermodynamics in the QM model we adopt a method based on the functional renormalization group (FRG). The FRG is based on an infrared regularization with the momentum scale parameter, where the full propagator is derived from a corresponding effective action.

We consider systems in which there is a true critical point in infinite volume. In finite volume, instead there is an *apparent* critical point (ACP). There is some degree of arbitrariness in how one defines an apparent critical point. We define the position of the apparent critical point from the maximum in the corresponding chiral susceptibility, which is equivalent to the minimum in the sigma mass. We stress, however, that unlike the case of infinite volume, that in finite volume other definitions will give different positions for the apparent critical point.

With our definition, we show that at some intermediate system size, the system has *two* apparent critical points, located at different values of T and μ. One of the apparent critical points, which we call ACP I, approaches the true critical point in the limit of infinite volume; we show that for the ACP I, it approaches the zero temperature axis as the volume decreases. The second apparent critical point, which we call ACP II, appears near the zero temperature axis, and evolves to *higher* temperature as the volume decreases. The location of the two apparent critical points is depicted in Fig. 1. The emergence of a second apparent critical point influences the cumulants of baryon number.

In Fig. 2, we show the dependence of the kurtosis χ_4/χ_2 on the temperature for different system sizes and different anisotropy parameters. The calculations are done for zero μ.

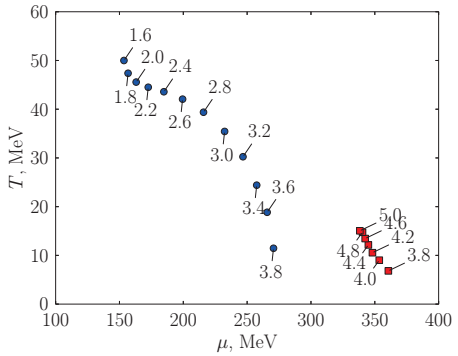

Fig. 1. The location of the apparent critical points (ACP) as a function of the system size, L. The squares (circles) denote ACP I (II), see text.

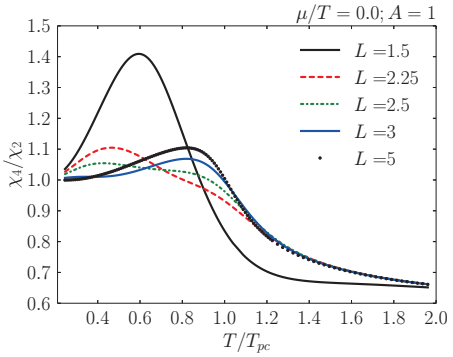

Fig. 2. The ratio of the fourth to the second order susceptibilities as a function of temperature for different systems sizes; the results are computed at zero chemical potential.

† Condensed from the article, 1612.04416

*1 RIKEN Nishina Center

ΛN and ΣN interactions from $2+1$ lattice QCD with almost physical masses †

H. Nemura*1

Description of the nuclear force from a fundamental perspective is a challenging problem in physics. Characterization of an atomic nucleus as a nucleonic many body system provides successful results although a nucleon is not a true rudimentary constituent of atomic nucleus but a composition of quarks and gluons defined in quantum chromodynamics (QCD). Especially, precise determination of the nucleon-nucleon (NN), hyperon-nucleon (YN), and hyperon-hyperon (YY) interactions has a large impact on the studies of both hypernuclei and hyperonic matter inside neutron stars since phenomenological descriptions of YN and YY interactions are not well constrained from experimental data because of the short life time of hyperons.

In the recent few years, 2+1 flavor lattice QCD calculations have been widely performed. This is an opportune moment to investigate beyond the baryon-baryon (BB) potentials at the flavor $SU(3)$ point since exploring breakdown of the flavor symmetry is not only an intriguing subject but also a major concern of the phenomenological YN and YY interaction models. Therefore, it is beneficial to take account of a large number of BB channels. We have proposed an approach for the efficient calculation of a large number of four-point correlation functions for various BB channels, and implemented a hybrid parallel C++ program at the very beginning (the first quarter of 2013) for calculating such a large number (e.g., 52 channels) for the BB interactions from NN to $\Xi\Xi$.[1)]

Based on those works, an extremely large scale lattice QCD calculation is now being performed to unveil the nature of nuclear forces with strangeness $S=0$ (NN) to -4 ($\Xi\Xi$) and almost physical quark masses corresponding to $(m_\pi, m_K) \approx (146, 525)$ MeV and large volume $(La)^4 = (96a)^4 \approx (8.1\ \mathrm{fm})^4$ with lattice spacing $a \approx 0.085$ fm.

Figure 1 shows preliminary result of $\Lambda N \to \Sigma N$ tensor potential in the ${}^3S_1 - {}^3D_1$ channel (top), ΣN central potential in the $I=1/2$, ${}^1S_0$ channel (middle), and ΣN central potential in the $I=3/2$, ${}^3S_1 - {}^3D_1$ channel (bottom). In the figure, the potentials are obtained at imaginary time $(t - t_0 = 5 - 12)$ in the lattice QCD, which might be slightly smaller than the region where the excited state contamination above pion production is suppressed because the statistics is not large enough at this moment. See Ref. 2 for detail. Calculation is underway to improve both the signal/noise ratio and the systematic uncertainty. Nevertheless, the present results show remarkable behaviors. For example, the top figure shows a sizable strength of $\Lambda N \to \Sigma N$ tensor interaction, which is expected to play an important role to have a light hypernucleus bounded. The lower two figures show that these two ΣN interaction channels are repulsive, which is consistent with the quark model's prediction. Hence, lattice QCD would be a promising approach to clarify the origin of repulsive nature of the ΣN interaction.

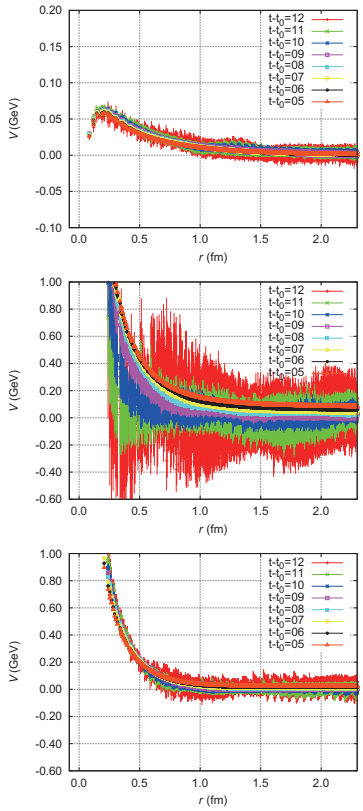

Fig. 1. Top: $\Lambda N - \Sigma N$ tensor potential in the ${}^3S_1 - {}^3D_1$ channel obtained with nearly physical point lattice QCD calculation on a volume $(96a)^4 \approx (8.1\ \mathrm{fm})^4$ with lattice spacing $a \approx 0.085$ fm and $(m_\pi, m_K) \approx (146, 525)$ MeV. Middle: ΣN central potential in the $I=1/2$, ${}^1S_0$ channel. Bottom: ΣN central potential in the $I=3/2$, ${}^3S_1 - {}^3D_1$ channel.

References
1) H. Nemura, Comput. Phys. Commun. **207**, 91 (2016) [arXiv:1510.00903 [hep-lat]].
2) H. Nemura *et al.*, arXiv:1702.00734 [hep-lat].

† Condensed from Ref. 1

*1 Center for Computational Sciences, University of Tsukuba

Nucleon form factors with large momenta from lattice QCD

S. Syritsyn*1,*2,*3 and B. Musch*3,*4

Vector form factors are among the most important features of a nucleon describing its distributions of charge and magnetization densities,

$$\langle P+q|\bar{q}\gamma^\mu q|P\rangle = \bar{u}_{P+q}\big[F_1(Q^2)\gamma^\mu + F_2(Q^2)\frac{i\sigma^{\mu\nu}}{2M_N}\big]u_P\,,$$

where $F_{1,2}$ are Dirac and Pauli form factors, respectively, and $Q^2 = -q^2 > 0$ is the momentum transfer squared in elastic nucleon-photon scattering. Although the proton and neutron form factors have been studied extensively, many puzzles remain. The behavior of form factors at high momenta is expected to transition to perturbative QCD scaling,[1,2] which has not been observed yet. The ratio the proton electric and magnetic form factors may cross zero around $Q^2 = 7\ldots 8\,\mathrm{GeV}^2$, placing constraints on nucleon models in the Dyson-Schwinger framework. There is a large qualitative difference of contributions between u- and d-quarks to both the F_1 and F_2 form factors[3]; understanding this phenomenon may also shed light on the internal organization of the nucleons. An upcoming experimental program at JLab will measure the nucleon form factors up to $Q^2 \approx 18\,\mathrm{GeV}^2$.

The study of high-momentum nucleon states on a lattice is complicated by statistical noise from cancellations and reduced energy gaps between the ground and excited states. A novel technique to study boosted nucleon states on a lattice has been recently introduced,[4] in which the quark fields used to construct the nucleon field are spatially "smoothed" with the momentum-translated covariant smearing operator,

$$\mathcal{S} = e^{\frac{1}{4}w^2\Delta} \to e^{+i\vec{k}_0\vec{x}}e^{\frac{1}{4}w^2\Delta}e^{-i\vec{k}_0\vec{x}}, \qquad (1)$$

where Δ is the gauge-covariant lattice Laplacian. Such an operator leads to a substantial improvement of the signal-to-noise ratio for boosted nucleon correlators.[4] We select $\vec{k}_0 = \frac{1}{3}\vec{P}$ assuming that quarks carry equal fractions of the nucleon momentum, although a larger value may be optimal.[4]

We have performed initial calculations on a $32^3\times 64$ lattice with $N_f = 2+1$ dynamical flavors of Wilson-clover quarks, lattice spacing $a = 0.091(2)\,\mathrm{fm}$ and pion mass $m_\pi = 278(3)\,\mathrm{MeV}$. With approximately 15,000 Monte Carlo samples, we can calculate nucleon-current correlators with source-sink separation up to $t_{\mathrm{sep}} = 10a = 0.9\,\mathrm{fm}$. Such a t_{sep} may be insufficient to suppress excited states, and we perform 2-state fits to extract matrix elements between the nucleon ground states. In the figure we show the ratio of the proton Pauli and Dirac form factors Q^2F_2/F_1 with the additional factor Q^2 compensating for the diffference in asymptotic scaling.[2] Quantum corrections modify the scaling by a factor $\log(Q^2/\Lambda^2)$,[1] which agrees with a recent analysis of JLab data.[3] Our lattice results agree qualitatively with this behavior. Different curves correspond to different $t_{\mathrm{sep}} = \{8,9,10\}a$ and different methods to extract the ground state. Remarkably, although the form factors $F_{1,2}$ are likely affected by excited states, their ratio does not change when excited states are suppressed by increasing t_{sep}. This is expected because perturbative QCD should not be able to discriminate between the ground and excited states of the nucleon, which are essentially nonperturbative, and the form-factor ratio may be universal for the ground and excited states.

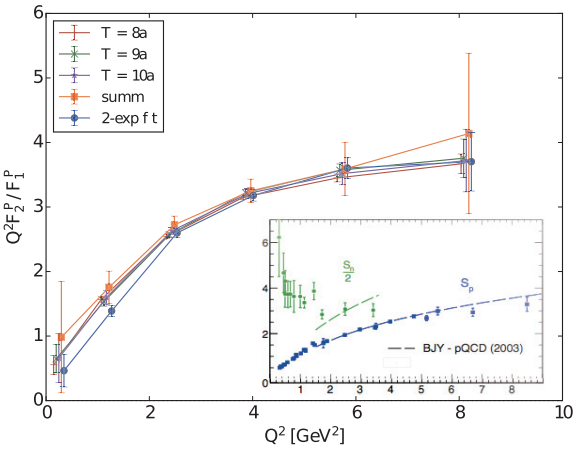

Fig. 1. Scaling of nucleon form factors with momentum transfer Q^2, lattice and phenomenology.[1]

Currently, this calculation is extended to include quark-disconnected contributions, variational analysis of excited states, improvement of the lattice quark vector current, selection of the optimal value for $\vec{k}_0$,[4] and study of the continuum limit. The calculation of high-momentum form factors from first principles will enable the comparison of the fundamental theory (QCD) and on-going experiments. In addition, it will validate the methodology for studying high-momentum nucleon states on a lattice. This method will be important for lattice calculations of TMDs and PDFs also requiring high-momentum nucleon initial and final states.

*1 RIKEN Nishina Center
*2 Department of Physics and Astronomy, Stony Brook University
*3 Institüt für Theoretische Physik, University of Regensburg
*4 Theory Group, Jefferson Lab

References
1) A. V. Belitsky et al, Phys. Rev. Lett. **91**, 092003 (2003).
2) S. Brodsky and G. Farrar, Phys. Rev. **D11**, 1309 (1975).
3) G. D. Cates et al, Phys. Rev. Lett. **106**, 252003 (2011).
4) G. S. Bali et al, Phys. Rev. **D93**, 094515 (2016).

Octet Baryon Magnetic Moments from an $SU(3)$ Flavor-Symmetric Lattice QCD Calculation†

B. Tiburzi*1 on behalf of the NPLQCD Collaboration

The external-field technique and its more recent generalizations are powerful tools with which to compute structural properties of hadrons using lattice QCD (LQCD). Such external magnetic field computations have been performed recently by NPLQCD, in particular: the first computation of the magnetic moments of light nuclei[1], the computation of the magnetic transition moment that dominates the $np \to d\gamma$ radiative-capture process[2], the determination of magnetic polarizabilities of light nuclei[3], and the evidence suggesting the unitary limit of two-nucleon interactions might be achieved in strong magnetic fields[4]. In this summary, however, we do not focus on few-nucleon physics; instead, we concern ourselves with the single-baryon sector in order to review the computation of magnetic moments within the lowest-lying octet of baryons.

In the limit of $SU(3)$ flavor symmetry, in which $m_u = m_d = m_s$, the octet baryon magnetic moments are determined by just two parameters. These are the Coleman-Glashow moments, μ_D and μ_F, which appear in the Hamiltonian density

$$\mathcal{H} = -\frac{e}{2M_B}\vec{\sigma}\cdot\vec{B}\left[\mu_D\langle\overline{B}\{Q,B\}\rangle + \mu_F\langle\overline{B}[Q,B]\rangle\right], \quad (1)$$

where: $Q = \mathrm{diag}(\frac{2}{3}, -\frac{1}{3}, -\frac{1}{3})$ is the quark electric charge matrix; the octet baryon fields are described by a matrix B, which can be expanded in terms of $SU(3)_F$ generators, $B = \sum_{a=1}^{8} B^a \frac{\lambda^a}{2}$; and, angled brackets are used to denote flavor traces.

The Coleman-Glashow moments are directly calculated by NPLQCD using an $SU(3)_F$-symmetric ensemble of gauge configurations with the octet meson mass $m_\pi \sim 800\,\mathrm{MeV}$, and with the addition of background magnetic fields coupled to the valence quarks. Aside from tiny electrodynamic effects $\lesssim 1\%$, there are no quark-disconnected contributions to the baryon magnetic moments at an $SU(3)_F$-symmetric point due to the condition $\langle Q\rangle = 0$. The determination of μ_D and μ_F at this quark mass is very precise, see Fig. 1.

Away from the limit of $SU(3)_F$ symmetry, the Coleman-Glashow moments can be obtained with additional assumptions. From calculations performed using an $N_f = 2+1$ ensemble of gauge configurations, with a corresponding pion mass of $m_\pi \sim 450\,\mathrm{MeV}$, the octet baryon magnetic moments are also determined. The nucleon moments are utilized to determine μ_D and μ_F, because $SU(3)_F$ breaking only arises from the strange quark in the sea. This effect is proportional to $(m_s - m)/N_c$, where $m = \frac{1}{2}(m_u + m_d)$, and N_c is the number of colors. The effect is estimated to be 6% on this ensemble. The same argument is applied to estimate the Coleman-Glashow moments from the experimental values of the nucleon moments, where the strange sea-quark effect is at the level of 11%.[a] The results obtained are depicted in Fig. 1.

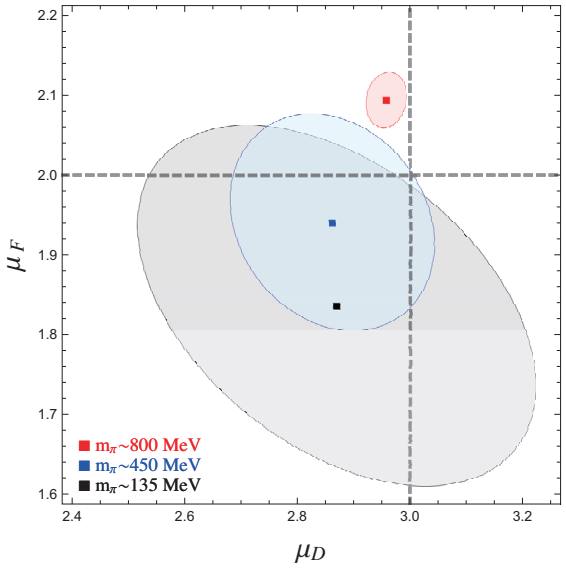

Fig. 1. Determined values of the Coleman-Glashow magnetic moments, μ_D and μ_F, as a function of the pion mass obtained from LQCD and experiment.

The integer values $\mu_D = 3$ and $\mu_F = 2$ arise from the $SU(6)$ symmetry of the nonrelativistic quark model. It is quite surprising how little quark-mass dependence exists in these moments, and how robust the nonrelativistic quark model appears to be as a function of the pion mass. Chiral-limit values of these moments are also estimated, but the large uncertainties from chiral extrapolation currently preclude definite conclusions.

References

1) S. R. Beane *et al.* [NPLQCD Collaboration], Phys. Rev. Lett. **113**, 252001 (2014), arXiv:1409.3556 [hep-lat].
2) S. R. Beane *et al.* [NPLQCD Collaboration], Phys. Rev. Lett. **115**, 132001 (2015), arXiv:1505.02422 [hep-lat].
3) E. Chang *et al.* [NPLQCD Collaboration], Phys. Rev. D **92**, 114502 (2015), arXiv:1506.05518 [hep-lat].
4) W. Detmold *et al.* [NPLQCD Collaboration], Phys. Rev. Lett. **116**, 112301 (2016), arXiv:1508.05884 [hep-lat].

† Condensed from the article arXiv:1609.03985

*1 Department of Physics, The City College of New York (CUNY); and RIKEN Nishina Center

a) Notice that $SU(3)_F$-breaking quark-disconnected contributions are proportional to $(m_s - m)/N_c^2$, and are hence subleading compared to those estimated above.

$\Lambda_b \to \Lambda\,\ell^+\ell^-$ form factors, differential branching fraction, and angular observables from lattice QCD with relativistic b quarks†

W. Detmold*1 and S. Meinel*2,*3

Decays of bottom hadrons involving the flavor-changing neutral-current transition $b \to s\,\ell^+\ell^-$ are highly suppressed in the Standard Model, so that small effects from new physics could cause significant changes in the observed decay rates and angular distributions. The recent precise experimental results from LHCb for the mesonic decays $B \to K\mu^+\mu^-$, $B \to K^*\mu^+\mu^-$, and $B_s \to \phi\mu^+\mu^-$ indeed show some deviations from the available Standard-Model predictions, but it remains unclear whether these deviations are caused by new fundamental physics or by problems with the calculations of the hadronic contributions[1].

The baryonic decay mode $\Lambda_b \to \Lambda(\to p\,\pi)\ell^+\ell^-$ can shed new light on these puzzles. Similarly to $B \to K^*(\to K\,\pi)\ell^+\ell^-$, this decay provides a wealth of angular observables that can be used to disentangle the contributions from individual operators in the $b \to s\,\ell^+\ell^-$ effective Hamiltonian[2]. At the same time, the theoretical description of $\Lambda_b \to \Lambda(\to p\,\pi)\ell^+\ell^-$ is cleaner than that of $B \to K^*(\to K\,\pi)\ell^+\ell^-$ because the Λ is stable under the strong interactions.

The $\Lambda_b \to \Lambda(\to p\,\pi)\ell^+\ell^-$ differential decay rate depends on the hadronic matrix elements

$$\langle\Lambda(p',s')|\,\bar{s}\,\gamma^\mu\,b\,|\Lambda_b(p,s)\rangle, \tag{1}$$
$$\langle\Lambda(p',s')|\,\bar{s}\,\gamma^\mu\gamma_5\,b\,|\Lambda_b(p,s)\rangle, \tag{2}$$
$$\langle\Lambda(p',s')|\,\bar{s}\,i\sigma^{\mu\nu}q_\nu\,b\,|\Lambda_b(p,s)\rangle, \tag{3}$$
$$\langle\Lambda(p',s')|\,\bar{s}\,i\sigma^{\mu\nu}q_\nu\gamma_5\,b\,|\Lambda_b(p,s)\rangle, \tag{4}$$

which can be decomposed into ten form factors. In this work, we performed a precise lattice QCD determination of these form factors, utilizing lattice gauge-field ensembles generated by the RBC and UKQCD Collaborations. Based on these form factors, we then calculated the $\Lambda_b \to \Lambda(\to p\,\pi)\ell^+\ell^-$ differential decay rate and the complete set of angular observables (for unpolarized Λ_b) in the Standard Model. Our results for the differential branching fraction $\mathrm{d}\mathcal{B}/\mathrm{d}q^2 = \tau_{\Lambda_b}\mathrm{d}\Gamma/\mathrm{d}q^2$ and for the lepton-side forward-backward asymmetry A_{FB}^ℓ are shown in Fig. 1. Also included in the plots are the measurements of these observables from the LHCb Collaboration[3].

In the high-q^2 region from 15 to 20 GeV^2, the magnitude of the lepton-side forward-backward asymmetry measured by LHCb is smaller than the theoretical value by 3.3σ. The measured differential branching fraction exceeds the theoretical value by 1.6σ. While the latter deviation is not yet statistically significant, it is in the opposite direction to what has been observed mesonic B decays[1]. More precise experimental results, including for the branching ratio of the normalization mode $\Lambda_b \to J/\psi\,\Lambda$, would be very useful in clarifying this aspect of the results.

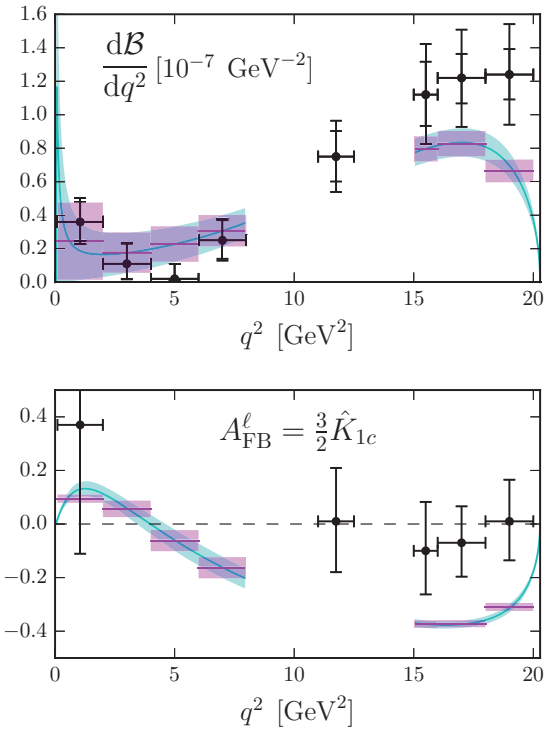

Fig. 1. The $\Lambda_b \to \Lambda(\to p\,\pi)\ell^+\ell^-$ differential branching fraction (top) and lepton-side forward-backward asymmetry (bottom). The cyan and magenta curves (without and with q^2-binning) show the Standard-Model predictions obtained from the form factors computed in lattice QCD; the black data points are the experimental results from LHCb[3]. The regions near $q^2 \sim m_{J/\psi}^2, m_{\psi'}^2$, where resonant long-distance effects are dominant, are excluded from the analysis.

References

1) T. Blake, G. Lanfranchi, D. M. Straub, Prog. Part. Nucl. Phys. **92**, 50 (2017).
2) P. Böer, T. Feldmann, D. van Dyk, JHEP **1501**, 155 (2015).
3) R. Aaij *et al.* [LHCb Collaboration], JHEP **1506**, 115 (2015).

† Condensed from the article in Phys. Rev. D **93**, 074501 (2016)

*1 Center for Theoretical Physics, Massachusetts Institute of Technology
*2 RIKEN Nishina Center
*3 Department of Physics, University of Arizona

$\Lambda_c \to \Lambda \ell^+ \nu_\ell$ form factors and decay rates from lattice QCD with physical quark masses†

S. Meinel*1,*2

The decays $\Lambda_c \to \Lambda \ell^+ \nu_\ell$, where $\ell = e, \mu$, are the most important baryonic $c \to s \ell^+ \nu_\ell$ transitions; their rates are proportional to the CKM matrix element $|V_{cs}|^2$ in the Standard Model. The motivations for studying $\Lambda_c \to \Lambda \ell^+ \nu_\ell$ include the following:

- Taking the precisely determined value of $|V_{cs}|$ from CKM unitarity, a comparison between calculated and measured $\Lambda_c \to \Lambda \ell^+ \nu_\ell$ decay rates provides a stringent test of the methods used to compute the heavy-baryon decay form factors.
- Combining the $\Lambda_c \to \Lambda \ell^+ \nu_\ell$ decay rates from experiment with a lattice QCD calculation of the $\Lambda_c \to \Lambda$ form factors gives a new direct determination of $|V_{cs}|$ and new constraints on physics beyond the Standard Model.

The BES III Collaboration has recently reported precise measurements of the $\Lambda_c \to \Lambda \ell^+ \nu_\ell$ branching fractions[1,2]:

$$\mathcal{B}(\Lambda_c \to \Lambda \ell^+ \nu_\ell) = \begin{cases} 0.0363(38)(20), & \ell = e, \\ 0.0349(46)(27), & \ell = \mu. \end{cases} \quad (1)$$

In the Standard Model, the decay rates depend on six form factors that parametrize the matrix elements $\langle \Lambda(p') | \, \bar{s} \gamma^\mu c \, | \Lambda_c(p) \rangle$ and $\langle \Lambda(p') | \, \bar{s} \gamma^\mu \gamma_5 c \, | \Lambda_c(p) \rangle$ as functions of $q^2 = (p - p')^2$. These form factors have previously been estimated using quark models and sum rules, giving branching fractions that vary substantially depending on the model assumptions. In this work, the first lattice QCD determination of the $\Lambda_c \to \Lambda$ form factors is reported. The calculation was performed with $2 + 1$ flavors of dynamical domain-wall fermions, using two different lattice spacings and a range of quark masses. Gauge-field ensembles generated by the RBC and UKQCD Collaborations were used, including one ensemble at the physical pion mass. The form factors were extrapolated to the continuum limit and are parametrized using model-independent z-expansions.

The resulting Standard-Model predictions for the $\Lambda_c \to \Lambda \ell^+ \nu_\ell$ differential decay rates, without the factor of $|V_{cs}|^2$, are shown in Fig. 1. The q^2-integrated rates are

$$\frac{\Gamma(\Lambda_c \to \Lambda \ell^+ \nu_\ell)}{|V_{cs}|^2} = \begin{cases} 0.2007(71)(74)\,\text{ps}^{-1}, & \ell = e, \\ 0.1945(69)(72)\,\text{ps}^{-1}, & \ell = \mu, \end{cases} \quad (2)$$

† Condensed from the article in arXiv:1611.09696 (accepted for publication in Phys. Rev. Lett.)

*1 RIKEN Nishina Center
*2 Department of Physics, University of Arizona

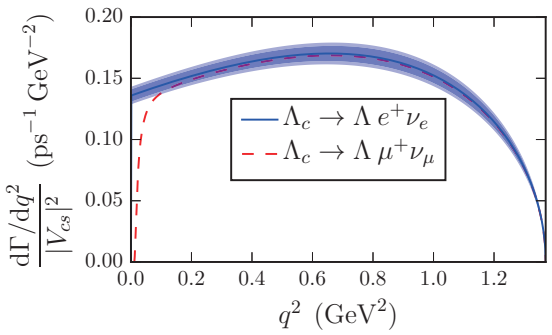

Fig. 1. Predictions for the $\Lambda_c \to \Lambda \ell^+ \nu_\ell$ differential decay rates (divided by $|V_{cs}|^2$) using the form factors from lattice QCD.

where the two uncertainties are from the statistical and total systematic uncertainties in the form factors. The branching fractions obtained from Eq. (2) using $|V_{cs}| = 0.97344(15)$ from a CKM unitarity global fit[3] and $\tau_{\Lambda_c} = 0.200(6)$ ps from experiments[4] are consistent with, and two times more precise than, the BES III measurements shown in Eq. (1). This is a valuable check of the lattice methods which were also used in Refs. 5-6.

Combining instead the BES III measurements (1) and $\tau_{\Lambda_c} = 0.200(6)$ ps with the results in Eq. (2) to determine $|V_{cs}|$ from $\Lambda_c \to \Lambda \ell^+ \nu_\ell$ gives

$$|V_{cs}| = \begin{cases} 0.951(24)_{\text{LQCD}}(14)_{\tau_{\Lambda_c}}(56)_{\mathcal{B}}, & \ell = e, \\ 0.947(24)_{\text{LQCD}}(14)_{\tau_{\Lambda_c}}(72)_{\mathcal{B}}, & \ell = \mu, \\ 0.949(24)_{\text{LQCD}}(14)_{\tau_{\Lambda_c}}(49)_{\mathcal{B}}, & \ell = e, \mu, \end{cases} \quad (3)$$

where the last line is the correlated average over $\ell = e, \mu$. This is the first determination of $|V_{cs}|$ from baryonic decays. The result is consistent with CKM unitarity, and the uncertainty can be reduced further with more precise measurements of the $\Lambda_c \to \Lambda \ell^+ \nu_\ell$ branching fractions.

References

1) M. Ablikim *et al.* [BESIII Collaboration], Phys. Rev. Lett. **115**, 221805 (2015).
2) M. Ablikim *et al.* [BESIII Collaboration], Phys. Lett. B, **767**, 42 (2017).
3) UTfit Collaboration, http://www.utfit.org/UTfit/ResultsWinter2016.
4) C. Patrignani *et al.* [Particle Data Group], Chin. Phys. C **40**, 100001 (2016).
5) W. Detmold, C. Lehner, S. Meinel, Phys. Rev. D **92**, 034503 (2015).
6) W. Detmold, S. Meinel, Phys. Rev. D **93**, 074501 (2016).

6. Particle Physics

Light scalar resonance from lattice simulation of SU(3) gauge theory with eight light fermions†

E. T. Neil*1,*2 for the LSD Collaboration

Studying the properties of strongly-coupled gauge theories with a large number of fermions has been an area of active research using lattice gauge theory techniques in recent years[1]. The screening of the gauge force by the presence of N_f light fermions is known to trigger a phase transition as N_f increases, with confinement and chiral symmetry breaking disappearing as the theory becomes scale invariant at long distances. Near the transition, such a theory can be confining (and therefore a useful candidate for the construction of composite Higgs models), but exhibit novel dynamical features associated with the onset of scale invariance.

Lattice gauge theory provides an ideal method to study these non-perturbative theories numerically. We consider an SU(3) gauge theory with $N_f = 8$ degenerate light fermions, charged under the fundamental representation. An earlier study of this same theory by the LatKMI collaboration[2] revealed evidence for a very light scalar resonance with $J^{PC} = 0^{++}$ quantum numbers. This is qualitatively different from QCD, where the lightest scalar resonance is heavy enough to decay into two pions.

Our lattice simulations are carried out with an nHYP-smeared staggered fermion action, and a plaquette gauge action which includes an adjoint plaquette term to reduce lattice artifacts associated with a lattice phase transition.[3] We use standard lattice spectroscopy techniques to calculate the resonance masses and decay constants. For the 0^{++} meson state, the fermion-line-disconnected contribution to the two-point correlation function is important, for which we employ the method of dilution with $U(1)$ stochastic sources. We simulate the theory at relatively light fermion masses, with the ratio $M_\rho/M_\pi \approx 2.1$ at our lightest point shown, requiring a $64^3 \times 128$ lattice volume in order to control finite-volume systematic effects.

One of the main results of our simulation is shown in figure 1, which gives the resonance masses as a function of the input fermion mass am. Over a wide range of input masses, the 0^{++} resonance is seen to be nearly degenerate with the pion, and both resonances are becoming light compared to the ρ and other heavier states seen in the spectrum. This confirms the LatKMI result[2] and demonstrates that the degeneracy between the 0^{++} and π states persists even to rather light fermion masses, approaching the chiral limit of the theory.

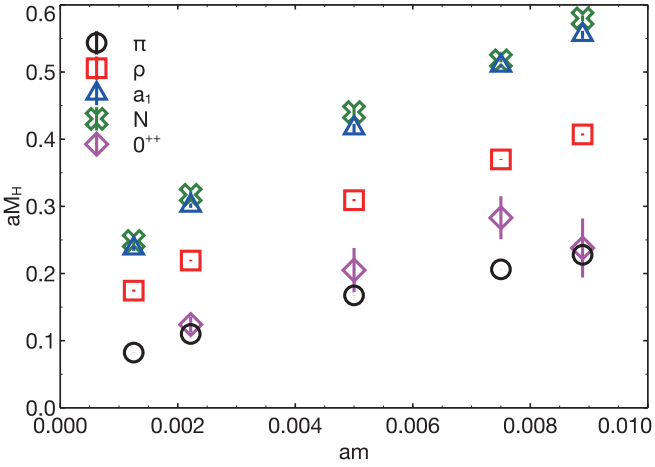

Fig. 1. Spectrum of the SU(3) $N_f = 8$ theory in lattice units, obtained from our simulations. The states shown are the lightest resonance in the pseudoscalar (π), scalar (0^{++}), vector (ρ), axial vector (a_1), and nucleon (N) channels. Error bars are shown for all results, but are often smaller than the size of the symbols used. The 0^{++} and π states are seen to be near-degenerate over a wide range of input fermion masses am and well-separated from the rest of the spectrum.

The separation of the 0^{++} and π states relative to the rest of the spectrum, which stands in stark contrast to the familiar case of QCD, raises the question of whether there is an effective field theory (EFT) containing both the 0^{++} and π degrees of freedom which can describe the low-energy dynamics of the $N_f = 8$ system. Identifying a novel EFT that contains a light scalar degree of freedom could provide a completely new approach to the construction of composite Higgs models, and might help to deepen our understanding of the confining-conformal transition in many-fermion gauge theories as well. As a next step in our study of this theory, lattice calculations of $\pi - \pi$ scattering are now underway, which will help to distinguish the possible EFT descriptions of this intriguing system.

† Condensed from the article in Phys. Rev. D **93** no. 11, 114514 (2016)
*1 RIKEN Nishina Center
*2 Department of Physics, University of Colorado, Boulder

References

1) T. DeGrand, Rev. Mod. Phys. **88** (2016), 015001.
2) Y. Aoki et al. (LatKMI Collaboration): Phys. Rev. **D89** (2014), 111502.
3) A. Cheng, A. Hasenfratz, and D. Schaich, Phys. Rev. **D85** (2012), 094509.

Using $\Lambda_b \to \Lambda\mu^+\mu^-$ data within a Bayesian analysis of $|\Delta B| = |\Delta S| = 1$ decays†

S. Meinel*1,*2 and D. van Dyk*3

The tensions between theory and experiment for P_5' [1,2], one of the angular observables in the kinematic distribution of the decay $\bar{B} \to \bar{K}^*(\to \bar{K}\pi)\mu^+\mu^-$, have sparked much interest in the determination of the short-distance couplings in flavor-changing neutral currents of the form $b \to s\ell^+\ell^-$. Several competing global analyses that use the available data on such rare decays of $\bar{B}$ mesons to various degrees find that a negative shift in one of the Wilson coefficients, $\mathcal{C}_9$, improves the agreement with the data[3]. However, it remains unclear whether this effect is caused by physics beyond the Standard Model, or merely by uncontrolled hadronic contributions.

The baryonic rare decay $\Lambda_b \to \Lambda(\to p\pi^-)\mu^+\mu^-$[4] offers complementary constraints compared to the commonly used mesonic channels. A recent lattice QCD calculation of the relevant $\Lambda_b \to \Lambda$ form factors[5] enables us to evaluate the $\Lambda_b \to \Lambda(\to p\pi^-)\mu^+\mu^-$ observables with high precision. In this work, we studied the constraining power of the b-baryon decay in a global analysis of $|\Delta B| = |\Delta S| = 1$ decays. Our analysis includes the following observables:

- For the baryonic decay $\Lambda_b \to \Lambda(\to p\pi^-)\mu^+\mu^-$ we used the LHCb measurements[4] of the differential branching fraction $\langle\mathcal{B}\rangle_{15,20}$, the fraction of longitudinally polarized dileptons $\langle F_L\rangle_{15,20}$, the lepton-side forward-backward asymmetry $\langle A_{\rm FB}^{\ell}\rangle_{15,20}$, and the hadron-side forward-backward asymmetry $\langle A_{\rm FB}^{\Lambda}\rangle_{15,20}$, all in the bin $15\,\text{GeV}^2 \le q^2 \le 20\,\text{GeV}^2 \simeq q^2_{\rm max}$.
- For the decay $\bar{B}_s \to \mu^+\mu^-$, we included the time-integrated branching ratio from a combined analysis of the CMS and LHCb collaborations[6].
- We use the Belle[7] and Babar[8] measurements of the branching ratio of the inclusive mode $\bar{B} \to X_s\ell^+\ell^-$ in the bin $1\,\text{GeV}^2 \le q^2 \le 6\,\text{GeV}^2$.

We performed a Bayesian analysis of several scenarios, including the Standard Model (where only nuisance parameters are fitted) and scenarios in which subsets of the Wilson coefficients are allowed to float. The 2D-marginalized posterior for the $\mathcal{C}_9$-$\mathcal{C}_{10}$ scenario is shown in Fig. 1. The best-fit point has $\mathcal{C}_9 - \mathcal{C}_9^{\rm SM} = +1.6^{+0.7}_{-0.9}$,

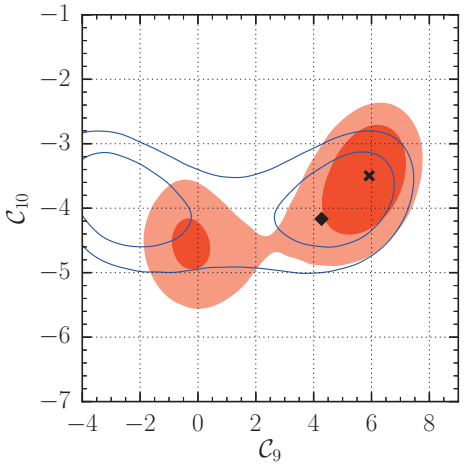

Fig. 1. The 2D-marginalized posterior in the $\mathcal{C}_9$-$\mathcal{C}_{10}$ plane. To demonstrate the impact of the baryonic decay in the analysis, we show the results from a fit to the $\bar{B} \to X_s\ell^+\ell^-$ and $\bar{B}_s \to \mu^+\mu^-$ branching ratios only (blue lines) and from the full fit including also the $\Lambda_b \to \Lambda(\to p\pi^-)\mu^+\mu^-$ observables (orange-red areas). The SM point is marked with a diamond, while the best-fit point from the full fit is marked with a cross.

which is opposite in sign compared to the global fits of mesonic-only decays[3]. Furthermore, the posterior odds favor the Standard Model over the scenarios in which Wilson coefficients are allowed to float. The uncertainties in our analysis of $\Lambda_b \to \Lambda(\to p\pi)\ell^+\ell^-$ are currently dominated by experiment, and will be reduced with higher-statistics results and a full angular analysis expected in the near future.

† Condensed from the article in Phys. Rev. D **94**, 013007 (2016)

*1 RIKEN Nishina Center
*2 Department of Physics, University of Arizona
*3 Physik-Institut, Universität Zürich

References

1) R. Aaij *et al.* [LHCb Collaboration], Phys. Rev. Lett. **111**, 191801 (2013).
2) R. Aaij *et al.* [LHCb Collaboration], JHEP **1602**, 104 (2016).
3) T. Blake, G. Lanfranchi, D. M. Straub, Prog. Part. Nucl. Phys. **92**, 50 (2017).
4) R. Aaij *et al.* [LHCb Collaboration], JHEP **1506**, 115 (2015).
5) W. Detmold, S. Meinel, Phys. Rev. D **93**, 074501 (2016).
6) V. Khachatryan *et al.* [CMS and LHCb Collaborations], Nature **522**, 68 (2015).
7) M. Iwasaki *et al.* [Belle Collaboration], Phys. Rev. D **72**, 092005 (2005).
8) J. P. Lees *et al.* [BaBar Collaboration], Phys. Rev. Lett. **112**, 211802 (2014).

Determination of $|V_{us}|$ from inclusive τ decay with lattice HVPs†

T. Izubuchi*1,*2 and H. Ohki*2

Precise deteminations of the CKM matrix element $|V_{us}|$ are important for flavor physics, which is relevant to the search for new physics beyond the standard model (SM) in particle physics. We propose a new method to determine $|V_{us}|$ from inclusive strange hadronic τ decay data and hadronic vacuum polarization functions (HVPs) computed on the lattice. The basic idea is to consider generalized dispersion relations for the experimentally observed us V+A inclusive distributions. In the SM, the differential distribution of τ decay, $dR_{V/A;us}/ds$, is related to the spectral function $\rho^{(J)}_{us;V/A}(s)$ by

$$\frac{dR_{us;V/A}}{ds} = \frac{12\pi^2|V_{us}|^2 S_{EW}}{m_\tau^2} \times \left[\omega_\tau(s)\rho^{0+1}_{us;V/A}(s) - \omega_L(y_\tau)\rho^{0}_{us;V/A}(s)\right], \quad (1)$$

where $y_\tau = s/m_\tau^2$, $\omega_\tau(y) = (1-y)^2(1+2y)$, $\omega_L(y) = 2y(1-y)^2$, and S_{EW} is a known short-distance electroweak correction. Using a weight function $\omega_N(s) = \frac{1}{\Pi_{k=1}^N(s+Q_k^2)}$ $(s = -Q_k^2 < 0)$, we obtain the following dispersion relation,

$$\int_0^\infty \rho_{us}(s)\omega_N(s)ds = \sum_k^N \mathrm{Res}\left(\Pi_{us}(-Q_k^2)\omega_N(-Q_k^2)\right) \quad (2)$$

Here, $\Pi_{us}(Q^2)$ is the HVP defined in space-like momentum $-Q^2$. The idea is to use the lattice QCD data for $\Pi_{us}(Q^2)$ on the RHS in Eq. (2) to compare with the LHS, which can be evaluated up to $s = m_\tau^2$ from the experimental $dR_{us;V+A}/ds$ distribution with an unknown $|V_{us}|^2$. The pQCD result is used to approximate the contribution from $s > m_\tau^2$. We use $\omega_N(s)$ with uniformly spaced poles, which is characterized by N, and the center value of Q^2, C in the interval, and the nearest-neighbor spacing is fixed to $\Delta = 0.2/(N-1)$ [GeV^2]. In Fig. 1, we plot some example values for spectrum contributions given in the LHS of Eq. (2). Increasing N or decreasing C can suppress the contributions from high-s modes that have larger errors, so that we can adjust the "inclusiveness", that is, the impact of the high multiplicity modes.

For the RHS in Eq. (2), we use the lattice HVPs measured near the physical quark masses on the $2+1$ flavor Mobius domain wall fermion ensembles by the RBC and UKQCD collaborations.[a] Here, $\Pi(Q^2)$ is obtained from the Fourier transformation of the lattice HVPs ($\Pi(t)$) in the coordinate space.

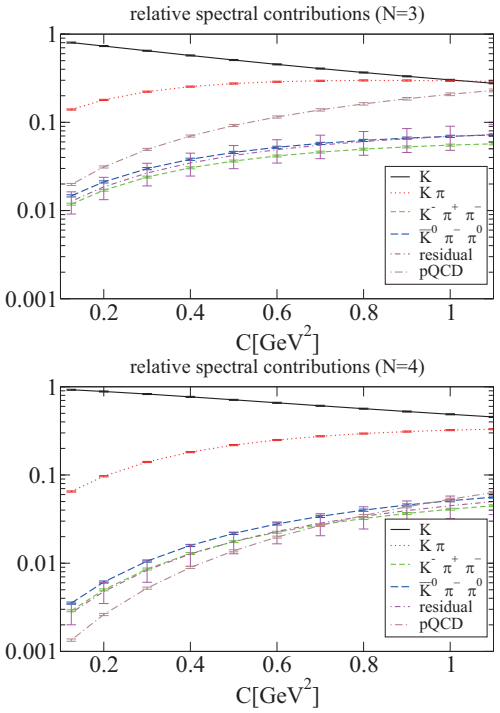

Fig. 1. Ratio of each spectrum integral.

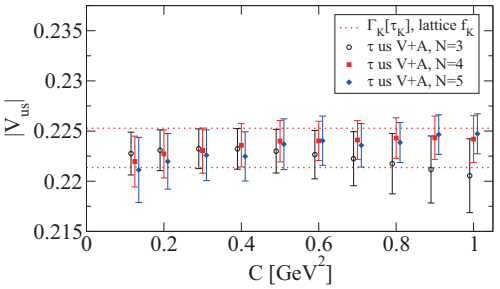

Fig. 2. Result of $|V_{us}|$ as a function of C for $N = 3, 4$, and 5. The result obtained from K is also shown.

Figure 2 shows our result for $|V_{us}|$. Our best value is $|V_{us}| = 0.2241(14)_{exp}(13)_{th}$, from the result with $C = 0.7$ [GeV^2] with $N = 4$. The theoretical error is comparable with the experimental one, and the total error is less than the previous inclusive τ decay determinations. [b] Moreover, the result is consistent with those obtained from analyses of kaon physics and 3-family CKM unitarities.

Reference

1) P. A. Boyle et al., Int. J. Mod. Phys. Conf. Ser. **35**, 1460441 (2014) doi:10.1142/S2010194514604414 [arXiv:1312.1716 [hep-ph]].

† Condensed from a paper by authors in preparation

*1 Physics Department, Brookhaven National Laboratory
*2 RIKEN Nishina Center

a) We thank RBC-UKQCD collaboration and Kim Maltman for providing lattice HVP and experimental data.

b) For a recent study of the inclusive τ decay by using the finite energy sum rule, see Ref. 1.

New insights on dark matter using lattice gauge theories

E. Rinaldi*1

Dark matter is thought to be the dominant form of matter in our universe today. Its energy density is about five times larger than common visible matter according to recent cosmological observations. However, dark matter is very elusive and it has not yet been detected despite large experimental efforts. Moreover, the particle dark matter candidate generally used as a template for all the experimental analysis, the so-called WIMP (weakly interacting massive particle) dark matter, is a product of supersymmetric theories and these theoris have not been discovered yet.

From the theoretical point of view, it is interesting to start exploring dark matter models where the candidates are more exotic than the usual WIMPs and that can naturally explain why all the experimental searches have turned out empty handed. This research program focuses on composite dark matter, a framework for dark matter models where the candidate new particle is a bound state of a new strong interaction. Composite dark matter has a non-trivial internal structure and its main properties are dictated by non-perturbative strong dynamics, which naturally include self interactions.

This type of picture is familiar to everyone working in Quantum Chromodynamics (QCD), the theory of quarks and gluons that explains how composite particles like protons and neutrons are created. Moreover, methods that are succesfull in exploring non-perturbative QCD properties can be applied to composite dark matter theories. This is the case for lattice gauge theory simulations. They provide a systematic way of solving the strong dynamics of the theory with improvable and controllable errors.

Applying lattice field theory methods to models of composite dark matter has been very fruitful. In particular, for the case of Stealth Dark Matter, they have helped determining the strength of the dominant interactions with the photon[1] and the Higgs boson[2]. Stealth Dark matter is a model with a SU(4) gauge group and dark fermions that have electric charges and are bound together into a heavy neutral four-fermion object that constitutes dark matter. Since this object has constituents with electric charge and mass, it will interact with Standard Model particles through the exchange of the corresponding gauge bosons, the photon and the Higgs. While the dominant interaction with the Higgs boson depends on unknown parameters of the model at high energy and can only be bound using existing experimental results, the electro-magnetic interaction between the dark matter and the nuclear matter in detectors like LUX or XENON1T can be directly calculated with lattice simulations.

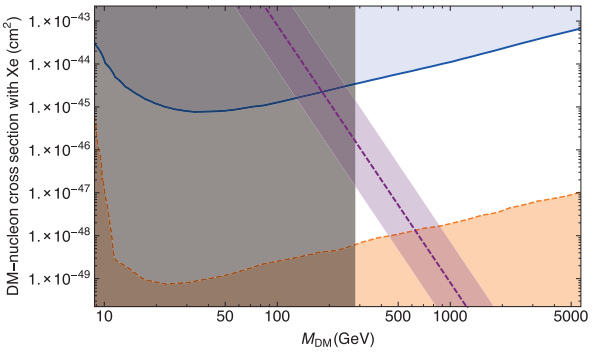

Fig. 1. The DM spin-independent scattering cross section per nucleon evaluated for xenon is shown as the purple band obtained from the SU(4) polarizability, where the width of the band corresponds to $1/3 < M_F^A < 3$ from low to high. The blue curve and the light blue region above it is excluded by the LUX constraints. The vertical, darker shaded region is excluded by the LEP II bound on charged mesons[1].

The operator

$$\mathcal{O}_F = C_F B^* B\, F^{\mu\alpha} F^{\nu}_{\alpha} v_\mu v_\nu \,, \qquad (1)$$

where C_F is the EM polarizability, corresponds to a cross section with a nucleon of

$$\sigma_{\rm nucleon}(Z,A) = \frac{Z^4}{A^2} \frac{144\pi\alpha^2\mu_{nB}^2 (M_F^A)^2}{M_{\rm DM}^6 R^2} [\alpha \tilde{m}_B^3 \tilde{C}_F]^2 \,, \qquad (2)$$

where Z and A are the usual atomic number and mass, while $M_{\rm DM}$ is the unknown dark matter mass. The cross section *per nucleus* scales as Z^4 and not A^2, and so the cross section *per nucleon* must be calculated for each nucleus separately in order to compare with experiments.

Comparing to LUX gives the cross section in Figure 1 as a function of the dark matter mass. Stealth Dark matter of mass 500 GeV is not excluded by experiments.

These results have been presented at the BNL Early Career Researcher Symposium in December 2016 and the presentation won an award for its originality[3].

*1 RIKEN Nishina Center

References
1) Lattice Strong Dynamics (LSD) Collaboration, Phys. Rev. Lett. **115**, 171803 (2015), Editors' Suggestion.
2) Lattice Strong Dynamics (LSD) Collaboration, Phys. Rev. D**92**, 075030 (2015), Editors' Suggestion.
3) Outstanding oral presentation award, Early Career Researcher Symposium 2016, Brookhaven National Laboratory.

Parity-doublet representation of Majorana fermions and neutron oscillation†

K. Fujikawa*1 and A. Tureanu*2

We present a parity-doublet theorem in the representation of the intrinsic parity of Majorana fermions, which is expected to be useful in condensed matter physics as well, and it is illustrated to provide a criterion of neutron-antineutron oscillation in a BCS-like effective theory with $\Delta B = 2$ terms. The CP violation influences the neutron electric dipole moment, but no direct CP violating effects appear in the oscillation itself, as demonstrated by an exact solution. An analogue of Bogoliubov transformation, which preserves P and CP, is crucial in the analysis.

The Majorana fermions are defined by the condition $\psi(x) = C\bar{\psi}^T(x) = \psi^c(x)$ where $C = i\gamma^2\gamma^0$ denotes the charge conjugation matrix. We start with a neutral Dirac fermion $n(x)$ and define the combinations $\psi_\pm(x) = \frac{1}{\sqrt{2}}[n(x) \pm n^c(x)]$, which satisfy $\psi^c_\pm(x) = \pm\psi_\pm(x)$, showing that $\psi_+(x)$ and $\psi_-(x)$ are Majorana fields. We treat the fermion with $\psi^c_-(x) = -\psi_-(x)$ also as a Majorana fermion. The common parity operation, which is called "γ^0-parity" here, is defined by $n(x) \to \gamma^0 n(t, -\vec{x})$ and $n^c(x) \to -\gamma^0 n^c(t, -\vec{x})$ and satisfies $\mathrm{P}^2 = 1$; it leads to a *doublet representation* $\{\psi_+(x), \psi_-(x)\}$, namely $\psi_\pm(x) \to \gamma^0\psi_\mp(t, -\vec{x})$. Only when the two fermions $\psi_\pm(x)$ are degenerate, this doublet representation is consistent with dynamics. The mass splitting in $\psi_\pm(x)$ inevitably breaks the γ^0-parity as a symmetry of the Lagrangian. The parity thus becomes crucial in the analysis of the neutron oscillation[1,2], which is based on the neutron expressed as a superposition of two Majorana-type fermions with different masses.

In the analysis of possible baryon number violation and neutron oscillation, one can study the quadratic effective Hermitian-Lagrangian

$$\begin{aligned}\mathcal{L} &= \overline{n}(x)i\gamma^\mu\partial_\mu n(x) - m\overline{n}(x)n(x) \\ &- \frac{i}{2}\epsilon_1[e^{i\alpha}n^T(x)Cn(x) - e^{-i\alpha}\overline{n}(x)C\overline{n}^T(x)] \\ &- \frac{i}{2}\epsilon_5[n^T(x)C\gamma_5 n(x) + \overline{n}(x)C\gamma_5\overline{n}^T(x)], \end{aligned} \tag{1}$$

where m, ϵ_1, ϵ_5 and α are real parameters. The first $\Delta B = 2$ term with a real ϵ_1 breaks the γ^0-parity while the second $\Delta B = 2$ term with a real ϵ_5 preserves γ^0-parity. The term with ϵ_5 in (1) preserves C and P, while $\alpha \neq 0$ implies CP violation. An analogy of the Lagrangian in (1) to BCS theory has been emphasized at the early stage of the study of neutron oscillation.[3]

The presence of the neutron oscillation $P(n \to \bar{n}) \propto \sin^2((\Delta M/2)t)$ implies the mass splitting of auxiliary Majorana-type fermions. In connection with this, we have established the γ^0-parity doublet representation $\{\psi_+(x;\epsilon_1), \psi_-(x;-\epsilon_1)\}$ of the solutions of (1),

$$\begin{aligned}&\psi_+(x;\epsilon_1) \to \gamma^0\psi_-(t, -\vec{x}; -\epsilon_1), \\ &\psi_-(x;-\epsilon_1) \to \gamma^0\psi_+(t, -\vec{x}; \epsilon_1), \end{aligned} \tag{2}$$

which satisfy $\mathrm{P}^2 = 1$. This representation is valid irrespective of whether the γ^0-parity is conserved or not. The γ^0-parity violation by $\epsilon_1 \neq 0$ in (1) is a *necessary condition* of neutron oscillation which requires $M_+ = M(\epsilon_1) \neq M(-\epsilon_1) = M_-$ (*parity-doublet theorem*) .

The solution of this Lagrangian with $\epsilon_1 = 0$ defines the Bogoliubov transformation

$$\begin{pmatrix} n(x) \\ n^c(x) \end{pmatrix} = \begin{pmatrix} \cos\phi N(x) - i\gamma_5 \sin\phi N^c(x) \\ \cos\phi N^c(x) - i\gamma_5 \sin\phi N(x) \end{pmatrix}, \tag{3}$$

with a Dirac fermion $N(x)$, the mass $M = \sqrt{m^2 + \epsilon_5^2}$, and $\sin 2\phi \equiv \epsilon_5/\sqrt{m^2 + \epsilon_5^2}$. To solve (1), we first use the Bogoliubov transformation (3) as a change of variables, which preserves C and P. We then obtain the exact mass formula

$$(M \pm \epsilon_1\sqrt{1 - (\tilde{\epsilon}_1/\epsilon_1)^2}) + i\tilde{\epsilon}_1\gamma_5 \equiv M_\pm e^{2i\theta_\pm\gamma_5}, \tag{4}$$

with $M_\pm = \left([M \pm \epsilon_1\sqrt{1 - (\tilde{\epsilon}_1/\epsilon_1)^2}]^2 + (\tilde{\epsilon}_1)^2\right)^{1/2}$ for two majorana fermions, where $\tilde{\epsilon}_1 \equiv \epsilon_1 \sin\alpha \sin 2\phi$.

The oscillation probability is given by ($\theta = \theta_+ - \theta_-$)

$$\begin{aligned}P(n(\vec{p}) \to n^c(\vec{p}); t) &= (1 - \sin^2 2\phi \cos^2\tilde{\alpha}) \cos^2\theta \\ &\times \sin^2(\frac{1}{2}\Delta E t), \end{aligned} \tag{5}$$

with $\sin\tilde{\alpha} = \sin\alpha\cos 2\phi/\sqrt{1 - (\sin\alpha \sin 2\phi)^2}$. Under CP transformation, which is equivalent to $\alpha \to -\alpha$, $\theta \to -\theta$, this oscillation formula with energy difference $\Delta E = \sqrt{\vec{p}^2 + M_+^2} - \sqrt{\vec{p}^2 + M_-^2}$ is invariant. We do not have a manifestation of CP violation in oscillation in vacuum, which is typically expressed by $P(n(\vec{p}) \to n^c(\vec{p}); t) \neq P(n^c(\vec{p}) \to n(\vec{p}); t)$.

References
1) R. N. Mohapatra, J. Phys. G: Nucl. Part. Phys. **36**, 104006 (2009).
2) D. G. Phillips II et al., arXiv:1410.1100.
3) L. N. Chang and N. P. Chang, Phys. Rev. Lett. **45**, 1540 (1980).

† Condensed from the article in K. Fujikawa and A. Tureanu, Phys. Rev. D **94** (2016) 115009

*1 RIKEN Nishina Center
*2 Department of Physics, University of Helsinki

Separability criteria with angular and Hilbert-space averages†

K. Fujikawa,*1 C.H. Oh,*2 K. Umetsu,*3 and Sixia Yu[2]

To characterize entanglement, the notions of separability and inseparability, which are the characteristic properties of state vectors in quantum mechanics, are commonly used. On the other hand, the notion of local realism based on local non-contextual hidden-variable models is also used to test properties such as locality and reduction.[1] Local hidden-variable models are generally different from quantum mechanics, and thus local realism tests the deviation from quantum mechanics also.

In the experimental study of local realism, which is commonly tested by the CHSH inequality,[2] it is customary to first confirm the consistency of the measured basic correlation such as the spin correlation $\langle \mathbf{a}\cdot\sigma\otimes\mathbf{b}\cdot\sigma\rangle$ with quantum mechanics and then test the CHSH inequality. If one confirms the consistency of $\langle \mathbf{a}\cdot\sigma\otimes\mathbf{b}\cdot\sigma\rangle$ for any unit vectors $\mathbf{a}$ and $\mathbf{b}$ with quantum mechanics, one can naturally apply the criterion of quantum mechanical separability to the correlation. In the present study, we discuss this aspect of the separability test in quantum mechanics. It is well known that the Peres criterion of the positivity of a partial transposed density matrix gives a necessary and sufficient condition for the separability of a general density matrix in $d = 2\times 2$[3] which we study in the present paper. However, it is also well-known from the days of Pauli that the reconstruction of the state vector or density matrix from measured data is generally very involved.[4] It is thus practically useful to derive simpler criteria that do not require precise state reconstruction. The purpose of the present paper is to derive such separability criteria. We assume the most general separable density matrix, but we use a limited set of two-point correlations and thus obtain only the necessary condition of separability in general. Nevertheless, we illustrate that our criteria are very useful when applied to the past experimental data of Aspect et al. in 1981[5] and Sakai et al. in 2006.[6]

To be specific, we study the general separable quantum mechanical states

$$\rho = \sum_k w_k \rho_k \tag{1}$$

in $d = 2\times 2 = 4$; all the states ρ_k are separable pure quantum states.[7] If the state is a separable pure state $\rho = |\psi\rangle\langle\psi|$, separability in (1) is quantified by the equality, which is necessary and sufficient,

$$G(\mathbf{a},\mathbf{b}) \equiv 4[\langle\psi|P(\mathbf{a})\otimes P(\mathbf{b})|\psi\rangle - \langle\psi|P(\mathbf{a})\otimes\mathbf{1}|\psi\rangle\langle\psi|\mathbf{1}\otimes P(\mathbf{b})|\psi\rangle] = 0 \tag{2}$$

for two arbitrary projection operators $P(\mathbf{a})$ and $P(\mathbf{b})$.

In the case of a general mixed ρ, we derive the useful criteria of separable mixed states, namely

$$\mathrm{Tr}\rho\{\mathbf{a}\cdot\sigma\otimes\mathbf{b}\cdot\sigma\} = (1/3)C\cos\varphi \tag{3}$$

for two spin 1/2 systems, and

$$4\mathrm{Tr}\rho\{P(\mathbf{a})\otimes P(\mathbf{b})\} = 1 + (1/2)C\cos 2\varphi \tag{4}$$

for two photon systems with linear polarization projectors $P(\mathbf{a})$ and $P(\mathbf{b})$, respectively. Here, $-1\le C\le 1$. The basic new ingredient in our derivation of criteria (3) and (4) is that we take a geometric *angular average* of unit vectors $\mathbf{a}$ and $\mathbf{b}$ with fixed $\cos\varphi = \mathbf{a}\cdot\mathbf{b}$. It is shown that this angular averaging, which was originally motivated by the specific experiment,[6] does not add a new burden on the measurements by analyzing the existing experimental data. The difference in the numerical coefficients 1/3 and 1/2 in (3) and (4) arises from the difference in rotational properties; the spinor rotational freedom is 3-dimensional, which agrees with the freedom of the $d = 2$ Hilbert space, while the rotational freedom of the photon is two-dimensional, which differs from the freedom of the $d = 2$ Hilbert space because it is confined in a plane perpendicular to the momentum direction. If one instead takes an average over the states in the $d = 2$ Hilbert space, the formula for the photon is replaced by

$$4\mathrm{Tr}\rho\{P(\mathbf{a})\otimes P(\mathbf{b})\} = 1 + (1/3)C\cos 2\varphi. \tag{5}$$

This difference between the geometrical angular average and the Hilbert space average is interesting, and it has an interesting implication on the separability issue of the entangled Werner state[7] which accommodates a specific local hidden-variable representation and thus satisfies the CHSH inequality. In the photon case, the Hilbert space average can judge the inseparability of the Werner state but the geometrical angular average cannot, while the geometric average can judge the Werner state in the case of spin 1/2 systems.

† Condensed from the article in K. Fujikawa, C.H. Oh, K. Umetsu, and Sixia Yu, Ann. of Physics 368, 248 (2016)

*1 RIKEN Nishina Center
*2 Department of Physics, National University of Singapore
*3 College of Science and Technology, Nihon University

References

1) J. S. Bell, Physics **1**, 195 (1964).
2) J. F. Clauser, M. A. Horne, A. Shimony, R. A. Holt, Phys. Rev. Lett. **23**, 880 (1969).
3) A. Peres, Phys. Rev. Lett. **77**, 1413 (1996). P. Horodecki, Phys. Lett. A**232**, 333 (1997).
4) D. F. V. James et al., Phys. Rev. A**64**, 052312 (2001).
5) A. Aspect, P. Grangier, G. Roger, Phys. Rev. Lett. **47**, 460 (1981).
6) H. Sakai et al., Phys. Rev. Lett. **97**, 150405 (2006).
7) R. F. Werner, Phys. Rev. A**40**, 4277 (1989).

7. Astrophysics and Astro-Glaciology

High-density kaonic-proton matter (KPM) composed of $\Lambda^* \equiv K^- p$ multiplets and its astrophysical connections

Y. Akaishi*1,*2 and T. Yamazaki*1,*3

We propose and examine a new high-density composite of $\Lambda^* \equiv K^- p = (s\bar{u}) \otimes (uud)$, which may be called kaonic proton matter (KPM), or simply Λ^*-*Matter*[1], where baryonic bound systems originating from the strong attraction of the $(\bar{K}N)^{I=0}$ interaction shrinks substantially,[2,3] providing a ground-state neutral baryonic system with a huge energy gap (see details in Ref. 1). Recent experimental data[4–6] support this view.

The mass of an ensemble of $(K^- p)_m$, where m, the number of the $K^- p$ pair, is larger than $m \approx 10$, is predicted to drop below its corresponding neutron ensemble, $(n)_m$, since the attractive interaction is further increased by the Heitler-London type molecular covalency[7], as well as by chiral symmetry restoration of the QCD vacuum.[8–11] Since the seed clusters ($K^- p$, $K^- pp$ and $K^- K^- pp$) are short-lived, the formation of such a stabilized relic ensemble, $(K^- p)_m$, may be conceived during the Big-Bang quark-gluon-plasma (QGP) period in the early universe before the hadronization and *quark-anti-quark* annihilation proceed.

At the final stage of baryogenesis a substantial amount of primordial $(\bar{u}, \bar{d})$s are transferred and captured into KPM, where the anti-quarks find places to survive forever. The expected KPM state may be *cold, dense and neutral $\bar{q}q$-hybrid (quark gluon bound (QGB)) states,* $[s(\bar{u} \otimes u)ud]_m$, to which the relic of the disappearing anti-quarks plays an essential role as hidden components. The KPM may also be produced during the formation and decay of neutron stars.

The formation of KPM from the primordial Big Bang proceeds, as $u, \bar{u}, d, \bar{d}, s, \bar{s}$ quarks are produced in QGP at high temperatures and densities. With decreasing temperature it changes to the pre-hadronization stage, where $K^- p$, $K^- pp$ and $K^- K^- pp$ with large binding energies are formed. Then, stable $(\Lambda^*)_{10}$ composites are formed, which eventually grow the increasingly larger, but become cold matter with eventual formation of QGB states. Three quark sectors in the early universe during the disappearance of anti-quark matter become i) the disappearing *ANTI-QUARK* sector ii) quark-anti-quark *HYBRID* sector, where *relic and stable* precursors of $K^- p = s\bar{u} - uud$ are formed, and iii) the remaining ordinary *QUARK* sector.

*1 RIKEN Nishina Center
*2 Institute for Particle and Nuclei, KEK
*3 Department of Physics, University of Tokyo

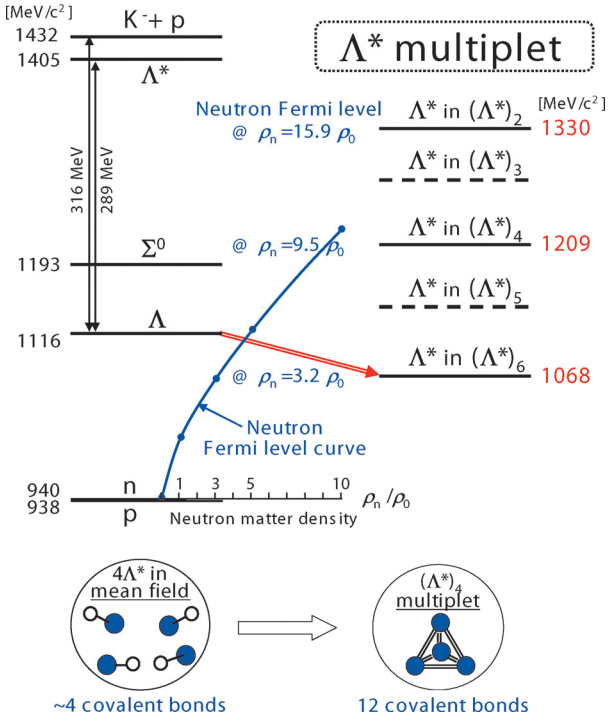

Fig. 1. Predicted energy levels of $\Lambda^* = K^- p$ in Λ^* multiplets calculated by a variational method. The corresponding nuclear densities and neutron Fermi levels are also shown, indicating that the Λ^* in $(\Lambda^*)_6$ cannot decay to a neutron in neutron matter at $\rho = 3.2 \times \rho_0$.

References

1) Excerpt from Y. Akaishi, T. Yamazaki, arXiv:1610.01249v3 [astro-ph.HE] 6 Jan 2017.
2) Y. Akaishi, T. Yamazaki, Phys. Rev. C **65**, 044005 (2002); further references in Ref.[3].
3) S. Maeda, Y. Akaishi, T. Yamazaki, Proc. Jpn. Acad. B **89**, 418-437 (2013) and references therein.
4) T. Yamazaki et al., Phys. Rev. Lett. **104**, 132502 (2010).
5) Y. Ichikawa et al., Prog. Exp. Theor. Phys., 021D01 (2015).
6) M. Hassanvand, Y. Akaishi, T. Yamazaki, in this report.
7) T. Yamazaki, Y. Akaishi, Proc. Jpn. Acad. B **83**, 144 (2007).
8) Y. Nambu, G. Jona-Lasinio, Phys. Rev. **122**, 345 (1961); **124**, 246 (1961).
9) T. Hatsuda, T. Kunihiro, Prog. Theor. Phys. **74**, 765 (1985).
10) U. Vogl, W. Weise, Prog. Part. Nucl. Phys. **27**, 195 (1991).
11) G.E. Brown, K. Kubodera, M. Rho, Phys. Lett. B **192**, 273 (1987).

Time-reversal measurement of the p-wave cross sections of the ^{7}Be$(n,\alpha)^4$He reaction for the cosmological Li problem†

T. Kawabata,[*1] Y. Fujikawa,[*2] T. Furuno,[*1] T. Goto,[*2] T. Hashimoto,[*1] M. Ichikawa,[*2] M. Itoh,[*2] N. Iwasa,[*3,*4] Y. Kanada-En'yo,[*1] A. Koshikawa,[*1,*2] S. Kubono,[*4] E. Miyawaki,[*2] E. Mizuno,[*2] K. Mizutani,[*1] T. Morimoto,[*1,*2] K. Murata,[*1] T. Nanamura,[*1,*2] S. Nishimura,[*4] S. Okamoto,[*2] Y. Sakaguchi,[*2] I. Sakata,[*2] A. Sakaue,[*1] R. Sawada,[*2] Y. Shikata,[*2] Y. Takahashi,[*2] D. Takechi,[*2] T. Takeda,[*1,*2] C. Takimoto,[*2] M. Tsumura,[*1] K. Watanabe,[*1,*2] and S. Yoshida[*2]

The primordial abundances of light elements produced in the Big Bang nucleosynthesis (BBN) provide important insights into the early universe. Accurate estimation of the primordial abundances is crucial for testing cosmological theories by comparing the predicted values with the observations.

A comparison between the theoretical predictions and observations is in good agreement with those for helium and deuterium. However, there remains a serious problem: the ^{7}Li abundance does not agree with any theoretical BBN calculations. This discrepancy is known as the cosmological lithium problem, and has been of great interest in recent years.[1] Several ideas have been proposed to solve this problem. One idea is to improve the current understanding of the stellar processes that exhaust lithium in metal-poor stars. Other ideas are to find new physics beyond the standard BBN model, e.g., a cosmological variation of the fundamental constants,[2] decay of supersymmetric particles,[3] and so on. However, there is no experimental evidence to confirm these models.

From the viewpoint of nuclear physics, nuclear-reaction rates involved in the BBN theory should be examined. The main process of the ^{7}Li production in the BBN is the electron-capture decay of ^{7}Be, which is synthesized in the ^{3}He(^{4}He,γ)^{7}Be reaction. Direct measurements of the cross section for the ^{3}He(^{4}He,γ)^{7}Be reaction were extensively carried out in the past, and uncertainties in this thermonuclear reaction rate are now very small. There is no room to modify the ^{7}Be production rate to solve the lithium problem.[4]

It was pointed out that the ^{7}Li abundance would be greatly reduced in the BBN calculation if the destruction rate of ^{7}Be is enhanced. One of the candidate channels for destroying ^{7}Be is the ^{7}Be$(n,\alpha)^4$He reaction. Unfortunately, the ^{7}Be$(n,\alpha)^4$He reaction at the cosmological energy has been scarcely examined.

Very recently, we have measured the total cross section for the ^{4}He$(\alpha,n)^7$Be reaction, which is the time reverse reaction of the ^{7}Be$(n,\alpha)^4$He reaction. Using the detailed balance principle, the total cross section of the ^{7}Be$(n,\alpha)^4$He reaction for p-wave neutrons at low energies down to $E_{c.m.} = 0.20$ MeV was obtained, as shown in Fig. 1, for the first time. The solid circles and squares show the total cross sections of the (n,α) reaction on the ground and first excited states in ^{7}Be. The shaded area presents the effective-energy window for the p-wave reaction at $T_9 = 0.6$–0.8.

The cross sections evaluated by the indirect methods are compared with the present results. The estimation from p + ^{7}Li scattering[5] is plotted by the open triangles in Fig. 1, whereas the cross section from the evaluated nuclear data library ENDF/B-VII.1[6] based on the R-matrix analysis of several indirect reactions is shown by the dashed line. It was found that these evaluated cross sections are very close to the present data for the ^{7}Be$_{g.s.}(n,\alpha)^4$He reaction.

The cross section for the ^{7}Be$(n,\alpha)^4$He reaction was first estimated by Wagoner,[7] as shown by the solid line in Fig. 1. Currently, this evaluation is widely used in the BBN calculations. The present values of the ^{7}Be$(n,\alpha)^4$He cross sections are much smaller than the Wagoner's calculation. Thus, we concluded that the present results suggest that the ^{7}Be$(n,\alpha)^4$He reaction does not solve the cosmological lithium problem.

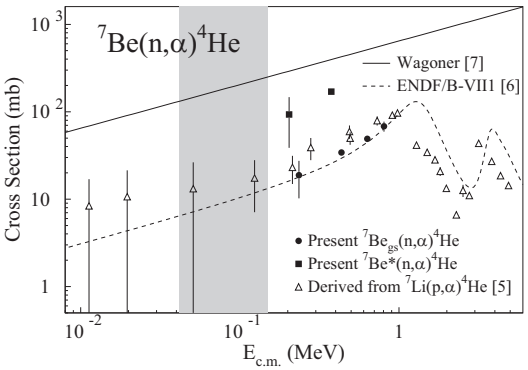

Fig. 1. Measured total cross sections for the ^{7}Be$(n,\alpha)^4$He reaction compared with the previous evaluations.

References
1) B. D. Fields, Ann. Rev. Nucl. Part. Sci. **61**, 47 (2011).
2) A. Coc et al., Phys. Rev. D **76**, 023511 (2007).
3) D. G. Yamazaki et al., Phys. Rev. D **90**, 023001 (2014).
4) R. H. Cyburt et al., Phys. Rev. C **78**, 064614 (2008).
5) S. Q. Hou et al., Phys. Rev. C **91**, 055802 (2015).
6) M. B. Chadwick et al., Nucl. Data Sheets **112**, 2887 (2011).
7) R. V. Wagoner, Astrophys. J. Suppl. **18**, 247 (1969).

† Condensed from the article in Phys. Rev. Lett. **118**, 052701 (2017)

*1 Department of Physics, Kyoto University
*2 Faculty of Science, Kyoto University
*3 Department of Physics, Tohoku University
*4 RIKEN Nishina Center

Box-model simulation for influence of solar proton events on the middle atmosphere

Y. Nakai,[*1] Y. Motizuki,[*1,*2] M. Maruyama,[*1] Y. Hasebe,[*1,*2] H. Akiyoshi,[*1,*3] and T. Imamura[*3]

In a solar proton event (SPE), high-energy particles precipitate into the atmosphere. A part of the high energy particles can induce an increase in the concentrations of radicals, such as odd nitrogen radicals (NOx) and odd hydrogen radicals (HOx), through ionic and neutral reactions in the middle atmosphere. Furthermore, ozone depletion through subsequent reactions with radicals lasts longer than the SPE. The concentration variations of trace gas components with SPEs have been observed and numerical simulation studies have been performed.[1–5)]

We have developed a box-model of multitudinous and homogeneous gas phase reactions of ionic and neutral chemical species in the middle atmosphere, but without transport processes, to investigate the variation of trace gas composition induced by SPEs.[6–8)] We adopted 79 chemical species including positive and negative ions and 608 chemical reactions including various types of ionic and neutral reactions in the latest version of the box-model. The detailed numbers of adopted chemical species and chemical reactions are listed in Tables 1 and 2, respectively. The simulations were performed using commercial software (FACSIMILE, MCPA Software Ltd).

Figure 1 shows the result for the variation of ozone concentration at an altitude of 50km in the northern polar region for an SPE known as the "Halloween" event, which occurred in October-November 2003. The solid line corresponds to the result of full calculation, and the dashed line corresponds to that of a calculation conducted by taking account only of neutral-species production in initial radiolysis processes. The difference between the two results indicates that ion production in initial radiolysis processes and subsequent ionic reactions are important in the quick ozone depletion in the SPE. In both cases, diurnal oscillations of concentrations are observed.

In the near future, the variations estimated by the box-model simulation during an SPE will be input into a three-dimensional chemical climate model[9)] as perturbations to investigate the spatial and temporal atmospheric influence of the SPE through transport processes, aerosol formation, and so on.

Table 1. The number of chemical species adopted in this model.

Neutral species	45
Positively charged species	17
Negatively charged species	17
Total adopted species	79

*1 RIKEN Nishina Center
*2 Department of Physics, Saitama Univ.
*3 National Institute for Environmental Studies

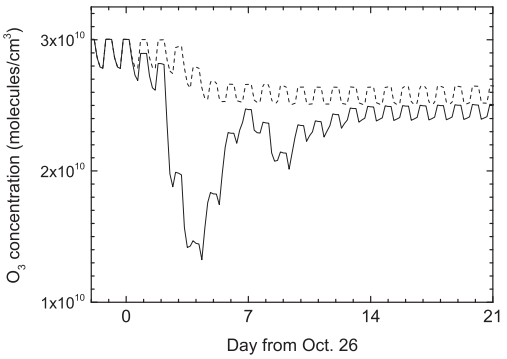

Fig. 1. Variation of the ozone concentration at an altitude of 50km in the northern polar region for the "Halloween" SPE in October-November 2003 (See text).

Table 2. The number of reactions adopted in this model for each reaction type.

Reaction type	# of reactions
Radioysis (initial processes in SPE)	12
Positive ion-neutral reactions	49
Negative ion-neutral reactions	65
Electron attachment on neutral species	8
Collisional and associative detachment	15
Electron-positive ion recombinations	26
Ion-ion recombinations	285
Photodissociation of negative ions[a]	3
Photo-detachment of electrons[a]	5
Solar UV photolysis of neutral species	24
Neutral reactions	116
Total adopted reactions	608

[a] Applied only above 70km.

References

1) K. A. Duderstadt et al., J. Geophys. Res. Atoms. **121**, 2994 (2016).
2) B. Funke et al., Atmos. Chem. Phys. **11**, 9089 (2011).
3) C. H. Jackman et al., Atmos. Chem. Phys. **8**, 765 (2008).
4) P. T. Verronen et al., Geophys. Res. Lett. **35**, L20809 (2008).
5) M. López-Puertas et al., J. Geophys. Res. **110**, A09S43 (2005).
6) K. Sekiguchi et al., RIKEN Accel. Prog. Rep. **46**, 124 (2013).
7) Y. Nakai et al., RIKEN Accel. Prog. Rep. **48**, 168 (2015).
8) Y. Nakai et al.:,RIKEN Accel. Prog. Rep. **49**, in press.
9) H. Akiyoshi et al., J. Geophys. Res. Atoms. **121**, 1361 (2016).

Characteristics of Na^+ and Cl^- distributions in shallow samples from an Antarctic ice core DF01 (Dome Fuji) drilled in 2001: Result of strong atmospheric high-pressure blocking events?†

Y. Motizuki,[*1] H. Motoyama,[*2] Y. Nakai,[*1] K. Suzuki,[*3] Y. Iizuka,[*4] and K. Takahashi[*1]

Ice cores record aspects of the geological history of the Earth, including past climate changes. Dome Fuji station, situated in inland Antarctica (77.3°S, 39.7°E; 3,810m above sea level), is one of the best drilling locations for obtaining ice cores to reconstruct past climates and environments. We present the concentration profiles of certain dissolved ions in samples of the part of a Dome Fuji ice core (DF01) drilled in 2001 that was 7.7m to 65.0m deep.

The anions analyzed were $HCOO^-$, CH_3COO^-, $CH_3SO_3^-$, F^-, Cl^-, NO_2^-, NO_3^-, SO_4^{2-}, $C_2O_4^{2-}$, and PO_4^{3-}, and the cations were Na^+, K^+, Mg^{2+}, Ca^{2+}, and NH_4^+. The temporal resolution of the depth profiles of the ionic concentrations was about one year (Fig. 1). No significant correlations were observed between any ions except for Na^+ and Cl^-.

The ratios of the averaged ionic concentrations in samples of the ice core differed from the ratios in sea salt, a result consistent with the findings of previous studies. This suggests that the ionic components of the samples may mainly be of stratospheric origin. Only several synchronous peaks appear in the concentrations of the Na^+ and Cl^- profiles (Fig. 1).

The Cl^-/Na^+ ratios of the DF01 ice core samples analyzed in this study are different from those reported previously for the surface snow at Dome Fuji[1]. This implies that Cl^-, but not Na^+, was redistributed after deposition[2]. High concentrations of SO_4^{2-} in some DF01 samples may account for the difference between the ice core Cl^-/Na^+ ratios and the surface snow Cl^-/Na^+ ratio.

There were indentifiable synchronous peaks of Na^+ and Cl^- in several samples of the DF01 ice core (Fig. 1). In the samples with synchronous peaks, the corresponding Cl^-/Na^+ ratios were confirmed to be close to the ratio in sea salt (=1.8), indicating the presence of strong sea salt components. This implies that the some critical climatic change in the troposphere occurred to cause precipitation with enhanced sea salt components to fall in the Dome Fuji area.

Our results suggest that there were, intermittently, large-scale intrusions of sea salt particles into the interior of Antarctica − the Dome Fuji station is about

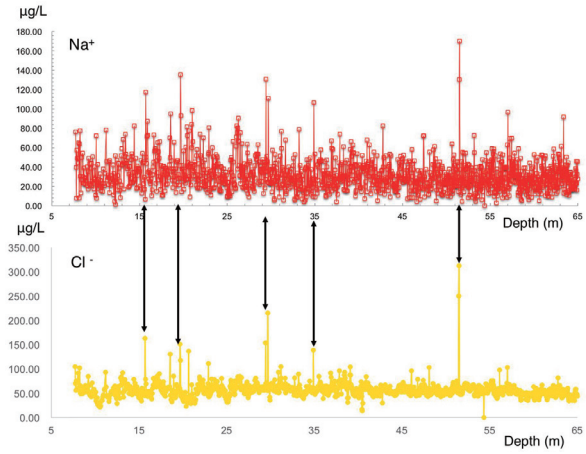

Fig. 1. Depth profiles of Na^+ and Cl^- of DF01 ice core with temporal resolution of about 1 year. Synchronous Na^+ and Cl^- peaks are shown by arrows; the Cl^-/Na^+ ratios of these samples were confirmed to be close to the ratio in sea salt.

1000 km from the coast. The intrusion events appear to have lasted for certain (cumulative) duration that affected one or two of time-resolution periods (Fig. 1). We conjecture that our analyses could be chemical evidence that the usual Antarctic airflow was distorted by high-pressure blocking events[3–6]. High-pressure blocking events convey warm and moist air masses from the Antarctic coast in the troposphere to inland. A blocking event at Dome Fuji was observed in 1997 to persist for about a week[3,4], but one particular event observed in 1994 lasted as long as several weeks[5]. Our findings may indicate that several much larger events occurred in the ∼1300-year period investigated in this study. Those events may have been unusually strong atmospheric high-pressure blocking events.

It is important that the same DF01 samples analyzed for Na^+ and Cl^- be analyzed for $\delta^{18}O$ and δD isotopes, so that the four profiles can be compared in order to confirm that blocking events actually caused the synchronous ionic peaks in our data.

† First part of this article was condensed from the paper in Geochemical J., **51**, 293 (2017) doi:10.2343/geochemj.2.0458
*1 RIKEN Nishina Center
*2 National Institute of Polar Research, Research Organization of Information and Systems
*3 Department of Environmental Sciences, Shinshu University
*4 Institute of Low Temperature Science, Hokkaido University

References
1) e.g., Y. Iizuka et al.: Tellus B **68**, 29285 (2016).
2) S. Fujita et al.: J. Glacilology, doi:10.1017/jog.2016.16.
3) N. Hirasawa et al.: Geophys. Res. Lett. **27**, 1911 (2000).
4) N. Hirasawa et al.: J. Geophys. Res. **118**, 6916 (2013).
5) H. Enomoto et al.: J. Geophys. Res. **103**, 23103 (1998).
6) K. Fujita et al.: Geophys. Res. Lett. **33**, L18503 (2006).

8. Accelerator

Beam test using new central region for energy upgrade at RIKEN AVF cyclotron†

J. Ohnishi,*1 A. Goto,*1 and Y. Kotaka*2

The structure of the central region of the AVF cyclotron was renovated in 2009 (S1), and the available energy for M/Q = 2 ions was increased from 9 MeV/u to 12 MeV/u.[1] After this modification, in order to further increase the beam energy of protons to 30 MeV, another structure (S2) which enables an acceleration with a harmonic number (h) of 1 instead of 2 was designed.[2] Figure 1 shows the superimposed plan views of the structures S1 and S2. In structure S2, the RF shield is smaller than that of S1, the second acceleration gap was moved downstream and the outside wall at the exit of the second gap was removed. Figure 2 shows the acceleration performance of the AVF cyclotron for the three structures of the central region. The acceleration of the 20–30 MeV proton uses the harmonic number h = 1.

We replaced the central region S1 with S2 and performed beam acceleration tests in August 2016. In addition to the acceleration test with h = 1, we investigated the influence on the transmission efficiencies through the cyclotron in the h = 2 operation. Table 1 presents a summary of the acceleration tests. A total of seven beams were accelerated. As the scheduled time for study was limited, the mean beam tuning time for the acceleration of one beam was approximately 4 h. In Table 1, I36 and C01 indicate the beam currents at Faraday cups FC-I36 and FC-C01 located at the injection and extraction beam lines of the AVF cyclotron. In the h = 1 operation, while 20-MeV protons were successfully accelerated with a beam current of 10 μA, the beam current for 30-MeV protons was as small as 1.1 μA because the dee voltage was insufficient owing to the deterioration of the RF cavities. In the h = 2 operation, the extracted beam currents at the FC-C01 for 14-MeV protons, 12-MeV/u deuterons and $^{22}Ne^{7+}$ were almost the same as those in the S1 configuration. However, the transmission

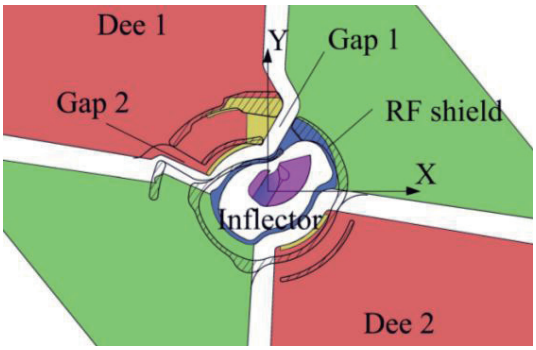

Fig. 1. Existing and tested geometries of the central region. The shaded area indicates the existing geometry.

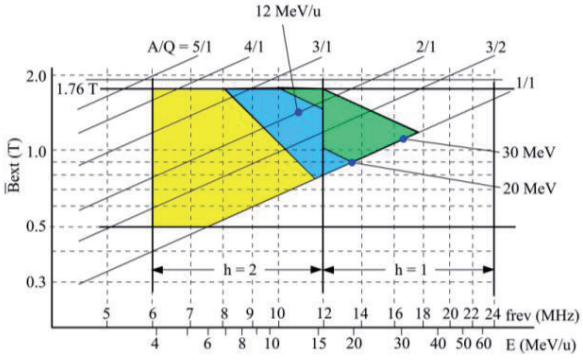

Fig. 2. Acceleration performance of the AVF cyclotron. The yellow, blue, and green areas correspond to the original (before 2009), existing (S1), and currently tested (S2) geometries, respectively.

Table 1. Summary of acceleration test.

Ion	Energy	RF frequency (MHz)	Harmonics	I36 (μA)	C01 (μA)
p	14 MeV	23	2	90	14.3
H_2^+	12 MeV/u	21.25	2	57	9.6
$^{22}Ne^{7+}$	6.0 MeV/u	15.05	2	42	7.5
$^{22}Ne^{5+}$	4.0 MeV/u	12.3	2	12	2
p	20 MeV	13.6	1	76	10
p	30 MeV	16.5	1	116	1.1
$^{56}Fe^{15+}$	5 MeV/u	13.8	2	1.2	0.12

efficiency for $^{22}Ne^{5+}$, which simulates $^{84}Kr^{20+}$, was approximately 60% of the peak performance to date. The transmission efficiency for $^{56}Fe^{15+}$ beams was only 10%, while its efficiency has so far greater than 20% or occasionally 30%. It can be concluded that the transmission efficiencies in the h = 2 operations with S2 were rather poor compared to those with S1, although the time for machine study was not sufficient. Therefore, we decided to revert the tested structure, S2, to the existing one, S1. At present, we are attempting to clarify the reason why the transmission efficiency was low and search for a new geometry that realizes higher transmission efficiencies for both h = 1 and h = 2 operations through a beam simulation study.

References

1) A. Goto et al., RIKEN Accel. Prog. Rep. **43**, 127 (2010).
2) S. B. Vorozhtsov et al., RIKEN Accel. Prog. Rep. **44**, 105 (2011).

† Condensed from the article in Proceedings of Cyclotrons 2016, Zurich, Switzerland, THP13

*1 RIKEN Nishina Center
*2 Center for Nuclear Study, the University of Tokyo

Injection-beam-orbit analysis of AVF cyclotron using 4-dimensional emittance

Y. Kotaka, *1 Y. Ohshiro, *1 H. Yamaguchi, *1 N. Imai, *1 Y. Sakemi, *1 T. Nagatomo, *2
M. Kase, *2 J. Ohnishi, *2 A. Goto, *2 K. Hatanaka, *3 H. Muto, *4 and S. Shimoura *1

For the purpose of increasing the beam intensity of the AVF cyclotron, the improvement of the injection beam intensity is essential because 80% of the beam intensity produced by ECRIS is lost in this injection line. In order to determine the reason for this loss and to optimize the injection beam orbit, the injection beam orbit is analyzed in view of the space charge effect.

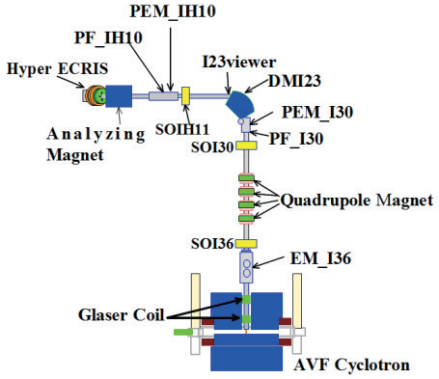

Fig. 1 Beam injection line of the AVF cyclotron.

Figure 1 shows the beam injection line of the AVF cyclotron. We measured the 4-dimensional emittance by the pepper-pot emittance monitor[1] (PEM_IH10) and calculated the injection beam orbit using the 4-dimensional emittance as the initial value. We adopted two types of calculation models for electromagnets. For the calculation in solenoid coils and quadrupole magnets, we adopted the calculated magnetic field. On the other hand, we adopted the hard-edge model for a dipole magnet (DMI_23). For the edge focus of DMI23, we used the correction indicated by TRANSPORT.[2] These calculation models were tested by a 25.4-keV $^4He^{2+}$ ion beam of 5 eμA. The calculated beam orbit was mostly consistent with the measurement results of the beam viewer (I23viewer), profile monitor (PF_I30) and 2-dimensional emittance monitor (EM_I36).[3]

To evaluate the performance of these models for the high-intensity beam, we tested them by a 15.4-keV $^4He^{2+}$ ion beam of 240 eμA. The calculated beam orbit was not consistent. The result was thought to be caused by the space charge effect.

There are some models for the space charge effect. In the model we adopted first, the beam cross section was circular, and the transverse and longitudinal beam densities were uniform.[3] Next, we adopted an ellipse instead of a circle because the beam cross section was not always circular.

*1 Center for Nuclear Study, University of Tokyo
*2 RIKEN Nishina Center
*3 RCNP, Osaka University
*4 Center of General Education, Tokyo University of Science, Suwa

The equation of the space charge effect is as follows:[4]

$$\frac{d^2x}{ds^2}=\frac{4\lambda r_p}{\beta^2\gamma^3 a(a+b)}x,\quad \frac{d^2y}{ds^2}=\frac{4\lambda r_p}{\beta^2\gamma^3 b(a+b)}y \quad \left(r_p=\frac{q^2}{4\pi\epsilon_0 mc^2}\right) \quad (1),$$

where s is the beam axis, (x, y) is the transverse phase-space coordinate, λ is the number of particles per unit length, β and γ are Lorentz factors, a and b are the ellipse axes of the beam, and r_p is the classical radius of the particle.

We solved the equation of the injection beam orbit including equation (1) and compared the 2-dimensional emittance measured by EM_I36. The coordinates (u, w) of EM_I36 are rotated by 45 degree against the coordinates (x, y). The comparisons of (u, u') and (w, w') are shown in Fig. 2 and Fig. 3, respectively. The shapes of the calculated 2-dimensional emittances are close to those of the 2-dimensional emittances measured by EM_I36. The model of the space charge effect is thought to be effective.

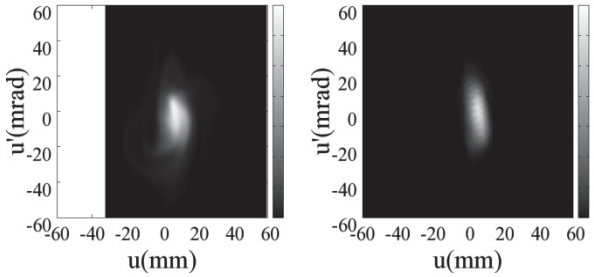

Fig. 2 (left) Image of (u, u') emittance measured by EM_I36. (right) Image of the (u, u') emittance calculated from the measured 4-dimensional emittance.

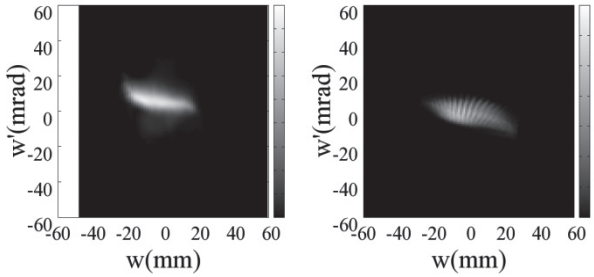

Fig. 3 (left) Image of (w, w') emittance measured by EM_I36. (right) Image of the (w, w') emittance calculated from the measured 4-dimensional emittance.

References

1) T. Hoffmann et al., Proc. 9th BIW, Cambridge, USA (2000), p. 432-439.
2) D. C. Carey et al., FERMILAB-Pub-98/310
3) Y. Kotaka et al., Proc. 13th Annual Meeting of PASJ, Chiba (2016).
4) S. Y. Lee: Accelerator Physics 1st ed. (Singapore, World Scientific, 1999).

Mg ion pumping effect during $^{24}Mg^{8+}$ ion beam production at the Hyper-ECR ion source

H. Muto,[*1] M. Kase,[*1] K. Kobayashi,[*2] M. Nishimura,[*2] S. Kubono,[*1]
Y. Ohshiro,[*3] Y. Kotaka,[*3] H. Yamaguchi,[*3] Y. Sakemi,[*3] and S. Shimoura[*3]

A grating monochromator with a photomultiplier has been used for beam tuning at the Center for Nuclear Study Hyper-Electron Cyclotron Resonance (ECR) ion source.[1,2] The Hyper-ECR ion source has been successfully used as an injector of the multi-charged ion beams of high intensity for the RIKEN AVF cyclotron.[3] $^{24}Mg^{8+}$ ions have been produced in the 14.2-GHz Hyper-ECR ion source. At the beginning of the chamber baking an RF power of 100 W was fed to the residual gas of the plasma chamber. The extraction voltage was set to 10 kV. Then the vacuum gauge reading rapidly dropped to less than 10^{-4} Pa from the order of 10^{-5} Pa and a brakedown of the high-voltage power supply occured because of the huge drain current. A few hours later the extraction voltage was recovered and the vacuum gauge reading was restored to the order of 10^{-5} Pa. The RF power was gradually increased to 600 W until a good vacuum condition (1~5 x 10^{-5} Pa) and low drain current of less than 2 mA were obtained. After baking the plasma chamber an MgO rod was gradually inserted into the chamber without excessive heat. The RF power ranges from 500 to 600 W for $^{24}Mg^{8+}$ ion production. A grating monochromator (JASCO CT-25C) and a photomultiplier (Photosensor module H11462-031, Hamamatsu Photonics) were used for light intensity observation during chamber baking and beam operation.[3] The wavelengths of the observed lines were determined in accordance with the NIST Atomic Spectra Database.[4] Figure 1 shows the optical line spectrum of the Hyper-ECR ion source under plasma chamber baking. This spectrum was taken three hours from baking start. The vacuum gauge reading was 5.7 x 10^{-5} Pa. The drain current was 12 mA. The RF power was 100 W. In this figure most of the peaks were from Fe I and Fe II. The relative intensities of those Fe I and Fe II peaks are quite high. Figure 2 shows an optical line spectrum of the ECR plasma during $^{24}Mg^{8+}$ ion beam tuning. The vacuum gauge reading was 1.7 x 10^{-5} Pa. The drain current was 1.8 mA. The RF power was 611 W. The line intensities of Fe I and Fe II almost decreased to zero and Mg line intensities appeared. Especially, the Mg VIII line spectrum (λ=279.64 nm) was clearly obtained to identify the existence of $^{24}Mg^{8+}$ ions in the ECR plasma. The ion source was tuned for the production of the $^{24}Mg^{8+}$ ions. The H^+ ions were also reduced during $^{24}Mg^{8+}$ ion beam operation. From these results the ion pumping effect of Mg ions was visually demonstrated by the optical grating monochromator with a photomultiplier.

*1 RIKEN Nishina Center
*2 Sumitomo Accelerator Service (SAS)
*3 CNS, University of Tokyo

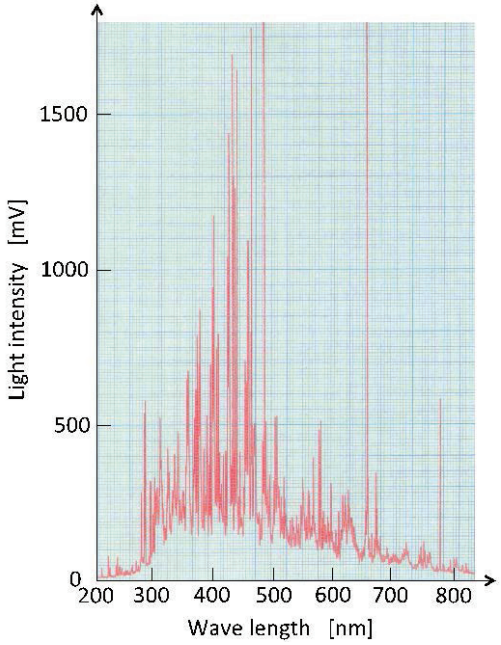

Figure 1. Light intensity spectrum of the residual gas ions during baking for three hours.

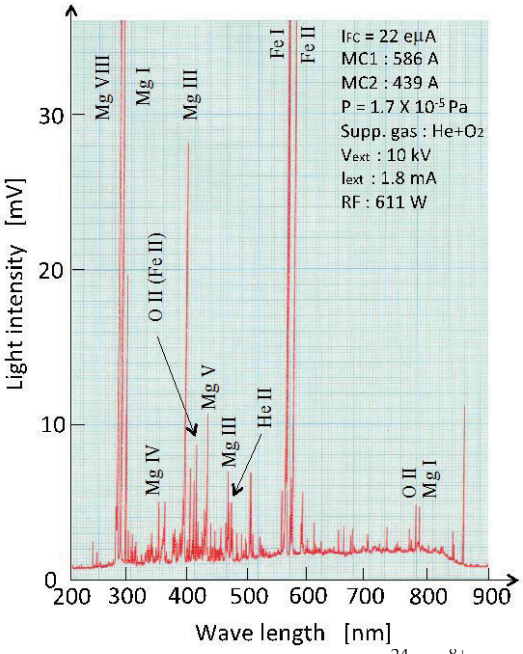

Figure 2. Optical line spectrum during $^{24}Mg^{8+}$ ion beam tuning.

References
1) H. Muto et al., Rev. Sci. Instrum. **84**, 073304 (2013).
2) H. Muto et al., Rev. Sci. Instrum. **85**, 02A905 (2014).
3) H. Muto et al., Physics Procedia **66**, 140 (2015).
4) www.nist.gov/pml/data/asd.cfm for NIST atomic spectrum data base.

Recent developments of RIKEN 28 GHz SC-ECRIS†

Y. Higurashi,*1 J. Ohnishi,*1 H. Haba,*1 M. Kidera,*1 K. Ozeki,*1 and T. Nakagawa*1

In the past two years, we have attempted to improve the performance of RIKEN 28GHz SC-ECRIS for the production of an intense U ion beam. Last year, we produced ~200 eμA of U^{35+} at an injected radio frequency (RF) power of ~2.6 kW. For the RIKEN RIBF experiment, we produced ~110 eμA of U^{35+} ions with the sputtering method for longer than one month without interruption. In this case, we surely require a very stable beam to increase the transmission efficiency in the accelerators and avoid any damage to the components of the accelerator due to the high-power beam. Very recently, we tested the production of a highly charged Zn ion beam to meet the requirements of the RIBF project and to produce an intense beam with a very low consumption rate.

Figures 1(a) and (b) show the extraction current of the ion source and the beam intensity of U^{35+} ions, respectively. The extracted current is quite stable, and the average beam intensity of U^{35+} was ~102 eμA over a long period of time. Under this condition, a maximum beam intensity of ~49 pnA was successfully extracted from the superconducting ring cyclotron for the RIBF experiment conducted last autumn[1].

For long-term operation, it is important to minimize the material consumption rate. To obtain the consumption rate, we operated the ion source with the same sputtering voltage for approximately one month. In 2012, we produced an intense beam of U^{35+} with a sputtering voltage of approximately –5 kV. In this experiment, we observed that the consumption rate of the material is higher than that in the oven method[2]. To minimize the consumption rate while maintaining the beam intensity, we systematically studied the consumption rate for several sputtering voltages. At a sputtering voltage of –1 kV, the consumption rate was ~2.1 mg/h for the production of approximately 100 eμA of U^{35+} ions, which is significantly lower than the consumption rate at approximately –5 kV (~5 mg/h) .

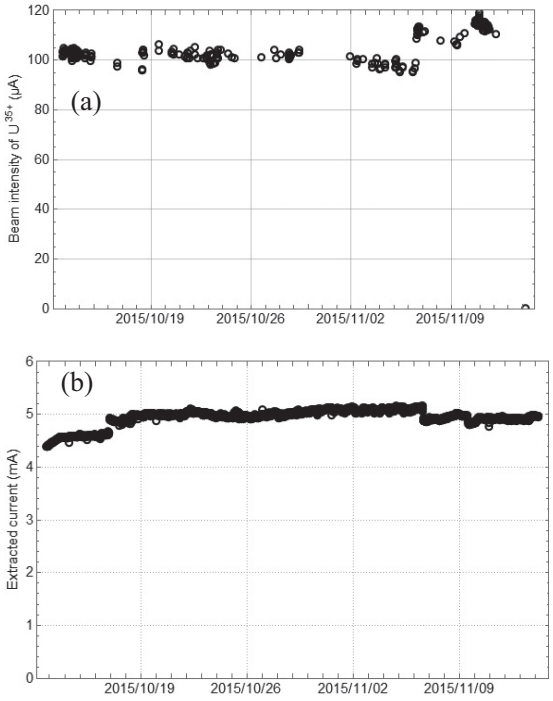

Fig. 1. (a) Beam intensity of U^{35+} ions and (b) the extracted current as a function of time.

For the production of Zn vapor, we used a low-temperature oven[3] of the same type as that used for the 18 GHz ECRIS at RIKEN. In the test experiment, we used He gas as a support gas and $_{nat}$ZnO as a sample. Fig. 2 shows the typical charge distribution of the highly charged Zn ions. The injected RF power was ~1.6 kW (28 GHz + 18 GHz). B_{inj}, B_{min}, B_{ext}, and B_r[4] were 3.1, 0.62, 1.78, and 1.94 T, respectively, and the typical gas pressure was 6.5–7.5×10^{-5} Pa. The average beam intensity was ~26 eμA of $^{64}Zn^{19+}$ ions, which is the required charge state of the Zn ions for RIBF experiments. The consumption rate of Zn was ~0.20 mg/h. If we assume the use of enriched ^{70}Zn, the beam intensity will be ~60 eμA, which is the required beam intensity. (the natural abundance of ^{64}Zn is about 48.6 %) Furthermore, the consumption rate for 28 GHz SC-ECRIS was almost same as that for 18 GHz ECRIS.

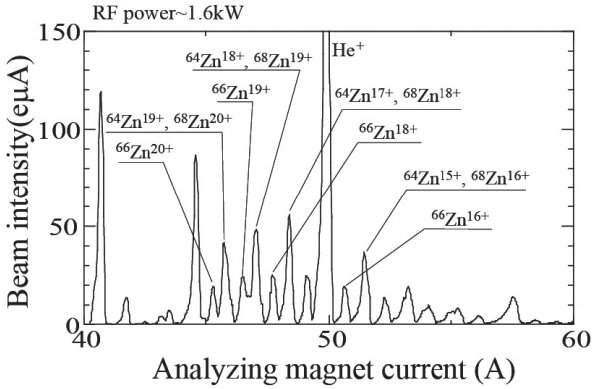

Fig. 2. Charge distribution of the highly charged Zn ion beam.

References

1) J. Ohnishi, Y. Higurashi, T. Nakagawa, Rev. Sci. Instrum. **87**, 02A709 (2016).
2) O. Kamigaito et al., IPAC2016, TUPMR022.
3) K. Ozeki, Y. Higurashi, M. Kidera, T. Nakagawa, HIAT2015, WEPB22.
4) G. D. Alton, D. N. Smithe, Rev. Sci. Instrum. 65, 775(1994).

† Condensed from the proceeding of the ECIRS2016

*1 RIKEN Nishina Center

Four-dimensional transverse phase space distribution changes with respect to degree of vacuum of LEBT†

T. Nagatomo,[*1] V. Tzoganis,[*1,*2,*3] M. Kase,[*1] T. Nakagawa,[*1] and O. Kamigaito[*1]

The four-dimensional transverse emittance ϵ_{4D} is a fundamental quantity, which is the degree of beam quality, and is invariant under linear symplectic transformations, such as beam optics components including solenoid lenses and skew quadrupole lenses. The emittance indicates the area of distribution in the phase space; thus, the smaller ϵ_{4D} is, the better the beam transport efficiency is. Because ϵ_{4D} is not decreased during the beam transport unless special techniques of beam cooling are used, it is essential to provide a beam having an emittance as small as possible at the extraction area of the ion source. Especially, at the beam-extraction area, the total current of the extracted ions reaches the order of milli-amperes; thus, the importance of the space-charge effect is considered to be serious at the present intensity.

The space-charge effect is induced by the repulsive forces between the positively charged ions inside of the beam and causes degradation of the beam quality, namely the emittance growth. The possibility to compensate for the space-charge effect by injecting a neutral gas into the low-energy beam transport (LEBT) following the ion source was discussed by Toivanen et al.[1] The electrons produced through collisions between the neutral gas and the beam are considered to moderate the electric repulsive forces. Based on that report, we intend to clarify how the ϵ_{4D} of multiply charged argon beams evolves with respect to the amount of krypton (Kr) gas injected in the LEBT of the RIKEN AVF cyclotron. The LEBT is connected to the 18-GHz superconducting ECR ion source (SC-ECRIS) and the RIKEN AVF cyclotron. We have measured ϵ_{4D} by the pepper-pot emittance meter[2] installed immediately behind a solenoidal lens following the analyzing magnet.

Figure 1 shows the change of emittances of $Ar^{8+,9+,11+}$-ion beams with respect to the gas pressure of LEBT, which represents the amount of injected Kr gas. The Kr gas was injected from a port attached at a vacuum chamber of the analyzing magnet, and the LEBT pressure was measured by a cold cathode gauge, which was also attached to the camber of the analyzing magnet. In Fig. 1, the emittances of $\epsilon_{x,y}$ and ϵ_{4D} were normalized by the values obtained under the condition of no Kr-gas injection, which were ϵ_{x0}, ϵ_{y_0}, and ϵ_{4D0}, respectively. In Fig. 1, all the obtained emittances decrease as the amount of Kr gas increases. Especially, it is noteworthy that the emittances decrease in spite of the increases of the observed beam currents in the Ar^{8+} and Ar^{9+} cases. Further, it is interesting that the ϵ_{4D} of all charge states seem to decrease similarly to each other, despite the fact that their projections ϵ_x and ϵ_y decrease differently for each charge state. In order to clarify the emittance-reduction mechanism, we are planning to conduct further experiments that would arrow us to distinguish between the space-charge compensation effect in the LEBT and the gas mixing effect of Kr gas penetrating the ECR plasma.

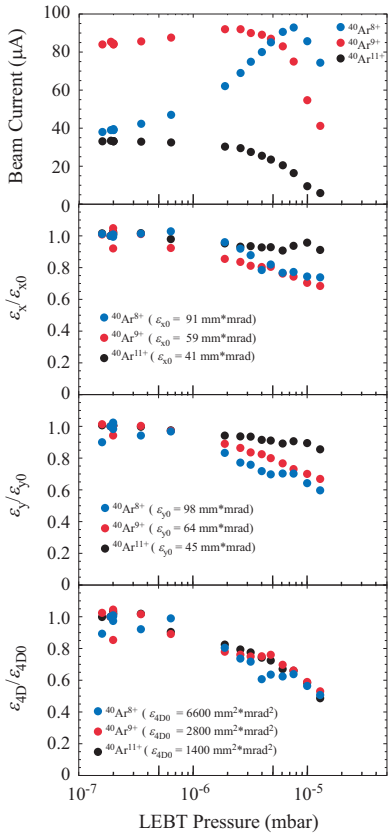

Fig. 1. Obtained beam currents and rms emittances ϵ_x, ϵ_y, and ϵ_{4D} of $^{40}Ar^{8+,9+,11+}$ with respect to the LEBT residual gas pressure.

References

1) V. Toivanen et al., Nucl. Instr. Meth. B **268**, 1508 (2010).
2) V. Tzoganis et al.: Proc. 7st Int. Particle Accelerator Conf. (IPAC'16), Busan, Korea, paper MOPMR048 (2016), p. 361

† Condensed from the article in the Proc. of 22nd Int. Workshop on ECR Ion Sources (ECRIS2016), Busan, Korea, August 2016, paper WEPP35, in press

*1 RIKEN Nishina Center
*2 Cockcroft Institute, Daresbury, Warrington
*3 Department of Physics, University of Liverpool

Beam energy measurement system using electrostatic pickups at the RIBF

T. Watanabe,[*1] N. Fukunishi,[*1] M. Fujimaki,[*1] and R. Koyama[*2]

It is important to measure the beam energy of heavy-ion beams at the RIBF. Monitors with plastic scintillators as sensors (scintillation monitors) were used to measure the energy and longitudinal profiles of heavy-ion beams.[1] However, the beam cannot be used while it is being measured, and there is a danger of melting the scintillator. For the purpose of real-time measurement of the beam energy, electrostatic pickups were newly designed, fabricated, and installed in the beam transport line (C01, C02) in the AVF cyclotron.[2] Two electrostatic pickup monitors installed in the beam transport line are used to measure the particle time- of-flight (TOF) between the paired monitors. Researchers who conduct experiments can always watch the beam energy in real time with a web browser even if they are in an experiment room.

When a charged-particle beam passed along the axis of the electrostatic pickup, the image charge is electrostatically induced on the pickup. The beam signals are amplified and transmitted via coaxial cables with a length of 46 m directly to the DAQ stage outside the radiation protected area. Finally, a high-speed digitizer board digitizes the beam signals and sends the date to a controller PC. We chose this digitizer for the signal processing instead of a standard oscilloscope because it has high transfer rates and large-capacity onboard memory. The electrical specifications of the digitizer and amplifier are listed in Table 1. The program for the data acquisition of the digitizer and for displaying results is written in LabVIEW. Since the controller PC in the DAQ stage is connected to an EPICS Ethernet LAN, the measured results can be watched with a web browser on any PC, only users have permissions. The obtained data are stored in a

Table 1. Electrical specifications of digitizer and amplifier.

Digitizer	
Model No.	NI PXIe-5160 (National Instruments)
Bandwidth	DC - 500 MHz
Sampling rates	2.5 GS/s (1 ch), 1.25 GS/s (4 ch)
Memory	2GB
Resolution	10-bit
Channels	4
Transfer Rates	600 MB/s
Amplifier	
Model No.	ABL0300-00-3230 (Dynamic RF Inc.)
Bandwidth	9 kHz - 3.0 GHz
Noise Figure	2.5dB typical, 3.0 dB Max @25 °C
Gain	32 dB @25 °C

*1 RIKEN Nishina Center
*2 SHI Accelerator Service Ltd.

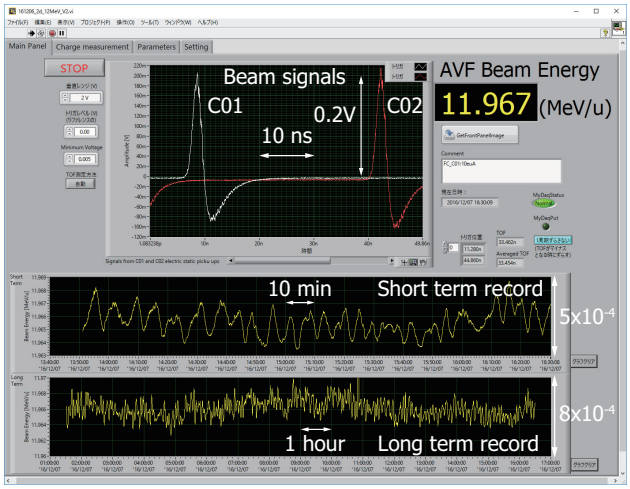

Fig. 1. Example of the measured results for the acceleration of a $^2H^+$ beam at an intensity of 10 μA.

MyDAC, which is a simple data-logging and display server. An example of the measured results for the acceleration of a $^2H^+$ (deuteron) beam with an intensity of 10 μA is shown in Fig. 1. In these results, the beam energy was found to be changed periodically with a period of about 6 min. This phenomenon was synchronized with a temperature change of cooling water, which was caused by a heat exchanger and temperature-control device. The temperature of cooling water was changed within ±0.4°C every 6 min. Although the investigation indicated that the beam-energy change might have been caused by the temperature change of the main coil of the cyclotron, more detailed investigation is necessary. The accuracy can reach better than 0.2% for the energy spread assuming precisions of the length ΔL = 1 mm and time Δt = 100 ps. The minimum detectable beam current with this system is approximately 50 nA.

In fiscal year 2016, we measured the beam energy 12 times for the cross section measurements for RI production experiments,[3–7] which typically lasted for 3 days. Those beam-energy measurements were performed using the scintillation monitors and electrostatic pickup monitors.

References

1) T. Watanabe et al.; Proc. IPAC'14 (2014), p. 3566.
2) T. Watanabe et al.; Proc. 12th Ann. Meet. of PASJ, (2015), p. 1198.
3) S. Takács et al., NIM B **383**, 213 (2016).
4) F. Ditrói et al., NIM B **385**, 1 (2016).
5) S. Takács et al., NIM B **397**, 33 (2017).
6) A. Usman et al. NIM B **399**, 34 (2017).
7) A. Saito et al., ARI **125**, 23 (2017).

Sensitivity improvement and miniaturization of HTc-SQUID beam current monitor

T. Watanabe,[*1] N. Fukunishi,[*1] S. Inamori,[*2] and K. Kon[*2]

To measure the DC current of heavy-ion beams non-destructively at high resolution, we have developed a high- critical- temperature (HTc) superconducting quantum interference device (SQUID) beam current monitor (SQUID monitor) for use in the RIBF. We have completed the development of a prototype of the SQUID monitor and installed it in one of the beam transport lines in the RIBF.[1] Presently, we have been using the SQUID monitor for current measurement of heavy-ion beams. Furthermore, with the aim of higher sensitivity and miniaturization of the SQUID monitor, we have started the investigation for developing a new method.[2]

We investigated a low- critical- temperature (LTc) SQUID monitor, which was expected to be use for monitoring the beam of the Antiproton Accumulator in the Fermi National Accelerator Laboratory.[3] Furthermore, we considered why an LTc SQUID monitor has a high sensitivity, which was developed for atomic-physics experiments on the electron-ion collision processes in the cooler synchrotron TARN II ring.[4] As a result of consideration, we concluded that it is essentially important to improve the coupling efficiency between the SQUID and the magnetic flux produced by a beam current. To achieve strong coupling, a highly permeable magnetic core with large inductance is necessary. Fig. 1 shows a new scheme of an HTc SQUID monitor. Both an HTc shielding ring and an HTc induction ring are fabricated by dip coating a thin Bi_2-Sr_2-Ca_1-Cu_2-O_x (Bi-2212) layer on a Ag substrate. The Bi-2212 layer is approximately 100-μm thick. When a charged-particle beam passes along the axis of the HTc induction ring, a shielding current produced by the Meissner effect flows in the opposite direction along the wall of the HTc induction ring. The shielding current acts to eliminate the magnetic field produced by the beam. The shielding current also flows on the shielding ring in the same manner. Since a permeable core with a magnetic gap is installed in the induction ring, the magnetic flux produced by the current flow is strongly coupled with the magnetic core. An HTc SQUID installed in the magnetic gap of the induction ring can detect the magnetic flux. We theoretically estimated the expected signal voltage[2] and made several parts (Fig. 2 (a)-(c)) to verify whether the theory is correct. After all parts were cooled by liquid nitrogen, the test was performed using a simulated beam current of 0.5 mA at 20 Hz. Fig. 2 (d) shows the output voltage from the HTc SQUID controller, which was analyzed in the frequency domain. Since the theoretically expected voltage was 2.6 V_{pp} and the measured voltage was 2.2 V_{pp}, it was confirmed that the theoretical estimation was correct.

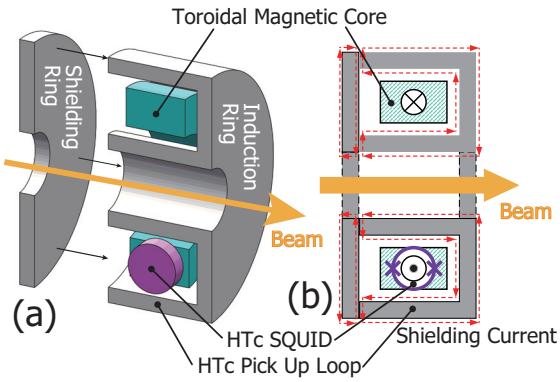

Fig. 1. New scheme of a HTc SQUID monitor.

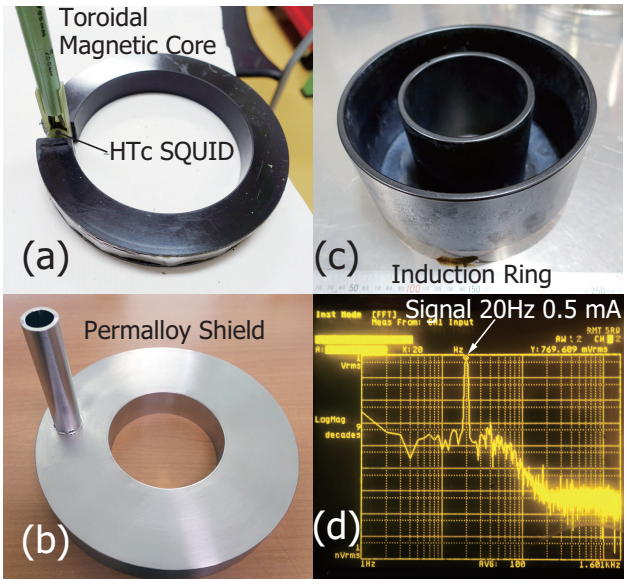

Fig. 2. Several parts for testing (a)-(c) and measured result (d).

The authors are grateful to Prof. S. Tanaka of Toyohashi university of technology for cooperation regarding the above mentioned test. This work was supported by JSPS KAKENHI Grant Number 15K04749.

References

1) T. Watanabe et al., Proc. 4th Int. Beam Instr. Conf. IBIC2015 (2014), p. 590.
2) T. Watanabe et al., Proc. 13th Ann. Meet. of Particle Accel. Society of Japan, (2016), p. 1127.
3) M. Kuchnir et al., IEEE Trans. Mag. MAG **21**, No.2, 997 (1985).
4) T. Tanabe et al., NIM A **427**, 445 (1999).

*1 RIKEN Nishina Center
*2 TEP Corporation

Radiation monitoring for cyclotrons in RIBF

M. Nakamura,[*1] K. Yamada,[*1] A. Uchiyama,[*1] H. Okuno,[*1] and M. Kase[*1]

In recent years, we attempted to monitor radiation due to beam loss in the RIBF by using ionization chambers (ICs). Thus far, we were able to perform simultaneous measurements of beam loss at several important components at RRC and SRC.[1] Especially, we investigated the radiation from the electrostatic diffraction channel (EDC) at RRC and SRC. Furthermore, we successfully input the alarm signal from these ICs to the beam interlock system (BIS).[2,3] On the other hand, the case of the $^{238}U^{86+}$ beam, for example, RRC, fRC, IRC and SRC are used. Hence, in this time, we newly installed the ICs near the EDC of fRC and IRC. We report here our recent attempt to monitor the beam loss at the EDC of RRC, fRC, IRC and SRC simultaneously.

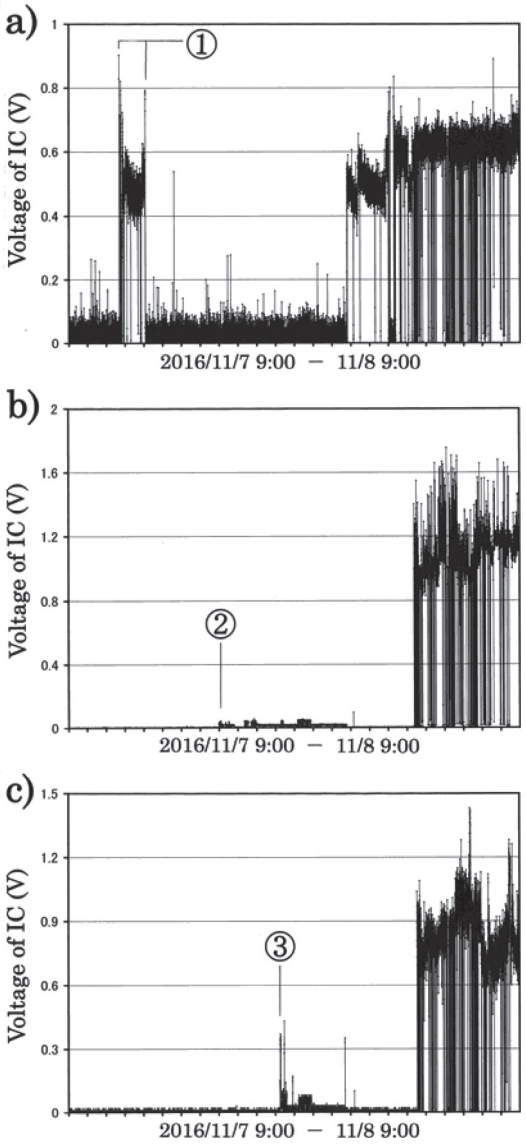

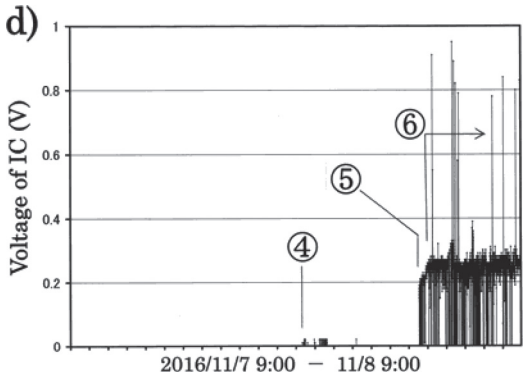

Fig. 1. Signals from ICs installed near the EDCs in RIBF a) EDC of RRC b) EDC of fRC c) EDC of IRC d) EDC of SRC.

From October 11 to November 11, the $^{238}U^{86+}$ beam was accelerated to 345 MeV/nucleon. The measured signals from 9:00 on 11/7/2016 to 9:00 on 11/8/2016 are shown in Fig. 1 a) – d), as the examples. In Fig. 1 a), we observed some noise around the baseline. The cause of the noise is unknown. However, we consider that this signal reflected the operating conditions of RRC well.

In these figures, the main occurrences are shown by ① - ⑥. These events are listed as follows.

① At 11:45 on 11/7, the beam reached RRC. After 13:10, the beam was reduced and RRC was adjusted.
② At 17:00 on 11/7, the reduced beam was transported to fRC and fRC adjustment was started.
③ At 19:00 on 11/7, the beam was transported to IRC and IRC adjustment was started.
④ At 21:00 on 11/7, the beam was transported to SRC and SRC was adjusted until 22:00.
⑤ At 3:00 on 11/8, the beam irradiation from SRC was started.
⑥ At 3:40 on 11/8, SRC adjustment for “High intensity beam tuning” was started.

We could confirm that these four ICs signals reflected the RIBF operations from 9:00 on 11/7 to 9:00 on 11/8. By observing the signals of ICs from 10/11/2016 to 11/11/2016, we also verified that these signals corresponded to the conditions of RIBF operations quite well.

In this experiment, we performed simultaneous measurements of beam loss near the EDC of RRC, fRC, IRC and SRC. We can use the signals of these four ICs to monitor the RIBF operations and adjust each EDC for ensuring the best conditions.

References

1) M. Nakamura et al., RIKEN Accel. Prog. Rep. **44**, 293 (2011)
2) M. Nakamura et al., RIKEN Accel. Prog. Rep. **45**, 228 (2012)
3) M. Nakamura et al., RIKEN Accel. Prog. Rep. **48**, 237 (2015)

[*1] RIKEN Nishina Center

Development of thin graphite carbon (GC) disks†

H. Hasebe,[*1] H. Okuno,[*1] A. Tatami,[*2] M. Tachibana,[*2] M. Murakami,[*2] H. Kuboki,[*1] H. Imao,[*1] N. Fukunishi,[*1] M. Kase,[*1] and O. Kamigaito[*1]

Graphite carbon sheet (GCS) disks have been used as the final charge stripper for U-beam acceleration since 2015 and have successfully provided stable U beams. Whereas the thickness of the GCS disk was 14 mg/cm^2 (two layers of 7.0-mg/cm^2-thick sheets)[1], disks with a thickness less than 4.45 mg/cm^2 are also required for other ion beams. A graphite carbon (GC) disk with a thickness of 2.2 mg/cm^2 was fabricated for trial by Kaneka Corporation[2]. The dimensions of the GC disk were identical to those of the GCS disk; the outer diameter was 110 mm with a hole at the center for mounting. The GC disk has sufficient flexibility and high mechanical strength considering its thickness. This GC disk was used for a Ca beam time in November 2015. The Ca^{16+} ions were stripped into Ca^{20+} with a fraction of 87% at an incident energy of 45 MeV/nucleon. A total of 3.31×10^{18} Ca particles were irradiated on one disk at 10-electric-μA intensity, which corresponded to a thermal load of 6.4 W. Fig. 1 shows the GC disk before (left) and after (right) Ca beam irradiation. There was no deterioration in appearance except for a slight color change and deformation. This deformation did not affect the beam intensity at the downstream. Therefore, the GC disk was still usable.

A thinner GC disk with a thickness of 0.91 mg/cm^2 has also been fabricated for trial use. Although its thickness was less than half that of the 2.2-mg/cm^2-thick GC disk, the mechanical strength was almost the same. This GC disk was tested for U-beam stripping at 50 MeV/nucleon in November 2015. In order to evaluate the thickness uniformity of the GC disk, the disk was rotated at a high speed, and the beam fluctuations were monitored at the downstream. The rotation speed was 300 rpm for the first 2 h, and it was increased up to 1000 rpm for five more minutes. No intensity fluctuation was observed during the measurement. In addition, charge distributions of U after passing through the GC disk was measured with the incident U^{64+} beam. The beam intensity was 10 electric μA, which corresponded to a thermal load of 8.5 W. Fig. 2 shows the GC disk after the test. No damage was observed, and it was in pristine condition. Fig. 3 shows the charge distributions of U after passing through GC disks with thicknesses of 0.91 (blue) and 2.2 mg/cm^2 (green), and a GCS disk with a thickness of 14 mg/cm^2 (red). The mean charge states of U behind the disks with thicknesses of 0.91, 2.2, and 14 mg/cm^2 were 78+, 82+, and 87+, respectively.

† Condensed from an article in the proceedings of the 28th world conference of the International Nuclear Target Development Society

*1 RIKEN Nishina Center

*2 Frontier Materials Development Laboratories, Kaneka Corporation

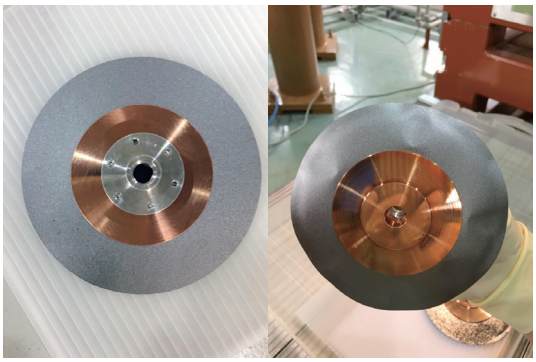

Fig. 1. GC disk with a thickness of 2.2 mg/cm^2 before (left) and after (right) usage in Ca beam irradiation.

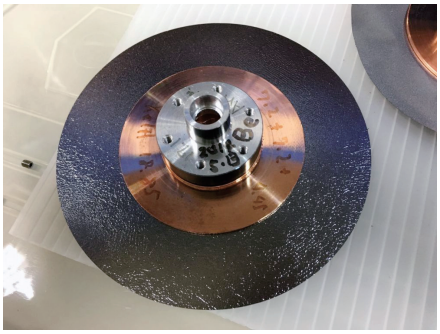

Fig. 2. GC disk with a thickness of 0.91 mg/cm^2 after the U beam irradiation test.

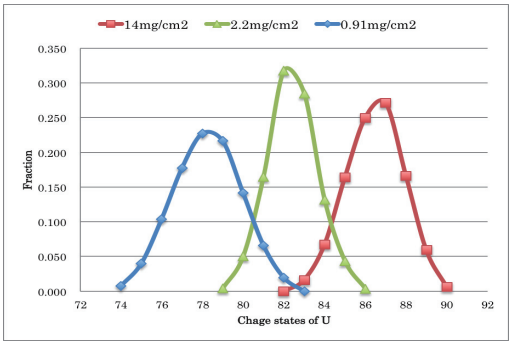

Fig. 3. Charge distributions of U behind GC disks with thicknesses of 0.91 (blue) and 2.2 mg/cm^2 (green), and a GCS disk with a thickness of 14 mg/cm^2 (red).

References

1) H. Hasebe et al., RIKEN Accel. Prog. Rep. **49**, 14 (2016).
2) Kaneka Corporation,
URL: http://www.elecdiv.kaneka.co.jp/english/index.html

Status of cryopumps in RIBF accelerator facilities (2016)

Y. Watanabe,*1 E. Ikezawa,*1 M. Kase,*1 S. Watanabe,*1 K. Yamada,*1
M. Nishida,*2 K.Oyamada,*2 J. Shibata,*2 K. Yadomi,*2 and A. Yusa*2

The RIBF accelerator facilities consist of three injectors (RILAC/CSM, RILAC2 and AVF) and four ring cyclotrons (RRC, fRC, IRC, and SRC), and more than 80 cryopumps are used for the main evacuation of these facilities[1-2]. The status of cryopumps in these facilities is listed in Table 1. The number of cryopumps and current vacuum pressures are the same as in 2015.[2] However, some facilities were affected by malfunctions and temporary shutdowns of cryopumps or cryopump compressors. In this paper, we report some cryopump problems encountered in 2016.

In the cryopump of RILAC-RF #6, the temperature has been fluctuating above 20 K since November. Though helium gas in the cryopump was replaced for improving purity, the fluctuations of temperature did not subside. The cause has still not been identified. As in 2015, a malfunction occurred again in the compressor of RILAC2-DTL3 in July, which was assumed to be due to the influence of ambient radiation caused by an increase in beam intensity. Therefore, a substitute compressor was relocated from the AVF vault to the mezzanine floor. Further, a malfunction occurred owing to age-related deterioration in the compressor of I-36 (AVF injection BT line) in December. Because the cryopump and compressor had been in operation for over 27 years, we plan to install a new compressor or a turbomolecular pump in FY2017.

In the cryopump of RRC, frequent helium leakages caused by age-related deterioration have been recently occurring in some flexible hoses and couplings. A helium leak occurred in a flexible hose on the compressor side for VN-CRP11, and we replaced the flexible hose with a substitute hose. A helium leak occurred in some couplings for RS-CRP11, RS-CRP22, and RN-CRP11, and we replaced the O-rings with new ones. Though a helium leak occurred in the cryopump for RN-CRP21, this leak was not investigated. We will repair it in February 2017. In the cryopump of fRC, the compressor of RE-CRP1 stopped temporarily once in April owing to overload, but is now operating in the local control mode. Subsequently, a malfunction occurred in this cryopump in October, but its source is not clear. We will repair it in February 2017. Since some components of the compressor deteriorated because of ambient radiation, the compressors of the IRC-NE valley were shifted a location just under the W-sector magnet in the summer of 2015.[2] However, the compressors of NEV-CP01 and CP03 stopped temporarily a few times in April. The radiation dose in this installed location may still be high. Therefore, these are offline from the IRC now. In the cryopump of SRC, many malfunctions and temporary shutdowns of the compressors frequently occurred in 2016 because some inverters and electrical components of the compressor deteriorated owing to ambient radiation and aging. A malfunction occurred in the compressors of RES1-CP02 and RES3-CP03 in December 2015, and two repaired compressors were reinstalled in August. Helium leakages occurred at RES2-CP03 in March and August, and helium gas was supplied accordingly. This leak has not been investigated in detail yet. The control boxes of a substitute compressor were replaced with a new box because of a malfunction in March. A malfunction occurred in the compressor of RES3-CP01 in September. This compressor is out of order now, and a substitute compressor has been installed. As listed in Table 2, some compressors stopped temporarily a few times in 2016, and almost all compressors are operating now in the local control mode. We plan to relocate the compressors to a location far from the region of high ambient radiation.

Table 2. Temporary shutdowns of compressors in SRC.

Device name	Month in which temporary shutdown occurred
RES1-CP04	February
RES3-CP02	February, April, and August
RES4-CP02	April and August
Substitute compressor for RES1-CP02	July
VLB2-CP01	August
VLB2-CP02	August

References
1) S. Yokouchi et al., Accel. Prog. Rep. **41**, 101 (2008).
2) Y. Watanabe et al., Accel. Prog. Rep. **49**, 142 (2015).

Table 1. Status of cryopumps in RIBF accelerator facilities.

	RILAC/CSM *	RILAC2 *	AVF *	RRC	fRC	IRC	SRC
Total volume (m^3) of facility	(72)	(6)	0.9	30	16	35	90
Number of cryopumps	13	9	2	14	6	14	22
Current vacuum pressure (Pa)	$0.1–1\times10^{-4}$ **	$4–7\times10^{-6}$	2×10^{-5}	$0.2–2\times10^{-5}$ **	$0.3–1\times10^{-5}$	$2–4\times10^{-6}$	$2–4\times10^{-6}$
Number of times problems occurred in 2016	1	1	0	5	2	3	12

* Excluding ion sources and beam transport lines.
** Vacuum leaks have been observed.

*1 RIKEN Nishina Center
*2 SHI Accelerator Service Ltd.

Operation report 2016 for Nishina and RIBF water-cooling systems

T. Maie,[*1] K. Kusaka,[*1] M. Ohtake,[*1] Y. Watanabe,[*1] E. Ikezawa,[*1] M. Kase,[*1]
M. Oshima,[*2] H. Hirai,[*2] K. Kobayashi,[*3] and J. Shibata[*3]

Operation condition

In FY2016, the Nishina and RIBF water-cooling systems were operated for six and five months, respectively. These operation periods correspond to the scheduled beam service time of RIBF, i.e., five months. In addition, Nishina's water-cooling system was used not only for full RIBF operation but also for the AVF standalone and AVF+RRC operations. During FY2016, there was no significant problem that resulted in beam service interruption for both Nishina and RIBF water-cooling systems. However, they were affected by minor problems.

Trouble report

Fortunately, we were not affected by the big trouble that canceled an experiment, but a water leak and cooling-water pump trouble occurred from a coupling and a connection part of the cooling plumbing. In addition, we encountered a movement defectiveness of the control valve which was damaged by radiation during the operation of the accelerator, and a trouble in the inverter for cooling-water pumps due to deterioration with, age accelerator driving depended on got up.

Periodic maintenance

Routine maintenance works listed below were performed during the scheduled summer and winter maintenance periods of the RIBF accelerators.

1) Cleaning of the cooling towers
2) Inspection and overhauling of the cooling-water pumps
3) Touch panel exchange for RIBF cooling system control
4) Inspection of the inverter of the RIBF water-cooling pumps
5) Inspection and overhauling of the air compressor
6) Replacement of some superannuated hoses, joints and valves used in the system
7) Cleaning of the strainers and filters used in the deionized water production system
8) Extension of the sensing wires of the water leakage alarm to floors of new areas

As usual, 2-3 times go the work that pro-backup, changes electricity and a cooling installation in a year during an accelerator outage to be affected by cooling facilities than a stop of steam and the cold water by rolling blackouts of RIKEN inside and a periodic inspection of the co-generation in the Nishina Center.

Establishment and improvememt

With the cooling facilities, we performed coolant pipelaying for K1 electromagnets in additionto an the update of the absorption-style refrigerator, the transference construction of the turbo system in the refrigerator this year. A high strength would improve the ability to cool the Faraday cup G01 which is a future plan, and RILAC upgrade plans the laying construction of cooling facilities for setting of cooling facilities for Helium refrigerator facilities for becoming it, GARIS2 to transfer.

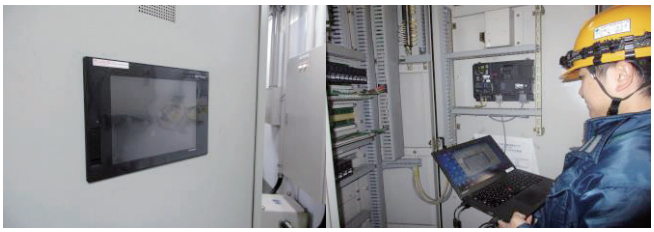

Fig. 1. Photograph of the touch panel exchange for control.

Fig. 2. Photograph of the inspection of the control system of the RIBF water-cooling system.

References

1) K.Ozeki et al., RIKEN Accel. Prog. Rep. 49 (2015) pp139.
2) T. Maie et al., RIKEN Accel. Prog. Rep. 49 (2015) pp143.
3) T. Maie et al., RIKEN Accel. Prog. Rep. 48(2014) pp197.

[*1] RIKEN Nishina Center
[*2] Nippon Kucho Service Co., Ltd
[*3] SHI Accelerator Service Co., Ltd

Integration of standalone control system into EPICS-based system at RIKEN RIBF†

A. Uchiyama,*1 M. Komiyama,*1 M. Fujimaki,*1 and N. Fukunishi*1

The major parts of the accelerator components developed for the RIBF have been integrated into the Experimental Physics and Industrial Control System (EPICS), but several standalone control systems were carried over and certain new components were provided with their own standalone control systems. These non-integrated systems are grouped into two major categories. The first is hard-wired control systems and the second is based on a two-layer remote control system, which consists of controllers and client PCs without a middle layer.The RILAC beam Faraday cup control was categorized as a hard-wired control system. We replaced the hard-wired devices with an N-DIM[1], and an EPICS input/output controller (IOC) provides the channel access (CA) service. Similarly, the Hyper ECRIS control system has been constructed as a standalone system with a closed network, for which the main controller was a MELSEC-A series programmable logic controller (PLC) as two-layer system. Hyper ECRIS is usually controlled with a Microsoft Windows-based client PC located in the ion source room. In this work, the conventional control method was not modified, and integration into the EPICS system was supplemented by introducing an EPICS IOC as a gateway between the RIBF control network and the closed network of the Hyper ECRIS control system. In the present study, we developed EPICS device support for a MELSEC-A series PLC. Thus, we could construct unified operator interfaces by utilizing CSS/BOY[2] because it is possible to also control the Hyper ECRIS control system to control from EPICS.

For the linear accelerator and the cyclotrons, the RF control systems are implemented as a two-layer system consisting of a client, based on Wonderware InTouch[3], and an OMRON PLC. Since the accelerator operators are familiar with the InTouch interface, it would not be beneficial to replace the GUIs to send output control commands to the PLCs. On the other hand, there is a need to monitor the RF data along with the other EPICS-based data, such as vacuum pressures, by creating charts and graphs. Therefore, the two-layer systems were left as they were for the accelerator operation, but we inserted a middle layer, based on EPICS, to monitor the data. When a new instrument is introduced, the control system may not be compatible with EPICS because human resources are required to develop the EPICS device support software. We mention that National Instrument LabVIEW is a suitable platform for the rapid prototyping of a system. In RIBF, LabVIEW-based systems with a two-layer structure are utilized for the monitoring of the beam phase and intensity[4], and other parameters. In addition, commercial systems are also implemented to monitor the temperature. To attain data integration, we considered an approach for handling and sharing the data. Since there is a need to store and analyze the data for a system with a two-layer structure, we introduced MyDAQ2 as a common DAQ system for small non-EPICS-based systems[5]. The MyDAQ2 system can store data in a MySQL-based database by sending an ASCII command and allow viewing of the stored data via a Web application. One of the beneficial features of MyDAQ2 is that it is possible to easily develop a program to store data from other client systems. In addition, by utilizing a JavaScript chart library, we realized a chart feature with a significantly higher level of performance than the original MyDAQ2 chart feature, which used gnuplot. Thus, the administrator can store data from LabVIEW-based and commercial systems via MyDAQ2. In order to integrate the data for LabVIEW-based and commercial systems, we developed a system capable of handling the data stored in a MyDAQ2 by using EPICS CA. This system is illustrated in Fig. 1. Simply by inserting data into MyDAQ2, data in the CA protocol can be flexibly acquired, even if the system is a non-EPICS-based system. In our study, the control system integration was successfully completed, and we can currently handle the data of nearly all the RIBF components in an integrated manner.

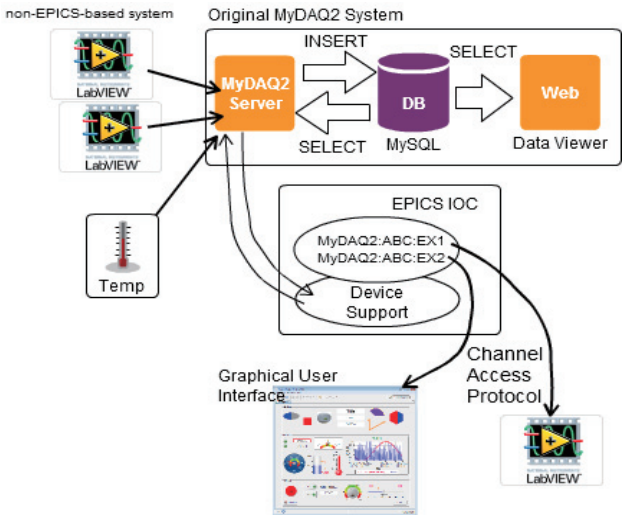

Fig. 1. EPICS IOC for MyDAQ2. Newly stored data can be obtained from the MySQL-based database via EPICS IOC.

References

1) M. Fujimaki et al., RIKEN Accel. Prog. Rep. **37**. 279 (2004).
2) M. Nishimura et al., Proc. PASJ16, Chiba, Japan, p. 660.
3) R. Koyama et al., RIKEN Accel. Prog. Rep. **37**. 122 (2007).
4) https://www.wonderware.com/hmi-scada/intouch/
5) T. Hirono et al., Proc. PCaPAC08, Ljubljana, Slovenia, p. 55.

† Condensed from the article in Proc. PCaPAC2016. No. WEPOPRPO11

*1 RIKEN Nishina Center

Introduction of visualization system for RIBF control network monitoring

A. Uchiyama,[*1] M. Komiyama,[*1] M. Fujimaki,[*1] and N. Fukunishi[*1]

The RIBF control system is a distributed control system consisting of various types of Ethernet-based modules, VME-based modules, programmable logic controllers, and so on.[1] In the case of the Ethernet-based module, the LAN is also utilized as a field bus of Ethernet-based modules. The network switches for the control system LAN are installed in the whole area of the RIBF accelerator facility including RILAC and AVF.

As mentioned above, since the control system LAN is used not only for various services, but also as a fieldbus, it is an essential part of the infrastructure of the RIBF control system. For this reason, in order to make the RIBF control system highly reliable, an alive monitoring feature for the LAN is necessary. On the other hand, when backing up a large amount of data such as the image file of the virtual OS, the usage rate of the network bandwidth and the response speed decrease in some cases. Therefore, network traffic monitoring between the network router and the switches is also needed for stable accelerator operation. Because the network monitoring and switch management are very important, we introduced a network visualization system for the RIBF control network.

Considering network monitoring, the following two key protocols are utilized to construct this visualization system. One is the simple network management protocol (SNMP). SNMP is adapted to monitor the network switch state. SNMP is an application layer protocol for monitoring and controlling communication devices connected to a TCP/IP network, such as a network router, switch, and server, via a network. For example, a network router sends the information of its system health, which includes memory usage, CPU load average, and so on, to the SNMP manager from the SNMP agent. Another is the NetFlow protocol, which is a feature to be introduced to correct network traffic data on Cisco routers and it can passively monitor traffic flowing over a network.[2] In the RIBF control system, the network topology is a star type, adopting Cisco Catalyst 4506 as the network router in the center of the LAN. It is suitable for monitoring with NetFlow because Cisco Catalyst 4506 has a feature of sending the data passed through the router from each network switch as NetFlow protocol, if only plug-in is installed. In order to visualize data of NetFlow and SNMP, we adopted the commercial software PRTG[3] and constructed a monitoring system. As a result of testing the NetFlow collection software, we confirmed that its implementation is inexpensive in term of both introduction and daily operation. In addition to low cost, the reason for adopting PRTG is that it is available to collect and visualize data of both SNMP and NetFlow protocols. Moreover, it can monitor the service port of the server, such as the address resolution protocol (ARP), hypertext transfer protocol (HTTP), and file transfer protocol (FTP). In the usual case, the PRTG is installed in the server computer and collects the NetFlow data, which is transmitted by UDP from the network router. The specifications of the server computer for PRTG are a Xeon E3-1220v3 CPU (3.1GHz), 16 GB memory, and a TB RAID1 hard disk. By utilizing a Web application as the user interface of PRTG, it is possible to view the data not only from the control system network but also from the office network via the proxy server.[4] A screen capture of the user interface for PRTG is shown in Fig. 1.

As a result, it possible to check the status of all the network switches via the Web by using SNMP, for example, the high load average for the network switches and fan failure situation. Since we can analyze the data traffic volume at the protocol level by using NetFlow, this network visualization system can help minimize the system risk such as network performance degradation caused by insufficient network bandwidth.

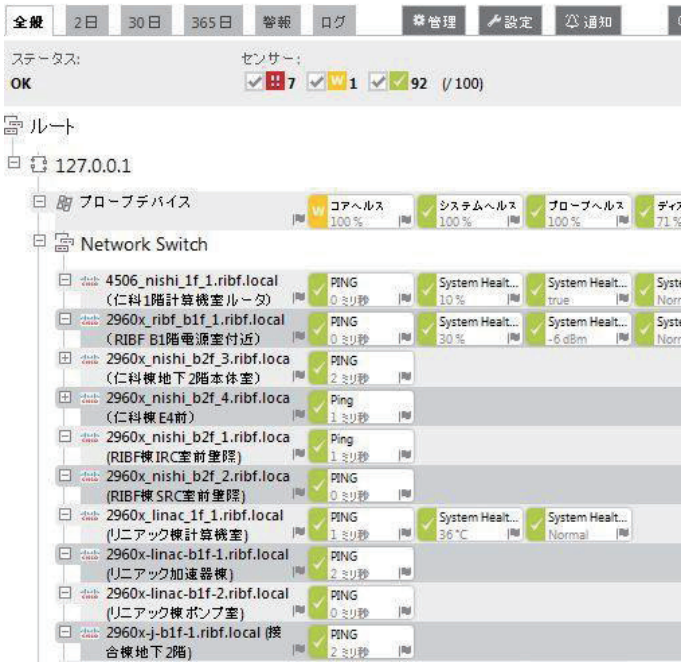

Fig. 1. Screen capture of Web-based user interface for PRTG.

References

1) M. Komiyama et al. Proc. ICALEPCS 2013, San Francisco, CA, USA (2013), p. 348.
2) http://www.cisco.com/go/netflow
3) https://www.paessler.com/
4) A. Uchiyama et al. Proc. ICALEPCS 2011, Grenoble, France (2011), p. 1161.

*1 RIKEN Nishina Center

Improvements of the RIBF control system

M. Komiyama,[*1] A. Uchiyama,[*1] M. Fujimaki,[*1] N. Fukunishi,[*1] and M. Hamanaka[*2]

We report on two improvements of the RIBF control system. One is the completion of update of an aged controller, DIM,[1] used in the RILAC control system, while the other is an improvement of the alarm system to support stable beam delivery during a long-term experiment.

In the RIBF control system, various types of old and new controllers are mixed for interfacing with each controlled object used in the RIBF accelerator complex. Because the supply of many parts used in these old controllers has been terminated, we have been successively replacing the old controllers with new ones every year. Especially, the DIM module, an in-house controller developed for beam diagnostic equipment, vacuum systems and magnet power supplies in our old facility, is the oldest controller in the RIBF control system. Hence, we have been replacing DIM with N-DIM[2], an in-house controller newly developed as a successor to DIM in 2003. As a result, most of the DIMs have been updated to N-DIMs up to last year. However, we found a problem in the data acquisition of the program used in the N-DIM system last year. After refurbishment of the program and repeated operation tests, we confirmed the normal operation of N-DIMs early in this year. Subsequently, we updated the remaining DIMs used for controlling the magnet power supplies of the RILAC accelerator complex to N-DIMs this summer. Consequently, the update of all the DIMs in the RILAC control system was completed, which results in a reduction of the number of the CAMAC crate controllers used in RIBF from 6 to 5. The model of the CAMAC crate controller in use[3] is not available commercially now and we should terminate its operation with DIM as soon as possible. N-DIM, when used as a controller of magnet power supplies, needs a slightly longer response time than DIM, even after recent updates of the program handling procedures of post-monitoring and the analysis of the network packet of N-DIM this year. We have not completely overcome the response-speed problem, and further improvements are needed.

The second improvement is related to hardware protection under high-intensity operations of the RIBF accelerator complex frequently performed in the past few years. Because the present typical beam intensity causes heat loads much higher than the allowable values for components used in the accelerators, malfunction and hardware troubles of the control system may seriously damage the hardware. Therefore, the malfunction of equipment should be detected as soon as possible, and when a problem occurs during an experiment, the operator is required to fix its cause and, if possible, remove it immediately. Therefore, we have started to upgrade the existing alarm system, which covers only some components of the ion source. We newly installed a distributed alarm system, the Best Ever Alarm System Toolkit (BEAST)[4] based on the Control System Studio (CSS)[5] platform. The BEAST was chosen taking into account the future extension of the CSS at the RIBF control system instead of upgrading the existing Alarm Handler[6]. As the first step of the alarm system upgrade, the vacuum status of the entire RIBF accelerator complex, including the status of vacuum pumps, gate valves, and vacuum pressures, was registered in the BEAST. The BEAST outputs a warning signal when the opening-closing status of a valve changes, a vacuum pump stops, or a change of vacuum pressure higher than its pre-determined limit is detected. In addition, the difference between the set and read-back value of the excitation currents of all the magnet power supplies of the RIBF accelerator complex was registered in the BEAST. The BEAST outputs a warning signal when the ratio of the read-back current value to the set value is less than 50%. We registered approximately 700 signals in the BEAST, and its test operation was started in April 2016. Toward more efficient operation, we are now investigating how to set the optimal alarm criterion patterns for each experiment in the BEAST. Since there are 65 beam operation patterns with different combinations of ion sources, accelerators, and experimental vaults, it is necessary to activate signals relevant to the experiment of running at a particular time.

References

1) K. Shimizu et al., Proc. Cyclotrons ’84, (1984), p. 392.
2) M. Fujimaki et al., RIKEN Accel. Prog. Rep. 37, 279 (2004).
3) http://www-online.kek.jp/~yasu/Parallel-CAMAC/
4) https://github.com/ControlSystemStudio/cs-studio/wiki/BEAST
5) http://controlsystemstudio.org/
6) http://www.aps.anl.gov/epics/extensions/alh/

*1 RIKEN Nishina Center
*2 SHI Accelerator Service Ltd.

Long term operation of low charge state laser ion source†

M. Okamura,*1,*2 S. Ikeda,*1,*3 and T. Kanesue*1

In March 2014, a laser ion source (LIS) that delivers high-brightness low charge state heavy ions for the hadron accelerator complex in Brookhaven National Laboratory (BNL) was comissioned. Since then, the LIS has provided many heavy ion species successfully. The induced low-charge-state (mostly singly charged) beams are injected to the electron beam ion Source (EBIS),[1] where ions are heavily ionized, e.g., Au^{32+}, to fit to the ensuring accelerator's Q/M acceptance. To provide various species[2] to NASA space radiation laboratory (NSRL), more than ten materials are installed in the laser irradiation chamber, and the target can be changed in a few seconds. In 2015, we installed another laser and an additional disk-shaped target to provide a gold beam to the relativistic heavy ion collider (RHIC). Now the LIS provides beams to two user facilities simultaneously.

Although the LIS was a newly conceptualized ion source and we encountered many minor difficulties as expected, we could provide various heavy-ion beams with almost no down time during the past runs. Table 1 shows the operation days. Run 17 has already started, and the LIS is providing beams to the following accelerators now.

Table 1: Total days of operation.

		Li	B	C	O	Al	Ca	Si	Ti	Fe	Ta	Au
Run14 (since March 25, 2014)	NSRL (days)			2				11	1	18	1	3
	RHIC (days)											33
Run15	NSRL (days)	1		2			1	18	4	30		6
	RHIC (days)					14						42
Run16	NSRL (days)		1	5	9			13	5	33	4	1
	RHIC (days)											198

We have experienced many types of the failures. Initially, we planned to rotate the gold disk target with a constant velocity. However, the continuous revolution of the mechanical shafts destroyed some bearings since they are in a vacuum condition. Therefore, we employed the step scanning of the rotating target. By applying an intermittent rest condition, accumulated heat can be conducted from bearings. We also replaced some ceramic ball bearings to Vespel bushings.

In 2016, we found heavy accumulation on the gold target. An enlarged photo of the accumulation is shown in Fig. 1. The shown build-up was formed from evaporated material, since we had operated the beam or almost two hundred days continuously. Unfortunately, some chunks of gold were stuck on the target surface and caused unstable beam condition. For the next run, we modified the target cover and installed a carbon fiber brush to scrape off the accumulations.

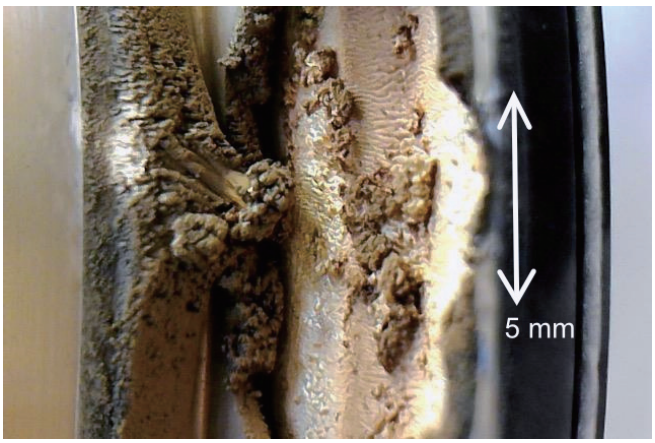

Fig. 1. Accumulation caused by vaporized gold.

The vacuum window for the laser path is one of the vulnerable parts in a laser ion source. The window is 1.8 m away from the target at an angle of 30° from the plasma expanding axis. Since the plasma expands within about 20°. the off-set position of the window helps to reduce direct exposure from the dense plasma. Even under this condition, after one season's exposure, the window was darkened. The outside surface has AR coating, but the inner surface has no coating since a slight accumulation could easily dirupt the AR condition. On the laser path, the deposited laser energy helps to keep clean the inner surface of the window. The laser transmission on the laser spot reduced to 4 %, the remaining area absorbs 9 % of the laser energy.

We also experienced an energy drop in one of the laser systems. The laser had been in standby mode for a month at a steady temperature of 38 °C. This warm water condition could cultivate algae in the water circulation system and degrade the reflectors installed around the laser flash lamps. Now, we avoid a long standby mode and apply UV sanitization when the cooling water is replaced.

The LIS has operated successfully since 2014. Although we had some failures, those experiences help us improve the overall reliability of the LIS.

References

1) J. Alessi *et al.*, *Rey. Sci. Insrtum.*, 81, 02A509 (2010).
2) M. Okamura *et al.*, *Rev. Sci. Instrum.*, *87, 02A901 (2016)*.

† Condensed from the article in Proceedings of North American Particle Accelerator Conference, MOA4I01 (2016)

*1 Collider-Accelerator Department, Brookhaven National Laboratory
*2 RIKEN Nishina Center
*3 Radiation Laboratory, RIKEN

RFQ and IH linac for SLOWRI post accelerator

S. Arai*1 and M. Wada*1

A post accelerator for SLOWRI [1] has been conceptually designed [2]. This accelerator has a 100% duty factor and is a normal conductive linear accelerator complex composed of a 79-MHz split-coaxial RFQ, a medium-energy beam transport, and a 158-MHz interdigital-H (IH) linac. In the review of this design, the following tasks have been performed: 1) the vane length of RFQ was made as short as possible without change of input and output energies and 2) the output beam energy of the IH linac was increased from 1.5 to 5 MeV/u. In order to shorten the vane length of RFQ, the maximum value of the mass-to-charge ratio (A/q) was changed from 9 to 8, the synchronous phase was changed from -30 to -25º, and the vane voltage was changed from 65.1 to 81.5 kV. On the other hand, the normalized emittance of the RFQ beam was increased to 0.06 π cm·mrad to ensure a capture efficiency higher than 90% of the beam from an ion source. As a result of the new design [3], the vane length of the RFQ was decreased by about 2 m, as indicated in Table 1.

Table 1. Main RFQ parameters of the 1st and 2nd versions

Parameter	1st version	2nd version
Mass to charge ratio: *A/q*	9	8
Normalized emittance (π·cm mrad)	0.047	0.06
Input and output energy (MeV/u)	0.005 and 0.5	0.005 and 0.5
Output synchronous phase (deg.)	-30	-25
Vane voltage (kV)	65.2	81.5
Kilpatrick factor	1.57277	1.6573
Transmission (%)	92.2	93.4
Number of cells	290	244
Vane length (m)	7.193	5.1925
Mean bore radius (cm)	0.541	0.6415
Cavity diameter (cm)	30	40
Number of cavity modules	18	15
RF power loss (kW)	186	179

In the new design, the IH linac accelerates ions with an A/q of 8 or less from 0.5 to 5 MeV/u. The IH linac comprises 18 tanks and 18 quadrupole doublets to make the output energy variable. Quadrupole doublets are placed in a short space of 42 cm between the tanks. The main parameters of the IH linac are listed in Table 2. The gap voltage of each tank was determined to be between 140 and 250 kV because X-rays due to electron field emission are controlled to a relatively low intensity. The gap length of each tank was determined to ensure that the gap electric field is 100 kV/cm. The phase spread of bunches along the beam axis depends on the number of gaps in each tank, especially in the low-energy region. To ensure that the phase spread is within ±25º around a synchronous phase of -25º, the number of gaps from the 1st to 6th tanks is determined to be 16, 8, 12, 12, 13, and 14. The number of gaps beyond the 6th tank is determined automatically to be as large as possible under the limit that the maximum number of gaps is 15 and the maximum tank length is 1 m. Transverse motion of the beam is controlled with quadrupole doublets. Phase advance of the betatron oscillation per focusing period composed of a tank and a quadrupole doublet is set at 54º, except for 36º at the 2nd period. The maximum magnetic field of the quadrupole doublet is about 5 kG/cm at the 18th focusing period. The four transverse ellipse parameters (α_x, α_y, β_x, β_y) should be varied smoothly over all focusing periods. Therefore, by using the four quadrupole magnets set in the 1st and 2nd periods, four parameters at the end of the 2nd period are adjusted to be equal to them at the beginning of the 3rd period. In the same manner, between the 4th and 5th periods, etc., four parameters are connected smoothly. Fig. 1 shows the results of beam simulation using 1000 particles.

Table 2. Main parameters of the IH linac

Parameter	Value
Mass to charge ratio: *A/q*	8
Normalized emittance (π·cm mrad)	0.06
Input and output energies (MeV/u)	0.5 and 5
Transmission (%)	99.9
Synchronous phase (deg.)	-25
Gap voltage (kV)	140 - 250
Gap length (mm)	14 - 25
Kilpatrick factor	0.74293
Drift-tube bore radius (mm)	10 - 14
Tank radius (mm)	190 - 203
Tank length (mm)	300 - 1008
Number of tanks	18
Quadrupole magnet (kG/cm)	3.22 - 5.05
RF power loss (kW)	1270

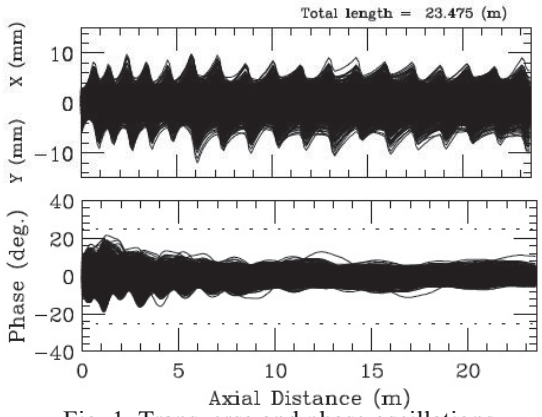

Fig. 1. Transverse and phase oscillations.

*1 RIKEN Nishina Center

References
1) M. Wada et al., Hyp. Int. **199**, 269 (2011).
2) S. Arai, M. Wada, RIKEN Accel. Prog. Rep. **47**, 206 (2014).
3) S. Arai, RIKEN-NC-AC-3, 2016.

Simultaneous acceleration of ions with different charge-to-mass ratio in the SLOWRI post accelerator

S. Arai*1 and M. Wada*1

To accelerate beams from SLOWRI, [1] a post accelerator consisting of a split-coaxial RFQ, a medium energy beam transport (MEBT) and an interdigital-H linac (IH) has been designed. [2] The main parameters of the accelerator are listed in Table 1. For the sake of experimental convenience, there is a demand to simultaneously accelerate the same element having different charges. Then, the transmission efficiencies of ions with charge-to-mass ratio (q/A) deviating from the design value of 0.125 are investigated by beam simulations. A calculation code PARMTEQ is used for RFQ simulation, and a calculation code TRACEP [3] is used for MEBT and IH simulations. PARMTEQ cannot calculate the motion of ions with q/A as a variable without

Table 1. Main parameters of the SLOWRI post accelerator.

Parameter	RFQ	MEBT	IH
Frequency (MHz)	79	79	158
Mass to charge ratio: *A*/*q*	8	8	8
Normalized emittance (π·cm mrad)	0.06	0.06	0.06
Energy (MeV/u)	0.005 - 0.5	0.5	0.5 - 5
Synchronous phase (deg)	-25	-90	-25
Electrode voltage (kV)	81.5	82.5	140-250
Number of cavities	1	1	18
Number of acceleration cells in each cavity	244	4	8 - 16
Length (m)	5.19	2.52	23.48
Cavity diameter (cm)	40	25	40

changing the vane parameters from the design values. However, the calculation with vane voltage as a variable is possible. Since the vane voltage is inversely proportional to the charge-to-mass ratio, for example, the simulation result obtained with a normalized vane voltage ($V_n=V/V_{design}$) of 1.08 can be regarded the same as the simulation result obtained with $V_n=1$ and q/A=0.135. By using the above characteristic, a beam simulation of the post accelerator, which accelerates ions with q/A different from the design value, is conducted using 500 ions as follows: 1) The operating parameters such as accelerating voltage, Q-magnet field strength, etc. are fixed to accelerate the design ions. 2) The phase space distributions of the output ions of RFQ calculated with V_n as a variable and the q/A corresponding to V_n are used as input data for MEBT simulation. 3) The phase space distributions and q/A of the output ions of MEBT are used as input data for IH simulation. Figure 1 shows the simulation result for the q/A=0.135 ions. From the number (297) of ions distributed in the IH output phase spaces, the beam transmission is found to be 59.4%. By using the above method, beam

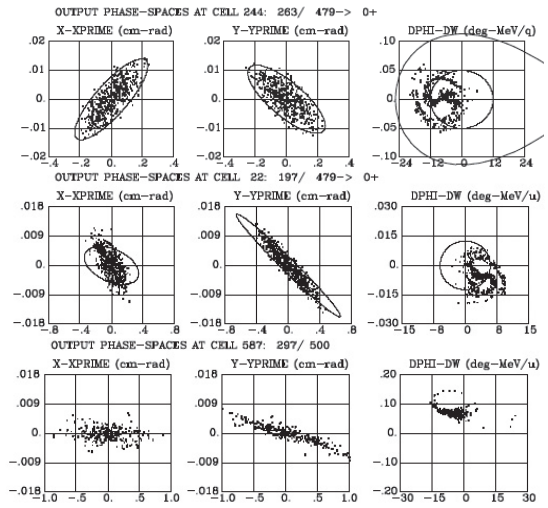

Fig. 1. From top to bottom, results of RFQ, MEBT and IH.

transmission is examined in the range of 0.1125≤q/A≤0.1525. The result drawn in red in Fig. 2 is obtained by assuming that the input energy of RFQ is 5 keV/u even for ions different from design ions. However, the kinetic energy per nucleon of ions extracted from the same ion source depends on the charge number of ions. The result of considering this is drawn in green in Fig. 2. The full width at half maximum of the transmission indicated by the green line is mainly determined by the acceleration characteristic of RFQ related to the input energy of ions. [4]

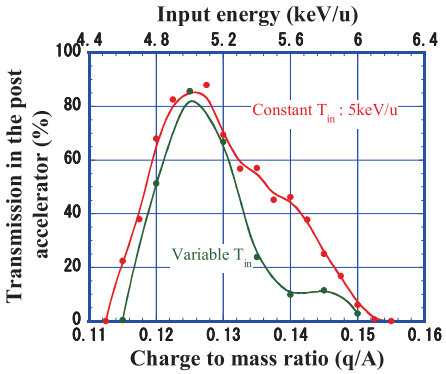

Fig. 2. The q/A dependence of the transmission.

References

1) M. Wada et al., Hyp. Int. **199**, 269-277 (2011).
2) S. Arai, RIKEN-NC-AC-3, 2016.
3) S. Yamada, NIRS HIMAC program manual No. 1, May, 1990, unpublished.
4) S. Arai, RIKEN-NC-AC-6, 2017.

*1 RIKEN Nishina Center

9. Instrumentation

Development of beam trigger detector with compact geometry

N. Chiga,[*1] A. Hirayama,[*1,*2] S. Takeuchi,[*1,*2] T. Sumikama,[*1] K. Yoshida,[*1] D. Ahn,[*1] H. Suzuki,[*1] and H. Otsu[*1]

A new scintillation detector used as a focal plane beam trigger detector was developed for the ImPACT experiment. The beam is spread over a wide acceptance of the ZeroDegree spectrometer in the momentum dispersive mode used in this experiment. This scintillation detector was required to cover a large effective area of 240×150 mm^2, which is the same as that of PPAC.[1] The effective area of the present scintillation detector[2] is 120×100 mm^2, which is smaller than that of PPAC. Because the vacuum chamber at F11 of ZeroDegree is not large enough to install a wide scintillator with the present PMT of H7195, the compact PMT of R11265U-200 is used for the new detector. The use of R11265U-200 has the following advantages compared with H7195: the length of 32.5 mm of this PMT is much smaller than that of 215 mm of H7195. The PMT has a transit time of 5.8 ns, which is shorter than that of 40 ns of H7195.

The specifications of the new beam line trigger detector are listed in Table 1. The new detector, which satisfies the requirement of the effective area, is smaller than present detector of 670 mm×100 mm. The new detector can be used at other focal planes on the beam line at BigRIPS, ZeroDegree, or SAMURAI.

Table 1. Specifications of the detector.

Effective area (H × V)	240 × 150 mm^2
Scintillator	EJ-200, 0.2 mm^t
PMT	R11265U-200 ×4
Size of detector (H × D)	524 mm × 100 mm
Requirement of time resolution	less than 100 ps

Figure 1 shows a schematic view of the new detector. Four PMTs of R11265U-200 were attached on the left and right side of the new detector. To ensure that light from the scintillator is effectively collected in the PMT, light guides are used as optical connection between them. The PMTs and light guides were bonded by an optical cement using a dedicated jig to provide a position accuracy within 0.5 mm. The light guides work as a support frame of a thin scintillator. The scintillator was mounted on the light guides using optical grease. It can be easily replaced with a different scintillator. A scintillator with a thickness of 0.1 - 0.5 mm can be mounted.

The new detector successfully worked in the ImPACT experiments in spring and autumn 2016. The time resolution of the difference between left and right timings, which was the average of up and down PMTs for each side, was 43 ps as shown in Fig. 2.

This work was funded by ImPACT Program of Council for Science, Technology and Innovation (Cabinet Office, Government of Japan).

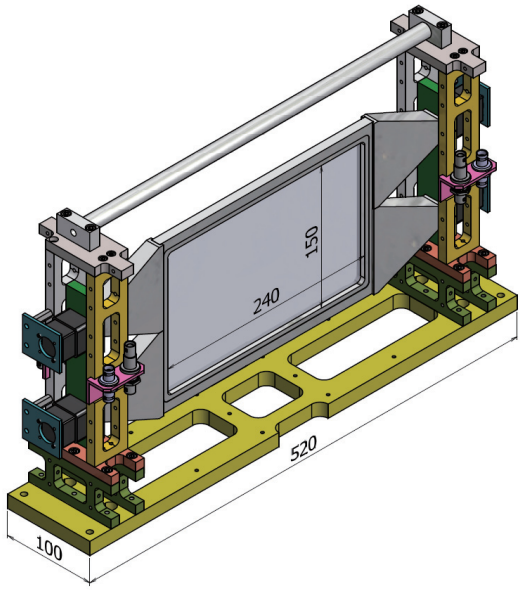

Fig. 1. Schematic 3D-CAD model of the new detector.

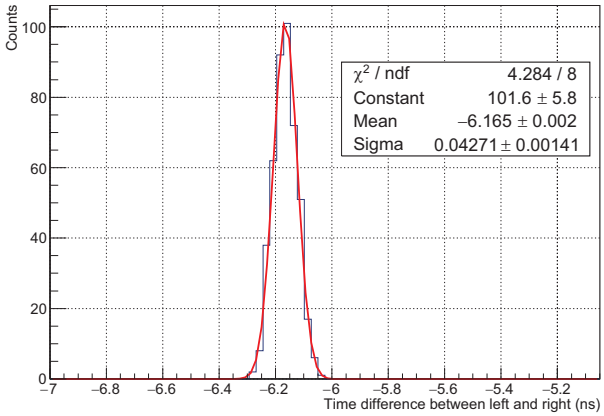

Fig. 2. Time difference between the left and right timings for the secondary beams in the vicinity of ^{93}Zr at 58 MeV/u. The timing average of two PMTs on each side was used.

*1 RIKEN Nishina Center
*2 Department of Physics, Tokyo Institute of Technology

References

1) H. Kumagai et al., Nucl. Instrum. Methods. **B317**, 717 (2013).
2) T. Ohnishi et al., RIKEN Accel. Prog. Rep. **42**, 159 (2009).

Development of new ionization chamber for low energy heavy ions

N. Chiga,[*1] A. Hirayama,[*1,*2] K. Chikaato,[*1,*3] K. Nakano,[*1,*4] J. Suwa,[*1,*4] S. Kawakami,[*1,*5] S. Takeuchi,[*1,*2] D. Suzuki,[*1] T. Sumikama,[*1] and H. Otsu[*1]

A new multiple-sampling ionization chamber (MUSIC) was developed for the ImPACT experiment[1] in which measurements at 50MeV/nucleon were performed. A charge is read from pads divided into fifteen units in the beam direction. All fragments produced by the secondary reaction at the F8 focal plane were stopped inside of the MUSIC, and a ranges and the energy loss of the incident particles were measured in each segmented pad. To measure the fragments of different ranges at the same time, the length of the effective area in the beam direction is required to be approximately 750 mm, although the length of a previous MUSIC[2] at F11 was 480 mm. The previous MUSIC had many anode and cathode films on the beam trajectory; therefore, a large energy loss in the films near the Bragg peak cannot be measured. In order to overcome these demerits, the new MUSIC, which has an effective length of approximately 750 mm and consists of only counter gas in the effective area, was developed. The size of the new ionization chamber is summarized in Table 1.

Figure 1 shows a field cage and a readout pad with Frisch-grid. A high voltage of 4 kV is applied between top and bottom plates, and the electrons are drifted to the top (anode) side. An entrance window with vapored Au electrodes on a Mylar film with uniform thickness of 4 μm was adopted to uniform a thickness of substance. Fig. 2 shows a contour plot of the electric-field gradient inside the detector by GARFIELD[3]. The electric-field gradient inside the cage was zero. The Frisch-grid was used to decrease the effect of charges induced by ions for readout pad. The Frisch-grid is made in consideration of the aperture to the pad and the uniformity of the electric field. The drifted electrons pass through the Frisch-grid and are detected in a readout pad. The readout pad show the backgammon electrode structure[4] for position sensitivity. The size of one unit is 50.5 × 280 mm. The readout pad consists of 15 units of electrodes, and the total size of the effective area is 757 × 280 mm. The MUSIC was successfully operated in the ImPACT experiments in autumn 2016[1]. Analysis of particle identification is in progress.

This work was funded by ImPACT Program of Council for Science, Technology and Innovation (Cabinet Office, Government of Japan).

Table 1. Specifications of ion chamber.

Effective area (X × Y × Z)	260 × 170 × 757 mm^3
Electric field cage size	369 × 194 × 780 mm^3
Gas box size	700 × 440 × 1000 mm^3

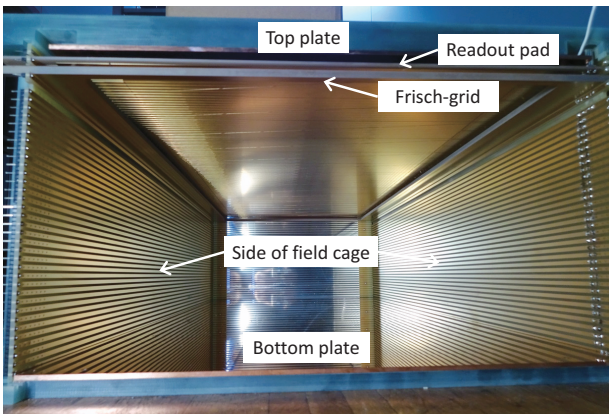

Fig. 1. Photograph of a field cage and a readout pad with a Frisch-grid.

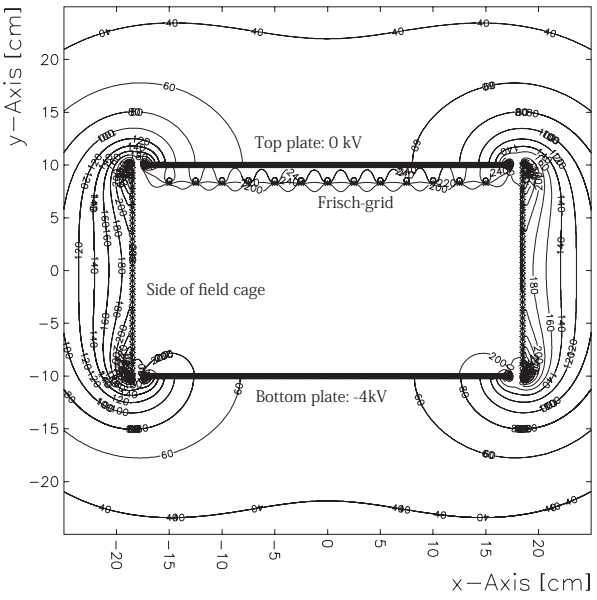

Fig. 2. Contour plot of the electric-field gradient calculated using GARFIELD.

*1 RIKEN Nishina Center
*2 Department of Physics, Tokyo Institute of Technology
*3 Department of Fundamental Sciences, Niigata University
*4 Department of Advanced Energy Engineering Sciences, Kyushu University
*5 Department of Applied Physics, Faculty of Engineering, University of Miyazaki

References

1) T. Sumikama et al., in this report.
2) H. Otsu et al., RIKEN Acc. Prog. Rep. **42**, 163 (2009).
3) R. Veenhof:, GARFIELD, a drift-chamber simulation program, CERN (1994).
4) R. Allemand, G. Thomas: Nucl. Instr. Meth. **137**, 141 (1976).

Development of energy-control method for slowed-down ^{93}Zr beam

T. Sumikama,[*1] D. S. Ahn,[*1] N. Fukuda,[*1] Y. Shimizu,[*1] H. Suzuki,[*1] H. Takeda,[*1] H. Wang,[*1] N. Chiga,[*1] H. Otsu,[*1] H. Sakurai,[*1] S. Kawase,[*2] Y. Togano,[*3] A. Saito,[*3] K. Yoshida,[*1] N. Inabe,[*1] S. Kubono,[*1] K. Nakano,[*2] J. Suwa,[*2] Y. Watanabe,[*2] S. Takeuchi,[*3] T. Tomai,[*3] A. Hirayama,[*3] M. Matsushita,[*4] S. Michimasa,[*4] S. Shimoura,[*4] M. Takechi,[*5] K. Chikaato,[*5] and J. Amano[*6]

The spallation reaction of the long-lived fission product (LLFP) in nuclear waste might be a key reaction for nuclear transmutation. The spallation cross sections for the LLFPs were measured on proton and deuteron targets via the inverse kinematics method using the RI beam with an energy of 185 MeV/u at RIBF.[1] For the cross-section measurement at ∼100 MeV/u,[2,3] the aluminum energy degrader was used to slow down the RI beam. At a lower energy such as 50 or 20 MeV/u, the inaccuracy of the energy-loss calculation becomes relatively larger. A new control method of the RI-beam energy was developed for quick and precise tuning.

The RI beam of ^{93}Zr was produced using a ^{238}U primary beam with 345 MeV/u impinging on a 7-mm Be target. The aluminum energy degraders were placed at foci F1 and F5, which were the momentum dispersive focal planes of the first and second stages of the BigRIPS separator. The thicknesses of the F1 and F5 degraders were 4 mm and 0.5 mm, respectively. The F1 slit was ±1 mm. A 90-mg/cm^2 carbon target was prepared supposing the spallation-reaction measurement. The goal energy at the center of the carbon target was 50 MeV/u, and the energy without the carbon target was expected to be 60 MeV/u using the energy-loss calculation in the target. The energy without the carbon target was measured to be 51.1 MeV/u by using the time of flight in the ZeroDegree spectrometer, as shown in Fig. 1. The magnetic rigidity $B\rho_{01}$ of the first dipole was increased by 1.24% based on the calculated relation between $B\rho_{01}$ and the energy in the ZeroDegree spectrometer. The magnetic rigidities of other dipoles were readjusted. The energy became 60.4 MeV/u, which was almost same as the goal energy of 60 MeV/u. Hence, $B\rho_{01}$ was changed again by −0.37% because the average of the energies with and without the carbon target, 53 MeV/u, was slightly large. The final energy average, 50.1 MeV/u, was remarkably close to the goal energy: it was obtained by averaging the peak energies of the two energy distributions as indicated by the red line in Fig. 1.

For the 20 MeV/u setting, the thickness of the F1 degrader was changed to 5 mm. Two energies with and without a CH_2 target with a 17-mg/cm^2 thickness

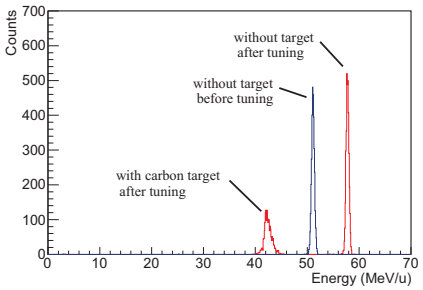

Fig. 1. Energy distributions of the ^{93}Zr beam before (blue) and after (red) the $B\rho$ tuning of dipoles in the BigRIPS separator. The goal energy at the center of the carbon target was 50 MeV/u, and 50.1 MeV/u was achieved.

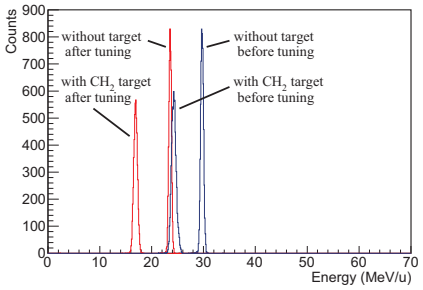

Fig. 2. Energy distributions before (blue) and after (red) the $B\rho$ tuning of dipoles for the 20 MeV/u setting of the ^{93}Zr beam.

were measured for an initial condition to obtain the average, which was 27.0 MeV/u, as shown in Fig. 2. An average energy of 20.2 MeV/u was successfully obtained after $B\rho_{01}$ was changed by −0.56%. The energy after the CH_2 target was 16.9 MeV/u and its width was 0.82 MeV/u (FWHM), which corresponds to 2.4% (FWHM) in momentum. The position and angle distributions on a secondary target were also optimized in a later experiment.[4]

This work was funded by ImPACT Program of Council for Science, Technology, and Innovation (Cabinet Office, Government of Japan).

References

1) H. Wang et al., Phys. Lett. B **754**, 104 (2016).
2) H. Wang et al., RIKEN Accel. Prog. Rep. **49**, 8 (2016).
3) S. Kawase et al., RIKEN Accel. Prog. Rep. **49**, 87 (2016).
4) T. Sumikama et al., RIKEN Accel. Prog. Rep. **50** (submitted).

*1 RIKEN Nishina Center
*2 Department of Physics, Tokyo Institute of Technology
*3 Faculty of Engineering Sciences, Kyushu University
*4 Center for Nuclear Study, University of Tokyo
*5 Department of Physics, Niigata University
*6 Department of Physics, Rikkyo University

Slowed-down RI beams of ^{93}Zr and ^{107}Pd at 50 MeV/u produced for spallation reaction

T. Sumikama,[*1] D. S. Ahn,[*1] N. Fukuda,[*1] Y. Shimizu,[*1] H. Suzuki,[*1]H. Takeda,[*1] and K. Yoshida[*1]
for ImPACT-RIBF collaboration

The spallation-reaction cross sections of long-lived fission products (LLFPs) on proton and deuteron were measured at ∼100 and 200 MeV/u at RIKEN RIBF to search for a method to transmute LLFPs in nuclear waste[1–3]. In the present study, RI beams of ^{93}Zr and ^{107}Pd were provided for the measurement at an energy of 50 MeV/u. The control method of the RI beam energy was established in a previous experiment[4]. This report gives an outline of RI beam production and new developments, and approaches.

Figure 1 shows a schematic view of the experimental setup. The RI beams of ^{93}Zr and ^{107}Pd were produced and separated in the BigRIPS separator using a ^{238}U primary beam and a 7-mm Be target. The thickness of the aluminum degraders at F1 and F5 were 5 mm and 0.5 mm, respectively. The maximum intensity of the primary beam was used to make the emittance of the RI beams small. Under the standard operation, the acceptance of the momentum and position distributions can be changed by the slits at the momentum dispersive and achromatic foci, respectively, but the angle distribution is retained. Two new methods were developed to control the angle distributions in the horizontal (X) and vertical (Y) directions. For the X direction, a narrow second slit (Joker slit) at F1 was used as shown in Fig. 2. The RI beams with a large angle were stopped in the Joker slit by the use of narrow slit widths. For the Y direction, the focus position of Y at F2 was changed from the F2 slit position. Because the defocus beam on the slit has a correlation between the angle and position, RI beams with a large angle were stopped in the F2 Y slits with a narrow width of ±2 mm. The position and distribution for ^{107}Pd are shown in Fig. 3.

Fragments measured in the ZeroDegree spectrometer are produced not only in a secondary target but also in the detectors at F7 and F8. Although the contribution from the detectors is subtracted by using the data without the secondary target, a thinner detector combination can increase the sensitivity of the measurement. The ionization chamber (140 mg/cm^2) at F7 for the atomic number Z determination of the RI beam was removed, because Z was determined from the energy loss in the F5 degrader instead[5].

The momentum dispersive mode in the ZeroDegree spectrometer was used to avoid the charge-state change in F9 detectors that was necessary for the achromatic mode. A wide plastic scintillator and ionization chamber at F11 were developed[6]. An analysis of the particle identification in the ZeroDegree spectrometer is in progress.

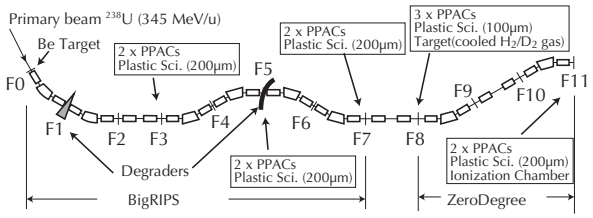

Fig. 1. Configuration of target, degrader, and detectors in the BigRIPS and ZeroDegree spectrometer.

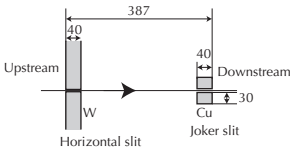

Fig. 2. Schematic top view of two sets of slits at F1. The position and angle were restricted by the narrow slit widths for both sets of slits. The widths of the upstream and downstream slits were ±2 mm and ±10 mm, respectively.

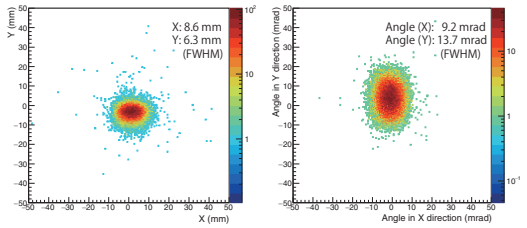

Fig. 3. Position (left) and angle (right) distributions on the secondary target at F8 for ^{107}Pd with 50 MeV/u.

This work was funded by ImPACT Program of Council for Science, Technology and Innovation (Cabinet Office, Government of Japan).

References

1) H. Wang et al., Phys. Lett. B **754**, 104 (2016).
2) H. Wang et al., RIKEN Accel. Prog. Rep. **49**, 8 (2016).
3) S. Kawase et al., RIKEN Accel. Prog. Rep. **49**, 87 (2016).
4) T. Sumikama et al., RIKEN Accel. Prog. Rep. **50** (2017).
5) S. Ota et al., RIKEN Accel. Prog. Rep. **49**, 15 (2016).
6) N. Chiga et al., RIKEN Accel. Prog. Rep. **50** (2017).

*1 RIKEN Nishina Center

Operation of GET system as main readout device for SπRIT experiment at 2016 spring campaign

T. Isobe,[*1] M. Kurata-Nishimura,[*1] H. Baba,[*1] M. Kaneko,[*2] T. Murakami,[*2] W.G. Lynch,[*3] J. Barney,[*3] J. Estee,[*3] S. Tangwancharoen,[*3] G. Jhang,[*4] and J.W. Lee[*4] for the SπRIT Collaboration

The SπRIT time projection chamber (TPC) is one of the main devices for the SπRIT project at RIKEN-RIBF.[1] The SπRIT project aims to study the density-dependent term of the symmetry energy using heavy RI collision. General electronics for TPC (GET)[2] is a novel readout system employed for the SπRIT-TPC[3] to capture the signals produced by charged particles passing through TPC. By using the GET system, it is possible to realize a high resolution, wide dynamic range, and stable operation of data acquisition. The GET system for SπRIT-TPC is composed of 48 AsAd boards, 12 CoBo boards and 2 MuTANT boards. 12 CoBo boards and 2 MuTANT boards are mounted in 2 μ-TCA shelves so that the trigger signal and sampling clock are synchronized among different CoBo boards.

During the spring season of 2016, the first physics experiment campaign was performed as well as the commissioning of the SπRIT system in a SAMURAI magnet. All the readout electronics on TPC worked under a magnetic field of 0.5 T without any problem, and full operation of the GET system was successfully performed for a two-week physics run. The analog part of the system was configured to have a dynamic range of 120 fC, shaping time of 117 ns, and sampling rate of 25 MHz. The trigger rate was ∼60 Hz, and the total beam rate was ∼10 kHz. The SπRIT-DAQ system sustained a data rate of 300 MByte/s. The data were copied to RIKEN HPC storage through a 10-Gbps network for the 1st/offline data analysis. The trigger rate of 60 Hz was expected to be improved after the integration of a partial readout mode, where the channel was digitized and can be selected event by event to reduce the conversion time. Since this functionality was not fully tested as of spring 2016, only the fully digitized readout mode was used.

Figure 1 and Fig. 2 show the event display of heavy RI collision taken with SπRIT-TPC and the typical shape of electric signals detected with GET electronics, respectively.

As shown in Fig. 1, a large number of charged particle tracks pass through TPC. There are several pads which seem to be dead. However, the positions of the dead pads vary from event to event. The pads above the beam trajectory become dead.

The drift electrons produced by the beam is supposed to be blocked by the gating grid wire plane of TPC. An excessively large amount of δ-ray electrons produced by the beam which can penetrate the gating grid and is expected to affect the readout system.

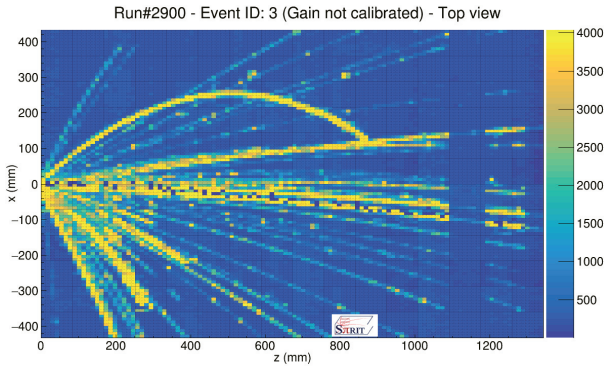

Fig. 1. Event display of heavy RI collision taken with SπRIT-TPC (top view). One dot corresponds to one of the channels. The color of each pad shows the maximum value of the signal. The Sn target is located at the left hand side of this display.

After a large effort to analyze TPC data, the ratio of charged pion production will be determined for setting the constraint on nuclear EoS.

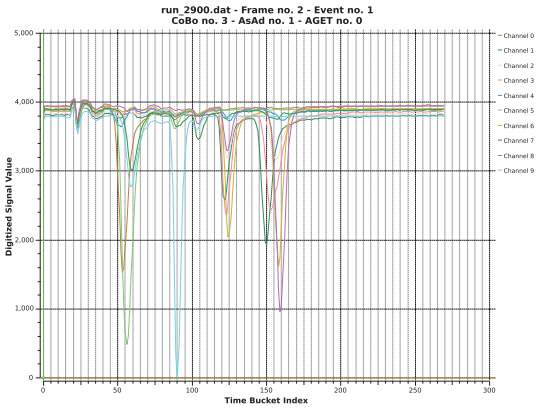

Fig. 2. Typical shape of electric signals produced by charged particles passing through TPC. Each color corresponds to each pad. Signals on 10 pads out of 12k pads are shown.

*1 RIKEN Nishina Center
*2 Department of Physics, Kyoto University
*3 National Superconducting Cyclotron Laboratory, Michigan State University
*4 Department of Physics, Korea University

References
1) S. Rebecca et al., Nucl. Inst. Met. A **784**, 513 (2015).
2) E. Pollacco et al., Physics Procedia **37**, 1799 (2012).
3) T. Isobe et al., RIKEN Accel. Prog. Rep. **48**, 204 (2015).

Vertex Correlation Between Beam Line Detector and SπRIT-TPC

M. Kurata-Nishimura,[*1] J. Barney,[*2,*1] G. Cerizza,[*2,*1] J. Estee,[*2,*1] B. Hong,[*3] T. Isobe,[*1] G. Jhang,[*3,*1] M. Kaneko,[*4,*1] P. Lasko,[*5,*6,*1] H.S. Lee,[*7] J.W. Lee,[*3,*1] J. Lukasik,[*5] W.G. Lynch,[*2] A.B. McIntosh,[*8] T. Murakami,[*4,*1] P. Paw lowski,[*5,*1] K. Pelczar,[*6] H. Sakurai,[*1] C. Santamaria,[*2,*1] R. Shane,[*2] D. Suzuki,[*1] M.B. Tsang,[*2] S.J. Yennello,[*8] Z.G. Xiao,[*9,*1] Y. Zhang,[*9,*1] and for SπRIT Collaboration

The main purpose of the SAMURAI Pion-Reconstruction and Ion-Tracker Time-Projection Chamber (SπRIT-TPC)[1] project is to constrain nuclear Equation of State (EOS) term in supra-density at around $\rho \approx 2 \cdot \rho_0$. In Spring 2016, the first experiments were performed at SAMURAI for different nuclear symmetry systems such as ^{132}Sn + ^{124}Sn and ^{108}Sn + ^{112}Sn. Since the experimental setup consisted of several independent detectors[2], data acquisition (DAQ) synchronization and relative position are one of the key concerns. Here, the correlation between beam line detectors and SπRIT-TPC will be reported to confirm them.

A schematic view of the experimental setup along the beam line is shown in Fig.1. There were two plastic scintillation counters and two Beam Drift Chambers (BDC), which determine the trigger timing and beam position in the target, respectively. The SπRIT-TPC was installed inside the SAMURAI dipole magnet. The reaction target was mounted on a ladder in front of the field cage window.

The absolute position of each detector in the SAMURAI laboratory frame was measured using a photogrammetry system[3]. Since SπRIT-TPC was placed inside the magnet and surrounded by the ancillary detectors, limited portion of the TPC was visible. Thus the outer and inner geometry measured beforehand were superimposed to visible reference target points to obtain the entire position.

A SπRITROOT analysis frameworkfor track reconstruction was developed. A reaction vertex was obtained as an intersection of multiple extrapolated tracks event by event. The reactions taking place at the target were chosen if the reaction vertex originated from the target. In Fig.2, X and Y correlations at the target between reconstructed vertices and beam positions measured by BDCs are shown. Clear correlations indicate success of DAQ synchronization and vertex reconstructions. The spatial resolution of the reconstructed vertex at the target was estimated to be of the order of 1mm after subtracting the BDC resolution. The good determination of the vertex position would enable us to improve the momentum resolution especially for low momentum particles. It was also confirmed that the TPC was aligned within 200 μm accuracy from the non-magnetic field data.

The correlation between beam position and reaction vertex indicates the successful operation of DAQ synchronization and vertex reconstruction.

This work is supported by the U.S. Department of Energy under Grant Nos. DE-SC0004835, DE-SC0014530, DE-NA0002923, US National Science Foundation Grant No. PHY-1565546, the Japanese MEXT KAKENHI (Grant-in-Aid for Scientific Research on Innovative Areas) grant No. 24105004, and the Polish National Science Center (NCN), under contract Nos. UMO- 2013/09/B/ST2/04064 and UMO-2013/10/M/ST2/ 00624.

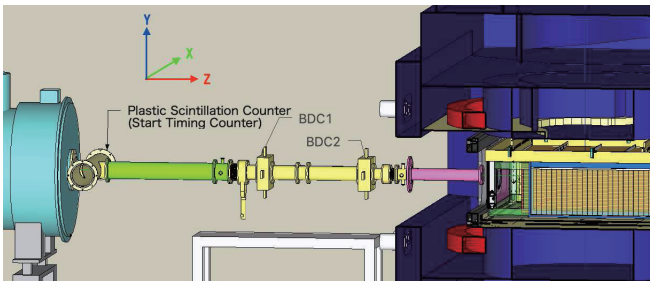

Fig. 1. Experimental setup at beam line in 2016. The coordinate is desccribed here.

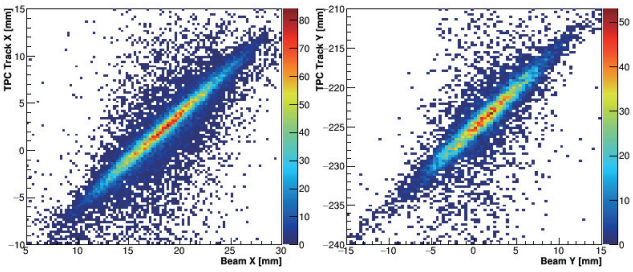

Fig. 2. Correlation at the target between vertex reconstructed by SπRIT-TPC and beam position measured by BDCs. Left and right sides show X and Y correlations, respectively.

*1 RIKEN Nishina Center
*2 NSCL and Dept. of Phys. & Ast., Michigan State University
*3 Department of Physics, Korea University
*4 Department of Physics, Kyoto University
*5 IFJ PAN, Kraków
*6 Faculty of Physics, Astronomy and Applied Computer Science, Jagiellonian University, Kraków
*7 Rare Isotope Science Project, Institute for Basic Science
*8 Cyclotron Institute, Texas A&M University
*9 Department of Physics, Tsinghua University

References

1) R. Shane et al.: Nucl. Instr. Meth. A **784** (2015) 513.
2) J. Barney et al.: in this report.
3) http://www.geodetic.com.

A Gating Grid Driver for Time Projection Chambers†

S. Tangwancharoen,[*1] W.G. Lynch,[*1] J. Barney,[*1,*2] J. Estee,[*1,*2] R. Shane,[*1] M.B. Tsang,[*1] Y. Zhang,[*3,*2] T. I sobe,[*2] M. Kurata-Nishimura,[*2] T. Murakami,[*4,*2] Z.G. Xiao,[*3,*2] Y.F. Zhang,[*5] and the SπRIT collaboration

The SπRIT (SAMURAI pion Reconstruction and Ion Tracker) experiment utilizes the SπRIT Time Projection Chamber (TPC)[1] as the main detector. The TPC operates within the uniform magnetic field of the SAMURAI magnet. Within its field cage, the TPC provides a uniform electric field anti-parallel to the magnetic field. When particles travel through the field cage, they ionize electrons from the counter gas, leaving tracks of electrons. These drift electrons move upwards to the detection region, which consists of wire planes which amplify the electron signal via avalanche process and a 2-D pad plane to readout the amplified signal. The avalanche process produces many positive ions, which can alter the electric fields in the detector. Both the electrons and positive ions cause aging effects on the wires. To avoid space charge problems and aging effects, a gating grid wire plane is used to close the detection region to prevent drift electrons from reaching the avalanche region unless a trigger has been provided. The gating grid operates with an average voltage V_a that matches the electric field from the field cage. In the open state, all wires are maintained at the average voltage V_a. In its closed state, the voltages of alternate wires are offset by voltage ΔV from V_a to voltage V_h, which is ΔV higher than V_a, and voltage V_l, which is ΔV lower than V_a. Drift electrons will be attracted to the wires at V_h and repelled from the wires at V_l, causing them to terminate at V_h. The time it takes to transition between closed and open must be minimized, as electrons which reach the detection region before the gating grid opens will not be detected. To control the opening and closing of the gating grid, a gating grid driver was developed at MSU to quickly drive the voltages from closed to open, and then back to closed again.

Key features of this gating grid driver include using a low-impedance transmission line, as well as using two pairs of N-type and P-type MOSFET switches to drive both the opening and closing of the gating grid. For the opening of the gating grid, the V_h and V_l wires are shorted together using an N-type and a P-type MOSFET switch, bringing them to the common voltage of V_a. These switches are denoted as $N1$ and $P1$ in Circuit A of Figure 1. To return the gating grid to the closed state, the switches $N2$ and $P2$ are used to quickly recharge the wires to V_h and V_l.

In the recent SπRIT experiment, the gating grid driver was used to drive the gating grid of the SπRIT TPC. Both the TPC and the gating grid driver are located inside the SAMURAI magnet. According to GARFIELD calculations, in a magnetic field of 0.5T, ΔV should be less than 10V to achieve 90% electron transparency, effectively opening the gating grid. This condition is achieved within 350 ns of providing the signal to open. The gating grid with the driver worked succesfully, with only a small pickup correction evidenced by the changing of V_a, which can be removed from the data at in offline analysis. The analysis of the performance of the gating grid is ongoing in offline analysis.

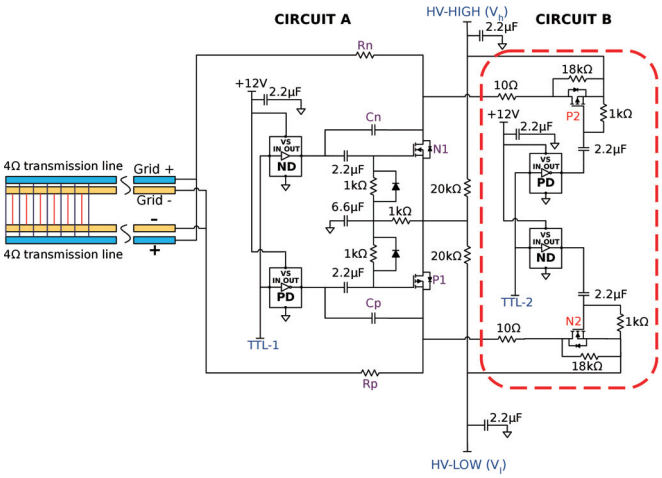

Fig. 1. The gating grid driver circuit design. Circuit A refers to the left side, while Circuit B refers to the circuit inside the red-dashed area.

This work is supported by the U.S. Department of Energy under Grant Nos. DE-SC0004835, DE-SC0014530, DE-NA0002923, US National Science Foundation Grant No. PHY-1565546 and the Japanese MEXT KAKENHI (Grant-in-Aid for Scientific Research on Innovative Areas) grant No. 24105004.

Reference

1) R. Shane et al.: Nucl. Instr. Meth. A **784**, 513 (2015).

† Condensed from the article in arXiv:1612.06708

*1 National Superconducting Cyclotron Laboratory and Department of Physics and Astronomy, Michigan State University
*2 RIKEN Nishina Center
*3 Department of Physics, Tsinghua University
*4 Department of Physics, Kyoto University
*5 College of Nuclear Science and Technology, Beijing Normal University

The Veto Collimator for the SπRIT-TPC

Y. Zhang,[*1,*2] J. Barney,[*3,*2] M. Kaneko,[*2,*4] M. Kurata-Nishimura,[*2] P. Lasko,[*5,*6,*2] J. Łukasik,[*5] P. Pawłowski,[*5,*2] Z.G. Xiao,[*1,*2] G. Cerizza,[*3,*2] J. Estee,[*3,*2] T. Isobe,[*2] G. Jhang,[*7,*2] W.G. Lynch,[*3] T. Murakami,[*4,*2] K. Pelczar,[*6] C. Santamaria,[*3,*2] M.B. Tsang,[*3] and the SπRIT Collaboration

The Veto Collimator, VC, is an ancillary detector of the SπRIT-TPC[1] (SAMURAI pion Reconstruction Ion-Tracker Time Projection Chamber), the main device used to study the nuclear Equation of State at RIKEN. It is located 22 cm upstream of the target and provides a veto condition for beam particles which do not hit the target and upstream reaction products. The VC consists of four BC408 scintillators with the size of 90×50×6 mm^3. Attached to each scintillator is an MPPC (S10931-100P) which is a new type of a photon-counting device made up of multiple APD (Avalanche PhotoDiode) pixels operating in Geiger mode[2]. The active area of this MPPC is 3×3 mm^2. The BC408 is a premium plastic scintillator with the highest light output and with the maximum emission at the wavelength of 425 nm, which is compatible to the peak sensitivity wavelength of the MPPC[2,3]. The gain of the MPPC amounts to about 2.4×10^6.

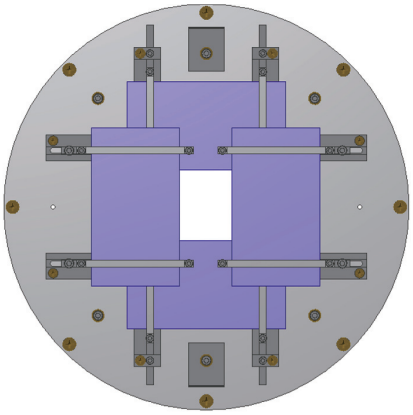

Fig. 1. Mechanical sketch of the veto collimator.

The mechanical sketch of the VC is shown in Fig. 1. Four scintillators, shown in purple, are mounted on adjustable support slots so they form a hole in the center where the beam particles can go through towards the target downstream. To ensure that beam particles pass through the hole will hit the target, the size is slightly smaller than the 30×40 mm^2 target.

For each scintillator, the analog signal produced by the MPPC is sent to a preamplifier (same as those used for the KATANA[4] array) and then to the leading edge discriminators of the trigger logic system. Any of the four scintillators firing above the threshold produce a veto signal preventing a trigger for the TPC.

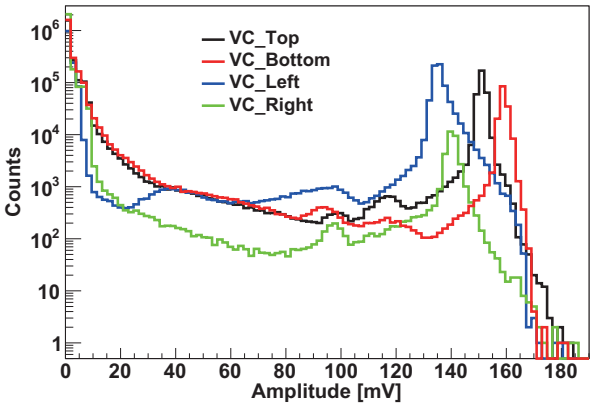

Fig. 2. The energy spectra of fragments hitting the VC.

During the experiment the MPPCs were biased at 71.51, 71.52, 71.41 and 71.40 V and the thresholds were set to 145, 155, 130 and 135 mV for the top, bottom, left and right paddles, respectively. The energy spectra of fragments hitting the four VC paddles are shown in Fig. 2. The presented data come from the commissioning runs of ^{132}Sn at 300 MeV/nucleon, for which the VC was operating in a triggering mode and thus the veto thresholds were not effective. The peaks at high amplitudes are due to the beam particles. The counts at smaller amplitudes correspond to slower and/or lighter upstream reaction products as well as to those backward emitted from the target and from the downstream material. The VC performed well during the two experiments and the commissioning run with the SπRIT-TPC in 2016, suppressing upstream reactions and off-target events.

This work is supported by the National Science Foundation of China under Grant No. U1332207, by the U.S. DOE under Grant Nos. DE-SC0004835, DE-SC0014530, DE-NA0002923, US NSF Grant No. PHY-1565546, by the Japanese MEXT KAKENHI grant No. 24105004 and by the Polish NSC Grants UMO-2013/09/B/ST2/04064 and UMO-2013/10/M/ST2/00624.

*1 Department of Physics, Tsinghua University
*2 RIKEN Nishina Center
*3 NSCL and Department of Physics and Astronomy, Michigan State University
*4 Department of Physics, Kyoto University
*5 IFJ PAN, Kraków
*6 Jagiellonian University, Kraków
*7 Department of Physics, Korea University

References

1) R. Shane *et al.*, Nucl. Instr. Meth. A **784**, 513 (2015).
2) `http://www.datasheetlib.com/datasheet/707358/s10931_hamamatsu-photonics.html`
3) `http://www.crystals.saint-gobain.com`
4) P. Lasko *et al.*, arXiv:1610.06682.

Zero suppression performance evaluation of GET electronics using SπRIT TPC experimental data

G. Jhang,[*1,*2] J. Barney,[*2,*3] G. Cerizza,[*2,*3] J. Estee,[*2,*3] B. Hong,[*1,*2] T. Isobe,[*2] M. Kaneko,[*2,*4] M. Kurata-Nishimura,[*2] J. W. Lee,[*1,*2] W. G. Lynch,[*2,*3] T. Murakami,[*2,*4] C. Santamaria,[*2,*3] M. B. Tsang,[*2,*3] and Y. Zhang[*2,*5] for the SπRIT collaboration

Zero suppression is of great importance in acquiring data with a TPC equipped with GET electronics[1] because of its huge data size. For example, the SπRIT TPC[2] has 12,096 channels, which result in an event size of ∼6.7 MB without zero suppression. With the average disk writing rate observed during the first series of the SπRIT experiment, ∼60 Hz, data throughput corresponds to ∼402 MB/s.[3]

The performance of three different types of zero suppression (two hardware and one software types) is evaluated through the software simulation of hardware zero suppression based on the observation from the experiment. Below is a brief explanation of the data structure from the GET electronics. Single channel data are composed of pairs of ADC and elapsed time from the trigger (time bucket, TB). Figure 1 shows the display of ADC-TB pairs from GET electronics. In full readout mode, ADC values are sorted sequentially so that TB information is omitted to reduce the data size. In the zero-suppression mode, however, TB information is indispensable because only some of the ADC-TB pairs are stored. As a result, the data size of a channel in the zero-suppression mode is greater than that in the full readout mode when the threshold is set to 0.

Hardware zero-suppression mode 1 writes all the ADC values in a channel above the threshold. The data size is greater than the size in the full readout mode unless the number of fired channels is less than half of the number of total channels. The mean number of fired channels of ^{132}Sn+^{124}Sn collision events is ∼6900 out of 12,096 with a threshold of 0.05% of the maximum ADC value. The data size of zero-suppression mode 1 is 114% of the full readout data size.

Mode 2 writes ADC values above the threshold only. With the same conditions as those used in mode 1, mode 2 results in merely 14% of the full readout data size. One disadvantage of this mode is that it is difficult to determine the baseline because the mode removes all the signals below the threshold.

The software zero-suppression mode we designed keeps 5 more ADC-TB pairs at every crossing point of the signal to the threshold value. For example, in Fig. 1 the largest pulse at the center cross the threshold at 90 TB and 115 TB. The software zero-suppression mode keeps not only 90∼115 TBs, but also 84∼89 and 116∼120 TBs. We also added a feature to reduce the data size using the fact that ADC-TB pairs above the threshold are not random but sequential from the point crossing the threshold. By writing the first TB of the crossing point and the number of TBs, we could make the data size 10% smaller than what it would be if we simply follow the rule of hardware zero suppression. The data size of software zero suppression is 21% of the full readout data size. Moreover, the suppression process is performed after the baseline is determined and matched to 0. However, the software zero suppression also has disadvantages in that it involves an additional process after acquiring data and consumes additional disk space for processing.

In summary, hardware zero-suppression mode 1 will be extremely useful when only a few tracks are generated. The use of zero-suppression mode 2 is efficient when the baseline determination is not a problem. The software zero suppression is more flexible but requires computational and storage resources and must be performed offline.

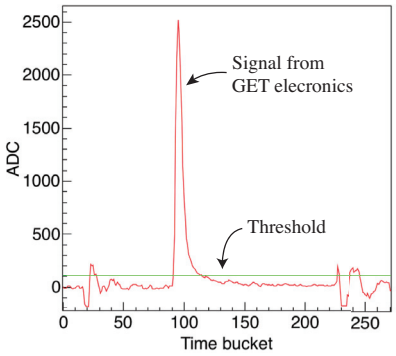

Fig. 1. Baseline-matched signal from GET electronics (red solid curve). Zero suppression mode 1 stores complete curves on the figure if there exists a part above the threshold (solid green line). On the other hand, mode 2 stores the parts above the threshold only. Software zero suppression stores 5 more ADC-TB pairs at each crossing point to the threshold.

*1 Department of Physics, Korea University
*2 RIKEN Nishina Center
*3 NSCL and Dept. of Physics and Astronomy, Michigan State University
*4 Department of Physics, Kyoto University
*5 Department of Physics, Tsinghua University

References
1) E. Pollacco et al.: Physics Procedia **37**, 1799 (2012).
2) R. Shane et al.: Nucl. Inst. Meth. A **784**, 513 (2015).
3) T. Isobe et al.: In this report.

Kyoto Multiplicity Array for the SπRIT experiment

M. Kaneko,[*1,*2] T. Murakami,[*1,*2] T. Isobe,[*2] M. Kurata-Nishimura,[*2] W. G. Lynch,[*3] M. B. Tsang,[*3] J. Barney,[*2,*3] J. Estee,[*2,*3] G. Cerizza,[*2,*3] C. Santamaria,[*2,*3] G. Jhang,[*4] J. W. Lee,[*4,*2] P. Lasko,[*5,*2] J. Łukasik,[*5] P. Pawłowski[*5,*2] and Y. Zhang[*6,*2] for the SπRIT collaboration

The SπRIT experiment, which aimed to investigate the nuclear equation of state at supra-saturation densities, was performed in the spring of 2016 at RIKEN-RIBF. The integral or momentum spectrum of π^-/π^+ produced in central heavy-ion (HI) collisions can be a useful probe[1] and was measured in this experiment. In order to identify multi fragments including charged pions generated from HI collision and to reconstruct their momenta, a large time projection chamber (SπRIT-TPC[2]) and ancillary trigger detectors were constructed. These detectors were used in the SAMURAI spectrometer with a magnetic field of 0.5 T.

The "Kyoto Multiplicity Array" has a sensitivity to sideward charged particle multiplicity which correlates with collision centrality. This detector consists of 2×30 plastic scintillator bars that are in close contact with both sides of the SπRIT-TPC. The enclosure of the SπRIT-TPC has 1-mm-thick aluminum window parts allowing light fragments from the reaction to pass through and be detected by the external triggering system. The dimensions of each plastic bar are 450×50×10 mm^3, and the plastic bars are coated with oxidized titanium for light reflection. Each bar has a hole of about 1.5 mmϕ centered along its length for a wavelength-shifting fiber as a light guide. The light propagated in the fiber of 1 mmϕ will be detected by a 1.3-mm^2 multi-pixel photon counter (MPPC) capable of use in a magnetic field. Figure 1 shows the geometrical setup of detectors in the SAMURAI magnet.

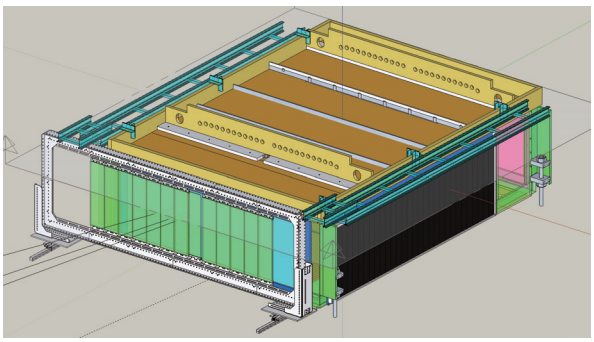

Fig. 1. Schematic drawing of SπRIT-TPC and ancillary detectors from beam-left downstream side. One-sided Kyoto Multiplicity Array is indicated by black, and the other side is behind the SπRIT-TPC.

*1 Department of Physics, Kyoto University
*2 RIKEN Nishina Center
*3 NSCL and Dept. of Phys. & Ast., Michigan State University
*4 Department of Physics, Korea University
*5 Institute of Nuclear Physics, PAN, Kraków
*6 Department of Physics, Tsinghua University

The ASD chip designed to readout photodiode type detectors - EASIROC - is used for shaping MPPC signals. For handling the EASIROC and its digital outputs from discriminators, FPGA is integrated in one board together with EASIROC (VME-EASIROC[3]). The number of digital signals, as charged-particle multiplicity, is calculated by a combination of ROMs and adder circuits, which is implemented in the FPGA. If the calculation result surpasses the user-set threshold, a trigger signal will be generated within about 52 ns for the whole electronics. In addition to the online triggering function, multi-hit TDC with 1 ns time resolution is also implemented in the FPGA for offline analysis. In the SπRIT experiment, triggered event multiplicity was required to be greater than 4.

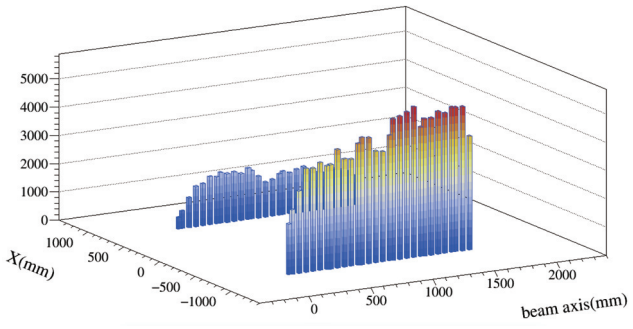

Fig. 2. Number of hits in each plastic bar in offline analysis from beam-right upstream side. The coordinates correspond to the position of each bar, and the target was located at X=0 mm and beam axis=–8.9 mm.

Although this was the first operation in the magnetic field, the data for TPC with ancillary detectors were acquired without major problems. The hit pattern obtained by the detector is presented in Fig. 2, where the effect of the magnetic field on charged particles can be observed. While there are some fluctuations, detailed analysis is necessary to understand the bias for triggered events and the impact parameter information.

This work is supported by the Japanese MEXT KAKENHI grant No. 24105004; the U.S. DOE under Grant Nos. DE-SC0004835, DE-SC0014530, and DE-NA0002923; the US NSF Grant No. PHY-1565546; and the Polish NSC Grant Nos. UMO-2013/09/B/ST2/04064 and UMO-2013/10/M/ST2/00624.

References

1) Bao-An Li et al., Phys. Rev. C **71**, 014608 (2005).
2) R. Shane et al., Nucl. Instr. Meth. A **784**, 513 (2015).
3) T. Shiozaki: Master's Thesis, Tohoku University (2015).

KATANA - a charge-sensitive triggering system for the SπRIT experiment†

P. Lasko,[*1,*2,*5] M. Adamczyk,[*2] J. Brzychczyk,[*2] P. Hirnyk,[*1] J. Łukasik,[*1] P. Pawłowski,[*1,*5] K. Pelczar,[*2] A. Snoch,[*3] A. Sochocka,[*2] Z. Sosin,[*2] J. Barney,[*4,*5] G. Cerizza,[*4,*5] J. Estee,[*4,*5] T. Isobe,[*5] G. Jhang,[*5,*6] M. Kaneko,[*5,*7] M. Kurata-Nishimura,[*5] W.G. Lynch,[*4] T. Murakami,[*5,*7] C. Santamaria,[*4,*5] M.B. Tsang,[*4] and Y. Zhang[*5,*8]

KATANA - the Krakow Array for Triggering with Amplitude discrimiNAtion - has been built and used as a trigger and veto detector for the SπRIT TPC at RIKEN. Its construction allows operating in magnetic field and providing fast response for ionizing particles, giving an approximate forward multiplicity and charge information.

The experiments with the SπRIT TPC at RIKEN were focused on investigation of the central and semi-central heavy-ion (HI) collisions at energies of about 300 MeV per nucleon. The target was located about 3 mm upstream of the entrance field cage window inside the SπRIT TPC, so that the HI beam passed through the chamber. To obtain sufficiently large gas amplification for pions and light charged particles, a high electric field is required inside the chamber. In such conditions the ionization produced by the HI beam would produce an excessive space charge leading to field distortion and could bring a risk of damage: the charge produced by gas ionization could exceed the safe limit for the pad planes of the TPC. For this reason, a gating grid wire plane is mounted below the pad plane[1,2]. The grid was normally 'closed' to keep the detector off until a desired collision occurs. When such an event happens, the opening of the gating grid can occur quickly (in ∼350 ns). Such operation should be performed whenever an incoming projectile reacts violently with the target nuclei.

The KATANA detector, located downstream of the TPC exit window, was designed to produce a logic signal to open the gating grid when a desired event occurs. During the experiment it played a double role: to produce a minimum bias or majority trigger, and to provide a veto signal whenever a beam particle or a fragment heavier than $Z \simeq 20$ passed through the chamber. To fulfill the requirements, the wall has been constructed of two parts: a Veto and a Trigger array. The KATANA-Veto part consisting of 3 thin (1 mm thick) plastic-scintillator paddles with the middle one centered on the beam, has been designed to produce a veto signal for heavy fragments. The KATANA-Trigger array, consisting of 12 thicker (10 mm thick) paddles, arranged on both sides of the beam, has been designed to produce a forward multiplicity trigger.

A technical design of the KATANA detector is presented in Fig. 1. Fifteen scintillators, each 10 cm wide and 40 cm high, are mounted on a rectanglular, aluminum frame. Each scintillator is wrapped in a sheet of a light-reflective, metalized Kapton foil. Three veto plastic bars, marked with dashed lines, are placed in the middle of the frame. Twelve trigger plastics are placed unevenly on both sides of the beam (7 on the left and 5 on the right side) to account for bending of the beam particles in the magnetic field. The Multi Pixel Photon Counter (MPPC) devices from Hamamatsu which are not sensitive to magnetic fields have been used as the light sensors.

During the experimental runs the device perfectly fulfilled its role.

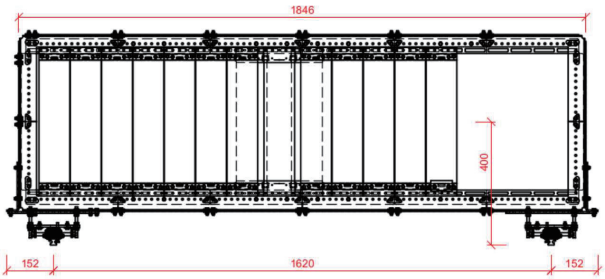

Fig. 1. A technical drawing of the KATANA detector with the external dimensions in mm.

This work was supported by the Polish National Science Center (NCN), under contract Nos. UMO-2013/09/B/ST2/04064 and UMO-2013/10/M/ST2/00624 as a part of the SπRIT Project supported by the U.S. Department of Energy under Grant Nos. DE-SC0004835, DE-SC0014530, DE-NA0002923, US National Science Foundation Grant No. PHY-1565546 and the Japanese MEXT KAKENHI (Grant-in-Aid for Scientific Research on Innovative Areas) grant No. 24105004.

References

1) R. Shane *et al.*, Nucl. Inst. Meth. A **784**, 513 (2015).
2) S. Tangwancharoen *et al.*, arXiv:1612.06708.

† Condensed from the article arXiv:1610.06682

*1 IFJ PAN, Kraków
*2 Faculty of Physics, Astronomy and Applied Computer Science, Jagiellonian University, Krakw
*3 Faculty of Physics and Astronomy, Wroclaw University
*4 NSCL and Department of Physics and Astronomy, Michigan State University
*5 RIKEN Nishina Center
*6 Department of Physics, Korea University
*7 Department of Physics, Kyoto University
*8 Department of Physics, Tsinghua University

Trigger logic for the SπRIT experiments

C. Santamaria,[*1,*2] P. Pawlowski,[*3,*2] W. Lynch,[*1] K. Pelczar,[*3] J. Barney,[*1,*2] G. Cerizza,[*1,*2] J. Estee,[*1,*2] T. Isobe,[*2] M. Kaneko,[*4,*2] M. Kurata-Nishimura,[*2] P. Lasko,[*3,*2] J. Lukasik,[*3] A.B. McIntosh,[*5] T. Murakami,[*4,*2] M. B. Tsang,[*1] S.J. Yennello,[*5,*6] Y. Zhang[*7,*2] for the SπRIT collaboration

The SπRIT experiments[1] require a trigger to select central collisions in order to probe the nuclear equation of state at high densities using heavy ion collisions. Central collisions are studied via a Time Projection Chamber (TPC) surrounded by ancillary detectors. They are triggered by suitable multiplicities of charged particles in the Kyoto plastic scintillators located on the sides of the TPC and KATANA plastic scintillator paddles located downstream of the TPC. An extensive description of the KATANA array is provided in Ref. 3. The trigger was vetoed by the presence of a projectile-like fragment in the three KATANA veto scintillators, which are downstream of the TPC and centered about the beam trajectory, or if there is a hit in the active collimator that shadows the target frame from the incident beam.

The ultimate trigger decision was made by an FPGA in a "trigger box", shown in Fig. 1 in the shaded gray box. The internal trigger logic of this trigger box is not shown. It required a signal from the beam in a Start Counter scintillator located upstream, a multiplicity signal from the EASIROC module servicing the Kyoto multiplicity array or a multiplicity in the KATANA plastic that exceeds a threshold multiplicity selected by user. For regular data runs, the trigger condition required a multiplicity greater than four in the Kyoto array and the multiplicity in KATANA was ignored. Moreover, this trigger was vetoed in the trigger box if heavy fragments hit any of the three KATANA veto scintillators or if the beam hit the active collimator upstream. To obtain minimum bias events and to study the trigger bias of this event selection, the values of the Kyoto multiplicity, the KATANA trigger multiplicity, and the KATANA beam veto paddle thresholds were varied in separate minimum bias runs for further analysis.

To avoid a loss of track information in the TPC, a Fast Trigger decision was made. This Fast Trigger AND coincidence, shown in the figure, required the Start Counter, none of the three KATANA veto signals and vetoed by a BUSY signal. This opened the gating grid driver (GGD)[2] via a TTL_open signal generated by the latch G&D 2. The TTL_open is normally terminated by G&D 1 after 11 μsec but can be shortened by the arrival of a random beam particle in one of the KATANA veto paddles or the lack of a trigger signal from the trigger box. The 11 μsec maximum length of the gate is calculated from the 9 μsec drift length of the TPC plus some safety margin to make sure all the volume of the TPC is included in the accepted time window. The TTL_close signal, generated by the G&D 4, starts on the trailing edge of the TTL_open signal and defines the closing of the GGD. The 5 μsec width of the TTL_close gate is calculated as the maximum drift time in the TPC for a heavy fragment to avoid these tracks from producing a signal in the next event.

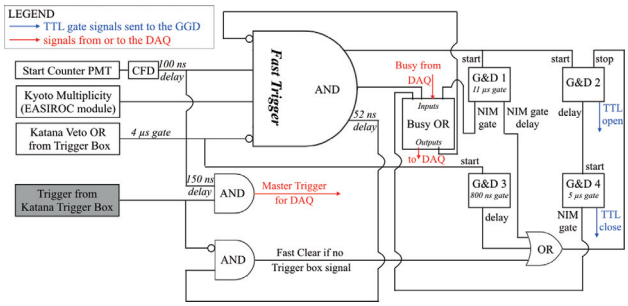

Fig. 1. Schematic circuit diagram of the trigger logic used during the SπRIT experiments.

Three data acquisitions (DAQ) are coupled during the experiment to write data from the TPC (SπRIT), the beam tracking counters and Kyoto array (RIKEN) and the KATANA array (KATANA). The BUSY signal is generated from an OR of the three DAQ BUSY signals plus the TTL_open and TTL_close. The trigger sent to the DAQ systems is a coincidence of the trigger from the trigger box, a NOT BUSY signal, and a delayed Start Counter signal in order to keep the Start Counter as the reference time for the DAQ.

During the experiment, the data acquisition successfully selected heavy ion collisions with on average a 800 μs dead time. Analysis of data runs will quantitatively determine the average impact parameter of the heavy ion collisions in our setup and a further study of the minimum bias runs will constrain the bias of our experimental detection system.

*1 NSCL and Department of Physics and Astronomy, Michigan State University
*2 RIKEN Nishina Center
*3 Institute of Nuclear Physics, PAN
*4 Department of Physics, Kyoto University
*5 Cyclotron Institute, Texas A&M University
*6 Department of Chemistry, Texas A&M University
*7 Department of Physics, Tsinghua University

References

1) R. Shane et al., Nucl. Instr. Meth. A **784**, 513 (2015).
2) S. Tangwancharoen et al., Nucl. Instr. Meth. A **853**, 44 (2017).
3) P. Lasko et al., Nucl. Instr. Meth. A **856**, 92 (2017).

Calibration of the SπRIT TPC with light fragments

J. Estee,[*1,*3] J. Barney,[*1,*3] G. Cerizza,[*1,*3] B. Hong,[*2] T. Isobe,[*3] G. Jhang,[*2,*3] M. Kaneko,[*4,*3] M. Kurata-Nishimura,[*3] P. Lasko,[*5,*3] J. W. Lee,[*2] J. Lukasik,[*5] W.G. Lynch,[*1] A.B. McIntosh,[*6] T. Murakami,[*4,*3] P. Pawlowski,[*5,*3] K. Pelczar,[*8] C. Santamaria,[*1,*3] D. Suzuki,[*3] M. B. Tsang,[*1] S.J. Yennello,[*6] Y. Zhang,[*7,*3] and the SπRIT collaboration

The SAMURAI Pion-Reconstruction and Ion-Tracker Time-Projection Chamber (SπRIT-TPC)[1)] was constructed to measure pions and light particle fragments resulting from heavy ion collisions. While the symmetry energy of the nuclear Equation of State is constrained at sub-saturation densities, large theoretical uncertainties still exist above nuclear saturation density. In an effort to constrain the symmetry energy at high densities, two experiments were performed at RIKEN in the spring of 2016 with the TPC inserted into the SAMURAI magnet.

To calibrate the gain of the TPC, a "cocktail" beam of (p,d,t,^{3}He,^{4}He,^{6}Li) light fragments was tuned for two different $B\rho$ settings. The BigRIPS fragment separator was able to provide the species listed in Table 1 with a momentum resolution of about 0.8% as estimated by LISE++. Because the momentum of each particle was well defined, we can also determine the energy loss distribution of each particle species.

Table 1. Mean momentum and momentum resolution from the BigRIPS separator as predicted by LISE++.

Particle	momentum [MeV/c]	$\frac{dp}{p}$ [%]
p	903.6	0.77
d	886.9	0.78
t	886.9	0.82
^{3}He	1795.7	0.78
^{4}He	1782.9	0.80
^{6}Li	2652.2	0.82

The energy loss distribution of a particle depends not only on a particle's momentum, but also on the analyzed segment length and is explained in extensive detail in Ref. 1. Such a technique is implemented in other TPC's such as STAR and ALICE[2)]. For our analysis, a C++ version of the Bichsel's FORTRAN code, in Ref. 3, was made and the resulting straggling functions were compared to the original Bichsel code to check for accuracy.

As the particle traverses the detection gas volume, the energy deposited is amplified and recorded over many readout pads[1)]. Thus, the energy loss of each track is broken up into smaller analyzed segments or clusters. The straggling function for a 903.63 MeV/c proton was created with a Monte Carlo simulation, and is shown as a blue curve in Fig. 1. To calibrate the TPC, we assign the energy deposited value D to a measured ADC value Q. We assume a linear relationship and minimize Pearson's χ^2 to fit the measured straggling function to the theoretical Bichsel straggling function yielding the relationship:

$$D = 0.45 * Q + 0.48 \quad (1)$$

The red curve in Fig. 1 shows the calibrated experimental straggling function of protons at 903.63 MeV/c.

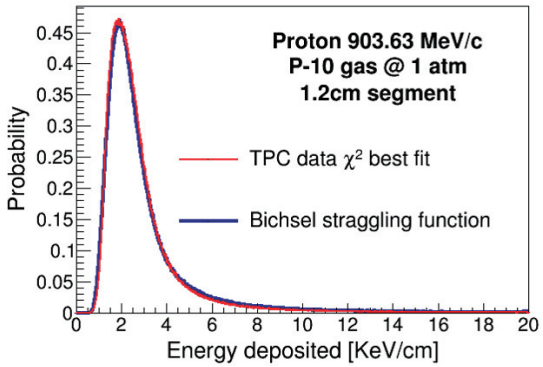

Fig. 1. Fitted TPC data and the Bichsel straggling function for P-10 gas over a track segment length of 1.2cm. Bin width is 10 [eV/cm]

In summary, good agreement between the energy loss distribution of the TPC and the expected Bichsel curve was found for the protons. In the near future, other particle species will be analyzed as well as the particles produced in the second $B\rho$ setting which provides higher momentum values.

This work is supported by the U.S. Department of Energy under Grant Nos. DE-SC0004835, DE-SC0014530, DE-NA0002923, US National Science Foundation Grant No. PHY-1565546 and the Japanese MEXT KAKENHI (Grant-in-Aid for Scientific Research on Innovative Areas) grant No. 24105004.

References

1) R. Shane et al. Nucl. Instr. Meth. A **784**, (2015) 513.
2) H. Bichsel Nucl. Instr. Meth. A **562**, (2006) 154.
3) Original code found under "Current research" section of home page http://faculty.washington.edu/hbichsel/

*1 NSCL and Dept. of Phys. and Ast., Michigan State University
*2 Department of Physics, Korea University
*3 RIKEN Nishina Center
*4 Department of Physics, Kyoto University
*5 IFJ PAN, Kraków
*6 Dept. of Physics and Astronomy, Texas A&M University
*7 Department of Physics, Tsinghua University
*8 Faculty of Physics, Astronomy and Applied Computer Science, Jagiellonian University

NeuLAND demonstrator performance in EOS experiments

I. Gašparić,[*1,*2] K. Boretzky,[*3] H. Törnqvist,[*2,*4] T. Aumann,[*3,*4] L. Atar,[*2,*4] A. Horvat,[*4] Y. Leifels,[*3] D. Rossi,[*4] H. Simon,[*3] and H. Scheit[*4] for the SπRIT and R^{3}B-NeuLAND Collaborations

The NeuLAND demonstrator is a fraction of the neutron detector R^{3}B-NeuLAND[1)], which is being built at FAIR in Germany. Since the beginning of 2015, it has been used within the SAMURAI experimental setup at RIKEN. It consists of 400 plastic scintillator bars arranged in 8 planes with 50 bars oriented either horizontally or vertically. The size of each bar is 250×250×5 cm^3, which makes the total depth of detector 40 cm.

The detector is usually placed at 0° to the beam line downstream of the SAMURAI magnet to detect neutrons from peripheral reactions of a radioactive beam particle on a target, whereas charged particles are bent away. A VETO detector consisting of eight 1-cm-thick plastic scintillator paddles is mounted in front of NeuLAND to reject background, mostly produced from beam-like particles in the fragment branch (typically ∼5% of events).

In the experiments S015 and S022 (April/May 2016),[2)] where the nuclear EOS was studied in central collisions of Sn isotopes, the detector was placed at 30° to the beam line. The proton/neutron and triton/^{3}He yield ratios and flows were measured. NeuLAND was used to detect light charged particles, such as hydrogen and helium ions, together with neutrons and gammas. The VETO detector in this study of central collisions plays an essential role for the distinction of charged and neutral particles in contrast to other experiments, where neutrons are expected to be dominant and the VETO serves for background discrimination only.

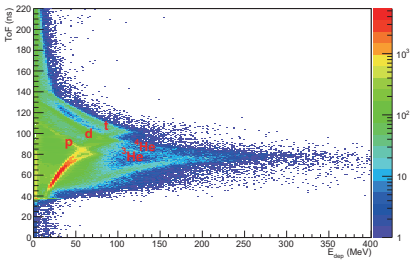

Fig. 1. Particle identification plot in the 1st plane.

A considerable amount of light charged particles (∼40% of events) with a large range of energies (from zero to the beam energy) was detected in the NeuLAND demonstrator. Figure 1 shows the time of flight vs. deposited energy in the first plane of NeuLAND. The spectrum exhibits characteristic lines for the various charged particles, and protons, deuterons, tritons, ^{3}He, and ^{4}He are identified.

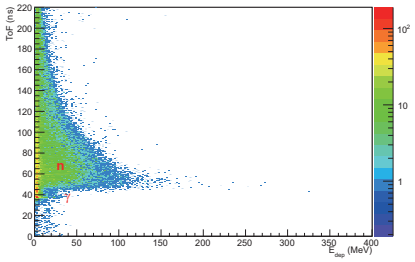

Fig. 2. Particle identification plot in the 1st plane with a strong VETO condition.

To check the performance of the suppression of charged particles, the same spectrum was produced again (Fig. 2) with a condition on events where no hit was recorded in the full VETO detector (strong VETO condition). A loss of neutrons with that condition was evaluated from Geant simulations, and it was on a percent level.

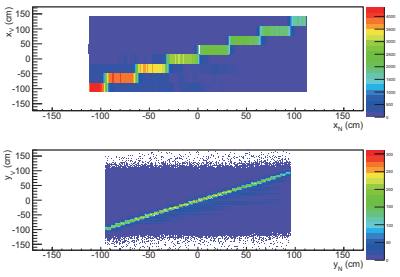

Fig. 3. Spatial correlation between hits in NeuLAND and VETO detectors.

In order to analyze charged particles and neutrons in the same events, a more elaborated VETO analysis is under investigation, including spatial correlation between hits in NeuLAND (x_N, y_N) and VETO (x_V, y_V) (Fig. 3), as well as timing correlations. The set of VETO hits needs to be linked to hits in NeuLAND to determine unambiguously which NeuLAND hits originate from charged particles and which from neutrons.

*1 Ruđer Bošković Institute, Zagreb
*2 RIKEN Nishina Center
*3 GSI Helmholtzzentrum für Schwerionenforschung, Darmstadt
*4 Institut für Kernphysik, TU Darmstadt

References

1) http://www.fair-center.de/fileadmin/fair/experiments/NUSTAR/Pdf/TDRs/NeuLAND-TDR-Web.pdf.
2) R. Shane et al. Nucl. Instr. Meth. A **784**, 513 (2015).

Upgrade of proton detector NINJA

N. Chiga,[*1] T. Kobayashi,[*1,*2] T. Saito,[*1,*3] A.T. Saito,[*1,*4] Y. Togano,[*1,*4] T. Isobe,[*1] and H. Otsu[*1]

The detector NINJA[1,2] is a plastic scintillator array positioned inside the SAMURAI gap chamber to measure protons that cannot to exit the gap chamber with the standard SAMURAI setup. NINJA is composed an X-layer and a Y-layer. The X- and Y-layers consist of 18 slots with dimensions of 60(w)× 720(l)mm^2× 10(t)mm^t and 12 slots with 60(w)× 1100(l)^2×10(t)mm^t, respectively. The X-layer is located 5 cm upstream of the Y-layer. Scintillation light signals from the plastic are transported to the MPPC through a wave-length-shifter rod in the scintillator. The details of the NINJA can be found in Ref. 2.

This report describes the upgrade of the readout circuits and the performance of NINJA. The readout circuit of NINJA was earlier the VME-EASIROC[3], witch was utilized to digitize the signals from NINJA. VME-EASIROC supplies HV to MPPC. Since we determined that the connection of the external HV supplier was the major noise source, the readout circuit has been changed to NIM-EASIROC,[4] which has an internal HV supplier. Since NIM-EASIROC is not equipped with an internal TDC, the V1190A TDC was used (as an external TDC) to accept the leading and trading edges of signals.

The timing resolution and the detection efficiency of NINJA for protons were evaluated by using the projectile-like protons produced in the ^{1}H(^{6}He,X) reaction in the SAMURAI13 experiment[5]. The detection efficiency ε of the X-layer was evaluated as $N(X\cap Y)/N(Y)$, where $N(X\cap Y)$ represents the number of events occurring at both the X- and Y-layers, and N(Y) the event firing the Y-layer. The Y-layer efficiency ε^Y was evaluated as $N(X\cap Y)/N(X)$. The efficiency of NINJA for protons was evaluated to be 98% for both layers.

The timing resolution was evaluated by using the time difference between the X- and Y-layers, since the distance between the two layers is small (50mm). Figure 1 shows the spectrum of time difference between the X- and Y-layers. One channel in the X-axis corresponds to 100 ps in this case. The red curve indicates the result of fitting using a Gaussian distribution. The resultant sigma of the Gaussian is 6.5 ch, corresponding to 650 ps. Assuming that the time resolutions the X- and Y-layers are identical, the time resolution of NINJA is estimated to be 460 ps. This resolution is mostly governed by one of the EASIROC circuits[3,4], and it can be further improved sightly vis correcting of the walk effect and adjusting the fine offsets of the individual TDC channels. NINJA is currently ready to be employed as the SAMURAI standard detector. It will be used to detect protons emitted from reactions of proton-rich unstable-nuclei beams, for example, for the study of exotic decay channels such as a d-bar (singlet s state of the p+n system) decay from excited states of nuclei. The momentum reconstruction of protons will be performed by combining NINJA with a drift chamber that is currently being developed, which will be positioned immediately in front of NINJA.

This work was funded by ImPACT Program of Council for Science, Technology and Innovation (Cabinet Office, Government of Japan).

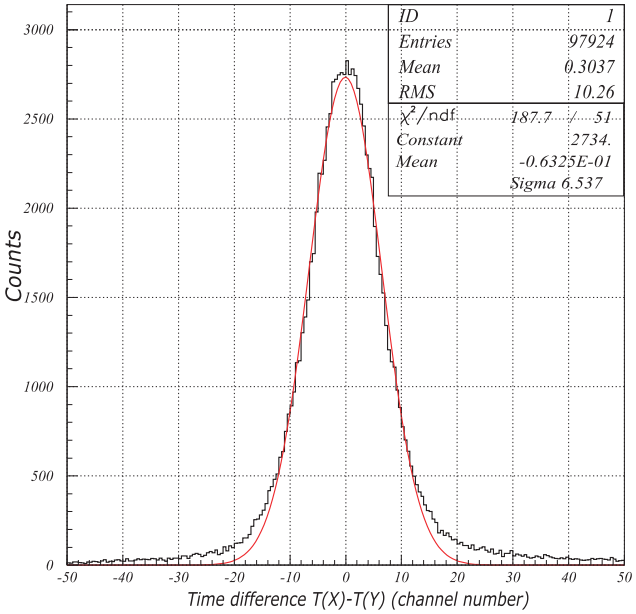

Fig. 1. Spectrum of time difference between X- and Y-layers of NINJA.

References
1) N. Chiga et al.: KEK Proceedings 2016-1, O-1-1 (2015), p.5.
2) N. Chiga et al.: RIKEN. Accel. Prog. Rep.**49**, 165 (2015).
3) T. Shiozaki, Master Thesis, Department of Physics, Tohoku university (2015).
4) N. Ishijima, Master Thesis, Department of Physics, Osaka university (2014).
5) S. Chebotaryov et al.: in this report.

*1 RIKEN Nishina Center
*2 Department of Physics, Tohoku University
*3 Department of Physics, University of Tokyo
*4 Department of Physics, Tokyo Institute of Technology

Measurement of light charged particle in the SAMURAI magnet gap with NINJA

T. Y. Saito,[*1,*2] N. Chiga,[*2] T. Isobe,[*2] R. Tamura,[*1] M. Usami,[*1] R. Higuchi,[*1] and H. Otsu[*2]

SAMURAI is a large-acceptance magnetic spectrometer aiming at coincidence measurements of charged particles and neutrons. SAMURAI has a standard detector setup for measuring heavy residual nuclei and neutrons, but it is practically impossible to measure more than three types of particles that have considerably different magnetic rigidities, such as neutrons, heavy residual nuclei, and protons. NINJA was designed to measure protons in their trajectory inside the SAMURAI vacuum chamber before they are incident on the side yoke of the dipole magnet.

NINJA consists of a 2-layer plastic scintillator with a thickness of 10 mm each and has a sensitive area of 1080×720 mm^2. Multi-pixel photon counters (MPPCs) located in the pole gap of the dipole magnet are used to count scintillation photons in a strong magnetic field.[1)] Signals from each MPPC are read by the VME-EASIROC frontend board,[2)] which equips an onboard TDC and voltage sensitive ADC.

The first online performance test of NINJA using protons and other fragments was performed at RIBF in 2015. Proton beams with energies of 110 MeV and 250 MeV generated by the fragmentation of a primary beam of ^{48}Ca irradiated NINJA. A particle identification (PID) test using NINJA for light fragments such as deuterons and ^{3}He produced at reactions between a secondary beam of ^{29}Ne and a liquid H_2 target was also performed.

In the present experiments, it was found that the data aquisition with the ADC remained to be developed. For the PID of light-charged ions, time over threshold (ToT) values were taken by the TDC instead of ADC. Figure 1 shows PID using the ToT value and the leading edge timing of a certain bar in the X layer measured by a plastic scintillator (F13 plastic) during the ^{29}Ne+H_2 run. One can clearly identify the proton, deuteron, ^{3}He, and ^{4}He by means of TOF-ΔE.

One can measure the X and Y positions of the light charged particle by taking the coincidence between the X layer and Y layer. Figure 2 shows the position of a 250-MeV proton beam measued by NINJA. Each pixel in Fig. 2 represents the coincidence of both layers. The peak position is consistent with a calculation of the proton trajectory.

Currentry, VME-EASIROC used in the present experiments is being replaced by NIM-EASIROC aiming at the easier handling of bias supply and low noise. The performance with NIM-EASIROC is reported in Ref. 3. Further developments are in progress to incorporate NINJA into standard detectors of SAMURAI.

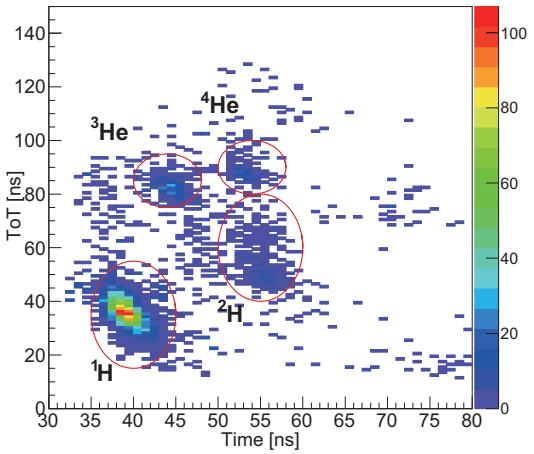

Fig. 1. Particle identification with NINJA. The horizontal axis represents the time of flight between F13 plastic and NINJA, and the vertical axis represents the ToT value for ΔE.

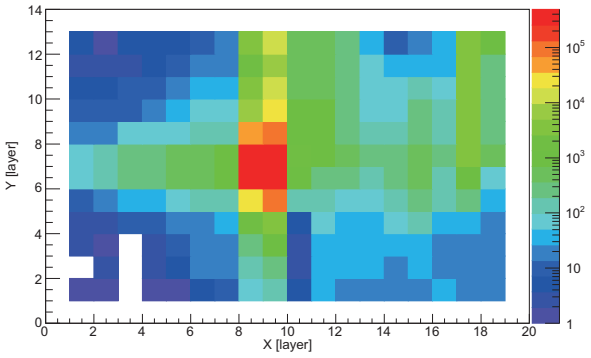

Fig. 2. Measured position of a proton beam with an energy of 250 MeV.

This work was funded by the ImPACT Program of the Council for Science, Technology and Innovation (Cabinet Office, Government of Japan).

References

1) N. Chiga et al.: RIKEN Accel. Prog. Rep. **49** (2015) 165.
2) T. Shiozaki: Master's thesis, Tohoku University (2014).
3) N. Chiga et al.: In this report.

*1 Department of Physics, the University of Tokyo
*2 RIKEN Nishina Center

Background estimation for multi-charged particle coincidence events with SAMURAI

S. Koyama[*1,*2] and H. Otsu[*2] for SAMURAI08 collaboration

Several experiments have been performed with the SAMURAI spectrometer[1] in recent years. Some of these experiments performed invariant-mass spectroscopy for the particle-unbound states of unstable nuclei. For the invariant-mass spectroscopy of multi-charged particles (MCPs) such as protons or α particles and residuals, it is important to select MCP coincidence events. Charged-particle events can be identified by a hodoscope (HOD)[1] composed of plastic scintillator slats, which is placed downstream of the SAMURAI magnet. Therefore, a value of more than two of HOD slats ($M2$) is able to select MCP coincidence events. In this report, we estimate the origins of the background for MCP coincidence events.

For the estimation, we analyzed the data of the SAMURAI08 experiment.[2] In this experiment, α-cluster levels in ^{16}C were investigated with a 200 MeV/nucleon ^{16}C beam and liquid He target. Here, we used down-scaled *Beam* trigger events. A *Beam* trigger is generated by the coincidence of two plastic scintillators SBT1 and SBT2[1] and the anti-coincidence of a perforated plastic scintillator SBV. The SBV is installed to reject events in which a ^{16}C beam hits the target cell frame. The averaged count rate of the *Beam* trigger is 100 kcps and the purity of the ^{16}C is more than 99 %. An $M2$ event is 2.5 % of the *Beam* trigger events for a 150 mg/cm^2-thick liquid He filled tearget and 2.3 % for empty. Therefore, the 8 % of $M2$ events are caused by the reaction between the ^{16}C and the He target. We define the other 92 % of $M2$ events as background.

The main component of the background is found to be fragmentation of the ^{16}C beam downstream of the SAMURAI magnet. The time of flight (ToF) versus the light output (LO) plot of a typical slat of HOD gated by a multiplicity of one and $M2$ is shown in Figs. 1(a) and (b), respectively. Several isotopes can be identified in Fig. 1(a), while loci in low LO events occupy the main part in Fig. 1(b). These loci are identified as light ions originating from the ^{16}C beam downstream of the SAMURAI magnet as follows. The positions and angles of these loci can be deduced by drift chamber FDC2.[1] Reaction points can be vertex-reconstructed when two positions and angles are deduced in one event, as shown in Fig. 2(a). In this figure, the coordinate origin ($x = z = 0$) is the box center of FDC2. Both the $x-$axis and $z-$axis are perpendicular to the gravity direction and the $x-$axis is parallel to the FDC2 entrance window. The red line

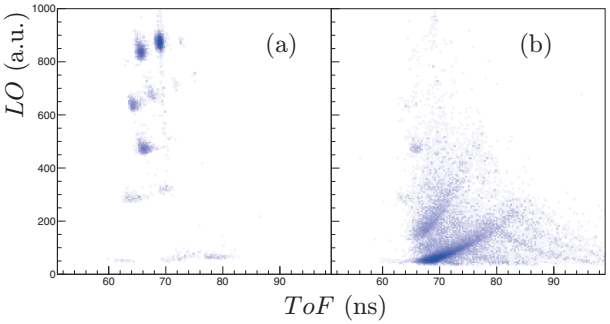

Fig. 1. ToF versus LO of a typical slat of HOD gated by (a) multiplicity of one and (b) $M2$.

in Fig. 2(a) is a typical trajectory of the ^{16}C beam which overlaps with the reaction points. The projection for the $z-$axis is shown in Fig. 2(b). Two peaks around $z = -440$ mm and $z = -930$ mm are significant. These values are consistent with the z positions of the FDC2 entrance window and the charged particle exit window of the SAMURAI magnet ,[3] and 92 % of the background is tagged as this component.

Other minor components of the background are single events including more than two beam particles (3 %) and one particle going through neighboring HOD slats (1 %). The other component (4 %) probably consists of reactions with materials upstream of the SAMURAI magnet other than the He target.

In conclusion, the origins of the background for MCP coincidence events are identified and the main component of the background is beam fragmentation downstream of the SAMURAI magnet.

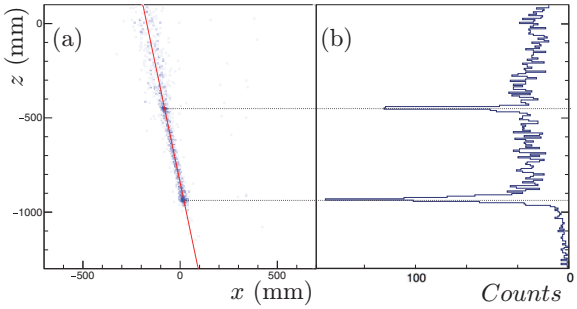

Fig. 2. (a) Reaction points deduced from the positions and angles of two fragments. The red line is a typical trajectory of the ^{16}C beam. (b) Projection for z of (a).

*1 Department of Physics, University of Tokyo
*2 RIKEN Nishina Center

References
1) T. Kobayashi et al., Nucl. Instrum. Meth. B **317** (2013).
2) H. Otsu et al., RIKEN Accel. Prog. Rep. **47**, xx (2014).
3) Y. Shimizu et al., RIKEN Accel. Prog. Rep. **47**, 175 (2014).

Helium filling method for SAMURAI spectrometer†

V. Panin,[*1] S. Chebotaryov,[*1,*2] S. Sakaguchi,[*3] E. Milman,[*1,*2] N. Chiga,[*1] Z. Elekes,[*4] B. Heffron,[*5] S. Leblond,[*6] T. Lokotko,[*6] and H. Otsu[*1]

A helium filling method was developed for the SAMURAI spectrometer and successfully tested in the SAMURAI13 experiment. The method allowed the use of an extra-large exit window to maximize the geometrical acceptance of the spectrometer and preserved the acceptable momentum resolution for charged particles by minimizing multiple scattering in the gas with a small Z number.

A schematic layout of the He-filling system is shown in Fig. 1. The vacuum extension duct, neutron window, and large "megane" flange of the spectrometer were replaced by a large window with a total area of 5.2×1 m^2. The design of the exit window was based on a previously tested prototype.[1)] Two O_2 sensors were placed inside the SAMURAI gap to monitor the concentration of air in a volume of $\sim$10 m^3. Helium was supplied into the gap at a rate of 20 L/min via an injection flange, which also contained feedthroughs for signal cables from the O_2 sensors. In addition, an internal pressure monitor was attached to the injection flange to control gas pressure inside the gap. Another external monitor measured ambient pressure in the experimental area. The data from the O_2 and pressure sensors were monitored and recorded on the external PC. During He injection, the air-He mixture was freely exhausted to the atmosphere via NW25 port. Slow gas ventilation allowed maintaining a pressure nearly equal to atmospheric pressure inside the gap without significant stress on the exit window.

The results are summarized in Fig. 2. The operation was performed in three stages. During the first period ($\sim$11 h), a He concentration of 76% was reached. Subsequently, He injection was interrupted, and the exhaust port was sealed for 11 h to check the leak rate. No leak was observed during this period, and the final ventilation was performed to reach the desired He content of $\sim$95%. The concentration was maintained at this level throughout 13 consecutive days without continuous gas supply and keeping a sealed ejection port. In the following, an insignificant air leak of $\sim$2 L/day into the gap was observed, which was partially compensated by adding small amounts of helium once per two days. No significant changes (<1 mbar) in the internal pressure relative to the exterior were observed during and after the ventilation procedure. Small fluctuations of the absolute pressure coincided with the ambient pressure due to changing weather conditions as can be seen in Fig. 2.

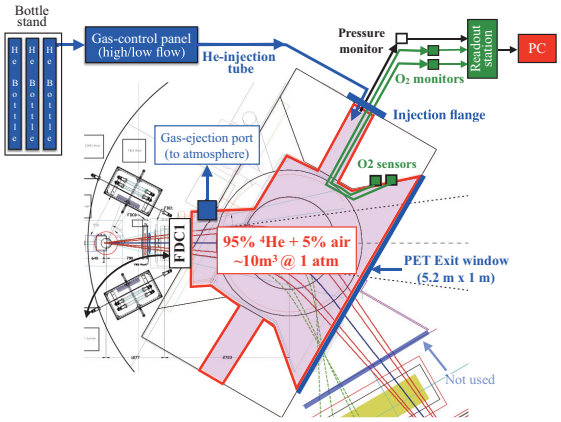

Fig. 1. Schematic layout of the He-filling system. The red shaded area indicates the volume filled by helium.

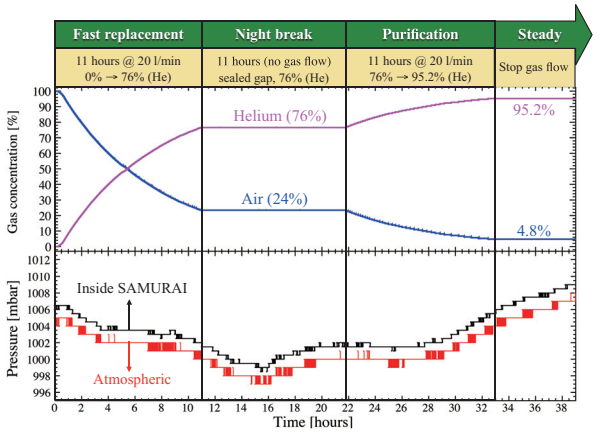

Fig. 2. He-filling performance with SAMURAI. Top figure: gas concentration in the gap as a function of time, estimated from the measurements in O_2 sensors. Bottom figure: data form the internal and external pressure monitors.

The presented results clearly demonstrate the feasibility of the He-filling of the SAMURAI spectrometer. The method can be potentially applied in the upcoming experiments at SAMURAI, for example, in heavy-ion-proton measurements, which require the maximum geometrical acceptance for protons in the focal plane owing to 90° rotation of the spectrometer.

*1 RIKEN Nishina Center
*2 Department of Physics, Kyungpook National University
*3 Department of Physics, Kyushu University
*4 Institute for Nuclear Research, MTA Atomki
*5 Oak Ridge National Laboratory
*6 Department of Physics, University of Hong Kong

Reference

1) V. Panin et al., RIKEN Accel. Prog. Rep. **49**, 168 (2016).

Improvement of the β-ion correlation algorithm in decay spectroscopy

J. Ha,[*1,*2] T. Sumikama,[*2] and S. Choi[*1]

Decay spectroscopy provides information about the decay properties of unstable nuclei on a nucleosynthesis path. Many experiments were performed under the EURICA collaboration at RIKEN RIBF. The Double-Sided Strip Si Detectors (DSSDs) called WAS3ABi were installed to measure the energy and time of implanted nuclei (ions) and β-rays.[1)] A β-ion correlation to determine the parent nucleus was performed using the position difference between the β-rays and ions. A new algorithm was developed to increase the correlated events and decrease background by selecting the β-ray origin from all detected positions. The outline of the algorithm is as follows:

(1) Categorize the β-ray events using the hit pattern of the DSSDs (see Fig. 1).
(2) For cases (category #=10* in Fig. 1) for which the maximum number of hits in one layer = 1, check whether the upstream/downstream plastic scintillator has detected the β-ray or not.
(2-1) If it has, the emitted β-ray has gone to the plastic scintillator. Therefore, the direction of the β-ray and the emitted position candidate can be determined explicitly.
(2-2) If it has not, if an energy deposition by a penetrated beta ray was also lower than one, it is selected as the emitted position candidate.
(3) If there is detection on only one side, detection of the β ray in the implanted layer is difficult because the passing distance in one DSSD is shorter than the DSSD with the penetrated β ray. When detection occurs on only one side of the DSSD, the position of the other side is estimated by trajectory extrapolation.
(4) For implanted ions, implanted events near the surface of DSSDs can be assigned.[2)] The implanted layer may not detect the emitted β-ray because the energy loss is too small to detect when the beta ray is emitted towards the near surface. Therefore, a layer difference of up to one between the ion and beta ray is accepted only for this surface-implantation case.

To compare the old and new algorithms, isotope ^{112}Nb was chosen (Fig. 2). In the previous algorithm, all β-ray hit positions were candidates for β-ion correlation, and it collected 38.7% of the total β decay by accepting the X(Y) position difference ΔX (ΔY)$\leq$1 strip. The new algorithm, using the same condition ΔX (ΔY)$\leq$1, detects more β-ion correlations, collecting 41.9% of the total β decay (option 1 in Fig. 1). The ratio of the number of detected parent decays to the number of background events in the first 10 ms was also compared. Figure 2 shows the improvement in this ratio obtained by the new algorithm. The new algorithm provides options, as described in the caption of Fig. 2, for different requirements. The improvement was achieved mainly by selecting the position candidates and considering the surface implantation of the ions.

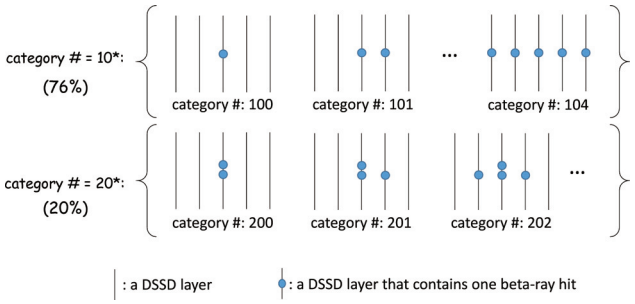

Fig. 1. β-ray events are categorized by category number. Numbers in the 100s indicate that the number of hits in a given layer is one or less. Numbers in the 200s indicate that the number of hits in a given layer is two or less. The total fraction of category 10* (100 to 104) is 76%.

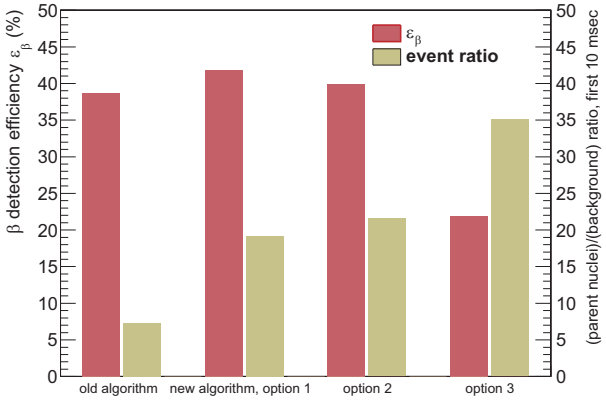

Fig. 2. β detection efficiency ε_β of the old and new algorithms for ^{112}Nb decay. Option 1 uses the position difference condition ΔX (ΔY)$\leq$1. Option 2 uses ΔX (ΔY)=0, and option 3 uses the events for which the β-ray was detected by upstream or downstream plastic scintillators and ΔX (ΔY)=0 to minimize background events.

*1 Department of Physics and Astronomy, Seoul National University
*2 RIKEN Nishina Center

References

1) P.-A. Söderström et al., Nucl. Instr. Meth. **317**, 649 (2013).
2) I. Nishizuka et al., JPS Conf. Proc. **6**, 030062 (2015).

Development of new analysis methods for EURICA data: γ-ray efficiency and γ-γ angular correlation

A. Yagi,[*1,*2] H. Kanaoka,[*1,*2] A. Odahara,[*1] R. Lozeva,[*3,*4] C.-B. Moon,[*5] H. Nishibata,[*1,*2] T. Shimoda,[*1] P. Lee,[*6] R. Daido,[*1,*2] Y. Fang,[*1,*2] S. Nishimura,[*2] P. Doornenbal,[*2] G. Lorusso,[*2] P.-A. Söderström,[*2] T. Sumikama,[*2] H. Watanabe,[*7] T. Isobe,[*2] H. Baba,[*2] H. Sakurai,[*8,*2] F. Browne,[*9,*2] Z. Patel,[*10,*2] S. Rice,[*10,*2] L. Sinclair,[*11,*2] J. Wu,[*12,*2] Z.Y. Xu,[*13] R. Yokoyama,[*14] T. Kubo,[*2] N. Inabe,[*2] H. Suzuki,[*2] N. Fukuda,[*2] D. Kameda,[*2] H. Takeda,[*2] D.S. Ahn,[*2] D. Murai,[*15] F.L. Bello Garrote,[*16] J.M. Daugas,[*2,*17] F. Didierjean,[*3] E. Ideguchi,[*18] T. Ishigaki,[*1,*2] H.S. Jung,[*19] T. Komatsubara,[*2,*20] Y.K. Kwon,[*20] C.S. Lee,[*6] S. Morimoto,[*1,*2] M. Niikura,[*8] I. Nishizuka,[*21] and K. Tshoo[*20]

The evolution of the nuclear shape as a function of N and Z numbers is one of the most important subjects in nuclear physics to date. In some regions, in particular for the neutron-rich Xe isotopes, not only the shape evolution but also the shape coexistence are expected to appear at low excitation energy region. To study these phenomena for nuclei in this neutron-rich mass region, an experiment was performed as a part of EURICA campaign[1]. The neutron-rich Xe nuclei were produced by the in-flight fission reaction of a ^{238}U beam and were implanted in five double-sided Si-strip detectors (WAS3ABi) with particle identification information. After the implantation, β-rays and γ-rays were detected by WAS3ABi and EURICA consisting of twelve cluster-type Ge detectors, respectively. As the beam spot size is large in WAS3ABi, it is difficult to exactly deduce the γ-ray efficiency and extract the γ-γ angular correlation for Ge detectors with large solid angles. To solve these problems, we developed the following new analysis methods.

The γ-ray efficiencies for all Ge detectors in EURICA were deduced from the data of γ-ray standard sources ^{152}Eu and ^{133}Ba, placed upstream and downstream of WAS3ABi as well as in-beam data to correct the positions of the γ-ray emission from widely distributed isotopes. In the latter case, if two consecutive γ-rays of γ_1 (with intensity of I_1 for 100 decays of the parent nuclei) and γ_2 (I_2) in a cascade are detected by two Ge detectors, the full-energy peak efficiency of γ_1 can be given by $\epsilon_{\gamma 1} = \frac{N_{\gamma 1 \gamma 2} I_{\gamma 2}}{N_{\gamma 2} I_{\gamma 1}}$, where $N_{\gamma 1}$ and $N_{\gamma 2}$ are counts in the full-energy peaks in the singles spectrum and $N_{\gamma 1 \gamma 2}$ is the full-energy peak count in a γ_1-γ_2 coincidence event. The absolute γ-ray efficiency of EURICA (closed circles with error bars) with efficiency curve obtained by source data (solid line) is shown in Fig. 1. In the low-energy region, absolute efficiency is smaller than source data, which may be caused by the spread of isotope distribution and decrease of the γ-ray intensity in WAS3ABi.

Next, we try to deduce the γ-γ angular correlation to obtain multiplicities of γ-ray transitions (ΔI between levels) and extract the spin of newly identified levels. Because of the large solid angle of each cluster-type Ge detector and widely implanted isotopes in WAS3ABi, correction of the γ-ray efficiency for each Ge detector and angle have to be performed. To correct γ-ray efficiency, the γ-γ angular correlation can be deduced by $W_{\gamma 1 \gamma 2}(\theta) = \frac{N_{\gamma 1 \gamma 2}(\theta)}{N_{\gamma 1} N_{\gamma 2}}$ for a γ_1-γ_2 coincidence event[2], because of this $W_{\gamma 1 \gamma 2}(\theta) \propto \frac{N_{\gamma 1 \gamma 2}(\theta)}{\epsilon_{tot\gamma 1} \epsilon_{tot\gamma 2}}$, where $\epsilon_{tot\gamma 1}$ and $\epsilon_{tot\gamma 2}$ are the efficiency of the total Ge detectors for γ_1 and γ_2, respectively. For the angle in two Ge detectors and an implanted isotope position in WAS3ABi, the angular spread is also obtained by event-by-event analysis. As an example, in Fig. 2, we show the γ-γ angular distribution between 403 ($4^+ \rightarrow 2^+$) and 287 ($2^+ \rightarrow 0^+$) keV γ rays in ^{142}Xe for angles of 28°, 54°, and 85°. These data points are found to be in agreement with the calculated values[3] (solid line in Fig. 2) for the case of $4^+ \rightarrow 2^+ \rightarrow 0^+$. The presented method allows a more effective analysis of the γ-γ angular distribution.

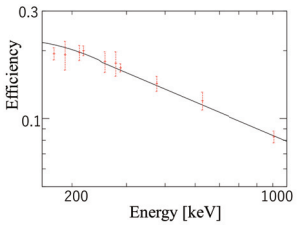

Fig. 1. Absolute γ-ray efficiency of EURICA.

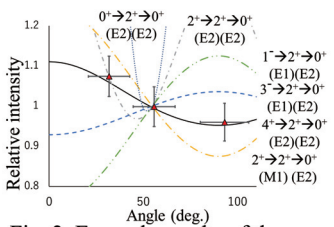

Fig. 2. Example results of the γ-γ angular correlation.

*1 Department of Physics, Osaka University
*2 RIKEN Nishina Center
*3 IPHC/CNRS and University of Strasbourg
*4 CSNSM/CNRS, University Paris-Sud
*5 Department of Display Engineering, Hoseo University
*6 Department of Physics, Chung-Ang University
*7 Department of Physics, Beihang University
*8 Department of Physics, University of Tokyo
*9 CEM, University of Brighton
*10 Department of Physics, University of Surry
*11 Department of Physics, University of York
*12 Department of Physics, Peking University
*13 Department of Physics, The University of Hong Kong
*14 CNS, University of Tokyo
*15 Department of Physics, Rikkyo University
*16 Department of Physics, University of Oslo
*17 CEA/DAM
*18 RCNP, Osaka University
*19 Department of Physics, University of Notre Dame
*20 IBS
*21 Department of Physics, Tohoku University

References

1) P.-A. Söderström et al., Nucl. Instrum. Methods Phys. Res. B **317**, 649 (2013).
2) M. Asai et al., Nucl. Instrum. Methods Phys. Res. A **398**, 265 (1997).
3) C. Goodin et al., Phys. Rev. C **79**, 034316 (2009).

Isochronism of Rare RI Ring

Y. Yamaguchi,[*1] M. Wakasugi,[*1] Y. Abe,[*1] A. Ozawa,[*1,*2] F. Suzaki,[*1] D. Nagae,[*1] S. Ohmika,[*1,*3] S. Naimi,[*1] Z. Ge,[*1,*3] S. Suzuki,[*1,*2] T. Uesaka,[*1] T. Yamaguchi[*1,*3] for the Rare RI Ring Collaboration

A precise isochronous condition for reference particles is essential to precisely determine the mass of nuclei using the Rare RI Ring (R3)[1]; therefore, one of the main purposes of a machine study for R3 is the isochronous tuning with beams. An isochronous field is formed by a combination of the edge-angle and gradient magnetic field of dipoles that are equipped with 10 trim coils.

In the first machine study, a first-order isochronous field tuned to a ^{78}Kr primary beam was successfully formed by adjusting the trim coils. The time-of-flight (TOF) spectrum after extraction as a function of momentum can be used to verify the isochronism, as shown in Fig. 1. Although it is natural that the secondary component remains in the distribution, the TOF width is broad overall. Because TOF width affects the experimental uncertainty of mass determination, it must be reduced as much as possible. Before conducting the third machine study,[2] we investigated the cause of the TOF broadening using simulation. It was found that the non-uniformity of the pole face of dipoles influence the TOF width. However, it could be improved by correcting the secondary component remaining in the distribution.

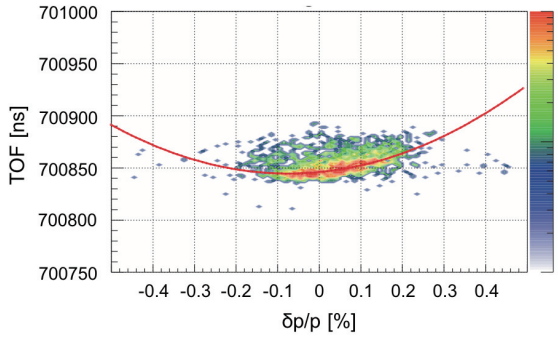

Fig. 1. TOF spectrum of ^{78}Kr after extraction as a function of momentum. The red line shows a quadratic fitting curve.

In the third machine study, we performed the isochronous tuning with ^{78}Ge, which was produced by in-flight U fission. The upper panel of Fig. 2 shows the TOF of extracted particles as a function of momentum before adjusting the isochronism by the second order. The full width of the TOF is almost as large as that of ^{78}Kr case. From this figure, it seems that isochronism is not satisfied on the high momentum side, in contrast to the low momentum side; thus, we tuned mainly the outer trim coils of R3. This resulted in the disappearance of the secondary component and the reduction of TOF width simultaneously as shown in the lower panel of Fig. 2. Consequently, the isochronism with the full momentum of 0.6% was improved. The TOF width after projection on the y-axis direction is 3.6 ns in sigma, and therefore, the degree of isochronism is approximately 5 ppm.

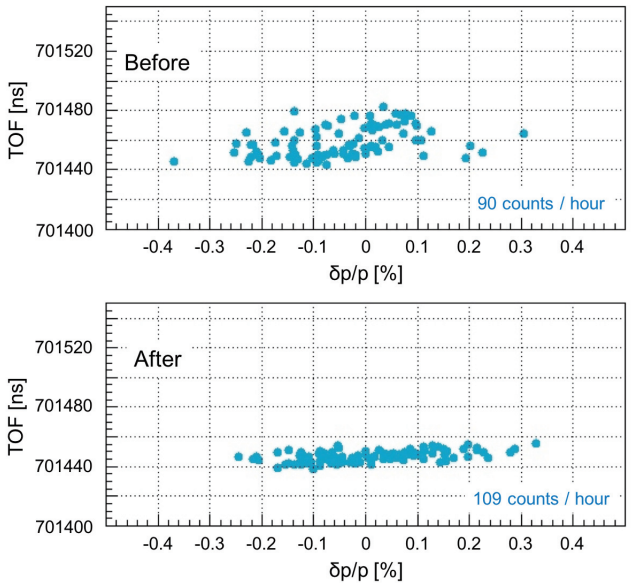

Fig. 2. TOF spectra of ^{78}Ge after extraction as a function of momentum. Upper and lower figures show the results obtained before and after adjusting the isochronism by the second order, respectively.

This value is at the level of the main magnetic-field fluctuation of R3 during the measurement time of about 1 day. There is no strong correlation between the TOF data and the fluctuation of magnetic field; however, it may be necessary to reduce the fluctuation of the magnetic field to further improve the isochronism. Another possibility is that the isochronism will further improve by third- or higher-order correction. The optimum value would be 1 ppm or less, which is quite challenging and requires step-by-step improvement.

*1 RIKEN Nishina Center
*2 Institute of Physics, University of Tsukuba
*3 Department of Physics, Saitama University

References

1) A. Ozawa et al., Prog. Theor. Exp. Phys. 2012, 03C009 (2012).
2) D. Nagae et al., In this report.

Momentum acceptance of the Rare RI Ring studied from revolution frequency measurements

F. Suzaki,[*1] Y. Abe,[*1] D. Nagae,[*1] S. Omika,[*1,*2] A. Ozawa,[*1,*3] T. Uesaka,[*1] M. Wakasugi,[*1] K. Yamada,[*1] T. Yamaguchi,[*2] Y. Yamaguchi,[*1] J. Zenihiro,[*1] for the Rare RI Ring collaboration

The Rare RI Ring was constructed[1,2] to investigate the nuclear structure and nucleosynthesis of unstable nuclei. The ring is a storage ring that measures the masses of unstable nuclei. Aiming at a relative mass precision of 10^{-6}, we employ the isochronous mass spectrometry method in the ring having precisely tuned isochronism. We developed a resonant Schottky pick-up for measuring revolution frequency.[3] Electromagnetic field is induced in the cavity by a circulating ion which periodically passes through it. The revolution frequency is obtained from frequency measurement of the field stored in the cavity. Basic parameters representing the performance of the resonant cavity, such as resonance frequency $f_{\rm res} = 172.9 \pm 1.6$ MHz, shunt impedance $R_{\rm sh} = 161$ kΩ, and unloaded quality factor $Q_0 = 1880$, were acquired.

The first commissioning of the Rare RI Ring using a 168-MeV/u Kr beam was conducted in June 2015. In the experiment, the signal of a single Kr nucleus was detected with the resonant Schottky pick-up. A frequency resolution of 1.3×10^{-6} was obtained from 32 ms-long measurements[4]. We observed that the revolution frequency gradually varies with time during the ion accumulation for 5 s. This is caused by the imperfection of isochronism and momentum change due to a finite vacuum condition. Under the current vacuum condition of 3.9×10^{-5} Pa, the momentum decrease shown in Fig. 1 is expected. This enables us to convert the time to the momentum change.

We acquired 14 events, each exhibiting their revolution frequencies as functions of time. Figure 2 shows the individual trajectories for the 14 events in a momentum change-frequency two-dimensional plane, for which the momentum change is obtained by the conversion from time according to Fig. 1. We note here that the initial momenta for the individual events are unknown and may not be identical, and some of the trajectories seem to be discontinued owing to possible hard collisions. Since the revolution frequency trajectories should be identical as far as the machine condition remains constant, each event in Fig. 2 has been appropriately shifted along the horizontal axis to conform to a single trajectory. The conformability is imperfect as evident in Fig. 2, because the momentum change shown in Fig. 1 is a stochastic process. Each event may not cover full momentum acceptance. The full momentum width in the total data, however, could be identified as the momentum acceptance of the ring. The estimated momentum acceptance is approximately 0.6%.

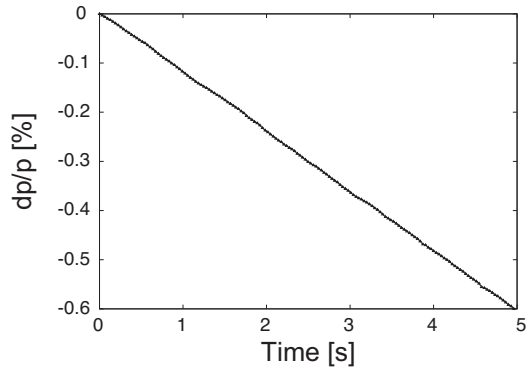

Fig. 1. Simulation result of momentum change as a function of time under the vacuum condition of 3.9×10^{-5} Pa.

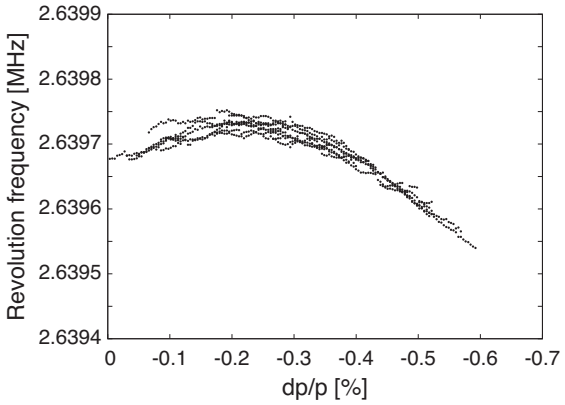

Fig. 2. 14 events of revolution frequency as a function of the momentum change obtained through the conversion from time according to Fig. 1.

References

1) A. Ozawa et al., Prog. Theor. Exp. Phys. 03C009 (2012).
2) Y. Yamaguchi et al., Nucl. Instrum. Methods Phys. Res. B **317**, 629 (2013).
3) F. Suzaki et al., JPS Conf. Proc. **6**, 030119 (2015).
4) F. Suzaki et al., Proceedings of 13th International Conference on Heavy Ion Accelerator Technology (HIAT).

*1 RIKEN Nishina Center
*2 Department of Physics, Saitama University
*3 Institute of Physics, University of Tsukuba

Development of a monitor for stored particles in the Rare RI Ring

S. Omika,[*1,*2] T. Yamaguchi,[*1] N. Tadano,[*1] T. Suzuki,[*1] Z. Ge,[*1,*2] K. Wakayama,[*1] Y. Abe,[*2] T. Uesaka,[*2] S. Naimi,[*2] F. Suzaki,[*2] D. Nagae,[*2] Y. Yamaguchi,[*2] M. Wakasugi,[*2] M. Amano,[*3] A. Ozawa,[*3] D. Kamioka,[*3] S. Suzuki,[*3] and T. Moriguchi[*3]

The precise mass measurements of neutron-rich nuclei are important for the study of the r-process and nuclear structure. The Rare RI Ring is a device for the precise mass measurements for short-lived nuclei.[1,2] In the mass measurements, the magnetic field in the ring is adjusted to be isochronous by using trim coils. Under this condition, the revolution time is constant and independent of the momentum of particles. This device determines the masses by comparing the revolution time of the reference particle with known mass and the particle of interest. First, we must optimize the septum magnets and the kicker magnet to enable the injection and storage of particles. For this purpose, a detector is needed to monitor the stored particle in the Rare RI Ring.

The required performance of a detector to confirm particle storage is high efficiency and low material density on beam line. In this report, we have developed a detector using a thin foil, scintillators and multi-pixel photon counters (MPPCs). This detector detects multiple turns by detecting secondary electrons including low-energy electrons to δ-rays using plastic scintillators and MPPCs. As a detector for the same purpose, a timing detector using a carbon foil and a micro-channel plate has been developed.[3] The advantage of the new detector is that it is free from the electrical noise of the kicker magnet because it uses a photo-sensor.

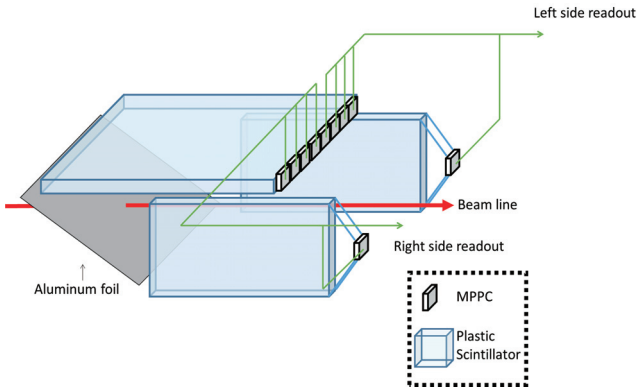

Fig. 1. Schematic view of the configuration of the δ-ray detector.

Figure 1 shows a schematic view of the developed detector. The thin foil consists of 3-μm-thick aluminum. The size of the top plastic scintillator is 100 × 100 mm^2 with 3-mm thickness. The size of plastic scintillators on both sides is 80 × 50 mm^2 with 3-mm thickness. We prepared ten MPPCs. Eight of them were connected to the upper side of the plastic scintillator and the other two were connected to the left and right sides. Ten MPPCs were divided into two units, the right half and the left half, and signals of five MPPCs are combined into one signal to reduce the number of readout channels. Hereafter, we refer to the developed detector as the δ-ray detector.

In November 2016, we conducted the third machine study of the Rare RI Ring[4] and measured revolution time using the δ-ray detector and the timing detector. In this experiment, we injected nuclei around ^{78}Ge with 175 MeV/nucleon. Figure 2(a) shows a histogram of the circulation of ^{78}Ge. This figure indicates the success of detection of circulating particles. The revolution time is calculated by the relationship between the turn numbers and total stored time (Fig. 2(b)). The revolution time measured by the δ-ray detector is consistent with the value measured by the timing detector. The precision of determining revolution time was 8 × 10 $^{-4}$. The future development goal is the improvement of time resolution.

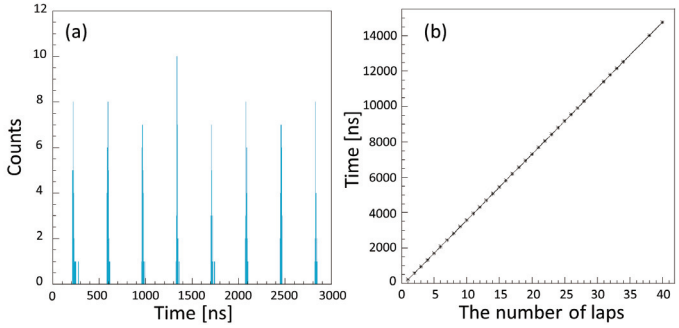

Fig. 2. (a) Zoomed histogram of the circulation of ^{78}Ge. (b) Time as a function of turn number, which is fit using a linear function.

*1 Department of Physics, Saitama University
*2 RIKEN Nishina Center
*3 Institute of Physics, University of Tsukuba

References

1) A. Ozawa et al., Prog. Theor. Exp. Phys. 2012, 03C009 (2012).
2) Y. Yamaguchi et al., Nucl. Instrum. Methods. Phys. Res. B **317**, 629 (2013).
3) D. Nagae et al., RIKEN Accel. Prog. Rep. **49**, 181 (2016).
4) D. Nagae et al., In this report.

Particle selection using RF signal for Rare RI Ring experiments

Y. Abe,[*1] D. Nagae,[*1] H. Baba,[*1] A. Ozawa,[*2] T. Uesaka,[*1] T. Yamaguchi,[*3] Y. Yamaguchi,[*1] M. Wakasugi[*1]
for the Rare RI Ring collaboration

We commissioned the Rare RI Ring by using secondary beams around ^{78}Ge nuclei in November.[1)] The secondary beams were produced via the in-flight fission of a 345 MeV/nucleon ^{238}U primary beam with a ^{9}Be target. To inject rare RI to the ring reliably, a self-trigger injection method was adopted in the ring. In this method, the RI of interest itself generates a trigger signal for the injection kicker at F3. It is necessary to perform a particle identification (PID) before generating the trigger signals and to transmit the trigger signal to the fast kicker system[2)] as soon as possible. The PID is based on the TOF-$B\rho$-ΔE method, in which the time-of-flight (TOF), magnetic rigidity ($B\rho$), and energy loss (ΔE) are measured. In order to perform PID, the TOF between F2 and F3 using a plastic scintillation counter and the ΔE at F3 using an ionization chamber were measured, as shown in Fig. 1. An acceptable momentum window of the ring is ±0.3%, which corresponds to the isotone region shown in the figure.

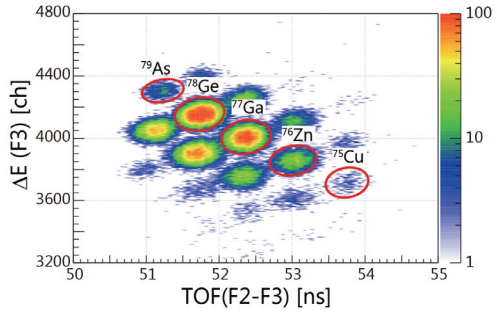

Fig. 1. PID plot of secondary particles with TOF and ΔE.

As can be seen from Fig. 1, the yield of nuclei on the neutron-rich side is very low. Because the purity of the neutron-rich nuclei is also low, the ratio included in the trigger signal, which was generated by the F3 plastic scintillation counter becomes lower. Because the maximum injection repetition frequency of the kicker system is 100 Hz, the measurement for such nuclei becomes time consuming. Therefore, we developed a new technique for restriction by TOF in order to efficiently measure such nuclei. We combined a radio frequency (RF) timing signal for accelerators with the trigger signal. This is because the timing of the RF signal and the arrival time of the RI beam have a certain time relationship so that only the RI arriving at a certain time can be used as a trigger signal by combining the RF signals. A conceptual diagram of the circuit is shown in Fig. 2. The adjustment of the particles to be restricted was carried out by changing the external delay in the circuit.

In the experiment, we demonstrated the technique. Figure 3 shows the difference in particles that generate trigger signals obtained when changing the external delay. When we changed the delay time every 2 ns, particles reaching at certain time do not participate in the trigger. By using this technique, for example, in the case of ^{75}Cu, we succeeded in improving the purity by more than one order of magnitude. From this result, it became possible to efficiently inject nuclei in the neutron-rich region. Moreover, this technique can be applied not only to the experiments of the Rare RI Ring but also to experiments in RI Beam Factory (RIBF). It is possible, for example, to acquire only event data of nuclides of interest.

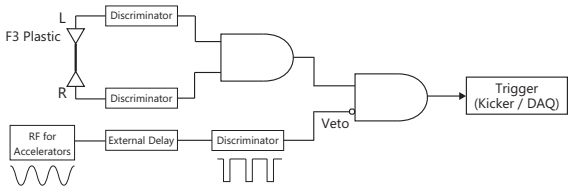

Fig. 2. Conceptual diagram of circuit for particle selection in generating trigger signal using RF signal for accelerators and timing signal at F3.

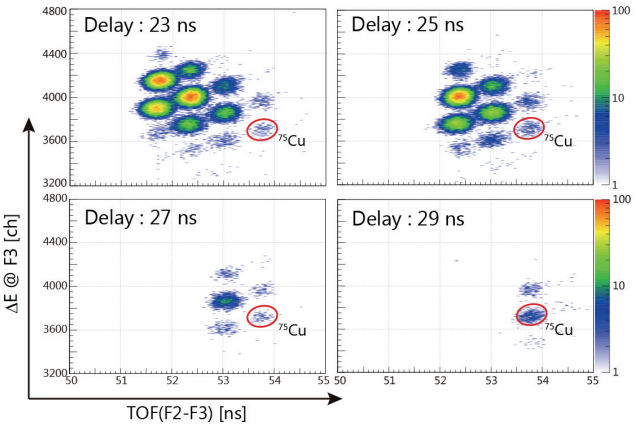

Fig. 3. Results of particle restriction using RF timing signal. The external delay time was different in each setting.

*1 RIKEN Nishina Center
*2 Institute of Physics, University of Tsukuba
*3 Department of Physics, Saitama University

References

1) D. Nagae et al. : In this report.
2) Y. Yamaguchi et al., Phys. Scr. **T166** 014056 (2015).

Simulation and design of a large area position sensitive TOF MCP detector at the Rare RI Ring

Z. Ge,[*1,*2] S. Naimi,[*1] D. Nagae,[*1] Y. Abe,[*1] T. Uesaka,[*1] T. Yamaguchi,[*2] F. Suzaki,[*1] Y. Yamaguchi,[*1] M. Wakasugi,[*1] S. Omika,[*1,*2] N. Tadano,[*2] K. Wakayama,[*2] A. Ozawa,[*1,*3] S. Suzuki,[*3] T. Moriguchi,[*1,*3] G. Lorusso,[*4] Y. Yano[*1] for the Rare RI Ring collaboration

In order to transport nuclei of interest individually to the central orbit of the Rare RI Ring[1](R3) with high efficiency and to improve the resolution of the in-ring TOF mass measurements at the R3, we plan to develop a large area (∼42mm x 190mm) position sensitive TOF MCP detector for R3, which has the properties of low energy loss, good timing and high position resolution.

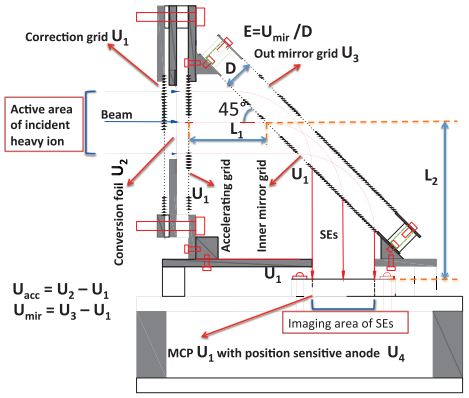

Fig. 1. Structure of the MCP detector and description of the parameters of the imaging mirror detector.

Information on the heavy ions that possess high energy can be reproduced by measuring the secondary electrons (SEs) induced from conversion foils with MCP which has a high intrinsic timing (20 ps-100 ps) and position resolution (0.1 mm). Detectors with magnetic field can't be used inside R3 because of the accumulation of the bending power of the magnet for the multi-turn circulation of fully stripped heavy ions and the influence on the homogeneity of the magnetic field of R3. Therefore, we chose a mirror-electrostatic-field-type detector for in-ring TOF position measurements. The detector consists of two chevron type micro-channel plates (MCPs) coupled with a position sensitive anode, a thin electron conversion foil, and a mirror electric field for bending the SEs ejected from a thin conversion foil (40 ug/cm^2) passing through by the highly charged heavy ion (^{78}Ni region with ∼ 170 MeV/nucleon energy for the next experiment).

To achieve high resolution, an isochronous condition[2] is chosen, at which the total time of flight consists of 3 parts: the accelerating grid to the inner mirror wires, bending path between the inner and outer mirror wires, free drift region from the inner mirror wires to the MCP. The relation of the so-called isochronous condition is $D/(L_1 + L_2) = 0.236\frac{U_{mir}}{U_{acc}}$[2]. U_{acc} and U_{mir} are, respectively the acceleration potentials between the conversion foil and the accelerating grid, and the mirror deflection potential between the mirrors are described in Fig. 1 together with L_1 and L_2.

To optimize the performance of the detector, a simulation was performed via SIMION.[3] By keeping the high voltage (HV) potential of the MCP, accelerating grid and inner mirror at -2500 V and by varying the accelerating HV of the foil and outer mirror grid at the isochronous condition we obtained the results shown in Fig. 1. With the increase of the accelerating HV, the resolution of timing and position is improved and reaches a plateau at a certain HV value. The Y position resolution is better than that of X, which is due to the mirror electric field effect in the Y direction. From the simulation results, the intended timing and position resolution of ∼100 ps in sigma and ∼1 mm in FWHM is satisfied, which is required for mass measurement (10^{-6}) and velocity reconstruction (10^{-4}). The detector has already been constructed and is now being tested.

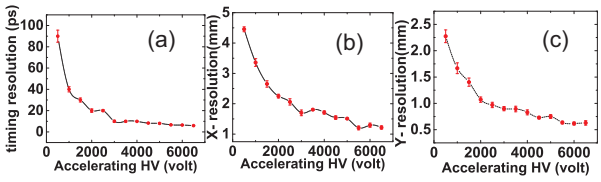

Fig. 2. Simulation results by *SIMION*[3] (with a mean energy value of 2 eV and a Gaussian distribution in energy of the SEs). (a) Timing resolution (in sigma) as function of the accelerating HV potential (the HV difference between the accelerating grid and conversion foil). (b) and (c) X- and Y-position resolution (in FWHM) dependence of the accelerating HV supply.

*1 RIKEN Nishina Center
*2 Department of Physics, Saitama University
*3 Institute of Physics, University of Tsukuba
*4 Department of Physics, University of Surrey

References

1) A. Ozawa et al., Prog. Theor. Exp. Phys. **2012**, 03C009 (2012).
2) N. Nankov et al., Wiss. Tech. Berichte FZR-423, 25 (2005) (Annual Report 2004).
3) http://www.simion.com.

Understanding bremsstrahlung spatial distribution of electron scaterring in the SCRIT experiment

T. Fujita,[*1] A. Enokizono,[*1,*2] K. Adachi,[*1] S. Ichikawa,[*2] N. Uchida,[*1] T. Ohnishi,[*2] K. Kasama,[*3] K. Kurita,[*1] S. Sasamura,[*1] T. Suda,[*2,*3] T. Tamae,[*2,*3] K. Tsukada,[*2,*3] M. Togasaki,[*1] K. Namba,[*3] M. Hara,[*2] M. Hori,[*1] T. Hori,[*2] K. Matsuda,[*3] K. Yamada,[*1] M. Watanabe,[*2] and M. Wakasugi[*2]

The self-confining RI ion target (SCRIT) electron scattering facility has been constructed to realize electron scattering off unstable nuclei[1]. In 2014, a luminosity monitor (LMon) was installed to measure the absolute luminosity value of electron scattering in the SCRIT experiment[2,3]. The luminosity is determined as

$$\frac{d^2N}{d\Omega dE} = L \cdot \frac{d^2\sigma}{d\Omega dE} \tag{1}$$

where N is the number of scattered electrons, L is the luminosity and σ is scattering cross section.The angular distribution of scattered electrons is measured by the window-frame spectrometer for electron scattering(WiSES)[4]. The required accuracy of the luminosity value is expected to be less than 5% which is comparable with the systematic uncertainty of WiSES.

To determine the luminosity with a total uncertainty less than 5%, it is necessary to measure the bremsstrahlung photon counts, energies and spatial distribution very precisely and accurately. The photon counts and energies are measured by a CsI calorimeter array. The CsI calorimeter consits of 7 pure CsI scintillators. The spatial distributions of the bremsstrahlung photons are measured by two layers of fiber scintillators. Each layer consits of 16 fiber scintillators and the cross section of each fiber is 3×3 mm^2. In the experiment, L is calculated as

$$L = \frac{N_{\mathrm{Brems.}}}{\sigma_{\mathrm{Brems.}}} \cdot \frac{1}{\varepsilon} \quad [\mathrm{cm}^{-2}\mathrm{sec}^{-1}] \tag{2}$$

where $N_{\mathrm{Brems.}}$ is the number of bremsstrahlung photons per second and $\sigma_{\mathrm{Brems.}}$ is the caluculated bremsstrahlung cross section[5]. Because LMon is located 7 m downstream of the vertex position and there are structures in the path of the photons such as a cryopanel in the beam chamber, it is necessary to evaluate the transmittance. ε is estimated as the number of photons detected with LMon divided by the number of radiated photons in the SCRIT calculated by GEANT4 simulations. It is important to understand several electron beam conditions such as electron beam energy and beam shape. In order to determine the parameters to be handled in the simulation, we compared experimental data and simulation data.

From 2015 to 2016, the experiment of electron scattering for ^{132}Xe and ^{208}Pb targets had been performed at electron beam energies Ee = 150 MeV, 200 MeV and 300 MeV. Figure 1 shows the experimental spatial distributions together with that calculated with GEANT4 simulations at E_{e} = 150 MeV. The red and blue closed circles in the upper panels in Fig. 1 represent the spatial distributions with and without target ions (Ion In and Ion Out), respectively. The lower panels show the spatial distributions of bremsstrahlung photons from ^{208}Pb estimated by subtracting Ion Out from Ion In. The systematic uncertainty of ε is estimated by varying the initial beam parameters within χ^2/ndf between exprimental data and GEANT4 spatial distributions. With a careful study of the initial beam condition, it has become possible to reproduce the spatial distributions of data by GEANT4 simulation, and the systematic uncertainty of ε was reduced to ∼ 6% , significantly less than the uncertainty of ∼ 10% achieved in a previous study. The key point to increase the reproducibilty and to reduce the systematic uncertainty is to understand the electron beam size according to the lattice function of the electron storage ring. In Fig. 1, the beam size is σ_{H} ∼ 2.13 mm, σ_{V} ∼ 0.60 mm and the spread of incident angle in the horizontal direction is +0.4 mrad in σ_{H} at the center of the SCRIT device.

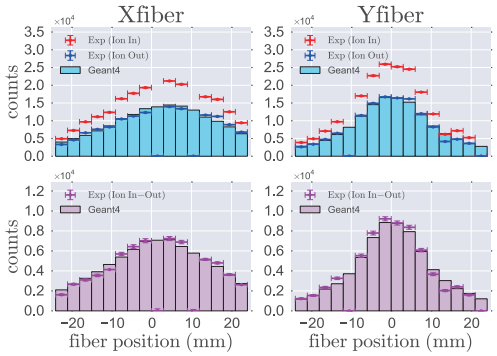

Fig. 1. Horizontal (X fiber) and vertical (Y fiber) spatial distributions. The histograms show simulation results.

In summary, we found that a careful treatment of the initial beam condition is key to reproduce the spatial distribution of bremsstrahlung photons and to reduce the systematic uncertainty in the determination of ε.

References

1) M. Wakasugi et al., Nucl. Instr. Meth. B**317**, 668 (2013).
2) S. Yoneyama et al., RIKEN Accel. Prog. Rep. **48**, 227 (2014).
3) A. Enokizono et al.: In this progress report.
4) K. Tsukada et al.: In this progress report.
5) Y. S. Tsai, Rev. Mod. Phys. **46** 815-851 (1974).

*1 Department of Physics, Rikkyo University
*2 RIKEN Nishina Center
*3 ELPH Tohoku University

Properties of ion trapping measured by the SCRIT LMon

A. Enokizono,[*1,*2] T. Fujita,[*1] K. Adachi,[*1] M. Hori,[*1] K. Kasama,[*3] K. Kurita,[*1] K. Namba,[*3] T. Ohnishi,[*2] S. Sasamura,[*1] T. Suda,[*2,*3] T. Tamae,[*3] N. Uchida,[*1] K. Tsukada,[*2,*3] M. Togasaki,[*1,*2] M. Wakasugi,[*2] M. Watanabe,[*2] and K. Yamada[*1]

The SCRIT detector is composed of a Window-frame Spectrometer for Electron Scattering (WiSES) to measure the angular distribution of scattered electrons[1] and a Luminosity Monitor (LMon) to measure the absolute luminosity of electron-RI scatterings.[2] LMon is measuring the bremsstrahlung photons and determine the luminosity as $L = N_{br}/t\sigma_{br}\epsilon$ ($\mathrm{cm^{-2}s^{-1}}$), where N_{br}/t is the number of bremsstrahlung photons per second, σ_{br} is the bremsstrahlung cross-section, and ϵ is the detector acceptance. σ_{br} can be calculated using a theoretical model[3], and LMon consists of two main components to measure the remaining factors: a CsI calorimeter to measure N_{br}/t and a two-dimensional fiber scintillator detector to measure the spatial distribution of bremsstrahlung photons which have to be compared with GEANT4 to determine ϵ. The first physics experiment using ^{132}Xe and ^{208}Pb targets was performed in 2015-2016. Results of the experiment using WiSES are reported elsewhere,[4] and progress on LMon with respect to the determination of ϵ and its uncertainty is described in a separate report.[5] In this article, detailed measurements of ion trapping by LMon using ^{132}Xe data are reported.

With a recent upgrade of LMon, it has acquired the ability to measure N_{br} as a function of trapping-time, which revealed detailed properties of the ion trapping. Figure 1 shows N_{br} as a function of the trapping-time measured at an electron beam energy (E_e) of 150 MeV for different beam currents. Here Ion IN and Ion OUT denote measurements with and without trapped ^{132}Xe ions, respectively. That is, Ion OUT is the background contribution from residual gases (e.g H_2, O_2), and the net amount of N_{br} from ^{132}Xe ions is estimated as Ion IN-OUT. The Ion IN-OUT decreases as a function of the trapping-time, implying that trapped target ^{132}Xe ions are depleted with time. On the other hand, the number of trapped residual gas ions, which is shown by Ion OUT, can be increased as a function of the trapping-time since there are virtually infinite neutral residual gas atoms inside the chamber, which are continuously ionized by the electron beam and trapped by the SCRIT device. Figure 2 shows the N_{br}/t of Ion IN-OUT as a function of the trapping-time for several currents and beam energies. N_{br}/t increases as the electron beam current/energy increases, which can be naturally explained by the fact that the beam density increases with increasing beam current/energy. It is interesting to note that there are fast and slow components in the trapping-time dependence, and the slow component becomes prominent as the beam energy and/or current increases. A feasible explanation is that the slow component originates from high-charged-state nuclei, which increase at time scales on the order of hundreds of milliseconds.

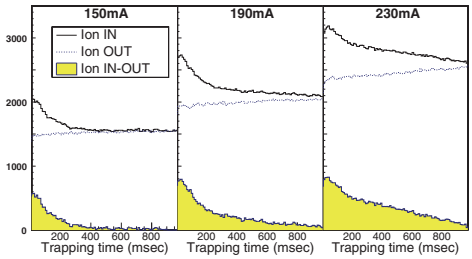

Fig. 1. Trapping-time dependence of N_{br} measured for different beam currents for ^{132}Xe at $E_e = 150$ MeV.

In summary, the properties of ion trapping at the SCRIT experiment have been measured by LMon. This information is useful for tuning the electron beam and SCRIT device parameters to optimize the ion trapping and maximize the luminosity, even though more detailed studies using simulations and calculations are required to reproduce the observation.

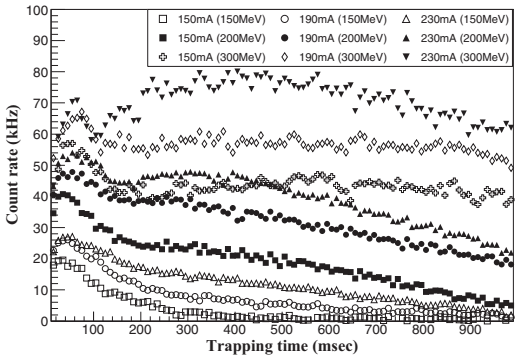

Fig. 2. Trapping-time dependence of N_{br}/t measured for different beam currents and energy regions.

*1 Department of Physics, Rikkyo University
*2 RIKEN Nishina Center
*3 Research Center for Electron-Photon Science, Tohoku University

References
1) T. Suda et al., Accel. Prog. Rep. **47**, 195 (2014).
2) S. Yoneyama et al., Accel. Prog. Rep. **48**, 227 (2015).
3) Y. S. Tsai, Rev. Mod. Phys. **46**, 815 (1974).
4) K. Tsukada et al., in this report.
5) T. Fujita et al., in this report.

Upgrade of electron gun at the SCRIT facility

M. Watanabe,[*1] M. Wakasugi,[*1] T. Oonishi,[*1] K. Adachi,[*2] A. Enokizono,[*1,*2] T. Fujita,[*2] M. Hori,[*2] K. Kurita,[*2] S. Sasamura,[*2] N. Uchida,[*2] and K. Yamada[*2]

We have been upgrading the electron beam source of the SCRIT facility.[1)] The electron beams from this source are used for electron injection into the electron storage ring (SR2) and for photofission at ERIS[2)] (electron-beam-driven RI separator for SCRIT). Particulaly for ERIS, the electron beam power forms one of the most important parameter in order to perform the electron scattering measurements of unstable nuclei, since the power affects the efficiency required to lead to photofission to generate the target nuclei.

In a previous work,[3)] we developed a new electronic circuit board for the trigger pulse of the electron gun. The driving frequency of the electron beam injector was subsequently increased from 10 Hz to 20 Hz by the new electronics; the total electron beam power was doubled.

In this work, we report on our modifications of two parts of the electron gun. The first is concerned the voltage power supply and pulser electronics for the extractor grid. With the new power supply, it is possible to increase the extractor voltage up to 650 V; the maximum previous extractor voltage was 200 V. As regards the equipment setup, the extractor grid is located about 1-2 mm above the cathode of the gun. Therefore, the electric field due to a higher voltage results in a higher electron current from the source, which yields higher electron-beam efficiency.

Secondly, we modified the shape of the extractor-grid electrode to generate focused rather than parallel electron beams. In the original design, the electrode could not shape concave equipotential surfaces in front of the extractor grid, since the top portion of the electrode was nearly flat. Consequently, it was not possible to generate a focused electron beam towards the DC acceleration electrode. An unfocused electron beam results in beam loss at the entrance of RF cavity of the race-track microtron (RTM).

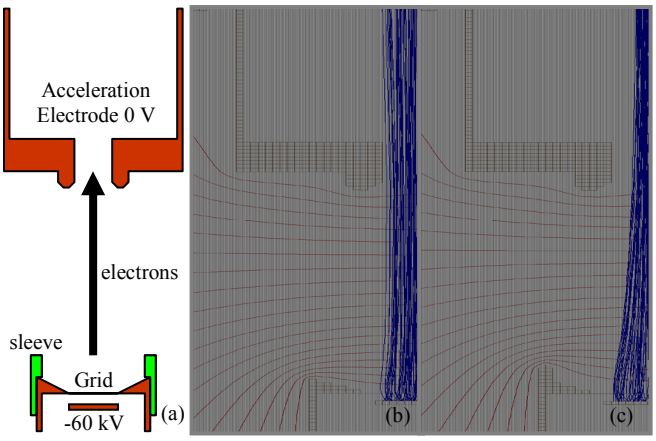

Fig. 1. (a) Schematic of electron gun, (b) simulation of electrons with original design, and simulation of electrons obtained with new grid electrode.

*1 RIKEN Nishina Center
*2 Department of Physics, Rikkyo University

In order to transport the electron beam from the source into the RTM, we installed a sleeve part atop the extractor grid, and fabricated a concave equipotential surface at the position corresponding to the beginning of DC acceleration of 60 kV. Figure 1(a) shows the schematic of the electron gun area. The protruding part denotes the sleeve. Figure 1(b) shows the beam simulation result without the space-charge effect as simulated by the software SIMION for the original design of the extractor grid. The blue lines indicate the trajectories of electrons, and red lines indicate the equipotential surfaces. From Fig. 1(c), We observe that the newly designed extractor grid affords a focused electron beam with small divergence inside the acceleration electrode.

In order to utilize this modification, we had to readjust the relevant parameters of the optics of the electron beam injector. The leakage field from the RTM magnet and gauge affects the beam transport in the 60-kV low-energy area. However, appropriate steerer magnets are utilized to direct the beam back to the center axis of the optics.

As a result of the extractor modification, we could increase the beam efficiency by 50% of the previous value at the beam monitor in the RTM. In addition, by applying a higher voltage to the grid, we expect to obtain a higher total yield of electron transport from the source to the RTM. The combination of the focused electron beam and higher grid voltage promises an increase in the ratio required to produce unstable nuclei at ERIS, and improved electron scattering measurements.

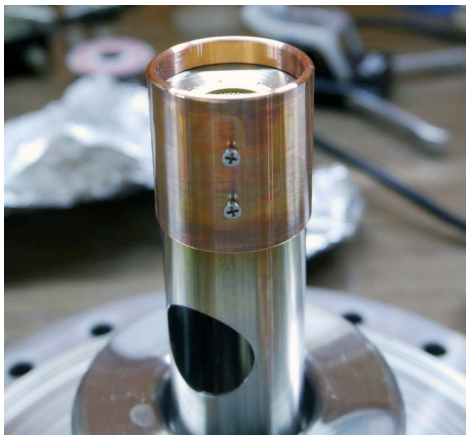

Fig. 2. Photograph of electron gun. The top cupper sleeve is the newly installed part for concave quipotential surface to generate a focused electron beam.

References

1) M. Wakasugi et al., Nucl. Instr. And Meth. **B317**, 668 (2013), and references therein.

2) T. Ohnishi et al., Nucl. Instr. Meth. **B317**, 357 (2013).

3) M. Watanabe et al., RIKEN Accel. Prog. Rep., **49**, 188 (2015).

Development of an ion beam Buncher for SCRIT experiment

K. Yamada,[*1] T. Ohnishi,[*2] K. Kurita,[*1] M. Togasaki,[*1] R. Toba,[*3] M. Watanabe,[*2] and M. Wakasugi[*2]

We have developed low-energy ion-beam buncher named FRAC (Fringing-RF-Field-Activated Ion-Beam Compressor)[1] for the SCRIT (Self-Confining Radioactive isotope Ion Target)[2]. FRAC is based on a linear RFQ ion trap widely used in the world[3], but is a new-type buncher without using buffer gas and making active use of fringing fields of RFQ.

Figure 1 schematically shows the experimental setup together with the longitudinal electrostatic potential diagrams. It consists of the ERIS (Electron-beam-driven RI separator for SCRIT)[4] ion source with a grid pulser, RFQ with endcap electrodes as its both edges, and two Faraday cups for measuring total charge. The ion source provides $^{132}Xe^{+}$ beams with accelerating energy of 6.0 keV. In this time, ERIS provided not only continuous beams but also pulsed beams with pulse width of 220 μs by switching grid pulser voltage $V_{\rm grid}$ with repetition frequency of 500 Hz. Averaged ion-beam current is identical in both cases. The voltages $V_{\rm barr1}$ and $V_{\rm barr2}$ are slightly lower than $V_{\rm acc}$ by a few volts, and higher than the $V_{\rm DC}$ applied to RFQ by about 15 V. The switching action of $V_{\rm barr1}$ is synchronized with arrival of each pulsed beam. At this situation, some parts of injected ions are longitudinally decelerated by fringing RF field and stacked in FRAC. For the extraction of the stacked ions from FRAC, the voltage of barrier 2 is switched to $V_{\rm acc} - 150$ V with appropriate frequency ($1 \sim 50$ Hz) depending on favorable stacking time. The conversion efficiency ε is defined as $\varepsilon = N_{\rm ext}/N_{\rm inj}$, where $N_{\rm inj}$ and $N_{\rm ext}$ are the number of ions injected into and extracted from FRAC, respectively. Figure 2 shows typical waveforms obtained at FC 1 and 2. Typical value of the efficiency ε at extraction frequency of 10 Hz is 5.7 % in case of continuous beam injection.

We aimed to improve the efficiency, and we tried to use synchronized pulsed beam injection. The efficiency ε was improved by a factor of 2.7 compared with continuous beam injection, and it is typically 15.3 % at extraction frequency of 10 Hz. The efficiency enhancement factor is nearly identical at any extraction frequency as shown in Figure 3.

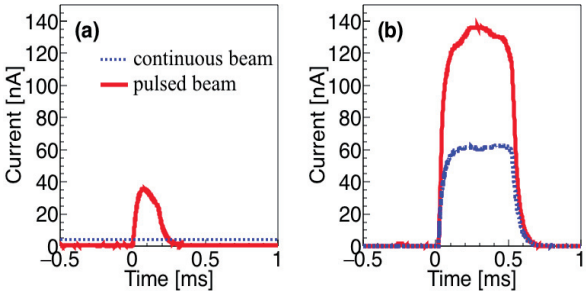

Fig. 2. Typical waveforms of injected continuous and pulsed ion beams measured at FC 1 (a), and extracted beams measured at FC 2 in case of extraction frequency of 10 Hz (b).

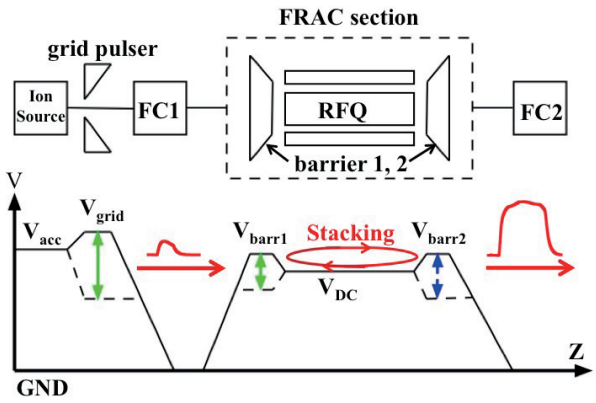

Fig. 1. Experimental setup of FRAC together with longitudinal electrostatic potential diagram for pulsed beam injection.

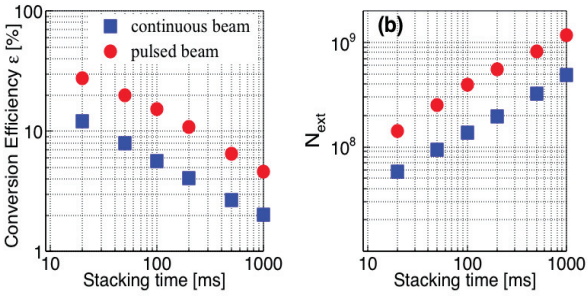

Fig. 3. Dependence on the extraction frequency of the conversion efficiency ε (a), and the number of ions extracted from FRAC $N_{\rm ext}$ (b) for both injection methods.

*1 Department of Physics, Rikkyo University
*2 RIKEN Nishina Center
*3 Department of Electrical Engineering, Nagaoka University of Technology

References

1) M. Togasaki et al., HIAT2015, WEPB25 (2015).
2) M. Wakasugi et al., Nucl. Instr. Meth. A**532**, 216 (2004).
3) F. Herfurth et al., Nucl. Instr. Meth. A**469**, 254 (2001).
4) T. Ohnishi et al., Nucl. Instr. Meth. B**317**, 357 (2013).

Ion stacking and pulse extraction at ERIS

T. Ohnishi,[*1] S. Ichikawa,[*1] M. Togasaki,[*1,*2] K. Yamada,[*1,*2] K. Kurita,[*1,*2] M. Watanabe,[*1] and M. Wakasugi[*1]

The ERIS (electron-beam-driven RI separator for SCRIT)[1] at the SCRIT electron scattering facility[2] is an online isotope separator system for the electron scattering of unstable nuclei. Ion beams from the ERIS are transported to the FRAC (fringing-RF-field-activated ion beam compressor).[3] The FRAC realizes the continuous injection followed by trapping, and after the appropriate accumulation time, pulsed beams from the FRAC are injected to the SCRIT system. During the accumulation inside the FRAC, some of the trapped ions escape through the entrance because the entrance potential is lower than the beam energy. In order to reduce the ratio of escaped ions to injected ions, it is necessary to shorten the opening period of the entrance and inject same number of ions as in the continuous injection. Ion stacking and pulse extraction[4] are proposed, and we report the results obtained at the ERIS in this paper.

Figure 1 shows a schematic drawing of the new ionization chamber of the ERIS. The new ionization chamber consists of a cathode, an ionization chamber (anode), and entrance and exit grids. The entrance and exit grids are connected to the ionization chamber through an insulator. The schematic potential structure of these electrodes is also shown in Fig. 1. The ion stacking and extraction are controlled by switching the voltage of the exit grid. Neutral atoms continuously enter the ionization chamber, passing through the cathode. They are ionized by electrons emitted from the surface of the cathode, which is kept at approximately 2000 °C. In the longitudinal direction, ions are trapped between the entrance and exit grids. The number of stacked ions inside the ionization chamber is determined by the ionization rate and ion-trapping lifetime.

The properties of the ion stacking and pulse extraction at the ERIS were studied using 6-keV ^{132}Xe ion beams. The voltages of the cathode, anode, and entrance grid were set to 0, 180, and 182 V, respectively. The exit-grid voltages at the stacking and extraction were 182 and 40 V, respectively. The typical pulse shape, measured at the entrance of the FRAC with a 1-ms stacking time and a 300-μs extraction period, is shown in Fig. 2(a). The pulse height is about five times larger than that of the continuous beam. Figure 2(b) shows the stacking ratio, which is the ratio of the total charge within a 300-μs pulse width to the total charge obtained by integrating the continuous beam over the stacking time and extraction period. This results shows that a pulsed beam with the same number of ions as those of the continuous injection is provided with a 1-ms stacking time and 300-μs pulse width. Using this scheme, the number of ions accumulated inside the FRAC is 2–3 times larger than when using continuous injection.[5]

The decay time of the stacking ratio corresponds to the ion-trapping lifetime, which is estimated to be 4 ms. In order to extend the ion-trapping lifetime, a transverse potential like an RFQ potential is needed.

In addition, in Fig. 2(b), the stacking ratio exceeds one when the stacking time is shorter than 1 ms. This is believed to be because the extraction efficiency is different from that in the continuous extraction. One possible reason for this is that the potential distribution inside the ionization chamber is modified by the charge of the stacked ions.

In summary, we performed ion stacking and pulse extraction at the ERIS. The obtained accumulation efficiency at FRAC is still half of the target value[5]. More detailed study and developments are in process.

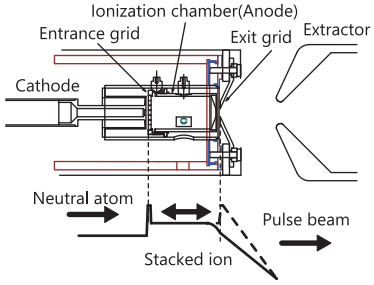

Fig. 1. Schematic drawing of the new ionization chamber of the ERIS. The schematic potential structure is also shown.

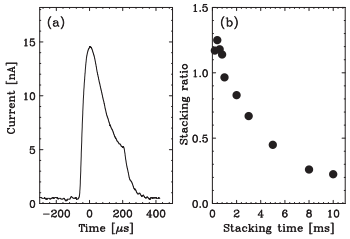

Fig. 2. (a) Pulse shape extracted from the ERIS after the stacking. (b) Stacking time dependence of the stacking ratio. Details are given in the main text.

*1 RIKEN Nishina Center
*2 Department of Physics, Rikkyo University

References

1) T. Ohnishi et al., Nucl. Instr. Meth. B**317**, 357 (2013).
2) M. Wakasugi et al., Nucl. Instr. Meth. B**317**, 668 (2013).
3) T. Togasaki et al., Proceedings of HIAT2015, WEPB25 (2015).
4) Y. Shirakabe et al., Nucl. Instr. Meth. A**337**, 11 (1993).
5) K. Yamada et al.: in this report.

Design work of rf ion guide system at the SLOWRI facility

A. Takamine,[*1] M. Rosenbusch,[*1] P. Schury,[*2] J. Y. Moon,[*3] M. Wada,[*1,*2] H. Miyatake,[*2] Y. Ito,[*1] T. Sonoda,[*1] Y. X. Watanabe,[*2] Y. Hirayama,[*2] T. Sato,[*1] T. M. Kojima,[*1] I. Katayama,[*1] H. Wollnik,[*1,*4] and H. Ueno[*1]

We are developing an rf ion guide[1] gas catcher cell at the SLOWRI facility towards online commissioning in FY2017. We initially designed a large traveling wave rf carpet for the ion transport in the gas cell. The carpet had such a large capacitance due to its large area of 600 cm^2 with 0.28 mm pitch and 0.14 mm separation for stripe electrodes that the resonance frequency was less than 1 MHz to obtain a voltage greater than100 $V_{p.p.}$.

We designed a new configuration that consists of three-stage rf transport electrodes as shown in Fig. 1 so as to reduce the areas of the rf carpets. The first electrode is composed of DC, RF+DC, gap, RF+DC, and DC parts with long strip electrodes. It produces a hemisphere's electrostatic potential to collect thermalized ions onto the central RF+DC parts. When the ions reach close to the electrode surface, they are guided to the gap by the rf ion guide method,[1] extracted from the gap, and pulled onto the second electrode by electrostatic fields between the first and the second electrodes. We utilize the ion surfing method[2] to transport the ions downstream with a traveling wave produced with superimposed RF and AF fields. When the ions arrive at the downstream edge, they are again pulled onto the third electrode, transported to an exit hole, and extracted to the outside of the gas cell. We plan to place a block in front of the third electrode to avoid the direct impinging of ion beams on the electrode. This scheme has an advantage in that He ions, which create space charge, produced by beam thermalization can be killed on the first electrode because of the small mobility of He ions. Although the ion surfing method provides faster transport compared with the conventional rf ion guide method, it is more susceptible to a space charge effect. This is why we selectively use the two methods.

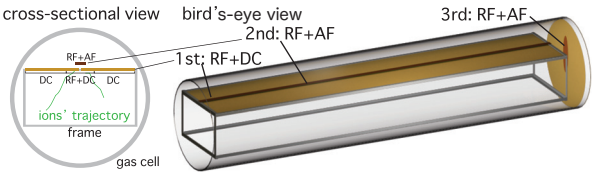

Fig. 1. New design of the rf ion guide system in the gas cell. The size of the cuboid frame is 160×260×1470 mm.

*1 RIKEN Nishina Center
*2 Wako Nuclear Science Center (WNSC), IPNS, KEK
*3 Institute for Basic Science
*4 Department of Chemistry & BioChemistry, New Mexico State University

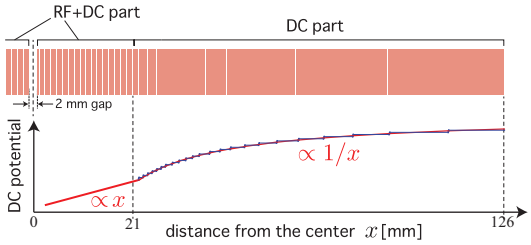

Fig. 2. Enlarged drawing of a part of the first-stage electrode.

The DC potential configuration on the first electrode determines the amount of ions collected in a narrow region, which is important to reduce the area of an RF part. Because the ion's motion simply follows the lines of the electric field, a $\propto 1/x$ potential produced by a point charge would be the best solution to focus ions. In order to emulate such a field, we designed a DC part as shown in the Fig. 2 by changing the width of each electrode. The blue line in Fig. 2 shows the potential with a constant voltage step between the adjacent electrodes and the red line shows a $\propto 1/x$ potential on the DC part and a $\propto x$ potential on the RF+DC part. We also confirmed that the $\propto 1/x$ potential produces the best focusing ion collection among three types of potentials ($\propto 1/x$, $\propto x$, and $\propto \log(x)$) in SIMION simulations. From the simulation result, we set the area of each RF+DC part as 121 cm^2 (25 mm×485 mm) with 0.32 mm pitch and 0.16 mm separation. We expect that the capacitance will be reasonably small and we can apply an rf voltage at several MHz with sufficient voltages for the rf ion guide. We will start an rf test with an actual electrode soon.

Simulations for space charge in this configuration are also in progress. The simulation is based on a state-of-art simulation code "3DCylPIC"[3] in coorperation with Dr. Ringle from NSCL. In the simulation for the case of the incoming beams in the mid-heavy mass region, preliminary results show that this system will be tolerable to an incoming beam intensity of 10^6 pps.

We finalized the design of the first-stage rf carpet. The designs of the second- and the third-stage electrode will also be finalized soon. We plan to start offline tests of the rf transport system using ion sources from Mar. 2017 and conduct online commissioning in the later half of FY2017.

References

1) M. Wada et al., Nucl. Instr. Meth. B **204**, 570 (2003).
2) G. Bollen: Int. J. Mass Spectrom. **299**, 131 (2011).
3) R. Ringle: Int. J. Mass. Spectrom. **303** 42 (2011).

First cooling test of rf ion guide gas cell at the SLOWRI facility

A. Takamine,[*1] M. Rosenbusch,[*1] P. Schury,[*2] J. Y. Moon,[*3] M. Wada,[*1,*2] H. Miyatake,[*2] Y. Ito,[*1] T. Sonoda,[*1] Y. X. Watanabe,[*2] Y. Hirayama,[*2] T. Sato,[*1] T. M. Kojima,[*1] I. Katayama,[*1] H. Wollnik,[*1,*4] and H. Ueno[*1]

Molecularization is a serious problem in gas catcher cells around the world. It is not so significant for nuclear mass measurements but crucial for laser spectroscopy. If a gas, typically a noble gas, contains a non-negligible amount of impurities such as water, hydrocarbons, nitrogen, and alcohol, thermalized ions have a fair chance to form molecules with impurities. Even though molecules can be broken up *via* collisions with residual gases by acceleration into the high-density region immediately after the gas-cell exit hole, molecular ions have a lower transportation efficiency on an rf carpet. This is because the repelling force produced by rf fields is proportional to the square of ions' mobilities[1)] which are generally much smaller for molecular ions than for atomic ions. Gas purification is, therefore, important to avoid the molecularization of injected ions.

We use the highest grade G1 He gas additionally purified through a getter-based gas purifier which provides 99.9999999% purity. Moreover it is desirable that the gas cell is pre-cooled to freeze out impurities onto the inner wall before catching RI beams. In order to cool down the rf ion guide gas cell at the SLOWRI facility, the chamber has a vacuum double-wall structure for vacuum thermal insulation. We prepared two 77-K cryocoolers (Sumitomo CH-110), "cryoU" and "cryoD," as shown in Fig. 1. The gas cell will be cooled by the cryocoolers through aluminum supporters and by a copper pipe winding around the gas cell to carry liquid nitrogen (LN_2). An indium sheet is placed between the supporters and the gas cell for heat conduction. Since the heat capacity of the gas cell is estimated to be as large as ∼300 kJ/K, we conducted a cooling test although only one cryocooler, "cryoD," was ready to use in Sep. 2016. For temperature measurements with the four-terminal resistance measuring method,

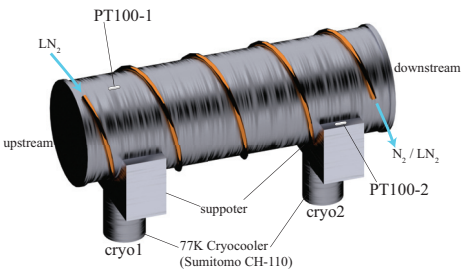

Fig. 1. Schematic of the gas cell cooling scheme.

*1 RIKEN Nishina Center
*2 Wako Nuclear Science Center (WNSC), IPNS, KEK
*3 Institute for Basic Science
*4 Department of Chemistry & BioChemistry, New Mexico State University

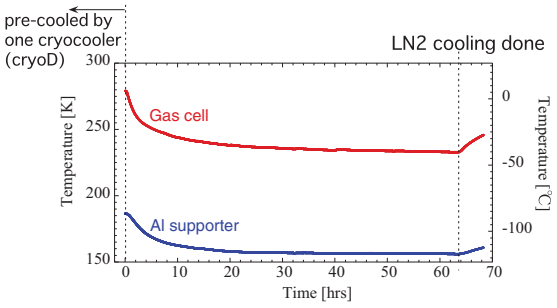

Fig. 2. Preliminary cooling test result.

thermo sensors of type PT100 have been attached at two positions: the gas-cell vessel and the Al support (see Fig. 1).

Figure 2 shows the result of the preliminary cooling test. The gas cell was pre-cooled by cryoD and then started to be cooled with LN_2 at time = 0 in the plot. We continuously kept supplying LN_2 while alternately using the two LN_2 tanks of 120 L and 100 L capacity. It was cooled down to 237 K in one day after the start of LN_2 cooling and to 233 K in 2.5 days. After stopping the cooling, the heating rate was 0.071 K/min. We estimated the conductive heat transfer from this value combined with the estimation of the radiation heat transfer. When object 1 with an outer surface area of A_1 is surrounded by object 2 with an inner surface area of A_2, the radiation heat transfer Q from 2 to 1 is expressed by $Q = \sigma A_1(T_2^4 - T_1^4)/(1/\varepsilon_1 + (A_1/A_2)(1/\varepsilon_2 - 1))$, where σ is the Stephan-Boltzmann constant, ε_i the emissivity of object i, and T_i the temperature of object i. Assuming $\varepsilon_1 = \varepsilon_2 = 0.1$ (typical value for stainless steel), $T_1 = 290$ K, $T_2 = 240$ K, $A_1 = 1.73$ m^2, and $A_2 = 6.72$ m^2, Q was calculated as 0.12 kW, which resulted in a heating rate of 0.024 K/min.. Therefore the heating rate of the conductive heat transfer was estimated to be 0.047 K/min, corresponding to a heat transfer of 0.24 kW, which is thought to be mainly responsible for the heat connection to the unused cryocooler.

Now both cryocoolers are ready to use. We continue the cooling test using both cryocoolers and will introduce many superinsulator layers between the gas cell and the outer vessel to suppress the radiation heat transfer.

Reference

1) M. Wada et al., Nucl. Instr. Meth. B **204**, 570 (2003).

Status of SLOWRI beamline construction

T. M. Kojima,[*1] I. Katayama,[*1] T. Sonoda,[*1] and M. Wada[*1,*2]

To utilize rare RIs generated at BigRIPS as slow (~10 keV) ion beams, we have been constructing a 60 m long beamline in parallel to the development of slow RI beam generators, such as PALIS (Parasitic RI-beam production by Laser Ion-Source) and other gas cell type ion stoppers. [1] The beamline will transport singly charged RI ions, which are separated and slowed by PALIS at the F2 chamber of BigRIPS, from F2 to the experimental area E11. It consists of four sector dipole magnets, two focal plane chambers, 62 electrostatic quadrupole singlets, and 11 electrostatic quadrupole quartets. Fourteen 450 L/s turbo molecular pumps evacuate the beamline, which is divided into nine sections (two of them are focal plane chambers) delimited by gate valves. The beamline was installed two years ago.

In contrast to the case of usual fast accelerator beams, it is very important to keep the beamline in a good vacuum since the collisional electron capture cross sections of ions with residual gas molecules are large for slow ions.[2] In some cases, the cross section reaches $\approx 1 \times 10^{-15}$ cm^2 at approximately 10 keV. [3] Assuming this value for the cross section, we estimated the beam fraction surviving after 60 m flight for some vacuum pressures at a temperature of 25℃. The results showed that beam fractions of 48.2%, 93.0%, and 99.3% survive through pressures of 5×10^{-4}, 5×10^{-5} and 5×10^{-6} Pa, respectively. Therefore, a vacuum of the order of 10^{-6} Pa should be sufficient. In order to realize such a good vacuum, the beamline was baked with wire heaters coiling the ducts at 120℃ for about 10 months.

Figure 1 shows a typical vacuum change of the beamline during the baking. Before baking, the vacuum pressure was about 1×10^{-4} Pa. When the heaters were turned on in the middle of October 2015, the pressure temporarily increased up to 3.3×10^{-4} Pa and then decreased gradually. Some dips of pressure appearing in Fig. 1 correspond to the days in which heaters were off because of Christmas holidays, RIKEN Open Day, and so on. Many of the beamline vacuum ducts (and electrostatic quadrupoles inside them) were previously used at other facilities and had been stored for about 15 years. Therefore many molecules were supposed to be stuck on their inside surfaces. Especially, it was considered that the Kapton (polyimide) insulators inside the ducts had adsorbed a considerable amount of H_2O molecules. It took almost 10 months to reach the range of 10^{-6} Pa. The heaters were turned off on August 10, 2016, when the vacuum was about 9×10^{-6} Pa, and then the vacuum became about 5×10^{-6} Pa. Some spikes (sudden rise of pressure) after baking were caused by the stoppage of evacuation pumps due to power outage and maintenance. Once water molecules stuck tight on the surface have been baked out, the vacuum can reach the range of 10^{-6} Pa easily even after ventilation of the beamline with dry nitrogen gas.

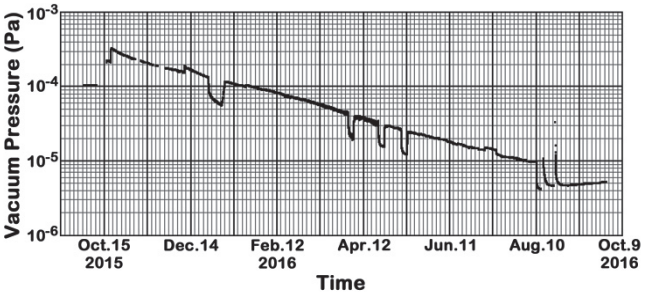

Fig. 1. Typical vacuum change of the beamline during baking. The dips correspond to the days in which baking heaters were turned off (see text).

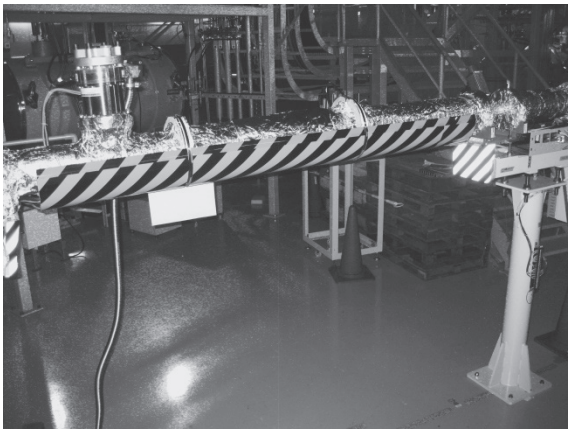

Fig. 2. Protector shell (zebra patterned) covering the beamline ducts over the passage.

Since the baking period was long, for the safety of experimental workers and tour visitors who pass under the beamline, the ducts over the passage were covered with a protector shell (see Fig. 2). The protector is made of aluminum and thermally insulated with thick glass wool rings. The surface of the protector is covered with zebra cushions to minimize physical damages if someone bumped his/her head against it.

In the next year, we will install a conventional ion source and beam profile monitors, following which beam transportation will be tested with some ions.

*1 RIKEN Nishina Center
*2 KEK Wako Nuclear Science Center

References

1) M. Wada et al., RIKEN Acc. Prog. Rep. **47**, 203 (2014).
2) E. W. McDaniel, J. B. A. Mitchell, M. Eugene Rudd: Atomic Collisions: Heavy Particle Projectiles (John Wiley & Sons, New York, 1993).
3) See, for example, data in the following Web Data Base:
CMOL (http://dbshino.nifs.ac.jp/nifsdb/cmol/top)
CHART (http://dbshino.nifs.ac.jp/nifsdb/chart/top)

Introduction of silver atoms into superfluid helium using laser ablation method

T. Fujita,[*1,*2] K. Imamura,[*1,*3] D. Tominaga,[*1,*4] T. Egami,[*1,*4] W. Kobayashi ,[*1,*4] Y. Nakamura,[*1,*3] M. Sanjo,[*1,*4] T. Kobayashi,[*5] A. Takamine,[*1] T. Furukawa,[*1,*6] H. Ueno,[*1] T. Shimoda,[*2] and Y. Matsuo[*1,*4]

The Optical Radioisotope atom Observation in Condensed Helium as Ion-catcher (OROCHI) utilizes superfluid helium (He II) as a stopping material of energetic ion beams of a few tens to hundreds of MeV/nucleon. Injected ion beams are neutralized during the stopping process, and neutralized atoms are confined in a region of 1 to several mm^2 over a second. There He II also serves as a host matrix of laser spectroscopy of stopped atoms[1]. Since He II is optically transparent in wide frequency region from ultraviolet (UV) to radio frequency (RF), it is possible to apply laser-RF and laser-microwave (MW) double resonance methods to atoms in He II to measure Zeeman and hyperfine splitting energies. From these splitting energies, values of nuclear spin and electromagnetic moment can be deduced.

The measured hyperfine splitting (HFS) energies were slightly shifted from those in vacuum for alkali atoms such as Rb and Cs owing to the effect of surrounding helium atoms[2]. However, the observed energy shift $\triangle$ E/E $\lesssim$ 1% was sufficiently small to discuss nuclear structures. Moreover, the preliminary results indicated that this method provides a high-precision measurement of a magnetic dipole hyperfine structure constant to derive a hyperfine anomaly which gives information on the distribution of nuclear charge and magnetization. Recently, we started to apply the method to group 11 atoms such as Au and Ag.[3,4] The observed shift of the HFS energy for Au atoms was even smaller than that for alkali atoms. The investigation of HFS of Ag atoms will lead to more detailed information because Ag has two stable isotopes, which are necessary to determine a hyperfine anomaly whereas Au has only one stable isotope.

In offline experiments, we adopted a two-step laser sputtering technique to introduce atoms into He II (Fig. 1). As the first step, a sample material placed 1 cm above the He II surface is ablated by either a third-harmonic or a second-harmonic pulse of a neodymium-doped yttrium aluminum garnet laser (wavelength: 355 or 532 nm, repetition rate: 10 Hz, pulse width: 8 ns, pulse energy: ∼5 mJ). Clusters out of the sample material immerse into He II. Next, the clusters are dissociated by a femtosecond titanium-doped sapphire laser (wavelength: 800 nm, repetition rate: 500 Hz, pulse width: ∼120 fs, pulse energy: ∼200 μJ). The method was successful in the previous experiments for Rb, Cs and Au atoms. However, a sufficient number of atoms were not introduced into He II in the case of Ag. In this experiment, the ablation plasma produced by the ablation laser irradiation was observed, whereas the plasma produced by the dissociation laser irradiation was not observed. We concluded almost no introduction of Ag atoms in this condition because this dissociation laser was not effective for Ag.

One of the possible reasons for the difficulty in the dissociation by the dissociation laser could be the difference in absorption efficiencies between Ag particles and other species. The Ag sample has a high reflectance ratio in infrared and visible regions. To achieve the measurement of HFS for Ag, we plan to change the dissociation laser to a second-harmonic pulse of the femtosecond laser (wavelength: 400 nm, repetition rate: 500 Hz, pulse width: ∼200 fs, pulse energy: ∼100 μJ) and a XeCl excimer laser pulse (wavelength: 308 nm, repetition rate: 10 Hz, pulse energy: ∼10 mJ) because, generally, UV pulses dissociate particles more efficiently.

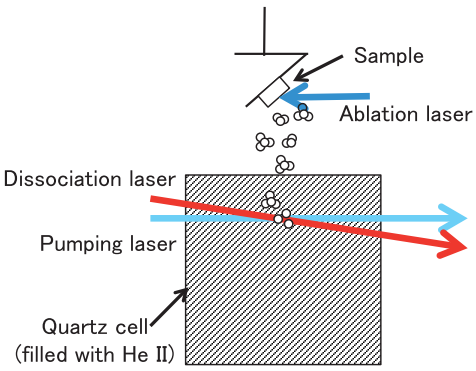

Fig. 1. Schematic of the two-step laser sputtering technique in our experimental setup. For details, see the text.

*1 RIKEN Nishina Center
*2 Department of Physics, Osaka University
*3 Department of Physics, Meiji University
*4 Department of Advanced Science, Hosei University
*5 RIKEN Center for Advanced Photonics
*6 Department of Physics, Tokyo Metropolitan University

References

1) X. F. Yang et al., Phys. Rev. A **90**, 052516 (2014).
2) K. Imamura et al., RIKEN Accel. Prog. Rep. **48**, 251 (2015).
3) T. Fujita et al., RIKEN Accel. Prog. Rep. **47**, 212 (2014).
4) T. Furukawa et al., RIKEN Accel. Prog. Rep. **42**, 194 (2009).

Fluorescence detection and double resonance spectroscopy using ^{85}Rb beam for the development of OROCHI

K. Imamura,[*1,*2] T. Egami,[*1,*3] W. Kobayashi,[*1,*3] M. Sanjo,[*1,*3] A. Takamine,[*1] T. Furukawa,[*1,*4] T. Fujita,[*1,*5] D. Tominaga,[*1,*3] Y. Nakamura,[*1,*2] Y. Ichikawa,[*1] T. Sato,[*1] H. Nishibata,[*1] A. Gladkov,[*1,*6] L. C. Tao,[*1,*7] T. Kawaguchi,[*1,*3] Y. Baba,[*1,*3] M. Iijima,[*1,*3] H. Gonda,[*1,*3] Y. Takeuchi,[*1,*3] R. Nakazato,[*1,*3] T. Wakui, [*1,*8] H. Ueno,[*1] H. Odashima,[*2] and Y. Matsuo[*1,*3]

Nuclear structure study using atomic laser spectroscopy has revealed the nuclear spins and moments of a wide variety of nuclei with high accuracy in the past decades. However, in order to apply these methods to nuclei with a production rate of less than 100 pps, a highly sensitive method is strongly desired.

To establish such a method, we are developing a laser spectroscopic method for a smaller number of atoms in superfluid helium (He II) to study their nuclear structure. We call this method OROCHI (Optical RI-atom Observation in Condensed Helium as Ion-catcher). In OROCHI, superfluid helium works as an effective stopper for highly energetic ion beams. Most of the immersed ions (nearly 100%) in He II are neutralized in the stopping process and are stopped as atoms. In addition, the center wavelengths of the absorption and emission spectra of the atoms in He II have an large difference because of the effect of the surrounding He II[1] We can detect emitted photons from the stopped atoms with an extremely low background using wavelength separation. From the features of He II mentioned above, OROCHI should achieve a highly sensitive detection of the fluorescence from atoms.

So far, we have shown the validity of the principle of our method by observing both laser-MW (microwave) and laser-RF (radio frequency) double resonance spectra using a $^{84-87}$Rb beam[2] However, we also found that the reduction of the stray laser light was not sufficient. Therefore, the applicable ion beam intensity was limited. In order to apply OROCHI to rare isotopes whose production rate is less than 100 pps, we have upgraded the fluorescence detection system to reduce the stray laser light more effectively[3]. Last December, we conducted an online experiment using an ^{85}Rb beam to confirm the validity of our development.

Figure 1(a) schematically shows the experimental setup. The ^{85}Rb ions delivered from RIPS were injected into He II and stopped at the center of the cryostat. In order to measure the ion beam intensity, we counted the number of injected Rb ions using two photomultiplier tubes (PMTs) and a plastic scintillator. The stopped atoms were subjected to a laser light whose wavelength corresponds to the Rb D1 line in He II, namely 780 nm[1] The fluorescence from the atoms was collected through two lenses and focused on the entrance of an optical fiber. The exit of the optical fiber was connected to the entrance of a monochoromator that was used to select 794-nm emission light. Finally, the fluorescence was detected using PMT. Figure 1(b) shows the detected photon intensity variation due to the switching of the ion beam and laser. The ion beam intensity and the irradiated laser power were approximately 10^4 pps and 400 mW, respectively. This result confirms the fluorescence detection using the upgraded system and effective background suppression. In addition, we also successfully observed laser-RF double resonance spectra by applying both a switching magnetic field and an RF field whose frequency was scanned. As shown in Fig. 1(c), the detected photon count rate clearly decreases with the production of the spin polarization when the magnetic field is ON. The degree of the polarization is approximately 35% which was comparable to that obtained in the previous experiment[2]

We are now analyzing these data to estimate the lower limit of the applicable beam intensity.

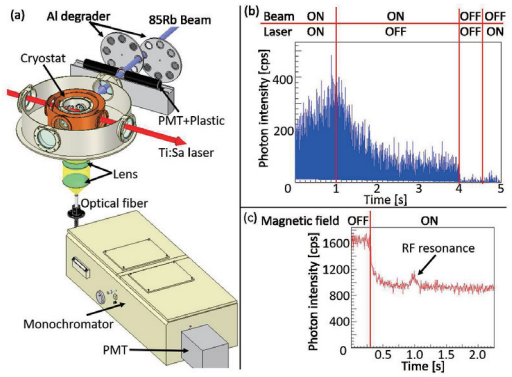

Fig. 1. Experimental setup and obtained result. (a) Experimental setup. (b) Variation of the detected photon intensity due to the switching of the ion beam and the laser. (c) the RF resonance spectrum.

*1 RIKEN Nishina Center
*2 Department of Physics, Meiji University
*3 Department of Advanced Science, Hosei University
*4 Department of Physics, Tokyo metropolitan University
*5 Department of Physics, Osaka University
*6 Department of Physics, Kyungpook National University
*7 School of Physics, Peking University
*8 National Institute for Quantum and Radiological Science and Technology(QST)

References

1) Y. Takahashi et al. Phys. Rev. Lett. **71**, 1035 (1993).
2) X. F. Yang et al. Phys. Rev. A **90**, 052516 (2014).
3) W. Kobayashi et al. in this report.

Effective suppression of stray laser light for fluorescence detection from ^{85}Rb atoms injected into superfluid helium

W. Kobayashi,[*1,*2] K. Imamura,[*1,*3] T. Egami,[*1,*2] M. Sanjo,[*1,*2] T. Fujita,[*1,*4] D. Tominaga,[*1,*2] Y. Nakamura,[*1,*3] A. Takamine,[*1] T. Furukawa,[*1,*5] T. Wakui,[*1,*6] H. Ueno,[*1] and Y. Matsuo[*1,*2]

We have been developing a laser spectroscopy technique named Optical RI-atom Observation in Condensed Helium as Ion-catcher (OROCHI) for the investigation of nuclear properties such as nuclear spins and moments. In OROCHI experiments, we catch highly energetic ion beams in superfluid helium (He II) to neutralize them and apply laser-rf and laser-microwave double resonance methods to the stopped atoms. It is known that the optical absorption spectrum of an atom in He II is greatly blue-shifted compared with the emission spectrum[1]. Therefore, the laser-induced fluorescence (LIF) from the atoms can be spectrally isolated from the stray laser light that results in a background in spectra. We have developed an LIF detection system (LDS) which enables the detection of LIF with an extremely low background. In a previous online experiment[2], we successfully observed LIF from $^{84-87}$Rb isotope atoms and double resonance spectra using LDS II[3,4] equipped with interference filters for wavelength selection (Fig. 1(a)). However, we observed background signals of $\approx 10^3$ counts with a laser radiation of 100 mW while the LIF intensity was also of the same order for the injected beam intensity of the order of 10^4 pps. This is because the filter transmission shifts to shorter wavelengths for oblique incident light. We require a higher wavelength selectivity for the application of OROCHI to lower-production yield nuclei.

In order to reduce the background due to stray laser light more efficiently, we developed LDS III (Fig. 1(b)). It consists of a set of lenses, bundled optical fibers and a monochromator. The fluorescence light is collected and collimated through lens1 and focused by lens2 onto the entrance of the fibers. It is resolved in the monochromator according to the wavelengths. The focal lengths of lens1 and lens2 are optimized for the LIF collection and transmission. This configuration makes it possible to suppress the stray laser light that reaches the monochromator through the fibers by a factor of 10^{-9}.

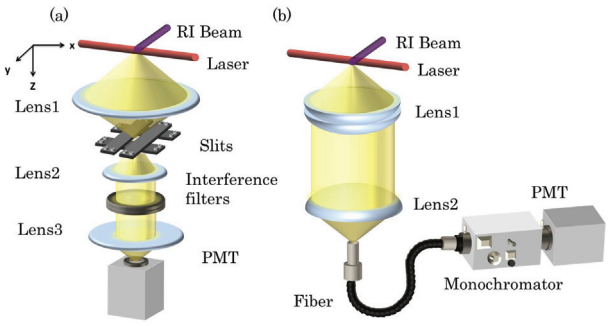

Fig. 1. Laser-induced fluorescence detection system (a) LDS II and (b) LDS III.

In order to confirm the effective reduction of the background, we investigated the background induced by the stray laser light in LDS III. We measured the dependence of a photomultiplier tube (PMT) signal on the irradiated laser power (Fig. 2). As shown in Fig. 2, the detected signal attributed to the stray laser light was four cps per 100-mW laser radiation power. From this result, we concluded that the stray laser light was reduced by three orders of magnitude compared with the case of LDS II and the background was near the level of dark counts in the PMT. After confirming the reduction of background counts, we installed LDS III for the online experiment using a ^{85}Rb beam delivered from RIPS[5]. The evaluation of the applicable ion beam intensity in the LDS III is in progress now.

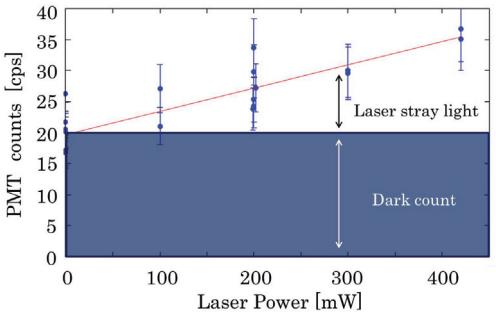

Fig. 2. Background signals due to the stray laser light in He II as a function of the incident laser power.

*1 RIKEN Nishina Center
*2 Department of Advanced Science, Hosei University
*3 Department of Physics, Meiji University
*4 Department of Physics, Osaka University
*5 Department of Physics, Tokyo Metropolitan University
*6 National Institutes for Quantum and Radiological Science and Technology

References

1) Y. Takahashi et al.: Phys. Rev. Lett. **71**, 1035 (1999).
2) X. F. Yang et al.: Phys. Rev. A **90**, 052516 (2014).
3) A. Sasaki et al.: RIKEN Accel. Prog. Rep. **44**, 204 (2011).
4) H. Tetsuka et al.: RIKEN Accel. Prog. Rep. **46**, 117 (2013).
5) K. Imamura et al.: in this report.

Experimental evaluation of laser-MW double resonance signal intensity in OROCHI project

T. Egami,[*1,*2] K. Imamura,[*1,*3] A. Takamine,[*1] W. Kobayashi,[*1,*2] T. Fujita,[*1,*4] D. Tominaga,[*1,*2] M. Sanjo,[*1,*2] Y. Nakamura,[*1,*3] T. Wakui,[*1,*5] T. Furukawa,[*1,*6] H. Ueno,[*1] and Y. Matsuo[*1,*2]

We are developing a laser spectroscopy technique named OROCHI to study the properties of low-production-yield nuclei. In the OROCHI experiment, energetic ions are injected into superfluid helium and are neutralized during their stopping process. We irradiate the neutralized atoms with a circularly polarized laser light to produce spin polarization and measure the atomic Zeeman splitting by laser-radio frequency (RF) double resonance method and the hyperfine splitting by laser-microwave (MW) double resonance method. The measurements enable us to deduce nuclear spin and moment values. We succeeded in observing the resonance signal by the double resonance methods in the online experiment using $^{84-87}$Rb ion beams of an order of 10^4 ions/s.[1,2] However, the resonance signal was smaller than that in the offline experiments, and difficulties were anticipated for the application of this method to lower-production yield nuclides. One of the possible causes for small resonance signal intensity was attributed to an insufficient MW radiation power. So we performed an offline test using Rb vapor which was enclosed in pyrex glass cell with He buffer gas (Rb cell) in order to find the experimental conditions to maximize the MW resonance signal intensity in our experimental setup.

We irradiated Rb atoms in the cell with a circularly polarized laser light for spin polarization and a MW radiation at a fixed frequency. Laser intensity was 1.0 mW (with the diameter 2 mm, wavelength 795 nm). In order to maintain spin polarization, a magnetic field was applied to the atoms in the direction coaxial with the laser axis. We detected fluorescence photons from Rb atoms by using a photomultiplier tube. By sweeping magnetic field strength, we obtained a MW resonance peak (y_r) and a maximum de-excitation peak which corresponds to the signal level of spin unpolarization (y_{max}).[1] We defined resonance intensity(I) as $I = (y_r - y_0)/(y_{max} - y_0)$, where y_0 is the background signal level. We measured the dependence of the resonance intensity on antenna position and MW power.

Figure 1 shows the resonance intensity as a function of distance between the antenna and observation region. MW power was 3.0(3) W. In the previous online experiment, MW of 2-3 W was applied and the antenna was placed about 4 cm away from the observation region. From this result, we estimate that the resonance intensity can be increased by a factor of approximately 5 by bringing the antenna 1 cm away from the observation region.

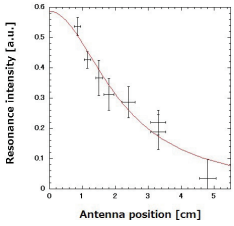

Fig. 1. Resonance intensity dependence on the antenna position. Horizontal axis indicates the distance between the MW antenna and observation region.

We also measured the resonance intensity with different applied MW power (Fig. 2). The Rb cell was placed at the observation region in our cryostat used for online experiments. The antenna was set about 1 cm away from the observation region. De-excitation light from Rb atoms was detected by the newly developed LIF detection system[3]. When the MW power of 8 W was applied to the atoms, the resonance intensity was increased by a factor of approximately 1.2 from that of 3 W.

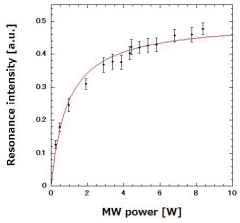

Fig. 2. Resonance intensity dependence on the MW applied power

The two results above showed different resonance intensities at the same condition of MW irradiation due to different optical pumping rates and slightly different antenna orientation. Nevertheless, taking into account of the two factors, namely optimizing antenna position and applied power, the MW resonance signal intensity increment is estimated to be able to reach at least 6 times higher than that of the previous online experiment. In next online experiment, we will evaluate the amplification of the resonance intensity discussed above.

*1 RIKEN Nishina Center
*2 Department of advanced science, Hosei University
*3 Department of Physics, Meiji University
*4 Department of Physics, Osaka University
*5 QST
*6 Department of Physics, Tokyo Metropolitan University

References

1) X. F. Yang *et al.*: Phys. Rev. A. **90**, 052516(2014).
2) K. Imamura *et al.*: JPS Conf. Proc. **6**, 030115(2015).
3) W. Kobayashi *et al.*: In this report.

70-m laser beam transport for the RIBF-PALIS experiment

T. Sonoda,[*1] H. Iimura,[*2] M. Reponen,[*3] M. Wada,[*1] I. Katayama,[*1] V. Sonnenschein,[*4] T. Takamatsu,[*4] H. Tomita,[*4] and T.M. Kojima[*1]

Laser beam transport is essential part of the operation of PALIS.[1,2] Figure 1 shows a stereoscopic view of the PALIS laser beam transport line. Because of the strong radiation in the beam line area, one cannot access to PALIS when BigRIPS is in operation. Therefore, the laser light source, which needs appropriate tuning during the experiment, was placed in the human-accessible area. As a result, the laser light source and the ionization area for PALIS are on different floors and different building foundations, which leads to a total laser beam path of up to 70 m. Hence even small beam fluctuations can cause the laser beam to miss the distant downstream optics.

We designed and implemented a simple optical system consisting of several mirrors equipped with compact stepping motor actuators, lenses, beam spot screens, and network cameras. The system enables multistep resonant laser ionization in a gas cell and gas jet with a collinear overlap of a few millimeters diameter between the laser photons and atomic beam at 70 m away from the laser light source.

The optical components used for the long laser beam transportation are only four mirrors and one lens to simplify the whole system. The mirrors are vapour-deposited aluminum flat mirrors that were designed for high reflectivity at any incident angle. To avoid divergence due to the long distance, the beam size has to be sufficiently large. The beam size at the exit of the dye laser is approximately 0.8 mm horizontally and 2 mm vertically. Then it expands to 7 mm × 17 mm using a telescope consisting of a concave lens and an achromatic lens. The laser beam size is finally collimated to 3 mmϕ by a concave lens to irradiate the resonance photoionization volume. In order to control the mirror angle remotely, each mirror has an actuator equipped with a high-performance compact stepping motor for both the horizontal axis and vertical axis. The single-pulse travel of the stepping motor is 1 μ m. All stepping motors can be remotely controlled by a PC with an automation program written in LabVIEW. The remote control interface is integrated with the LAN platform, so that control is possible from any place where a LAN connection is available. Using a dichroic mirror and polarizing cube beam splitter, laser beams with different wavelengths are combined at the starting location in the laser laboratory and transported to the ionization volume.

We have achieved a transmission efficiency of 53 % from B1F laser laboratory to BigRIPS F2 room, for which the total flight path corresponds to about 66 m. We also confirmed that the position stability of the laser beam stays within a permissible range for a dedicated resonant ionization experiment. The system will be finalized in several on-line experiments for robust and efficient handling operations.

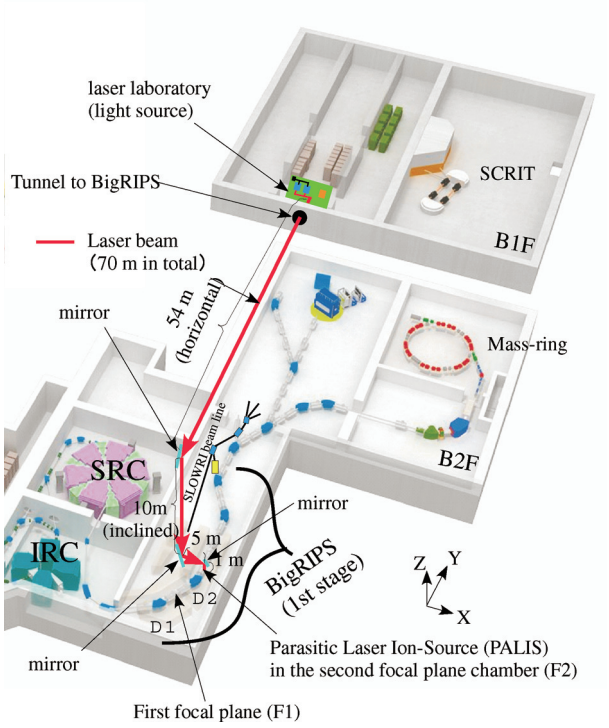

Fig. 1. Stereoscopic view of the 70-m laser beam transport line on the RIBF experimental floors. Multi-color laser beams are sent from the PALIS laser laboratory (B1F) to the PALIS located in the second focal plane chamber in the fragment separator BigRIPS (B2F-F2).

*1 RIKEN Nishina Center
*2 Japan Atomic Energy Agency
*3 Department of Physics, University of Jyvaskyla
*4 Faculty of Engineering, Nagoya University

References

1) T. Sonoda et al., AIP Conf. Proc. Vol. **1104** 132(2009).
2) T. Sonoda et al., Nucl. Instr. and Meth. B**295** 1(2013).

Gas circulation and purification system for RIBF-PALIS experiment†

T. Sonoda,*1 T. Tsubota,*2 M. Wada,*1 I. Katayama,*1 T.M. Kojima*1 and M. Reponen*3

A gas circulation and purification system was developed for the parasitic low-energy RI-beam production system (PALIS).[1,2] The development was motivated by the following three requirements; 1) to avoid pollution by radioactive Ar gas (^{41}Ar, $T_{1/2}$=109.61(4)min) diffusing into the air, which is created by the reaction of ^{40}Ar and an intense neutron flux; 2) to reduce consumption of the buffer gas, since the exhausted buffer gas ejected from the gas cell was thus far disposed of via a differential pumping system; and 3) to enhance the gas purity to avoid a loss in the low-energy RI-beam extraction efficiency.

An overview of the gas cell, differential pumping system, and the gas circulation and purification system is shown in Fig. 1. The main part of the gas circulation system is located 5 m away from the BigRIPS F2 room. The interfaces between the PALIS gas cell and circulation system consist of several long gas tubes and compressed air tubes for valve control. During on-line beam experiments, the radiation level in the F2 room increases by several hundred mSv, whereby the main contribution to the radiation is the high-intensity neutron flux. Therefore, it is not possible to access the F2 room during experiments, and all devices should be controlled remotely. A high-flow-rate gas cell filled with 1 atm of buffer gas (argon or helium) is used for the deceleration and thermalization of high-energy RI-beams in PALIS experiments. The exhausted buffer gas is efficiently collected using a compact dry pump and returned to the gas cell. The buffer gas is efficiently purified using two gas purifiers as well as through collision cleaning, which eliminates impurities including gas.

We have achieved a gas recovery efficiency of 97% for Ar, when the pressure of the gas cell was set at 10^5 Pa. This value falls within the permissible range considering the natural abundance of ^{41}Ar in air. In addition, the consumption of the expensive, high-purity buffer gas was drastically reduced. The replacement rate of Ar gas to a new bottle (47 L, 15 MPa) amounts to just one bottle per week, even if a gas flow rate of 15 L/min is spent continuously to maintain a pressure of 1 atm in the gas cell. Moreover, the achieved gas purity was 99.9999999% (grade 9.0; impurity level: 1 part per billion (ppb)), which was evaluated from the moisture content in the gas using a dew-point transmitter.

This system can be extended to any application based on a gas cell and is feasible for any type of gas. Particularly, in the semiconductor production process, highly pure argon gas is indispensable for use as atomospheric gas, but the gas is usually used once and then disposed of. The reduction of cost of highly pure argon gas is expected on implementing the gas circulation and purification system.[3]

Detail information on this work can be founded in a published article.[4]

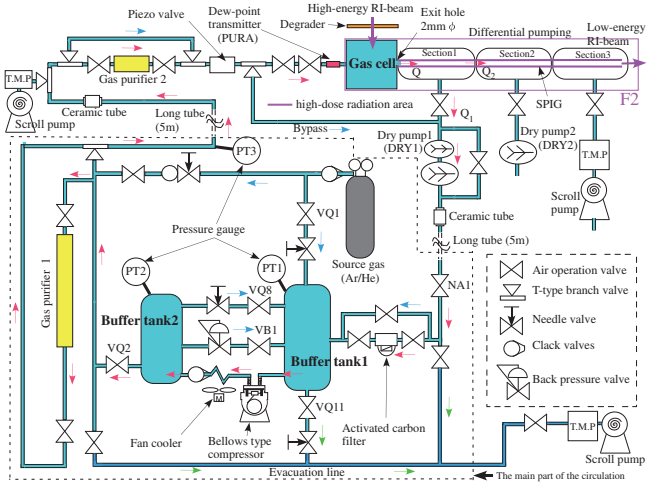

Fig. 1. Overview of the gas cell and the gas circulation and purification system. The red arrows indicate the regular direction of circulation, and the green arrows indicate the direction of the evacuation line. The blue arrows indicate the direction of gas flow under some special conditions.

References
1) T. Sonoda et al., AIP Conf. Proc. **1104** 132 (2009).
2) T. Sonoda et al., Nucl. Inst. and Meth. B **295** 1 (2013).
3) Japan Chemical Daily, Aug. 23, (2016).
4) T. Sonoda, T. Tsubota et al., Rev. Sci. Instrum. **87**, 065104 (2016).

† Condensed from the article in Rev. Sci. Instrum. **87**, 065104 (2016)

*1 RIKEN Nishina Center
*2 Tokyo KOATSU Co., Ltd.
*3 Department of Physics,University of Jyvaskyla

Concept design for cold highly charged ion generation toward time variation detection of fine structure constant α

N. Kimura,[*1,*2] K. Okada,[*1] N. Nakamura,[*3] N. Ohmae,[*4,*5,*6] H. Katori,[*4,*5,*6] and M. Wada[*7,*2]

A ground unification theory approves that fundamental physical constants have a time dependence.[1] Over recent decades, time-variation detections of fundamental physical constants have been attempted through several approaches. In astrophysical research, J. K. Webb et al. reported that a variation of fine-structure constant α was observed as $\delta\ \alpha/\alpha = 0.72(\pm 0.18) \times 10^{-5}$ by comparison with quasar spectra.[2] Recently, V. V. Flambaum et al. have focused on achieving a high enhancement factor K of highly charged ion(HCI) atomic transitions and suggested high-sensitivity measurements for the detection of α-time variation by Ho^{14+} precision spectroscopy.[3] Additionally, they proposed special enhanced measurements using highly charged Actinide ions Cf^{15+} and Es^{16+}.[4]

As mentioned above, HCI precision spectroscopy is expected to be a candidate for the next-generation atomic clock for conducting the constancy test of fundamental physical constants. We plan to measure the frequency difference between a Sr optical lattice clock and a clock transition of HCI using an optical-frequency comb[3,5] in the detection of α-time variation during a realistic experimental period. In this experiment, we have to prepare an HCI Coulomb crystal for Doppler-shift reduction. However, there are few studies on HCI Coulomb crystals awing to experimental difficulties. In 2015, Ar^{13+} Coulomb crystallization in laser-cooled Be^+ ions was demonstrated by an external HCI injection system from an electron beam ion trap via a deceleration tube.[6] For the demonstration of HCI Coulomb crystallization and clock transition detection, we also set a plan to generate an HCI Coulomb crystal using a sympathetic cooling method via laser cooled Be^+ in a compact instrument as explained below.

Figure 1 shows a temporary assembled ion trap without a solenoid coil and a flexible printed circuit. It will be mounted on the 4K cryogenic chamber as shown in Figure 2,under an ultra-high-vacuum condition with superconductive driving. This ion trap based on the linear Paul trap is divided into three areas and is combined with the Penning ion trap. In the 1st area, HCI and Be^+ are generated by laser ablation and an electron beam. The off-axis cold cathode injects an electron beam into a trap region while maintaining the cryogenic thermal condition and cooling laser path. A superconductive Nb:Ti wire will be looped on quadrupole rods directly. This wire will become a solenoid coil and generate a strong magnetic field for Penning trap driving and the concentration of the electron beam. Generated HCI ions are transported to the 3rd area by electrical manipulation and cooled by the prepared Be^+ Coulomb crystal.

A function test of this instrument will be performed by observations of Be^+ trapping and cooling. After this test, we will try to perform HCI generation and sympathetic crystallization.

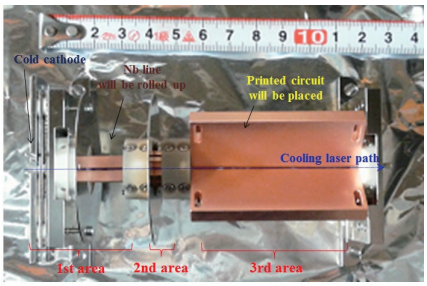

Fig. 1. HCI trap (without coils and print circuits).

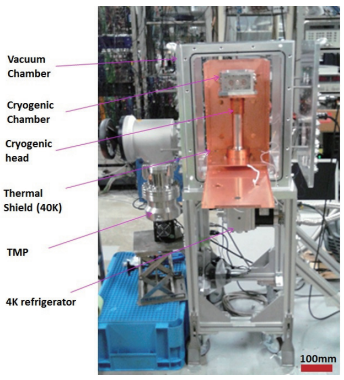

Fig. 2. Cryogenic chamber system.

*1 Department of Physics, Sophia University
*2 RIKEN Nishina Center
*3 Institute for Laser Science, The University of Electro-Communications
*4 Quantum Metrology Laboratory, RIKEN
*5 Innovative Space-Time Project, ERATO
*6 Department of Applied Physics, Graduate School of Engineering, The University of Tokyo
*7 Wako Nuclear Science Center (WNSC), Institute of Particle and Nuclear Studies (IPNS), High Energy Accelerator Research Organization (KEK)

References

1) J. -P. Uzan, Rev. Mod. Phys. **75**, 403(2003).
2) J. K. Webb, et al., Phys. Rev. Lett. **87**, 091301(2001).
3) V. A. Dzuba, et al., Phys. Rev. **A 91**, 022119 (2015).
4) V. A. Dzuba, et al., Phys. Rev. **A 92**, 060502(R) (2015).
5) N. Nemitz, et al., Nature Photonics **10**, 258261 (2016).
6) L. Schmoger, et al., Science **347**, 12331236 (2015).

Reduction in contaminants originating from primary beam by using beam stoppers in GARIS-II

S. Kimura,[*1,*2] D. Kaji,[*2] Y. Ito,[*2] H. Miyatake,[*3] K. Morimoto,[*2] and M. Wada[*2,*3]

An apparatus consisting of a multireflection time-of-flight mass spectrograph (MRTOF-MS) and a gas-filled recoil ion separator GARIS-II[1] has been developed to measure the masses of superheavy elements[2]. The MRTOF-MS is connected to GARIS-II via a gas cell and an ion transport system. It is known that the ion extraction efficiency of the gas cell decreases as the incoming rate increases[3]. If some charge states of the primary beam have $B\rho$-values that are close to the target nuclide's values, the gas cell efficiency could be drastically reduced by the huge contaminants and space charge. In addition, the intense contaminant beam could lead to breakage of the thin Mylar window foils located at both the exit of GARIS-II and the gas cell entrance.

To avoid this situation, two water-cooled primary beam stoppers, Stopper1 and Stopper2, were installed in the first dipole (D1) of GARIS-II as shown in Fig. 1. Stopper1 installed at the entrance of the D1 chamber consisted of a copper plate of 80 mm width and 30 mm height and could vary its effective area to the beam by rotating. Stopper2, located near the D1 chamber exit, was made of a 400 mm wide and 60 mm high copper board mounted on a linear manipulator to change its position, and had tantalum fins on its surface to prevent scattering of the colliding particles.

The performance of the both stoppers was evaluated by using the ^{208}Pb(^{18}O, 3n) ^{223}Th reaction. In this reaction, the 4+ state of the ^{18}O beam after the targets has a $B\rho$-value that is close to the optimum one for ^{223}Th. A silicon detector array was employed to count both the incoming ^{223}Th and the contaminants at the GARIS-II focal plane. The primary beam was chopped to measure the α-decay from ^{223}Th in low background conditions. The evaluation results are shown in Fig. 2. An intensity ratio of contaminants to ^{223}Th of ∼20 was reached without both stoppers. As the Stopper1 effective area began to increase, the intensity of the contaminants rapidly decreased, in contrast with the ^{223}Th counting rate, which varied gradually (Fig. 2 (top)). As a result, we could suppress ∼95% of the contaminants from reaching the focal plane by using Stopper1, while ∼80% of ^{223}Th was still transported. The same measurements were conducted by changing the Stopper2 position as shown in Fig. 2 (bottom). When measuring the Stopper2 performance, the Stopper1 effective area was set to the maximum value: 2400 mm^2. The Stopper2 measurement shows results similar to those obtained with Stopper1. Thus, we can improve the signal noise ratio up to ∼250 times higher than before by using both stoppers.

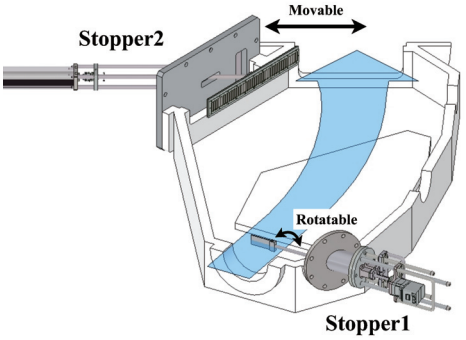

Fig. 1. Schematic view of the primary beam stoppers. The D1 chamber is shown as a cross-sectional view. The blue arrow indicates the beam direction.

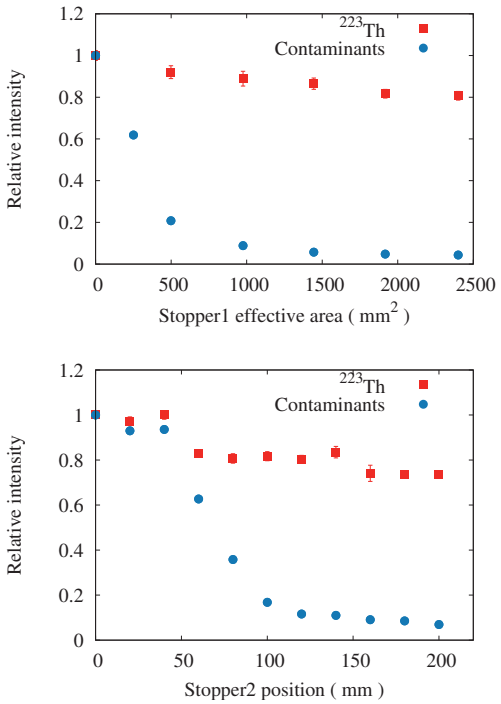

Fig. 2. Results of both stoppers' performance evaluations. The figures indicate the dependencies of the counting rates on the Stopper1 effective area (top) and on the Stopper2 position (bottom).

*1 Institute of Physics, University of Tsukuba
*2 RIKEN Nishina Center
*3 Wako Nuclear Science Center (WNSC), Institute of Particle and Nuclear Studies (IPNS), High Energy Accelerator Research Organization (KEK)

References
1) D. Kaji et. al., NIM B **317**, 311(2013).
2) P. H. Schury et. al., PRC **95**, 011305 (2017).
3) A. Takamine et. al., RSI **76**(10) 103503 (2005).

Separated flow operation of the SHARAQ spectrometer for in-flight proton-decay experiments†

M. Dozono,[*1] T. Uesaka,[*2] S. Michimasa,[*1] M. Takaki,[*1] M. Kobayashi,[*1] M. Matsushita,[*1] S. Ota,[*1] H. Tokieda,[*1] and S. Shimoura[*1]

The SHARAQ spectrometer[1] is a high-resolution magnetic spectrometer designed for radioactive isotope (RI) beam experiments at the RI Beam Factory (RIBF). The spectrometer has opened up new experimental opportunities in combination with the high-resolution beam line. One interesting example is a new type of missing-mass spectroscopy with an RI beam used as a probe. To date, investigations of spin-isospin properties in nuclei have been strongly promoted by RI-induced charge-exchange reactions such as $(t, {}^3\mathrm{He})$, $({}^{12}\mathrm{N}, {}^{12}\mathrm{C})$, $({}^{10}\mathrm{C}, {}^{10}\mathrm{B})$, and $({}^{8}\mathrm{He}, {}^{8}\mathrm{Be})$.

We have developed a new ion-optical mode of SHARAQ operation. The new mode, called the "*separated flow mode*", enables the invariant-mass spectroscopy of proton-unbound states with SHARAQ and thus extends the research field of the nuclear chart toward proton-rich nuclei. In addition, proton-unbound nuclei can be used as probe particles. One interesting example is the parity-transfer reaction $({}^{16}\mathrm{O}, {}^{16}\mathrm{F}(0^-, \mathrm{g.s.}))$[2]. This reaction has a unique sensitivity to unnatural parity states and can be used as a powerful tool to probe 0^- states in a target nucleus.

In the separated flow mode, the SHARAQ spectrometer is used as two spectrometers with different magnet configurations of "QQD" and "QQDQD" at the same time (see Fig. 1). The reaction products from the target (S0) are separated and analyzed in either of these two configurations depending on their mass-to-charge ratios (A/Z). The particles with $A/Z \sim 1$, such as protons, are analyzed in the "Q1-Q2-D1" configuration and detected in the S1 focal plane, which is located on the low-momentum side downstream of the D1 magnet. On the other hand, the heavy-ion products are analyzed in the "Q1-Q2-D1-Q3-D2" configuration to increase the resolving power and detected at the S2 final focal plane. Therefore, this new technique enables us to perform coincidence measurements of the proton and heavy-ion pairs produced in the decays of proton-unbound states in nuclei. Details of the ion-optical properties and the focal-plane detector systems can be found in our published paper.

The separated flow mode was successfully introduced in an experiment with the reaction $({}^{16}\mathrm{O}, {}^{16}\mathrm{F})$ at a beam energy of 247 MeV/u (SHARAQ08 experiment). The outgoing $^{15}\mathrm{O} + p$ produced in the decay of $^{16}\mathrm{F}$ were measured in coincidence with SHARAQ.

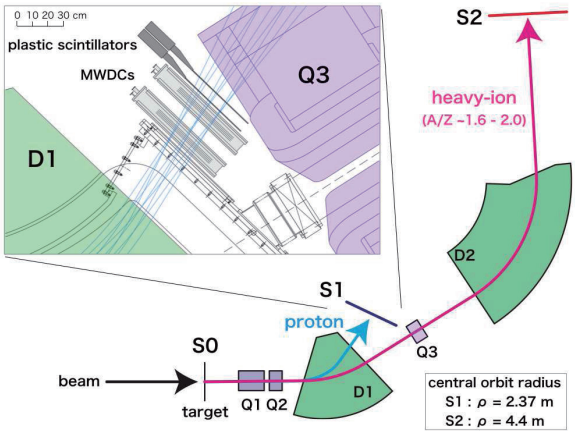

Fig. 1. Schematic layout of the SHARAQ spectrometer. The SHARAQ spectrometer consists of two superconducting quadrupole magnets (Q1 and Q2), one normal conducting quadrupole magnet (Q3), and two dipole magnets (D1 and D2) in a "QQDQD" configuration. In the separated flow mode, the protons and the heavy-ion products from the target (S0) are separated and measured in coincidence at two different focal planes (S1 and S2) of SHARAQ. The inset shows the tracking detector system at S1, which consists of two multi-wire drift chambers (MWDCs) and two plastic scintillators.

For the relative energy between the $^{15}\mathrm{O}$ particle and the proton, a resolution of 100 keV (FWHM) was achieved, and the 0^- g.s. of $^{16}\mathrm{F}$ ($E_{\mathrm{rel}} = 0.535$ MeV) was clearly separated from the excited states, the 1^- state at 0.193 MeV ($E_{\mathrm{rel}} = 0.728$ MeV) and the 2^- state at 0.424 MeV ($E_{\mathrm{rel}} = 0.959$ MeV). In addition, a high resolution of ~2 MeV (FWHM) was achieved for a $^{16}\mathrm{F}$ kinetic energy of 3,940 MeV. Such an accurate missing-mass measurement combined with an invariant-mass method gives unique opportunities to explore little-studied excitation modes in nuclei using new types of reaction probes with particle-decay channels.

References

1) T. Uesaka, S. Shimoura, and H. Sakai, Prog. Theor. Exp. Phys. **2012**, 03C007 (2012).
2) M. Dozono et al., RIKEN Accel. Prog. Rep. **45**, 10 (2012).

† Condensed from the article in Nucl. Instrum. Meth. A **830**, 233 (2016)

*1 Center for Nuclear Study, University of Tokyo
*2 RIKEN Nishina Center

Development of multiwire drift chambers and the readout system for focal-plane tracking detectors in BigRIPS

S. Y. Matsumoto,[*1,*2] H. Fujioka,[*1,*2] K. Itahashi,[*1] T. Kawabata,[*2] T. Nishi,[*1] A. Sakaue,[*1,*2] M. Takaki,[*3] Y. K. Tanaka,[*1,*5] T. Uesaka,[*1] Y. N. Watanabe,[*1,*4] K. Yako,[*3] and J. Zenihiro[*1]

We are developing a new focal-plane detector and readout system, aiming at searching for double Gamow–Teller giant resonance (DGTGR) via the $\left({}^{12}\mathrm{C}, {}^{12}\mathrm{Be}\left(0_2^+\right)\right)$ reaction and systematic high-precision spectroscopy of pionic atoms (piAF) via the $\mathrm{Sn}\left(d, {}^3\mathrm{He}\right)$ reaction.

Both experiments use the same detector configuration for missing-mass spectroscopy. The particles emitted in the nuclear reactions are momentum-analyzed in F0–F5 of BigRIPS and detected at the F5 dispersive focal plane. The tracking detector at F5 (i) should detect light ions and (ii) should work under high rate background conditions (on the order of megahertz for tritons in the DGTGR experiment and protons in the piAF experiment). In order to satisfy these conditions, we adopt multiwire drift chambers (MWDCs) instead of the standard tracking detector, PPACs.

We decided to develop low-pressure MWDCs that can be operated in vacuum[1]. In the preceding experiment of pionic atom spectroscopy in 2014, MWDCs with a gas pressure of 1 atm were operated in air. A vacuum window (50-μm-thick stainless) located upstream caused multiple scattering. While the intrinsic tracking resolution was found to be $\sim$ 0.1 mm (FWHM), the effect of multiple scattering resulted in the deterioration of the position resolution up to 4.1 mm (FWHM) at maximum. This deterioration is suppressed by using the low-pressure MWDC.

Our new MWDCs have configurations with sets of 1/3-cell staggered three-layer structures, (XX'X"(0°), UU'U"(+30°), VV'V"(−30°)), as schematically shown in Fig. 1. The previous MWDCs had sets of 1/2-cell staggered two-layer structures and showed a nonnegligible inhomogeneity in the spectra originating in an analytic bias in the proximity of both the sense and potential wires. The asymmetric probability distribution of the estimated drift length near the wires due to the boundary condition ($0 \leq$ drift length $\leq$ wire interval) caused a bias for the reconstructed track, disfavoring the close proximity of the wires. This effect is expected to be exhibited even with an exactly known drift-time-to-length conversion with a finite resolution, as demonstrated by a simple Monte Carlo simulation[2] and becomes prominent in extremely high-statistics data. For each set of layers in the new MWDCs, we use the drift length information of two of the three layers by neglecting the data of the layer where the trajectory is closest to a wire. On the basis of the previous experiment, we expect a high-rate capability (0.1–1MHz) and sufficient plane resolution (0.3 mm (FWHM)) for the detector.

An upgrade of the readout system for the new MWDCs is necessary to realize high-speed data handling. As for the hardware of the system, we are developing a new all-in-one board[3] that handles a higher triggering rate ($\sim$10kHz). The board reads 64 channels of MWDC analog signals and amplifies, discriminates, and digitizes them by FADC and TDC. The board also receives trigger tag information from an event tagging system and transfers data by an SiTCP[4] network processor implemented by an FPGA. There are two modes for reading data, raw and suppress modes. The raw mode is an option for recording all of the data of FADC, and the suppress mode, which is used in our experiments, is prepared for lowering the data size by collecting the data of channels with more than one TDC hit. We have been working on building a DAQ system with eight boards and combining this system with the standard RIBF DAQ[5].

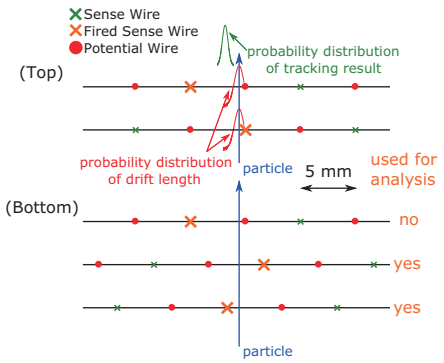

Fig. 1. Schematics of the old (top) and new (bottom) MWDC wire configurations. The new (old) MWDC has sets of 1/3-cell (1/2-cell) staggered three(two)-layer structures. The new MWDC has a redundant design to avoid the analytical bias originating from the asymmetric probability density distribution of the estimated drift length in the proximity of the wires.

*1 RIKEN Nishina Center
*2 Department of Physics, Kyoto University
*3 Center for Nuclear Study, University of Tokyo
*4 Department of Physics, University of Tokyo
*5 GSI Helmholtzzentrum für Schwerionenforschung GmbH

References

1) H. Miya *et al.*, Nucl. Instr. Meth. B **317**, 701 (2013).
2) Y. K. Tanaka: Ph. D. thesis, Univ. Tokyo (2016).
3) H. Yamakami: Master's thesis, Kyoto Univ. (2015).
4) T. Uchida, IEEE Trans. Nucl. Sci. **55**, 3, 1631 (2008).
5) H. Baba *et al.*, Nucl. Instr. Meth. A **616**, 65 (2010).

Development of control system for magnetic field of the BigRIPS separator with a feedback algorithm

Y. Shimizu[*1] D.S. Ahn,[*1] N. Fukuda,[*1] N. Inabe,[*1] K. Kusaka,[*1] M. Ohtake,[*1] H. Suzuki,[*1] H. Takeda,[*1] Y. Yanagisawa,[*1] and K. Yoshida[*1]

We have designed and constructed a new control system for magnetic field of the BigRIPS separator[1] at RIKEN. The absolute $B\rho$ value was derived from the magnetic field of a dipole magnet measured with an NMR probe and the central trajectory radius of the dipole magnet determined from the magnetic-field map.[2] A new control system has been designed to satisfy zero deviation between the preset and measured $B\rho$ values. Furthermore, the control system is required to show not only high stability but also high reproducibility within a reasonably short time, since the settings of the BigRIPS separator are frequently changed during an experiment.

In order to enhance the reproducibility of the $B\rho$ value of the dipole magnet, a new control system was designed with a proportional-integral-derivative (PID) algorithm.[3] The output current I_n of the power supply after the nth sampling is given by

$$\begin{aligned} I_n &= I_{n-1} + \Delta I_n, \\ \Delta I_n &= -K_P(B_n - B_{n-1}) + K_I \Delta T_n (S_n - B_n) \\ &\quad - \frac{K_D}{\Delta T_n}(B_n - 2B_{n-1} + B_{n-2}), \end{aligned}$$

where ΔT_i is the sampling time, S_i is the preset $B\rho$ value, and B_i is the measured $B\rho$ value in the ith sampling. K_P, K_I, and K_D, all non-negative, denote the parameters of the PID feedback algorithm corresponding to the proportional, integral, and derivative components, respectively. Note that the integral action only responds to changes in the preset $B\rho$ value because the proportional and derivative actions produce a large unwanted spike when the preset $B\rho$ value is changed.[3]

The magnetic field is required to be changed and stabilized so that the position of the central particle in the focal plane is set within 0.0±0.5 mm in 3 min. The 0.5 mm at the 5th focal plane of the BigRIPS separator corresponds to 6×10^{-4} Tm at 4 Tm. Therefore the values of the parameters K_P, K_I, and K_D were optimized such that the magnetic field is changed and stabilized within $\pm 5 \times 10^{-4}$ Tm in 3 min.

Figure 1 shows typical magnetic-field responses of the 2nd dipole magnet of the BigRIPS separator as functions of time. The red and blue solid lines show the results changed from 6.93 Tm and 7.07 Tm to 7.00 Tm. Some overshoots remained because an NMR probe could not work owing to a rapid change of magnetic field in the beginning when the preset $B\rho$ value

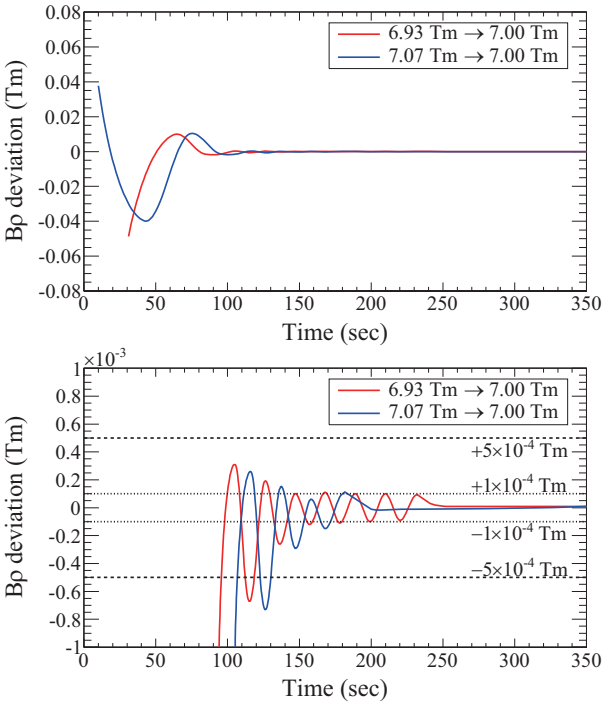

Fig. 1. Typical magnetic-field responses of the 2nd dipole magnet of the BigRIPS separator as functions of time. The bottom panel shows the plots enlarged around $\pm 1 \times 10^{-3}$ Tm.

was changed. However, they were negligibly small in the BigRIPS tuning. The bottom panel of Fig. 1 shows the plots enlarged around $\pm 1 \times 10^{-3}$ Tm. Dashed and dotted lines show the values of $\pm 5 \times 10^{-4}$ Tm and $\pm 1 \times 10^{-4}$ Tm, respectively. The PID feedback system successfully functions, and the magnetic field is stabilized in 2.5 min within $\pm 5 \times 10^{-4}$ Tm. The fluctuations of the magnetic fields are limited within $\pm 1 \times 10^{-4}$ Tm after 4 min.

A new control system for the magnetic field of the BigRIPS separator with a PID feedback algorithm is currently operational well.

References

1) T. Kubo et al., Nucl. Instr. Meth. B **204**, 97 (2003).
2) Y. Yanagisawa et al., RIKEN Accel. Prog. Rep. **41**, 125 (2008).
3) T. Kitamori, Journal of The Society of Instrument and Control Engineers, 19(4), 382 (1980).

*1 RIKEN Nishina Center

Fast beam interlock system at BigRIPS separator

K. Yoshida,[*1] Y. Yanagisawa,[*1] K. Kusaka,[*1] K. Tanaka,[*1] and T. Kubo[*1,*2]

A fast beam interlock system (FBIS) with a response time less than 1 ms has been developed and installed at BigRIPS in order to cope with the recent increase of beam intensity at RIBF. If an intensive beam such as ^{238}U and ^{48}Ca beams with an energy of 345 MeV/nucleon and intensity of 1 particle μA was mis-steered and incident on the beam duct owing to a failure of magnet power supplies, the duct will be melted within 1- 5 ms. The fast interlock system detects the failure and cuts off the beam within 1 ms to prevent severe damage.

The FBIS at BigRIPS utilizes a compact RIO system (cRIO) of National Instrument Co. Ltd to achieve a fast response and flex configuration capability. A prototype of the system was developed in 2013 and tested.[1)] Based on the successful test results,[1)] the FBIS was constructed to monitor the analog and digital signals from the production target system and power supplies of the 34 magnets placed at the primary beam line and BigRIPS where a high-power primary beam is transported. The system consists of 5 cRIOs (three cRIO-9075 and two cRIO-9068) and sends the beam stop signal to the beam chopper system as well as the normal beam interlock system (BIS).[2)] NI-9222 ADC modules and NI-9401 digital I/O modules are used for analog and logical signal processing respectively.

Figure 1 shows the logic diagram of the FBIS. The diagram is almost same as that for the prototype system but two enhancements were made. A digital filtering algorithm was added to analog signal processing in order to eliminate the noise in analog inputs. The moving average method was employed as the filtering algorithm. Another improvement was in the pulse rate measurement. A periodic counter was formed in the control logic and logical signal pulses were counted. The counter had a special function to produce an error signal immediately when the counting number exceeded the limit. Thus, one can set a rate limit to logical signal pulses unless waiting for the counting to end. All these control logics were stored in a field-programmable gate array (FPGA) of the cRIO-9075 and cRIO-9068 modules and executed at fast speed.

The control conditions such as limit values of analog inputs and pulse rates, enable/disable flags, and positive/negative logic selections are dynamically set from the comprehensive control system of BigRIPS.[3)] The status of faults and digitized values of the analog inputs are monitored and logged by the control system of BigRIPS.

In the operation of the FBIS, current monitor outputs and fault signals of magnet power supplies are connected to the analog and logical signal inputs, respectively. The temperature monitor and rotating speed signals of the BigRIPS rotating target system[4)] are also connected to the analog input of the FBIS. Interlock windows of analog signals are set to ±0.3% for dipole magnets and ±1.5% for quadrupole magnets. Windows of ±15% are set for the rotation speeds of the rotating targets and an upper limit of 700 ℃ is set for the target temperature.

The response time of the FBIS was measured using beams at RIBF. A logical test signal was applied as the logical input of the FBIS. Signals from the beam trigger counter, which measures the secondary beam produced from the accelerated beam at the third focus (F3) of the BigRIPS separator, was monitored to determine the beam stopping timing. Measurements were performed for ^{48}Ca and ^{238}U primary beams, and in both cases, time differences from the test signal input to the disappearance of the beam trigger signal were about 250 μs. Thus, the response time of the FBIS is sufficiently low to prevent the severe damage of the equipment.

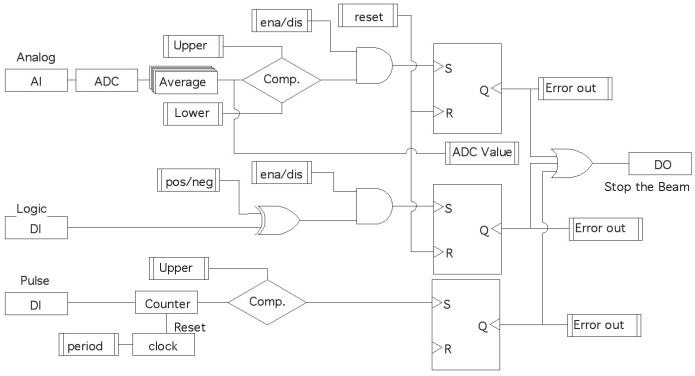

Fig. 1 Logic diagram of the fast beam interlock system.

References

1) K. Yoshida, et. al., RIKEN Accel. Prog. Rep., **47**, 169 (2014) .
2) M. Komiyama, et. al., RIKEN Accel. Prog. Rep. **41**, 242(2008).
3) K. Yoshida, RIKEN Accel. Prog. Rep. **44**, 131 (2011).
4) A. Yoshida, et. al., Nucl. Instr. and Meth. **A521**, 65 (2004).
5) A. Yoshida, et. al., Nucl. Instr. and Meth. **A590**, 204 (2008).
6) A. Yoshida, et. al., Nucl. Instr. and Meth. **A655**, 10 (2011).

[*1] RIKEN Nishina Center
[*2] FRIB/NSCL, Michigan State University

Isomer identification under high-rate-counting environment

S. Terashima,[*1,*2] J. Zenihiro,[*1] S. Ota,[*3] A. Bracco,[*4,*5] F. Camera,[*4,*5] S. Chebotaryov,[*1] M. Dozono,[*3] T. Harada,[*6] C. Iwamoto,[*3] K. Kawata,[*3] N. Kitamura,[*3] M. Kobayashi,[*3] A. Krasznahorkay,[*8] S. Leblond,[*8] T. Lokotko,[*8] Y. Maeda,[*9] S. Masuoka,[*3] Y. Matsuda,[*10] M. Matsushita,[*3] S. Michimasa,[*3] E. Milman,[*1] T. Murakami,[*1,*11] H. Nasu,[*10] J. Okamoto,[*10] H. Sakaguchi,[*12] S. Sakaguchi,[*13] M. Takaki,[*3] K. Taniue,[*9] H. Tokieda,[*3] M. Tsumura,[*11] T. Uesaka,[*1] O. Wieland,[*5] Z.H. Yang,[*1] Y. Yamaguchi,[*3] and R. Yokoyama[*3]

RIBF can provide a new opportunity to study small-cross-section measurement with a highly intense secondary beam. In spring 2016, a series of experiments RIBF113 and RIBF79 with a ^{132}Sn secondary beam was performed with a new technique called the TOF-Bρ-Bρ method[1]. Full identification of atomic number Z and mass over charge A/Q can be achieved by a combination of time-of-flight(TOF) between F3 and F7 and magnetic rigidity(Bρ) by tracking detectors before and after the degrader at F5, even under an extremely high counting rate of approximately 200 kHz at F7. In RIBF79, the μs isomer ^{132}Sn(8^+) identification was also investigated. The existence of the isomer in ^{132}Sn forms a potential background for the study of density distribution by proton elastic scattering. The isomer ratio of ^{132}Sn in U-fission products had already been measured at RIKEN several years ago to be of the order of 3%[2].

Four large-volume LaBr(Ce) detectors called Hector$^+$ which was developed by INFN-Milano[3], were installed around the plastic stopper where all ejectiles from the secondary hydrogen target were stopped. The distance between the stopper to the detector surface is about 10 cm. Signals from the PMT output of the Hector$^+$ were connected to a flash-ADC SIS3350(FADC). The total time window was approximately 8 μs with 2048 samplings with 250-MHz frequency used for analysis, which is sufficiently long for our isomer of interest ^{132}Sn(8^+), the half life of which is 2.04 μs. The DAQ for FADC was operated separately with a common trigger from the main system. The typical trigger rate and dead time were 100 Hz and 1.5 ms, respectively. Separately obtained data are merged with the time-stamp information of the LUPO module[4]. The single rate of one Hector$^+$ was typically 50 kHz for a beam condition with a total intensity of 200 kHz. The purity of ^{132}Sn was approximately 30%.

*1 RIKEN Nishina Center
*2 School of Physics and Nuclear Energy Engineering, Beihang University
*3 Center for Nuclear Study, University of Tokyo
*4 Dipartimento di Fiscia dell Universit degli Studi di Milano
*5 Istituto Nazionale di Fisica Nucleare Serione di Milano
*6 Department of Physics, Toho University
*7 MTA ATOMKI, Debrecen
*8 Department of Physics, University of Hong Kong
*9 Department of Applied Physics, University of Miyazaki
*10 CYRIC, Tohoku University
*11 Department of Physics, Kyoto University
*12 RCNP, Osaka University
*13 Department of Physics, Kyushu University

Figure 1 shows a typical waveform of the FADC. An FFT filter is applied to eliminate high-frequency components in the waveform. We can identify each sequential γ-ray correctly, even under a high single rate. Figure 2 shows an example plot of time-energy correlation of one Hector$^+$ gated by ^{132}Sn with the TOF-Bρ-Bρ method as shown in the right panel of Fig. 2. Delayed sequential γ-decays of 133/299/374 keV from ^{132}Sn(8^+), which are indicated by red arrows, are observed weakly following prompt timings within a huge background. Further analysis combined with proton scattering is in progress.

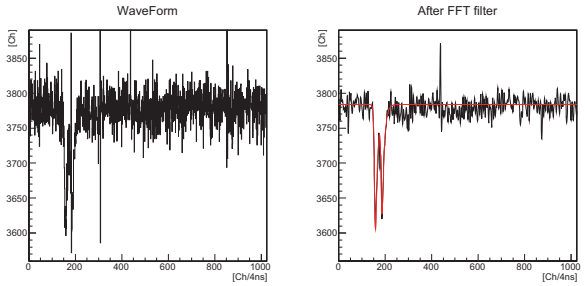

Fig. 1. Sample of raw waveform(left) and after FFT filter(right) with fitting in Hector$^+$ for a sequential event with an energy of approximately 100 keV with 200-ns time difference.

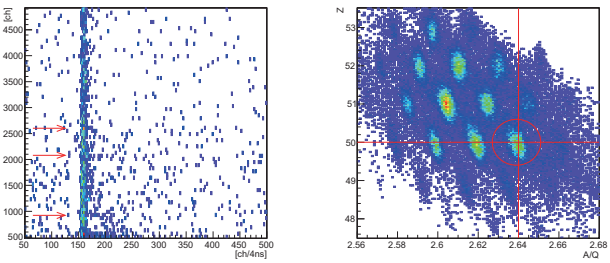

Fig. 2. Time-energy correlation in FADC(left) with ^{132}Sn gate by TOF-Bρ-Bρ method(right). Arrows indicate the expected γ-decay line from ^{132}Sn(8^+).

References

1) S. Ota et al. RIKEN Accel. Prog. Rep. **49**, 15 (2015).
2) D. Kameda et al. RIKEN Accel. Prog. Rep. **43**, 1 (2010).
3) A. Gias et al. Nucl.Instr. Meth. A **729**, 910 (2013).
4) H. Baba et al. Nucl.Instr. Meth. A **777**, 75 (2015).

Channeling effect in ultra-thin monolithic silicon telescopes

F. Parnefjord Gustafsson,[*1] B. Dolachay,[*2] V. Ho Phong,[*3] S. Nishimura,[*3] and T. Ikeda[*3]

Determining the cross section of the ^{8}Li$(\alpha, n)^{11}$B reaction in the low energy regime $E_{\rm cm} < 2$ MeV has been of particular interest in recent decades.[1,2] In a potential inhomogenous Big Bang scenario, this reaction could bridge the mass gap at $A = 8$, leading to the evolution of heavier nuclei in the very early universe. Furthermore, full network calculations indicate that this reaction could play a vital role in enhancing the r-process nucleosynthesis in supernovae.[3,4]

Multiple experiments have been performed to determine the low-energy cross section using the inverse kinematics of a ^{8}Li beam incident on a ^{4}He gas target.[2,5,6] However, data are scarce and show remarkable discrepancy below $E_{\rm cm} < 1.7$ MeV owing to difficulties with the accurate identification of the low-energy reaction products.[2] A new method was proposed at RIKEN to study the low-energy resonances using ultra-thin ΔE-E monolithic silicon telescopes (MSTs)[1]. Each telescope consists of five ultra-thin $\sim$1 μm (ΔE) silicon detector pads on a $\sim$500-μm-thick (E) silicon detector. Experiments performed in 2005 show promising results for identifying the reaction at even a low energy of $E_{\rm cm} \cong 0.5$ MeV.[7]

To assure optimal detector performance for the final cross-section measurement, it is crucial to determine the MST characteristics and response for particles incoming at different angles of incidence. Ultra-thin silicon detectors are particularly prone to the channeling effect, which degrades the detector signal for particles incident along the detector crystal planes or axis by significantly reducing the stopping power. Moreover, the exact detector characteristics remain unknown, and determining the thickness of the two dead layers in the telescope could reveal the detector threshold for particle identification.

The tandem Pelletron accelerator at the Nishina Center, RIKEN was used to accelerate 4-MeV ^{11}B, 9-MeV ^{63,65}Cu, and 7- and 25.5-MeV ^{197}Au ions into the MST. The telescope was attached to a rotation stage within the target chamber allowing accurate remote angular control with respect to the ion beam. Approximately 30000 coincidence events in the ΔE and E detector were collected at varying angles of incidence for each selected ion beam.

Our study reveals the influence of the channeling effect in the ΔE-E particle identification spectrum with respect to detector orientation (see Fig. 1). A tail extending from the 4-MeV ^{11}B main peak in the spectrum was observed at specific detector angles, and it was attributed to the channeling effect. The channeling ratio was defined as the ratio of the number of events in this tail ($N_{\rm chan}$) to the number of events within the main peak ($N_{\rm peak}$). By determining the channeling ratio as a function of detector angle the silicon crystal orientation could be deduced. Our results indicate that the channeling effect can be significantly reduced by orienting the silicon detector at 10° facing the anisotropic silicon crystal orientation in between the crystal axis [111] and ⟨231⟩.

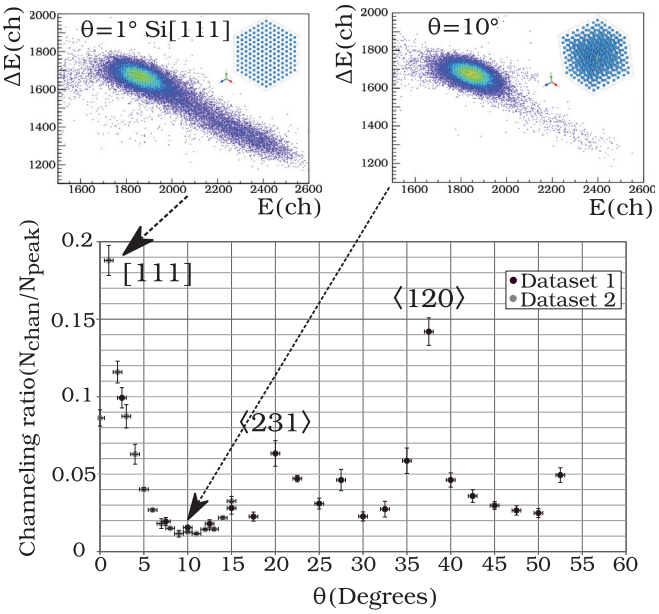

Fig. 1. Channeling ratio versus detector angle θ for 4-MeV ^{11}B. The ΔE-E particle identification spectrum is displayed for the [111] silicon crystal axis and at 10° with the minimal channeling ratio. The peaks with high channeling ratio are indicated with the corresponding silicon crystal axis.

References

1) M. Kurata-Nishimura et al., Nucl. Phys. A **758**, 162 (2005).
2) M. La Cognata et al., Phys. Lett. B **664.3**, 157 (2008).
3) M. Terasawa et al., Astrophys. J. **562**, 470 (2001).
4) T. Kajino et al., Nucl. Phys. A **704**, 165c (2002).
5) Y. Mizoi et al., Phys. Rev. C **6206**, 5801 (2000).
6) S. Cherubini et al., Eur. Phys. J. A **20**, 355 (2004).
7) S. Nishimura et al., RIKEN Accel. Prog. Rep. **39**, 43 (2006).

*1 Department of Physics, Lund University
*2 Department of Physics, University of Paris-Sud
*3 RIKEN, Nishina Center

Pulse height defect in the sc CVD diamond detector versus the applied electric field measured with fission fragments from ^{252}Cf

O.Beliuskina,[*1] N.Imai,[*1] H.Haba,[*2] S.Heinz,[*3] M.Kis,[*3] and M.Traeger[*3]

The response of semiconductor detectors to the energy lost by heavy ions is complicated because the kinetic energy of the ion is not completely converted into an electric signal. The emerging pulse-height defect (PHD) depends on the energy, mass, and charge of the ion as well as on the applied electric field. The PHD is defined as the energy difference ΔE between the kinetic energy E_k of an ion incident in the detector and the apparent energy E_{DD} derived from the measured electric signal.

Most detailed studies of PHD were performed for Si detectors.[1–3] Another promising detector material that appears to extend the possible applications for heavily-ionizing particles compared to Si is chemical vapor deposition (CVD) diamond.[4,5] However, the use of diamond detectors (DDs) as detectors for low-energetic heavy ions is still at its beginning. There are only few publications about PHD in DD.[6–8]

The use of DD as fission fragment detectors was studied by Fregeau et al.[7] The authors concluded that all their DDs showed inadequate energy resolution and suffered from extensive PHDs. The detected pulse height never exceeded about 30 % of what they expected from a simulation of the stopping of ^{252}Cf fission fragments in DD.

In an earlier experiment at the FLNR, Dubna, we investigated the PHD for fission fragments of a ^{252}Cf source at different electric fields.[8] Values between 0.7-$-$2.5 V/μm were used. The charge collection slowly increased towards saturation, but it was not yet saturated at 2.5 V/μm. At 0.7 V/μm, the PHD is about 70 % of the kinetic energy for heavy (HF) and light (LF) fragment groups of ^{252}Cf and about 59 % at 2.5 V/μm.

The aim of our new measurements at the HotLab, RIKEN, was to study the dependencies of the PHD caused by fission products of ^{252}Cf versus the applied electric field up to the highest possible bias and to compare these results with those of previous studies obtained with another single-crystal (sc) CVD DD.

The experiment was carried out at the HotLab, RIKEN. The dependence of the peak positions for the fission fragments of the ^{252}Cf source of 0.5 MBq activity on the electric field were measured with a sc DD manufactured at the GSI detector laboratory. The charge sensitive preamplifier CSTA2, the ORTEC spectroscopic amplifier, and the multichannel analyzer Kromek K102 were used. Detector dimensions were 3 $\times$ 3 mm^2 with a thickness of 200 μm. The DD had CrAu electrodes with thicknesses of 40 nm. The ^{252}Cf source was placed at a distance of 10 cm from the DD. The energy calibration was performed with α particles from a mixed source that has energies of 4.780, 5.480, and 5.795 MeV. The calibration of the electronics was performed with a precision pulser. The mean energies of the heavy and light fragment groups of ^{252}Cf were measured. The difference between the measured energies and the values reported in the literature[1,9] was defined as the PHD.

The working electric field for DDs is about 1.0-$-$2.0 V/μm[10] although its breakdown value for DDs is much higher. All the charge created by α particles with energy of about 5 MeV has already been collected at 0.5 V/μm, and the pulse height remains the same at all values of the electric field from 0.5 to 5.0 V/μm (applied in our experiment). In contrary, for fission fragments of the ^{252}Cf with an increasing electric field from 1.0 to 2.0 V/μm, the pulse height increased by 8 %, indicating that the created charge is not fully collected. Further, PHD dependency on the applied electric field, which has a quite steep slope in the region 1.0$-$2.0 V/μm goes almost to its saturation between 2.5 and 3.5 V/μm. Namely, the PHD decreases in this region only by about 1 % for LF and about 2 % for HF. It was not possible to use an electric field higher than 3.5 V/μm for fission fragments of ^{252}Cf because occasional breakdowns started to occur.

We conclude that the application of an electric field higher than 2 V/μm slightly improves the charge collection efficiency of DDs for fission fragments of ^{252}Cf.

References

1) H. W. Schmitt, W. E. Kiker, C. W. Williams, Phys. Rev. **137**, B837 (1965).
2) S. B. Kaufman et al., NIM **115**, 47 (1974).
3) E. C. Finch et al., NIM **142**, 539 (1977).
4) M. Pomorski et al., Phys. Stat. Sol. **(a)202**, 2199 (2005).
5) M. Pomorski et al., Phys. Stat. Sol. **(a)203**, 3152 (2006).
6) Y. Sato et al., Euro. Phys. Let. **104**, 22003 (2013).
7) M. O. Fregeau et al., NIM A **791**, 58 (2015).
8) O. Beliuskina et al., Eur. Phys. J. A **53** (2017).
9) G. N. Knyazheva et al., NIM B **248**, 7 (2006).
10) The Element Six Diamond Handbook (www.e6.com).

*1 CNS, University of Tokyo
*2 RIKEN Nishina Center
*3 GSI, Darmstadt

PANDORA project - low-energy neutron detector with real-time neutron-gamma discrimination

L. Stuhl,[*1,2] M. Sasano,[*2] K. Yako,[*1] J. Yasuda,[*3] H. Baba,[*2] S. Ota,[*1] and T. Uesaka[*2]

Recent nuclear physics studies are increasingly focusing on the region far from the valley of stability, requiring an increase of the intensity of available exotic isotopes. This advancement opens up the possibility to investigate phenomena with low cross sections, such as charge-exchange reactions.

The (p, n) charge-exchange reaction at intermediate energies is a powerful tool to study the spin-isospin excitations of nuclei. The technique of inverse kinematics[1,2] enables us to study the (p, n) reactions on exotic nuclei with high luminosity. In this technique, neutron detectors are used for measuring the time of flight (ToF) of low-energy (0.1–10 MeV) recoil neutrons. This method was successfully applied to study the Gamow–Teller strength distribution from ^{56}Ni[2,3] and ^{132}Sn[4] isotopes. In the latter experiment, the secondary beam intensity was 10^4 particles/s, the (p, n) reaction event rate was a few Hz, and the random gamma background produced an additional trigger rate of about 1 kHz.[4] For future experiments with higher beam intensities, this background event rate will lead to higher trigger rates and a large dead time of data acquisition. To solve this problem, clear tagging of recoil neutrons in real time i necessary before recording the event data. Our work focuses on the development of the particle analyzer neutron detector of real-time acquisition (PANDORA). Our goals were

- in online data processing: to reduce the trigger rate by one order of magnitude by removing the random gamma background, leading to a smaller data size and the capability to handle high-intensity beams
- in offline analysis: to fully remove the gamma ray background using the pulse shape discrimination (PSD) parameter.

PANDORA consists of an EJ-299-34 plastic scintillator bar[5] with dimensions of 2.5×5×30 cm^3 coupled to a Hamamatsu H7195 photomultiplier tube on each end. Detector signals from the anode output of both PMTs are read out with a digital data acquisition system (CAEN V1730 digitizer and digital pulse processing for pulse shape discrimination firmware). In order to measure the neutron kinetic energies using the ToF technique with an energy resolution of $\sim 5\%$ ΔE/E for neutron energies below 5 MeV, a ToF resolution better than 0.6 ns (FWHM) is required, while the angular resolution must be less then 1.5°.

*1 Center for Nuclear Study, University of Tokyo
*2 RIKEN Nishina Center
*3 Department of Physics, Kyushu University

The PSD parameter is defined as follows:

$$\mathrm{PSD} = \frac{Q_{Long} - Q_{Short}}{Q_{Long}}, \quad (1)$$

where Q_{Long} is the charge integrated in the long gate. Typically, it contains all charges in the signal. Q_{Short} is the charge integrated in the short gate. Defining PSD_{mean} value as the arithmetic mean of PSD values of two single-end readouts, PANDORA exhibits PSD capability comparable to those presented in literature.

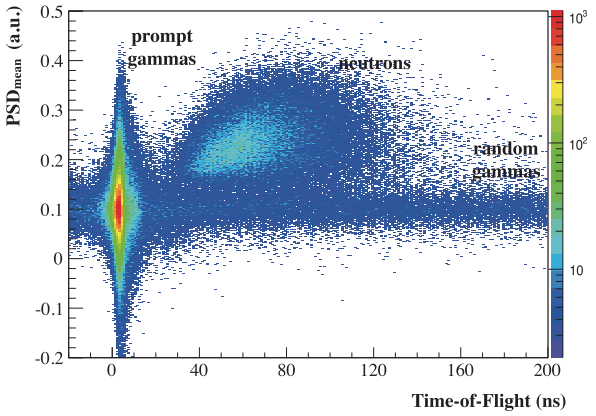

Fig. 1. PSD_{mean} vs. ToF spectrum showing the separation of neutron- and gamma-like events. The sharp peak below 4 ns corresponds to prompt gamma rays, while the distribution in the higher ToF and PSD_{mean} region corresponds to neutron-like events. A large random gamma background can also be observed.

The selection efficiency of neutrons or gammas can be defined as the ratio of the number of selected particles to the total number of detected particles. The ToF distributions acquired using a ^{252}Cf fission source proved that at a given PSD threshold (PSD_{mean} = 0.15) and 10-keV$_{ee}$ detection threshold, the selection efficiency of PANDORA is 91±1% for all detected neutrons. It decreases to about 87±2% in the neutron kinetic energy region below 1 MeV. About 91±1% of the detected gamma-rays can be excluded resulting in background reduction by one order of magnitude.[6]

References

1) G. Perdikakis et al. IEEE Trans. Nucl. Sci. **56**, 3 (2009).
2) M. Sasano et al., Phys. Rev. Lett. **107**, 202501 (2011).
3) M. Sasano et al., Phys. Rev. C **86**, 034324 (2012).
4) J. Yasuda, Study of Gamow-Teller transitions from ^{132}Sn via the (p,n) reaction in inverse kinematics, PhD thesis, Dept. of Physics, Kyushu University (2017).
5) N. Zaitseva et al., Nucl. Instr. Meth. A **668**, 88 (2012).
6) L. Stuhl et al., Nucl. Instr. Meth. A **866**, 164 (2017).

Development of co-existing ^{129}Xe and ^{131}Xe nuclear spin masers with active feedback scheme for the Xe atomic EDM search

T. Sato,[*1,*2] Y. Ichikawa,[*1,*2] T. Inoue,[*3,*4,*1] A. Uchiyama,[*4,*1] A. Gladkov,[*1,*5] A. Takamine,[*1] S. Kojima,[*2] C. Funayama,[*2] S. Tanaka,[*2] Y. Sakamoto,[*2] Y. Ohtomo,[*2] C. Hirao,[*2] M. Chikamori,[*2] E. Hikota,[*2] T. Furukawa,[*6] A. Yoshimi,[*7,*1] C.P. Bidinosti,[*8] T. Ino,[*9] H. Ueno,[*1] Y. Matsuo,[*10,*1] T. Fukuyama,[*11] N. Yoshinaga,[*12] Y. Sakemi,[*13,*4] and K. Asahi[*1,*2]

Astronomical observations reveal that the matter to photon ratio in the Universe is many orders of magnitude larger than the prediction based on broadly accepted cosmological scenarios. The extra CP-violation, which may come from physics beyond the Standard Model (SM), will contribute to understanding of the origin of matter. The electric dipole moment (EDM) of a particle is one of the cleanest probes for new physics, because the SM contribution to the EDM is undetectably small while most of proposed candidates for new physics predict detectable sizes of EDM. There are only three CP-violating effective operators at the hadron level that can enter EDMs of diamagnetic atoms.[1] Therefore, a combination of measurements for at least three different atoms is essential to distinguish the new physics beyond the SM. The improvement of the upper limits of the EDMs of diamagnetic atoms has a significant impact on the study of new physics in the nucleon-nucleon and nucleon-electron interactions. Thus, we aim to improve the current upper limit on the Xe atomic EDM, $|d(\mathrm{Xe})| < 4.1 \times 10^{-27} e\mathrm{cm}$,[2] by more than one order of magnitude.

To detect the EDM of a Xe atom, the frequency of spin precession in a static magnetic field and an electric field is measured. The presence of an EDM of a size 10^{-28} $e$cm, for instance, in a 10 kV/cm electric field would change the frequency of the Xe spin precession on the level of nanohertz. In order to detect such an extremely small frequency change, an experimental scheme, a nuclear spin maser with an active feedback was developed.[3–5] The spin maser enables the elongation of the spin coherence time to an infinitely long duration, and thus, the statistical sensitivity can be improved rapidly with time compared to repeated short measurements. In addition, in order to eliminate the effect of the drift in the magnetic field, the ^{131}Xe spin maser was introduced as a reference system (co-magnetometer). For this purpose, ^{3}He is often used[2] as its small EDM compared to that of Xe due to the small atomic number is suitable for the reference atom. However, there remains a difficulty due to the difference in the magnitudes of the frequency shifts caused by the contact interaction with polarized Rb atoms. This limitation can be eased by using ^{131}Xe. Since the magnitude of the polarized Rb interaction is almost the same between ^{129}Xe and ^{131}Xe,[6] the systematic errors arising from the polarized Rb interaction will be reduced dramatically.

The operation of the co-existing ^{129}Xe and ^{131}Xe masers with the active feedback scheme was realized for the first time, as shown in Fig. 1. By taking the frequency difference between the ^{129}Xe and ^{131}Xe masers, the dependence of the frequency on the cell temperature, which virtually limits the measurement sensitivity in our ^{129}Xe/^{3}He masers, was mitigated significantly in the ^{129}Xe/^{131}Xe case. The study on the optimization of the maser operation is ongoing. We expect that further improvement in the maser stability can be achieved by increasing the magnitude of the polarization and elongating the spin coherence times for ^{129}Xe and ^{131}Xe.

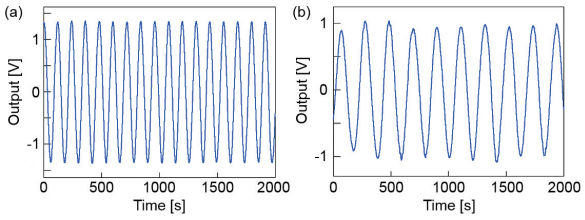

Fig. 1. Maser signals obtained for (a) ^{129}Xe and (b) ^{131}Xe. Beat signals from the lock-in amplifiers which were employed to improve the signal-to-noise ratio were observed at the reference frequency of 33.036 Hz for ^{129}Xe and 9.797 Hz for ^{131}Xe.

*1 RIKEN Nishina Center
*2 Department of Physics, Tokyo Institute of Technology
*3 FRIS, Tohoku University
*4 CYRIC, Tohoku University
*5 Department of Physics, Kyungpook National University
*6 Department of Physics, Tokyo Metropolitan University
*7 RIIS, Okayama University
*8 Department of Physics, University of Winnipeg
*9 Institute of Material Structure Science, KEK
*10 Department of Advanced Sciences, Hosei University
*11 RCNP, Osaka University
*12 Department of Physics, Saitama University
*13 CNS, University of Tokyo

References

1) T. Chupp and M. Ramsey-Musolf: Phys. Rev. C **91**, 035502 (2014).
2) M. A. Rosenberry and T. E. Chupp: Phys. Rev. Lett. **86**, 22 (2001).
3) A. Yoshimi et al.: Phys. Lett. A **304**, 13 (2002).
4) A. Yoshimi et al.: Phys. Lett. A **376**, 1924 (2012).
5) T. Inoue et al.: Eur. Phys. J. D **70**, 129 (2016).
6) M. Bulatowicz et al.: Phys. Rev. Lett. **111**, 102001 (2013).

Towards two-neutron transfer reactions with a tritium target: Characterization of a prototype $TiD_{0.24}$ target

T. Koiwai,[*1] T. Kumon,[*1] Y. Shimizu,[*1] N. Imai,[*2] M. Niikura,[*1] K. Wimmer,[*1] and Y. Hatano[*3]

Two-nucleon transfer reactions are well-suited to investigate specific nuclear structure properties, like shape coexistence and pairing correlations. In particular neutron-adding reactions are of great interest because they can populate very exotic systems. The large neutron excess combined with the rather simple structure of the tritium nucleus makes it an ideal probe or target nucleus for two-neutron pair transfer reactions. With radioactive ion beams two-neutron transfer reactions have to be performed in inverse kinematics and therefore a radioactive tritium target is required. After pioneering work at REX-ISOLDE,[1,2] tritium targets are now also available at ATLAS at Argonne National Laboratory and TRIUMF's ISAC II facility. Transfer reactions are best performed at beam energies close to the Coulomb barrier. At RIBF, the full potential of this spectroscopic tool will be exploited with the completion of the OEDO facility.[3] Here, the high-intensity radioactive beam produced by projectile fragmentation and in-flight fission will be slowed down in a degrader. Re-bunching and focusing devices are used to restore the beam quality. The challenge in building a radioactive tritium target for RIBF is twofold. First the size of the target has to be sufficiently large. At RIBF, typical beam spot sizes are approximately 2 cm in FWHM, in stark contrast to the values of approximately 1 mm that are achieved through post-acceleration at ISOL facilities. In order to perform two-neutron transfer reactions at RIBF a tritium target with an area of 2.5 x 2.5 cm^2 is required. Secondly, the effective thickness of the tritium target material has to be sufficient to achieve reasonable luminosities for experiments with radioactive beams at RIBF. The target thickness has to result in a total activity below the limit of 10 TBq, but it also has to be suitable for a wide variety of experiments with different physics goals as well as beam energies. The approach used for RIBF is the loading of a titanium foil with hydrogen. Theoretically a hydrogen to titanium ratio H:Ti = 2:1 can be reached. However the large amount of hydrogen critically affects the mechanical stability.[4] This is a challenge for the construction of a large-area tritium target. In order to establish a production and handling method for a tritium target, prototypes containing non-radioactive deuterium instead of tritium are used.

At the Hydrogen Isotope Research Center at Toyama University a deuterated target with an intended ratio of D:Ti = 0.24:1 has been produced, the thickness of which is 20 μm Ti before loading. In order to characterize the properties of the target, and in-beam experiment has been performed.

*1 Department of Physics, University of Tokyo
*2 Center for Nuclear Study, University of Tokyo
*3 Hydrogen Isotope Science Center, Toyama University

The goal of the experiment was to (i) independently determine the deuteron content of the target, (ii) examine the behavior under high beam current, and (iii) investigate other possible types of radioactive contamination of the target due to fusion reactions of the Ti carrier material. The experiment was performed at the E7b beam line. A ^{20}Ne beam at an energy of 8.2 MeV/u was irradiated on the TiD target. Elastically scattered deuterons were detected in three pin diodes in the forward direction. In the backward direction an array of Si strip detectors was placed to detect protons from (d,p) transfer reactions.

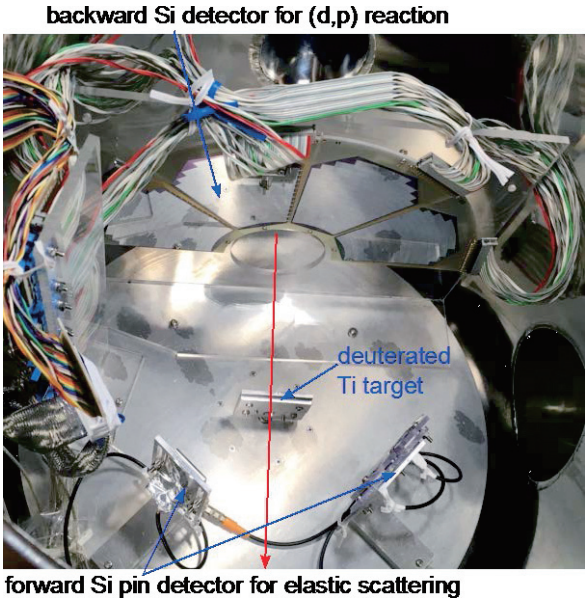

At the end of the beam line, the unreacted beam was impinged on two additional Ti foils to investigate the background that could be created by fusion reactions on the Ti material. In order to establish a limit on the beam current that might cause the release of hydrogen from the Ti material, the mass distribution of the residual gas was monitored in a quadrupole mass spectrometer. The beam intensity was varied from 5 pnA to 200 pnA. Up to 20 pnA (1.3 $x10^{11}$ pps) the partial pressure of A/q =2 was stable at background level. At higher currents the release of deuterium from the target was observed.

The analysis of the scattering as well as the activation data is ongoing. New prototype targets with different D:Ti loading ratios are being produced. The production of the final tritium target is envisioned for 2018.

References

1) K. Wimmer et al., Phys. Rev. Lett. **105** 252501 (2010).
2) K. Nowak et al., Phys. Rev. C **93** 044335 (2016).
3) S. Shimoura, Letter of Intent for OEDO project, the 14th NPPAC for nuclear physics experiment at RIBF, June 2014.
4) I. Lewkowicz, Solid State Phenomena, **49-50** 239 (1996).

Isotope identification in nuclear emulsion plate for double-hypernuclear study (isotope track-angle dependence)

R. Murai,[*1] S. Kinbara,[*1] H. Ekawa,[*2] T. Fujita,[*3] S. Hayakawa,[*4] S. H. Hwang,[*5] Y. Ichikawa,[*3] K. Imamura,[*3] H. Itoh.[*1] H. Kobayashi,[*1] M. K. Soe,[*1] A. Takamine,[*3] A. M. M. Theint,[*1] H. Ueno,[*3] J. Yoshida,[*1] and K. Nakazawa[*1]

Double-Λ and Ξ hypernuclei, so-called double hyper nuclei, are quite important sources to understand baryon- baryon interaction in a unified manner under SU(3)*f* symmetry. Although the Nagara event [1,2] and the Kiso event [3] were the uniquely identified samples for the sequential decay of the double-Λ and Ξ hypernucleus, respectively, knowledge from them has thus far been limited. To systematically study double-strangeness nuclear physics, it is necessary to detect as many uniquely identified double hypernuclei as possible in the emulsion. Therefore, we are going to develop a method for the identification of daughter nuclei from the decay of double hypernuclei by measuring their ionization losses from the viewpoint of track width under a microscope. However, the widths can be changed by the defocusing halo image, which will depend on the track angle in the emulsion, even for the same nucleus. In this report, we will present a preliminary result on the angle dependence of track widths.

Nuclear emulsion sheets (3 × 7 cm^2) were irradiated by 8 nuclear species with charges from one to five, which were ^{1}H, ^{2}H, ^{3}H, ^{3}He, ^{4}He, ^{7}Li, ^{9}Be, and ^{11}B, at RIPS (NP1406-RRC32). Carbon (^{12}C) at 68 MeV/nucleon and 10 pnA was incident on a ^{9}Be target with 0.5-mm thickness. To nominate the secondary nuclides, we utilized wedge-shaped degraders of 962 and 426 mg/cm^2 and iron and/or aluminum plates in front of the emulsion stack. The stacks consist of 6 emulsion sheets, where the sheet size is 30 (*x*) × 70 (*y*) × 1 (*z*) mm^3. The z-direction was at angles (θ) of 0°, 25°, 50°, and 75° with respect to the beam direction (z'). To understand the angle-dependent effect for the width, the stack exposed by ^{1}H was studied.

To measure track widths, we developed a method for image processing with the help of OpenCV24-11. Firstly, we produced a track image consisting of the most focused points in sliced track images taken by moving a 100× objective lens with an 8-bits CCD camera at a pitch of 0.1 μm along the optical axis (z). In Fig. 1 (a), a sliced image is presented. To obtain the most focused point of the track, we applied a Gaussian function for the track illumination of the image along the z direction and obtained the minimum sigma value by fitting with a quadratic function in sigma data, as shown in Fig. 1(b). By summing up those images, the most focused image of a track can be obtained as shown in Fig. 1(c).

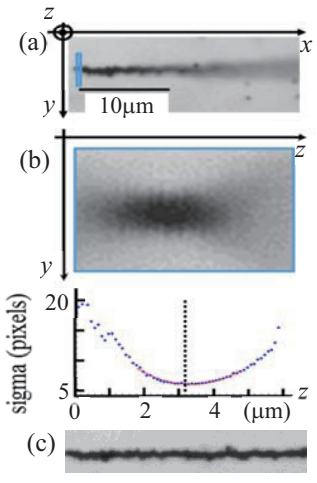

Fig. 1. Process for producing a focused image of the track.

Secondly, we measured the widths along the track as follows. A Gaussian operator is applied to the contrast-enhanced image of Fig.1 (c) to obtain a blurred image with a kernel size of 47 × 47 pixels, where the size of one pixel is 0.080(x) × 0.080(y) μm^2. Each of those images is shown in Fig. 2(a) and (b), respectively. To obtain a uniform background, we produce the image shown in Fig.2 (c) by subtracting Fig. 2(a) from (b). We apply the function $F(x) = A\cdot\tanh(\mathrm{Gauss}(x,\mu,s))$ for the brightness of Fig. 2(c) in each pixel line vertically along the x direction. The width can be obtained as the distance between inflection points of the applied function, as shown in Fig. 2(d).

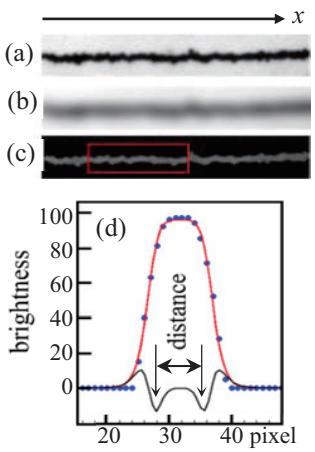

Fig. 2 Process for obtaining track width.

Finally, we set a window with 2-μm range along the track and acquire the minimum track width, so-called *minimum tracking*, to avoid accidental grains associated with the track. The window is shifted by 1 pixel in the range of 10 to 100 μm from the stopping point, and a sample of measured widths is shown in Fig. 3 for the area shown in the box of Fig. 2(c). The dotted line and the solid line are the widths based on the distance between inflection points and for minimum tracking, respectively.

Assuming the track is constructed by many cylinders with the diameter of the width given by the minimum tracking, we obtain the track volume by summing such cylinders. The measured result for track volumes is shown in Fig. 4, for ^{1}H with θ = 0°, 25°, 50°, and 75°. As a preliminary result, we obtained a clear angle dependence (log(1/sinθ)) of the track volume measured by our microscope. In the near future, this work should be applied for other nuclides, and the method for their identification with angle dependence will be published.

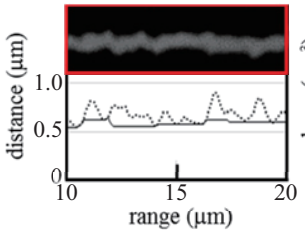

Fig. 3. Minimum tracking.

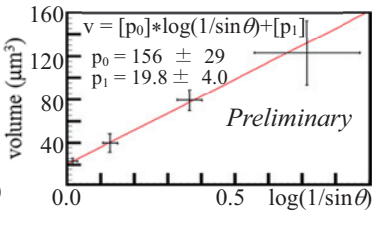

Fig. 4. Angle dependence of volume.

*1 Physics Department, Gifu University
*2 Department of Physics, Kyoto University
*3 RIKEN Nishina Center
*4 Department of Physics, Osaka University
*5 Japan Atomic Energy Research Institute

References
1) H. Takahashi et al., Phys. Rev. Lett. **87**, 212502 (2001).
2) J. K. Ahn et al., Phys. Rev. C **88**, 014003 (2013).
3) K. Nakazawa et al., Prog. Theor. Exp. Phys., 033D02. (2015).

Measurement of the activation of helium gas stripper by ^{238}U beam irradiation at 11 A MeV

A. Akashio,[*1] K. Tanaka,[*1] H. Imao,[*1] and Y. Uwamino[*1]

The activation of the helium gas stripper setup[1] for uranium beam was evaluated. At RIBF, a charge stripper of helium gas has been applied for the uranium beam as a substitute for one of solid material to avoid the limited lifetime of solid material charge stripper[1]. However, the residual dose around the setup is a serious problem for maintenance. Radiation properties such as the strong source point and lifetime of radioactive nuclei were obtained in this study. The activation around the gas stripper setup was measured using activation samples. The activation was evaluated using the PHITS Monte-Carlo simulation code[2] and the result was compared with the measured one.

A uranium beam with an energy of 10.75 MeV/u and intensity of 0.86 particle μA irradiated and passed through the helium gas cell. The helium-gas pressure in the region of highest pressure was 7 kPa, and the thickness of the helium layer was about 500 mm, which corresponds to 0.7 mg/cm^2. The helium gas was irradiated with 5.4×10^{18} uranium ions (20% accuracy) during about 18 days of the operation of the accelerator in 2015.

The activation samples were located inside the gas stripper chamber. The aluminum and bismuth samples were 10 × 10 mm in size and 1 mm thick. Figure 1 shows the setup of the helium stripper by PHITS. The distance of the samples from the beam axis was 47.25 mm. After the beam irradiation on the helium gas, the γ-rays from the samples were measured using a Ge detector after about three months of cooling. In addition, the several source RIs in the samples were identified and the number of RI nuclei were counted. The identified nuclei are listed in Table 1.

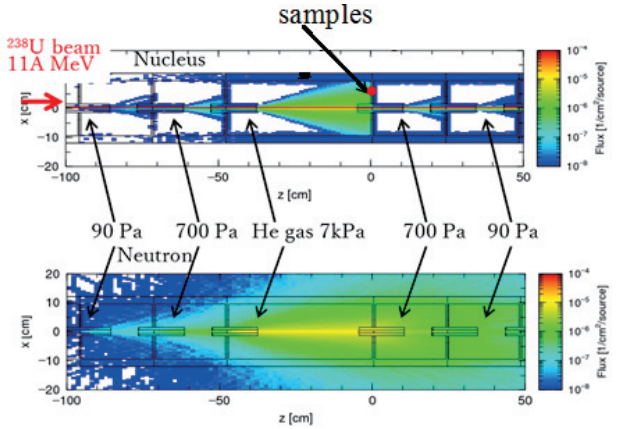

Fig.1 Flux of the nuclei (upper) and neutrons (lower) calculated by PHITS.

The calculation was performed using PHITS ver. 2.76[1] for the geometry shown in Fig. 1, which shows the flux of the generated nuclei and neutrons. The fission products were generated from uranium beam nuclei. Part of the fission products reached and were stopped at the samples. The number of generated RIs at the samples were counted and compared with the observed number of RIs. Figure 2 shows the preliminary ratios of the number of nuclei calculated by PHITS to the observed number of nuclei at the samples. The errors in the plots arise mainly from the statistics of the γ-ray and PHITS calculations and the 20% accuracy of the beam intensity. The PHITS result for the fission products of uranium beam irradiation on helium gas reproduced well the observed nuclei. These nuclides mainly concentrate the downward interior of the helium stripper chamber.

Table 1. Identified nuclei of fission products in the aluminum sample after about three months of cooling.

Nuclide	Half-life	Nuclide	Half-life
^{91}Y	58.5 day	^{134}Cs	2.06 year
^{95}Zr	64.0 day	^{137}Cs	30.1 year
^{103}Ru	39.3 day	^{141}Ce	32.5 day
^{106}Ru	371 day	^{144}Ce	285 day
^{124}Sb	60.2 day	^{155}Eu	4.75 year
^{125}Sb	2.76 year		

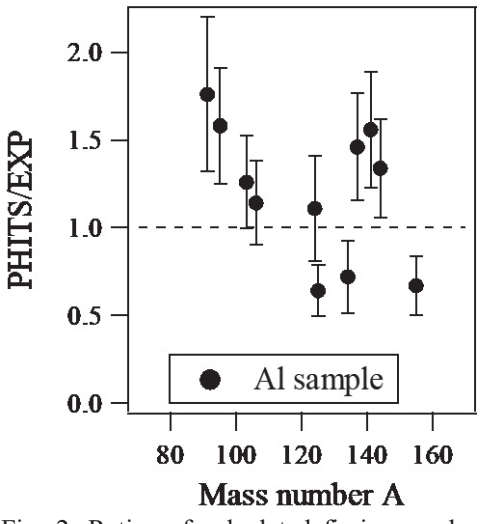

Fig. 2. Ratios of calculated fission products to the observed fission products.

References

1) H. Imao et al. Proc. of IPAC2013, Shanghai, China, May 2013 THPWO038, p.3851 (2013).
2) D. Sato et al., Nucl. Inst. Meth. A, **583**, 507 (2007).

*1 RIKEN Nishina Center

Radiation evaluation for RILAC irradiation room

K. Tanaka,[*1] A. Akasiho,[*1] H. Sakamoto,[*1] H. Mukai,[*1] R. Suzuki,[*1] H. Haba,[*1] K. Morimoto,[*1] S. Yanou,[*1] D. Kaji,[*1] and Y. Uwamino[*1]

The radiation doses at and around the irradiation room at RILAC facility were measured and evaluated. The permitted maximum intensity is 10 particle μA at 7.0 MeV/nucleon. The maximum energy in the room is 7.5 MeV/nucleon at which the permitted intensity reduced to 5 particle μA. Monte-Carlo simulations, such as PHITS[1)], are often applied for radiation evaluations. However, their accuracy would not be good at these energies in general. Therefore, we measured the neutron dose rates using an ^{18}O beam at 6.8 MeV/nucleon. The ^{18}O beam can provide a higher neutron dose than other beam nuclides in this room. Three types of measurements were performed. Firstly, neutron dose rates near the radiation sources were measured using several target materials. Secondly, the neutron dose rates inside and outside the radiation shield wall of the irradiation room were measured. Thirdly, the high-energy neutron flux was measured using bismuth samples.

The neutron dose from thick targets of aluminum, carbon, copper, and tantalum were measured using a neutron survey meter at GARIS-II. Table 1 lists the preliminary result of measured and calculated dose at a 90 degree direction of beam axis and a beam intensity of 5 particle μA. A TPC-451C neutron survey meter (HITACHI Co Ltd.) was located on the top of the target chamber. Its distance from the beam axis was 31 cm. The width and height of the targets were 25 mm and 25 mm commonly, and the thicknesses are listed in Table 1. Another neutron survey meter is located in the beam direction immediately after the GARIS-II D1 magnet. The beam stopped in the thick targets and then only the neutrons from the targets irradiated the survey meter. Because the neutron scattering at the magnet affects the dose measurement, the analysis of beam direction is ongoing.

Table 1. Measured neutron dose rates and comparison with values calculated using by PHITS code

Target and thickness	measured dose (mSv/h)	PHITS result (mSv/h)	ratio PHITS/measurement
C 150μm	3300	6100	1.8
Al 200μm	3100	5500	1.8
Cu 50μm	2500	4400	1.8
Ta 100 μm	1600	1900	1.2

The distribution of neutron dose rates in and around the shield wall of the irradiation room were measured. The ^{18}O beam irradiated the tantalum beam dump of GARIS and GARIS-II individually. Figure 1 and 2 show measured dose results on the top view of the experimental room. The maximum doses on the roof and basement are also shown. The neutron dose outside the shield wall was less than about 1/1000 of inside dose.

The evaluation for bismuth samples is ongoing.

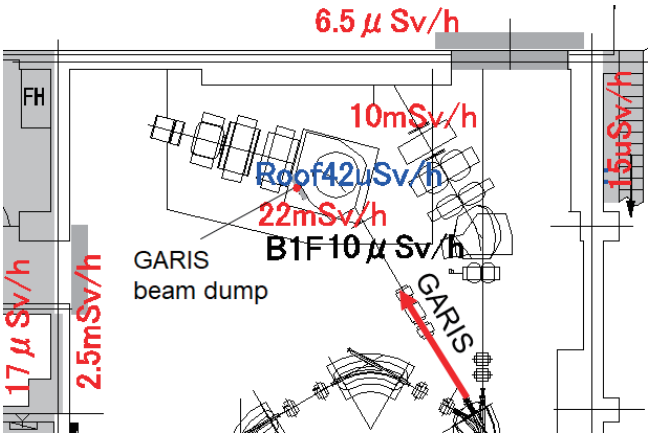

Fig. 1. Measured result for neutron dose rate from the GARIS beam dump. The red values show the dose rates at the beam level of GARIS which was at the first floor. The blue value indicates the maximum measured dose on the roof and the black value indicates that on the first basement level.

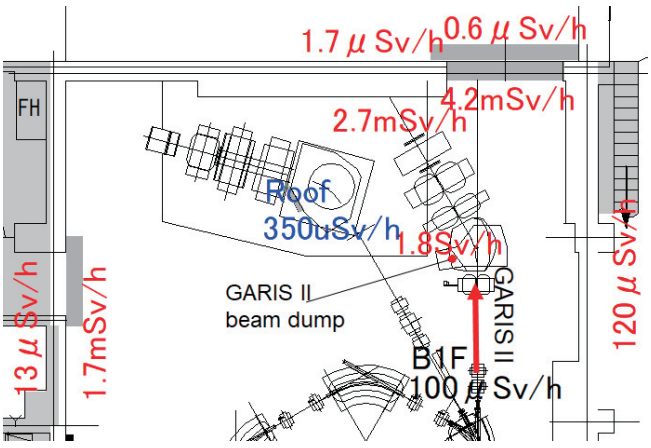

Fig. 2. Measured results for neutron dose rate from the GARISII beam dump.The legendisthe same as for Fig. 1.

Reference

1) T. Sato et al., J. Nucl. Sci. Technol. **50**, 913 (2013).

*1 RIKEN Nishina Center

Status report on the developement of the high-resolution missing-mass spectroscopy for the (p,2p) reaction in inverse kinematics

S. Reichert,[*1,*2] M. Sako,[*2] M. Sasano,[*2] R. Gernhäuser,[*1] H. Baba,[*2] C. Berner,[*1] M. Böhmer,[*1] N. Chiga,[*2] W. F. Henning,[*4] T. Kobayashi,[*2,*5] Y. Kubota,[*2,*6] R. Lang,[*1] L. Maier,[*1] D. Mücher,[*3] V. Panin,[*2] L. Stuhl,[*2] E. Takada,[*7] T. Uesaka,[*2] L. Werner, [*1] and J. Yasuda[*2,*8]

A new detector setup for high-resolution missing-mass measurements was tested at the HIMAC facility in February 2016 with the reaction ^{16}O$(p, 2p)^{15}$N in inverse kinematics at E = 290 MeV/nucleon and with a beam intensity of 10^5 pps. The concept is a detector setup having two arms each to measure the momentum vector of a proton emitted from the (p,2p) reaction. Each arm consists of three layers of single-sided 100 μm thick silicon detectors featuring a strip pitch of 100 μm. Two arrays of 9 scintillator rods for TOF mounted at a distance of 2 m outside the vacuum chamber for the target and silicon trackers complete each arm. Measuring the light particle's velocity $|\vec{v}|$ and their directions $\vec{v}/|\vec{v}|$, the missing-mass in a quasi-free scattering kinematic is defined rather well. Downstream in the beam-line, a $dE-dE$ detector measures the remaining heavy residues and therefore, one is even able to determine the exclusive excitation function. In the experiment, background especially arises from inelastic $(p, 2p)$ reactions in the CH_2 target. For a detailed description of the setup, see[1].

The major goal for the test experiment at HIMAC was to prove the capability of the setup to reach a resolution of $\sigma_{E_X} \sim 1$ MeV for the excitation energy. Achieving such a high excitation energy resolution is a major prerequisite for studying fission barrier heights induced by the $(p, 2p)$ reaction in future experiments at RIBF/RIKEN.[2]

Preliminary results for the resolution are for an opening angle of 3.2 mrad (σ_{open}) and for an energy of 3.3% (σ_{ENY}). They are slightly greater than the targeted values of 3.0 mrad (σ_{open}) and 2.5% (σ_{ENY}), respectively. The opening angle depends strongly on the inner-target multiple scattering. Therefore, 125-μm-thick target foils and vertical fiber targets (D = 150 μm) were accurately positioned to evaluate the vertex-position reconstruction performance of the silicon trackers. Geant4 simulations predict a vertex resolution of $\sigma_{pos} = 165$ μm. In the experiment we could reconstruct reactions in the fibers with a precision of $\sigma_{pos} = 175\,\mu$m[3].

As a result of the quasi-free knockout reaction ^{16}O$(p, 2p)^{15}$N, we were able to demonstrate the missing-mass spectroscopy based on our setup by reconstructing kinetic curves for the ground state and the excited states at 6.3 MeV and 9.9 MeV with an uncertainty better than $\sigma = 1.7$ MeV, as shown in Fig. 1.

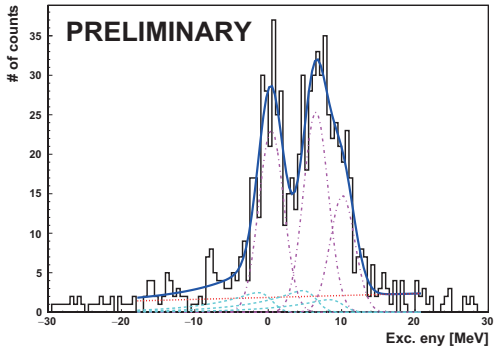

Fig. 1. Distribution of the excitation energies in ^{15}N, reconstructed from the missing-mass spectroscopy. Data are compared to a superposition of the three most prominent states and a constant background (red dotted line). Signal shapes were empirically fit by a gaussian (purple dotted) and a left tail (blue dotted).

The differential cross sections $d\sigma/dE_X$ are listed in Table 1 and so far do not match with the ratio of the spectroscopic factors in $(e, e'p')$ reactions in[4].

Table 1. Comparison between preliminary diff. CS $d\sigma/dE_X$ and spectroscopic factors for the first discrete peaks

E_x (MeV)	J^π	CS Exp. (mbarn)	S_α Ref.[4]
0.00	$\frac{1}{2}^-$	4.6±1	1.260(13)
6.32	$\frac{3}{2}^-$	5.2±1	2.348(19)
9.93	$\frac{3}{2}^-$	3.1±1	0.133(15)

The next step is the replacement of the first layer with new 50 μm silicon wafers to reduce multiple scattering and to improve the resolution of the missing-mass.

*1 Department of Physics, Technical University Munich
*2 RIKEN Nishina Center
*3 Department of Physics, University of Guelph
*4 ANL
*5 Department of Physics, Tohoku University
*6 Center for Nuclear Studies, University of Tokyo
*7 NIRS
*8 Department of Physics, Kyushu University

References

1) S. Reichert, M. Sako et al.: RIKEN Accel. Prog. Rep. 48, 47 (2015).
2) D. Mücher, M. Sasano et al.: RIBF NP-PAC-12 (2013).
3) L. Werner, Master's Thesis, *A silicon tracker system for (p,2p) reactions*, TU Munich (2016).
4) M. Leuschner et al.: Phys. Rev. C, 49,955 (1994).

Preparation status of the J-PARC E16 experiment in 2016

S. Yokkaichi*1 for the J-PARC E16 Collaboration

We have proposed the experiment E16[1] to measure the vector meson decays in nuclei in order to investigate the chiral symmetry restoration in dense nuclear matter. The experiment will be performed at the J-PARC Hadron Experimental Facility. Scientific ("stage 1") approval was granted to the experiment E16 by PAC in March 2007. For the full approval, we were required to demonstrate the experimental feasibility and show the prospects of acquiring sufficient funds and of beam-line construction. Toward the full approval, the technical design report was submitted to PAC in May 2014, and the revision was performed twice, as per the requirements of PAC. The most recent revision has been submitted to PAC in Jan. 2017.

The aim of the experiment is to perform to systematically study the spectral modification of vector mesons, particularly the ϕ meson, in nuclei by using the e^+e^- decay channel with statistics that are two orders larger in magnitude than those of the precedent E325[2] experiment performed at KEK–PS. In other words, the aim is to accumulate 1×10^5 to 2×10^5 events for each nuclear target (H, C, Cu, and Pb) and to deduce the dependence of the modification on the matter size and the meson momentum. At the same time, the e^+e^- decays of the ρ, ω, and J/ψ mesons can be measured, while the yields depend on the trigger condition required to suppress the background e^+e^- pairs.

In order to increase the statistics by a factor of 100, we plan to use a 30-GeV primary proton beam with 1×10^{10} particle per spill (2-s duration and 5.52-s cycle) of in the high-momentum beam line and 0.2%-interaction targets, which brings a background particle rate of 5 kHz/mm^2 at the most forward region of the trackers. In order to cope with such a high rate, the GEM tracker has been adopted. [a]

The construction of the high-momentum beam line, where we will perform the experiment, was started in JFY 2013 by KEK and scheduled for completion in JFY 2015. However, the construction has been delayed owing to a radiation accident at J-PARC in May 2013 and the budgetary limitation partly caused by the accident. The current target date of the first beam is Mar. 2019 in the most optimistic scenario. While such a tight budgetary situation, the spectrometer magnet reconstruction was completed in JFY 2015 by KEK.

Our spectrometer has 26 modules. Owing to the budget limitations, our first goal of the staged construction plan is to construct eight modules, which covers approximately one third of the full acceptance.

The development of the detectors was completed, and we have been in the production phase since 2013. For the GEM Tracker (GTR),[3] the production of GEM and the read-out strip board has been underway since 2013. Parts for six modules (out of eight, as mentioned above) have been completed. The CFRP frames, which are used to install the GEM chambers in the spectrometer, have also been made for two modules. For the HBD,[4] which is one of our electron ID detectors, two modules are currently under construction at RIKEN. The read-out electronics including preamplifier for the two GEM detectors, GTR and HBD, have also been purchased, for six and two modules, respectively. They use an APV25 chip and SRS, both of which are CERN-made. We joined the RD51[5] collaboration in CERN which aims to develop multi-pixel gas detectors including GEM.

The lead-glass (LG) EM Calorimeter, another electron ID detector, utilizes the recycled LG from the TOPAZ experiment. The reshaping of LG blocks for eight modules (330 blocks) was completed at the KEK engineering center. Electronics for two modules has been purchased, and it uses the DRS4 chip.[6]

The development of trigger electronics is still underway.[7] The trigger signal for vector mesons consists of two electron candidates. An electron candidate is defined by the coincidence of corresponding hits in LG, HBD, and the outermost layer of GTR, located immidiately in front of HBD. ASICs for the amp-shaper-discriminator to generate the trigger primitive of the two GEM detectors have been produced in cooperation with the KEK e-sys group. To generate a global trigger signal, an FPGA board "UT3"(developed by Belle II) is used. To transfer the trigger primitives to UT3, we developed another module called "TRG-MRG." The development of firmware for these modules is underway, and a system test connecting all the modules with detectors is planned for the end of JFY 2017.

*1 RIKEN Nishina Center

a) At the COMPASS experiment, the GEM tracker was operated at a particle rate of 25 kHz/mm^2.[8]

References

1) S. Yokkaichi et al., J-PARC proposal No. 16 (`http://j-parc.jp/researcher/Hadron/en/pac_0606/pdf/p16-Yokkaichi_2.pdf`), Y. Morino et al., JPS Conf. Proc. **8**, 022009 (2015).
2) R. Muto et al., Phys. Rev. Lett. **98**, 042501 (2007).
3) W. Nakai et al., RIKEN Accel. Prog. Rep. **49**, 195 (2015).
4) K. Kanno et al., Nucl. Instrum. Meth. A **819**, 20-24 (2016).
5) `http://rd51-public.web.cern.ch/RD51-Public/`
6) `https://www.psi.ch/drs/drs-chip/`
7) T. N. Takahashi et al., J. Phys.: Conf. Ser. (JPCS) **664**, 082053 (2015).
8) B. Ketzer et al., Nucl. Instrum. Meth. A **535** 314-318 (2004).

Hadron blind detector using a finely segmented pad readout†

K. Kanno*1,*2 for the J-PARC E16 Collaboration

We developed a hadron blind detector (HBD) using a finely segmented pad readout for the J-PARC E16 experiment.[1] The HBD is a Cherenkov detector that does not require mirrors or transparent windows.[2] Our HBD is used to identify electrons and to reject pions in the momentum region of 0.4–3.0 GeV/c. The finely segmented pad readout enabled us to perform an advanced analysis using the number of signal-detecting pads in addition to the usual analysis with the total amount of collected charge. With this advanced analysis method, the pion rejection factor is increased while keeping the electron detection efficiency.

Our HBD consists of a 50-cm-long CF_4 radiator, a mesh electrode, a CsI photocathode, three layers of GEM foils and a pad readout. The mesh and three layers of GEM foils are stacked together onto the readout pad. The CsI photocathode is evaporated on the top surface of the top GEM foil to detect Cherenkov photons and convert them into photoelectrons. An incident electron emits Cherenkov photons, whereas an incident pion does not in the momentum region of interest. Thus, a pion can induce a signal only through the ionization electrons. However, this signal is greatly suppressed by controlling the electric field of the gap between the mesh and the top GEM foil such that the ionization electrons produced in the gap are swept into the mesh. The pad readout consists of 25 square pads. The size of each pad is 10×10 mm^2. This size is smaller than that of the circular image of the Cherenkov photons, which is 34 mm in diameter in our HBD. Thus, an incident electron is expected to induce multiple signal-detecting pads, whereas an incident pion is expected to leave no signal-detecting pad. The pion rejection factor is expected to be improved by applying a threshold on the size of a charge cluster. This analysis method is called cluster size analysis.

To measure the responses of the detector to electrons and pions, we performed a beam test at J-PARC K1.1BR with a negatively charged secondary beam at 1.0 GeV/c containing approximately 20% electrons. A signal-detecting pad was defined as a pad with the induced charge larger than that of the pedestal by 7σ, corresponding to 0.22 e. The cluster size is defined as the number of neighboring signal-detecting pads. Two pads which share at least a corner are considered as neighbors. Our HBD was operated under a reverse bias of 5 V/mm. The mean primary charge for incident electrons and pions is 7.3 e and 0.7 e, respectively.

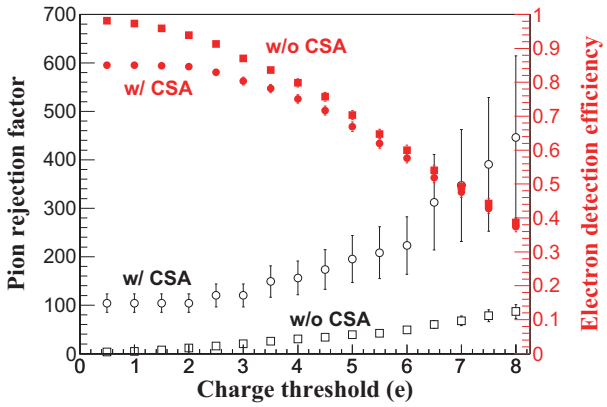

Fig. 1. Electron detection efficiency and pion rejection factor with and without the cluster analysis as a function of the threshold on the primary charge. The notation "CSA" represents the cluster size analysis. The open and closed symbols represent the pion rejection factor and electron detection efficiency, respectively.

This mean primary charge for incident electrons was consistent with the expected result calculated based on the performance of each detector element including the quantum efficiency of the CsI photocathode. Thus, the primary charge induced by an incident electron was considered to be due to photoelectrons. The mean cluster size for incident electrons and pions was 4.3 pads and 0.5 pads, respectively. An electron had a larger cluster size than a pion.

We calculated the electron detection efficiency and the pion rejection factor with and without the cluster size analysis as shown in Fig. 1. We achieved an electron detection efficiency of 83% with a pion rejection factor of 120 when we applied a threshold of 2.5 e on the primary charge and required a cluster size of three or more. The pion rejection factor with the cluster size analysis was improved by a factor of approximately five.

Based on this result, we constructed a production model of the HBD for the J-PARC E16 experiment with hexagonal pads with a side length of 10 mm. The pion rejection factor of the HBD was evaluated as 160 with a simulation, which satisfies the requirement of the experiment.

† Condensed from the article in Nucl. Instr. and Meth. A **819**, 20 (2016)
*1 Department of Physics, Graduate School of Science, The University of Tokyo
*2 RIKEN Nishina Center

References

1) S. Yokkaichi et al.: In this report.
2) W. Anderson et al., Nucl. Instr. and Meth. A **646**, 35 (2011).

Expected energy resolution and its trigger dependence for very forward neutron measurements in $\sqrt{s} = 510$ GeV polarized proton-proton collisions at the RHICf experiment

M. H. Kim[*1,*2] for the RHICf collaboration

The single spin asymmetry, A_N, of very forward neutrons in polarized proton-proton collisions plays an important role in the study of the production mechanism of very forward neutrons, particularly diffractive and non-diffractive interactions. A_N is a left-right asymmetry,

$$A_N = \frac{d\sigma^{\uparrow} - d\sigma^{\downarrow}}{d\sigma^{\uparrow} + d\sigma^{\downarrow}} \quad (1)$$

for yields observed with proton polarization, where $d\sigma^{\uparrow}(d\sigma^{\downarrow})$ is the production cross section when the protons are polarized up (down). To measure the A_N of very forward neutrons precisely, an electromagnetic calorimeter was installed in front of the ZDC hadron calorimeter[1] at the STAR experiment to improve the limited position resolution of ZDC ($\sim$ 1 cm). This detector was originally developed for the LHCf experiment[2] at CERN and will be called the RHICf detector[3] hereafter. RHICf is not designed to provide good energy resolution to neutrons with an interaction length of 1.6 λ. However, its energy resolution can be well recovered by compensating for the shower leakage of RHICf caused by ZDC, the interaction length of which is 2 λ. Here, we report the result of a Monte-Carlo (MC) study of the expected performance of neutron energy measurement when both RHICf and ZDC are used together as well as its trigger dependence with respect to the threshold energy.

In the MC study, 10^6 neutrons with energies of 100, 150, 200, 250, and 350 GeV were generated as it passed through the center point of the first GSO plate and their energies were reconstructed using the correlation between energy to energy deposit (edep) sum of RHICf and the total number of photoelectrons (Npe) of ZDC. Energy resolution was evaluated in the following three cases: 1) RHICf only, 2) ZDC only, and 3) the combined system.

Simulation results for the threshold energy dependence of neutron energy resolution and the ratio of the selected to the total events at 250 GeV are shown in Fig. 1 (a). A higher threshold energy results in lower trigger efficiency and better energy resolution. The red dashed line indicates the intrinsic ZDC resolution (18.2%). The energy resolution becomes as good as the intrinsic resolution of ZDC even though the shower leakage of RHICf is measured by ZDC and combined later.

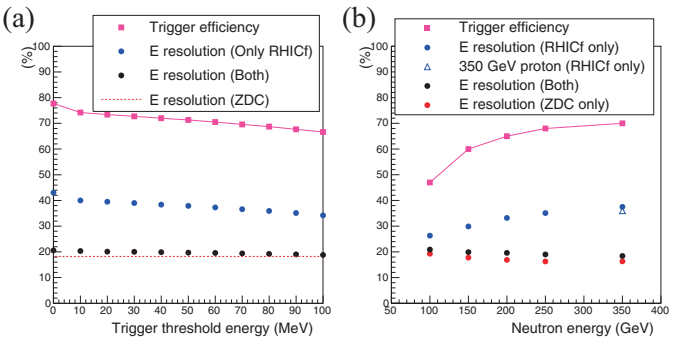

Fig. 1. (a) Trigger-threshold-energy dependence of the expected neutron energy resolution and the trigger efficiency. (b) Incident-neutron-energy dependence at a trigger threshold energy of 90.6 MeV.

The energy resolution at different neutron energies is plotted in Fig. 1 (b). The threshold energy of the trigger was set at 90.6 MeV in order to compare with a previous LHCf test result of 350-GeV protons shown as a blue open triangle. However, it will be optimized later for only the RHICf experiment. The MC prediction, 37.5 %, for 350-GeV neutrons shows good consistency with the LHCf result, 36.0 %, within statistical error. A better energy resolution is obtained with a lower neutron energy because the same threshold energy was applied to the trigger. When only ZDC is used, the resolution at 100 GeV also shows good agreement with a previous experimental result for polarized pp collision at $\sqrt{s} = 200$ GeV.[4] Finally, because the simulation result corresponds with experimental results in both the 1) RHICf only and 2) ZDC only cases, for neutrons with an energy of 100-250 GeV in the RHICf experiment, we expect an energy resolution of approximately 20% with a threshold of 90.6 MeV when both detectors are used.

References

1) C. Adler et al., Nucl. Instrum. Meth. A**470**, 488 (2001).
2) Y. Itow, H. Menjo, T. Sako, N. Sakurai et al., arXiv:1409.4860 [physics.ins-det].
3) K. Kawade et al., arXiv:1312.5950v1 [physics.ins-det].
4) A. Adare et al., Phys. Rev. D **88**, 032006 (2013).

*1 RIKEN Nishina Center
*2 Department of Physics, Korea University

Sensor module prototype for Silicon INTT for sPHENIX

Y. Akiba,[*1] T. Hachiya,[*1] Y. Kawashima,[*1*2] E. Mannel,[*3] H. Masuda,[*1*2] G. Mitsuka,[*1] I. Nakagawa,[*1] D. Nemoto,[*1*2] R. Nouicer,[*3] and Y. Yamaguchi[*1]

We are developing a new silicon intermediate tracker INTT[1,2] for sPHENIX, a new experiment at the Relativistic Heavy Ion Collider at Brookhaven National Laboratory. In this article we report on the research and development of the silicon module of the INTT.

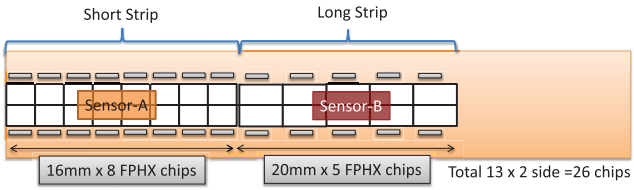

Fig. 1. Conceptual design of the sensor module for layers 1 to 3 of the INTT detector.

Figure 1 illustrates the conceptual design of the sensor module for layers 1 to 3 of the INTT detector. The module consists of two pieces of silicon sensors, named type-A and type-B, and 26 read-out chips (FPHX chips) placed on a fexlible circuit board called high-density interconnect (HDI).

The sensors are single sided, AC coupled sensors. The active area of the type-A and type-B sensors are 128 mm × 19.96 mm and 100 mm × 19.96 mm, respectively. The active area of the type-A (type-B) sensor is divided into 8×2 (5×2) blocks. Each block has 128 short strips that are 78 μm in pitch and 16.0 mm (type-A) or 20 mm (type-B) long, and run parallel to the z (beam) direction. In Fig. 1, the strip runs horizontally. The read-out lines of the strips run perpendicular to the strips and bring the signals to the read-out chips placed on the HDI at the upper and lower edge of the sensor.

FPHX chips, which were used for the Forward VerTeX (FVTX) silicon tracker of PHENIX, are utilized to read out the sensor. An FPHX chip has 128 channels of 3 bit ADCs and it can read out 128 mini-strips in one block of the sensor. The read-out pad pitch of the sensor is thus matched to that of the FPHX chip (75 μm). The FPHX chip has a low power consumption of about 64 mW per chip, which reduces the need for cooling the sensor module. The analog signal of each strip is digitized in the FPHX chip, and the digitized data of 128 channels are sent out through the 200 MHz data-out port of the FPHX chip.

The HDI is a 7 layer flexible circuit board used to read out these two sensors. One type-A and one type-B sensor and 26 FPHX chips are placed on an HDI. The type-A (type-B) sensor is read out by 16 (10) FPHX chips: 8 (5) at the upper edge and 8 (5) at the lower edge of the sensor. The data from the FPHX chips are sent to the front end module though the high speed data bus in the HDI.

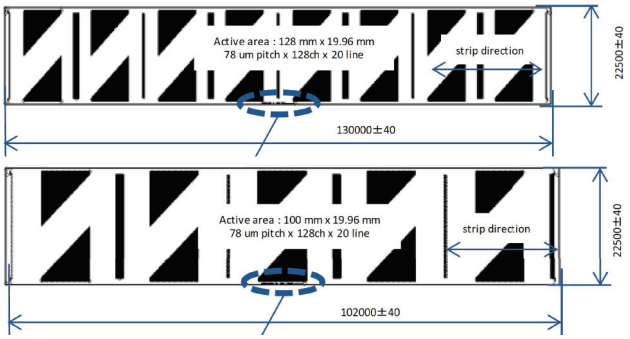

Fig. 2. Part of the sensor design drawings made by HPK.

The sensors will be manufactured by Hamamatsu Photonics Co. (HPK). Fig. 2 shows a part of the design drawings of the sensor made by HPK.

We will produce both type-A and type-B sensors with two thicknesses. One is 320-μm thick, which is the standard thickness of wafers that HPK uses. The other is 200-μm thick, which is made by thinining the 320 μm sensors. The thinner sensor results in lower scattering of charged particles and thus improves the momentum resolution of tracks. However, the signal generated by a hit will be reduced. We will evaluate the S/N ratio for MIP particles for both types of sensors to determine which one we will use for the production.

The design of the sensor at HPK has been completed and they are manufacturing the sensors. We expect the delivery of the sensors by early 2017.

The HDI will be manufactured by Yamashita Co. They will be delivered by early 2017.

The sensors and HDIs are assembed into sensor modules at Brookhaven National Laboratory, where they will be tested with a test bench.

References

1) I. Nakagawa: In this report.
2) Y. Yamaguchi: In this report.

*1 RIKEN Nishina Center
*2 Department of Physics, Rikkyo University
*3 Brookhaven National Laboratory

Intermediate Silicon Strip Tracker for sPHENIX Experiment

I. Nakagawa,[*1] Y. Akiba,[*1] T. Hachiya,[*1] Y. Kawashima,[*1*2] E. Mannel,[*3] H. Masuda,[*1*2] G. Mitsuka,[*1] D. Nemoto,[*1*2] R. Nouicer,[*3] and Y. Yamaguchi[*1]

After 16 years of continuous operation, the PHENIX experiment completes its original mission and was decommissioned at the end of Run16. In combination with other RHIC experiments, results from PHENIX show that the quarks and gluons are liberated from protons and neutrons in nucleus forming Quark Gluon Plasma (QGP). These strong interactions make the plasma flow like a nearly "perfect" liquid. On the other hand, the understanding exactly how the QGP's perfect fluidity and other collective properties emerge from its point-like constituent particles remains a compelling mystery.

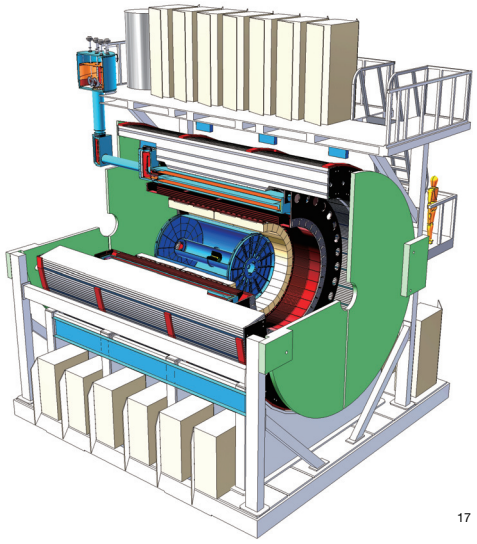

Fig. 1. Latest design of sPHENIX detector complex.

Alternative QGP studies in the large hadron collider experiments which launched a decade later than RHIC experiments indicated the direct observing potential of QGP using jets as a probe. To address remaining open questions of QGP[1)], a new scientific collaboration was formed to upgrade the PHENIX detector, i.e. building a brand new detector called super-PHENIX (sPHENIX)[2)] in the same experimental hall at RHIC after disassembling the PHENIX. The latest design of sPHENIX detector complex is shown in Fig. 1. This central arm detector is designed to cover the rapidity range of $|\eta| < 1.1$ with full azimuthal coverage.

The sPHENIX tracker reference design consists of MAPS (monolithic active pixel sensors) and a time projection chamber (TPC) for the inner- and outer-tracking system, respectively, with an intermediate silicon strip tracker (INTT). The momentum of a charged particle is primarily measured by TPC detector, whereas the inner most MAPS detector measures the decay vertex of heavy flavor mesons. The INTT interconnects the tracks between MAPS and TPC independently observed as illustrated in Fig. 2. The present time resolution of 4∼10 beam clocks prevents us from connecting track candidates between MAPS and TPC under the high multiplicity circumstances. The INTT is to be built by the well established technology, i.e. silicon strip sensors which gives better than 1 beam clock timing resolution.

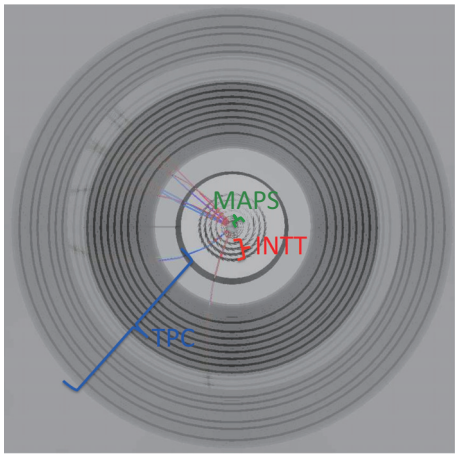

Fig. 2. Cross section of the sPHENIX tracking system.

The radius of the each detector layers are tabulated in the Table. The MAPS and INTT detectors consist of 3 and 4 layers, respectively. The TPC detector tracking volume runs about 58 cm to the radial direction.

Table 1. Radius of each detector layers.

Detector	layer	radius [cm]
MAPS	0	2.3
MAPS	1	3.1
MAPS	2	3.9
INTT	0	6
INTT	1	8
INTT	2	10
INTT	3	12
TPC	-	20∼78

*1 RIKEN Nishina Center
*2 Department of Physics, Rikkyo University
*3 Brookhaven National Laboratory

References

1) I. Nakagawa, Accelerator Progress Report vol.48 (2015).
2) sPHENIX pre-Conceptual Dsign Report (2015).

Development of data-collection and data-analysis systems for time-resolved ESR experiments

T. L. Tang,[*1] K. Tateishi, [*1] T. Uesaka,[*1] and K. Yamada [*1,2]

Nuclear magnetic resonance (NMR) is a valuable tool for biochemistry and medical science. The signal strength of NMR can be boosted significantly using dynamic nuclear polarization, which transfers the electron polarization to that of the nucleus. However, the conventional and well-understood polarization molecule pentacene[1] is not water solvable, and that limits its biological application. Various water-solvable pentacene derivatives have been synthesized (from collaborations) and their molecular structure needs to be studied via the electron spin resonance (ESR) spectrum. We are developing a data-collection system to simplify the labor of this task.

The data-collection system is illustrated in Fig. 1. The sample of pentacene derivative is placed inside a dielectric microwave chamber with a narrow resonance frequency band. A pulsed laser[2] is fed into the chamber to excite the electrons from the ground singlet state to the excited triplet state. The laser also triggers the oscilloscope to record the time-resolved ESR signal. The strength of an external magnetic field is fixed for each measurement, but it can vary from 0.0 T to 3.8 T and is controlled by a DC voltage power supply. The DC voltage is fed to a voltage-to-current convertor to supply a steady current to the magnetic coil. The magnitude of the magnetic field is measured using a Hall probe. A typical ESR signal is show in Fig. 2.

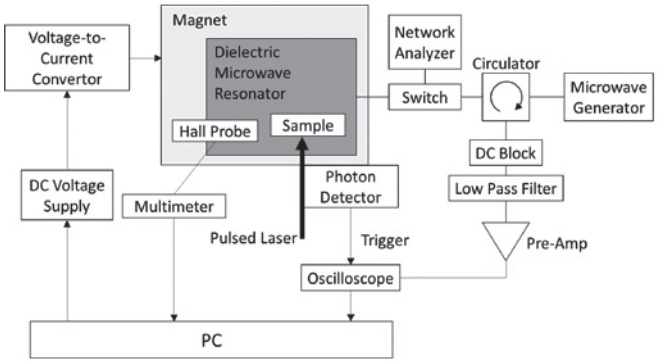

Fig. 1. Illustration of the ESR system.

A custom-built data-collection program with a graphical user interface (GUI) sets the control voltage, gets the Hall probe voltage, obtains the time-resolved ESR signal from the oscilloscope, and saves the signal into a file for analysis. Using the program, the strength of the magnetic field can be swapped and the data-collection process is fully automatic once the initial setup is done.

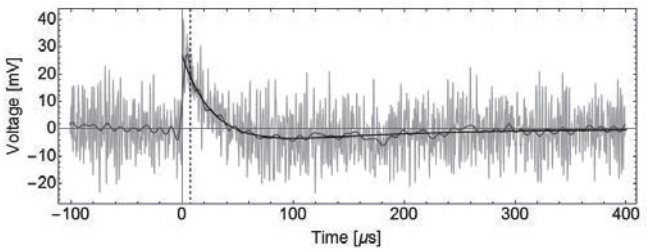

Fig. 2. Typical ESR signal (light gray). The gray line indicates the 100 kHz cutoff obtained using a Fourier transform. The black line is fit to the gray line using Eq. (1). The fitting uses the region after the dashed line.

The 2-dimensional data (time-resolved signal for each magnetic field setting) can be analyzed using a custom-built cross-platform GUI analysis program. The time-domain signal has the form

$$f(t) = a\exp\left(-\frac{t}{T_a}\right) - b\exp\left(-\frac{t}{T_b}\right), \quad (1)$$

where a and b are the relative populations of the energy levels and T_a and T_b are the lifetimes of the corresponding energy levels. The Levenberg—Marquardt algorithm is used to fit the non-linear function against the time-resolved signal. The effective magnitude of the electron polarization is

$$P = \frac{|a| - |b|}{|a| + |b|}. \quad (2)$$

The program also has other functions. It can be used as a plotting tool, for example, to plot the contour of the data. The program also provides a 2-dimensional Fourier transform[3] and different digital filters for noise elimination, for example, a sharp-cut low/high-pass filter and conventional low/high-pass filter. The filter can be applied as many times as needed to create filters such as a band-pass filter.

We are now developing a cross-platform GUI database program. The database stores the properties of the samples and their measurements. Other denoising methods such as discrete wavelet transformation will be evaluated.

References

1) K. Tateishi *et al.*: Angew. Chem. Int. Ed. **52** (2013) 13307.
2) N. Saito *et al.*: Opt. Lett. **32** (2007) 1965.
3) FFTW3.35, www.fftw.org.

*1 RIKEN Nishina Center
*2 Physics Department, Toho University

Parallel Readout VME DAQ system

H. Baba,[*1] T. Ichihara,[*1] T. Isobe,[*1] T. Ohnishi,[*1] K. Yoshida,[*1] Y. Watanabe,[*1] S. Ota,[*2] S. Shimoura,[*2] S. Takeuchi,[*3] R. Yokoyama,[*2] and J. Zenihiro[*1]

We have been developing the data acquisition (DAQ) system at RIBF. The parallel readout VME DAQ system was constructed to improve the DAQ performance. The system is based on RIBFDAQ,[1] and the data readout of all VME modules is completely parallelized by a mountable controller (MOCO).[2] A conceptual design of the system is shown in Fig. 1. A typical VME-based system adopts a controller board to read out data from multiple VME modules, whereas this system uses MOCO together with a front-end computer: this combination acts as a readout controller to each VME module. This system was introduced in the NP1312-RIBF113 and NP1512-RIBF79R1 experiments. CAT[3] and ESPRI[4] detectors were installed at the F8 and F12 focal planes, respectively. The DAQ systems of both detectors worked independently, but the data of the DAQ system for beam-line detectors (beam-DAQ) were common. To synchronize absolute time information, a time-stamping system[5] was used. After the measurements, separately taken data are merged based on time information. In this case, the live time ratio of the combined system will be worse because the dead time of each system is not shared on an event-by-event basis. The trigger rate of beam-DAQ is relatively high because the trigger signals from CAT, ESPRI and the beam-line detectors (down-scaled) were applied. Therefore, we have introduced the parallel readout VME DAQ system for the beam-line detector to minimize the dead time.

In the experiments, VME modules of CAEN V1190 TDC, CAEN V1290 TDC and Niki-glass LUPO[9] were used together with MOCO as front-end systems. Figure 2 shows the installation of VME modules. As in the standard RIBFDAQ system, the dead time of each event, which is managed by a generic trigger operator (GTO),[6,7] is determined by the slowest front-end system. The slowest one was CAEN V1190 TDC + MOCO for LP-MWDC[8] at the F3 focal plane. Its dead time consists of the TDC time window (6 μs), the latency from the end of the TDC time window until the time when the data is ready (2 μs), and data readout time by MOCO (the number of hits $\times$ 0.2 μs). Each module's data are buffered in MOCO once, after it is acquired by a front-end computer through the USB bus. Next, the front-end computer packs data to conform to the RIBFDAQ-data format, and sends the data to the back-end system (i.e., the event builder in RIBFDAQ). If the data throughput of the front-end computer is sufficiently high, additional dead time does not occur. In these experiments, a Raspberry Pi (Version 2, Model B) which is a very cheap computer was adopted. In fact, MOCO is capable of data throughput up to 320 Mbps, but it is limited to 64 Mbps because of the limitations of Raspberry Pi. The total data rate of beam-DAQ was 22 Mbps (typically 2 Mbps per front-end system). This rate is much lower than the limitation caused by Raspberry Pi. A live-time ratio of 99% could be achieved with respect to the generated triggers.

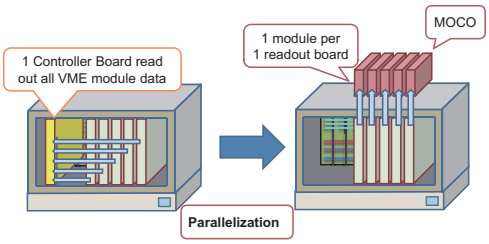

Fig. 1. Conceptual design of the system.

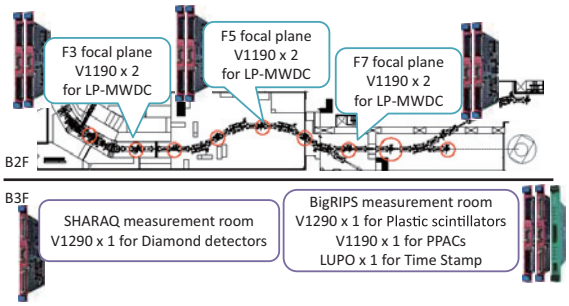

Fig. 2. VME modules for the experiments.

In summary, the parallel readout VME DAQ system successfully worked with very good performance. This system was temporally installed during the NP1312-RIBF113 and NP1512-RIBF79R1 experiments. We plan to install this system for the beam-line detectors permanently.

*1 RIKEN Nishina Center
*2 Center for Nuclear Study, University of Tokyo
*3 Department of Physics, Tokyo Institute of Technology

References

1) H. Baba et al., Nucl. Instr. Meth. A **616**, 65 (2010).
2) H. Baba et al., RIKEN Acc. Prog. Rep. **45**, ix (2012).
3) S. Ota et al., J. Radio. Nucl. Chem. **305**, 907 (2015).
4) Y. Matsuda et al., Phys. Rev. C **87**, 034614 (2013).
5) H. Baba et al., Nucl. Instr. and Meth. A **777**, 75 (2015).
6) H. Baba et al., RIKEN Acc. Prog. Rep. **46**, 213 (2013).
7) H. Baba et al., RIKEN Acc. Prog. Rep. **47**, 235 (2014).
8) H. Miya et al., Nucl. Instr. Meth. B **317**, 701 (2013).
9) H. Baba et al., RIKEN Acc. Prog. Rep. **43**, 222 (2010).

CCJ operations in 2016

S. Yokkaichi,*1 H. En'yo,*1 T. Ichihara,*1 and Y. Watanabe*1

1 Overview

The RIKEN Computing Center in Japan (CCJ)[1] commenced operations in June 2000 as the largest offsite computing center for the PHENIX[2] experiment being conducted at RHIC. Since then, CCJ has been providing numerous services as a regional computing center in Asia. We have transferred several hundred TBs of raw data files and nDST [a] files from the RHIC Computing Facility (RCF)[3] to CCJ.

Many analysis and simulation projects are being carried out at CCJ, and these projects are listed on the web page `http://ccjsun.riken.go.jp/ccj/proposals/`. As of December 2016, CCJ has contributed to 38 published papers and 41 doctoral theses.

2 Computing hardware and software

The computing hardware (nodes and RAIDs) and software (OS, batch queuing systems, database engine, etc.) have not been changed in 2016 from those described in the previous APR.[1] In summary, we have 28 computing nodes, two login servers, one main server (users' home directory, NIS, DNS, NTP), two disk servers, and 10 computing nodes provided by the RIKEN ACCC.[4] In total, 422 (= 384 + 72) jobs can be processed simultaneously by these computing nodes.

Table 1 lists the number of malfunctioning SATA or SAS disks in the HP servers, namely, computing nodes and NFS/AFS servers.

Table 1. Number of malfunctioning HDDs in 2011-2016

Type	Size	Total	2016	'15	'14	'13	'12	'11
SATA	1 TB	192	8	14	11	16	20	9
	2 TB	120	2	10	0	2	5	4
SAS	146 GB	38	5	3	2	0	1	1
	300 GB	24	0	1	1	0	0	1

One database (postgreSQL[5]) server and one AFS[6] server are operated in order to share the PHENIX computing environment. Now, only the SL5[7] environment is shared by the computing nodes, which have approximately 0.9 TB of library files. We have two data-transfer servers, on which the grid environment[8] is installed for the data transfer to/from RCF. One of them will be retired in March 2017.

The new NFS server HP DL380eGen8 and Infortrend 16TB SAS RAID, deployed in October 2015, have not posed any trouble as of December 2016.

Batteries of three 10 KVA UPS were replaced in March 2016, and a UPS of 7.5 KVA was retired. Thus, the current total power is 40 KVA for all the four UPSs.

The main network switch was also replaced by the same model in June 2016. In early 2017, a login server machine will be replaced. Also, the two machine rooms (258/260 in Main Bldg.) currently used will be downsized to one room (260) in the fall of 2017.

3 HOKUSAI and network environment

CCJ and the RIKEN Integrated Cluster of Clusters (RICC) have been jointly operated since July 2009. In April 2015, a new system named "HOKUSAI Greatwave" was launched by RIKEN ACCC and the joint operation with CCJ has been successful. A new hierarchical archive system and 10 dedicated PC nodes were provided to CCJ by them. Approximately 900 TB of CCJ data are archived in the system. The 10 nodes are the legacy of RICC and will be operated until June 2017, when the system replacement is planned.

The network configuration is shown in Fig. 1. Between the CCJ main switch and HOKUSAI, two 10G Ethernet links are used. Toward the outside of RIKEN, one 10G line is used between the main switch and the zen-riken net. Another 10G line of our grid server for data transfer between RCF has also been retained.

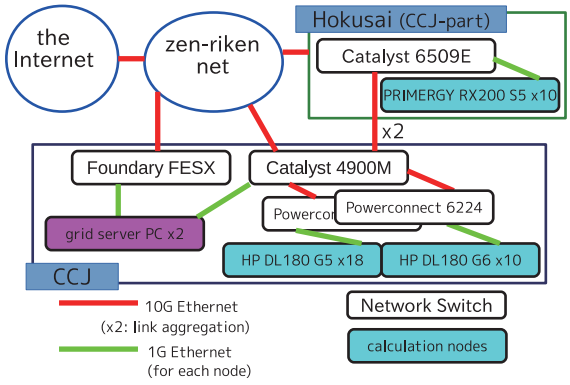

Fig. 1. Schematic view of the network configuration as of December 2016.

*1 RIKEN Nishina Center

a) term for a type of summary data files in PHENIX

References

1) S. Yokkaichi et al.: RIKEN Accel. Prog. Rep. **49**, 204 (2016).
2) `http://www.phenix.bnl.gov/`
3) `https://www.racf.bnl.gov/`
4) `http://accc.riken.jp/`
5) `http://www.postgresql.org/`
6) `http://www.openafs.org/`
7) `http://www.scientificlinux.org/`
8) `http://www.globus.org/toolkit/docs/latest-stable/gridftp/`

Computing and network environment at the RIKEN Nishina Center

T. Ichihara,*1 Y. Watanabe,*1 and H. Baba*1

We are operating Linux NIS/NFS cluster systems[1,2] at the RIKEN Nishina Center (RNC).

Figure 1 shows the current configuration of the Linux servers at the RNC. We have adopted Scientific Linux (SL), which is a clone of Red Hat Enterprise Linux (RHEL), as the operating system. Since the support of SL5 is scheduled to be terminated in March 2017, the SL5 OS installed in some servers is planned to be replaced with SL7 by the end of March 2017.

The host *RIBF.RIKEN.JP* is used as the mail server, NFS server of the user home directory /rarf/u/, and the NIS master server. This is the core server for the RIBF Linux cluster with approximately 700 registered user accounts. Because five years have passed since the installation of this sever, we are preparing to replace the server and RAID file system.

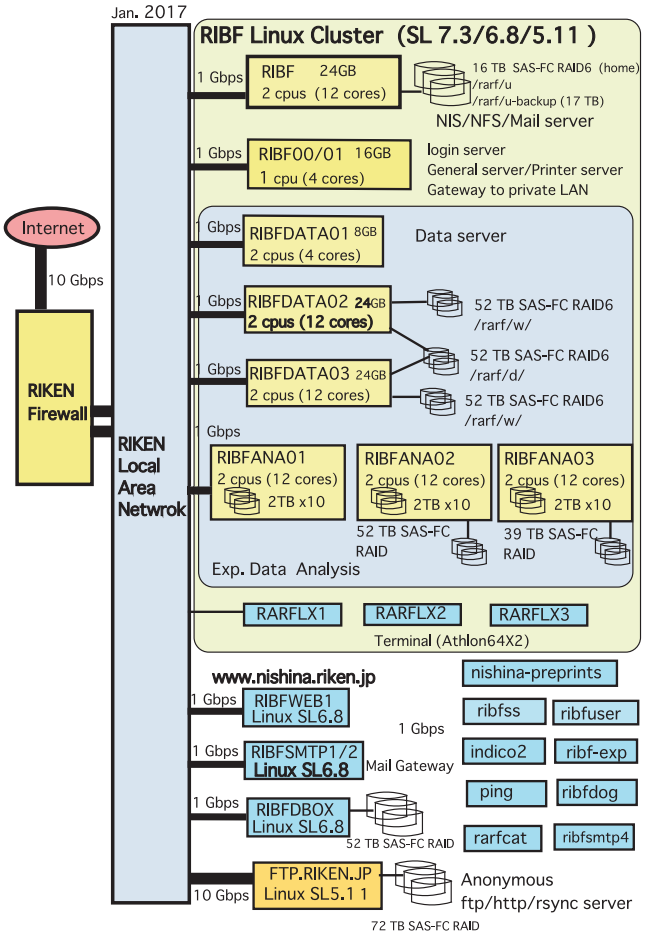

Fig. 1. Configuration of the RIBF Linux cluster.

The hosts *RIBFSMTP1/2* are the mail front-end servers, which are used for tagging spam mails and isolating virus-infected mails. The latest version of Sophos Email Protection-Advanced (PMX 6.3.3) has been installed on these servers.

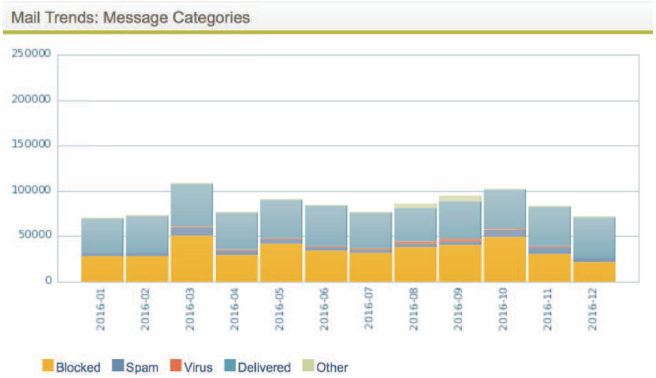

Fig. 2. Mail trends:message categories in 2016

We noticed that virus-infected mails were occasionally not detected by PMX in the case of new types of virus. Therefore, we added a new rule to PMX to isolate and remove executable image files attached in mail because they are often aimed at virus infection. As a result, most of the viruses in mails are successfully blocked by PMX. Figure 2 shows the mail trends of PMX in 2016. Approximately 1.5% of the incoming mails were infected by viruses in the year 2016, which is 14 times the yearly average for 2015.

An anonymous ftp server, *FTP.RIKEN.JP*, is managed and operated at the RNC. Major Linux distributions, including Scientific Linux, Ubuntu and CentOS, are mirrored daily for the convenience of their users and for facilitating high-speed access. An HP PloLiant DL-380G6 server was installed in 2009, and it is scheduled to be replaced by DL-380G9 in March 2017. Simultaneously, the OS will be upgraded from SL 5.11 to SL 7.3 .

We have been operating approximately 70 units of wireless LAN access points in RNC[3]. Almost the entire radiation-controlled area of the East Area of RIKEN Wako campus is covered by wireless LAN for the convenience of experiments and daily work. Since the devices used for the Wireless LAN access points became obsolete, all of them were replaced by WAPM-1166D or WAPS-APG-600H in 2016, which supports the protocols of 802.11b, 11g, 11a, 11n, and 11ac.

*1 RIKEN Nishina Center

References

1) https://ribf.riken.jp/comp/
2) T. Ichihara et al., RIKEN Accel. Prog. Rep. **49**, 205 (2016).
3) https://ribf.riken.jp/comp/net/wireless.html

III. RESEARCH ACTIVITIES II
(Material Science and Biology)

1. Atomic and Solid State Physics (Ion)

Site occupancy of hydrogen in Ta-rich Ta-Nb alloys as observed by the channelling method†

Y. Okada,[*1, *2] E. Yagi,[*1, *2] H. Matsuba,[*2] C. Sugi,[*2] S. Koike,[*3] S. Nakamura,[*1, *2] T. Sugawara,[*4] T. Shishido,[*4] and K. Ogiwara[*1]

In metal-hydrogen systems, alloying with substitutional or interstitial solutes has significant effects on various hydrogen properties in these systems, e.g., the terminal solubility of hydrogen, hydrogen diffusivity etc. One of the important factors controlling such effects is hydrogen-solute interaction. As an example for substitutional solutes, the interaction in the Nb-based Nb-Mo and Nb-Ta alloys has hitherto been studied systematically in the solute concentration range up to 60 at. % through the observation of a change in the lattice location of hydrogen. Information on the lattice location of hydrogen had been extremely limited, because of experimental difficulties. Therefore, the channelling method utilizing a nuclear reaction of $^{1}H(^{11}B,\alpha)\alpha\alpha$ with a $^{11}B^{+}$ beam of about 2 MeV with a Tandem accelerator was developed.[1] Hydrogen can be detected by measuring emitted α particles.

Both Nb-based Nb-Mo and Nb-Ta alloy systems form a solid solution over the entire solute concentration (C_{Mo} and C_{Ta}) range, maintaining a bcc crystal structure, although the lattice parameter changes. Their atomic radii are 1.43 Å for Nb, 1.36 Å for Mo (undersized solute) and 1.44 Å for Ta (slightly oversized solute). It has been demonstrated that, in the Nb-Mo alloys, the lattice location of hydrogen changes very sensitively to C_{Mo}, whereas, in the Nb-Ta alloys, the C_{Ta} dependence of the site change is very weak. With the help of measurement of X-ray reflection line width, such a change was interpreted on the basis of lattice distortion induced by alloying.[2] Broadening of reflection lines serves as a measure of lattice distortion averaged over the whole specimen. Hydrogen is located at tetrahedral (*T*) sites in Nb and Ta.

In the Nb-Mo alloys, at low C_{Mo}, lattice is strongly distorted around individual undersized Mo atoms. Hydrogen is trapped by a Mo atom so as to reduce the lattice distortion around the Mo atom, and is located at a site displaced from a *T* site by about 0.6 Å (T_{tr} site) towards the Mo atom, indicating a strong attractive interaction between hydrogen and Mo atoms.[3] With increasing C_{Mo}, the lattice distortion is reduced owing to interference between strain fields around individual Mo atoms, and most of the H atoms occupy *T* sites as in Nb. For C_{Mo}>39 at. %, the lattice distortion gradually increases again with increasing C_{Mo}, because of an increase in the number of undersized Mo atoms in a unit cell, but not so strongly as that at low C_{Mo}, i.e., up to an intermediate level. In this case, hydrogen is distributed over *T* and *d*-*T* sites, where *d*-*T* sites are displaced from *T* sites to the nearest neighbour octahedral (*O*) sites by about 0.25 Å. Hydrogen preferentially occupies *T* sites in the undistorted or very weakly distorted region, but, as the concentration of available *T* sites is limited, excess H atoms occupy *d*-*T* sites in the region distorted at the intermediate level.[2]

In the Nb-Ta alloys, at low C_{Ta}, hydrogen is distributed over *T* and *d*-*T* sites as in the case of the Nb-Mo alloys with C_{Mo}>39 at. %. At low C_{Ta}, the lattice distortion was observed to be at the intermediate level from the measurement of X-ray reflection line width. In the 50 at. % Ta alloys, where lattice is less distorted, hydrogen is located at *T* sites. Therefore, there exists no attractive interaction between hydrogen and an oversized Ta atom.[4]

According to the above-stated interpretation, it is expected that, in the Ta-rich Ta-Nb alloys, hydrogen is distributed over *T* and *d*-*T* sites, because a size difference between Nb and Ta atoms is small, although a Nb atom is an undersized solute. In this study, therefore, the lattice location of hydrogen in the Ta-rich Ta-Nb alloy with 3 at. % Nb was investigated. This alloy is symmetrical in the solute concentration to the hitherto studied Nb-rich Nb-Ta alloys containing 2 or 5 at. % Ta atoms. The following results were obtained. Hydrogen atoms occupy *T* and *d*-*T* sites, which are displaced by 0.25–0.3 Å from *T*-sites. Hydrogen preferentially occupies *T* sites and excess H atoms enter *d*-*T* sites. This is compatible with the above-stated expectation, and is different from the case in Nb alloyed with 3 at. % undersized Mo atoms. There exists no strong attractive interaction between hydrogen and undersized Nb atoms in Ta. Considering also the results obtained for the Nb-Mo alloys, the Nb-50 at. % Ta and Nb-(2–5) at. % Ta alloys, it is concluded that, in the Nb-Mo and Nb-Ta alloys, the site occupancy of hydrogen and the interaction between hydrogen and solute atoms can be well explained on the basis of the lattice distortion induced by alloying.

References

1) E. Yagi, T. Kobayashi, S. Nakamura, Y. Fukai, and K. Watanabe: J. Phys. Soc. Jpn. **52**, 3441 (1983).
2) E. Yagi, et al.: J. Phys. Soc. Jpn. **79**, 044602 (2010).
3) E. Yagi, S. Nakamura, F. Kano, T. Kobayashi, K. Watanabe, Y. Fukai, and T. Matsumoto: Phys. Rev. B **39**, 57 (1989).
4) C. Sugi, E. Yagi, Y. Okada, S. Koike, T. Sugawara, T. Shishido and T. Ogiwara: J. Phys. Soc. Jpn. **82**, 074601 (2013).

† Condensed from the article in J. Phys. Soc. Jpn. **83** 064602 (2014).

*1 RIKEN Nishina Center
*2 School of Science and Engineering, Waseda University.
*3 Department of Physics II, Tokyo University of Science.
*4 Institute for Materials Research, Tohoku University.

Nb/rare-earth bilayers: RKKY systems in proximity to an *s*-wave superconductor

H. Yamazaki*1

We have been studying the superconducting proximity effects in Nb/rare-earth (RE) bilayers, where RE indicates Gd, Tb, Dy, or Ho (the first four heavy RE elements in the periodic table). The RKKY interaction is common mechanism responsible for the magnetic structures in the RE elements. The Nb/RE bilayers can thus be regarded as RKKY systems in proximity to an *s*-wave superconductor (Nb). Recent theoretical studies showed that a new class of superconducting systems based on RKKY interactions exhibits topological superconductivity and hosts Majorana fermions. This result may unexpectedly shed light on the understanding of the superconducting proximity effects in Nb/RE bilayers.

The details of the sample preparation have been reported in the previous APR. The superconducting transition temperature T_c of each sample was measured, and we performed a periodicity analysis on the $T_c(t_{RE})$ data using a quantitative fast Fourier transform (FFT) method, where t_{RE} is the thickness of the RE layer. In Fig. 1, the vertical bars indicate the periods of the oscillation components in $T_c(t_{RE})$. With the exception of the longest period (~3.5 nm) for Gd, two types of variations are confirmed in the element dependence of the period. Here, we refer to the longer periods (more than 1 nm) as λ_L and the shorter ones (about 1 nm) as λ_S. The spin modulation period intrinsic to Ho, λ_{spin}^{Ho}(=3.4 nm; closed circle: ref. 1), is located within a broad distribution of λ_L for Ho. We identify a linear change in λ_L (shown as a broken line) from Gd to Dy. The line is extrapolated to Ho, giving an extrapolated value of 2.45 nm. The distribution of λ_L for Ho can be explained by the two unresolved peaks at 3.4 and 2.45 nm.

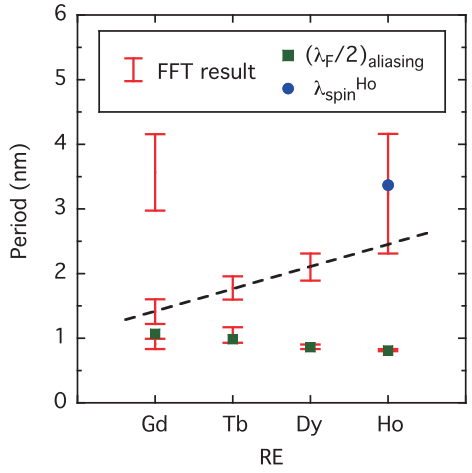

Fig. 1. Summary of the FFT analysis: periods of the oscillation components in $T_c(t_{RE})$ for Gd, Tb, Dy, and Ho. The closed circle (λ_{spin}^{Ho}) shows literature data.[1)]

*1 RIKEN Nishina Center

According to the picture of the RKKY interaction between conduction electrons and 4*f* moments, the exchange energy E_{ex} at 0 K scales linearly with the 4*f* spin moment *S*, where *S*=7, 6, 5, and 4 μ_B for Gd, Tb, Dy, and Ho, respectively. The spatial period of the FFLO-like oscillation, λ_{FFLO}, in the REs therefore increases from Gd to Ho, as long as $\lambda_{FFLO}=\pi\hbar v_F/2E_{ex}$ holds and the Fermi velocity v_F is almost unchanged for the REs. The broken line actually suggests that λ_L increases as $S(\propto E_{ex})$ decreases. Further, the values of λ_L for Ho and Gd are consistent with the literature data for λ_{FFLO}.[1, 2)] We infer that the broken line indicates the element dependence of λ_{FFLO}.

The Fermi wavelength λ_F of each RE was calculated from λ_{FFLO} (the broken line) and the experimental values of E_{ex} for the Δ_2 valence states[3)] by using the above equation and $v_F=2\pi\hbar/m_e\lambda_F$ (m_e: electron mass). Note that there is little experimental data of v_F and λ_F for REs to date. Our calculations show that v_F=1.25, 1.46, 1.33, and 1.36 ($\times10^6$ m/s) for Gd, Tb, Dy, and Ho, respectively. These values are close to those predicted by the nearly free-electron model. The closed squares in Fig. 1 show the calculated results of $(\lambda_F/2)_{aliasing}$, i.e., the $\lambda_F/2$ aliased by discrete-thickness (Δt_{RE}=0.4 nm) sampling. We recognize that the values of $(\lambda_F/2)_{aliasing}$ reproduce λ_S values very well. Naively, therefore, λ_S reflects the formation of quantum well states in the RE layer, as observed in the superconducting Pb film.[4)]

The above discussion is simple, but provides a reasonable explanation for the two oscillation components λ_L and λ_S regardless of the RE. When we recall the intricate Fermi surface (FS) of RE as well as of Nb, however, the basis for the free-electron-like aspect is not obvious. The Fermi wave vector mismatch between two materials, in general, has a large influence on the proximity effect, and the FS which contributes to the proximity effect is mainly determined by the smaller one among the two materials.[5)] In our case, it would be difficult to extract a spherical-like FS from the intricate FSs of RE and Nb. We also have to explain the use of the bare electron mass instead of the effective mass for m_e, since the mass enhancement of the conduction electrons due to electron-phonon interaction has been calculated for bulk RE metals.[6)] This issue deserves further consideration.

References

1) F. Chiodi et al., Europhys. Lett. **101**, 37002 (2013).
2) J. S. Jiang et al., Phys. Rev. Lett. **74**, 314 (1995).
3) C. Schüßler-Langeheine et al., Phys. Rev. Lett. **84**, 5624 (2000).
4) Y. Guo et al., Science **306**, 1915 (2004).
5) Y. Tanaka, M. Tsukada, Phys. Rev. B **42**, 2066 (1990).
6) H. L. Skriver, I. Mertig, Phys. Rev. B **41**, 6553 (1990).

Investigation of non-catastrophic failure mode observed in SiC diodes

Y. Nakada,[*1] E. Mizuta,[*1] H. Shindou,[*1] S. Kuboyama[*1] and K. Suzuki[*1]

Power devices are widely used for the power handling portion of the electronic devices for space systems as well as ground-based commercial devices. In our previous study, we investigated the fatal destruction mode called single-event effects (SEEs) in the SiC schottky barrier diode (SiC-SBD) and SiC metal-oxide-semiconductor field-effect transistor (SiC-MOSFET). SiC is expected to be a candidate material the next-generation semiconductor devices. It is applicable to high-voltage and high-temperature applications because of its inherent wide energy band gap. In addition, SiC is suitable for use in ultra-high frequency applications.

However, experimental date on SiC properties for radiation are rare. If we elucidate the mechanism of SEEs, it will be an innovative achievement.

In our previous study, 3 regions were revealed in the failure mode of SiC diodes as shown in Fig. 1. Region 1 is a non-destructive region, and collected charge is reproducibly measured with no damage. In region 2, there is a permanent increase in leakage current. We define the permanent damage region, region 2 in Fig. 1, as a non-catastrophic failure region. Further, region 3 in Fig. 1 is defined as a catastrophic failure region in which a single event burnout (SEB) occures. SEB is a failure mechanism caused by a large current arising from the irradiation of heavy ion. In a previous study, it was reported that the failure mode of SiC diodes is due to local heating.[1)] By irradiating heavy ions, high density electron-hole pairs and many defects (traps) are generated along its track. The resulting current flow contributes to local heating, and carriers are generated by trap-assisted tunneling. However, little is known about which factors the mechanism is depends on, its structure, applied voltage, and energy and fluences of ions.

Thus, in this experiment, to evaluate the difference of structures of SiC diodes and the effect of fluence, 4 types of commercial SiC-SBDs were prepared. Table 1 lists the electrical characteristic of the samples. The test sample was irradiated with a Kr-ion beam with an energy of 2304 MeV using the RIKEN RILAC+RRC. The total fluence was set to 2.5×10^4 or 3×10^5 ions/cm^2 at the chip surface. The reverse voltage, V_R, was increased with an interval of 20 V.

The result of this experiment is presented Fig. 2. It shows the leakage current of all test samples. Solid lines show that the total fluence at each V_R is 2.5×10^4 ions/cm^2 and dashed lines show that it is 3×10^5 ions/cm^2 at each V_R. We defined the device as broken when the leakage current deviated from the rated current. It can be seen that the leakage current increases permanently with increasing reverse voltage. Finally, for example, the leakage current of SiC-SBD C deviated from its rated current at 400 V. The leakage current of SiC-SBD D deviated at 460 V.

Moreover, Fig. 2 shows that there are some effects of difference of radiation fluence. The leakage current increases with increasing fluence. These results correspond with the previous experimental results. Generated electron-hole pairs tended to increase with increasing radiation fluence. A greater number of electron-hole pairs causes greater damage to devices. Finally, the leakage current at 3×10^5 ions/cm^2 is greater than that at 2.5×10^4 ions/cm^2.

In this experiment, non-catastrophic failure is observed in all samples. However, for use in space, it is important to clarify the long-term reliability of SiC diodes in region 2, and additional careful experiments are required in the future.

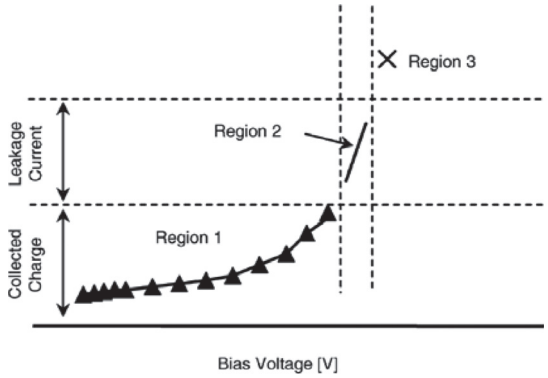

Fig. 1. Characteristic regions observed by heavy ion irradiations on SiC Schottky diodes.

Table 1. Test sample

	SiC-SBD A	SiC-SBD B	SiC-SBD C	SiC-SBD D
V_{BR}	1200 V	600 V	1200 V	1200 V
I_R	200 uA	100 uA	400 uA	200 uA
Diode Type	Schottky Barier			

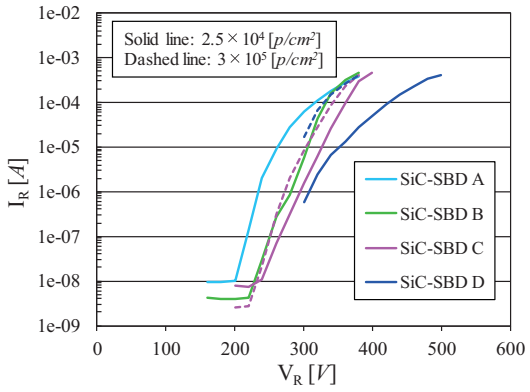

Fig. 2. Leakage current of SiC diodes.

Reference

1) S. Kuboyama et al., IEEE Trans., vol. 53, No. 6, 2006.

*1 Japan Aerospace Exploration Agency

Behavior of Cu impurity in Si studied by the β-NMR of ^{58}Cu

M. Mihara,[*1,*2] M. Tanaka,[*1,*2] Y. Tanaka,[*1,*2] H. Du,[*1,*2] T. Sugihara,[*1,*2] K. Ohnishi,[*1,*2] S. Yagi,[*1,*2] T. Hori,[*1,*2] S. Nakamura,[*1,*2] R. Yanagihara,[*1,*2] Y. Ishibashi,[*2] Y. Abe,[*2] H. Ueno,[*2] K. Yamada,[*2] D. Nagae,[*2] Y. Ichikawa,[*2] M. Fukuda,[*1,*2] K. Matsuta,[*1,*2] A. Ozawa,[*3,*2] T. Izumikawa,[*4] T. Ohtsubo,[*5] M. Takechi,[*5] S. Momota,[*6,*2] D. Nishimura,[*7,*2] T. Suzuki,[*8] T. Yamaguchi,[*8,*2] T. Nagatomo,[*2] T. Minamisono,[*1] K. Matsukawa,[*9] K. Shirai,[*10] and T. Fujimura[*10]

Cu impurities in Si devices are known as serious contaminants because of the unique diffusivity of Cu, which is the fastest among transition-metal impurities, enabling them to easily spread over a Si wafer of standard size only in a few hours.[1)] Short-lived β emitter ^{58}Cu ($I^\pi = 1^+$, $T_{1/2} = 3.2$ s) is an attractive option for a β-NMR probe nucleus for studying the behavior of Cu impurities in Si, which will provide unique information on the mechanism of fast Cu diffusion or the properties of the Cu-dopant complex which is related to the gettering technique.[2)] Using the β-NMR technique, which relies on magnetic dipole moment μ and electric quadrupole moment Q of the probe nucleus, local internal magnetic fields or electric field gradients (EFGs) at a probe nucleus can be observed. In the present case of ^{58}Cu in Si, measurement of the static EFG is essential for examining the structure of a complex such as a B-Cu pair or of off-center substitutional (S) site of implanted Cu ions suggested by β-ray emission channeling.[3)]

We have been performing the ^{58}Cu β-NMR experiments since 2010 using the Riken Projectile Fragment Separator (RIPS) at the RIBF operated by the RIKEN Nishina Center and CNS, University of Tokyo. In previous works, we have shown NMR signals of ^{58}Cu in Si at 15 K in 2010[4)] and signals implying a quadrupole splitting ν_Q, detected in 2013.[5)] In the present study, we have tried to confirm the reproducibility and a beta nuclear quadrupole (β-NQR) spectrum was obtained, as shown in Fig. 1. In the case of ^{58}Cu, which has a nuclear spin $I = 1$, the quadrupole interaction generates a splitting into two NMR lines with frequencies of $\nu_0 \pm \nu_Q/2$, where ν_0 and ν_Q are described as $\nu_0 \simeq \mu B_0/h$ and $\nu_Q = (3/4)eqQ/h(3\cos 2\theta - 1)$, respectively. The spectrum in Fig. 1 was obtained by applying multi RF pulses as a function of ν_Q. Owing to the remarkable progress in the recent μ and Q measurements for ^{58}Cu by laser spectroscopy,[6)] the center frequency ν_0 of approximately 4.04 MHz at $B_0 = 0.93$ T was estimated, and our result supports the value of $\mu[^{58}\mathrm{Cu}] = +(0.570 \pm 0.002)\mu_N$ in Ref. 6. A ν_Q of approximately 2.5 MHz was obtained from the present ν_Q spectrum. This supports the idea that implanted Cu atoms in the Si lattice are not located in a spatially symmetric configuration, as proposed by the β-ray emission channeling.[3)] The EFG (q) cannot be determined because the angle between the main axis of the EFG and the direction of B_0 is unknown. The EFG for ^{58}Cu in Si is determined from the crystal orientation dependence of ν_Q relative to B_0 and the value of $Q = (15 \pm 3)\ e\mathrm{fm}^2$ in Ref. 6.

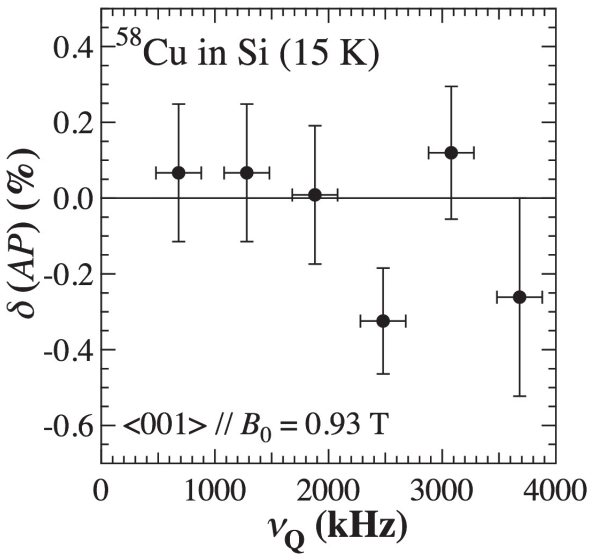

Fig. 1. β-NQR spectrum of ^{58}Cu in Si.

*1 Department of Physics, Osaka University
*2 RIKEN Nishina Center
*3 Department of Physics, University of Tsukuba
*4 Radioisotope Center, Niigata University
*5 Department of Physics, Niigata University
*6 School of Environmental Science and Engineering, Kochi University of Technology
*7 Department of Physics, Tokyo University of Science
*8 Department of Physics, Saitama University
*9 SUMCO, Co.
*10 ISIR, Osaka University

References
1) E. R. Weber, Appl. Phys. **A30**, 1 (1983).
2) S. M. Myers et al., J. Appl. Phys. **88**, 3795 (2000).
3) U. Wahl et al., Phys. Rev. Lett. **84**, 1495 (2000).
4) M. Mihara et al., Hyperfine Interact. **197**, 143 (2010).
5) M. Mihara et al., JPS Conf. Proc. **6**, 030114 (2015).
6) P. Vingerhoets et al., Phys. Lett. **B703**, 34 (2011).

2. Atomic and Solid State Physics (Muon)

μSR study of impurity effects on the Cu-spin correlation and superconductivity in the undoped superconductor T'-$La_{1.8}Eu_{0.2}CuO_4$

T. Kawamata,[*1,*2] K. Ohashi,[*2] T. Adachi,[*1,*3] T. Takamatsu,[*2] M. Kato,[*2] I. Watanabe,[*1] and Y. Koike[*1,*2]

It has long been believed that high-T_c superconductivity appears through hole and electron doping into antiferromagnetic mother compounds Ln_2CuO_4 (Ln: lanthanide elements) with the K_2NiF_4-type (T-type) and Nd_2CuO_4-type (T'-type) structures, respectively. Recently, however, in adequately reduced thin films of T'-$Nd_{2-x}Ce_xCuO_4$, superconductivity was observed in a wide range of x and even in the undoped mother compound of $x = 0$.[1)] In undoped T'-Ln_2CuO_4, it was suggested that the electronic state is explained based on the strong electronic correlation:[2)] carriers are induced at the Fermi level by the collapse of the charge-transfer gap between the upper Hubbard band of Cu3$d_{x^2-y^2}$ and the O2p band.[2)] The electronic state and superconductivity in undoped T'-Ln_2CuO_4 have, therefore, attracted great interest.

For the undoped superconductor T'-$La_{1.8}Eu_{0.2}CuO_4$ (T'-LECO), our recent study of impurity effects on the superconducting critical temperature, T_c, has revealed that T'-LECO shows d-wave superconductitiy mediated by the spin fluctuation and that the electronic state is similar to that in optimally hole-doped and overdoped T-LSCO.[3)] A previous μSR study using a T'-LECO sample ($T_c = 15$ K) showed that a short-range magnetic order appears in the almost whole region of the sample.[4)] Accordingly, in order to investigate the electronic state and superconductivity, the effect of impurities on the development of the Cu-spin correlation in undoped T'-LECO was studied. We performed the zero-field (ZF) and longitudinal-field μSR measurements for another sample of T'-LECO ($T_c = 20$ K) and impurity-substituted samples of T'-$La_{1.8}Eu_{0.2}Cu_{1-y}M_yO_4$ (M = Ni, Zn) at RIKEN-RAL.

Figure 1 shows the ZF spectra of T'-$La_{1.8}Eu_{0.2}Cu_{1-y}$-M_yO_4 (M = Ni, Zn; $y = 0, 0.01$). In all samples, we find that (a) the spectra at 150 K show a slow depolarization of muon spins, (b) the depolarization becomes faster gradually with decreasing temperature, and (c) the spectra show an exponential-like depolarization at 1.5 K, indicating the development of the magnetic order. The volume fraction of the magnetic order at 1.5 K is estimated to be almost the same in all samples. This shows that the magnetic order does not appear around Ni and Zn in the superconducting regions of the impurity-substituted samples. This behavior has been observed in overdoped T-LSCO[5)] and is consistent with the results of impurity effects on T_c.[3)]

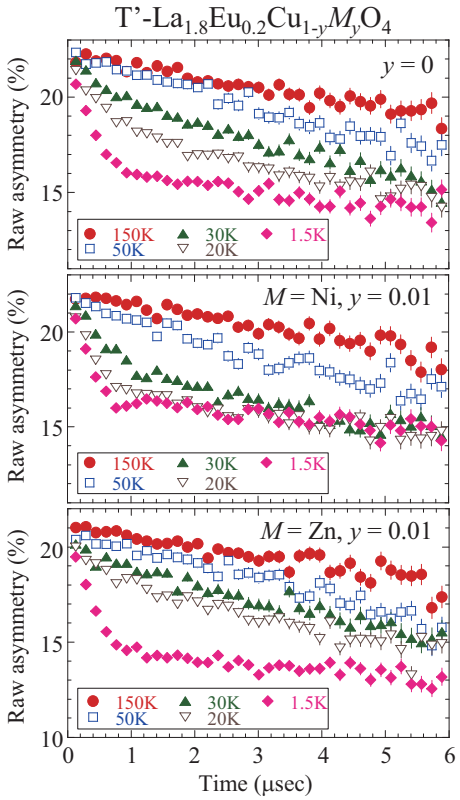

Fig. 1. Zero-field μSR time spectra of T'-$La_{1.8}Eu_{0.2}Cu_{1-y}$-M_yO_4 (M = Ni, Zn; $y = 0, 0.01$).

From the temperature dependence of the depolarization change, moreover, it is found that the magnetic order develops in the Ni- (Zn-) substituted sample below the temperature higher (lower) than that in the non-substituted sample. These impurity effects indicate that the magnetic order is due to the nearest exchange interaction in a localized spin system. The development of the magnetic order is enhanced by Ni with a larger magnetic moment than that of Cu, while the order is suppressed owing to the spin-dilution effect by the substitution of nonmagnetic Zn. These results indicate a strong electronic correlation and suggest the occurrence of phase separation into superconducting and magnetic-ordered regions in T'-LECO. The strong electronic correlation model[2)] in undoped T'-Ln_2CuO_4 is strongly supported.

*1 RIKEN Nishina Center
*2 Department of Applied Physics, Tohoku University
*3 Department of Engineering and Applied Sciences, Sophia University

References
1) O. Matsumoto et al.: Physica C **469**, 924 (2009).
2) T. Adachi et al.: J. Phys. Soc. Jpn. **82**, 063713 (2013).
3) K. Ohashi et al.: J. Phys. Soc. Jpn. **85**, 093703 (2016).
4) T. Adachi et al.: J. Phys. Soc. Jpn. **85**, 114716 (2016).
5) T. Adachi et al.: Phys. Rev. B **78**, 134515 (2008).

μSR study of ferromagnetic fluctuations in heavily overdoped Bi-2201 cuprates

K. Kurashima,[*1] T. Adachi,[*2,*3] T. Kawamata,[*1,*2] T. Noji,[*1] I. Watanabe,[*2] and Y. Koike[*1,*2]

High-temperature superconductivity in cuprates is known to emerge by hole doping into the antiferromagnetic (AF) Mott insulators. Superconducting (SC) transition temperature T_c indicates the maximum in the optimally doped regime and the superconductivity disappears with heavy overdoping. Theoretical studies in this decade[1,2] have suggested that the decrease in T_c with hole doping in the overdoped (OD) regime is related to the development of ferromagnetic (FM) fluctuations. In fact, it has been reported from zero-field (ZF) μSR, ab-plane electrical resistivity ρ_{ab} and magnetization measurements that the FM fluctuations are observed in non-SC heavily overdoped (HOD) $La_{2-x}Sr_xCuO_4$.[3] However, because the FM fluctuations have been observed only in $La_{2-x}Sr_xCuO_4$ thus far, the universality of the FM fluctuations in cuprates is still unclear.

To investigate the universality of the FM fluctuations, we performed ρ_{ab}, magnetization, and μSR measurements on Bi-2201 cuprates.[4] It was found that the temperature dependence of ρ_{ab} is proportional to $T^{4/3}$ in the OD and HOD regimes in a wide temperature range between 2-310 K. This dependence is a characteristic of metals with two-dimensional FM fluctuations according to the self-consistent renormalization (SCR) theory.[5] The magnetization curves in the HOD regime show a tendency to be saturated in high magnetic fields below 20 K. This is a precursor phenomenon to the formation of a possible FM order. Transverse-field (TF) μSR measurements on HOD Bi-2201 also show that muon spin relaxation rate λ increases with decreasing temperature below 100 K and that the enhancement of λ is more pronounced in 9.5 T than in 3 T. These results suggest that the spin correlation is enhanced by the application of a magnetic field, which is consistent with the existence of FM fluctuations. To further investigate the temperature and doping dependences of the FM fluctuations in Bi-2201, we performed ZF-μSR measurements on non-SC HOD (T_c < 2 K) and SC OD (T_c = 13 K) $Bi_{1.76}Pb_{0.35}Sr_{1.89}CuO_{6+\delta}$ single crystals (Bi-2201[A]) using a MiniCryo and a ^{3}He cryostat at RIKEN-RAL. The hole concentration per Cu of p was estimated from the thermoelectric power at 290 K.

Figure 1 shows the temperature dependence of λ in the single crystals of non-SC HOD (p = 0.274) and SC OD (p = 0.236) Bi-2201[A]. The results of HOD $Bi_{1.71}Pb_{0.32}Sr_{1.97}CuO_{6+\delta}$ (Bi-2201[B]) with p = 0.264 at J-PARC, Japan, are also shown. In the HOD Bi-2201[A] and HOD Bi-2201[B], the enhancement of λ is observed below 200 K, suggesting development of the spin correlation. For the OD Bi-2201[A], we find that λ shows a small increase with decreasing temperature. These results suggest that the spin correlation develops with hole doping in the HOD and OD regime, which is consistent with the existence of FM fluctuations in the HOD regime. In light of the resistivity results, the enhancement of λ below 200 K is due to the development of the two-dimensional FM correlation.

From the temperature and doping dependences of λ, we conclude that the FM fluctuations exist in HOD and OD Bi-2201, and that the FM fluctuations are enhanced with hole doping. The existence of FM fluctuations is, therefore, a universal feature in HOD cuprates.

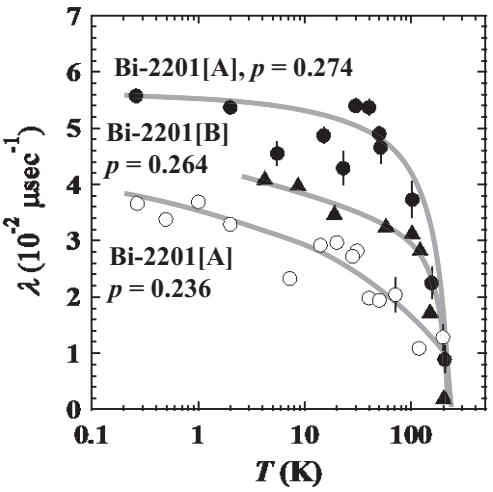

Fig. 1. Temperature dependence of λ in HOD and OD Bi-2201[A] and HOD Bi-2201[B].

References

1) A. Kopp et al., Proc. Natl. Acad. Sci. USA **104**, 6123 (2007).
2) B. Barbiellini, T. Jarlborg, Phys. Rev. Lett. **101**, 157002 (2008).
3) J. E. Sonier et al., Proc. Natl. Acad. Sci. USA **107**, 17131 (2007).
4) K. Kurashima et al., J. Phys: Conf. Ser. **568**, 022003 (2014).
5) Y. Hatatani, T. Moriya, J. Phys. Soc. Jpn. **64**, 3434 (1995).

*1 Department of Applied Physics, Tohoku University
*2 RIKEN Nishina Center
*3 Department of Engineering and Applied Sciences, Sophia University

μSR studies of the barium iridate $Ba_3MIr_2O_9$ (M = Y, Sc)

H. Guo,[*1] R. Asih,[*2,*3] D. P. Sari,[*2,*3] I. Watanabe,[*2] and A. C. Komarek[*1]

Iridates with $5d$ electron systems have drawn much attention recently because these materials may show spin orbit coupling (SOC)-driven novel phases such as Mott-insulators, Weyl semimetals and topological insulators. In addition to the SOC effect, crystal structure is an important factor that induces novel properties. Therefore, compounds with large SOC and special structures may provide another direction to search for unconventional properties. A series of $Ba_3MIr_2O_9$ (M = Sc, Y and rare earth elements) compounds are such candidates, which show Ir-Ir dimers within the unit cell.[1)] Furthermore, the valence of Ir ions can be tuned by choosing different ions at the M site and possible charge ordering of Ir^{4+} and Ir^{5+} ions has been suggested for some compounds. A previous NMR experiment suggested a magnetic ordering in the Y sample while the magnetic ground state of the Sc sample is unclear.[2)]

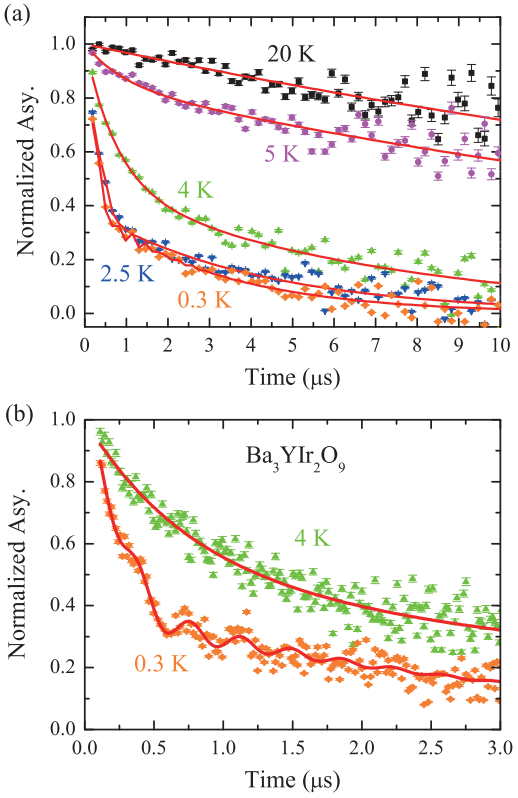

Fig. 1. Typical time spectra for the Y sample measured in the zero-field condition.

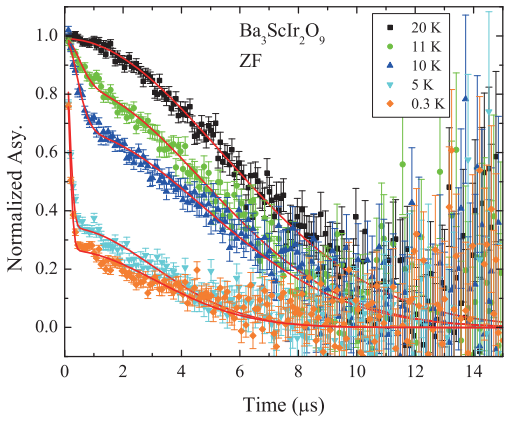

Fig. 2. Typical time spectra for the Sc sample measured in the zero-field condition.

Here, we studied the magnetic ground state of these compounds by means of μSR. Figure 1 shows the typical time spectra for the Y sample measured at various temperatures. The muon spin relaxation rate becomes faster below 5 K and clear spontaneous muon spin precession was observed below about 4 K, as can be seen from Fig. 1(b), indicating long-range magnetic ordering in this compound. The transition temperature is consistent with the specific heat measurement which shows a λ-like anomaly at 4 K. The detailed magnetic structure needs to be clarified in future studies. Figure 2 shows the time spectra for the Sc sample measured in the zero-field condition as well as a preliminary analysis. The muon spin relaxation rate becomes faster below about 10 K, but no spontaneous muon spin precession was observed down to 0.3 K. Therefore, the spin fluctuations slow down below 10 K, but no long range magnetic ordering was formed in this material. More detailed analyses of the spectra are needed.

From powder x-ray diffraction measurements, a site mixture between the Sc and Ir ions of about 8% has been observed, while no site mixture for the Y sample was observed. Such a site mixture may be the origin of the absence of magnetic ordering in the Sc sample.

References

1) Y. Doi, Y. Hinatsu, J. Phys.: Condens. Matter **16**, 2849-2860 (2004)
2) T. Dey, R. Kumar, A. V. Mahajan, S. D. Kaushik, V. Siruguri, Phys. Rev. B. **89**, 205101-1-205101-8 (2014)

*1 MPI Chemical Physics of Solids
*2 RIKEN Nishina Center
*3 Department of Physics,Osaka University

μSR investigation of a quantum criticality in the coupled spin ladder Ba_2CuTeO_6

Y. S. Choi, *1 S.-H. Do,*1 Dita Puspita Sari,*2,*3 I. Watanabe,*2 and K.-Y. Choi*1, *2

Quantum spin ladders consisting of leg and rung couplings offer an outstanding opportunity to investigate quantum-critical spin dynamics and have far-reaching relevance to diverse fields of physics such as Tomonaga-Luttinger liquids, magnon fractionalization, unconventional superconductivity, and quark confinement.[1)-3)] Isolated two-leg ladders have a short-range resonating valence bond state.[4)] With growing interladder couplings, a quantum phase transition is anticipated to occur to the magnetically ordered state.[5)]

Ba_2CuTeO_6 is a prime candidate material for a three-dimensionally networked spin ladder, allowing addressing quantum criticality in coupled two-leg ladders. Ba_2CuTeO_6 features both a long-range ordering at T_N =15 K and the spin-gap excitation of Δ=50 K at finite temperatures.[6)-7)] However, the magnetic transition is largely hidden, while showing no magnetic Bragg peaks and no apparent λ-like anomaly in the specific heat. Thus, it is highly desired to identify the occurrence of the static magnetic ordering. To resolve these issues, we performed zero-field μSR experiments on the ARGUS spectrometer of RIKEN-RAL. The collected data were analyzed using the software package WiMDA.

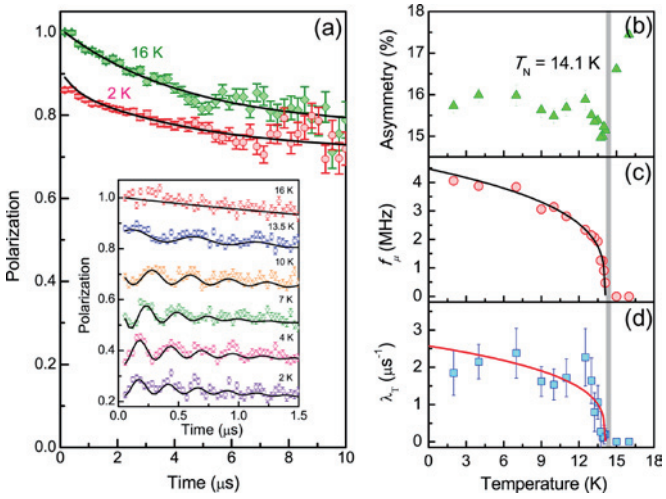

Fig. 1. (a) Representative data of the muon polarization of Ba_2CuTeO_6 measured above and below T_N. The solid lines are fits described in the text. The inset zooms the early-time behavior at various temperatures. The spectra are vertically shifted. (b),(c),(d) The asymmetry, the muon spin precession frequency f_μ, and the transverse relaxation rate λ_T as a function of temperature. The vertical bar indicates the onset of magnetic ordering at T_N =14.1 K.

The time decay of the muon spin polarization P(t) at temperatures above and below T_N is shown in Fig. 1(a). Upon cooling towards T_N, we observe muon-spin precession together with a drop in the early-time asymmetry [see the inset of Fig. 1(a)], confirming the development of static local magnetic fields at the muon stopping sites. The polarization curves can be well described by the sum of an exponentially relaxing cosine function and a simple exponential function:

$$P(t)=(1-\alpha)\exp(-\lambda_L t)+\alpha\exp(-\lambda_T t)\cos(2\pi f_\mu t+\phi),$$

where the two terms represent muons polarized transverse and parallel to the local magnetic fields. The temperature dependence of the asymmetry, the muon-spin precession frequency f_μ, and the transverse relaxation rate λ_T is plotted in Fig. 1(b)-(d). All μSR parameters display distinct changes at T_N. The initial asymmetry drops rapidly on cooling to T_N. The missing asymmetry is ascribed to an unresolved precession signal within the pulsed muon beam time window.

f_μ(T), corresponding to the magnetic order parameter, is fitted to the phenomenological form $f_\mu(T)= f_0(1-(T/T_N))^\beta$, f_0=4.3 MHz is the frequency at T=0 K and β=0.29(1) is the critical exponent. The obtained critical exponent is not much different from the value β=0.365, expected for the 3D Heisenberg model. T_N =14.1 K is slightly lower than the transition temperature of 15 K determined from the uniform susceptibility. The temperature dependence of λ_T(T) can be also modeled with the same order-parameter fit as plotted in Fig. 1(d). Taken together, a ground state of Ba_2CuTeO_6 is characterized by a conventional antiferromagnetic order, while having persisting spin fluctuations in the ordered state.

In this report, we have presented a combined study of ZF-μSR measurements on the coupled two-leg spin ladder Ba_2CuTeO_6. We observe unambiguously an oscillating signal in the ZF-μSR time spectra, suggesting that Ba_2CuTeO_6 lies close to a quantum critical point from a magnetically ordered side.

References

1) S. Maekawa: Science **273**, 1515 (1996).
2) B. Lake et al.: Nature Phys. **6**, 50 (2009).
3) M. Jeong et al.: Phys. Rev. Lett. **111**, 106404 (2013).
4) S. R. White et al.: Phys. Rev. Lett. **73**, 886 (1994).
5) B. Normand and T. M. Rice, Phys. Rev. B **54**, 7180 (1996).
6) A. S. Gibbs et al.: arXiv:1511.01477 (2015).
7) G. Narsinga Rao et al.: Phys. Rev. B **93**, 104401 (2016).

*1 Department of Physics, Chung-Ang University
*2 RIKEN Nishina Center
*3 Department of Physics, Osaka University

Study of the spin dynamics of a honeycomb ruthenate using spin polarized muons

S. Yoon,[*1,*2] S.-H. Do,[*3] K.-Y. Choi,[*3] B. J. Suh,[*2] and I. Watanabe[*1,*2]

Honeycomb ruthenate α-$RuCl_3$ was recently suggested as a candidate to realize the Kitaev-Heisenberg spin model for the following reasons.[1] Ru^{3+} ions can be in the low spin state because of the competition between the spin orbit coupling and the electronic correlation on the octahedral environment surrounded by Cl^- ions. Also, they form a nearly two-dimensional honeycomb network for the weak coupling by a van der Waals force among honeycomb layers. These environments are expected to serve the bond-dependent anisotropic exchange coupling between Ru^{3+} ions by an orthogonally bridged Cl^- ion in the honeycomb network.

We prepared a single crystal sample of α-$RuCl_3$ with a rhombohedral lattice observed by the X-ray diffraction. In this lattice, the anisotropic exchange can be revealed for the close cubic environment in the two-dimensional honeycomb layer. In addition, we carried out the measurements for DC susceptibility and specific heat. The DC susceptibility result shows a magnetic anomaly around 6 K. The specific heat result also exhibits a sharp peak around 6 K, as well as two broad humps around 10 K and 13 K. These anomalies are lower than previously presented results.[2-4]

In order to obtain details of the magnetic ordered states, we performed a local probe investigation using spin polarized muons at the RIKEN-RAL Muon Facility because muons are highly sensitive to a small magnetic field. In the muon polarization at zero field, we confirmed results similar to the previous experiment,[5] two magnetic transitions around 6 K and 13 K. It was also found that both transitions are close to the two dimensional Ising spin state by fitting the phenomenological equation of the magnetic ordered state.

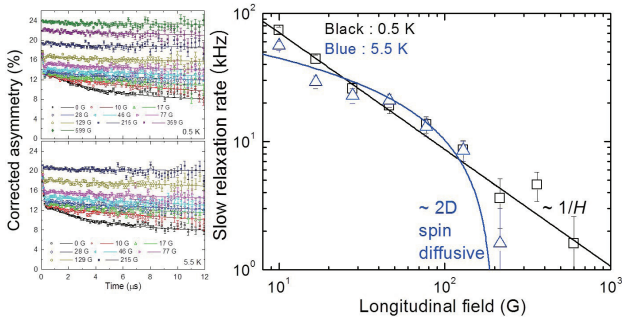

Fig. 1. (Left panel) Muon polarization spectra in several longitudinal fields at 0.5 K (up), and 5.5 K (down), respectively. (Right panel) Longitudinal field dependences of the slow relaxation rates with their fits at 0.5 K and 5.5 K, respectively.

*1 RIKEN Nishina Center
*2 Department of Physics, The Catholic University of Korea
*3 Department of Physics, Chung-Ang University

In addition, we obtained information about the electronic spin fluctuations from the muon polarization in the external longitudinal field by fitting with the superposition of two exponential functions. We then extracted the relaxation rate of the slow-relaxing component on the latter time region. As shown in Fig. 1, the slow relaxation rates of the whole spectra are strongly dependent on the external longitudinal field. The spin diffusive model is used to describe the behavior of the electronic spin fluctuation.[6] It was found that the result of the relaxation rates at 5.5 K is close to the two-dimensional diffusive model rather than the result at 0.5 K which is almost inversely proportional to the longitudinal field.

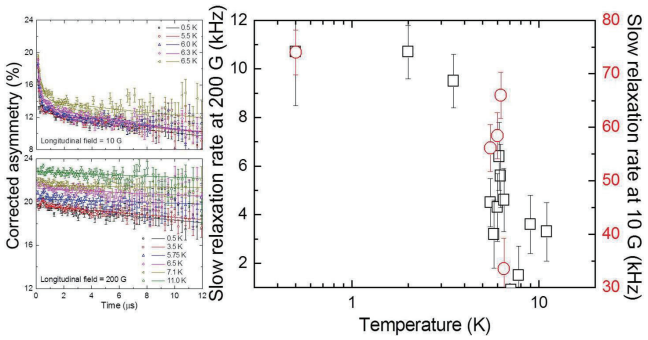

Fig. 2. (Left panel) Several time differential spectra of the muon polarization at some temperatures in the longitudinal fields of 10 G and 200 G, respectively. (Right panel) Temperature dependence of the slow relaxation rates from the muon polarization at longitudinal fields of 10 G and 200 G, respectively.

Moreover, we also extracted the relaxation rate on the latter time region by fitting with the superposition of two exponential functions from the muon polarization at several temperatures in the longitudinal fields of 10 G and 200 G, as shown in Fig. 2. Both relaxation rates on latter times in the longitudinal fields of 10 G and 200 G are dependent on the temperature and exhibit a sharp peak around 6 K. Then, as the temperature cools, both relaxation rates increase, and become almost saturated below 2 K.

References

1) K. W. Plumb et al., Phys. Rev. B **90**, 041112 (2014).
2) Y. Kubota et al., Phys. Rev. B **91**, 094422 (2015).
3) J. A. Sears et al., Phys. Rev. B **91**, 144420 (2015).
4) M. Majumder et al., Phys. Rev. B **91**, 180401 (2015).
5) R491 in the 2015 RIKEN Accelerator Program Report.
6) F. L. Pratt et al., Hyperfine Interact. **106**, 33 (1997).

Successive magnetic phase transition of the new frustrated compound $KCu_3OCl(SO_4)_2$

H. Kikuchi,[*1] K. Kunieda,[*1] Y. Fujii,[*2] F. Astuti,[*3] D. P. Sari,[*3] and I. Watanabe[*3]

Geometrically frustrated magnets have attracted much interest recently because some new physical states including spin liquids are expected to be realized in them. One of the most studied spin lattices is the pyrochlore lattice, in which spin tetrahedrons are connected by their vertices to form a 3D frustrated lattice. If tetrahedrons are coupled only along one direction, we have a one-dimensional (1D) pyrochlore lattice in which new quantum phases or states can be generated by both low-dimensional and frustration effects.

We attempted to find model compounds for the 1D pyrochlore and found $KCu_3OCl(SO_4)_2$ (mineral name, kamchatkite).[1)] The copper ions form distorted tetrahedra that are connected along the crystallographic c axis to form 1D pyrochlore. We synthesized a kamchatkite powder sample and measured its magnetic susceptibility and specific heat.[2)] The specific heat result revealed three successive phase transitions at about T_c=15, T_m=11, and T_N = 3 K. The 15 K and 3 K transitions are considered to be weak ferromagnetic and antiferromagnetic transitions, respectively. These complex successive phase transitions including the magnetic transition originate from the spin frustration. A new phase may appear due to the interplay between the spin frustration and characteristic crystal structure of kamchatkite.

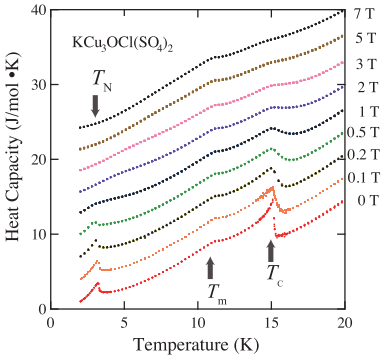

Fig. 1. Temperature dependence of the specific heat of kamchatkite measured under various magnetic fields up to 7 T.

In order to investigate the properties of these phase transitions from microscopic and dynamic points of view, tentative μSR measurements under zero magnetic field were carried out. Contrary to the first expectation that μSR would show anomalies at the three phase temperatures, the relaxation rate λ and asymmetry parameter show an anomaly at only one temperature around T_c =15 K. Moreover, drastic changes of these parameters suggest that the transition at T_c is a first order transition, although no thermal hysteresis is observed in the specific heat. We need further relaxation data including LF measurements to determine the nature of the transition at T_c.

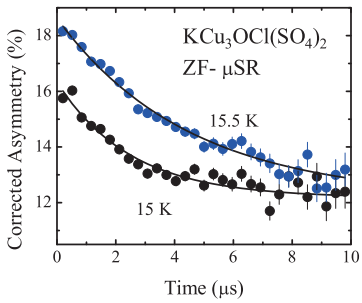

Fig. 2. ZF-μSR spectra measured at 15 and 15.5 K. Drastic change is observed at around T_c=15 K.

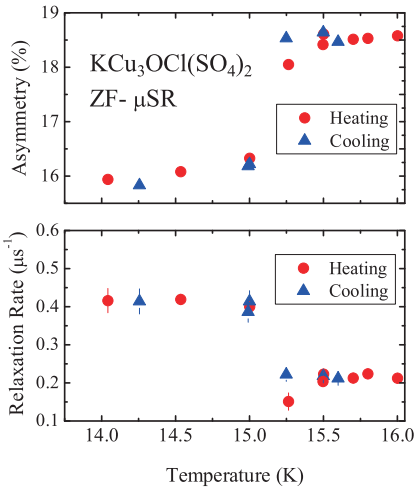

Fig. 3. Temperature dependence of the asymmetry parameter and relaxation time λ obtained from ZF-μSR spectra.

*1 Department of Applied Physics, University of Fukui
*2 FIR Center, University of Fukui
*3 RIKEN Nishina Center

References

1) T. V. Varaksina et al.: Mineralogical Magazine **54**, 613 (1990).
2) H. Kikuchi, K. Kunieda, Y Fujii, A. Matsuo, K. Kindo: submitted to Proc. HFM2016 (Taipei, 2016).

Investigation of the magnetic ground state in a new one-dimensional quantum spin system $K_2Cu_3O(SO_4)_3$

M. Fujihala,[*1] S. Mitsuda,[*1] I. Watanabe,[*2] and R. Aish[*2]

The magnetic ground states of linear chain systems are known to follow the Haldane's conjecture [1] that the half-integer spin chains are gapless and integer spin chains are gapped, which is supported by a vast amount of theoretical and experimental results. On the other hand, competing interactions or inter-chain interactions can often induce a spin gap, even in half-integer spin systems.[2] These exciting results indicate that exotic quantum states will be discovered in one-dimensional spin systems with competing magnetic interactions based on the unique arrangement of magnetic ions. In zero-dimensional $S = 1/2$ spin systems on an isolated spin cluster, the magnetic ground state can be determined exactly. If a cluster contains many spins, it is difficult to intuitively understand, and there is a possibility of the presence of an exotic quantum state. In the present study, we report the magnetism of the edge-sharing $S = 1$ tetrahedral cluster chain system $K_2Cu_3O(SO_4)_3$. The unique competing interaction in a spin edge-sharing tetrahedron and the weak one-dimensional inter-cluster couplings lead to the exotic quantum state.

Single-phase $K_2Cu_3O(SO_4)_3$ was verified to possess a monoclinic crystal structure identical to the mineral (Fig. 1). As illustrated in Figs. 1(b) and (c), magnetic ions of Cu^{2+} form the edge-sharing spin tetrahedral cluster that are connected with each other by SO_4^{2-} ions along the b-axis direction. The inter-cluster magnetic interactions should be weaker than intra-cluster magnetic interactions because they are next-nearest-neighbor magnetic interactions through the Cu-O-S-O-Cu exchange paths, hence we called this system the "edge-sharing spin tetrahedral cluster chain." The nonmagnetic potassium ions are located as shown Fig. 1(b), thus resulting in a long inter-chain distance along the a-axis. In this compound, Cu^{2+} ions have tetra-coordination, as shown Fig. 1(d). Therefore, only the presence of very weak inter-chain magnetic interactions through the Cu-O-K-O-Cu exchange paths is expected. Therefore, we conclude that $K_2Cu_3O(SO_4)_3$ has good one dimensionally.

We observed a Schottky-like anomaly at around 4 K, and any anomaly indicative of long-range ordering is absent down to at least 0.7 K. The anomalies at around 4 K and 100 K were seen in the temperature dependence of the magnetic susceptibility. Moreover, a clear spin-gap is seen in the inelastic neutron scattering spectrum.[3] In order to investigate the spin dynamics in $K_2Cu_3O(SO_4)_3$, we performed muon spin rotation and relaxation (μSR) measurements at the RIKEN-RAL Muon facility at the Rutherford-Appleton Laboratory, UK.

*1 Department of Physics, Tokyo University of Science
*2 RIKEN Nishina Center

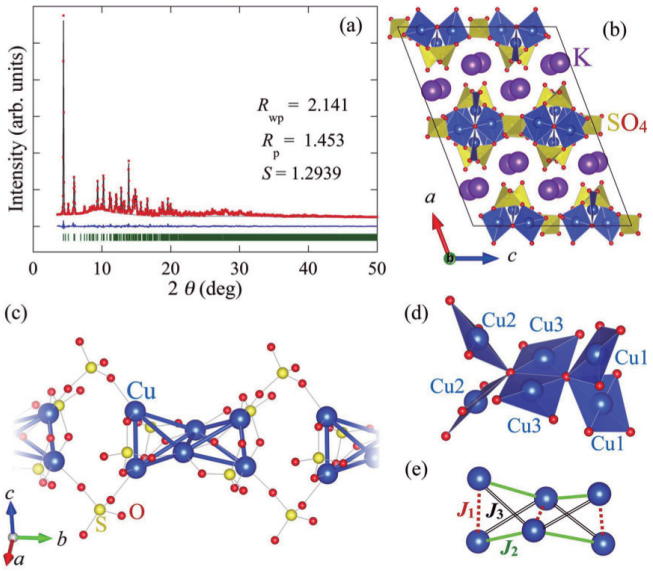

Fig. 1. (a) The observed synchrotron x-ray diffraction intensity pattern for $K_2Cu_3O(SO_4)_3$ and the result of the calculated Rietveld structure refinements. (b), (c), (d) The crystal structure of $K_2Cu_3O(SO_4)_3$. (e) An edge-sharing tetrahedron with nearest-neighbor exchange couplings.

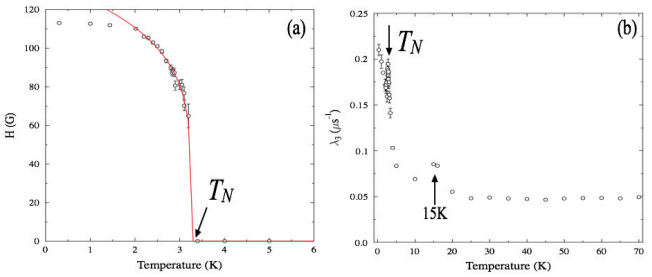

Fig. 2. (a) Temperature dependence of the internal field in $K_2Cu_3O(SO_4)_3$. (b) Temperature dependences of the relaxation rate.

Surprisingly, the μSR results are quite different from the results of the other experiments. A clear oscillation indicative of the long-range magnetic order was observed at 3.2 K (Fig. 2(a)). In addition, the anomaly was observed at around 15 K (Fig. 2(b)). Further detailed studies are required. At this point, we suspect that the sample was deteriorated by moisture.

References

1) F. D. M. Haldane, Phys. Rev. Lett. **50**, 1153 (1983).
2) M. Azuma, Z. Hiroi, M. Takano, K. Ishida, and Y. Kitaoka, Phys. Rev. Lett. 73, 3463 (1994).
3) M. Fujihala *et al.*: unpublished.

Investigation on spin dynamics of a staircase kagome material by using spin polarized muons

S. Yoon,[*1,*2] S.-H. Do,[*3] K.-Y. Choi,[*3] B. J. Suh,[*2] and I. Watanabe[*1,*2]

$PbCu_3TeO_7$ was suggested as a Cu-based anisotropic kagome material with the staircase kagome lattice.[1)] The crystal structure of $PbCu_3TeO_7$ is an orthorhombic lattice with the space group, *Pnma*, No. 62.[2)] $PbCu_3TeO_7$ is formed by a buckled kagome layer, and each layer is alternatively arranged Cu^{2+} ions in the different environments of surrounding O^{2-} ions, the octahedral, and the tetrahedral crystal environments, respectively.[1), 2)] Since all buckled kagome layers are not only stacked along the *a* axis, but also separated by Pb, and Te atoms, they can be in a two dimensional network of Cu^{2+} ions. Therefore, it is expected that several magnetic anomalies emerge for different crystal environments.[1)]

We synthesized a $PbCu_3TeO_7$ polycrystalline sample, and we found several magnetic anomalies from the DC magnetic susceptibility and the specific heat results. The DC susceptibility exhibits three distinct anomalies at 17 K, 25 K, and 36 K, and the Weiss temperature is extracted approximately 180 K by the Curie Weiss law, indicating a highly frustrated spin state. The specific heat result also indicates that the magnetic entropy over 36 K remains around 50 %. The experimental results of the nuclear magnetic resonance also support a frustrated spin state.[3)] With the consideration of previous experimental results, it can be suggested that $PbCu_3TeO_7$ is in the frustrated spin state with several magnetic anomalies, as revealed in anisotropic kagome materials.[1)] However, it is unrevealed the nature of magnetic anomalies in the Cu-based staircase kagome material.

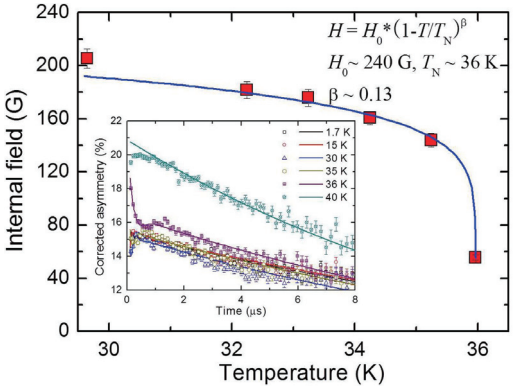

Fig. 1. Temperature dependence of the internal field obtained by the muon polarization at zero field with a fit obtained using the phenomenological equation of the magnetic ordered state, and the inset of exhibiting several time differential spectra of the muon polarization at zero field.

*1 RIKEN Nishina Center
*2 Department of Physics, The Catholic University of Korea
*3 Department of Physics, Chung-Ang University

In order to understand the nature of the magnetic anomalies, we conduct a microscopic investigation using spin-polarized muons at the RIKEN-RAL Muon Facility. Because the muon is highly sensitive of the small magnetic field, the muon is expected to provide a clue for the characteristics of magnetic anomalies.

In Fig. 1, it shows the temperature dependence of the internal field around 36 K obtained from the muon polarization at zero field by fitting with the oscillation function to represent the magnetic ordered state. This anomaly can be described by the two-dimensional Ising spin state with a phenomenological function to express the magnetic ordered state in the range from 32 K to 36 K. It is suggested that the anomaly at 36 K is induced by the two dimensional network including Cu^{2+} ions in the tetrahedral environment.

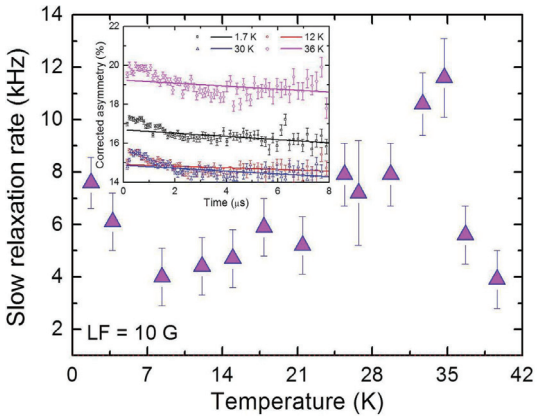

Fig. 2. Temperature dependence of the slow relaxing component obtained by the muon polarization at a longitudinal field (LF) of 10 G, and the inset of revealing several spectra of the muon polarization at LF = 10 G.

Exhibited in Fig. 2, it was extracted the temperature dependence of the relaxation rate from the relaxation component on a latter time region of the muon polarization at a weak longitudinal field for the exclusion of the contribution of the nuclear dipole moment. It supports that the behavior of the ordered state at 36 K is close to the second-order phase transition. Furthermore, a slight increase of the relaxation rate below 5 K was found, suggesting a frustrated spin state.

References

1) B. Koteswararao et al., J. Phys.: Condens. Matter **25**, 336003 (2013).
2) B. Wedel and H. Mueller-Buschbaum, Z. Naturf. B **51**, 1587 (1996).
3) DAI Jia et al., Chin. Phys. Lett. **32**, 127503 (2015).

Magnetic ordering and spin dynamics driven by *p*-orbital in RbO_2

F. Astuti,[*1,*3] D. P. Sari[*2,*3] I. Watanabe,[*1,*3] M. Miyajima,[*4] and T. Kambe[*4]

Magnetism in the π-electron system has attracted attention for the possibility of the new kinds of the magnetic informative materials. Alkali-metal superoxides AO_2 (A= Na, K, Rb, Cs) present an interesting example of magnetic materials on the basis of *p*-elements. These systems have a dumbbell-type bonding state of O atoms forming the valence state of O_2^- and resulting in one unpaired π-electron on the O_2^- dumbbell. They further show the changing of crystal structure introducing the splitting of the *p*-orbital degeneracy, similar to the Jahn-Taller effect. Beside the crystallographic phase transition due to molecular ordering of the disordered O_2^-, the magnetic order in alkali metal superoxide is interesting to study. In the case of superoxides, the number of unpaired electrons is only one on the O_2^- dumbbell, and magnetic superexchange interaction is expected between those unpaired spins through the A metal. Accordingly, a different magnetically ordered state from that observed in the solid oxygen molecule[1] is expected in superoxides, but detailed information on magnetic properties is still missing. The magnetic ordering of KO_2, RbO_2, and CsO_2 have been observed at temperatures of 7 K, 15 K, and 9.6 K, respectively, using specific heat measurement.[2] The Tomonaga Luttinger Liquid (TLL) model suggests that a field-induced magnetic order should appear in the CsO_2 that is related to the TLL state.[3]

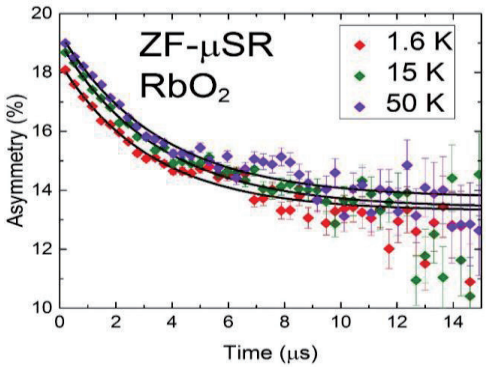

Fig. 1. ZF-μSR time spectra for CsO_2 for the first microsecond from 10 K down to base temperature.

Therefore, a detailed investigation on the magnetic properties near or in the zero-field (ZF) condition is strongly required to describe the magnetically ordered state that appears in the CsO_2 and other alkali metal superoxides.

*1 Department of Physics, Hokkaido University
*2 Department of Physics, Osaka University
*3 RIKEN Nishina Center
*4 Department of Physics, Okayama University

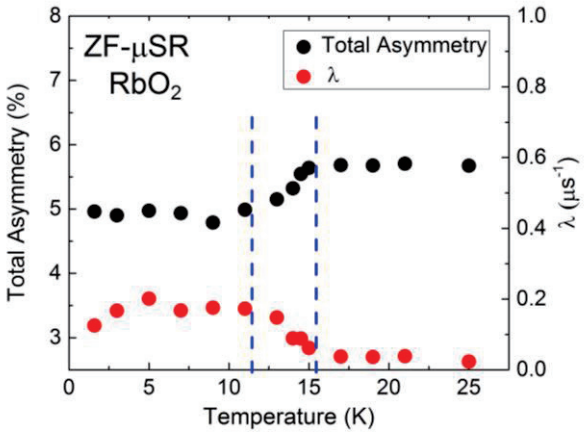

Fig. 2. Temperature dependence of the initial asymmetry and relaxation rate (λ) of the ZF-μSR time spectra measured at the RIKEN-RAL Muon Facility. The anomaly in the μSR measurement is observed in between 10 and 15 K around the suggested T_N.

We carried out μSR measurements in CsO_2 at the PSI Switzerland using the continuous muon beam. Clear spontaneous muon-spin precession behavior indicates the appearance of a long-range magnetic ordered state. This is evidence of the coherent static magnetically ordered state of π-electrons in oxygen molecules. Another alkali-metal superoxide, RbO_2, which has a crystal structure similar to that of CsO_2 (CaC_2-like), was tested at the RIKEN-RAL. In this system, only a type of anomaly in the magnetic susceptibility of RbO_2 is reported at T_N ~ 15 K, as indicated.[4] Unfortunately, we could not observe clear muon-spin precession as shown in Fig.1, although the decrease in the initial asymmetry around the suggested T_N was observed, as displayed in Fig. 2. The decrease in the initial asymmetry and increase in the relaxation rate (λ) possibly means the magnetically ordered state appears, causing a depolarization behavior that is faster than the time limitation of the pulsed muon facility. This ordered state might accommodate the fast muon-spin precession as well as the case of CsO_2. Therefore, it is necessary to test RbO_2 at PSI using the continuous muon beam in order to detect clear evidence of the appearance of magnetically ordered states.

References

1) C. Uyeda et al., JPSJ, **54** (1985)

2) A. Zumsteg et al., Phys. Cond. Matter, 267-291 (1974)

3) M. Klansjek et al., PRL **115**, 057205 (2015)

4) M. Labhart et al., PRB **20**, 53 (1979)

Study of muon spin rotation of the superconducting state of organic superconductor λ-$(BETS)_2GaCl_4$

D. P. Sari,[*1,*2] R. Asih,[*1,*2] K. Hiraki,[*3] Y. Ishii,[*4] T. Nakano,[*2] Y. Nozue,[*2] and I. Watanabe[*1]

The Cooper pairing symmetry of the third-generation organic superconductor λ-$(BETS)_2GaCl_4$ has attracted interest owing to the strongly correlated nature of this system lying near the Mott insulating phase.[1] A recent high-resolution thermodynamic measurement reported *d*-wave pairing symmetry [2] whereas other experiments such as microwave conductivity measurement reported *s*-wave.[3] We report our experimental result of zero field (ZF) and transverse field (TF) μSR in the fields of 30 G down to 0.3 K at the RIKEN-RAL Muon Facility in the UK. From ZF-μSR, a slight increase in the muon-spin relaxation rate was observed below T_C = 5 K indicating a signature of the appearance of an unconventional SC state. The TF-μSR time spectrum at the base temperature of 0.3 K shows a damping behavior in comparison with that of the one at the normal state at 10 K owing to the appearance of the flux state, which produces a distribution of penetrated magnetic fields in the sample, as shown in Fig. 1.

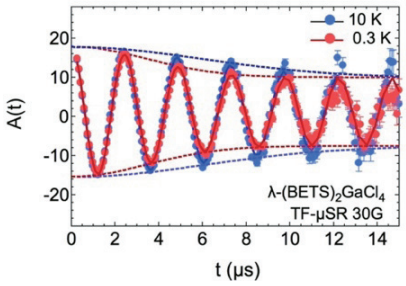

Fig. 1. TF-μSR time spectra of λ-$(BETS)_2GaCl_4$ in TF = 30 G at 0.3 K and 10 K. The red and blue dashed line are the results of fitting the data with Eq. (1).

We analyse the time spectra by using the following function

$$P^{TF}(t) = A_1 e^{-(\sigma^2 t^2)} \cos(\gamma_\mu H_1 t + \phi) + A_2 \cos(\gamma_\mu H_2 t + \phi) \quad (1)$$

Here, σ is the Gaussian damping rate representing the symmetric field distribution in the vortices felt by muons. The H_1 is the averaged field at the muon site in the sample and H_2 is the one in the Ag foil. A_1 and A_2 are initial asymmetry parameters of the Gaussian-type damping and the background components, respectively. A_2 was fixed to be that achieved at 0.3 K, and ϕ is the phase of the muon-spin precession. In the normal state, σ was estimated to be 0.1172 ± 0.0023 μs^{-1}.

The Gaussian damping rate in the SC state at 0.3 K, σ_{SC}, is estimated to be 0.1708 ± 0.0022 μs^{-1} by the relation $\sigma^2 = \sigma_{SC}^2 + \sigma_{NM}^2$ where σ_{NM} is the Gaussian damping rate by the nuclear moment in the normal state. For a pollycrystalline sample and large Ginzburg-Landau parameter κ ≫70, σ_{SC} is related to the superconducting penetration depth by the relation $\sigma_{SC} = \sqrt{0.00371}\,\Phi_0/\lambda^2$, where Φ_0= 2.07 x 10^{-15} is the flux quantum.

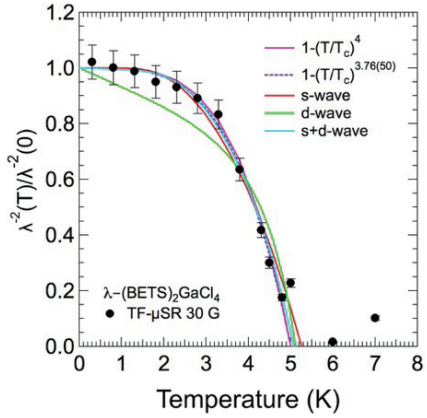

Fig. 2. Extracted temperature dependence of the normalized inverse magnetic penetration depth squared. The red, blue, and green solid lines show the result of fit using Eq. (2).

We could find a *d*–wave pairing contribution in the power-law fitting of λ(T) as a deviation from that expected for a typically full-gap *s*–wave pairing, power-value of which is 4. Furthermore, λ(T) curves can be fit in the clean limit using the following expression [4]:

$$\frac{\lambda^{-2}(T)}{\lambda^{-2}(0)} = 1 + \frac{1}{\pi}\int_0^{2\pi}\int_{\Delta(T)}^{\infty}\left(\frac{\partial f}{\partial E}\right)\frac{E dE d\phi}{\sqrt{E^2-\Delta^2(\phi,T)}} \quad (2)$$

where $f = [1+\exp(E/k_BT)]^{-1}$ is the Fermi function and the temperature dependence of the gap is approximated by $\Delta(T) = \Delta(0)\tanh\{1.82[1.018(T_C/T-1)]^{0.51}\}$. The angular function $\Delta(\phi) = \Delta_0$ in the *s*-wave model and $\Delta(\phi) = \Delta_0\cos(2\phi)$ in the *d*-wave model, where Δ_0 is constant. The curve can be well fit by the *s*-wave model. Interestingly, the data just below the T_c down to about 3 K well follow the fitting of the *d*-wave model and show a close agreement with the extracted critical temperature T_C = 5.1(1) K. Furthermore, we attempted to fit the data by using a simple superposition of a single-gap s-wave and single-gap *d*-wave, as shown in Fig. 2, in order to study if there is any hint of coexistence of *s*- and *d*-wave. Further experiments on TF-μSR under different fields and with higher statistics may be needed to make the current experimental results convincing.

*1 RIKEN Nishina Center
*2 Department of Physics, Osaka University
*3 Department of Physics, Gakushuin University
*4 Department of Physics, Shibaura Institute of Technology

References

1) H. Kobayashi et al., Phys. Rev. B. **56,** 8526(R) (1997).
2) S. Imajo et al., J. Phys. Soc. Jpn., **85**, 043705 (2016).
3) T. Suzuki et al., Physica C. **440,** 17 (2006).
4) S. Chandrasekhar, D. Einzel, Ann. Phys. **505,** 535 (1993).

Na diffusion in Na_xFeO_2

J. Sugiyama,[*1] I. Umegaki,[*1] H. Nozaki,[*1] M. Månsson,[*2] O. K. Forslund,[*2] Y. Sassa,[*3] K. Ishida, [*4] and I. Watanabe [*4]

In order to develop next-generation Na-ion batteries,[1] we have attempted to measure Na diffusion in several candidate materials with μ^+SR.[2] The present target compound, α-$NaFeO_2$, has a layered rocksalt structure with the trigonal space group $R\bar{3}m$ (Fig. 1). The isostructural compound, $NaCoO_2$, works as a positive electrode material owing to reversible Na^+ deintercalation from and intercalation into the lattice.[3] Furthermore, μ^+SR clearly detected Na diffusive behavior in Na_xCoO_2 at high T,[2] which is consistent with electron diffraction and neutron scattering results.[4] However, α-$NaFeO_2$ does not exhibit reversible Na deintercalation and intercalation behavior.[5]

The following two explanations were proposed for such behavior in α-$NaFeO_2$, 1) Na ions do not diffuse, or 2) Na ions diffuse, but electrons are not transferred for charge compensation. Since α-$NaFeO_2$ is an antiferromagnetic insulator,[6,7] the second explanation is more reasonable.

Figure 2 shows the T dependences of the field fluctuation rate (ν) and field distribution width (Δ) for α-$NaFeO_2$ and $Na_{0.7}CoO_2$ extracted from the μ^+SR spectra measured on ARGUS. Here, ν corresponds to the spin-lattice relaxation rate (T_1^{-1}) of NMR, and Δ corresponds to the spin-spin relaxation rate (T_2^{-1}). For $Na_{0.7}CoO_2$, ν increases with T particularly above 325 K, while Δ decreases with T. This is a typical motional narrowing behavior due to Na diffusion.

For α-$NaFeO_2$, both ν and Δ are scattered in the whole T range measured. In particular, there is no acceptable reason for the increase in Δ above 300 K. Note that even for stoichiometric $NaFeO_2$, there are interstitial sites between two adjacent Na^+ ions, to which Na^+ ions jump, as in the case for $LiNiO_2$.[8] Back to the data analysis, the ZF- and LF-spectra were fitted by a combination of an exponentially relaxing dynamic Kubo-Toyabe signal and a time-independent background signal from the muons stopped in the sample holder. This indicates the presence of two muon sites in the lattice, although the muon sites are unknown at present. However, owing to the large exponential relaxation of the two terms caused by the fluctuation of the Fe^{3+} moments, it is very difficult to extract ν and Δ from the present μ^+SR spectrum with the statistics of 18M events. Thus, we need additional data with higher statistics.

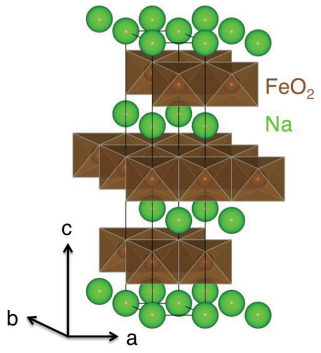

Fig. 1. Crystal structure of α-$NaFeO_2$ consisting of a two-dimensional triangular lattice of FeO_2 layers formed by edge sharing FeO_6 octahedra separated by the Na layer.

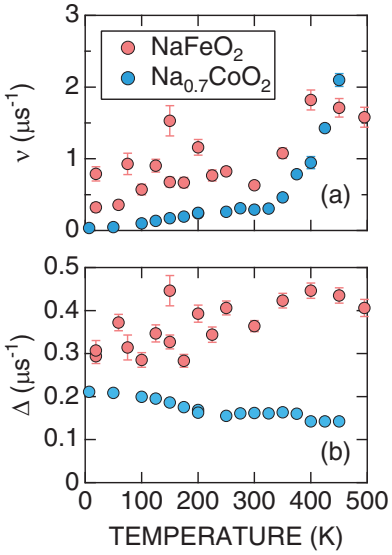

Fig. 2. T dependences of the field fluctuation rate (ν) and field distribution width (Δ) for α-$NaFeO_2$ and $Na_{0.7}CoO_2$.

*1 Toyota Central Research and Development Labs., Inc.,
*2 Department of Materials and Nanophysics, KTH Royal Institute of Technology,
*3 Department of Physics and Astronomy, Uppsala University,
*4 RIKEN Nishina Center

References
1) S-W. Kim et al., Adv. Energy Mater. **2**, 710 (2012).
2) M. Månsson, J. Sugiyama, Phys. Scr. **88**, 068509 (2013).
3) L. W. Shacklette et al., J. Electrochem. Soc. **135**, 2669 (1988).
4) M. Medarde et al., Phys. Rev. Lett. **110**, 266401 (2013).
5) M. C. Blesa et al., Solid State Ionics **126**, 81 (1999).
6) T. Ichida et al., J. Phys. Soc. Jpn. **29**, 795 (1970).
7) T. McQueen et al., Phys. Rev. B **76**, 024420 (2007).
8) J. Sugiyama et al., Phys. Rev. B **82**, 224412 (2010).

Solute-vacancy clustering in Al-Mg-Si and Al-Si alloys

K. Nishimura,[*1,*3] K. Matsuda, [*1,*3] T. Namiki,[*1] S. Lee,[*1] N. Nunomura,[*2]
I. Watanabe,[*3] M. A. Jaward,[*3] S. Yoon,[*3] and T. Matsuzaki[*3]

Al-Mg-Si (6xxx series) aluminum alloys are in high demand as materials for vehicles because of their low weight, excellent formability and age hardenability. The usual process for heat treatment is solution heat treatment at approximately 820 K followed by quick quenching in water, resulting in a supersaturated solid solution (SSSS). After inevitable storage at room temperature (called natural aging, NA), the alloy is subjected to artificial aging (AA) at approximately 420 K, leading to a precipitation sequence:[1)]
SSSS $\rightarrow$Mg/Si/vacancy cluster $\rightarrow$Guinier Preston (GP) zone $\rightarrow\beta''\rightarrow\beta'\rightarrow\beta(Mg_2Si)$.

It is well known that the early stage of solute clustering of Mg and Si proceeds quite quickly and is completed in less than an hour even at room temperature.[2-4)] A long-standing problem for the industry is that NA treatment often results in a negative effect on the mechanical strength in the subsequent AA treatment.[1, 5)] From various studies on Al-Mg-Si alloys, vacancy behavior is considered to play an important role in the aging process, stimulating the diffusion of solute Mg and Si atoms and nucleation of clusters. Positron annihilation spectroscopy (PAS)[3, 4)] and muon spin relaxation spectroscopy (μSR)[6, 7)] have been successfully used to investigate the vacancy and clustering behavior in Al-Mg-Si alloys.

New observations of time dependent muon spin relaxation and direct current (DC) magnetization of an Al-1.6%Mg_2Si alloy in the isothermal condition at 280, 290, or 300K are presented in this report. All the samples underwent heat treatment at 848 K for 1 h and subsequently quenching in ice water (STQ). Approximately 10 min after STQ, the sample was inserted into the ARGUS muon spectrometer, and then zero-field μSR measurement was started at a constant temperature. The observed spin relaxation spectra were fit using a Gaussian function with standard deviation $1/\sigma$ using the WIMDA program,[8)] where σ is a measure of the depolarization rate of the muon spins as shown in Fig. 1(a). A similar sample treatment was performed in the magnetization measurements, which were carried out with a superconducting quantum interference device (SQUID) magnetometer (Quantum Design, MPMS-XL7) (Fig. 1(b)[9)]). The M_0 value is approximately 0.04 Am^2/kg. The time variations of the depolarization rates and the magnetizations at the corresponding measurement temperature appear to resemble each other. We attempted to estimate the migration energy of Mg/Si/vacancy in the non-equilibrium condition, assuming that the time variation of σ is brought about by the diffusion of these elements with the relations $\sigma=\sigma_0\exp(-\tau t)$ and $\tau=\tau_0\exp(-E/kT)$ (τ: reaction rate, and E: migration energy). From the recent studies of time dependent magnetizations[9)] and positron annihilation spectroscopy[3)] the Mg/Si/vacancy clustering (stage III) was found to proceed in a certain time window depending on the aging temperature. In the present σ vs. t curves we set the time windows as above 400, 70-500, and 30-150 min at 280, 290 and 300 K, respectively. The selected data points in Fig. 1(a) are marked with filled symbols. Fig. 2 shows an Arrhenius plot of ln(τ) vs T which yields E = 0.18 eV. Further μSR experiments of Al-Mg-Si-Cu, Al-Si and Al-Mg samples have been conducted to investigate the details of solute elements and vacancy kinetics.

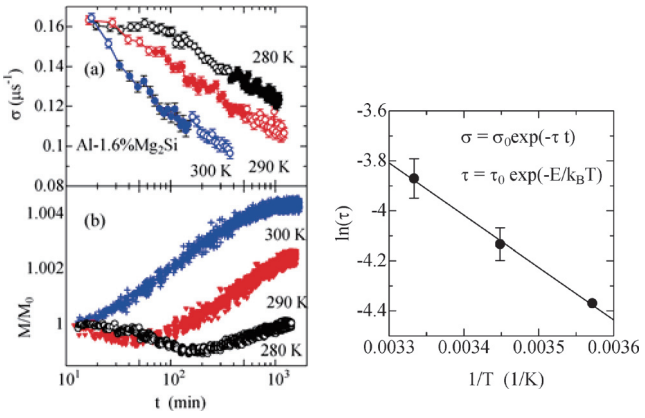

Fig. 1 (left). Aging time dependences of (a) zero-field spin relaxation rate and (b) normalized DC magnetization with an Al-1.6%Mg2Si sample at constant temperatures of 280, 290 and 300 K.

Fig. 2 (right). An Arrhenius plot for the reaction rate against temperature.

References

1) S. Pogatscher et al., Acta Mater. **59**, 3352 (2011).
2) H. Seyedrezai et al., Mater. Sci. Eng. **A525**, 186 (2009).
3) J. Banhart et al., Phys. Rev. B **83**, 014101 (2011).
4) A. Somoza et al., Phys. Rev. B **61**, 14454 (2000).
5) S. Pogatscher et al., Phy. Rev. Lett. **112**, 225701 (2014).
6) S. Wenner et al., Phys. Rev. B **86**, 104201 (2012).
7) S. Wenner et al., Acta Mater. **61**, 6082 (2013).
8) F. L. Pratt, Physica B**289,** 710 (2000).
9) K. Nishimura et al., Mater. Trans. **56,** 1307 (2015).

*1 Department of Materials Science and Engineering, U. Toyama
*2 Information Technology Center, U. Toyama
*3 RIKEN Nishina Center

Beamline tune for muonium emission from silica aerogel towards ultra-slow muon project at RIKEN-RAL

S. Okada,[*1] S. Aikawa,[*2] G. Beer,[*3] J. Brewer,[*4] K. Ishida,[*2] M. Iwasaki,[*2] S. Kanda,[*5] H. Kawai,[*6] R. Kitamura,[*5] Y. Ma,[*2] G. Marshall,[*4] T. Mibe,[*7] Y. Oishi,[*8] A. Olin,[*4] M. Otani,[*7] N. Saito,[*7] M. Sato,[*9] M. Tabata,[*6] and T. Tsukihana[*10]

A sharp low-energy muon beam may be realized by accelerating several-eV positive muons, so-called ultra-slow muons, generated by the laser ionization of thermal muonium atoms in vacuum.[1,2] This technology is the focus of attention in material science using μSR techniques and particle physics, e.g., measurement of the muon anomalous magnetic moment, g-2, and electric dipole moment at J-PARC.[3]

Continued research on muonium emission into vacuum from several stopping materials revealed that silica aerogel with a laser-ablated surface is a good candidate.[4] To demonstrate the actual ultra-slow muon production with silica aerogel, a new experimental setup has been prepared at RIKEN-RAL, as previously reported.[5] Here, we report the results of a commissioning run conducted in September 2016.

Positive muons stopping in the surface region of the aerogel target contribute to muonium emission into vacuum. To maximize this for the beam at RIKEN-RAL,[6] we adjusted the thickness of a degrader so that the number of muons stopping in the aerogel is approximately half of the full stop, while the remainder passed through mostly to regions beyond those of interest for muonium decay in vacuum. Since aerogel is the only material capable of muonium production installed in the setup, we can assess the amount of muonium produced by measuring asymmetry amplitudes at time zero of the muonium precession signal with a frequency of 13.9 GHz/T, well separated from the frequency of muons, 136 MHz/T.

Figure 1(a) shows our experimental setup. A three-axis Helmholtz coil system is used for the cancellation of stray magnetic fields, and for applying a transverse field of 0.18 mT to rotate the spin of muonium. Figure 1(b) shows a typical muonium spin rotation asymmetry distribution measured by a set of μSR counters. The fit result shows a rotation cycle of 400 ns being consistent with our expectation for muonium with 0.18 mT. Figure 1(c) shows the measured range curve as a function of the total thickness of aluminum-foil degraders, where degrader thicknesses for "full-stop" and "half-stop" conditions are indicated. The aerogel target has a density of 28 mg/cm^3 and thickness of 7.8 mm which corresponds approximately to the full stop range. The obtained curve was consistent with a momentum bite of 2% assuming a Gaussian distribution at RIKEN-RAL.[6] The absolute values of muonium asymmetry amplitudes are also comparable with what we assessed with a Monte Carlo simulation.

Now we have established the method of degrader tuning and are ready for a laser ionization study.

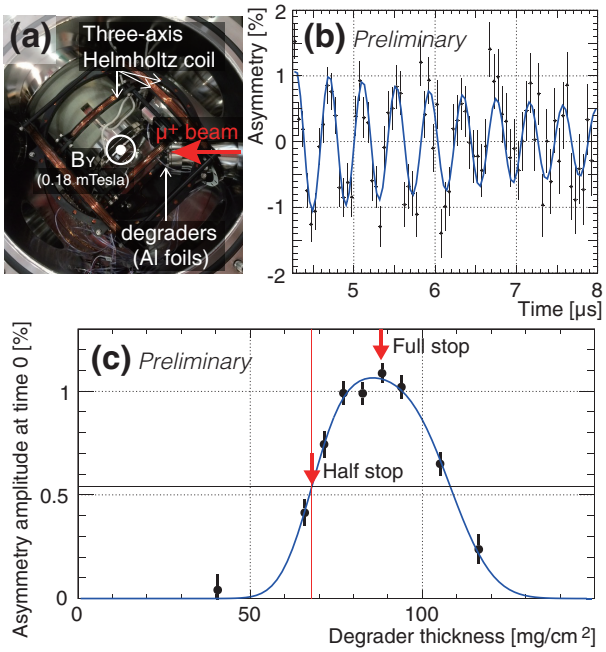

Fig. 1. (a) Photograph of the experimental setup at the Port 3 beamline of the RIKEN-RAL muon facility. (b) A typical muonium spin rotation asymmetry distribution, where the muon exponential decay time dependence has been removed. (c) Range curve obtained by measuring the asymmetry of muonium produced at a silica aerogel target as a function of degrader thickness.

*1 AMO Physics Laboratory, RIKEN
*2 RIKEN Nishina Center
*3 Department of Physics and Astronomy, UVic
*4 Science Division, TRIUMF
*5 Department of Physics, The University of Tokyo
*6 Department of Physics, Chiba University
*7 IPNS, KEK
*8 IMSS, KEK
*9 Condensed Molecular Materials Laboratory, RIKEN
*10 RIKEN Center for Advanced Photonics

References

1) K. Nagamine et al., Phys. Rev. Lett. **74**, 4811 (1995).
2) P. Bakule et al., NIM B **266**, 355 (2008).
3) M. Aoki et al., Conceptual Design Report for The Measurement of the Muon Anomalous Magnetic Moment g−2 and Electric Dipole Moment at J-PARC, (2011).
4) G. A. Beer et al., PTEP **2014**, 091C01 (2014).
5) S. Okada et al., RIKEN Accel. Prog. Rep. **49**, 228 (2015).
6) T. Matsuzaki et al., NIM A **465**, 365 (2001).

Background study with negative muons in RIKEN-RAL for the laser spectroscopy of hyperfine splitting energy in muonic hydrogen

M. Sato,[*1] S. Aikawa,[*2,*3] K. Ishida,[*2] M. Iwasaki,[*2,*3] S. Kanda,[*4] Y. Ma,[*2] Y. Matsuda,[*5] K. Midorikawa,[*6] Y. Oishi,[*7] S. Okada,[*8] N. Saito,[*6] A. Takamine,[*2] K. Tanaka,[*9] H. Ueno,[*2] S. Wada,[*6] and M. Yumoto[*6]

We are planning a new measurement of the hyperfine splitting energy in ground-state muonic hydrogen in the RIKEN-RAL muon facility. This project was motivated by *the proton radius puzzle*, which is an unsettled problem on the root-mean-square charge radius of protons. Conventionally, the charge radius has been determined by electron-proton scattering and atomic hydrogen spectroscopy as compiled in CODATA.[1] However, the charge radius determined from the Lamb shift in muonic hydrogen has a value smaller by 4 %, which corresponds to 7 times the standard deviation.[2,3] Thus far, there has been no definitive explanation for this puzzling discrepancy.

In our proposed experiment, we will determine the proton Zemach radius, which is a convolution of the proton charge and magnetic moment distributions. Since the Zemach radius can be determined from the hyperfine splitting energy in hydrogen-like atoms, we derive it from muonic hydrogen which is a Coulomb bound system consisting of a negative muon and a proton. Then, we can obtain information on the magnetic structure inside the proton by probing with muons.

For laser spectroscopy, muon spin is re-polarized by a circularly polarized laser in the laser-induced transition between hyperfine sub-levels. The polarized muons have a spatial asymmetry in the electron emission from the muon decay ($\mu^- \rightarrow e^- + \overline{\nu_e} + \nu_\mu$). The resonance can be identified by detecting the spatial distribution of electrons.

In the experiment, pulsed negative-muons are stopped in a hydrogen target to form muonic hydrogen. The pulsed laser used to induce the transition between hyperfine sublevels is irradiated with a delay of 1 μs from muon stoppage to suppress background events caused by muon stoppage due to materials in other than the hydrogen target. Since the negative muon capture rate is proportional to Z^4, muons stopped in high-Z materials around the target are quickly captured. In this manner, we aim to achieve a reduction factor greater than 10^{-4} at 1 μs compared to the prompt timing events at the time of muon stoppage.

*1 Condensed Molecular Materials Laboratory, RIKEN
*2 RIKEN Nishina Center
*3 Department of Physics, Tokyo Institute of Technology
*4 Department of Physics, The University of Tokyo
*5 Graduate School of Arts and Science, The University of Tokyo
*6 RIKEN Center for Advanced Photonics
*7 Institute of Materials Structure Science, KEK
*8 AMO Physics Laboratory, RIKEN
*9 Cyclotron and Radioisotope Center, Tohoku University

For the study of the background level, the timing spectrum after muon stoppage was measured in the RIKEN-RAL PORT-4 beam line. In the beam time in March 2016, we acquired data using an existing μSR spectrometer in PORT-4 (CHRONUS), which consists of segmented plastic scintillation counters. Each segment was viewed using a photomultiplier tube with wavelength shifting fiber.[4] The timing spectrum obtained by CHRONUS is shown by the red line in Fig. 1. The inset shows a close-up of the prompt timing which shows peaks caused by electrons and muons in a double pulse. In the spectrum, there is an unknown long-tail component which is the severe background of the measurement. To suppress this background, we prepared another type of counters in the successive beam time in May 2016. It has two-layered plastic scintillation counters with photomultiplier tubes on both sides. We acquired the timing spectrum with the coincidence of the two counters. As shown by the blue line in Fig. 1, the long-tail component was drastically suppressed. The reduction factor is greater than 10^{-4}, which is sufficient for the measurement. The origin of the component is still not understood, but it may be caused by neutral particles coming along with a negative muon pulse. Further investigation will be conducted in RIKEN-RAL, and the design of the electron counter will be finalized based on these studies.

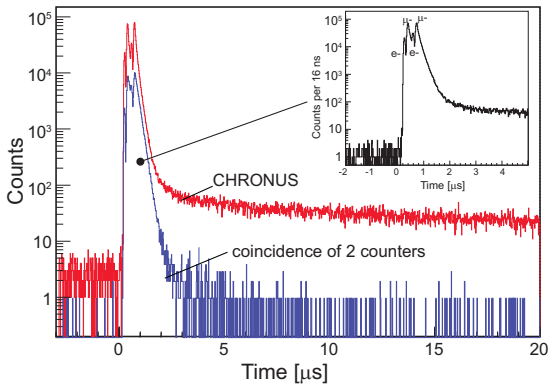

Fig. 1. Time spectra with negative muons obtained by CHRONUS (red) and coincidence counters (blue).

References

1) P. J. Mohr, B. N. Tylor, D. B. Newell, Rev. Mod. Phys. **84**, 1527 (2012).
2) R. Pohl et al., Nature **466**, 213 (2010).
3) A. Antognini et al., Science **339**, 417 (2013).
4) D. Tomono et al., J. Phys. Conf. Ser. **225**, 012056 (2010).

3. Radiochemistry and Nuclear Chemistry

Observation of the extraction of Fr^{2+} from a cryogenic gas cell†

P. Schury,[*1] M. Wada,[*1,*2] Y. Ito,[*2] H. Haba,[*2] Y. Hirayama,[*1] D. Kaji,[*2] S. Kimura,[*1,*2,*3] H. Koura,[*4] H. Miyatake,[*1] J.Y. Moon,[*7,*1] K. Morimoto,[*2] K. Morita,[*2,*5] A. Ozawa,[*2,*3] M. Rosenbusch,[*2] M. Reponen,[*2] A. Takamine,[*2] T. Tanaka,[*2,*5] Y. X. Watanabe,[*1] and H. Wollnik[*6]

The SHE-mass project is a joint effort between KEK and RIKEN with a long-term goal of identifying new superheavy element (SHE) isotopes produced via hot fusion. It makes use of cryogenic-capable, high-purity helium gas cell to convert the energetic (5∼50 MeV) evaporation products of fusion reactions into thermal ions. The evaporation products are separated from projectile-like fragments by use of the GARIS-II[1] gas-filled recoil ion separator. The thermalized ions are transferred to a multi-reflection time-of-flight mass spectrograph[2] (MRTOF) which can analyze the ions with a mass resolving power of $R_{\rm m} > 100\,000$. The SlowSHE system is described in some detail in[3].

To identify such low-yield species as new SHE will require an extremely low stable ion background rate. The primary source for stable background ions being charge exchange with contaminants in the gas cell, the gas cell has been designed to operate at cryogenic temperatures down to 50 K. At such temperatures, contaminants in the gas are expected to freeze out.

During the first commissioning runs of the SHE-mass project, masses of several isotopes of Fr, Rn, At, Po, and Bi were measured[3] as singly-charged ions. At that time the gas cell was operated near room temperature, as upon cooling the gas cell the radioactive ions ceased to be observed. One preliminary conjecture was that thermal contraction during cooling may be lead to misalignment of the gas cell extraction optics.

In December 2016, ions of short-lived Ac isotopes were produced with the reaction ^{169}Tm(^{48}Ca, xn)$^{217-x}$Ac with a bombarding energy of 232 MeV to study the gas cell system under cryogenic conditions, T≈150 K. As the 11.8 eV second ionization potential of actinium[4] is well-below the 24.6 eV first ionization potential of He, the system was optimized for Ac^{2+}. In the time-of-flight (ToF) spectrum, the intensity of the peak associated with a given Ac isotope could then be used to optimize the magentic field settings of GARIS-II and the thickness of the energy degrader between GARIS-II and the gas cell. Peaks were observed in the ToF spectra corresponding to a range of A/q, not all making the same number of laps in the MRTOF. By scaling the known period of circulation for a $^{133}Cs^{+}$ reference, it was possible to identify peaks corresponding to ions making different numbers of laps than the reference. Unexpectedly, fairly intense peaks were identified corresponding to $^{208-210}Fr^{2+}$, as shown in Fig. 1.

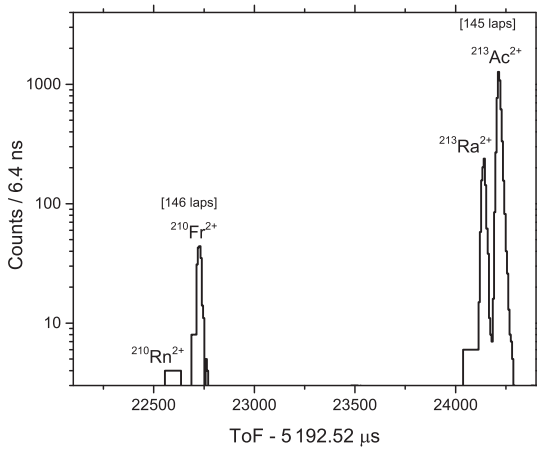

Fig. 1. Portion of observed ToF spectrum from the reaction ^{169}Tm(^{48}Ca, xn)$^{217-x}$Ac.

The production of Fr isotopes via ^{169}Tm(^{48}Ca, αxn)$^{213-x}$Fr is not unexpected[3]. However, francium being an alkali element with a second ionization potential of 22.4 eV[4], merely 2.2 eV below the first ionization potential of He, it was a surprise to observe Fr^{2+} ions. As the production yield of Fr could not be easily determined due to being the α daughter of Ac, the fraction of Fr ions extracted as doubly-charged could not be inferred from this measurement.

In a followup measurement with a ^{165}Ho target, Fr isotopes were directly produced. Preliminary analysis of these data indicate that Fr^{2+} was the dominant charge state. From this observation it can be inferred that in cryogenic operation, most elements should be expected to be extracted as 2+ or even 3+ ions.

References

1) D. Kaji, K. Morimoto, N. Sato, A. Yoneda, K. Morita, Nucl. Inst. and Methods in Phys. Res. B **317** (2013) 311-314.
2) P. Schury et al., Nucl. Inst. and Methods in Phys. Res. B **335** (2014) 39-53.
3) P. Schury et al., Phys. Rev. C **95** (2017) 011305(R).
4) A. Kramida, Yu. Ralchenko, J. Reader, and NIST ASD Team (2014). NIST Atomic Spectra Database (ver. 5.2), [Online]. Available: http://physics.nist.gov/asd [2016, December 27]. National Institute of Standards and Technology, Gaithersburg, MD.

† Condensed from 10.1016/j.nimb.2017.06.014

*1 KEK Wako Nuclear Science Center (WNSC)
*2 RIKEN Nishina Center
*3 Institute of Physics, University of Tsukuba
*4 Advanced Science Research Center, JAEA
*5 Dept. Physics, Kyushu University
*6 New Mexico State University
*7 Institute for Basic Science

On-line column chromatography of ^{88}Nb with 52 wt% Aliquat 336 resin from HF media for Db experiment

D. Sato,[*1,*2] M. Murakami,[*1] S. Goto,[*1] K. Ooe,[*1] R. Motoyama,[*1] K. Shirai,[*1] S. Tsuchiya[*5]
H. Haba,[*2] Y. Komori,[*2] S. Yano,[*2] A. Toyoshima,[*3] A. Mitsukai,[*3] H. Kikunaga,[*4] and H. Kudo[*5]

The elements with atomic number ≥ 104 are called super-heavy elements. Aqueous chemistry experiments with these elements have been performed often by using the Automated Rapid Chemical Apparatus (ARCA). In particular, an anion-exchange experiment of element 105, Db was successfully performed in 13.9 M hydrofluoric acid solution.[1] However, the complex formation of Db with the fluoride ion is still not clear, and further investigation of extraction behavior of Db in various concentrations of HF is needed. We have been studying the solid-liquid extraction behavior of group-5 elements, Nb and Ta, which are lighter homologues of Db, with Aliquat 336 resin in various HF solutions.[2] The obtained results showed that this extraction system is applicable to the on-line column chromatographic experiment of Db with ARCA. In this work, the solid-liquid extraction of Nb was conducted with 52 wt% Aliquat 336 resin in HF solution by the batch method and by using ARCA.

A 52 wt% Aliquat 336 resin was prepared by mixing MCI GEL CHP20/P30 with Aliquat 336 dissolved in methanol for about 1 day, which was followed by drying in an oven at 80 °C.[3] The isotope ^{88}Nb was produced in the ^{nat}Ge (^{19}F,xn)^{88}Nb reaction, at the RIKEN K70 AVF Cyclotron. The batch experiment and on-line column chromatographic experiment of ^{88}Nb were conducted to ermine the suitable experimental condition for the Db experiment. The experimental procedure of the batch experiment was almost the same as described in ref. [4]. In the on-line column chromatographic experiment of Nb with ARCA, the reaction products transported by the He/KCl gas-jet system were deposited on the collection part in ARCA for 300 s. Then, the products were dissolved in 2.7-27 M HF solutions and loaded on a chromatographic column (1.6 mm i.d. × 7.0 mm height) filled with the 52 wt% Aliquat 336 resin at a flow rate of 1.0 mL/min. The effluent was collected into 7 sample tubes as primary fractions for a few seconds each. The remaining products in the column were stripped with 6 M HNO_3/0.015 M HF solution at a flow rate of 1.0 mL/min. The effluent was collected in another sample tube as a secondary fraction. These samples were then subjected to γ-ray spectrometry using a Ge detector.

Figure 1 shows the distribution coefficients, K_d, of ^{88}Nb obtained in the batch experiment as a function of initial HF concentration, $[HF]_{ini}$. The K_d values of long-lived ^{95g}Nb and ^{179}Ta isotopes obtained in the previous batch experiment at 1.0-27 M HF[4] are also shown in Fig. 1. The K_d values of ^{88}Nb at 2.7 M and 27 M HF obtained in the present batch experiment are in good agreement with those of ^{95g}Nb obtained in the previous study. However, at 5.4 M and 10 M HF, the K_d values of ^{88}Nb showed higher values compared to those of ^{95g}Nb. The reason for this discrepancy is under investigation. In the on-line column chromatographic experiment, the elution curves for ^{88}Nb were measured at 2.7 M HF, and the K_d value of ^{88}Nb was calculated from eluted the volume peak, V_p, based on the Glückauf equation.[2] The obtained K_d value for ^{88}Nb in column experiment at 2.7 M HF is in accordance with the results of batch experiment of both ^{88}Nb and ^{95g}Nb. Therefore, the same fluoride complex of Nb may be formed in both on-line and batch experiments at 2.7 M HF. After these experiments, a Db experiment with 52 wt% Aliquat 336 resin in 2.7 M HF was conducted. The results of the Db experiment are now under analysis.

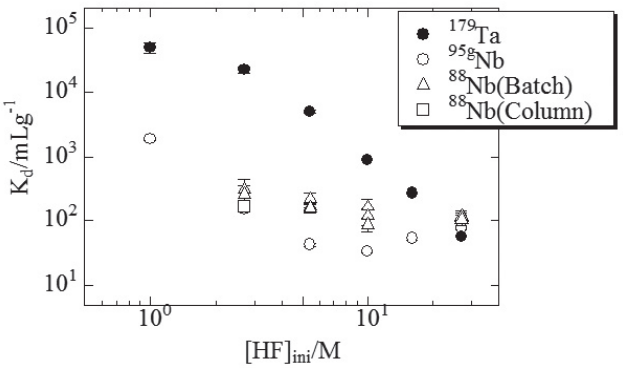

Fig. 1. Comparison of adsorption behavior of ^{88}Nb with that of ^{95g}Nb on 52 wt% Aliquat 336 resin as a function of $[HF]_{ini}$.

References

1) K. Tsukada et al., Radiochim. Acta. **97**, 83-89, 2009.
2) D. Sato et al., 59th Japan Society of Nuclear and Radiochemical Sciences, September 25-29, 2015, Sendai, Japan.
3) H. Haba et al., Radiochim. Acta. **95**, 1, 2007.
4) D. Sato et al., In this report.

[*1] Graduate School of Science and Technology, Niigata University
[*2] RIKEN Nishina Center
[*3] Japan Atomic Energy Agency
[*4] Research Center for Electron Photon Science, Tohoku University
[*5] Department of Chemistry, Faculty of Science, Niigata University

On-line solvent extraction of Re with a rapid solvent extraction apparatus coupled to the GARIS gas-jet system

Y. Komori,[*1] H. Haba,[*1] K. Ooe,[*2] D. Kaji,[*1] Y. Kasamatsu,[*3] H. Kikunaga,[*4] A. Mitsukai,[*5] K. Morimoto,[*1] R. Motoyama,[*2] J. P. Omtvedt,[*6] Z. Qin,[*7] D. Sato,[*2] N. Sato,[*1] Y. Shigekawa,[*3] T. Tanaka,[*1] A. Toyoshima,[*5] K. Tsukada,[*5] Y. Wang,[*7] K. Watanabe,[*1] S. Wulff,[*6] S. Yamaki,[*1] S. Yano,[*1] and Y. Yasuda[*3]

To enable aqueous chemistry studies of Sg (atomic number Z = 106) and Bh (Z = 107), we have been developing a continuous rapid solvent extraction apparatus coupled to the GARIS gas-jet transport system.[1)] This apparatus consists of a continuous dissolution apparatus called the Membrane DeGasser (MDG)[2)], a Flow Solvent Extractor (FSE), and liquid scintillation detectors for the α/SF-spectrometry. The FSE consists of a Teflon capillary (i.d. = 0.5 mm) and a phase separator. In our previous study,[1)] we investigated the performances of the MDG and FSE using lighter homologs of Bh, ^{92,94m}Tc ($T_{1/2}$ = 4.25, 293 min) and ^{181}Re ($T_{1/2}$ = 19.9 h), produced in the ^{nat}Mo(d,xn) and ^{nat}W(d,xn) reactions, respectively, at the AVF cyclotron. In this work, we coupled the MDG and FSE to the GARIS gas-jet system and performed on-line solvent extraction of the ^{174,176}Re ($T_{1/2}$ = 2.4, 5.3 min) produced in the ^{nat}Gd(^{23}Na,xn) reactions.

The $^{nat}Gd_2O_3$ target with a thickness of 349 μg/cm^2 was prepared by electrodeposition onto a 3-μm Ti foil. The $^{23}Na^{7+}$ ion beam was extracted from RILAC. The beam energy was 124.3 MeV at the middle of the target, and the typical beam intensity was 1.6 particle μA. The nuclear reaction products after preseparation with GARIS were guided into a gas-jet chamber (100-mm i.d.×20-mm depth) through a 2.5-μm Mylar window. The products were then transported to the MDG, which was placed in a chemistry laboratory through a Teflon capillary (2.0-mm i.d. × 10-m length) by He carrier gas at a flow rate of 1.5 L/min with KCl aerosols. In the MDG, they were continuously dissolved in 0.5 M HNO_3 at 1 mL/min. The effluents from the MDG were mixed with 1 mL/min of tri-*n*-octylamine (TOA) in toluene in the Teflon capillary of the FSE. After the phase separation, both aqueous and organic phases from the FSE were subjected to γ-ray spectrometry with a Ge detector to determine the distribution ratios (D) in the solvent extraction. We measured the D values of ^{174,176}Re by varying the capillary length of the FSE from 30 cm to 100 cm to change the extraction time. We also varied the concentration of TOA from 0.005 M to 0.1 M to determine the applicable D range using the 40-cm capillary of the FSE. These D values were compared with those in equilibrium obtained in the off-line batch extractions with ^{181}Re. The chemical yields (C.Y.) of ^{174,176}Re were determined as C.Y. = ($[A]_{org.}$ + $[A]_{aq.}$)×100/$[A]_{fil.}$, where $[A]_{org.}$ and $[A]_{aq.}$ indicate the radioactivities in the organic and aqueous phases, respectively, and $[A]_{fil.}$ is the radioactivity in the aerosols collected on the glass fiber filter in the chemistry laboratory.

Figure 1 shows the variation of the D values of ^{174,176}Re as a function of the capillary length. The dashed line indicates the D value of ^{181}Re in equilibrium obtained in the batch extraction. We found that the extraction equilibrium of ^{174,176}Re in 0.5 M HNO_3 - 0.01 M TOA in toluene can be attained with a 0.5-mm i.d. × 30-cm capillary at 1 mL/min for both aqueous and organic solutions. However, for TOA concentrations ≥ 0.05 M, it was found that the 40-cm capillary was too short to reach the extraction equilibrium. When using the 100-cm capillary of the FSE, the D values of ^{174,176}Re were consistent with those in equilibrium in the wide range of D = 0.3–20 in TOA concentrations of 0.005–0.1 M. The average chemical yields are 71 ± 15% for ^{174}Re and 79 ± 18% for ^{176}Re. Very recently, we performed solvent extraction with the short-lived ^{170}Re ($T_{1/2}$ = 9.2 s) produced in the ^{152}Gd(^{23}Na,5n) reaction with the GARIS gas-jet + MDG and FSE system as a model experiment for ^{266}Bh ($T_{1/2}$ = 10.3 s).[3)] The result of this experiment is under analysis.

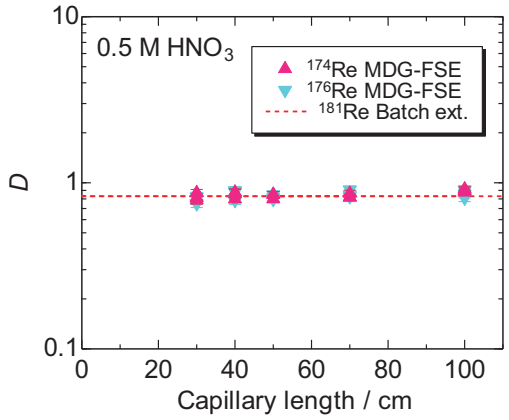

Fig. 1. Variation of the D values of ^{174,176}Re as a function of capillary length. The concentrations of HNO_3 and TOA are 0.5 M and 0.01 M, respectively. The dashed line indicates the D value of ^{181}Re in equilibrium obtained in the batch extraction.

*1 RIKEN Nishina Center
*2 Graduate school of Sci. and Technol., Niigata Univ.
*3 Graduate school of Sci., Osaka Univ.
*4 ELPH, Tohoku Univ.
*5 JAEA
*6 Univ. Oslo
*7 Institute of Modern Physics, Chinese Academy of Sciences

References

1) Y. Komori et al., RIKEN Accel. Prog. Rep. **49**, 21 (2016).
2) K. Ooe et al., J. Radioanal. Nucl. Chem. **303**, 1317 (2015).
3) H. Haba et al., 9th International Conference on Nuclear and Radiochemistry, P2-17, Helsinki, Finland, Aug.–Sep., 2016.

Extraction behavior of ^{93m}Mo and ^{179}W from HF / HCl into Aliquat336 as model experiments for seaborgium (Sg)

A. Mitsukai,[*1,*2] A. Toyoshima,[*2] Y. Komori,[*3] S. Yano,[*3] H. Haba,[*3] M. Asai,[*2] K. Tsukada,[*2] T.K. Sato,[*2] and Y. Nagame[*1,*2]

Chemical studies of superheavy elements with atomic numbers $Z \geq 104$ provide not only crucial and challenging opportunities to advance our understanding of the properties of matter at the limits of existence but also elucidate the influence of relativistic effects on atomic electrons and the architecture of the farthest of the periodic table of elemetnts.[1,2] These elements are all artificial and synthesized at accelerators using nuclear reactions of heavy-ion beams with heavy element target materials. As both the half lives and cross sections of these nuclides are rapidly decreasing with increasing Z, they are usually available in quantities of only a few atoms or often one atom at a time.

Recently, we started studying the aqueous chemistry of element 106, seaborgium (Sg), to clarify its complex formation and redox reactions in aqueous phases. In this work, the solvent extraction behavior of molybdenum (Mo) and tungsten (W), which are lighter homologs of Sg, from a HF/HCl mixed solution into toluene with an amine extractant Aliquat336 is studied by a batch wise method to elucidate the complex formation of these homologs.

At the RIKEN AVF cyclotron, ^{93m}Mo and ^{179}W were produced in the ^{93}Nb(d, $2n$)^{93m}Mo and ^{nat}Ta(d, xn)^{179}W reactions, respectively. The reaction products were transported to the laboratory by a gas-jet method and deposited on a small Naflon® sheet. The deposited products were dissolved with 700 μL of HF/HCl and the solution was collected in a plastic tube. Then the same volume of Aliquat336/toluene solution was added to this HF/HCl solution. The mixture was shaken for 60 s. (In a separate experiment, we confirmed that the chemical equilibrium of this reaction was accomplished within 60 s in the present system.)[3] After centrifugation, the aqueous and organic solutions were separately taken in plastic tubes for γ-ray spectrometry with a Ge detector. The distribution ratio (D) is defined as the ratio of radioactivity per unit volume between two phase as $D = (A_{org} / V_{org}) / (A_{aq} / V_{aq})$, where A_{org} and A_{aq} denote radioactivities in the organic and aqueous phases, respectively, and V_{org} and V_{aq} represent the volumes of the organic and aqueous phases, respectively.

In the batch experiments, the concentration of HF was varied from 10^{-4} to 5 M, while those of HCl and Aliquat336 were fixed to be 1 M and 0.2 M, respectively. In Fig. 1, variations of the D values of Mo and W are shown as a function of HF concentration, [HF]. The D values of both elements start to increase steeply at approximately [HF] = 10^{-2} M, indicating that anionic fluoride complexes are formed beyond that concentration. Above [HF] = 10^{-1} M, on the other hand, the D values of Mo and W decrease with increasing [HF]. This is due to the increase of the HF_2^- concentration; the extraction of HF_2^- is competed with that of anionic fluoride complexes of Mo and W. Under the present conditions, we clearly observed the formation of anionic fluoride complexes of Mo and W. In the next step, the extraction behavior of Mo and W will be investigated while varying the Aliquat336 concentration in the HF/HCl solution to obtain information on chemical forms of the anionic fluoride complexes of Mo and W

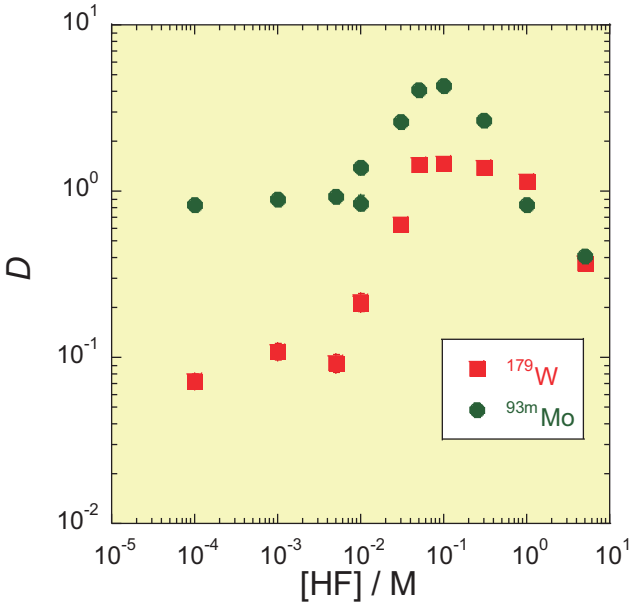

Fig. 1. Variation of the D values of Mo and W as a function of [HF].

References

1) A. Türler, V. Pershina, Chem. Rev. **113**, 1237 (2013).
2) M. Schädel, D. Schaughnessy (eds.): The Chemistry of Superheavy Elements, 2nd edition (Springer, Berlin, 2014).
3) A. Mitsukai, Master's Thesis (2017) (unpublished).

*1 Graduate School of Science and Technology, Ibaraki University
*2 Advanced Science Research Center, Japan Atomic Energy Agency
*3 RIKEN Nishina Center

Batch solid-liquid extraction of Nb and Ta with 52 wt% Aliquat 336 resin from HF solutions

D. Sato,[*1,*2] M. Murakami,[*1] K. Ooe,[*1] R. Motoyama,[*1] H. Haba,[*2] Y. Komori,[*2] A. Toyoshima,[*3] A. Mitsukai,[*3] H. Kikunaga,[*4] S. Goto,[*1] and H. Kudo[*5]

The elements with atomic number ≥ 104 are called super-heavy elements. Aqueous-chemistry experiments with these elements have been performed often by using the Automated Rapid Chemical Apparatus (ARCA).[1), 2)] In particular, an anion-exchange experiment of element 105, Db was successfully performed in 13.9 M hydrofluoric acid solution.[2)] However, the chemical species of Db in HF solution were still not clear. Therefore, we studied the liquid-liquid extraction behavior of Nb and Ta, which are lighter homologues of Db, with Aliquat 336 for investigating the charge of complexes of these elements extracted from HF solution.[3)] The results showed that univalent anionic complexes such as $NbOF_4^-$ and TaF_6^- were extracted. Applying this extraction system to the solid-liquid extraction with Aliquat 336 resin, on-line column chromatography experiments of Nb and Ta with 32 wt% Aliquat 336 resin from HF solutions were conducted using ARCA.[4)] In these experiments, the distribution coefficients (K_d) of Nb and Ta in 1-27 M HF solution were calculated from elution peak volume (V_p) and were compared with the results of a batch experiment. The results showed that the K_d values of Nb in 5.4 M HF and 10 M HF with ARCA were lower than those obtained from the batch experiment. This probably suggests that the K_d values of Nb in these HF concentrations were too low because the volume of the resin in micro-columns of ARCA is very small. Therefore, it is necessary to increase the K_d values of Nb by increasing the amount of Aliquat 336 in the resin. In this work, the batch solid-liquid extraction of Nb and Ta with 52 wt% Aliquat 336 resin was performed.

Long-lived radiotracers, ^{95g}Nb ($T_{1/2}$ = 34.97 d) and ^{179}Ta ($T_{1/2}$ = 665 d), were produced by deuteron irradiation on Zr and Hf metallic foil targets with natural isotopic abundance, respectively, using the RIKEN K70 AVF Cyclotron. These radiotracers in the targets were chemically isolated by ion exchange. A 52 wt% Aliquat 336 resin was prepared by mixing MCI GEL CHP20/P30 with Aliquat 336 dissolved in methanol for about 1 day, which was followed by drying in an oven at 80 ˚C.[5)] The ^{95g}Nb and ^{179}Ta tracers were dissolved in 400 μL of 1-27 M HF and then mixed with 10-15 mg of the 52 wt% Aliquat 336 resin in a syringeless filter tube. After shaking for 5 min, the solution was separated from the resin by filtration, and 250 μL of the solution in each sample was pipetted into another sample tube. For measurement of initial radioactivity, A_{ini}, in the aqueous solutions, control experiments without the Aliquat 336 resin were also conducted. The radioactivities of these samples were measured with a Ge detector. The K_d of ^{95g}Nb and ^{179}Ta were obtained using the following equation:

$$K_d = \frac{(A_{ini} - A_s)/m_r}{A_s/V_s}. \quad (1)$$

Here, A_s is the radioactivity of the solution, m_r is the weight of the resin used and V_s is the volume of a liquid phase.

The dependences of K_d values of ^{95g}Nb and ^{179}Ta on the initial HF concentration, $[HF]_{ini}$ were investigated with the 52 wt% Aliquat 336 resin from 1-27 M HF solutions. The obtained results are shown in Fig. 1. In addition, the previous results with 32 wt% Aliquat 336 resin are also shown in Fig. 1.The K_d values of ^{179}Ta decreased with increasing $[HF]_{ini}$, while those of ^{95g}Nb show a minimum at 10 M HF. The obtained behaviors of both elements were similar to those with 32 wt% Aliquat 336 resin, and therefore, the extraction species of those elements are the same for both resins. The lowest K_d value obtained in this study was about 34 at 10 M HF for Nb. In the previous experiment, the K_d values obtained from the elution curves in an on-line column experiment were in good agreement with those obtained in a batch experiment in the K_d value range of 30-80. Therefore, it is expected that consistent results between on-line column and batch experiments would be obtained with 52 wt% Aliquat 336 resin. Recently, an on-line column experiment of Nb and Ta with 52 wt% Aliquat 336 resin was performed using ARCA.[6)]

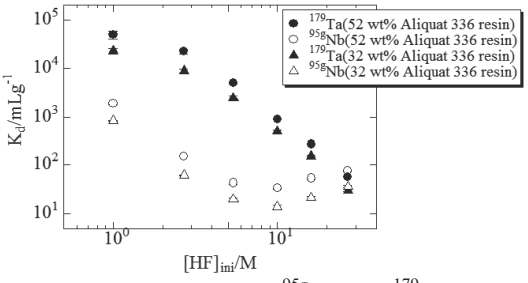

Fig. 1. Adsorption behavior of ^{95g}Nb and ^{179}Ta on 32 wt% and 52 wt% Aliquat 336 resin as a function of $[HF]_{ini}$.

References

1) W. Paulus et al., Radiochim. Acta. **84**, 69 (1999).
2) K. Tsukada et al., Radiochim. Acta. **97**, 83 (2009).
3) D. Sato et al., Accel. Prog. Rep. **47**, 247 (2014).
4) D. Sato et al., 59th Japan Society of Nuclear and Radiochemical Sciences, September 25-29, 2015, Sendai, Japan.
5) H. Haba et al., Radiochim. Acta. **95**, 1 (2007).
6) D. Sato et al., In this report.

[*1] Graduate School of Science and Technology, Niigata University
[*2] RIKEN Nishina Center
[*3] Japan Atomic Energy Agency
[*4] Research Center for Electron Photon Science, Tohoku University
[*5] Department of Chemistry, Faculty of Science, Niigata University

Extraction behaviors of Nb and Ta with triisooctyl amine from hydrochloric acid solution

R. Motoyama,[*1,*2] K. Ooe,[*1] Y. Komori,[*2] M. Murakami,[*3] H. Haba,[*2] S. Goto,[*1] and H. Kudo[*4]

Of the studies of the 105th element, Db, only three reports have been published on the chloride complexes of Db in the aqueous phase.[1–3] In two of the reported experiments, chloride complex formation and its extraction behavior with triisooctyl amine (TiOA) were investigated.[1,2] The observed sequence of the extraction was Ta > Nb > Db > Pa. However the influence of fluoride ions on the extraction sequence was suggested because a mixed HCl/HF solution was used in the extraction.[4] Only one experiment using a pure HCl solution has been reported so far, where a reversed-phase column chromatographic experiment using 6 M HCl and Aliquat 336 on an inert support was performed.[3] The sequence of extraction was Pa > Nb ≧ Db > Ta. This is a reversal of the earlier observed sequence. To clarify the complex formation mechanism of Db with chloride ions, it is important to study the behavior of Db in pure HCl solutions.

We have already started investigating the extraction behaviors of Nb and Ta as lighter homologues of Db from pure HCl solutions with TiOA on a tracer scale. As a result of the liquid-liquid extraction using radiotracers ^{95g}Nb ($T_{1/2}$ = 34.991 d) and ^{179}Ta ($T_{1/2}$ = 1.82 y) preserved in concentrated HCl after purification by ion exchange separation with HF solution, the behavior of Ta, influenced by the remaining fluoride ions, was observed.[5] In this paper, we report on the extraction behaviors of Nb and Ta using radiotracers transported by a He/KCl gas-jet method, which makes it possible to observe the extraction behaviors of these two elements without the effects of HF.

Radiotracers of ^{90g}Nb ($T_{1/2}$ = 14.60 h) and ^{178}Ta ($T_{1/2}$ = 2.36 h) were produced in the ^{nat}Zr(d,xn) and ^{nat}Hf(d,xn) reactions, respectively, using a 24-MeV deuteron beam supplied by the RIKEN AVF cyclotron. Nuclear reaction products recoiling out of the targets were transported by a He/KCl gas-jet method at a He gas flow rate of 2.5 L/min. The transported products were collected on a Naflon® sheet for 1.5 min. The collected products were then dissolved in 1 mL of 2–10 M HCl. From this solution, 300 μL aliquots were pipetted to a polypropylene tube in which 300 μL of 2–10 M HCl and 600 μL of 0.12 M TiOA in xylene had been added. After shaking with a Voltex mixer for 10 min, the mixture was centrifuged for 1 min. From each phase, 420 μL aliquots were separated into sample tubes. The radioactivity of each phase was measured with a Ge detector. We calculated the distribution ratios (D) of ^{90g}Nb and ^{178}Ta using the following equation:

$$D = (A_{org} / V_{org}) / (A_{aq} / V_{aq}),$$

where A_{org} and A_{aq} are the radioactivities in the organic and aqueous phases, respectively, and V_{org} and V_{aq} are the volumes of the organic and aqueous phases, respectively.

The dependence of the D values of ^{90g}Nb and ^{178}Ta extracted into 0.12 M TiOA in xylene is shown in Fig. 1 as a function of the HCl concentration ([HCl]). The D values of both elements increase with increasing [HCl]. The D values of ^{178}Ta are greater than the values in the literature[6] for relatively high [HCl], although those of ^{90g}Nb are in agreement with those in the literature.[6] It is presumed that the formed Ta complexes differ in the present experiment and reported experiment,[6] which was performed on a macro scale. To obtain further information on the extracted complexes of Nb and Ta and the differences between the D values of Ta in the present experiment and the literature,[6] we need to conduct a detailed investigation. We will then investigate the behavior of Db and discuss the complex Db formation mechanism.

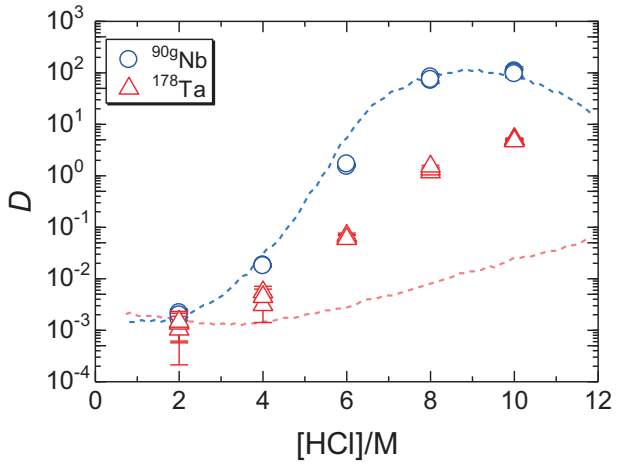

Fig. 1. Distribution ratios of ^{90g}Nb and ^{178}Ta extracted into 0.12 M TiOA in xylene as a function of the HCl concentration ([HCl]). Dashed lines indicate the values of Nb (blue) and Ta (red) reported in the literature.[6]

References

1) J. V. Kratz et al., Radiochim. Acta **48**, 121 (1989).
2) H. P. Zimmermann et al., Radiochim. Acta **60**, 11 (1993).
3) W. Paulus et al., Radiochim. Acta **84**, 69 (1999).
4) V. Pershina et al., Radiochim. Acta **64**, 37 (1994).
5) R. Motoyama et al., RIKEN Accel. Prog. Rep. **49**, 238 (2016).
6) T. Ishimori et al., J. At. Energy Soc. Japan **3**, 698 (1961).

*1 Graduate School of Science and Technology, Niigata University
*2 RIKEN Nishina Center
*3 Japan Atomic Energy Agency
*4 Faculty of Science, Niigata University

Chelate extraction of zirconium and hafnium using flow injection analysis technique for aqueous chemistry of element 104, rutherfordium

R. Yamada,[*1] K. Ooe,[*1] S. Goto,[*1] H. Haba,[*2] Y. Komori,[*2] and H. Kudo[*3]

We have been investigating the solvent extraction behavior of Zr and Hf, which are lighter homologues of rutherfordium (Rf, element 104), with chelating agents 2-thenoyltrifluoroacetone (HTTA) and di(2-ethylhexyl)phosphoric acid (HDEHP). In our previous study, the extraction mechanisms of Zr and Hf with TTA[1] and HDEHP[2] from 3 M acid solution were investigated using the batch method. The plots of the logarithm of distribution ratio (D) of Zr and Hf (log D) against log [TTA or $(HDEHP)_2$] showed a linear relation with a slope of approximately 4, suggesting that the extraction species of Zr and Hf were $M(TTA)_4$ or $M(HDEHP{\cdot}DEHP)_4$ (M = Zr or Hf). However, it took about tens of minutes to several hours to reach extraction equilibrium with these chelating agents. For extraction studies with a short-lived Rf isotope, more rapid extraction is required. In our previous study,[3] rapid extraction equilibrium was attained using a flow injection analysis (FIA) technique for the extraction of ^{95g}Nb from hydrochloric acid into Aliquat 336/1,2-dichloroethane. In this study, we applied this rapid solvent extraction apparatus for Zr and Hf extraction with HDEHP.

Radiotracers of ^{88}Zr ($T_{1/2}$ = 83.4 d) and ^{175}Hf ($T_{1/2}$ = 70 d) were produced in the bombardment of metallic ^{89}Y and ^{nat}Lu foils, respectively, with a 24-MeV deuteron beam from the RIKEN K70 AVF cyclotron. These radiotracers were chemically separated from the target materials through anion exchange and the solvent extraction method. A schematic view of the FIA apparatus used in this study is shown in Fig. 1. Three molar concentrations of perchloric acid containing the tracers and 1.5×10^{-3} M HDEHP in toluene were used as aqueous and organic phases, respectively. These solutions were pumped with double-plunger pumps at the same flow rate of 0.10 or 0.50 mL min^{-1} and mixed in the extraction coil (Teflon capillary) with an inner diameter of 0.17 mm. The length of the extraction coil was changed from 0.5 to 10 m to vary the contact time of the two phases. The aqueous and organic solutions eluting from the extraction coil were collected in a sample tube, which was subsequently centrifuged. The aliquots of these two phases were separately pipetted into other sample tubes and subjected to γ-ray spectrometry using a Ge detector. Because the flow rate of the aqueous phase was the same as that of the organic phase, the D values of Zr and Hf were evaluated from the following simple equation:

$$D = A_o/A_a,$$

where A denotes the radioactivity of either ^{88}Zr or ^{175}Hf, and the subscripts a and o refer to the aqueous and organic phases, respectively.

Figure 2 shows the dependences of the D values of Zr and Hf on the contact time of the two phases in the extraction coil. The results obtained with the batch extraction method are also shown in Fig. 2. The dashed and solid lines in the figure show the D values of Zr and Hf, respectively, at the extraction equilibrium. The D values of Zr and Hf obtained with the FIA apparatus increase more rapidly than those obtained in the batch extraction, showing that the extraction reaction was enhanced by the FIA apparatus. However, extraction equilibrium was not attained with the FIA apparatus within the contact time of approximately 1 min, which corresponded to the half-life of ^{261}Rf ($T_{1/2}$ = 68 s). Therefore, further enhancement of the extraction reaction through heating or vigorous agitation of the two phases in the extraction coil is required.

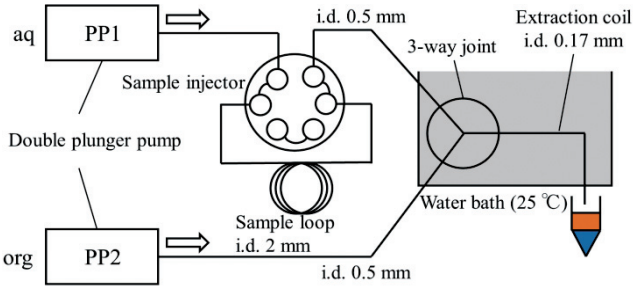

Fig. 1. Schematic view of the FIA apparatus setup.

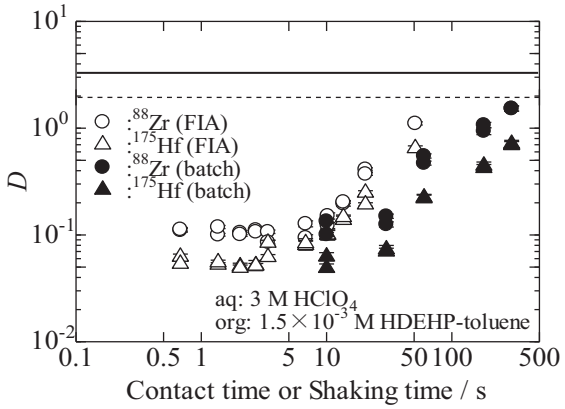

Fig. 2. Dependences of the D values of ^{88}Zr and ^{175}Hf on the contact time in the FIA apparatus or shaking time in the batch experiment. The dashed and solid line indicate the D values of ^{88}Zr and ^{175}Hf at equilibrium, respectively.

*1 Institute of Science and Technology, Niigata University
*2 RIKEN Nishina Center
*3 Faculty of Science, Niigata University

References

1) A. Tanaka et al., RIKEN Accel. Prog. Rep. **48**, 288 (2015).
2) R. Yamada et al., RIKEN Accel. Prog. Rep. **49**, 241 (2016).
3) T. Koyama et al., RIKEN Accel. Prog. Rep. **47**, 275 (2014).

Coprecipitation experiment with Sm hydroxide using a multitracer produced by nuclear spallation reaction: A tool for chemical studies with superheavy elements†

Y. Kasamatsu,[*1] T. Yokokita,[*1] K. Toyomura,[*1] Y. Shigekawa,[*1] H. Haba,[*2] J. Kanaya,[*2] M. Huang,[*2] Y. Ezaki,[*2] T. Yoshimura,[*3] K. Morita,[*2] and A. Shinohara[*1]

The chemical properties of superheavy elements (SHEs) are expected to deviate from the periodicity of their lighter homologues in the periodic table because of the strong relativistic effects on the valence electronic shells of the heavy atoms. However, it is difficult to perform chemical experiments of SHEs because these nuclides are short-lived and their production rates by nuclear reactions are quite low. These conditions create the need for rapid chemical experiments on a one-atom-at-a-time basis. In addition, for unambiguous identifications of these elements existing as single atoms, it is necessary to detect α particles with characteristic energies. These experimental difficulties limit the variety of chemical investigations of SHEs. So far, most of the methodologies in aqueous chemistry were limited to the ion-exchange method or solvent extraction. The purpose of the present study is to establish a coprecipitation method as a new methodology to explore the chemistry of SHEs. In the present study, a multitracer which contains various radioisotopes (various homologues of SHEs) was used to investigate the applicability of the coprecipitation experiment with Sm hydroxide to SHE chemistry.

The multitracer was produced by irradiating ^{nat}Ta targets (2-μm thickness × 30 foils) with $^{14}N^{7+}$ ions accelerated to 135 MeV per nucleon by the RIKEN ring cyclotron (~1.6 electric μA) for 40 h. Various nuclides, namely various elements, with $Z \leq 73$ (Ta) were produced by nuclear spallation reactions. Only the nuclear reaction products recoiling out of the target foils were attached to KCl aerosols seeded in a He gas and transported from the nuclear reaction chamber to the chemical laboratory by a He gas jet through a PTFE capillary tube.[1)] The transported products were collected on glass filter paper, and were dissolved in 1 mL of 0.01 M HCl.

In a polypropylene (PP) beaker, 20 μL of Sm standard solution (1000 mg L^{-1}, 1 M HNO_3) was added into 220 μL of the prepared multitracer solution. The solution was stirred, and then, 2 mL of the basic solution (dilute and concentrated aqueous NH_3, and 0.10, 1.0, 6.0, and 12 M NaOH solutions) was added. The solution was stirred for 10 s or 10 min at room temperature to determine the chemical reaction time required to reach equilibrium. Then, the solution containing the precipitate was filtrated by suction with a PP membrane filter (eichrom, Resolve® Filters 0.1 μm). Both the precipitate and filtrate were dried using a heater at 100 ºC. The precipitate, filtrate, and PP beaker used were subjected to γ-ray spectrometry with Ge semiconductor detectors. The standard activities of the radiotracers were also determined. The precipitation yields were evaluated from these radioactivities.

The product nuclides were identified based on their characteristic γ-ray energies and corresponding half-lives. In total, we identified 34 elements containing more than 60 nuclides as follows: ^{24}Na, ^{42}K, ^{82m}Rb, ^{127,129}Cs {group 1}, ^{28}Mg, ^{47}Ca, $^{128,(131)}$Ba {group 2}, ^{44,47,48}Sc, $^{(86),87g,(m)}$Y {group 3}, (^{132}La), ^{132,135}Ce, $^{145,146,(147)}$Eu, ^{146,147,149}Gd, $^{149\text{-}153,155}$Tb, ^{152,155,157}Dy, (^{160m}Ho), ^{161}Er, $^{165,(166),167}$Tm, $^{166,(169)}$Yb, $^{169,(170),171,172}$Lu {group 3 (lanthanides)}, $^{(86,87)89}$Zr, ^{170,173}Hf {group 4}, ^{90}Nb, ^{176}Ta {group 5}, ^{93m}Mo {group 6}, ^{96}Tc {group 7}, $^{99m,100,(101m)}$Rh {group 9}, ^{65}Zn {group 12}, ^{67}Ga, ^{110,111}In {group 13}, ^{71,72}As, ^{118m,120m}Sb {group 15}, ^{73}Se, and ^{119m}Te {group 16}. The nuclides listed in parentheses are ones for which the coprecipitation yields could not be determined. Various elements belonging to various groups in the periodic table were included in the multitracer used. The presently prepared multitracer contains the homologues of various (nine) SHEs (group 4–18), and thus, this study is beneficial for the model experiment toward the chemical study on the SHEs.

The coprecipitation yields of radionuclides of groups 1–7, 9, 12, 13, 15, 16 elements with Sm hydroxide and their dependence on the kind and concentration of the prepared basic solutions qualitatively reflect the hydroxide precipitation properties (formation of ammine and hydroxide complexes) of the elements in macro amounts. This finding suggests that the coprecipitation behavior of an element whose chemical properties are unknown can be investigated using the present method, and we can discuss its general hydroxide precipitation properties based on the results obtained for coprecipitation. In addition, the chemical reactions of the majority of the elements in the coprecipitation are sufficiently fast to reach equilibrium within 10 s of stirring although for Mo and Se, relatively slow chemical reactions were observed. Based on the results in the present experiment, we can say that the present coprecipitation method with Sm hydroxide is applicable to SHE chemistry. This methodology will open new chemistry routes (various precipitates) for SHEs.

† Condensed from the article in Appl. Radiat. Isot. **118**, 105 (2016)

*1 Graduate School of Science, Osaka University
*2 RIKEN Nishina Center
*3 Radioisotope Center, Osaka University

Reference

1) H. Haba et al.: Radiochim. Acta **93**, 539 (2005).

Fundamental study on DFO complexation of Zr : Application to the behavior of geochemical pairs in aquatic environment

J. Inagaki, [*1] A. Sakaguchi, [*1] H. Haba, [*2] Y. Komori, [*2] and S. Yano [*2]

The zirconium (Zr)-hafnium (Hf) pair is known as a "geochemical twin"[1] with Zr/Hf ratios in various systems being theoretically the same as that of the chondrite meteorite. However, owing to the ongoing development of analytical techniques, significant fractionation of the two elements between seawater (Zr/Hf ～ 180–350)[2] and ferromanganese crusts (FMCs) (Zr/Hf ～57–87)[3] has been observed. In addition, these elements are found to undergo fractionation between crustal rock and seawater. [4]

To clarify the fractionation of Zr and Hf at the water-rock interface, the behavior of the siderophore complexes of these elements has been studied, given that these refractory elements are thought to exist as siderophore complexes in environmental water.[4] However, even the complexation formation constants of siderophore-Zr/Hf have not been established owing to experimental difficulties. In this research, we have attempted to devise a method for obtaining such complexation formation constants.

To gain an improved understanding of the behaviour of Zr, first, a radiochemical tracer was used in laboratory experiments. ^{88}Zr ($T_{1/2}$ = 83.4 day) was produced in the reaction ^{89}Y(d, 3n)^{88}Zr by using the AVF cyclotron at RIKEN. ^{88}Zr was chemically separated from an Y foil [5] and mixed with stable Zr to produce a radiotracer solution with a total Zr concentration of 12.5 μM.

About 40 μL of tracer solution was added to 50 mL of 0.01 M NaCl solution, and ^{88}Zr γ-ray (393 keV) in the solution was assayed using a Ge detector. The pH value of this solution was adjusted to pH 8 using HCl and NaOH solutions to obtain hydrolysed Zr. The solution was filtered using a membrane filter (pore size of 0.2 μm) after stirring for 30 min. The ^{88}Zr in the filtered solution was determined, and the amount of hydrolysed Zr on the filter was estimated.

The hydrolysed Zr was transferred to 50 mL of 0.01 M NaCl solution containing 100 nM of siderophore, and the resulting solution was stirred for 90 h. As an analogous ligand to the siderophore, desferrioxamine B (DFO) was employed for this experiment. A portion of the solution was sub-sampled at t = 1, 4, 9, 16, 27, 66, and 90 h, and the sub-samples were filtered using a membrane filter (GTBP01300, Merck Millipore). The ^{88}Zr γ-ray intensities in the filtered solutions were measured using a Ge detector. The amount of filtered Zr was considered to represent the concentration of the DFO-Zr complexes.

The chemical yield of ^{88}Zr from the Y foil was found to be very low, a few percent, in the first experiment. This low yield might have been caused by Zr fixation at the bottom of the PFA vial owing to complete evaporation of the solution in the first step of the procedure. Subsequently, in the first step, evaporation to dryness was avoided, and the sample solution was carefully treated to prepare the chloride complex, $ZrCl_6^{2-}$.[6] Thus, a high chemical yield of 95% was realized.

The amount of hydrolysed Zr on the filter was estimated to be 59%, and the absolute amount was 295 pmol. The remainder of the Zr (41%) had passed through the membrane filter in the form of dissolved species and/or colloidal material.

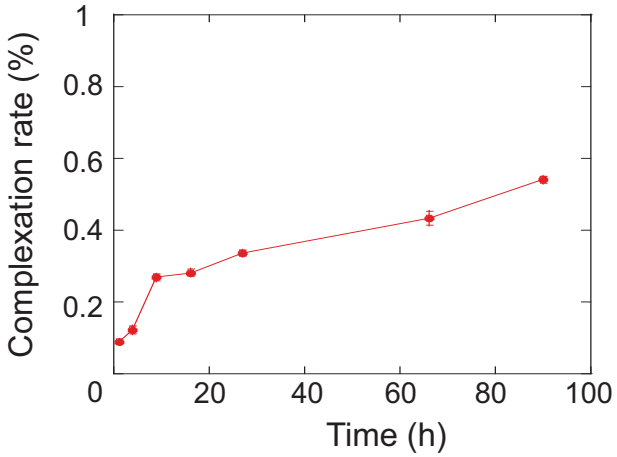

Fig. 1. DFO-Zr complexation rate as a function of stirring time.

The complexation rate of Zr with DFO is outlined as a function of stirring time in Fig. 1. As can be seen, the complexation rate of Zr with DFO increased with time, and an equilibrium condition was not established. Moreover, the percent complexation rate was quite low. Here, the ratio between Zr and DFO (in moles) was about 20 and the competitive reaction between OH^- and DFO did not seem to have been operating. Thus, for future experiments, the concentration of DFO should be increased to study more precisely the complexation of Zr with DFO. An additional work is definitely needed to clarify the complexation behavior of Zr and Hf.

References

1) V. M. Goldschmidt, Chem. Soc. **1**, 655 (1937).
2) M. L. Firdaus et al., Nat. Geosci. **4**, 227 (2011).
3) K Schmidt et al., Geochem. Cosmochim. Acta **140**, 468 (2014).
4) D. Kraemer et al., Geochem. Cosmochim. Acta **165**, 263 (2015).
5) H. Haba et al., Radiochim. Acta **89**, 733 (2001).
6) H. Haba et al., Bull. Chem. Soc. Jpn **6,** 698 (2009).

*1 Graduate School of Pure and Applied Sciences, University of Tsukuba
*2 RIKEN Nishina Center

Production and purification of ^{88}Zr and ^{121m}Te

T. Kubota,[*1,*2] S. Yanou,[*2] S. Shibata,[*2] H. Haba,[*2] and S. Takahashi[*1]

Zirconium and tellurium are produced as a result of nuclear fission. Experimental investigations of their migration in the environment are rarer than those of cesium, strontium, and plutonium and require, if possible, carrier-free radionuclides, which mean they are undiluted with naturally occurring isotopes. Such radionuclides can be produced by bombardment with protons, deuterons, or alpha particles. In this report, we present investigations of purification methods for zirconium and tellurium from yttrium and antimony, respectively, as target material.

Radionuclides, ^{88}Zr and ^{121m}Te, were produced at the RIKEN AVF cyclotron and transferred to the Kyoto University Research Reactor Institute and then separated from target materials, yttrium and antimony. The purification was estimated by using the decontamination factor, DF, which is defined as the ratio of the radioactivity of X in the initial sample to that in the purified sample, where X is the target material, yttrium or antimony. The radioactivity was determined by γ-spectrometry.

Zirconium-88 was produced by the bombardment of yttrium foil (purity: 99%, size: 18 mm x 18 mm x 0.15 mm) with 24-MeV[1] deuterons at 4.1 particle-μA for 2 h. ^{88}Zr was purified from an yttrium matrix by solvent extraction after the by-product ^{89}Zr decayed out to ^{89}Y. The yttrium foil was dissolved in c.HCl, and a black residue was removed by centrifugation. The supernatant was diluted to 0.1 M HCl, which was used as the initial solution. ^{88}Zr in the initial solution was extracted into 0.5 M 2-thenoyltrifluoroacetone (TTA) in xylene.[2] The xylene solution was washed with 0.1 M HCl and diluted with xylene to 0.05 M TTA. ^{88}Zr was extracted into c.HCl and the aqueous solution was washed with cyclohexane to remove TTA. The c.HCl solution was vapored and then the solution of ^{88}Zr in 0.1 M HCl was prepared.

Tellurium-121m was produced by a bombardment of an Sb_2O_3 pellet[3] (diameter 15 mm), which was prepared by pressing Sb_2O_3 powder (purity 99.999%) at 3 t for 5 min, with deuterons. ^{121m}Te was purified from an antimony matrix by anion exchange chromatography.[4] The Sb_2O_3 pellet was dissolved in c.HCl, following which NaClO was added to regulate the atomic valence to Sb(V) and Te(VI). This oxidized solution was loaded onto anion exchange resin (50-100 mesh Cl^-form). The pentavalent of antimony in c.HCl forms $SbCl_6^-$ and strongly adsorbs onto anion exchange resin, while H_2TeO_4, which has Te(VI), is not adsorbed. However, some fraction of tellurium was adsorbed onto anion exchange resin, which could have been caused by incomplete oxidation. In order to recover tellurium, the anion exchange resin was washed with a mixture of c.HCl and 5% NaClO solution several times.

The radioactivity of ^{88}Zr in the initial solution was 2.4 MBq excluding the radioactivity in the undissolved material, which is the black residue. ^{88}Zr completely remained in the organic solution in the extraction with 0.5 M TTA and washing with 0.1 M HCl, while yttrium completely remained in the aqueous solution. This showed that a high purity of ^{88}Zr solution can be obtained. In the back extraction from 0.05 M TTA, 75% of ^{88}Zr was extracted into c.HCl in one process. This recovery rate is sufficiently high; however, if necessary, the repeat of back extraction would yield a higher value. The DF evaluated from the distribution of ^{88}Y, which is produced in the Y(d, 2np) reaction, was greater than 10^4.

The radioactivity of ^{121m}Te produced was 2.8 MBq. The DF was 10^3 at most, and the recovery of tellurium was 50%. Moreover, the low DF value of approximately 10 was often obtained. This low recovery ratio and selectivity could be ascribed to the redox reaction of antimony and tellurium, and further investigation is required. As another purification method, solvent extraction methods are planned to be applied.

In this investigation, ^{88}Zr and ^{121m}Te without the dilution of naturally occurring isotopes were produced, and these nuclides were purified. ^{88}Zr was purified by solvent extraction with TTA, while ^{121m}Te was incompletely purified by anion exchange chromatography.

References

1) M. S. Uddin et al., Radiochim. Acta. **95**, 187 (2007).
2) H. Onish et al., Talanta. **19,** 473 (1972).
3) S. Takács et al., Nucl. Instr. and Meth. Phys. Res. B. **278** 93 (2012).
4) D. Downs et al., J. Radio. Nucl. Chem. **262,** 241 (2004).

*1 Kyoto University Research Reactor Institute
*2 RIKEN Nishina Center

^{99}Ru Mössbauer spectroscopy of Na-ion batteries of Na_2RuO_3 (III)

K. Takahashi,[*1] Y. Kobayashi,[*1,*2] H. Haba,[*2] and H. Ueno[*2]

Sodium-ion batteries are attractive energy storage media owing to its abundance of sodium, compared with lithium-ion batteries. There have been many investigations of the development of Na^+-containing electrodes as new cathodes.[1,2] We recently reported the electrochemical properties of Na_2RuO_3 as the cathode material.[3] Na_2RuO_3 has a layered structure in which the first layer is composed of Na while the second layer contains Na and Ru in the ratios 1:3 and 2:3, respectively. It was known that layered Na_2RuO_3 has two phases in the $[Na_{1/3}Ru_{2/3}]O_2$ layers, namely *ordered* and *disordered* arrangements, depending on the sintering time. The *ordered* Na_2RuO_3 phase has honeycomb-type cation ordering in the $[Na_{1/3}Ru_{2/3}]O_2$ layers. On the other hand, the *disordered* Na_2RuO_3 phase has a random distribution of Na and Ru in $[Na_{1/3}Ru_{2/3}]O_2$ layers. The two polymorphs exhibit significant differences in electrochemical properties.

In this study, the *disordered* Na_2RuO_3 phase and the Na-deficient oxides that imitate discharged samples of Na_2RuO_3, which were obtained after a short sintering time of 12 h were characterized by XRD and ^{99}Ru Mössbauer spectroscopy to understand the change of oxidation state and coordination environment of the Ru atoms caused by the deficiency of Na^+ ions.

Disordered Na_2RuO_3 and non-stoichiometric Na-Ru oxides (atomic ratios of Na/Ru = 1.5, 1.0, 0.5, and 0.2) were synthesized by conventional solid-state reaction.[2] RuO_2 and $NaHCO_3$ were mixed with different atomic ratios of Na/Ru thoroughly and sintered at 850ºC for 12 h in an Ar atmosphere. The source nuclide, ^{99}Rh ($T_{1/2}$=15.0 d) of ^{99}Ru Mössbauer spectroscopy was produced by the ^{99}Ru(p,n)^{99}Rh reaction at the AVF Cyclotron. After p-irradiation for 24 h, the target was used as the Mössbauer source with no chemical treatment. ^{99}Ru Mössbauer spectra were obtained by a conventional arrangement, but both the source and the absorbers were maintained at 4.2 K in a liquid He cryostat during the measurements.[4,5]

The XRD pattern of *disordered* Na_2RuO_3 showed a trigonal structure with a = 0.313 nm and c = 1.605 nm. The parameters were consistent with those reported in Ref. 3. The ^{99}Ru Mössbauer spectrum of *disordered* Na_2RuO_3 obtained at 5.0 K is shown in Fig. 1 (a). The spectrum is similar to that of *ordered* Na_2RuO_3, reported in Ref. 4, and is reasonably fitted by a doublet with an isomer shift (δ) of –0.34(1) mm/s and a quadrupole splitting (ΔE_Q) of 0.30(5) mm/s. The linewidth of 0.44(5) mm/s was slightly broadened compared to that *ordered* Na_2RuO_3 owing to the shorter sintering time.

The XRD of non-stoichiometric Na-Ru oxides sintered with Na/Ru = 1.5 indicated that the sample crystallized in two phases of Na_2RuO_3 (85%) and $NaRu_2O_4$ (15%). $NaRu_2O_4$ is in the orthorhombic space group *Pnm* and consists of double chains of edge sharing RuO_6 octahedra.[6] The Mössbauer spectrum of Na-Ru oxides with Na/Ru = 1.5 is shown in Fig. 1 (b). It was difficult to analyze the two separated components, Na_2RuO_3 and $NaRu_2O_4$. However, assuming that the spectrum consists of one component, the Mössbauer spectrum could have δ = −0.42(1) mm/s and ΔE_Q = 0.49(1) mm/s. The value of δ indicated that the oxidation state of Ru ions was reduced from Ru^{4+} to $Ru^{3.5+}$ on average. The detailed discussion between the oxidation states of the Ru atoms and the Na/Ru ratios of non-stoichiometric Na-Ru oxides is under consideration.

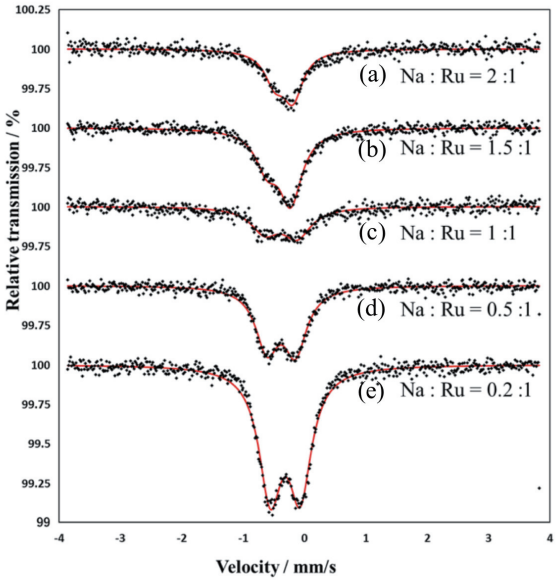

Fig. 1. ^{99}Ru Mössbauer spectra of (a) *disordered* Na_2RuO_3 and non-stoichiometric Na-Ru oxides (Na/Ru = (b) 1.5, (c) 1.0, (d) 0.5, and (e) 0.2) obtained by sintering at 850 ºC for 12 h in an Ar atmosphere.

References

1) K. M. Mogare et al., Z. Anorg. Allg. Chem. **630**, 547 (2004).
2) M. Tamaru et al., Electrochem. Commun. **33**, 23 (2013).
3) B. M. de Boisse et al., Nature Commun. doi 10.1038/ncomms 11397 (2016).
4) K. Takahashi et al., RIKEN Accel. Prog. Rep. **48**, 242 (2015) .
5) Y. Kobayashi et al., J. Phys. **217**, 012023 (2010).
6) K. A. Regan et al., J. Solid Stat. Chem. **179,** 195 (2006).

*1 Dep. of Eng. Sci., University of Electro-Commun.
*2 RIKEN Nishina Center

Excitation functions of ^{nat}Cu(α, x)$^{57,58g+m}$Co nuclear reactions†

A. R. Usman,[*1,*2] M. U. Khandaker,[*1,*2] H. Haba,[*1] N. Otuka,[*1,*3] M. Murakami,[*1] and Y. Komori[*1]

Studies on radionuclides production cross-sections through the (*p,x*) route is relatively more active compared to the other light-charged particles production-routes, though sometimes, the production of the same radionuclides are more effective via the (*d,x*) or (α,x) reaction process. Using copper (Cu) as a target material, several important radionuclides can be produced. Some of such radionuclides are gallium (Ga) and cobalt (Co) radionuclides. In particular, ^{66}Ga was recently tested in in vivo studies as ^{66}Ga-labeled nano-graphene and reported to be a good candidate for imaging (PET) of vascular system[1]. The radionuclide ^{67}Ga ($T_{1/2}$ = 3.2617 d) is useful due to its short half-life and the Auger and Coster-Kronig electron emissions, making ^{67}Ga-labeled radiopharmaceuticals more appropriate to patients (in clinical terms) compared to its prototype ^{125}I ($T_{1/2}$ = 59.4 d) equivalent [2]. Additionally, ^{57}Co is a popular candidate in Mössbauer spectroscopy and also as a calibration standard in γ-ray spectrometry as well as in single photon emission computed tomography (SPECT) [3].

Our extensive literature survey of previous experimental data shows that Cu have been used as target in radionuclides production. However, these studies reported mainly the production of Ga and Zn radionuclides for α beam monitoring purposes. In addition, there are also obvious discrepancies among the studies in the reported data. More so, the reported studies on cobalt (Co) radionuclides through this route is relatively less. Present work therefore reports new α-particle-induced reaction cross-sections on ^{nat}Cu to reduce the observed discrepancies and also to enrich Co production cross-sections database.

The stacked-foil activation method and γ-ray spectrometry were used for the excitation functions measurements. The stack was irradiated for 2.0 hours by a 50.4 MeV α beam in a Faraday cup-like water-cooled target holder using AVF cyclotron of the RIKEN RI Beam Factory, Japan. The intensity of the beam was determined from the measured activities of the front Ti of the stack, the foil directly facing the incident beam. The ^{nat}Ti(*α,x*)^{51}Cr IAEA [4] recommended monitor reaction (σ = 26.4 mb at E_d = 50.0 MeV) was used for the evaluation of the beam intensity. The intensity was considered as a constant in the stack and was used to deduce cross-sections of the ^{51}Cr from each Ti foil of the stack.

The production cross-sections of ^{66,67}Ga, ^{65}Zn, and $^{57,58g+m,60}$Co have been assessed and presented with their relevant total uncertainties in Tables of Ref.[4] while the corresponding excitation factions of these radionuclides have been presented in the Figures of Ref.[4].

The present results were compared with the previous experimental data as well as the extracted theoretical TENDL-2014 data. Due to space constrain, only excitation functions of ^{57}Co and $^{58g+m}$Co are presented in this report. The cross-sections of ^{57}Co ($T_{1/2}$ = 271.74 d) were assessed using its interference-free γ line (E_γ = 122.0607 keV; I_γ = 85.60%). The evaluated TENDL-2014 library data indicate that the ^{57}Co production is due to the ^{63}Cu(α,2n2α)^{57}Co process below 50 MeV. Two earlier studies[5,6] have been reported for the production of ^{57}Co. The TENDL-2014 library reproduced the excitation function of $^{58g+m}$Co more closely as compared to ^{57}Co.

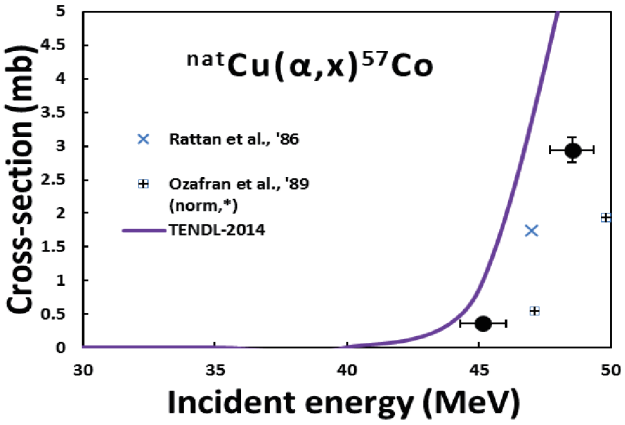

Fig. 1. Excitation function of the ^{nat}Cu(α,x)^{57}Co reaction.

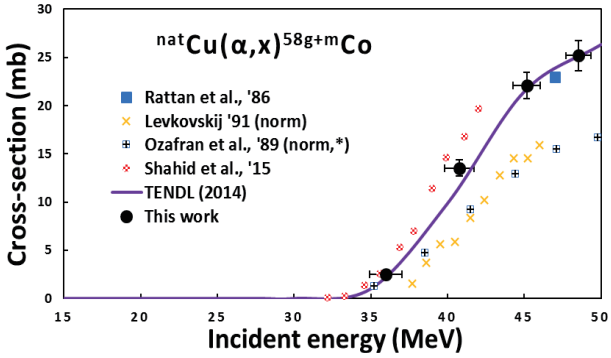

Fig. 2. Excitation function of the ^{nat}Cu(α,x)$^{58g+m}$Co reaction.

References

1) H. Hong et al.: Biomaterials **33**, 4147 (2012).
2) E. Koumarianou et al.: Nucl. Med. Bio. **41**, 441 (2014).
3) A. R. Usman et al.: Nucl. Instr. Meths Phys. B **368**, 112 (2016).
4) A. R. Usman, et al.: Appl. Radiat. Isot. **114,** 104 (2016).
5) S. S. Rattan etal.: Radiochimica Acta **39**, 61 (1986).
6) M. J. Ozafrán et al.: J. Radioanal. Nucl. Chem. **131**, 467 (1989).

† Condensed from the article in Appl. Radiat. Isot. **114,** 104 (2016)

*1 RIKEN Nishina Center
*2 Department of Physics, University of Malaya
*3 Nuclear Data Section, International Atomic Energy Agency

Activation cross sections of α-induced reactions on ^{nat}Zn for ^{68}Ge production

M. Aikawa,[*1,*2] M. Saito,[*1,*2] S. Ebata,[*1] Y. Komori,[*2] and H. Haba[*2]

Radioactive isotopes are used in nuclear medicine for therapy and diagnosis. A positron emitter, ^{68}Ga ($T_{1/2}$ = 67.71 min), is applied for positron emission tomography (PET).[1] In addition to ^{68}Ga, its long-lived parent, ^{68}Ge ($T_{1/2}$ = 270.95 d), is useful as a ^{68}Ga generator.[2] A possible reaction route to produce ^{68}Ge (Z = 32) comprises alpha-induced reactions on zinc isotopes (Z = 30), cross sections of which have been investigated previously.[3,4] However, the amplitudes of the previous data are slightly different from each other. We therefore measured cross sections of the alpha-induced reactions on natural zinc for ^{68}Ge production.

The experiment was performed at the AVF cyclotron of the RIKEN RI Beam Factory by using the stacked foil technique and the activation method. ^{nat}Zn foils (purity: 99.9%, Nilaco, Japan) were stacked with ^{nat}Ti monitor foils (purity: 99.6%, Nilaco, Japan). The thicknesses of the Zn and Ti foils were estimated from the measured area and weight of large foils (50 × 50 mm^2 and 50 × 100 mm^2) and found to be 18.64 mg/cm^2 and 2.25 mg/cm^2, respectively. The stacked target consisted of 14 sets of the Zn-Ti-Ti foils (8 × 8 mm^2) cut off from the large foils. The first Ti monitor foils at the downstream side of the beam were assumed to compensate for losses of recoil products. The target was irradiated for 2 h by a 51.5 MeV alpha beam with an average intensity of 41.0 pnA, which was measured by a Faraday cup. The beam energy was measured by the time-of-flight method using a plastic scintillator monitor.[5] The irradiated foils were subjected to γ-ray spectrometry by HPGe detectors.

The decay data[6] are summarized in Table 1. The measurement of the 1077.34 keV γ-line (3.22%) from the ^{68}Ga decay, which is in equilibrium with that of its parent ^{68}Ge, was performed after a long cooling time of about 80 days. Each Zn foil with its Ti catcher foil was simultaneously measured to collect the recoiled products. In the cooling time, all ^{68}Ga produced directly through the ^{nat}Zn(α,x) reaction during the irradiation could be considered to have decayed completely. The cross sections derived from the measurement are shown in Fig. 1 together with the previous experimental data (open squares and triangles)[3,4] and the TENDL-2015 data (dashed line).[7] The present result is slightly different from the previous experimental data, although the peak position of approximately 30 MeV is consistent with them. In contrast, the TENDL-2015 data shows a different tendency from the experimental data, probably because of underestimation of the contribution from the ^{nat}Zn(α,3n) reaction.

Table 1. Decay data of ^{68}Ge and ^{68}Ga

Nuclide	$T_{1/2}$	E_γ (keV)	I_γ (%)
^{68}Ge	270.95 d	-	-
^{68}Ga	67.71 min	1077.34	3.22

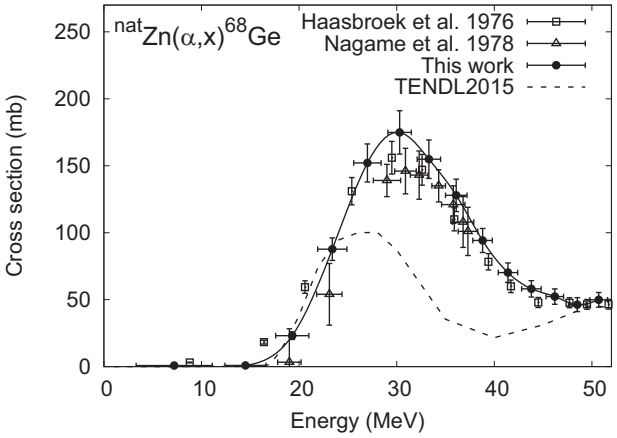

Fig. 1. Excitation function of the ^{nat}Zn(α,x)^{68}Ge reaction. The result is compared with the previous experimental data[3,4] and TENDL-2015.[7]

In summary, we performed an experiment on the alpha-induced reactions on natural zinc to produce ^{68}Ge, a generator of a positron emitter, ^{68}Ga. The excitation function of the ^{nat}Zn(α,x)^{68}Ge reaction was measured up to 51.5 MeV, and the peak position was found to be consistent with that of previous experiments.

*1 Graduate School of Science, Hokkaido University
*2 RIKEN Nishina Center

References

1) S.R. Banerjee, M.G. Pomper, Appl. Radiat. Isot. **76**, 1 (2013).
2) F. Rösch, Appl. Radiat. Isot. **76**, 24 (2013).
3) F.J. Haasbroek et al., CSIR Research Report, FIS 89 (1976).
4) Y. Namage et al., Appl. Radiat. Isot. **29**, 615 (1978).
5) T. Watanabe et al.: Proc. 5th Int. Part. Accel. Conf. (IPAC2014), 3566 (2014).
6) National Nuclear Data Center: the NuDat 2 database, http://www.nndc.bnl.gov/nudat2/.
7) A.J. Koning et al.: TENDL-2015: TALYS-based evaluated nuclear data library.

Activation cross sections of deuteron-induced reactions on natural palladium for ^{103}Ag production

N. Ukon,*1,*2 M. Aikawa,*2,*3 Y. Komori,*2 and H. Haba*2

^{103}Pd with a half life of 16.991 days decays (100% electron capture (EC)) to ^{103m}Rh (100% isomeric transition to ^{103}Rh with 39.5-keV γ-ray emission) is a medical radioisotope (RI) for brachytherapy. For the effective production of ^{103}Pd, a variety of reactions should be investigated. They also include reactions to produce ^{103}Ag ($T_{1/2}$ = 65.7 min), a parent of ^{103}Pd. A process to produce ^{103}Ag is a deuteron-induced reaction on natural palladium, which has only been studied up to 20.3 MeV.[1] Therefore, we measured the activation cross sections of the ^{nat}Pd(d,x)^{103}Ag reaction using a 24-MeV deuteron beam.

The excitation function of the ^{nat}Pd(d,x)^{103}Ag reaction was measured by the stacked-foil method, activation method and high-resolution γ-ray spectroscopy. ^{nat}Pd foils (purity: 99.95%, Nilaco Corp., Japan) were stacked with ^{nat}Ti (purity: 99.6%, Nilaco Corp., Japan) and ^{nat}Zn foils (purity: 99.95%, Nilaco Corp., Japan) for monitoring the beam parameters and degrading the beam energy. The thicknesses of Pd, Ti and Zn foils were 8.15, 4.93 and 25.14 mg/cm^2, respectively.

The irradiation was performed at the RIKEN AVF cyclotron. A 24-MeV deuteron beam with an average intensity of 174.74 nA was irradiated on the target for 20 min. The incident beam energy was measured by the time-of-flight method using plastic scintillator monitors. The beam energy degraded in the stacked target was calculated using the polynomial approximation of stopping-power data.[2] The γ-ray spectra of the activated foils were measured by HPGe detectors. Nuclear decay data are summarized in Table 1 and are taken from the online NuDat 2.6 database.[3]

From the net peak area of the 118.75-keV γ-ray, the activation cross sections for the ^{nat}Pd(d,x)^{103}Ag reaction were deduced using the standard activation formula

$$\sigma = \frac{T_\gamma \lambda}{\varepsilon_d \varepsilon_\gamma \varepsilon_t N_t N_b (1 - e^{-\lambda t_b}) e^{-\lambda t_c} (1 - e^{-\lambda t_m})}$$

where N_t denotes the surface density of target atoms: N_b the number of bombarding particles per unit time: T_γ the number of counts in photo-peak: ε_d the detector efficiency: ε_γ the gamma ray abundances: ε_t the measurement dead time, which is the ratio of live time to real time: λ the decay constant: t_b the bombarding time: t_c the cooling time: and t_m acquisition time.

*1 Nuclear Reaction Data Center (JCPRG), Hokkaido University
*2 RIKEN Nishina Center
*3 Faculty of Science, Hokkaido University

Table 1. Decay data of ^{103}Ag.

Nuclide	$T_{1/2}$	E_γ (keV)	I_γ (%)
^{103}Ag	65.7 min	118.74	31.2
		148.2	28.3
		266.86	13.3
		531.92	8.8
		1273.83	9.4

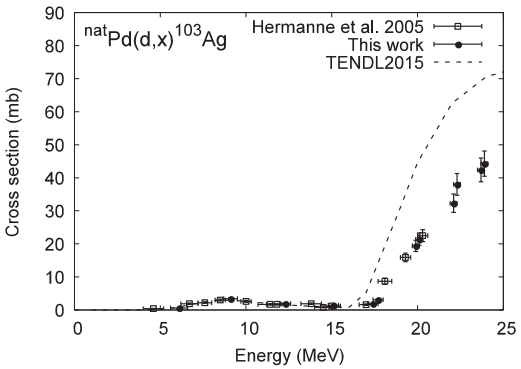

Fig.1. Excitation function of the ^{nat}Pd(d,x)^{103}Ag reactions. The result is compared with a previous study[1] and TENDL-2015.[4]

We found that our result is in good agreement with previous data obtained by Hermanne et al.[1] up to 20.3 MeV.

On the other hand, the theoretical calculation reproduces well the experimental cross sections up to 15 MeV, while at higher energies, the calculation overestimates the cross section. This is probably because the theoretical calculation overestimates cross section of the ^{104}Pd (d,3n)^{103}Ag reaction.

In conclusion, we performed an experiment of deuteron-induced reactions on natural palladium to produce ^{103}Ag. The excitation function of the ^{nat}Pd(d,x)^{103}Ag reaction was measured for the first time from 22 MeV to 24 MeV.

References

1) A. Hermanne et al., Radiochim. Acta **92**, 215 (2004).
2) H. H. Andersen, J. F. Ziegler: Hydrogen Stopping Powers and Ranges in All Elements, Vol. 3 (Pergamon, Oxford, 1997).
3) National Nuclear Data Center: the NuDat 2 database, http://www.nndc.bnl.gov/nudat2/.
4) A. J. Koning et al.: TENDL-2015: TALYS-based evaluated nuclear data library.

Production cross sections of ^{169}Yb in deuteron-induced reactions on ^{169}Tm

M. Saito,[*1,*2] M. Aikawa,[*1,*2] Y. Komori,[*2] H. Haba,[*2] and S. Takács[*3]

Radioactive isotopes (RI) are used in many application fields such as engineering and medicine. The medical RI ^{169}Yb ($T_{1/2}$ = 32.018 d, EC = 100%) is an Auger electron and X-ray emitter suitable for use in brachytherapy.[1,2] The proton-,[3–5] deuteron-,[6–8] and α-induced reactions[9] on a monoisotopic ^{169}Tm target were investigated by several research groups. Based on the experimental cross-section data, the deuteron-induced reaction on ^{169}Tm is one of the best candidates for the production of ^{169}Yb owing to the large cross section of the (d,2n) reaction.[6–8] However, the experimental cross-section data for the ^{169}Yb production by deuteron-induced reactions show relatively large uncertainties and scattering; therefore, the excitation function has not been defined properly yet. In this paper, we report cross-section data of the ^{169}Tm(d,2n)^{169}Yb reaction using thin metallic thulium foils to reduce the uncertainty of the experimental data.

The excitation function of the deuteron-induced reactions on ^{169}Tm were measured by the stacked-foil activation method using high-resolution γ-ray spectroscopy to assess the activity of the irradiated target foils. ^{169}Tm metallic foils (purity: 99%, Goodfellow Co., Ltd., UK) were stacked with ^{nat}Ti (purity: 99.9%, Goodfellow Co., Ltd., UK) and ^{27}Al foils (purity: >99.95%, Nilaco Corp., Japan) for monitoring the beam parameters and for degrading the beam energy. The average thicknesses of Tm, Ti, and Al foils were determined by measuring the surface area and weight of a larger piece of each foil and found to be 28.65, 4.95, and 13.44 mg/cm^2, respectively. The irradiation was performed at the AVF cyclotron of the RIKEN RI Beam Factory. The target was irradiated in a Faraday-cup with a deuteron beam of 24.36 MeV and an average beam intensity of 135.6 nA for 75 min. The beam intensity was increased by 6.4% in agreement with the ^{nat}Ti(d,x)^{48}V monitor reaction. The incident beam energy was measured by the time-of-flight method using plastic scintillator monitors.[10]

Nuclear decay data of ^{169}Yb are taken from the online NuDat 2.6 database.[11] The energy-dependent cross sections of the ^{169}Tm(d,2n)^{169}Yb reaction were derived from the γ-line at 177.21 keV (22.28%). Results are shown in Fig. 1 together with the previously measured experimental data[6–8] and the extracted result of the TALYS calculation (TENDL-2015[12]). The lowest measured cross section was 0.20 mb at 5.1 MeV while the highest measured cross section was 682.8 mb at 13.5 MeV. This peak energy is in good agreement with the previous data,[6–8] although the present cross sections are slightly higher.

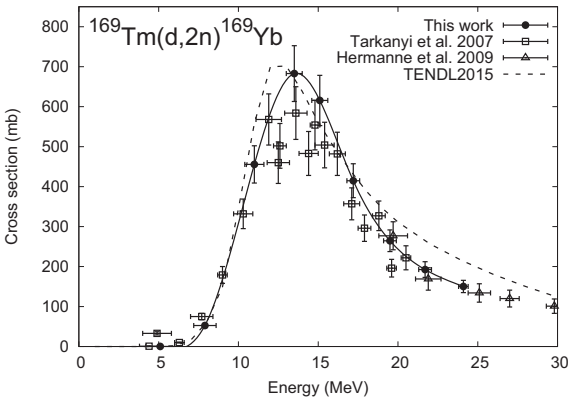

Fig. 1. The excitation function of the ^{169}Tm(d,2n)^{169}Yb reaction is shown with a spline fit over our experimental data. The result is compared with the previous experimental data[6–8] and TENDL-2015.[12]

In summary, we have measured the cross sections of the deuteron-induced reactions on ^{169}Tm to produce ^{169}Yb by using the stacked foil activation method. Thin metallic Tm foils were irradiated by a 24.36-MeV deuteron beam, and the activity of the produced radioisotopes was determined by high-resolution γ-ray spectrometry. The obtained excitation functions were compared with the earlier experimental data,[6–8] and good agreements were found in general.

*1 Graduate School of Science, Hokkaido University
*2 RIKEN Nishina Center
*3 MTA ATOMKI, Hungarian Academy of Sciences

References

1) F.H. DeLand et al., J. Nucl. Med. **12**, 683 (1971).
2) G. Lymperopoulou et al., Med. Phys. **33**, 4583 (2006).
3) C. Birattari et al., Nucl. Phys. A **201**, 579 (1973).
4) I. Spahn et al., Appl. Radiat. Isot. **63**, 235 (2005).
5) F. Tárkányi et al., Appl. Radiat. Isot. **70**, 309 (2012).
6) F. Tárkányi et al., Appl. Radiat. Isot. **65**, 663 (2007).
7) A. Hermanne et al., Nucl. Instr. Meth. B **267**, 727 (2009).
8) A. Hermanne et al., Nucl. Instr. Meth. B **383**, 81 (2016).
9) A.V. Mohan Rao et al., Pramana - J. Phys. **38**, 279 (1992).
10) T. Watanabe et al., Proc. 5th Int. Part. Accel. Conf. (IPAC2014), 3566 (2014).
11) National Nuclear Data Center: the NuDat 2 database, http://www.nndc.bnl.gov/nudat2/.
12) A.J. Koning et al.: TENDL-2015: TALYS-based evaluated nuclear data library.

No-carrier-added purification of ^{28}Mg using co-precipitation and cation exchange method

H. Kikunaga,[*1,*2] Y. Komori,[*2] H. Haba,[*2] S. Shibata,[*2] and S. Yano[*2]

The isotope ^{28}Mg is useful in biological sciences as a radioactive tracer.[1,2] Generally, ^{28}Mg is produced for each use in nuclear reactions because of its short half life of 21.6 h.[3] The reaction ^{27}Al(α,3p)^{28}Mg is often chosen for the production of ^{28}Mg owing to its potential to produce no-carrier-added ^{28}Mg tracer with a convenient and low-cost target. Several groups have reported separation methods of ^{28}Mg from Al targets based on adsorption,[4,5] co-precipitation,[6] solvent extraction,[7] and the cation exchange column method.[8] Although the cation exchange column method should yield a high purity tracer, it requires a large column and an eluant volume of a few hundred milliliters. In this work, we applied a co-precipitation method before the cation exchange column method to downsize the column volume. Downsizing chemistry leads to the reduction of waste and labor in separation procedures and the quality improvement of the tracer.

Magnesium-28 was produced in the ^{27}Al(α,3p)^{28}Mg reaction. An α-particle beam was delivered from either the RIKEN K70 AVF Cyclotron or the AVF Cyclotron at CYRIC, Tohoku University. The target stack of 7 Al foils (99.9% pure) with a thickness of 100 μm was irradiated with an α-particle beam with a beam energy of 50 MeV and a mean current of approximately 3 μA.

After the irradiation, the Al targets were dissolved in 12 M (mol/dm^3) HCl diluted with water to 15 mL. The ^{28}Mg isotopes were co-precipitated with iron hydroxide by adding 2 mg of Fe(III) and 25 mL of 6 M NaOH and separated from $[Al(OH)_4]^-$ ions. After centrifugal separation, the precipitation of iron hydroxide was dissolved in 9 M HCl. The solution was passed through an anion exchange resin column (Dowex 1×8, 100-200 mesh, 1 mL), which adsorbs Fe(III) ions, and the resin was washed with additional 9 M HCl. The eluate was heated to dryness and adjusted to 0.5 M oxalic acid. Note that the solution includes non-radioactive Na ions entering from the co-precipitation process. To investigate the behavior of the Na ions, 300 Bq of ^{22}Na tracer was added to the solution. The solution was passed through a cation exchange resin column (Dowex 50w×8, 100-200 mesh, 1 mL) to adsorb ^{28}Mg isotopes. The resin was washed with 10 mL of 0.5 M oxalic acid to eliminate Al ions and then with 0.5 M HCl to eliminate Na ions. The elution curves of the cation exchange separation for Na and Mg are shown in Fig. 1. The Na ions are eluted completely within 10 mL of 0.5 M HCl whereas the Mg ions are retained onto the column. The ^{28}Mg isotopes were eluted from the column with 6 mL of 2 M HCl.

The chemical yield of the separation procedure, determined by γ-spectrometry of ^{28}Mg, was higher than 85%. However, the Mg fraction obtained in the chemical procedure includes a small amount of ^{7}Be radioactivity. We will attempt to improve this chemical procedure to eliminate Be isotopes from the Mg fraction completely.

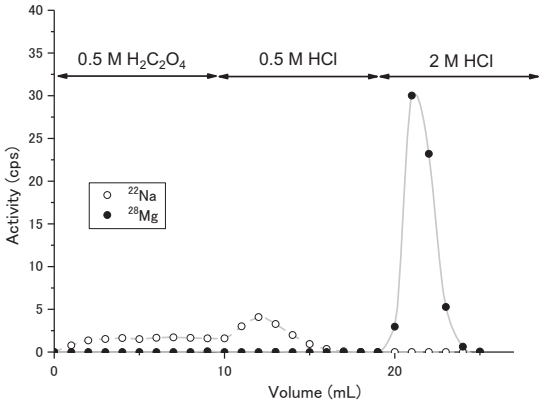

Fig. 1. Elution curves for the cation exchange separation for Na and Mg.

References

1) C. Schimansky, J. Plant Nutr. **8**, 467 (1985).
2) K. Tanoi et al., Plamt Soil **384**, 69 (2014).
3) R. B. Firestone, V. S. Shirley: Table of Isotopes, 8th ed. (John Wiley and Sons, New York, 1996).
4) J. Hudis, J. Inorg. Nucl. Chem. **4**, 237 (1957).
5) T. Nozaki, Int. J. Appl. Radiat. Isot. **26**, 17 (1975).
6) H. Lundqvist, P. Malmborg, Int. J. Appl. Radiat. Isot. **30**, 33 (1979).
7) K. Mukhopadhyay, S. Lahiri: Radiochim. Acta **90**, 65 (2002).
8) R. Iwata et al., J. Radioanal. Nucl. Chem. **159**, 233 (1992).

*1 Research Center for Electron Photon Science, Tohoku University
*2 RIKEN Nishina Center

Specification of ^{67}Cu produced in the ^{70}Zn($d,\alpha n$)^{67}Cu reaction

S. Yano,[*1] H. Haba,[*1] S. Shibata,[*1] Y. Komori,[*1] K. Takahashi,[*1] Y. Wakitani,[*2] T. Yamada,[*2] and M. Matsumoto[*2]

Copper-67 (half life $T_{1/2}$ = 61.83 h and β⁻-decay branch $I_{\beta-}$ = 100%) is one of the promising radioisotopes for radiotherapy and radiodiagnosis.[1] In our preliminary study,[2] about 70 kBq of ^{67}Cu was produced in the ^{70}Zn($d,\alpha n$)^{67}Cu reaction at the AVF cyclotron. The production yield of ^{67}Cu was 4.0 MBq/μA h at 24-MeV deuteron beam energy. We also investigated a chemical purification procedure for ^{67}Cu. The chemical yield of ^{67}Cu was 97%, and the decontamination factors for Ga and Zn were evaluated to be ~10^3 and >10^3, respectively. In this work, we developed a new irradiation chamber to produce a larger amount of ^{67}Cu (> 100 MBq) with a more intense deuteron beam. About 100 MBq of the purified ^{67}Cu was obtained and its radionuclidic purity, specific radioactivity, and chemical purity were evaluated.

A schematic of the ^{67}Cu production chamber is shown in Fig. 1. The 24-MeV deuteron beam with an intensity of 4 μA was extracted from the AVF cyclotron. The ^{70}Zn-enriched oxide (^{70}ZnO) powder was prepared as a disk with 10-mm diameter and 340-mg cm^{-2} thickness at a pressure of 2×10^3 kg cm^{-2} for 3 min. The isotopic composition of the ^{70}Zn target was 96.87% ^{70}Zn, 1.55% ^{68}Zn, 0.09% ^{67}Zn, 0.55% ^{66}Zn, and 0.94% ^{64}Zn. As shown in Fig. 1, the ^{70}ZnO disk placed on a Ta beam stopper was covered by a high-purity Al foil 10 μm in thickness. During the irradiation, the ^{70}ZnO target was cooled with circulating helium gas (30 L min^{-1}) and water (1.5 L min^{-1}). The beam axis was continuously rotated in 3-mm diameter at 2 Hz to avoid local heating of the target using electromagnets on the beam line of the AVF cyclotron. After the 10-h irradiation, ^{67}Cu was separated from the target material and by-products such as ^{67}Ga, ^{69m}Zn, and ^{71}Zn through the chemical procedure reported in Ref.[2] The purified ^{67}Cu was obtained as 300 μL of 0.1 M CH_3COOH for synthesis of the ^{67}Cu-labeled antibody.[3] The radioactivity and radionuclidic purity was determined by γ-ray spectrometry using a Ge detector. The specific radioactivity and chemical purity were also evaluated by chemical analysis using an inductively coupled plasma mass spectrometer (Agilent Technologies 7700x).

A γ-ray spectrum of the purified ^{67}Cu is shown in Fig. 2. 135 MBq of ^{67}Cu was produced at the end of bombardment (EOB). The major radionuclidic impurity in the purified ^{67}Cu was ^{64}Cu ($T_{1/2}$ = 12.70 h). The radioactivity ratio A(^{64}Cu)/A(^{67}Cu) was 1.2×10^{-2} at EOB, which decreased to 8.9×10^{-4} at 60 h after EOB (a typical time for its application studies). The present A(^{64}Cu)/A(^{67}Cu) ratio is smaller than the typical value of 6.7 in the ^{68}Zn(p,2p)^{67}Cu reaction.[4] The radionuclidic purity of the ^{67}Cu solution was then evaluated to be >99.9% 60 h after EOB. In the ICP-MS analysis, only Cu (2.1 ppm) and Br (1.0 ppm) were detected with concentrations >1 ppm among the elements having atomic number $Z \geq 20$. The specific radioactivity of ^{67}Cu was then determined to be 220 MBq μg^{-1} at EOB. Hundreds of MBq of the purified ^{67}Cu are ready for application studies. The results of synthesis of the ^{67}Cu-labeled antibody will be reported elsewhere.[3]

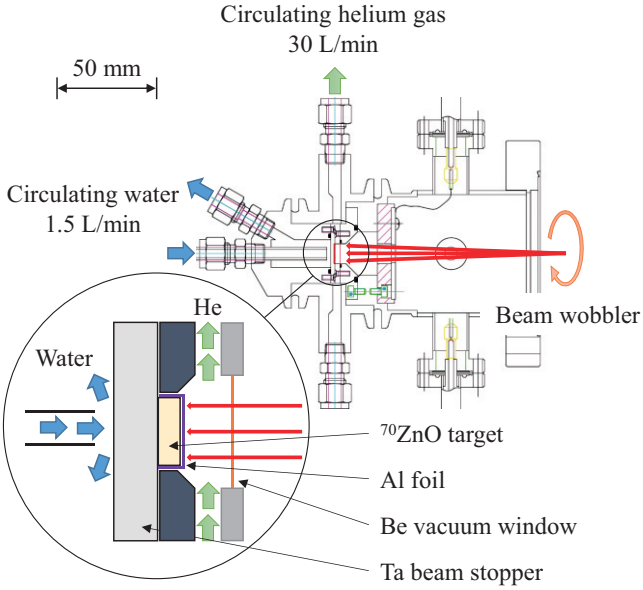

Fig. 1. Schematic of the new ^{67}Cu production chamber.

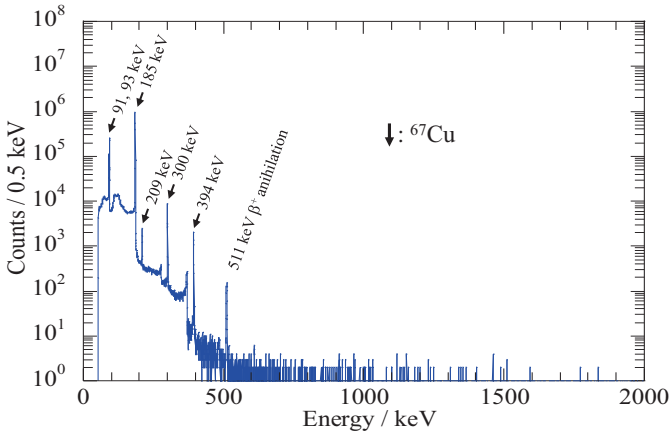

Fig. 2. Typical γ-ray spectrum of the purified ^{67}Cu.

References

1) I. Novak-Hofer et al., Eur. J. Nucl. Med. **29**, 821 (2002).
2) S. Yano et al., RIKEN Accel. Prog. Rep. **49**, 22 (2016).
3) K. Fujiki et al., private communication.
4) In *Cyclotron Produced Radionuclides: Physical Characteristics and Production Methods*, IAEA Technical Reports Series **468**, 100 (2009).

*1 RIKEN Nishina Center
*2 Japan Radioisotope Association

Development of a production technology of ^{211}At at the RIKEN AVF cyclotron: (i) Production of ^{211}At from the ^{209}Bi(α,2n)^{211}At reaction

N. Sato,[*1] S. Yano,[*1] A. Toyoshima,[*1,*2,*3] H. Haba,[*1] Y. Komori,[*1] S. Shibata,[*1] K. Watanabe,[*1] D. Kaji,[*1] K. Takahashi,[*1] and M. Matsumoto[*4]

Astatine-211 (^{211}At, $T_{1/2}$ = 7.214 h) is one of the promising radionuclides for the α-particle therapy of diseases. The 5.9- and 7.5-MeV α-particle emissions occur with intensities of 42% and 58%, respectively, associated with the ^{211}At decay.[1] Owing to the proper ranges of these α-particles in tissue (60–80 μm), the ^{211}At-labeled medicine is effective in killing focus cells. For the pre-clinical and clinical trials, a large amount of ^{211}At-labeled compounds is needed.

We have started to produce ^{211}At from the ^{209}Bi(α,2n)^{211}At reaction at the RIKEN AVF cyclotron and to distribute it to researchers in universities and institutes in Japan. Figure 1 shows the irradiation system for the ^{211}At production. An 18-μm beryllium window was placed to separate the vacuum beam line and the He-filled ^{211}At production chamber. A metallic ^{209}Bi target (chemical purity: >99.999%, typical thickness: 20 mg/cm^2) was prepared by vacuum evaporation onto an Al backing plate of 1-mm thickness. The Bi target was placed at an angle of 15° with respect to the beam axis. A 29.36-MeV α beam was delivered from the AVF cyclotron; the beam energy on the center of the target surface was calculated to be 28.4 MeV with the SRIM-2013 program.[2] To obtain ^{211}At with a high radionuclidic purity, the α-beam energy was controlled at 28–29 MeV to prevent the production of ^{210}At ($T_{1/2}$ = 8.1 h), which decays to a highly toxic α emitter ^{210}Po ($T_{1/2}$ = 138 d); the threshold energy for the ^{209}Bi(α,3n)^{210}At reaction is 28.6 MeV. Thus, electrostatic pickups were used for an accurate evaluation of the beam energy.[3] The target was cooled with circulating water (1.5 L/min) and He gas (30 L/min) during the irradiation. A beam wobbler system was used to rotate the beam spot on the target and to prevent heat concentration. The Bi targets were irradiated for 20–30 min at beam intensities between 1 and 10 particle μA. After the irradiation, the targets were subjected to γ-ray spectrometry with a Ge detector.

Figure 2 shows the thick-target yield of ^{211}At as a function of the α-beam energy on the target. Our experimental data almost agree with the IAEA recommended values.[4] The deduced yield of ^{211}At was 7.2 ± 0.5 GBq/C at 28.4 MeV, which was nearly constant upto 10 particle μA. According to this work,

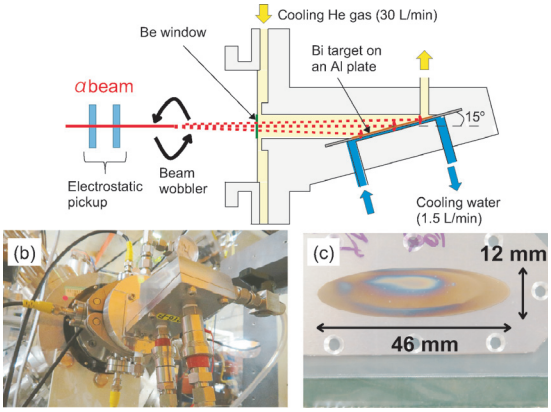

Fig. 1. (a) Schematic view of the irradiation system. (b) Photograph of the ^{211}At production chamber. (c) Vacuum-evaporated Bi target on an Al plate (after irradiation).

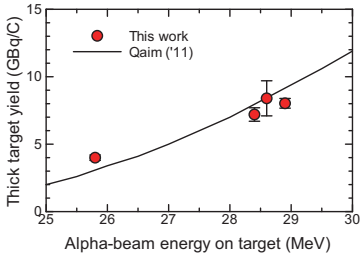

Fig. 2. Thick target yield of ^{211}At as a function of α-beam energy. The solid curve indicates the IAEA recommended value.[4]

about 500 MBq of ^{211}At could be obtained under 10 particle μA irradiation for 1 h. The atomic ratio of ^{210}At/^{211}At at the end of bombardment (EOB) was estimated to be $< 1 \times 10^{-5}$, which satisfied the medical requirement of $< 1 \times 10^{-3}$ at EOB.[5] After the irradiation, ^{211}At was purified by a dry distillation method, which is reported in our succeeding paper.[6]

*1 RIKEN Nishina Center
*2 Advanced Science Research Center, Japan Atomic Energy Agency
*3 Graduate School of Science, Osaka Univ.
*4 Japan Radioisotope Association

References

1) R. B. Firestone et al.: Table of Isotopes CD-ROM, 8th ed. (John Wiley and Sons, New York, 1998).
2) J. F. Ziegler et al.: Nucl. Instrum. Meth. Phys. Res. B **268**, 1818 (2010).
3) T. Watanabe et al.: Proc. 12th Annual Meeting of Particle Accelerator Society of Japan (2015), p. 1198.
4) S. M. Qaim et al. (eds.): IAEA Technical Report Series No. 473, IAEA, Vienna, Austria (2011).
5) A. Hermanne et al.: Appl. Radiat. Isot. **63**, 1 (2005).
6) S. Yano et al.: In this report.

Development of a production technology of ^{211}At at the RIKEN AVF cyclotron: (ii) Purification of ^{211}At by a dry distillation method

S. Yano,[*1] N. Sato,[*1] A. Toyoshima,[*1,2,3] H. Haba,[*1] Y. Komori,[*1] S. Shibata,[*1] K. Takahashi,[*1] and M. Matsumoto[*4]

Astatine-211 is one of the promising radioisotopes for targeted cancer therapy[1] because ^{211}At has a suitable half life of $T_{1/2}$ = 7.214 h for medical applications and a high α-particle emission probability of 100% in addition to its short-lived decay daughter ^{211g}Po ($T_{1/2}$ = 516 ms). We have started to develop a production technology of ^{211}At at the RIKEN RI Beam Factory to distribute this useful radioisotope to the general public. In a separate paper,[2] we have reported the production technology of ^{211}At from the ^{209}Bi(α,2n)^{211}At reaction using the AVF cyclotron. In this report, we describe a chemical purification procedure of ^{211}At from the irradiated ^{209}Bi target by a dry distillation method. A schematic of the dry distillation apparatus is shown in Fig. 1. After the irradiation,[2] the ^{209}Bi target was placed on a copper tray in a quartz tube (28-mm i.d. × 200-mm length) and heated up to 850°C using an electric furnace. ^{211}At sublimated from the target material was extracted from the quartz tube to a PFA tube (1-mm i.d. × 1-m length) through a quartz capillary (1.95-mm i.d. × 130-mm length) with O_2 gas flow at a flow rate of 20 mL min^{-1}. The PFA tube was cooled at –72°C in a mixture of dry ice and ethanol to collect the gaseous ^{211}At. After distillation for 30 min at 850°C, the quartz capillary was removed from the quartz tube, and the inside of the quartz capillary and the PFA trap tube were washed with 1 mL of water to recover ^{211}At. The chemical yield of ^{211}At was determined by γ-ray spectrometry using a Ge detector. The radionuclidic purity was determined by α-particle spectrometry and γ-ray spectrometry using Si and Ge detectors, respectively.

The chemical purity and the decontamination factor of ^{209}Bi from ^{211}At were evaluated based on a chemical analysis using ICP-MS. The α-particle and γ-ray spectra of the purified ^{211}At are shown in Figs. 2A and 2B, respectively. Only the peaks corresponding to ^{211}At are observed in the spectra. The chemical yield of ^{211}At was approximately 60%; the major loss of ^{211}At was due to the low trap yield of the PFA tube. The radionuclidic purity of the ^{211}At solution was >99.9%, and the atomic ratio of ^{210}At/^{211}At was < 1.0×10^{-5} at the end of irradiation. Among the elements having atomic number $Z \geq 13$ (Al), Cu (405 ppb), Al (23 ppb), Tl (20 ppb), Bi (9 ppb), and Zn (8 ppb) were detected with a concentration >5 ppb. The decontamination factor of ^{209}Bi from the purified ^{211}At was 3.0×10^{-7}. We are ready to distribute 1 GBq of ^{211}At for researches in nuclear medicine.

*1 RIKEN Nishina Center
*2 Advanced Science Research Center, Japan Atomic Energy Agency
*3 Graduate School of Science, Osaka Univ.
*4 Japan Radioisotope Association

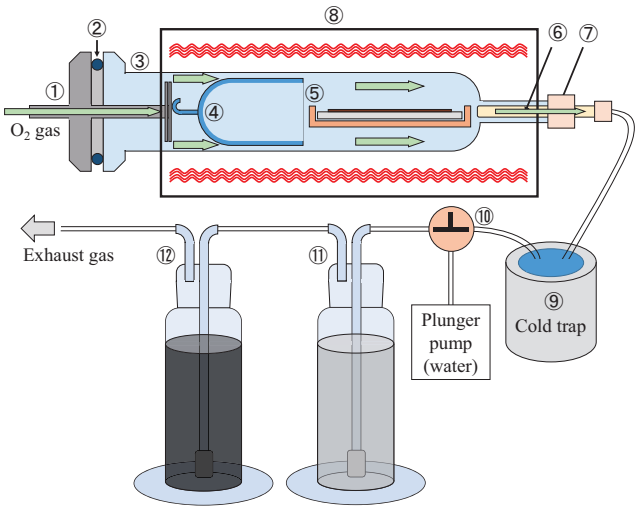

Fig. 1. Schematic of the dry distillation system of ^{211}At. ①: KF40 flange with a heat sink for preheating of the O_2 gas. ②: O-ring. ③: Quartz tube (28-mm i.d. × 200-mm length). ④: Quartz spacer. ⑤: Bi target on an Al plate in Cu tray. ⑥: Quartz capillary (2-mm i.d. × 130-mm length). ⑦: PFA connector. ⑧: Electric furnace. ⑨: PFA trap tube (1-mm i.d. × 1-m length) cooled in a mixture of ethanol and dry ice. ⑩: PFA three-way valve. ⑪: 1 M $Na_2S_2O_5$ gas wash bottle. ⑫: Charcoal gas wash bottle.

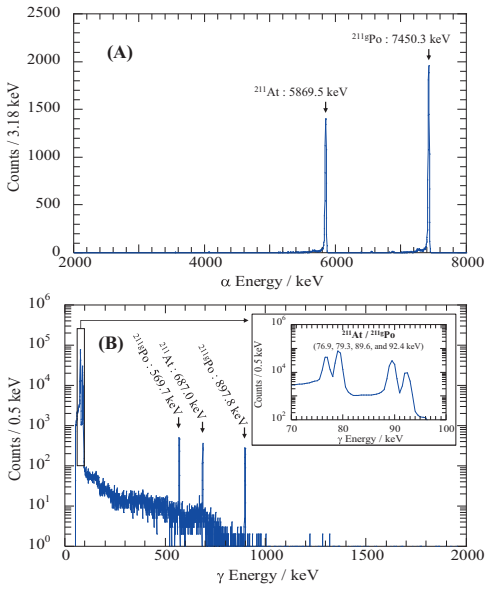

Fig. 2. Typical (A) α-particle and (B) γ-ray spectra of the purified ^{211}At obtained from a Bi target.

References

1) S. Huclier-Markai, Curr. Top. Med. Chem. **23**(12), 1 (2012).
2) N. Sato et al., in this report.
3) K. Nagatsu et al., Appl. Radiat. Isot. **94**, 363 (2014).

4. Radiation Chemistry and Biology

Focus formation of Rad51 and phosphorylated DNA-PK after heavy-ion irradiation in mammalian cells.

M. Izumi[*1] and T. Abe[*1]

Accelerated heavy-ion particles with high linear energy transfer (LET) induce complex clustered DNA damage, which is considered an obstacle to efficient repair. DNA double-strand breaks (DSB), the most dangerous DNA damage, are repaired primarily by non-homologous end joining (NHEJ), homologous recombination (HR), or microhomology mediated end joining in mammalian cells.[1] Our previous studies using the wild-type CHO cell and two CHO mutant lines deficient in HR or NHEJ suggest that HR is primarily involved in the repair pathway induced by high-LET ionizing radiation.[2,3] However, several studies suggest that NHEJ is also involved in DSB repair caused by high-LET ionizing radiation,[4,5] and the repair mechanism is still controversial in higher eukaryotes.

In this study, we investigated the foci formation of Rad51 and phosphorylated DNA-PK, which are involved in HR and NHEJ, respectively (Fig. 1). In human normal fibroblast NB1RGB cells synchronized at the G0 phase by serum starvation, the formation of Rad51 foci was not observed after X-ray or Ar-ion irradiation since HR is dependent on the S phase. The number of Rad51 foci reached maximum 8 h after X-ray irradiation and decreased gradually thereafter in both HeLa cells and logarithmically growing NB1RGB cells. On the other hand, the number of Rad51 foci increased immediately after Ar-ion irradiation (LET = 300 keV/μm), suggesting that the high LET radiation stimulates HR. The number of Rad51-positive cells in the population of HeLa and logarithmically growing NB1RGB cells also reached maximum at 8 h after X-ray irradiation. In contrast, the number of Rad51-positive cells in the population of HeLa cells increased with time after Ar-ion irradiation, whereas that in the population of logarithmically growing NB1RGB cells decreased as time proceeded because DNA damage caused by Ar-ion irradiation induced prolonged cell cycle arrest at the G2 and G1 phase in HeLa and NB1RGB cells, respectively.

The number of phosphorylated DNA-PK foci in quiescent NB1RGB cells was twice that in logarithmically growing NB1RGB cells 1 h after X-ray irradiation, suggesting that NHEJ and HR work competitively. In contrast, the number of phosphorylated DNA-PK foci in quiescent cells was slightly higher than that in logarithmically growing cells after Ar-ion irradiation. These results suggest that HR works mainly after Ar-ion irradiation, which is consistent with our previous report[5]. All the irradiated HeLa and quiescent NB1RGB cells had the DNA-PK foci 1 h after X-ray irradiation, whereas only 57% of logarithmically growing NB1RGB cells had the DNA-PK foci 1 h after irradiation, suggesting that the foci formation of phosphorylated DNA-PK occurs only in the G1-S phase in NB1RGB cells after X-ray irradiation. In contrast, the foci of phosphorylated DNA-PK were observed in all irradiated cells 1 h after Ar-ion irradiation, suggesting that the foci formation of phosphorylated DNA-PK occurs even in the G2 phase after Ar-ion irradiation. These results also suggest that the regulation of formation of DNA-PK foci was different between X-ray and Ar-ion irradiation. Now we are investigating the localization of the other repair proteins involved in the selection of repair pathways for DSB repair.

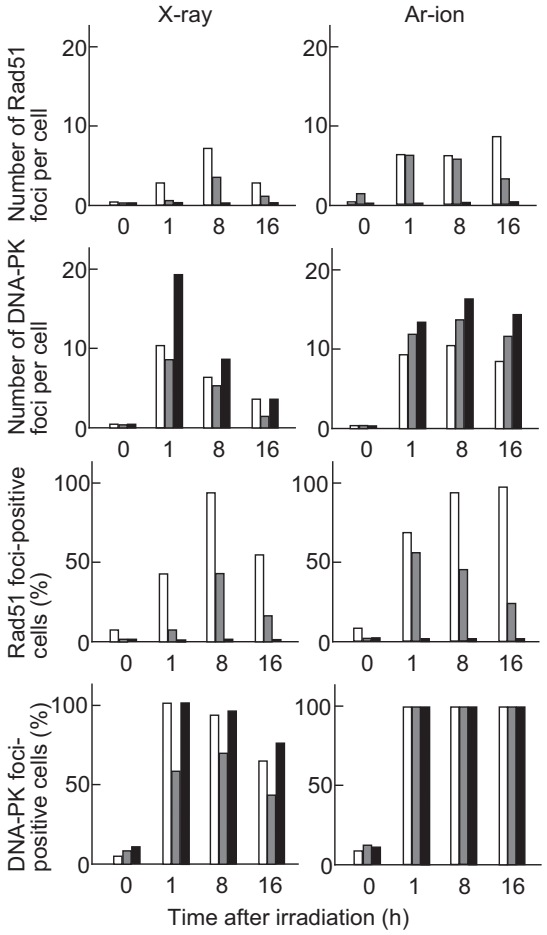

Fig. 1 Kinetics of the foci formation of Rad51 and phosphorylated DNA-PK in HeLa cells (open box), logarithmically growing NB1RGB cells (gray box), and synchronized NB1RGB cells at the G0 phase (closed box). The foci were detected by indirect immunofluorescent staining 1-16 h post irradiation.

References

1) L. S. Symington, J. Gautier, Annu. Rev. Genet. **45,** 247 (2011).
2) M. Izumi, T. Abe, RIKEN Accel. Prog. Rep. **47,** 253 (2014).
3) M. Izumi, T. Abe, RIKEN Accel. Prog. Rep. **49,** 251 (2016).
4) A. Takahashi et al., Radiat. Res. **182,** 338 (2014).
5) A. Bajinskis et al., Mut. Res. **731,** 125 (2012).

*1 RIKEN Nishina Center

Low-dose high-LET heavy ion-induced bystander signaling (III)

M. Tomita,[*1,*2] T. Tsukada,[*2] and M. Izumi[2]

Radiation-induced bystander response (RIBR) is a cellular response induced in non-irradiated cells that received bystander signals from directly irradiated cells within an irradiated cell population.[1)] RIBR induced by low doses of high-LET radiation is an important issue for the health of astronauts and in hadrontherapy. Here, we investigated the underlying molecular mechanisms and biological implications of RIBR induced by such low doses of high-LET radiation.

We established an optimal system to assess the low doses of high-LET radiation-induced bystander cell killing, and reported that gap-junction intercellular communication (GJIC), cyclooxygenase-2 (COX-2), and nitric oxide (NO) are involved in its signal transfer.[2)] Figure 1 shows the results obtained in these experiments. Normal human fibroblasts, WI-38, were irradiated with 0.1 Gy of 90 MeV/u Fe ions (1000 keV/μm). Cells were harvested 16–24 h after irradiation and plated on cell culture dishes to allow colony formation. The surviving fraction decreased to 0.84 ± 0.02 by the bystander cell killing effects (Fig.1, control). Lindane (Lin) and NS-398 (inhibitors of GJIC and COX-2, respectively) were dissolved in DMSO (a scavenger of reactive oxygen species). c-PTIO is a scavenger of NO. DMSO (0.1%), Lin (50 μM), c-PTIO (20 μM), or NS-398 (50 μM) was added to the medium 2 h before irradiation.[3)] DMSO did not significantly suppress bystander cell killing. In contrast, Lin, NS-398, and c-PTIO significantly ($P < 0.05$) suppressed cell death to similar levels. Cells pretreated with both c-PTIO and Lin did not survive more than those pretreated with Lin or c-PTIO alone. These results support our previous suggestion that GJIC is involved in bystander signaling and the cell culture medium induces the bystander cell killing effect in a coordinated manner.[2)]

The fluence (number of ion tracks/cm^2) was calculated as the dose (Gy)/LET (keV/μm)/(1.6×10^{-9}). The area of the cell nucleus was 188 μm^2. The average number of ion tracks per cell nucleus was calculated as 0.11 when cells were irradiated with 0.1 Gy of Fe ions (1000 keV/μm).[4)] To confirm this result, we measured the number of ion hits per cell nucleus using a plastic ion-track detector, CR-39. The CR-39 film was irradiated with 0.1 Gy of Fe ions and then cells were cultured on the film. After cells were fixed and stained with the DAPI solution, the opposite surface of the film was etched with an alkaline-ethanol solution.[5)] Figure 2 shows the images of cell nuclei and the etch pits of the CR-39 film. The number of ion hits per cell nucleus was 0.11 ± 0.01 (n=5), which corresponded with the calculated results. Therefore, the cell surviving fraction at a dose of 0.1 Gy was lower than the number of Fe-ions hit on the cell nucleus, suggesting that cell death was induced in non-hit cells by RIBR.

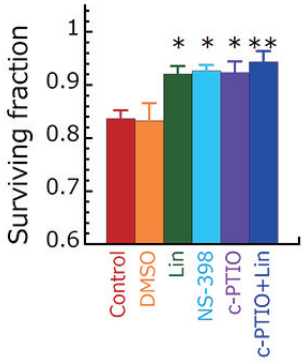

Fig. 1. Effect of inhibitors or scavengers on cell survival. WI-38 cells pretreated with inhibitors or scavengers were irradiated with 0.1 Gy of Fe ions (1000 keV/μm). Error bars represent the standard errors of the means (SEMs) (n=4–6).*$P < 0.05$ and **$P < 0.01$, for comparison with control and drug-treated cultures.

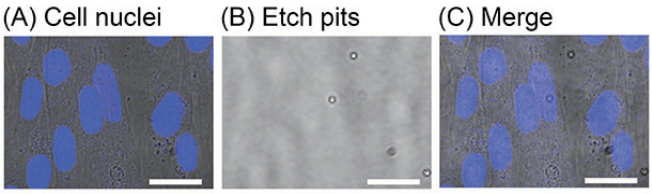

Fig. 2. Microscopic images of WI-38 cell nuclei and etch pits of the CR-39 irradiated with 0.1 Gy of Fe ions (1000 keV/μm). Panel A shows the fluorescence image of WI-38 cell nuclei stained with DAPI. Panel B shows the etch pits of the CR-39 film. Panel C shows the overlay of A and B. Scale bar is 20 μm

*1 Radiation Safety Research Center, Central Research Institute of Electric Power Industry
*2 RIKEN Nishina Center

References

1) M. Tomita and M. Maeda: J. Radiat. Res. **56**, 205 (2015).
2) M. Tomita et al.: RIKEN Accel. Prog. Rep. **48**, 302 (2015).
3) M. Tomita et al.: Radiat. Res. **179**, 200 (2013).
4) M. Tomita et al.: RIKEN Accel. Prog. Rep. **42**, 276 (2009).
5) T. Funayama et al.: Radiat. Res. **163**, 241 (2005).

Results of whole-genome analysis of *pink* and *ebony* mutant

K. Tsuneizumi,[*1] H. Ichida,[*1] R. Morita,[*1] and T. Abe[*1]

Heavy-ion-beam mutagenesis is generally recognized as an effective method for mutation breeding.[1, 2] Although this method was greatly successful with plants, its application is limited for animals. Therefore, we plan to acquire more basic data to set up optimal conditions for the heavy-ion-beam irradiation system by using *Drosophila melanogaster* (fruit fly) as the model.

In our previous study, we determined that 1-3 Gy irradiation using a carbon-ion beam is suitable for the large-scale screening of mutant lines.[3] To elucidate the biological effect of heavy-ion-beam irradiation to the genome, we analyzed the whole-genome sequencing of several mutants established by the condition of 1-3 Gy irradiation. In this report, we applied the high-performance bioinformatics pipeline, which was developed for analyzing rice exome sequencing results obtained in our laboratory[4], to fly genome analysis. Mutants are established using the third chromosome balancer, which is a unique genetic tool for fruit fly. Because the third chromosome balancer is known to prevent homologous recombination only on the third chromosome, the following results are limited to third chromosome events.

In this report, we show the result of *pink* [Fig. 1] and *ebony* [Fig. 2] mutants. Each mutation is summarized in Fig. 1c and Fig. 2c. These data suggest that 1-3 Gy dose is sufficient for several mutations such as single base substitution, deletion, insertion, rearrangement, and large deletion. These diversities of mutations indicate an advantage in screening by the heavy-ion-beam mutagenesis. Both mutants contain 11 or 12 mutations, and then the third chromosome consists of 5.2 x 10^7 base pairs (bp). This means that the heavy-ion-beam irradiation introduces a mutation into the genome at a frequency of approximately 4.5 x 10^6 bp.

Among 11 or 12 mutations, an alteration in protein sequence was observed in only one gene. We purchased several mutants of the same gene from the *Drosophila* stock center. Through the complementation test known as a genetic technique for fruit fly to determine whether two mutants belong to the same gene, we determined that the causal genes are *pink* and *ebony*. Though it is thought that the fruit fly has about 15000 genes, we could easily identify the causal genes of mutants by using whole-genome sequencing and the pipeline. These results suggest that the pipeline technique is a powerful tool for mutation analysis.

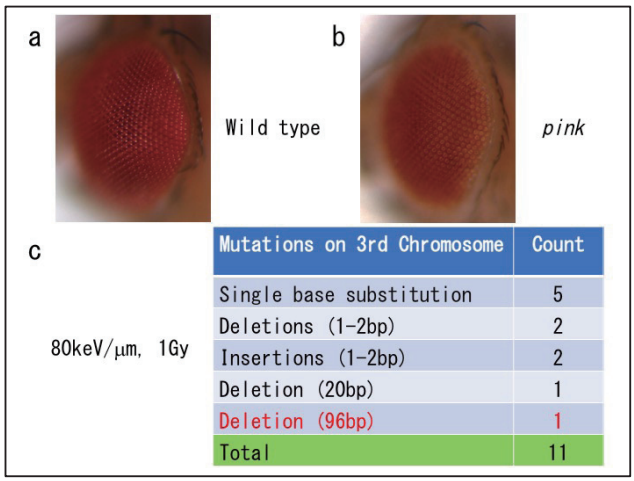

Mutations on 3rd Chromosome	Count
Single base substitution	5
Deletions (1-2bp)	2
Insertions (1-2bp)	2
Deletion (20bp)	1
Deletion (96bp)	1
Total	11

Fig. 1. Phenotype of the *pink* mutant and the result of whole-genome analysis.

a) Wildtype eye color is vivid red. b) The mutant eye color becomes lighter than wildtype. c) The mutant is established by the condition with 80 keV/μm linear energy transfer at 1 Gy dose level. Whole-genome analysis revealed 11 mutations caused by heavy-ion-beam irradiations. Each mutation was categorized into substitution, deletion and insertion. The causal mutation of *pink* was classified into large deletion with red text.

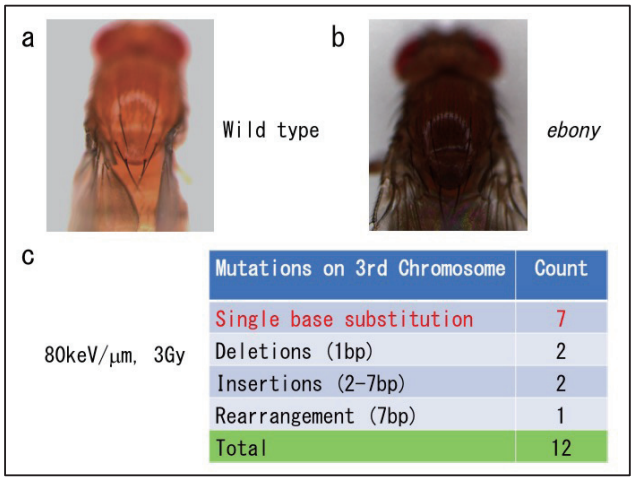

Mutations on 3rd Chromosome	Count
Single base substitution	7
Deletions (1bp)	2
Insertions (2-7bp)	2
Rearrangement (7bp)	1
Total	12

Fig. 2. Phenotype of the *ebony* mutant and the result of whole-genome analysis.

a) Wildtype body color is yellowish brown. b) The mutant body color becomes darker than wildtype. c) The mutant is established by the condition with 80 keV/μm linear energy transfer at 3 Gy dose level. Whole-genome analysis revealed 12 mutations caused by heavy-ion-beam irradiations. Each mutation was categorized into substitution, deletion, insertion and rearrangement. The causal mutation of *ebony* was classified into single base substitution with red text.

References

1) T. Abe et al., in Plant Mutation Breeding and Biotechnology, edited by Q. Y. Shu et al. (CABI, Oxfordshire, 2012), p. 99.
2) A. Tanaka et al., J. Radiat. Res. **51**, 223 (2010).
3) K. Tsuneizumi et al., RIKEN Accel. Prog. Rep. **49**, 253 (2016).
4) H. Ichida et al., RIKEN Accel. Prog. Rep. **49**, 254 (2016).

*1 RIKEN Nishina Center

Effect of carbon-ion irradiation on the mycelial growth of *Tricholoma matsutake* in the form of spawn

H. Murata,[*1] T. Abe,[*2] H. Ichida,[*2] Y. Hayashi,[*2] T. Yamanaka,[*1] T. Shimokawa,[*1] and H. Neda[*1]

Tricholoma matsutake is a filamentous fungus that produces gourmet mushrooms, commonly known as "matsutake," during mycorrhizal association with conifers, most notably red pines *Pinus densiflora* in the Far East Asia and *Pinus sylvestris* in Scandinavia. [1-3] Currently, neither cultivars nor cultivation methods that allow *T. matsutake* to fruit artificially are available, unlike some wood-rotting edible fungi, such as *Lentinula edodes*, commonly known as "shiitake," and *Pleurotus ostreatus*, commonly known as "oyster mushroom." Because we solely harvest the wild fruiting body for trading, the matsutake yield has devastatingly decreased over the past few decades in Japan and other countries that export the commodity. Developing cultivars that are suitable for spawn cultivation to yield matsutake will greatly contribute to countermeasures against overharvesting of the wild mushroom. *Lyophyllum shimeji*, an ectomycorrhizal edible fungus that produces another gourmet mushroom commonly known as "shimeji," are artificially cultivated for commercial trading after selecting a few extraordinary strains suitable for spawn cultivation. [4]

Since particle beams have been used widely in crop breeding to generate superb cultivars and industrial microbes with practical uses, we hypothesized that particle beams could be useful in breeding *T. matsutake* cultivars for fruiting during spawn cultivation; note that classical breeding does not work on the fungus because of complex variable nuclear phases and the lack of information on the mating system. [5] In the present study, as a prerequisite for generating *T. matsutake* mutants, we analyzed the lethality of carbon-ion irradiation and its corresponding doses using the fungal spawn.

Fig. 1. *T. matsutake* spawn. The mycelia axenically cultured in a mayonnaise jar (left) were transferred to a sterile plant tissue culture box (right) for irradiation.

[*1] Forestry and Forest Products Research Institute
[*2] RIKEN Nishina Center

T. matsutake mycelia were cultured as spawn in a mayonnaise jar according to a protocol for *L. shimeji* (Fig. 1), [4] which could be more practical for cultivar selection than agar plate culture. Prior to the irradiation, the spawn was transferred into either a sterile plant tissue culture box (60 × 60 × 60 mm) containing sheets (10 mm thick) of hardwood or a sterile plastic Petri dish (90 × 15 mm) so that the particles pass through the spawn (Fig. 1). After irradiation, the spawn was divided into 10 portions as seeds, inoculated into fresh sterile substrates, and incubated at 22 °C for 60 days (Fig. 2). The extent of mycelial growth in the spawn was scored (Fig. 2).

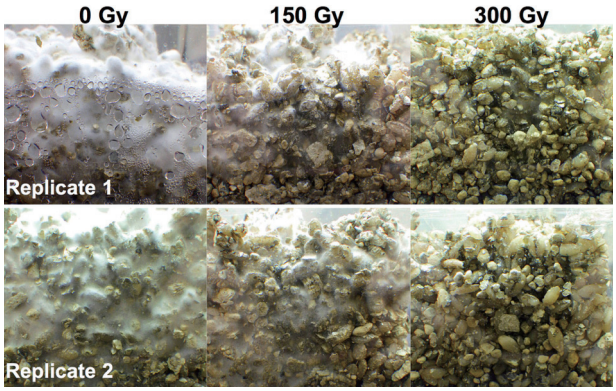

Fig. 2. *T. matsutake* growth after the carbon-beam irradiation. The irradiated spawn was divided as seeds, inoculated into fresh substrates and incubated for 60 days.

The 300-Gy irradiation dose resulted in little growth, as the fungal mycelia only colonized the inoculated area on the surface, while the 150-Gy dose resulted in growth to a certain extent by thinly invading the substrate (Fig. 2). In the controls, the fungal mycelia grew well throughout the substrate (Fig. 2). Therefore, we conclude that the carbon ion irradiation may be useful in generating mutants from *T. matsutake* that is cultured as spawn with a barley grain-based substrate.

References

1) L. Vaario et al., Mycorrhiza **20**, 511 (2010).
2) A. Yamada et al., Mycoscience **55**, 27 (2014).
3) M. Yamaguchi et al., Mycorrhiza **26**, 847 (2016).
4) A. Ohta, Mycoscience **35**, 147 (1994).
5) H. Murata et al., Mycoscience **56**, 287 (2015).

Flotation of *Botryococcus braunii* after ionizing irradiation

Y. Kazama,[*1] K. Ikeda,[*2] K. Kaya,[*2] Y. Sakakura,[*2] and T. Abe[*1]

Botoryococcus braunii is a green microalga having the ability to produce high amounts of oil, making it suitable for biofuel production. Aiming at the industrial use of this species, several studies, including one on the development of new strains having a high growth rate and cost-effective cultivation methods, are being conducted.[1,2] Another important issue is the harvesting method of *B. braunii* after cultivation. Since this alga contains much oil after cultivation, its specific gravity is low. Thus, the collection of the algae using centrifugation is difficult. Here, we have reported a novel phenomenon of *B. braunii*, in which *B. braunii* floats on the surface of media after the irradiation of ionizing radiation. By applying this phenomenon, an effective method for the collection of the algae can be developed.

The flotation of *B. braunii* was first observed after Ar-ion irradiation. A strain, Hojo, derived from the Hojo-Oh pond in Tsukuba city was cultured and irradiated with Ar ion beams with an LET of 290 keV/μm and a dose range of 25-150 Gy. The flotation was observed 2 h after irradiation. The ratio of floated algae increased in a dose-dependent manner. For example, 11.9% of the algae floated with 25-Gy irradiation, whereas 100% of the algae floated with 100-Gy irradiation. This phenomenon was observed after X-ray irradiation as well. We adopted X-ray irradiation at a dose of 50 Gy for further investigation, in which both floated and sunken algae were observed 2 h after irradiation.

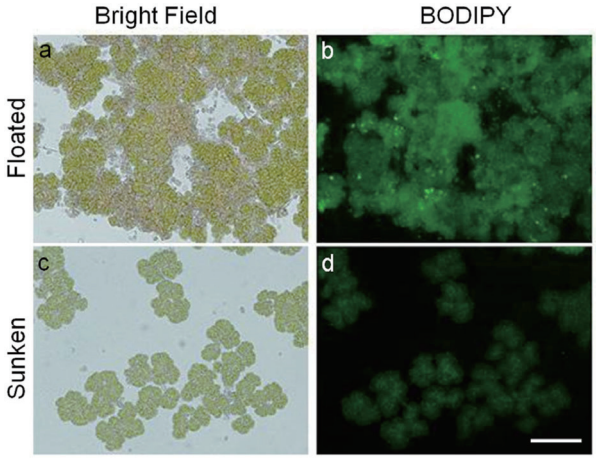

Fig. 1 Microscopic observation of *B. braunii* colonies after X-ray irradiation. Floated and sunken algae were stained with BODIPY and observed by fluorescent microscopy. Scale bar = 50 μm.

The colonies of floated and sunken algae were observed by microscopy after staining with the lipophilic green fluorescent dye, BODIPY (Fig. 1). The colonies of floated algae had large extracellular matrices. These matrices showed higher intensities of BODIPY fluorescence under fluorescent microscopy, indicating that oil was accumulated in the matrices. By contrast, the colonies of sunken cells had less extracellular matrices. This result indicates that floated algae may accumulate more oil than sunken ones.

To investigate the relationship between oil contents and the flotation of the algae, we measured the dry weight and oil weight of both floated algae and sunken algae after irradiation, respectively (Table 1). We also measured the dry weight and oil weight of the algae before the irradiation of X-rays. From these measurements, the oil content in each sample was calculated. Before the irradiation, the oil content was 34.8%. However, 2 h after irradiation, the floated algae showed an oil content of 53.1%. Such an increase of oil content was not observed in the sunken algae. These data indicate that the floated algae accumulate more oil.

By applying this phenomenon, algae having high oil contents can be selectively harvested. Moreover, the sunken algae can be continuously cultured after the removal of the floated algae for the next harvesting. Thus, we suggest that an efficient method of the collection of *B. braunii* can be developed with this approach. To clarify why and how the algae are floated after irradiation, further studies will be needed.

Table 1 Oil contents of irradiated and non-irradiated algae.

	Dry weight (mg)	Oil weight (mg)	Oil content (%)
Before irradiation	71.8	25.0	34.8
Floated algae	30.9	16.4	53.1
Sunken algae	72.5	21.0	29.0

References
1) W. Khatri et al., Biotechnol. and Bioeng. **111**, 493 (2013).
2) P. Cheng et al., Biores. Technol. **138**, 95 (2013).

[*1] RIKEN Nishina Center
[*2] Sea Act Co. Ltd

Effects of LET-dose (Gy) combination on germination and viability rates in durum wheat irradiated by heavy-ion beam

K. Murai,[*1] Y. Kazama,[*2] and T. Abe[*2]

Durum wheat (*Triticum turgidum* ssp. *durum*) is a tetraploid species with the genome constitution AABB that was derived from two wild diploid ancestral species: the A genome from *T. urartu* and the B genome from *Aegilops speltoides* or another species classified in the Sitopsis section. Therefore, the tetraploid durum wheat genome contains duplicated homoeologous genes, and this characteristic may increase the difficulty of screening for mutants in durum wheat. To avoid this problem, we have chosen to use cultivated diploid einkorn wheat (*T. monococcum*) with the A^m genome, similar to the A genome in bread wheat, for developing a large-scale mutant panel[1], and screened and analyzed several mutants from the mutant panel[2]. However, durum wheat is an important crop species for making pasta, and we have started to make a mutant panel of durum wheat by heavy-ion beam irradiation. First, we examined the effects of the LET-Dose (Gy) combination of ion beam irradiation using Carbon (C) and Argon (Ar) as nuclei on the germination and viability rates in M_1 generation.

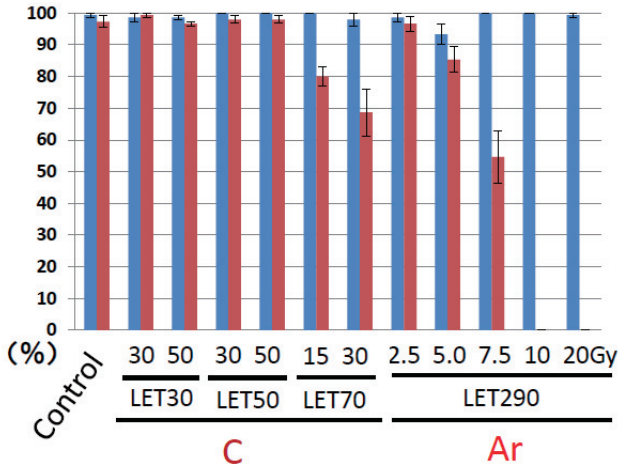

Fig. 1. Effects of heavy-ion beam irradiation on the germination and viability rates in M_1 generation of durum wheat. Percentages (%) of M_1 individuals are shown in each LET-Gy combination of heavy-ion beam irradiation using Carbon (C) and Argon (Ar) as nuclei. Brue and red bars indicate germination and viability rates, respectively.

*1 Department of Bioscience, Fukui Prefectural University
*2 RIKEN Nishina Center
This work was supported by Council for Science, Technology and Innovation (CSTI), Cross-ministerial Strategic Innovation Promotion Program (SIP), "Technologies for creating next-generation agriculture, forestry and fisheries".

Dry seeds of the durum wheat cultivar "Langdon" were irradiated with 15, 30, or 50 Gy and 30, 50, or 70 keV μm^{-1} LET for $^{12}C^{6+}$ ions or 2.5, 5.0, 7.5 10, or 20 Gy of $^{40}Ar^{17+}$ ions (290 keV μm^{-1}) to determine the optimal conditions for mutant generation, using the E5 beam line of Ring Cyclotron (RRC) in the RIKEN RI-beam factory. The germination rate was examined using the irradiated seeds (called M_1 seeds) that were sown in wet-paper-containing petri-dishes. 150 seeds (50 seeds with three replications) were tested for each treatment. The germination rate was not affected by heavy-ion beam irradiation conditions (Fig. 1). Surprisingly, seeds treated with a high dose of the Ar ion beam also showed a normal germination rate.

The M_1 seedlings were planted in the field in October 2014, and the survival ratio (viability rate) was observed in May 2015 at the heading stage with three replications (Fig. 1). The viability rate was reduced to less than 80 % when the LET of the C ion beam was 70 keV μm^{-1}. For the Ar ion beam, the viability rate was reduced to less than 60% with dose greater than 7.5 Gy, and all plants were killed when the dose was 10 and 20 Gy. Based on a previous result of the relationship between viability rate and mutation rate in diploid wheat (K. Murai, unpublished data), the LET-Gy condition with 80% viability is optimal for mutant generation. As a follow up study, therefore, we are now examining the condition with LET50-70Gy for the C ion beam in addition to LET70-15Gy.

Durum wheat cultivars are usually late-heading and not suitable for cultivation in Japan, because of a rainy season from June to July. All known cultivars of durum wheat show pre-harvest sprouting when exposed to prolonged rainfall before harvest. Furthermore durum wheat cultivars are susceptible to Fusarium head blight disease. Because of these disadvantages, durum wheat has not been cultivated in Japan. Recently, one durum wheat cultivar "Setodure" was developed by the National Agriculture and Food Organization. However, "Setodure" is still susceptible to Fusarium head blight, and was therefore released in a limited manner in the Seto-uchi region which receives little rain.

To develop durum wheat cultivars suitable for wide regions in Japan, we are focusing on identifying mutations of early heading, short culm, and resistance against pre-harvest sprouting and Fusarium head blight in durum wheat using heavy-ion beam mutagenesis.

References

1) K. Murai et al., Nucl. Instrum. Meth. Phys. Res. B **314**, 59 (2013).
2) A. Nishiura et al., Breeding Sci. **64**, 213 (2014).

Whole genome sequencing of 12 morphological rice mutants from carbon-ion irradiations

H. Ichida,[*1] Y. Shirakawa,[*1] R. Morita,[*1] Y. Hayashi,[*1] and T. Abe[*1]

Heavy-ion beams are one of the physical mutagens that are classified in high-LET radiations and known to induce double strand breaks of DNA in a cell along with its track. The resulting mutations, including deletions, insertions, inversions and base substitutions, that occurr on the genome can cause the inactivation and/or temporal change of gene expressions that are necessary for morphogenesis. We previously reported the design and implementation of high-performance bioinformatics pipeline for massively parallel (aka "next generation") DNA sequences obtained from mutants. We irradiated a carbon-ion beam from RRC ($^{12}C^{6+}$, 135 MeV/u) on dry and wet seeds of rice (*Oryza sativa* 'Nipponbare') plants and isolated morphological mutants in the M_2 generation. Of those mutants, we selected 12 morphological mutants for comprehensive mutation analysis by whole genome sequencing and subsequent bioinformatics analysis.

We utilized the whole-genome shotgun strategy using an Illumina HiSeq X system. Leaf blades were collected from each M_3 plant grown in a paddy field in September 2016, shipped in dry ice, and stored at -80°C until use. Genomic DNA was purified from 100 mg of bulked frozen tissue of each line using MagExtractor plant genome DNA extraction kits (Toyobo, Japan). The purified DNA was quantified and quality-checked, follwing which it was subjected to random fragmentation by sonication and subsequent processes to attach the adapter sequences necessary for Illumina sequencing. We aimed at an average insert size of 350 bp and a total of 30 billion bases of clean sequences (the sequences that passed filtering by mean quality and read length) from each mutant line. This corresponds to approximately 80 times the equivalent of rice genome and is expected to be sufficient for accurate variant calling according to the current recommendations in variant calling programs. The data were analyzed using our bioinformatics pipeline[1] built and operated on the Hokusai GreatWave system operated by the Advanced Center for Computing and Communication, RIKEN.

The statistics of sequencing, mapping, and variant calling are summarized in Table 1. We could obtain a similar amount of sequencing reads as well as other mapping metrics, indicating that the procedure is quite stable and robust. The number of mutations identified by the Genome Analysis Took Kit (GATK)[2] was also similar among the mutants sequenced. Roughly 52,000 to 53,000 mutations were reported by the GATK program. However, as expected, most of those were artifacts from the intra-cultivar variations between the sequenced and our mutagenized Nipponbare cultivars of different origins. Our filtering strategy removed such false positives very effectively: only 175 to 549 mutations were likely to be the actual mutations caused by heavy-ion beam irradiations. These results demonstrate that our approach using whole genome sequencing and the high-performance bioinformatics pipeline is well suited for the mutation analysis in rice.

References

1) H. Ichida et al., RIKEN Accel. Prog. Rep. **49**, 254 (2016).
2) A. McKenna et al., Genome Res. **20**, 1297–1303 (2010).

Table 1. Sequencing, mapping, and variant calling statistics of whole genome sequencing from 12 rice mutants

Seed condition	Mutant	Irradiation condition		Total reads	Aligned (%)	Mismatch ($\times10^{-3}$)	Indel ($\times10^{-5}$)	Num. of mutations	
		LET[*1]	Dose (Gy)					Total	Line specific
Wet	C-249	50	15	243,240,586	99.53	3.21	5.00	53,600	191
Dry (9%[*2])	7-80	30	50	233,349,445	99.43	3.71	5.10	52,404	175
	7-84	30	50	231,042,177	99.44	3.94	5.00	52,365	202
	7-92	30	50	227,590,774	99.52	3.70	5.00	52,476	210
Dry (13%[*2])	14-34	30	150	236,257,550	98.40	3.59	5.10	53,135	276
	14-55	30	150	234,303,120	99.05	4.05	5.00	52,593	193
	14-64	30	150	234,084,341	99.38	3.84	5.00	53,273	273
	14-70	30	150	233,143,578	99.25	3.31	4.80	53,196	294
	15-16	30	175	235,733,926	99.52	3.33	5.00	52,373	404
	15-17	30	175	233,910,879	99.14	3.43	4.90	52,601	549
	15-65	30	175	232,386,380	99.43	3.38	4.90	52,174	280
	15-74	30	175	233,696,581	99.49	3.38	4.90	52,115	258

[*1] keV/μm; [*2] water content of the irradiated seed

[*1] RIKEN Nishina Center

Analysis of a temperature sensitive virescent mutant of rice induced by heavy-ion beam†

R. Morita,[*1] M. Nakagawa, [*2] H. Takehisa, [*3] Y. Hayashi, [*1] H. Ichida, [*1] S. Usuda, [*1] K. Ichinose, [*1] H. Abe, [*1] Y. Shirakawa, [*1] T. Sato, [*1,*4] M. Fujiwara, [*1,*5] R. Itoh [*6] and T. Abe [*1]

In plants, several leaf-color mutants such as albino, xantha, pale green, stripe, and virescence have been found. Among them, virescent mutants are intriguing because they exhibit white chlorotic leaves during the early growth stages, but produce normal green leaves as they grow. To date, an increasing number of genes responsible for virescent phenotypes have been identified from a number of species. For example, eight genes were recognized as causative genes for the virescent phenotype in rice. Among them, only three genes were reported until 2010, and the remaining five genes were identified recently (since 2011). However, little is known about the mechanism underlying this phenotype. To gain insight into the molecular mechanism of the virescent phenotype, we isolated and characterized a novel rice mutant named 22-4Y.

22-4Y was obtained from a mutant population generated by heavy-ion irradiation ($^{12}C^{6+}$ ions, 20 Gy, LET: 22.5 keV μm^{-1}).[1)] This mutant exhibited chlorotic leaves only during an early growth period, especially the second, third, and fourth leaves at 25°C. After the fifth-leaf stage, the mutants produced normal green leaves. In addition, the mutant shows temperature sensitivity. At 30°C, 22-4Y produced third and fourth leaves with slight chlorosis. However, at 20°C, almost all leaves of the mutant were white. Interestingly, the mutant transferred from 30°C to 20°C conditions at the fifth leaf stage produced chlorotic leaves as the sixth and subsequent leaves, indicating that this mutant responded to low temperature in the early growth and tillering stages. We performed transmission electron microscopy to compare the chloroplast ultrastructure of the mutant grown at 30°C and 20°C. At 30°C, mutant plants possessed normally developed chloroplasts. However, the chloroplasts in the mutant at 20°C displayed undeveloped membrane structures. These observations demonstrate that the chlorotic phenotype of the mutant is attributable to aberrant chloroplast development during leaf formation. Genetic analysis revealed that there are two genes altered by translocation (deletion for LOC_Os05g34040 and insertion for LOC_Os12g31810) (Fig. 1). A complementation test revealed that the causative gene for the virescent phenotype is LOC_Os05g34040.[2)] Since LOC_Os05g34040 is a newly identified causative gene for the virescent phenotype, we named this gene *Cold Sensitive Virescent1* (*CSV1*). The protein domain analysis of CSV1 showed that this protein belongs to the large family of FAD-dependent pyridine nucleotide reductases (FADPNR). Since the FADPNR family includes a broad range of oxidoreductase enzymes, it is difficult to infer the molecular function of CSV1 simply from its amino acid sequence homology. ChloroP program predicted that the N-terminal region of the CSV1 protein might function as a chloroplast transit peptide. To verify its ability, we constructed a fusion gene expressing the N-terminal region of CSV1 fused to the N-terminus of the cyan fluorescent protein (CFP), under the control of a strong promoter (named 35S::TP_{CSV1}-CFP). We co-introduced 35S::TP_{CSV1}-CFP with 35S::$TP_{AtFtsZ1}$-YFP, positive control encoding the plastid-targeted yellow fluorescent protein (YFP), into an onion epidermal cell. The fluorescent signals of CFP were clearly co-localized with those of YFP (Fig. 2). In contrast, the fluorescent signals were observed in the cytoplasm and nucleus when we introduced the plasmid DNA for a non-fused CFP or YFP as a control. These observations demonstrated that CSV1 is a plastid-localizing protein. Our findings indicate that *CSV1* is an important gene for chloroplast development under cold stress, both in the early growth stage and in the tillering stage.

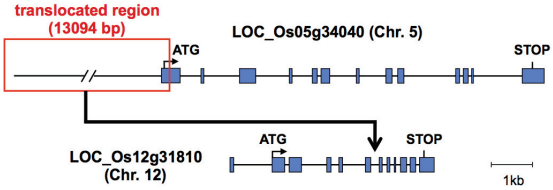

Fig. 1. Schematic representation of the translocation induced in 22-4Y. The boxes indicate exons. ATG and STOP indicate the start and stop codon, respectively.

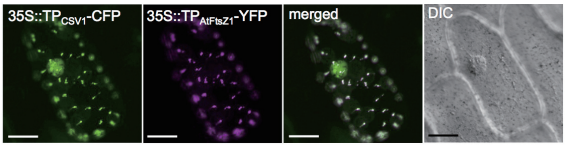

Fig. 2. Intracellular localization of CSV1. 35S::TP_{CSV1}-CFP, CFP with the putative transit peptide of CSV1 (pseudo-coloured in green); 35S::$TP_{AtFtsZ1}$-YFP, YFP with the transit peptide of plastid-targeted AtFtsZ1 (magenta); Merged, merged images of the CFP and YFP images; DIC, differential interference contrast. Scale bars = 50 μm.

References

1) M. Nakagawa et al.: RIKEN Accel. Prog. Rep. **43**, 281 (2010).
2) R. Morita et al.: RIKEN Accel. Prog. Rep. **46**, 259 (2013).

† Condensed from the article in Biosci. Biotech. Biochem. **81**, 271 (2017)

*1 RIKEN Nishina Center
*2 Faculty of Science and Technology, Ishinomaki Senshu University
*3 Institute of Crop Science, National Agriculture and Food Research Organization
*4 Graduate School of Agricultural Science, Tohoku University
*5 Faculty of Science and Technology, Sophia University
*6 Faculty of Science, University of the Ryukyus

Low polyphenol oxidase mutant induced by $^{12}C^{6+}$ ion beam irradiation to protoplasts of lettuce (*Lactuca sativa* L.)†

R. Sawada,[*1,*2] T. Hirano, [*3*4] K. Iimure,[*1] T. Abe,[*4] and Y. Ozaki[*5]

Lettuce is one of the most important vegetables in Japan and has been established as a designated vegetable by the Ministry of Agriculture, Forestry and Fisheries. Lettuce is often eaten raw in dishes such as salads, and the browning of the cut section is one of the causes of quality loss during storage. In the cut section, activated phenylalanine ammonia-lyase (PAL) produces cinnamic acid, and polyphenols are synthesized from the cinnamic acid. The browning is due to the accumulation of pigments derived from the oxidation of the polyphenols by polyphenol oxidase (PPO). Since PAL and PPO are key enzymes for the browning, the suppression of enzyme activity can prevent the browning.[1)] In the present study, the induction of *PPO* gene mutation by heavy-ion beam irradiation was attempted for the production of lettuce plants with a low browning property as a cut vegetable.

We used protoplasts as plant materials for the irradiation to prevent of chimera mutants. Protoplasts of *L. sativa* 'Round' were embedded at a density of 0.75×10^4/ml in modified Murashige and Skoog medium[3)] supplemented with 0.3% gellan gum and 100 mg/l cefotaxime sodium. The protoplasts were stored overnight at 4°C in the dark. Then, the protoplasts were transported at room temperature and cultured at 25°C in the dark until irradiation. The protoplasts were irradiated with $^{12}C^{6+}$ ions (135 MeV/nucleon, corresponding to 22.5 keV/μm linear energy transfer) at a dose of 0.5, 1.0, 2.0, and 5.0 Gy. The irradiated protoplasts were cultured according to the methods described by Nishio et al. (Ref. 2). Twenty three days after the irradiation, the number of colonies (> 0.1 mm in diameter) in each sample was counted, and colony formation rates were calculated as percentages relative to values in unirradiated protoplasts. In the calli derived from the protoplasts, mutation in the *PPO* gene was detected by the Targeting Induced Local Lesions IN Genomes (TILLING) method[3)] with Surveyor Mutation Detection kits (Transgenomic, Inc).

The colony formation rates decreased with increasing dose (Fig. 1); the colony formation rate was approximately 64% at 2.0 Gy and 26% at 5.0 Gy. A total of 869 calli formed from the colonies were used for mutation detection by TILLING, and two of them, 2Gy-3-36 from 2.0-Gy irradiation and 5Gy-2-27 from 5.0-Gy irradiation, showed positive fragments due to mutation in the *PPO* gene. The mutation frequencies for 2.0-Gy and 5.0-Gy irradiation were 0.41% and 1.10%, respectively.

We obtained regenerated M_1 plants from the callus of 2Gy-3-36, and their M_2 progenies were produced by self-pollination. When PPO activity in the leaves was measured according to the method of Dan et al. (Ref. 4) with modification, the M_1 plants show about half the PPO activity of the control. In the M_2 progenies, the segregation of individual genotypes was estimated by TILLING analysis and PPO activity; homozygous dominant plants showed no cleavage fragment in TILLING analysis and showed similar or higher PPO activity compared with the control, heterozygous plants showed the cleavage fragment and similar or lower PPO activity, and homozygous recessive plants showed no cleavage fragment and markedly lower PPO activity. These results suggest that mutation in the *PPO* gene is cause of the PPO activity decrease.

The reverse genetic approach combined with the carbon ion beam has been thought to be effective in *Arabidopsis thaliana*.[5)] It is revealed in the present study that this approach is also useful in horticultural crops. The homozygous recessive plants are promising as breeding materials for low-browning lettuce.

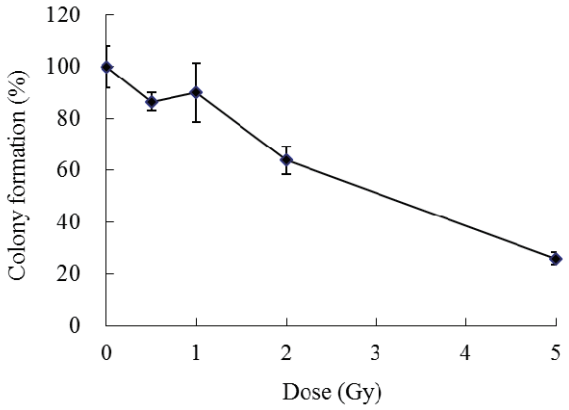

Fig. 1 Effect of carbon ion irradiation on colony formation. Data are represented as mean ± standard error of three individual experiments.

References

1) H. Hashimoto et al., Biosci. Biotechnol. Biochem. **65**, 1016 (2001).
2) T. Nishio et al., Japan. J. Breed. **38**, 165 (1988).
3) B. J. Till et al., Genome Res. **13**, 524 (2003).
4) K. Dan et al., Food Preser. Sci. **25**, 209 (1999).
5) Y. Kazama et al., BMC Plant Biol. **11**, 161 (2011).

† Condensed from the article in Hort. Res. (Japan) **15**, 347 (2016)

*1 Kumamoto Prefectural Agricultural Research Center.
*2 Graduate School of Bioresource and Bioenvironmental Sciences, Kyushu University
*3 Faculty of Agriculture, University of Miyazaki.
*4 RIKEN Nishina Center
*5 Faculty of Agriculture, Kyushu University

Production of flower color mutants of spray-mum 'Southern Chelsea' by Ar-ion beam irradiation

M. Tamari,[*1] Y. Tanokashira,[*1] Y. Hayashi ,[*2] T. Hirano,[*2,*3] and T. Abe[*2]

Heavy-ion beam irradiation effectively induces mutations of plants and has been used in plant breeding.[1] Ar-ion beam irradiation is expected to expand the spectrum of mutant phenotypes and mutation rate owing to its higher LET compared to a C-ion beam. We previously reported the induction of flower-color mutants of spray-mum cultivar 'Southern Chelsea' cuttings using Ar-ion beam irradiation.[2] In addition, we reported the effects of Ar-ion beam irradiation on the regeneration from leaf blades[3] and speculated that Ar-ion beam irradiation on leaf blades was not practical because of the low relative regeneration fequency of less than 10% at doses of 2 Gy Ar-ion beam irradiation.[4] Here, we report the production of flower-color mutants by the irradiation of stem segments of 'Southern Chelsea.'

Eighty and forty stem segments of 'Southern Chelsea,' were irradiated with Ar-ion beams (LET: 280 keV/μm) at doses of 0.5, 1, 2, and 3 Gy and C-ion beams (LET: 23 keV/μm) at doses of 1, 2, and 3 Gy, respectively. After irradiation, these tissues were cultured in vitro, and 3 nodes that had axillary buds cut out from an extended shoot were subcultured to separate mutation sites. This subculture step was repeated when shoots sprouted from axillary buds were extended sufficiently. Plantlets grown from re-subcultred nodes were transferred to a greenhouse to investigate flower- color mutation.

Table 1. Flower-color mutation induced by heavy-ion beam irradiation.

Variation source		Number of plants[1] (%)	Number of flower-color mutants						Number of mutants	Mutation rate(%)
Line class	Dose (Gy)		White	Yellow	Orange	Yellowish pink	Light pink	Other		
Ar	0.5	171							0	0
	1	165						1	1	0.6
	2	151	2	1	2	8		1	14	9.3
	3	74	1		4		1		6	8.1
	Total	561	3	1	6	8	1	2	21	3.7
C	0	12							0	0
	1	111							0	0
	2	102							0	0
	3	101			1				1	1.0
	Total	314	0	0	1	0	0	0	1	0.3
	0	46						1	1	2.2

1) Regenerated and flowered plants after irradiation.

*1 Kagoshima Prefectural Institute for Agricultural Development
*2 RIKEN Nishina Center
*3 Faculty of Agriculture, University of Miyazaki

The numbers of flower-color mutants obatined by Ar-ion beam irradiation at 1, 2, and 3 Gy were 1, 14, and 6, respectively (Table 1). On the other hand, only one flower-color mutant was obtained by C-ion beam irradiation at all doses (Table 1).

The flower colors of mutants obtained by Ar-ion beam irradiation were white, yellow, orange, yellowish pink, and light pink (Table 1). This fact suggests that the direction of flower-color mutation by Ar-ion beam irradiation is the decrease or disappearance of anthocyanin and increase of carotenoid. Especially, one yellow-flower mutant, which was thought to be difficult to obtain from 'Southern Chelsea,' having pink flowers, appeared after Ar-ion beam irradiation at 2 Gy (Table 1). It is thought that this yellow-flower mutant was caused by the disappearance of anthocyanin and simultaneous increase of carotenoid. Some mutants also showed the morphological variation of flower shape because of Ar-ion beam irradiation (data not shown). The growth of many mutants from stem segments with Ar-ion beam irradiation was equal to that of control plants (data not shown). Because the growth of almost all mutants from leaf blades by the same irradiation condition was lower than that of control plants,[4] this result suggests that stem segments will be more suitable for producing mutants of spray-mum using Ar-ion beam irradiation.

From the results presented above, it has become possible to produce many flower-color mutants of spray-mum by Ar-ion beam irradiation to stem segments. On the basis of these results, it is supposed that the low rate of regeneration and mutation by Ar-ion beam irradiation in several spray-mum cultivars will be improved by using stem segments as irradiation targets.

The present study was supported by the Council for Science, Technology and Innovation (CSTI), Cross-ministerial Strategic Innovation Promotion Program (SIP), "Technologies for creating next-generation agriculture, forestry and fisheries" (funding agency: Bio-oriented Technology Research Advancement Institution, NARO).

References

1) T. Abe et al.: Breed. Res. **16**, 67 (2014).
2) Y. Tanokashira et al.: RIKEN Accel. Prog. Rep. **47**, 297 (2014).
3) Y. Tanokashira et al.: RIKEN Accel. Prog. Rep. **48**, 306 (2015).
4) Y. Tanokashira et al.: RIKEN Accel. Prog. Rep. **49**, 261(2016)

New cherry blossom cultivars induced by C-ion beam irradiation

S. Ishii, [*1] Y. Hayashi, [*2] T. Hirano, [*2,3] Y. Kazama, [*2] and T. Abe[*2]

A new color cherry blossom with pale-yellow flowers, 'Nishina Zao' was created by irradiating the greenish 'Gyoiko' scions with C ions.[1] It became the first plant to be registered under the Seeds and Seedlings Law by RIKEN a decade ago. Another cultivar of the cherry blossom tree, 'Nishina Otome' does not require a certain period of cold winter weather to induce flowering in the spring.[2] The winter temperatures have not been sufficiently low due to the global warming in recent years. This climate change has resulted in a decrease in the number of cherry blossoms in spring. These two cultivars are propagated clone plants of the mutant branch. We have succeeded in creating three new cherry blossom cultivars by irradiating cherry scions with C ions. With the original cultivars, 'Shungetsuka' and 'Beniyutaka', it is difficult to obtain seeds with germination capacity. The irradiation treatment on scions increased the germination rates of seeds from 0.5 to 12% and 0 to 56%, in 'Sungetsuka' and 'Beniyutaka', respectively. Three new cultivars were selected from the progeny plants of the irradiated plants.

'Nishina Haruka' and 'Nishina Komachi'

'Shungetsuka' is a Japanese ornamental cherry cultivar having double flowers (ϕ 3–3.5 cm) with 21 to 50 petals. Its scions were irradiated with carbon-ions (135 MeV/u, LET 22.6 keV/μm) at the doses of 5, 7.5, and 10 Gy. The irradiated scions were grafted on rootstocks. Twenty of the irradiated plants showed no change in their flower color and shape in 2008. Subsequently, we attempted natural crossing between irradiated plants from 2008 to 2009. Plants irradiated at a dose of 5 Gy showed good growth and bore 300 – 500 cherries per plant. The original cultivar 'Shungetsuka' bears cherry fruits with low germination capacity. Specifically, only 23 plants were grown from approximately 5000 cherry seeds of the original cultivar. On the other hand, 296 plants were grown from approximately 2500 cherry seeds from the fruits borne by the irradiated plants. The progeny plants bloomed in 2012, and the characteristics of the mutant lines were confirmed to be stable. We produced two new cultivars, named 'Nishina Haruka' and 'Nishina Komachi', from the mutant lines irradiated at 5 Gy. 'Nishina Haruka' had double flowers (ϕ 4.1–4.2 cm) with 23 to 25 petals: they were 1.3 times larger than the flowers of the original cultivar. This cultivar also bore sweet cherries (ϕ 1cm). 'Nishina Komachi' had small single flowers (ϕ 1.3–1.4 cm) with five petals, which do not open fully. These two cultivars were submitted for cultivar registration in September 2012.

'Nishina Tomoka'

'Beniyutaka' (*Prunus lannesiana*) has double flowers (ϕ 5 cm) with 15 – 20 petals. Its scions were irradiated with carbon-ions (135 MeV/u, LET 22.6 keV/μm) at a dose of 10 Gy in 2005. The irradiated scions were grafted on the rootstock. No change was observed in the flower color and shape of the three irradiated plants in 2007. Even though the original cultivar 'Beniyutaka' does not bear cherries, one of the irradiated plants bore 9 cherries. We sowed the seeds from these cherries. Of these nine seeds, five germinated. Three of these germinated seeds grew into progeny plants that bloomed in 2011. One mutant line, named 'Nishina Tomoka', had single flowers (ϕ 3.2–3.6 cm) with 5 petals. The rim of its flowers was deep pink. 'Beniyutaka' was bred in the Hokkaido area because the cold region was suitable for its cultivation. However, 'Nishina Tomoka' showed good growth even in the relatively warmer Shizuoka Prefecture. This cultivar was easy to propagate by cuttings, and was submitted for cultivar registration in September 2016.

Fig. 1. Flowers of new cultivars.
(a) Nishina Haruka, (b) Nishina Komachi, (c) Nishina Tomoka

*1 JFC Ishii Garden
*2 RIKEN Nishina Center
*3 Faculty of Agriculture, University of Miyazaki

References

1) S. Ishii et al.; RIKEN Accel. Prog. Rep. 42, xi (2009).
2) S. Ishii et al.; RIKEN Accel. Prog. Rep. 44, xiii (2011).

Current status of development of ion microbeam device to fatally damage the small active organs of insects

T. Ikeda,[*1] M. Hamagaki,[*1] I. Hakamada,[*1,*2] H. Sato,[*1] and T. Abe[*1]

In the bodies of living organisms, there exist left-right-symmetric organ structures, or repetitions as in the spine and ribs. The structures are generated by genes that work only in a specific phase during the development of the organism. The study of identifying these genes is considerably important in developmental biology including the field of medicine. One of the methods to specify the gene in an organ corresponding to morphogenesis (the development of the structure or shape) involves damaging the candidate gene before the gene works actively. For example, *Drosophilidae* (fruit fly) has a bristle that can be seen from outside. The growth of this bristle is realized by genes having their corresponding RNA and proteins localized at small parts (~1 μm) of the bristle. If the bristle growth is stopped after one of the parts is damaged by ions with an energy of a few MeV, the RNA and proteins are found to play an important role in the growth. For this purpose, a micrometer-sized He ion beam with an energy of a few MeV energy is used as a tool for causing precise damage within a volume of ~μm^3 order because of the Bragg peak in the stopping-power distribution. Alternatively, if the target is damaged thermally or physically, no further development can be expected because of cellular necrosis.

Before the experiment above, *C. elegans* (nematode) will be targeted because it is easier to irradiate a relatively larger area (~50 μm) by H^+ beams and to observe real-time changes in pharyngeal pumping activity. An experiment with carbon-ion microbeams (18.3 MeV/u) was reported but not yet performed with light ions of a few MeV. We developed a device to damage a small part near pharynges using microbeams of H ions with MeV energies generated by the Pelletron accelerator at RIKEN. The pin-point damaging is provided by tapered glass capillary optics, as shown by a blue thin object in Fig. 1. [1-4] A glass capillary is the same as an injection needle used for biological experiments. Ions with MeV energy can be transmitted through a total capillary length of ~100 mm. Its inlet diameter is typically 0.8 mm. The outlet can have a thin end-window (1-200 μm in diameter and a few to 15 μm in thickness) for targets in liquid or air. We employ a combination of MeV energy H / He ions from the Pelletron accelerator and glass capillary optics because of the following advantages: the Pelletron facility has a beam port accessible during the irradiation, a H / He ion with MeV energy stops at a low depth in the target, and the capillary makes pin-point damaging possible. In the cases of H (He) ions, the stopping power of 80 (240) keV/μm with a short range of ~130 (~20) μm in the target is expected. In order to realize the above advantages, some points should be taken into account. For reliability, the acceleration voltage (1-1.5 MV) should be stabilized with a fluctuation less than 0.1%. Furthermore, beam divergence should be known to avoid mis-hitting any object neighboring the target.[5] The acceleration voltage of the Pelletron was found to be 0.31% in April 2016. After modification including overhaul, it became 0.095%, which is at the level of our requirement. The microbeam divergence was examined using MeV H^+ and pieces of the solid track detector CR-39 for each capillary. The beam profile was analyzed by comparing with the simulation data to estimate the mis-hitting probability. Moreover, usability, such as the method to irradiate, observe, manipulate, etc. must be considered. Figure 1 shows the setup installed at the West 30° beam line in the Pelletron room. The capillary axis is aligned to the initial beam axis by the linear motion of X and Y as well as the rotational motion of θ and ϕ. A microscope is located around the target. The orientation of the microscope will be determined according to the sample. When the sample is transparent, the microscope view will be obtained from the downstream. The method to fix the target is discussed in detail with a group from the QST Takasaki institute.[6]

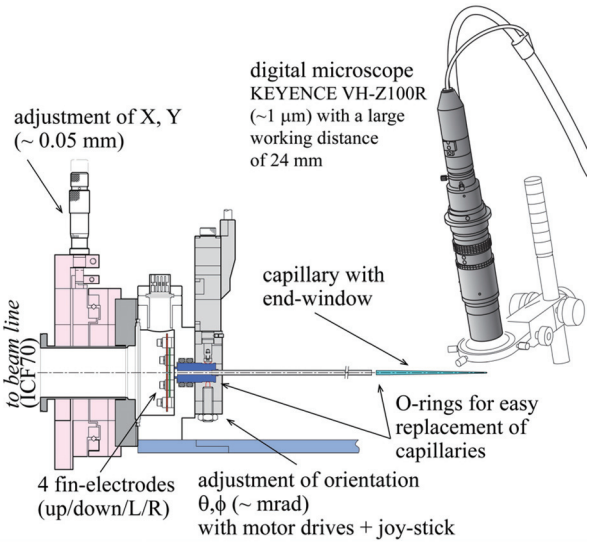

Fig. 1. Experimental setup with the irradiation sample below the microscope.

*1 RIKEN Nishina Center
*2 Nuclear Engineering and Management, The University of Tokyo

References

1) T. Nebiki et al., J. Vac. Sci. Technol. A **21** (5), 1671 (2003).
2) Y. Iwai et al., Appl. Phys. Lett. **92**, 023509 (2008).
3) M. Kato et al., Appl. Phys. Lett. **100**, 193702 (2012).
4) V. Mäckel et al., Rev. Sci. Instrum. **85**, 014302 (2014).
5) T. Ikeda et al., RIKEN Accel. Prog. Rep. **49**, 267 (2016).
6) M. Suzuki et al., JAEA Takasaki Annu. Rep. 2011 JAEA-Rev. 2012-**046**, 77 (2013).

IV. OPERATION RECORDS

Program Advisory Committee meetings for nuclear physics and for materials and life experiments

K. Yoneda, [*1] K. Ishida, [*1] H. Yamazaki, [*1] N. Imai, [*2] Y.X. Watanabe, [*3] K. Yako, [*2] H. Miyatake, [*3] M. Iwasaki, [*1] H. Ueno, [*1] and H. Sakai[*1]

The Program Advisory Committees (PAC) is in charge of reviewing scientific proposals submitted for use of the accelerator facility of RIKEN Nishina Center (RNC). In Fiscal Year 2016, two PAC meetings were held; one for proposals of nuclear physics (NP-PAC), and one for proposals of materials and life experiments (ML-PAC). The NP-PAC reviewed experimental proposals at RIBF, whereas the ML-PAC reviewed proposals at Rutherford Appleton Laboratory (RAL) and RIBF.

NP-PAC

The 17th NP-PAC meetings were held on December 1–3, 2016[1]. From this 17th NP-PAC, the experimental proposals which utilize the Rare RI Ring were called for the first time.

In the 17th NP-PAC meeting, 25 proposals were reviewed, and 17 proposals were approved as grade S or A. There was a proposal which requrested beam time for both RIPS and BigRIPS, and only RIPS part was approved. The outcome of these NP-PAC meetings is summarized in Table 1.

The 17th NP-PAC members are as follows:
B.M. Sherrill (NSCL, MSU, the chair), A. Andreyev (University of York), A. Bracco (INFN), I. Hamamoto (University of Lund/RNC), H. Iwasaki (MSU), W. Loveland (Oregon State University), S. Nakamura (Tohoku University), T. Nilsson (Chalmers University of Technology), K. Ogata (RCNP, Osaka University), T. Rauscher (University of Hertfordshire), H. Simon (GSI), O. Sorlin (GANIL, absent), A. Tamii (RCNP, Osaka University), Y. Utsuno (JAEA), P. Van Duppen (KU Leuven), Y.-H. Zhang (IMP).

Table 1. Summary of the outcome of the 17th NP-PAC meeting. The proposals ranked with S and A are treated as the "approved" proposals. There was a proposal which requested beam time for both RIPS and BigRIPS.

17th NP-PAC (December 1–3, 2016)	requested proposals (days)	approved proposals (days)
GARIS (RILAC)	2 (29)	2 (29)
CRIB (AVF)	2 (27)	0 (0)
RIPS	2 (15.5)	2 (10.5)
KISS	2 (19.5)	2 (14.5)
BigRIPS/ZD	11(12) (104)	7 (49)
Rare RI Ring	2 (29.5)	1 (10)
SAMURAI	4 (38)	3 (25)
Construction	0 (-)	0 (-)
Total	25(26) 262.5	17 (138)

ML-PAC

The 13th ML-PAC meeting was held on January 19–20, 2017[2]. This was the first ML-PAC meeting where the proposals were reviewed only with documents submitted, i.e. no presentation was made by the proponents. In this meeting, 25 RAL proposals and 5 RIBF proposals were reviewed. The summary of the outcome of the meeting is given in Table 2.

The 13th ML-PAC members are as follows:
A. Hiller (ISIS, RAL, the chair), T. Azuma (RIKEN), R. Kadono (KEK), A. Kawamoto (Hokkaido University), N. Kojima (Toyota RIKEN), K. Kubo (ICU), P. Mendels (University of Paris), A. Shinohara (Osaka University), S. Sulaiman (Universiti Sains Malaysia, absent), H. Yamase (NIMS), S. Yoshida (Thera Projects Associates, absent), and X.G. Zheng (Saga University).

Table 2. Summary of the outcome of the 13th ML-PAC meeting.

13th ML-PAC (January 19–20, 2017)	requested proposals (days)	approved proposals (days)
RAL	25 (171)	17 (54)
RIBF	5 (28)	5 (28)
Total	30 (199)	22 (82)

References

1) http://www.nishina.riken.jp/RIBF/NP-PAC/index.html
2) http://www.nishina.riken.jp/RIBF/ML-PAC/index.html

*1 RIKEN Nishina Center
*2 Center for Nuclear Study, the University of Tokyo
*3 Wako Nulcear Science Center, Institute of Particle and Nuclear Studies, KEK

Beam-time statistics of RIBF experiments

K. Yoneda *1 and H. Sakai*1

This report describes the statistics of the beam times (BTs) at the RIBF facility in Fiscal Year (FY) 2016. In the following, the BTs are categorized into two groups: high-energy-mode and low-energy-mode BTs. In the former mode, the beams were delivered in the acceleration scheme of AVF, RILAC, or RILAC2 → RRC → (fRC → IRC →) SRC, where the accelerators in parentheses can be skipped in the cascade acceleration, depending on the beam species used. In the latter mode, the acceleration scheme is AVF or RILAC (→ RRC).

BTs in the high-energy mode were scheduled from April to June, from October to December 2016, and in the last week of March 2016, considering the restriction of utility-power use, budgetary constraints, maintenance schedule of the accelerator system and co-generation system, as well as other constraints. In the series of experiments in spring, the primary beams of ^{238}U, ^{124}Xe, and ^{18}O were provided to users, and in the autumn series, the primary beams of ^{238}U and ^{48}Ca were provided. 14 experiments approved by the RIBF Program Advisory Committees[1] with the approved beam time of 79 days were conducted in total. Five days were used for the facility development programs, defined as machine study (MS) experiments. Other than these, a new isotope search experiment and two nuclear transmutation experiments were conducted as the Nishina Center mission programs.

The summary of the high-energy-mode BTs in FY2016 is given in Fig. 1 as a bar chart. Compared to the beam time in FY2015, the user time increased, reflecting the longer total running time in FY2016. The decrease of the machine study is partly due to cancellation of 3 machine studies in spring (4.5 days in total), which was caused by an accelerator trouble.

The summary for the low-energy mode is shown in Fig. 2. Here the BTs are classified by the accelerator operation modes, AVF standalone, RILAC standalone, and RRC. In FY2016, the total beam time length of the low-energy mode was almost the same as in FY2015. A long shutdown of RILAC is expected to begin in spring 2017. A lot of RILAC-use experiments were scheduled to finish prior to the shutdown.

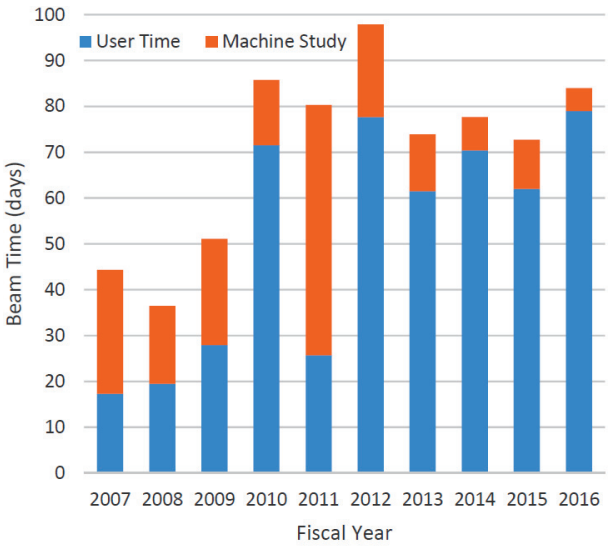

Fig. 1. Bar chart showing the BT statistics for high-energy-mode experiments from FY2007 to FY2016. The accelerator tuning time and Nishina Center mission time are not included.

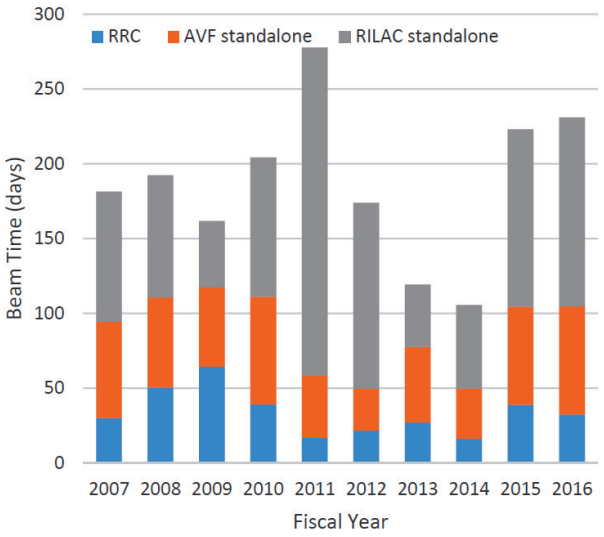

Fig. 2. Bar chart showing the BT statistics for low-energy-mode experiments from FY2007 to FY2016.

Reference

1) K. Yoneda, K. Ishida, H. Yamazaki, N. Imai, Y. Watanabe, K. Yako, H. Miyatake, H. Ueno, and H. Sakai: In this report.

*1 RIKEN Nishina Center

Electric power condition of Wako campus in 2016

E. Ikezawa, *[1] M. Kato, *[1] H. Yamasawa, *[1] and M. Kase*[1]

The monthly electrical power consumption data for the RIKEN Wako campus (Wako) and RIKEN Nishina Center (RNC) and the energy supply by the cogeneration systems (CGSs) are shown in Fig. 1. The hourly average electrical power consumption in a day for RNC in 2016 is shown in Fig. 2. The annual data of the electrical power consumption and energy supply in 2016 are listed in Table 1. The total electrical power consumption of Wako in 2016 was 159,384 MWh, which is approximately the same as that in 2015. However, the total electrical power consumption of RNC in 2016 was 77,877 MWh, which is 4% higher than that in 2015. When the RI Beam Factory (RIBF) experiments using an uranium (^{238}U) beam were conducted, the maximum electrical power supply to Wako from the Tokyo electric power corporation (TEPCO) reached 21.5 MW with a CGS output of 6.5 MW on June 10, 2016, and the maximum electrical power consumption of RNC reached 17.9 MW on October 31, 2016.

A complete overhaul of the gas turbine of CGS #1 after 4,000 h of operation was performed from 31 August to 3 September 2016.

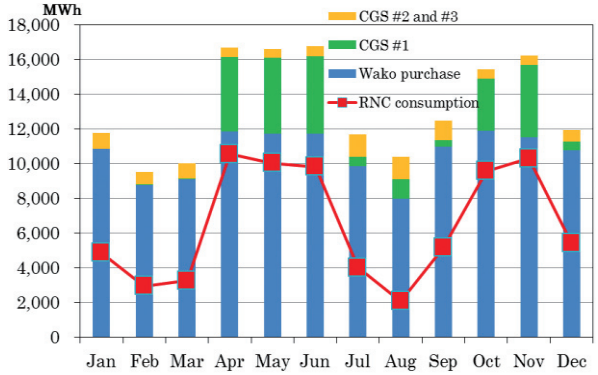

Fig. 1. Monthly electrical power consumption and energy supply by CGSs in 2016.

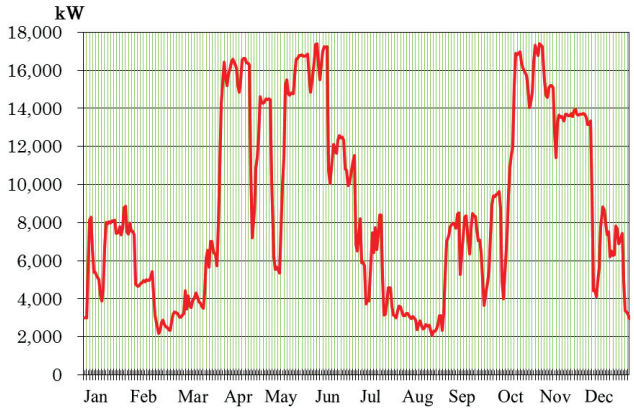

Fig. 2. Hourly average electrical power consumption of RNC in a day in 2016.

Table 1. Annual data of electrical power consumption and energy supply in 2016.

	Total (MWh)	Note	% of 2015
Wako purchase	126,878	Total electrical power supply to Wako from TEPCO	94%
Wako consumption	159,384	Wako electrical power consumption (CGSs + TEPCO)	100%
RNC purchase	54,881	Total electrical power supply to RNC from TEPCO	95%
CGS #1	22,996	CGS #1 total electrical power output	134%
CGS #2 and #3	9,510	CGS #2 and #3 total electrical power output	145%
RNC consumption	77,877	RNC total electrical power consumption	104%

*[1] RIKEN Nishina Center

Operation report on the ring cyclotrons in the RIBF accelerator complex

K. Yadomi,[*3] K. Suda,[*1] T. Dantsuka,[*1] M. Fujimaki,[*1] T. Fujinawa,[*1] N. Fukunishi,[*1] S. Fukuzawa,[*3] M. Hamanaka,[*3] H. Hasebe,[*1] Y. Higurashi,[*1] E. Ikezawa,[*1] H. Imao,[*1] S. Ishikawa,[*3] O. Kamigaito,[*1] M. Kase,[*1] M. Kidera,[*1] K. Kobayashi,[*3] M. Komiyama,[*1] Y. Kotaka,[*2] R. Koyama,[*3] K. Kumagai,[*1] T. Maie,[*1] M. Nagase,[*1] T. Nagatomo,[*1] T. Nakagawa,[*1] M. Nakamura,[*1] T. Nakamura,[*3] M. Nishida,[*3] M. Nishimura,[*3] J. Ohnishi,[*1] H. Okuno,[*1] K. Ozeki,[*1] N. Sakamoto,[*1] J. Shibata,[*3] N. Tsukiori,[*3] A. Uchiyama,[*1] S. Watanabe,[*1] T. Watanabe,[*1] Y. Watanabe,[*1] K. Yamada,[*1] and H. Yamasawa[*1]

Table 1. Summary of the accelerated beams in 2016

Beam particle	Energy (MeV/u)	Acceleration mode	Beam course	Beam current(particle nA)		Beam time(h)		Down time (h)	Availability (%)
				Requested	Actual	Scheduled	Actual		
^{4}He	7.3	RILAC2-RRC	A02(MS)	N/A	47.5	24.0	39.1	0.0	162.8
^{12}C	135	AVF-RRC	E5B(Biology)	1.0	583.3	41.5	47.0	0.0	113.3
^{22}Ne	70		E6(RIPS)	250.0	167.0	114.0	112.1	7.6	91.7
^{40}Ar	66		E5A(MS)	N/A	8.2	36.0	42.6	0.0	118.2
^{40}Ar	95		E5B(Biology)	1.0	91.2	28.0	28.3	0.0	100.9
^{40}Ar	95		E5A(Industry)	0.1	91.2	48.0	45.6	0.0	95.0
^{40}Ar	160	AVF-RRC-IRC	E5B(Biology)	1.0	55.5	8.0	8.2	0.0	102.5
^{48}Ca	63	RILAC-RRC	E6(RIPS)	150.0	352.9	120.0	127.2	1.0	105.1
^{51}V	6	RILAC2-RRC	A02(MS)	N/A	150.0	84.0	114.2	0.0	136.0
^{56}Fe	90	AVF-RRC	E5B(Biology)	1.0	6.3	25.0	27.2	0.0	108.8
^{58}Ni	63	RILAC-RRC	E6(RIPS)	200.0	97.8	63.0	75.1	0.0	119.2
^{84}Kr	70	AVF-RRC	E5A(Industry)	0.1	7.8	72.0	75.3	1.1	103.0
^{85}Rb	66		E6(RIPS)	1.0	0.7	48.0	56.3	0.2	117.0
^{86}Kr	36	RILAC-RRC	E3A(JAXA)	1.0	5.1	24.0	21.9	0.0	91.3
^{86}Kr	66	AVF-RRC		1.0	5.8	24.0	23.9	0.0	99.5
^{136}Xe	10.75	RILAC2-RRC	E2B(KEK/KISS)	50.0	47.5	147.0	149.0	4.1	98.6
^{238}U	10.75			140.0	4.9	48.0	46.6	0.0	97.0
^{18}O	230	AVF-RRC-SRC	BigRIPS/SAMURAI/SHARAQ	>650	838.0	336.0	351.0	18.4	99.0
^{48}Ca	345	RILAC2-RRC-IRC-SRC	BigRIPS/SAMURAI/ZDS/Rare-RI Ring	500.0	738.0	492.0	504.1	29.4	96.5
^{124}Xe	345	RILAC2-RRC-fRC-IRC-SRC	BigRIPS/SAMURAI/ZDS/F12	>10	102.0	168.0	180.0	3.5	105.1
^{238}U(1st)	345		BigRIPS/SAMURAI/ZDS/F12	5~60	37.0	372.0	384.0	56.9	87.9
^{238}U(2nd)	345		BigRIPS/SAMURAI/ZDS/F12	5~60	39.0	612.0	665.6	97.8	86.9
^{238}U(3rd)	345		BigRIPS/SAMURAI/ZDS/Rare-RI Ring	>35	41.0	600.0	600.0	88.8	85.2
					total	3534.5	3724.2	344.8	95.61

In this report, the operation of the ring cyclotrons in the RIBF from January to December 2016 is presented. Table 1 presents a summary of the beams accelerated by these cyclotrons (the upper part until ^{238}U at 10.75 MeV/u is for the old facility, and the lower part from ^{18}O at 230 MeV/u for the new facility). The availability in the table is defined by the ratio of actual beam time to scheduled beam time, which is an index of the reliability. The total beam supply time in 2016 was 3724.2 h. In the old facility, the actual beam time was 1025.4 h, and the availability was 107.4 %. In the new facility, the total beam supply time was 2580.0 h, and the availability was 91.2%.

For the experiments at the old facility, ^{22}Ne, ^{58}Ni, ^{48}Ca and ^{85}Rb for RIPS group, ^{40}Ar and ^{84}Kr for the industrial use (E5A), ^{86}Kr for JAXA group (E3A), and ^{136}Xe and ^{238}U for KEK/KISS group (E2B) were supplied. In addition, biological experiments (E5B) were conducted as usual.

The ^{18}O (230 MeV/u) beam was supplied to two experiments (Jun. 16th to 30th). The maximum intensity was 838 particle nA achieved by using the ion source SCECR.[1)] The intensity was two times that in the previous operation (March 2012)[2)]. The availability was 99.0% including the extension time of 15 h. The major troubles were caused by radiation: the failures of EIC / EDC and the main power supply for RRC, and a malfunction of the filament power supply for SRC-RES1.

The ^{48}Ca beam was supplied to six experiments (Nov. 15th to Dec. 6th). The maximum intensity was 738 particle nA. The availability was 96.5 % and the down time was 29.4 h. Most of the down time was due to the replacement of the charge stripper foils.

The ^{124}Xe beam was supplied to one experiment (Apr. 28th to May 6th). The maximum intensity was 102 particle nA. Owing to the improvement in transmission efficiencies, the intensity was increased by a factor of 2.7 compared with that in the previous experiment of June 2013. Since the tuning time was shortened, the beam was supplied for a duration 12 h longer than scheduled. Consequently, the availability became 105%.

The ^{238}U beam was supplied for three periods as follows: 1) Apr. 6th to Apr. 22nd for two experiments, 2) May 16th to Jun. 13th for five experiments, and 3) Oct. 17th to Nov. 12th for four experiments. The maximum beam intensity was 41 particle nA. The beam was supplied for 1370.1 h in total, and the availability was 86.5%. The reason that the availability became relatively low was that it took time to deal with several failures which frequently occurred. The major troubles were 1) the failure of output capacitors of the amplifier for RRC RF No. 1, 2) an interlock system of SRC He-refrigerator, 3) the power feeder of the S6 rebuncher, and 4) damages of the power feeder lines and directional couplers caused by a high-power operation of the acceleration resonators for SRC.

[*1] RIKEN Nishina Center
[*2] Center for Nuclear Study, the University of Tokyo
[*3] SHI Accelerator Service Ltd.

References

1) T. Nakagawa et al.: RSI **75,** 1394 (2004).

2) M. Kase et al.: Proc. PASJ9, WEPS004, p. 350.

RILAC operation

E. Ikezawa,*1 T. Ohki,*2 M. Kase,*1 T. Nakagawa,*1 N. Sakamoto,*1 H. Okuno,*1 N. Fukunishi,*1 M. Komiyama,*1 A. Uchiyama,*1 T. Maie,*1 M. Nagase,*1 M. Fujimaki,*1 T. Watanabe,*1 H. Hasebe,*1 H. Imao,*1 K. Ozeki,*1 K. Suda,*1 Y. Higurashi,*1 K. Yamada,*1 Y. Watanabe,*1 S. Watanabe,*1 M. Kidera,*1 T. Nagatomo,*1 H. Yamauchi,*2 K. Oyamada,*2 M. Tamura,*2 A. Yusa,*2 K. Kaneko,*2 and O. Kamigaito*1

The RIKEN heavy-ion linac (RILAC) has operated steadily throughout the reporting period and has supplied various ion beams for different experiments. Some statistics regarding the RILAC operation from January 1 to December 31, 2016 are presented in Table 1. The total beam service time of the RILAC accounted for 89.7% of its operation time. The two operation modes of the RILAC, the standalone mode and the injection mode, in which the beam is injected into the RIKEN Ring Cyclotron (RRC), accounted for 77.5% and 22.5% of the total beam service time of the RILAC, respectively. For experiments, a 2.675-MeV/nucleon ^{48}Ca-ion beam accelerated by the RILAC was injected into the RRC from November 12 to December 6. Table 2 lists the beam service times in the standalone mode of the RILAC allotted to the e2 and e3 beam courses in target room no. 1 in 2016. The e2 beam course was used in experiments with the GARIS2. The e3 beam course was used in experiments with the GARIS. Table 3 lists the operation time of the 18-GHz ECR ion source in 2016.

We performed the following improvements and overhauls during the reporting period.

1) In the RF systems, DC high-voltage power supplies were subjected to annual inspection. The major components with mechanical parts were subjected to simple inspection.
2) The water pumps for the RFQ, RILAC, and CSM were subjected to annual inspection. All cooling towers were subjected to monthly inspection and annual cleaning.
3) All the turbomolecular pumps were subjected to annual inspection. Cryogenic pumps used for the RILAC no. 3, RILAC no. 4, RILAC no. 6, CSM A5, and CSM A6 cavities were overhauled.

Table 1. Statistics of RILAC operation from January 1 to December 31, 2016.

Operation time of RILAC	4127.8	h
Mechanical problems	64.9	h
Standalone RILAC	2868.0	h
Injection into RRC	834.3	h
Total beam service time of RILAC	3702.3	h

We faced the following mechanical problems during the reporting period.

1) Water was found to have splashed in the end drift tube of the CSM A3-A6 cavities because of leakage from each cooling pipe. We repaired the pipes with a repair material as a stopgap measure. In addition, the faulty part of the end drift tube of the CSM A4 cavity was replaced.
2) A section of the air-pressure pipe for the contact fingers of the rf shorting plate in the RILAC no. 4 and the RILAC no. 6 cavities had a vacuum leak because of a deteriorated O-ring. We replaced it with a new one.

Table 2. Beam service time of the standalone RILAC allotted to each beam course in target room no. 1 in 2016.

Beam course	Total time (h)	%
e2	1674.6	59.2
e3	1154.6	40.8
Total	2829.2	100.0

Table 3. Operation time of the 18-GHz ECR ion source in 2016.

Ion	Mass	Charge state	Total time (h)
He	4	2	24.0
O	18	5,6	300.9
Ne	22	7	528.0
Na	23	7	416.2
Mg	24	7	129.2
Ar	36	10	216.6
Ar	40	9,11	207.2
Ca	40	10	192.0
Ca	48	10,11	1959.9
Ti	50	11	329.7
V	51	11	216.0
Ni	58	13	120.0
Kr	86	18	84.6
Au	197	26	24.0
U	238	35	82.1
	Total		4830.4

*1 RIKEN Nishina Center
*2 SHI Accelerator Service Ltd.

AVF operations in 2016

S. Ishikawa,[*1] K. Ozeki,[*2] M. Fujimaki,[*2] N. Fukunishi,[*2] S. Fukuzawa,[*1] M. Hamanaka,[*1] H. Hasebe,[*2] Y. Higurashi,[*2] E. Ikezawa,[*2] H. Imao,[*2] O. Kamigaito,[*2] M. Kase,[*2] M. Kidera,[*2] K. Kobayashi,[*1] M. Komiyama,[*2] Y. Kotaka,[*3] R. Koyama,[*1] K. Kumagai,[*2] T. Maie,[*2] M. Nagase,[*2] T. Nakamura,[*1] T. Nagatomo,[*2] T. Nakagawa,[*2] M. Nakamura,[*2] M. Nishida,[*1] N. Tsukiori,[*1] M. Nishimura,[*1] J. Ohnishi,[*2] Y. Ohshiro,[*3] H. Okuno,[*2] N. Sakamoto,[*2] J. Shibata,[*1] K. Suda,[*2] A. Uchiyama,[*2] S. Watanabe,[*2] T. Watanabe,[*2] Y. Watanabe,[*2] K. Yadomi,[*1] K. Yamada,[*2] and S. Yamaka[*3]

In 2016, the total annual operation time of the K70 AVF cyclotron (denoted as AVF hereafter) was 3366 hours, as indicated in Table 1. The beam supply time was classified into four categories: “Injection to RRC,” “Injection to RRC-SRC,” “Injection to RRC-IRC-E5,” and “AVF standalone.” The total beam supply time was 2112 hours, which was increased by 62 hours compared with that in 2015. The increase in the beam supply time was mainly due to the CRIB experiments. The time supplied to CRIB was three times longer than that in 2015. “Injection to RRC-IRC-E5” was a new beam course, and the beam was supplied for the first time in January 2016. The supplied time for “AVF standalone” was 1321 hours, which was 266 hours shorter than that in 2015.

All of the beams accelerated by the AVF in 2016 are listed in Table 2. In this table, the following beams were accelerated for the first time in 2016: ^{26}Mg (6.6 MeV/u) and ^{86}Kr (3.77 MeV/u). The supplied courses were (in order of the supplied time): C03 (RI production), RRC-SRC, RRC-IRC-E5, E7A (CRIB), RRC-E5, RRC-E6, and E7B (Student experiment).

Table 1. AVF operation statistics in 2016

	2015	2016
Total operation time (h)	3282	3366
Beam tuning (AVF)	785	788
Beam tuning (others)	446	466
Injection to RRC	324	430
Injection to RRC-SRC	124	350
Injection to RRC-IRC-E5	15	11
AVF standalone	1587	1321
Beam course (AVF standalone) (h)		
E7A (CRIB)	1097	686
E7B (Student experiment)	28	73
C03 (RI production)	462	562

The total fault time was 5 hours (included in the operation time in Table 1). The main faults are listed in Table 3, in descending order of time spent for restoration.

Table 2. AVF beam list in 2016

Particle	E (MeV/u)	Course
p	12	RI production
p	14	RI production
d	7.25	RI production
d	12	RI production
α	6.5	Student experiment
α	7.25	RI production
α	12.5	RI production
^{7}Li	5	CRIB
^{7}Li	5.6	CRIB
^{12}C	7	RRC-E5
^{18}O	4.64	RRC-SRC
^{18}O	8	CRIB
^{19}F	6.768	RI production
^{20}Ne	8.2	E7B
^{22}Ne	3.97	RRC-E6
^{26}Mg	6.6	CRIB
^{40}Ar	5.2	RRC-E5
^{40}Ar	3.78	RRC-E5
^{40}Ar	3.78	RRC-IRC-E5
^{56}Fe	5.01	RRC-E5
^{84}Kr	3.97	RRC-E5
^{85}Rb	3.78	RRC-E6
^{86}Kr	3.777	RRC-E3

Table 3. AVF faults in 2016

Date	Time for restoration (h)	Matter
May 8th	3	Damage on compressed-air pipe installed in AVF-RF #1.
Nov. 21st	2	Re-filling of Li material in the ion source.

*1 SHI Accelerator Service Ltd.
*2 RIKEN Nishina Center
*3 Center for Nuclear Study, the university of Tokyo

Present status of the liquid-helium supply and recovery system†

T. Dantsuka,[*1] H. Okuno,[*1] M. Nakamura,[*1] M. Kase,[*1] S. Tsuruma,[*1]
M. Ohshima,[*2] H. Miura,[*2] H. Shiraki,[*2] H. Hirai,[*2] and H. Hazama[*2]

The liquid-helium supply and recovery system,[1)] which can produce liquid helium at a liquefaction rate of 200 L/h from pure helium gas, has been under stable operation since the beginning of April 2001. The volumes of liquid helium supplied each year from 2001 to 2015 are shown in Fig. 1. The volume gradually increased from 2001 to 2013, with two declines in 2009 and 2011. In 2014, the supplied volume decreased because of a malfunction of the system. In 2015, the supplied volume returned to its original supply volume.

The purity of helium gas recovered from the laboratories gradually improved after the construction of the system was completed. Currently, the impurity concentration in the recovered gas rarely exceeds 200 ppm. The volume of helium gas recovered from each building in the Wako campus as well as the volume transported to the liquid helium supply and recovery system were measured. The recovery efficiency, which is defined as the ratio of the amount of recovered helium gas to the amount of supplied liquid helium, was calculated.

The recovery efficiency for the buildings on the south side of the Wako campus, such as the Cooperation Center building of the Advanced Device Laboratory, Chemistry and Material Physics building, and Nanoscience Joint Laboratory building, increased to more than 90%.

At the end of November 2015, the system experienced a malfunction. We found an inflow of oil in the helium liquefier. One cause for the oil separator failure was deterioration due to age. We changed the oil separator of the recovery compressor in December 2016.

Reference

1) K. Ikegami et al.: RIKEN Accel. Prog. Rep. 34, 349 (2001).

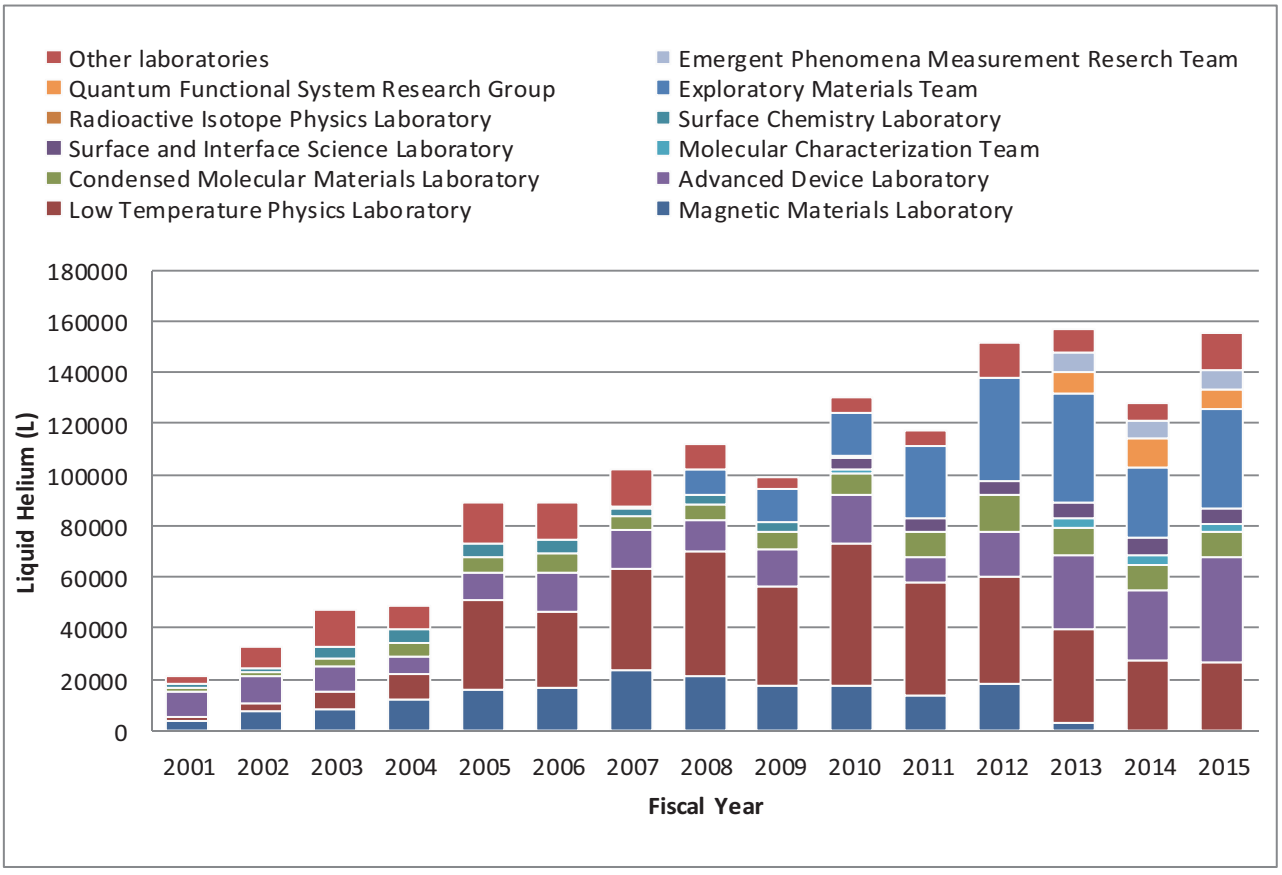

Fig.1. Volumes of liquid helium supplied to the various laboratories for each fiscal year from 2001 to 2015.

*1 RIKEN Nishina Center
*2 Nippon Air Conditioning Service K.K

Operation of the BigRIPS cryogenic plant

K. Kusaka,[*1] M. Ohtake,[*1] K. Yoshida,[*1] M. Ohshima,[*2] A. Mikami,[*2] H. Hazama,[*2]
H. Miura,[*2] H. Shiraki,[*2] H. Hirai,[*2] M. Haneda,[*2] R. Sasaki,[*2] and M. Nakayama[*2]

In 2016, we have operated the BigRIPS cryogenic plant according to the RIBF beam time schedule. We started continuous operation in March, and, after about 100 days of steady state operation, the main compressor was stopped in July. After the summer maintenance,[1)] we restarted the cryogenic plant in September and stopped the compressor in December. The total operation time of the compressor unit was 59,276 h.

During these continuous operations, we faced three significant incidents. One incident was the sudden stop of the compressor unit on Oct. 12 that was caused by a power outage. This large power outage in the Tokyo metropolitan area was caused by a power transmission cable of the Tokyo Electric Power Co. (TEPCO) that caught on fire. Although the power of all the cryogenic plants and most of the water cooling system in the RIBF facility is supplied by the independent RIBF co-generation system (CGS), a momentary voltage drop arose from the power switching system interlock between the TEPCO- and the CGS-power lines. The momentary voltage drop stopped some cooling water pumps and our compressor unit stopped at the same time. The reason for the failure of the mechanical components caused by the momentary voltage drop is under investigation.

Another incident consisted of the sudden stops of the expansion turbines in the refrigerator, which were false interlock stops caused by the failure of the temperature transducer for the helium gas at the exit of the second turbine, T2. We replaced the temperature transducer and continued the operation. The temperature at the T2 exit is one of the most important parameters for the refrigerator system and is usually set to 11.6 K for optimum cooling capacity. However, we had to change the T2 temperature parameter to 10.5 K for optimum cooling capacity during the ^{48}Ca beam time. At this parameter setting, we operated the cryogenic system with a beam heat load fluctuation of more than 100 W. We calibrate the T2 temperature transducer and test the cooling capacity using the stand alone operation of the TCF200 cold-box in 2017.

The third incident was an unusual noise that was produced by the main motor of the compressor unit. We first noticed the noise in mid-November and the noise level gradually increased daily, even though we had greased the motor unit. Since 2015, we have regularly measured the vibrations of the main compressor unit using an OH-580A hand-held vibration tester.[4)] The vibration acceleration in the vertical and horizontal directions as a function of the total operation time is shown in Fig. 1. Measurements were performed both at the high-pressure and low-pressure sides of the compressor. It is clear that the vibration acceleration increased drastically after hour 58,630 of operation, which corresponds to Nov. 14. On Dec. 5, the acceleration exceeded more than 20 m/s^2 and the noise level became dangerously large, so we decided to cancel the beam time and stop the compressor unit on Dec. 6. After a 6-h recovery operation after the expansion turbines were stopped, the compressor was safely stopped. Using a temporary recovery line, evaporated helium gas from the STQ cryostats was successfully transferred to the RIKEN liquid-helium supply and recovery system.

The main motor unit was disassembled on site to investigate the origin of the unusual vibrations. In a baring unit on the anti-coupling side, damage was found on a surface of its inner ring (Fig. 2). The motor unit was reassembled with a new bearing unit. After careful mechanical and electrical checks of the whole compressor unit, the test operation was successfully performed and the vibration acceleration was measured to be less than 8 m/s^2. The origin of the bearing damage is under investigation.

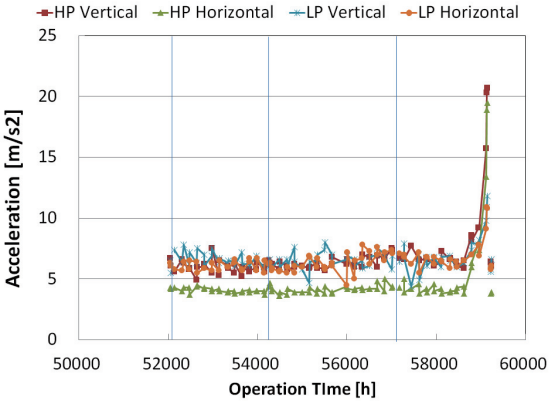

Fig. 1. Vibration acceleration of the compressor unit.

Fig. 2. Damaged bearing unit, disassembled from the anti-coupling side of the motor unit.

References

1) K. Kusaka et al.: RIKEN Accel. Prog. Rep. **49**, 330 (2016).
2) http://www.testo.jp.

[*1] RIKEN Nishina Center
[*2] Nippon Kucho Service Co., Ltd.

Present status of the BigRIPS cryogenic plant

K. Kusaka,[*1] M. Ohtake,[*1] K. Yoshida,[*1] M. Ohshima,[*2] A. Mikami,[*2] H. Hazama,[*2] H. Miura,[*2] H. Shiraki,[*2] H. Hirai,[*2] M. Haneda,[*2] R. Sasaki,[*2] M. Nakayama[*2] M. Noguchi,[*3] and N. Suzuki[*3]

Periodic maintenance of the oil-removal module in the helium compressor unit is crucial to ensure the long-term continuous operations of BigRIPS[1]. The oil-removal module comprises a bulk oil separator (an oil vessel with a demister), three coalescer vessels, and two adsorbent vessels (4SP and 5SP) that contain activated carbon and molecular sieves. The periodic replacement of coalescer filters and adsorbents ensure low oil contamination in helium gas. We report our studies on oil contamination performed over the past 9 years.

Each coalescer vessel contains four coalescer filters, manufactured by Domnick Hunter,[2] and all the filters were replaced every 2 years since 2008. However, the filters used for 6 years were discontinued and replaced with the successive product of Domnick Hunter in 2014. The drain oil separated from the helium gas is sent to the compressor via a drain line with solenoid valves, depending on the oil level in the vessel. By measuring the operation interval of the solenoid valves, the oil contamination level of the coalescer vessels is evaluated.[3]

Figure 1 shows an estimate of the oil contamination level at the entrance of the third coalescer vessel as a function of the coalescer filter operation time. The navy blue, green, and yellow diamonds represent the estimates for the 2008-2009, 2010-2011, and 2012-2013 operations, respectively. The coalescer filters used in those periods were discontinued.[2] The estimate for the 2014-2015 operation with the new coalescer filters is shown with pink diamonds. The oil contamination values measured using the oil check kit are also shown. The open triangles, squares, circles, and diamonds represent the results for the 2008-2009, 2010-2011, 2012-2013, and 2014-2015 operations, respectively. Both estimates of the coil contamination level are consistent with each other and the performance efficiency of the new filter elements seems to be similar to or better than that of the discontinued ones.

In addition to replacing the coalescer filters, we have replaced the adsorbent in 4SP and 5SP to maintain the performance of the oil-removal modules. The 4SP adsorbent vessel contains activated carbon and molecular sieves, and they are replaced with new ones every year. On the other hand, the 5SP vessel contains activated carbon only, which we replaced in 2009, 2011, 2013, and 2016. Used adsorbent was sampled and sent to the adsorbent manufacturer for degradation analysis. Sampled activated carbon was tested and the following items were measured and reported: bulk density, loss on drying, and volatile matter content.

*1 RIKEN Nishina Center
*2 Nippon Kucho Service Co., Ltd.
*3 Mayekawa Mfg. Co., Ltd.

We show, as an example, results of the volatile matter content, which we consider a good index of the amount of oil adsorbed in activated carbon. Figure 2 shows the volatile matter content of the activated carbon sampled from 4SP. In each analysis, activated carbon was sampled from three different parts of the adsorbent vessel. The results for the sample from the upper, middle, and lower part of the vessel are indicated by blue, brown, and green bars, respectively. The total operation time of each adsorbent is also indicated.

Before summer 2008 only two coalescer vessels were used in the oil-removal module and the whole cryogenic plant suffered from oil-contamination. The volatile matter content of 8.7% indicates that the activated carbon was badly degraded. All the results except that for the sample taken in 2008 are in the range of 2–3% and indicate the degradation of the adsorbent in its early stage. This result suggests that the three coalescer vessels work with sufficient oil-separation efficiency.

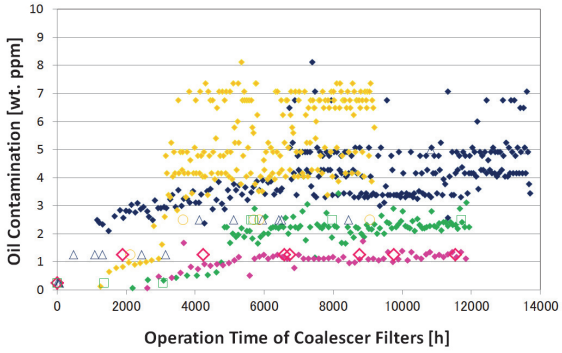

Fig. 1. Oil contamination at the entrance of the third coalescer vessel.

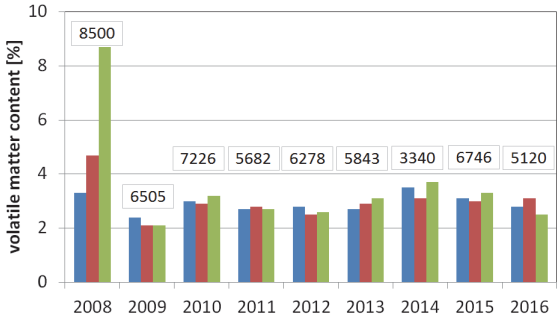

Fig. 2. Volatile matter content of the activated carbon sampled from the 4SP adsorbent vessel.

References

1) K. Kusaka et al., RIKEN Accel. Prog. Rep. **43**, 244 (2008).
2) http://www.parker.com/
3) K. Kusaka et al., RIKEN Accel. Prog. Rep. **41**, 309 (2010).

Radiation safety management at RIBF

K. Tanaka,[*1] Y. Uwamino,[*1] H. Sakamoto,[*1] R. Hirunuma-Higurashi,[*1] H. Mukai,[*2] A. Akashio,[*1] T. Okayasu,[*1] R. Suzuki,[*3] M. Takekoshi,[*3] Y. Yamauchi,[*3] S. Fujita,[*1] H. Aiso,[*1] K. Igarashi,[*1] S. Iizuka,[*1] and N. Usudate[*1]

The results of radiation monitoring at RIBF, carried out at the border of the facility and radiation-controlled area, are reported. The residual doses along the accelerator setups are also presented. In 2016, on average, a 345 MeV/u ^{238}U beam was provided at an intensity of 30 particle nA in April, May, October, and November. A ^{124}Xe beam of 100 particle nA was used in May, an ^{18}O beam of 1000 particle nA was used in June, and a ^{48}Ca beam of 300 particle nA was used in November and December.

The dose rates at the boundary of the radiation-controlled area were monitored. Neutron and γ-ray monitors were used on the roofs at three locations: RRC, IRC, and BigRIPS. Figure 1 shows the annual neutron dose at these positions. In 2016, even the highest annual dose of 120 μSv/y at the IRC roof was lower than the legal limit of 5.2 mSv/y. The γ-ray dose of these positions were background level.

The dose rates at the site boundary, where the legal limit is 1 mSv/y, were monitored. Neutron and γ-ray monitors were used, and the annual dose in 2016 was found to be smaller than the detection limit after background correction. The detection limit of the neutron monitor is 2 μSv/y and that of the γ-ray monitor is 8 μSv/y. Therefore, it was inferred that the annual dose at the boundary was less than 10 μSv/y, which is considerably lower than the legal limit.

The residual radioactivity at the deflectors of the cyclotrons was measured just before the maintenance work. The residual dose depends on factors such as the beam intensity, accelerator operation time, and cooling time.

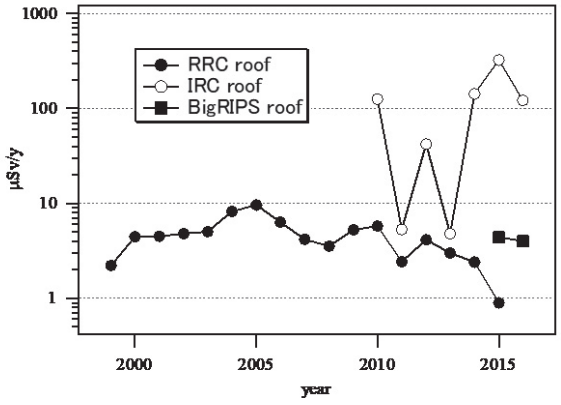

Fig. 1. Radiation dose at the boundary of the radiation-controlle area.

The dose rates from 1986 are shown in Fig. 2. The dose rates for FRC, IRC, and SRC are shown after the year 2006, when the RIBF operation started. For the AVF, the dose rate increased in 2006 because radioisotope production was started and the beam intensity increased. In 2008, the residual dose measurements were highest because high intensity N_2 beam of 500 particle nA was accelerated for RI production just before the measurement.

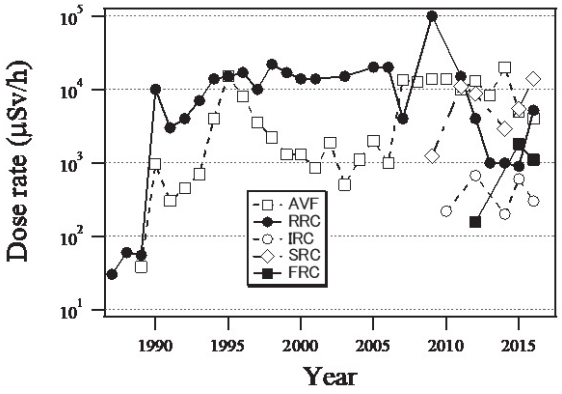

Fig. 2. Dose rates of the residual radioactivity at the deflectors of five cyclotrons.

The residual radioactivity along the beam lines was measured after almost every experiment. Figure 3 shows the locations of measurement points where high residual doses were observed. Table 1 lists the dose rates, beam conditions, and cooling time at these measurement points. The beam conditions are beam nuclides, energies, and maximum intensity in the experiments just before the measurements. The maximum dose was 50 mSv/h at point 12, which is in the vicinity of the G01 Faraday cup.

The radioactivity in the closed cooling system at BigRIPS was measured. The water for the F0 target, exit beam dump, and sidewall dump were sampled in September. The water in the closed cooling systems was replaced in February 2015; therefore, the detected radioisotopes were generated during one and a half years operation in RIBF. The results are shown in Table 2. A liquid scintillation counter was used for the low energy β ray of 18 keV from H-3 nuclide. A Ge detector was also used for γ rays emitted from other radionuclides. The radionuclides, except for H-3, were already filtered by an ion exchange resin in the closed cooling systems. Although the overall value of contamination was less than the legal limit for drain water, as shown in Table 2, the water from the closed cooling system will be dumped into a drain tank before the next

*1 RIKEN Nishina Center
*2 Japan Environment Research Corporation
*3 Daiwa Atomic Engineering Corporation

operation to prevent contamination in the room in case of a water leakage.

An E-learning module that can be accessed anytime and anywhere, even from outside RIKEN, has been used for retraining the radiation workers at RIBF. About 600 radiation workers completed the training in 2016.

Table 1. Residual dose rates measured at beam lines in 2016. Points 1−26 indicate the locations where measurements were taken as shown in Fig. 3. At points 24-27, secondary radioactive-isotope beams (RI) were provided whose intensities were limited to 10^7 particles per second.

Point	Dose rate (μSv/h)	Date (M/D)	Particle	Energy (MeV/u)	Intensity (pnA)	Cooling time (h)
1	400	7/28	p	20	2000	77
2	1500	7/28	p	20	2000	77
3	210	7/22	U-238	11	42	74
4	1500	7/6	O-18	80	1320	133
5	1400	7/6	O-18	80	1320	133
6	180	7/6	O-18	80	1320	133
7	110	7/6	O-18	230	837	134
8	320	12/15	Ca-48	345	700	222
9	350	12/15	Ca-48	345	700	222
10	700	7/6	O-18	230	837	134
11	10000	7/6	O-18	230	837	134
12	50000	7/6	O-18	230	837	134
13	300	7/6	O-18	230	837	137
14	350	7/6	O-18	230	837	137
15	1200	12/15	Ca-48	345	700	222
16	450	7/6	O-18	230	837	137
17	450	7/6	O-18	230	837	137
18	1500	7/6	O-18	230	837	136
19	150	7/6	O-18	230	837	136
20	350	7/6	O-18	230	837	136
21	4100	12/15	Ca-48	345	700	222
22	5700	12/15	Ca-48	345	700	222
23	31000	12/15	Ca-48	345	700	222
24	760	12/15	Ca-48	345	700	222
25	260	12/15	Ca-48	345	700	222
26	240	12/15	Ca-48	345	700	222

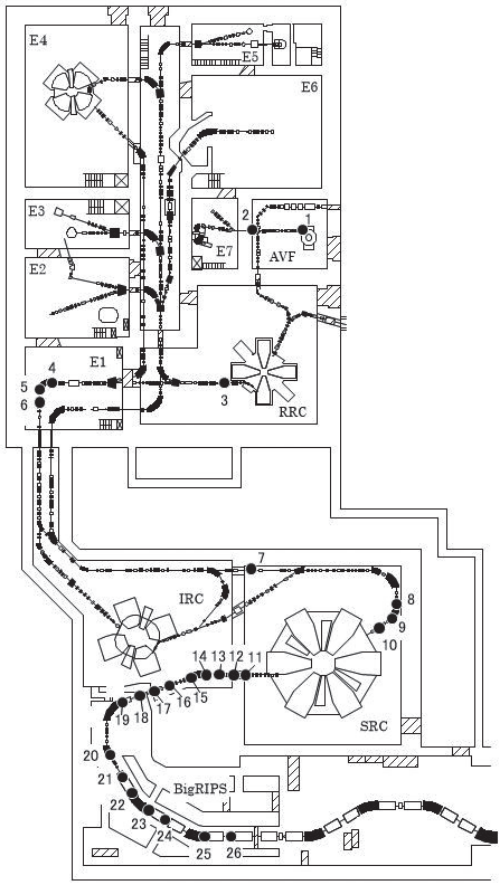

Fig. 3. Layout of the beam lines at RIBF. The measurement locations listed in Table 1 are indicated.

Table 2. Concentrations of radionuclide in the cooling water at BigRIPS, the allowable legal limits for drain water, and the ratios of concentration to the allowable limit.

Cooling water	Nuclide	Concentration[a] (Bq/cm^3)	Limit[b] (Bq/cm^3)	Ratio to limit [a/b]
BigRIPS F0 target	H-3	25	60	0.42
	Co-57	8.7e-4[1)]	4	2.2e-4
	Co-58	7.7e-4	1	7.7e-4
	Mn-54	7.5e-4	1	7.5e-4
			summation	0.42
BigRIPS exit beam dump	H-3	17	60	0.29
	Co-57	1.5e-3	4	3.8e-4
	Co-58	8.9e-4	1	8.9e-4
	Mn-54	2.0e-3	1	2.0e-3
			summation	0.29
BigRIPS side-wall beam dump	H-3	25	60	0.42
	Co-57	1.3e-3	4	3.2e-4
	Co-58	1.4e-3	1	1.4e-3
	Co-60	6.1e-4	0.2	3.1e-3
	Mn-54	8.5e-4	1	8.5e-4
			summation	0.43

1) read as 8.7×10^{-4}

Maintenance of vacuum equipment for accelerators

S. Watanabe,*1 Y. Watanabe,*1 E. Ikezawa,*1 N. Sakamoto,*1 N. Yamada,*1
M. Kase,*1 K. Oyamada,*2 M. Nishida*2 K. Yadomi,*2 J. Shibata,*2 and A. Yusa*2

We have been maintaining the vacuum equipment of the accelerators in good condition. We report the maintenance of the vacuum for the accelerators in 2016.

First, the maintenance of vacuum equipment in RILAC is described. In January, the pressure at the X-re-buncher (X-REB) increased to 5 x 10^{-5} Pa after a joint for cooling the inner cylinder was repaired. When the X-REB was searched, leak points were found downstream of the duct of beam. The leak points were found in an O-ring of a Penning gauge, an O-ring of a Pirani gauge, and an O-ring between a rotary pump and turbo-molecular pump. These O-rings were replaced with new ones and no further leaks could be found using a helium leak detector. However, the pressure did not improve. The cause of the pressure increase lay elsewhere and remained unknown until April, when a shaft on a bottom plate of the outer cylinder was disassembled and reconstructed. The bolts and screws of this part were tightened and the pressure improved. In February, a leak was confirmed in cavity No. 5 using a helium leak detector. However, the leak points could not be identified. Because the helium leak detector takes some time to respond after the helium gas has been shot, the leak point could be different from the place where the helium was shot. To identify the leak point, a dye penetrant inspection (color check) was used. A color check is a method for searching scratches and cracks on metal. First, special colored liquid is sprayed on the metal. Next, the liquid is wiped off. Finally, the scratches and cracks appear if they exist. When the liquid was sprayed on a welded area of the RF feeders, red color appeared on the reverse side of the painted area. This indicated that the liquid had passed though the chamber wall. These scratches were treated with vacuum sealing agent. However, the vacuum pressure could not be improved. This indicated other paths that linked outside of the chamber to its inside. If these paths through the chamber wall were the cause of the vacuum leak, the chamber wall should be changed to improve the leak completely. In April, a vacuum leak was found on a part of the welded joint of flanges near cavity No. 6 in an area called e42. However, it was difficult to repair the leak because the access space was narrow. The leak could not be repaired. Because the pressure was kept at the order of 10^{-5} Pa, the vacuum leak did not influence the experiments.

In February, the pressure increased in the AVF cyclotron. The cause of the pressure increase was a vacuum leak. Vacuum leaks in the AVF cyclotron had occurred previously. Leak often happened because of a deformation of the flange. Hence, the flange was supported by pillars so that it would not deform. In this case, the cause of the leak was not the condition of the pillars. Therefore, an O-ring of the flange was greased and the vacuum leak was fixed. In March, a rotary pump used at the AVF cyclotron stopped suddenly. The rotary pump was replaced with a spare. However, the reduction in pressure obtained by the spare was not sufficient. Hence, the spare pump was replaced with the former one which worked normally. The cause of this incident remains unknown.

In March, a cryopump did not work at the SRC. The cause of this problem was a compressor malfunction. To fix the compressor, its head unit was replaced. The cryopump worked normally again.

At the IRC in April, several cryopumps failures occurred. A cryopump failed to work properly. When the circuit breaker was turned off and reset, the pump worked again. However, it soon failed to work again. The pump was replaced with a spare one. Another cryopump also failed to work. After the circuit breaker was turned off and on, the pump was restarted.

At the fRC in April, a cryopump failed to work. After a switch in front of a compressor was turned off and on, the cryopump was restarted.

At the RRC, a bellows connected with RF No. 2 had a leak point. Vacuum leaks from this part occurred frequently. The leak was treated with a vacuum sealing agent. However, the leak happened repeatedly, especially during experimental beam time. In November, the pressure increased during beam time. The ion beam was stopped and the leak point was investigated. The cause of the pressure increase was a leak on the bellows. The leak point was treated with vacuum sealing agent. Then the pressure decreased. To solve this problem completely, RF No. 2 have to be taken apart, and the bellows will need to be replaced. A large-scale repair is needed to solve this problem. It is not easy to solve this problem; therefore, the treatment using vacuum sealing agent will be continued.

*1 RIKEN Nishina Center
*2 SHI Accelerator Service LTD

Operation of fee-based activities by the industrial cooperation team

A. Yoshida,[*1] T. Kambara,[*1] H. Haba,[*1] and S. Yano[*1]

The fee-based activities operated by the industrial cooperation team in 2016, which are the utilization of heavy-ion beams in the industry and the distribution of radioisotopes, are summarized below.

RIKEN Nishina Center allows the use of the AVF cyclotron, RILAC, and RIKEN Ring Cyclotron (RRC) by private companies in Japan for a fee.[1)] In October, two fee-based beamtimes to test space-use semiconductor devices were successfully performed at the E5A beamline of RRC. A 70-MeV/A ^{84}Kr beam was delivered for about 60 h and a 95-MeV/A ^{40}Ar beam was delivered for about 30 h. The clients irradiated their samples in the atmosphere with a beam of uniform flux distribution and specified LET. The beamline setup was the same as before,[2)] and the beam handling was reported previously.[3)]

Since 2007, RIKEN has distributed radioisotopes (RIs) to users in Japan for a fee in collaboration with the Japan Radioisotope Association[4)] (JRIA). The nuclides are ^{65}Zn ($T_{1/2}$ = 244 days), ^{109}Cd ($T_{1/2}$ = 463 days), ^{88}Y ($T_{1/2}$ = 107 days), and ^{85}Sr ($T_{1/2}$ = 65 days), produced by the RI Applications Team at the AVF cyclotron. According to a material transfer agreement (MTA) drawn between JRIA and RIKEN, JRIA mediates the transaction of the RIs and distributes them to users. ^{65}Zn and ^{109}Cd are delivered about two weeks after the acceptance of an order. ^{85}Sr and ^{88}Y, which have shorter half-lives are not stocked like ^{65}Zn and ^{109}Cd but are produced in a scheduled beamtime after an order is accepted. Therefore they are delivered two months or more after order. Details can be found on the online ordering system J-RAM[5)] of JRIA.

In 2016, we delivered two shipments of ^{109}Cd with a total activity of 12 MBq, five shipments of ^{65}Zn with a total activity of 24 MBq, two shipments of ^{88}Y with a total activity of 2 MBq, and a shipment of ^{85}Sr with an activity of 1 MBq. The final recipients of the RIs were seven universities and one medical research center. The shipment of ^{85}Sr was the first since April 2015 when the distribution of this radioisotope was formalized.

Figure 1 shows the yearly trends in the number of orders and the amounts of distributed RIs. Compared with 2015, the amount of distributed ^{109}Cd increased by a factor of 3, that of ^{65}Zn by 2.4, and that of ^{88}Y by 2. Information on the RIs can be obtained from JRIA JRAM or FAX (03-5395-8055).

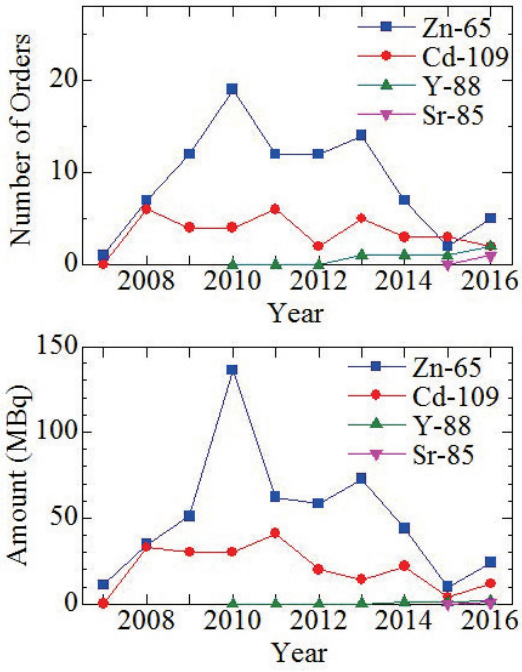

Fig. 1. Number of orders (upper) and amount (lower) of the RIs distributed yearly from 2007 to 2016. The distribution of ^{88}Y started in 2010 and that of ^{85}Sr in 2015.

References

1) http://ribf.riken.jp/sisetu-kyoyo/ (Japanese).
2) T. Kambara, A. Yoshida, RIKEN Accel. Prog. Rep. **48**, 239 (2015).
3) T. Kambara, A. Yoshida, RIKEN Accel. Prog. Rep. **49**, 193 (2016).
4) http://www.jrias.or.jp/ (Japanese), http://www.jrias.or.jp/e/ (English).
5) https://www.j-ram.net/jram/DispatchTopPage.do (Japanese).

*1 RIKEN Nishina Center

Operation of the Pelletron tandem accelerator

T. Ikeda,[*1] M. Hamagaki,[*1] and H. Sato[*1]

The tandem accelerator (Pelletron 5SDH-2, 1.7 MV max.) in Nishina R&D Building (Fig. 1) has been managed by the Detector Team, RNC since April 1st, 2016. The accelerator has three beam lines for (1) RBS (Rutherford backscattering) spectrometry/ERDA (elastic recoil detection analysis), (2) microbeam port, and (3) multi-purpose use. So far, the ion species of H, He, Li, B, C, N, O, Si, Ti, Ni, Cu, and Au have been accelerated.

The total machine time including sample irradiation was 37 days during the annual reporting period from Jan. 1 to Dec. 31, 2016, excluding repair of the high-voltage system. In addition, a precise alignment of the beam elements as well as the ion source was performed. The experiments in machine time and details of the maintenance are described in this report.

Fig. 1. Pelletron tandem accelerator and beamline.

The ion species accelerated in this year were H^+, B^{3+}, and Au^{6+}, with energies ranging from 1.0 to 10.5 MeV, as summarized in Table 1.

Experimental studies including a machine study on the following subjects were performed. (Machine studies without beam delivery to beam ports are not counted.)

(1) Performance test of a thin Si detector (11 days)
(2) Educational experiment of proton capture by carbon nucleus for Nishina School (Fig. 2) (5 days)
(3) Metallic nanoparticle formation by ion irradiation in liquid (5 days)
(4) Microbeam irradiation to single cells (6 days)
(5) Machine study of proton microbeam using tapered glass capillaries (10 days)
(6) Analyses using elastic scattering (RBS/ERDA) as Wako joint-use equipment (0 days = no user)

In April, the stability over 700 s of the acceleration voltage was examined, as shown in Fig. 3(a). The horizontal axis shows the monitored voltage, which is proportional to the acceleration voltage (5.95 V corresponding to 1.5 MV). The fluctuation σ (standard deviation of the data) was found to be more than 0.3%, which was worse than the specification of 0.1% guaranteed by the manufacturer. After a maintenance overhaul (cleaning in the acceleration tank to avoid discharge and replacing a broken ground level shaft with a new one), it improved, as shown in Fig. 3(b), for a 9,000-s operation. In December, the locations of all beam elements (ion source, triplet-Q, dipole magnet, and beam ducts) were measured precisely. Because of the position adjustment of the ion source, the beam intensity at the irradiation port improved by two orders of magnitude.

Table 1 Beam conditions and experiments conducted in the tandem accelerator (*experiments that used more than one ion species per day.)

Ion	Energy [MeV]	Beam current [nA]	Experiment	Operation time [days]
$^{1}H^{+}$	1.0–3.0	0.01–50	Irradiation	37
$^{4}B^{3+}$	1.5–2.3	0.01–1	Irradiation	*3
$^{197}Au^{6+}$	7.0–0.5	0.01–1	Irradiation	*2

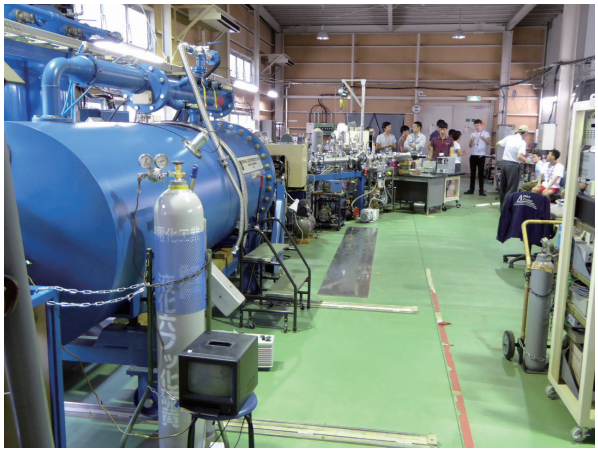

Fig. 2. Educational experiment for Nishina School.

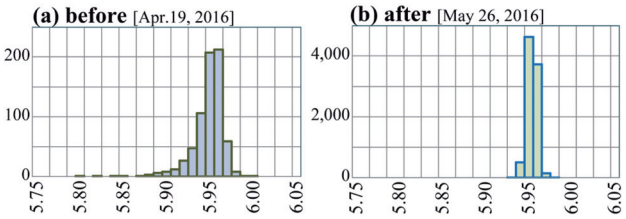

Fig. 3. Acceleration voltage monitoring results (a) before and (b) after the repair. Fluctuation σ improved from (a) σ = 0.312% to (b) 0.095%.

*1 RIKEN Nishina Center

V. EVENTS

Users Meeting to Memorize the 25-Years of the RIKEN-RAL Muon Facility Project in the UK

I. Watanabe,[*1] K. Ishida,[*1] and M. Iwasaki[*1]

The RIKEN-RAL Muon Facility project was started from 1990. This project was the biggest scientific international collaboration in between Japan and the UK in that year. The facility construction has been successfully completed in 1994 and the user program has been running until now after that. The facility operation is still on going and many researchers and students are enjoying the muon science at the RIKEN-RAL on the collaboration basis. In the beginning of the history of the facility operation, Japanese collaborators were mainly using the facility. Recently, Asian and worldwide groups were joining to this RIKEN-RAL project year by year making scientific activities and human resource exchanges wider and bigger.

The year of 2015 is the memorial year as a milestone of the 25-years of the RIKEN-RAL project. In order to memorize this milestone, we planned to organize the celebration ceremony and users workshop inviting all staffs, researchers and students who are related to and/or have used the RIKEN-RAL Muon Facility in this 25 years. The cerebration event has been held at the RIKEN Wako Campus on 16th and 17th of Feb in 2016 which is the end of the fiscal year of 2015. The event was organized with the 12th the RIKEN-RAL PAC meeting in order to invite all committee members.

As the beginning of the memorial event for the RIKEN-RAL, the ASIA-RIKEN workshop was organized with Indonesian and Malaysian collaborators from the afternoon on 16th of Feb. More than 40 people including students attended this meeting and discussed recent scientific achievement on the muon science by Asian groups as shown in Fig. 1.

Figure 1: The ASIA-RIKEN workshop held on 16th of Feb .

The RIKEN-RAL celebration ceremony was organized on 17th in conjunction with the RIKEN-RAL Users Workshop as the RIKEN Symposium. Attendances to the Users Workshop presented posters to introduce their scientific achievements. Figure 2 shows the atmosphere of the workshop. Eighty-eight scientific posters were presented during the workshop and more than 150 researchers, students and administrators enjoyed

Figure 2: RIKEN-RAL Users Workshop

communications and discussions.

The 25-Years celebration of the RIKEN-RAL project was organized after the Users Workshop. Celebration talks were given from the Executive Director of RIKEN, Director of Nihina Center, Director of the RIKEN-RAL and a guest representative from KEK. A letter of the congratulatory address from the Ambassador of British Embassy was also introduced by the chief administrator.

A celebration cake was prepared by laboratory students and secretaries and served in the ceremony. After celebration talks, we cut the cake and celebrate the RIKEN-RAL Muon Facility as shown Fig. 3.

Figure 3: Photograph of the cake-cut event. The cake was hand made by students who are studying at the RIKEN-RAL.

The RIKEN-RAL Muon Facility is still being operated e delivering pulsed muon beams for a wide range of the muon science. We continuously have new users opening doors to new sciences. Recently, Ph.D. students are continuously joining from Asian countries to the RIKEN-RAL Project. They are working at the experimental side by using the RIKEN-RAL Muon Facility and/or at the computational side by using RIKEN supercomputing resources. The muon-science activity is expanding to the world and young human resources are growing up year by year from the RIKEN-RAL Muon Facility even after this 25-years memorial celebration.

*1 RIKEN Nishina Center

The 14th International Symposium on Nuclei in the Cosmos

S. Nishimura[*1] and T. Kajino[*2]

The Nuclei in the Cosmos is the foremost bi-annual symposium of nuclear physics, astrophysics, astronomy, cosmo-chemistry, and other related fields and it is considered as the most important international symposium in the research field of nuclear astrophysics. In 2016, the 14th International Symposium on Nuclei in the Cosmos (NIC-XIV) was held on 19th – 24th June at the Toki Messe in Niigata, Japan. The NIC-XIV[a)] was jointly organized by two major institutes in Japan: the National Astronomical Observatory of Japan (NAOJ) and the RIKEN Nishina Center for Accelerator-Based Science (RNC).

The symposium was started on 19th June with a welcome reception. The scientific program from 20th – 24th June started with the opening ceremony overseen by the director general of NAOJ, M. Hayashi, and the director of RNC, H. En'yo, who introduced variety of research activities related to the nuclear astrophysics in Japan. On 20th June, Professor T. Kajita, the 2015 Nobel Laureate in Physics for the discovery of neutrino masses, gave a special lecture on "The Discovery of Neutrino Oscillations" in the main conference hall to an audience of NIC participants and the general public, including thirty students from super science high schools in Niigata. A special invited talk was given by Professor K. Morita with the title "The Discovery of Super-Heavy Element of Atomic Number Z = 113 Nihonium and Beyond" on 22nd June.

In NIC-XIV, fifteen sessions of the symposium were devoted to thirty-seven plenary talks and fifty-nine oral talks to cover a wide range of subjects relevant to nuclear astrophysics: (a) Big-Bang Cosmology, Nucleosynthesis, Dark Matter, and Dark Energy, (b) Neutrino Astrophysics and Weak Processes, (c) Novae and X-Ray Bursts, (d) Stellar Evolution and Hydrostatic Nuclear Burning Processes, (e) Radioactive Nuclei Far From Stability, (f) Explosive nucleosynthesis in Stars, (g) Nuclear Theory and Experiments in Astrophysics, (h) Supernovae, Gamma-Ray Bursts and Mergers, (i) Nuclear Data and Astrophysics, (j) First Generations of Stars and Galactic Chemo-Dynamical Evolution, (j) Neutron Stars and Hadron Physics, (k) Meteoritic Abundances, Interstellar Gas and Dust Astronomy, and (l) X- and γ-Ray Astronomy and Cosmic Ray Astrophysics.

Two poster sessions were also held on 21st and 23rd June with 189 poster presentations; six young scientists were awarded prizes (Cupper, Silver, and Gold) for excellent poster presentations delivered on the last day of the symposium. Many discussions and debates were shared during the symposium. One of the highlighted topics was related to the rapid neutron-capture process (r process) and the equation of state (EOS) in high density matter. In relation to the question "Where is the site of the r-process?", the candidates of the r-process site, the supernovae and neutron-star merger scenarios, were discussed deeply. It was decided that the next NIC symposium would be held in Gran Sasso, Italy and will be announced in due time.

Associated with the NIC symposium, the NIC School was conducted at Niigata University immediately before NIC-XIV, where lectures were given by internationally recognized experts on theories, experiments, and observations, which covered the areas of research relevant to nuclear astrophysics. Moreover, public lectures associated with the NIC symposium were organized on 11th June at Hitotsubashi hall after the post symposiums (SEA, 2nd NAOJ-ECT*, MOTO16) around Tokyo.

The poster presentations and the invited and oral talks of NIC-XIV were published in the conference proceedings[1)].

Figure 1. Participants of the NIC-XIV symposium at Toki Messe

Figure 2. Posters (from left) for NIC-XIV, special lecture of Prof. Kajita, and public lecture, respectively (designed by N. Miyauchi)

[1] JPS Conf. Proc. Vol. 14 (2017); http://jpscp.jps.jp

*1 Vice-Chair, RIKEN Nishina Center
*2 Chair; National Astronomical Observatory of Japan / Univ. of Tokyo

a) The NIC-XIV was supported by IUPAP, Physical Society of Japan (JPS), RIKEN iTHES, Niigata Prefecture, the Japan World Exposition 1970 Commemorative Fund, European Physical Journal (EPJ), KAKENHI Grant-In-Aid for Scientific Research on Innovative Area (2404), Japan Radioisotope Association, Nuclear Reaction Data Center Hokkaido University, CNS, RCNP, JAEA, KEK, JINA-CEE, JRIA, JCPRG. Sponsors of NIC-Xiv were SEIKO EG&G Co. Ltd., REPIC Corp. PTEP, Burbon Corp., Canberra Japan KK, Techno AP Co. Ltd. Clear Pulse Co. Ltd. G-Tech Corp. Fuji Diamond Int. Co. Ltd.

International Symposium on Modern Technique and its Outlook in Heavy Ion Science (MOTO16)

H. Sakurai, on behalf of MOTO16 organizers

International Symposium on Modern Technique and its Outlook in Heavy Ion Science (MOTO16) was organized by Rikkyo University and RIKEN Nishina Center (RNC), on 26th and 27th June 2016 at Rikkyo University, to commemorate Prof. Tohru Motobayashi's outstanding scientific achievements during his lifelong dedication to the field of heavy ion science.

Since the dawn of the history of fast radioactive isotope beams (RIB) about 30 years ago, multitudes of radioactive nuclei have been experimentally investigated and their exotic structure revealed at the heavy-ion accelerator facilities worldwide. The rapid growths of this field can be attributed to the enthusiasm of many physicists who aspired to develop new techniques. The techniques would overcome experimental difficulties in terms of intensity and quality of RIB. Emphasis should be given not only to experimental methods but also to instrumentation developments and reliable theoretical-models, all of which should be worked out closely together to promote further progress in the field.

This Symposium provided both reviews and contribution talks on modern technique and its outlook for both experimental and theoretical studies of nuclear structure, reactions and nuclear astrophysics, and encouraged discussions on perspectives of future growths at the facilities around the world.

This Symposium was started from opening address by S. Kitamoto, the Dean, Faculty of Science, Rikkyo Univ. and by H. En'yo, the Director of RNC. The first session was arranged to cover Tohru's pioneering works of Coulomb dissociation and excitation with fast RIB. S. Shimoura, N. Iwasa and R. Casten overviewed the works. The second and third sessions were dedicated to present activities running at RIBF and theoretical works; SEASTAR (A. Obertelli), resonant scattering (T. Teranishi), shell model work (T. Suzuki), SCRIT (K. Kurita), missing and invariant mass spectroscopy (D. Beaumel), Coulomb dissociation for halo nuclei (T. Nakamura).

The last session of the 1st day had one-hour lecture given by Tohru Motobayashi, entitled "Technological and methodological developments in reaction studies with fast radioactive-ion beams -their application to nuclear spectroscopy and nuclear astrophysics -".

About 80 persons joined the Symposium Dinner. The venue was the No.1 Dining Hall in Rikkyo Univ. campus. Speeches and special gifts were given to Tohru by H. Sakai, Z. Fulop, R. Casten, K. Hahn, R. Yamukhamedov, N. Aoi, M. Kurokawa, S. Takeuchi. Tohru and his colleagues (H. Baba, N. Nakagawa, Y. Watanabe) gave a music performance. Music pieces presented were "Beachcomber" (Clive Richardson), "A ce Joy Moys de May" (Clement Janequin) and "Now is the Month of Maying" (Thomas Morley). The pleasant, friendly and unforgettable Dinner was finished by a speech of Tohru.

The second day covered recent activities associated with the early works of Tohru; invariant mass method (Y. Kondo), transfer reaction (K. Wimmer), mean-field theory (M. Yamagami), reaction theory (T. Fukui), Coulomb dissociation (Y. Togano), nuclear astrophysics (K. Hahn, Z. Fulop), detector R&D (M.Kurokawa), ANC (R. Yamukhamedov), high-energy gamma (O. Wieland). Other people who have connection with Tohru gave interesting talks; T-violation search in beta-decay (J. Murata), medical application (A. Saito), SHARAQ (M. Dozono) and double-gamma decay (H. Scheit). The last talk in this Symposium was overview of DALI2, given by S. Takeuchi. At the end of this Symposium, two co-chairmen, K. Ieiki and H. Sakurai, gave closing remarks.

Organizers of this Symposium were N. Aoi (RCNP, Osaka Univ.), K. Ieki (Rikkyo Univ., co-chair), K. Kurita (Rikkyo Univ.), S. Nishimura (RIKEN), H. Sakurai (RIKEN, co-chair), S. Shimoura (CNS, Univ. of Tokyo), T. Uesaka (RIKEN), Y. Yanagisawa (RIKEN) and K. Yoneda (RIKEN). Special thanks would be given to a secretary E. Isogai (RIKEN) and N. Miyauchi (RIKEN) for photos.

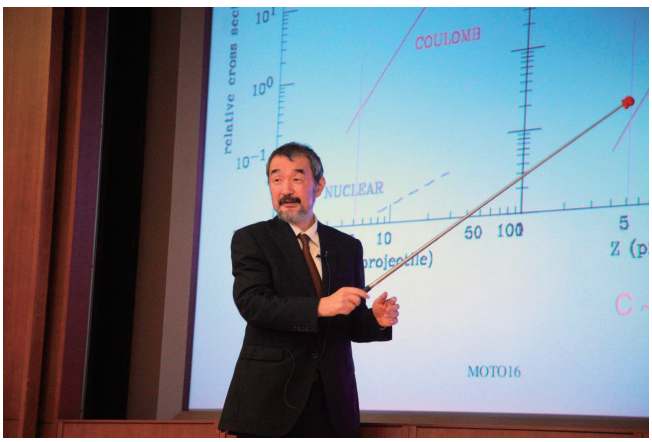

The 14th International Conference on Meson-Nucleon Physics and the Structure of the Nucleon (MENU2016) †

S. Yokkaichi*1

The 14th International Conference on Meson-Nucleon Physics and the Structure of the Nucleon (MENU 2016) was held at Kyoto University Clock Tower Centennial Hall from July 25th to July 30th, 2016. The conference was co-hosted by Kyoto University and RIKEN Nishina Center (RNC), and supported by the Research Center for Nuclear Physics, Osaka University (RCNP), and the Kyoto University Foundation. This conference series had been launched in 1983 at Karlsruhe, Germany. We were very pleased to host at Kyoto, where Hideki Yukawa had first arrived the idea of the "meson" about 80 years ago.

The conference had 142 participants from 20 countries. There were 29 plenary talks and 80 parallel talks (including 11 invited talks) in seven parallel sessions as "Meson-Nucleon Interactions," "Baryons," "Mesons," "Pentaquarks," "Nucleon structure," "Fundamental symmetries," and "Few body systems." From RNC, T. Izubuchi (Lattice QCD), I. Nakagawa (RHIC spin physics) and F. Sakuma (K-pp bound states) were invited as plenary speakers. About three-quarters of all the talks are summarized in the proceedings published online: JPS Conference Proceedings volume 13. The full program and presentation files are available at the conference website (`http://menu2016.riken.jp/`).

The recent progress in meson-nucleon physics, especially hadron spectroscopy, was well summarized at the conference by the presenters covering high-precision photo-, electro-, and hadroproduction data. There were overview talks on spectroscopy from CLAS, BESIII, CBELSA/TAPS, and COMPASS experiments. As the key topics, multi-quark states or hadronic molecular states such as X, Y, and Z states or pentaquarks were discussed. Based on the recent observation of the pentaquark at LHCb, possible explanations and future prospects of hidden charm pentaquarks were discussed. Furthurmore, the current status of the pentaquark at LEPS was reported. New results of K-pp bound states and related results were also presented from four J-PARC and LEPS experiments. In addition, developments in η/η'-N bound state searches were reviewed from experimental and theoretical points of view. It should be noted that there were inspiring talks reporting the recent study of lattice QCD, which has advanced dramatically over the past 5 years. On the last day, there were numerous discussions on prospects at a variety of future facilities: CLAS12, Belle II, PANDA, Electron-Ion Collider, and the J-PARC Hadron-Hall extension. The conference gave us a very unique opportunity to discuss a wide range of topics and its intersections.

A satellite workshop "Meson In Nuclei 2016" followed MENU 2016 at Yukawa Institute of theoretical physics, Kyoto University (YITP), from July 31st to August 2nd (`http://www2.yukawa.kyoto-u.ac.jp/~min2016/`). Topics focused on "mesonic atoms/nuclei" and "meson properties in nuclear matter" were discussed intensively.

The conference was also supported by a subsidy from Kyoto City and the Kyoto Convention and Visitors Bureau, and was held as a part of the RIKEN Symposium Series. We thank INFN, Italy, for their endorsement and financial help. We appreciate the supportive works by the young-physicist and student team and secretaries from RNC. We are very grateful to Dr. N. Miyauchi from the User Liaison Team of RNC, who designed a stylish logo (Fig. 1 left) and a chic poster with a motif of the Nanzenji temple (Fig. 1 right).

The next MENU conference is scheduled to be held in the USA in 2019.

† Modified from the preface of JPS. Conf. Proc. 13 (Copyright reserved by JPS), based on the Creative Commons Attribution 4.0 International License.

*1 RIKEN Nishina Center

Fig. 1. From left to right, the conference logo; an opening address by Dr. H. En'yo (Conference Chair); and the supporting team from Kyoto University, Osaka University, and RIKEN Nishina Center.

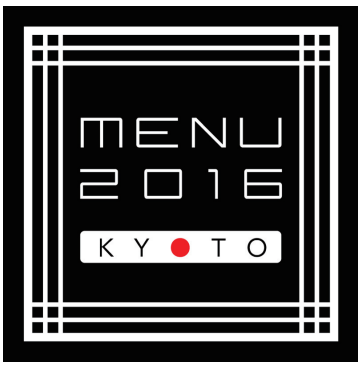

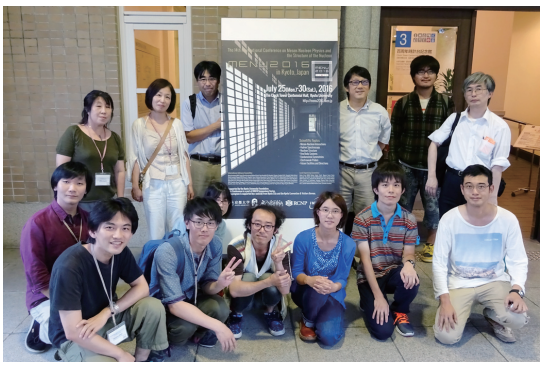

Nishina School 2016

T. Motobayashi*1 and H. Ueno*1

The Nishina School aims at contributing to the development of nuclear physics research in Asia by encouraging undergraduate students who are deciding their future field of study. It started in 2008 after intense discussions among scientists and officers of RIKEN and Peking University, China. Seoul National University, Korea joined the School in 2012, and Honkong University newly became a Nishina School member in this 10th School held from August 1 to 12, 2016. A photograph taken at the beginning of the School is shown in Fig. 1. In addition to the students from the three universities, high-school students from Phillips Exeter Academy, USA with their teacher participated in most of the School programs.

Fig. 1. Photograph of Nishina School 2016 participants.

The two-weeks program of the 10th School started with a welcome address by Shigeharu Kato, RIKEN's Executive Director, and the introduction of participating universities by the professors supervising the students, followed by other welcome statements by Hideto En'yo, Nishina Center Director. The school program consisted of lectures, trainings, and a nuclear reaction experiment using proton beams from the Pelletron accelerator at RIKEN Nishina Center. The lectures were given in the first week. They were on a few basic topics for research including overviews of nuclear physics and nuclear astrophysics, the function of particle accelerators, and methods of radiation measurements. Other lectures were devoted to radiation safety, important issues in paper writing and oral presentation, and issues that researchers may encounter. The subjects of training were electronic-pulse propagation and radiation detection. The detectors, electronics, and data acquisition systems to be used in the experiment in the following week were employed in the training.

The second-week program was focused on the one-day reaction experiment. The students were divided into four teams, which were in charge of four types of measurements. They evaluated the feasibility of measurements by themselves before the experiment, analyzed the data obtained in the experiments, and finally made presentations. The reaction they studied is the proton radiative capture by the ^{12}C nucleus, which is relevant to the CNO cycle hydrogen burning in stars.

Figure 2 is an example of the γ ray spectra measured with a NaI(Tl) scintillator. Proton beams with 1 MeV or 2 MeV energy bombarded a carbon target, which stopped the protons to provide a so-called thick target yield of the ^{12}C(p,γ)^{13}N reaction. Two methods were employed for resonance yield measurements: detection of "in-beam" γ rays emitted during the collision of the beam with the carbon target and measurement of ^{13}N activities by detecting positron-anihiration photons or the 511-keV γ line, known as the "activation" technique. The four teams took care of four independent measurements: "in-beam" and "activation" at the two proton energies. Within the limited time, the teams could reach the stage of extracting the capture cross sections at the two resonances in ^{13}N and comparing them with the data published in the 1970s.

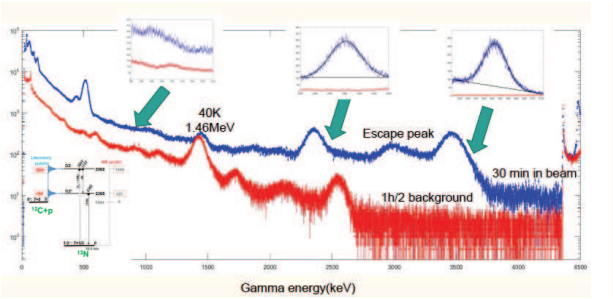

Fig. 2. An example of the γ-ray spectra. The histogram in blue color was obtained in the "in-beam" measurement for the ^{12}C(p,γ)^{13}N reaction with a 2 MeV proton beam. Two γ ray peaks corresponding to the two low-lying resonances in ^{13}N (see the inset for the level diagram) are clearly seen. The other peaks are of the natural background, which is identified in the spectrum taken without the beam (in red color).

The school was operated by the Nishina School Steering Committee headed by Hideki Ueno, in collaboration with many staff members of the Nishina Center. Takashi Kisida had been the School master for 8 years until the last School in 2015. Tohru Motobayashi suceeded him and served as the master of this 10th School in 2016.

*1 RIKEN Nishina Center

RIBF Users Meeting 2016

T. Isobe,[*1] M. Asai,[*1] P. Fallon,[*1] N. Imai,[*1] Y. Kanada-En'yo,[*1] M. Kimura,[*1] J. Lee,[*1] T. Nakamura,[*1] A. Obertelli,[*1] K. Ogata,[*1] S. Ota,[*1] and K. Yoshida[*1]

The RIBF Users Meeting 2016 was held on September 8th and 9th in 2016. This meeting aims at mutual understanding among RIBF users through discussion on the latest results obtained every year at RIBF. We, the RIBF User Group Executive Committee (UEC), organize the Users Meeting independently from RIKEN Nishina Center. While we sought help from the RIBF user liaison, the meeting was held by the RIBF user community for RIBF users. The number of participants was about 70, which is less than usual for an RIBF Users Meeting. The program mainly consists of status reports from each of the following collaborations: EURICA, SAMURAI, MRTOF, SCRIT, KISS, Super Heavy, BigRIPS, ImPACT, SUNFLOWER, SπRIT, OEDO/SHARAQ, CRIB, and R3. The details of each report were presented in the poster session held in conjunction with the get-together party on the evening of the first day. Fig. 1 shows the number of time slots for each type of presentation.

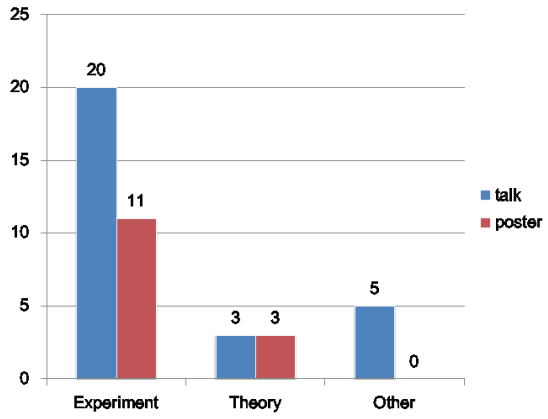

Fig. 1. Number of talks/posters presented at the Users Meeting. "Other" corresponds to the activity report, opening/closing remarks, and so on.

In addition to the report by each group, a ceremony to present the RIBF thesis award to two winners was conducted, as shown in Fig. 2, together with a special talk by the recipients. The awards honor the achievements of Dr. Kosho Minomo (Research Center for Nuclear Physics, Osaka University) and Dr. Clementine Santamaria (National Superconducting Cyclotron Laboratory, Michigan State University) for the Ph.D theses titled "Determination of deformed and halo structure of unstable nuclei by fully microscopic theory" (Kyushu University in 2013) and "Quest for new nuclear magic numbers with MINOS" (Universite Paris Sud XI in 2015), respectively. The RIBF Thesis Award is co-hosted by UEC and Nishina Center from this year. Plates for the award were newly prepared.

Fig. 2. Ceremony for RIBF Thesis award 2016. It was presented to Dr. Clementine Santamaria (2nd from left hand side) and Dr. Kosho Minomo (3rd from left hand side). Certification and plates were given to winners.

Finally, we conducted a session to discuss the post-RIBF activities. In this session, after the status report and upgrade plan of the RIBF accelerator were presented, we discussed how we will endorse the physics of exotic nuclei in Japan.

The next RIBF Users Meeting will be held at the beginning of December in 2017. As the year 2017 is the 10th year since the first experiment at RIBF, a special symposium to celebrate the 10th year of RIBF is planned.

Reference

1) https://indico2.riken.jp/indico/conferenceDisplay.py?confId=2340

*1 RIBF User Group Executive Committee

VI. ORGANIZATION AND ACTIVITIES OF RIKEN NISHINA CENTER

(Activities, Members, Publications & Presentations)

1. Organization

1.1 Organization Chart as of March 31, 2017 (End of FY2016)

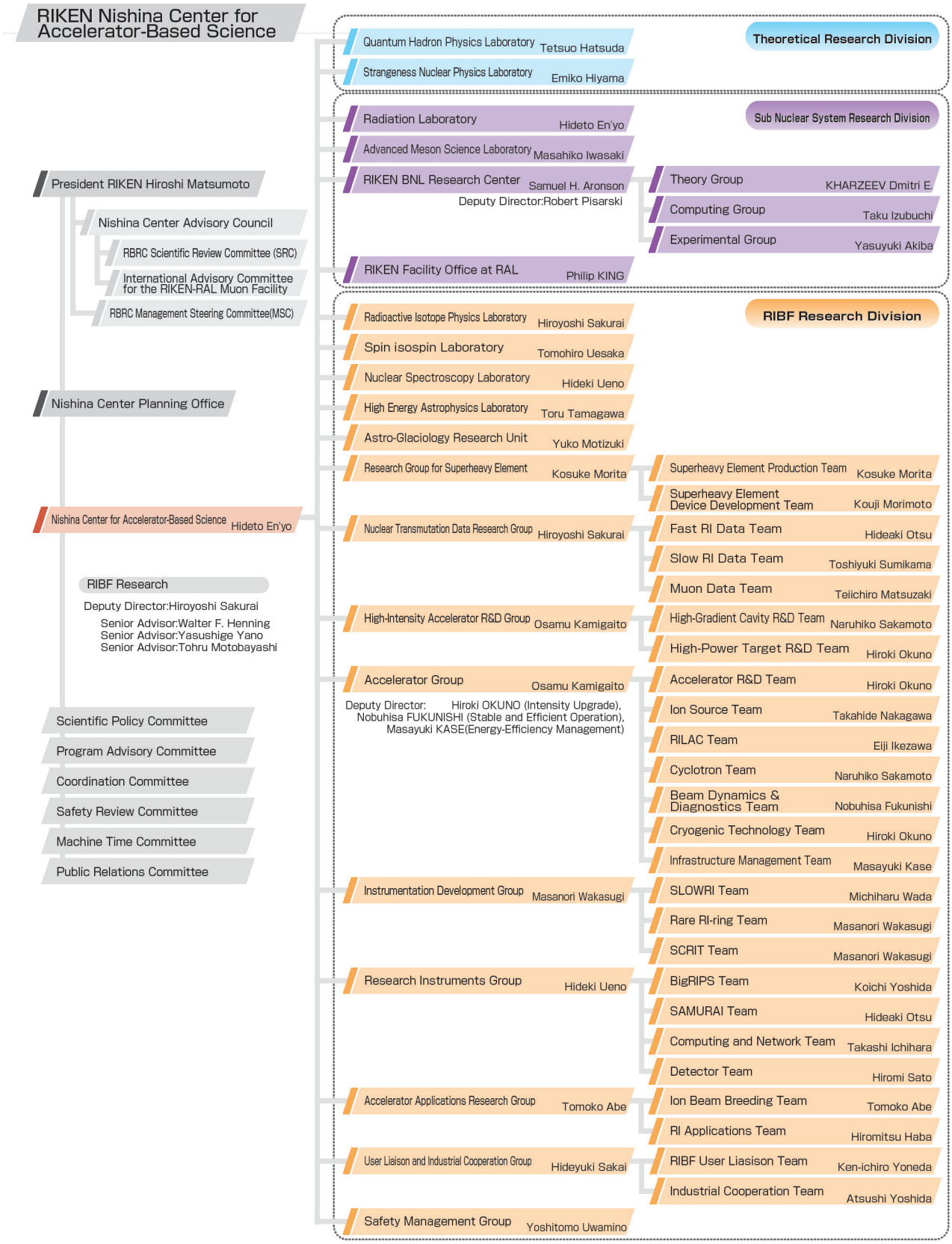

1.2 Topics in FY2016

In fiscal year 2016, the International Union of Pure and Applied Chemistry (IUPAC) officially approved the name (nihonium) and chemical symbol (Nh) proposed earlier this year for element 113 by a research group led by Group Director Kosuke Morita, Research Group for Superheavy Element. A ceremony to commemorate the naming of element 113 as “nihonium” was held at the Japan Academy in Tokyo on March 14, 2017, with His Imperial Highness the Crown Prince in attendance.

Five months operation was achieved as had been planned at the beginning of FY2016. The number of RIBF users from home and abroad was the highest ever. RIBF utilization rate exceeding 70% has been maintained.

A key development in accelerator technology was achieved by the Accelerator Group, whereby the use of new “graphene” carbon foils has enabled RIBF to reach an unprecedented, worldwide record in the intensity of 50 pnA for a 238U beam.

Year	Date	Topics in Management
2016	Apr. 1	New appointment Director of Research Instruments Group: Hideki UENO
	Sep. 1	New appointment Team Leader of Slow RI Data Team: Toshiyuki SUMIKAMA
	Oct. 31	Step down from the position of Deputy Director of RNC: Tetsuo HATSUDA
	Dec. 5	Final Report of the former Associate Chief Scientist, Takashi NAKATSUKASA
2017	Jan. 30	Research Review of the Chief Scientist, Tetsuo HATSUDA

2. Finances

As mentioned in “1.2 Administrative Topic in FY2016”, RNC executed five months of RIBF operation. A transition of the RNC budget for the past four years is shown in following graph.

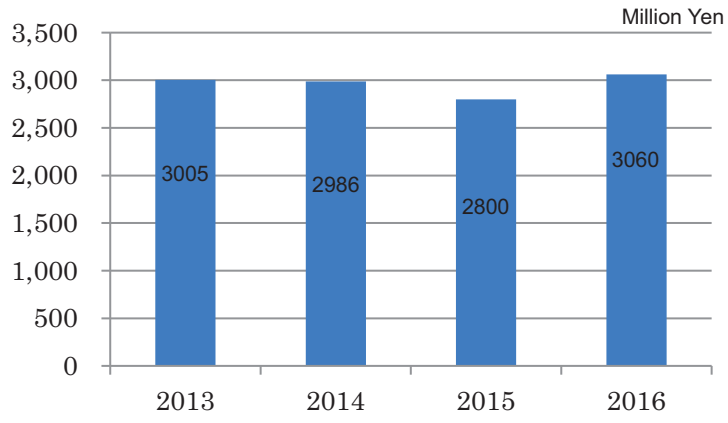

3. Staffing

At the start of FY 2016, there were 187 personnel affiliated with RNC and 376 researchers visiting RNC for research purpose. The following graphs show a breakdown of personnel into six categories as of April 1, 2016, and a transition of the number of each category.

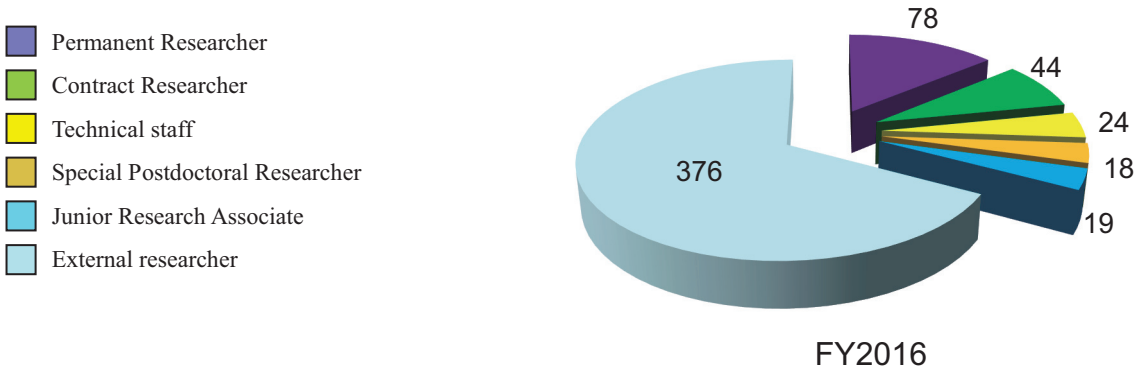

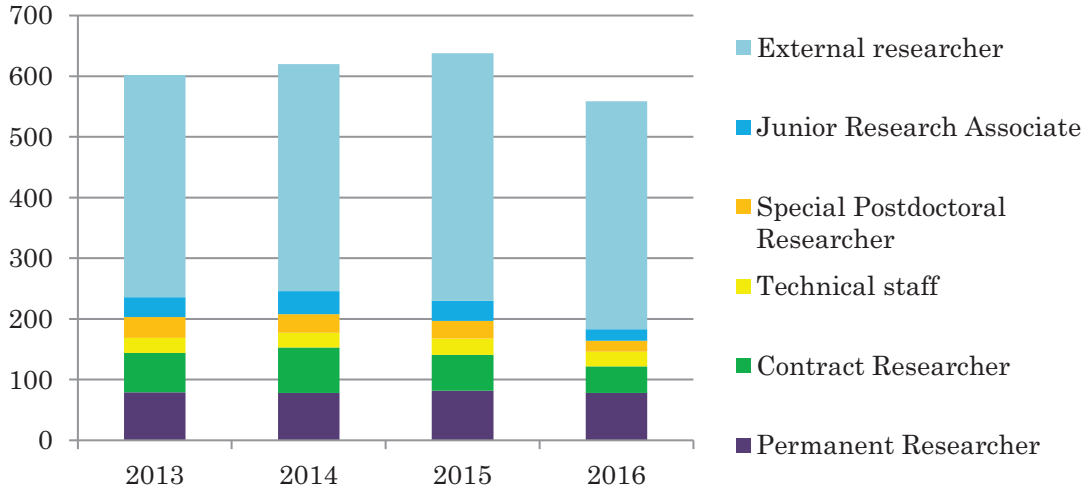

4. Research publication

The number of papers published annually from RNC is shown graphically using the data obtained from Thomson Reuters' Web of Science Documents.

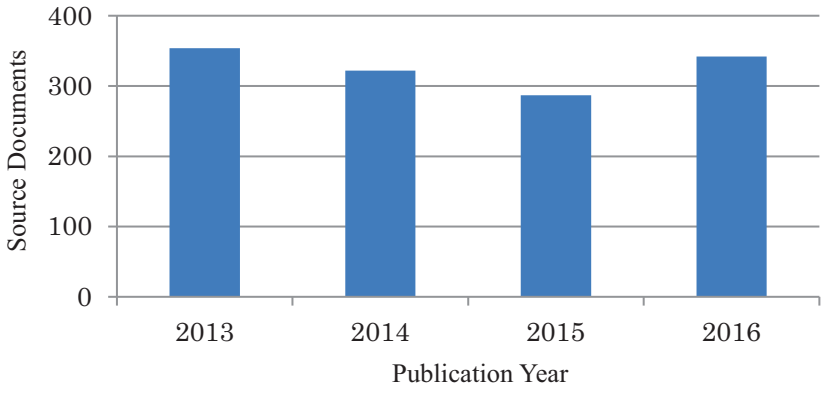

Citation analysis for the past four years

As of April 29, 2017

Indicators \ Year	2013	2014	2015	2016
Total number of papers	354	322	287	342
Total number of citations	4126	3190	1710	687
Number of papers in top 10%	59	62	50	40
Percentage of papers in top 10%	16.7	19.3	17.4	12.2
Number of papers in top 1%	8	5	3	3
Percentage of papers in top 1%	2.26	1.55	1.05	0.91

5. Management

Headed by the RNC Director Hideto En'yo, the RIKEN Nishina Center for Accelerator-Based Science (RNC) consists of:

8 Laboratories
1 Research unit
9 Groups with 25 Teams
2 overseas research center with 3 Groups

as of the latter half of FY2016. There are also three 'Partner Institutes' which conduct research in the laboratories set up in RNC.

RNC is managed by its Director who takes into consideration the majority decision of the RNC Coordination Committee. The Nishina Center Planning Office under the auspices of President of RIKEN is responsible for administrative matters of RNC.

The management of RNC is supported by the following committees:

Scientific Policy Committee
Program Advisory Committee
Safety Review Committee
RIBF Machine Time Committee
Public Relations Committee

There are also committees to support the President of RIKEN and/or the Director of RNC such as:

Nishina Center Advisory Council with two subcommittees
RBRC Scientific Review Committee (SRC) and
International Advisory Committee for the RIKEN-RAL Muon Facility
RBRC Management Steering Committee (MSC)

Nishina Center for Accelerator-based Science

Executive Members (as of March 31, 2017)

Hideto EN'YO	Director RNC; Chief Scientist, Director of Radiation Laboratory
Hiroyoshi SAKURAI	Deputy Director (RIBF Research), RNC; Chief Scientist, Director of Radioactive Isotope Physics Laboratory; Group Director, Nuclear Transmutation Data Research Group
Walter F. HENNING	Senior Advisor
Yasushige YANO	Senior Advisor
Tohru MOTOBAYASHI	Senior Advisor
Minami IMANISHI	Assistant

RNC Coordination Committee

The following subjects relevant to the RNC management are deliberated under the chairmanship of the RNC Director:

Establishment of the new organization or reorganization in RNC
Personnel management of RNC researchers
Research themes and research budget
Approval of the Partner Institutes
Evaluation of the management of RNC and the response to the recommendations by external evaluation

The RNC Coordination Committee is held monthly.

Members (as of March 31, 2017)

Hideto EN'YO	Director, RNC; Chief Scientist, Radiation Laboratory
Hiroyoshi SAKURAI	Deputy Director, RNC; Chief Scientist, Radioactive Isotope Physics Laboratory; Group Director, Nuclear Transmutation Data Research Group
Walter F. HENNING	Senior Advisor, RNC
Yasushige YANO	Senior Advisor, RNC
Tohru MOTOBAYASHI	Senior Advisor, RNC
Tetsuo HATSUDA	Chief Scientist, Quantum Hadron Physics Laboratory
Masahiko IWASAKI	Chief Scientist, Advanced Meson Science Laboratory
Tomohiro UESAKA	Chief Scientist, Spin isospin Laboratory
Hideki UENO	Chief Scientist, Nuclear Spectroscopy Laboratory; Group Director, Research Instruments Group
Toru TAMAGAWA	Associate Chief Scientist, High Energy Astrophysics Laboratory
Emiko HIYAMA	Associate Chief Scientist, Strangeness Nuclear Physics Laboratory
Kosuke MORITA	Group Director, Research Group for Superheavy Element; Team Leader, Superheavy Element Production Team
Osamu KAMIGAITO	Group Director, Accelerator Group; Group Director, High-Intensity Accelerator R&D Group
Hideyuki SAKAI	Group Director, User Liaison and Industrial Cooperation Group
Hiroki OKUNO	Deputy Group Director, Accelerator Group; Team Leader, Accelerator R&D Team; Team Leader, Cryogenic Technology Team; Team Leader, High-Power Target R&D Team
Nobuhisa FUKUNISHI	Deputy Group Director, Accelerator Group; Team Leader, Beam Dynamics & Diagnostics Team
Masayuki KASE	Deputy Group Director, Accelerator Group; Team Leader, Infrastructure Management Team
Tomoko ABE	Group Director, Accelerator Applications Research Group; Team Leader, Ion Beam Breeding Team
Yoshitomo UWAMINO	Group Director, Safety Management Group
Toshiyuki KUBO	Group Director, Research Instruments Group; Team Leader, Detector Team
Masanori WAKASUGI	Group Director, Instrumentation Development Group; Team Leader, Rare RI-ring Team; Team Leader, SCRIT Team
Eiji IKEZAWA	Team Leader, RILAC Team
Takashi ICHIHARA	Team Leader, Computing and Network Team; Vice Chief Scientist, Radioactive Isotope Physics Laboratory
Hideaki OTSU	Team Leader, SAMURAI Team; Team Leader, Fast RI Data Team
Naruhiko SAKAMOTO	Team Leader, Cyclotron Team; Team Leader, High-Gradient Cavity R&D Team
Hiromi SATO	Team Leader, Detector Team
Toshiyuki SUMIKAMA	Team Leader, Slow RI Data Team
Takahide NAKAGAWA	Team Leader, Ion Source Team
Hiromitsu HABA	Team Leader, RI Applications Team
Teiichiro MATSUZAKI	Team Leader, Muon Data Team
Koji MORIMOTO	Team Leader, Superheavy Element Device Development Team
Atsushi YOSHIDA	Team Leader, Industrial Cooperation Team
Koichi YOSHIDA	Team Leader, BigRIPS Team
Ken-ichiro YONEDA	Team Leader, RIBF User Liasison Team
Michiharu WADA	Team Leader, SLOWRI Team
Yasuyuki AKIBA	Vice Chief Scientist, Radiation Laboratory; Group Leader, Experimental Group, RIKEN BNL Research Center
Katsuhiko ISHIDA	Vice Chief Scientist, Advanced Meson Science Laboratory
Tsukasa TADA	Vice Chief Scientist, Quantum Hadron Physics Laboratory
Yuko MOTIZUKI	Research Unit Leader, Astro-Glaciology Research Unit
Kanenobu TANAKA	Deputy Group Director, Safety Management Group
Yasushi WATANABE	Deputy Team Leader, RIBF User Liaison Team
Noriko SHIOMITSU	Director, Nishina Center Planning Office

Nishina Center Planning Office

The Nishina Center Planning Office is responsible for the following issues:

- Planning and coordination of RNC's research program and system
- Planning and management of RNC's use of budget
- Public relations activities

Members (as of March 31, 2017)

Noriko SHIOMITSU	Director, Nishina Center Planning Office
Kazunori MABUCHI	Manager, Nishina Center Planning Office; Administration Manager, RBRC; Administration Manager, RIKEN Facility Office at RAL
Keiko IWANO	Deputy Manager, Nishina Center Planning Office
Yasutaka AKAI	Chief, Nishina Center Planning Office; Deputy Administration Manager, RBRC
Yukari ONISHI	Chief, Nishina Center Planning Office
Kumiko SUGITA	Special Administrative Employee
Yuko OKADA	Task-Specific Employee
Aiko KAWAMURA	Task-Specific Employee
Masatoshi MORIYAMA	Consultant
Rie KUWANA	Temporary Staff

Scientific Policy Committee

The Scientific Policy Committee deliberates on the following issues:
Research measures and policies of RNC
Administration of research facilities under RNC's management
The Committee members are selected among professionals within and outside RNC. The members were not chosen nor the Committee held in FY2016.

Program Advisory Committee

The Program Advisory Committee reviews experimental proposals submitted by researchers and reports the approval/disapproval of the proposals to the RNC Director. The Committee also reports to the RNC Director the available days of operation at RIBF or the Muon Facility at RAL allocated to researchers.

The Committee is divided into three categories according to the research field.
(1) Nuclear Physics Experiments at RIBF (NP-PAC): academic research in nuclear physics
(2) Materials and Life Science Researches at RNC (ML-PAC): academic research in materials science and life science
(3) Industrial Program Advisory Committee (In-PAC): non-academic research

Program Advisory Committee for Nuclear Physics Experiments at RI Beam Factory (NP-PAC)

The 17th NP-PAC was held on December 1-3, 2016 at RIBF.
Members (as of March 31, 2017)

Bradley. M.SHERRILL (Chair)	Prof., Director, Michigan State University
Andrei ANDREYEV	Prof., The University of York
Angela BRACCO	Prof., The Istituto Nazionale di Fisica Nucleare
Ikuko Hamamoto	Prof. Emeritus, The Lund University, Senior Visiting Scientist, RNC
Hironori Iwasaki	Associate Prof., Michigan State University
Walter D. LOVELAND	Prof., Oregon State University
Satoshi Nakamura	Prof., Tohoku University
Thomas NILSSON	Prof., Chalmers University of Technology
Kazuyuki Ogata	Associate Prof., Osaka University
Thomas Rauscher	University of Basel
Haik Simon	GSI
Olivier Sorlin	GANIL(Grand Accélérateur National d'Ions Lourds)
Atsushi TAMII	Associate Prof., OsakaUniversity
Yutaka UTSUNO	Senior Scientist, JAEA
Piet Van Duppen	Prof., University of Leuven (K.U.Leuven)
Yuhu Zhang	Institute of Modern Physics, Chinese Academy of Sciences

Program Advisory Committee for Materials and Life Science Researches at RIKEN Nishina Center (ML-PAC)

The 13th ML-PAC was held on January 19-20, 2017 at RIBF.
Members (as of March 31, 2017)

Adrian HILLIER (Chair)	ISIS, RAL
Toshiyuki AZUMA	Chief Scientist, RIKEN
Ryosuke KADONO	Prof., Institute of Materials Structure Science, KEK
Atsushi KAWAMOTO	Prof., Hokkaido University
Norimichi KOJIMA	Full Time Research Fellow, Toyota Physical and Chemical Research Institute
Kenya KUBO	Prof., International Christian University
Philippe MENDELS	Prof., Universite Paris-SUD
Atsushi SHINOHARA	Prof., Osaka University
Shukri SULAIMAN	Prof., Universiti Sains Malaysia
Hiroyuki YAMASE	Senior Researcher, National Institute for Materials Science
Shigeo YOSHIDA	Research Consultant, RIKEN
Xu-Guang ZHENG	Prof., Saga University

Industrial Program Advisory Committee (In-PAC)

The 6th In-PAC was held on January 13, 2017 at RNC.
Members (as of March 31, 2017)

Akihiro IWASE (Chair)	Prof., Osaka Prefecture University
Toshiyuki AZUMA	Chief Scientist, RIKEN
Kenya KUBO	Prof., International Christian University
Hitoshi NAKAGAWA	Central Research Laboratory, Hamamatsu Photonics K.K.
Nobuhiko NISHIDA	Full Time Research fellow, Toyota Physical and Chemical Research Institute
Toshinori MITSUMOTO	Chief Engineer, Sumitomo Heavy Industries, Ltd

Safety Review Committee

The Safety Review Committee is composed of two sub committees, the Safety Review Committee for Accelerator Experiments and the Hot-Lab Safety Review Committee. These Committees review the safety regarding the usage of radiation generating equipment based on the proposal submitted to the RNC Director from the spokesperson of the approved experiment.

Safety Review Committee for Accelerator Experiments

Members (as of March 31, 2017)

Hiromi SATO (Chair)	Team Leader, Detector Team
Kouji MORIMOTO	Team Leader, Superheavy Element Device Development Team
Eiji IKEZAWA	Team Leader, RILAC Team
Hiromitsu HABA	Team Leader, RI Applications Team
Shinichiro MICHIMASA	Assistant Prof., Center for Nuclear Study, University of Tokyo
Hidetoshi YAMAGUCHI	Lecturer, Center for Nuclear Study, University of Tokyo
Hiroshi WATANABE	Lecturer, Radioactive Nuclear Beam Group, IPNS, KEK
Atsushi YOSHIDA	Team Leader, Industrial Cooperation Team
Koichi YOSHIDA	Team Leader, BigRIPS Team
Naoki FUKUDA	Nishina Center Research Scientist, BigRIPS Team
Naruhiko SAKAMOTO	Team Leader, Cyclotron Team
Daisuke SUZUKI	Research Scientist, Radioactive Isotope Physics Laboratory
Juzo ZENIHIRO	Research Scientist, Spin Isospin Laboratory
Yuichi ICHIKAWA	Research Scientist, Nuclear Spectroscopy Laboratory

Ex officio members

Yoshitomo UWAMINO	Group Director, Safety Management Group
Kanenobu TANAKA	Deputy Group Director, Management Group
Hisao SAKAMOTO	Nishina Center Technical Scientist, Safety Management Group

Hot-Lab Safety Review Committee

Members (as of March 31, 2017)

Masako IZUMI (Chair)	Senior Research Scientist, Radiation Biology Team
Yoshitomo UWAMINO	Group Director, Safety Management Group
Hisao SAKAMOTO	Nishina Center Technical Scientist, Safety Management Group
Hiroki MUKAI	Assigned Employee, Safety Management Group
Kanenobu TANAKA	Deputy Group Director, Safety Management Group
Hiromitsu HABA	Team Leader, RI Applications Team

RIBF Machine Time Committee

Upon request of the RNC Director, the RIBF Machine Time Committee deliberates on the machine time schedule of RIBF, and reports the results to him.

Members (as of March 31, 2017)

Hideyuki SAKAI (Chair)	Group Director, User Liaison and Industrial Cooperation Group
Tomoko ABE	Group Director, Accelerator Applications Research Group; Team Leader, Ion Beam Breeding Team
Nobuhisa FUKUNISHI	Deputy Group Director, Accelerator Group; Team Leader, Beam Dynamics & Diagnostics Team
Osamu KAMIGAITO	Group Director, Accelerator Group; Group Director, High-Intensity Accelerator R&D Group
Masayuki KASE	Deputy Group Director, Accelerator Group
Kouji MORIMOTO	Team Leader, Superheavy Element Research Device Development Team
Hiroki OKUNO	Deputy Group Director, Accelerator Group; Team Leader, Accelerator R&D Team; Team Leader, Cryogenic Technology Team; Team Leader, High-Power Target R&D Team
Hiroyoshi SAKURAI	Deputy Director, RNC; Chief Scientist, Radioactive Isotope Physics Laboratory; Group Director, Nuclear Transmutation Data Research Group
Hideki UENO	Chief Scientist, Nuclear Spectroscopy Laboratory; Group Director, Research Instruments Group
Tomohiro UESAKA	Chief Scientist, Spin Isospin Laboratory
Yoshitomo UWAMINO	Group Director, Safety Management Group
Masanori WAKASUGI	Group Director, Instrumentation Development Group; Team Leader, Rare RI-ring Team; Team Leader, SCRIT Team
Ken-ichiro YONEDA	Team Leader, RIBF User Liasion Team

External members

Susumu SHIMOURA	Professor, Center for Nuclear Study, University of Tokyo
Hidetoshi YAMAGUCHI	Lecturer, Center for Nuclear Study, University of Tokyo
Hiroari MIYATAKE	Professor, Radioactive Nuclear Beam Group, IPNS, KEK

Observers

Hideto EN'YO	Director, RNC; Chief Scientist, Radiation Laboratory
Nobuaki IMAI	Chair, RIBF-UEC, Associate Prof. Center for Nuclear Study, University of Tokyo
Hiromitsu HABA	Team Leader, RI Applications Team
Kosuke MORITA	Group Director, Research Group for Superheavy Element; Team Leader, Superheavy Element Production Team
Tohru MOTOBAYASHI	Senior Advisor, RNC
Koichi YOSHIDA	Team Leader, BigRIPS Team
Kanenobu TANAKA	Deputy Group Director, Safety Management Group
Hideaki OTSU	Team Leader, Fast RI Data Team
Kazunori MABUCHI	Manager, Nishina Center Planning Office

Public Relations Committee

Upon request of the RNC Director, the Public Relations Committee deliberates and coordinates the following matters:
(1) Creating public relations system for RNC
(2) Prioritization of the public relations activities for RNC
(3) Other general and important matters concerning the public relations of RNC

Members (as of March 31, 2017)

Noriko SHIOMITSU (Chair)	Director, Nishina Center Planning Office
Hiroyoshi SAKURAI	Deputy Director, RNC; Chief Scientist, Radioactive Isotope Physics Laboratory; Group Director, Nuclear Transmutation Data Research Group
Tetsuo HATSUDA	Deputy Director, RNC; Chief Scientist, Quantum Hadron Physics Laboratory
Tohru MOTOBAYASHI	Senior Advisor
Walter F. HENNING	Senior Advisor
Yasushige YANO	Senior Advisor
Masahiko IWASAKI	Chief Scientist, Advanced Meson Science Laboratory
Tomohiro UESAKA	Chief Scientist, Spin isospin Laboratory
Hideki UENO	Chief Scientist, Nuclear Spectroscopy Laboratory; Group Director, Research Instruments Group
Toru TAMAGAWA	Associate Chief Scientist, High Energy Astrophysics Laboratory
Emiko HIYAMA	Associate Chief Scientist, Strangeness Nuclear Physics Laboratory
Kosuke MORITA	Group Director, Research Group for Superheavy Element; Team Leader, Superheavy Element Production Team
Osamu KAMIGAITO	Group Director, Accelerator Group; Group Director, High-Intensity Accelerator R&D Group
Hideyuki SAKAI	Group Director, User Liaison and Industrial Cooperation Group

RBRC Management Steering Committee (MSC)

RBRC MSC is set up according to the Memorandum of Understanding between RIKEN and BNL concerning the collaboration on the Spin Physics Program at the Relativistic Heavy Ion Collider (RHIC). The 22nd MSC was held on June 3, 2016 at Brookhaven National Laboratory.

Members (as of March 31, 2017)

Yoichiro MATSUMOTO	Executive Director, RIKEN
Shoji NAGAMIYA	Science Advisor, RIKEN
Hideto EN'YO	Director, RNC
David LISSAUER	Deputy Chair, Physics Department, BNL
Berndt MUELLER	Associate Laboratory Director for Nuclear and Particle Physics, BNL
Satoshi OZAKI	Senior Advisor, BNL

Nishina Center Advisory Council (NCAC)

NCAC 2016 is the 4th AC meeting since the establishment of RNC which promotes RIKEN's accelerator based science including the RIKEN BNL Research Center and the RIKEN-RAL Muon Facility. NCAC has two sub-councils for the RBRC and the RAL Muon Facility respectively. The 1st NCAC was held in January, 2009. The 2nd NCAC was held in May, 2011. The 3rd NCAC was held in July, 2014.

The mission of NCAC 2016 is set by the Terms of Reference presented by President Matsumoto based on the Initiative for Scientific Excellence and the fundamental issues about research activities and research administration. NCAC submits its report to the President Matsumoto, and to the RNC Director if necessary.

The members of NCAC are recommended by the RNC Director to the President of RIKEN from among highly knowledgeable individuals and experts worldwide.

Members (as of March 31, 2017)

Sydney GALES (Chair)	Scientific Director, Research IPN Orsay CNRS, Scientific Director, ELI-N
Robert V.F. JANSSENS	Division Director, Argonne National Laboratory (ANL)
Jochen WAMBACH	Director, ECT*
Witold NAZAREWICZ	Prof., Michigan State University
Kinichi IMAI	Prof. Emeritus, Kyoto University
Richard G. MILNER	Prof., MIT
Angella BRACCO	Prof., The Istituto Nazionale di Fisica Nucleare
Reiner KRÜCKEN	Deputy Director, TRIUMF
Hirokazu TAMURA	Prof., Tohoku University
Tokushi SHIBATA	Adviser, Chiyoda Technol Corporation, Oarai Research Laboratory
Elvezio MORENYONI	Prof., Paul Scherrer Institut
Yoshitaka ITOW	Prof., Nagoya University
Lia MERMINGA	Accelerator Directorate, SLAC National Accelerator Laboratory
Akira YAMAMOTO	Prof. Emeritus, High Energy Accelerator Research Organization, KEK
Hidenori TAKAGI	Prof., Max-Planck Institute for Solid State Research

RBRC Scientific Review Committee (SRC)

Members (as of March 31, 2017)

Richard MILNER (Chair)	Prof., MIT
Shinya AOKI	Prof., Yukawa Institute for Theoretical Physics, Kyoto University
Alfred MUELLER	Prof., Columbia University
Albert De ROECK	Prof., CERN
Xiandong JI	Prof., University of Maryland
Julia VELKOVSKA	Prof., Vanderbilt University

International Advisory Committee for the RIKEN-RAL Muon Facility (RAL-IAC)

Members (as of March 31, 2017)

Andrew D TAYLOR (Chair)	Executive Director, STFC National Laboratories
Jean-Michel POUTISSOU	Senior research scientist Emeritus, TRIUMF
Klaus P. JUNGMANN	Prof., University of Groningen
Roberto De RENZI	Prof., University of Parma
Yasuyuki MATSUDA	Assoc. Prof., the University of Tokyo
Jun SUGIYAMA	Principal Research Scientist, Toyota Central R&D Labs., INC

6. International Collaboration

Country	Partner Institute	Objects	RNC contact person
Austria	Stefan Meyer Institute for Subatomic Physics	Experimental and theoretical hadron physics, especially in exotic hadronic atoms and meson and baryon nuclear bound states	Masahiko IWASAKI, Chief Scientist, Director of Advanced Meson Science Laboratory
China	China Nuclear Physics Society	Creation of the council for China -Japan research collaboration on nuclear physics	Hiroyoshi SAKURAI, Deputy Director, Chief Scientist, Radioactive Isotope Physics Laboratory
	Peking University	Nuclear Science	Hiroyoshi SAKURAI, Deputy Director, Chief Scientist, Radioactive Isotope Physics Laboratory
	Institute of Modern Physics, Chinese Academy of Science	Physics of heavy ions	Hiroyoshi SAKURAI, Deputy Director, Chief Scientist, Radioactive Isotope Physics Laboratory
	School of Nuclear Science and Technology, Lanzhou University	Framework	Yue MA, Advanced Meson Science Laboratory
	School of Physics, Nanjing University	Framework	Emiko HIYAMA, Associate chief scientist, Strangeness Nuclear Physics Laboratory
	Department of Physics, Faculty of Science, The Univ. of Hong Kong	Experimental and educational research collaboration in the area of experimental nuclear physics	Hiroyoshi Sakurai, Deputy Director, Chief Scientist, Radioactive Isotope Physics Laboratory
	School of physics, Nankai University	Framework	
Finland	University of Jyvaskyla	Basic nuclear physics and related instrumentation	Michiharu WADA, Team Leader, SLOWRI Team

Country	Partner Institute	Objects	RNC contact person
France	National Institute of Nuclear Physics and Particle Physics (IN2P3)	Physics of heavy ions	Tohru MOTOBAYASHI, RIBF synergetic-use coordinator
	CNRS, CEA,GANIL, Université Paris Sud, etc.	Creation of an International Associated Laboratory (LIA) French-Japanese International Associated Laboratory for Nuclear Structure Problems	Tohru MOTOBAYASHI, RIBF synergetic-use coordinator
	CEA-DSM	The use of MINOS device at RIKEN	Tomohiro UESAKA, Chief Scientist, Spin Isospin Laboratory
	SIMEM Graduate School, Department of Physics, Caen University	Framework	Tomohiro UESAKA, Chief Scientist, Spin Isospin Laboratory
	Centre National de la Rocherche Scientifique (CSRS) Commissariat A L'Energie Atomique Et Aux Energies Alternatives (CEA)	Research Collaboration in EXPAND (Exploration Across the Neutron Dripline) project	Tomohiro UESAKA, Chief Scientist, Spin Isospin Laboratory
Germany	Technische Universität München	Nuclear physics, hadron physics, nuclear astrophysics	Emiko HIYAMA, Associate chief scientist, Strangeness Nuclear Physics Laboratory
	GSI	Physics of heavey ions and accelerator	Hiroyoshi SAKURAI, Deputy Director, Chief Scientist, Radioactive Isotope Physics Laboratory
	GSI and Reactions with Relativistic Radioactive Beam Collaboration (R3B)	The use of NeuLAND device at RIBF	Tomohiro Uesaka, Chief Scientist, Spin Isospin Laboratory
	Department of Physics, Technische Universität Darmstadt	Framework	Emiko Hiyama, Associate chief scientist, Strangeness Nuclear Physics Laboratory
	European Gamma-Ray Spectroscopy Pool Owners Committee	The use of Euroball ditector at RIKEN	Shunji NISHIMURA, Radioactive Isotope Physics Laboratory
Hungary	The Institute of Nuclear Research of the Hungarian Academy of Sciences (ATOMKI)	Nuclear physics, Atomic Physics	Tomohiro UESAKA, Chief Scientist, Spin Isospin Laboratory
Indonesia	ITB, UNPAD, ITS, UGM, UI	Material science using muons at the RIKEN-RAL muon facility	Isao WATANABE, Advanced Meson Science Laboratoy
	Universitas Hasanuddin	Agricultural science and related fields involving heavy-ion beam mutagenesis using Indonesian crops	Tomoko ABE, Group Director, Accelerator Applications Research Group
Italy	Applied Physics Division, National Institute for New Technologies, Energy and Environment (ENEA)	Framework	Tohru MOTOBAYASHI, RIBF synergetic-use coordinator
	European Center for Theoretical Studies in Nuclear Physics and Related Areas (ECT*)	Theoretical physics	Tetsuo HATSUDA, Deputy Director, Chief Scientist, Quantum Hadron Physics Laboratory
Korea	Seoul National University	Nishina School	Hiroyoshi SAKURAI, Deputy Director, Chief Scientist, Radioactive Isotope Physics Laboratory
	Institute of Basic Science, Rare Isotope Science Project	Rare ion accelerator and related fields	Hiroyoshi SAKURAI, Shunji NISHIMURA
	Department of Physics, Kyungpook National University	Framework	Tomohiro UESAKA, Chief Scientist, Spin Isospin Laboratory
	College of Science, Yonsei University	Framework	Tomohiro UESAKA, Chief Scientist, Spin Isospin Laboratory
	Department of Physics, Korea University	Framework	Yuji GOTO, Radiation Laboratory
	College of Natural Science, Ewha Women's University	Framework	Tomohiro UESAKA, Chief Scientist, Spin Isospin Laboratory
	College of Natural Sciences, INHA Univ.	Framework	Emiko Hiyama, Associate chief scientist, Strangeness Nuclear Physics Laboratory
Malaysia	Universiti Sains Malaysia	Muon Science	Isao WATANABE, Advanced Meson Science Laboratoy
Poland	the Henryk Niewodniczanski Institute of Nuclear Physics, Polish Academy of Sciences(IFJ PAN)	Framework	Hiroyoshi SAKURAI, Deputy Director, Chief Scientist, Radioactive Isotope Physics Laboratory
Romania	"Horia Hulubei" National Institute of Physics and Nuclear Engineering Bucharest-Magurele, Romania	Framework	Tomohiro UESAKA, Chief Scientist, Spin Isospin Laboratory
Russia	Joint Institute for Nuclear Research (JINR)	Framework	Tomohiro UESAKA, Chief Scientist, Spin Isospin Laboratory
	Russian Research Center "Kurchatov Institute"	Framework	Hiroyoshi SAKURAI, Tomohiro UESAKA, Osamu KAMIGAITO, Masanori WAKASUGI
Switzerland	Paul Scherrer Institute	Improve the performance and reliability of accelerator systems	Osamu KAMIGAITO, Director, Chief Scientist, Accelerator Group
	CERN	RD-51:R&D programme for micro-pattern gas detectors (MPGD)	Satoshi YOKKAICHI, Senior Research Scientist, Radiation Laboratory
	CERN	Collaboration in the ALICE Experiment as an Associate Member	Satoshi YOKKAICHI, Senior Research Scientist, Radiation Laboratory
UK	The Science and Technology Facilities Council	Muon science using the ISIS Facility at the Rutherford Appleton Laboratory	Philip KING, Director of RIKEN-RAL muon facility
	University of Surrey	Theoretical physics	Tetsuo HATSUDA, Deputy Director, Chief Scientist, Quantum Hadron Physics Laboratory

Country	Partner Institute	Objects	RNC contact person
USA	BNL	The Spin Physics Program at the Relativistic Heavy Ion Collider(RHIC)	Hideto EN'YO, Director of RNC
	Columbia University	The development of QCDCQ	Taku IZUBUCHI, Group Leader, Computing Group, RBRC
	Michigan State University	Comprehensive The use of TPC(Time Projection Chamber)	Tomohiro Uesaka, Chief Scientist, Spin Isospin Laboratory Hiroyoshi Sakurai, Deputy Director, Chief Scientist, Radioactive Isotope Physics Laboratory & Tadaaki Isobe, Radioactive Isotope Physics Laboratory
Vietnam	Vietnam Atomic Energy Commission	Framework	Tohru MOTOBAYASHI, RIBF synergetic-use coordinator
	Institute of Physics, Vietnam Academy of Science and Technology	Framework	Hiroyoshi SAKURAI, Deputy Director, Chief Scientist, Radioactive Isotope Physics Laboratory

7. Awards

Awardee, Laboratory / Team	Award	Organization	Date
Kosuke Morita, Group Director, Research Group for Superheavey Element	The Commendation for Science and Technology by the Minister of Education, Culture, Sports, Science and Technology for FY2016	Science and Technology by the Minister of Education, Culture, Sports, Science and Technology	Apr. 20
Kosuke Morita, Group Director, Research Group for Superheavey Element	The Japan Academy Prize	The Japan Academy	June 5
Tadashi Fujinawa, Research Consultant, Accelerator Group	The 12th PASJ Award for Significant Contributions	Particle Accelerator Society of Japan	Aug. 9
Yoshitaka Yamaguchi, Nishina Center Research Scientist, Rare RI-Ring Team	The 12th PASJ Award for Technical Contributions	Particle Accelerator Society of Japan	Aug. 9
Shinya Yanou, Technical Staff , RI Application Team	The Young Scientist Award	The Japan Society of Nuclear and Radiochemical Sciences	Sep. 12
Liang Haozhao, Research Scientist, Quantum Hadron Physics Laboratory	The International Union of Pure and Applied Physics (IUPAP) Young Scientist Prize 2016	International Union of Pure and Applied Physics (IUPAP)	Sep. 14
Kosuke Morita, Group Director, Research Group for Superheavey Element	The Oita Godo Shimbun Special Culture Award	The Oita Godo Shimbun	Nov. 13
Kosuke Morita, Group Director, Research Group for Superheavey Element	The Best Team of the Year 2016	The Best Team of the Year	Nov. 16
Yoshimasa Hidaka, Senior Research Scientist, Quantum Hadron Physics Laboratory	The 31st Nishinomiya-Yukawa Memorial Prize	Nishinomiya City	Dec. 3
Kosuke Morita, Group Director, Research Group for Superheavey Element	The 2016 Asahi Prize	The Asahi Shimbun Company	Jan. 30
Kosuke Morita, Group Director, Research Group for Superheavey Element	The Sai-no-Kuni Academic and Cultural Achievement Award	Saitama Prefecture	Jan. 31
Takahide Nakagawa, Team Leader, Ion Source Team	The 2016 Suwa Award	The Foundation for High Energy Accelerator Science	Feb. 14
Yuko Motizuki, Research Unit Leader, the Astro-Glaciology Research Unit	The 4th Toshiko Yuasa Prize	Ochanomizu University with the cooperation of the High Energy Accelerator Research Organization (KEK)	Feb. 24
Kosuke Morita, Group Director, Research Group for Superheavey Element	The Special Commendation for Outstanding Paper Award of the Physical Society of Japan	The Physical Society of Japan	Mar. 19

8. Brief overview of the RI Beam Factory

Intensity of Primary Beams

Achieved beam intensities (as of March 2017)

^{238}U	49 pnA (345 MeV/u, Oct. 2015)
^{124}Xe	102 pnA (345 MeV/u, Apr. 2016)
^{86}Kr	30 pnA (345 MeV/u, Nov. 2007)
^{78}Kr	486 pnA (345 MeV/u, May. 2015)
^{70}Zn	123 pnA (345 MeV/u, Jun. 2014)
^{48}Ca	730 pnA (345 MeV/u, Nov. 2016)
^{18}O	1000 pnA (345 MeV/u, Jun. 2010)
^{14}N	400 pnA (250 MeV/u, Oct. 2010)
^{4}He	1000 pnA (250 MeV/u, Oct. 2009)
d	1000 pnA (250 MeV/u, Oct. 2010)
pol. d	120 pnA, P~80% (250 MeV/u, May. 2015)

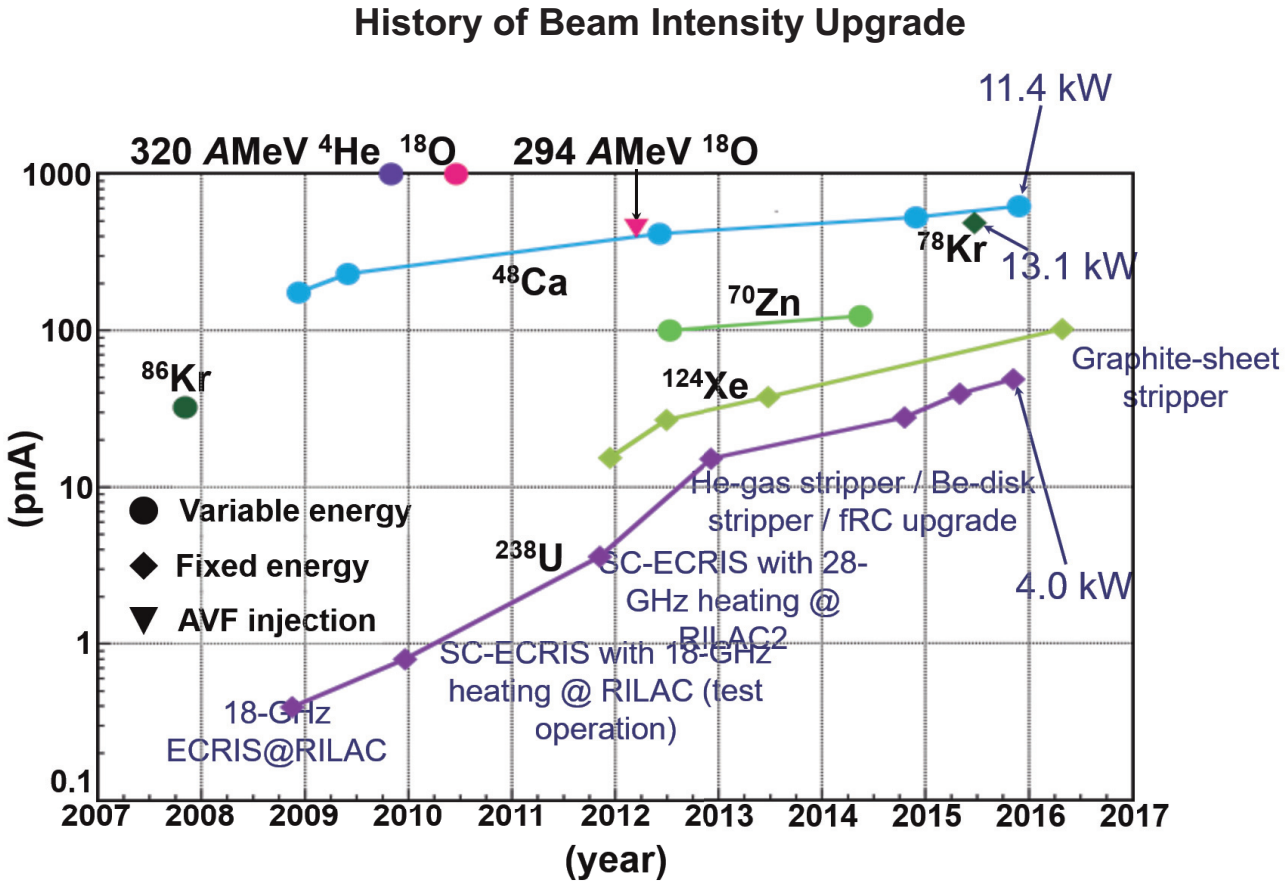

Total beam time for experiments

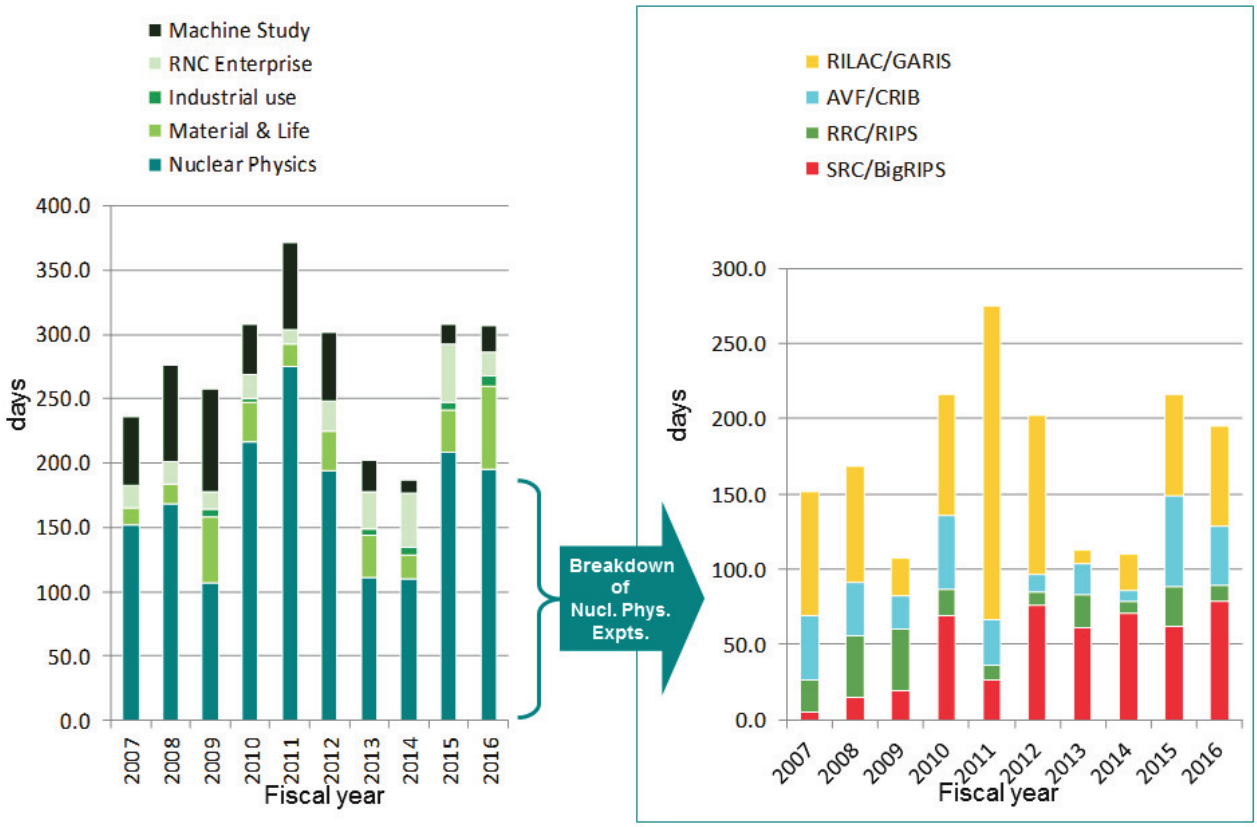

Total beam time allocated to BigRIPS experiments

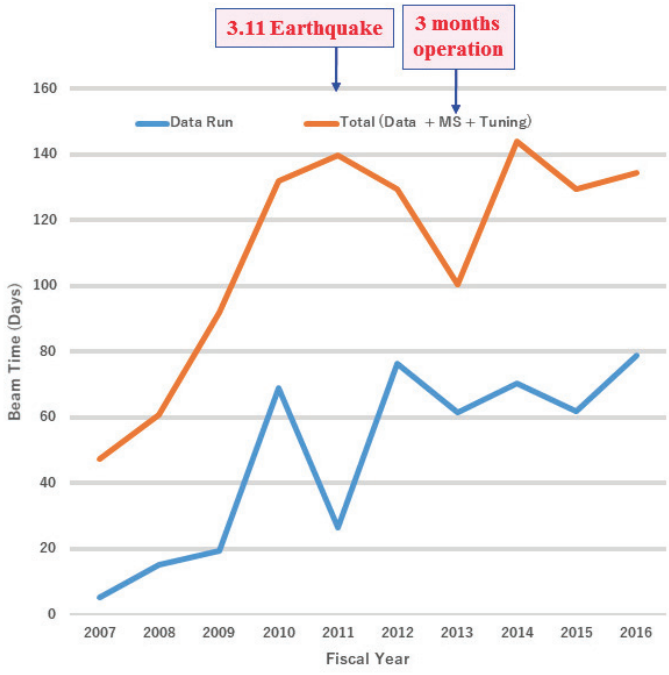

Theoretical Research Division
Quantum Hadron Physics Laboratory

1. Abstract

Atomic nuclei are made of protons and neutrons bound by the exchange of pion and other mesons. Also, protons and neutrons are made of quarks bound by the exchange of gluons. These strong interactions are governed by the non-Abelian gauge theory called the quantum chromodynamics (QCD). On the basis of theoretical and numerical analyses of QCD, we study the interactions between the nucleons, properties of the dense quark matter realized at the center of neutron stars, and properties of the hot quark-gluon plasma realized in the early Universe. Strong correlations common in QCD and cold atoms are also studied theoretically to unravel the universal features of the strongly interacting many-body systems. Developing perturbative and non-perturbative techniques in quantum field theory and string theory are of great importance not only to solve gauge theories such as QED and QCD, but also to find the theories beyond the standard model of elementary particles. Various theoretical approaches along this line have been attempted.

2. Major Research Subjects

(1) Perturbative and non-perturbative methods in quantum field theories
(2) Theory of spontaneous symmetry breaking
(3) Lattice gauge theory
(4) QCD under extreme conditions
(5) Nuclear and atomic many-body problems

3. Summary of Research Activity

(1) Perturbative and non-perturbative methods in quantum field theories

(1-1) 10^{th} order QED calculation and the lepton anomalous magnetic moments

First preliminary value of the tenth-order QED contribution to the electron anomalous magnetic moment $a_e=(g-2)/2$ was reported by us in 2012. Since then, we have been improving and establishing its accuracy: We reevaluated the most difficult and large set of the Feynman diagrams by using advanced techniques of numerical calculation especially suitable to RIKEN's supercomputer. As a result, we have obtained precise values for the eighth- and tenth-order terms. Assuming the validity of the standard model, it leads to the world-best value of the fine-structure constant $\alpha^{-1}(a_e)=137.035\ 999\ 1570(29)(27)(18)(331)$, where uncertainties are from the eighth-order term, tenth-order term, hadronic and electroweak terms, and the experimental measurement of a_e. This is the most precise value of α available at present in the world and provides a stringent constraint on possible theories beyond the standard model.

(1-2) Picard–Lefschetz theory and the sign problem

Understanding strongly-correlated quantum field theories and many-body systems has been one of the ultimate goals in contemporary physics. Exact diagonalization of a Hamiltonian provides us with complete information on the system; however, it usually requires the huge computational cost and is limited to small systems. For large systems, numerical simulation on discretized spacetime lattice with quantum Monte Carlo method is a powerful ab initio tool based on the importance sampling. In many quantum systems of great interest, however, it suffers from the so-called sign problem; large cancellation occurs between positive and negative quantities to obtain physical signals, so that the computational time grows exponentially with the system size. So far, many attempts have been proposed overcome the sign problem, which include the two promising candidates, the complex Langevin method and the Lefschetz-thimble method. In particular, the Lefschetz-thimble approach is a generalization of the steepest descent method for multiple oscillatory integrals. In the past few years, we have studied extensively the mathematical basis of the Lefschetz-thimble method as well as its practical applications to quantum systems such as the real-time path integral for quantum tunneling, zero-dimensional bosonic and fermionic models, the one-site Hubbard model, and Polyakov-loop effective models for QCD. We have shown that the interference among multiple Lefschetz thimbles is important to reproduce the general non-analytic behavior of the observables as a function of the external parameter. Such an interference is a key to understand the sign problem of finite-density QCD.

(1-3) Functional renormalization group

- BEC-BCS crossover in cold fermionic atoms

We have developed a fermionic functional renormalization group (FRG) and applied this method to describe the superfluid phase transition of the two-component fermionic system with an attractive contact interaction. The connection between the fermionic FRG approach and the conventional Bardeen-Cooper-Schrieffer (BCS) theory with Gorkov and Melik-Barkhudarov (GMB) correction was clarified in the weak coupling region by using the renormalization group flow of the fermionic four-point vertex with particle-particle and particle-hole scatterings. To go beyond the BCS+GMB theory, coupled FRG flow equations of the fermion self-energy and the four-point vertex are studied under an Ansatz concerning their frequency/momentum dependence. We found that the fermion self-energy turns out to be substantial even in the weak coupling regime, and the frequency dependence of the four-point vertex is essential to obtain the correct asymptotic-ultraviolet behavior of the flow for the self-energy. The superfluid transition temperature and the associated chemical potential were evaluated in the region of negative scattering lengths.

- Tricritical point of the superconducting transition

The order of the phase transition in the Abelian Higgs model with complex scalar fields became of interest because of the analyses of the spontaneous symmetry breaking due to radiative corrections in 3+1 dimensions, and of a superconductor near the critical point with the dimensionally reduced Ginzburg-Landau theory. Indeed, the fluctuations of the gauge field were of great importance and may even turn the second-order transition to first-order at least for strongly type-I superconductors. We analyzed the order of the superconducting phase transition via the functional renormalization group approach: We derived for the first time fully analytic expressions for the β functions of the charge and the self-coupling in the Abelian Higgs model with N-component scalar field in $d = 3$ dimensions. The result supports the existence of two charged fixed-points: an infrared (IR) stable fixed point describing a second-order phase transition and a tricritical fixed

point controlling the region of the parameter space that is attracted by the former one. It was found that the region separating first and second-order transitions can be uniquely characterized by the critical Ginzburg-Landau parameter, $\kappa_c \approx 0.62/\sqrt{2}$ for N=1.

- Chiral dynamics under strong magnetic field

The magnetic field is not only interesting as a theoretical probe to the dynamics of QCD, but also important in cosmology and astrophysics: A class of neutron stars called magnetars has a strong surface magnetic field of order 10^{10} T while the primordial magnetic field in early Universe is estimated to be even as large as ~ 10^{19} T. In non-central heavy-ion collisions at RHIC and LHC, a magnetic field of the strength ~ 10^{15} T perpendicular to the reaction plane could be produced and can have impact on the thermodynamics and transport properties of the quark-gluon plasma. We investigated the quark-meson model in a magnetic field using the functional renormalization group equation beyond the local-potential approximation. We considered anisotropic wave function renormalization for mesons in the effective action, which allows us to investigate how the magnetic field distorts the propagation of neutral mesons. We found that the transverse velocity of mesons decreases with the magnetic field at all temperatures. Also, the constituent quark mass is found to increase with magnetic field, resulting in the crossover temperature that increases monotonically with the magnetic field.

(1-4) Emergent spacetime

In quantum field theories, symmetry plays an essential and exceptional role. Focusing on some proper symmetry and delving into its meaning have been proven to be one of the most fruitful strategies. A recent example is the SO(2, 4) symmetry in AdS/CFT correspondence which leads to unexpected connection between gravity and gauge theory defined in different dimensions. We offer another example of quantum field theory where symmetry plays a central role and reveals interesting phenomena: Our focal point is the global conformal symmetry in two dimensional conformal field theory (2d CFT), which is homomorphic to SL(2, R). We have shown that 2d CFT admits a novel quantization which we call dipolar quantization. Usually the study of the quantum field theory starts by defining the spacetime where the field is situated. On the other hand, in our case, we first obtain quantum system and then the nature of spacetime emerges. This is in accordance with the general ideas of emergent spacetime such as those discussed in matrix models.

(2) Theory of spontaneous symmetry breaking

(2-1) Dispersion relations of Nambu-Goldstone modes at finite temperature and density

We clarified the dispersion relations of Nambu-Goldstone (NG) modes associated with spontaneous breaking of internal symmetries at finite temperature and/or density. We showed that the dispersion relations of type-A and type-B NG modes are linear and quadratic in momentum, whose imaginary parts are quadratic and quartic, respectively. In both cases, the real parts of the dispersion relations are larger than the imaginary parts when the momentum is small, so that the NG modes can propagate for long distances. We derived the gap formula for NG modes in the presence of explicit symmetry breaking. We also discussed the gapped partners of type-B NG modes, when type-A and type-B NG modes coexist.

(2-2) Effective field theory for spacetime symmetry breaking

We studied the effective field theory for spacetime symmetry breaking from the local symmetry point of view. By gauging spacetime symmetries, the identification of Nambu-Goldstone (NG) fields and the construction of the effective action were performed based on the breaking pattern of diffeomorphism, local Lorentz, and isotropic Weyl symmetries as well as the internal symmetries including possible central extensions in nonrelativistic systems. Such a local picture provides a correct identification of the physical NG fields, while the standard coset construction based on global symmetry breaking does not. We also revisited the coset construction for spacetime symmetry breaking: Based on the relation between the Maurer-Cartan one-form and connections for spacetime symmetries, we classified the physical meanings of the inverse Higgs constraints by the coordinate dimension of broken symmetries. Inverse Higgs constraints for spacetime symmetries with a higher dimension remove the redundant NG fields, whereas those for dimensionless symmetries can be further classified by the local symmetry breaking pattern.

(2-3) Nambu-Goldstone modes in dissipative systems

Spontaneous symmetry breaking (SSB) in Hamiltonian systems is a universal and widely observed phenomena in nature, e.g., the electroweak and chiral symmetry breakings, superconductors, ferromagnets, solid crystals, and so on. It is also known that the SSB occurs even in dissipative systems such as reaction diffusion system and active matters. The translational symmetry in the reaction diffusion system is spontaneously broken by a spatial pattern formation such as the Turing pattern in biology. The rotational symmetry is spontaneously broken in the active hydrodynamics which describes collective motion of biological organisms. We found that there exist two types of NG modes in dissipative systems corresponding to type-A and type-B NG modes in Hamiltonian systems. By taking the O(N) scalar model obeying a Fokker-Planck equation as an example, we have shown that the type-A NG modes in the dissipative system are diffusive modes, while they are propagating modes in Hamiltonian systems. We pointed out that this difference is caused by the existence of two types of Noether charges, Q^{α}_{R} and Q^{α}_{A} : Q^{α}_{R} are symmetry generators of Hamiltonian systems, which are not generally conserved in dissipative systems. Q^{α}_{A} are symmetry generators of dissipative systems described by the Fokker-Planck equation and are conserved. We found that the NG modes are propagating modes if Q^{α}_{R} are conserved, while those are diffusive modes if they are not conserved.

(3) Lattice gauge theory

(3-1) Hadron interactions from lattice QCD

One of the most important goals in nuclear physics is to determine baryon-baryon interactions directly from QCD. To achieve this goal, the HAL QCD Collaboration has been developing a novel lattice QCD formulation (HAL QCD method) and performing first-principles numerical simulations. We have calculated the spin-orbit forces for the first time from QCD by the HAL QCD method, and have observed the attraction in the $^3P_2$ channel related to the P-wave neutron superfluidity in neutron star cores. Our calculation of the N-Ω interaction shows that this system is bound in the $^5S_2$ channel. We have shown that the Ω-Ω interaction in the spin-singlet channel is in the unitary region where the scattering length becomes large. Three-nucleon forces have been calculated for several heavy quark masses. Our lattice calculations was extended to the heavy quark systems, e.g. the exotic tetraquark, T_{cc} and T_{cs}. Properties of the light and medium-heavy nuclei (^{4}He, ^{16}O, ^{40}Ca) have been calculated by combining the nuclear many-body techniques and the nuclear forces obtained from lattice QCD. Also, we have theoretically and numerically shown that the Luscher's method traditionally used in studying the hadron-hadron interactions does not lead to physical results for baryon-baryon interactions unless the lattice volume is unrealistically large, so that the HAL QCD method is the only reliable approach to link QCD to nuclear physics.

As a part of the High Performance Computing Infrastructure (HPCI) Project 5, we have completed the generation of (2+1)-flavor full QCD configurations with a large box, V=(8 fm)^3, and with nearly physical pion mass, 145MeV, on the 10Pflops super computer "K". We are currently in the process of calculations of baryon-baryon interactions using these configurations.

(3-2) Momenta and Angular Momenta of Quarks and Gluons inside the Nucleon

Determining the quark and gluon contributions to the spin of the nucleon is one of the most challenging problems in QCD both experimentally and theoretically. Since the quark spin is found to be small (~ 25% of the total proton spin) from the global analysis of deep inelastic scattering data, it is expected that the rest should come from the gluon spin and the orbital angular momenta of quarks and gluons. We made state-of-the-art calculations (with both connected and disconnected insertions) of the momenta and the angular momenta of quarks and gluons inside the proton. The u and d quark momentum/angular momentum fraction extrapolated to the physical point is found to be 0.64(5)/0.70(5), while the strange quark momentum/angular momentum fraction is 0.024(6)/0.023(7), and that of the gluon is 0.33(6)/0.28(8). This implies that the quark spin carries a fraction of 0.25(12) of the proton spin. Also, we found that the quark orbital angular momentum, which turned out to be dominated by the disconnected insertions, constitutes 0.47(13) of the proton spin.

(4) QCD under extreme conditions

(4-1) Production and Elliptic Flow of Dileptons and Photons in the semi-Quark Gluon Plasma

A notable property of peripheral heavy-ion collisions at RHIC and LHC is the elliptic flow which is a measure of the transfer of initial spatial anisotropy to momentum anisotropy. Both the PHENIX experiment at RHIC and the ALICE experiment at LHC have announced a puzzling observation; a large elliptic flow for photons, comparable to that of hadrons. We considered the thermal production of dileptons and photons at temperatures above the QCD critical temperature (T_c) on the basis of semi-QGP, a theoretical model for describing the quark-gluon plasma (QGP) near T_c. With realistic hydrodynamic simulations, we have shown that the strong suppression of photons in semi-QGP due to the inhibition of colored excitations tends to bias the elliptical flow of photons to that generated in the hadronic phase. This increases the total elliptic flow for thermal photons significantly towards the experimental data.

(4-2) Deriving relativistic hydrodynamics from quantum field theory

Hydrodynamics describes the spacetime evolution of conserved quantities, such the energy, the momentum, and the particle number. It does not depend on microscopic details of the system, so that it can be applied to many branches of physics from condensed matter to high-energy physics. One of the illuminating examples is the recent success of relativistic hydrodynamics in describing the evolution of QGP created in heavy-ion collisions. Inspired by the phenomenological success of relativistic hydrodynamics in describing QGP, theoretical derivations of the relativistic hydrodynamics have been attempted on the basis of the kinetic theory, the fluid/gravity correspondence, the non-equilibrium thermodynamics, and the projection operator method. In our study, a most microscopic and non-perturbative derivation of the relativistic hydrodynamics from quantum field theory was given on basis of the density operator with local Gibbs distribution at initial time. Performing the path-integral formulation of the local Gibbs distribution, we derived the generating functional for the non-dissipative hydrodynamics microscopically. Moreover, we formulated a procedure to evaluate dissipative corrections.

(4-3) Hadron-quark crossover in cold and hot neutron stars

We studied bulk properties of cold and hot neutron stars (NS) on the basis of the hadron-quark crossover picture where a smooth transition from the hadronic phase to the quark phase takes place at finite baryon density. By using a phenomenological equation of state (EOS) "CRover" which interpolates the two phases at around 3 times the nuclear matter density (ρ_0), it is found that the cold NSs with the gravitational mass larger than two solar mass can be sustained. This is in sharp contrast to the case of the first-order hadron-quark transition. The radii of the cold NSs with the CRover EOS are in the narrow range (12.5±0.5) km which is insensitive to the NS masses. Due to the stiffening of the EOS induced by the hadron-quark crossover, the central density of the NSs is at most 4 ρ_0 and the hyperon-mixing barely occurs inside the NS core. This constitutes a solution of the long-standing hyperon puzzle first pointed out by Takatsuka et al. The effect of color superconductivity (CSC) on the NS structures was also examined with the hadron-quark crossover picture. For the typical strength of the diquark attraction, a slight softening of the EOS due to two-flavor CSC takes place and the maximum mass is reduced by about 0.2 solar mass. The CRover EOS is generalized to the supernova matter at finite temperature to describe the hot NSs at birth. The hadron-quark crossover was found to decrease the central temperature of the hot NSs under isentropic condition. The gravitational energy release and the spin-up rate during the contraction from the hot NS to the cold NS were also estimated.

(5) Nuclear and atomic many-body problems

(5-1) Giant dipole resonance in hot nuclei

Over the last several decades, extensive experimental and theoretical works have been done on the giant dipole resonance (GDR) in excited nuclei covering a wide range of temperature (T), angular momentum (J) and nuclear mass. A reasonable stability of the GDR centroid energy and an increase of the GDR width with T (in the range ~1−3 MeV) and J are the two well-established results. Some experiments have indicated the saturation of the GDR width at high T: The gradual disappearance of the GDR vibration at much higher T has been observed. Experiments on the Jacobi transition and the GDR built on superdeformed shapes at high rotational frequencies have been reported in a few cases. We have demonstrated that thermal pairing included in the phonon damping model (PDM) is responsible for the nearly constant width of GDR at low temperature T < 1 MeV. We have also shown that the enhancement observed in the recent experimentally extracted nuclear level densities in ^{104}Pd at low excitation energy and various angular momenta is the first experimental evidence of the pairing reentrance in finite (hot rotating) nuclei. The results of calculations within the PDM were found in excellent agreement with the latest experimental data of GDR in the compound nucleus ^{88}Mo.

(5-2) Hidden pseudospin symmetries and their origins in atomic nuclei

The quasi-degeneracy between single-particle orbitals, (n,l,j=l+1/2) and (n−1,l+2,j=l+3/2), indicates a hidden symmetry in atomic nuclei, the so-called pseudospin symmetry (PSS). Since the introduction of the concept of PSS in atomic nuclei, there have been comprehensive efforts to understand its origin. Both splittings of spin doublets and pseudospin doublets play critical roles in the evolution of magic numbers in exotic nuclei discovered by modern spectroscopic studies with radioactive ion beam facilities. Since the PSS was recognized as a relativistic symmetry in 1990s, many special features, including the spin symmetry (SS) for anti-nucleon, and other new concepts have been introduced. We have published a comprehensive review article (Liang et al., Phys. Rept. 2015) on the PSS and SS in various systems, including extensions of the PSS study from stable to exotic nuclei, from non-confining to confining potentials, from local to non-local potentials, from central to tensor potentials, from bound to resonant states, from nucleon to anti-nucleon spectra, from nucleon to hyperon

spectra, and from spherical to deformed nuclei. We also summarized open issues in this field, including the perturbative nature, the supersymmetric representation with similarity renormalization group, and the puzzle of intruder states.

(5-3) Efimov Physics in cold atoms

For ultra-cold atoms and atomic nuclei, the pairwise interaction can be resonant. Then, universal few-body phenomena such as the Efimov effect may take place. We carried out an exploratory study suggesting that the Efimov effect can induce stable many-body ground states whose building blocks are universal clusters. We identified a range of parameters in a mass and density imbalanced two-species fermionic mixture for which the ground state is a gas of Efimov-related universal trimers. An explicit calculation of the trimer-trimer interaction reveals that the trimer phase is an SU(3) Fermi liquid stable against recombination losses. We proposed to experimentally observe this phase in a fermionic mixture of ^{6}Li-^{53}Cr atoms. We have also written a comprehensive review article on theoretical and experimental advances in Efimov physics.

(5-4) Supersymmetric Bose-Fermi mixtures

Some special Bose-Fermi mixtures of cold atoms and molecules in optical lattices could be prepared in such a way as they exhibit approximate supersymmetry under the interchange of bosons and fermions. Since supersymmetry is broken at finite temperature and/or density, an analog of the Nambu-Goldstone excitation, dubbed the “Goldstino”, should appear. We evaluated the spectral properties of the Goldstino in a Bose-Fermi mixture of cold atoms and molecules. We derived model independent results from sum rules obeyed by the spectral function. Also, by carrying out specific calculations with random phase approximation, analytic formula for the dispersion relation of Goldstino at small momentum was obtained.

Members

Chief Scientist (Lab. Head)

Tetsuo HATSUDA

Vice Chief Scientist

Tsukasa TADA

Research & Technical Scientists

Takumi DOI (Senior Research Scientist)
Yoshimasa HIDAKA (Senior Research Scientist)
Pascal Raphaël Gabriel NAIDON (Senior Research Scientist)
Haozhao LIANG (Research Scientist)

Nishina Center Research Scientists

Makiko NIO
Dang NGUYEN DINH

Special Postdoctoral Researchers

Noriaki OGAWA
Yuya TANIZAKI
Kazuhiko KAMIKADO
Shingo TORII
Shinya GONGYO
Hiromichi NISHIMURA

Foreign Postdoctoral Researcher

Di-Lun YANG

Postdoctoral Researchers

Yoichi IKEDA
Koichi HATTORI
Takumi IRITANI

Junior Research Associate

Masaru HONGO (Univ. of Tokyo)

International Program Associate

Shihang SHEN (Peking University)
Zhaoxi LI (Beihang University)

Visiting Researchers

Kanako YAMAZAKI (JSPS Fellow)
Kei SUZUKI (JSPS Fellow)

Senior Visiting Scientist

Koichi YAZAKI (Univ. of Tokyo)

Visiting Scientists

Noriyoshi ISHII (Osaka Univ.)
Kanabu NAWA (Univ. of Tokyo)
Motoi TACHIBANA (Saga Univ.)
Tomoya HAYATA (Univ. of Tokyo)
Toichiro KINOSHITA (Cornell Univ.)
Takashi SANO (AIST)
Tatsumi AOYAMA (Nagoya Univ.)
Keitaro NAGATA (Hiroshima Univ.)
Hiroshi SUZUKI (Kyushu Univ.)
Kazuyuki KANAYA (Univ. of Tsukuba)
Takeo INAMI (National Taiwan University)
Shinsuke YOSHIDA (Los Alamos National Laboratory)
Koji HASHIMOTO (Osaka Univ.)
Takayuki MATSUKI (Tokyo Kasei Univ.)
Daisuke KADOH (Keio Univ.)
Takumi IRITANI (Stony Brook University)
Yoichi IKEDA (Osaka Univ.)
Shinya GONGYO (Centre national de la recherche scientifique)
Tatsuyuki TAKATSUKA (Iwate Univ.)

Hiroshi TOKI (Osaka Univ.)
Makoto TAKIZAWA (Showa Pharm. Univ.)
Shoichi SASAKI (Tohoku Univ.)

Yoshitaka HATTA (Univ. of Tsukuba)
Masashi HAYAKAWA (Nagoya Univ.)
Kenji SASAKI (Univ. of Tsukuba)
Shinya AOKI (Kyoto Univ.)
Atsushi NAKAMURA (Hiroshima Univ.)
Hung NGUYEN (Duy Tan University)
Keiko MURANO (Osaka Univ.)
Minoru ETO (Yamagata Univ.)
Norisuke SAKAI (Keio Univ.)
Arata YAMAMOTO (Univ. of Tokyo)

Sho OZAKI (Yonsei University)
Gergely FEJOS (Osaka Univ.)
Takashi OKA (Univ. of Tokyo)
Takashi INOUE (Nihon Univ.)
Sachiko TAKEUCHI (Japan College of Social Work)
Toshifumi NOUMI (The Hong Kong University of Science and Technology)
Rhine Kumar Arayakkandi Keechiprath (Tata Institute of Fundamental Research)
Yoichi KAZAMA (Univ. of Tokyo)
Tetsuo MATSUI (The Open Univ. of Japan)
Teiji KUNIHIRO (Kyoto Univ.)
Kazuo FUJIKAWA (Nihon Univ.)

Student Trainees

Bruno CHARRON (Univ. of Tokyo)
Ryuichi KURITA (Univ. of Tokyo)
Terukazu ICHIHARA (Kyoto Univ.)
Takaya MIYAMOTO (Kyoto Univ.)
Tan Phuc LE (University of Science. Vietnam National University)

Yuya TANIZAKI (Univ. of Tokyo)
Kota MASUDA (Univ. of Tokyo)
Shoichiro TSUTSUI (Kyoto Univ.)
Min SHI (Anhui University)

Part-time Workers

Koichi MURASE

Kayo YAMAJI

List of Publications & Presentations

Publications

[Journal]

(Original Papers) *Subject to Peer Review

W. Bentz, A. Kotzinian, H.H. Matevosyan, Y. Ninomiya, A.W. Thomas and K. Yazaki, "Quark-Jet model for transverse momentum dependent fragmentation functions," Physical Review D94 (2016) no.3, 034004.*

N. Ishibashi, T. Tada, “Dipolar quantization and the infinite circumference limit of two-dimensional conformal field theories,” International Journal of Modern Physics A 31, 1650170 (2016).*

Y. Kazama, S. Komatsu, and T. Nishimura, "Classical Integrability for Three-point Functions: Cognate Structure at Weak and Strong Couplings," Journal of High Energy Physics 1610, 042 (2016).*

Yoshimasa Hidaka, Shi Pu, Di-Lun Yang , Relativistic Chiral Kinetic Theory from Quantum Field Theories, Physical Review D 95, 091901 (2017).*

Ioannis Iatrakis, Elias Kiritsis, Chun Shen, Di-Lun Yang , Holographic Photon Production in Heavy Ion Collisions, Journal of High Energy Physics 1704 (2017) 035.*

Tomoya Hayata, Yoshimasa Hidaka, "Kinetic derivation of generalized phase space Chern-Simons theory," Physical Review B 95, 125137 (2017)*

Kenji Fukushima, Yoshimasa Hidaka, “Magnetic shift of the chemical freezeout and electric charge fluctuations,” Physical Review Letters 117, 102301 (2016).*

Tomoya Hayata, Yoshimasa Hidaka, Yuya Tanizaki,“Complex saddle points and the sign problem in complex Langevin simulation,” Nuclear Physics B911, 94 (2016)*.

T.Blum, N.Christ, M.Hayakawa, T.Izubuchi, L.Jin, C.Jung and C.Lehner, "Connected and Leading Disconnected Hadronic Light-by-Light Contribution to the Muon Anomalous Magnetic Moment with a Physical Pion Mass," Physical Review Letters 118, no. 2, 022005 (2017).*

Y. Ikeda, S. Aoki, T. Doi, S. Gongyo, T. Hatsuda, T. Inoue, T. Iritani, N. Ishii, K. Murano, and K. Sasaki (HAL QCD Collaboration), "Fate of the Tetraquark Candidate Zc (3900) in Lattice QCD," Physical Review Letters 117, 242001 (2016).*

T. Iritani, T. Doi, S. Aoki, S. Gongyo, T. Hatsuda, Y. Ikeda, T. Inoue, N. Ishii, K. Murano, H. Nemura and K. Sasaki (HAL QCD Collaboration) "Mirage in Temporal Correlation functions for Baryon-Baryon Interactions in Lattice QCD," Journal of High Energy Physics 1610, 101 (2016).*

F. Okiharu, T. Doi, H. Ichie, H. Iida, N. Ishii, M. Oka, H. Suganuma and T. T. Takahashi, "Tetraquark and Pentaquark Systems in Lattice QCD," Journal of Modern Physcs 7 (2016) 774.*

Masakiyo Kitazawa, Takumi Iritani, Masayuki Asakawa, Tetsuo Hatsuda, Hiroshi Suzuki, “Equation of State for SU(3) Gauge Theory via the Energy-Momentum Tensor under Gradient Flow”, Physical Review D94, 114512 (2016), arXiv:1610.07810 [hep-lat] (12 pages).*

K. Fujikawa and A. Tureanu, "Naturalness in see-saw mechanism and Bogoliubov transformation", arXiv:1609.03309, Physics Letters B767 (2017) 199-204. *

K. Fujikawa and A. Tureanu, "Parity-doublet representation of Majorana fermions and neutron oscillation", Physical Review D94 (2016) 115009.*

K. Fujikawa, “Dimensional regularization is generic”, International Journal of Modern Physics A31 (2016) no.25, 1630042. *

K. Fujikawa, “Nambu-Goldstone theorem and spin-statistics theorem”, International Journal of Modern Physics A31 (2016) no.13, 1630018. (Special article in memory of Yoichiro Nambu).

K. Fujikawa, "BCS, Nambu-Jona-Lasinio, and Han-Nambu -- A sketch of Nambu's works in 1960-1965", Progress of Theoretical and Experimental Physics 2016 (2016) no.6, 06A101. *

Norihiro Iizuka, Toshifumi Noumi and Noriaki Ogawa,"Entanglement entropy of de Sitter space α-vacua”, Nuclear Physics B 910, 23 (2016).*

N. Quang Hung, N. Dinh Dang, T. V. Nhan Hao, and L. Tan Phuc, Physical Review C 94, 064312 (2016).*

N. Quang Hung, N. Dinh Dang, and L. T. Quynh Huong, Physical Review C 94, 024341 (2016).*
N. Quang Hung, N. Dinh Dang, and L. T. Quynh Huong, Physical Review Letters 118, 022502 (2017).*
D. Chakrabarty, N. Dinh Dang, and V.M. Datar, Giant dipole resonance in hot nuclei (invited review) Eur. Phys. Jour. A 52 (2016) : 143.*
V. Vorobyev, et al. (Belle Collaboration), “Measurement of the CKM angle ϕ_1in B^0 → D¯^((*)0) h^0 , D¯^0→ K_S^0 π^+ 〖 π〗^- decays with time-dependent binned Dalitz plot analysis,” Physical Review D 94, 052004-1-15 (2016).*
J. Yelton, et al. (Belle Collaboration), “Studies of excited Ξ_c states decaying into Ξ_c^0 and Ξ_c^+ baryons,” Physical Review D 94, 052011-1-14 (2016).*
R. Mizuk, et al. (Belle Collaboration), “Energy Scan of the e^+ e^-→ h_b (nP) π^+ π^- (n=1,2) Cross Sections and Evidence for ϒ (11020) Decays into Charged Bottomoniumlike States,” Physical Review Letters 117, 142001-1-7 (2016).*
Y. Sato et al. (Belle Collaboration), “Measurement of the branching ratio of B¯^0 → D^(*+) τ^- ν¯_τ relative to B¯^0 → D^(*+) l^- ν¯_l decays with a semileptonic taging method,”Physical Review D 94, 072007-1-12 (2016).*
E. Won, et al. (Belle Collaboration), “Search for a dark vector gauge boson decaying to π^+ π^- using η → π^+ π^- γ decays,” Physical Review D 94, 092006-1-6 (2016).*
S. Takeuchi and M. Takizawa, “The hidden charm pentaquarks are the hidden color-octet uud baryons?” Physics Letters B 764, 254-259 (2017).*
Y.-T. Lai, et al. (Belle Collaboration), “Search for the 0^(--) glueball in Y(1S) and Y(2S) decays,”Physical Review D 95, 011102(R)-1-8 (2017).*
S. Jia, et al. (Belle Collaboration), “Search for D^0 decays to invisible final states at Belle,”Physical Review D 95, 012001-1-13 (2017).*
T. Nanut, et al. (Belle Collaboration), “Observation of D^0 → ρ^0 γ and Search for CP Violation in Radiative Charm Decays,” Physical Review Letters 118, 051801-1-8 (2017).*
S. Wehle, et al. (Belle Collaboration), “Lepton-Flavor-Dependent Angular Analysis of B → K^* l^+ l^-,” Physical Review Letters 118, 111801-1-7 (2017).*
S. Gongyo, Y. Kikuchi, T. Hyodo and T. Kunihiro, “Effective field theory and the scattering process for magnons in ferromagnets, antiferromagnets, and ferrimagnets,” Progress of Theoretical and Experimental Physics 2016 (2016) no.8, 083B01.*
M.N. Chernodub, S. Gongyo, “Interacting fermions in rotation: chiral symmetry restoration, moment of inertia and thermodynamics”, Journal of High Energy Physics 1701 (2017) 136.*
M.N. Chernodub, S. Gongyo, “Effects of rotation and boundaries on chiral symmetry breaking of relativistic fermions”, Physical Review D95 (2017) no.9, 096006.*
Dian-Yong Chen, Xiang Liu, and Takayuki Matsuki, "Search for missing ϕ(4S) ϕ(4S) in the e+e-→ π + π - ϕ(2S) process", Physical Review D93, 034028-1-10 (2016).*
T. Matsuki, Qi-Fang L¥"u, Yubing Dong, and T. Morii, "Approximate degeneracy of heavy-light mesons with the same L", Physics Letter B758, 274 (2016).*
Hao Zu, Xiang Liu, Takayuki Matsuki, "Understanding B→X(3823)K^- via rescattering mechanism and predicting B→η _{c2}(1D2)/ϕ _3(3D3)K^-", Physical Review D94, 034005 (2016).*
Jun-Zhang Wang, Dian-Yong Chen, Qin-Tao Song, Xiang Liu, and Takayuki Matsuki, "Revealing the inner structure of the newly observed D^*_2(3000)", Phys. Rev. D94, 094044 (2016).*
S.H. Shen, J.N. Hu, H.Z. Liang, J. Meng, P. Ring, and S.Q. Zhang, “Relativistic Brueckner-Hartree-Fock Theory for Finite Nuclei”, Chinese Physics Letter 33, 102103 (2016).*
N. Li, M. Shi, J.Y. Guo, Z.M. Niu, and H.Z. Liang, “Probing resonances of the Dirac equation with complex momentum representation”, Physical Review Letters 117, 062502 (2016).*
Z.M. Niu, B.H. Sun, H.Z. Liang, Y.F. Niu, and J.Y. Guo, “Improved radial basis function approach with odd-even corrections”, Physical Review C 94, 054315 (2016).*
Z. Fang, M. Shi, J.Y. Guo, Z.M. Niu, H.Z. Liang, and S.S. Zhang, “Probing the resonance in the Dirac equation with quadruple-deformed potentials by complex momentum representation method”, Physical Review C 95, 024311 (2017).*
M. Shi, X.X. Shi, Z.M. Niu, T.T. Sun and J.Y. Guo, “RMF-CGF method for resonances in deformed nuclei”, The European Physical Journal A 53, 40 (2017) .*

(Review)

T. Doi and T. Inoue,"Baryon-Baryon Interactions from Lattice QCD: The Bridge from Quarks to Nuclei and Cosmos," Nuclear Physics News 27, 13 (2017).*
Pascal Naidon, Shimpei Endo, “Efimov physics: a review” Reports on Progress in Physics 80 (2017) 056001.*
H.Z. Liang, “Pseudospin symmetry in nuclear structure and its supersymmetric representation”, Physica Scripta 91, 083005 (2016).*

[Proceedings]

(Original Papers) *Subject to Peer Review

Ioannis Iatrakis, Elias Kiritsis, Chun Shen, Di-Lun Yang , Holographic Photon Production and Anisotropic Flow, to appear in Nuclear and Particle Physics Proceedings by Elsevier. [Contribution to the proceedings of Hard Probes 2016].*
Ioannis Iatrakis, Elias Kiritsis, Chun Shen, Di-Lun Yang , Direct-Photon Spectra and Anisotropic Flow in Heavy Ion Collisions from Holography, to appear in European Physical Journal Web of Conferences. [Contribution to the proceedings of XII Quark Confinement and Hadron Spectrum].*
Shi Pu, Di-Lun Yang, Analytic Solutions of Transverse Magneto-hydrodynamics under Bjorken Expansion, to appear in European Physical Journal Web of Conferences. [Contribution to the proceedings of XII Quark Confinement and Hadron Spectrum].*
L.Jin, T.Blum, N.Christ, M.Hayakawa, T.Izubuchi, C.Jung and C.Lehner,"The connected and leading disconnected diagrams of the hadronic light-by-light contribution to muon g-2," Proceedings of Science (LATTICE 2016), 181 (2016), 34rd International Symposium on Lattice Field Theory (LATTICE 2016),July 24-30, 2016, University of Southampton, Southampton, UK.
T. Doi, S. Aoki, S. Gongyo, T. Hatsuda, Y. Ikeda, T. Inoue, T. Iritani, N. Ishii, T. Miyamoto, K. Murano, H. Nemura and K. Sasaki "Baryon interactions from lattice QCD with physical masses -- Overview and S = 0, −4 sectors --" Proceeding of Science LATTICE2016, 110 (2017).*

N. Ishii, S. Aoki, T. Doi, S. Gongyo, T. Hatsuda, Y. Ikeda, T. Inoue, T. Iritani, T. Miyamoto, K. Murano, H. Nemura and K. Sasaki,"Baryon interactions from lattice QCD with physical masses -- S = －3 sector: XiSigma and XiLambda - XiSigma --," Proceeding of Science LATTICE2016, 127 (2017).*
K. Sasaki, S. Aoki, T. Doi, S. Gongyo, T. Hatsuda, Y. Ikeda, T. Inoue, T. Iritani, N. Ishii, T. Miyamoto and K. Murano "Baryon interactions from lattice QCD with physical masses -- S = －2 sector --" Proceeding of Science LATTICE2016, 116 (2017).*
H. Nemura, S. Aoki, T. Doi, S. Gongyo, T. Hatsuda, Y. Ikeda, T. Inoue, T. Iritani, N. Ishii, T. Miyamoto, K. Murano and K. Sasaki "Lambda-Nucleon and Sigma-Nucleon interactions from lattice QCD with physical masses" Proceeding of Science LATTICE2016, 101 (2017).*
S. Aoki, T. Doi and T. Iritani, for HAL QCD Collaboration "Luscher's finite volume test for two-baryon systems with attractive interacions" Proceeding of Science LATTICE2016, 109 (2016).*
T. Doi, S. Aoki, S. Gongyo, T. Hatsuda, Y. Ikeda, T. Inoue, T. Iritani, N. Ishii, T. Miyamoto, K. Murano, H. Nemura and K. Sasaki "First results of baryon interactions from lattice QCD with physical masses (1) -- General overview and two-nucleon forces --" Proceeding of Science LATTICE2015, 086 (2016).*
N. Ishii, S. Aoki, T. Doi, S. Gongyo, T. Hatsuda, Y. Ikeda, T. Inoue, T. Iritani,T. Miyamoto, K. Murano, H. Nemura and K. Sasaki "First results of baryon interactions from lattice QCD with physical masses (2) -- S=－3 and S=－4 sectors (XiXi, XiSigma, XiLambda - XiSigma channels)--" Proceeding of Science LATTICE2015, 087 (2016).*
K. Sasaki, S. Aoki, T. Doi, S. Gongyo, T. Hatsuda, Y. Ikeda, T. Inoue, T. Iritani, N. Ishii, T. Miyamoto and K. Murano "First results of baryon interactions from lattice QCD with physical masses (3) -- Strangeness S=-2 two-baryon system" Proceeding of Science LATTICE2015, 088 (2016).*
K. Fujikawa and A. Tureanu, “Lorentz invariant CPT violation in the Dirac equation”, arXiv: 1607.01409. [Contribution to the Proceedings of the Memorial Meeting for Abdus Salam’s 90th Birthday, Nanyang Technological University, Singapore].
H.Z. Liang, “Microscopic studies on nuclear spin-isospin properties---a personal perspective on covariant density functional theory”, (Proceedings of INPC2016, Adelaide, Australia, 11-16 September, 2016), PoS (INPC2016) 361.
X. Roca-Maza, G. Colo, H.Z. Liang, J. Meng, P. Ring, H. Sagawa, and P. W. Zhao, “Towards the improvement of spin-isospin properties in nuclear energy density functionals”, (Proceedings of the XXI International School on Nuclear Physics and Applications & International Symposium on Exotic Nuclei (ISEN-2015), Varna, Bulgaria, 6-12 September 2015), Journal of Physics: Conference Series 724, 012041 (2016).

[Book]
(Original Papers) *Subject to Peer Review
風間洋一、「宇宙の統一理論を求めて」(岩波現代文庫/学術 353、岩波書店).

[Others]
風間洋一、「物理にたずさわるすべての人が知っておくべき超弦理論の基礎」、(翻訳：Edward Witten, " What every physicist know about string theory")パリティ 2016 年 7 月号、31(7), 4-12.
早川雅司, 「ミューオンの異常磁気能率」, 数理科学 2016 年 9 月号 No.639.
T. Doi and editorial committee "20xx A Space Odyssey: from Quarks to Nuclei and Cosmos,"The Physical Society of Japan Membership Journal Vol.71 No. 8, 522 (2016).
藤川和男、「ファインマン図，反粒子，CPT の破れ」、数理科学 2016 年 7 月号 34 ページ（サイエンス社）.

Oral Presentations
[International Conference etc.]
Tsukasa Tada, "Dipolar Quantization of conformal field theories,” YITP Workshop String and Fields, August 10th, 2016.
Tsukasa Tada, "Dipolar quantization of conformal field theories,” KEK Theory workshop 2016, December 6th, 2016.
Di-Lun Yang,“Side-Jumps and Collisions in Chiral Kinetic Theory from Quantum Field Theories”, Chirality Workshop, UCLA, March 27, 2017, Los Angel, U.S.
Di-Lun Yang, “Holographic photon production and flow in strongly coupled quark gluon plasmas”, Hard Probes 2016, East Lake International Conference Center, September 24th, 2016, Wuhan, China
Di-Lun Yang, “Holographic photon production in heavy ion collisions”, XII Quark Confinement and Hadron Spectrum, Makedonia Palace, September 2nd, 2016, Thessaloniki, Greece.
Yoshimasa Hidaka, “Spatially modulated chiral condensates in quark matter,” Quarkyonic matter, from theory to experiment, Oct 24-28, Central China Normal University, Wuhan, China.
Yoshimasa Hidaka, “The power of symmetry,” Big Waves of Theoretical Science in Okinawa, July 8 (Fri.) - July 11 (Mon), 2016, Okinawa Institute of Science and Technology Graduate University, Okinawa, Japan.
Y. Tanizaki, Y. Hidaka, T. Hayata, "Lefschetz-thimble approach to the Silver Blaze problem of one-site fermion model", 34th International Symposium on Lattice Field Theory (Lattice2016), Southampton, UK, 24-30 July 2016.
M. Hayakawa,"Standard model prediction for the muon g-2; QCD and QED contributions", The 1st KEK-KIAS-NCTS Joint WorkShop on Particle Physics Phenomenology, May 26-29, 2016, National Center for Theoretical Physics, Taiwan.
M. Hayakawa,"Hadronic light-by-light scattering contribution to the muon g-2 from lattice QCD"The 2nd Durham-KEK-KIPMU-KIAS Joint WorkShop, Octorber 24-28, 2016, KIAS, Korea.
M. Hayakawa, "Attempt to calculate hadronic light-by-light scattering contribution to the muon g-2 from lattice QCD,"Towards high precision muon g-2/EDM measurement at J-PARC, 28-29 November 2016, J-PARC, Tokai.
T. Doi, for HAL QCD Collaboration "Baryon-Baryon Interactions from Lattice QCD" Invited Talk given at KEK theory center workshop on "Hadron and Nuclear Physics in 2017", KEK, Tsukuba, Japan, 7-10 Jan. 2017.
T. Doi, for HAL QCD Collaboration "Baryon-Baryon Interactions from Lattice QCD" Invited Talk given at First Tsukuba-CCS-RIKEN joint workshop on "microscopic theories of nuclear structure and dynamics",RIKEN, Saitama, Japan, 12-16 Dec. 2016.
T. Doi, for HAL QCD Collaboration "Baryon-Baryon Interactions from Lattice QCD" Talk given at International Molecule-type Workshop "Realistic hadron interactions in QCD", YITP, Kyoto, Japan, 21, Nov. - 02 Dec. 2016.

T. Doi, for HAL QCD Collaboration "Two- and Three-Baryon Forces from Lattice QCD" Invited Talk given at YIPQS long-term and Nishinomiya-Yukawa memorial workshop on "Nuclear Physics, Compact Stars, and Compact Star Mergers (NPCSM) 2016",YITP, Kyoto, Japan, 17 Oct. - 18 Nov. 2016.

T. Doi, for HAL QCD Collaboration "Baryon interactions from lattice QCD with physical masses -- Overview and S=0, －4 sectors --" Talk given at "The 34th International Symposium on Lattice Field Theory (Lattice 2016)", Southampton, UK, 24-30 Jul. 2016.

T. Doi, for HAL QCD Collaboration "Baryon Interactions from Lattice QCD with physical masses" Talk given at INT Program "Nuclear Physics from Lattice QCD", Institute for Nuclear Theory (INT), Seattle, USA, 17, Mar. - 27 May 2016.

T. Iritani, Current status for two baryon-systems in lattice QCD II: HAL QCD potential method and diagnosis of the direct method, First Tsukuba-CCS-RIKEN joint workshop on microscopic theories of nuclear structure and dynamics, December 12-13, 2016, RIKEN Nishina Center, 14-16, 2016, Center for Computational Science, University of Tsukuba, Japan.

T. Iritani, "Lattice studies of Z_N-symmetric QCD", ECT* Workshop "Gauge Topology: from Lattice to Colliders", November 7-11, 2016, ECT*, Trento, Italy.

T. Iritani, "Baryon interactions in lattice QCD: the direct method vs. the HAL QCD potential method", The 34th International Symposium on Lattice Field Theory, July 24-30, 2016, Highfield Campus, University of Southampton, Southampton, UK.

T. Iritani, "Baryon interactions from Luscher's finite volume method and HAL QCD method", INT-16-1 Nuclear Physics from Lattice QCD, April 18, 2016, Institute for Nuclear Theory, University of Washington, Seattle, USA.

K. Fujikawa, "Higgs and neutrino masses in the Standard Model", Invited talk, YITP 50th Anniversary Symposium, Stony Brook University, Stony Brook, New York, USA, October 10-11, 2016.

K. Fujikawa, "Chiral anomaly and Berry phase", Invited talk, International Symposium "Chiral Matter 2016", RIKEN, Wako, Japan, December 5-8, 2016.

K. Fujikawa, "Path Integrals in Particle and Condensed Matter Physics: Quantum Anomalies and Related Topics", Invited talk, International Workshop "Path Integrals in Complex Systems", Lorentz Center, Leiden University, February 6-10, 2017.

Pascal Naidon, "From the Yukawa to the Efimov attraction", Invited talk, Workshop on "Quantum Many-Body Problems in Particle, Nuclear, and Atomic Physics", Duy Tan University, Danang, Vietnam, March 8-11, 2017.

Pascal Naidon, "Interacting Bose polarons: from the Yukawa to the Efimov attraction", Invited talk, Workshop on "Dynamics of hightly unstable exotic light nuclei and few-body systems", CEA Saclay, France, January 30 - February 3, 2017.

Pascal Naidon, "Universal clusters of mass-imbalanced fermions" Invited talk, "Few-body physics in cold-atomic gases", Beijing, China, Apr. 14-16, 2016.

Noriaki Ogawa,"Physical Modeling of Growing Cellular Mosaic Patterns in Fish Retina",

Workshop "Big Waves of Theoretical Science in Okinawa", Okinawa Institute for Science and Technology, 2016 July 9.

N. Quang Hung, "Nuclear Theory Group at Duy Tan University", Oral talk, International Workshop on Quantum Many-Body Problems in Particle, Nuclear, and Atomic Physics, Danang city, Vietnam, Mar. 8-11, 2017.

M. Takizawa, for Belle Collaboration, "New results on the XYZ states and B-decays from Belle," Invited talk, "Helmholts International Summer School - Dubna International Advanced School of Theoretical Physics", Dubna, Russia, July 18-30, 2016

Takayuki Matsuki, "String point of view for heavy-light mesons", XIIth Quark Confinement and the Hadron Spectrum, Thessaloniki, Greece, Aug. 29-Sept. 3

Shihang Shen, "Relativistic Brueckner-Hartree-Fock Theory for Finite Nuclei", Recent Progresses in Nuclear Structure Physics 2016 (NSP2016), Yukawa Institute for Theoretical Physics, Kyoto University, Kyoto, Japan, December 5-23, 2016.

Shihang Shen, "Relativistic Brueckner-Hartree-Fock Theory for Finite Nuclei", First Tsukuba-CCS-RIKEN joint workshop on microscopic theories of nuclear structure and dynamics, Wako & Tsukuba, Japan, December 12-16, 2016.

Min Shi, "Probing Resonances of the Dirac Equation with Complex Momentum Representation", First Tsukuba-CCS-RIKEN joint workshop on microscopic theories of nuclear structure and dynamics, Wako & Tsukuba, Japan, December 12-16, 2016.

Min Shi, "Probing Resonances of the Dirac Equation with RMF-CSM and RMF-CMR Method", Recent Progresses in Nuclear Structure Physics 2016 (NSP2016), Yukawa Institute for Theoretical Physics, Kyoto University, Kyoto, Japan, December 5-23, 2016.

Zhongming Niu, "High-precision nuclear physics inputs and their influences on the r-process simulations", Recent Progresses in Nuclear Structure Physics 2016 (NSP2016), Yukawa Institute for Theoretical Physics, Kyoto University, Kyoto, Japan, December 5-23, 2016.

Zhongming Niu, "Microscopic description of nuclear beta-decay half-lives", First Tsukuba-CCS-RIKEN joint workshop on microscopic theories of nuclear structure and dynamics, Wako & Tsukuba, Japan, December 12-16, 2016.

Haozhao Liang, "From Functional Renormalization Group to Density Functional Theory--- a case study of 0D anharmonic oscillator", Invited talk, ECT* Workshop: Unraveling the complexity of nuclear systems: single-particle and collective aspects through the looking glass, ECT*, Trento, Italy, February 6-10, 2017.

Haozhao Liang, "From Functional Renormalization Group to Density Functional Theory--- a case study of 0D anharmonic oscillator", First Tsukuba-CCS-RIKEN joint workshop on microscopic theories of nuclear structure and dynamics, Wako & Tsukuba, Japan, December 12-16, 2016.

Haozhao Liang, "From Functional Renormalization Group to Density Functional Theory--- a case study of 0D anharmonic oscillator", Recent Progresses in Nuclear Structure Physics 2016 (NSP2016), Yukawa Institute for Theoretical Physics, Kyoto University, Kyoto, Japan, December 5-23, 2016.

Haozhao Liang, "Microscopic studies on nuclear spin-isospin properties---a personal perspective on covariant density functional theory", Invited talk, The 26th International Nuclear Physics Conference (INPC2016), Adelaide, Australia, September 11-16, 2016.

Haozhao Liang, "Relativistic Brueckner-Hartree-Fock theory for finite nuclei", The 10th APCTP-BLTP/JINR-RCNP-RIKEN Joint Workshop on Nuclear and Hadronic Physics, RIKEN, Wako, Japan, August 17-21, 2016.

M. Nio, "Higher-order QED contributions to muon g-2," invitead talk, international workshop on "Towards high precision muon g-2/EDM measurement at J-PARC", J-PARC, Tokai, Japan, November 28-29, 2016.

[Domestic Conference]

日高義将, 南佑樹, "量子散逸系における南部・ゴールドストンの定理," 日本物理学会 第 72 回年次大会(2017 年) (大阪大学) 3 月 17-20 日.

日高義将, 福嶋健二, "Magnetic shift of the chemical freezeout and electric charge fluctuations," 日本物理学会 2016 年秋季大会, 宮崎大学,

2016 年 9 月 21-24 日.
早川雅司,"Hadronic light-by-light scattering contribution to muon g-2 from lattice QCD: pogress and challenges," New Physics Forum (Muon), January 19, 2016, KEK, Tsukuba.
早川雅司,"Is the theoretical prediction for the muon g-2 really correct ?", PPP2016, 2016 年 9 月 5 日~9 日, 京都大学基礎物理学研究所, 京都.
T. Doi, for HAL QCD Collaboration,"Baryon Forces from Lattice QCD," Invited Talk given at Workshop on "Advances of nuclear structure and reaction physics based on the realistic nuclear forces", Yukawa Institute of Theoretical Physics (YITP), Kyoto, Japan, 27-29 Mar. 2017.
T. Doi, for HAL QCD Collaboration "Baryon forces from physical point lattice QCD [4] -- General overview and S=0, －4 sectors --"Talk given at JPS meeting, Osaka University, Osaka, Japan, 17-20 Mar. 2017.
T. Doi, for HAL QCD Collaboration "Interactions between clusters on a lattice" Invited Talk given at Workshop on "Clusters connecting quarks, hadrons, nuclei and atoms", Osaka University, Osaka, Japan, 16, Mar. 2017.
T. Doi, for HAL QCD Collaboration "Lattice QCD calculations for Three-Nucleon Forces" Talk given at JPS meeting, University of Miyazaki, Miyazaki, Japan, 21-24 Sep. 2016.
T. Doi, for HAL QCD Collaboration,"Baryon forces from physical point lattice QCD [3] -- General overview and S=0, －4 sectors --" Talk given at JPS meeting, University of Miyazaki, Miyazaki, Japan, 21-24 Sep. 2016.
T. Doi, for HAL QCD Collaboration, "Baryon Interactions from Lattice QCD" Invited Talk given at Symposium on "Forefront of researches with supercomputers HOKUSAI and Shoubu", RIKEN, Saitama, Japan, 08 Jun. 2016.
T. Doi, "Baryon-Baryon Interactions from Lattice QCD" Seminar at Niigata University, Niigata, Japan, 6 Dec. 2016.
T. Doi, "Hadron Interactions from Lattice QCD" Seminar at "QCD Club", RIKEN, Wako, Saitama, Japan, 28 Oct. 2016.
T. Doi,"Baryon Interactions from Lattice QCD with physical masses" Seminar at Nagoya University, Nagoya, Japan, 17 May 2016.
入谷匠、"Current status for two baryon systems in lattice QCD II: HAL QCD potential method", 日本物理学会第 72 回年次大会、大阪大学豊中キャンパス、2017 年 3 月 17-20 日.
入谷匠、"格子 QCD による核子２体計算の現状と展望"、素粒子・原子核・宇宙「京からポスト京に向けて」シンポジウム、筑波大学東京キャンパス、2017 年 2 月 16-17 日
Pascal Naidon, “From the Yukawa to the Efimov attraction”, Japan Physical Society meeting, Osaka, March 17, 2017.
Pascal Naidon, “Interacting Bose polarons”, Cold-atom one-day workshop at RIKEN, Wako, August 25th 2016.
小川軌明, 初田哲男, 望月敦史, 立川正志,“Dynamical Pattern Selection of Growing Cellular Mosaic in Fish Retina",日本物理学会年次大会, 大阪大学, 2017 年 3 月 17 日.
M. Takizawa, “Structure of Y(4260) by the quark model,” Workshop on "Structures and Interactions of Heavy Quark Hadrons", KEK Tokai Campus, Tokai, Japan March 1-3, 2017.

Poster Presentations

[International Conference etc.]

Di-Lun Yang,“Direct-Photon Spectra and Anisotropic Flow in Heavy Ion Collisions from Holography “, Quark Matter 2017, Hyatt Regency, February 2, 2017, Chicago, U.S.
Di-Lun Yang,“Transverse flow induced by inhomogeneous magnetic fields in the Bjorken expansion “, XII Quark Confinement and Hadron Spectrum, Makedonia Palace, August 30, 2016, Thessaloniki, Greece.
Pascal Naidon, “Two impurities in a Bose-Einstein condensate: from Yukawa to Efimov attracted polarons”, 25th International Conference on Atomic Physics (ICAP2016), Seoul, South Korea, July 24-29, 2016.
Noriaki Ogawa, Tetsuo Hatsuda, Atsushi Mochizuki, Masashi Tachikawa,"Dynamical Pattern Selection of Growing Cellular Mosaic in Fish Retina”, Annual Conference of Japan Society of Mathematical Biology 2016, Kyushu University, 2016 Sep 7-8.
Shihang Shen, “Relativistic Brueckner-Hartree-Fock Theory for Finite Nuclei”, poster presentation at the NIC-XIV School 2016, June 15, 2016, Niigata University, Niigata, Japan.

[Domestic Conference]

小川軌明,「魚類網膜錐体モザイク形成のモデル化と解析」、研究会「熱場の量子論」, 理研和光, 2016 年 8 月 23 日.
小川軌明, 初田哲男, 望月敦史, 立川正志,「網膜錐体モザイク形成のモデル化と解析」,日本物理学会秋季大会, 金沢大学, 2016 年 9 月 16 日.

Theoretical Research Division
Strangeness Nuclear Physics Laboratory

1. Abstract

We proposed accurate calculation method called 'Gaussian Expansion Method using infinitesimally shifted Gaussian lobe basis function'. When one proceeds to four-body systems, calculation of the Hamiltonian matrix elements becomes much laborious. In order to make the four-body calculation tractable even for complicated interactions, the infinitesimally-shifted Gaussian lobe basis function has been proposed. The GEM with the technique of infinitesimally-shifted Gaussians has been applied to various three-, four- and five-body calculations in hypernuclei, the four-nucleon systems, and cold-atom systems. As results, we succeeded in extracting new understandings in various fields.

2. Major Research Subjects

(1) Hypernuclear structure from the view point of few-body problem
(2) Structure of exotic hadron system
(3) quantum atomic system and ultra cold atomic system
(4) Equation of state for neutron star

3. Summary of Research Activity

(1) Recently, at RIBF, they observed tetra neutron system to be bound or resonant state. Theoretically, it is requested to study this system theoretically. We performed four-body calculation using NN realistic force and a phenomenological three-body force. We found that we need unrealistically strong three-body force to describe 4n system.
(2) We investigate the effects of the odd-state part of bare ΛΛ interactions on the structure of neutron stars by constructing equations of state (EOSs) for uniform nuclear matter containing Λ and Σ⁻ hyperons with use of the cluster variational method. The EOS obtained for NS matter becomes stiffer as the odd-state ΛΛ interaction becomes more repulsive, and correspondingly the maximum mass of NSs increses.
(3) We calculate the universal spectrum of trimer and tetramer states in heteronuclear mixture of ultracold atoms with different masses in the vicinity of the heavy-light dimer threshold. We find that trimer and tetramer cross into the heavy-light dimer threshold at the same point and that as the mass ratio M/m decreases, the distance between the thresholds for trimer and tetramer states become smaller.

Members

Associate Chief Scientist (Lab. Head)
Emiko HIYAMA

Research Scientists
Hiroya SUNO (Research Scientist, concurrent: Strangeness Nuclear Physics Laboratory, Main: Field Theory Research Team)

Contract Researchers
Yasuro FUNAKI
Hyun-Chul KIM

Special Postdoctoral Researchers
Masahiro ISAKA
Hajime TOGASHI
Shin WATANABE
Masahiro YAMAGUCHI

Postdoctoral Researchers
Hajime TOGASHI
Tingting SUN

Junior Research Associates
Saori MAEDA (Tokyo Tech.)
Tetsuya YOSHIDA (Tokyo Tech.)
Jehee LEE (Inha University)

International Program Associate
Christiane SCHMICKLER (TU Darmstadt)
Qian WU (Nanjing University)

Visiting Researcher
Naoyuki SAKUMICHI (JSPS Fellow)

Visiting Scientists
Masayuki ASAKAWA (Osaka Univ.)
Yasuro FUNAKI (Beihang University)
Takayuki MYO (Osaka Inst. of Tech.)
Hidekatsu NEMURA (Univ. of Tsukuba)
Masakiyo KITAZAWA (Osaka Univ.)
Taiichi YAMADA (Kanto Gakuin Univ.)
Takenori FURUMOTO (Yokohama National Univ.)
Yasuo YAMAMOTO (Tsuru Univ.)
Makoto OKA (Tokyo Tech.)
Atsushi UMEYA (Nihon Inst. of Tech.)

Tetsuo HYODO (Kyoto Univ.)
Soichi ISHIKAWA (Hosei Univ.)
Atsushi HOSAKA (Osaka Univ.)
Akinobu DOTE (KEK)
Ying ZHANG (Tianjin University)
Jinniu HU (Nankai Univ.)
Wolfram WEISE (TUM)
Masahiro ISAKA (JSPS)
Javier ROCAMAZA (Univ. of Milan)
Xian-Rong ZHOU (East China Normal Univ.)
Kei KOTAKE (Fukuoka Univ.)
Hans-Josef SCHULZE (INFN)
Tingting SUN (Zhengzhou University China)
Jirina STONE (Univ, of Tennessee Knoxville)
Chengjun XIA (Zhejiang University)
Satoru HIRENZAKI (Nara Women's Univ.)
Kiyomi IKEDA (Niigata Univ.)
Daisuke JIDO (Tokyo Met. Univ.)
Thomas Adriaan RIJKEN (Radboud Univ. Nijmegen)
Shoji SHINMURA (Gifu Univ.)
Kazuma NAKAZAWA (Gifu Univ.)
Toru SATO (Osaka Univ.)
Philipp GUBLER (ECT*)
Toshio MOTOBA (Osaka Elec.-Com. Univ.)
Shuichi GOJUKI (SGI Japan Ltd.)
Hyun-Chul KIM (Inha Univ.)
Petr VESELY (Academy of Science of the Czech Republic Institute of the Nuclear Physcis)
Jean-Marc RICHARD (Lyon University)
Ulugbek YAKHSHIEV (Inha University)
Jiwei CUI (Xidian University)
Satoshi NAKAMURA (Tohoku Univ.)
Tomokazu FUKUDA (Osaka Elec.-Com. Univ.)

Student Trainees

Akira YOKOTA (Tokyo Tech.)
Karl SALLMEN (TIT)
Christiane SCHMICKLER (TU Darmstadt)

List of Publications & Presentations

Publications

[Journal]

(Original Papers) *Subject to Peer Review

S. Maeda, M. Oka, A. Yokota, E. Hiyama and Y-R. Liu, “A model of charmed baryon-nucleon potential and two- and three-body bound states with charmed baryon”, Progress of Theoretical and experimental Physics, 2016, 023D02 (2016).*

H. Togashi, E. Hiyama, Y. Yamamoto and M. Takano, “Equation of state for neutron stars with hyperons using a variational method”, Physical Review C, 93, 035808 (2016).*

E. Hiyama, R. Lazauskas, J. Carbonell and M. Kamimura, “Possibility of generating a 4-resonance with a $T=3/2$ isospin 3-neutron force”, Physical Review C 93, 044004 (2016).*

H. Togashi, K. Nakazato, Y. Takehara, S. Yamamuro, H. Suzuki and M. Takano, “Nuclear equation of state for core-collapse supernova simulations with realistic nuclear forces”, Nuclear Physics A, 961, 78, (2017).*

Oral Presentations

[International Conference etc.]

E. Hiyama, “Recent progress and future prospect of hypernuclear physics --from theory view point--”, The 31st Reimei Workshop on Hadron Physics in Extreme Conditions at J-PARC, Tokai, Japan, January, 2016.

E. Hiyama, “Clustering aspect of hypernuclei”, International workshop on Clustering effects of nucleons in nuclei and quarks in multi-quark states, Beijing, China, April, 2016.

H. Togashi, E. Hiyama and M. Takano, “Hyperon equation of state for supernovae and neutron stars with the variational method”, 4th DTA Symposium on Compact stars and gravitational wave astronomy, Mitaka, Japan, May, 2016.

H. Togashi, “Microscopic equation of state for core-collapse supernovae and neutron stars with realistic nuclear interactions”, Key Laboratory Seminar in Institute of Theoretical Physics, Beijing, China, June, 2016.

H. Togashi, E. Hiyama and M. Takano, “Variational study for the equation of state of hot nuclear matter with hyperons”, J-PARC Workshop 2016: From Exotic hadrons to QGP, Incheon, Korea, June, 2016.

H. Togashi, E. Hiyama and M. Takano, “Variational study of the supernova equation of state with hyperons”, 14th Symposium on Nuclei in the Cosmos (NIC XIV), Niigata, Japan, June, 2016.

H. Togashi, E. Hiyama and M. Takano, “Microscopic equation of state for hot dense matter in core-collapse supernovae”, The 10th APCTP-BLTP/JINR-RCNP-RIKEN Joint Workshop on Nuclear and Hadron Physics, Wako, Japan, August, 2016.

H. Togashi, E. Hiyama and M. Takano, “Variational study of hyperon effects on the nuclear equation of state at finite temperature”, International Nuclear Physics Conference (INPC2016), Adelaide, Australia, September, 2016.

H. Togashi, K. Nakazato, Y. Takehara, S. Yamamuro, H. Suzuki and M. Takano, “New nuclear equation of state for core-collapse supernovae with realistic nuclear forces”, International conference on Compact stars and gravitational waves, Kyoto, Japan, October, 2016.

H. Togashi, E. Hiyama and M. Takano, “Variational study of hyperon mixing in neutron stars and supernova cores”, NSMAT 2016, Sendai, Japan, November, 2016.

H. Togashi, K. Nakazato, Y. Takehara, S. Yamamuro, H. Suzuki and M. Takano, “New table of supernova equation of state using a variational method and its application to astrophysical compact objects”, QCS2017, Kyoto, Japan, February, 2017.

H. Togashi, “Nuclear equation of state with the variational method and the effect of Lambda hyperons in supernova cores”, International Workshop on Quantum Many-Body Problems in Particle, Nuclear, and Atomic Physics, Danang, Vietnam, March, 2017.

H. Togashi, E. Hiyama and M. Takano, “Hyperon stars at zero and finite temperatures with the variational method”, SNP2017, Neyagawa, Japan, March, 2017.

T. Oyamada, E. Hiyama and M. Tachikawa, “Three-Body Gaussian Expansion Method Calculations for He Atom”, International Workshop on Quantum Many-Body Problems in Particle, Nuclear, and Atomic Physics, Danang, Vietnam, March, 2017.

Y. Yamaguchi, A. Giachino, E. Santopinto and A. Hosaka, “Hidden-charm meson-baryon molecules with the five-quark bare field potential”, Workshop on Structures and Interactions of Heavy Quark Hadrons, Tokai, Japan, March, 2017.
Y. Yamaguchi and T. Hyodo, “Quark mass dependence of H-dibaryon in Lambda-Lambda scattering”, SNP2017, Neyagawa, Japan, March, 2017.
S. Watanabe, T. Matsumoto, K. Ogata, and M. Yahiro, “Four- and three-body breakup mechanism of ^{6}Li elastic scattering”, 11th International Conference on Clustering Aspects of Nuclear Structure and Dynamics, Napoli, Italy, May, 2016.
S. Watanabe, K. Minomo, M. Shimada, S. Tagami, M. Kimura, M. Takechi, M. Fukuda, D. Nishimura, T. Suzuki, T. Matsumoto, Y. R. Shimizu, and M. Yahiro, “Deformation and halo structure through reaction cross sections”, Direct Reactions with Exotic Beams (DREB2016), Halifax, Canada, July, 2016.
S. Watanabe, T. Matsumoto, K. Ogata, and M. Yahiro, “Four-body dynamics of ^{6}Li scattering”, The 10th APCTP-BLTP/JINR-RCNP-RIKEN Joint Workshop on Nuclear and Hadron Physics, Wako, Japan, August, 2016.
S. Watanabe, T. Matsumoto, K. Ogata, and M. Yahiro, “Four- and three-body dynamics in ^{6}Li scattering”, International Nuclear Physics Conference (INPC2016), Adelaide, Australia, September, 2016.
S. Watanabe, T. Matsumoto, K. Ogata, and M. Yahiro, “Four-body reaction mechanism of ^{6}Li scattering”, Workshop on Nuclear Cluster Physics (WNCP2016), Yokohama, Japan, November, 2016.
S. Watanabe, K. Ogata, T. Matsumoto, “Dynamic and static core excitation effects on deformed halo nuclei”, International Workshop on Quantum Many-Body Problems in Particle, Nuclear, and Atomic Physics, Danang, Vietnam, March, 2017.

[Domestic Conference]
富樫甫, “Nuclear equation of state for neutron stars and core-collapse supernovae with the variational method”, 筑波大学原子核理論研究室セミナー, 筑波, 6 月, 2016.
富樫甫, 肥山詠美子, 鷹野正利, “変分法によるハイペロン混合を考慮した有限温度核物質状態方程式の研究”, 日本物理学会 2016 年秋季大会, 宮崎, 9 月, 2016.
富樫甫, 肥山詠美子, 鷹野正利, “変分法による有限温度ハイペロン物質状態方程式と原始中性子星への適用”, 日本物理学会第 72 回年次大会, 大阪, 3 月, 2017.
富樫甫, “変分法による核物質状態方程式 –Supernova EOS テーブル完成までの道のり–“, 研究会「原子核のサイズと状態方程式の物理」, 福岡, 3 月, 2017.
山口康宏, A. Giachino, 竹内幸子, 瀧澤誠, E. Santopinto, 保坂淳, “反 D 中間子とチャームバリオンによるハドロン分子状態の解析”, 日本物理学会第 72 回年次大会, 大阪, 3 月, 2017.
渡邉慎, “^{6}Li 弾性散乱における動的性質”, 法政大学セミナー, 東京, 4 月, 2016.
渡邉慎, “CDCC calculations of ^{6}Li elastic scattering: Effects of four- and three-body breakup channels”, 東京工業大学セミナー, 東京, 6 月, 2016.
渡邉慎, “反応断面積で探る核構造研究の進展”, 日本物理学会 2016 年秋季大会, 宮崎, 9 月, 2016.
渡邉慎, “Reaction cross sections as a probe of deformation and shell structures”, RIKEN RIBF Nuclear Physics Seminar, 埼玉, 12月, 2016.
渡邉慎, “変形や殻進化のプローブとしての反応断面積”, 法政大学セミナー, 東京, 12 月, 2016.
渡邉慎, 松本琢磨, 緒方一介, 八尋正信, “連続状態離散化チャネル結合法を用いた弱束縛原子核の記述”, 研究会「クラスター・平均場 の両側面からみる原子核構造の多様性とそのダイナミクス」, 大阪, 1 月, 2017.
渡邉慎, “変形ハロー核の動的背性質と静的性質”, 九大原子核セミナー, 福岡, 3 月, 2017.
渡邉慎, 緒方一介, 松本琢磨, “1 中性子ハロー核に対する芯核励起の効果”, 日本物理学会第 72 回年次大会, 大阪, 3 月, 2017.

Sub Nuclear System Research Division
Radiation Laboratory

1. Abstract

Nucleons, such as protons and neutrons, are a bound state of constituent quarks glued together with gluons. The detail structure of nucleons, however, is not well understood yet. Especially the mechanism to build up the spin of proton, which is 1/2, is a major problem in physics of the strong force. The research goal of Radiation Laboratory is to solve this fundamental question using the world first polarized-proton collider, realized at RHIC in Brookhaven National Laboratory (BNL) in USA. RHIC stands for Relativistic Heavy Ion Collider, aiming also to create Quark Gluon Plasma, the state of Universe just after the Big Bang, and study its property. RIKEN-BNL Research Center (RBRC) directed by S. Aronson carries our core team at BNL for those exciting researches using the PHENIX detector. We have observed that the proton spin carried by gluons is finite and indeed sizable. We also identified W bosons in the electron/positron decay channel and in the muon decay channel, with which we are about to conclude how much anti-quarks carry the proton spin. Other than the activities at RHIC we are preparing and starting new experiments at J-PARC and Fermilab to study the nature of hadron. We are also performing technical developments such as novel ion sources, fine-pitch silicon pixel detectors and high-performance trigger electronics.

2. Major Research Subjects

1) Spin physics with relativistic polarized-proton collisions at RHIC
2) Study of nuclear matter at high temperature and/or at high density
3) Technical developments on radiation detectors and accelerators

3. Summary of Research Activity

(1) Experimental study of spin structure of proton using RHIC polarized proton collider

[See also RIKEN-BNL Research Center Experimental Group for the activities at BNL]

The previously published central pion double spin asymmetries at the highest collision energies at RHIC of 510 GeV have been augmented with the publication of the first forward double spin asymmetries on J/Psi mesons in 2016 by PHENIX. The forward rapidities increase the probed gluon momentum fractions at RHIC down to regions not accessible until the planned electron-ion collider. While statistically limited, there is an indication of a positive gluon spin contribution also at such low momentum fractions and together with the previous measurements would indicate a rather dominant gluon contribution to the nucleon spin.

With the valence quark spin contribution already reasonably well known, the contributions from sea quarks and orbital angular momenta remain to be understood. PHENIX has collected data to access the sea quark polarizations via leptonic decays of W bosons. Preliminary results have been obtained using all the data taken so far. The central rapidity electron decay channel results have been published while the forward muon decay channel results are now finalized and will be published soon.

While orbital angular momentum cannot be directly accessed at RHIC, several transverse spin phenomena have been observed which relate to orbital angular momentum and the three-dimensional structure of the nucleon. These phenomena by themselves have become a major field of research as the dynamics of the strong interaction. During the 2015 RHIC operation, collisions of transversely polarized protons with Au and Al nuclei were provided for the first time. The observed asymmetries in very forward neutron production showed surprisingly strong nuclear-size dependence. It could be explained by a contribution of electromagnetic interactions which may be sizable for heavy nuclei. The results have been prepared for publication.

To further investigate these effects the PHENIX experiment proposes substantial detector upgrades to go along the expected accelerator improvements. The proposed upgrade replaces the present magnet with the Babar solenoid, and we are considering to build an open-geometry forward spectrometer which has both hadronic and electromagnetic calorimetry as well as tracking, designed with a focus on the measurement of charged tracks and fully reconstructed jets in pea and pap collisions. Key measurements of this upgrade are forward Drell-Yan di-electrons to study sea quarks in nuclei and transverse-spin asymmetries for forward inclusive jets to study spin-momentum correlations in the proton.

As a pilot measurement, some of us are participating in the Fermilab Sea Quest experiment which has been collecting muon pairs using a 120-GeV unpolarized proton at Fermilab. By measuring the unpolarized Drell-Yan process, we can study quark spin-orbit effects which supplement what can be learned in the polarized Drell-Yan process. For many jet related measurements fragmentation functions are necessary to gain spin and or flavor sensitivity. Those are currently extracted by some of us using the Belle data. In addition to using the fragmentation results with RHIC measurements, they will also provide the basis of several of the key measurements to be performed at the electron-ion collider.

(2) Experimental study of quark-gluon plasma using RHIC heavy ion collider

[See also RIKEN-BNL Research Center Experimental Group for the activities at BNL]

We have completed several key measurements in the study of quark-gluon plasma at RHIC. As the top of them, we lead the analysis of the first thermal photon measurement in heavy ion collisions. The measurement indicates that the initial temperature reached in the central Au+Au collision at 200 GeV is about 350MeV, far above the expected transition temperature Tc~170MeV, from hadronic phase to quark-gluon plasma. This work was rewarded by Nishina Memorial Prize given to Y. Akiba in 2011. We also measured direct photons in d+Au and direct photon flow strength v2 and v3 in Au+Au.

We lead measurement of heavy quark (charm and bottom) using VTX, a 4 layer silicon vertex tracker which we jointly constructed with US DOE. The detector was installed in PHENIX in 2011. Analysis of heavy quark using the silicon vertex detector is ongoing. The final results of the 2011 run was published in Physical Review C (PRC93, 034904 (2016). This is the

first publication from VTX. The result showed that the electrons from bottom quark decay is suppressed for pT>4 GeV/c, but the suppression factor is smaller than that of charm decay electrons for 3<pT<4 GeV/c. This is the first observation of bottom electron suppression in heavy ion collisions, and the first result that shows the bottom and charm suppression is different. PHENIX recorded approximately 10 times more data of Au+Au collisions in the 2014 run than the 2011 run. We report preliminary results of about 1/4 of the 2014 data in QM2017 conference, confirming the published results with 3 times of statistics. PHENIX recorded high statistics p+p and p+A data in 2015, and the doubled the Au+Au in 2016. PHENIX concluded its data taking in the 2016 run.

In Wako we are operating a cluster computer system (CCJ) specialized to analyze huge data sets taken with the PHENIX detector. It consists of 28 nodes (18 old nodes and 10 new nodes) each of which has two CPUs and 10 sets of local disk for data repository (old node: quad-core CPU, 1TB disk, new node: six-core CPU, 2TB disk). There are 264 CPU cores and 380 TB disks in total. This configuration ensures the fastest disk I/O when each job is assigned to the node where the required data sets are stored. It is also important that this scheme doesn't require an expensive RAID system and network. Through this development we have established a fast and cost-effective solution in analyzing massive data.

0.9 PB of data for the PHENIX experiment is stored in a hierarchical storage system which is a part of HOKUSAI GreatWave supercomputer system operated by the Advanced Center for Computing and Communication (ACCC). ACCC also provides 10 dedicated PC nodes for CCJ.

(3) Study of properties of mesons and exotic hadrons with domestic accelerators

Preparation of the experiment E16 at J-PARC 50-GeV PS is underway with several Grant-in-Aids. This experiment aims to perform a systematic study of the spectral modification of low-mass vector mesons in nuclei to explore the chiral symmetry breaking in dense nuclear matter, namely, the mechanism proposed by Nambu to generate the major part of hadron mass.

Gas Electron Multiplier (GEM) technology is adopted for the two key detectors, GEM Tracker (GTR) and Hadron-blind Cherenkov detector (HBD). With cooperation with Japanese industries, large GEM foils (30cm x 30cm, the world-largest size at that time) were newly developed. We have joined the CERN-RD51 collaboration for the joint-development of the GEM and its readout technology. For the electron ID, lead-glass calorimeter (LG) is also used. The lead-glass blocks are recycled from the TOPAZ experiment. The development phase of the detectors is over and we are in the production phase. The parts for six modules of GTR and two modules of HBD are delivered and some of their assemblies have started. The “Scalable Readout System” developed by RD51 is adopted and purchased for the readout electronics modules of GEM. For LG readout, a flush ADC module using DRS4 ASIC has been developed and the first batch of production was delivered. Trigger logic modules and the trigger preamp ASIC are still under the test.

Due to the budgetary limitation, we aim to install a part of detectors, eight modules of GTR/HBD/LG out of 26 modules in the full installation, at the beginning of experiment. The construction of the beam line will be completed in 2019, with a significant delay from the original plan which aimed for March 2016. The yield of phi mesons and sensitivity to the possible spectral modification with the eight-module configuration under the expected high-rate environment was evaluated by the Geant4 simulation including the achieved performance of each detector and by using a newly-developed GEM-signal simulator.

(4) Detector development for PHENIX experiment

The PHENIX experiment proposes substantial detector upgrades to go along the expected accelerator improvements, including the future electron-ion collider “eRHIC”. The present PHENIX detector is repurposed to the sPHENIX (super PHENIX) detector replacing the present magnet with the Babar solenoid magnet at SLAC, and will be covered by the hadronic calorimeter which was absent in present RHIC experiment. The sPHENIX project is now funded by DOE, and RIKEN will participate in the construction of the inner silicon tracker.

We are considering to build an open-geometry forward spectrometer to be added to the sPHENIX detector. With this addition the fsPHENIX (sPHENIX with forward) detector will have both hadronic and electromagnetic calorimetry as well as tracking in the forward rapidity, which is suited to full reconstruction of p+A and p+p collisions. .The fsPHENIX detector will further improved to the ePHENIX detector in the era of eRHIC.

(5) Development of beam source

Under the collaboration with Brookhaven National Laboratory, we are developing various techniques for a laser ion source (LIS) to provide high quality heavy-ion beams to the accelerators. In 2014, we installed a new LIS which provides various species of singly charged ions to the RHIC-AGS complex. Since the beam commissioning was very successful, the LIS was upgraded to provide high repetition rate Au beam to the RHIC in 2015. At the moment, all the ion beams except proton, neon and uranium are being supplied by the LIS and the capability of the fast switching species contributes enhanced versatility and uniqueness of the at the RHIC-AGS. Besides, we are studying the highly charged ionization and magnetic field confinement of laser ablation plasma, and testing a linear accelerator model which selectively accelerates charge states.

Members

Chief Scientist (Lab. Head)
Hideto EN'YO (Director, RNC)

Vice Chief Scientist
Yasuyuki AKIBA

Research & Technical Scientists
Yasushi WATANABE (Senior Research Scientist)
Yuji GOTO (Senior Research Scientist)
Itaru NAKAGAWA (Senior Research Scientist)
Satoshi YOKKAICHI (Senior Research Scientist)
Ralf SEIDL (Senior Research Scientist)
Hiroaki ONISHI (Senior Research Scientist, concurrent; Advanced Meson Science Lab.)

Research Associates
Yusuke KOMATSU

Foreign Postdoctoral Researchers
Sanghwa PARK

Junior Research Associates
Yuko SEKIGUCHI (Univ. of Tokyo)
Koki KANNO (Univ. of Tokyo)
Wataru NAKAI (Univ. of Tokyo)
Tomoya HOSHINO (Hiroshima Univ.)
Shunsuke IKEDA (Tokyo Tech.)
Masafumi KUMAKI (Waseda Univ.)
Satoshi YANO (Hiroshima Univ.)
Daisuke WATANABE (Univ. of Tsukuba)
Kohei TERASAKI (Univ. of Tokyo)
Kazuya NAGASHIMA (Hiroshima Univ.)
Hikari MURAKAMI (Univ. of Tokyo)
Hiroshi NAKAGOMI (Univ. of Tsukuba)

International Program Associates
Inseok YOON (Seoul Nat'l Univ.)
Minjung KIM (Seoul Nat'l Univ.)
Minho KIM (Korea Univ.)
Taebong MOON (Yonsei Univ.)
Se Young HAN (Ewha Womans Univ.)
Jaehee YOO (Korea University)

Senior Visiting Scientists
Toshiaki SHIBATA (Tokyo Tech.)
Takashi NAKANO (Osaka Univ.)

Visiting Scientists
Kyoichiro OZAWA (KEK)
Susumu SATO (JAEA)
Megumi NARUKI (Kyoto Univ.)
Yoshinori FUKAO (KEK)
Michiko SEKIMOTO (KEK)
Kiyoshi TANIDA (JAEA)
Hirotsugu KASHIWAGI (National Institute for Quantum and Radiological Science and Technology)
Taku GUNJI (Univ. of Tokyo)
Junpei TAKANO (KEK)
Kazuya AOKI (KEK)
Masashi KANETA (Tohoku Univ.)
Munehisa OHTANI (Kyorin Univ.)
Yorito YAMAGUCHI (Univ. of Tokyo)
Youngil KWON (Yonsei Univ.)
Kenichi NAKANO (Tokyo Tech.)
Maya SHIMOMURA (Nara Women's Univ.)
Noriyosu HAYASHIZAKI (Tokyo Tech.)
Yuhei MORINO (KEK)
Kenji FUKUSHIMA (Univ. of Tokyo)
Ryo ICHIMIYA (KEK)
Tomohiro NISHITANI (Nagoya Univ.)
Tomonori TAKAHASHI (Osaka Univ.)
Tsutomu MIBE (KEK)
Makoto KUWAHARA (Nagoya Univ.)
Masahiro OKAMURA (BNL)
Shunzo KUMANO (KEK)
Bentz WOLFGANG (Tokai Univ.)
Alexander BAZILEVSKY (BNL)
Shin-ya SAWADA (KEK)
Ryotaro MUTO (KEK)
Masanori HIRAI (Tokyo Univ. of Sci.)
Kenta SHIGAKI (Hiroshima Univ.)
Sanghwa PARK (Stony Brook University)
Robert JAMESON (Goethe Universitat Frankfurt)
Takuya SUZUKI (Waseda Univ.)

Student Trainees
Shoichiro NISHIMURA (Univ. of Tokyo)
Yuki OBARA (Univ. of Tokyo)
Mana UENO (Nagoya Univ.)
Qidong Zhou (Nagoya Univ.)
Seiya MIYATA (Univ. of Tokyo)
Yosuke UEDA (Hiroshima Univ.)
Key NAGAI (Tokyo Tech.)
Koji IGARASHI (Tokyo Tech)
Kenta SATO (Nagoya Univ.)
Kazuya NAGASHIMA (Hiroshima Univ.)

Interns
Junsang PARK (Seoul Nat'l Univ.)
Daisuke NEMOTO (Rikkyo Univ.)
Jaehee YOO (Korea University)
Hidekazu MASUDA (Rikkyo Univ.)
Naoki FUJIYAMA (Rikkyo Univ.)
Ryota KAWASHIMA (Rikkyo Univ.)
Minho KIM (Korea Univ.)

Part-time Workers

Toru NAGASHIMA (Rikkyo Univ.)
Hidemitsu ASANO
Wataru NAKAI (Univ. of Tokyo)
Yusuke KOMATSU
Hidekazu MASUDA (Rikkyo Univ.)
Koki KANNO (Univ. of Tokyo)
Michiko SEKIMOTO

Assistant

Keiko SUZUKI

List of Publications & Presentations

Publications

[Journal]

(Original Papers) *Subject to Peer Review

Measurement of the Vector Meson Spectral Modification in the Nuclear Medium at J-PARC. By Yusuke Komatsu et al.. JPS Conf.Proc. 13 (2017) 020005.

Angular decay coefficients of J/ψ mesons at forward rapidity from p+p collisions at √s=510$ GeV. By PHENIX Collaboration (A. Adare et al.). Phys.Rev. D95 (2017) 092003.

Measurement of the relative yields of ψ(2S) to ψi(1S) mesons produced at forward and backward rapidity in p+p, p+Al, p+Au, and ^{3}He+Au collisions at $\sqrt{s_{NN}}$=200 GeV. By PHENIX Collaboration (A. Adare et al.). Phys.Rev. C95 (2017) no.3, 034904.

Nonperturbative-transverse-momentum effects and evolution in dihadron and direct photon-hadron angular correlations in p+p collisions at√s=510 GeV. By PHENIX Collaboration (A. Adare et al.). Phys.Rev. D95 (2017) no.7, 072002.

Measurement of long-range angular correlations and azimuthal anisotropies in high-multiplicity p+Au collisions at $\sqrt{s_{NN}}$ =200 GeV. By C. Aidala et al. Phys.Rev. C95 (2017) no.3, 034910.

Measurements of double-helicity asymmetries in inclusive J/ψ production in longitudinally polarized p+p collisions at √s =510$ GeV. By PHENIX Collaboration (A. Adare et al.). Phys.Rev. D94 (2016) no.11, 112008.

Precision study of the $\eta \to \mu^+\mu^-\gamma$ and $\omega \to \mu^+\mu^-\pi^0$ electromagnetic transition form-factors and of the $\rho \to \mu^+\mu^-$ line shape in NA60. By NA60 Collaboration (R. Arnaldi et al.). Phys.Lett. B757 (2016) 437-444.

Inclusive cross section and double-helicity asymmetry for π^0 production at midrapidity in p+p collisions at √s =510$ GeV. By PHENIX Collaboration (A. Adare et al.). Phys.Rev. D93 (2016) no.1, 011501.

Azimuthally anisotropic emission of low-momentum direct photons in Au+Au collisions at $\sqrt{s_{NN}}$ =200$ GeV. By PHENIX Collaboration (A. Adare et al.). Phys.Rev. C94 (2016) no.6, 064901.

Scaling properties of fractional momentum loss of high-p_T hadrons in nucleus-nucleus collisions at $\sqrt{s_{NN}}$ from 62.4 GeV to 2.76 TeV. By PHENIX Collaboration (A. Adare et al.). Phys.Rev. C93 (2016) no.2, 024911.

Transverse energy production and charged-particle multiplicity at midrapidity in various systems from $\sqrt{s_{NN}}$ =7.7 to 200 GeV. By PHENIX Collaboration (A. Adare et al.). Phys.Rev. C93 (2016) no.2, 024901.

ϕ meson production in the forward/backward rapidity region in Cu+Au collisions at $\sqrt{s_{NN}}$ =200$ GeV. By PHENIX Collaboration (A. Adare et al.). Phys.Rev. C93 (2016) no.2, 024904.

Centrality-dependent modification of jet-production rates in deuteron-gold collisions at $\sqrt{s_{NN}}$ =200 GeV. By PHENIX Collaboration (A. Adare et al.). Phys.Rev.Lett. 116 (2016) no.12, 122301.

Measurement of higher cumulants of net-charge multiplicity distributions in Au+Au collisions at $\sqrt{s_{NN}}$ =7.7-200$ GeV. By PHENIX Collaboration (A. Adare et al.). Phys.Rev. C93 (2016) no.1, 011901.

Measurement of parity-violating spin asymmetries in W^{+-} production at midrapidity in longitudinally polarized p+p collisions. By PHENIX Collaboration (A. Adare et al.). Phys.Rev. D93 (2016) no.5, 051103.

Performance of the Low Charge State Laser Ion Source in BNL. By Masahiro Okamura et.al.10.18429/JACoW-HIAT2015-THM1C03.

Control of Laser Ablation Plasma by Pulsed Magnetic Field for Heavy Ion Beam Production. By Shunsuke Ikeda et al. 10.18429/JACoW-HIAT2015-WEPB28.

Development of a hadron blind detector using a finely segmented pad readout. By Koki Kanno et al. Nuclear Instruments and Methods in Physics Research A, 819 (2016) 20-24.

[Proceedings]

(Original Papers) *Subject to Peer Review

Polarized nucleon-structure physics at RHIC-PHENIX. By Yuji Goto (PHENIX Collaboration). Proceedings of Science (Hadron 2013) 155.

Cross Section and Asymmetry Measurement of Very Forward Neutral Particle Production at RHIC. By Yuji Goto (RHICf collaboration). International Journal of Modern Physics, Conference Series 40, 1660110 (2016).Spin Physics. By Ralf Seidl, PoS DIS2016 (2016) 007

Measurement of double helicity asymmetries (ALL) at mid- and forward rapidities in longitudinally polarized p+p collisions at s√ = 510 GeV with PHENIX experiment. By Ralf Seidl and Taebong Moon, PoS DIS2016 (2016) 007

Oral Presentations

[International Conference etc.] [Domestic Conference]

S. Yokkaichi (JPARC E16 collaboration), “Systematic study of the vector meson spectral modification in the nuclear medium at J-PARC” in MENU2016, July 27th, 2016 at Kyoto, Japan.

S. Yokkaichi (JPARC E16 collaboration), “Measurements of spectral change of vector mesons in nuclear matter” in HINT2016, Dec 05th, 2016 at Tokai, Japan.

Yuji Goto, “GPDs and TMDs at Electron-Ion Collider” in Hadron Tomography at J-PARC and KEKB, Jan. 6th, 2017 at Tsukuba, Japan.

Ralf Seidl, “Spin Physics” in 24th International Workshop on Deep-Inelastic Scattering and Related Subjects, Apr. 11th, 2016, at Hamburg,

Germany.

Ralf Seidl, “Measurement of double helicity asymmetries (A_{LL}) in π^0 and π^{+-} production at mid-rapidity in longitudinally polarized p+p collisions at √s = 510 GeV with PHENIX experiment” in 24th International Workshop on Deep-Inelastic Scattering and Related Subjects, Apr. 13th, 2016, at Hamburg, Germany.

Ralf Seidl, “RHIC spin and Belle” in Workshop on hadron tomography, July 31st, 2016 at Kyoto, Japan.

Ralf Seidl, “The fragmentation function program at Belle” in 22th international spin symposium, Sep. 28th, 2016 at Urbana-Champaign, Il, USA.

Ralf Seidl, “The fragmentation function program at Belle” in 22th international spin symposium, Sep. 28th, 2016 at Urbana-Champaign, Il, USA.

Ralf Seidl, “Fragmentation function measurements in Belle” in KEK Hadron and nuclear physics workshop, Jan. 7th at Tsukuba, Japan.

[Domestic Conference]

Yuji Goto (RHICf collaboration), “RHICf experiment: Very forward measurement of particle production at RHIC” in Japan Physical Society Meeting, 20th March, 2016 at Sendai, Japan

Yuji Goto (PHENIX Collaboration),”Double-helicity asymmetry measurement of J/ψ production in √s = 510 GeV polarized p+p collisions at PHENIX” in Japan Physical Society Meeting, Sep. 23rd, 2016 at Miyazaki, Japan

Ralf Seidl, “Fragmentation function measurements in Belle” in JPS Fall Meeting, Sep. 23rd, 2016 at Miyazaki, Japan.

Sub Nuclear System Research Division
Advanced Meson Science Laboratory

1. Abstract

Particles like muons, pions, and kaons have finite life times, so they do not exist in natural nuclei or matters. By implanting these particles into nuclei/matters, exotic phenomena in various objects can be studied from new point of view.

Kaon is the second lightest meson, which has strange quark as a constituent quark. It is expected that if one embed mesons into nuclei, the sizes of the nuclei become smaller and one can form a high-density object beyond the normal nuclear density. Study of this object could lead to better understanding of the origin of the mass of the matter, and may reveal the quark degree of freedom beyond the quark-confinement. The other example is the weak interaction in nuclear matter. It can only be studied by the weak decay of hypernuclei, which have Lambda particle in the nuclei.

Muon provides even wider scope of studies, covering condensed matter physics as well as nuclear and atomic physics, and we are trying to extend the application field further into chemical and biological studies. For instance, stopping positively charged muon in a material, we obtain information on the magnetic properties or the local field at the muon trapped site (μSR). Injecting negatively charged muon to hydrogen gas, muonic hydrogen atom (μp) is formed. We are planning to measure μp hyperfine splitting energy to measure proton magnetic radius, which is complementary quantity to the proton charge radius and its puzzle lately attracts strong interest. We are also interested in precision measurement of muon property itself, such as muon anomalous magnetic moment (g-2).

In our research, we introduce different kind of impurities into nuclei / matters, and study new states of matter, new phenomena, or the object properties.

2. Major Research Subjects

(1) Study of meson property and interaction in nuclei
(2) Origin of matter mass / quark degree of freedom in nuclei
(3) Condensed matter and material studies with muon
(4) Nuclear and particle physics studies via muonic hydrogen
(5) Development of ultra cold muon beam, and its application from material science to particle physics

3. Summary of Research Activity

(1) Hadron physics at J-PARC, RIKEN-RIBF, GSI and SPring-8

Kaon and pion will shed a new insight to the nuclear physics. The recent discovery of deeply bound pionic atom enables us to investigate the properties of mesons in nuclear matter. At RIKEN-RIBF, we are preparing precise experimental study of the pionic atom. We have also started next generation kaon experiments (E15 and E31) at J-PARC. In these experiments, we are aiming to determine the $K^{bar}N$ interaction precisely, clarify the nature of kaon in nuclei, and Λ(1405) that could be K^-p bound state. At Spring-8 and at GSI, we are also aiming to study omega and eta' nuclei. By these experiments, we aim to be a world-leading scientific research group using these light meta-stable particles.

(1-A) Deeply bound kaonic nuclei

We have performed experimental exploration of theoretically predicted deeply bound kaonic nuclear states, such as the $<K^-pp>$ bound state. One of the most interesting features of the kaonic nucleus is the strong attraction of the $K^{bar}N$ interaction. Because of this strong attraction, the kaon in nucleus will attract surrounding nucleons resulting in extremely high-density object, which is several times larger than normal nuclear density. Measurement of the kaon properties at such high energy density will provide precious information on the origin of hadron masses and the chiral symmetry breaking and its partial restoration.

The experiment J-PARC E15 aims to identify the nature of the $<K^-pp>$ bound state by the in-flight ^{3}He(K^-, n) reaction, which allows us to investigate such state both in the formation via the missing-mass spectroscopy using the emitted neutron, and in its decay via the invariant-mass spectroscopy by detecting decay particles from $<K^-pp>$. For the experiment, we constructed a dedicated spectrometer system at the secondary beam-line, K1.8BR, in the hadron hall of J-PARC.

The first physics data-taking was carried out in March and May, 2013 with 6×10^9 kaons on ^{3}He target, corresponding to a ~1% of the approved proposal. We successfully obtained semi-inclusive ^{3}He(K^-, n) X missing-mass spectrum, and found a tail structure just below the mass threshold of ($K^- + p + p$) which cannot be explained by well-known processes and backgrounds. We also demonstrated an exclusive analysis by reconstructing ^{3}He(K^-, Λp) n events. To derive more information on the $K^{bar}N$ interaction by the exclusive measurement, we carried out the second physics data-taking in November-December, 2015 with 43×10^9 kaon on ^{3}He target, in which 7 times more data was accumulated. We have been analyzing the new data set focusing on the ^{3}He(K^-, Λp)n channel, and a significant bump structure below the ($K^- + p + p$) mass threshold has been observed in the Λp invariant-mass spectrum. To confirm whether or not the observed structure is the $<K^-pp>$ bound state, further analysis is currently in progress.

(1-B) Precision X-ray measurement of kaonic atom

Simultaneously with the above experiment (1-A), we have performed an X-ray spectroscopy of atomic $3d\rightarrow2p$ transition of negatively charged K-mesons captured by helium atoms. However, the energy resolution of the conventional semiconductor spectrometers is insufficient to see the K^- - nucleus potential observed by atomic levels at zero energy. This is closely related to the problem on the existence of deeply bound kaonic states in nuclei, well below the atomic levels, and this is one of the biggest problems in strangeness nuclear physics. Aiming to provide a breakthrough from atomic level observation, we will perform high-resolution X-ray spectroscopy of kaonic atoms at a J-PARC hadron beam line using a novel cryogenic X-ray spectrometer: an array of superconducting transition-edge-sensor (TES) micro-calorimeters. The spectrometer offers unprecedented energy resolution, which is about two orders of magnitude better than that of

conventional semiconductor detectors. A spectrometer array of 240 pixels will have an effective area of about 20 mm^2. Very recently, we have performed a proof-of-principle experiment by measuring pionic-atom X rays with a TES array at the PiM1 beam line at the Paul Scherrer Institut (PSI), and successfully demonstrated the feasibility of TES-based exotic-atom x-ray spectroscopy in a hadron-beam environment. Based on the results, we are preparing for the kaonic-atom experiment at J-PARC.

Another important X-ray measurement of kaonic atom would be $2p \rightarrow 1s$ transition of kaonic deuteron. We have measured same transition of kaonic hydrogen, but the width and shift from electro-magnetic (EM) value reflect only isospin average of the $K^{bar}N$ interaction. We can resolve isospin dependence of the strong interaction by the measurement. We are presently preparing a proposal to J-PARC PAC to measure kaonic deuteron X-ray.

(1-C) Deeply bound pionic atoms and η' mesonic nuclei

We have been working on precision spectroscopy of pionic atoms systematically, that leads to understanding of hidden non-trivial structure of the vacuum and origin of hadron masses. The precision data set stringent constraints on the chiral condensate at nuclear medium. We are presently preparing for the systematic high precision measurement of pionic tin isotopes at RIBF. A pilot experiment was performed in 2010, and showed a very good performance of the system. A main experiment was performed in 2014 and we achieved unprecedented resolution with much reduced systematic errors. A new experiment is being prepared with a improved setup.

We are also working on spectroscopy of η' mesonic nuclei in GSI/FAIR. Theoretically, peculiarly large mass of η' is attributed to UA(1) symmetry and chiral symmetry breaking. As a result, large binding energy is expected for η' meson bound states in nuclei (η'-mesonic nuclei). First experiment was conducted in 2014 in GSI. We accumulated very high quality data in terms of the spectral resolution and the statistics and set constraints in the η'-nucleus interaction.

(1-D) Hadron physics at SPring-8/LEPS2

Photo production of meson in nuclei is known to be a powerful tool to investigate property of the hadron in nuclear media. For this study, we started a new experimental project named LEPS2 (Laser Electron Photon at SPring-8 II) in this RIKEN Mid-term. The experimental hutch for LEPS2 at SPring-8 was constructed in March 2011, lead by RIKEN. The Large solenoid spectrometer magnet (2.96 m inner diameter x 2.22 m length) was successfully transported from BNL (US) to SPring-8 and installed into LEPS2 hutch in 2011.

One of the first physics programs is photo-production of η' in nuclei. Especially (γ, p) is most important reaction channel, where we can perform missing mass spectroscopy by detecting forward going proton. One of the big advantages of photo-production reaction is that the initial reaction is expected to be much cleaner than the hadron channel.

Detector construction for the first physics program is in progress. The 4π Electro-Magnetic calorimeter has been constructed and proton counter to detect forward going proton produced via (γ,p) reaction was partially installed in November 2013. Engineering run for the first experiment was performed in December 2013 to confirm performance of our detector system. Detector construction have been completed and 1st physics data taking was starting since 2014. Based on data collected, detail analysis to extract signal of η'-mesic nucleus, photoproduction of η etc are in progress.

(2) Muon science at RIKEN-RAL branch

The research area ranges over particle physics, condensed matter studies, chemistry and life science. Our core activities are based on the RIKEN-RAL Muon Facility located at the Rutherford-Appleton Laboratory (UK), which provides intense pulsed-muon beams. We have variety of important research activities such as particle / nuclear physics studies with muon's spin and condensed matter physics by muon spin rotation / relaxation / resonance (μSR).

(2-A) Condensed matter/materials studies with μSR

Two μSR spectrometer named CHRONUS and ARGUS are working together with ISIS standard data acquisition system, DAEII, with the front-end control system, SECI. Running a pulse-kicker system, we can perform two independent μSR experiments in Port-2 and 4 at the same time, splitting double-pulse to share beam between the two.

Among our scientific activities on μSR studies from year 2015 to 2017, following five subjects of material sciences are most important achievements at the RIKEN-RAL muon facility:

1) Novel superconducting state having partial nodal gaps in the two-dimensional organic superconductor λ-$[BETS]_2GaCl_4$.
2) Tiny magnetic moments and spin structures of Ir^{4+}, Nd^{3+} in carrier doped pyrochlore iridates $(Nd_{1-x}Ca_x)_2Ir_2O_7$.
3) Magnetism and spin dynamics in superoxides CsO_2, NaO_2 and RbO_2.
4) Magnetic properties of the nano-cluster gold in the border of macro- and micro- scale
5) Effects of the spatial distributions of magnetic moments and muon positions estimated from density functional theory (DFT) and dipole-field calculations.

(2-B) Nuclear and particle physics studies via ultra cold muon beam and muonic atoms

If we can improve muon beam emittance, timing and energy dispersion (*so-called* "ultra-slow muon"), then the capability of μSR study will be drastically improved. The ultra-slow muon beam can stop in thin foil, multi-layered materials and artificial lattices, so one can apply the μSR techniques to surface and interface science. The development of ultra-slow muon beam is also very important as the source of ultra-cold (pencil-like small emittance) muon beam for muon g-2 measurement. Therefore, we have been working on R&D study.

We have been working on the "ultra-slow muon" generation by laser ionization of muonium atoms in vacuum (bound system of μ^+ and electron) emitted after stopping "surface muon beam" in a material. In this mid-term, we are developing two key components, namely, high efficiency muonium generator at room temperature and high intensity ionization laser. The study of muonium generator has been done in collaboration with TRIUMF and KEK. In 2013, we demonstrated at least 10 times increase of the muonium emission efficiency by fabricating fine laser drill-holes on the surface of silica aerogel. We also developed a high power Lyman-α laser in collaboration with laser group at RIKEN. In this laser development, we succeeded to synthesize novel laser crystal Nd:YGAG, which has an ideal wavelength property for laser amplification to generate Lyman-α by four-wave mixing in Kr gas cell. We already achieved 10 times increase of

Lyman-α generation than before. We are working on the growth of large laser amplifying crystal so we can increase the Lyman-α by 10 times further. In order to fully apply these new developments to slow muon generation, we installed a new ultra-slow muon source chamber dedicated for silica aerogel in Port-3 with new features such as spin manipulation. We already demonstrated a method of maximizing the muon stopping in silica aerogel even under muon decay background from surrounding materials by using the spin rotation of muonium formed in aerogel.

Concerning the muonic atom, we are planning a new precise measurement of proton radius. A large discrepancy was found recently in the proton charge radius between the new precise value from muonic hydrogen atom at PSI and those from normal hydrogen spectroscopy and e-p scattering. We propose a precise measurement of Zemach radius (with charge and magnetic distributions combined) using the laser spectroscopy of hyperfine splitting energy in the muonic hydrogen atom**.** Preparation of the hydrogen target, mid-infrared laser and muon spin polarization detectors is in progress. We measured the delayed background in the detectors, which could overshadow the signal. We confirmed it is low enough if a coincidence detection is used. Port-1, previously used for muon catalysed fusion, is now being converted for the dedicated use by the proton radius measurement involving laser.

Members

Chief Scientist (Lab. Head)
Masahiko IWASAKI

Vice Chief Scientist
Katsuhiko ISHIDA

Research & Technical Scientists
Isao WATANABE (Senior Research Scientist)
Kenta ITAHASHI (Senior Research Scientist)
Haruhiko OUTA (Senior Research Scientist)
Hiroaki OHNISHI (Senior Research Scientist)
Fuminori SAKUMA (Senior Research Scientist)
Yue MA (Research Scientist)

Contract Researchers
Masaharu SATO

Special Postdoctoral Researchers
Tadashi HASHIMOTO
Sohtaro KANDA
Takahiro NISHI

Research Consultants
Yoshinori AKAISHI
Hironari MIYAZAWA
Masayasu KAMIMURA
Eiichi YAGI

Junior Research Associates
Kazuo TANAKA (Univ. of Tokyo)
Takuya SHIBUKAWA (Univ. of Tokyo)
Hirotomo HAMANO (Osaka Univ.)
Nam TRAN (Osaka Univ.)
Fahmi ASTUTI (Hokkaido Univ.)
Ryo KITAMURA (Univ. of Tokyo)
Dita PUSPITA SARI (Osaka Univ.)
Retno ASIH (Osaka Univ.)
Shu AIKAWA (Tokyo Tech.)
Shintaro TANAKA (Osaka Univ.)
Juila ANGEL (Hokkaido Univ.)

International Program Associates
Edi SUPRAYOGA (Bandung Inst. Tech.)
Zhang QI (Lanzhou Univ.)
Noraina ADAM(Universiti Sains Malaysia)
Sungwon YOON (Catholic Univ. of Korea)
Saidah Sakinah Mohd Tajudin (Universiti Sains Malaysia)

Senior Visiting Scientist
Kazuhiro TANAKA (KEK)

Visiting Scientists
Toshimitsu YAMAZAKI (Univ. of Tokyo)
Mototsugu MIHARA (Osaka Univ.)
Donald George FLEMING (Univ. of British Columbia/TRIUMF)
Yasuo NOZUE (Osaka Univ.)
Takehito NAKANO (Osaka Univ.)
Tadashi ADACHI (Sophia Univ.)
Zyun Francis EZAWA (Tohoku Univ.)
Yasuyuki ISHII (Shibaura Inst. of Tech.)
Johann ZMESKAL (SMI)
Risdiana (UNPAD)
Norimichi KOJIMA (Univ. of Tokyo)
Takao SUZUKI (Shibaura Inst. of Tech.)
Masami IIO (KEK)
Georg Peter BERG (Univ. of Notre Dame)
Takayuki GOTO (Sophia Univ.)
Masaya ENOMOTO (Tokyo Univ. of Sci.)
Hiroyuki FUJIOKA (Kyoto Univ.)
Takayuki KAWAMATA (Tohoku Univ.)
Lee CHOW (UCF)
Helmut WEICK (GSI)
Harry W. K. TOM (UC Riverside)
Agustinus NUGROHO (ITB)
Kawakami Kenji ROLAND (Univ. of California, Riverside)
Ichiro SHIRAKI (Univ. of Yamanashi)

Kensuke SUZUKI (Tohoku Univ.)
Kyosuke ISODA (Kagawa Univ.)
Ken SUZUKI (SMI)
Irwan DHARMAWAN (UNPAD)
Koji YOKOYAMA (Queen Marry Univ.)
Catalina Oana Curceanu(INFN)
Maryam Hassanvand(IUT)
Kazuki UENO (KEK)
Lusy SAFRIANI (UNPAD)
Hiroyuki NOUMI (Osaka Univ.)
Zhuan XU (Zhejiang Univ.)
Hiroshi TANIDA (Hiroshima Univ.)
Kenji KOJIMA (KEK)
Atsushi OKAZAWA (Univ. of Tokyo)
Tobat Parasian Irianto SARAGI (Univ. of Kassel)
Hiroko ARIGA (Hokkaido Univ.)
Yoshiki TANAKA(GSI)
Katsuhiko NISHIMURA (Univ. of Toyama)
Kenji MATSUDA (Univ. of Toyama)
Hexi SHI (LNF)
Mohamed Ismail MOHAMED IBRAHIM (USM)
Shukri SULAIMAN (USM)
Ayi BAHTIAR (UNPAD)
Eberhard WIDMANN(SMI)
Tsutomu MIBE (KEK)
Koichi ICHIMURA (Hokkaido Univ.)
Youichi IGARASHI (KEK)
Makoto YOKOYAMA (Ibaraki Univ.)
KwangYong CHOI (Chung-Ang Univ.)
Peklan TOH (Univ. Sains Malaysia)
Emma HAETTNER (GSI)
Andrea VACCHI (INFN)
Seungwon LEE (Univ. of Toyama)
Takahiro NAMIKI (Univ. of Toyama)
Naohito SAITO (KEK)
Kouichirou SHIMOMURA (KEK)
Satoru HIRENZAKI (Nara Women's Univ.)
Eiko TORIKAI (Univ. of Yamanashi)
Ryousuke KADONO (KEK)
Wataru HIGEMOTO (JAEA)
Yoji KOIKE (Tohoku Univ.)
Kazuhiko SATOH (Saitama Univ.)
Masaru YOSOI (Osaka Univ.)
Dai TOMONO (Kyoto Univ.)
Kazuki OHISHI (Comprehensive Res. Org. for Sci. and Soc.)
Yasuhiro MIYAKE (KEK)
Prasad Tara DAS (SUNY)
Yu OISHI (KEK)
Seiko KAWAMURA(JAEA)
Hideyuki TATSUNO (Lund Univ.)

Visiting Technicians

Kazuo OOYAMA (JOHO com.)

Research Fellows

Yuta SADA (Osaka Univ.)
Yuki NOZAWA (Osaka Univ.)
Natsuki HIROE (RCNP)

Student Trainees

Sohtaro KANDA (Univ. of Tokyo)
Kentaro INOUE (Osaka Univ.)
Yoshiki TANAKA (Univ. of Tokyo)
Hiroyuki YAMADA (Univ. of Tokyo)
Yuni WATANABE (Univ. of Tokyo)
Xingliang Xu (Saga Univ.)
Shingo KAWASAKI (Osaka Univ.)
Ryo KITAMURA (Univ. of Tokyo)
Kazuki MATSUI (Sophia Univ.)
Ainul Fauzeeha Binti ROZLAN (Univ. Saints Malaysia)
Saidah Sakinah Binti MOHD TAJUDIN (Univ. Saints Malaysia)
Shu AIKAWA (Tokyo Tech.)
Hiroshi HORII (Univ. of Tokyo)
Kazuya KATAYAMA (Tokyo Tech.)
Koshi KURASHIMA (Tohoku Univ.)
Tomotaka UEHARA (Saitama Univ.)
Takuro FUJIMAKI (Yamanashi Univ.)
Govinda KHANAL (Yamanashi Univ.)
Akane SAKAUE (Kyoto Univ.)
Isao YANAGIHARA (Kitasato Univ.)
Muhamad UMAR (Hokkaido Univ.)
Fahmi ASTUTI (Hokkaido Univ.)
Edi SUPRAYOGA (Bandung Inst. Tech.)
Taehyung KIM (Tokyo Tech.)
Go MISHIMA (Univ. of Tokyo)
Irwan RAMLI (Hokkaido Univ.)
Harison Binti ROZAK (UTM)
Juila ANGEL (Hokkaido Univ.)

Part-time Workers

Makoto TOKUDA (Tokyo Tech.)
Taehyung KIM (Tokyo Tech.)
Yuki NOZAWA (Osaka Univ.)
Fahmi ASTUTI (Hokkaido Univ.)
Takahiro NISHI (Univ. of Tokyo)
Juila ANGEL (Hokkaido Univ.)

Assistants

Tomoko IWANAMI
Yoko FUJITA
Mitsue YAMAMOTO

List of Publications & Presentations

Publications

[Journal]

(Original Papers) *Subject to Peer Review

Y. Sada et al., “Structure near the K^-+p+p threshold in the in-flight 3He(K^-,Λp)n reaction”, Prog. Theor. Exp. Phys., 051D01 (2016). DOI 10.1093/ptep/ptw040 *

Y.K. Tanaka, K. Itahashi et al. (for eta-PRiME/Super-FRS collaboration), "Measurement of excitation spectra in the 12C(p,d) reaction near the η′ emission threshold", Physical Review Letters 117 (2016) 202501 *

J. Äystöet al. (Super-FRS of NUSTAR@FAIR Collaboration), "Experimental program of the Super-FRS Collaboration at FAIR and developments of related instrumentation", Nucl. Instrum. Meth. B376 (2016) 111-115, DOI: 10.1016/j.nimb.2016.02.042 *

N. Saito, Y. Oishi, K. Miyazaki. K. Okamura, J. Nakamura, M. Iwasaki, S. Wada, "Photoionization pathways and thresholds in generation of Lyman-α radiation by resonant four-wave mixing in Kr-Ar mixture",

O. A. Louchev, AIP Advances 6, 095018/1-10 (2016). *

Norihito Saito, Yu Oishi, Koji Miyazaki, Kotaro Okamura, Jumpei Nakamura, Oleg A. Louchev, Masahiko Iwasaki and Satoshi Wada, ”High-efficiency generation of pulsed Lyman-α radiation by resonant laser wave mixing in low pressure Kr-Ar mixture”, Optics Express 24, 7566 (2016); DOI:10.1364/OE.24.007566 *

[Proceedings]

(Original Papers) *Subject to Peer Review

T. Yamaga et al., “Study of the elementary (K^-, n) reactions to search for the $K^{bar}NN$ bound state via the ^{3}He(K^-, n) reaction at J-PARC”, Proceedings of XVI International Conference on Hadron Spectroscopy (Hadron2015), AIP Conf. Proc. 1735, 040007 (2016). *

Yuni N. Watanabe et al.," Spectroscopy of Pionic Atoms Via (p, 2He) Reaction", JPS Conf.Proc. 13 (2017) 020015

Kenta Itahashi et al. (η-PRiME/SuperFRS Collaboration), "Excitation Spectra of Carbon Nuclei near η′ Emission Threshold", JPS Conf. Proc. 13 (2017) 020030, DOI: 10.7566/JPSCP.13.020030 *

Kenta Itahashi et al., "Precision spectroscopy of pionic atoms and chiral symmetry in nuclei", EPJ Web Conf. 130 (2016) 01017, DOI: 10.1051/epjconf/201613001017 *

Yoshiki K. Tanaka et al., "Search for η′ mesic nuclei by missing-mass spectroscopy of the 12C(p,d) reaction", EPJ Web Conf. 130 (2016) 02010 *

Hiroyuki Fujioka, Tomokazu Fukuda, Toru Harada, Emiko Hiyama, Kenta Itahashi, Shunsuke Kanatsuki, Tomofumi Nagae, Takuya Nanamura, Takahiro Nishi , "Search for Tetraneutron by Pion Double Charge Exchange Reaction at J-PARC" , JPS Conf.Proc. 13 (2017) 020058, DOI: 10.7566/JPSCP.13.020058 *

Oral Presentations

[International Conference etc.]

F.Sakuma, "Experimental studies on the $K^{bar}N$ interaction", International Workshop on Strangeness Nuclear Physics 2017 (SNP2017), , Osaka, March 2017

K.Inoue, "Analysis status of d(K^-,n)"πΣ" at J-PARC K1.8BR beam line", International Workshop on Strangeness Nuclear Physics 2017 (SNP2017), , Osaka, March 2017

M.Iwasaki, "News about Latest Experiment at J-PARC", 55th International Winter Meeting on Nuclear Physics, Bormio, Italy, January 2017

H.Outa, "Search for Deeply-bound K-pp States in 3He(K- ,Λp)n Reaction - Recent Results from J-PARC E15 Experiment -", International Symposium on Neutron Star Matter (NSMAT2016), Sendai, November 2016

T.Yamaga, "Improved ^{3}He(K^-,Λp)n Spectroscopy to Search for the KbarNN Bound State with J-PARC E15-2nd Data", The 26th International Nuclear Physics Conference (INPC2016), Adelaide, Australia, September 2016

M.Iwasaki, "Kaonic nuclear state search by kaon reaction on ^{3}He target at 1GeV/c", Meson in Nucleus 2016 (MIN16), Kyoto, August 2016

T.Yamaga, "Recent result of an exclusive measurement of ^{3}He(K^-,Λp)n reaction to search for $K^{bar}NN$ bound state at J-PARC", The 14th International Conference on Meson-Nucleon Physics and the Structure of the Nucleon (MENU2016), Kyoto. July 2016

F.Sakuma, "$K^{bar}NN$ bound state search at J-PARC", The 14th International Conference on Meson-Nucleon Physics and the Structure of the Nucleon (MENU2016), Kyoto, July 2016

S.Kawasaki, "Spectroscopic experiment of Λ(1405) via in-flight d(K^-,n) reaction at J-PARC K1.8BR", The 14th International Conference on Meson-Nucleon Physics and the Structure of the Nucleon (MENU2016), Kyoto. July 2016

K.Itahashi, Transregio symposium, Bonn, 2016

K. Itahashi, "Meson-nuclear bound states", The 71st Fujihara Seminar, Shimoda, July 2016

K. Itahashi, "Precision spectroscopy of pionic atoms and chiral symmetry in nuclei", 14th International WOrkshop on Meson Production, Properties and Interaction (MESON 2016), Krakow, June 2016

[Domestic Conference]

K. Itahashi, "π 中間子原子、η'中間子原子核分光実験", 日本物理学会第 71 回年次大会, 東北学院大学, 3 月(2016)

Y.Ma, "Study of KbarN interaction at J-PARC K1.8BR beam line", ELPH 研究会「マルチフレーバーで探るエキゾチックハドロンとハドロン多 体系の物理」, 東北大学, 仙台, 12 月(2016)

山我拓巳, "[シンポジウム:K 中間子クラスターと高密度物質への展開] K^-pp クラスター実験研究の最前線", 日本物理学会第 72 回年次大会, 大阪大学, 大阪, 3 月(2017)

川﨑新吾, "J-PARC K1.8BR ビームラインにおける d(K^-,n)反応による Λ(1405)粒子 の精密分光実験の $\pi^0\Sigma^0$ 終状態に関する解析状況", 日本物理学会第 72 回年次大会, 大阪大学, 大阪, 3 月(2017)

Sub Nuclear System Research Division
RIKEN-BNL Research Center

1. Abstract

The RIKEN BNL Research Center was established in April 1997 at Brookhaven National Laboratory with Professor T. D. Lee of Columbia University as its initial Director. It is funded by the Rikagaku Kenkyusho (RIKEN, The Institute of Physical and Chemical Research) of Japan. The Center is dedicated to the study of strong interactions, including spin physics, lattice QCD and RHIC physics through the nurturing of a new generation of young physicists. Professor Lee was succeeded by BNL Distinguished Scientist, N. P. Samios, who served until 2013. The current director is Dr. S. H. Aronson. After strong and significant leadership for 4 years, S. Aronson steps down from Director in March 31st 2017. Hideto En'yo succeeds as an acting Director from JFY 2017.Support for RBRC was initially for five years and has been renewed three times, and presently extends to 2018. The Center is located in the BNL Physics Department. The RBRC Theory Group activities are closely and intimately related to those of the Nuclear Theory, High Energy Theory, and Lattice Gauge Theory Groups at BNL. The RBRC Experimental Group works closely with Radiation Laboratory at RIKEN, Wako, the RHIC Spin Group at BNL, the RHIC Spin Physics community, and the PHENIX collaboration. BNL provides office space, management, and administrative support. In addition, the Computational Science Center (CSC) and Information Technology Division (ITD) at BNL provide support for computing, particularly the operation and technical support for the RBRC 400 Teraflop QCDCQ (QCD Chiral Quark) lattice gauge theory computer. The Deputy Director of RBRC is R. Pisarski (BNL). D. Kharzeev (Stony Brook/BNL) is leader of the Theory Group. Y. Akiba (RIKEN) is Experimental Group leader with A. Deshpande (Stony Brook) deputy. T. Izubuchi (BNL) is Computing Group leader.

2. Major Research Subjects

Major research subjects of the theory group are
(1) Heavy Ion Collision
(2) Perturbative QCD
(3) Phenomenological QCD

Major research subjects of the computing group are
(1) Search for new law of physics through tests for Standard Model of particle and nuclear physics
(2) Dynamics of QCD and related theories
(3) Theoretical and algorithmic development for lattice field theories, QCD machine design

Major research subject of the experimental group are
(1) Experimental Studies of the Spin Structure of the Nucleon
(2) Study of Quark-Gluon Plasma at RHIC
(3) sPHENIX detector construction as

3. Summary of Research Activity

Summary of Research Activities of the three groups of the Center are given in the sections of each group.

Members

Director
Samuel H. ARONSON

Deputy Director
Robert PISARSKI

Administrative Staff
Kazunori Mabuchi (Administration Manager, Nishina Center Planning Office)
Yasutaka AKAI (Deputy Administration Manager, Nishina Center Planning Office)
Colleen MICHAEL (Administrative Assistant)
Pamela ESPOSITO (Administrative Assistant)

Sub Nuclear System Research Division
RIKEN-BNL Research Center
Theory Group

1. Abstract

The efforts of the RBRC theory group are concentrated on the major topics of interest in High Energy Nuclear Physics. This includes: understanding of the Quark-Gluon Plasma; the nature of dense quark matter; the initial state in high energy collisions, the Color Glass Condensate; its evolution through a Glasma; spin physics, as is relevant for polarized hadronic collisions; physics relevant to electron-hadron collisions.

Theory Group hosted many joint tenure track positions with universities in U.S. and Japan.

2. Major Research Subjects

(1) Heavy Ion Collision
(2) Perturbative QCD
(3) Phenomenological QCD

3. Summary of Research Activity

(1) Spin Physics

The experimental program at RBRC is strongly focused on determining the origin of spin in the proton and neutron. To extract the spin content of nucleon requires both precise data and precise computation. Dr. Jianwei Qiu of the Nuclear Theory group is one of the world's leading theorists in perturbative QCD, and leading the effort at BNL in spin physics. Their effort will continue to concentrate on computing perturbative QCD effects to sufficient precision that one can reliably extract information from the evolving experimental program. In addition they are developing ideas which might be tested in an electron-hadron collider, such as the one proposed to be built by adding an electron ring to RHIC.

(2) Matter at High Energy Density

The RHIC experimental heavy ion program is designed to study the properties of matter at energy densities much greater than that of atomic nuclei. This includes the initial state of nucleus-nucleus collisions, the Color Glass Condensate, the intermediate state to which it evolves, the Glasma, and lastly the thermal state to which it evolves, the Quark-Gluon Plasma. Theorists at the RBRC have made important contributions to all of these subjects.

Matter at high temperature has been studied by a variety of techniques involving both numerical and analytic methods. Much of the high precision work on numerical simulations of lattice QCD at nonzero temperature and density such matter have been done by members of the Lattice Gauge Theory Group at BNL, including Frithjof Karsch, Peter Petreczsky, Swagato Mukherjee, and postdoctoral assistants. These groups, along with collaborators at Columbia University, the University of Bielefeld, and other groups, have computed numerous properties of QCD in thermodynamic equilibrium. This includes the equation of state for physical quark masses, susceptibilies with respect to quark chemical potentials, and transport coefficients.

Phenomenological theories of the Quark-Gluon Plasma, based upon results from lattice simulations, have been developed by R. Pisarski of the Nuclear Theory Group, in collaboration with Dr. Y. Hidaka (previously of RBRC/BNL, and now a permanent member at RIKEN in Waco), Shu Lin, Daisuke Sato, and other postdoctoral research assistants at RBRC/BNL.

The theory of the Color Glass Condensate and Glasma was largely developed by RBRC scientists. This theory has been successfully applied to a wide variety of experimental results involving high energy collisions of hadrons, electrons and nuclei. There is recent data on heavy ion collisions that are naturally explained by such matter, including data on proton (or deuteron) nucleus collisions. Much of the effort here will be aimed towards excluding or verifying the Color Glass Condensate and Glasma hypothesis in RHIC and LHC experiments.

Thermal matter at high temperature and baryon density has been traditionally conjectured to be of two phases: confined and deconfined, with a direct correlation between deconfinement and the restoration of chiral symmetry. RBRC scientists have recently conjectured a third phase, of quarkyonic matter. This is baryonic matter at energy densities very high compared to the QCD scale. It has a pressure and energy density typical of quarks, yet it is confined. The name arises because it shares properties of confined baryonic matter with unconfined quark matter. This hypothesis is new and predicts new classes of phenomena that might be observed in collisions of nuclei of relatively low energy at RHIC. There are a number of first principle theoretical issues also to be understood.

Efforts on RHIC phenomenology proceed on a broad front. Recent efforts include improving hydrodynamic computations using state of the art equations of state derived from lattice gauge theory. Understanding the nature of matter at high baryon number density has generated the idea of Quarkyonic Matter, that may have implications for an upcoming low energy run at RHIC and eventual experiments in the future at FAIR and NICA. An issue being studied is the nature of mass generation and the breaking of translational invariance. A central focus of work at RBRC, the Color Glass Condensate and the Glasma, matter that controls the high energy limit of QCD, is being realized in experiments at RHIC. Much activity focuses on the relation between observations at LHC and the implications made at RHIC.

Members

Group Leader (Lab. Head)
Dmitri KHARZEEV

Deputy Group Leader
Robert PISARSKI (concurrent : Deputy Director, RBRC)

RBRC Researchers
Jinfeng LIAO (RHIC Physics Fellow)
Ho-Ung YEE (RHIC Physics Fellow)
Yuya TANIZAKI (Special Postdoctoral Researcher)
Hiromichi Nishimura (Special Postdoctoral Researcher)
Daniel PITONYAK (Research Associates)
Vladimir SKOKOV (Special Postdoctoral Researcher)
Ryutaro FUKUDA (Junior Research Associate)

Visiting Scientists
Koichi Hattori (Fudan Univ.)

Sub Nuclear System Research Division
RIKEN-BNL Research Center
Computing Group

1. Abstract

The computing group founded in 2011 as a part of the RIKEN BNL Research Center established at Brookhaven National Laboratory in New York, USA, and dedicated to conduct researches and developments for large-scale physics computations important for particle and nuclear physics. The group was forked from the RBRC Theory Group.

The main mission of the group is to provide important numerical information that is indispensable for theoretical interpretation of experimental data using the theories of particle and nuclear physics. Their primary area of research is lattice quantum chromodynamics (QCD), which describes the sub-atomic structures of hadrons, which allow us the ab-initio investigation for strongly interacting quantum field theories beyond pertrubative analysis.

The RBRC group and its collaborators have emphasized the necessity and importance of precision calculations, which will precisely check the current understandings of nature, and will have a potential to find a physics beyond the current standard model of fundamental physics. We have therefore adopted techniques that aim to control and reduce any systematic errors. This approach has yielded many reliable results.

The areas of the major activities are R&D for high performance computers, developments for computing algorithms, and researches of particle, nuclear, and lattice theories. Since the inception of RBRC, many breakthroughs and pioneering works has carried out in computational forefronts. These are the use of the domain-wall fermions, which preserve chiral symmetry, a key symmetry for understanding nature of particle nuclear physics, the three generations of QCD devoted supercomputers, pioneering works for QCD calculation for Cabibbo-Kobayashi-Maskawa theory, QCD+QED simulation for isospin breaking, novel algorithm for error reduction in general lattice calculation. Now the chiral quark simulation is performed at the physical up, down quark mass, the precision for many basic quantities reached to accuracy of sub-percent, and the group is aiming for further important and challenging calculations, such as the full and complete calaution for $K\rightarrow\pi\pi$ decay, ε'/ε, or hadronic contributions go muon's anomalous magnetic moment, or Nucleon's shape and structures related to physics for future Electron Ion Collider (EIC).

2. Major Research Subjects

(1) Search for new law of physics through tests for Standard Model of particle and nuclear physics, especially in the framework of the Cabibbo–Kobayashi–Maskawa (CKM), hadronic contributions to the muon's anomalous magnetic moment (g-2).
(2) Dynamics of QCD and related theories, including study for the structures of nucleons related to physics for Electron Ion Collider (EIC or eRHIC).
(3) Theoretical and algorithmic development for lattice field theories, QCD machine design.

3. Summary of Research Activity

In 2011, QCD with Chiral Quarks (QCDCQ), a third-generation lattice QCD computer that is a pre-commercial version of IBM's Blue Gene/Q, was installed as an in-house computing resource at the RBRC. The computer was developed by collaboration among RBRC, Columbia University, the University of Edinburgh, and IBM. Two racks of QCDCQ having a peak computing power of 2 × 200 TFLOPS are in operation at the RBRC. In addition to the RBRC machine, one rack of QCDCQ is owned by BNL for wider use for scientific computing. In 2013, 1/2 rack of Blue Gene/Q is also installed by US-wide lattice QCD collaboration, USQCD. The group has also used the IBM Blue Gene supercomputers located at Argonne National Laboratory and BNL (NY Blue), and Hokusai and RICC, the super computers at RIKEN (Japan), Fermi National Accelerator Laboratory, the Jefferson Lab, and others. From 2016, the group started to use the institutional cluster both GPU and Intel KnightLanding (KNL) clusters installed at BNL extensively.

Such computing power enables the group to perform precise calculations using up, down, and strange quark flavors with proper handling of the important symmetry, called chiral symmetry, that quarks have. The group and its collaborators carried out the first calculation for the direct breaking of CP (Charge Parity) symmetry in the hadronic K meson decay ($K\rightarrow\pi\pi$) amplitudes, ε'/ε which provide a new information to CKM paradigm and its beyond. They also provide the hadronic contribution in muon's anomalous magnetic moment $(g-2)_\mu$. These calculation for ε'/ε hadronic light-by-light of (g-2), are long waited calculation in theoretical physics delivered for the first time by the group. The $K\rightarrow\pi\pi$ result in terms of ε'/ε currently has a large error, and deviates from experimental results by 2.1 σ. Hadronic Light-by-light contribution to $(g-2)_\mu$ is improved by more than two order of magnitudes compared to our previous results. Other projects including flavor physics in the framework of the CKM theory for kaons and B mesons that include the new calculation of b-baryon decay, $\Lambda_b\rightarrow p$; the electromagnetic properties of hadrons; the proton's and neutron's formfactors and structure function including electric dipole moments; proton decay; nucleon form factors, which are related to the proton spin problem; Neutron-antineutron oscillations; τ inclusive decay; nonperturbative studies for beyond standard model such composite Higgs or dark matter models from strong strongly interacting gauge theories; a few-body nuclear physics and their electromagnetic properties; and QCD thermodynamics in finite temperature/density systems such as those produced in heavy-ion collisions at the Relativistic Heavy Ion Collider.

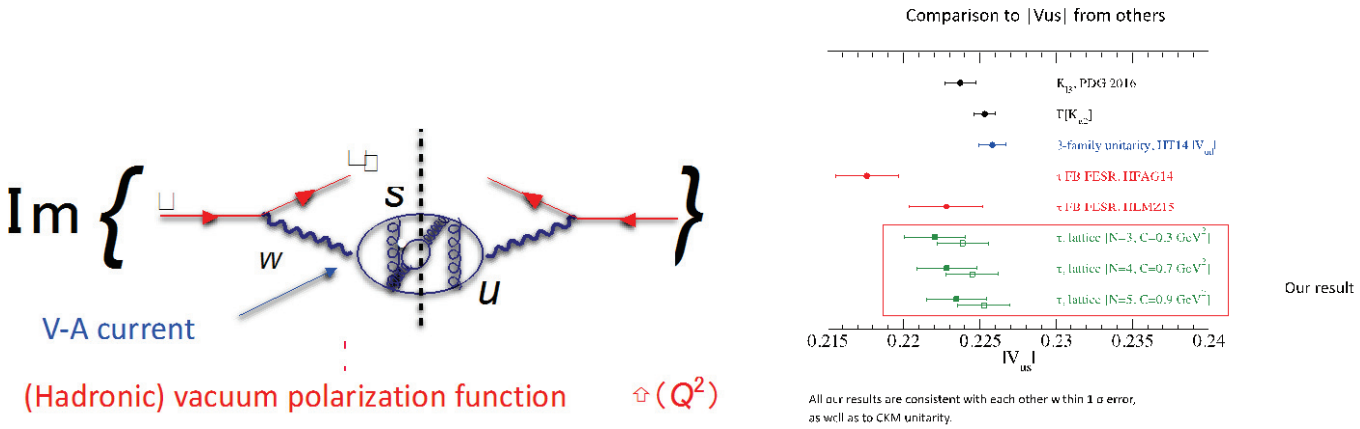

Figure : Hadronic inclusive decay of tau lepton (left), the new results of CKM matrix element Vus (right).

Theme	Significant Outcomes	Expected Impacts & Extensions
(a) DWF QCD ensemble generation and measurements of basic quantities.	hadron spectrum, f_π, f_K, K_{13}, B_K, and ChPT LECs, with smaller systematic errors	Basis of physical observables such as below
(b) Operator Renormalization	Precise matrix elements, bag parameters quark masses, and coupling constants	Reduced systematic error in *e.g.* $K \to \pi\pi$ amplitudes
(c) Computational Algorithms, Software, and Machines	Fast and Cost-Effective Computing All-Mode Averaging (AMA) PhySyHCAl	Unprecedented precision and new physical quantities (see below)
(d) K physics	K_{13},$\Delta I = 1/2, 3/2$, $K \to \pi\pi$ amplitudes, ϵ'/ϵ $K_L - K_S$ Mass Difference	New constraints *e.g.* on CKM from rare Kaon decay $K \to \pi\nu\bar{\nu}$
(e) B physics	Matrix elements for (semi-)leptonic decays and $B^0 - \overline{B^0}$ oscillations	CKM matrix, e.g., V_{ub}, V_{ts}, V_{td}.
(f) QED and Isospin breaking effects	Better determination of quark masses Proton-Neutron Mass Difference	A step towards sub-% precision groundwork for $(g-2)_\mu$
(g) Muon Anomalous Magnetic Moment $(g-2)_\mu$	Hadronic Vacuum Polarization contribution Light-by-Light contribution	$(g-2)_\mu$ experiments at BNL, FNAL, J-PARC
(h) Proton/Neutron Physics Electric Dipole Moments, ProtonDecay	Nucleon structure, Parton Distribution Functions (PDF) EM properties, Electric Dipole Moment (EDM)	Electron-Ion Collider (eRHIC) Spin Physics, Kamiokande Origin of matter in Universe

Table: Summery of current physics program and their impacts

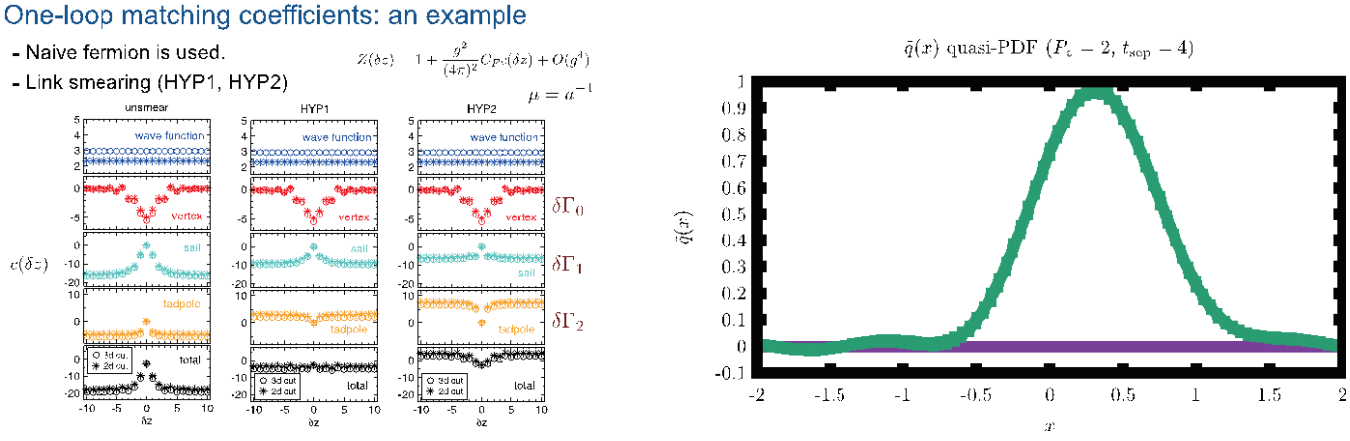

Figure: Renormalization of quasi Parton Distribution Function (PDF) operator (left), preliminary result of pion PDF (right)

The RBRC group and its collaborators have emphasized the necessity and importance of precision calculations, which will precisely check the current understandings of nature, and will have a potential to find physics beyond the current standard model of fundamental physics. We have therefore adopted techniques that aim to control and reduce any systematic errors. This approach has yielded many reliable results, many of basic quantities are now computed within sub-percent accuracies.

The group also delivers an algorithmic breakthrough, which speed up generic lattice gauge theory computation. In this novel technique called All Mode Averaging (AMA), the whole calculation is divided into frequent approximated calculations, and infrequent expensive and accurate calculation using lattice symmetries. Together with another formalism, zMobius fermion, which approximate chiral lattice quark action efficiently, the typical calculation is now improved by a couple of orders of magnitudes compared to the traditional methods.

Members

Group Leader (Lab. Head)
Taku IZUBUCHI

RBRC Researcher
Tomomi ISHIKAWA (RIKEN BNL Fellow)
Yasumichi AOKI (RIKEN BNL Fellow, KEK)
Brian TIBURZI (RHIC Physics Fellow)
Ethan NEIL (RHIC Physics Fellow)
Stefan MEINEL (RHIC Physics Fellow)
Hiroshi OKI (Special Postdoctoral Researcher)
Sergey SYRITSYN (Special Postdoctoral Researcher)
Enrico RINALDI (Special Postdoctoral Researcher)

Visiting Scientists
Yasumichi AOKI (Nagoya Univ.)
Thomas BLUM (Univ. of Connecticut)
Chulwoo JUNG (BNL)
Christoph LEHNER (BNL)
Meifeng LIN (Yale Univ.)
Robert MAWHINNEY (Columbia)
Shigemi OHTA
Sergey SYRITSYN (Thomas Jefferson National Laboratory)
Tomomi ISHIKAWA (Shanghai Jiao-Tong Univ.)

List of Publications & Presentations

Publications
[Journal]
(Original Papers) [* Currently subject to peer review]

Thomas Blum, Norman Christ, Masashi Hayakawa, Taku Izubuchi, Luchang Jin, Chulwoo Jung, and Christoph Lehner
"Connected and Leading Disconnected Hadronic Light-by-Light Contribution to the Muon Anomalous Magnetic Moment with a Physical Pion Mass", Phys. Rev. Lett. 118, 022005 – Published 11 January 2017.

T. BlumP. A. BoyleL. Del DebbioR. J. HudspithT. IzubuchiA. JüttnerC. LehnerR. LewisK. MaltmanM. Krstić MarinkovićA. PortelliM. Spraggs, "Lattice calculation of the leading strange quark-connected contribution to the muon g−2g−2", Published in JHEP 1604 (2016) 063, Erratum: JHEP 1705 (2017) 034

T. Blum , P.A. Boyle, T. Izubuchi, L. Jin, A. Jüttner, C. Lehner, K. Maltman, M. Marinkovic, A. Portelli, M. Spraggs, "Calculation of the hadronic vacuum polarization disconnected contribution to the muon anomalous magnetic moment ", Published in Phys.Rev.Lett. 116 (2016) no.23, 232002

Eigo Shintani, Thomas Blum, Taku Izubuchi, Amarjit Soni, "Neutron and proton electric dipole moments from Nf=2+1Nf=2+1 domain-wall fermion lattice QCD", Phys.Rev. D93 (2016) no.9, 094503

Michael G. Endres, Andrea Shindler, Brian C. Tiburzi, Andre Walker-Loud, "Massive photons: an infrared regularization scheme for lattice QCD + QED", Physical Review Letters, Volume 117, Article 072002, 2016/8/10*

Matthew E. Matzelle, Brian C. Tiburzi, "Finite-volume corrections to electromagnetic masses for larger-than-physical electric charges", Physical Review D Volume 95, Article 094510 2017/5/30*

Asumpta Parreño, Martin J. Savage, Brian C. Tiburzi, Johnas Wilhelm, Emmanuel Chang, William Detmold, Kostas Orginos
(NPLQCD Collaboration), "Octet baryon magnetic moments from lattice QCD: Approaching experiment from a three-flavor symmetric point", Physical Review D, in press, 2017*

Martin J. Savage, Phiala E. Shanahan, Brian C. Tiburzi, Michael L. Wagman, Frank Winter, Silas R. Beane, Emmanuel Chang, Zoreh Davoudi, William Detmold, Kostas Orginos (NPLQCD Collaboration), "Proton-proton fusion and tritium beta decay from lattice quantum chromodynamics", arXiv:1610.04545v1 [hep-lat] 2016/10/14

T. DeGrand, M. Golterman, W. I. Jay, E. T. Neil, Y. Shamir and B.Svetitsky.
"Radiative contribution to the effective potential in composite Higgs models from lattice gauge theory." Phys. Rev. D94:5, 054501 (2016). arXiv:1606.02695.

T. DeGrand, M. Golterman, E. T. Neil and Y. Shamir. "One-loop Chiral Perturba-tion Theory with two fermion representations", Phys. Rev. D94:2, 025020(2016).arXiv:1605.07738.

G. D. Kribs and E. T. Neil. "Review of strongly-coupled composite dark matter models and lattice simulations", IJMPA 31:22, 1643004 (2016).arXiv:1604.04627.

Jeremy Green, Nesreen Hasan, Stefan Meinel, Michael Engelhardt, Stefan Krieg, Jesse Laeuchli, John Negele, Kostas Orginos, Andrew Pochinsky, Sergey Syritsyn,""Up, down, and strange nucleon axial form factors from lattice QCD", Accepted by Phys. Rev. D arXiv:1703.06703 [hep-lat]

A. Datta, S. Kamali, S. Meinel, A. Rashed. "Phenomenology of $\Lambda b \to \Lambda c \tau \bar{\nu}_\tau$ using lattice QCD calculations", arXiv:1702.02243 [hep-ph] Submitted to JHEP RBRC-1228

S. Meinel. “Λc → Λl+νl form factors and decay rates from lattice QCD with physical quark masses”, arXiv:1611.09696 [hep-lat] Phys. Rev. Lett. 118, no. 8, 082001 (2017) RBRC-1216

T.Ishikawa, Y.Q.Ma, J.W.Qiu and S.Yoshida, “Practical quasi parton distribution functions," arXiv:1609.02018 [hep-lat] (* under peer review)

Yasumichi Aoki, Tatsumi Aoyama, Ed Bennett, Masafumi Kurachi, Toshihide Maskawa, Kohtaroh Miura, Kei-ichi Nagai, Hiroshi Ohki, Enrico Rinaldi, Akihiro Shibata, Koichi Yamawaki, Takeshi Yamazaki (the LatKMI Collaboration), “Light flavor-singlet scalars and walking signals in Nf=8 QCD on the lattice”

Y. Aoki et al. “Review of lattice results concerning low-energy particle physics “, Jul 1, 2016. 383 pp. Published in Eur.Phys.J. C77 (2017) no.2, 112

[Proceedings]

(Original Papers) *Subject to Peer Review

Taku Izubuchi, Michael Abramczyk, Tom Blum, Hiroshi Ohki, Sergey Syritsyn, “Calculation of Nucleon Electric Dipole Moments Induced by Quark Chromo-Electric Dipole Moments”, PoS LATTICE2016 (2017) 398

Kim Maltman, Renwick Hudspith, Taku Izubuchi, Randy Lewis, Hiroshi Ohki, James Zanotti. “VusVus from inclusive determinations based on hadronic tau data”, PoS LATTICE2016 (2017) 279

Jonathan Flynn, Taku Izubuchi, Andreas Juttner, Taichi Kawanai, Christoph Lehner, Edwin Lizarazo, Amarjit Soni, Justus Tobias Tsang, Oliver Witzel. “Form factors for semi-leptonic BB decays”, PoS LATTICE2016 (2016) 296.

Matthew Spraggs, Peter A. Boyle, Luigi Del Debbio, Taku Izubuchi, Andreas Jüttner, Christoph Lehner, Kim Maltman, Marina Krstic Marinkovic, Antonin Portelli. “Computing the muon anomalous magnetic moment using the hybrid method with physical quark masses”, PoS LATTICE2016 (2016) 184

Luchang Jin, Thomas Blum, Norman Christ, Masashi Hayakawa, Taku Izubuchi, Chulwoo Jung, Christoph Lehner. “The connected and leading disconnected diagrams of the hadronic light-by-light contribution to muon g−2”, PoS LATTICE2016 (2016) 181

Kim Maltman, Renwick James Hudspith, Randy Lewis, Taku Izubuchi, Hiroshi Ohki, James M. Zanotti. “Determinations of Vuu using inclusive hadronic τ decay data”, Published in Mod.Phys.Lett. A31 (2016) no.29, 1630030

Kim Maltman, Renwick J. Hudspith, Randy Lewis, Taku Izubuchi, Hiroshi Ohki, James Zanotti, “Determinations of VusVus from Hadronic τ Decay Data”, PoS FPCP2016 (2017) 023

Martin J. Savage, Phiala E. Shanahan, Brian C. Tiburzi, Michael L. Wagman, Frank Winter, Silas R. Beane, Emmanuel Chang, Zoreh Davoudi, William Detmold, Kostas Orginos, (NPLQCD Collaboration). “Axial-current matrix elements in light nuclei from lattice QCD”, Proceedings of the 38th International Conference on High Energy Physics, PoS (ICHEP2016), 506

Amy Nicholson, Evan Berkowitz, Chia Cheng Chang, M. A. Clark, Balint Joo, Thorsten Kurth, Enrico Rinaldi, Brian Tiburzi, Pavlos Vranas, Andre Walker-Loud,(CalLat Collaboration), “Neutrinoless double beta decay from lattice QCD” Proceedings of the 34th International Symposium on Lattice Field Theory, PoS (LATTICE2016), 017

C. C. Chang et al. (Fermilab Lattice/MILC Collaborations). “D-Meson Mixing in 2+1-Flavor Lattice QCD.” Proceedings of Science (LATTICE 2016).FERMILAB-CONF-17-017-T.

J. Komijiani et al. (Fermilab Lattice/MILC Collaborations). “Decay constants fB and fBs and quark masses mb and mc from HISQ simulations.” Proceedings of Science (LATTICE 2016). FERMILAB-CONF-16-545-T.

E. Gamiz et al. (Fermilab Lattice/MILC Collaborations). “Kaon semileptonic decays with Nf = 2 + 1 + 1 HISQ fermions and physical light-quark masses.” Proceedings of Science (LATTICE 2016). FERMILAB-CONF-16-544-T.

T. A. DeGrand, D. Hackett, W. I. Jay, E. T. Neil, Y. Shamir, and B. Svetitsky. “Towards Partial Compositeness on the Lattice: Baryons with Fermions in Multiple Representations.” Proceedings of Science (LATTICE 2016).

N. Hasan, M. Engelhardt, J. Green, S. Krieg, S. Meinel, J. Negele, A. Pochinsky, S. Syritsyn, “Computing the nucleon Dirac radius directly at Q2 = 0” arXiv:1611.01383 [hep-lat] PoS LATTICE 2016, 147 (2016) RBRC-1216

Luka Leskovec, Constantia Alexandrou, Giannis Koutsou, Stefan Meinel, John W. Negele, Srijit Paul, Marcus Petschlies, Andrew Pochinsky, Gumaro Rendon, Sergey Syritsyn. “A study of the radiative transition ππ → πγ∗ with lattice QCD” arXiv:1611.00282 [hep-lat], PoS LATTICE 2016, 159 (2016)RBRC-1214

A. Peters, P. Bicudo, L. Leskovec, S. Meinel, M. Wagner. “Lattice QCD study of heavy-heavy-light-light tetraquark candidates”, arXiv:1609.00181 [hep-lat], PoS LATTICE 2016, 104 (2016), RBRC-1213

S. Meinel, G. Rendon. “Lattice QCD calculation of form factors for Λb → Λ(1520)l+l− decays”, arXiv:1608.08110 [hep-lat], PoS LATTICE, 2016, 299 (2016), RBRC-1203

T. Ishikawa, Y. Q. Ma, J. W. Qiu and S. Yoshida, “`Matching issue in quasi parton distribution approach”, PoS LATTICE2016, 177 (2016).

S. Syritsyn, A. Gambhir, B. Musch, K. Orginos,"Constructing Nucleon Operators on a Lattice for Form Factors with High Momentum Transfer", in proceedings of International Symposium LATTICE2016, Southampton, July 24-30; PoS LATTICE2016 (2017) 176.

T. Izubuchi, M. Abramczyk, T. Blum, H. Ohki, S. Syritsyn, "Calculation of Nucleon Electric Dipole Moments Induced by Quark Chromo-Electric Dipole Moments", in proceedings of International Symposium LATTICE2016, Southampton, July 24-30; PoS LATTICE2016 (2017) 398; arXiv:1702.00052.

L. Leskovec, C. Alexandrou, G. Koutsou, S. Meinel, J. W. Negele, S. Paul, M. Petschlies , A. Pochinsky, G. Rendon, S. Syritsyn, "A study of the radiative transition pi pi to pi gamma star with lattice QCD", in proceedings of International Symposium LATTICE2016, Southampton, July 24-30; PoS LATTICE2016 (2017) 159 ; arXiv:1611.00282.

Oral Presentations

[International Conference etc.]

Taku Izubuchi. “Lattice calculation for the light-by-light hadronic contribution to muon g-2”, 14th international workshop on Tau Lepton Physics, IHEP, Beijing, China,19-23 September.

Taku Izubuchi. “Search for beyond standard model and QCD”, the 14th international conference on Menuson-Nucleon Physics and Structure of the Nucleon MENU2016, Kyoto University, Japan July 25-30

Taku Izubuchi. “Muon g-2 Light-by-light on Lattice and Related Topics” Precision for New discoveries, TRIUMF, Vancouver, Canada, June 8-10.

Taku Izubuchi. “Muon g-2 theory status”, Flavor Physics and CP violation 2016 (FPCP) 2016, at Caltech, Pasadena, CA, June 6-9.

Taku Izubuchi, ”Muon g-2 Hadronic Light by Light: Lattice QCD”, Invited talk, Symposium on Effective Field Theories and Lattice Gauge Theory at Institute for Advanced Study, Technical University Munich, May 18-21.

Brian C. Tiburzi. “Going to Extremes: Lattice QCD in External Fields”, Invited talk, Maryland Center for Fundamental Physics, University of Maryland, 11/16/2016.

Brian C. Tiburzi. “Going to Extremes: Lattice QCD in External Fields”, Invited talk, Lawrence Berkeley National Laboratory, Berkeley, California, 11/8/2016.

Brian C. Tiburzi. “New features of baryon magnetic moments uncovered from lattice QCD”, Invited talk, TP Program “Frontiers in Nuclear Physics”, Kavli Institute for Theoretical Physics, Santa Barbara, California, 9/16/2016.

Brian C. Tiburzi. “Magnetic properties of light nuclei from lattice QCD”, Invited talk, INT Program 16-1 “Nuclear Physics from Lattice QCD”, Institute for Nuclear Theory, Seattle, Washington, 5/15/2016.

Ethan Neil. “Lattice study of gauge theory with multiple fermion representations.”, RIKEN Lunch Seminar, Brookhaven National Laboratory, Upton, NY. May 2017.

Ethan Neil. “Lattice Insights for Composite BSM Models.” High Energy/Cosmology Seminar, University of Wisconsin, Madison, WI. March 2017.

Ethan Neil “Lattice Insights for Composite BSM Searches.” Future Colliders Seminar series, Fermilab, Batavia, IL. December 2016.

Stefan Meinel. “Heavy baryon decay form factors from lattice QCD,” International Workshop on Hadronic Contributions to New Physics Searches, Puerto de la Cruz, Spain (invited talk) September 27, 2016.

Stefan Meinel “Flavor physics with Λb baryons,” 38th International Conference on High Energy Physics, Chicago, USA (invited talk) August 5 2016,

Stefan Meinel “Lattice QCD calculation of form factors for $\Lambda_b \to \Lambda(1520) l^+ l^-$ decays,” 34th International Symposium on Lattice Field Theory, University of Southampton, UK, July 29, 2016,

Stefan Meinel “Flavor physics with Λb baryons,” Fermilab Theory Seminar, Batavia, USA (invited talk) June 2, 2016.

Stefan Meinel “Heavy Baryons on the Lattice,” International Conference on the Structure of Baryons, Florida State University, Tallahassee, USA (invited talk) May 18, 2016.

Stefan Meinel “Lattice results and outlook,” Prospects and challenges for semitauonic decays at LHCb, CERN, Geneva, Switzerland (invited talk, given remotely) April 28, 2016,

T. Ishikawa. "Matching for quasi parton distribution functions”, 22nd International Spin Symposium 2016, 25-30 September 2016, University of Illinois, Urbana-Champaign, USA.

T. Ishikawa, "Matching issue in quasi parton distribution approach”, The 34th International Symposium on Lattice Field Theory, 24-30 July 2016, University of Southampton, UK.

S. Syritsyn, "Nucleon Form Factors at High Momentum Transfer", parallel presentation at the International Symposium LATTICE2016, Southampton, July 24-30.

S. Syritsyn, "On Lattice Calculation of Nucleon Electric Dipole Moments", HET Lunch seminar, Brookhaven National Laboratory, March 2, 2017.

S. Syritsyn, "On Lattice Calculation of Nucleon Electric Dipole Moments", Nuclear Theory seminar at Stony Brook University, March 2, 2017.

Ohki Hiroshi. “Determination of |Vus| from hadronic tau decays”, The international workshop on future potential of high intensity accelerators for particle and nuclear physics (HINT2016), J-PARC, Tokai-village, Ibaraki, Japan, Dec. 6, 2016.

Ohki Hiroshi. “Lattice calculation of Vus from inclusive strangeness changing tau decay”, The 14th International Workshop on Tau Lepton Physics (Tau2016), IHEP, Beijing, September 19, 2016.

Ohki Hiroshi “Vus from inclusive strange tau decay data and lattice HVP”, The 34the International Symposium on Lattice Field Theory, Highfield Campus, University of Southampton, July 28, 2016.

Ohki Hiroshi. “Many-flavor QCD dynamics on the lattice”, Lattice for Beyond the Standard Model Physics 2016, Argonne National Laboratory, April 21, 2016.

E. Rinaldi, “Lattice Gauge Theory insights on Dark Matter”, at the Dark Interactions Workshop, BNL, Upton, NY, 10/06/2016

E. Rinaldi, “Dark Interactions and the Lattice”, at the Frontiers in Nuclear Physics Program, KITP, Santa Barbara, CA, 11/03/2016

E. Rinaldi, “An overview of lattice field theory applications to dark matter searches”, RIKEN lunch seminar, BNL, 11/10/2016

E. Rinaldi, “Dark Interactions and Lattice Gauge Theories”, at the Early Career Researcher Symposium, BNL, Upton, NY, 12/13/2016

E. Rinaldi, “What lattice gauge theory can do for Dark Matter searches”, at Università di Roma “La Sapienza”, Rome, Italy, 02/23/2017

E. Rinaldi, “Beyond the Standard Model Physics with Lattice Simulations”, at Università di Roma “Tor Vergata”, Rome, Italy, 03/01/2017

[Domestic Conference]

Taku Izubuchi. “Lattice QCD computation for muon’s anomalous magnetic moment”, Talk at seminar, Yukawa Institute, Kyoto University, March 24.

Taku Izubuchi. “Lattice QCD computation for muon’s anomalous magnetic moment”, Talk at seminar, Kanazawa University, March 21.

Taku Izubuchi, “Lattice QCD computation for muon’s anomalous magnetic moment” Invited talk, Japan Physics Society annual meeting, Osaka University, March 19.

青木 保道 “素粒子質量起源の理論探索 (Theoretical exploration of the origin of mass of elementary particles)”, 第 3 回「京」を中心とする HPCI システム利用課題成果報告会, コクヨホール（東京都）2016/10/21

青木 保道 “QCD の有限温度相転移とトポロジー”, 素粒子・原子核・宇宙「京からポスト京に向けて」シンポジウム,筑波大学東京キャンパス（東京都）2017/2/17

青木 保道 “有限温度 2 フレーバーQCD のトポロジカル感受率 (Topological susceptibility of the finite-temperature two-flavor QCD)”, 大阪大学 日本物理学会第 72 回年次大会 (JPS meeting 2017/3/18)

大木 洋. “物質優勢宇宙の謎解明のための核子構造精密計算”, 2016 年度, 理研シンポジウム「スーパーコンピューターHOKUSAI と Shoubu、研究開発の最前線」和光市理化学研究所, 2016 年 6 月 8 日.

大木 洋. “核子(chromo) EDM 演算子の格子計算”, 日本物理学会第 72 回年次大会、大阪大学, March 19, 2017.

Sub Nuclear System Research Division
RIKEN-BNL Research Center
Experimental Group

1. Abstract

RIKEN BNL Research Center (RBRC) Experimental Group studies the strong interactions (QCD) using RHIC accelerator at Brookhaven National Laboratory, the world first heavy ion collider and polarized p+p collider. We have three major activities: Spin Physics at RHIC, Heavy ion physics at RHIC, and detector upgrades of PHENIX experiment at RHIC.

We study the spin structure of the proton using the polarized proton-proton collisions at RHIC. This program has been promoted by RIKEN's leadership. The first focus of the research is to measure the gluon spin contribution to the proton spin. Recent results from PHENIX pi0 measurement and STAR jet measurement has shown that gluons in the proton carry about 30% of the proton spin. This is a major milestone of RHIC spin program. The second goal of the spin program is to measure the polarization of anti-quarks in the proton using W→e and W→μ decays. The results of W->e measurement was published.

The aim of Heavy ion physics at RHIC is to re-create Quark Gluon Plasma (QGP), the state of Universe just after the Big Bang. Two important discoveries, jet quenching effect and strong elliptic flows, have established that new state of dense matter is indeed produced in heavy ion collisions at RHIC. We are now studying the property of the matter. Recently, we have measured direct photons in Au+Au collisions for $1<p_T<3$ GeV/c, where thermal radiation from hot QGP is expected to dominate. The comparison between the data and theory calculations indicates that the initial temperature of 300 MeV to 600 MeV is achieved. These values are well above the transition temperature to QGP, which is calculated to be approximately 160 MeV by lattice QCD calculations.

We had major roles in detector upgrades of PHENIX experiment, namely, the silicon vertex tracker (VTX) and muon trigger upgrades. Both of the upgrade is now complete. The VTX is the main device to measure heavy quark (charm and bottom) production and the muon trigger is essential for W→μ measurement. The results from the first run with VTX detector in 2011 was published. The results show that electrons from bottom quark decay is strongly suppressed at high pT, but the suppression is weaker than that of charm decay electron for $3<pT<4$ GeV/c. We have recorded 10 times as much Au+Au collisions data in each of the 2014 run and 2016 run. The large dataset will produce definitive results on heavy quark production at RHIC.

PHENIX completed its data taking in 2016. We are now working on R&D of intermediate silicon tracker INTT for sPHENIX, a new experiment at RHIC that will be installed in the PHENIX IR.

2. Major Research Subjects

(1) Experimental Studies of the Spin Structure of the Nucleon
(2) Study of Quark-Gluon Plasma at RHIC
(3) PHENIX detector upgrades

3. Summary of Research Activity

We study the strong interactions (QCD) using the RHIC accelerator at Brookhaven National Laboratory, the world first heavy ion collider and polarized p+p collider. We have three major activities: Spin Physics at RHIC, Heavy ion physics at RHIC, and detector upgrades of PHENIX experiment.

(1) Experimental study of spin structure of proton using RHIC polarized proton collider

How is the spin of proton formed with 3 quarks and gluons? This is a very fundamental question in Quantum Chromodynamics (QCD), the theory of the strong nuclear forces. The RHIC Spin Project has been established as an international collaboration between RIKEN and Brookhaven National Laboratory (BNL) to solve this problem by colliding two polarized protons for the first time in history. This project also has extended the physics capabilities of RHIC.

The first goal of the Spin Physics program at RHIC is to determine the gluon contribution to proton spin. It is known that the spin of quark accounts for only 25% of proton spin. The remaining 75% should be carried either by the spin of gluons or the orbital angular momentum of quarks and gluons. One of the main goals of the RHIC spin program has been to determine the gluon spin contribution. Before the start of RHIC, there was little experimental constraint on the gluon polarization, ΔG.

PHENIX measures the double helicity asymmetry (A_{LL}) of π^0 production to determine the gluon polarization. Our most recent publication of pi0 ALL measurement at 510 GeV shows non-zero value of ALL, indicating that gluons in the proton is polarized. Global analysis shows that approximately 30% of proton spin is carried by gluons.

RHIC achieved polarized p+p collisions at 500 GeV in 2009. The collision energy increased to 510 GeV in 2012 and 2013. The main goal of these high energy p+p run is to measure anti-quark polarization via single spin asymmetry A_L of the W production. We upgraded the muon trigger system to measure W→m decays in the forward direction. With the measurement of W→ e and W→μ, we can cover a wide kinematic range in anti-quark polarization measurement. The 2013 run is the main spin run at 510 GeV. PHENIX has recorded more than 150/pb of data in the run. The final results of the A_L measurement in W→ e channel in combined data of 2011 to 2013 was published. The high statistics results give strong constraints on the polarization of anti-quarks in the proton. The analysis of W→μ is in progress.

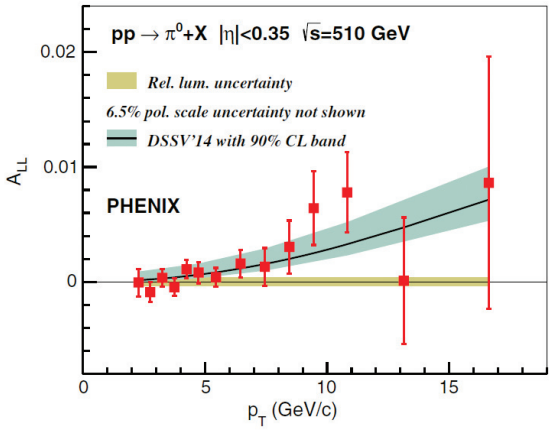

Figure 1 Double spin asymmetry ALL in π^0 production as function of transverse momentum pT. The non-zero ALL indicates that gluons in the proton is polarized. Published in Physical Review D93,011501 (2016)

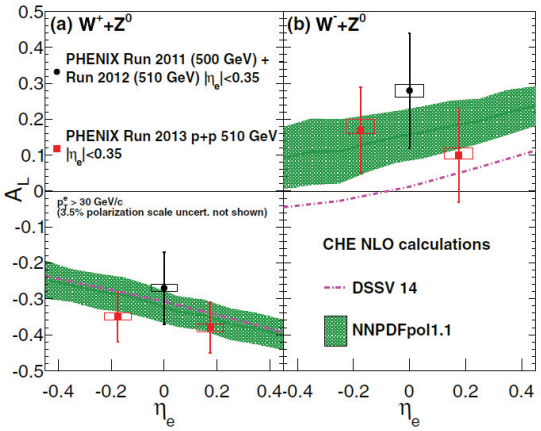

Figure 2 Single spin asymmetry AL of electrons from W and Z decays. The AL is sensitive to the polarization of anti-quarks in the proton. The curves and green shaded region show theoretical calculations based on various polarized parton distribution (PDF) sets. Published in Physical Review D93, 051103(R) (2016)

(2) Experimental study of Quark-Gluon Plasma using RHIC heavy-ion collider

The goal of high energy heavy ion physics at RHIC is study of QCD in extreme conditions i.e. at very high temperature and at very high energy density. Experimental results from RHIC have established that dense partonic matter is formed in Au+Au collisions at RHIC. The matter is very dense and opaque, and it has almost no viscosity and behaves like a perfect fluid. These conclusions are primarily based on the following two discoveries:

- Strong suppression of high transverse momentum hadrons in central Au+Au collisions (jet quenching)
- Strong elliptic flow

These results are summarized in PHENIX White paper, which has approximately 2400 citations to date.

The focus of the research in heavy ion physics at RHIC is now to investigate the properties of the matter. RBRC have played the leading roles in some of the most important results from PHENIX in the study of the matter properties. These include (1) measurements of heavy quark production from the single electrons from heavy flavor decay (2) measurements of J/Psi production (3) measurements of di-electron continuum and (4) measurements of direct photons.

The most important recent result is the measurement of direct photons for $1<p_T<5$ GeV/c in p+p and Au+Au through their internal conversion to e+e- pairs. If the dense partonic matter formed at RHIC is thermalized, it should emit thermal photons. Observation of thermal photon is direct evidence of early thermalization, and we can determine the initial temperature of the matter. It is predicted that thermal photons from QGP phase is the dominant source of direct photons for $1<p_T<3$ GeV/c at the RHIC energy. We measured the direct photon in this p_T region from measurements of quasi-real virtual photons that decays into low-mass e+e- pairs. Strong enhancement of direct photon yield in Au+Au over the scaled p+p data has been observed. Several hydrodynamical models can reproduce the central Au+A data within a factor of two. These models assume formation of a hot system with initial temperature of Tinit = 300 MeV to 600 MeV. This is the first measurement of initial temperature of quark gluon plasma formed at RHIC. These results are recently published in Physical Review Letters. Y. Akiba is the leading person of the analysis and the main author of the paper. **He received 2011 Nishina memorial Prize mainly based on this work.**

(3) PHENIX detector upgrade

The group had major roles in several PHENIX detector upgrades, namely, the silicon vertex tracker (VTX) and muon trigger upgrades. VTX is a high precision charged particle tracker made of 4 layers of silicon detectors. It is jointly funded by RIKEN and the US DOE. The inner two layers are silicon pixel detectors and the outer two layers are silicon strip detectors. Y. Akiba is the project manager and A. Deshpande is the strip system manager. The VTX detector was completed in November 2010 and subsequently installed in PHENIX. The detector started taking data in the 2011 run. With the new detector, we measure heavy quark (charm and bottom) production in p+p, A+A collisions to study the properties of quark-gluon plasma. The final result of the 2011 run was published. The result show that single electrons from bottom quark decay is suppressed, but not as strong as that from charm decay in low pT region (3<pT<4 GeV/c). This is the first measurement of suppression of bottom decay electrons at RHIC and the first observation that bottom suppression is smaller than charm. We have recorded 10 times as much Au+Au collisions data in each of the 2014 run and 2016 run. The large dataset will produce definitive results on heavy quark production at RHIC.

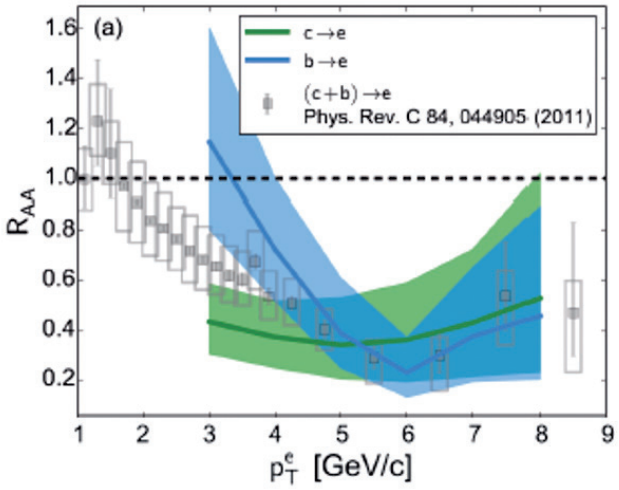

Figure 3. Nuclear modification factor RAA for single electrons from charm (green band) and bottom (blue band) decays. Published in Physical Review C93, 034904 (2016)

PHENIX completed its data taking in 2016. We are now working on R&D of intermediate silicon tracker INTT for sPHENIX, a new experiment at RHIC that will be installed in the PHENIX IR.

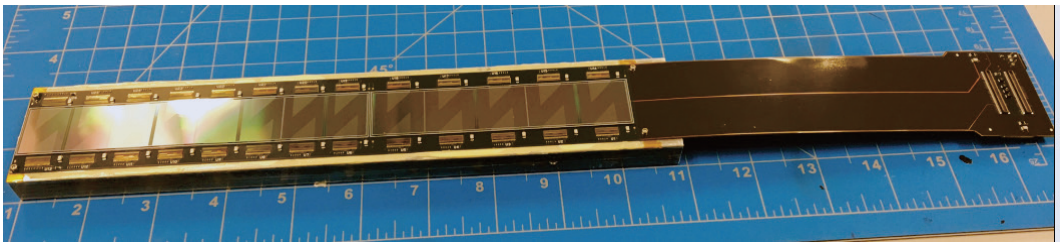

Figure 4. A prototype of sensor module of INTT silicon tracker for sPHENIX experiment

Members

Group Leader (Lab. Head)

Yasuyuki AKIBA (Deputy Chief Scientist)

Deputy Group Leader

Abhay DESHPANDE

RBRC Researcher

Xiaorong WANG (RHIC Physics Fellows)
Takashi HACHIYA
Yorito YAMAGUCHI
Gaku MITSUKA
Yasushi WATANABE (RIKEN Spin Program Researcher, concurrent: Radiation Lab.)
Yuji GOTO (RIKEN Spin Program Researcher, concurrent: Radiation Lab.)

Itaru NAKAGAWA (RIKEN Spin Program Researcher, concurrent: Radiation Lab.)
Takashi ICHIHARA (RIKEN Spin Program Researcher, concurrent: RI Physics Lab.)
Atsushi TAKETANI (RIKEN Spin Program Researcher, concurrent: Neutoron Beam Technology Team, Advanced Photonics Technology development Group, RAP)
Satoshi YOKKAICHI (RIKEN Spin Program Researcher, concurrent: Radiation Lab.)
Ralf SEIDL (RIKEN Spin Program Researcher, concurrent: Radiation Lab.)

Visiting Scientists

Stefan BATHE (Baruch College University of New York)
Ady HERSHCOVITCH (RBRC Collaborating Scientist, BNL)
Akio OGAWA (BNL)
Rachid NOUICER (RBRC Collaborating Scientist)
Masahiro OKAMURA (concurrent: BNL)
Takao SAKAGUCHI (BNL)

List of Publications & Presentations

Publications

[Journal]

(Original Papers)

G Mitsuka ”Recently measured large AN for forward neutron in pA collisions at sqrt(s)=200 GeV explained through simulations of ultraperipheral collisions and hadronic interactions”, Physical Review C95, 044908 (2017)

Oral Presentations

[International Conference etc.]

Takashi Hachiya, “Recent results on open and closed heavy flavor from PHENIX at RHIC”, ICHEP2016
Takashi Hachiya, “Recent heavy flavor measurements from PHENIX at RHIC”, ISMD2016
Takashi Hachiya, “Recent results on heavy flavor production at RHIC-PHENIX”, INPC2016
Gaku Mitsuka, ”Disentangling transverse single spin asymmetry for very forward neutrons in polarized pA collisions using ultra-peripheral collisions ”, 25th International Workshop of Deep Inelastic Scattering (DIS2017)

[Domestic Conference]

Gaku Mitsuka, “RHIC 単スピン非対称測定に対する ultra-peripheral collision の影響” , 日本物理学会 第 72 回年次大会

Posters Presentations

[International Conference etc.]

Gaku Mitsuka ”sPHENIX Intermediate silicon tracker INTT” Quark Matter 2017

Sub Nuclear System Research Division
RIKEN Facility Office at RAL

1. Abstract

Our core activities are based on the RIKEN-RAL Muon Facility located at the Rutherford Appleton Laboratory (UK), which provides intense pulsed-muon beams. Muons have their own spins with 100% polarization, and can detect local magnetic fields and their fluctuations at muon stopping sites very precisely. The method to study characteristics of materials by observing time dependent changes of muon spin polarization is called "Muon Spin Rotation, Relaxation and Resonance (μSR method), and is applied to study electro-magnetic properties of insulating, metallic, magnetic and superconducting systems. Muons reveal static and dynamic properties of the electronic state of materials in the zero-field condition, which is the ideal magnetic condition for research on magnetism. We have carried out μSR investigations on frustrated pyrochlore systems, which have a variety of exotic ground states of magnetic spins, so the magnetism study of this system using muons is quite unique.

The ultra-slow muon beam can be stopped in thin foil, multi-layered materials and artificial lattices, which enables us to apply the μSR techniques to surface and interface science. The development of an ultra-slow muon beam is also very important as a source of ultra-cold (pencil-like small emittance) muon beam for muon g-2/EDM measurement. We have been developing muonium generators to create more muonium atoms in vacuum even at room temperature to improve beam quality compared with the conventional hot-tungsten muonium generator. We demonstrated a tremendous increase of the muonium emission efficiency by fabricating fine laser drill-holes on the surface of silica aerogel. We also developed a high power Lyman-alpha laser in collaboration with the Advanced Photonics group at RIKEN. The new laser will ionize muonium atoms 100 times more efficiently for slow muon beam generation.

2. Major Research Subjects

(1) Materials science by muon-spin-relaxation method
(2) Hyperfine interactions at muon sites studied by the computation science
(3) Nuclear and particle physics studies via muonic atoms and ultra-cold muon beam

3. Summary of Research Activity

(1) Material Science at the RIKEN-RAL Muon Facility

Muons have their own spins with 100% polarization, and can detect local magnetic fields and their fluctuations at muon stopping sites very precisely. The μSR method is applied to studies of newly fabricated materials. Muons enable us to conduct (1) material studies under external zero-field condition, (2) magnetism studies with samples without nuclear spins, and (3) measurements of muon spin relaxation changes over a wide temperature range with same detection sensitivity. The detection time range of local field fluctuations by μSR is 10^{-6} to 10^{-11} second, which is an intermediate region between neutron scattering methods (10^{-10}-10^{-12} second) and Nuclear Magnetic Resonance (NMR) (longer than 10^{-6} second). At Port-2 and 4 of the RIKEN-RAL Muon Facility, we have been performing μSR research on strong correlated-electron systems, organic molecules and biological samples to study electron structures, superconductivity, magnetism, molecular structures and crystal structures.

In the period from 2015 to 2017, we have obtained excellent results, and the highlights are listed in the following,

1) The superconducting gap state of λ-$[BETS]_2GaCl_4$ has both the *s*- and *d*-wave characters.
2) A static ordering in the Ca-doped pyrochlore iridate; $(Nd_{1-x}Ca_x)_2Ir_2O_7$ is strongly suppressed by the carrier doping.
3) A long-range magnetic ordering is observed in alkali-metal superoxides of CsO_2 and RbO_2 but not in NaO_2.
4) Missing of a static ordering is confirmed in both Au144 and Au25 nano-clusters.
5) The quantum spatial distribution of the muon by the zero-point vibration energy is clarified by density functional theory calculations by using the RIKEN supercomputing system. HOKUSAI.

Result-1) One dimensional organic superconductor, λ-$[BETS]_2GaCl_4$, has a unique Fermi-surface structure with the four-fold nodal points. The estimation of the superconducting gap from computational analysis of μSR experimental data indicates a unique view of the supeconducting gap to be a mixed state of the major *s*-wave component and the minor *d*-wave one. Result-2) Static orderings of both Nd and Ir magnetic spins are strongly suppressed by the carrier doping. A quantum critical change to the non-magnetic ground state is expected around x=0.10 being accompanied by changes in the transport properties. Result-3) The π electrons which are widely distributed on the O_2 dumbbell in superoxides CsO_2 and RbO_2 are found to form static long-range orderings. The magnetic moment is quantitatively estimated in conjunction with density functional theory calculations and confirmed to shrink to less than a half in the magnetically ordered state. Result-4) Ground states of nano-cluster of Au with 144 and 25 atoms are concluded to be still nonmagnetic down to 0.3 K from both the magnetic susceptibility and μSR measurements although those systems have been argued to show some static magnetic states. Result-5) The muon trapped in materials is confirmed to be spatially distributed around the local minimum potential position by the zero-point vibration energy, which is due to the muon's physics character as a light particle. This quantum spatial distribution is now taken into account for the μSR data analysis with the similar quantum spatial distribution of magnetic moments.

We are developing international collaborations on the muon science with Asian groups in order to organize new μSR experimental research themes and to develop muon-site calculation activities using computational method. We renewed MOU's with Indonesian and Malaysian universities to enhance collaborative researches on the muon science at the RIKEN-RAL Muon Facility. We formed a new MOU with Universitus Indonesia (UI) as a new partner to work on the muon science and student education. We are developing new collaborations in μSR experiments on strongly correlated systems with researchers from China, Taiwan and Korea including graduate students.

(2) Ultra Slow (low energy) Muon Beam Generation and Applications

A positive muon beam with thermal energy has been produced by laser ionization of muonium atoms (bound system of μ^+ and electron) emitted from hot tungsten surface with stopping surface muon beam at Port-3. The method generates a positive muon beam with acceleration energy from several 100 eV to several 10 keV, small beam size (a few mm) and good time resolution (less than 8 nsec). By stopping the ultra-slow muon beam in thin foil, multi-layered materials and artificial lattices, we can precisely measure local magnetic field in the materials, and apply the μSR techniques to surface and interface science. Since there has been no appropriate probe to study magnetism at surface and interface, the ultra-slow muon beam will open a new area of these research fields. In addition, the development of ultra-slow muon beam is very important as the source of ultra-cold (pencil-like small emittance) muon beam for muon g-2/EDM measurement. It is essential to increase the slow muon beam production efficiency by 100 times for these applications. There are three key techniques in ultra-slow muon generation: production of thermal muonium, high intensity Lyman-alpha laser and the ultra-slow muon beam line.

In the period from 2011 to 2016, we developed a high power Lyman-alpha laser in collaboration with the Advanced Photonics group at RIKEN. The new laser will ionize muoniums 100 times more efficiently for slow muon beam generation. This development was funded mostly by the Grant-in-Aid for Scientific Research on Innovative Areas “Frontier in Materials, Life and Particle Science Explored by Ultra Slow Muon Microscope”. This Grant-in-Aid research group is a complex of research institutions from universities together with J-PARC muon group and RIKEN. The new laser system was installed to J-PARC slow muon beam line and is being used for the generation of ultra-slow muons. In this development, we succeeded in synthesizing a novel ceramic-based Nd:YGAG crystal. We already achieved 10 times increase in Lyman-alpha intensity and are waiting the growth of a large crystal to achieve the goal of 100 times increase. This crystal can also be applicable to the flash-lamp based Lyman-alpha laser system of RIKEN-RAL to realize substantial improvement of the laser power at a much reduced cost based on our experience so far.

We also aimed to realize drastic improvements on the ultra-slow muon source with much reduced emittance. We have been developing muonium generators to create more muoniums in vacuum even at room temperature. In 2013, we demonstrated at least 10 times increase of the muonium emission efficiency in one of the silica aerogel samples with fine holes fabricated on the surface. The measurement was carried out at TRIUMF in collaboration with J-PARC muon g-2/EDM group. In 2016 we studied the method of stable production of various laser drill-holes with Canadian collaborators so we can increase the muonium emission by systematic study of muonium emission under various target conditions.

We are planning to feed these new techniques to RIKEN-RAL ultra-slow muon beam line to realize further improvement of ultra-slow muon technology. The muonium production target section, which had been designed with hot tungsten, was completely redesigned and rebuilt to use advantages of the new room temperature silica aerogel target, such as no need of thermal shielding and spin control by applying weak magnetic field, etc. Also, we adopted an all-cylindrical beam-transport design, because of its simpler optics and better manufacture precision, which will contribute to the ultimate cold muon source required for muon g-2/EDM. In test experiments with the muon beam in 2016, we demonstrated a new powerful method of the muon stopping optimization in silica aerogel using muonium spin rotation.

(3) New Proposal for Fundamental Physics

We proposed the measurement of the proton radius by using the hyperfine splitting of the 1S states of muonic hydrogen. Recent measurement of the proton radius using muonic hydrogen at PSI revealed that the proton radius is surprisingly smaller than the radius so far measured using normal hydrogen spectroscopy and e-p scattering by more than 5 times their experimental precision. In contrast to the conventional measurement by means of electron, measurement with muonic hydrogen has larger sensitivity to the proton radius because the negative muon orbits closer to the proton, although there is no reason why these measurements can yield inconsistent results. The cause of the discrepancy is not understood yet, thus a new measurement with independent method is much anticipated.

There are two independent experimental proposals to RIKEN-RAL PAC to measure the hyperfine splitting energy of the 1S energy levels by laser excitation from singlet ground state to triplet state. This energy splitting is sensitive to the Zemach radius, which is a convolution of charge and magnetic distributions inside proton. Both commonly search resonant excitation from singlet 1S (F=0) to triplet 1S (F=1) using high intensity 6.7 μm excitation laser, but different schemes are proposed to detect the resonance. One is to detect muon transfer to the surrounding impurity atom by x-ray (European group), and the other is to detect the muon decay asymmetry recovery along the circularly polarized excitation laser, which selectively excites one of the F=1 states and regenerates the muon spin polarization (RIKEN group). RIKEN-RAL PAC accepted both proposals for feasibility studies.

RIKEN laser group made basic design of the laser system, based on their recent success on mid-infared (6 μm) high-power pulse laser system. There is no direct way to produce 6.7 μm lasers, so we started to test the wavelength conversion efficiency of the laser key components. Other important progress is the background measurement. Since we need to stop muons in extremely low-density hydrogen target to substantially reduce the polarization quenching effect due to the atomic collision, all the muons stopped in the material other than the target can be a background source. Thus, we plan to use high Z materials for the target cell construction, so as all the muons stopping in surrounding materials quickly die out before the laser is introduced. We carried out the measurement of long-life background level, and confirmed that the background level can be made low enough by using coincidence detection method. The RIKEN-RAL Port 1 experimental area was refurbished for the proton radius experiments in 2016 and the muon beam was reestablished in March 2017.

(4) Other topics

New demand is emerging utilizing the muon beam for electronic chip radiation effect studies. Recent progress of semiconductor devices has produced electronic chips with very fine structure. It is anticipated that the single memory upset by the ionization effect of a single muon may result in malfunction or errors of advanced electronics. The muon is the main component of cosmic rays in our ordinary life and difficult to be removed. Measurements are being performed at RIKEN-RAL to measure such an error rate. Already several groups

carried out measurements on several different electronics. Although the sensitivity differs from chip to chip, in most cases, the error rate increases when the muon beam momentum is chosen so that the muon nearly stops in the chip itself (Bragg peak effect).

There were also demands for the use of negative muons for the non-destructive elements analysis using muonic x-rays. Especially its good depth sensitivity was clearly demonstrated. The applied objects so far are archaeological coins, sword, and oxygen concentration measurement in levers, movement of Li concentration in batteries, etc. The first paper on this work has recently been published ('Probing beneath the surface without a scratch — bulk non-destructive elemental analysis using negative muons', AD Hillier et al., Microchemical Journal 125 (2016) 203) which describes the technique's development and potential capabilities. A project has been initiated with STFC's Technology Department to develop detectors for this application and already demonstrated use of pixel detector for imaging.

Members

Director
Philip KING

Research & Technical Scientist
Isao WATANABE (concurrent: Advanced Meson Science Lab.)

Administration Manager
Mitsuru KISHIMOTO (concurrent: Nishina Center Planning Office)
Kazunori MABUCHI (concurrent: Nishina Center Planning Office)

List of Publications & Presentations

Publications

[Journal]

(Original Papers) *Subject to Peer Review

A. Adamczak et al., "Steps towards the hyperfine splitting measurement of the muonic hydrogen ground state: pulsed muon beam and detection system characterization", Journal of Instrumentation, 11, P05007 (2016); doi:10.1088/1748-0221/11/05/P05007 *

K.M. Suzuki, T. Adachi, H. Sato, I. Watanabe, and Y. Koike, "Successive Magnetic Transitions Relating to Itinerant Spins and Localized Cu Spins in $La_{2-x}Sr_xCu_{1-y}Fe_yO_4$: Possible Existence of Stripe Correlations in the Overdoped Regime" J. Phys. Soc. Jpn. **85**, 124705-1-7 (2016).*

Xing-Liang Xu, Xu-Guang Zheng, and I. Watanabe, "Utilizing Muon-Spin-Relaxation to Probe Ferroelectric Transition in Hydroxyl Salt $Co_2(OD)_3Cl$" Ferroelectrics **505**, 1255131-1-6 (2016). *

T. Adachi, A. Takahashi, K.M. Suzuki, M.A. Baqiya, T. Konno, T. Takamatsu, M. Kato, I. Watanabe, A. Koda, M. Miyazaki, R. Kadono, and Y. Koike, "Strong Electron Correlation Behind the Superconductivity in Ce-Free and Ce-Underdoped High-Tc T'-Cuprates" J. Phys. Soc. Jpn. **85**, 124705-1-7 (2016). *

M. Enomoto, I. Watanabe, and N. Kojima, "Dynamical Behavior of the Charge Transfer Phase Transition in Dithiooxalato-Bridged Iron Mixed-Valence System", Current Inorganic Chemistry **6**, 49-60 (2016). *

Sunaryono, Ahmad Taufiq, Edy Giri Rahman Putra, A. Okazawa, I. Watanabe, N. Kojima, Supagorn Rugmai, Siriwat Soontaranon, Mohammad Zainuri, Triwikantoro, Suminar Pratapa, and Darminto, "Small-Angle X-Ray Scattering Study on PVA/Fe_3O_4 Magnetic Hdrogels" NANO **11**, 1650027-1-12 (2016). *

I. Kawasaki, K. Fujimura, I. Watanabe, M. Avdeev, K. Tenya, and M. Yokoyama, "Muon Spin Relaxation and Neutron Diffraction Studies of Cluster-Glass State in $Sr_{1-x}La_xRuO_3$" J. Phys. Soc. Jpn. **85**, 054701-1-8 (2016). *

T. Uehara, M. Ito, J. Angel, J. Shimada, N. Komakine, T. Tsuchiya, H. Taniguchi, K. Satoh, K. Triyana, Y. Ishii, and I. Watanabe, "Studies on Magnetism of the Layered Organic Antiferromagnet Bordered on a Superconducting Phase by Muon Spin Rotation and Magnetization Measurements", J. Phys. Soc. Jpn. **85**, 024710-1-6 (2016). *

[Proceedings]

(Original Papers) *Subject to Peer Review

M. Bagatin, S. Gerardin, A. Paccagnella, A. Visconti, S. Beltrami, M. Bertuccio, K. Ishida, C. D. Frost, A. Hillier, V. Ferlet-Cavrois Reliability Physics Symposium (IRPS), 2016 IEEE International , 10.1109/IRPS.2016.7574552 *

Oral Presentations

[International Conference etc.]

K. Ishida, " Muon g-2/EDM at J-PARC " , Seventh Meeting on CPT and Lorentz Symmetry, Bloomington, USA, June 2016

K. Ishida, "Muon catalyzed d-t fusion ", The 6th Yamada Conference on Muonic X and Gamma ray Spectroscopy, Osaka, Sep 2016

[Domestic Conference]

北村遼他, " J-PARC ミューオン g-2/EDM 精密測定実験におけるミューオン加速実現に向けた低速ミューオン生成実験の結果報告と展望"、日本物理学会年次大会、東北学院大学、3 月(2016)

Posters Presentations

[International Conference etc.]

Alexandre Bosser, Viyas Gupta, Arto Javanainen, Georgios Tsiligiannis, Helmut Puchner, Frédéric Saigne, Frédéric Wrobel, Ari Virtanen , Luigi Dilillo; "Comparison of the Effects of Muon and Low-Energy Proton Irradiation on a 65 nm Low-Power SRAM", . RADECS: Radiation and Its Effects on Components and Systems, Sep 2016, Bremen, Germany.

RIBF Research Division
Radioactive Isotope Physics Laboratory

1. Abstract

This Laboratory works as one of core research groups conducting programs at the world-premiere heavy-ion accelerator facility of RIKEN “RI Beam Factory (RIBF)”. The Laboratory explores exotic nuclear structures and dynamics in exotic nuclei that have never been investigated before, such as those with largely imbalanced proton and neutron numbers. Our aim is to develop new experimental techniques utilizing fast radioactive isotope (RI) beams at RIBF, to discover new phenomena and properties in exotic nuclei. The Laboratory is focusing three major subjects; shell evolution of very neutron-rich nuclei, the r-process path and equation-of-state in asymmetric nuclear matter. The Laboratory has initiated international collaborations for in-beam gamma spectroscopy, decay spectroscopy and heavy-ion induced reactions, and has formed a discussion forum for next generation gamma detectors.

2. Major Research Subjects

(1) Study of structure and dynamics of exotic nuclei through developments of new tools in terms of reaction- and technique-based methodology
(2) Research on EOS in asymmetric nuclear matter via heavy-ion induced reactions
(3) Detector developments for spectroscopy and reaction studies

3. Summary of Research Activity

(1) In-beam gamma spectroscopy

In the medium and heavy mass region explored at RIBF, collective natures of nuclei are one of important subjects, which are obtained through production and observation of high excited and high spin states. To populate such states, heavy-ion induced reactions such as fragmentation, fission are useful. So far, we have developed two-step fragmentation method as an efficient method to identify and populate excited states, and lifetime measurements to deduce transition strength.

Devices utilized for the in-beam gamma spectroscopy are ZeroDegree Spectrometer (ZDS) and a NaI array DALI2. Since the end of 2008, the first spectroscopy on nuclei island-of-inversion region was performed, we have explored step-by-step new and unknown regions in the nuclear chart. The second campaign in 2009 was organized to study background components originating from atomic processes in a heavy target. Neutron-rich nuclei at N=20 to 28 were studied in 2010. In 2011-2013, we conducted experiment programs for Ca-54, Ni-78, neutron-rich nuclei at N=82 and neutron-deficient nuclei at Z=50.

A multitude of data obtained with inelastic, nucleon knock-out, fragmentation channels have been analyzed and published. In 2011-2013, collective natures of Mg-36, 38 and Si-42 were both published in PRL. Excited states firstly observed in Ca-54 were reported in Nature to demonstrate a new nuclear magic number of 34. Fragmentation reaction has been found efficient for nuclei with A>100 and low-lying excited state in Pd-126 has been successfully observed and reported in PRC.

To further strengthen the in-beam gamma spectroscopy at RIBF, we have proposed a new setup of MINOS + DALI2 to search for the 1st excited states in even-even neutron-rich nuclei with Z~20 to 40. The program was submitted to the PAC 2013 as a new category “proposal for scientific program” and was S-ranked. A dedicated collaboration “SEASTAR” has been established as a subset of in-beam gamma collaboration “SUNFLOWER”. The two campaigns were organized in 2014 and 2015 to study very neutron-rich isotopes.

Concerning a next generation detector, a discussion forum has been established to write up a white paper on tracking germanium detectors and high-efficient crystal detectors such LaBr3 and GAGG.

(2) Decay spectroscopy

Beta- and isomer-spectroscopy is an efficient method for studying nuclear structure, especially for non-yrast levels. We had accumulated experimental techniques at the RIPS facility to investigate nuclear structure in light mass region via beta-gamma and beta-p coincidence. Concerning the medium and heavy mass region available at RIBF, we have developed two position-sensitive active-stoppers, strip-silicon detectors and a cylindrical active stopper called CAITEN, to achieve a low-background measurement by taking correlation between heavy ion stop position and beta-ray emission position. A site of decay-spectroscopy at the new facility of RIBF is the final focal plane of ZDS, where high precision of TOF in particle identification is obtained due to a long flight path from BigRIPS to ZDS.

At the end of 2009, the first decay spectroscopy was organized with a minimum setup of four clover gamma detectors and silicon strip detectors, to study neutron-rich nuclei with A~110. The first campaign was found successful and efficient to publish four letter articles in 2011, two PRL’s and two PLB’s. One of the PRL papers is associated to the r-process path where half-lives for 18 neutron-rich nuclei were determined for the first time. The other PRL paper reported a finding of deformed magic number 64 in the Zr isotopes.

The success of the first decay-spectroscopy campaign stimulated to form a new large-scale collaboration “EURICA”, where a twelve Euroball cluster array is coupled with the silicon-strip detectors to enhance gamma efficiency by a factor of 10. A construction proposal of “EURICA” was approved in the PAC 2011, and the commissioning was successfully organized in spring 2012. Since then, physics runs have been conducted for programs approved to survey nuclei of interest as many as possible, such as Ni-78, Pd-128, Sn-100. So far, 34 papers including 11 PRL’s and 8 PLB’s were published. One of the highlights is discovery of a seniority isomer in Pd-128, of which cascade gamma decay gives the energy of 1st excited state and robustness of N=82 magic number, and the other is a half-life measurement for 110 neutron-rich nuclei across the N=82 shell gap, which shows implications for the mechanism and universality of the r-process path. The EURICA collaboration finished its physics programs in summer 2016.

Beta-delayed neutron emission probability of medium and heavy neutron-rich nuclei is important to understand nuclear structure and the r-process path. In 2013, a new collaboration “BRIKEN” has been established to form a He-3 detector array. A present design of the array has neutron efficiency as high as 70% up to 3 MeV. The array will be coupled with the AIDA silicon strip system. A construction

proposal was approved at the PAC 2013 and three physics proposals have been approved. The commissioning run was conducted in autumn 2016.

The CAITEN detector was successfully tested with fragments produced with a Ca-48 beam in 2010.

(3) Equation-of-state via heavy-ion central collisions

Equation-of-state in asymmetric nuclear matter is one of major subjects in physics of exotic nuclei. Pi-plus and pi-minus yields in central heavy ion collisions at the RIBF energy are considered as one of EOS sensitive observables at the RIBF energy. To observe charged pions, a TPC for the SAMURAI spectrometer is being constructed under an international collaboration "SπRIT". Construction proposal was submitted at the PAC 2012, and physics proposals were approved at the PAC 2012 and 2013. The physics runs were successfully conducted in spring 2016.

An international symposium "NuSYM" on nuclear symmetry energy was organized at RIKEN July 2010 to invite researchers in three sub-fields, nuclear structure, nuclear reaction and nuclear astrophysics, and to discuss nuclear symmetry energy together. Since then, the symposium series have been held every year and been useful to encourage theoretical works and to strengthen the collaboration.

(4) Nucleon correlation and cluster in nuclei

Nucleon correlation and cluster in nuclei are matters of central focus in a "beyond mean-field" picture. The relevant programs with in-beam gamma and missing-mass techniques are to depict nucleon condensations and correlations in nuclear media as a function of density as well as temperature. Neutron-halo and –skin nuclei are objects to study dilute neutron matter at the surface. By changing excitation energies in neutron-rich nuclei, clustering phenomena and role of neutrons are to be investigated.

In 2013, two programs were conducted at the SAMURAI spectrometer. One is related to proton-neutron correlation in the C-12 nucleus via p-n knockout reaction with a carbon target. The other is to search for a cluster state in C-16, which was populated via inelastic alpha scattering. The data is being analyzed.

Members

Chief Scientist (Lab. Head)

Hiroyoshi SAKURAI (Deputy Director, RNC)

Vice Chief Scientist

Takashi ICHIHARA

Research & Technical Scientists

Yoichi NAKAI (Senior Research Scientist)
Akihisa KOHAMA (Senior Research Scientist)
Takashi KISHIDA (Senior Research Scientist)
Shunji NISHIMURA (Senior Research Scientist)
Tadaaki ISOBE (Senior Research Scientist)
Pieter Christiaan DOORNENBAL (Research Scientist)
Daisuke SUZUKI (Research Scientist)

Contract Researchers

David STEPPENBECK
Mizuki NISHIMURA

Foreign Postdoctoral Researchers

Paer-Anders SOEDERSTROEM
He WANG

Research Consultants

Masayasu ISHIHARA
Akitsu IKEDA
Hiroyuki MURAKAMI
Kenichi MATSUYANAGI

Junior Research Associate

Yoshiaki SHIGA (Rikkyo Univ.)
Noritsugu NAKATSUKA (Kyoto Univ.)
Keishi MATSUI (Univ. of Tokyo)
Masanori KANEKO (Kyoto Univ.)

International Program Associates

Ian MURRAY (Univ. Paris Sud)
Sidong CHEN (Peking Univ.)
Xiaohui SUN (Peking Univ.)
Phong VI (Hanoi University of Science,)
Longchun TAO (Peking University)

Visiting Researchers

Gabor KISS (JSPS Fellow)
Martha Liliana CORTES SUA (JSPS Fellow)
David STEPPENBECK (JSPS Fellow)
Frank BROWNE (JSPS Fellow)

Senior Visiting Scientists

Kengo OGAWA (Chiba Univ.)
Koichiro ASAHI (TIT)
Shigeru KUBONO (Univ. of Tokyo)

Visiting Scientists

Hooi Jing ONG (RCNP)
Megumi NIIKURA (Univ. of Tokyo)

Silivio CHERUBINI (Univ. of Catania)
Hyo Soon JUNG (Univ. of Notre Dame)
Daiki NISHIMURA (Tokyo Univ. of Sci.)
Takashi KISHIDA (Aoyama Univ.)
Naohiko OTSUKA (Intl. Atomic Energy Agency, Austria)
Giuseppe LORUSSO (National Physics Lab., UK)
Hiu Ching LEE (Univ. of Hong Kong)
Zhengyu XU (Univ. of Hong Kong)
Indranil MAZUMDAR (GSI)
Byungsik HONG (Korea Univ.)
Prabhakar PALNI (MSU)
Rebecca SHANE (MSU)
Alan MCINTOSH (Texas A & M Univ.)
Michael YOUNG (Texas A & M Univ.)
Thomas DAVINSON (Univ. of Edinburgh)
Yassid AYYAD (Osaka Univ.)
Kathrin WIMMER (Univ. of Tokyo)
Tetsuya MURAKAMI (Kyoto Univ.)
Kazuo IEKI (Rikkyo Univ.)
Mitsunori FUKUDA (Osaka Univ.)
Nori AOI (RCNP)
Khiem Hong LE (Vietnam Academy of Sci. and Tech.)
Evgueni NIKOLSKI (RRC Kurchatov Inst.)
Alexey OGLOBLIN (RRC Kurchatov Inst.)
Hiroshi WATANABE (Beihang Univ.)
Akira ONO (Tohoku Univ.)
Kazuhiro OYAMATSU (Aichi Shukutoku University)
Clementine SANTAMARIA (Michigan State University)
Kei IIDA (Kochi University)
Natsumi IKENO (Tottori Univ.)
Yont Jin KIM (Institute for Basic Science)
Pawlowski PIOTR (Institute of Nuclear Physics PAN)
Giordano CERIZZA (NSCL)
Marisa GULINO (Universita di Enna Kore Italy)
Satoshi TAKEUCHI (TIT)
Hyo Sang LEE (Institute for Basic Science)

Visiting Technicians

Ivan KOJOUHAROV (GSI)

Student Trainees

Hiroki NISHIBATA (Osaka Univ.)
Tetsuya YAMAMOTO (Osaka Univ.)
Ayumi YAGI (Osaka Univ.)
Ryo TANIUCHI (Univ. of Tokyo)
Jin-hee CHANG (Korea University)
Akira HOMMA (Niigata Univ.)
Satoru MOMIYAMA (Univ. of Tokyo)
Shintaro YAMAOKA (Osaka Univ.)
Kouta WATANABE (Osaka Univ.)
Justin ESTEE (Michigan State University)
MasanoriKANEKO (Kyoto Univ.)
Suwat TANGWANCHAROEN (Michigan State University)
JungWoo LEE (Korea University)
Takashi ANDO (Univ. of Tokyo)
Shunpei KOYAMA (Univ. of Tokyo)
Hang DU (Osaka Univ.)
Yuutaro TANAKA (Osaka Univ.)
Jonathan BARNEY (Michigan State University)
Hiroyuki OIKAWA (Tokyo Univ. of Science)
Toshiki YOSHINOBU (Tokyo Univ. of Science)
Yuki KANKE (Tokyo Univ. of Science)
Junya NAGUMO (Tokyo Univ. of Science)
Jiajian LIU (The University of Hong Kong)
Shinnosuke KANAYA (Osaka Univ.)
Hiroshi KANAOKA (Osaka Univ.)
Yan ZHANG (Tsinghua University)
Shunsuke NAGAMINE (Univ. of Tokyo)
TakeshiSAITO (Univ. of Tokyo)
Eri MIYATA (Niigata Univ.)
Yuta KUNIMOTO (Rikkyo Univ.)
Yohei TANAKA (Rikkyo Univ.)
Sean SWEANY (Michigan State University)
Shoichi YAGI (Osaka Univ.)
Yuki TAKEI (Tokyo Univ. of Science)
Pawel LASKO (Jagiellonian University)
Krzyszto PELCZAR (Jagiellonian University)
Ryo HIGUCHI (Univ. of Tokyo)
Riku TAMURA (Univ. of Tokyo)
Masashi USAMI (Univ. of Tokyo)
KousukeONISHI (Osaka Univ.)
Takanobu SUGIHARA (Osaka Univ.)
Juan MANFREDI (Michigan State University)
FredrikPARNEFJORD GUSTAFSSON (HKU)
Chun Yuen TSANG (CUHK)
Kosuke MAEDA (Rikkyo Univ.)
Ryunosuke BANNAY (Rikkyo Univ.)
Sakiko ASHIKAGA (Kyoto Univ.)
Kento INABA (Kyoto Univ.)
Shota MATSUMOTO (Kyoto Univ.)
Ken WATANABE (Kyoto Univ.)
Yu TAKAHASHI (Kyoto Univ.)
Ami KOSHIKAWA (Kyoto Univ.)
Andrea JEDEL (Texas A & M University)
Taku KUMON (Univ. of Tokyo)
Takuma KOIWAI (Univ. of Tokyo)
Yuma SHIMIZU (Univ. of Tokyo)
SoomiCHA (Sungkyunkwan University)
Taichi HORI (Osaka Univ.)
Shoken NAKAMURA (Osaka Univ.)
Rikuto YANAGIHARA (Osaka Univ.)
Naoto KANDA (Niigata Univ.)
Suharu HOSHINO (Niigata Univ.)
Ryohei HOSODA (Niigata Univ.)
Masaki SHIOTA (Niigata Univ.)
Taro WADA (Niigata Univ.)
Toshiki MOCHIZUKI (Univ. of Tokyo)
Tomoaki KASUGA (Univ. of Tokyo)
Ryohei ITO (Univ. of Tokyo)
Herrera Wilmar RODRIGUEZ (Univ.Nacional de Colombia)
Yusuke FUJINO (Rikkyo Univ.)

Interns

Dolachai BONIFACE (Univrsite Paris SUD)

Part-time Workers

Yukiya SAITO (Univ.of Tokyo)

List of Publications & Presentations

Publications

[Journal]

(Original Papers) *Subject to Peer Review

G. Jhang, J. Barney, J. Estee, T. Isobe, M. Kaneko, M. Kurata-Nishimura, G. Cerizza, C. Santamaria, J.W. Lee, P. Lasko, J. Lukasik, W.G. Lynch, A.B. McIntosh, T. Murakami, P. Pawlowski, R. Shane, S. Tangwancharoen, M.B. Tsang, H. Baba, B. Hong, Y.J. Kim, H.S. Lee, H. Otsu, K. Pelczar, H. Sakurai, D. Suzuki, Z. Xiao, S.J. Yennello, Y. Zhang et. al., "Beam Commissioning of the SpiRIT Time Projection Chamber", Journal of the Korean Physical Society, Vol. 69, No. 2, 144 (2016) *

J. W. Hwang, S. Kim, Y. Satou, N. A. Orr, Y. Kondo, T. Nakamura, J. Gibelin, N. L. Achouri, T. Aumann, H. Baba, F. Delaunay, P. Doornenbal, N. Fukuda, N. Inabe, T. Isobe, D. Kameda, D. Kanno, N. Kobayashi, T. Kobayashi, T. Kubo, S. Leblond, J. Lee, F. M. Marques, R. Minakata, T. Motobayashi, D. Murai, T. Murakami, K. Muto, T. Nakashima, N. Nakatsuka, A. Navin, S. Nishi, S. Ogoshi, H. Otsu, H. Sato, Y. Shimizu, H. Suzuki, K. Takahashi, H. Takeda, S. Takeuchi, R. Tanaka, Y. Togano, A. G. Tuff, M. Vandebrouck, and K. Yoneda. 'Single-neutron knockout from 20C and the structure of 19C.' Phys.Lett. B, 769:503, 2017.

H. N. Liu, J. Lee, P. Doornenbal, H. Scheit, S. Takeuchi, N. Aoi, K. A. Li, M. Matsushita, D. Steppenbeck, H. Wang, H. Baba, E. Ideguchi, N. Kobayashi, Y. Kondo, G. Lee, S. Michimasa, T. Motobayashi, A. Poves, H. Sakurai, M. Takechi, Y. Togano, J. A. Tostevin, and Y. Utsuno. 'Intruder configurations in the ground state of 30Ne.' Phys.Lett. B, 767:58, 2017.

N. Paul, A. Corsi, A. Obertelli, P. Doornenbal, G. Authelet, H. Baba, B. Bally, M. Bender, D. Calvet, F. Chateau, S. Chen, J. -P. Delaroche, A. Delbart, J. -M. Gheller, A. Giganon, A. Gillibert, M. Girod, P. -H. Heenen, V. Lapoux, J. Libert, T. Motobayashi, M. Niikura, T. Otsuka, T. R. Rodriguez, J. -Y. Rousse, H. Sakurai, C. Santamaria, N. Shimizu, D. Steppenbeck, R. Taniuchi, T. Togashi, Y. Tsunoda, T. Uesaka, T. Ando, T. Arici, A. Blazhev, F. Browne, A. M. Bruce, R. Carroll, L. X. Chung, M. L. Cortes, M. Dewald, B. Ding, F. Flavigny, S. Franchoo, M. Gorska, A. Gottardo, A. Jungclaus, J. Lee, M. Lettmann, B. D. Linh, J. Liu, Z. Liu, C. Lizarazo, S. Momiyama, K. Moschner, S. Nagamine, N. Nakatsuka, C. Nita, C. R. Nobs, L. Olivier, Z. Patel, Z. Podolyak, M. Rudigier, T. Saito, C. Shand, P. -A. Soderstrom, I. Stefan, R. Orlandi, V. Vaquero, V. Werner, K. Wimmer, and Z. Xu. 'Are There Signatures of Harmonic Oscillator Shells Far from Stability? First Spectroscopy of 110Zr.' Phys.Rev.Lett., 118:032501, 2017.

H. Wang, N. Aoi, S. Takeuchi, M. Matsushita, T. Motobayashi, D. Steppenbeck, K. Yoneda, H. Baba, Zs. Dombradi, K. Kobayashi, Y. Kondo, J. Lee, H. Liu, R. Minakata, D. Nishimura, H. Otsu, H. Sakurai, D. Sohler, Y. Sun, Z. Tian, R. Tanaka, Zs. Vajta, Z. Yang, T. Yamamoto, Y. Ye, and R. Yokoyama. 'First spectroscopic information from even-even nuclei in the region "southeast" of 132Sn: Neutron-excitation dominance of the 2+ 1 state in 132Cd.' Phys.Rev. C, 94:051301, 2016.

D.Q. Fang, Y.G. Ma, X.Y. Sun, P. Zhou, Y. Togano, N. Aoi, H. Baba, X.Z. Cai, X.G. Cao, J.G. Chen, Y. Fu, W. Guo, Y. Hara, T. Honda, Z.G. Hu, K. Ieki, Y. Ishibashi, Y. Ito, N. Iwasa, S. Kanno, T. Kawabata, H. Kimura, Y. Kondo, K. Kurita, M. Kurokawa, T. Moriguchi, H. Murakami, H. Ooishi, K. Okada, S. Ota, A. Ozawa, H. Sakurai, S. Shimoura, R. Shioda, E. Takeshita, S. Takeuchi, W.D. Tian, H.W. Wang, J.S. Wang, M. Wang, K. Yamada, Y. Yamada, Y. Yasuda, K. Yoneda, G.Q. Zhang, T. Motobayashi: 'Proton-proton correlations in distinguishing the two-proton emission mechanism of 23Al and 22Mg', Phys. Rev. C 94 (2016) 044621

Y. Togano, T. Nakamura, Y. Kondo, J. A. Tostevin, A. T. Saito, J. Gibelin, N. A. Orr, N. L. Achouri, T. Aumann, H. Baba, F. Delaunay, P. Doornenbal, N. Fukuda, J. W. Hwang, N. Inabe, T. Isobe, D. Kameda, D. Kanno, S. Kim, N. Kobayashi, T. Kobayashi, T. Kubo, S. Leblond, J. Lee, F. M. Marques, R. Minakata, T. Motobayashi, D. Murai, T. Murakami, K. Muto, T. Nakashima, N. Nakatsuka, A. Navin, S. Nishi, S. Ogoshi, H. Otsu, H. Sato, Y. Satou, Y. Shimizu, H. Suzuki, K. Takahashi, H. Takeda, S. Takeuchi, R. Tanaka, A. G. Tuff, M. Vandebrouck, and K. Yoneda. 'Interaction cross section study of the two-neutron halo nucleus 22C.' Phys.Lett. B, 761:412, 2016.

P. Doornenbal, H. Scheit, S. Takeuchi, N. Aoi, K. Li, M. Matsushita, D. Steppenbeck, H. Wang, H. Baba, E. Ideguchi, N. Kobayashi, Y. Kondo, J. Lee, S. Michimasa, T. Motobayashi, A. Poves, H. Sakurai, M. Takechi, Y. Togano, and K. Yoneda. 'Mapping the deformation in the "island of inversion": Inelastic scattering of 30Ne and 36Mg at intermediate energies.' Phys.Rev. C, 93:044306, 2016.

H. Wang, H. Otsu, H. Sakurai, D.S. Ahn, M. Aikawa, T. Ando, S. Araki, S. Chen, N. Chiga, P. Doornenbal, N. Fukuda, T. Isobe, S. Kawakami, S. Kawase, T. Kin, Y. Kondo, S. Koyama, S. Kubono, Y. Maeda, A. Makinaga, M. Matsushita, T. Matsuzaki, S. Michimasa, S. Momiyama, S. Nagamine, T. Nakamura, K. Nakano, M. Niikura, T. Ozaki, A. Saito, T. Saito, Y. Shiga, M. Shikata, Y. Shimizu, S. Shimoura, T. Sumikama, P.-A. Söderström, H. Suzuki, H. Takeda, S. Takeuchi, R. Taniuchi, Y. Togano, J. Tsubota, M. Uesaka, Ya. Watanabe, Yu. Watanabe, K. Wimmer, T. Yamamoto, and K. Yoshida. 'Spallation reaction study for the long-lived fission product ^{107}Pd', Progress in Theory and Experiment Physics 2017(2), 021D01 (2017).

S. Hayakawa, S. Kubono, D. Kahl, H. Yamaguchi, D. N. Binh, T. Hashimoto, Y. Wakabayashi, J. J. He, N. Iwasa, S. Kato, T. Komatsubara, Y. K. Kwon, and T. Teranishi. "First direct measurement of the 11C(α, p)14N stellar reaction by an extended thick-target method", : Phys. Rev. C 93 (2016) 065802 (8)

W.P. Liu, Z.H. Li, J.J. He, X.D. Tang, G. Lian, Z. An, J.J. Chang, H. Chen, Q.H. Chen, X.J. Chen, Z.J. Chen, B.Q. Cui, X.C. Du, C.B. Fu, L. Gan, B. Guo, G.Z. He, A. Heger, S.Q. Hou, H.X. Huang, N. Huang, B.L. Jia, L.Y. Jiang, S. Kubono, J.M. Li, K.A. Li, T. Li, Y.J. Li, M. Lugaro, X.B. Luo, H.Y. Ma, S.B. Ma, D.M. Mei, Y.Z. Qian, J.C. Qin, J. Ren, Y.P. Shen, J. Su, L.T. Sun, W.P. Tan, I. Tanihata, S. Wang, P. Wang, Y.B. Wang, Q. Wu, S.W. Xu, S.Q. Yan, L.T. Yang, Y. Yang, X.Q. Yu, Q. Yue, S. Zeng, H.Y. Zhang, H. Zhang, L.Y. Zhang, N.T. Zhang, Q.W. Zhang, T. Zhang, X.P. Zhang, X.Z. Zhang, Z.M. Zhang, W. Zhao, Z. Zhao, and C. Zhou (JUNA Collaboration). "Progress of Jinping Underground laboratory for Nuclear Astrophysics (JUNA)", SCIENCE CHINA - Physics, Mechanics & Astronomy 59 (2016) 642001.

X. Xu, P. Zhang, P. Shuai, R.J. Chen, X.L. Yan, Y.H. Zhang, M. Wang, Yu.A. Litvinov, H.S. Xu, T. Bao, X.C. Chen, H. Chen, C.Y. Fu, S. Kubono, Y.H. Lam, D.W. Liu, R.S. Mao, X.W. Ma, M.Z. Sun, X.L. Tu, Y.M. Xing, J.C. Yang, Y.J. Yuan, Q. Zeng, X. Zhou, X.H. Zhou, W.L. Zhan, S. Litvinov, K. Blaum, G. Audi, T. Uesaka, Y. Yamaguchi, T. Yamaguchi, A. Ozawa, B.H. Sun, Y. Sun, A. C. Dai, and F.R. Xu. "Identification of the Lowest T=2, Jπ =0+ Isobaric Analog State in 52Co and Its Impact on the Understanding of β-Decay Properties of 52Ni", Phys. Rev. Lett. 117 (2016) 182503.

P. Zhang, X. Xu, P. Shuai, R.J. Chen, X.L. Yan, Y.H. Zhang, M. Wang, Yu.A. Litvinovc, K. Blaum, H.S. Xu, T. Bao, X.C. Chen, H. Chena, C.Y. Fua, J.J. He, S. Kubono, Y.H. Lam, D.W. Liua, R.S. Mao, X.W. Ma, M.Z. Suna, X.L. Tu, Y.M. Xing, J.C. Yang, Y.J. Yuan, Q. Zenga, X. Zhoua, X.H. Zhou, W.L. Zhan, S. Litvinov, G. Audi, T. Uesaka, Y. Yamaguchi, T. Yamaguchi, A. Ozawa, B.H. Sun, Y. Sun, F.R. Xu. "High-precision QECvalues of super-allowed 0+→0+ β-emitters 46Cr, 50Fe and 54Ni", Phys. Lett. B 767 (2017) 20.

T. Kawabata, T. Kawabata, Y. Fujikawa, T. Furuno, T. Goto, T. Hashimoto, M. Ichikawa, M. Itoh, N. Iwasa, Y. Kanada-En'yo, A. Koshikawa, S. Kubono, E. Miyawaki, M. Mizuno, K. Mizutani, T. Morimoto, M. Murata, T. Nanamura, S. Nishimura, S. Okamoto, Y. Sakaguchi, I. Sakata, A.

Sakaue, R. Sawada, Y. Shikata, Y. Takahashi, D. Takechi, T. Takeda, C. Takimoto, M. Tsumura, K. Watanabe, and S. Yoshida. “Time-Reversal Measurement of the p-Wave Cross Sections of the ^{7}Be(n,α)^{4}He Reaction for the Cosmological Li Problem”, Phys. Rev. Lett. 118 (2017) 052701.

P. Russotto, S. Gannon, S. Kupny, P. Lasko, L. Acosta, M. Adamczyk, A. Al-Ajlan, M. Al-Garawi, S. Al-Homaidhi, F. Amorini, L. Auditore, T. Aumann, Y. Ayyad, Z. Basrak, J. Benlliure, M. Boisjoli, K. Boretzky, J. Brzychczyk, A. Budzanowski, C. Caesar, G. Cardella, P. Cammarata, Z. Chajecki, M. Chartier, A. Chbihi, M. Colonna, M.D. Cozma, B. Czech, E.De Filippo, M.Di Toro, M. Famiano, I. Gasparic, L. Grassi, C. Guazzoni, P. Guazzoni, M. Heil, L. Heilborn, R. Introzzi, T. Isobe, K. Kezzar, M. Kis, A. Krasznahorkay, N. Kurz, E. La Guidara, G. Lanzalone, A. Le Fevre, Y. Leifels, R.C. Lemmon, Q.F. Li, I. Lombardo, J. Lukasik, W.G. Lynch, P. Marini, Z. Matthews, L. May, T. Minniti, M. Mostazo, A. Pagano, E. V. Pagano, M. Papa, P. Pawlowski, S. Pirrone, G. Politi, F. Porto, W. Reviol, F. Riccio, F. Rizzo, E. Rosato, D. Rossi, S. Santoro, D.G. Sarantites, H. Simon, I. Skwirczynska, Z. Sosin, L. Stuhl, W. Trautmann, A. Trifiro, M. Trimarchi, M.B. Tsang, G. Verde, M. Veselsky, M. Vigilante, Y. Wang, A. Wieloch, P. Wigg, J. Winkelbauer, H.H. Wolter, P. Wu, S. Yennello, P. Zambon, L. Zetta, M. Zoric, "Results of the ASY-EOS experiment at GSI: The symmetry energy at suprasaturation density", Physical Review C 94 (2016) 034608.

M.B. Tsang, J. Estee, H. Setiawan, W.G. Lynch, J. Barney, M.B. Chen, G. Cerizza, P. Danielewicz, J. Hong, P. Morfouace, R. Shane, S. Tangwancharoen, K. Zhu, T. Isobe, M. Kurata-Nishimura, J. Lukasik, T. Murakami, Z. Chajeck, "Pion Production in Rare Isotope Collisions", Physical Review C 95 (2016) 044614.

S. Tangwancharoen, W.G. Lynch, J. Barney, J. Estee, R. Shane, M.B. Tsang, Y. Zhang, T. Isobe, M. Kurata-Nishimura, T. Murakami, Z.G. Xiao, Y.F. Zhang, the SpiRIT collaboration, "A gating grid driver for time projection chambers", Nuclear Instruments and Methods A 853 (2017) 44.

P. Lasko, M. Adamczyk, J. Brzychczyk, P. Hirnyk, J. Lukasik, P. Pawlowski, K. Pelczar, A. Snoch, A. Sochocka, Z. Sosin, J. Barney, G. Cerizza, J. Estee, T. Isobe, G. Jhang, M. Kaneko, M. Kurata-Nishimura, W.G. Lynch, T. Murakami, C. Santamaria, M.B. Tsang, Y. Zhang, "KATANA – A charge-sensitive triggering system for the SpiRIT experiment", Nuclear Instruments and Methods A 856 (2017) 92.

A. Tarifeno-Saldivia, J.L. Tain, Domingo-Pardo, F. Calvino, G. Cortes, V.H. Phong, A. Riego, J. Agramunt, A. Algora, N. Brewer, R. Caballero-Folch, P.J. Coleman-Smith, T. Davinson, I. Dillmann, A. Estrade, C.J. Griffin, R. Grzywacz, L.J. Harkness-Brennan, G.G. Kiss, M. Kogimtzis, M. Labiche, I.H. Lazarus, G. Lorusso, K. Matsui, K. Miernik, F. Montes, A.I. Morales, S. Nishimura, R.D. Page, Z.S. Podolyak, V.F.E. Pucknell, B.C. Rasco, P. Regan, B. Rubio, K.P. Rykaczewski,d Y. Saito,c;g H. Sakurai,c J. Simpson,k E. Sokol,t R. Surman,A. Svirkhin, S.L. Thomas, A. Tolosa and P. Woods "Conceptual design of a hybrid neutron-gamma detector for study of beta-delayed neutrons at the RIB facility of RIKEN" Journal of Instrumentation 12 (2016) P04006.

T. Goigoux, P. Ascher, B. Blank, M. Gerbaux, J. Giovinazzo, S. Grevy, T. Kurtukian Nieto, C. Magron, P. Doornenbal, G. G. Kiss, S. Nishimura, P.-A. Söderström, V. H. Phong, J. Wu, D. S. Ahn, N. Fukuda, N. Inabe, T. Kubo, S. Kubono, H. Sakurai, Y. Shimizu, T. Sumikama, H. Suzuki, H. Takeda, J. Agramunt, A. Algora, V. Guadilla, A. Montaner-Piza, A. I. Morales, S. E. A. Orrigo, B. Rubio, Y. Fujita, M. Tanaka, W. Gelletly, P. Aguilera, F. Molina, F. Diel, D. Lubos, G. de Angelis, D. Napoli, C. Borcea, A. Boso, R. B. Cakirli, E. Ganioglu, J. Chiba, D. Nishimura, H. Oikawa, Y. Takei, S. Yagi, K. Wimmer, G. de France, S. Go, and B. A. Brown "Two-proton radioactivity of 67Kr" PHYSICAL REVIEW LETTERS 117 (2016) 162501.

B. Blank, T. Goigoux, P. Ascher, M. Gerbaux, J. Giovinazzo, S. Grevy, T. Kurtukian Nieto, C. Magron, J. Agramunt, A. Algora, V. Guadilla, A. Montaner-Piza, A. I. Morales, S. E. A. Orrigo, B. Rubio, D. S. Ahn, P. Doornenbal, N. Fukuda, N. Inabe, G. Kiss, T. Kubo, S. Kubono, S. Nishimura, V. H. Phong, H. Sakurai, Y. Shimizu, P.-A. Soderstrom, T. Sumikama, H. Suzuki, H. Takeda, J. Wu, Y. Fujita, M. Tanaka, W. Gelletly, P. Aguilera, F. Molina, F. Diel, D. Lubos, G. de Angelis, D. Napoli, C. Borcea, A. Boso, R. B. Cakirli, E. Ganioglu, J. Chiba, D. Nishimura, H. Oikawa, Y. Takei, S. Yagi, K. Wimmer, G. de France, and S. Go "New neutron-deficient isotopes from 78Kr fragmentation" PHYSICAL REVIEW C 93 (2016) 061301(R)

Y. Nakai, H. Hidaka, N. Watanabe, T. M. Kojima: “Stepwise formation of $H_3O^+(H_2O)_n$ in an ion drift tube: empirical effective temperature of association/dissociation reaction equilibrium in an electric field”, Journal Chemical Physics 144, (2016) 224306.

P.J. Davies, H. Grawe , K. Moschner, A. Blazhev, R. Wadsworth , P. Boutachkov, F. Ameil, A. Yagi, H. Baba, T. Bäck, M. Dewald, P. Doornenbal, T. Faestermann, A. Gengelbach, J. Gerl, R. Gernhäeuser, S. Go, M. Górska, E. Gregor, T. Isobe, D.G. Jenkins, H. Hotaka, J. Jolie, I. Kojouharov, N. Kurz, M. Lewitowicz, G. Lorusso, L. Maier, E. Merchan, F. Naqvi, H. Nishibata, D. Nishimura, S. Nishimura, F. Nowacki, N. Pietralla, H. Schaffner, P.-A. Söderström, H.S. Jung, K. Steiger, T. Sumikama, J. Taprogge, P. Thöle, N. Warr, H. Watanabe, V. Werner, Z.Y. Xu, K. Yoshinaga, Y. Zhu: “The role of core excitations in the structure and decay of the 16+ spin-gap isomer in 96Cd” , Phys. Lett. B 767 (2017) 474-479.

J. Wu, S. Nishimura, G. Lorusso, P. Möller, E. Ideguchi, P.-H. Regan, G. S. Simpson, P.-A. Söderström, P. M. Walker, H. Watanabe, Z. Y. Xu, H. Baba, F. Browne, R. Daido, P. Doornenbal, Y. F. Fang, G. Gey, T. Isobe, P. S. Lee, J. J. Liu, Z. Li, Z. Korkulu, Z. Patel, V. Phong, S. Rice, H. Sakurai, L. Sinclair, T. Sumikama, M. Tanaka, A. Yagi, Y. L. Ye, R. Yokoyama, G. X. Zhang, T. Alharbi, N. Aoi, F. L. Bello Garrote, G. Benzoni, A. M. Bruce, R. J. Carroll, K. Y. Chae, Z. Dombradi, A. Estrade, A. Gottardo, C. J. Griffin, H. Kanaoka, I. Kojouharov, F. G. Kondev, S. Kubono, N. Kurz, I. Kuti, S. Lalkovski, G. J. Lane, E. J. Lee, T. Lokotko, G. Lotay, C.-B. Moon, H. Nishibata, I. Nishizuka, C. R. Nita, A. Odahara, Zs. Podolyák, O. J. Roberts, H. Schaffner, C. Shand, J. Taprogge, S. Terashima, Z. Vajta, and S. Yoshida : “94 β-Decay Half-Lives of Neutron-Rich 55Cs to 67Ho: Experimental Feedback and Evaluation of the r-Process Rare-Earth Peak Formation” , Phys. Rev. Lett. 118, 072701 (2017) 1-7.

A.I. Morales, G. Benzoni, H. Watanabe, Y. Tsunoda, T. Otsuka, S. Nishimura, F. Browne, R. Daido, P. Doornenbal, Y. Fang, G. Lorusso, Z. Patel, S. Rice, L. Sinclair, P.-A. Söderström, T. Sumikama, J. Wu, Z.Y. Xu , A. Yagi, R. Yokoyama, H. Baba, R. Avigo, F.L. Bello Garrote, N. Blasi, A. Bracco, F. Camera, S. Ceruti, F.C.L. Crespi, G. de Angelis, M.-C. Delattre, Zs. Dombradi, A. Gottardo, T. Isobe , I. Kojouharov , N. Kurz, I. Kuti, K. Matsui, B. Melon , D. Mengoni , T. Miyazaki , V. Modamio-Hoybjor, S. Momiyama, D.R. Napoli, M. Niikura, R. Orlandi, H. Sakurai, E. Sahin, D. Sohler, H. Schaffner, R. Taniuchi, J. Taprogge , Zs. Vajta, J.J. Valiente-Dobón, O. Wieland , M. Yalcinkaya : Type II shell evolution in A = 70 isobars from the $N \geq 40$ island of inversion, Phys. Lett. B 765 (2017) 328-333.

E. Ideguchi, G. S. Simpson, R. Yokoyama, Mn. Tanaka, S. Nishimura, P. Doornenbal, G. Lorusso, P.-A. So¨derstro¨m, T. Sumikama, J. Wu, Z. Y. Xu, N. Aoi, H. Baba, F. L. Bello Garrote, G. Benzoni, F. Browne, R. Daido, Y. Fang, N. Fukuda, A. Gottardo, G. Gey, S. Go, N. Inabe,T. Isobe, D. Kameda, K. Kobayashi, M. Kobayashi, I. Kojouharov, T. Komatsubara, T. Kubo, N. Kurz, I. Kuti, Z. Li, M. Matsushita, S. Michimasa, C.-B. Moon, H. Nishibata, I. Nishizuka, A. Odahara, Z. Patel, S. Rice, E. Sahin, H. Sakurai, H. Schaffner, L. Sinclair, H. Suzuki, H. Takeda, J. Taprogge, Zs. Vajta, H. Watanabe, and A. Yagi : ”µs isomers of 158,160Nd”, Phys Rev. C 94, 064322 (2016) 1-5.

J. Taprogge, A. Jungclaus, H. Grawe, I.N. Borzov, S. Nishimura, P. Doornenbal, G. Lorusso, G.S. Simpson, P.-A. So¨derstro¨m, T. Sumikama, Z.Y. Xu, H. Baba, F. Browne, N. Fukuda, R. Gernha user, G. Gey, N. Inabe, T. Isobe, H.S. Jung, D. Kameda, G.D. Kim, Y.-K. Kim, I.

Kojouharov, T. Kubo, N. Kurz, Y.K. Kwon, Z. Li, H. Sakurai, H. Schaffner, Y. Shimizu, K. Steiger, H. Suzuki, H. Takeda, Zs. Vajta, H. Watanabe, J. Wu, A. Yagi, K. Yoshinaga, G. Benzoni, S. Bo¨nig, K.Y. Chae, L. Coraggio, J.-M. Daugas, F. Drouet, A. Gadea, A. Gargano, S. Ilieva, N. Itaco, F.G. Kondev, T. Kro¨ll, G.J. Lane, A. Montaner-Piza´, K. Moschner31, D. Mu¨cher, F. Naqvi, M. Niikura, H. Nishibata, A. Odahara, R. Orlandi, Z. Patel, Zs. Podolya´k, and A. Wendt : Proton-hole and core-excited states in the semi-magic nucleus 131In82 , Eur. Phys. J. A 52, 347 (2016) 1-10.

P.-A. Söderström, P.M. Walker, J. Wu, H.L. Liu, P.H. Regan, H. Watanabe, P. Doornenbal, Z. Korkulu, P. Lee, J.J. Liu, G. Lorusso, S. Nishimura, V.H. Phong, T. Sumikama, F.R. Xu, A. Yagi, G.X. Zhang, D.S. Ahn, T. Alharbi, H. Baba, F. Browne, A.M. Bruce, R.J. Carroll , K.Y. Chae, Zs. Dombradi, A. Estrade , N. Fukuda, C.J. Griffin, E. Ideguchi, N. Inabe, T. Isobe, H. Kanaoka, S. Kanaya, I. Kojouharov, F.G. Kondev, T. Kubo, S. Kubono, N. Kurz, I. Kuti, S. Lalkovski, G.J. Lane, E.J. Lee , C.S. Lee, G. Lotay, C.-B. Moon, I. Nishizuka, C.R. Nit¸a˘, A. Odahar, Z. Patel, Zs. Podolyák, O.J. Roberts, H. Sakurai, H. Schaffner, C.M. Shand, H. Suzuki, H. Takeda, S. Terashima, Zs. Vajta, J.J. Valiente-Dòbon, Z.Y. Xu : "*K*-mixing in the doubly mid-shell nuclide 170Dy and the role of vibrational degeneracy", Phys. Lett. B 762 (2016) 404-408.

J. Lee, H. Liu, P. Doornenbal, M. Kimura, K. Minomo, K. Ogata, Y. Utsuno, N. Aoi, M. Matsushita, H. Scheit, D. Steppenbeck, S. Takeuchi, H. Wang, H. Baba, E. Ideguchi, N. Kobayashi, Y. Kondo, S. Michimasa, T. Motobayashi, H. Sakurai, M. Takechi, Y. Togano:"Asymmetry dependence of reduction factors from single-nucleon knockout of 30Ne at similar to 230 MeV/nucleon", Prog. Theo. and Exp Physics 8 (2016) 083D01.

A. Jungclaus, H. Grawe, S. Nishimura, P. Doornenbal, G. Lorusso, G. S. Simpson, P.-A. So¨derstro¨m, T. Sumikama, J. Taprogge, Z. Y. Xu, H. Baba, F. Browne, N. Fukuda, R. Gernha¨user, G. Gey, N. Inabe, T. Isobe, H. S. Jung, D. Kameda, G. D. Kim, Y.-K. Kim, I. Kojouharov, T. Kubo, N. Kurz, Y. K. Kwon, Z. Li, H. Sakurai, H. Schaffner, Y. Shimizu, K. Steiger, H. Suzuki, H. Takeda, Zs. Vajta, H. Watanabe, J. Wu, A. Yagi, K. Yoshinaga, G. Benzoni, S. Bo¨nig, K. Y. Chae, L. Coraggio, J.-M. Daugas, F. Drouet, A. Gadea, A. Gargano, S. Ilieva, N. Itaco, F. G. Kondev, T. Kro¨ll, G. J. Lane, A. Montaner-Piza´, K. Moschner, D. Mu¨cher, F. Naqvi, M. Niikura, H. Nishibata, A. Odahara, R. Orlandi, Z. Patel, Zs. Podolya´k, and A. Wendt: "β decay of semi-magic 130Cd: Revision and extension of the level scheme of 130In", Phys. Rev. C 94, 024303 (2016) 1-8.

H. Watanabe, G.X. Zhang, K. Yoshida, P.M. Walker, J.J. Liu, J. Wu, P.H. Regan, P.-A. Söderström, H. Kanaoka, Z. Korkulu, P.S. Lee, S. Nishimura, A. Yagi, D.S. Ahn, T. Alharbi, H. Baba, F. Browne, A.M. Bruce, R.J. Carroll, K.Y. Chae, Zs. Dombradi, P. Doornenbal, A. Estrade, N. Fukuda, C. Griffin, E. Ideguchi, N. Inabe, T. Isobe, S. Kanaya, I. Kojouharov, F.G. Kondev, T. Kubo, S. Kubono, N. Kurz, I. Kuti, S. Lalkovski, G.J. Lane, C.S. Lee , E.J. Lee, G. Lorusso, G. Lotay, C.-B. Moon , I. Nishizuka, C.R. Nita, A. Odahara , Z. Patel , V.H. Phong , Zs. Podolyák , O.J. Roberts , H. Sakurai , H. Schaffner , C.M. Shand , Y. Shimizu , T. Sumikama , H. Suzuki , H. Takeda , S. Terashima , Zs. Vajta , J.J. Valiente-Dóbon , Z.Y. Xu : "Long-lived *K* isomer and enhanced γ vibration in the neutron-rich nucleus 172Dy: Collectivity beyond double midshell", Phys. Lett. B 760 (2016) 641-646.

H. Otsu, S. Koyama, N. Chiga, T. Isobe, T. Kobayashi, Y. Rondo, M. Kurokawa, W.G. Lynch, T. Motobayashi, T. Murakami, T. Nakamura, M. Kurata-Nishimura, V. Panin, H. Sato, Y. Shimizu, H. Sakurai, M.B. Tsang, K. Yoneda, H. Wang :"SAMURAI in its operation phase for RIBF users", Nucl. Instrum and Methods B 376 (2016) 175-179

I. Čeliković, M. Lewitowicz, R. Gernhäuser, R. Krücken, S. Nishimura, H. Sakurai, D.S. Ahn, H. Baba, B. Blank, A. Blazhev, P. Boutachkov, F. Browne, G. de France, P. Doornenbal, T. Faestermann, Y. Fang, N. Fukuda, J. Giovinazzo, N. Goel, M. Górska, S. Ilieva, N. Inabe, T. Isobe, A. Jungclaus, D. Kameda, Y.-K. Kim, Y. K. Kwon, I. Kojouharov, T. Kubo, N. Kurz, G. Lorusso, D. Lubos, K. Moschner, D. Murai, I. Nishizuka, J. Park, Z. Patel, M. Rajabali, S. Rice, H. Schaffner, Y. Shimizu, L. Sinclair, P.-A. Söderström, K. Steiger, T. Sumikama, H. Suzuki, H. Takeda, Z. Wang, H. Watanabe, J. Wu, and Z. Xu : "New Isotopes and Proton Emitters–Crossing the Drip Line in the Vicinity of 100Sn", Phys. Rev. Lett. 116, 162501 (2016) 1-6.

Y. L. Sun, J. Lee, Y. L. Ye, A. Obertelli, Z. H. Li, N. Aoi, H. J. Ong, Y. Ayyad, C. A. Bertulani, J. Chen, A. Corsi, F. Cappuzzello, M. Cavallaro, T. Furono, Y. C. Ge, T. Hashimoto, E. Ideguchi, T. Kawabata, J. L. Lou, Q. T. Li, G. Lorusso, F. Lu, H. N. Liu, S. Nishimura, H. Suzuki, J. Tanaka, M. Tanaka, D. T. Tran, M. B. Tsang, J. Wu, Z. Y. Xu, and T. Yamamoto : "Experimental study of the knockout reaction mechanism using 14O at 60 MeV/nucleon", Phys. Rev. C 93, 044607 (2016) 1-8.

A. Jungclaus, A. Gargano, H. Grawe, J. Taprogge, S. Nishimura, P. Doornenbal, G. Lorusso, Y. Shimizu, G. S. Simpson, P.-A. So¨derstro¨m, T. Sumikama, Z. Y. Xu, H. Baba, F. Browne, N. Fukuda, R. Gernha¨user,G. Gey, N. Inabe, T. Isobe, H. S. Jung, D. Kameda, G. D. Kim, Y.-K. Kim, I. Kojouharov, T. Kubo, N. Kurz, Y. K. Kwon, Z. Li, H. Sakurai, H. Schaffner, K. Steiger, H. Suzuki, H. Takeda, Zs. Vajta, H. Watanabe, J. Wu, A. Yagi, K. Yoshinaga, S. Bo¨nig, L. Coraggio, J.-M. Daugas, F. Drouet, A. Gadea, S. Ilieva, N. Itaco, T. Kro¨ll, A. Montaner-Piza´, K. Moschner, D. Mu¨cher, H. Nishibata, A. Odahara, R. Orlandi, and A. Wendt : "First observation of γ rays emitted from excited states south-east of 132Sn: The π $g_{9/2}^{-1}$ ⊗ ν $f_{7/2}$ multiplet of 132In83", Phys. Rev. C 93, 041301(R) (2016) 1-6

[Proceedings]

(Original Papers) *Subject to Peer Review

T. Isobe, *et al.,* "Constraint on Nuclear Symmetry Energy through Heavy RI Collision Experiment by Using SpiRIT Device at RIBF-SAMURAI", JPS Conf. Proc. 14, 010802 (2017) *

H. Wang, "In-beam gamma-ray spectroscopy and cross section measurement strategy for long-lived fission products at RIBF", Proceedings of the 2014 Symposium on Nuclear Data, 69 (2016).

D. Suzuki et al., "Cluster structure of neutron-rich ^{10}Be and ^{14}C via resonant alpha scattering", Il Nuovo Cimento C 39, 372 (2016).

P.-A. Söderström, P. M. Walker, J. Wu, H. L. Liu, P. H. Rega, H. Watanabe, P. Doornenbal, Z. Korkulu, P. Lee, J. J. Liu, G. Lorusso, S. Nishimura, V. H. Phong, T. Sumikama, F. R. Xu, A. Yagi, G. X. Zhang, D. S. Ahn, T. Alharbi, H. Baba, F. Browne, A. M. Bruce, R. J. Carroll, K. Y. Chae, Zs. Dombradi, A. Estrade, N. Fukuda, C. Griffin, E. Ideguchi, N. Inabe, T. Isobe, H. Kanaoka, S. Kanaya, I. Kojouharov, F. G. Kondev, T. Kubo, S. Kubono, N. Kurz, I. Kuti, S. Lalkovski, G. J. Lane, E. J. Lee, C. S. Lee, G. Lotay, C.-B. Moon, I. Nishizuka, C. R. Nit¸a˘, A. Odahara*l*, Z. Patel, Zs. Podolyák, O. J. Roberts, H. Sakurai, H. Schaffner, C. M. Shand, H. Suzuki, H. Takeda, S. Terashima, Zs. Vajta, J. J. Valiente-Dòbon and Z. Y. Xu : "Collective And Single-particle Structures In The Neutron-rich Doubly Mid-shell Nucleus 170Dy", In *Proceedings of International Nuclear Physics Conference, PoS (INPC2016)*, page 072. Sissa, (2017).

V. H. Phong, S. Nishimura, G.Lorusso and A. Algora, "Impact of the β-Delayed Neutron Emission Probabilities Around A= 100–125 on the r-Process and the BRIKEN Project" In Proceedings of the 14th International Symposium on Nuclei in the Cosmos (NIC2016), 020620 (2017).

[Others]

The Proceedings of the 14th International Symposium on Nuclei in the Cosmos NIC2016 (Niigata, 19-24 June, 2016), JPS Conference Proceedings No. 14 (2017) edited by S. Kubono, T. Kajino, S. Nishimura, T. Isobe, S. Nagataki, T. Shima, and Y. Takeda

櫻井博儀, “2 重に魔法数をもったニッケル-78“、パリティ 2016 年 12 月号

櫻井博儀, “百年の計“、Isotope News [特別号 No.1] 2017 年 1 月号

本林透、櫻井博儀, “魔法数の帰趨をめぐって“、原子核研究第 61 巻 2 号 1, 2017

Oral Presentations

[International Conference etc.]

T. Isobe, “Constraint on Nuclear Symmetry Energy through Heavy RI Collision Experiment by Using SpiRIT Device at RIBF-SAMURAI”, 14th International Symposium on Nuclei in the Cosmos XIV, 19-24 Jun 2016, Toki-Messe, Niigata, Japan

H. Wang, “Nuclear structure study for the neutron-rich nuclei beyond ^{132}Sn”, The international conference on Direct Reactions with Exotic Beams (DREB2016), July 11-15, 2016, Halifax, Canada

H. Wang, “Spallation reaction study for fission products in nuclear waste: Cross section measurements for ^{137}Cs, ^{90}Sr and ^{107}Pd on proton and deuteron at different reaction energy”, International conference on nuclear data and technology (ND2016), September 11-16, 2016, Brugge, Belgium

H. Wang, “Measurement of Spallation Cross Sections for ^{137}Cs, ^{90}Sr and ^{107}Pd on Proton and Deuteron Using the Inverse Kinematic Method”, Asian Nuclear Prospects 2016 (ANUP2016), October 24-27, 2016, Sendai, Japan

H. Wang, “Spallation Reaction Study for the Long-Lived Fission Products in Nuclear Waste: Cross Section Measurement for ^{137}Cs, ^{90}Sr and ^{107}Pd Using the Inverse Kinematic Method”, The Fifth International Symposium on Innovative Nuclear Energy Systems (INES-5), October 31-November 2, 2016, Tokyo Institute of Technology, Tokyo, Japan

D. Suzuki, “Second 0^+ state of unbound ^{12}O via the (p,t) reaction”, The international conference on Direct Reactions with Exotic Beams (DREB2016), July 11-15, 2016, Halifax, Canada

D. Suzuki, “Tetra-proton cluster and mirror symmetry”, Third LISE/ICC workshop, December 12-14, 2016 GANIL, Caen, France

D. Suzuki, “Gaseous detectors for radioactive beam experiment”, GDS Topical Meeting: GDS coupling to auxiliary detection systems, January 25-27, 2017 INFN Laboratori Nazionali di Legnaro, Italy

S. Kubono, “Challenge to Explore the Mechanism of Evolution of the Universe and the Origin of Elements”: The 20th International Conference on Accelerators and Beam Utilizations, Nov. 2 - 4, 2016, Gyeongju, Korea, Nov, 2016

S. Kubono, “Problems in BigBang nucleosynthesis; Heavy element synthesis and Li problem”, The 40th ASRC International Workshop on Experimental and Theoretical Advances in Fission and Heavy Nuclei, JAEA, Tokai, 12 – 13th December, 2016

T. Isobe, “DAQ and computing infrastructure for high multiplicity tracking with SpiRIT", Workshop on Software for Time Projection Chambers for Nuclear Physics Experiments, 8-10 Aug 2016, FRIB-MSU, East Lansing, Michigan, USA

T. Isobe, “Experimental study of density dependent nuclear symmetry energy by using heavy RI collision at RIBF-SpiRIT", KPS annual meeting, 19-21 Oct 2016, Kim-Daejon Convension Center, Guanjin, Korea

T. Isobe, “Experimental Study of Neutron Rich Matter EOS at RIKEN-RIBF", APPC-AIP 2016 is the Asia Pacific Physics Conference and 22nd Australian Institute of Physics Congress, 4-8 Dec 2016, Brisbane Convention and Exhibition Centre, Brisbane, Australia

T. Isobe, “Application of transport model to design experiment",Transport 2017: International Workshop on Transport Simulations for Heavy Ion Collisions under Controlled Conditions, 27-31 Mar 2017, FRIB-MSU, East Lansing, Michigan, USA

Y. Nakai, H. Hidaka, N. Watanabe, T.M. Kojima, “Equilibrium of association/dissociation reactions of a water molecule to/ from $H_3O^+(H_2O)_n$ cluster ions in an ion drift tube”, 12th Asian International Seminar on Atomic and Molecular Physics, 6-10 September 2016, Changchun, China

G. G. Kiss, “Beta-delayed neutron emission probability measurements at RIKEN” Hungarian Wayfarer Meeting on Physics 2016, Aug. 24-27; Szeged, Hungary

G. G. Kiss, “Introduction to the Briken project” 3rd EURICA collaboration workshop 2016, Sept. 7-8; Wako, Japan

G. G. Kiss, “Beta delayed neutrons and the astrophysical r process” 3. Annual meeting of the Hungarian Nuclear Physics Community (2016, Dec. 7-9; Paks, Hungary

S. Nishimura, “Experimental beta-decay rates of r-process nuclei”, Neutron star mergers: From gravitational waves to nucleosynthesis, (2017, January 15-21; Hirshegg, Austria

S. Nishimura, “b-decay properties of neutron-rich nulei: impact on r-process abundance”, The 14th International Symposium on Nuclei in the Cosmos (NIC-XIV), 2016, June 19-24; Niigata, Japan

H. Sakurai, "Nuclear magic numbers", The 71st Fujihara Seminar-Shimoda 2016, Shimoda, July 2016

H. Sakurai, "RIB Experiments", ICTP-IAEA workshop on Nuclear Structure and Decay Data: Experiment, Theory and Evaluation, Trieste, Aug. 2016

H. Sakurai, "Decay studies of exotic nuclei at RIKEN", The 2016 Zakopane Conference on Nuclear Physics "Extremes of the Nuclear Landscape", Zakopane, Aug. 2016

H. Sakurai, "Post RIBF project", RIBF Users Meeting 2016, Wako, Sept. 2016

H. Sakurai, "Long-lived Fission Product Transmutation", 21st International Conference on Cyclotrons and their applications, Zurich, Sept. 2016

H. Sakurai, "Recent highlights and future projects at RIBF", Shapes and Symmetries in Nuclei: from Experiment to Theory, Orsay, Nov., 2016

H. Sakurai, "Recent Activities and Plans at RIBF", IBS-RIKEN Conference on Recent Developments in RI Physics, Daejeon, Nov. 2016

H. Sakurai, "The status and future of RIBF", ANPhA2916 Symposium, Sendai, Nov. 2016

H. Sakurai, "New Magicity and Magicity Loss in Atomic Nuclei", Joint 13th Asia Pacific Physics Conference and 22nd Australian Institute of Physics Congress, Brisbane, Dec. 2016

[Domestic Conference]

磯部忠昭, “高密度原子核物資の対称エネルギー”, 「熱場の量子論とその応用研究会」, 23-Aug-16, RIKEN

H. Wang, “Reaction study for fission products in nuclear waste: Cross section measurements for the spallation of ^{137}Cs, ^{90}Sr and ^{107}Pd on proton and deuteron”, JPS meeting 2016 autumn, September 21-24, 2016, Miyazaki University

D. Suzuki, “Missing mass spectroscopy with radioactive isotope beam”, CNS Summer School 2016 (CNSSS2016), August 24 through 30, Riken Wako campus
D. Suzuki, “Overview of the RIBF facility”, CNS Summer School 2016 (CNSSS2016), August 24 through 30, Riken Wako campus
磯部忠昭, "中性子過剰核物質の状態方程式解明に向けた重 RI 衝突実験用タイムプロジェクションチェンバーの開発", 日本物理学会 2016 年秋季大会、21-24-Sep-16、宮崎大学
磯部忠昭, "世界最先端の研究と未来", 社会人講演会、細田学園高校、埼玉県志木市、2016 年 11 月
磯部忠昭, “中性子物質をさぐる時間射影型３次元飛跡検出器の開発”, 「先端物理計測開発室　キックオフワークショップ」, 22-Dec-16, 東京工業大学
磯部忠昭, "科学者になるという事", SSH キャリア講演会、新潟県立長岡高校、新潟県長岡市、2017 年 2 月
磯部忠昭, “SpiRIT 検出器の読み出し回路系”, 「新学術領域中性子星核物質 第二回検出器ワークショップ」, 4-Mar-17, 東京工業大学
Y. Nakai, N. Watanabe, Y. Oba, “Hydrogenation of a thin foil C_{60} under low temperature condition”, 72th Annual meeting of the physical society of Japan, March 2017, Osaka University
金子雅紀, "重イオン衝突を用いた高密度非対称核物質における対称エネルギー研究の解析状況", 日本物理学会 2016 年秋季大会, 21-24-Sep-16, 宮崎大学
櫻井博儀,”理研 RIBF における核物理研究”、東海・重イオン科学シンポジウムータンデム加速器成果報告会ー、東海、2017 年 1 月
櫻井博儀, “親子一緒に"先端研究者から科学を学ぼう“、本郷、2016 年 7 月
櫻井博儀, "魔法数研究　RIPS から RIBF への展開と今後"、日本物理学会秋の分科会、宮崎大学、2016 年 9 月

Posters Presentations

[International Conference etc.]

M. Kaneko, “Experimental Study on the Symmetry Energy of Nuclear Matter with SpiRIT-TPC”, 14th International Symposium on Nuclei in the Cosmos XIV, 19-24 Jun 2016, Toki-Messe, Niigata, Japan

RIBF Research Division
Spin isospin Laboratory

1. Abstract

The Spin Isospin Laboratory pursues research activities putting primary focus on interplay of spin and isospin in exotic nuclei. Understanding nucleosyntheses in the universe, especially those in r- and rp-processes is another big goal of our laboratory.

Investigations on isospin dependences of nuclear equation of state, spin-isospin responses of exotic nuclei, occurrence of various correlations at low-densities, evolution of spin-orbit coupling are main subjects along the line. We are leading a mass measurement project with the Rare RI Ring project, too. Through the experimental studies, we will be able to elucidate a variety of nuclear phenomena in terms of interplay of spin and isospin, which will in turn, lead us to better understanding of our universe.

2. Major Research Subjects

(1) Direct reaction studies of neutron-matter equation of state
(2) Study of spin-isospin responses with RI-beams
(3) R-process nucleosynthesis study with heavy-ion storage ring
(4) Application of spin-polarization technique to RI-beam experiments and other fields
(5) Development of special targets for RI-beam experiments

3. Summary of Research Activity

(1) Direct reaction studies of neutron matter equation of state

Direct reactions induced by light-ions serve as powerful tools to investigate various aspects of nuclei. We are advancing experimental programs to explore equation of state of neutron matter, via light-ion induced reactions with RI-beams.

(1-a) Determination of a neutron skin thickness by proton elastic scattering

A neutron skin thickness is known to have strong relevance to asymmetry terms of nuclear equation of state, especially to a term proportional to density. The ESPRI project aims at determining density distributions in exotic nuclei precisely by proton elastic scattering at 200−300 MeV/nucleon. An experiment for ^{132}Sn that is a flagship in this project has been successfully performed in 2016.

(1-b) Asymmetry terms in nuclear incompressibility

Nuclear incompressibility represents stiffness of nuclear matter. Incompressibility of symmetric nuclear matter is determined to be 230±20 MeV, but its isospin dependence still has a large uncertainty at present. A direct approach to the incompressibility of asymmetric nuclear matter is an experimental determination of energies of isoscalar giant monopole resonances (GMR) in heavy nuclei. We have developed, in close collaboration with Center for Nuclear Study (CNS) of University of Tokyo, an active gas target for deuteron inelastic scattering experiments to determine GMR energies. The active gas target has been already tested with oxygen and xenon beams at HIMAC and finally has been applied to a ^{132}Sn experiment in 2016.

(1-c) Multi-neutron and α-cluster correlations at low densities

Occurrences of multi-neutron andα-cluster correlations are other interesting aspects of nuclear matter and define its low-density behavior. The multi-neutron and α-cluster correlations can be investigated with the large-acceptance SAMURAI spectrometer. The SAMURAI has been already applied to experiments to explore light neutron-rich nuclei close to the dripline. We plan to reinforce experimental capabilities of the SAMURAI by introducing advanced devices such as MINOS (Saclay) and NeuLAND (GSI).

(1-d) Fission barrier heights in neutron-rich heavy nuclei

The symmetry energy has a strong influence on fission barrier heights in neutron-rich nuclei. Knowledge on the fission barrier heights, which is quite poor at present, is quite important for our proper understanding on termination of the r-process. We are planning to perform, in collaboration with the TU Munich group, (p,2p)-delayed fission experiments at the SAMURAI to determine the fission barrier heights in neutron-rich nuclei in Pb region.

(2) Study of spin-isospin responses with RI-beams

The study of spin-isospin responses in nuclei forms one of the important cores of nuclear physics. A variety of collective states, for example isovector giant dipole resonances, isobaric analogue states, Gamow-Teller resonances, have been extensively studied by use of electromagnetic and hadronic reactions from stable targets.

The research opportunities can be largely enhanced with light of availabilities of radioactive isotope (RI) beams and of physics of unstable nuclei. There are three possible directions to proceed. The first direction is studies of spin-isospin responses of unstable nuclei via inverse-kinematics charge exchange reactions. A neutron-detector array WINDS has been constructed, under a collaboration of CNS, Tokyo and RIKEN, for inverse kinematics (p,n) experiments at the RI Beam Factory. We have already applied WINDS to the (p,n) experiments for ^{12}Be, ^{132}Sn and plan to extend this kind of study to other exotic nuclei.

The second direction is studies with RI-beam induced charge exchange reaction. RI-beam induced reactions have unique properties which are missing in stable-beam induced reactions and can be used to reach the yet-to-be-discovered states. We have constructed the SHARAQ spectrometer and the high-resolution beam-line at the RI Beam Factory to pursue the capabilities of RI-beam induced reactions as new probes to nuclei. One of the highlights is an observation of β^+ type isovector spin monopole resonances (IVSMR) in ^{208}Pb and ^{90}Zr

via the (t, ^{3}He) reaction at 300 MeV/nucleon.

The third direction is studies of neutron- and proton-rich nuclei via stable-beam induced charge exchange reactions, which is conducted under collaboration with Research Center for Nuclear Physics (RCNP), Osaka University. We have performed the double charge exchange ^{12}C(^{18}O, ^{18}Ne)^{12}Be reaction at 80 MeV/nucleon to investigate structure of a neutron-rich ^{12}Be nucleus. Peaks corresponding to ground and excited levels in ^{12}Be have been clearly observed. Another double charge exchange reaction, (^{12}C, ^{12}Be(0_2^+)) are being used to search for double Gamow-Teller resonances.

(3) R-process nucleosynthesis study with heavy-ion storage ring

Most of the r-process nuclei become within reach of experimental studies for the first time at RI Beam Factory at RIKEN. The Rare RI Ring at RIBF is the unique facility with which we can perform mass measurements of r-process nuclei. Construction of the Rare RI Ring started in FY2012 in collaboration with Tsukuba and Saitama Universities. A major part of the ring has been completed and the commissioning run is planned in FY2014.

We are planning to start precise mass measurements of r-process nuclei soon. A series of experiments will start with nuclei in the A=80 region and will be extended to heavier region.

(4) Application of spin-polarization technique to RI-beam experiments and other fields

A technique to produce nuclear polarization by means of electron polarization in photo-excited triplet states of aromatic molecules can open new applications. The technique is called “Tripletd-DNP”. A distinguished feature of Triplet-DNP is that it works under a low magnetic field of 0.1—0.7 T and temperature higher than 100 K, which exhibits a striking contrast to standard dynamic nuclear polarization (DNP) techniques working in extreme conditions of several Tesla and sub-Kelvin.

We have constructed a polarized proton target system for use in RI-beam experiments. Recent experimental and theoretical studies have revealed that spin degrees of freedom play a vital role in exotic nuclei. Tensor force effects on the evolution of shell and possible occurrence of p-n pairing in the proton-rich region are good examples of manifestations of spin degrees of freedom. Experiments with the target system allow us to explore the spin effects in exotic nuclei. It should be noted that we have recently achieved a proton polarization of 40% at room temperature in a pentacene-d_{14} doped p-terphenyl crystal.

Another interesting application of Triplet-DNP is sensitivity enhancement in NMR spectroscopy of biomolecules. We started a new project in 2016 to apply the Triplet-DNP technique to study protein-protein interaction via two-dimensional NMR spectroscopy, in close collaboration with biologists and chemists.

(5) Development of special targets for RI-beam experiments

For the research activities shown above, we are developing and hosting special targets for RI-beam experiments listed below:

a) Polarized proton target (described in (4))
b) Thin solid hydrogen target
c) MINOS (developed at Saclay and hosted by the Spin Isospin Laboratory)

Members

Chief Scientist (Lab. Head)

Tomohiro UESAKA

Research & Technical Scientists

Ken-ichiro YONEDA (Senior Research Scientist, concurrent ; Team Leader, User Support Office)
Masaki SASANO (Research Scientist)
Juzo ZENIHIRO (Research Scientist)
Sarah NAIMI (Research Scientist)

Contract Researcher

Daisuke NAGAE

Special Postdoctoral Researchers

Kenichiro TATEISHI
Yuki KUBOTA
Yuma KIKUCHI

Foreign Postdoctoral Researchers

Zaihong YANG

Postdoctoral Researchers

Valerii PANIN
Fumi SUZAKI

Research Associate

Masami SAKO
Takahiro NISHI
Kenichiro TATEISHI
Tsz Leung TANG

Junior Research Associates

CheongSoo LEE (Univ. of Tokyo)
Fumi SUZAKI (Saitama Univ.)
Shunichiro OMIKA (Saitama Univ.)
Yuki KUBOTA (Univ. of Tokyo)

International Program Associates

Sergey CHEBOTARYOV (Kyungpook Nat'l Univ.)
Evgeniy Vladimirovich MILMAN (Kyungpook Nat'l Univ.)
Zhuang GE (Institute of Modern Physics Chinese Academy of Sciences,)
Julian KAHLBOW (Technical University Darmstadt)

Research Consultant

Harutaka SAKAGUCHI
Kazuko TANABE

Visiting Researchers

Stuhl LASZLO (JSPS Fellow)
Keiichi KISAMORI (JSPS Fellow)

Senior Visiting Scientists

Hiroyuki SAGAWA (Aizu Univ.)

Visiting Scientists

Didier BEAUMEL (IPN)
Yasuyuki SUZUKI (Niigata Univ.)
Yosuke KONDO (Tokyo Tech.)
Zoltan ELEKES (ATOMKI)
Hidetoshi AKIMUNE (Konan Univ.)
Yohei MATSUDA (Osaka Univ.)
Yasuhiro TOGANO (Tokyo Tech.)
Satoshi SAKAGUCHI (Kyusyu Univ.)
Kenjiro MIKI (TU Darmstadt)
Valerie LAPOUX (CEA Saclay)
Alexandre OBERTELLI (CEA Saclay)
Alain GILLIBERT (CEA Saclay)
Emanuel POLLACCO (CEA Saclay)
Anna CORSI (CEA Saclay)
Dennis MUECHER (TUM)
Yuma KIKUCHI (Osaka City Univ.)
Yury LITVINOV (GSI)
Yuhu ZHANG (CAS)
Igor GASPARIC (Ruder Boskovic Inst. Zagreb Croatia)
Hans Toshihide TOERNQVIST (TU Darmstadt)
Christoph CAESAR (GSI)
Haik SIMON (GSI)
Matthias HOLL (TU Darmstadt)
Takayuki YAMAGUCHI (Saitama Univ.)
Takashi NAKAMURA (Tokyo Tech.)
Atsushi TAMII (Osaka Univ.)
Attila KRASZNAHORKAY (ATOMKI)
Takashi WAKUI (Tohoku Univ.)
Kimiko SEKIGUCHI (Tohoku Univ.)
Dorottya KUNNE SOHLER (Institute of Nuclear Research Hungarian Academy of Sciences (ATOMKI))
Satoru TERASHIMA (Beihang University)
Valdir GUIMARAES (Instituto de Fisica da Universidade de Sao Paulo)
Yasutaka TANIGUCHI (Nihon Institute of Medical Science)
Tetsuaki MORIGUCHI (Univ. of Tsukuba)
Kazuyuki OGATA (Osaka Univ.)
Shinji SUZUKI (Univ. of Tsukuba)
Zsolt VAJTA (Institute of Nuclear Research Hungarian Academy of Sciences (ATOMKI))
Istvan KUTI (Institute of Nuclear Research Hungarian Academy of Sciences (ATOMKI))
Makoto NEGORO (Osaka Univ.)
Konstanze BORETZKY (GSI)
Zsolt FULOP (Institute of Nuclear Research Hungarian Academy of Sciences (ATOMKI))
Zsolt DOMBRADI (Institute of Nuclear Research Hungarian Academy of Sciences (ATOMKI))
Akinori KAGAWA (Osaka Univ.)
Baohua SUN (Beihang Univ.)
Leyla ATAR (TU Darmstadt)
Zoltan HALASZ (ATOMKI)
Li-Gang CAO (North China Electric Power Univ.)
Kaori KAKI (Shizuoka Univ.)

Visiting Technicians

Tomomi KAWAHARA (Toho Univ.)
Gilles AUTHELET (CEA Saclay)
Jean-Marc GHELLER (CEA Saclay)
Cedric PERON (CEA Saclay)
Jean-Yves ROUSSE (CEA Saclay)
Denis CALVET (CEA Saclay)
Alan PEYAUD (CEA Saclay)
Alain DELBART (CEA Saclay)
Frederic CHATEAU (CEA Saclay)
Caroline LAHONDE-HAMDOUN (CEA Saclay)
Arnaud GIGANON (CEA Saclay)
Daniel KOERPER (GSI)
Clement HILAIRE (CEA Saclay)

Student Trainees

Yasunori WADA (Tohoku Univ.)
Tatsuya FURUNO (Kyoto Univ.)
Miho TSUMURA (Kyoto Univ.)
Jumpei YASUDA (Kyushu Univ.)
Mizuki SHIKATA (Tokyo Tech.)
Junichi TSUBOTA (Tokyo Tech.)
Yuuki TAKEUCHI (Saitama Univ.)
Syunichirou OHMIKA (Saitama Univ.)
Hiroshi MIURA (Saitama Univ.)
Takuma NISHIMURA (Saitama Univ.)
Motoki MURATA (Kyoto Univ.)
Syunsuke KAWAKAMI (Miyazaki Univ.)
Daijiro ETO (Tohoku Univ.)
Junki TANAKA (Osaka Univ.)
Sebastian Benedikt REICHERT (TU Munchen)
Tomoyuki OZAKI (Tokyo Tech.)
Atsumi SAITO (Tokyo Tech.)
Yusuke SHINDO (Kyushu Univ.)
Munemi TABATA (Kyushu Univ.)
Atomu WATANABE (Tohoku Univ.)
Ayaka OHKURA (Kyushu Univ.)
Yukina ICHIKAWA (Univ. of Tsukuba)
Kotaro YAMADA (Toho Univ.)
Tomoaki KANEKO (Toho Univ.)

Julian KAHLBOW (TU Darmstadt)
Taras LOKOTKO (Univ. of Hong Kong)
Dahee KIM (Ewha Womans Univ.)
Natsuki TADANO (Saitama Univ.)
Ikuma KATO (Saitama Univ.)
Tomomi AKIEDA (Tohoku Univ.)
Hiroshi KON (Tohoku Univ.)
Tomoyuki MUKAI (Tohoku Univ.)
Shinnosuke NAKAI (Tohoku Univ.)
Takato TOMAI (Tokyo Tech.)
Akihiro HIRAYAMA (Tokyo Tech.)
Yoshiyuki TAJIRI (Univ. of Tsukuba)
Kentaro HIRAISHI (Univ. of Tsukuba)
Simon LINDBERG (Chalmers University of Technology)
Masamichi AMANO (Univ. of Tsukuba)
Daisuke SAKAE (Kyushu Univ.)
Yasuaki NORIMATSU (Kyushu Univ.)
Takahiro FUKUTA (Kyushu Univ.)
Youhei AKIYAMA (Kyushu Univ.)
Kiyoshi WAKAYAMA (Saitama Univ.)
Han Hagen MAYER (University of Cologne)
Takahiro MORIMOTO (Kyoto Univ.)
Katsuyoshi HEGURI (Konan Univ.)
Takuya MATSUMOTO (Univ. of Tsukuba)
Tomoya HARADA (Toho Univ.)
Kosei TANIUE (Univ. of Miyazaki)
Masahiro YASUDA (Tokyo Tech.)
Hiroki YAMADA (Tokyo Tech)
Jun OKAMOTO (Tohoku Univ.)
Yu NASU (Tohoku Univ.)
Shota MATSUMOTO (Kyoto Univ.)
Simon GIRAUD (Université de Nantes)
Yu ANDO (Kyungpook National Univ.)
Sonja STORCK (TU Darmstadt)
Ina Josephine SYNDIKUS (TU Darmstadt)
Mayuko MATSUMOTO (Tokyo Tech.)
Daiki KAMIOKA (Univ. of Tsukuba)
Christopher LEHR (TU Darmstadt)
Tomoya FUJII (Saitama Univ.)
Kunimitsu NISHIMURO (Saitama Univ.)
Ryo IGOSAWA (Saitama Univ.)
Kumi INOMATA (Saitama Univ.)
Hiroki ARAKAWA (Saitama Univ.)
Jan Daniel STEINHAUSER (Tokyo Tech.)

Interns

Lily SIEGENBERG (Univ. of Surrey)
Quentin Nathanael DESHAYES (Universite de Caen Normandie)
David HEGEDUES (Eotvos Lorand Univ.)

Part-time Worker

Kotaro YAMADA

Assistants

Emiko ISOGAI
Yu NAYA
Yuri TSUBURAI
Noriko KIYAMA

List of Publications & Presentations

Publications

[Journal]

(Original Papers) *Subject to Peer Review

P. Moller, A.J. Sierk, T. Ichikawa, H. Sagawa, Nuclear ground-state masses and deformations: FRDM(2012), Atomic Data and Nuclear Data Tables, Volume 109, 1 (2016).

J. Yasuda, M. Sasano, R.G.T. Zegers, H. Baba, W. Chao, M. Dozono, N. Fukuda, N. Inabe, T. Isobe, G. Jhang, D. Kameda, T. Kubo, M. Kurata-Nishimura, E. Milman, T. Motobayashi, H. Otsu, V. Panin, W. Powell, H. Sakai, M. Sako, H. Sato, Y. Shimizu, L. Stuhl, H. Suzuki, S. Tangwancharoen, H. Takeda, T. Uesaka, K. Yoneda, J. Zenihiro, T. Kobayashi, T. Sumikama, T. Tako, T. Nakamura, Y. Kondo, Y. Togano, M. Shikata, J. Tsubota, K. Yako, S. Shimoura, S. Ota, S. Kawase, Y. Kubota, M. Takaki, S. Michimasa, K. Kisamori, C.S. Lee, H. Tokieda, M. Kobayashi, S. Koyama, N. Kobayashi, T. Wakasa, S. Sakaguchi, A. Krasznahorkay, T. Murakami, N. Nakatsuka, M. Kaneko, Y. Matsuda, D. Mucher, S. Reichert, D. Bazin, J.W. Lee, Inverse kinematics reactions studies using the WINDS slow neutron detector and the SAMURAI spectrometer, Nuclear Instruments and Methods in Physics Research Section B: Beam Interactions with Materials and Atoms, Volume 376, 393 (2016).

E. Minaya Ramirez, P. Alfaurt, M. Aouadi, P. Ascher, B. Blank, K. Blaum, J.-F. Cam, P. Chauveau, L. Daudin, P. Delahaye, F. Delalee, P. Dupre, S. El Abbeir, M. Gerbaux, S. Grevy, H. Guerin, D. Lunney, F. Metz, S. Naimi, L. Perrot, A. de Roubin, L. Serani, B. Thomas, J.-C. Thomas, Conception of PIPERADE: A high-capacity Penning-trap mass separator for high isobaric contamination at DESIR, Nuclear Instruments and Methods in Physics Research Section B: Beam Interactions with Materials and Atoms, Volume 376, 298 (2016).

H. Otsu, S. Koyama, N. Chiga, T. Isobe, T. Kobayashi, Y. Kondo, M. Kurokawa, W.G. Lynch, T. Motobayashi, T. Murakami, T. Nakamura, M. Kurata-Nishimura, V. Panin, H. Sato, Y. Shimizu, H. Sakurai, M.B. Tsang, K. Yoneda, H. Wang, SAMURAI in its operation phase for RIBF users, Nuclear Instruments and Methods in Physics Research Section B: Beam Interactions with Materials and Atoms, Volume 376, 175 (2016).

Yusuke Tanimura and Hiroyuki Sagawa, Three-body model for an isoscalar spin-triplet neutron-proton pair in 102Sb, Physical Review C **93**, 064319 (2016)

E. Ganioğlu, H. Fujita, B. Rubio, Y. Fujita, T. Adachi, A. Algora, M. Csatlós, J. M. Deaven, E. Estevez-Aguado, C. J. Guess, J. Gulyás, K. Hatanaka, K. Hirota, M. Honma, D. Ishikawa, A. Krasznahorkay, H. Matsubara, R. Meharchand, F. Molina, H. Okamura, H. J. Ong, T. Otsuka, G. Perdikakis, C. Scholl, Y. Shimbara, G. Susoy, T. Suzuki, A. Tamii, J. H. Thies, R. G. T. Zegers, and J. Zenihiro, High-resolution study of Gamow-Teller transitions in the 48Ti(3He,t)48V reaction, Physical Review C **93**, 064326 (2016)

J.W. Zhao, B.H. Sun, I. Tanihata, S. Terashima, L.H. Zhu, A. Enomoto, D. Nagae, T. Nishimura, S. Omika, A. Ozawa, Y. Takeuchi, T. Yamaguchi, Reaching time resolution of less than 10ps with plastic scintillation detectors, Nuclear Instruments and Methods in Physics Research Section A: Accelerators, Spectrometers, Detectors and Associated Equipment, Volume 823, 41 (2016).

Y H Zhang, Yu A Litvinov, T Uesaka and H S Xu, Storage ring mass spectrometry for nuclear structure and astrophysics research, Physica

Scripta **91**, 073002 (2016).
H Sagawa, C L Bai and G Colò, Isovector spin-singlet (T = 1, S = 0) and isoscalar spin-triplet (T = 0, S = 1) pairing interactions and spin-isospin response, Physica Scripta **91**, 083011 (2016)
Xian-Rong Zhou, E. Hiyama, and H. Sagawa, Exotic structure of medium-heavy hypernuclei in the Skyrme Hartree-Fock model, Physical Review C **94**, 024331 (2016)
E Hiyama, Y Yamamoto and H Sagawa, The structure of hypernuclei and hyperon mixing in neutron-star matter, Physica Scripta **91**, 093001 (2016)
M. Dozono, T. Uesaka, S. Michimasa, M. Takaki, M. Kobayashi, M. Matsushita, S. Ota, H. Tokieda, and S. Shimoura, Separated flow operation of the SHARAQ spectrometer for in-flight proton-decay experiments, Nuclear Instruments and Methods in Physics Research Section A: Accelerators, Spectrometers, Detectors and Associated Equipment, Volume 830, 233 (2016)
Yuma Kikuchi, Kazuyuki Ogata, Yuki Kubota, Masaki Sasano, and Tomohiro Uesaka, Determination of a dineutron correlation in Borromean nuclei via a quasi-free knockout (p,pn) reaction, Progress of Theoretical and Experimental Physics **2016**, 103D03 (2016)
X. Roca-Maza, Li-Gang Cao, G. Colò, and H. Sagawa, Fully self-consistent study of charge-exchange resonances and the impact on the symmetry energy parameters, Physical Review C **94**, 044313 (2016).
Zhen-Yu Zhu, Ang Li, Jin-Niu Hu, and Hiroyuki Sagawa, Δ(1232) effects in density-dependent relativistic Hartree-Fock theory and neutron stars, Physical Review C **94**, 045803 (2016).
H. Sagawa, T. Suzuki, and M. Sasano, Effect of isoscalar spin-triplet pairings on spin-isospin responses in sd-shell nuclei, Physical Review C **94**, 041303(R) (2016).
X. Xu, P. Zhang, P. Shuai, R. J. Chen, X. L. Yan, Y. H. Zhang, M. Wang, Yu. A. Litvinov, H. S. Xu, T. Bao, X. C. Chen, H. Chen, C. Y. Fu, S. Kubono, Y. H. Lam, D. W. Liu, R. S. Mao, X. W. Ma, M. Z. Sun, X. L. Tu, Y. M. Xing, J. C. Yang, Y. J. Yuan, Q. Zeng, X. Zhou, X. H. Zhou, W. L. Zhan, S. Litvinov, K. Blaum, G. Audi, T. Uesaka, Y. Yamaguchi, T. Yamaguchi, A. Ozawa, B. H. Sun, Y. Sun, A. C. Dai, and F. R. Xu, Identification of the Lowest T = 2, Jπ = 0+ Isobaric Analog State in 52Co and Its Impact on the Understanding of β-Decay Properties of 52Ni, Physical Review Letters **117**, 182503 (2016)
T. Uesaka, Spins in exotic nuclei: RI beam experiments with polarized targets, The European Physical Journal Plus 131, 403 (2016)
D. T. Tran, H. J. Ong, T. T. Nguyen, I. Tanihata, N. Aoi, Y. Ayyad, P. Y. Chan, M. Fukuda, T. Hashimoto, T. H. Hoang, E. Ideguchi, A. Inoue, T. Kawabata, L. H. Khiem, W. P. Lin, K. Matsuta, M. Mihara, S. Momota, D. Nagae, N. D. Nguyen, D. Nishimura, A. Ozawa, P. P. Ren, H. Sakaguchi, J. Tanaka, M. Takechi, S. Terashima, R. Wada, and T. Yamamoto, Charge-changing cross-section measurements of 12–16C at around 45 AMeV and development of a Glauber model for incident energies 10 A–2100 AmeV, Physical Review C **94**, 064604 (2016)
J.C. Zamora, T. Aumann, S. Bagchi, S. Bヲhnig, M. Csatlos, I. Dillmann, C. Dimopoulou, P. Egelhof, V. Eremin, T. Furuno, H. Geissel, R. Gernhaeuser, M.N. Harakeh, A.-L. Hartig, S. Ilieva, N. Kalantar-Nayestanaki, O. Kiselev, H. Kollmus, C. Kozhuharov, A. Krasznahorkay, Th. Kroll, M. Kuilman, S. Litvinov, Yu.A. Litvinov, M. Mahjour-Shafiei, M. Mutterer, D. Nagae, M.A. Najafi, C. Nociforo, F. Nolden, U. Popp, C. Rigollet, S. Roy, C. Scheidenberger, M. von Schmid, M. Steck, B. Streicher, L. Stuhl, M. Thurauf, T. Uesaka, H. Weick, J.S. Winfield, D. Winters, P.J. Woods, T. Yamaguchi, K. Yue, J. Zenihiro, First measurement of isoscalar giant resonances in a stored-beam experiment, Physics Letters B, Volume 763, 16 (2016).
T. T. Sun, E. Hiyama, H. Sagawa, H.-J. Schulze, and J. Meng, Mean-field approaches for Ξ−hypernuclei and current experimental data, Physical Review C **94**, 064319 (2016)
H. Sagawa and T. Uesaka, Sum rule study for double Gamow-Teller states, Physical Review C **94**, 064325 (2016).
Y. F. Niu, G. Colò, E. Vigezzi, C. L. Bai, and H. Sagawa, Quasiparticle random-phase approximation with quasiparticle-vibration coupling: Application to the Gamow-Teller response of the superfluid nucleus 120Sn, Physical Review C **94**, 064328 (2016).
N. Paul, A. Corsi, A. Obertelli, P. Doornenbal, G. Authelet, H. Baba, B. Bally, M. Bender, D. Calvet, F. Château, S. Chen, J.-P. Delaroche, A. Delbart, J.-M. Gheller, A. Giganon, A. Gillibert, M. Girod, P.-H. Heenen, V. Lapoux, J. Libert, T. Motobayashi, M. Niikura, T. Otsuka, T. R. Rodríguez, J.-Y. Roussé, H. Sakurai, C. Santamaria, N. Shimizu, D. Steppenbeck, R. Taniuchi, T. Togashi, Y. Tsunoda, T. Uesaka, T. Ando, T. Arici, A. Blazhev, F. Browne, A. M. Bruce, R. Carroll, L. X. Chung, M. L. Cortés, M. Dewald, B. Ding, F. Flavigny, S. Franchoo, M. Górska, A. Gottardo, A. Jungclaus, J. Lee, M. Lettmann, B. D. Linh, J. Liu, Z. Liu, C. Lizarazo, S. Momiyama, K. Moschner, S. Nagamine, N. Nakatsuka, C. Nita, C. R. Nobs, L. Olivier, Z. Patel, Zs. Podolyák, M. Rudigier, T. Saito, C. Shand, P.-A. Söderström, I. Stefan, R. Orlandi, V. Vaquero, V. Werner, K. Wimmer, and Z. Xu, Are There Signatures of Harmonic Oscillator Shells Far from Stability? First Spectroscopy of 110Zr, Physical Review Letters **118**, 032501 (2017).
K. Hagino and H. Sagawa, New concept for the pairing anti-halo effect as a localized wave packet of quasiparticles, Physical Review C **95**, 024304 (2017).
P. Zhang, X. Xu, P. Shuai, R.J. Chen, X.L. Yan, Y.H. Zhang, M. Wang, Yu.A. Litvinov, K. Blaum, H.S. Xu, T. Bao, X.C. Chen, H. Chen, C.Y. Fu, J.J. He, S. Kubono, Y.H. Lam, D.W. Liu, R.S. Mao, X.W. Ma, M.Z. Sun, X.L. Tu, Y.M. Xing, J.C. Yang, Y.J. Yuan, Q. Zeng, X. Zhou, X.H. Zhou, W.L. Zhan, S. Litvinov, G. Audi, T. Uesaka, Y. Yamaguchi, T. Yamaguchi, A. Ozawa, B.H. Sun, Y. Sun, and F.R. Xu, High-precision QEC values of superallowed 0+ → 0+ β-emitters 46Cr, 50Fe and 54Ni, Physics Letters B, Volume 767, 20 (2017).
S. Chen, P. Doornenbal, A. Obertelli, T. R. Rodríguez, G. Authelet, H. Baba, D. Calvet, F. Château, A. Corsi, A. Delbart, J.-M. Gheller, A. Giganon, A. Gillibert, V. Lapoux, T. Motobayashi, M. Niikura, N. Paul, J.-Y. Roussé, H. Sakurai, C. Santamaria, D. Steppenbeck, R. Taniuchi, T. Uesaka, T. Ando, T. Arici, A. Blazhev, F. Browne, A. M. Bruce, R. Caroll, L. X. Chung, M. L. Cortés, M. Dewald, B. Ding, F. Flavigny, S. Franchoo, M. Górska, A. Gottardo, A. Jungclaus, J. Lee, M. Lettmann, B. D. Linh, J. Liu, Z. Liu, C. Lizarazo, S. Momiyama, K. Moschner, S. Nagamine, N. Nakatsuka, C. R. Nita, C. Nobs, L. Olivier, R. Orlandi, Z. Patel, Zs. Podolyak, M. Rudigier, T. Saito, C. Shand, P.-A. Söderström, I. Stefan, V. Vaquero, V. Werner, K. Wimmer, and Z. Xu, Low-lying structure and shape evolution in neutron-rich Se isotopes, Physical Review C **95**, 041302(R) (2017).
M. Scott, R. G. T. Zegers, R. Almus, Sam M. Austin, D. Bazin, B. A. Brown, C. Campbell, A. Gade, M. Bowry, S. Galès, U. Garg, M. N. Harakeh, E. Kwan, C. Langer, C. Loelius, S. Lipschutz, E. Litvinova, E. Lunderberg, C. Morse, S. Noji, G. Perdikakis, T. Redpath, C. Robin, H. Sakai, Y. Sasamoto, M. Sasano, C. Sullivan, J. A. Tostevin, T. Uesaka, and D. Weisshaar, Observation of the Isovector Giant Monopole Resonance via the 28Si(10Be, 10B∗[1.74 MeV]) Reaction at 100 AmeV, Physical Review Letters **118**, 172501 (2017).
N. Nakatsuka, H. Baba, T. Aumann, R. Avigo, S.R. Banerjee, A. Bracco, C. Caesar, F. Camera, S. Ceruti, S. Chen, V. Derya, P. Doornenbal, A. Giaz, A. Horvat, K. Ieki, T. Inakura, N. Imai, T. Kawabata, N. Kobayashi, Y. Kondo, S. Koyama, M. Kurata-Nishimura, S. Masuoka, M. Matsushita, S. Michimasa, B. Million, T. Motobayashi, T. Murakami, T. Nakamura, T. Ohnishi, H.J. Ong, S. Ota, H. Otsu, T. Ozaki, A. Saito, H. Sakurai, H. Scheit, F. Schindler, P. Schrock, Y. Shiga, M. Shikata, S. Shimoura, D. Steppenbeck, T. Sumikama, I. Syndikus, H. Takeda, S.

Takeuchi, A. Tamii, R. Taniuchi, Y. Togano, J. Tscheuschner, J. Tsubota, H. Wang, O. Wieland, K. Wimmer, Y. Yamaguchi, K. Yoneda, and J. Zenihiro, Observation of isoscalar and isovector dipole excitations in neutron-rich 20O, Physics Letters B, Volume 768, 387 (2017).

K. Sawahata, A. Ozawa, Y. Saito, Y. Abe, Y. Ichikawa, N. Inaba, Y. Ishibashi, A. Kitagawa, S. Matsunaga, T. Moriguchi, D. Nagae, S. Okada, S. Sato, S. Suzuki, T. Suzuki, Y. Takeuchi, T. Yamaguchi, J. Zenihiro, Investigations of charge-changing processes for light proton-rich nuclei on carbon and solid-hydrogen targets, Nuclear Physics A, Volume 961, 142 (2017).

J. Li, Y. L. Ye, Z. H. Li, C. J. Lin, Q. T. Li, Y. C. Ge, J. L. Lou, Z. Y. Tian, W. Jiang, Z. H. Yang, J. Feng, P. J. Li, J. Chen, Q. Liu, H. L. Zang, B. Yang, Y. Zhang, Z. Q. Chen, Y. Liu, X. H. Sun, J. Ma, H. M. Jia, X. X. Xu, L. Yang, N. R. Ma and L. J. Sun, Selective decay from a candidate of the σ-bond linear-chain state in 14C, Physical Review C **95**, 021303(R) (2017).

G. Audi, F.G. Kondev, Meng Wang, W.J. Huang, and S. Naimi, The NUBASE2016 evaluation of nuclear properties, Chinese Physics C **41**, 030001 (2017).

W.J. Huang, G. Audi, Meng Wang, F.G. Kondev, S. Naimi, and Xing Xu, The AME2016 atomic mass evaluation (I). Evaluation of input data; and adjustment procedures, Chinese Physics C **41**, 030002 (2017).

Meng Wang, G. Audi, F.G. Kondev, W.J. Huang, S. Naimi, and Xing Xu, The AME2016 atomic mass evaluation (II). Tables, graphs and references, Chinese Physics **41**, 030003 (2017).

[Proceedings]

(Original Papers) *Subject to Peer Review

J. Yasuda, T. Wakasa, M. Dozono, T. Fukunaga, S. Gotanda, K. Hatanaka, Y. Kanaya, Y. Maeda, Y. Maeda, K. Miki, Y. Nishio, T. Noro, K. Ohnaka, S. Sakaguchi, Y. Sakemi, K. Sekiguchi, A. Tamii, T. Taguchi, Y. Wada, Development of Neutron Polarization Measurement System for Studying NN interaction in Nuclear Medium, International Journal of Modern Physics: Conference Series **40**, 1660073 (2016).

Satoshi Sakaguchi, Tomohiro Uesaka, Takashi Wakui, Sergey Chebotaryov, Tomomi Kawahara, Shoichiro Kawase, Evgeniy Milman, Tsz Leung Tang, Kenichiro Tateishi, and Takashi Teranishi, Studies of Unstable Nuclei with Spin-Polarized Proton Target, International Journal of Modern Physics: Conference Series **40**, 1660071 (2016).

K. Sekiguchi, Y. Wada, A. Watanabe, D. Eto, T. Akieda, H. Kon, K. Miki, N. Sakamoto, H. Sakai, M. Sasano, Y. Shimizu, H. Suzuki, T. Uesaka, Y. Yanagisawa, M. Dozono, S. Kawase, Y. Kubota, C. S. Lee, K. Yako, Y. Maeda, S. Kawakami, T. Yamamoto, S. Sakaguchi, T. Wakasa, J. Yasuda, A. Ohkura, Y. Shindo, M. Tabata, E. Milman,S. Chebotaryov, H. Okamura, and T. L. Tang, Deuteron Analyzing Powers for dp Elastic Scattering at Intermediate Energies and Three-Nucleon Forces, The 23rd European Conference on Few-Body Problems in Physics, 48 (2017).

Oral Presentations

[International Conference etc.]

T. Uesaka, ``R-process studies at RIBF'', ICNT Workshop “The r-process nucleosynthesis: connecting FRIB with the cosmos”, East Lansing, USA, 6—10 June, 2016

T. Uesaka, ``RIBF's challenge to the r-process nucleosynthesis'', 14th International Symposium on Nuclei in the Cosmos (NIC-XIV), Niigata, Japan, 19—24 June 2016.

T. Uesaka, ``(d,p) and Knockout reactions with high momentum transfer'', ECT* Workshop ``Three-body systems in reactions with rare isotopes'', Trento, Italy, 3—7 October, 2016

T. Uesaka, ``Studies of neutron-rich nuclei at RIBF – from tetraneutron to fission'', 6th International Conference on Fission and properties of neutron-rich nuclei, Florida, USA, 6—12 November 2016.

T. Uesaka, Y. Yamazaki, H. Katori, S. Ulmer, ``Extreme precision to Explore fundamental physics with Exotic particles'', Symposium for exploring prospective research ``Pioneering New Fields: Forefront of RIKEN's Science and Beyond'', Saitama, Japan, 21—22 Novemeber 2016

T. Uesaka, ``Looking Through Double Charge Exchange Reactions'', ISOLDE Workshop and Users meeting 2016, Zurich, 7—9 December 2016.

H. Sagawa and P. Moller, ``New mass model FRDM2012 and symmetry energy'', 14th International Symposium on Nuclei in the Cosmos (NIC-XIV), Niigata, Japan, 19—24 June 2016.

H. Sagawa, ``Three-body model for exotic nuclei'', XXIII Nuclear Physics Workshop, Kazimeirz, Poland, 17 Sept.—1 Oct. 2016.

H. Sagawa, ``Pairing and di-neuron correlations in Exotic Nuclei'', RAON/RISP workshop, Deajone, Korea, 28 Oct., 2016.

H. Sagawa, ``Nuclear models and Hyperons'', invited seminar, Soongsil University, Seoul, Korea, 31 Oct., 2016.

H. Sagawa, ``Isoscalar pairing and spin-isospin response'', 1st RIKEN-Tsukuba-CNS workshop, Japan, 12—15 December 2016.

H. Sagawa, ``Three-body model for nuclei near and beyond drip line'', Recent Progresses in Nuclear Structure Physics 2016 (NSP2016), Kyoto, Japan, 21 December 2016.

H. Sagawa, ``Isoscalar pairing and spin-isospin response'', Workshop on spin-isospin excitations and related nuclear structure problems, Milano, Italy, 13—14 March 2017.

M. Sasano, ``Study Of Gamow-Teller Transitions from 132Sn Via The Inverse Kinematics (p,n) Reaction'', INPC2016, Adelaide, Australia, 11—16 Spetember 2016.

M. Sasano, ``Status report on studies of GT transitions via the (p,n) reaction and (p,2p) fission at SAMURAI'',SAMURAI international workshop 2016 , Kyushu, Japan, 5—6 September 2016.

M. Sasano, ``Fission study project in RIKEN RIBF: towards the “complete” measurement of fission observables'', 6th Workshop on Nuclear Fission and Spectroscopy of Neutron-Rich Nuclei, Chamrousse, Fracne, 20—24 March 2017.

L. Stuhl, ``A New Low-energy Plastic Scintillation Neutron Detector For Real Time Pulse Shape Discrimination'', INPC2016, Adelaide, Australia, 11—16 Spetember 2016.

Y. Kubota, ``Study of neutron-neutron correlation in Borromean nucleus 11Li via the (p,pn) reaction'', DREB2016, Halifax, Canada, 11—15 July 2016

Y. Kubota, ``Study On Neutron-neutron Correlation In Borromean Nucleus 11Li Via The Quasi-free (p,pn) Reaction'', INPC2016, Adelaide, Australia, 11—16 Spetember 2016.

Y. Kubota, ``Probing neutron-neutron correlation in Borromean nuclei via the quasi-free (p,pn) reaction'',SAMURAI international workshop 2016 , Kyushu, Japan, 5—6 September 2016.

J. Zenihiro, ``Proton elastic scattering and nucleon density distributions'', International Symposium on Neutron Star Matter (NSMAT2016), Sendai, Japan, 21—24 November 2016.
D. Nagae, `` The rare-RI ring at RIKEN RI beam factory'', International Symposium on Neutron Star Matter (NSMAT2016), Sendai, Japan, 21—24 November 2016.
V. Panin, ``Heavy-ion-proton experiments at SAMURAI: challenges and perspectives'',SAMURAI international workshop 2016 , Kyushu, Japan, 5—6 September 2016.
J. Yasuda, ``Study of Gamow Teller strength from 132Sn via the inverse kinematics (p,n) reaction'', DREB2016, Halifax, Canada, 11—15 July 2016
T. Tang, ``Quasi-free proton knockout of 23,25F'', DREB2016, Halifax, Canada, 11—15 July 2016
Y. Zaihong, `` Study on the Dineutron Decay in 8He'', Workshop on Nuclear Clustering, Beijing, China, 2—3 July 2016.
Y. Zaihong, ``Study on the cluster structure in nuclei using direct reactions'', Cluster16, Napoli, Italy, 23—27 May 2016.
Y. Zaihong, ``Status and Results of SAMURAI018'', 5th Sunflower workshop, Hongkong, China, 18—20 September 2016.
Y. Zaihong, ``Study of cluster structure in light nuclei by using neutron-rich Carbon isotope beams'',SAMURAI international workshop 2016 , Kyushu, Japan, 5—6 September 2016.
T. Lokotko, ``Spectroscopy of 69,71,73Co isotopes'', 5th Sunflower workshop, Hongkong, China, 18—20 September 2016.
M. Tsumura, ``Search for the rare g-decay mode in 12C'', Cluster16, Napoli, Italy, 23—27 May 2016.
T. Furuno, `` An active target MAIKo to investigate cluster structures in unstable nuclei'', Cluster16, Napoli, Italy, 23—27 May 2016.
S. Sakaguchi, ``Polarized proton target at SAMURAI: elastic scattering of 6He from polarized proton'',SAMURAI international workshop 2016 , Kyushu, Japan, 5—6 September 2016.

[Domestic Conference]
M. Sasano, “Study of nuclear fission via the (p,2p) reaction at RIBF”, 第8回 停止・低速RIビームを用いた核分光研究会(SSRI), Wako, Japan, 4—5 March 2016
上坂友洋, “トリプレットDNP法の最近の進展と生物学研究への応用”, 日本物理学会 2016年秋季大会, 宮崎, 日本, 2016年9月21日−9月24日.
上坂友洋、立石健一郎、``トリプレットDNP ~新たな核偏極法の可能性~'', 第18回CROSSroads Workshop 「偏極ターゲットと偏極中性子技術開発」, 東海村, 日本, 2016年6月15日
上坂友洋、立石健一郎、``トリプレットDNP ~高温・低磁場での核偏極生成とタンパク質研究における展望~'', 新世代研究所2016年度水和ナノ構造・バイオ単分子合同研究会, 東京, 日本, 2017年3月27日
S. Chebotaryov, “Experiment on elastic scattering of polarized protons from neutronrich 6He isotopes at 200 MeV/nucleon”, 日本物理学会 2016年秋季大会, 宮崎, 日本, 2016年9月21日—9月24日.
E. Milman, “Search for low-lying resonances in 10N structure via 9C + p resonant scattering”, 日本物理学会 2016年秋季大会, 宮崎, 日本, 2016年9月21日—9月24日.
津村美保, “12C原子核における稀γ崩壊モード探索のためのテスト実験”, 日本物理学会 2016年秋季大会, 宮崎, 日本, 2016年9月21日−9月24日.
佐川弘幸, “スピンアイソスピン応答から探る対相関とテンソル力”, 日本物理学会 (シンポジウム講演) 2016年秋季大会, 宮崎, 日本, 2016年9月21日—9月24日
Y. Zaihong, “Two-neutron decay of 8He excited states”, Workshop on Cluster Physics 2016 (WNCP2016), Yokohama, Japan, 14—17 November 2016.
大甕舜一朗, “稀少RIリングのための粒子周回モニターの開発”, 日本物理学会 2017年春季大会, 豊中, 日本, 2017年3月17日—3月20日.
Zhuang GE, “Development of Large area position sensitive MCP detector at Rare RI Ring”, 日本物理学会 2017年春季大会, 豊中, 日本, 2017年3月17日—3月20日.
那須裕, “崩壊α粒子測定による炭素13のαクラスターガス状態の探索”, 日本物理学会 2017年春季大会, 豊中, 日本, 2017年3月17日−3月20日.
古野達也, “MAIKoアクティブ標的を用いた10Cの質量欠損分光”, 日本物理学会 2017年春季大会, 豊中, 日本, 2017年3月17日−3月20日.
S. Chebotaryov, “Status of data analysis from experiment on p-6He elastic scattering at 200 MeV/nucleon”, 日本物理学会 2017年春季大会, 豊中, 日本, 2017年3月17日—3月20日.
立石健一郎, “信号増大比660倍を超える光励起三重項電子を用いたDNP" (招待講演) 第44回 日本磁気共鳴医学会大会スタディグループ（超偏極による他核MRSIの高感度計測), 大宮ソニックシティ 2016年9月10日.
立石健一郎, “光励起三重項電子スピンを用いた動的核偏極による室温での1Hスピン偏極率40%の達成” 日本物理学会 2016年秋季大会, 金沢大学 2016年9月16日.
立石健一郎, “光励起三重項電子を用いた動的核偏極 −660倍を超える偏極増大”, 日本物理学会（シンポジウム講演）2017年春季大会, 豊中, 日本, 2017年3月17日−3月20日.
上坂友洋, ``トリプレットDNP ~新たな核偏極法の可能性~'', 北海道大学原子核理論グループセミナー, 札幌, 日本, 2016年10月26日
上坂友洋、立石健一郎, ``トリプレットDNP ~高温・低磁場での核偏極が拓く世界~'', 山形大学クォーク核物理学研究室セミナー, 山形, 日本, 2017年1月12日
佐川弘幸, “原子核の対相関”, 平成28年度第19回先導原子力研コロキウム, 東京, 日本, 2016年10月13日.

Posters Presentations
[International Conference etc.]
M. Tsumura, ``Search for the rare gamma-decay mode in 12C'', 14th International Symposium on Nuclei in the Cosmos (NIC-XIV), Niigata, Japan, 19—24 June 2016.
M. Murata, ``The measurement of 4He photodisintegration with MAIKo active target'', 14th International Symposium on Nuclei in the Cosmos (NIC-XIV), Niigata, Japan, 19—24 June 2016.

RIBF Research Division
Nuclear Spectroscopy Laboratory

1. Abstract

The research group has conducted nuclear-physics studies utilizing stopped/slowed-down radioactive-isotope (RI) beams mainly at the RIBF facility. These studies are based on the technique of nuclear spectroscopy such as β-ray-detected NMR, γ-PAD (Perturbed Angular Distribution), laser, and Mössbauer among other methods that takes advantage of intrinsic nuclear properties such as nuclear spins, electromagnetic moments, and decay modes. In particular, techniques and devices for the production of spin-controlled RI beams have been developed and combined to the spectroscopic studies, which enable high-sensitivity measurements of spin precessions/resonances through a change in the angular distribution of radiations. Anomalous nuclear structures and properties of far unstable nuclei are investigated from thus determined spin-related observables. The group also aims to apply such techniques to interdisciplinary fields such as fundamental physics and materials science by exploiting nuclear probes..

2. Major Research Subjects

(1) Nuclear spectroscopy with spin-oriented RI beams
(2) R&D studies for laser spectroscopy of stopped/slowed-down RI beams
(3) Application of RI probes
(4) Fundamental physics: Study of symmetry

3. Summary of Research Activity

(1) Nuclear spectroscopy with spin-oriented RI beams

Measurements of static electromagnetic nuclear moments over a substantial region of the nuclear chart have been conducted for structure studies on the nuclei far from the β-decay stability. Utilizing nuclear spin orientation phenomena of RIs created in the projectile-fragmentation reaction, ground- and excited-state nuclear moments of nuclei far from the stability have been determined by means of the β-ray-detected nuclear magnetic resonance (β-NMR) and the γ-ray time differential perturbed angular distribution (γ-TDPAD) methods. To extend these observations to extremely rare RIs, development of a new apparatus to produce highly spin-polarized RI beams will be conducted by extending the atomic beam resonance method to fragmentation-based RI beams.

(2) R&D studies for laser spectroscopy of stopped/slowed-down RI beams

For the measurement of electromagnetic nuclear properties such as spin, isotope shift, and electromagnetic nuclear moments at RIBF, we have been conducting R&D studies on nuclear laser spectroscopy. One is development of a new laser-spectroscopy system utilizing superfluid helium (He II) as a stopping medium of energetic RI beams, where characteristic atomic properties of ions surrounded by liquid helium enable us to perform unique nuclear laser spectroscopy. The other is a system for collinear laser spectroscopy for a large variety of elements using slowed-down RI beams produced via projectile-fragmentation reaction at RIBF, which can be achieved only by a universal low-energy RI-beam delivery system SLOWRI.

(3) Application of RI probes

The application of RI and heavy ion beams as a probe for condensed matter studies is also conducted by the group. The microscopic material dynamics and properties have been investigated through the deduced internal local fields and the spin relaxation of RI probes based on various spectroscopies utilizing RI probes such as the β-NMR/nuclear quadrupole resonance (NQR) methods, in-beam Mössbauer spectroscopy and the γ-ray time differential perturbed angular correlation (γ-TDPAC) spectroscopy.

(4) Fundamental physics: Study of symmetry

The nuclear spins of stable and unstable isotopes sometimes play important roles in fundamental physics research. New experimental methods and devices have been developed for studies of the violation of time reversal symmetry (T-violation) using spin-polarized nuclei. These experiments aim to detect the small frequency shift in the spin precession arising from new mechanisms beyond the Standard Model.

Members

Chief Scientist (Lab. Head)
Hideki UENO

Research & Technical Scientists
Hiroki YAMAZAKI (Senior Research Scientist)
Yuichi ICHIKAWA (Research Scientist)
Aiko TAKAMINE (Research Scientist)

Research Consultant
Takuya OKADA

Special Postdoctoral Researcher
Tomoya SATO

Junior Research Associates
Kei IMAMURA (Meiji Univ.)
Tomomi FUJITA (Osaka Univ.)

International Program Associates
Ian MURRAY (Univ. Paris Sud)
Aleksey GLADKOV (Kyungpook National Univ.)

Part-time Worker
Yoko ISHIBASHI (Univ. of Tsukuba)

Senior Visiting Scientist
Yukari MATSUO (Hosei Univ.)

Visiting Researcher
Hiroki NISHIBATA (JSPS Fellow)

Visiting Scientists
Wataru SATO (Kanazawa Univ.)
Kensaku MATSUTA (Osaka Univ.)
Jin NAKAMURA (Univ. of Elec.-Com.)
Atsushi HATAKEYAMA (Tokyo Univ. of Agric. and Tech.)
Takeshi FURUKAWA (Tokyo Met. Univ.)
Satoshi TSUTSUI (JASRI)
Takamasa MOMOSE (Univ. of British Columbia)
Jean-Michel DAUGAS (CEA)
Yoshio KOBAYASHI (Univ. of Elec.-Com.)
Jiro MURATA (Rikkyo Univ.)
Jun MIYAZAKI (Hokuriku Univ.)
Yasuhiro YAMADA (Tokyo Univ. of Sci.)
Kenya KUBO (ICU)
Akihiro YOSHIMI (Okayama Univ.)
Dimiter Loukanov BALABANSKI (IHIN)
Naoki NISHIDA (Tokyo Univ. of Science)
Boulay FLORENT (CNRS GANIL)
Yasuaki EINAGA (Keio Univ.)
Kei IMAMURA (Meiji Univ.)
Takashi ABE (Univ. Of Tokyo)

Student Trainees
Yoko ISHIBASHI (Univ. of Tsukuba)
Masaomi TANAKA (Osaka Univ.)
Ryosuke KANBE (Osaka Univ.)
Yukiko SATO (Univ. of Elec.-Com.)
Shotaro TANIGAWA (Univ. of Elec.-Com.)
Daiki NATORI (Univ. of Elec.-Com.)
Kenichi TANABE (Tokyo Univ. of Sci.)
Miho SATO (Tokyo Univ. of Sci.)
Takafumi TABATA (Tokyo Univ. of Sci.)
Tomoya SATO (Tokyo Tech.)
Daiki TOMINAGA (Hosei Univ.)
Ippei KUBONO (Tokyo Univ. of Sci.)
Shota AMAGASA (Tokyo Univ. of Sci.)
Tsuyoshi EGAMI (Hosei Univ.)
Takafumi KAWAGUCHI (Hosei Univ.)
Yuka KOBAYASHI (Tokyo Univ. of Science)
Masanari SEKI (Tokyo Univ. of Science)
Takaya KOIZUMI (Univ. of Elec.-Com.)
Kenya TAKAHASHI (Univ. of Elec.-Com.)
Yuki MINATO (Univ. of Elec.-Com.)
Ryouhei KOZU (Univ. of Elec.-Com.)
Takayuki KAWAMURA (Osaka Univ.)
Makoto SANJO (Hosei Univ.)
Wataru KOBAYASHI (Hosei Univ.)
Masato SUZUKI (Univ. of Elec.-Com.)
Taishi NISHIZAKA (Hosei Univ.)
Shuichiro KOJIMA (Tokyo Tech.)
Chikako FUNAYAMA (Tokyo Tech.)

Interns
Yig JIANG (Peking University)
Cheng CHEN (Peking University)
Xudong LYU (Peking University)
Chenguang WU (Peking University)
Bo DAI (Peking University)
Yunxiang WANG (Peking University)
Younsik KIM (Seoul National University)
Young Ju CHO (Seoul National University)
Yun Gi JEONG (Seoul National University)
Seugho HAN (Seoul National University)
Jung Hwan LEE (Seoul National University)
Taekeun YOON (Seoul National University)
Alfred AMRUTH (University of Hong Kong)
CALVIN (University of Hong Kong)
Sen Yu CHANG (University of Hong Kong)
Frederik O. A. PARNEFJORD GUSTAFSSON (University of Hong Kong)
Xinzhi TENG (University of Hong Kong)
Jia-Shian WANG (University of Hong Kong)

Assistant
Yuri TSUBURAI

List of Publications & Presentations

Publications
[Journal]
(Original Papers) *Subject to Peer Review

A. Kusoglu, G. Georgiev, C. Sotty, D. L. Balabanski, A. Goasduff, Y. Ishii, Y. Abe, K. Asahi, M. Bostan, R. Chevrier, M. Chikamori, J. M. Daugas, T. Furukawa, H. Nishibata, Y. Ichikawa, Y. Ishibashi, R. Lozeva, H. Miyatake, D. Nagae, T. Nanao, M. Niikura, T. Niwa, S. Okada, A. Ozawa, Y. Saito, H. Shirai, H. Ueno, D. T. Yordanov, N. Yoshida, “Magnetic moment of the $13/2^+$ isomeric state in ^{69}Cu: Spin alignment in the one-nucleon removal reaction”, Phys. Rev. C 93, 054313 (2016).*

A. Takamine, M. Wada, K. Okada, Y. Ito, P. Schury, F. Arai, I. Katayama, K. Imamura, Y. Ichikawa, H. Ueno, H. Wollnik, H. A. Shuessler, “Towards high precision measurements of nuclear g-factors for the Be isotopes”, Nucl. Instr. Meth. Phys. Res. B 376, 307 (2016).*

T. Inoue, T. Furukawa, A. Yoshimi, T. Nanao, M. Chikamori, K. Suzuki, H. Hayashi, H. Miyatake, Y. Ichikawa, M. Tsuchiya, N. Hatakeyama, S. Kagami, M. Uchida, H. Ueno, Y. Matsuo, T. Fukuyama, K. Asahi, "Frequency characteristics of nuclear spin oscillator with an artificial feedback toward search for ^{129}Xe atomic electric dipole moment", Eur. Phys. J. D 70, 129 (2016).*

H. Heylen, M. De Rydt, G. Neyens, M. L. Bissell, L. Caceres, R. Chevrier, J. M. Daugas, Y. Ichikawa, Y. Ishibashi, O. Kamalou, T. J. Mertzimekis, P. Morel, J. Papuga, A. Poves, M. M. Rajabali, C. St¨odel, J. C. Thomas, H. Ueno, Y. Utsuno, N. Yoshida, and A. Yoshimi, "High-precision quadrupole moment reveals significant intruder component in ^{33}Al ground state", Phys. Rev. C 94, 034312 (2016).*

H. Ishiyama, S. C. Jeong, Y. X. Watanabe, Y. Hirayama, N. Imai, H. Miyatake, M. Oyaizu, I. Katayama, A. Osa, Y. Otokawa, M. Matsuda, K. Nishio, H. Makii, T. Sato, N. Kuwata, J. Kawamura, A. Nakao, H. Ueno, Y. H. Kim, S. Kimura, and M. Mukai, "Direct measurement of nanoscale lithium diffusion in solid battery materials using radioactive tracer of ^{8}Li", Nucl. Instr. Meth. Phys. Res. B 376, 307-310 (2016)

K. Asahi, T. Sato, and Y. Ichikawa, "EDMS of Closed-shell Atoms: An Example of Xe Atom", Asian Journal of Physics 25, 1403-1412 (2016).*

(Review)

[Proceedings]
(Original Papers) *Subject to Peer Review

Oral Presentations

[International Conference etc.]

H. Ueno, "Nuclear moment measurements using radioactive ion beams", International Conference on Hyperfine Interactions and their Applications (HYPERFINE2016), Leuven, Belgium, July 3–8, 2016.

A. Takamine, "Determination of the hyperfine anomaly for the one-neutron halo nucleus ^{11}Be", 2016 SSRI-PNS collaboration meeting, Wako, Japan, September 2-3, 2016.

A. Takamine, "Collinear laser spectroscopy at SLOWRI", 2016 SSRI-PNS collaboration meeting, Wako, Japan, September 2-3, 2016.

A. Takamine, "Measurements of nuclear moments by using RI atomic beam (RIAB)", 2016 SSRI-PNS collaboration meeting, Wako, Japan, September 2-3, 2016.

Y. Ichikawa, "Magnetic moment measurement using spin-aligned beam at RIBF", RIBF Users Meeting, Wako, Japan, September 8-9, 2016.

Y. Ichikawa, A. Takamine, H. Nishibata, K. Imamura, T. Fujita, T. Sato, S. Momiyama, Y. Shimizu, D. S. Ahn, K. Asahi, H. Baba, D. L. Balabanski, F. Boulay, J. M. Daugas, T. Egami, N. Fukuda, C. Funayama, T. Furukawa, G. Georgiev, A. Gladkov, N. Inabe, Y. Ishibashi, Y. Kobayashi, S. Kojima, A. Kusoglu, T. Kawaguchi, T. Kawamura, I. Mukul, M. Niikura, T. Nishizaka, A. Odahara, Y. Ohtomo, D. Ralet, T. Shimoda, G. S. Simpson, T. Sumikama, H. Suzuki, H. Takeda, L. C. Tao, Y. Togano, D. Tomonaga, H. Ueno, H. Yamazaki and X. F. Yang, "Magnetic moment of isomeric state of ^{75}Cu measured with highly spin-aligned beam", International Nuclear Physics Conference (INPC) 2016, Adelaide, Australia, September 11-16, 2016.

T. Sato, Y. Ichikawa, S. Kojima, C. Funayama, S. Tanaka, Y. Sakamoto, Y. Ohtomo, C. Hirao, M. Chikamori, E. Hikota, T. Furukawa, A. Yoshimi, C. P. Bidinosti, T. Ino, H. Ueno, Y. Matsuo, T. Fukuyama, K. Asahi, "Development of ^{131}Xe comagnetometry for Xe atomic EDM search", International Nuclear Physics Conference (INPC) 2016, Adelaide, Australia, September 11-16, 2016.

K. Imamura, T. Fujita, T. Egami, T. Nishizaka, D. Tominaga, T. Kawaguchi, A. Takamine, T. Furukawa, Y. Ichikawa, T. Wakui, H. Odashima, H. Ueno, Y. Matsuo, "Development of laser spectroscopy technique using superfluid helium for the study of low-yield nuclei", International Nuclear Physics Conference (INPC) 2016, Adelaide, Australia, September 11-16, 2016.

H. Nishibata, "Various structures of the neutron-rich nucleus ^{31}Mg investigated by beta-gamma spectroscopy of spin-polarized ^{31}Na", 22nd International Spin Symposium (SPIN2016), Illinois, USA, September 25-30, 2016.

H. Ueno, "Nuclear moments and their applications", 2016 IBS Annual Meeting - IBS-RIKEN Conference on Recent Developments in RI Physics, Daejeon, Korea, November 17-18, 2016.

H. Ueno, "Nuclear-moment measurements at RIBF utilizing spin-oriented RI beams", First Tsukuba-CCS-RIKEN joint workshop on microscopic theories of nuclear structure and dynamics, Wako & Tsukuba, Japan, December 12-16, 2016.

T. Sato, Y. Ichikawa, T. Inoue, A. Uchiyama, A. Gladkov, A. TAkamine, S. Kojima, C. Funayama, S. Tanaka, Y. Sakamoto, Y. Ohtomo, C. Hirao, M. Chikamori, E. HIkota, T. Furukawa, A. Yoshimi, C. P. Bidinosti, T. Ino, H. Ueno, Y. Matsuo, T. Fukuyama, N. Yoshinaga, Y. Sakemi, K. Asahi, "Search for Xe atomic EDM using nuclear spin masers of xenon-129 and -131", 9th International Workshop on "Fundamental Physics Using Atoms" (FPUA 2017), Kyoto, Japan, January 9-10, 2017.

K. Imamura, T. Egami, T. Nishizaka, A. Takamine, D. TOminaga, T. Kawaguchi, W. Kobayashi, M. Sanjo, T. Furukawa, Y. Ichikawa, T. Sato, H. Nishibata, A. Gladkov, L. C. Tao, T. Wakui, H. Odashima, H. Ueno, Y. Matsuo, "Development of laser spectroscopy technique of atoms in superfluid helium for the study of low production yield nuclei", 9th International Workshop on "Fundamental Physics Using Atoms" (FPUA 2017), Kyoto, Japan, January 9-10, 2017.

A. Takamine, "Laser Spectroscopy at the SLOWRI facility in RIKEN", CSNSM/IPN seminar, Orsay, France, March 28, 2017.

[Domestic Conference]

上野秀樹, 「核電磁モーメントで探る原子核構造研究」, 「分子システム研究」第５回春季研究会, 熱海, 2016 年 5 月 13-16 日

北村徳隆, 今井伸明, 下浦享, K. Wimmer, 道正新一郎, 大田晋輔, O. Beliuskina, P. Schrock, 小林幹, 清川裕, 山口勇貴, 増岡翔一朗, 上野秀樹, 米田健一郎, 市川雄一, 寺西高, 清水則孝, 宇都野穣, 「陽子共鳴散乱を用いた ^{35}Si の核構造の研究」, 日本物理学会 2016 年秋季大会, 宮崎, 2016 年 9 月 21-24 日

Evgeniy Milman, Takashi Teranishi, Satoshi Sakaguchi, Sergey Chebotaryov, B, Tomohiro Uesaka, Kenichiro Tateishi, Yuichi Ichikawa, Masaki Sasano, Wooyoung Kim, Reii Kaku, Yasuaki Norimatsu, Youhei Akiyama, Takahiro Fukuta, Daisuke Sakae, Nobuaki Imai, Hidetoshi Yamaguchi, Seiya Hayakawa, Daid Miles Kahl, Yuji Sakaguchi, Keijiro Abe, Noritaka Kitamura, Tomoaki Kaneko, Kotaro Yamada, Sanghoon Hwang, Dahee Kim, G, Alfredo Galindo-Uribarri, Elisa Romero-Romero, Didier Beaumel, "Search for low-lying resonances in ^{10}N structure via ^{9}C + p resonant scattering", 日本物理学会 2016 年秋季大会, 宮崎, 2016 年 9 月 21-24 日

金原慎二, NP1406 RRC-32-02 collaborators, 「ハイパー核の核種同定における荷電粒子識別法の開発」, 日本物理学会 2016 年秋季大会, 宮崎, 2016 年 9 月 21-24 日

村井李奈, 吉田純也, Myint Kyaw Soe, Aye Moh Moh Theint, 金原慎二, 大橋正樹, 長瀬雄一, 仲澤和馬, NP1406-RRC32 Collaborators, 「原

子核乾板中のハイパー核同定のための娘粒子の識別(角度依存性)」, 日本物理学会 2016 年秋季大会, 宮崎, 2016 年 9 月 21-24 日
長瀬雄一, 金原慎二, 村井李奈, 仲澤和馬, 他理研 NP1406-RRC32 Collaborators, 「原子核乾板中飛跡の核種同定(特に ^{6}He について)」, 日本物理学会 2016 年秋季大会, 宮崎, 2016 年 9 月 21-24 日
今村慧, 藤田朋美, 江上魁, 西坂大志, 高峰愛子, 富永大樹, 川口貴史, 小林航, 三條真, 古川武, 市川雄一, 佐藤智哉, 西畑洸希, A. Gladkov, L. C. Tao, 涌井崇, 小田島仁司, 上野秀樹, 松尾由賀利, 「超流動ヘリウム環境を用いた原子分光と核構造研究手法(OROCHI)の開発」, 第 9 回停止・低速不安定核ビームを用いた核分光研究, 東海, 2017 年 3 月 5-6 日
高峰愛子,「インフライト核反応生成 RI を対象としたコリニアレーザー分光 (Collinear laser spectroscopy for the nuclides provided from an in-flight RI beam separator)」, 第 9 回停止・低速不安定核ビームを用いた核分光研究, 東海, 2017 年 3 月 5-6 日
江上魁, 今村慧、高峰愛子、小林航、藤田朋美、富永大樹、三條真、中村祐太郎、涌井崇志、古川武、上野秀樹、松尾由賀利, 「超流動ヘリウム中に打ち込まれた低収量核原子の超微細構造間隔測定に向けた光学クライオスタットの開発」, 日本物理学会第 72 回年次大会, 大阪, 2017 年 3 月 17-20 日
佐藤智哉, 市川雄一, 井上壮志, 内山愛子, 高峰愛子, 小島修一郎, 舟山智歌子, 田中俊也, 坂本雄, 大友祐一, 平尾千佳, 近森正敏, 彦田絵里, 古川武, 吉見彰洋, C.P. Bidinosti, 猪野隆, 上野秀樹, 松尾由賀利, 福山武志, 吉永尚孝, 酒見泰寛, 旭耕一郎,「能動帰還型核スピンメーザーにおける帰還磁場印加方式と周波数安定性」, 日本物理学会第 72 回年次大会, 大阪, 2017 年 3 月 17-20 日
伊藤由太, 和田道治, P. Schury, 加治大哉, 森本幸司, 羽場宏光, I. Murray, M. Rosenbusch, 木村創大, 高峰愛子, 宮武宇也, 山木さやか, 新井郁也, H. Wollnik, 「MRTOF 質量分析器による八重極変形核 ^{223,224}Th の精密原子質量測定」, 日本物理学会第 72 回年次大会, 大阪, 2017 年 3 月 17-20 日

Posters Presentations

[International Conference etc.]

Y. Ichikawa, A. Takamine, H. Nishibata, K. Imamura, T. Fujita, T. Sato, S. Momiyama, Y. Shimizu, D. S. Ahn, K. Asahi, H. Baba, D. L. Balabanski, F. Boulay, J. M. Daugas, T. Egami, N. Fukuda, C. Funayama, T. Furukawa, G. Georgiev, A. Gladkov, N. Inabe, Y. Ishibashi, Y. Kobayashi, S. Kojima, A. Kusoglu, T. Kawaguchi, T. Kawamura, I. Mukul, M. Niikura, T. Nishizaka, A. Odahara, Y. Ohtomo, D. Ralet, T. Shimoda, G. S. Simpson, T. Sumikama, H. Suzuki, H. Takeda, L. C. Tao, Y. Togano, D. Tomonaga, H. Ueno, H. Yamazaki and X. F. Yang, "Magnetic moment of ^{75m}Cu and collectivity around ^{78}Ni", 14th International Symposium on Nuclei in the Cosmos XIV, Niigata, Japan, June 19-24, 2016.

A. Takamine, M. Wada, K. Okada, Y. Ito, P. Schury, I. Katayama, K. Imamura, Y. Ichikawa, H. Ueno, H. Wollnik, H. A. Schuessler, "Precision laser spectroscopy for laser-cooled radioactive beryllium isotopes" International Nuclear Physics Conference (INPC) 2016, Adelaide, Australia, September 11-16, 2016

[Domestic Conference]

今村慧, 早坂美希, 藤田朋美, 小林徹, 古川武, 上野秀樹, 松尾由賀利,「パルス Ti:Sa レーザーによる超流動ヘリウム環境中原子のスピン偏極生成」, 原子・分子・光（AMO）科学討論会, 和光, 2016 年 6 月 3-4 日.
江上魁, 今村慧, 藤田朋美, 西坂太志, 富永大樹, 川口高史, 高峰愛子, 古川武, 上野秀樹, 松尾由賀利, 「低収量原子核の核構造研究に向けた超流動ヘリウム環境におけるレーザー核分光法の開発」, 原子・分子・光（AMO）科学討論会, 和光, 2016 年 6 月 3-4 日.
富永大樹, 今村慧、藤田朋美、高峰愛子、小林徹、上野秀樹、松尾由賀利, 「超流動ヘリウム中レーザーアブレーション法による Ba+イオンの発生と蛍光観測」, イオンビーム工学研究所シンポジウム, 東京, 2016 年 12 月 7 日.
小林航, 今村慧, 江上魁, 西坂太志, 三條真, 藤田朋美, 富永大樹, 中村祐太郎, 高峰愛子, 涌井崇志, 古川武, 上野秀樹, 松尾由賀利, 「低収量原子核の核構造研究に向けた超流動ヘリウム中原子のレーザー誘起蛍光検出系の高度化」, 日本物理学会第 72 回年次大会, 大阪, 2017 年 3 月 17-20 日.

RIBF Research Division
High Energy Astrophysics Laboratory

1. Abstract

Immediately after the Big Bang, the beginning of our universe, only hydrogen and helium existed. However, nuclear fusion in the interior of stars and the explosion of supernovae in the universe over the course of 13.8 billion years led to the evolution of a world brimming with the many different elements we have today. By using man-made satellites to observe X-rays and gamma-rays emitted from celestial objects, we are observing the synthesis of the elements at their actual source. Our goal is to comprehensively elucidate the scenarios for the formation of the elements in the universe, together with our research on sub-atomic physics through the use of an accelerator.

2. Major Research Subjects

(1) Connect missing links of nucleosynthesis in our universe
(2) Reveal the particle acceleration mechanism in astronomical objects, planets and inter-planetary space
(3) Discover new physics in extremely strong magnetic and gravitational environment
(4) Research and development of innovative X-ray and gamma-ray detectors

3. Summary of Research Activity

High Energy Astrophysics Laboratory started in April 2010. The goal of our research is to reveal the mechanism of nucleosynthesis and the evolution of elements in our universe, to study the particle acceleration mechanisms by shockwaves or electrical potential, and to observe/discover exotic physical phenomena in extremely strong magnetic and/or gravitational fields. We have observed supernova remnants, strongly magnetized neutron stars, pulsars, black holes, galaxies, and planets of the solar system with UV, X-ray, and gamma-ray astronomical satellites and/or ground-based telescopes. In FY2016, we have following achievements.

(1) Ultra high-resolution spectroscopy

The microcalorimeter, Soft X-ray Spectrometer (SXS), onboard the Hitomi (ASTRO-H) X-ray satellite was launched in February 2016. Our laboratory contributed to the mission, in particular to the development of the SXS. The SXS consisted of a semiconductor sensor cooled down around 50 mK, and measuring X-ray energy with a very sensitive thermometer. Soon after the Hitomi launch, SXS achieved the operation temperature and observed the Perseus galaxy cluster and some other celestial objects for verifying the detector system. Although the Hitomi satellite was lost in March 2016 due to a tragic accident, the data obtained in the verification phase was analyzed and published to Nature. This analysis demonstrated the excellent capability of the microcalorimeter in spectroscopy: A recovery mission is planned for the launch in 2021.

(2) X-ray polarimeter development

X-ray polarimeter is one of our key devices developing for more than 12 years. We have evaluated the basic performance of the X-ray polarimeter for Relativistic Astrophysical X-ray Sources (PRAXyS) small explorer. PRAXyS is the NASA's mission designed to probe the space-time geometry in strong gravitational field and strong magnetic field of high-energy astronomical objects in the universe, such as black holes and neutron stars, via X-ray polarimetry in the energy band of 2-10 keV. An engineering model of the polarimeter was tested at the Brookhaven National Laboratory and NASA's Goddard Space Flight Center. We measured its modulation factor, the most important indicator of polarimetry, and successfully verified that the measured values were consistent with the ones obtained with simulations, which well meets the mission requirement.

(3) Observations of Jupiter's aurora

We made an international observing campaign for Jupiter's space environment by using the Hisaki satellite, Hubble Space Telescope (HST), and Juno explorer in mid-2016. Continuous monitoring of Jupiter's aurora with Hisaki indicated an explosive auroral brightening within a few hours, of which structure was found expanding in longitude and latitude in the HST high-resolution imaging. During the auroral explosion, Juno detected a forward shock in the solar wind plasma propagating to Jupiter. We interpret the observations as a release of electromagnetic energy stored at <100 Jovian radii from Jupiter, followed by Jupiter-ward transport of the released energy as the hot plasma population, which finally excites the auroral explorsion. This rapid energy release and transport could universally take place at other magnetized rotating bodies, e.g., exoplanets, neutron stars, and white dwarfs.

(4) Observations of neutron stars

We have analyzed the X-ray data of the Neutron Star Low-Mass X-ray Binary (NS-LMXB) Aquila X-1 obtained by the Japanese X-ray satellite Suzaku. The spectrum was represented by an optically thick disk emission (multi-color blackbody) and a Comptonized emission by a corona around the neutron star as shown in the previous studies, but we discovered small hump structure around 30 keV for the spectrum obtained in the hard state, in which the Comptonized emission is dominant. The structure was well represented by a single Gaussian model or a recombination edge emission mode. One of the possible interpretations of the hump is the florescence line or K-edge recombination of the heavy element that is produced in a rapid proton capture process (rp-process) in Type-I X-ray bursts or superbursts occurred on the neutron star surface of Aql X-1.

(5) Observations of supernova remnants

We have performed a systematic X-ray study of nine evolved supernova remnants in the Magellanic Clouds, DEM L238, DEM L249, 0534−69.9, 0548−70.4, B0532−71.0, B0532−67.5, 0103−72.6, 0049−73.6, and 0104−72.3, using archival data of the Suzaku satellite. Although Suzaku does not spatially resolve the SN ejecta from the swept-up ISM due to the limited angular resolution, its excellent energy resolution has enabled clear separation of emission lines in the soft X-ray band. The Fe/Ne mass ratios clearly divide the observed SNRs into the Type Ia and core-collapse groups, confirming some previous typing made by Chandra observations that had utilized its extremely

high angular resolution. This demonstrates that spatially integrated X-ray spectra of old SNRs can also be used to discriminate their progenitor type.

(6) Development of a new analysis method for gravitational weak lensing

We developed a new weak gravitational lensing shear analysis method which can correct pixel noise effect. The gravitational lensing analysis is a great tool to direct measurement of mass information, and it can be applied to constrain the cosmological parameters by measuring cosmic shear, it is distortion by the large scale structure. Because the mass concentration of the structure is very weak, so the lensing effect is also very weak, so precise shear analysis method is needed for stronger constraining. The pixel noise effect is shear measurement error from random counts on galaxy images from Poisson noises of sky count. We studied pixel noise correction method with an analytical approach, and the new method has 10 times high precision about pixel noise effect.

Members

Associate Chief Scientist (Lab. Head)

Toru TAMAGAWA

Contract Researchers

Yuki OKURA
Asami HAYATO

Special Postdoctoral Researchers

Kumi ISHIKAWA
Hirofumi NODA
Takayuki YUASA
Tomoki KIMURA
Toshio NAKANO

Part-time Workers

Megu KUBOTA
Kazuki NISHIDA
Naoto MURATA
Sonoe ODA
Yuanhui ZHOU
Tatsuya YOSHIDA

Visiting Researcher

Wataru IWAKIRI (JSPS Fellow)

Visiting Scientists

Yukikatsu TERADA (Saitama Univ.)
Yujin NAKAGAWA (JAXA)
Masaki WAKABAYASHI (Jakulin Commercial Company LC)
Aya BAMBA (Aoyama Gakuin Univ.)
Naohisa INADA (National Institute of Tech., Nara College)
Rohta TAKAHASHI (Tomakomai Nat'l College of Tech.)
Toru MISAWA (Shinshu Univ.)
Hiroya YAMAGUCHI (Harvard Univ.)
Satoru KATSUDA (JAXA)
Shin'ya YAMADA (Tokyo Met. Univ.)
Takao KITAGUCHI (Hiroshima Univ.)
Teruaki ENOTO (Kyoto Univ.)
Hirofumi NODA (Tohoku Univ.)
Yuzuru Tawara (Nagoya Univ.)
Ikuyuki Mitsuishi (Nagoya Univ.)
Harufumi TSUCHIYA (JAEA)
Teruaki ENOTO (Kyoto Univ.)
Yuzuru TAWARA (Nagoya Univ.)

Student Trainees

Yoko TAKEUCHI (Tokyo Univ. of Sci.)
Megu KUBOTA (Tokyo Univ. of Sci.)
Kazuki NISHIDA (Tokyo Univ. of Sci.)
Sonoe ODA (Tokyo Univ. of Sci.)
Ryouta MICHIGAMI (Nagasaki Institute of Applied Science)
Naoto MURATA (Tokyo Univ. of Sci.)
Yuanhui ZHOU (Tokyo Univ. of Sci.)

List of Publications & Presentations

Publications

[Journal]

(Original Papers) *Subject to Peer Review

The Hitomi collaboration; "The quiescent intracluster medium in the core of the Perseus cluster", Nature, 535, 117-121 (2016).*

The Hitomi collaboration; "Hitomi Constraints on the 3.5 keV Line in the Perseus Galaxy Cluster", The Astrophysical Journal Letters, 837, L15, (2017).*

Takeuchi, Yoko; Yamaguchi, Hiroya; Tamagawa, Toru; "A systematic study of evolved supernova remnants in the large and small Magellanic Clouds with Suzaku", Publications of the Astronomical Society of Japan, 68, S9 (2016).*

Iwakiri, W. B.; Black, J. K.; Cole, R.; Enoto, T.; Hayato, A.; Hill, J. E.; Jahoda, K.; Kaaret, P.; Kitaguchi, T.; Kubota, M.; Marlowe, H.; McCurdy, R.; Takeuchi, Y.; Tamagawa, T.: "Performance of the PRAXyS X-ray polarimeter", Nuclear Inst. and Methods in Physics Research, A, 838, 89 (2016). *

Terada, Y.; Maeda, K.; Fukazawa, Y.; Bamba, A.; Ueda, Y.; Katsuda, S.; Enoto, T.; Takahashi, T.; Tamagawa, T.; Röpke, F. K.; Summa, A.; Diehl, R.; "Measurements of the Soft Gamma-Ray Emission from SN2014J with Suzaku", The Astrophysical Journal, 823, 43, (2016).*

Okura, Yuki; Futamase, Toshifumi: "The Systematic Error Test for PSF Correction inWeak Gravitational Lensing Shear Measurement By the ERA Method By Idealizing PSF" The Astrophysical Journal, 827, 138 (2016). *

Okura, Yuki; Petri, Andrea; May, Morgan; Plazas, Andrs A.; Tamagawa, Toru: "Consequences of CCD Imperfections for Cosmology Determined by Weak Lensing Surveys: From Laboratory Measurements to Cosmological Parameter Bias" The Astrophysical Journal, 825, 61 (2016). *

Furusawa, Hisanori; Kashikawa, Nobunari; Kobayashi, Masakazu A. R.; Dunlop, James S.; Shimasaku, Kazuhiro; Takata, Tadafumi; Sekiguchi, Kazuhiro; Naito, Yoshiaki; Furusawa, Junko; Ouchi, Masami; Nakata, Fumiaki; Yasuda, Naoki; Okura, Yuki; Taniguchi, Yoshiaki; Yamada, Toru; Kajisawa, Masaru; Fynbo, Johan P. U.; Le Fvre, Olivier: "A New Constraint on the Ly α Fraction of UV Very Bright Galaxies at Redshift 7" The Astrophysical Journal, 822, 46 (2016). *

Tao, Chihiro; Kimura, Tomoki; Badman, Sarah V; Murakami, Go; Yoshioka, Kazuo; Tsuchiya, Fuminori; Andre, Nicolas; Yoshikawa, Ichiro; Yamazaki, Atsushi; Shiota, Daikou; "Variation of Jupiter's aurora observed by Hisaki/EXCEED: 1. Observed characteristics of the auroral electron energies compared with observations performed using HST/STIS", Journal of Geophysical Research: Space Physics, 121, 4041-4054, (2016). *

Kita, Hajime; Kimura, Tomoki; Tao, Chihiro; Tsuchiya, Fuminori; Misawa, Hiroaki; Sakanoi, Takeshi; Kasaba, Yasumasa; Murakami, Go; Yoshioka, Kazuo; Yamazaki, Atsushi; "Characteristics of solar wind control on Jovian UV auroral activity deciphered by long-term Hisaki EXCEED observations: Evidence of preconditioning of the magnetosphere?", Geophysical Research Letters, 43, 6790-6798, (2016). *

Gray, RL; Badman, Sarah Victoria; Bonfond, Bertrand; Kimura, Tomoki; Misawa, H; Nichols, JD; Vogt, MF; Ray, LC; "Auroral evidence of radial transport at Jupiter during January 2014", Journal of Geophysical Research: Space Physics, 121, 9972-9984, (2016). *

Yoshikawa, Ichiro; Yoshioka, Kazuo; Murakami, Go; Suzuki, Fumiharu; Hikida, Reina; Yamazaki, Atsushi; Kimura, Tomoki; Tsuchiya, Fuminori; Kagitani, Masato; Sakanoi, Takeshi; "Properties of hot electrons in the Jovian inner magnetosphere deduced from extended observations of the Io Plasma Torus", Geophysical Research Letters, 43, 11,552{11,557, (2016). *

Yoshioka, K; Tsuchiya, F; Kimura, T; Kagitani, M; Murakami, G; Yamazaki, A; Kuwabara, M; Suzuki, F; Hikida, R; Yoshikawa, I; "Radial variation of sulfur and oxygen ions in the Io plasma torus as deduced from remote observations by Hisaki", Journal of Geophysical Research: Space Physics, 122, 2999-3012, (2017). *

Kuwabara, Masaki; Yoshioka, Kazuo; Murakami, Go; Tsuchiya, Fuminori; Kimura, Tomoki; Yamazaki, Atsushi; Yoshikawa, Ichiro; "The geocoronal responses to the geomagnetic disturbances", Journal of Geophysical Research: Space Physics, 122, 1269-1276, (2017). *

笠羽康正; 三澤浩昭; 土屋史紀; 笠原禎也; 井町智彦; 木村智樹; 加藤雄人; 熊本篤志; 小嶋浩嗣; 八木谷聡; 尾崎光紀; 石坂圭吾; 垰千尋; 三好由純; 阿部琢美; 諸岡倫子, 「みんなでふたたび木星へ, そして氷衛星へその 4 電波・プラズマ波動観測器 RPWI の飛翔へ」, 日本惑星科学会誌遊星人, 25, 96-107, (2016). *

Serino, Motoko; Iwakiri, Wataru; Tamagawa, Toru; Sakamoto, Takanori; Nakahira, Satoshi; Matsuoka, Masaru; Yamaoka, Kazutaka; Negoro, Hitoshi; "MAXI observations of long X-ray bursts", Publications of the Astronomical Society of Japan, 68, 95 (2016). *

Nakano, Toshio; Murakami, Hiroaki; Furuta, Yoshihiro; Enoto, Teruaki; Masuyama, Miyu; Shigeyama, Toshikazu; Makishima, Kazuo; "Study of the progenitor of the magnetar 1E 2259+586 through Suzaku observations of the associated supernova remnant CTB 109", Publications of the Astronomical Society of Japan, 69, 40 (2017).*

Makishima, Kazuo; Enoto, Teruaki; Murakami, Hiroaki; Furuta, Yoshihiro; Nakano, Toshio; Sasano, Makoto; Nakazawa, Kazuhiro; " Evidence for a 36 ks phase modulation in the hard X-ray pulses from the magnetar 1E 1547.0-5408", Publications of the Astronomical Society of Japan, 68, S12 (2016).*

[Proceedings]

(Original Papers) *Subject to Peer Review

Fujimoto, Ryuichi; Takei, Yoh; Mitsuda, Kazuhisa; Yamasaki, Noriko Y.; Tsujimoto, Masahiro; Koyama, Shu; Ishikawa, Kumi; Sugita, Hiroyuki; Sato, Yoichi; Shinozaki, Keisuke; Okamoto, Atsushi; Kitamoto, Shunji; Hoshino, Akio; Sato, Kosuke; Ezoe, Yuichiro; Ishisaki, Yoshitaka; Yamada, Shinya; Seta, Hiromi; Ohashi, Takaya; Tamagawa, Toru; Noda, Hirofumi; Sawada, Makoto; Tashiro, Makoto; Yatsu, Yoichi; Mitsuishi, Ikuyuki; Kanao, Kenichi; Yoshida, Seiji; Miyaoka, Mikio; Tsunematsu, Shoji; Otsuka, Kiyomi; Narasaki, Katsuhiro; DiPirro, Michael J.; Shirron, Peter J.; Sneiderman, Gary A.; Kilbourne, Caroline A.; Porter, F. Scott; Chiao, Meng P.; Eckart, Megan E.; Kelley, Richard L.; "Performance of the helium dewar and cryocoolers of ASTRO-H SXS", Proceedings of the SPIE, 9905, 99053S (2016).

Hill, J. E.; Black, J. K.; Jahoda, K.; Tamagawa, T.; Iwakiri, W.; Kitaguchi, T.; Kubota, M.; Kaaret, P.; McCurdy, R.; Miles, D. M.; Okajima, T.; Soong, Y.; Olsen, L.; Sparr, L.; Mosely, S. J.; Nolan, D.; "The x-ray polarimeter instrument on board the Polarimeter for Relativistic Astrophysical X-ray Sources (PRAXyS) mission", Proceedings of the SPIE, 9905, 99051B (2016).

Jahoda, Keith; Kallman, Timothy R.; Kouveliotou, Chryssa; Angelini, Lorella; Black, J. Kevin; Hill, Joanne E.; Jaeger, Theodore; Kaaret, Philip E.; Markwardt, Craig B.; Okajima, Takashi; Petre, Robert; Schnittman, Jeremy; Soong, Yang; Strohmayer, Tod E.; Tamagawa, Toru; Tawara, Yuzuru; "The Polarimeter for Relativistic Astrophysical X-ray Sources", Proceedings of the SPIE, 9905, 990516 (2016).

Tsujimoto, Masahiro; Mitsuda, Kazuhisa; Kelley, Richard L.; den Herder, Jan-Willem A.; Akamatsu, Hiroki; Bialas, Thomas G.; Boyce, Kevin R.; Brown, Gregory V.; Chiao, Meng P.; Costantini, Elisa; de Vries, Cor P.; DiPirro, Michael J.; Eckart, Megan E.; Ezoe, Yuichiro; Fujimoto, Ryuichi; Haas, Daniel; Hoshino, Akio; Ishikawa, Kumi; Ishisaki, Yoshitaka; Iyomoto, Naoko; Kilbourne, Caroline A.; Kitamoto, Shunji; Koyama, Shu; Leutenegger, Maurice A.; McCammon, Dan; Mitsuishi, Ikuyuki; Murakami, Hiroshi; Murakami, Masahide; Noda, Hirofumi; Ogawa, Mina; Ota, Naomi; Paltani, Stéphane; Porter, Frederick S.; Sato, Kosuke; Sato, Yoichi; Sawada, Makoto; Seta, Hiromi; Shinozaki, Keisuke; Shirron, Peter J.; Sneiderman, Gary A.; Sugita, Hiroyuki; Szymkowiak, Andrew E.; Takei, Yoh; Tamagawa, Toru; Tashiro, Makoto S.; Terada, Yukikatsu; Yamada, Shinya; Yamasaki, Noriko Y.; Yatsu, Yoichi; "In-orbit operation of the ASTRO-H SXS", Proceedings of the SPIE, 9905, 99050Y (2016).

Kelley, Richard L.; Akamatsu, Hiroki; Azzarello, Phillipp; Bialas, Tom; Boyce, Kevin R.; Brown, Gregory V.; Canavan, Edgar; Chiao, Meng P.; Costantini, Elisa; DiPirro, Michael J.; Eckart, Megan E.; Ezoe, Yuichiro; Fujimoto, Ryuichi; Haas, Daniel; den Herder, Jan-Willem; Hoshino, Akio; Ishikawa, Kumi; Ishisaki, Yoshitaka; Iyomoto, Naoko; Kilbourne, Caroline A.; Kimball, Mark O.; Kitamoto, Shunji; Konami, Saori; Koyama, Shu; Leutenegger, Maurice A.; McCammon, Dan; Mitsuda, Kazuhisa; Mitsuishi, Ikuyuki; Moseley, Harvey; Murakami, Hiroshi; Murakami, Masahide; Noda, Hirofumi; Ogawa, Mina; Ohashi, Takaya; Okamoto, Atsushi; Ota, Naomi; Paltani, Stéphane; Porter, F. S.; Sakai, Kazuhiro; Sato, Kosuke; Sato, Yohichi; Sawada, Makoto; Seta, Hiromi; Shinozaki, Keisuke; Shirron, Peter J.; Sneiderman, Gary A.; Sugita, Hiroyuki; Szymkowiak, Andrew E.; Takei, Yoh; Tamagawa, Toru; Tashiro, Makoto; Terada, Yukikatsu; Tsujimoto, Masahiro; de Vries, Cor P.; Yamada, Shinya; Yamasaki, Noriko Y.; Yatsu, Yoichi; "The Astro-H high resolution soft x-ray spectrometer", Proceedings of the SPIE, 9905, 99050V (2016).

The Hitomi Collaboration, "The ASTRO-H (Hitomi) x-ray astronomy satellite", Proceedings of the SPIE, 9905, 99050U (2016).

Watanabe, Shin; Tajima, Hiroyasu; Fukazawa, Yasushi; Blandford, Roger; Enoto, Teruaki; Goldwurm, Andrea; Hagino, Kouichi; Hayashi, Katsuhiro; Ichinohe, Yuto; Kataoka, Jun; Katsuta, Junichiro; Kitaguchi, Takao; Kokubun, Motohide; Laurent, Philippe; Lebrun, François; Limousin, Olivier; Madejski, Grzegorz M.; Makishima, Kazuo; Mizuno, Tsunefumi; Mori, Kunishiro; Nakamori, Takeshi; Nakano, Toshio; Nakazawa, Kazuhiro; Noda, Hirofumu; Odaka, Hirokazu; Ohno, Masanori; Ohta, Masayuki; Saito, Shinya; Sato, Goro; Sato, Rie; Takeda, Shin'ichiro; Takahashi, Hiromitsu; Takahashi, Tadayuki; Tanaka, Takaaki; Tanaka, Yasuyuki; Terada, Yukikatsu; Uchiyama, Hideki; Uchiyama, Yasunobu; Yamaoka, Kazutaka; Yatsu, Yoichi; Yonetoku, Daisuke; Yuasa, Takayuki; " The soft gamma-ray detector (SGD) onboard ASTRO-H", Proceedings of the SPIE, 9905, 990513 (2016).

Nakazawa, Kazuhiro; Sato, Goro; Kokubun, Motohide; Enoto, Teruaki; Fukazawa, Yasushi; Hagino, Kouichi; Harayama, Atsushi; Hayashi, Katsuhiro; Kataoka, Jun; Katsuta, Junichiro; Laurent, Philippe; Lebrun, François; Limousin, Olivier; Makishima, Kazuo; Mizuno, Tsunefumi; Mori, Kunishiro; Nakamori, Takeshi; Nakano, Toshio; Noda, Hirofumi; Odaka, Hirokazu; Ohno, Masanori; Ohta, Masayuki; Saito, Shinya; Sato, Rie; Tajima, Hiroyasu; Takahashi, Hiromitsu; Takahashi, Tadayuki; Takeda, Shin'ichiro; Terada, Yukikatsu; Uchiyama, Hideki; Uchiyama, Yasunobu; Watanabe, Shin; Yamaoka, Kazutaka; Yatsu, Yoichi; Yuasa, Takayuki; " The hard x-ray imager (HXI) onboard ASTRO-H", Proceedings of the SPIE, 9905, 990511 (2016).

Oral Presentations

[International Conference etc.]

Tomoki Kimura, Kazuo Yoshioka, Fuminori Tsuchiya, Yasutaka Hiraki, Chihiro Tao, Go Murakami, Atsushi Yamazaki, Masaki Fujimoto, Sarah Victoria Badman, Peter A Delamere, Fran Bagenal, "Response of tail reconnection and energetic event to plasma mass loading monitored by Hisaki", NASA Participating Scientist Program meeting for Hisaki/EXCEED, Boulder, USA, January (2017).

Tomoki Kimura, Go Murakami, Atsushi Yamazaki, Fuminori Tsuchiya, Kazuo Yoshioka, Chihiro Tao, Hajime Kita, Sarah V Badman, Masaki Fujimoto, Hisaki Science Team, "Continuous Monitoring of Jupiter's Aurora and Io Plasma Torus with the Hisaki Satellite: Recent Results and Future Coordination with JUNO" 8th International Workshop on Planetary, Solar and Heliospheric Radio Emissions (PRE VIII), Graz, Austria, October (2017).

Tomoki KIMURA, "Substorm like events seen as auroras and their responses to the plasma mass loading from Io", The influence of Io on Jupiter's Magnetosphere, International Space Science Institute Meeting, Zurich, Switzerland, September (2016).

Tomoki Kimura, Kazuo Yoshioka, Go Murakami, Atsushi Yamazaki, Fuminori Tsuchiya, Chihiro Tao, Masaki Fujimoto, "Hisaki Science team, Synergetic Multi-Wavelength Observation of Jupiter's Magnetosphere Driven by Hisaki: Recent Results and Plans for JUNO Mission", Japan Geoscience Union Meeting 2016, Makuhari, Japan, May (2016).

Yuki Okura; "Ellipticity of Re-smeared Articial image (ERA) Method", HSC collaboration meeting 2016 August, IPMU, Japan, August (2016).

Yuki Okura; "Current Status of ERA method and Pixel Noise Study", HSC WLWG f2f meeting at Princeton, IPMU, Japan, August (2016).

Toru Tamagawa, "X-ray polarimetry mission PRAXyS", 7 years of MAXI : monitoring X-ray transients conference, RIKEN, Japan, December (2016).

Toru Tamagawa, "A Modulated X-ray Generator for Possible Industrial Applications", IEEE NSS/MIC conference 2016, Strasbourg, France, November (2016).

[Domestic Conference]

玉川徹, 早藤麻美, 岩切渉, 中野俊男, 深沢泰司, 水野恒史, 北口貴雄, 田中慎之, 戸田皓陽, 榎戸輝揚, 窪田恵, 西田和樹, 田原譲, 三石郁之, 菅沼亮紀, 幅良統, 林田清, 井上翔太, Keith Jahoda, Joanne Hill-Kittle, ほか PRAXyS 衛星チーム, 「X 線偏光観測衛星 PRAXyS の進捗(4)" 日本天文学会 2017 年春季年会, 九州大学, 3 月(2017).

三石郁之, 菅沼亮紀, 二村泰介, 松本浩典, 田原譲, 立花一志, 大西崇文, 立花健二, 中野俊男, 玉川徹, 岡島崇, William Chang, Keith Jahoda, 「X 線偏光観測衛星 PRAXyS 搭載 X 線望遠鏡用サーマルシールドの開発」 日本天文学会 2017 年春季年会, 九州大学, 3 月(2017).

北口貴雄, 深沢泰司, 水野恒史, 玉川徹, 早藤麻美, 岩切渉, 中野俊男, 窪田恵, 榎戸輝揚, 他 PRAXyS チーム, 「PRAXyS 衛星に搭載する光電子追跡型 X 線偏光計の偏光角再構成法" 日本天文学会 2017 年春季年会, 九州大学, 3 月(2017).

中野俊男, 玉川徹, 早藤麻美, 岩切渉, 窪田恵, 北口貴雄, 田中慎之, 戸田皓陽, 深沢泰司, 水野恒史, 三石郁之, 田原譲, 井上翔太, 林田清, 榎戸輝揚, Keith Jahoda, Joanne Hill-Kittle, ほか PRAXyS 衛星チーム, 「PRAXyS 衛星搭載の X 線ミラーと偏光計のビームラインによる性能評価」 日本天文学会 2017 年春季年会, 九州大学, 3 月(2017).

菅沼亮紀, 二村泰介, 田原譲, 松本浩典, 三石郁之, 立花一志, 大西崇文, 立花健二, 中野俊男, 玉川徹, 「PRAXyS 衛星搭載 X 線望遠鏡サーマルシールド用ポリイミドフィルムの 特性評価" 日本天文学会 2017 年春季年会, 九州大学, 3 月 (2017).

窪田めぐ, 玉川徹, 牧島一夫, 芹野素子, 岩切渉, 杉崎睦, 中野俊男, 小野光, 「中性子星大気中における Z=52 付近の重元素の存在」 日本天文学会 2017 年春季年会, 九州大学, 3 月 (2017).

玉川徹, 岩切渉, 中野俊男, 早藤麻美, 北口貴雄, 水野恒史, 深沢泰司, 榎戸輝揚, 窪田恵, 西田和樹, 田原譲, 三石郁之, 幅良統, 林田清, Keith Jahoda, Joanne Hill, ほか PRAXyS 衛星チーム, 「X 線偏光観測衛星 PRAXyS の進捗状況」 日本天文学会 2016 年秋季年会, 愛媛大学, 9 月(2016).

田原譲, 二村泰介, 菅沼亮紀, 三石郁之, 松本浩典, 玉川徹, 岡島崇, 「PRAXyS 搭載用 X 線望遠鏡のためのサーマルシールドの開発」 日本天文学会 2016 年秋季年会, 愛媛大学, 9 月 (2016).

玉川徹, 早藤麻美, 岩切渉, 中野俊男, 窪田恵, 西田和樹, 田原譲, 三石郁之, 菅沼亮紀, 深沢泰司, 水野恒史, 北口貴雄, 田中慎之, 戸田皓陽, 榎戸輝揚, 林田清, 井上翔太, 渡辺伸, PRAXyS team, 「X 線偏光観測衛星 PRAXyS」 第 17 回宇宙科学シンポジウム, 宇宙科学研究所, 1 月 (2017).

木村智樹, 「Dynamics of Jupiter's aurora unveiled by the Hisaki-JUNO-Hubble collaboration: initial results」, Symposium on Planetary Science 2017, 東北大学, 2 月 (2017).

木村智樹, 吉岡和夫, 土屋史紀, 平木康隆, 垰千尋, 北元, 村上豪, 山崎敦, 藤本正樹, 「ひさき衛星によるオーロラとプラズマ供給率の連続監視で明らかにする木星サブストームライクイベントの動力学」, 地球電磁気・地球惑星圏学会第 138 回総会・講演会, 九州大学, 11 月 (2016).

中野俊男: 「長周期 CCO を伴う SNR RCW103 とマグネターSNR CTB109 の比較" 山形県蔵王アストリアホテル 9 月 (2016)

RIBF Research Division
Astro-Glaciology Research Unit

Summary of Research Activities

Our Astro-Glaciology Research Unit promotes both experimental and theoretical studies to open up the new interdisciplinary research field of astro-glaciology, which combines astrophysics and glaciology.

On the experimental side, we analyze ice cores drilled at the Dome Fuji station, in Antarctica, in collaboration with the National Institute of Polar Research (NIPR, Tokyo). These ice cores are time capsules. In particular, the ice cores obtained at Dome Fuji are known to be unique because they contain much more information on conditions in the stratosphere than any other ice cores recovered from other locations in either hemisphere. This means that there are significant advantages in using Dome Fuji ice cores if we wish to study astronomical phenomena of the past. Since gamma-rays and high-energy protons that are emitted in certain astronomical processes affect the chemical and isotopic compositions in the stratosphere but not those in the troposphere, we have been measuring:

(1) Variations in the nitrate ion (NO_3^-) concentrations in the ice cores, in an effort to establish a new proxy for supernova explosions in our own galaxy as well as past solar activity.
(2) Variations in the water isotopes (^{18}O and ^{2}H) in the ice cores, in order to construct in more detail records of past changes in the temperature of the surface of the earth; and
(3) Variations in the nitrogen isotope (^{15}N) in the nitrates contained in the ice cores, in order to investigate the possibility of utilizing ^{15}N as a new and more stable proxy for galactic supernovae explosions and past solar activity.

In the case of items (1), (2), and (3), our analyses of Dome Fuji ice cores cover the most recent 2000 years. The temporal resolution of the results of our research is currently 12 months. We intend to compare the results obtained in item (1) with those in item (2), in order to understand better the relationships between solar activity and long-term changes in the temperature of the earth. The underlying assumptions in item (2) are already well accepted in glaciology. Item (3) refers to one of the very first measurements of ^{15}N concentrations in ice cores.

On the theoretical side, we are simulating numerically:

(4) Changes in the chemical composition of the stratosphere induced by gamma-rays and/or high-energy particles emitted from explosive astronomical phenomena, such as galactic supernovae and solar proton events; and
(5) The explosive nucleosynthesis (including the r-process, the rapid neutron capture process, which creates elements heavier than iron) that arises in the environment of core-collapse supernova explosions.

Items (4) and (5) in our list, the chemical composition of the stratosphere and explosive nucleosynthesis, are very important in solar–terrestrial research and nuclear astrophysics; furthermore, these simulations provide a theoretical support when considering the characteristics of supernova explosions and solar activity, as seen in our ice core data. These studies are also important because it is necessary to discount the effects of the meteorological noise.

It is noteworthy that the as yet not fully understood frequency of supernova explosions in our galaxy is crucial to an understanding of the r-process nucleosynthesis. The results obtained from items (1) and (3) are expected to reveal the average rate of supernova explosions in our galaxy during the past million years of ice deposition.

Members

Research Unit Leader (Lab. Head)
Yuko MOTIZUKI

Research & Technical Scientists
Kazuya TAKAHASHI (Concurrent: RI Application Team, Senior Research Scientist)
Yoichi NAKAI (Concurrent: RI Physics Lab., Senior Research Scientist)

Part-time Workers
Manami MARUYAMA
Yuma HASEBE
Satomi NEGISHI
Sachiko MIYAZAKI
Yoko HOSHINO
Emi NISHIZAWA

Visiting Scientists
Yasushige YANO (Concurrent)
Akira HORI (Kitami Inst. of Tech.)
Hideharu AKIYOSHI (Nat ‘l Inst. for Environ. Studies)
Hideki MADOKORO (Mitsubishi Heavy Ind., Ltd.)

Research Consultant
Kenji Tanabe

Student Trainees
Yuma HASEBE (Saitama Univ.)

List of Publications & Presentations

Publications

[Journal]

(Original Papers) *Subject to Peer Review

Y. Motizuki, H. Motoyama, Y. Nakai, K. Suzuki, Y. Iizuka and K. Takahashi: “Overview of the chemical composition and characteristics of Na^+ and Cl^- distributions in shallow samples from Antarctic ice core DF01 (Dome Fuji) drilled in 2001”, Geochemical J., 51, 3, 293-298, 2017, doi:10.2343/geochemj.2.0458 (Open Access article)*

Shuji Fujita, Kumiko Goto-Azuma, Motohiro Hirabayashi, Akira Hori, Yoshinori Iizuka, Yuko Motizuki, Hideaki Motoyama, Kazuya Takahashi: “Densification of layered firn of the ice sheet at Dome Fuji, Antarctica”, Journal of Glaciology, 21 pages, 2016, doi:10.1017/jog.2016.16 (Open Access article)*

Y. Nakai, Y. Motizuki, M. Maruyama, Y. Hasebe, H. Akiyoshi, T. Imamura: “Box-model simulation for influence of solar proton events on the middle atmosphere”, RIKEN Accel. Prog. Rep. 50, in press*

Y. Motizuki, H. Motoyama, Y. Nakai, K. Suzuki, Y. Iizuka and K. Takahashi: “Characteristics of Na^+ and Cl^- distributions in shallow samples from an Antarctic ice core DF01 (Dome Fuji) drilled in 2001: Result of strong atmospheric high-pressure blocking events?”, RIKEN Accel. Prog. Rep. 50, in press*

Y. Motizuki, K. Takahashi, Y. Nakai, Y. Iizuka, K. Suzuki, H. Motoyama: “Overview of the chemical composition and characteristics of Na^+ and Cl^- distributions in samples from Antarctic ice core DF01 (Dome Fuji) drilled in 2001”, RIKEN Accel. Prog. Rep. 49, 133, 2017*

Y. Nakai, Y. Motizuki, M. Maruyama, H. Akiyoshi, T. Imamura: “Box-model simulation for variation of atmospheric chemical composition caused by solar energetic particles”, RIKEN Accel. Prog. Rep. 49, 132, 2017*

Y. Hasebe, Y. Motizuki, Y. Nakai, K. Takahashi: “Diagnose oscillation properties observed in an annual ice-core oxygen isotope record obtained from Dronning Maud Land, Antarctica”, RIKEN Accel. Prog. Rep. 49, 131, 2017*

[Book]

(Original Papers) *Subject to Peer Review

望月優子、佐藤勝彦：『人類の住む宇宙 第2版』（シリーズ現代の天文学 第1巻）、pp. 99-144（「第3章 元素の起源」）、岡村定矩他編、日本評論社、2017年3月*

望月優子：「ナイスステップな研究者から見た変化の新潮流」、文部科学省機関紙STI Horizon、2017年第3巻1号、pp. 17-20*

Oral Presentations

[International Conference etc.]

(Invited talk) Yuko Motizuki: “Solar signatures in ice cores”, The 10th East Asian Meeting on Astronomy, Seoul, Korea, Sep. 26-30, 2016.

(Invited talk) Yuko Motizuki: “Women astronomers in Japan”, The 10th East Asian Meeting on Astronomy, Seoul, Korea, Sep. 26-30, 2016.

(Invited talk) Yuko Motizuki: “Astronomical signatures embedded in ice cores", Baymfest in Tokyo -Exploring Extreme Forms of Matter-, Tokyo, Japan, Mar. 14, 2016.

H. Akiyoshi, Y. Nakai, Y. Motizuki, T. Imamura, Y. Yamashita: “A preliminary result of NOx and ozone change simulation for a solar proton event using a nudged CCM and box chemistry model”, Int. Workshop on Solar Cycle Activity and Impact on Climate for The 2nd PSTEP International symposium (PSTEP-2) , Kyoto, March 22, 2017.

Shuji Fujita, Kumiko Goto-Azuma, Hiroyuki Enomoto, Kotaro Fukui, Motohiro Hirabayashi, Akira Hori, Yu Hoshina, Yoshinori Iizuka, Yuko Motizuki, Hideaki Motoyama, Fumio Nakazawa, Shin Sugiyama, Sylviane Surdyk, Kazuya Takahashi: “Metamorphism of layered firn at Dome Fuji, Antarctica: Evolution of relations between Near-infrared reflectivity and the other textural/chemical properties”, The 7th Symposium on Poler Science, Tachikawa, Nov. 29 - Dec. 2, 2016.

Shuji Fujita, Kumiko Goto-Azuma, Hiroyuki Enomoto, Kotaro Fukui, Motohiro Hirabayashi, Akira Hori, Yu Hoshina, Yoshinori Iizuka, Yuko Motizuki, Hideaki Motoyama, Fumio Nakazawa, Shin Sugiyama, Sylviane Surdyk, Kazuya Takahashi: “Metamorphism of layered firn at Dome Fuji, Antarctica: Evolution of relations between Near-infrared reflectivity and the other textural/chemical properties”, XXXIV SCAR(Scientific Committee on Antarctic Research) Open Science Conference, Kuala Lumpur, Malaysia, Aug. 20-30, 2016.

[Domestic Conference]

望月優子、中井陽一、高橋和也、ほかドームふじ氷床コア解析チーム：「南極氷床コアに刻まれた超新星カシオペアA の爆発年代」、日本天文学会春季年会、福岡、2017年3月17日.

(招待講演) 望月優子：埼玉大学理学部物理量子力学特別講義「アイスコアからさぐる天文・宇宙のサイエンス −過去の超新星爆発と太陽活動、地球への影響−」、さいたま、2017年1月23日.

(招待講演) 中井陽一：第36回北海道大学低温科学研究所セミナー「太陽プロトン現象に誘起される地球中層大気の微量成分濃度変化 −ボックスモデルシミュレーションによるイオン化学反応の影響の研究−」、札幌、2017年1月19日.

(招待講演) 中井陽一、望月優子、丸山真美、秋吉英治、今村隆史：「太陽プロトン現象が引き起こす中層大気でのイオン化学反応の影響：ボックスモデルシミュレーションによる研究」、平成28年度「MTI研究集会」「宇宙空間からの地球超高層大気観測に関する研究会」合同研究会、小金井、2016年8月29日.

高橋和也、望月優子、中井陽一、本山秀明：「南極ドームふじ基地で掘削されたアイスコアの水同位体比分析に基づく過去2000年の高時間分解能気温変動」、“The isotopic measuremants of oxygen and hydrogen in Dome-Fuji (Antarctica) ice core:Annually-resolved temperature reconstructions of the past 2000 years”、日本地球惑星科学連合2016年連合大会、千葉、2016年5月22-26日.

中井陽一、望月優子、丸山真美、秋吉英治、今村隆史：「太陽高エネルギー粒子の大気への影響に関するボックスモデルシミュレーション：中層大気での微量化学種の変動」、“Box-model simulation for atmospheric effect of solar energetic particles: variation of trace chemical species in the middle atmosphere”、日本地球惑星科学連合2016年連合大会、千葉、2016年5月22-26日.

Shuji Fujita, Kumiko Goto-Azuma, Hiroyuki Enomoto, Kotaro.Fukui, Motohiro Hirabayashi, Akira Hori, Yu Hoshina, Yoshinori Iizuka, Yuko Motizuki, Hideaki Motoyama, Fumio Nakazawa, Shin Sugiyama, Sylviane Surdyk, Kazuya Takahashi: “Metamorphism of layered firn at Dome Fuji, Antarctica: Evolution of relations between Near-infrared reflectivity and the other textural and chemical properties”、日本地球惑星科学連合2016年連合大会、千葉、2016年5月22-26日.

三宅 芙沙、増田 公明、堀内 一穂、本山 秀明、松崎 浩之、望月 優子、高橋 和也、中井 陽一：「ドームふじアイスコアの^{10}Be分析による単年宇宙線イベントの調査」 、日本地球惑星科学連合2016年連合大会、千葉、2016年5月22-26日.

Posters Presentations

[International Conference etc.]

Yuko Motizuki, Kazuya Takahashi, Yoichi Nakai, and Hideaki Motoyama: “Annually-resolved temperature reconstructions of the past 2000 years from Dome-Fuji, East Antarctica” (A poster paper), EGU General Assembly 2016, Vienna, Austria, Apr. 17-22, 2016.

[Domestic Conference]

長谷部憂磨、望月優子、中井陽一、高橋和也：「南極および北極アイスコアの酸素同位体比から得られる気温変動周期」（ポスター発表）、“Diagnose oscillation properties of δ18O embeded in ice cores from Antarctica and Greenland”、日本地球惑星科学連合2016年連合大会、千葉、2016年5月22-26日.

RIBF Research Division
Research Group for Superheavy Element

1. Abstract

The elements with their atomic number Z>103 are called as trans-actinide or superheavy elements. The chemical properties of those elements have not yet been studied in detail. Those elements do not exist in nature. Therefore, they must be produced by artificially for the scientific study of those elements. In our laboratory, we have been studying the physical and chemical properties of the superheavy elements utilizing the accelerators in RIKEN and various methods of efficient production of the superheavy elements.

2. Major Research Subjects

(1) Search for new superheavy elements
(2) Decay spectroscopy of the heaviest nuclei
(3) Study of the chemical properties of the heaviest elements
(4) Study of the reaction mechanism of the fusion process (theory)

3. Summary of Research Activity

(1) Searching for new elements

To expand the periodic table of elements and the nuclear chart, we will search for new elements.

(2) Spectroscopic study of the nucleus of heavy elements

Using the high sensitivity system for detecting the heaviest element, we plan to perform a spectroscopic study of nuclei of the heavy elements.

(3) Chemistry of superheavy elements

Study of chemistry of the trans-actinide (superheavy element) has just started world-wide, making it a new frontier in the field of chemistry. Relativistic effects in chemical property are predicted by many theoretical studies. We will try to develop this new field.

(4) Study of a reaction mechanism for fusion process

Superheavy elements have been produced by complete fusion reaction of two heavy nuclei. However, the reaction mechanism of the fusion process is still not well understood theoretically. When we design an experiment to synthesize nuclei of the superheavy elements, we need to determine a beam-target combination and the most appropriate reaction energy. This is when the theory becomes important. We will try to develop a reaction theory useful in designing an experiment by collaborating with the theorists.

(5) Research Highlight

The discovery of a new element is one of the exciting topics both for nuclear physicists and nuclear chemists. The elements with their atomic number Z>103 are called as trans-actinides or superheavy elements. The chemical properties of those elements have not yet been studied in detail. Since those elements do not exist in nature, they must be produced by artificially, by using nuclear reactions for the study of those elements. Because the production rate of atoms of those elements is extremely small, an efficient production and collection are key issues of the superheavy research. In our laboratory, we have been trying to produce new elements, studying the physical and chemical properties of the superheavy elements utilizing the accelerators in RIKEN.

Although the Research Group for Superheavy element has started at April 2013, the Group is a renewal of the Superheay Element Laboratory started at April 2006, based on a research group which belonged to the RIKEN accelerator research facility (RARF), and had studied the productions of the heaviest elements. The main experimental apparatus is a gas-filled recoil ion separator GARIS. The heaviest elements with their atomic numbers, 107 (Bohrium), 108 (Hassium), 109 (Meitnerium), 110 (Darmstadtium), 111 (Roentogenium), and 112 (Copernicium) were discovered as new elements at Helmholtzzentrum für Schwerionenforschung GmbH (GSI), Germany by using ^{208}Pb or ^{209}Bi based complete fusion reactions, so called “cold fusion” reactions. We have made independent confirmations of the productions of isotopes of 108th, 110th, 111th, and 112th elements by using the same reactions performed at GSI. After these work, we observed an isotope of the 113th element, ^{278}113, in July 2004, in April, 2005, and in August 2012. The isotope, ^{278}113, has both the largest atomic number, (Z = 113) and atomic mass number (A = 278) which have determined experimentally among the isotopes which have been produced by cold fusion reactions. We could show the world highest sensitivity for production and detection of the superheavy elements by these observations. Our results that related to ^{278}113 has been recognized as a discovery of new element by a Joint Working Party of the International Union of Pure and Applied Chemistry (IUPAC) and International Union of Pure and Applied Physics (IUPAP). Finally, we named the 113th element as “Nihonium”.

We decided to make one more recoil separator GARIS-II, which has an acceptance twice as large as existing GARIS, in order to realize higher sensitivity. The design of GARIS-II has finished in 2008. All fabrication of the separator will be finished at the end of fiscal year 2008. It has been ready for operation after some commissioning works.

Preparatory work for the study of the chemical properties of the superheavy elements has started by using the gas-jet transport system coupled to GARIS. The experiment was quite successful. The background radioactivity of unwanted reaction products has been highly suppressed. Without using the recoil separator upstream the gas-jet transport system, large amount of unwanted radioactivity strongly prevents the unique identification of the event of our interest. This new technique makes clean and clear studies of chemistry of the heaviest elements promising.

The spectroscopic study of the heaviest elements has started by using alpha spectrometry. New isotope, ^{263}Hs (Z=108), which has the smallest atomic mass number ever observed among the Hassium isotopes, had discovered in the study. New spectroscopic information for ^{264}Hs and its daughters have obtained also. The spectroscopic study of Rutherfordium isotope ^{261}Rf (Z=104) has done and 1.9-s isomeric state has directly produced for the first time.

Preparatory works for the study of the new superheavy elements with atomic number 119 and 120 have started in 2013. We measured the reaction products of the ^{248}Cm (^{48}Ca, xn) $^{296-x}$Lv (Z=116) previously studied by Frelov Laboratory of Nuclear Reaction, Russia, and GSI. We observed 5 isotopes in total which tentatively assigned to ^{293}Lv, and ^{292}Lv.

Members

Group Director
Kosuke MORITA

Visiting Scientist
Kunihiro FUJITA (Kyushu Univ.)

Student Trainees
Taiki TANAKA (Kyushu Univ.)
Kenyu WATANABE (Kyushu Univ.)
Yuki YAMANO (Kyushu Univ.)

Publications

[Journal]

D. Kaji, K. Morita, K. Morimoto, H. Haba, M. Asai, K. Fujita, Z. Gan, H. Geissel, H. Hasebe, S. Hofmann, M. Huang, Y. Komori, L. Ma, J. Maurer, M. Murakami, M. Takeyama, F. Tokanai, T. Tanaka, Y. Wakabayashi, T. Yamaguchi, S. Yamaki, and A. Yoshida “Study of the Reaction 48Ca + 248Cm → 296Lv* at RIKEN-GARIS” Journal of the Physical Society of Japan, 86, 034201 (2017).

[解説、和文]

D. Kaji, K. Morimoto “気体充填型反跳イオン分離装置 GARIS-II” 放射化学 The Japan Society of Nuclear and Radiochemical Sciences, Vol.34, pp. 12-23

森本幸司「新元素“ニホニウム”の発見」真空ジャーナル p. 20-21,159, 2017 年 1 月

森本幸司「新元素発見までの道のり」兵庫教育 3 月号 No.793, p. 17-19

Oral Presentations

[International Conference etc.]

K. Morita, "Discovery of Element 113 and Future Research Direction at RIKEN", Nobel Symposia, NS160: Chemistry and Physics of Heavy and Superheavy Elements, Scania Sweden, May 29 to June 3, 2016

K. Morita, "The Discovery of Super-Heavy Element of Atomic Number Z=113 and Beyond", Nuclei in the Cosmos XIV (NIC XIV), TokiMesse, Niigata Japan, June 22, 2016

T. Tanaka, Y. Narikiyo, K. Morita, K. Fujita, D. Kaji, K. Morimoto, S. Yamaki, Y. Wakabayashi, K. Tanaka, M. Takeyama, A. Yoneyama, H. Haba, Y. Komori, S. Yanou, B. J. P. Gall, Z. Asfari, H. Faure, H. Hasebe, M. Huang, J. Kanaya, M. Murakami, A. Yoshida, T. Yamaguchi, T. Tokanai, T. Yoshida, Z. Gan, L. Ma, H. Geissel, S. Hofmann, Y. Maurer, S. Yamamoto, Y. Yamano, K. Watanabe, S. Ishizawa, M. Asai, R. Aono, S. Goto, K. Katori "Study of barrier distribution in heavy reaction system at the RIKEN-GARIS", Fusion17, Hobart Australia, February 23 2017

K. Morimoto “The discovery of element 113 at RIKEN” 26th International Nuclear Physics Conference (INPC2016) Sep. 11-16, 2016, Adelaide Convention Center, Australia (Plenary talk)

T. Tanaka, "Study of barrier distribution in heavy reaction system at the RIKEN-GARIS", 40th ASRC International Workshop ‘Experimental and Theoretical Advances in Fission and Heavy Nucei ’, Tokai Japan, December 13 2016

[Domestic Conference]

K. Morita, "Journey to the Discovery of Element 113", 64th General Meeting of Japanese Society of Chemotherapy, Kobe Japan, June 9, 2016

K. Morita, "Discovery of Element 113", JAIF General Meeting (2016), Tokyo Japan, June 21, 2016

K. Watanabe, D. Kaji, T. Niwase, T. Hirano, K. Fujita, Y. Yamano, S. Mitsuoka, K. Morimoto, K. Morita "Search for barrier distributions of Ti+Cm and V+Cm reaction", 122th Annual Meeting of Kyushu Branch of JPS, Fukuoka University Japan, December 10 2016

Y. Yamano, K. Morita, K. Fujita, K. Watanabe, T. Niwase, T. Hirano, S. Mitsuoka, K. Morimoto, D. Kaji, H. Haba, "Barrier distributions of 50Ti + 248Cm and 51V+ 248Cm reactions", JPS 72th Annual Meeting(2017), Osaka University Japan, March 20 2017

K. Fujita, "Present Status and Future Prospects of GARIS", JPS 72th Annual Meeting (2017), Osaka University Japan, March 17 2017

K. Morimoto, T. Tanaka, "理研における超重元素研究の今後", RIBF ミニ・ワークショップ「超重核生成反応の理論的理解に向けて」, RIKEN Japan, August 31 2016

T. Tanaka, "RIBF ミニ・ワークショップ「超重核生成反応の理論的理解に向けて」の報告", 日本物理学会 2016 秋季大会 SSRI インフォーマルミーティング, Miyazaki University Japan, September 22 2016

T. Tanaka, "新元素合成のための核融合反応における入射核依存性", 東海・重イオン科学シンポジウム ―タンデム加速器成果報告会―, JAEA Japan, January 6 2017

T.Niwase, K.Morita, K.Fujita, Y.Yamano, K.Watanabe, S.Mitsuoka, T.Hirano, D.Kaji, K.Morimoto, H.Haba, B.J.P.Gall, Z.Asfari”Measurement of barrier distribution for 208Pb (51V,xn)259-xDb reaction”, JPS 72th Annual Meeting (2017), Osaka University Japan, March 20 2017

D. Kaji, K. Morita, K. Morimoto, H. Haba “Frontline in superheavy element study using a gas-filled recoil separator GARIS” 第 60 回放射化学討論会, Tohoku University Japan, September 10-12 2016 (invited)

D. Kaji, K. Morimoto, H. Haba, Y. Wakabayashi, M. Takeyama, S. Yamaki, Y. Komori, S. Yano, S. Goto “Study on hot fusion reaction of 48Ca+238U→286Cn* using GARIS-II” 第 60 回放射化学討論会, Tohoku University Japan, September 10-12 2016

森本幸司 理研における超重元素合成実験の現状と計画 “Status and future plan of Superheavy element research at RIKEN”「第 9 回停止・低速 RI ビームを用いた核分光研究会」 & 「2017 超重元素の科学研究会」 合同研究会
原子力機構・先端基礎研究センター 茨城県東海村・原子力科学研究所 2017 年 3 月 6 日

K. Morimoto “Status and future plan of Superheavy element research at RIKEN” RIBF Users Meeting 2016, September 8, 2016, RIKEN JAPAN
森本幸司「113 番元素の合成と確認」AMO 討論会、理研、和光 2016 年 6 月 3 日

Posters Presentations

[International Conference etc.]
S. Ishizawa, K. Morimoto, D. Kaji, F. Tokanai "Development of time-of-flight detector for studying on superheavy nuclei", The 77th JSAP Autumn Meeting (2016), TOKI MESSE (Niigata Convention Center), Japan, September 13 2016
S. Ishizawa, K. Morimoto, D. Kaji, F. Tokanai "Development of time-of-flight detector for studying on superheavy nuclei II",The 64th JSAP Spring Meeting(2017), PACIFICO Yokohama, Japan, March 15 2017

[その他]
森本幸司「日本初、新元素“ニホニウム”の発見」IUPAC 賛助会員委員会 2016 年 11 月 2 日東京、明治大学紫紺館
森本幸司「113 番新元素の生成と確認」真空シンポジウム(VACUUM2016)2016 年 9 月 9 日、神奈川、パシフィコ横浜
森本幸司「日本初、原子番号 113"ニホニウム"の発見と、新元素がもたらす未来の産業創造への展望」JST フェア 2016, 東京ビッグサイト、2016/8/26 基調講演
森本幸司「113 番新元素の発見」アトムサイエンスフェア講演会 2016、京都、熊取交流センター、2016 年 10 月 22 日
森本幸司「113 番新元素ニホニウムの発見」平成 28 年度 大学等における放射線安全管理研修会、東京大学 農学部 弥生講堂 一条ホール、2016 年 8 月 30 日
森本幸司「ニホニウム発見物語」東北大学大学院理学研究科公開サイエンス講座東北大学川内キャンパス、仙台、2016 年 12 月 10 日

RIBF Research Division
Research Group for Superheavy Element
Superheavy Element Production Team

1. Abstract

The elements with their atomic number Z>103 are called as trans-actinide or superheavy elements. The chemical properties of those elements have not yet been studied in detail. Those elements do not exist in nature. Therefore, they must be produced by artificially for the scientific study of those elements. In our laboratory, we have been studying the physical and chemical properties of the superheavy elements utilizing the accelerators in RIKEN and various methods of efficient production of the superheavy elements.

2. Major Research Subjects

(1) Search for new supreheavy elements
(2) Decay spectroscopy of the heaviest nuclei
(3) Study of the chemical properties of the heaviest elements
(4) Study of the reaction mechanism of the fusion process (theory)

Summary of Research Activity

(1) Searching for new elements

To expand the periodic table of elements and the nuclear chart, we will search for new elements.

(2) Spectroscopic study of the nucleus of heavy elements

Using the high sensitivity system for detecting the heaviest element, we plan to perform a spectroscopic study of nuclei of the heavy elements.

(3) Chemistry of superheavy elements

Study of chemistry of the trans-actinide (superheavy element) has just started world-wide, making it a new frontier in the field of chemistry. Relativistic effects in chemical property are predicted by many theoretical studies. We will try to develop this new field.

(4) Study of a reaction mechanism for fusion process

Superheavy elements have been produced by complete fusion reaction of two heavy nuclei. However, the reaction mechanism of the fusion process is still not well understood theoretically. When we design an experiment to synthesize nuclei of the superheavy elements, we need to determine a beam-target combination and the most appropriate reaction energy. This is when the theory becomes important. We will try to develop a reaction theory useful in designing an experiment by collaborating with the theorists.

Members

Team Leader
Kosuke MORITA (concurrent; Group Director, Research Group for Superheavy Element)

Research & Technical Scientist
Kouji MORIMOTO (Senior Research Scientist, concurrent; Team Leader, Superheavy Element Device Development Team)

Nishina Center Research Scientist
Daiya KAJI (concurrent; Superheavy Element Device Development Team)

Nishina Center Technical Scientist-Consultant
Akira YONEDA

Research Consultant
Kenji KATORI

Junior Research Associate
Taiki TANAKA(Kyushu Univ.)

Visiting Scientists
Hiroyuki KOURA (JAEA)
Benoit Jean-Paul GALL (Strasbourg Univ.)
Marc ASFARI (Institut Pluridisciplinaire Hubert Curien)
Mirei TAKEYAMA (Yamagata Univ.)

Student Trainees
Toshitaka NIWASE (Kyushu Univ.)
Takeshi HIRANO (Kyushu Univ.)
Shun MITSUOKA(Kyushu Univ.)
Pierre BRIONNET (Strasbourg University)

Publications

[Journal]

D. Kaji, K. Morita, K. Morimoto, H. Haba, M. Asai, K. Fujita, Z. Gan, H. Geissel, H. Hasebe, S. Hofmann, M. Huang, Y. Komori, L. Ma, J. Maurer, M. Murakami, M. Takeyama, F. Tokanai, T. Tanaka, Y. Wakabayashi, T. Yamaguchi, S. Yamaki, and A. Yoshida “Study of the Reaction 48Ca + 248Cm → 296Lv* at RIKEN-GARIS” Journal of the Physical Society of Japan, 86, 034201 (2017).

[解説、和文]

D. Kaji, K. Morimoto “気体充填型反跳イオン分離装置 GARIS-II” 放射化学 The Japan Society of Nuclear and Radiochemical Sciences, Vol.34, pp. 12-23

森本幸司「新元素“ニホニウム”の発見」真空ジャーナル p. 20-21,159, 2017 年 1 月

森本幸司「新元素発見までの道のり」兵庫教育 3 月号 No.793, p. 17-19

Oral Presentations

[International Conference etc.]

K. Morita, "Discovery of Element 113 and Future Research Direction at RIKEN", Nobel Symposia, NS160: Chemistry and Physics of Heavy and Superheavy Elements, Scania Sweden, May 29 to June 3, 2016

K. Morita, "The Discovery of Super-Heavy Element of Atomic Number Z=113 and Beyond", Nuclei in the Cosmos XIV (NIC XIV), TokiMesse, Niigata Japan, June 22, 2016

T. Tanaka, Y. Narikiyo, K. Morita, K. Fujita, D. Kaji, K. Morimoto, S. Yamaki, Y. Wakabayashi, K. Tanaka, M. Takeyama, A. Yoneyama, H. Haba, Y. Komori, S. Yanou, B. J. P. Gall, Z. Asfari, H. Faure, H. Hasebe, M. Huang, J. Kanaya, M. Murakami, A. Yoshida, T. Yamaguchi, T. Tokanai, T. Yoshida, Z. Gan, L. Ma, H. Geissel, S. Hofmann, Y. Maurer, S. Yamamoto, Y. Yamano, K. Watanabe, S. Ishizawa, M. Asai, R. Aono, S. Goto, K. Katori "Study of barrier distribution in heavy reaction system at the RIKEN-GARIS", Fusion17, Hobart Australia, February 23 2017

K. Morimoto “The discovery of element 113 at RIKEN” 26th International Nuclear Physics Conference (INPC2016) Sep. 11-16, 2016, Adelaide Convention Center, Australia (Plenary talk)

T. Tanaka, "Study of barrier distribution in heavy reaction system at the RIKEN-GARIS", 40th ASRC International Workshop ‘Experimental and Theoretical Advances in Fission and Heavy Nucei ’, Tokai Japan, December 13 2016

[Domestic Conference]

K. Morita, "Journey to the Discovery of Element 113", 64th General Meeting of Japanese Society of Chemotherapy, Kobe Japan, June 9, 2016

K. Morita, "Discovery of Element 113", JAIF General Meeting (2016), Tokyo Japan, June 21, 2016

K. Watanabe, D. Kaji, T. Niwase, T. Hirano, K. Fujita, Y. Yamano, S. Mitsuoka, K. Morimoto, K. Morita "Search for barrier distributions of Ti+Cm and V+Cm reaction", 122th Annual Meeting of Kyushu Branch of JPS, Fukuoka University Japan, December 10 2016

Y. Yamano, K. Morita, K. Fujita, K. Watanabe, T. Niwase, T. Hirano, S. Mitsuoka, K. Morimoto, D. Kaji, H. Haba, "Barrier distributions of 50Ti + 248Cm and 51V+ 248Cm reactions", JPS 72th Annual Meeting(2017), Osaka University Japan, March 20 2017

K. Fujita, "Present Status and Future Prospects of GARIS", JPS 72th Annual Meeting (2017), Osaka University Japan, March 17 2017

K. Morimoto, T. Tanaka, "理研における超重元素研究の今後", RIBF ミニ・ワークショップ「超重核生成反応の理論的理解に向けて」, RIKEN Japan, August 31 2016

T. Tanaka, "RIBF ミニ・ワークショップ「超重核生成反応の理論的理解に向けて」の報告", 日本物理学会 2016 秋季大会 SSRI インフォーマルミーティング, Miyazaki University Japan, September 22 2016

T. Tanaka, "新元素合成のための核融合反応における入射核依存性”, 東海・重イオン科学シンポジウム ―タンデム加速器成果報告会―, JAEA Japan, January 6 2017

T.Niwase, K.Morita, K.Fujita, Y.Yamano, K.Watanabe, S.Mitsuoka, T.Hirano, D.Kaji, K.Morimoto, H.Haba, B.J.P.Gall, Z.Asfari”Measurement of barrier distribution for 208Pb (51V, xn) 259-xDb reaction”, JPS 72th Annual Meeting (2017), Osaka University Japan, March 20 2017

D. Kaji, K. Morita, K. Morimoto, H. Haba “Frontline in superheavy element study using a gas-filled recoil separator GARIS” 第 60 回放射化学討論会, Tohoku University Japan, September 10-12 2016 (invited)

D. Kaji, K. Morimoto, H. Haba, Y. Wakabayashi, M. Takeyama, S. Yamaki, Y. Komori, S. Yano, S. Goto “Study on hot fusion reaction of 48Ca+238U→286Cn* using GARIS-II” 第 60 回放射化学討論会, Tohoku University Japan, September 10-12 2016

森本幸司 理研における超重元素合成実験の現状と計画 “Status and future plan of Superheavy element research at RIKEN”「第 9 回停止・低速 RI ビームを用いた核分光研究会」 & 「2017 超重元素の科学研究会」 合同研究会

原子力機構・先端基礎研究センター 茨城県東海村・原子力科学研究所 2017 年 3 月 6 日

K. Morimoto “Status and future plan of Superheavy element research at RIKEN” RIBF Users Meeting 2016, September 8, 2016, RIKEN JAPAN

森本幸司「113 番元素の合成と確認」AMO 討論会、理研、和光 2016 年 6 月 3 日

Posters Presentations

[International Conference etc.]

S. Ishizawa, K. Morimoto, D. Kaji, F. Tokanai "Development of time-of-flight detector for studying on superheavy nuclei", The 77th JSAP Autumn Meeting (2016), TOKI MESSE (Niigata Convention Center), Japan, September 13 2016

S. Ishizawa, K. Morimoto, D. Kaji, F. Tokanai "Development of time-of-flight detector for studying on superheavy nuclei II",The 64th JSAP Spring Meeting(2017), PACIFICO Yokohama, Japan, March 15 2017

[その他]

森本幸司「日本初、新元素“ニホニウム”の発見」IUPAC 賛助会員委員会 2016 年 11 月 2 日東京、明治大学紫紺館

森本幸司「113 番新元素の生成と確認」真空シンポジウム(VACUUM2016)2016 年 9 月 9 日、神奈川、パシフィコ横浜

森本幸司「日本初、原子番号 113"ニホニウム"の発見と、新元素がもたらす未来の産業創造への展望」JST フェア 2016, 東京ビッグサイト、2016/8/26 基調講演

森本幸司「113 番新元素の発見」アトムサイエンスフェア講演会 2016、京都、熊取交流センター、2016 年 10 月 22 日
森本幸司「113 番新元素ニホニウムの発見」平成 28 年度 大学等における放射線安全管理研修会、東京大学 農学部 弥生講堂 一条ホール、2016 年 8 月 30 日
森本幸司「ニホニウム発見物語」東北大学大学院理学研究科公開サイエンス講座東北大学川内キャンパス、仙台、2016 年 12 月 10 日

RIBF Research Division
Research Group for Superheavy Element
Superheavy Element Device Development Team

1. Abstract

A gas-filled recoil ion separator has been used as a main experimental device for the study of superheavy elements. This team is in charge of maintain, improve, develop and operate the separators and related devices. There are two gas-filled recoil ion separators installed at RILAC experimental hall. One is GARIS that is designed for symmetric reaction such as cold-fusion reaction, and the other is newly developed GARIS-II that is designed for an asymmetric reaction such as hot-fusion reaction. New elements ^{278}113 were produced by ^{70}Zn + ^{209}Bi reaction using GARIS. Further the new element search Z > 118 are preparing by using GARIS-II.

2. Major Research Subjects

(1) Maintenance of GARIS and development of new gas-filled recoil ion separator GARIS-II.
(2) Maintenance and development of detector and DAQ system for GARIS and GARIS-II.
(3) Maintenance and development of target system for GARIS and GARIS-II.

3. Summary of Research Activity

The GARIS-II is newly developed which has an acceptance twice as large as existing GARIS, in order to realize higher sensitivity for asymmetric reaction such as a hot fusion reaction. After some commissioning works, the GARIS-II has been ready for new element research. We will also offer user-support if a researcher wishes to use the devices for his/her own research program.

Members

Team Leader
Kouji MORIMOTO

Nishina Center Research Scientist
Daiya KAJI

Junior Research Associate
Sayaka YAMAKI (Saitama Univ.)

Visiting Scientists
Fuyuki TOKANAI (Yamagata Univ.)

Student Trainee
Satoshi ISHIZAWA (Yamagata Univ.)
Ryutaro ITO (Yamagata Univ.)
Yuichiro INOMATA (Yamagata Univ

Publications

[Journal]

D. Kaji, K. Morita, K. Morimoto, H. Haba, M. Asai, K. Fujita, Z. Gan, H. Geissel, H. Hasebe, S. Hofmann, M. Huang, Y. Komori, L. Ma, J. Maurer, M. Murakami, M. Takeyama, F. Tokanai, T. Tanaka, Y. Wakabayashi, T. Yamaguchi, S. Yamaki, and A. Yoshida “Study of the Reaction 48Ca + 248Cm → 296Lv* at RIKEN-GARIS” Journal of the Physical Society of Japan, 86, 034201 (2017).

[解説、和文]

D. Kaji, K. Morimoto “気体充填型反跳イオン分離装置 GARIS-II” 放射化学 The Japan Society of Nuclear and Radiochemical Sciences, Vol.34, pp. 12-23
森本幸司「新元素“ニホニウム”の発見」真空ジャーナル p. 20-21,159, 2017 年 1 月
森本幸司「新元素発見までの道のり」兵庫教育 3 月号 No.793, p. 17-19

Oral Presentations

[International Conference etc.]

K. Morita, "Discovery of Element 113 and Future Research Direction at RIKEN", Nobel Symposia, NS160: Chemistry and Physics of Heavy and Superheavy Elements, Scania Sweden, May 29 to June 3, 2016

K. Morita, "The Discovery of Super-Heavy Element of Atomic Number Z=113 and Beyond", Nuclei in the Cosmos XIV(NIC XIV), TokiMesse, Niigata Japan, June 22, 2016

T. Tanaka, Y. Narikiyo, K. Morita, K. Fujita, D. Kaji, K. Morimoto, S. Yamaki, Y. Wakabayashi, K. Tanaka, M. Takeyama, A. Yoneyama, H. Haba, Y. Komori, S. Yanou, B. J. P. Gall, Z. Asfari, H. Faure, H. Hasebe, M. Huang, J. Kanaya, M. Murakami, A. Yoshida, T. Yamaguchi, T. Tokanai, T. Yoshida, Z. Gan, L. Ma, H. Geissel, S. Hofmann, Y. Maurer, S. Yamamoto, Y. Yamano, K. Watanabe, S. Ishizawa, M. Asai, R. Aono, S. Goto, K. Katori "Study of barrier distribution in heavy reaction system at the RIKEN-GARIS", Fusion17, Hobart Australia, February 23 2017

K. Morimoto “The discovery of element 113 at RIKEN” 26th International Nuclear Physics Conference (INPC2016) Sep. 11-16, 2016, Adelaide Convention Center, Australia (Plenary talk)

T. Tanaka, "Study of barrier distribution in heavy reaction system at the RIKEN-GARIS", 40th ASRC International Workshop ‘Experimental

and Theoretical Advances in Fission and Heavy Nucei ', Tokai Japan, December 13 2016

[Domestic Conference]

K. Morita, "Journey to the Discovery of Element 113", 64th General Meeting of Japanese Society of Chemotherapy, Kobe Japan, June 9, 2016

K. Morita, "Discovery of Element 113", JAIF General Meeting(2016), Tokyo Japan, June 21, 2016

K. Watanabe, D. Kaji, T. Niwase, T. Hirano, K. Fujita, Y. Yamano, S. Mitsuoka, K. Morimoto, K. Morita "Search for barrier distributions of Ti+Cm and V+Cm reaction", 122th Annual Meeting of Kyushu Branch of JPS, Fukuoka University Japan, December 10 2016

Y. Yamano, K. Morita, K. Fujita, K. Watanabe, T. Niwase, T. Hirano, S. Mitsuoka, K. Morimoto, D. Kaji, H. Haba, "Barrier distributions of 50Ti + 248Cm and 51V+ 248Cm reactions", JPS 72th Annual Meeting(2017), Osaka University Japan, March 20 2017

K. Fujita, "Present Status and Future Prospects of GARIS", JPS 72th Annual Meeting(2017), Osaka University Japan, March 17 2017

K. Morimoto, T. Tanaka, "理研における超重元素研究の今後", RIBF ミニ・ワークショップ「超重核生成反応の理論的理解に向けて」, RIKEN Japan, August 31 2016

T. Tanaka, "RIBF ミニ・ワークショップ「超重核生成反応の理論的理解に向けて」の報告" , 日本物理学会 2016 秋季大会 SSRI インフォーマルミーティング, Miyazaki University Japan, September 22 2016

T. Tanaka, "新元素合成のための核融合反応における入射核依存性", 東海・重イオン科学シンポジウム ―タンデム加速器成果報告会―, JAEA Japan, January 6 2017

T.Niwase, K.Morita, K.Fujita, Y.Yamano, K.Watanabe, S.Mitsuoka, T.Hirano, D.Kaji, K.Morimoto, H.Haba, B.J.P.Gall, Z.Asfari "Measurement of barrier distribution for 208Pb(51V,xn)259-xDb reaction", JPS 72th Annual Meeting (2017), Osaka University Japan, March 20 2017

D. Kaji, K. Morita, K. Morimoto, H. Haba "Frontline in superheavy element study using a gas-filled recoil separator GARIS" 第 60 回放射化学討論会, Tohoku University Japan, September 10-12 2016 (invited)

D. Kaji, K. Morimoto, H. Haba, Y. Wakabayashi, M. Takeyama, S. Yamaki, Y. Komori, S. Yano, S. Goto "Study on hot fusion reaction of 48Ca+238U→286Cn* using GARIS-II" 第 60 回放射化学討論会, Tohoku University Japan, September 10-12 2016

森本幸司 理研における超重元素合成実験の現状と計画 "Status and future plan of Superheavy element research at RIKEN"「第 9 回停止・低速 RI ビームを用いた核分光研究会」 & 「2017 超重元素の科学研究会」 合同研究会
原子力機構・先端基礎研究センター 茨城県東海村・原子力科学研究所 2017 年 3 月 6 日

K. Morimoto "Status and future plan of Superheavy element research at RIKEN" RIBF Users Meeting 2016, September 8, 2016, RIKEN JAPAN

森本幸司「113 番元素の合成と確認」AMO 討論会、理研、和光 2016 年 6 月 3 日

Posters Presentations

[International Conference etc.]

S. Ishizawa, K. Morimoto, D. Kaji, F. Tokanai "Development of time-of-flight detector for studying on superheavy nuclei", The 77th JSAP Autumn Meeting(2016), TOKI MESSE (Niigata Convention Center), Japan, September 13 2016

S. Ishizawa, K. Morimoto, D. Kaji, F. Tokanai "Development of time-of-flight detector for studying on superheavy nuclei II",The 64th JSAP Spring Meeting(2017), PACIFICO Yokohama, Japan, March 15 2017

[その他]

森本幸司「日本初、新元素"ニホニウム"の発見」IUPAC 賛助会員委員会 2016 年 11 月 2 日東京、明治大学紫紺館
森本幸司「113 番新元素の生成と確認」真空シンポジウム(VACUUM2016)2016 年 9 月 9 日、神奈川、パシフィコ横浜
森本幸司「日本初、原子番号 113"ニホニウム"の発見と、新元素がもたらす未来の産業創造への展望」JST フェア 2016, 東京ビッグサイト、2016/8/26 基調講演
森本幸司「113 番新元素の発見」アトムサイエンスフェア講演会 2016、京都、熊取交流センター、2016 年 10 月 22 日
森本幸司「113 番新元素ニホニウムの発見」平成 28 年度 大学等における放射線安全管理研修会、東京大学 農学部 弥生講堂 一条ホール、2016 年 8 月 30 日
森本幸司「ニホニウム発見物語」東北大学大学院理学研究科公開サイエンス講座東北大学川内キャンパス、仙台、2016 年 12 月 10 日

RIBF Research Division
Nuclear Transmutation Data Research Group

1. Abstract

The disposal of high-level radioactive wastes from nuclear power plants is a problem considered to be one of the most important issues at both national and international levels. As a fundamental solution to the problem, the establishment of nuclear transmutation technology where long-lived nuclides can be changed to short-lived or stable ones will be vital. Progress in R & D in the transmutation of long-lived fission products (LLFP) in the nuclear wastes however, has been slow. Our group aims to obtain reaction data of LLFP at RIBF and other facilities which may lead to a new discovery and invention for peaceful use of nuclear power and the welfare of humanity.

2. Major Research Subjects

The Group is formed by three research teams. The first two Teams, “Fast RI Data Team” and “Slow RI Data Team”, are in charge of proton- and deuteron-induced reaction data for LLFP in inverse kinematics at RIBF. The third Team “Muon Data Team” is to obtain muon capture data of LLFP at muon facilities. All the teams are focusing to obtain high-quality data which are essentially necessary to establish reliable reaction models. Each team has its own subjects and promotes LLFP reaction programs based on their large experiences, techniques and skills.

3. Summary of Research Activity

In 2014, all the teams polished up experimental strategies, formed collaboration and prepared experiments. Physics runs for spallation reaction and Coulomb breakup reaction with the beams at 100-200 MeV/u were successfully organized by using the ZeroDegree and SAMURAI spectrometers at RIBF in 2015-2016. In 2017, a physics run with an energy-decelerated radioactive beam will be conducted under collaboration with CNS, Univ. of Tokyo. The muon program started at J-PARC and RCNP (Osaka University) in spring 2016. A neutron detection array was newly developed to measure evaporation neutrons after muon capture process, and was utilized at an experiment at RCNP in February 2017. In 2017 and 2018, experiments will be organized at both RAL and RCNP to have complete sets of the muon data for a specific LLFP nuclide.

Members

Group Director

Hiroyoshi SAKURAI (concurrent: Chief Scientist, RI Physics Lab.)

Assitant

Izumi YOSHIDA (Apr. 1, 2015 –)
Asako TAKAHASHI (Apr. 1, 2015 –)

RIBF Research Division
Nuclear Transmutation Data Research Group
Fast RI Data Team

1. Abstract

Fast RI team aims at obtaining and accumulating the cross section data for long lived fission products (LLFPs) in order to explore the possibility of using accelerator for nuclear transmutation.

LLFPs as nuclear waste have been generated continuously in nuclear power plants for wealth for human lives, while people noticed the way of disposal has not necessarily been established, especially after the Fukushima Daiichi power plant disaster. One of the ways to reduce the amount of LLFP or to recover them as recycled resources is nuclear transmutation technique.

RIBF facility has a property to generate such LLFP as a secondary beam and the beam species are identified by event by event. Utilizing the property, absolute values of the cross section of various reactions on LLFPs are measured and accumulated as database.

2. Major Research Subjects

1) Measurement of reaction products by the interaction of LLFPs with proton, deuteron, and photon to explore candidate reactions for transmutation of LLFPs.
2) Evaluation of the cross section data for the neutron induced reactions from the obtained data.

3. Summary of Research Activity

1) Acting as collaboration hub on many groups which plan to take data using fast RI beam in RIBF facility.
2) Concentrating on take data for proton and deuteron induced spallation reactions with inverse kinematics.
3) Accumulating the cross section data and evaluating them as evaluated nuclear data.
4) Evaluating cross section of neutron induced reaction on LLFP by collaborating with the nuclear model calculation and evaluation group.

Members

Team Leader

Hideaki OTSU (Concurrent: Team Leader, SAMURAI Team)

Technical Staff I

Nobuyuki CHIGA

Student Trainees

Shouhei ARAKI (Kyushu Univ.)
Tatsuya YAMAMOTO (Miyazaki Univ.)
Keita NAKANO (Kyushu Univ.)
Ayaka IKEDA (Niigata Univ.)
Kazuya CHIKAATO (Niigata Univ.)
Hiroki TAKAHASHI (Niigata Univ.)
Yoshiki SOUDO（Miyazaki Univ.）
Kenji NISHIZUKA (Niigata Univ.)
Junki SUWA (Kyushu Univ.)
Masamichi AMANO (Rikkyo Univ.)
Junki AMANO (Rikkyo Univ.)
Akira HOMMA(Niigata Univ.)
Naoto KANDA(Niigata Univ.)

List of Publications & Presentations

Publications

[Journal]

(Original Papers)

H. Wang, H. Otsu, H. Sakurai, D. Ahn, M. Aikawa, T. Ando, S. Araki, S. Chen, N. Chiga, P. Doornenbal, N. Fukuda, T. Isobe, S. Kawakami, S. Kawase, T. Kin, Y. Kondo, S. Koyama, S. Kubono, Y. Maeda, A. Makinaga, M. Matsushita, T. Matsuzaki, S. Michimasa, S. Momiyama, S. Nagamine, T. Nakamura, K. Nakano, M. Niikura, T. Ozaki, A. Saito, T. Saito, Y. Shiga, M. Shikata, Y. Shimizu, S. Shimoura, T. Sumikama, P.A. Söderström, H. Suzuki, H. Takeda, S. Takeuchi, R. Taniuchi, Y. Togano, J. Tsubota, M. Uesaka Y. Watanabe, Y. Watanabe, K. Wimmer, T. Yamamoto, K. Yoshida, ''Spallation reaction study for the long-lived fission product ^{107}Pd'', Prog Theor Exp Phys (2017) 2017 (2): 021D01.

H. Wang, H. Otsu, H. Sakurai, D.S. Ahn, M. Aikawa, P. Doornenbal, N. Fukuda, T. Isobe, S. Kawakami, S. Koyama, T. Kubo, S. Kubono, G. Lorusso, Y. Maeda, A. Makinaga, S. Momiyama, K. Nakano, M. Niikura, Y. Shiga, P.-A. Söderström, H. Suzuki, H. Takeda, S. Takeuchi, R. Taniuchi, Ya. Watanabe, Yu. Watanabe, H. Yamasaki, K. Yoshida, “Spallation reaction study for fission products in nuclear waste: Cross section measurements for ^{137}Cs and ^{90}Sr on proton and deuteron”, Phys. Lett. B 754 (2016), 104-108.

(Proceedings)

H. Wang, H. Otsu, H. Sakurai et al., Spallation reaction study for fission products in nuclear waste: Cross section measurements for ^{137}Cs, ^{90}Sr and 107Pd on proton and deuteron, accepted, the Proceeding of ND2016, October, 2016

H. Wang, H. Otsu, H. Sakurai et al., Spallation reaction study for the long-lived fission products in nuclear waste: Cross section measurements for ^{137}Cs, ^{90}Sr and ^{107}Pd using inverse kinematics method, accepted, the Proceeding of INES-5, January 2017

S. Kawase et al., "Cross section measurement of residues produced in proton- and deuteron-induced spallation reactions on ^{93}Zr at 100MeV/u using the inverse kinematics method", Proceedings of ND2016 International Conference on NUCLEAR DATA FOR SCIENCE

AND TECHNOLOGY
K. Nakano et al., "Cross sections for nuclide production in proton- and deuteron-induced reactions on niobium-93 measured using the inverse kinematics method", Proceedings of ND2016 International Conference on NUCLEAR DATA FOR SCIENCE AND TECHNOLOGY

Oral Presentations

[International Conference]

H. Wang, Spallation reaction study for fission products in nuclear waste: Cross section measurements for ^{137}Cs, ^{90}Sr and ^{107}Pd on proton and deuteron at different reaction energy, International conference on nuclear data and technology (ND2016), September 11-16, 2016, Brugge, Belgium
H. Wang, Measurement of Spallation Cross Sections for ^{137}Cs, ^{90}Sr and ^{107}Pd on Proton and Deuteron Using the Inverse Kinematic Method, Asian Nuclear Prospects 2016 (ANUP2016), October 24-27, 2016, Sendai, Japan
H. Wang, Spallation Reaction Study for the Long-Lived Fission Products in Nuclear Waste: Cross Section Measurement for ^{137}Cs, ^{90}Sr and ^{107}Pd Using the Inverse Kinematic Method, The Fifth International Symposium on Innovative Nuclear Energy Systems (INES-5), October 31-November 2, 2016, Tokyo Institute of Technology, Tokyo, Japan
S. Takeuchi, "Status report of ImPACT experiments" , SAMURAI International Collaboration Workshop 2016, Kyushu
S. Kawase et al., "Cross section measurement of residues produced in proton- and deuteron-induced spallation reactions on ^{93}Zr at 100MeV/u using the inverse kinematics method", ND2016: International Conference on Nuclear Data for Science and Technology, Bruges, Belgium, Sep. 2016
S. Kawase et al., "Measurement of Isotopic Production Cross Sections through Proton- and Deuteron-Induced Spallation Reactions on ^{93}Zr and ^{93}Nb using the Inverse Kinematics Method", The Fifth International Symposium on Innovative Nuclear Energy Systems (INES5), Tokyo, Japan, Nov. 2016

[Domestic Conference]

H. Wang, Reaction study for fission products in nuclear waste: Cross section measurements for the spallation of ^{137}Cs, ^{90}Sr and ^{107}Pd on proton and deuteron, JPS meeting 2016 autumn, September 21-24, 2016, Miyazaki, Japan
平山晃大、^{79}Se, ^{80}Se のクーロン分解反応, 2017 年 3 月 日本物理学会年次大会, 大阪
武内聡、 クーロン分解反応による 107,108Pd および 93,94Zr の光吸収断面積, 2016 年 3 月日本物理学会年次大会, 仙台
尾崎友志、 ^{238}U の飛行核分裂によって生成される ^{107}Pd,^{79}Se のアイソマー比 2016 年 3 月日本物理学会年次大会, 仙台
川瀬頌一郎, 他 11 名, "陽子・重陽子に対する 100 MeV/u ^{93}Zr 入射核破砕反応による同位体生成断面積の測定", 日本物理学会 2015 年秋季大会, 大阪市, 2015 年 9 月
中野敬太, 他 9 名, ImPACT-RIBF Collaboration, "水素・重水素に対する 100 MeV/u^{93}Zr 及び ^{93}Nb 入射核破砕反応の残留核生成断面積測定", 日本原子力学会九州支部第 34 回研究発表講演会, O-02, 福岡市, 2015 年 12 月
川瀬頌一郎, 他 9 名, ImPACT-RIBF Collaboration, "逆運動学的手法を用いた陽子・重陽子による核破砕反応の残留核生成断面積測定 (2)100 MeV/u^{93}Zr 入射反応",日本原子力学会 2016 年春の年会, 2J12, 仙台市, 2016 年 3 月
中野敬太, 他 9 名, ImPACT-RIBF Collaboration, "逆運動学的手法を用いた陽子・重陽子による核破砕反応の残留核生成断面積測定 (3)100 MeV/u^{93}Nb 入射反応",日本原子力学会 2016 年春の年会, 2J13, 仙台市, 2016 年 3 月
中野敬太, 他 9 名, ImPACT-RIBF Collaboration, "^{93}Zr 及び ^{93}Nb に対する陽子・重陽子入射核破砕反応の同位体生成に関する研究", 日本原子力学会九州支部第 35 回研究発表講演会,O-05, 春日市,2016 年 12 月
諏訪純貴, 他 3 名,ImPACT-RIBF Collaboration, "陽子・重陽子に対する 91Y 核破砕反応の同位体生成断面積測定" 日本原子力学会 2017 春の年会, 平塚市, 2017 年 3 月
千賀信幸、相関陽子検出器の開発、平成 27 年度高エネルギー加速器研究機構技術研究会、KEK つくばキャンパス、平成 28 年 3 月 17 日
渡辺幸信、逆運動学手法を用いた陽子・重陽子による核破砕反応の残留核生成断面積測定 (1) 実験目的と概要、日本原子力学会春の大会、東北大学、2016 年 3 月
川瀬頌一郎、逆運動学手法を用いた陽子・重陽子による核破砕反応の残留核生成断面積測定 (2) 100 MeV/u ^{93}Zr□射反応、日本原子力学会春の大会、東北大学、2016 年 3 月
中野敬太、逆運動学手法を用いた陽子・重陽子による核破砕反応の残留核生成断面積測定 (3) 100 MeV/u ^{93}Nb 入射反応、日本原子力学会春の大会、東北大学、2016 年 3 月
武内聡、クーロン分解反応による 107,108Pd および 93,94Zr の光吸収断面積、日本物理学会年次大会、東北学院大学、2016 年 3 月
尾崎友志、^{238}U の飛行核分裂によって生成される ^{107}Pd,^{79}Se のアイソマー比、日本物理学会年次大会、東北学院大学、2016 年 3 月

Posters Presentations

[Domestic Conference]

平山晃大 不安定核の分解反応のための荷電フラグメント用ホドスコープの開発 2016 年 3 月日本物理学会年次大会, 仙台
中野敬太、逆運動学的手法を用いた陽子・重陽子による核破砕反応の残留核生成断面積測定、日本原子力学会春の大会、東北大学、2016 年 3 月
尾崎友志、^{238}U の飛行核分裂によって生成される ^{107}Pd,^{79}Se のアイソマー比、2016 年 8 月 第 62 回原子核三者若手夏の学校
平山晃大、不安定核分解反応のための荷電フラグメント粒子識別用ホドスコープの開発、2016 年 8 月 第 62 回原子核三者若手夏の学校

修士論文

四方瑞紀 93,94Zr のクーロン分解反応による光吸収断面積の測定、東京工業大学
中野敬太, "Cross section measurement of isotope production in proton- and deuteron-induced reactions on ^{93}Nb using the inverse kinematics method" 九州大学大学院総合理工学府先端エネルギー理工学専攻

卒業論文

平山晃大 学士論文：荷電フラグメントの粒子識別用ホドスコープの開発、東京工業大学
諏訪純貴,"陽子・重陽子に対する ^{93}Zr 入射核破砕反応による核種生成実験データの予備解析" 九州大学工学部エネルギー科学科 卒業論文, 2016 年 2 月

RIBF Research Division
Nuclear Transmutation Data Research Group
Slow RI Data Team

1. Abstract

This team is in charge of the development of low-energy RI beams of long-lived fission fragments (LLFP) from the ^{238}U by means of degrading the energy of beams produced by the BigRIPS fragment separator.

2. Major Research Subjects

Studies of the slowing down and purification of RI beams are the main subjects of the team. Developments of devices used for the slowing down of RI beams are also an important subject.

3. Summary of Research Activity

1) Study and development of the slowed-down methods for LLFP.
2) Development of the devices used for the slowing down.
3) Operation of the BigRIPS separator and supply the low energy LLFP beam to the experiment in which the cross sections of LLFP are measured at the low energy.

Members

Team Leader

Koichi YOSHIDA (– Aug. 31, 2016, concurrent: BigRIPS Team)
Toshiyuki SUMIKAMA (Sep. 1, 2016 –)

List of Publications & Presentations

Publications

[Proceedings]

(Original Papers)

T. Sumikama, D.S. Ahn, N. Fukuda, N. Inabe, T. Kubo, Y. Shimizu, H. Suzuki, H. Takeda, N. Aoi, D. Beaumel, K. Hasegawa, E. Ideguchi, N. Imai, T. Kobayashi, M. Matsushita, S. Michimasa, H. Otsu, S. Shimoura, T. Teranishi, “First test experiment to produce the slowed-down RI beam with the momentum-compression mode at RIBF”, Nuclear Instruments and Methods in Physics Research B 367, 180-184, (2016).

Oral Presentations

[International Conference etc.]

T. Sumikama, “Slowed-down RI beam produced from fast projectile fragment at RIBF”, Fragment separator expert meeting, Grand Rapids, Michigan, USA, August 30 – September 1, 2016.

T. Sumikama, “Spectroscopy of neutron-rich isotope around ^{108}Zr”, EURICA collaboration meeting, RIKEN, Wako, Saitama, Japan, September 6-7, 2016.

T. Sumikama et al., “Shape evolution of neutron-rich nuclei in the vicinity of ^{110}Zr”, the 26th International Nuclear Physics Conference (INPC 2016), Adelaide, Australia, September 11-16, 2016.

[Domestic Conference]

炭竈聡之 他, “中性子過剰 Mo 同位体の崩壊核分光”, 日本物理学会第 72 回年次大会, 大阪大学, 大阪, 2017 年 3 月 17 日-20 日。

RIBF Research Division
Nuclear Transmutation Data Research Group
Muon Data Team

1. Abstract

Dr. Yoshio Nishina observed muons in the cosmic rays in 1937. The muon is an elementary particle belonging to the lepton group. The muon has positive or negative electric charge, and the lifetime is 2.2 μsec. The negative muon is 207 times heavier than the electron, and behaves as a "heavy electron" in materials. The negative muon is caught by a nucleus (atomic number: Z) in materials to form a muonic atom, and is then captured by the nucleus. The muon is combined with a proton in the nucleus to convert to a neutron and a neutrino. The muon rest-mass energy is transferred to the nucleus with Z-1 to create the excited nuclear states. Emissions of neutrons and γ-rays are followed to produce several isotopic nuclei with Z-1. From a viewpoint of the nuclear physic, the nuclear reaction is very unique and interesting. High energy is suddenly introduced in the nuclei associated with the conversion process of proton to the neutron and the neutrino. Many experiments have been so far reported, but the reaction mechanism is not yet well clarified. The research team aims at obtaining the experimental data to understand the reaction mechanism of muon nuclear capture as well as at establishing the nuclear reaction theory.

2. Major Research Subjects

(1) Experimental clarification on the reaction mechanism of nuclear muon capture
(2) Establishment of the reaction theory on nuclear muon capture
(3) Interdisciplinary application of the nuclear muon capture reaction

3. Summary of Research Activity

There are two experimental methods to study the reaction mechanism of muon nuclear capture. The first one is "muon in-beam method". The neutron and γ-ray emissions from the excited states of nucleus with Z-1 are prompt events, and are observed by the "muon in-beam method" employing DC muon beam. The DC muon beam in Japan is obtained at the MuSIC (Muon Science Innovative Channel) muon facility constructed at Research Center for Nuclear Physics (RCNP) at Osaka University. The second one is "muon activation method" employing the pulsed muon beam. The unstable nuclei with Z-1 produced in the muon nuclear capture reaction make $\beta^{+/-}$ decay to stable nuclei. The γ-rays associated with the $\beta^{+/-}$ decay from the unstable nuclei are observed, and the γ-ray build-up (at beam-on) and decay (at beam-off) curves are measured. Since the half-lives and the absolute decay branches of $\beta^{+/-}$-γ decays are known, the production ratio of the isotopic Z-1 nuclei is extracted from the curves. The pulsed muon beam is obtained at the RIKEN-RAL Muon Facility in the UK and J-PARC MLF MUSE muon facility in Japan.

3.1 Test experiment at the MuSIC in early 2016

We made a test experiment of γ-ray observation associated with the muon nuclear capture reaction on isotope enriched Pd targets (^{104,105,106,108,110}Pd) at the MuSIC muon facility in the Osaka University. The DC muon beam is appropriate to observe the prompt neutron and γ-ray emissions. The primary proton beam intensity was 20 nA, and the capture solenoid magnets of the MuSIC were not fully energized because of the quench problem. The stopping muon number at Pd targets was 8 μ^-/second. Under such a severe experimental condition, we successfully observed the prompt γ-rays from ^{A}Pd (μ-,xn ν)$^{A-x}$Rh reactions and the muonic K, L, M and N X-rays from muonic Pd atoms.

3.2 Experiment at the MuSIC in late 2016

At the MuSIC muon facility, the radiation shield structure was improved around the production target, and the primary proton beam intensity to the MuSIC was raised up to 1 μA from 20 nA. The muon intensity is expected to be increased by 50 times, and the experimental data with good quality is obtained. In addition, we have installed a radiation shield wall at the end of the MuSIC beam line to reduce the background to the detection system. The wall consists of 30cm thick concrete block with 5 mm thick lead plate at the downstream side.

We performed the experiment concentrated to ^{108}Pd (μ-, xn ν)$^{108-x}$Rh reactions. Employing a newly built neutron spectrometer, the prompt neutron and γ-ray were measured to obtain the reaction branching ratios of
^{108}Pd (μ-,xn ν)$^{108-x}$Rh reactions.

For the neutron and γ-ray measurement, we have constructed a neutron spectrometer named "Seamine": **S**cintillator **E**nclosure **A**rray for **M**uon **I**nduced **N**eutron **E**mission. The spectrometer consists of 21 liquid scintillation counters, 2 Ge γ-ray detectors, 7 BaF_2 counters. The Pd target assembly including the muon beam counters and degraders is located at the center of the spectrometer. The neutron counter is a BC-501A liquid scintillation counter with 20cm diameter and 5cm depth, and is connected to a 5" photo multiplication tube (H4144-01). The total neuron detection efficiency is estimated 5%, where the distance is 4 cm between the neutron counter and the target. The Ge γ-ray detectors are placed at 10 cm form the target, and the typical detection efficiency is 0.5% for 200 keV γ-ray. The BaF_2 counters are located beneath the target to obtain fast γ-ray signals associated with muon nuclear capture reaction, which give the time spectrum of γ-rays emitted from the compound nucleus.

Signals from the liquid scintillation counters for neutron detection are processed in a CAEN V1730B waveform digitizer (16channel, 14bit, 500M samplings/sec.). The neuron-γ discrimination is performed on-line during the experiment, and the detailed analysis is conducted off-line after the experiment. The neutron energy spectrum is also constructed simultaneously. Signals from Ge γ-ray detectors are also processed in the CAEN V1730B waveform digitizer to obtain the energy and the time spectrum of γ-rays associated with muon

nuclear capture reaction. Signals from the BaF_2 counters and muon beam counters are sent to the CAEN V1730B waveform digitizer to make fast timing signals. The accumulated data is about 6.6 TB in the experiment, and the detailed off-line analysis is now in progress.

3.3 Test experiment at J-PARC MLF MUSE

We made a test experiment for a few hours at D2 beam line in the J-APRC MLF MUSE muon facility. The ^{108}Pd target was placed at the center of the vacuum chamber designed for muonic X-ray observation experiment. In spite of the long distance between the target and Ge γ-ray detectors, we successfully observed some γ-rays originated from the β^- decays of unstable Rh nuclei produced by ^{108}Pd (μ-, xn ν) $^{108-x}$Rh reactions. The γ-ray yield build-up curve at beam-on and the decay curve at beam-off were obtained by the off-line data analysis. The experimental technique for the muon activation method was established by the test experiment.

The experiments employing the muon activation method are scheduled in late 2017 at the RIKEN-RAL Muon Facility and J-PARC MLF MUSE muon facility.

3.4 Comparison with theory

The muon activation method gives the reaction branching ratios. The muon in-beam method gives the neutron multiplicity distribution (reaction branching ratio) and the neutron energy spectrum. We will compare the experimental results with theoretical calculations of the statistical compound nuclear model for the first step.

Members

Team Leader
Teiichiro MATSUZAKI

List of Publications & Presentations

Publications

[解説、和文]

松崎禎市郎“原子力分野への負ミュオンの応用；負ミュオンによる核変換・核融合・核分裂”、日本原子力学会誌 Vol. 58 No.10 (2016) P.612

Oral Presentations

[International Conference etc.]

松崎禎市郎、“Nuclear Transmutation by Muon Nuclear Capture Reaction” Muonic X and Gamma ray Spectroscopy (MXG16)、茨木市、2016 年 9 月 27 日

斎藤岳志、松崎禎市郎、櫻井博儀、新倉潤、他、“Muon Nuclear Capture Reaction on Pd Isotopes” Muonic X and Gamma ray Spectroscopy (MXG16)、茨木市、2016 年 9 月 27 日

[Domestic Conference]

松崎禎市郎、“負ミュオンによる原子核変換”、負ミュオン研究会、東海村、2016 年 7 月 11 日

松崎禎市郎、“原子力分野へのミュオン応用：原子核変換と触媒核融合”、日本原子力学会 2016 年春の年会、仙台市、2016 年 3 月 28 日

斎藤岳志、“松崎禎市郎、櫻井博儀、新倉潤、他、RCNP MuSIC における安定 Pd 同位体の μ^- 捕獲現象の研究”、日本物理学会第７２回年次大会（2017 年）、2017 年 3 月 17 日

特許出願

特許の名称: 「ミュオン照射による放射性物質の製造方法およびその製造物質」
発明者: 松崎禎市郎、櫻井博儀
出願人：理化学研究所
出願番号：JP2017/003226
出願年月日：2017 年 1 月 30 日
出願国：国際出願
共同出願人：なし

RIBF Research Division
High-Intensity Accelerator R&D Group

1. Abstract

The R&D group, consisting of two teams, develops elemental technology of high-power accelerators and high-power targets, aiming at future applications to nuclear transmutations of long-lived fission product into short-lived nuclides. The research subjects are superconducting rf cavities for low-velocity ions, design of high-power accelerators, high-power target systems and related technologies.

2. Major Research Subjects

(1) R&D of elemental technology of high-power accelerators and high-power targets

3. Summary of Research Activity

(1) Based on the discussion with other research groups, R&D study of various accelerator components and elements is under progress.

Members

Group Director

Osamu KAMIGAITO (concurrent: Chief Scientist, Group Director, Accelerator Gr.)

List of Publications & Presentations

Oral Presentations

[Domestic Conference]

上垣外修一、他、加速器システムの要素技術開発、日本物理学会秋季大会、宮崎大学、木花キャンパス、2016 年 9 月 22 日

RIBF Research Division
High-Intensity Accelerator R&D Group
High-Gradient Cavity R&D Team

Abstract

We develop new components for accelerators dedicated for low-beta-ions with very high intensity. Specifically, we are designing and constructing a cryomodule for superconducting linac efficient for acceleration of low-beta-ions. In parallel, we try to optimize an rf acceleration system by making computer simulations for acceleration of very high intensity beams.

Major Research Subjects

-Development of high-gradient cavites for low beta ions
-Development of power saving cryomodules

Summary of Research Activity

Development of highly efficient superconducting accelerator modules

Members

Team Leader

Naruhiko SAKAMOTO (concurrent: Cyclotron Team)

Research & Technical Scientists

Kazunari YAMADA (concurrent: Senior Technical Scientist, Beam Dynamics & Diagnostics Team)
Kazutaka OZEKI (concurrent: Technical Scientist, Cyclotron Team)
Yutaka WATANABE (concurrent: Senior Technical Scientist, RILAC team)

Nishina Center Research Scientist

Kenji SUDA (concurrent: Cyclotron Team)

Postdoctoral Researchers

Xingguang LIU

List of Publications & Presentations

Oral Presentations

[International Conference etc.]

Naruhiko Sakamoto, et al., Reduction and Resource Recycling of High-level Radioactive Wastes through Nuclear Transmutation-Development of Superconducting Quarter-Wave Resonators and their Cryomodules for Accelerator of Intense Low-β Ion-Beams、The 5th International Conference on Asian Nuclear Prospects（ANUP2016）, Sendai, Japan, October 26 2016.

Kazutaka Ozeki, et al., Design and fabrication status of RIKEN SC-Linac cryomodule, 2017 TESLA Technology Collaboration meeting, East Lansing, USA, February 21 2017

Kazutaka Ozeki et al., Cavity fabrication, processing and VT result of RIKEN QWR, 2017 TESLA Technology Collaboration meeting, East Lansing, USA, February 22 2017

Posters Presentations

[International Conference etc.]

Kazutaka Ozeki, et al., Cryomodule and power coupler for RIKEN Superconducting QWR, 28th Linear Accelerator Conference, East Lansing, USA, September 27 2016

Kazunari Yamada et al., First Vertical Test of Superconducting QWR Prototype at RIKEN, 28th Linear Accelerator Conference, East Lansing, USA, September 29 2016

.

RIBF Research Division
High-Intensity Accelerator R&D Group
High-Power Target R&D Team

1. Abstract

The subjects of this team cover R&D studies with respect to target technology for the transmutation of the LLFPs.

2. Major Research Subjects

(1) Liquid lithium target for production of neutron or muon
(2) Beam window without solid structure

3. Summary of Research Activity

(1) Liquid lithium target for production of neutron or muon
(H. Okuno, N. Ikoma)
(2) Beam window with solid structure
(H. Imao, N. Ikoma)

Members

Team Leader

Hiroki OKUNO (concurrent: Deputy Group Director, Accelerator Gr.)

Research and Technical Scientist

Kanenobu TANAKA (concurrent: Deputy Group Director, Safety Management Group)
Hiroshi IMAO (concurrent: Senior Research Scientist, Accelerator R&D Team)
Takashi NAGATOMO (concurrent: Technical Scientist, Ion Source Team)

Part-time Worker

Naoya IKOMA

RIBF Research Division
Accelerator Group

1. Abstract

The accelerator group, consisting of seven teams, pursues various upgrade programs of the world-leading heavy-ion accelerator facility, RI-Beam Factory (RIBF), to enhance the accelerator performance and operation efficiency. The programs include the R&D of superconducting ECR ion source, charge stripping systems, beam diagnostic devices, radiofrequency systems, control systems, and beam simulation studies. We are also maintaining the large infrastructure to realize effective operation of the RIBF, and are actively promoting the applications of the facility to a variety of research fields.

Our primary mission is to supply intense, stable heavy-ion beams for the users through effective operation, maintenance, and upgrade of the RIBF accelerators and related infrastructure. The director members shown below govern the development programs that are not dealt with by a single group, such as intensity upgrade and effective operation. We also promote the future plans of the RIBF accelerators along with other laboratories belonging to the RIBF research division.

2. Major Research Subjects

(1) Intensity upgrade of RIBF accelerators (Okuno)
(2) Effective and stable operation of RIBF accelerators (Fukunishi)
(3) Operation and maintenance of infrastructures for RIBF (Kase)
(4) Promotion of the future plan (Kamigaito, Fukunishi, Okuno)

3. Summary of Activity

(1) The maximum intensity of the calcium beam reached 738 pnA at 345 MeV/u, which corresponds to 12.2 kW.
(2) The maximum intensity of the xenon beams reached 102 pnA at 345 MeV/u.
(3) The overall beam availability for the RIBF experiments has been kept above 90 % since 2014.
(4) The large infrastructure was properly maintained based on a well-organized cooperation among the related sections.
(5) An intensity-upgrade plan of the RIBF has been further investigated in coorperation with the experimental groups.

Members

Group Director
Osamu KAMIGAITO

Deputy Group Directors
Hiroki OKUNO (Intensity upgrade)
Nobuhisa FUKUNISHI (Stable and efficient operation)
Masayuki KASE (Energy-efficiency management)

Research Consultant
Tadashi FUJINAWA

Visiting Researchers
Akira GOTO (Yamagata Univ.)
Toshiyuki HATTORI (TIT)
Kensei UMEMORI (KEK)
Hirotaka NAKAI (KEK)
Eiji KAKO (KEK)

Assistant
Karen SAKUMA

RIBF Research Division
Accelerator Group
Accelerator R&D Team

1. Abstract

We are developing the key hardware in upgrading the RIBF accelerator complex. Our primary focus and research is charge stripper which plays an essential role in the RIBF accelerator complex. Charge strippers remove many electrons in ions and realize efficient acceleration of heavy ions by greatly enhancing charge state. The intensity of uranium beams is limited by the lifetime of the carbon foil stripper conventionally installed in the acceleration chain. The improvement of stripper lifetimes is essential to increase beam power towards the final goal of RIBF in the future. We are developing the low-Z gas stripper. In general gas stripper is free from the lifetime related problems but gives low equilibrium charge state because of the lack of density effect. Low-Z gas stripper, however, can give as high equilibrium charge state as that in carbon foil because of the suppression of the electron capture process. Another our focus is the upgrade of the world's first superconducting ring cyclotron.

2. Major Research Subjects

(1) Development of charge strippers for high power beams (foil, low-Z gas)
(2) Upgrade of the superconducting ring cyclotron
(3) Maintenance and R&D of the electrostatic deflection/inflection channels for the beam extraction/injection

3. Summary of Research Activity

(1) Development of charge strippers for high power beams (foil, low-Z gas)

(Hasebe, H., Imao, H. Okuno., H.)

We are developing the charge strippers for high intensity heavy ion beams. We are focusing on the developments on carbon or berrilium foils and gas strippers including He gas stripper.

(2) Upgrade of the superconducting ring cyclotron

(Ohnishi, J., Okuno, H.)

We are focusing on the upgrade of the superconducting ring cyclotron.

(3) Maintenance and R&D of the electrostatic deflection/inflection channels for the beam extraction/injection

(Ohnishi, J., Okuno, H.)

We are developing high-performance electrostatic channels for high power beam injection and extraction.

Members

Team Leader

Hiroki OKUNO (concurrent: Deputy Group Director, Accelerator Gr.)

Research & Technical Scientists

Hiroshi IMAO (Senior Research Scientist)
Jun-ichi OHNISHI (Senior Technical Scientist)

Nishina Center Technical Scientist

Hiroo HASEBE

Visiting Scientists

Andreas ADELMANN (PSI)
Noriyosu HAYASHIZAKI (TIT.)
Hironori KUBOKI (KEK)

Junior Research Associate

Naoya IKOMA (Nagaoka Univ. of Technology)

List of Publications & Presentations

Publications

[Journal]

(Original Papers) *Subject to Peer Review

H. Hasebe, H. Okuno, H. Kuboki, H. Imao, N. Fukunishi, M. Kase, O. Kamigaito, “Development of rotating beryllium disk stripper”, Journal of .Radioanalytical and Nuclear Chemistry, 305, 825 (2015).

[Proceedings]

(Original Papers) *Subject to Peer Review

H. Hasebe, H. Okuno, H. Kuboki, H. Imao, N. Fukunishi, M. Kase, O. Kamigaito, “History of Solid Disk Improvement for Rotating Charge Stripper”, Proceeding of HIAT2015, Yokohama, Japan (2015) MOA1C01.

Oral Presentations

[International Conference etc.]

H. Hasebe, H. Okuno, H. Kuboki, H. Imao, N. Fukunishi, M. Kase, O. Kamigaito, “History of Solid Disk Improvement for Rotating Charge Stripper”, HIAT2015, Yokohama, Japan (2015) MOA1C01.

Posters Presentations

[International Conference etc.]

H. Imao, H. Kuboki, H. Hasebe, O. Kamigaito, M. Kase, H. Okuno, “Operation of Gas Strippers at RIBF ; Thining Effect of High-Intensity Very Heavy Ion Beams“ , HIAT2015, Yokohama, Japan (2015) MOPA32.

RIBF Research Division
Accelerator Group
Ion Source Team

1. Abstract

Our aim is to operate and develop the ECR ion sources for the accelerator-complex system of the RI Beam Factory. We focus on further upgrading the performance of the RI Beam Factory through the design and fabrication of a superconducting ECR ion source for production of high-intensity heavy ions.

2. Major Research Subjects

(1) Operation and development of the ECR ion sources
(2) Development of a superconducting ECR heavy-ion source for production of high-intensity heavy ion beams

3. Summary of Research Activity

(1) Operation and development of ECR ion sources

(T. Nakagawa, M. Kidera, Y. Higurashi, T. Nagatomo, and H. Haba)

We routinely produce and supply various kinds of heavy ions such as zinc and calcium ions for the super-heavy element search experiment as well as uranium ions for RIBF experiments. We also perform R&D's to meet the requirements for stable supply of high-intensity heavy ion beams.

(2) Development of a superconducting ECR ion source for use in production of a high-intensity heavy ion beam

(T. Nakagawa, J. Ohnishi, M. Kidera, Y. Higurashi, and T. Nagatomo)

The RIBF is required to supply heavy ion beams with very high intensity so as to produce RI's and for super-heavy element search experiment. We have designed and are fabricating an ECR ion source with high magnetic field and high microwave- frequency, since the existing ECR ion sources have their limits in beam intensity. The coils of this ion source are designed to be superconducting for the production of high magnetic field. We are also designing the low-energy beam transport line of the superconducting ECR ion source.

Members

Team Leader
Takahide NAKAGAWA

Research & Technical Scientist
Takashi NAGATOMO (Technical Scientist)

Nishina Center Research Scientists
Masanori KIDERA, Yoshihide HIGURASHI

Special Postdoctoral Researcher
Tatsuya URABE (Apr. 1, 2014 –)

List of Publications & Presentations

Publications

[Proceedings]
(Original Papers) *Subject to Peer Review

A.Uchiyama, K. Ozeki, Y. Higurashi, M. Kidera, M. Komiyama, and T. Nakagawa, 'Control system renewal for efficient operation in RIKEN 18 GHz electron cyclotron resonance ion source', Rev. Sci. Instrum. 87(2016)02A722*

J. Ohnishi, Y. Higurashi, T. Nakagawa, 'Progress in high-temperature oven development for 28 GHz electron cyclotron resonance ion source', Rev. Sci. Instrum. 87(2016)02A709*

Oral Presentations

[International Conference etc.]

T. Nakagawa, 'Optimization of Magnetic Field Distribution of RIKEN 28 GHz SC-ECRIS for Intense Beam Production', ECRIS2016, Aug.28–Sept 2, 2016, Busan, Korea

Y. Higurashi, 'Recent development of RIKEN 28GHz ECRIS', ECRIS2016, Aug.28–Sept 2, 2016, Busan, Korea

Posters Presentations

[International Conference etc.]

T. Nagatomo, 'Transverse Four-Dimension Phase-Space Distribution Measured by the Pepper-Pot Type Emittance Meter', ECRIS2016, Aug.28–Sept. 2, 2016, Busan, Korea

RIBF Research Division
Accelerator Group
RILAC Team

1. Abstract

The operation and maintenance of the RIKEN Heavy-ion Linac (RILAC) have been carried out. There are two operation modes: one is the stand-alone mode operation and the other is the injection mode operation. The RILAC has been used especially as an injector for the RIKEN RI- Beam Factory accelerator complex. The RILAC is composed of the ECR ion source, the frequency-variable RFQ linac, six frequency-variable main linac cavities, and six energy booster cavities (CSM).

2. Major Research Subjects

(1) The long term high stability of the RILAC operation.
(2) Improvement of high efficiency of the RILAC operation.

3. Summary of Research Activity

The RILAC was started to supply ion beams for experiments in 1981. Thousands hours are spent in a year for delivering many kinds of heavy-ion beams to various experiments.

The RILAC has two operation modes: one is the stand-alone mode operation delivering low-energy beams directly to experiments and the other is the injection mode operation injecting beams into the RRC. In the first mode, the RILAC supplies a very important beam to the nuclear physics experiment of “the research of super heavy elements”. In the second mode, the RILAC plays a very important role as upstream end of the RIBF accelerator complex.

The maintenance of these devices is extremely important in order to keep the log-term high stability and high efficiency of the RILAC beams. Therefore, improvements are always carried out for the purpose of more stable and more efficient operation.

Members

Team Leader
Eiji IKEZAWA

Research & Technical Scientist
Yutaka WATANABE (Senior Technical Scientist)

Research Consultants
Masatake HEMMI
Toshiya CHIBA

RIBF Research Division
Accelerator Group
Cyclotron Team

1. Abstract

Together with other teams of Nishina Center accelerator division, maintaining and improving the RIBF cyclotron complex. The accelerator provides high intensity heavy ions. Our mission is to have stable operation of cyclotrons for high power beam operation. Recently stabilization of the rf system is a key issue to provide 10 kW heavy ion beam.

2. Major Research Subjects

(1) RF technology for Cyclotrons
(2) Operation of RIBF cyclotron complex
(3) Maintenance and improvement of RIBF cyclotrons
(4) Single turn operation for polarized deuteron beams
(5) Development of superconducting cavity

3. Summary of Research Activity

・Development of the rf system for a reliable operation
・Development of highly stabilized low level rf system
・Development of superconducting rebuncher cavity
・Development of the intermediate-energy polarized deuteron beams.

Members

Team Leader
Naruhiko SAKAMOTO

Research & Technical Scientist
Kazutaka OZEKI (Technical Scientist)

Nishina Center Research Scientist
Kenji SUDA

List of Publications & Presentations

Publications

[Proceedings]

K. Yadomi, S. Fukuzawa, M. Hamanaka, S. Ishikawa, K. Kobayashi, R. Koyama, T. Nakamura, M. Nishida, M. Nishimura, J. Shibata, N. Tsukiori, K. Suda, T. Dantsuka, M. Fujimaki, T. Fujinawa, N. Fukunishi, H. Hasebe, Y. Higurashi, E. Ikezawa, H. Imao, M. Kase, O. Kamigaito, M. Kidera, M. Komiyama, K. Kumagai, T. Maie, M. Nagase, T. Nagatomo, T. Nakagawa, M. Nakamura, J. Ohnishi, H. Okuno, K. Ozeki, N. Sakamoto, A. Uchiyama, S. Watanabe, T. Watanabe, Y. Watanabe, K. Yamada, H. Yamasawa, “Status report of the operation of the RIBF ring cyclotrons”, Proceedings of the 13th annual meeting of Particle Accelerator Society of Japan, Chiba (2016) p1339.

S. Ishikawa, K. Kobayashi, R. Koyama, J. Shibata, N. Tsukiori, T. Nakamura, M. Nishida, M. Nishimura, M. Hamanaka, S. Fukuzawa, K. Yadomi, A. Uchiyama, K. Ozeki, J. Ohnishi, H. Okuno, M. Kase, O. Kamigaito, K. Kumagai, M. Komiyama, N. Sakamoto, K. Suda, T. Nakagawa, M. Nagase, T. Nagatomo, N. Fukunishi, M. Fujimaki, T. Maie, K. Yamada, T. Watanabe, Y. Watanabe, Y. Ohshiro, Y. Kotaka, S. Yamaka, “Status report on operation of RIKEN AVF cyclotron”, Proceedings of the 13th annual meeting of Particle Accelerator Society of Japan, Chiba (2016) p1344.

Posters Presentations

[Domestic Conference]

K. Yadomi, S. Fukuzawa, M. Hamanaka, S. Ishikawa, K. Kobayashi, R. Koyama, T. Nakamura, M. Nishida, M. Nishimura, J. Shibata, N. Tsukiori, K. Suda, T. Dantsuka, M. Fujimaki, T. Fujinawa, N. Fukunishi, H. Hasebe, Y. Higurashi, E. Ikezawa, H. Imao, M. Kase, O. Kamigaito, M. Kidera, M. Komiyama, K. Kumagai, T. Maie, M. Nagase, T. Nagatomo, T. Nakagawa, M. Nakamura, J. Ohnishi, H. Okuno, K. Ozeki, N. Sakamoto, A. Uchiyama, S. Watanabe, T. Watanabe, Y. Watanabe, K. Yamada, H. Yamasawa, “Status report of the operation of the RIBF ring cyclotrons”, Proceedings of the 13th annual meeting of Particle Accelerator Society of Japan, Chiba (2016) FSP008.

S. Ishikawa, K. Kobayashi, R. Koyama, J. Shibata, N. Tsukiori, T. Nakamura, M. Nishida, M. Nishimura, M. Hamanaka, S. Fukuzawa, K. Yadomi, A. Uchiyama, K. Ozeki, J. Ohnishi, H. Okuno, M. Kase, O. Kamigaito, K. Kumagai, M. Komiyama, N. Sakamoto, K. Suda, T. Nakagawa, M. Nagase, T. Nagatomo, N. Fukunishi, M. Fujimaki, T. Maie, K. Yamada, T. Watanabe, Y. Watanabe, Y. Ohshiro, Y. Kotaka, S. Yamaka, “Status report on operation of RIKEN AVF cyclotron”, Proceedings of the 13th annual meeting of Particle Accelerator Society of Japan, Chiba (2016) FSP009.

RIBF Research Division
Accelerator Group
Beam Dynamics & Diagnostics Team

1. Abstract

The cascaded cyclotron system at RIKEN RI Beam Factory (RIBF) requires not only strict matching of operation parameters but also high stability of all the accelerator components in order to establish stable operation of the world's most intense heavy-ion beams. Beam Dynamics and Diagnostics Team is responsible for power supplies, beam instrumentation, computer control and beam dynamic of the RIBF accelerator complex and strongly contributes to the performance upgrade of the RIBF.

2. Major Research Subjects

(1) Extracting the best performance of the RIBF accelerator complex based on the precise beam dynamics study.
(2) Maintenance and developments of the beam instrumentation, especially non-destructive monitors.
(3) Upgrade of the computer control system of the RIBF accelerator complex.
(4) Maintenance and improvements of the magnets and power supplies.
(5) Upgrade of the existing beam interlock system for higher intensity beams.

3. Summary of Research Activity

(1) High-intensity heavy-ion beams including 55-pnA uranium, 102-pnA xenon, 486-pnA krypton, and 740-pnA calcium beams have been obtained.
(2) The world-first high-Tc SQUID beam current monitor has been developed.
(3) The bending power of the fixed-frequency Ring Cyclotron has been upgraded to 700 MeV. It enables us to accelerate $^{238}U^{64+}$ ions obtained by the helium gas stripper.
(4) An EPICS-based control system and a homemade beam interlock system have been stably operated. Replacements of the existing legacy control system used in the old half of our facility is ongoing. Construction of the new control system for the new injector RILAC2 was successfully completed, where the embedded EPICS system running on F3RP61-2L CPU module, developed by KEK and RIKEN control group, was used.
(5) We replaced some dated power supplies of RIKEN Ring Cyclotron by new ones, which have better long-term stability than the old ones. The other existing power supplies (~900) are stably operated owing to elaborate maintenance work.
(6) We have contributed to RILAC2 construction, especially in its beam diagnosis, control system, magnet power supplies, vacuum system, high-energy beam transport system etc.

Members

Team Leader
Nobuhisa FUKUNISHI (concurrent; Deputy Group Director, Accelerator Gr.)

Research & Technical Scientists
Masaki FUJIMAKI (Senior Technical Scientist)
Keiko KUMAGAI (Senior Technical Scientist)
Tamaki WATANABE (Senior Technical Scientist)
Kazunari YAMADA (Senior Technical Scientist)

Nishina Center Technical Scientists
Misaki KOMIYAMA
Akito UCHIYAMA

Special Postdoctoral Researcher

Part-time Workers
Makoto NAGASE

Visiting Scientists
Kenichi ISHIKAWA (Univ. of Tokyo)
Shin-ichiro HAYASHI (Hiroshima Int'l Univ.)
Hiromichi RYUTO (Kyoto Univ.)
Takuya MAEYAMA (Kitasato Univ.)

Visiting Technician
Jun-ichi ODAGIRI (KEK)

List of Publications & Presentations

Publications

[Journal]

(Original Papers) *Subject to Peer Review

Maeyama T., Fukunishi N., Ishikawa K.L., Furuta T., Fukasaku K., and Fukuda S., "Radiological properties of nanocomposite Fricke gel dosimeters for heavy ion beams", Journal of Radiation Research **57**, pp. 318–324 (2016)*.

Uchiyama A., Ozeki K., Higurashi Y., Kidera M., Komiyama M., and Nakagawa T., "Control System Renewal for Efficient Operation in RIKEN 18 GHz Electron Cyclotron Resonance Ion Sourve", Rev. Sci. Instrum. **87**, 02A722 (2016)*.

Posters Presentations

[International Conference etc.]

Komiyama M., Fukunishi N., Uchiyama A., "Recent Improvements to the RI Beam Factory Control System", The 11th International Workshop on Personal Computers and Particle Accelerator Controls (PCaPAC2016), Campinas, Brazil, October 2016, WEPOPRPO11 (2016).

Uchiyama A., Komiyama M., Fujimaki M., Fukunishi N., "Integration of Standalone Control Systems into EPICS-based System at RIKEN RIBF", The 11th International Workshop on Personal Computers and Particle Accelerator Controls (PCaPAC2016), Campinas, Brazil, October 2016, WEPOPRPO12 (2016).

[Domestic Conference]

Watanabe T., Fukunishi N., Inamori S., Kon K., "Sensitivity Improvement and Miniaturization of HTc-SQUID Beam Current Monitor", 13th Annual Meeting of Particle Accelerator Society of Japan, August 2016, Chiba, Japan, pp. 1127-1133 (2016).

Uchiyama A., Komiyama M., "An Attempt to Implement the Alive Monitoring System for Reliable EPICS-based Control System", 13th Annual Meeting of Particle Accelerator Society of Japan, August 2016, Chiba, Japan, pp. 664-667 (2016).

Nishimura M., Uchiyama A., Ohshiro Y., "Upgrade of HyperECR Ion Source Control System for System Integration at RIBF", 13th Annual Meeting of Particle Accelerator Society of Japan, August 2016, Chiba, Japan, pp. 660-663 (2016).

RIBF Research Division
Accelerator Group
Cryogenic Technology Team

1. Abstract

We are operating the cryogenic system for the superconducting ring cyclotron in RIBF. We are operating the helium cryogenic system in the south area of RIKEN Wako campus and delivering the liquid helium to users in RIKEN. We are trying to collect efficiently gas helium after usage of liquid helium.

2. Major Research Subjects

(1) Operation of the cryogenic system for the superconducting ring cyclotron in RIBF
(2) Operation of the helium cryogenic plant in the south area of Wako campus and delivering the liquid helium to users in Wako campus.

3. Summary of Research Activity

(1) Operation of the cryogenic system for the superconducting ring cyclotron in RIBF
(Okuno, H., Dantsuka, T., Nakamura, M., Maie, T.)
(2) Operation of the helium cryogenic plant in the south area of Wako campus and delivering the liquid helium to users in Wako campus.
(Dantsuka, T., Tsuruma, S., Okuno, H.).

Members

Team Leader
Hiroki OKUNO (concurrent: Deputy Group Director, Accelerator Gr.)

Research & Technical Scientist
Masato NAKAMURA (Senior Technical Scientist)

Nishina Center Technical Scientist
Takeshi MAIE

Technical Staff I
Tomoyuki DANTSUKA

Part-time Worker
Shizuho TSURUMA

RIBF Research Division
Accelerator Group
Infrastructure Management Team

1. Abstract

The RIBF facility is consisting of many accelerators and its infrastructure is very important in order to make an efficient operation of RIBF project. We are maintaining the infrastructure of the whole system and to support the accelerator operation with high performance. We are also concerning the contracts of gas- and electricity-supply companies according to the annual operation plan. The contracts should be reasonable and also flexible against a possible change of operations. And we are searching the sources of inefficiency in the operation and trying to solve them for the high-stable machine operation.

2. Major Research Subjects

(1) Operation and maintenance of infrastructure for RIBF accelerators.
(2) Renewal of the old equipment for the efficient operation.
(3) Support of accelerator operations.

Members

Team Leader
Masayuki KASE (concurrent; Deputy Group Director, Accelerator Gr.)

Research & Technical Scientists
Shu WATANABE (Senior Technical Scientist)

Research Consultant
Hideyuki YAMASAWA

Visiting Scientist
Hideshi MUTO (Tokyo Univ. of Sci. Suwa)

RIBF Research Division
Instrumentation Development Group

1. Abstract

This group develops core experimental installations at the RI Beam factory. They are a slow-RI beam facility (SLOWRI), and highly program specific facilities of SCRIT and Rare-RI Ring (R3). All were designed to maximize the research potential of the world's most intense RI beams, made possible by the exclusive equipment available at the RI Beam Factory. While SLOWRI is under preparation for commissioning, physics experiments conducted in storage rings have been just started at SCRIT and R3 facilities. Beam manipulation techniques, such as a beam accumulation and a beam cooling, will be able to provide opportunities of new experimental challenges and the foundation for future developments of RIBF.

2. Major Research Subjects

(1) SCRIT Project
(2) SLOWRI Project
(3) Rear RI Ring Project

3. Summary of Research Activity

We are developing beam manipulation technology in carrying out above listed project. They are the high-quality slow RI beam production (SCRIT and SLOWRI), the beam cooling and stopping (SCRIT and SLOWRI), and the beam accumulation technology (SCRIT and R3). The technological knowhow accumulated in our projects will play a significant role in the next generation RIBF. Status and future plan for each project is described in subsections. SCRIT is now under test experimental phase in which the angular distribution of scattered electrons from ^{132}Xe isotopes has been successfully measured and the nuclear charge density distribution has been obtained. Electron scattering off unstable nuclei is now under preparation for the first experiment in 2017. Rare RI Ring was commissioned in three-times machine-study experiments, and we have demonstrated that the ring has an ability for precision mass measurement with the accuracy of the order of 10 ppm. We will be able to try to measure masses of nuclei $^{74-78}$Ni in 2017-2018 and continuously make improvement in the accuracy. Construction of the SLOWRI system has been almost completed in 2014. PALIS device was commissioned in 2015 and 2016, and basic functions such as the RI-beam stopping in argon gas cell and the extraction with the gas flow were confirmed. Other devices are now under setting up for the first commissioning.

Members

Group Director
Masanori WAKASUGI

Visiting Scientist
Akira OZAWA (Univ. of Tsukuba)

Student Trainees
Mitsuki HORI (Rikkyo Univ.)
Nobuaki UCHIDA (Rikkyo Univ.)
Shin-nosuke SASAMURA (Rikkyo Univ.)

List of Publications & Presentations

Publications and presentations for each project team are listed in subsections.

RIBF Research Division
Instrumentation Development Group
SLOWRI Team

1. Abstract

SLOWRI is a universal low-energy RI-beam facility at RIBF that provides a wide variety of short-lived nuclei as high-purity and low-emittance ion beams or stored ions in a trap, including a parasitic operation mode. The SLOWRI team develops and manages the facility and performs high-precision spectroscopy experiments. The construction of the SLOWRI facility began in FY2013 and commissioning work has been ongoing. Two major online prototype setups have been successfully tested. The first was a large room-temperature gas cell with RF-carpet structure. With this setup, the hyperfine structure constants of all odd Be isotopes were precisely measured by laser-microwave double resonance spectroscopy of trapped Be ions, followed by the first online mass measurement with a multi-reflection time-of-flight mass spectrograph (MRTOF) performed on $^{8}Li^{+}$ ions. The second prototype is a medium-sized cryogenic RF-carpet gas cell for the SHE-Mass project that aims to measure masses of trans-uranium elements at the GARIS-II facility. This prototype showed that a traveling-wave RF-carpet works fine and the cryogenic gas cell dominantly provides doubly charged ions even for Fr isotopes.

2. Major Research Subjects

(1) Construction of stopped and low-energy RI-beam facility, SLOWRI.
(2) Laser spectroscopy of trapped radioactive beryllium isotopes.
(3) Development of a multi-reflection time-of-flight mass spectrograph for precision mass measurements of short-lived nuclei.
(4) Development of collinear laser spectroscopy apparatus.
(5) Development of parasitic slow RI-beam production method using resonance laser ionization.

3. Summary of Research Activity

(1) Construction of stopped and low-energy RI-beam facility (SLOWRI)

Installation of SLOWRI began in FY2013. It consists of two gas catchers (RF Carpet gas cell and PALIS gas cell), magnetic mass separators, a 50-m beam transport line, a beam cooler-buncher, an isobar separator, and a laser system. The RF Carpet gas cell will be installed at the exit of the D5 dipole magnet of BigRIPS. This gas catcher comprises a large cryogenic He gas cell with a large traveling wave rf-carpet. It will convert main beams of BigRIPS to low-energy, low-emittance beams without any restrictions from the chemical properties of the elements. The PALIS gas cell will be installed in the vicinity of the second focal plane slit of BigRIPS. It will provide parasitic RI-beams from the ions normally lost in the slits during other experiments. In this gas catcher, thermalized RI quickly become neutralized and will be selectively re-ionized by resonant laser radiations. These gas catchers have been tested off-line. The 50 m beam transport line consists of four dipole magnets (SD1 to SD4), two focal plane chambers, 62 electrostatic quadrupole singlets, 11 electrostatic quadrupole quartets (EQQ1 to EQQ11) and 7 beam profile monitors (BPM). SD1 and SD2, located right after the gas catchers, will be used for isotope separation. After eliminating contaminant ions at the focal plane chamber, the low energy beam will be transported by a FODO lattice structure with phase space matching using EQQs. The EQQs have multipole elements made of 16 rods on which various potentials can be applied to produce 6-pole and 8-pole fields simultaneously, to compensate ion optical aberrations. This multipole element can also produce dipole fields for steering and scanning the beam. The BPM have a classical cross-wire beam monitor as well as a channel electron multiplier with a pinhole collimator. Combining the scanning capability of the EQQs and the pinhole detector, we can observe a beam profile even for a very low-intensity RI-beams. Off- and on-line commissioning is underway.

Based on test experiments with the prototype setups, the large RF-carpet gas cell contains a three stage rf-carpet structure: a gutter rf carpet for collection of thermal ions in the cell into a small slit, a narrow (≈10 mm) traveling-wave rf-carpet for collection of ions from the gutter carpet and for transporting the ions toward the exit, and a small rf carpet for extraction from the gas cell. An offline test of the gutter structure has shown a high collection efficiency of ions in the gas cell.

(2) Laser spectroscopy of trapped radioactive beryllium isotope ions

As a first application of the prototype SLOWRI setup, we applied hyperfine structure spectroscopy to the beryllium isotopes to determine, in particular, the anomalous radius of the valence neutron of the neutron halo nucleus ^{11}Be, and to determine the charge radii of these beryllium isotopes through laser-laser double resonance spectroscopy of laser-cooled ions. Laser cooling is an essential prerequisite for these planned experiments. The first laser spectroscopy experiments for beryllium isotopes were performed to measure the resonance frequencies of the 2s $^{2}S_{1/2}$ - 2p $^{2}P_{3/2}$ transition in ^{7}Be+, ^{9}Be+, $^{10}Be^{+}$ and ^{10}Be+ ions and the nuclear charge radii of these isotopes were determined. The hyperfine structures of $^{11}Be^{+}$ and $^{7}Be^{+}$ ions were also performed using the laser-microwave double resonance spectroscopy and the magnetic hyperfine constants of $^{7}Be^{+}$ and $^{11}Be^{+}$ ions were determined with accuracies of better than 10^{-7}. A new combined-trap setup for high-precision determination of nuclear g-factors of the odd Be isotopes using a superconducting Helmholtz magnet is under preparation at the SLOWRI experimental area in collaboration with Ueno nuclear spectroscopy laboratory.

(3) Development of a multi-reflection TOF mass spectrograph for short-lived nuclei

The atomic mass is one of the most important quantities of a nucleus and has been studied by various methods since the early days of modern physics. From among many methods we have chosen a multi-reflection time-of-flight (MR-TOF) mass spectrometer. Slow RI beams extracted from the RF ion-guide are bunched and injected into the spectrometer with a repetition rate of ~100 Hz. The spectrometer consists of two electrostatic mirrors between which the ions travel back and forth repeatedly. These mirrors are designed such that energy-isochrononicity in the flight time is guaranteed during the multiple reflections while the flight time varies with the masses of ions. A

mass-resolving power of 170,000 has been obtained within a 2 ms flight time for the $^{40}K^{+}$ and $^{40}Ca^{+}$ isobaric doublet. This mass-resolving power should allow determination of ion masses with an accuracy of $\leq 10^{-7}$. An online mass measurement for the radioactive isotope ^{8}Li has been carried out at the prototype SLOWRI setup.

The MR-TOF mass spectrograph has been placed under the GARIS-II separator with the goal of direct mass measurements of trans-uranium elements. A cryogenic gas catcher cell was placed at the focal plane box of GARIS-II and bunched low-energy heavy ion beams were transported to the trap of MR-TOF. In online commissioning experiments using No isotopes, more than 30% extraction efficiency from the cryogenic gas cell was achieved. In FY2016, mass measurements of more than 80 nuclides, including short-lived ($T_{1/2}$ =10 ms) isotopes of Ra and several isotopes of the trans-uranium elements Fm, Es, No and Md were performed at GARIS-II in collaboration with the KEK Wako Nuclear Science Center and the Super Heavy Element Synthesis team of RIKEN. The highest precisions, achieved for Ga isotopes, reached a level of 0.03 ppm. For most of the well-known nuclides, agreement with the literature mass values was found. However, discrepancies were found in some literature values derived from pre-1980 indirect measurements. This suggests that such indirect measurements must be revised with comprehensive direct mass measurements. The masses of four isotopes of Es and Md were measured for the first time, allowing for confirmation of the N = 152 shell closure in Md. Using these new mass data as anchor-points, the masses of seven isotopes of super-heavy elements up to Mt were indirectly determined and comparisons with various nuclear mass models were performed.

(4) Development of collinear fast beam apparatus for nuclear charge radii measurements

The root-mean-square charge radii of unstable nuclei have been determined exclusively by isotope shift measurements of the optical transitions of singly-charged ions or neutral atoms by laser spectroscopy. Many isotopes of alkali, alkali-earth, and noble-gas elements in addition to several other elements have been measured by collinear laser spectroscopy since these ions all have good optical transitions and are available at conventional ISOL facilities. However, isotopes of other elements, especially refractory and short-lived ones, have not been investigated so far.

In SLOWRI, isotopes of all atomic elements will be provided as well collimated, mono-energetic ion beams. This should expand the range of nuclides available for laser spectroscopy. In the first years of the RIBF project, elements in the vicinity of Ni, such as Ni, Co, Fe, Cr, Cu, Ga, and Ge are planned to be investigated. They all have possible optical transitions in the ground states of neutral atoms with presently available laser systems. Some of them have so called recycling transitions, which enhance the detection probabilities noticeably. Also, the multistep resonance ionization (RIS) method can be applied to the isotopes of Ni as well as those of some other elements. The required minimum intensity for this method can be as low as 10 atoms per second.

An off-line mass separator and a collinear fast beam apparatus with a large solid-angle fluorescence detector was built previously. A 617 nm transition of the metastable Ar+ ion at 20 keV was measured with both collinear and anti-collinear geometry that allowed determination of the absolute resonant frequency of the transition at rest with a relative accuracy of more than 10^{-8}. A new setup is under preparation at the SLOWRI experiment area in collaboration with the Ueno nuclear spectroscopy laboratory.

(5) Development of parasitic slow RI-beam production scheme using resonance laser ionization

More than 99.9% of RI ions produced in projectile fission or fragmentation are simply dumped in the first dipole magnet and the slits. A new scheme, named PALIS, meant to rescue such precious RI using a compact gas catcher cell and resonance laser ionization, was proposed as a part of SLOWRI. The thermalized RI ions in a gas cell filled with Ar gas can be quickly neutralized and transported to the exit of the cell by gas flow. Irradiation of resonance lasers at the exit ionizes neutral RI atoms efficiently and selectively. The ionized RI ions can be further selected by a magnetic mass separator and transported to the SLOWRI experimental area for various experiments. The resonance ionization scheme itself can also be a useful method to perform hyperfine structure spectroscopy of RI of many elements.

A prototype setup has been used to test resonance ionization schemes of several elements, extraction from the cell, and transport to a high-vacuum chamber. An online setup was fabricated in FY2013 and the first online commissioning took place in FY2015. It was confirmed that the PALIS gas cell is not deleterious for BigRIPS experiments, and a reasonable amount of radioactive Cu isotopes were extracted from the cell by gas flow. Mechanical problems discovered in the commissioning have been solved by modification of the gas cell, bellows structure, and laser path. Next online commissioning is scheduled in October 2017.

Members

Team Leader
Michiharu WADA

Research & Technical Scientist
Takao KOJIMA (Senior Research Scientist)
Aiko TAKAMINE (concurrent; UENO laboratory)

Nishina Center Research Scientists
Tetsu SONODA
Kensuke KUSAKA (concurrent; BigRIPS Team)

Nishina Center Technical Scientist
Takeshi MAIE (concurrent; Cryogenic Technology Team)

Special Postdoctoral Researcher
Yuta ITO

Part-time Workers
Shigeaki ARAI
Sota KIMURA
Ichiro KATAYAMA

Visiting Researcher
Mikael REPONEN (JSPS)

Visiting Scientists
Hans A SCHUESSLER (Texas A&M Univ.)
Hermann WOLLNIK (Univ. of Giessen)
Hideki IIMURA (JAEA)
Hideki TOMITA (Nagoya Univ.)
Klaus WENDT (Johannes Gutenberg Univ. Mainz)
Kunihiro OKADA (Sophia Univ.)
Volker SONNENSCHEIN (Nagoya Univ.)

Student Trainees
Naoki KIMURA (Sophia Univ.)
Takuma NOTO (Nagoya Univ.)
Yoshitaka ADACHI (Nagoya Univ.)
Takahide TAKAMATSU (Nagoya Univ.)
Daiki MATSUI (Nagoya Univ.)

List of Publications & Presentations

Publications

[Journal]

(Original Papers) *Subject to Peer Review

P. Schury, M. Wada, Y. Ito, D. Kaji, F. Arai, M. MacC ormick, I. Murray, H. Haba, S. Jeong, S. Kimura, H. Koura, H. Miyatake, K. Morimoto, K. Morita, A. Ozawa, M. Rosenbusch, M. Reponen, P.-A. Söderström, A. Takamine, T. Tanaka, H. Wollnik, “First online multireflection time-of-flight mass measurements of isomer chains produced by fusion-evaporation reactions: Toward identification of superheavy elements via mass spectroscopy”, Physical Review C 95, 011305(R) (2017)*

T. Sonoda, T.Tsubota, M. Wada, I. Katayama, T.M. Kojima, M. Reponen, « A gas circulation and purification system for gas-cell-based low-energy RI-beam production », Review of Scientific Instruments, 87 (2016) 065104.*

A Hamaker, M. Brodeur, J.M. Kelly, J. Long, C. Nicoloff, S. Syan, B.E. Schult, P. Schury, M. Wada, «Experimental investigation of the repelling force from RF carpets », International Journal Mass Spectrometry, 404 (2016) 14-19.*

[Proceedings]

(Original Papers) *Subject to Peer Review

A. Takamine, M. Wada, K. Okada, Y. Ito, P. Schury, F. Arai, I. Katayama, K. Imamura, Y. Ichikawa, H. Ueno, H. Wollnik, H.A. Schuessler, « Towards high precision measurements of nuclear g-factors for the Be isotopes », Nucl. Inst. Meth. B376 (2016) 307-310. *

Y. Hirayama, Y.X. Watanabe, N. Imai, H. Ishiyama, S.C. Jeong, H.S. Jung, H. Miyatake, M. Oyaizu, S. Kimura, M. Mukai, Y.H. Kim, T. Sonoda, M. Wada, M. Huyse, Yu. Kudryavtsev,P. van Duppen, « On-line experimental results of an argon gas cell-based laser ion source (KEK Isotope Separation System) », Nucl. Inst. Meth. B376 (2016) 52-56.*

M. Mukai, Y. Hirayama, H. Ishiyama, H.S. Jung, H. Miyatake, M. Oyaizu, Y.X. Watanabe, S. Kimura, A. Ozawa, S.C. Jeong, T. Sonoda, « Search for efficient laser resonance ionization schemes of tantalum using a newly developed time-of-flight mass spectrometer in KISS », Nucl. Inst. Meth B376 (2016) 73-76.*

S. Kimura, H. Ishiyama, H. Miyatake, Y. Hirayama, Y.X. Watanabe, H.S. Jung, M. Oyaizu, M. Mukai, S.C. Jeong, A. Ozawa, « Development of the detector system for image-decay spectroscopy at the KEK Isotope Sepaator System », Nucl. Inst. Meth. B376 (2016) 338-340.*

Y. Hirayama, H. Miyatake, Y.X. Watanabe, N. Imai, H. Ishiyama, S.C. Jeong, H.S. Jung, M. Oyaizu, M. Mukai, S. Kimura, T. Sonoda, M. Wada, Y.H. Kim, M. Huyse, Yu Kudryavtsev, P. van Duppen, « Deta-decay spectroscopy of r-process nuclei around N=126 », EPJ Web Conf. 109 (2016) 08001, 1-6.*

Oral Presentations

[International Conference etc.]

Y. Ito et al., « First online mass measurements of isobar chains via MRTOF-MS : Toward direct identification of SHE », International Nuclear Physics Conference, Sept. 11-16, 2016, Adelaide, Australia.

P. Schury et al., « Gas Catcher Systems Status: SLOWRI/PALIS, SlowSHE, and KISS”, Fragment Separator Expert Meeting, Aug. 30 – Sept. 2, 2016, Grand Rapids, Michigan, USA.

T. Sonoda et al., “Parasitic low-energy RI-beam production using gas catcher and resonance ionization”, Stopping and Manipulation of Ions and related topics (SMI-2016), June 8-10, 2016, IMP, Lanzhou, China.

[Domestic Conference]

M. Wada, « Possibility of comprehensive mass measurements of heavy elements », Symposium on Perspective of super heavy element science, Mar. 17-20, Osaka, Japan.

M. Wada et al., “High precision nuclear spectroscopy with trapped radioactive ions”, The 2nd Cicily East Asia Workshop on Low-energy Nuclear Physics”, June 26-28, 2016, RIKEN, Japan.

RIBF Research Division
Instrumentation Development Group
Rare RI-ring Team

1. Abstract

Mass measurement is one of the most important contributions to a nuclear property research especially for short-lived unstable nuclei far from the beta-stability line. In particular, a high-precision mass measurement for nuclei located around the r-process pass (rare-RI) is required in nucleosynthesis point of view. We chose a method of isochronous mass spectrometry (IMS) to make a measurement time shorter than 1 ms. Heavy-ion storage ring named "Rare-RI Ring (R3)" has been constructed until end of 2014 and commissioning experiments were successfully performed in 2015. Our target performance in the mass determination is to achieve accuracy of the order of 1 ppm (~100 keV) even if we get only one event. Since an isochronism in R3 is established over a wide range of the momentum, rare-RIs with a large momentum spread, $\Delta p/p=\pm 0.5$ %, are acceptable. Another significant feature of the R3 system is an individual injection scheme in which a produced rare-RI itself triggers the injection kicker. In the first commissioning experiment using primary ^{78}Kr beam, we demonstrated a high ability of R3 as a storage ring and succeed in establishing the individual injection scheme for the first time. In the second experiment using secondary beams of ^{36}Ar and ^{35}Cl, we successfully demonstrated mass determination by measuring revolution time for both isotopes with the accuracy of ~20 ppm. In last year, we performed the third experiment using isotopes around ^{78}Ge. We successfully extracted several kinds of isotopes, ^{79}As, ^{77}Ga, ^{76}Zn, and ^{75}Cu from the R3 in the same setting and established the mass measurement method. We are going to try to measure masses for isotopes around ^{78}Ni region in near future.

2. Major Research Subjects

(1) Developments of heavy-ion storage ring
(2) Precision mass measurement for rarely produced isotopes related to r-process.

3. Summary of Research Activity

Since the lattice design of R3 is based on the cyclotron motion, it can provide an isochronism in a wide range of the momentum. We expect a great improvement in mass resolution in IMS as long as the isochronous field is precisely formed in R3. Therefore, IMS using R3 is capable of both a high-precision measurement and a fast measurement. All the devices in R3 was designed under the assumption that an incoming beam has an energy of less than 200 MeV/u and a charge to mass ratio, m/q, of less than 3. The ring structure was designed with a similar concept of a separate-sector ring cyclotron. It consists of six sectors and 4.02-m straight sections, and each sector consists of four rectangular bending magnets. A radially homogeneous magnetic field is produced in the magnet, and a magnetic rigidity is 6.5 Tm at maximum, for instance, ^{78}Ni with the magnetic rigidity of 5.96 Tm. Two magnets at both ends of each sector are additionally equipped with ten trim coils to form a precise isochronous magnetic field. For $\Delta p=0$ particle, the circumference is 60.35 m and the betatron tunes are $\nu x=1.21$ and $\nu y=0.84$ in horizontal and vertical directions, respectively. The momentum acceptance is $\Delta p/p=\pm 0.5$ %, and the transverse acceptances are 20π mmmrad and 10π mmmrad in horizontal and vertical directions, respectively.

Another performance required for R3 is to efficiently seize hold of an opportunity of the measurement for rare-RIs produced unpredictably. We adopted an individual injection scheme in which the produced rare-RI itself triggers the injection kicker magnets. Full activation of the kicker magnetic field has to be completed within the flight time of the rare-RI from an originating point (F3 focal point in BigRIPS) of the trigger signal to the kicker position in R3. We successfully developed an ultra-fast response kicker system working with the repetition rate of 100 Hz.

Since R3 accumulates, in principle, only single ion, we need high-sensitive beam diagnostic devices in the ring, and they should be applicable even for a single particle circulation. One of them is a cavity type of Schottky pick-up installed for tuning of isochronous field. A resonance frequency is 171 MHz, a measured quality factor is about 1945, and shunt impedance is 190 kΩ. Another is a timing monitor, which detects secondary electrons emitted from thin carbon foil placed on the accumulation orbit. The thickness of the foil will be 50 $\mu g/cm^2$. The rare-RI with the energy of 200 MeV/u survives only for first 100 turns because of an energy loss at the foil.

In 2015, we had two times of commissioning experiments. In the first experiment, we use primary $^{78}Kr^{36+}$ beam with the energy of 168 MeV/u. We succeeded in beam injection particle by particle in individual injection scheme, beam extraction after 700-μs accumulation (~1860 turns), and measurements of the TOF from the injection to the extraction. It was demonstrated that R3 works well as a storage ring and a single particle is certainly manipulated in this storage ring system. The individual injection scheme was established for the first time in the world. In addition, the Schottky pick-up monitored a single $^{78}Kr^{36+}$ particle circulation with the measuring time of less than 10 ms. That demonstrated that our pick-up is world most sensitive non-destructive monitor. In this experiment, we could tune completely the first order isochronism, but higher order components were remained, consequently, the 10-ppm accuracy of the isochronism was obtained. More precise tuning is possible with reference the Schottky data. In the second experiment, we injected two isotopes, ^{36}Ar and ^{35}Cl, selected in the secondary beams into the ring, in which the isochronism is tuned for ^{36}Ar. It was obviously demonstrated that the mass of ^{35}Cl relative to ^{36}Ar is determined by comparing the TOF values for both isotopes, and the accuracy was ~20 ppm, which is one-order less than our target value of a few ppm. We found that the imperfection of isochronism significantly contributes to the time resolution of measured TOF values.

In 2016, we performed the third commissioning experiment using unstable nuclei. In this experiment, the 5-ppm accuracy of isochronism was obtained for the reference isotope ^{78}Ge by adjusting the isochronism up to second order. In addition, we derived the masses of ^{79}As, ^{77}Ga, ^{76}Zn, and ^{75}Cu relative to ^{78}Ge by determining its revolution time with beta correction. We found that not only the imperfection of isochronism but also the insufficient resolution of beta measurement significantly contributes to the mass resolution.

Detailed analysis is ongoing. In next time, we will try to improve the accuracy of isochronism and the beta measurement resolution. We plan to try mass measurements for isotopes related r-process pass around ^{78}Ni region after conducting the forth commissioning experiment.

Members

Team Leader
Masanori WAKASUGI (concurrent; Group Director, Instrumentations Development Gr.)

Nishina Center Research Scientists
Yoshitaka YAMAGUCHI

Nishina Center Technical Scientists
Takeshi MAIE (concurrent; Cryogenic Technology Team)

Contract Researcher
Daisuke NAGAE (Spin-Isospin Lab.)

Special Postdoctoral Researcher
Yasushi ABE

Postdoctoral Researcher
Fumi SUZAKI (Spin-Isospin Lab.)

Research Consultant
Akira NODA

List of Publications & Presentations

Publications

[Journal]

(Review)

Y. Yamaguchi, M. Wakasugi, Y. Abe, F. Suzaki, D. Nagae, S. Omika, H. Miura, S. Naimi, Z. Ge, T. Yamaguchi, A. Ozawa, T. Uesaka, J. Ohnishi, T. Kikuchi, M. Komiyama, K. Kumagai, A. Tokuchi, T. Fujinawa, T. Maie, H. Yamasawa, Y. Yanagisawa, T. Watanabe, Y. Watanabe, and Y. Yano, “Construction of the rare-RI ring at RIKEN RI Beam” , Journal of Particle Accelerator of Japan, Vol.12, No.3, 132-141 (2015).

[Proceedings]

(Original Papers) *Subject to Peer Review

S. Suzuki, A. Ozawa, T. Moriguchi, Y. Ichikawa, M. Amano, D. Kamioka, Y. Tajiri, K. Hiraishi, T. Matsumoto, D. Nagae, Y. Abe, S. Naimi, T. Yamaguchi, S. Omika, Z. Ge, N. Tadano, K. Wakayama, A. Kitagawa, S. Sato, “Development of secondary electron time detector for ion beams”, Proceedings of Science, INPC2016 (2016) 111. *

F. Suzaki, J. Zenihiro, Y. Abe, A. Ozawa, T. Suzuki, T. Uesaka, M. Wakasugi, K. Yamada, T. Yamaguchi, and Y. Yamaguchi, “Performance of a resonant Schottky pick-up for the Rare-RI Ring project”, JPS Conference Proceedings Vol.6 (2015) 030119.*

T. Yamaguchi, “Present status of Rare-RI Ring facility at RIBF”, Physica Scripta T166 (2015) 014039.*

Y. Abe, Y. Yamaguchi, M. Wakasugi, T. Uesaka, A. Ozawa, F. Suzaki, D. Nagae, H. Miura, and T. Yamaguchi, “Isochronous field study of the Rare-RI Ring”, Physica Scripta T166 (2015) 014039.*

F. Suzaki, J. Zenihiro, A. Ozawa, T. Suzuki, T. Uesaka, M. Wakasugi, K. Yamada, T. Yamaguchi, Y. Abe, and Y. Yamaguchi, “A resonant Schottky pick-up for Rare-RI Ring at RIKEN”, Physica Scripta T166 (2015) 014059.*

Y. Yamaguchi, H. Miura, M. Wakasugi, Y. Abe, A. Ozawa, F. Suzaki, A. Tokuchi, T. Uesaka, T. Yamaguchi, and Y. Yano, “Fast-kicker system for rare-RI ring” Physica Scripta T166 (2015) 014056.*

H. Miura, Y. Abe, Z. Ge, K. Hiraishi, Y. Ishikawa, I. Kato, T. Moriguchi, D. Nagae, S. Naimi, T. Nishimura, S. Omika, A. Ozawa, F. Suzaki, S. Suzuki, “Performance of a fast kicker magnet for rare-RI ring”, Proceedings of the HIAT2015 (2015) 95-97.

F. Suzaki, Y. Abe, Z. Ge, D. Nagae, S. Naimi, T. Uesaka, T. Watanabe, M. Wakasugi, K. Yamada, Y. Yamaguchi, J. Zenihiro, Y. Yano, I. Kato, H. Miura, T. Nishimura, S. Omika, T. Suzuki, N. Tadano, Y. Takeuchi, T. Yamaguchi, K. Hiraishi, Y. Ichikawa, T. Moriguchi, A. Ozawa, S. Suzuki, and Y. Tajiri, “Performance of a resonant Schottky pick-up in the commissioning of rare-RI ring”, Proceedings of the HIAT2015 (2015) 98-100.

Y. Yamaguchi, Y. Abe, and rare-RI ring collaborators, “The rare-RI ring at RIKEN RI Beam Factory”, Proceedings of the HIAT2015 (2015) 121-123.

T. Yamaguchi, T. Izumikawa, S. Miyazawa, T. Suzuki, F. Tokanai, H. Furuki, N. Ichihashi, C. Ichikawa, A. Kitagawa, T. Kuboki, S. Momota, D. Nagae, M. Nagashima, Y. Nakamura, R. Nishikiori, T. Ohtsubo, A. Ozawa, K. Sato, S. Sato, and S. Suzuki, “Performance of high-resolution position-sensitive detectors developed for storage-ring decay experiments”, Nuclear Instruments and Methods in Physics Research Section B 317 (2013) 697-700.*

F. Suzaki, J. Zenihiro, T. Yamaguchi, A. Ozawa, T. Uesaka, M. Wakasugi, K. Yamada, Y. Yamaguchi, and rare-RI ring collaboration, “Design

study of a resonant Schottky pick-up for the Rare-RI Ring project", Nuclear Instruments and Methods in Physics Research Section B317 (2013) 636-639.*
D. Nagae, S. Okada, A. Ozawa, T. Yamaguchi, H. Suzuki, T. Moriguchi, Y. Ishibashi, S. Fukuoka, R. Nishikiori, T. Niwa, T. Suzuki, K. Sato, H. Furuki, N. Ichihashi, S. Miyazawa, Y. Yamaguchi, T. Uesaka, and M. Wakasugi, "Time-of-flight detector applied to mass measurements in Rare-RI Ring", Nuclear Instruments and Methods in Physics Research Section B 317 (2013) 640-643.*
Y. Yamaguchi, M. Wakasugi, T. Uesaka, A. Ozawa, Y. Abe, T. Fujinawa, M. Kase, M. Komiyama, T. Kubo, K. Kumagai, T. Maie, D. Nagae, J. Ohnishi, F. Suzaki, A. Tokuchi, Y. Watanabe, K. Yoshida, K. Yamada, T. Yamaguchi, H. Yamasawa, Y. Yanagisawa, J. Zenihiro, and Y. Yano, "Construction of rare-RI ring at RIKEN RI Beam Factory", Nuclear Instruments and Methods in Physics Research Section B 317 (2013) 629-635.*
Yu.A. Litvinov, S. Bishop, K. Blaum, F. Bosch, C. Brandau, L.X. Chen, I. Dillmann, P. Egelhof, H. Geissel, R.E. Grisenti, S. Hagmann, M. Heil, A. Heinz, N. Kalantar-Nayestanaki, R. Knoebel, C. Kozhuharov, M. Lestinsky, X.W. Ma, T. Nilsson, F. Nolden, A. Ozawa, R. Raabe, M.W. Reed, R. Reifarth, M.S. Sanjari, D. Schneider, H. Simon, M. Steck, T. Stoehlker, B.H. Sun, X.L. Tu, T. Uesaka, P.M. Walker, M. Wakasugi, H. Weick, N. Winckler, P.J. Woods, H.S. Xu, T. Yamaguchi, Y. Yamaguchi, and Y.H. Zhang, "Nuclear physics experiments with ion storage rings", Nuclear Instruments and Methods in Physics Research Section B 317 (2013) 603-616.*
T. Yamaguchi, Y. Yamaguchi, and A. Ozawa "The challenge of precision mass measurements of short-lived exotic nuclei: Development of a new storage-ring mass spectrometry", Journal of Mass Spectrometry 349-350 (2013) 240-246.*
M. Wakasugi, and rare-RI ring collaborators, "Construction of the rare-RI ring at the RIKEN RI beam factory", Proceedings of Cyclotron2013 (2013) 477-481.
Y. Abe, D. Nagae, and rare-RI ring collaboration, "Developments of time-of-flight detectors for Rare-RI Ring", Proceedings of the 12th Asia Pacific Physics Conference 1 (2013) 013059.*
F. Suzaki, T. Yamaguchi, and rare-RI ring collaboration, "Storage-ring mass spectrometry in Japan", Proceedings of the 12th Asia Pacific Physics Conference 1 (2013) 013058.*
M. Komiyama, A. Uchiyama, N. Fukunishi, M. Wakasugi, M. Hamanaka, and M. Nishimura, "Status of the RIKE RI Beam Factory Control System", Proceedings of ICALEPCS2013 (2013) 348-351.

Oral Presentations

[International Conference etc.]

Y. Yamaguchi, M. Wakasugi, Y. Abe, D. Nagae, F. Suzaki, A. Ozawa, T. Uesaka, T. Yamaguchi, S. Naimi, and rare-RI ring collaborators, "The rare-RI ring at RIKEN RI beam factory", International Nuclear Physics Conference (INPC2016), Adelaide, Australia, September (2016).
S. Suzuki, A. Ozawa, T. Moriguchi, Y. Ichikawa, M. Amano, D. Kamioka, Y. Tajiri, K. Hiraishi, T. Matsumoto, D. Nagae, Y. Abe, S. Naimi, T. Yamaguchi, S. Omika, Z. Ge, N. Tadano, K. Wakayama, A. Kitagawa, S. Sato, "Development of secondary electron time detector for ion beams", International Nuclear Physics Conference (INPC2016), Adelaide, Australia, September (2016).
D. Nagae, S. Omika, F. Suzaki, Y. Abe, Y. Yamaguchi, S. Naimi, T. Yamaguchi, A. Ozawa, T. Uesaka, M. Wakasugi, and rare-RI ring collaborators, "The rare-RI ring at RIKEN RI beam factory", International Symposium on Neutron Star Matter (NSMAT2016), Sendai, Japan, November (2016).
T. Yamaguchi, "RI beam experiments with storage rings -present and future-", International Symposium on Interplay between Hadronic, Nuclear and Atomic Physics, Shimoda, Japan, July (2016).
T. Yamaguchi, "Rare-RI Ring at RIKEN present status", NUSTAR annual meeting, Darmstadt, Germany, February (2017).
Y. Yamaguchi, "The Rare RI Ring at RI Beam Factory", 13th International Conference on Heavy Ion Accelerator Technology, Yokohama, Japan, September (2015).
Y. Yamaguchi, "Commissioning of the Rare-RI Ring at RI Beam Factory", International Workshop on Beam Cooling and Related Topics, Newport News, USA, October (2015).
Y. Yamaguchi, "Commissioning of the Rare-RI Ring at RI Beam Factory", The 9th Japan-China Joint Nuclear Physics Symposium, Osaka, Japan, November (2015).
Ozawa, and rare-RI ring collaboration, "Mass measurement with Rare-RI Ring at RIKEN", SKLTP-BLTP Joint Workshop on Physics of Strong Interaction, Guangxi, China, November (2015).
Y. Yamaguchi, and rare-RI ring collaboration, "Present status of Rare-RI Ring", RIBF Users Meeting 2015, Wako, Japan, September (2015).
M. Wakasugi, and rare-RI ring collaboration, "The Rare-RI Ring Facility at RIKEN RI Beam Factory", 2nd Conference on Advances in Radioactive Isotope Science, Tokyo, Japan, June (2014).
Y. Yamaguchi, and rare-RI ring collaboration, "Rare-RI Ring at RIKEN RI Beam Factory", The 6th International Conference on Trapped Charged Particles and Fundamental Physics, Takamatsu, Japan, Desember (2014).
Y. Abe, Y. Yamaguchi, M. Wakasugi, T. Uesaka, A. Ozawa, F. Suzaki, H. Miura, T. Yamaguchi, and Y. Yano, "Isochronous study of the Rare-RI Ring", 9th International Conference on Nuclear Physics at Storage Rings, St. Goar, Germany, September (2014).
Ozawa, "Mass measurement with Rare-RI Ring", Science and Next Generation Experiments at FRIB and RIBF, Hawaii, USA, October (2014).
Y. Abe, "Mass measurement of RI with Rare-RI Ring at RIKEN", Post-TCP PMM Workshop, Wako, Japan, December (2014).
M. Wakasugi, and rare-RI ring collaborators, "Construction of the Rare RI Ring (R3) at the RIKEN RI Beam Factory", The 20th International Conference on Cyclotrons and Their Applications, Vancouver, Canada, September (2013).
T. Yamaguchi, "Rare-RI Ring project in RIKEN", Sino-German Symposium on (High precision experiments with stored exotic and stable nuclei), Lanzhou, China, November (2013).
Y. Yamaguchi, and rare-RI ring collaboration, "Construction status of the Rare-RI Ring", RIBF Users Meeting 2013, Wako, Japan, June (2013).
Ozawa, and rare-RI ring collaboration, "Rare-RI Ring for Mass measurements at RIBF", The 12th International Symposium on Origin of Matter and Evolution of Galaxies, Tsukuba, Japan, November (2013).

[Domestic Conference]

若山清志、阿部康志、天野将道、上岡大起、北川敦志、長江大輔、大甕舜一朗、小沢顕、佐藤眞二、鈴木伸司、鈴木健、只野奈津生、山口貴之、「ファイバーシンチレータと MPPC による簡易な重イオンビーム位置検出器の開発」日本物理学会第 72 回年次大会、大阪市、3 月 (2017).

大甕舜一朗、山口貴之、只野奈津生、鈴木健、若山清志、阿部康志、上坂友洋、Naimi Sarah、Ge Zhuang、洲嵜ふみ、長江大輔、山口由高、若杉昌徳、天野将道、小沢顕、上岡大起、鈴木伸司、森口哲朗、北川敦志、佐藤眞二、「稀少 RI リングのための粒子周回モニターの開発」日本物理学会第 72 回年次大会、大阪市、3 月 (2017).

Ge Zhuang、Naimi Sarah、長江大輔、阿部康志、大甕舜一朗、上坂友洋、洲嵜ふみ、山口由高、若杉昌徳、若山清志、山口貴之、小沢顕、鈴木伸司、森口哲朗、矢野安重、「Development of a large area position sensitive (TOF) detector at the Rare RI Ring at RIBF」日本物理学会第 72 回年次大会、大阪市、3 月 (2017).

大甕舜一朗、山口貴之、若杉昌徳、山口由高、阿部康志、上坂友洋、小沢顕、洲嵜ふみ、鈴木健、長江大輔、三浦宙、柳澤善行、「稀少 RI リング個別入射方式のための同軸菅の開発」日本物理学会 2015 年秋季大会、大阪市、9 月 (2015).

鈴木伸司、市川ゆきな、長江大輔、小沢顕、阿部康志、森口哲朗、岡田俊祐、石橋陽子、松本拓也、田尻芳之、斎藤祐多、稲葉成紀、沢畑克樹、山口貴之、鈴木健、河野準平、山木さやか、松本達、榎本彩乃、大甕舜一朗、竹内勇貴、加藤郁磨、只野奈津生、西村拓真、北川敦志、佐藤眞二、「RI ビーム飛行時間検出器の開発」日本物理学会 2015 年秋季大会、大阪市、9 月 (2015).

阿部康志、山口由高、上坂友洋、小沢顕、洲嵜ふみ、山口貴之、若杉昌徳、稀少 RI リングコラボレーション、「稀少 RI リングの性能評価」日本物理学会第 71 回年次大会、仙台市、3 月 (2016).

洲嵜ふみ、阿部康志、Ge Zhuang、平石健太郎、市川ゆきな、加藤郁磨、三浦宙、森口哲朗、長江大輔、Naimi Sarah、西村拓真、大甕舜一朗、小沢顕、鈴木伸司、鈴木健、只野奈津生、田尻芳之、竹内勇貴、上坂友洋、若杉昌徳、渡邊環、山田一成、山口貴之、山口由高、銭廣十三、矢野安重、「稀少 RI リングのための共鳴ショットキーピックアップのオンライン性能評価」日本物理学会第 71 回年次大会、仙台市、3 月 (2016).

鈴木伸司、小沢顕、市川ゆきな、森口哲朗、田尻芳之、平石健太郎、松本拓也、長江大輔、阿部康志、Naimi Sarah、Ge Zhuang、山口貴之、松本達、鈴木健、大甕舜一朗、竹内勇貴、加藤郁磨、只野奈津生、西村拓真、北川敦志、佐藤眞二、「質量測定用飛行時間検出器の開発」日本物理学会第 71 回年次大会、仙台市、3 月 (2016).

小沢顕、「Present status of Rare-RI Ring project at RIBF」実験と観測で解き明かす中性子星の核物質 第 4 回研究会、葉山、9 月 (2015).

山口貴之、「稀少 RI リングによる r プロセス核の測定計画」宇宙核物理連絡協議会 研究会、三鷹市、2 月 (2016).

Naimi Sarah、「Mass measurement in connection to the nuclear astrophysics」宇宙核物理連絡協議会 研究会、三鷹市、2 月 (2016).

洲嵜ふみ、阿部康志、Naimi Sarah、三浦宙、小沢顕、鈴木健、上坂友洋、若杉昌徳、山田一成、山口貴之、山口由高、銭廣十三、Chen Xiangcheng、「稀少 RI リングの共鳴ショットキーピックアップのオフライン性能試験」日本物理学会第 70 回年次大会、東京、3 月 (2015).

三浦宙、山口由高、若杉昌徳、阿部康志、小沢顕、洲嵜ふみ、徳地明、上坂友洋、山口貴之、長江大輔、柳澤善行、鈴木健、「稀少 RI リングのためのキッカーマグネットの開発」日本物理学会第 70 回年次大会、東京、3 月 (2015).

阿部康志、長江大輔、岡田俊祐、小沢顕、山口貴之、石橋陽子、斎藤祐多、沢畑克樹、鈴木健、河野準平、山木さやか、山口由高、上坂友洋、若杉昌徳、「稀少 RI リングのビームモニターの開発」日本物理学会 2013 年秋季大会、高知市、9 月 (2013).

洲嵜ふみ、銭廣十三、小沢顕、鈴木健、上坂友洋、若杉昌徳、山田一成、山口貴之、山口由高、「稀少 RI リングの共鳴ショットキーピックアップ設計のための電磁場シミュレーション」日本物理学会 2013 年秋季大会、高知市、9 月 (2013).

洲嵜ふみ、銭廣十三、小沢顕、鈴木健、上坂友洋、若杉昌徳、山田一成、山口貴之、山口由高、「稀少 RI リングの共鳴ショットキーピックアップの性能試験」日本物理学会第 69 回年次大会、平塚市、3 月 (2014).

Posters Presentations

[International Conference etc.]

S. Suzuki, A. Ozawa, Y. Ichikawa, T. Moriguchi, Y. Tajiri, K. Hiraishi, T. Matsumoto, D. Nagae, Y. Abe, S. Naimi, T. Yamaguchi, T. Suzuki, S. Omika, Z. Ge, Y. Takeuchi, N. Tadano, I. Kato, T. Nishimura, A. Kitagawa, S. Sato, “Development of time-of-flight detector for mass measurements of short-lived nuclei with the rare-RI ring”, International Symposium on Neutron Star Matter (NSMAT2016), Sendai, Japan, November (2016).

H. Miura and rare-RI ring collaborators, “Development of a Fast Kicker System for Rare-RI RIng”, 13th International Conference on Heavy Ion Accelerator Technology, Yokohama, Japan, September (2015).

F. Suzaki and rare-RI ring collaborators, “Performance of a resonant Schottky pick-up in the commissioning of Rare-RI Ring”, 13th International Conference on Heavy Ion Accelerator Technology, Yokohama, Japan, September (2015).

Z. Ge and rare-RI ring collaborators, “Rare-RI Ring at RIKEN”, The 13th International Symposium on Origin of Matter and Evolution of Galaxies, Beijing, China, June (2015).

Y. Yamaguchi, H. Miura, M. Wakasugi, Y. Abe, A. Ozawa, F. Suzaki, A. Tokuchi, T. Uesaka, T. Yamaguchi, and Y. Yano, “Fast-kicker system for Rare-RI Ring”, 9th International Conference on Nuclear Physics at Storage Rings, St. Goar, Germary, September (2014).

F. Suzaki, J. Zenihiro, A. Ozawa, T. Suzuki, T. Uesaka, M. Wakasugi, K. Yamada, T. Yamaguchi, Y. Abe, and Y. Yamaguchi, “A resonant Schottky pick-up for Rare-RI Ring at RIKEN”, 9th International Conference on Nuclear Physics at Storage Rings, St. Goar, Germany, September (2014).

F. Suzaki, J. Zenihiro, A. Ozawa, T. Suzuki, T. Uesaka, M. Wakasugi, K. Yamada, T. Yamaguchi, Y. Abe, and Y. Yamaguchi, “Performance of a resonant Schottky pick-up for Rare-RI Ring project”, 2nd Conference on Advances in Radioactive Isotope Science, Tokyo, Japan, June (2014).

Y. Abe, and D. Nagae, “Developments of time-of-flight detectors for Rare-RI Ring”, The 12th Asia Pacific Physics Conference, Chiba, Japan, July (2013).

T. Yamaguchi, F. Suzaki, and rare-RI ring collaborators, “Storage-ring mass spectrometry in Japan”, The 12th Asia Pacific Physics Conference, Chiba, Japan, July (2013).

T. Yamaguchi, “Cherenkov light detection as a velocity selector for uranium fission products at intermediate energies”, 8th International workshop on Ring imaging Cherenkov Detectors, Hayama, Japan, Desember (2013).

[Domestic Conference]

山口由高、若杉昌徳、阿部康志、洲嵜ふみ、藤縄雅、加瀬昌之、込山美咲、熊谷桂子、眞家武士、長江大輔、大西純一、小沢顕、上坂友洋、渡邉裕、山口貴之、山澤秀行、柳澤善行、銭廣十三、矢野安重、「理研 RIBF における稀少 RI リングの現状」第 11 回日本加速器学会年会、青森市、8 月 (2014).

RIBF Research Division
Instrumentation Development Group
SCRIT Team

1. Abstract

The SCRIT Electron Scattering Facility has been constructed at RIKEN RIBF. This aims at investigation of internal nuclear structure for short-lived unstable nuclei by means of electron scattering. SCRIT (Self-Confining RI Ion Target) is a novel method to form internal targets in an electron storage ring. This is a unique method for making electron scattering experiments for unstable nuclei possible. Construction of the facility has been started in 2009. This facility consists of an electron accelerator (RTM), a SCRIT-equipped electron storage ring (SR2), an electron-beam-driven RI separator (ERIS), and a detector system consisting of a high-resolution magnetic spectrometer, drift chambers and trigger scintillators. Installation of all components in the facility was completed in 2015, and it is now under comprehensive test experiment phase. In the test experiments, the luminosity was reached to 3×10^{27} /(cm^2s) with the number of injected ions of 3×10^8. In 2016, we successfully completed a measurement of diffraction of scattered electrons from ^{132}Xe nuclei and determined the charge density distribution for the first time. The facility is now under setting up to move the first experiment for unstable nuclei.

2. Major Research Subjects

Development of SCRIT electron scattering technique and measurement of the nuclear charge density distributions of unstable nuclei.

3. Summary of Research Activity

SCRIT is a novel technique to form internal target in an electron storage ring. Positive ions are three dimensionally confined in the electron beam axis by transverse focusing force given by the circulating electron beam and applied electrostatic longitudinal mirror potential. The created ion cloud composed of RI ions injected from outside works as a target for electron scattering. Construction of the SCRIT electron scattering facility has been started in 2009. The electron accelerators RTM and the storage ring SR2 were successfully commissioned in 2010. Typical accumulation current in SR2 is 250-300 mA at the energy range of 100-300 MeV that is required energy range in electron scattering experiment. The SCRIT device was inserted in the straight section of SR2 and connected to an ISOL named ERIS (Electron-beam-driven RI separator for SCRIT) by 20-m long low energy ion transport line. A buncher system based on RFQ linear trap was inserted in the transport line to convert the continuous beam from ERIS to pulsed beam, which is acceptable for SCRIT. A detector system consisting of a high-resolution magnetic spectrometer, drift chambers and trigger schintillators was constructed, and this has a solid angle of 100 msr, energy resolution of 10^{-3}, and the scattering angle coverage of 25-55 degrees. A wide range of momentum transfer, 80-300 MeV/c, is covered by changing the electron beam energy from 150 to 300 MeV. Installation of all the components in the facility has been completed in last year, and we are now under comprehensive test experiments.

We successfully measured a diffraction pattern in the angular distribution of scattered electron from ^{132}Xe isotope at the electron beam energy of 150MeV, 200MeV, and 300MeV, and derived the nuclear charge distribution by assuming two-parameters Fermi model for the first time. At this time, luminosity was reached to 3×10^{27}/(cm^2s) at maximum and the averaged value was 1.2×10^{27}/(cm^2s) with the number of injected target ions of 3×10^8.

We are now under preparation for going to the experiments for unstable nuclei. There are some key issues for that. They are increasing the intensity of the RI beams from ERIS, efficient DC-to-pulse conversion at the buncher, and effective suppression of the background in measurement of scattered electrons. RI beam intensity will be improved by upgrading the electron beam power from 10W to 60W, increasing the contained amount of U in the target ion source, and some modifications in mechanical structure in the ion source. For efficient DC-to-pulse conversion, we will innovate two-step bunching method, which is time compression at the buncher in combination with pre-bunching at the ion source using grid action, and was already demonstrated in off-line test. Since one of significant contribution to the background for scattered electron is scattering from massive structural objects around the trapping region originated from halo components of the electron beam, we will remodel the SCRIT electrodes. Luminosity for radioactive Xe isotopes is expected to be more than 10^{26}/(cm^2s) after these improvements. Then, we will be able to start experiments for unstable nuclei. When further upgrading in the RTM power planed to be 3kW will be achieved, we can extend the measurements to more exotic nuclei.

Members

Team Leader

Masanori WAKASUGI (concurrent; Group Director, Instrumentations Development Gr.)

Research & Technical Scientists

Masamitsu WATANABE (Senior Research Scientist)

Tetsuya OHNISHI (Senior Technical Scientist)

Nishina Center Research Scientist

Akitomo ENOKIZONO

Research Consultants

Tadaaki TAMAE
Shin-ichi ICHIKAWA
Masahiro HARA
Takashi EMOTO

Senior Visiting Scientist

Toshitada HORI (Hiroshima University)

Visiting Scientists

Shuo WANG (Shandong University)
Yuki HONDA (Tohoku University)
Kyo TSUKADA (Tohoku University)
Toshimi SUDA (Tohoku University)
Kazuyoshi KURITA (Rikkyo University)

Research Fellow

Mamoru TOGASAKI (Rikkyo University)

Student Trainees

Keita KASAMA (Tohoku University)
Kazuki NAMBA (Tohoku University)
Mitsuki HORI (Rikkyo University)
Nobuaki UCHIDA (Rikkyo University)

List of Publications & Presentations

Publications

[Journals]

K. Tsukada, A. Enokizono, T. Ohnishi, K. Adachi, T. Fujita, M. Hara, M. Hori, T. Hori, S. Ichikawa, K. Kurita, K. Matsuda, T. Suda, T. Tamae, M. Togasaki, M. Wakasugi, M. Watanabe, and K. Yamada, “First Elastic Electron Scattering from ^{132}Xe at the SCRIT Facility”, Physical Review Letters **118**, 262501, 27 June (2017)

T. Suda and Haik Simon, “Prospects for electron scattering on unstable, exotic nuclei”, Progress in Particle and Nuclear Physics, in press (2017)

[Proceedings]

(Original Papers) *Subject to Peer Review

M. Togasaki, K. Kurita, K. Yamada, R. Toba, M. Hara, T. Ohnishi, and M. Wakasugi, “Development of a buffer-gas-free buncher for low energy RI ion beam”, HIAT2015 proceedings, 253 (2015).

T. Ohnishi, S. Ichikawa, and M. Wakasugi, “Electron-beam-driven RI separator for SCRIT at RIKEN RI Beam Factory”, HIAT2015 proceedings, 194 (2015).

T. Ohnishi, A. Enokizono, M. Hara, T. Hori, S. Ichikawa, K. Kurita, S. Matsuo, T. Suda, T. Tamae, M. Togasaki, K. Tsukada, T. Tsuru, S. Wang, S. Yoneyama, and M. Wakasugi, “The SCRIT electron scattering facility project at RI Beam Factory”, Physca Scripta, T166 , 014071 (2015).*

T. Suda, A. Enokizono, M. Hara, Y. Haraguchi, S. Ichikawa, K. Kurita, S. Matsuo, T. Ohnishi, T. Tamae, M. Togasaki, K. Tsukada, T. Tsuru, S. Wang, S. Yoneyama, and M. Wakasugi, “SCRIT Electron Scattering Facility”, JPS Conf. Proc. 6, 030100 (2015).*

Oral Presentations

[International Conference etc.]

A. Enokizono, K. Adachi, T. Fujita, M. Hara, M. Hori, T. Hori, S. Ichikawa, K. Kasama, K. Kurita, K. Namba, T. Ohnishi, S. Sasamura, T. Suda, T. Tamae, K. Tsukada, M. Togasaki, N. Uchida, M. Wakasugi, S. Wang, M. Watanabe, K. Yamada, “Results of the first physics experiment with ^{132}Xe and ^{208}Pb targets at the SCRIT facility”, ARIS2017, Keystone, Colorado, May 30th, (2017)

A. Enokizono, K. Adachi, T. Fujita, M. Hara, M. Hori, T. Hori, S. Ichikawa, K. Kasama, K. Kurita, K. Nam
T. Suda, T. Tamae, K. Tsukada, M. Togasaki, N. Uchida, M. Wakasugi, M. Watanabe, K. Yamada, "The Performance Of The Scrit Detectors For Electron-RI Scattering Experiment", International Nuclear Physics Conference (INPC2016), Adelaide Convention Centre, Australia, Data: September 11-16, (2016).

T Ohnishi, M. Hara, T. Hori, S. Ichikawa, M. Watanabe, M. Wakasugi, K. Adachi, A. Enokizono, T. Fujita, M. Hori, S. Sasamura, M. Togasaki, N. Uchida, K. Yamada, K. Kurita, K. Kasama, K. Namba, K. Tsukada, T. Tamae, T. Suda, S. Wang, T. Kikuchi, “The SCRIT Electron Scattering Facility at the Riken RI Beam Factory”, International Nuclear Physics Conference (INPC2016), Adelaide Convention Centre, Australia, Data: September 11-16, (2016).

K. Tsukada, K. Kasama, K. Namba, T. Suda, T. Tamae, M. Hara, T. Hori, S. Ichikawa, T. Ohnishi, M. Wakasugi, M. Watanabe, K. Adachi, A. Enokizono, T. Fujita, M. Hori, K. Kurita, S. Sasamura, M. Togasaki, N. Uchida, K. Yamada, “First result from SCRIT electron scattering facility:Charge density distribution of ^{132}Xe”, International Nuclear Physics Conference, Adelaide Convention Centre, Australia, September 11-16, (2016).

K. Kurita, “How SCRIT came into reality”, International Symposium on Modern technique and its Outlook in Heavy Ion Science (MOTO16), Rikkyo University, Tokyo, Japan, June (2016).

T. Suda, “SCRIT electron scattering facility : present status and future perspectives”, Neutron Skin of Nuclei, Mainz, Germany, May 17 – 27, (2016).

T. Suda, “Electron scattering off short-lived nuclei at SCRIT facility”, Seminar at GANIL, CAEN, France. April 29, 2016.

K. Tsukada, “Physics program with SCRIT”, Electron-radioactive ion collisions : theoretical and experimental challenges, Saclay, France, April 25 – 27, (2016).

T. Suda, “Future perspectives of the SCRIT facility”, Electron-radioactive ion collisions : theoretical and experimental challenges, Saclay, France, April 25 – 27, (2016).

M. Wakasugi, “The SCRIT Facility at RIKEN”, Int. Workshop on Electron Radioactive Collision, Apr. 25-27, CEA Saclay, France (2016).

M. Wakasugi, T. Ohnishi, M. Watanabe, S. Ichikawa, M. Hara, T. Hori, M. Togasaki, K. Yamada, T. Fujita, K. Adachi, M. Hori, A, Enokizono,

K. Kurita, K. Tsukada, T. Tamae, and T. Suda, “Current status of electron-RI collision project at RIKEN“, Int. Workshop on Beem Cooling and Related Topics COOL15, Sep.28-Oct.2, JLab Newport News, Virginia, USA (2015).

T. Ohnishi, A. Enokizono, M. Hara, T. Hori, S. Ichikawa, K. Kurita, S. Matsuo, T. Suda, T. Tamae, M. Togasaki, K. Tsukada, T. Tsuru, S. Wang, S. Yoneyama, and M. Wakasugi, “The SCRIT electron scattering facility project at RI Beam Factory”, 9th Int. Conf. on Nuclear Physics at Storage Ring, Sep.28-Oct.2, Schloss Rheinfels, St. Goar, Germany (2015).

[Domestic Conference]

山田耕平，大西哲哉，栗田和好，戸ケ崎衛，鳥羽僚太，原雅弘，渡邊正満，若杉昌徳 SCRIT 実験のためのイオンビームバンチャーの開発”，日本物理学会、3月、大阪大学、大阪(2017).

藤田峻広，足立江介，市川進一，内田信昭，榎園昭智，大西哲哉，笠間桂太，栗田和好，笹村薪之介，須田利美，玉江忠明，塚田暁，戸ヶ崎衛，南波和希，原雅弘，堀利匡，堀充希，松田一衛，山田耕平，若杉昌徳，渡邊正満，“電子蓄積リングにおける電子散乱実験の制動輻射を用いたルミノシティ測定”，日本物理学会、3月、大阪大学、大阪(2017).

塚田暁、足立江介、市川進一、榎園昭智、大西哲哉、笠間桂太、栗田和好、笹村薪之介、須田利美、玉江忠明、戸ケ崎衛、南波和希、原雅弘、藤田峻広、堀利匡、堀充希、松田一衛、山田耕平、若杉昌徳、渡邊正満、”SCRIT法を用いた^{132}Xeの電荷分布測定”，日本物理学会、9月、宮崎大学、宮崎(2016).

藤田峻広，足立江介，市川進一，榎園昭智，大西哲哉，栗田和好，須田利美，玉江忠明，塚田暁，戸ヶ崎衛，原雅弘，堀利匡，堀充希，松田一衛，山田耕平，若杉昌徳，渡邊正満，“SCRIT 法を用いた Xe 同位体標的・電子散乱実験における ルミノシティ測定”，日本物理学会、9月、宮崎大学、宮崎(2016).

塚田暁、足立江介、市川進一、榎園昭智、大西哲哉、栗田和好、須田利美、玉江忠明、水流輝明、戸ケ崎衛、原雅弘、藤田峻広、堀利匡、堀充希、松田一衛、山田耕平、若杉昌徳、渡邊正満、”SCRIT 法を用いたXe同位体標的における電子散乱の角度分布測定“、日本物理学会、3月、東北学院大、仙台(2016).

榎園昭智、足立江介、市川進一、大西哲哉、栗田和好、須田利美、玉江忠明、塚田暁、水流輝明、戸ケ崎衛、原雅弘、藤田峻広、堀利匡、堀充希、松田一衛、山田耕平、若杉昌徳、渡邊正満、”SCRIT 法を用いた電子・不安定 Xe 核散乱実験におけるルミノシティの測定“、日本物理学会、3月、東北学院大、仙台(2016).

塚田暁、市川進一、榎園昭智、大西哲哉、栗田和好、須田利美、玉江忠明、水流輝明、戸ケ崎衛、原雅弘、藤田峻広、堀利匡、松田一衛、山田耕平、若杉昌徳、渡邊正満、”SCRIT 法を用いた電子・不安定核散乱実験に向けた電子スペクトロメータのアクセプタンス評価“、日本物理学会、9月、大阪市立大、大阪(2015).

榎園昭智、足立江介、市川進一、大西哲哉、栗田和好、須田利美、玉江忠明、塚田暁、水流輝明、戸ケ崎衛、原雅弘、藤田峻広、堀利匡、松田一衛、山田耕平、若杉昌徳、渡邊正満、”SCRIT 法を用いた電子・不安定核散乱実験に向けたルミノシティ決定精度の評価“、日本物理学会、9月、大坂市立大、大坂(2015).

戸ケ崎衛、大西哲哉、栗田和好、鳥羽瞭太、原雅弘、山田耕平、若杉昌徳、“イオンビームクーラー・バンチャーの開発”、日本物理学会、9月、大坂市立大、大坂(2015).

塚田暁、市川進一、榎園昭智、大西哲哉、栗田和好、須田利美、玉江忠明、水流輝明、戸ケ崎衛、堀利匡、原雅弘、松尾咲希、松田一衛、森谷洋祐、米山俊平、若杉昌徳、”SCRIT 電子スペクトロメータの運動量分解能とアクセプタンス評価“、日本物理学会、3月、早稲田大、東京(2015).

米山俊平、榎園昭智、大西哲哉、栗田和好、須田利美、玉江忠明、塚田暁、水流輝明、戸ケ崎衛、松尾咲希、松田一衛、森谷洋祐、若杉昌徳、”SCRIT 実験用ルミノシティーモニタ“、日本物理学会、3月、早稲田大、東京(2015).

松尾咲希、市川進一、榎園昭智、大西哲哉、栗田和好、須田利美、玉江忠明、塚田暁、水流輝明、戸ケ崎衛、原雅弘、堀利匡、松田一衛、森谷洋祐、米山俊平、若杉昌徳、”SCRIT 実験における散乱電子スペクトロメータの開発“、日本物理学会、3月、早稲田大、東京(2015).

Posters Presentations

[International Conference etc.]

M. Togasaki, K. Kurita, K. Yamada, R. Toba, M. Hara, T. Ohnishi, and M. Wakasugi, “Development of a buffer-gas-free buncher for low energy RI ion beam”, 13th Int. Conf. on Heavy Ion Accelerator Technorogy HIAT2015, Sep. 7-11, Yokohama, Japan (2015).

T. Ohnishi, S. Ichikawa, and M. Wakasugi, “Electron-beam-driven RI separator for SCRIT at RIKEN RI Beam Factory”, 13th Int. Conf. on Heavy Ion Accelerator Technorogy HIAT2015, Sep. 7-11, Yokohama, Japan (2015).

RIBF Research Division
Research Instruments Group

1. Abstract

The Research Instruments Group is the driving force at RI Beam Factory (RIBF) for continuous enhancement of activities and competitiveness of experimental research. Consisting of four teams, we are in charge of the operation, maintenance, and improvement of the core research instruments at RIBF, such as the BigRIPS in-flight RI separator, ZeroDegree spectrometer and SAMURAI spectrometer, and the related infrastructure and equipment. We are also in charge of the production and delivery of RI beams using the BigRIPS separator. The group also conducts related experimental research as well as R&D studies on the research instruments.

2. Major Research Subjects

Design, construction, operation, maintenance, and improvement of the core research instruments at RIBF and related R&D studies. Experimental studies on exotic nuclei.

3. Summary of Research Activity

The current research subjects are summarized as follows:
(1) Production and delivery of RI beams and related research
(2) Design, construction, operation, maintenance, and improvement of the core research instruments at RIBF and their related infrastructure and equipment
(3) R&D studies on the core research instruments and their related equipment at RIBF
(4) Experimental research on exotic nuclei using the core research instruments at RIBF

Members

Group Directors
Toshiyuki KUBO (– Mar. 31, 2016)
Hideki UENO (Apr. 1, 2016 –)

Junior Research Associates
Daichi MURAI (Rikkyo Univ.)
Momo MUKAI (Tsukuba Univ.)

Special Temporary Employee
Toshiyuki KUBO

Senior Visiting Scientists
Toshio KOBAYASHI (Tohoku Univ.)
Jerry NOLEN (Argonne National Lab.)

Visiting Scientist
Toshiyuki KUBO (Michigan State Univ.)

Student Trainee
Katrina Elizabeth KOEHLER (West Michigan University)

RIBF Research Division
Research Instruments Group
BigRIPS Team

1. Abstract

This team is in charge of design, construction, development and operation of BigRIPS in-flight separator and its related research instruments at RI beam factory (RIBF). They are employed not only for the production of RI beams but also the experimental studies using RI beams.

2. Major Research Subjects

Design, construction, development and operation of BigRIPS in-flight separator, RI-beam transport lines, and their related research instruments

3. Summary of Research Activity

This team is in charge of design, construction, development and operation of BigRIPS in-flight separator, RI-beam transport lines, and their related research instruments such as ZeroDegree spectrometer at RI beam factory (RIBF). They are employed not only for the production of RI beams but also various kinds of experimental studies using RI beams.
The research subjects may be summarized as follows:
(1) General studies on RI-beam production using in-flight scheme.
(2) Studies on ion-optics of in-flight separators, including particle identification of RI beams
(3) Simulation and optimization of RI-beam production.
(4) Development of beam-line detectors and their data acquisition system.
(5) Experimental studies on production reactions and unstable nuclei.
(6) Experimental studies of the limits of nuclear binding.
(7) Development of superconducting magnets and their helium cryogenic systems.
(8) Development of a high-power production target system.
(9) Development of a high-power beam dump system.
(10) Development of a remote maintenance and remote handling systems.
(11) Operation, maintenance and improvement of BigRIPS separator system, RI-beam transport lines, and their related research instruments such as ZeroDegree spectrometer and so on.
(12) Experimental research using RI beams.

Members

Team Leader
Koichi YOSHIDA

Research & Technical Scientists
Yoshiyuki YANAGISAWA (Senior Research Scientist)
Masao OHTAKE (Senior Technical Scientist)
Naohito INABE (Senior Technical Scientist)

Nishina Center Research Scientists
Hiroyuki TAKEDA
Naoki FUKUDA
Kensuke KUSAKA

Contract Researchers
Toshiyuki SUMIKAMA
Yohei SHIMIZU
Hiroshi SUZUKI

Postdoctoral Researchers
Deuk Soon AHN
Zeren KORKULU

Research Consultant
Hidekazu KUMAGAI

Part-time Worker
Tetsuro Komatsubara

Senior Visiting Scientist
Jerry NOLEN (Argonne National Lab.)

Visiting Scientists

Daisuke KAMEDA (TOSHIBA Corp.)
Michael A. FAMIANO (Western Michigan Univ.)
Daniel Pierre BAZIN (NSCL, MSU)
Oleg Borisovich TARASOV (NSCL, MSU)
Hans GEISSEL (GSI)
David Joseph MORRISSEY (NSCL, MSU)
Bradley Marc SHERRILL (NSCL, MSU)
Martin Alfred WINKLER (GSI)
Mauricio PORTILLO (NSCL, MSU)
Alan Matthew AMTHOR (Bucknell Univ.)
Tuomas Arne Santeri GRAHN (Univ. of Jyvaskyla)
Alfredo ESTRADE VAZ (Central Michigan Univ.)
Yutaka MIZOI (Osaka Elec.-Com. Univ.)
Naohito IWASA (Tohoku Univ.)
Sadao MOMOTA (Kochi Univ. of Tech.)
Kazuo IEKI (Rikkyo Univ.)

Student Trainees

Daichi MURAI (Rikkyo Univ.)
Ha JEONGSU (Seoul National Univ.)
Kousei ASADA (Tohoku Univ.)
Junki AMANO (Rikkyo Univ.)
Takahiro SAKAKIBARA (Tohoku Univ.)
Shunki ISHIKAWA (Tohoku Univ.)

List of Publications & Presentations

Publications

[Journal]

(Original Papers) *Subject to Peer Review

B. Blank, T. Goigoux, P. Ascher, M. Gerbaux, J. Giovinazzo, S. Grévy, T. Kurtukian Nieto, C. Magron, J. Agramunt, A. Algora, V. Guadilla, A. Montaner-Piza, A. I. Morales, S. E. A. Orrigo, B. Rubio, D. S. Ahn, P. Doornenbal, N. Fukuda, N. Inabe, G. Kiss, T. Kubo, S. Kubono, S. Nishimura, V. H. Phong, H. Sakurai, Y. Shimizu, P.-A. Söderström, T. Sumikama, H. Suzuki, H. Takeda, J. Wu, Y. Fujita, M. Tanaka, W. Gelletly, P. Aguilera, F. Molina, F. Diel, D. Lubos, G. de Angelis, D. Napoli, C. Borcea, A. Boso, R. B. Cakirli, E. Ganioglu, J. Chiba, D. Nishimura, H. Oikawa, Y. Takei, S. Yagi, K. Wimmer, G. de France, and S. Go, "New neutron-deficient isotopes from ^{78}Kr fragmentation", Physical Review C93, 061301(R), (2016).*

A. Jungclaus, A. Gargano, H. Grawe, J. Taprogge, S. Nishimura, P. Doornenbal, G. Lorusso, Y. Shimizu, G. S. Simpson, P.-A. Söderström, T. Sumikama, Z. Y. Xu, H. Baba, F. Browne, N. Fukuda, R. Gernhäuser, G. Gey, N. Inabe, T. Isobe, H. S. Jung, D. Kameda, G. D. Kim, Y.-K. Kim, I. Kojouharov, T. Kubo, N. Kurz, Y. K. Kwon, Z. Li, H. Sakurai, H. Schaffner, K. Steiger, H. Suzuki, H. Takeda, Zs. Vajta, H. Watanabe, J. Wu, A. Yagi, K. Yoshinaga, S. Bönig, L. Coraggio, J.-M. Daugas, F. Drouet, A. Gadea, S. Ilieva, N. Itaco, T. Kröll, A. Montaner-Pizá, K. Moschner, D. Mücher, H. Nishibata, A. Odahara, R. Orlandi, and A. Wendt, "First observation of γ rays emitted from excited states south-east of ^{132}Sn: The $\pi g^{-1}_{9/2} \otimes \nu f_{7/2}$ multiplet of $^{132}In_{83}$", Physical Review C93, 041301(R), (2016).*

R. Lozeva, H. Naïdja, F. Nowacki, J. Dudek, A. Odahara, C.-B. Moon, S. Nishimura, P. Doornenbal, J.-M. Daugas, P.-A. Söderström, T. Sumikama, G. Lorusso, J. Wu, Z. Y. Xu, H. Baba, F. Browne, R. Daido, Y. Fang, T. Isobe, I. Kojouharov, N. Kurz, Z. Patel, S. Rice, H. Sakurai, H. Schaffner, L. Sinclair, H. Watanabe, A. Yagi, R. Yokoyama, T. Kubo, N. Inabe, H. Suzuki, N. Fukuda, D. Kameda, H. Takeda, D. S. Ahn, D. Murai, F. L. Bello Garrote, F. Didierjean, E. Ideguchi, T. Ishigaki, H. S. Jung, T. Komatsubara, Y. K. Kwon, P. Lee, C. S. Lee, S. Morimoto, M. Niikura, H. Nishibata, and I. Nishizuka, "New isomer found in $^{140}_{51}Sb_{89}$: Sphericity and shell evolution between N=82 and N=90", Physical Review C93, 014316, (2016).*

N. Kobayashi, T. Nakamura, Y. Kondo, J. A. Tostevin, N. Aoi, H. Baba, R. Barthelemy, M. A. Famiano, N. Fukuda, N. Inabe, M. Ishihara, R. Kanungo, S. Kim, T. Kubo, G. S. Lee, H. S. Lee, M. Matsushita, T. Motobayashi, T. Ohnishi, N. A. Orr, H. Otsu, T. Sako, H. Sakurai, Y. Satou, T. Sumikama, H. Takeda, S. Takeuchi, R. Tanaka, Y. Togano, and K. Yoneda, "One-neutron removal from ^{29}Ne: Defining the lower limits of the island of inversion", Physical Review C93, 014613, (2016).*

A. Jungclaus, H. Grawe, S. Nishimura, P. Doornenbal, G. Lorusso, G. S. Simpson, P.-A. Söderström, T. Sumikama, J. Taprogge, Z. Y. Xu, H. Baba, F. Browne, N. Fukuda, R. Gernhäuser, G. Gey, N. Inabe, T. Isobe, H. S. Jung, D. Kameda, G. D. Kim, Y.-K. Kim, I. Kojouharov, T. Kubo, N. Kurz, Y. K. Kwon, Z. Li, H. Sakurai, H. Schaffner, Y. Shimizu, K. Steiger, H. Suzuki, H. Takeda, Zs. Vajta, H. Watanabe, J. Wu, A. Yagi, K. Yoshinaga, G. Benzoni, S. Bönig, K. Y. Chae, L. Coraggio, J.-M. Daugas, F. Drouet, A. Gadea, A. Gargano, S. Ilieva, N. Itaco, F. G. Kondev, T. Kröll, G. J. Lane, A. Montaner-Pizá, K. Moschner, D. Mücher, F. Naqvi, M. Niikura, H. Nishibata, A. Odahara, R. Orlandi, Z. Patel, Zs. Podolyák, and A. Wendt, "β decay of semi-magic ^{130}Cd: Revision and extension of the level scheme of ^{130}In", Physical Review C94, 024303, (2016).*

I. Čeliković, M. Lewitowicz, R. Gernhäuser, R. Krücken, S. Nishimura, H. Sakurai, D.S. Ahn, H. Baba, B. Blank, A. Blazhev, P. Boutachkov, F. Browne, G. de France, P. Doornenbal, T. Faestermann, Y. Fang, N. Fukuda, J. Giovinazzo, N. Goel, M. Górska, S. Ilieva, N. Inabe, T. Isobe, A. Jungclaus, D. Kameda, Y.-K. Kim, Y. K. Kwon, I. Kojouharov, T. Kubo, N. Kurz, G. Lorusso, D. Lubos, K. Moschner, D. Murai, I. Nishizuka, J. Park, Z. Patel, M. Rajabali, S. Rice, H. Schaffner, Y. Shimizu, L. Sinclair, P.-A. Söderström, K. Steiger, T. Sumikama, H. Suzuki, H. Takeda, Z. Wang, H. Watanabe, J. Wu, and Z. Xu, "New Isotopes and Proton Emitters–Crossing the Drip Line in the Vicinity of ^{100}Sn", Physical Review Letters 116, 162501, (2016).*

Y. Kondo, T. Nakamura, R. Tanaka, R. Minakata, S. Ogoshi, N. A. Orr, N. L. Achouri, T. Aumann, H. Baba, F. Delaunay, P. Doornenbal, N. Fukuda, J. Gibelin, J. W. Hwang, N. Inabe, T. Isobe, D. Kameda, D. Kanno, S. Kim, N. Kobayashi, T. Kobayashi, T. Kubo, S. Leblond, J. Lee, F. M. Marqués, T. Motobayashi, D. Murai, T. Murakami, K. Muto, T. Nakashima, N. Nakatsuka, A. Navin, S. Nishi, H. Otsu, H. Sato, Y. Satou, Y. Shimizu, H. Suzuki, K. Takahashi, H. Takeda, S. Takeuchi, Y. Togano, A. G. Tuff, M. Vandebrouck, and K. Yoneda, "Nucleus ^{26}O: A Barely Unbound System beyond the Drip Line", Physical Review Letters 116, 102503, (2016).*

K. Kisamori, S. Shimoura, H. Miya, S. Michimasa, S. Ota, M. Assie, H. Baba, T. Baba, D. Beaumel, M. Dozono, T. Fujii, N. Fukuda, S. Go, F. Hammache, E. Ideguchi, N. Inabe, M. Itoh, D. Kameda, S. Kawase, T. Kawabata, M. Kobayashi, Y. Kondo, T. Kubo, Y. Kubota, M. Kurata-Nishimura, C. S. Lee, Y. Maeda, H. Matsubara, K. Miki, T. Nishi, S. Noji, S. Sakaguchi, H. Sakai, Y. Sasamoto, M. Sasano, H. Sato, Y. Shimizu, A. Stolz, H. Suzuki, M. Takaki, H. Takeda, S. Takeuchi, A. Tamii, L. Tang, H. Tokieda, M. Tsumura, T. Uesaka, K. Yako, Y. Yanagisawa, R. Yokoyama, and K. Yoshida, "Candidate Resonant Tetraneutron State Populated by the ^{4}He(^{8}He,^{8}Be) Reaction", Physical Review Letters 116, 052501, (2016).*

T. Goigoux, P. Ascher, B. Blank, M. Gerbaux, J. Giovinazzo, S. Grévy, T. Kurtukian Nieto, C. Magron, P. Doornenbal, G. G. Kiss, S. Nishimura,

P.-A. Söderström, V. H. Phong, J. Wu, D. S. Ahn, N. Fukuda, N. Inabe, T. Kubo, S. Kubono, H. Sakurai, Y. Shimizu, T. Sumikama, H. Suzuki, H. Takeda, J. Agramunt, A. Algora, V. Guadilla, A. Montaner-Piza, A. I. Morales, S. E. A. Orrigo, B. Rubio, Y. Fujita, M. Tanaka, W. Gelletly, P. Aguilera, F. Molina, F. Diel, D. Lubos, G. de Angelis, D. Napoli, C. Borcea, A. Boso, R. B. Cakirli, E. Ganioglu, J. Chiba, D. Nishimura, H. Oikawa, Y. Takei, S. Yagi, K. Wimmer, G. de France, S. Go, and B. A. Brown, “Two-Proton Radioactivity of ^{67}Kr”, Physical Review Letters 117, 162501, (2016).*

Z. Patel, Zs. Podolyák, P.M. Walker, P.H. Regan, P.-A. Söderström, H. Watanabe, E. Ideguchi, G.S. Simpson, S. Nishimura, F. Browne, P. Doornenbal, G. Lorusso, S. Rice, L. Sinclair, T. Sumikama, J. Wu, Z.Y. Xu, N. Aoi, H. Baba, F.L. Bello Garrote, G. Benzoni, R. Daido, Zs. Dombrádi, Y. Fang, N. Fukuda, G. Gey, S. Go, A. Gottardo, N. Inabe, T. Isobe, D. Kameda, K. Kobayashi, M. Kobayashi, T. Komatsubara, I. Kojouharov, T. Kubo, N. Kurz, I. Kuti, Z. Li, H.L. Liu, M. Matsushita, S. Michimasa, C.-B. Moon, H. Nishibata, I. Nishizuka, A. Odahara, E. Şahin, H. Sakurai, H. Schaffner, H. Suzuki, H. Takeda, M. Tanaka, J. Taprogge, Zs. Vajta, F.R. Xu, A. Yagi, R. Yokoyama, ”Decay spectroscopy of ^{160}Sm: The lightest four-quasiparticle *K* isomer”, Physics Letter B753, 182, (2016).*

H. Wang, H. Otsu, H. Sakurai, D.S. Ahn, M. Aikawa, P. Doornenbal, N. Fukuda, T. Isobe, S. Kawakami, S. Koyama, T. Kubo, S. Kubono, G. Lorusso, Y. Maeda, A. Makinaga, S. Momiyama, K. Nakano, M. Niikura, Y. Shiga, P.-A. Söderström, H. Suzuki, H. Takeda, S. Takeuchi, R. Taniuchi, Ya. Watanabe, Yu. Watanabe, H. Yamasaki, K. Yoshida, ”Spallation reaction study for fission products in nuclear waste: Cross section measurements for ^{137}Cs and ^{90}Sr on proton and deuteron”, Physics. Letter B754, 104, (2016).*

H. Watanabea, G.X. Zhang, K. Yoshida, P.M. Walker, J.J. Liu, J. Wu, P.H. Regan, P.-A. Söderström, H. Kanaoka, Z. Korkulu, P.S. Lee, S. Nishimura, A. Yagi, D.S. Ahn, T. Alharbi, H. Baba, F. Browne, A.M. Bruce, R.J. Carroll, K.Y. Chae, Zs. Dombradi, P. Doornenbal, A. Estrade, N. Fukuda, C. Griffin, E. Ideguchi, N. Inabe, T. Isobe, S. Kanaya, I. Kojouharov, F.G. Kondev, T. Kubo, S. Kubono, N. Kurz, I. Kuti, S. Lalkovski, G.J. Lane, C.S. Lee, E.J. Lee, G. Lorusso, G. Lotay, C.-B. Moon, I. Nishizuka, C.R. Nita, A. Odahara, Z. Patel, V.H. Phong, Zs. Podolyák, O.J. Roberts, H. Sakurai, H. Schaffne, C.M. Shand, Y. Shimizu, T. Sumikama, H. Suzuki, H. Takeda, S. Terashima, Zs. Vajta, J.J. Valiente-Dóbon, Z.Y. Xu, “Long-lived *K* isomer and enhanced *γ* vibration in the neutron-rich nucleus ^{172}Dy: Collectivity beyond double midshell”, Physics Letter B760, 641, (2016).*

Y. Toganoa, T. Nakamura, Y. Kondo, J.A. Tostevin, A.T. Saito, J. Gibelin, N.A. Orr, N.L. Achouri, T. Aumann, H. Baba, F. Delaunay, P. Doornenbal, N. Fukuda, J.W. Hwang, N. Inabe, T. Isobe, D. Kameda, D. Kanno, S. Kim, N. Kobayashi, T. Kobayashi, T. Kubo, S. Leblond, J. Lee, F.M. Marqués, R. Minakata, T. Motobayashi, D. Murai, T. Murakami, K. Muto, T. Nakashima, N. Nakatsuka, A. Navin, S. Nishi, S. Ogoshi, H. Otsu, H. Sato, Y. Satou, Y. Shimizu, H. Suzuki, K. Takahashi, H. Takeda, S. Takeuchi, R. Tanaka, A.G. Tuff, M. Vandebrouck, K. Yoneda, “Interaction cross section study of the two-neutron halo nucleus ^{22}C”, Physics Letter B761, 412, (2016).*

P.-A. Söderström, P.M. Walker, J. Wu, H.L. Liu, P.H. Regan, H. Watanabe, P. Doornenbal, Z. Korkulu, P. Lee, J.J. Liu, G. Lorusso, S. Nishimura, V.H. Phong, T. Sumikama, F.R. Xu, A. Yagi, G.X. Zhang, D.S. Ahn, T. Alharbi, H. Baba, F. Browne, A.M. Bruce, R.J. Carroll, K.Y. Chae, Zs. Dombradi, A. Estrade, N. Fukuda, C.J. Griffin, E. Ideguchi, N. Inabe, T. Isobe, H. Kanaoka, S. Kanaya, I. Kojouharov, F.G. Kondev, T. Kubo, S. Kubono, N. Kurz, I. Kuti, S. Lalkovski, G.J. Lane, E.J. Lee, C.S. Lee, G. Lotay, C.-B. Moon, I. Nishizuka, C.R. Niţă, A. Odahara, Z. Patel, Zs. Podolyák, O.J. Roberts, H. Sakurai, H. Schaffner, C.M. Shand, H. Suzuki, H. Takeda, S. Terashima, Zs. Vajta, J.J. Valiente-Dòbon, Z.Y. Xu, “*K*-mixing in the doubly mid-shell nuclide ^{170}Dy and the role of vibrational degeneracy”, Physics Letter. B762, 404, (2016).*

J. Taprogge, A. Jungclaus, H. Grawe, I. N. Borzov, S. Nishimura, P. Doornenbal, G. Lorusso, G. S. Simpson, P. -A. Söderström, T. Sumikama, Z. Y. Xu, H. Baba, F. Browne, N. Fukuda, R. Gernhäuser, G. Gey, N. Inabe, T. Isobe, H. S. Jung, D. Kameda, G. D. Kim, Y. -K. Kim, I. Kojouharov, T. Kubo, N. Kurz, Y. K. Kwon, Z. Li, H. Sakurai, H. Schaffner, Y. Shimizu, K. Steiger, H. Suzuki, H. Takeda, Zs. Vajta, H. Watanabe, J. Wu, A. Yagi, K. Yoshinaga, G. Benzoni, S. Bönig, K. Y. Chae, L. Coraggio, J. -M. Daugas, F. Drouet, A. Gadea, A. Gargano, S. Ilieva, N. Itaco, F. G. Kondev, T. Kröll, G. J. Lane, A. Montaner-Pizá, K. Moschner, D. Mücher, F. Naqvi, M. Niikura, H. Nishibata, A. Odahara, R. Orlandi, Z. Patel, Zs. Podolyák, and A. Wendt, “Proton-hole and core-excited states in the semi-magic nucleus $^{131}In_{82}$”, European Physics Journal A 52, 347, (2016).*

[Proceedings]

(Original Papers) *Subject to Peer Review

T. Kubo, “Recent progress of in-flight separators and rare isotope beam production”, Nuclear Instruments & Methods B 376, 102 (2016).*

T.Sumikama, D.S. Ahn, N. Fukuda, N. Inabe, T. Kubo, Y. Shimizu, H. Suzuki, H. Takeda, N. Aoi, D. Beaumel, K. Hasegawa, E. Ideguchi, N. Imai, T. Kobayashi, M. Matsushita, S. Michimasa, H. Otsu, S. Shimoura, T. Teranishi, ”First test experiment to produce the slowed-down RI beam with the momentum-compression mode at RIBF”, Nuclear Instruments & Methods B 376, 180 (2016).*

Oral Presentations

[International Conference etc.]

K. Yoshida, ”Preset Status of the target and beam dump system at BigRIPS fragment separator”, The 6th High Power targetry Workshop, Oxford, UK, April 11 – 15, 2016.

Z. Korkulu, ”ANSYS code calculations of the beam spot temperature at BigRIPS separator”, The 6th High Power targetry Workshop, Oxford, UK, April 11 – 15, 2016.

N. Fukuda, "Operational Experiences with BigRIPS”, 6th Fragment Separator Expert Meeting, Grand Rapids, MI, USA, August 30 – September 1, 2016.

H. Suzuki, ”Ion optics development-1 (high resolution PID mode)”, 6th Fragment Separator Expert Meeting, Grand Rapids, MI, USA, August 30 – September 1, 2016.

H. Takeda, "Ion optical developments at BigRIPS -Additive and Subtractive Modes”, 6th Fragment Separator Expert Meeting, Grand Rapids, MI, USA, August 30 – September 1, 2016.

K. Yoshida, ”High-power Issues: Status and Simulations”, 6th Fragment Separator Expert Meeting, Grand Rapids, MI, USA, August 30 – September 1, 2016.

Y. Shimizu, ”Production yields and cross sections at the BigRIPS separator”, 6th Fragment Separator Expert Meeting, Grand Rapids, MI, USA, August 30 – September 1, 2016.

Y. Shimizu, ”New isotope search in the EURICA campaign at RIKEN RIBF”, EURICA Celebration and Collaboration Meeting, RIKEN, Wako, Saitama, Japan, September 6, 2016.

[Domestic Conference]

小山俊平, 大津秀暁, 清水陽平, 米田健一郎, 佐藤広海, 本林透, 西村美月, 銭廣十三, 櫻井博儀, 武内聡, 磯部忠昭, 馬場秀忠, 日下健祐, 大西純一, 笹野匡紀, P. Doornenbal, 福田直樹, 小林俊雄, 炭竈聡之, 松田洋平, 佐藤義輝, J. Hwang, 近藤洋介, 中村隆司, 梅野泰宏, 南方亮吾, 生越駿, 村上哲也, 中塚徳継, J. Gibelin, L. Sylvain, 新倉潤, 小林信之, H. Liu, J. Lee, E. Nikolskii, 坂口聡志, D. Beaumel, 「不変質量法を用いた ^{16}C のクラスター状態の研究」, 日本物理学会　第 71 回年次大会(2016), 東北学院大学、宮城県、3/19 – 22, 2016.

市川雄一, 高峰愛子, 西畑洸希, 今村慧, 藤田朋美, 佐藤智哉, 籾山悟至, 清水陽平, D.S.Ahn, 旭耕一郎, 馬場秀忠, D.L.Balabanski, F.Boulay, J.M.Daugas, 江上魁, 福田直樹, 舟山智歌子, 古川武, G.Georgiev, A.Gladkov, 稲辺尚人, 石橋陽子, 小林義男, 小島修一郎, A.Kusoglu, 川口高史, 河村嵩之, I.Mukul, 新倉潤, 西坂太志, 小田原厚子, 大友祐一, D.Ralet, 下田正, G.S.Simpson, 炭竈聡之, 鈴木宏, 竹田浩之, L.C.Tao, 梅野泰宏, 富永大樹, 上野秀樹, 山崎展樹, X.F.Yang, 「中性子過剰核 ^{75}Cu のアイソマー状態の核磁気モーメント」, 日本物理学会　第 71 回年次大会(2016), 東北学院大学、宮城県、3/19 – 22, 2016.

武内聡, 四方瑞紀, 中村隆司, 梅野泰宏, 近藤洋介, 坪田潤一, 尾崎友志, 齊藤敦美, 大津秀暁, Wang He, 渡辺幸信, 川瀬頌一郎, ImPACT-RIBF コラボレーション, 「クーロン分解反応による ^{107,108}Pd および ^{93,94}Zr の光吸収断面積」, 日本物理学会　第 71 回年次大会(2016), 東北学院大学、宮城県、3/19 – 22, 2016.

阿部康志, 山口由高, 上坂友洋, 小沢顕, 洲嵜ふみ, 山口貴之, 若杉昌徳, 稀少 RI リングコラボレーション,「稀少 RI リングの性能評価」, 日本物理学会　第 71 回年次大会(2016), 東北学院大学、宮城県、3/19 – 22, 2016.

T. L. Tang, S. Kawase, T. Uesaka, D. Beaumel, M. Dozono, T. Fujii, N. Fukada, T. Fukunaga, A. Galinda-Uribarri, S. H. Hwang, N. Inabe, D. Kameda, T. Kawahara, W. Y. Kim, K. Kisamori, M. Kobayashi, T. Kubo, Y. Kubota, K. Kusaka, C. S. Lee, Y. Maeda, H. Matsubara, S. Michimasa, H. Miya, T. Noro, A. Obertelli, S. Ota, E. Padilla-Rodal, S. Sakaguchi, H. Sakai, M. Sasano, S. Shimoura, S. S. Stepanyan, H. Suzuki, M. Takaki, H. Takeda, H. Tokieda, T. Wakasa, T. Wakui, K. Yako, Y. Yanagisawa, J. Yasuda, R. Yokoyama, K. Yoshia, and J. Zenihiro, "Quasi-free proton knockout of ^{23,25}F", 日本物理学会　第 71 回年次大会(2016), 東北学院大学、宮城県、3/19 – 22, 2016.

村井大地, 家城和夫, 久保敏幸, 稲辺尚人, 福田直樹, 竹田浩之, 鈴木宏, 安得順, 清水陽平, 佐藤広海, 佐藤優樹, 日下健祐, 柳澤善行, 大竹政雄, 吉田光一, 大津秀暁, 岩佐直仁, 中村隆司, Oleg B. Tarasov, Brad M. Sherrill, Dave J. Morrissey, Hans Geissel, 「大強度 ^{48}Ca ビームを用いた中性子ドリップライン探索 II」, 日本物理学会　第 71 回年次大会(2016), 東北学院大学、宮城県、3/19 – 22, 2016.

清川裕, 道正新一郎, 小林幹, 西村太樹, 横山輪, 小林和馬, 水上淳, 笈川浩之, 馬場秀忠, G.P.A. Berg, 堂園昌伯, 福田直樹, 古野達也, 井手口栄治, 稲辺尚人, 川畑貴裕, 川瀬頌一郎, 木佐森慶一, 久保敏幸, 久保田悠樹, 李清秀, 松下昌史, 宮裕之, 永倉弘康, 大田晋輔, 酒井英行, 下浦享, A. Stolz, 鈴木宏, 高木基伸, 竹田浩之, 武内聡, 時枝紘史, 上坂友洋, 矢向謙太郎, 山口勇貴, 柳澤善行, 吉田光一, 「SHARAQ における中性子過剰 ^{Sc} 近傍核の核異性体 γ 線分光」, 日本物理学会　第 71 回年次大会(2016), 東北学院大学、宮城県、3/19 – 22, 2016.

安田淳平, 笹野匡紀, R.G.T. Zegars, 馬場秀明, W. Chao, 福田直樹, 稲辺尚人, 磯部忠明, G. Jhang, 亀田大輔, 久保敏幸, 西村美月, E. Milman, 本林透, 大津秀暁, V. Panin, W. Powell, 酒井英行, 酒向正巳, 佐藤広海, 清水陽平, L. Stuhl, 鈴木宏, S. Tangwancharoen, 竹田浩之, 上坂友洋, 米田健一郎, 銭廣十三, 小林俊雄, 炭竈聡之, 田高義, 中村隆司, 近藤洋介, 梅野泰宏, 四方瑞紀, 坪田潤一, 矢向謙太郎, 下浦享, 大田晋輔, 川瀬頌一郎, 久保田悠樹, 高木基伸, 道正新一郎, 木佐森慶一, 李清秀, 時枝紘史, 堂園昌伯, 小林幹, 小山俊平, 小林信之, 若狭智嗣, 坂口聡, A. Krasznahorkay, 村上哲也, 中塚徳継, 金子雅紀, 松田洋平, D. Mucher, S. Reichert, D. Bazin, J.W. Lee, 「^{132}Sn(p,n)反応によるガモフテラー遷移の研究」、日本物理学会　第 71 回年次大会(2016), 東北学院大学、宮城県、3/19 – 22, 2016.

尾崎友志, 中村隆司, 武内聡, 近藤洋介, 梅野泰宏, 四方瑞紀, 坪田潤一, 齊藤敦美, 大津秀暁[A], 王赫[A], 渡辺幸信[B], 他 ImPACT-RIBF コラボレーション, 「^{238}U の飛行核分裂によって生成される ^{107}Pd,^{79}Se のアイソマー比」, 日本物理学会　第 71 回年次大会(2016), 東北学院大学、宮城県、3/19 – 22, 2016.

秋枝智美, 関口仁子, 和田泰敬, 江藤大二朗, 渡邉跡武, 今紘史, 坂本成彦, 酒井英行, 上坂友洋, 鈴木宏, 柳澤善行, 堂園昌伯, 久保田悠樹, 若狭智嗣, 坂口聡志, 安田淳平, 進藤佑輔, 田端心海, 大倉綾華, 前田幸重, 川上駿介, 山本達也, Evgeniy Milman, Sergey Chebotaryov, 「186.6 MeV/nucleon 重陽子-陽子弾性散乱における重陽子偏極分解能測定と三体力」, 日本物理学会　第 71 回年次大会(2016), 東北学院大学、宮城県、3/19 – 22, 2016.

小林幹, 道正新一郎, 清川裕, 馬場秀忠[A], G.P.A. Berg[B], 堂園昌伯, 福田直樹[A], 古野達也[C], 井手口栄治[D], 稲辺尚人[A], 川畑貴裕[C], 川瀬頌一郎, 木佐森慶一, 小林和馬[E], 久保敏幸[A], 久保田悠樹, 李清秀, 松下昌史, 宮裕之, 水上淳[F], 永倉弘康[E], 西村太樹[F], 笈川浩之[F], 大田晋輔, 酒井英行[A], 下浦享, A. Stolz[G], 鈴木宏[A], 高木基伸, 竹田浩之[A], 武内聡[A], 時枝紘史, 上坂友洋[A], 矢向謙太郎, 山口勇貴[E], 柳澤善行[A], 横山輪, 吉田光一, 「飛行時間法を用いた中性子数 34 近傍 Ca 同位体の質量測定」, 日本物理学会　2016 年秋季大会, 宮崎大学、宮崎県、9/21 – 24, 2016.

横山輪, 井手口栄治, G. Simpson, 田中まな, 西村俊二, P. Doornenbal, P-A Söderström, G. Lorusso, Z. Y. Xu, J. Wu, 炭竈聡之, 青井考, 馬場秀忠, F. Bello, F. Browne, 大道理恵, Y. Fang, 福田直樹, G. Gey, 郷慎太郎, 稲辺尚人, 磯部忠昭, 亀田大輔, 小林和馬, 小林幹, 小松原哲郎, 久保敏幸, I. Kuti, Z. Li, 松下昌史, 道正新一郎, C.-B. Moon, 西畑洸希, 西塚一平, 小田原厚子, Z. Patel, S. Rice, Sahin, L. Sinclair, 鈴木宏, 竹田浩之, J. Taprogge, E. Z. Vajta, 渡邉寛, 八木彩祐未, 「中性子過剰 Nd 同位体の変形進化における十六重極変形の効果」, 日本物理学会　2016 年秋季大会, 宮崎大学、宮崎県、9/21 – 24, 2016.

RIBF Research Division
Research Instruments Group
SAMURAI Team

1. Abstract

In collaboration with research groups in and outside RIKEN, the team designs, develops and constructs the SAMURAI spectrometer and relevant equipment that are and will be used for reaction experiments using RI beams at RI Beam Factory. The SAMURAI spectrometer consists of a large superconducting dipole magnet and a variety of detectors to measure charged particles and neutrons. After the commissioning experiment in March 2012, the team prepared and conducted, in collaboration with researchers in individual experimental groups, the first series of experiments with SAMURAI in May 2012. Then, several numbers of experiments were well performed until now utilizing the property of SAMURAI. The team also provides basis for research activities by, for example, organizing collaboration workshops by researchers who are interested in studies or plan to perform experiments with the SAMURAI spectrometer.

2. Major Research Subjects

Design, operation, maintenance and improvement of the SAMURAI spectrometer and its related research instruments. Support and management for SAMURAI-based research programs.

3. Summary of Research Activity

The current research subjects are summarized as follows:

(1) Operation, maintenance and improvement of a large superconducting dipole magnet that is the main component of the SAMURAI spectrometer
(2) Design, development and construction of various detectors that are used for nuclear reaction experiments using the SAMURAI spectrometer.
(3) Preparation for planning experiments using SAMURAI spectrometer.
(4) Maintenance and improvement of the SAMURAI beam line.
(5) Formation of a collaboration platform called "SAMURAI collaboration"

Members

Team Leader
Hideaki OTSU

List of Publications & Presentations

Publications

[Journal]

(Original Papers)

J.W. Hwang, S. Kim, Y. Satou, N.A. Orr, Y. Kondo, T. Nakamura, J. Gibelin, N.L. Achouri, T. Aumann, H. Baba, F. Delaunay, P. Doornenbal, N. Fukuda, N. Inabe, T. Isobe, D. Kameda, D. Kanno, N. Kobayashi, T. Kobayashi, T. Kubo, S. Leblond, J. Lee, F.M. Marqués, R. Minakata, T. Motobayashi, D. Murai, T. Murakami, K. Muto, T. Nakashima, N. Nakatsuka, A. Navin, S. Nishi, S. Ogoshi, H. Otsu, H. Sato, Y. Shimizu, H. Suzuki, K. Takahashi, H. Takeda, S. Takeuchi, R. Tanaka, Y. Togano, A.G. Tuff, M. Vandebrouck, K. Yoneda,"Single-neutron knockout from 20C and the structure of 19C", Phys. Lett. B 769, 503 (2017).

Y. Togano, T. Nakamura, Y. Kondo, J.A. Tostevin, A.T. Saito, J. Gibelin, N.A. Orr, N.L. Achouri, T. Aumann, H. Baba, F. Delaunay, P. Doornenbal, N. Fukuda, J.W. Hwang, N. Inabe, T. Isobe, D. Kameda, D. Kanno, S. Kim, N. Kobayashi, T. Kobayashi, T. Kubo, S. Leblond, J. Lee, F.M. Marqués, R. Minakata, T. Motobayashi, D. Murai, T. Murakami, K. Muto, T. Nakashima, N. Nakatsuka, A. Navin, S. Nishi, S. Ogoshi, H. Otsu, H. Sato, Y. Satou, Y. Shimizu, H. Suzuki, K. Takahashi, H. Takeda, S. Takeuchi, R. Tanaka, A.G. Tuff, M. Vandebrouck,K. Yoneda, "Interaction cross section study of the two-neutron halo nucleus 22C", Phys. Lett. B 761, 412 (2016).

Y. Kondo, T.Nakamura, R.Tanaka, R.Minakata, S.Ogoshi, N.A.Orr, N.L.Achouri, T.Aumann, H.Baba, F.Delaunay, P.Doornenbal, N.Fukuda, J.Gibelin, J.W.Hwang, N.Inabe, T.Isobe, D.Kameda, D.Kanno, S.Kim, N.Kobayashi, T.Kobayashi, T.Kubo, S.Leblond, J.Lee, F.M.Marques, T.Motobayashi, D.Murai, T.Murakami, K.Muto, T.Nakashima, N.Nakatsuka, A.Navin, S.Nishi, H.Otsu, H.Sato, Y.Satou, Y.Shimizu, H.Suzuki, K.Takahashi, H.Takeda, S.Takeuchi, Y.Togano, A.G.Tuff, M.Vandebrouck, K.Yoneda, " Nucleus 26O: A Barely Unbound System beyond the Drip Line", Phys. Rev. Lett 116, 102503 (6pages) (2016).

H. Otsu, S. Koyama, N. Chiga, T. Isobe, T. Kobayashi, Y. Kondo, M. Kurokawa, W.G. Lynch, T. Motobayashi, T. Murakami, T. Nakamura, M. Kurata-Nishimura, V. Panin, H. Sato, Y. Shimizu, H. Sakurai, M.B. Tsang, K. Yoneda, H. Wang, "SAMURAI in its operation phase for RIBF", NIMB 376, (2016), 175-179.

J. Yasuda, M. Sasano, R.G.T. Zegers, H. Baba, W. Chao, M. Dozono, N. Fukuda, N. Inabe, T. Isobe, G. Jhang, D. Kameda, T. Kubo, M. Kurata-Nishimura, E. Milman, T. Motobayashi, H. Otsu, V. Panin, W. Powell, H. Sakai, M. Sako, H. Sato, et al., "Inverse kinematics (p,n) reactions studies using the WINDS slow neutron detector and the SAMURAI spectrometer",NIMB 376 (2016), 393-396.

T. Nakamura, Y. Kondo, "Large acceptance spectrometers for invariant mass spectroscopy of exotic nuclei and future developments", NIMB 376 (2016), 156-161.

(Review)
T. Motobayashi, "Study of weakly bound nuclei at RIKEN RIBF”, Few-Body Systems 57, 337-341 (2016).
(Proceedings)
S. Sakaguchi, T. Uesaka, T. Wakui, S. Chebotaryov, T. Kawahara, S. Kawase, E. Milman, T. L. Tang, K. Tateishi and T. Teranishi, “Studies of Unstable Nuclei with Spin-Polarized Proton Target”, International Journal of Modern Physics 40, 1660071 (2016).
L. Stuhl et al., A New Low-energy Plastic Scintillation Neutron Detector For Real Time Pulse Shape Discrimination, PoS Proceeding of Science (INPC2016) 085 (2017).

Oral Presentations

[International Conference etc.]
T. Nakamura, (Invited) “Weakly bound and unbound nuclei near the neutron drip line“, INPC2016, 11-16, Sep, 2016, Adelaide, Australia
T.Nakamura, (Invited) “Recent Experiments and Perspectivefs of SAMURAI“, RIBF Users Meeting 2016, 8-9, Sep, 2016, Wako, Saitama
T.Nakamura, (Invited) “Spectroscopy of weakly bound and unbound nuclei“, Physics beyond the limits of stability: exploring the contiunum, 17-21, Oct.,2016, ECT*, Trento, Italy
T.Nakamura, (Invited) “Nuclear structure near and beyond the neutron drip line“, 1st Tsukuba-CCS-RIKEN joint workshop on microscopic theories of nuclear structure and dynamics, 12-16, Dec., 2016, Wako, Saitama
T.Nakamura, (Invited) “Neutron-star matter and related physics studied by neutron-rich nuclei“, International Symposium on Neutron Star Matter (NSMAT2016), 21-23, Nov.,2016, Sendai
T.Nakamura, (Invited) “Structure of neutron drip-line nuclei probed by breakup reactions“, APPC-APC 4-8,Dec.,2016, Brisbane, Australia
T.Nakamura, (Invited) “Structure of nuclei along and beyond the neutron drip line“, ESNT Workshop on Dynamics of highly unstable exotic light nuclei and few-body systems 30,Jan-3,Feb,2017, ESNT, Saclay, France
Y.Kondo, (Invited) “Experimental study of 25-28O with SAMURAI“, Direct Reactions with Exotic Beams (DREB2016)11-15,Jul.,2016, Halifax, Canada
M. Sasano et al., (Invited) "Study of Gamow-Teller transitions from 132Sn via the (p,n) reaction", ECT* workshop " Unraveling the complexity of nuclear systems: single-particle and collective aspects through the looking glass", Torento Italy, February 10 to 17, 2017.
M. Sasano et al., (Invited) "Gamow-Teller giant resonances in 132Sn", Advances in Radioactive Isotope Science (ARIS) 2017, Keystone CO US, May 28 to June 2, 2017.
Y. Kubota, (Invited) “Two-neutron correlation in Borromean nuclei via the quasi-free (p,pn) reaction”, in ESNT Workshop, Dynamics of highly unstable exotic light nuclei and few-body systems (Saclay, France, 2017)
Y. Kondo, “Recent experimental studies using SAMURAI at RIBF”, Current Activities and Future Prospects on Unstable Nuclei: Japan-Korea Exchange Program (JPS meeting), Tohoku gakuin University, 21, March, 2016
Y. Kondo, “Experimental study of unbound oxygen isotopes beyond the drip line”, International Workshop on "Critical Stability in Few-Body Systems", RIKEN, 4 Feb, 2016
Y. Kubota, “Study on neutron-neutron correlation in Borromean nucleus 11Li via the quasi-free (p,pn) reaction”, in International Nuclear Physics Conference (INPC2016) (Adelaide, Australia, 2016).
Y. Kubota, “Probing neutron-neutron correlation in Borromean nuclei via the quasi-free (p,pn) reaction”, in SAMURAI International Collaboration Workshop 2016 (Fukuoka, Japan, 2016).
Y. Kubota, “Study of neutron-neutron correlation in Borromean nucleus 11Li via the (p,pn) reaction”, in Direct Reactions with Exotic Beams (DREB2016) (Halifax, Canada, 2016).
Y. Kubota, “Direct measurement of two neutron correlation in 11Li via the (p,pn) reaction”, in International Workshop on “Critical Stability in Few-Body Systems” (Saitama, Japan, 2016).
S. Chebotaryov, S. Sakaguchi, et.al., “Elastic scattering of neutron-rich 6He nuclei from polarized protons at 200 A MeV”, 22nd International Spin Symposium, University of Illinois, 27 September 2016.
S. Sakaguchi, S. Chebotaryov, et.al., ”Polarized proton target at SAMURAI: Elastic scattering of 6He from polarized proton”, SAMURAI International Collaboration Workshop 2016, Kyushu University, 5 September 2016.
M. Sasano et al., “Study of Gamow-Teller transitions from 132Sn via the inverse kinematics (p,n) reaction”, The 26th International Nuclear Physics Conference (INPC2016) Adelaide, Australia, 2016.
L. Stuhl et al., A new low-energy plastic scintillation neutron detector for real time pulse shape discrimination, The 26th International Nuclear Physics Conference (INPC2016) Adelaide, Australia, 2016.
Yasuhiro Togano, ‘Reaction cross section of the two-neutron halo nucleus 22C at 235 MeV/nucleon’, INPC2016, September 2016, Adelaide, Australia
S. Koyama, H. Otsu, et.al, “Cluster structure on neutron rich nuclei 16C”, 11th international Conference on Clustering Aspects of Nuclear Structure and Dynamics, 23rd May 2016, Naples, Italy
S. Koyama, H. Otsu, et.al., “Study of cluster structure in 16C via α inelastic scattering”, Direct Reactions with Exotic Beams, 15th July 2016, Halifax, Canada
M. Kurata-Nishimura, “SpRIT-TPC experiments at RIKEN 2016”, Transport 2017, 2017/3/27 -30, MSU/FRIB, USA
M. Kurata-Nishimura, “First Experiments with The SpRIT-TPC at SAMURAI in RIKEN-RIBF”, 新学術領域「中性子星核物質」第 5 回ウィンタースクール・研究会「中性子星の核物質」, 2017/2/16-18, Fukushima, Japan
M. Kurata-Nishimura, “First Experiment with the SPiRIT-TPC”, The 26th International Nuclear Physics Conference, 2016/9/11-16, Adelaide, Australia
M. Kurata-Nishimura, “Preliminary results of SPiRIT-TPC experiment at RIBF-SAMURAI”, The 14th International Symposium on Nuclei in the Cosmos XIV, 2016/6/19 – 24, Niigata, Japan
Z. Yang, "Status and Results of SAMURAI018", 5th Sunflower workshop, Hongkong China 2016, Sep.18-20
Z. Yang, “Study on the cluster structure in nuclei using direct reactions”, Cluster 2016, Napoli Italy 2016, May 23-27

[Domestic Conference]

梅野泰宏, “γ-ray detector CATANA and E1 response of n-rich Ca isotopes”, 梅野泰宏, 宇宙核物理連絡協議会 研究会, 2016 年 2 月 国立天文台

梅野泰宏, “新γ線検出器 CATANA”, 日本物理学会第 71 回年次大会, 2016 年 3 月 東北学院大学

Y, Togano, ”Study of nuclear astrophysics by Coulomb dissociation”, MOTO16, June 2016, Rikkyo Univ.

梅野泰宏, “22C 反応断面積の高統計測定”, 日本物理学会 2016 年秋季大会, 2016 年 9 月 宮崎大学

梅野泰宏, “中性子過剰核の E1 応答と新γ線検出器 CATANA”, 新学術領域「中性子星核物質」第 5 回ウィンタースクール, 2017 年 2 月, 福島

Y. Kubota, (Invited) , ”Two-neutron correlation in Borromean nuclei via the quasi-free (p,pn) reaction”, 日本物理学会第 72 回年次大会シンポジウム New aspects of direct reactions in probing exotic nuclei, 2017 年 2 月大阪大学豊中キャンパス

久保田悠樹, “ボロミアン核(p,pn)反応を用いた二中性子運動量相関の研究”, 日本物理学会第 71 回年次大会 東北学院大学 泉キャンパス, 2016 年 3 月 東北学院大学泉キャンパス

小山俊平, 大津秀暁, 他, “不変質量法を用いた 16C のクラスター状態の研究”, 日本物理学会年次大会春季, 2016 年 3 月 20 日, 仙台

小山俊平, 大津秀暁, 他, “16C のクラスター構造”, 日本物理学会年次大会春季, 2017 年 3 月 18 日, 大阪

齋藤岳志, 千賀信幸, 田村陸, 宇佐見正志, 樋口諒, 大津秀暁, “SAMURAI 実験における陽子検出器 NINJA の開発状況”,日本物理学会年次大会, 2016 年 3 月 21 日 仙台

齋藤敦美、中村隆司、近藤洋介他, “反跳陽子のトラッキングを用いた高分解能中性子検出器の開発”,日本物理学会 第７２回年次大会 2017 年 3 月 17 日–20 日, 大阪府豊中市 大阪大学

平山晃大、中村隆司、武内聡他 “79Se,80Se のクーロン分解反応” 日本物理学会 第７２回年次大会 2017 年 3 月 17 日-21 日, 大阪府豊中市 大阪大学

斗米貴人、中村隆司、梅野泰宏他, “分解反応を用いた 31Ne の核分光”,日本物理学会 第７２回年次大会 2017 年 3 月 17 日-22 日, 大阪府豊中市 大阪大学

山田啓貴、中村隆司、梅野泰宏、近藤洋介他“不安定核反応実験のためのγ線検出器アレーCATANA の性能評価”,日本物理学会 第７３回年次大会 2017 年 3 月 17 日–23 日, 大阪府豊中市 大阪大学

安田昌弘、近藤洋介、中村隆司他, “中性子ドリップライン近傍のフッ素・ネオン同位体のインビームガンマ線核分光”,日本物理学会 第７４回年次大会, 2017 年 3 月 17 日–24 日, 大阪府豊中市 大阪大学

近藤洋介 "中性子ドリップラインを超えた領域での酸素同位体の不変質量核分光", 基研研究会「核力に基づく核構造、核反応物理の展開」, 2017 年 3 月 27 日–29 日,京都府京都市 京都大学

Posters Presentations

[International Conference etc.]

L. Stuhl et al., "PANDORA, a large volume low-energy neutron detector with real-time neutron-gamma discrimination", Advances in Radioactive Isotope Science (ARIS) 2017, Keystone CO US, May 28 to June 2, 2017.

Doctoral Dissertation

J. Yasuda, "Study of Gamow-Teller transitions from 132Sn via the (p,n) reaction in inverse kinematics", PhD thesis, Kyushu University, March 2017.

Y. Kubota, "Neutron-neutron correlation in Borromean nucleus 11Li via the (p,pn) reaction", PhD thesis, University of Tokyo, March 2017.

Master Thesis

S. Koyama, “不変質量法を用いた 16C のクラスター状態の研究 Study for cluster states in 16C via invariant mass method, 2016”, 東京大学

坪田 潤一 26F の不変質量核分光, 東京工業大学

尾崎友志 三中性子非束縛系 27O の核分光, 東京工業大学

齊藤敦美 ダイニュートロン相関探索に向けた高分解能中性子検出器 HIME の開発, 東京工業大学

Bachelor Thesis

斗米 貴人 不安定核反応実験のための大立体角中性子検出器の性能評価, 東京工業大学

平山 晃大 荷電フラグメントの粒子識別用ホドスコープの開発, 東京工業大学

安田昌弘 中性子ドリップライン近傍のフッ素・ネオン核の線核分光, 東京工業大学

山田啓貴 不安定核反応実験のためのγ線検出器アレーCATANA の性能評価, 東京工業大学

RIBF Research Division
Research Instruments Group
Computing and Network Team

1. Abstract

This team is in charge of development, management and operation of the computing and network environment, mail and information servers and data acquisition system and management of the information security of the RIKEN Nishina Center.

2. Major Research Subjects

(1) Development, management and operation of the general computing servers
(2) Development, management and operation of the mail and information servers
(3) Development, management and operation of the data acquisition system
(4) Development, management and operation of the network environment
(5) Management of the information security

3. Summary of Research Activity

This team is in charge of development, management and operation of the computing and network environment, mail and information servers and data acquisition system and management of the information security. The details are described elsewhere in this progress report.

(1) Development, management and operation of the general computing servers

We are operating Linux/Unix NIS/NFS cluster system for the data analysis of the experiments and general computing. This cluster system consists of eight computing servers with 64 CPU cores and totally 200 TB RAID of highly-reliable Fibre-channel interconnection. Approximately 700 user accounts are registered on this cluster system. We are adopting the latest version of the Scientific Linux (X86_64) as the primary operating system, which is widely used in the accelerator research facilities, nuclear physics and high-energy physics communities in the world.

(2) Development, management and operation of the mail and information servers

We are operating RIBF.RIKEN.JP server as a mail/NFS/NIS server. This server is a core server of RIBF Linux cluster system. Postfix has been used for mail transport software and dovecot has been used for imap and pop services. These software packages enable secure and reliable mail delivery. Because six years have passed since the installation of this sever, we are preparing to replace the server and RAID file system. Sophos Email Security and Control (PMX) installed on the mail front-end servers which tags spam mails and isolates virus-infected mails. The probability to identify the spam is approximately 95-99%. We noticed that virus-infected mails were occasionally not detected by PMX in the case of new types of virus. Therefore, we added a new rule to PMX to isolate and remove executable image files attached in mail because they are often aimed at virus infection. As a result, most of the viruses in mails are successfully blocked by PMX. We are operating several information servers such as Web servers, Integrated Digital Conference (INDICO) server, Wiki servers, Groupware servers, Wowza streaming servers. An anonymous ftp server, FTP.RIKEN.JP , is managed and operated at the RNC. Major Linux distributions, including Scientific Linux, Ubuntu and CentOS, are mirrored daily for the convenience of their users and for facilitating high-speed access. An HP PloLiant DL-380G6 server was installed in 2009, and it is scheduled to be replaced by DL-380G9 in June 2017. Simultaneously, the OS will be upgraded from SL 5.11 to SL 7.3. We have been operating approximately 70 units of wireless LAN access points in RNC. Almost the entire radiation-controlled area of the East Area of RIKEN Wako campus is covered by wireless LAN for the convenience of experiments and daily work. Since the devices used for the Wireless LAN access points became obsolete, all of them were replaced by WAPM-1166D or WAPS-APG-600H in 2016, which supports the protocols of 802.11b, 11g, 11a, 11n, and 11ac.

(3) Development, management and operation of the data acquisition system

We have developed the standard data-acquisition system named as RIBFDAQ. This system can process up to 40 MB/s data. By using parallel readout from front-end systems, the dead time could be small. To synchronize the independent DAQ systems, the time stamping system has been developed. The resolution and depth of the time stamp are 10 ns and 48 bit, respectively. This time stamping system is very useful for beta decay experiments such as EURICA and BRIKEN projects. The current main task is the DAQ coupling, because detector systems with dedicated DAQ systems are transported to RIBF from foreign facilities. In case of SAMURAI Silicon (NSCL/TUM/WUSTL), the readout system is integrated into RIBFDAQ. The projects of MUST2 (GANIL), MINOS (CEA Saclay), NeuLAND (GSI) and TRB3 (TUM) cases, data taken by their DAQ systems are transferred to RIBFDAQ. For SPIRIT (RIKEN/GANIL/CEA Saclay/NSCL), RIBFDAQ is controlled from the NARVAL-GET system that is a large-scale signal processing system for the time projection chamber. EURICA (GSI), BRIKEN (GSI/Univ. Liverpool/IFIC) and VANDLE (UTK) projects, we adopt the time stamping system to use individual trigger for each detector system. In this case, data are merged in offline. In addition to the development DAQ system, we are developing intelligent circuits based on FPGA. Mountable Controller (MOCO) is a very fast readout controller for VME modules. General Trigger Operator (GTO) is an intelligent triggering NIM module. Functions of “common trigger management”, “gate and delay generator”, “scaler” are successfully implemented on GTO.

(4) Development, management and operation of the network environment

We have been managing the network environment collaborating with Advanced Center for Computing and Communications (ACCC). All the Ethernet ports of the information wall sockets are capable of the Gigabit Ethernet connection (10/100/1000BT). In addition, a 10 Gbps network port has been introduced to the RIBF Experimental area in for the high speed data transfer of RIBF experiment to ACCC in near future. Approximately 60 units of wireless LAN access points have been installed to cover the almost entire area of Nishina Center.

(5) Management of the information security

It is essential to take proper information security measures for information assets.
We are managing the information security of Nishina Center collaborating with ACCC.

Members

Team Leader

Takashi ICHIHARA (concurrent; Vice Chief Scientist, RI Physics Lab.)

Research & Technical Scientist

Yasushi WATANABE (concurrent; Senior Research Scientist, Radiation Lab.)

Nishina Center Research Scientist

Hidetada BABA

List of Publications & Presentations

Publications

[Journal]

(Original Papers) *Subject to Peer Review

Inclusive cross section and doulble helicity asymmetry for π^0 production in p+p collisions at $\sqrt{s}$ =510 GeV. By PHENIX Collaboration (A. Adare *et al.*). Phys. Rev. D 93 (2016), 011501(R)

e+e- pair production in Au+Au collisions at $\sqrt{s}$NN = 200 GeV A. By Adare *et al.* By PHENIX Collaboration (A. Adare *et al.*). Phys. Rev. C 93 (2016), 014904

Measurement of higher cumulants of net-charge multiplicity distributions in Au+Au collisions at $\sqrt{s_{NN}}$ = 7.7 to 200 GeV. By PHENIX Collaboration (A. Adare *et al.*). Phys. Rev. C 93 (2016), 011901(R)

Charged particle multiplicity and transverse energy production in heavy ion collisions spanning $\sqrt{s_{NN}}$ = 7.7 GeV to 200 GeV. By PHENIX Collaboration (A. Adare *et al.*). Phys. Rev. C 93 (2016), 024901

Nuclear matter effects on φ meson production in Cu+Au collisions at $\sqrt{s_{NN}}$ = 200 GeV. By PHENIX Collaboration (A. Adare *et al.*). Phys. Rev. C 93 (2016), 024904

System dependence of fractional momentum loss of high pT hadrons in relativistic heavy ion collisions. By PHENIX Collaboration (A. Adare *et al.*). Phys. Rev. C 93 (2016), 024911

System size dependence of the forward J/psi production in PHENIX. By PHENIX Collaboration (A. Adare *et al.*). Phys. Rev. C 93 (2016), 034903

Single electron yields from semileptonic charm and bottom hadron decays in Au+Au collisions at $\sqrt{s_{NN}}$ =200 GeV. By PHENIX Collaboration (A. Adare *et al.*). Phys. Rev. C 93 (2016), 034904

Measurement of parity violating spin asymmetries in $W^{\pm}$ production at mid-rapidity in longitudinally polarized p+p collisions at $\sqrt{s}$ =510 GeV By PHENIX Collaboration (A. Adare *et al.*). Phys. Rev. D 93 (2016), 051103(R)

Jet Production in d+Au Collisions at $\sqrt{s_{NN}}$ = 200 GeV. By PHENIX Collaboration (A. Adare *et al.*). Phys. Rev. Lett. 116 (2016), 122301

Measurements of identified particle higher harmonic flow in Au+Au collisions at $\sqrt{s_{NN}}$ =200GeV. By PHENIX Collaboration (A. Adare *et al.*). Phys. Rev. C 93 (2016), 051902(R)

Measurement of 1st, 2nd and 3rd azimuthal anisotropy in Cu+Au collisions. By PHENIX Collaboration (A. Adare *et al.*). Phys. Rev. C 94 (2016), 054910

Elliptical and triangular flow of soft direct photons in Au+Au collisions at $\sqrt{s_{NN}}$ =200 GeV. By PHENIX Collaboration (A. Adare *et al.*). Phys. Rev. C 94 (2016), 064901

J/ψ longitudinal double spin asymmetry measurement at forward rapidity in p+p collisions at $\sqrt{s}$ =510 GeV. By PHENIX Collaboration (A. Adare *et al.*). Phys. Rev. D 94 (2016), 112008

Oral Presentations

[International Conference etc.]

H. Baba, “Isospin character of low-energy dipole strength in 20O”, First Tsukuba-CCS-RIKEN joint workshop on microscopic theories of nuclear structure and dynamics, Saitama/Ibaraki, Japan, 12-16th December, 2016 (Invited)

H. Baba, “Status of experiments RIBF56 and RIBF64”, 5th SUNFLOWER Workshop, 18-20th September, 2016, Hong Kong, China, 2016

Posters Presentations

[International Conference etc.]

H. Baba, T. Ichihara, T. Ohnishi, K. Yoshida, Y. Watanabe, S. Ota, S. Shimoura, R. Yokoyama, S. Takeuchi, D. Nishimura and A. Tokiyasu, “Complete Parallel Readout VME DAQ System”, IEEE 20th Real Time Conference, 5-10th June, 2016

RIBF Research Division
Research Instruments Group
Detector Team

1. Abstract

This team is in charge of development, fabrication, and operation of various detectors used for nuclear physics experiments at RIBF. Our current main mission is maintenance and improvement of detectors which are used at BigRIPS separator and its succeeding beam lines for beam diagnosis and particle identification of RI beams. We are also engaged in R&D of new detectors that can be used for higher-intensity RI beams. In addition, we are doing the R&D which uses the pelletron accelerator together with other groups.

2. Major Research Subjects

Development, fabrication, and operation of various detectors for nuclear physics experiments, including beam-line detectors which are used for the production and delivery of RI beams (beam diagnosis and particle identification). R&D which uses the pelletron accelerator.

3. Summary of Research Activity

The current research subjects are summarized as follows:

(1) Maintenance and improvement of the beam-line detectors which are used at BigRIPS separator and its succeeding beam lines.
(2) Development of new beam-line detectors with radiation hardness and tolerance for higher counting rates
(3) Management of the pelletron accelerator and R&D which uses the pelletron

Members

Team Leader
Hiromi SATO

Research and Technical Scientist
Tokihiro IKEDA (Senior Research Scientist)

Special Temporary Employee
Manabu HAMAGAKI

Visiting Scientist
Takeshi KOIKE (Tohoku Univ.)

Student Trainee
Itaru HAKAMADA (Tokyo Univ.)

List of Publications & Presentations

Publications

[Journal]

(Original Papers) *Subject to Peer Review

R. Yokoyama, S. Go, D. Kameda, T. Kubo, N. Inabe, N. Fukuda, H. Takeda, H. Suzuki, K. Yoshida, K. Kusaka, K. Tanaka, Y. Yanagisawa, M. Ohtake, H. Sato, Y. Shimizu, H. Baba, M. Kurokawa, D. Nishimura, T. Ohnishi, N. Iwasa, A. Chiba, T. Yamada, E. Ideguchi, T. Fujii, H. Nishibata, K. Ieki, D. Murai, S. Momota, Y. Sato, JW. Hwang, S. Kim, O.B. Tarasov, D.J. Morrissey, B.M. Sherrill, G. Simpson, C.R. Praharaj, “New K isomers in the neutron-rich N=100 isotones Sm-162, Eu-163, and Gd-164”, Physical Review C 95, 034313 (2017). *

T. Ikeda, T.M. Kojima, Y. Natsume, J. Kimura, and T. Abe, “Stable transmission of slow highly charged ions through tapered glass capillary with active discharging method for sub-micron sized beams”, Applied Physics Letters 109, 133501 (2016). *

Y. Kazama, K. Ishii, W. Aonuma, T. Ikeda, H. Kawamoto, A. Koizumi, D. Filatov, M. Chibalina, R. Bergero, D. Charlesworth, T. Abe, and S. Kawano, “A new physical mapping approach refines the sex-determining gene positions on the Silene latifolia Y-chromosome”, Scientific Reports 6, 18917 (2016). *

S.J. Wickramarachchi, T. Ikeda, B.S. Dassanayake, D. Keerthisinghe, and J. A. Tanis, “Incident energy and charge deposition dependences of electron transmission through a microsized tapered glass capillary”, Nuclear Instruments and Methods in Physics Research Section B 82, 60 (2016). *

K. Ishii, Y. Kazama, R. Morita, T. Hirano, T. Ikeda, S. Usuda, Y. Hayashi, S. Ohbu, R. Motoyama, Y. Nagamura, and T. Abe, “Linear Energy Transfer-dependent Change in Rice Gene Expression Profile after Heavy-ion Beam Irradiation”, PLOS ONE 11 (7): e0160061 (2016).*

S.J. Wickramarachchi, T. Ikeda, B. S. Dassanayake, D. Keerthisinghe, and J. A. Tanis, “Electron-beam transmission through a micrometer-sized tapered-glass capillary: Dependence on incident energy and angular tilt angle”, Physical Review A 94, 022701 (2016). *

Oral Presentations

[International Conference etc.]

H. Sato : “Status of PID detectors at BigRIPS", Fragment Separator Expert Meeting 2016, (Amway Grand Plaza Hotel), Grand Rapids, USA, August (2016).

[Domestic Conference]

八木彩祐未, 小田原厚子, R. Lozeva, C. Moon, 方一帆, 大道理恵, 西畑洸希, 金岡裕志, P. Lee, 下田正, 西村俊二, P. Doornenbal, G. Lorusso, 炭竈聡之, 渡辺寛, P.S. derstrm, J. Wu, F. Brown, Z.Y. Xu, 横山輪, 磯部忠昭, 馬場秀忠, 櫻井博儀, 鈴木宏, 稲辺尚人, 亀田大輔, 福田直樹, 竹田浩之, 安得順, 清水陽平, 佐藤広海, 久保敏幸, 石垣知樹, 森本翔太, 井手口栄治, 小松原哲郎, 新倉潤, 西塚一平, C.S. Lee, and the EURICA collaborators: “中性子過剰な Xe 同位体における集団運動状態の系統的変化”, 日本物理学会第 72 回年次大会, (大阪大学), 大阪, 3 月 (2017).

小山俊平, 大津秀暁, 清水陽平, 米田健一郎, 佐藤広海, 本林透, 西村美月, 銭廣十三, 櫻井博儀, 武内聡, 磯部忠昭, 馬場秀忠, 日下健祐, 大西純一, 笹野匡紀, P. Doornenbal, 福田直樹, 小林俊雄, 炭竈聡之, 松田洋平, 佐藤義輝, J. Hwang, 近藤洋介, 中村隆司, 梅野泰宏, 南方亮吾, 生越駿, 村上哲也, 中塚徳継, J. Gibelin, L. Sylvain, 新倉潤, 小林信之, H. Liu, J. Lee, E. Nikolskii, 坂口聡志, D. Beaumel: “16C のクラスター構造”, 日本物理学会第 72 回年次大会, (大阪大学), 大阪, 3 月 (2017).

池田時浩, 小島隆夫, 夏目好夫, 木村純, 阿部知子: “電極付きガラスキャピラリー光学系による低速マイクロイオンビーム安定供給のためのアクティブ放電法”, ビーム物理研究会 2016, (SPring-8), 佐用郡佐用町, 11 月 (2016).

池田時浩, 小島隆夫, 夏目好夫, 木村純, 阿部知子: “ Active discharging method for stable transmission of ion beams through tapered glass capillary optics”, 第 17 回「イオンビームによる表面・界面解析」特別研究会, (京都府立大学), 京都市, 12 月 (2016).

池田時浩, 小島隆夫, 夏目好夫, 木村純, 阿部知子: “ ガラスキャピラリーによる低速多価イオンビームのサブミクロン化と安定供給のためのアクティブガイディング”, 原子衝突学会第 41 回年会, (富山大学), 富山市, 12 月 (2016).

池田時浩, 小島隆夫, 夏目好夫, 木村純, 阿部知子: “ 高機能ガラスキャピラリー光学系による低速多価イオンマイクロビームの安定供給”, 日本物理学会第 72 回年次大会, (大阪大学), 豊中市, 3 月 (2017).

池田時浩, 小島隆夫, 夏目好夫, 木村純, 阿部知子: “招待講演: キャピラリマイクロイオンビームの放射線生物学応用”, 平成 28 年度弥生研究会「量子ビームの技術と利用」, (東京大学), 東海村, 3 月 (2017).

RIBF Research Division
Accelerator Applications Research Group

1. Abstract

This group promotes various applications of ion beams from RI Beam Factory (RIBF). Radiation Biology Team studies various biological effects of fast heavy ions and develops new technology to breed plants and microbes by heavy-ion irradiations. RI Applications Team studies production and application of radioisotopes for various research fields, development of trace element analysis and its application, and development of chemical materials for ECR ion sources of RIBF accelerators.

2. Major Research Subjects

Research and development in biology, chemistry and materials science utilizing heavy-ion beams from RI Beam Factory.

3. Summary of Research Activity

(1) Biological effects of fast heavy ions.
(2) Research and development of heavy-ion breeding.
(3) RI application researches
(4) Research and development of RI production technology at RIBF.
(5) Developments of trace elements analyses.
(6) Development of chemical materials for ECR ion sources of RIBF accelerators.

Members

Group Director
Tomoko ABE

RIBF Research Division
Accelerator Applications Research Group
Ion Beam Breeding Team

1. Abstract

Ion beam breeding team studies various biological effects of fast heavy ions. It also develops new technique to breed plants and microbes by heavy-ion irradiations. Fast heavy ions can produce dense and localized ionizations in matters along their tracks, in contrast to photons (X rays and gamma rays) which produce randomly distributed isolated ionizations. These localized and dense ionization can cause double-strand breaks of DNA which are not easily repaired and result in mutation more effectively than single-strand breaks. A unique feature of our experimental facility at the RIKEN Ring Cyclotron (RRC) is that we can irradiate living tissues in atmosphere since the delivered heavy-ion beams have energies high enough to penetrate deep in matter. This team utilizes a dedicated beam line (E5B) of the RRC to irradiate microbes, plants and animals with beams ranging from carbon to iron. Its research subjects cover physiological study of DNA repair, genome analyses of mutation, and development of mutation breeding of plants by heavy-ion irradiation. Some new cultivars have already been brought to the market.

2. Major Research Subjects

(1) Study on the biological effects by heavy-ion irradiation
(2) Study on the molecular nature of DNA alterations induced by heavy-ion irradiation
(3) Innovative applications of heavy-ion beams

3. Summary of Research Activity

We study biological effects of fast heavy ions from the RRC using 135A MeV C, N, Ne ions, 95A MeV Ar ions, 90A MeV Fe ions and from the IRC using 160A MeV Ar ions. We also develop breeding technology of microbes and plants. Main subjects are:

(1) Study on the biological effects by heavy-ion irradiation

Heavy-ion beam deposits a concentrated amount of dose at just before stop with severely changing the linear energy transfer (LET). The peak of LET is achieved at the stopping point and known at the Bragg peak (BP). It is well known to be good for cancer therapy to adjust the BP to target malignant cells. On the other hand, a uniform dose distribution is a key to the systematic study for heavy-ion mutagenesis, and thus to the improvement of the mutation efficiency. Therefore plants and microbes are treated using ions with stable LET. We investigated the effect of LET ranging from 23 to 640 keV/μm, on mutation induction using dry seeds of the model plants *Arabidopsis thaliana*. The most effective LET (LETmax) was 30 keV/μm. LETmax irradiations showed the same mutation rate as that by chemical mutagens, which typically cause high mutation rate. The LETmax of imbibed rice (*Oryza sativa* L.) seeds, dry rice seeds and dry wheat (*Triticum monococcum*) seeds were shown to be 50-63 keV/μm, 23-30 keV/μm and 50 keV/μm, respectively. In the case of microbe (*Mesorhizobium lothi*), the results showed a higher incidence of deletion mutations for Fe ions at 640 KeV/μm than for C ions at 23-40 keV/μm. Thus, the LET is an important factor to be considered in heavy-ion mutagenesis.

(2) Study on the molecular nature of DNA alterations induced by heavy-ion irradiation

Detailed analyses on the molecular nature of DNA alterations have been reported as an LET-dependent effect for induced mutation. The most mutations were deletions ranging from a few to several tens of base pairs (bp) in the *Arabidpsis thaliana* mutants induced by irradiation with C ions at 30 keV/μm and rice mutants induced by irradiation with C ions at 50 keV/μm or Ne ions at 63 keV/μm. LETmax is effective for breeding because of its very high mutation frequency. Since most mutations are small deletions, these are sufficient to disrupt a single gene. Thus, irradiation can efficiently generate knockout mutants of a target gene, and can be applied to reverse genetics. On the other hand, irradiation with Ar ions at 290 keV/μm showed a mutation spectrum different from that at LETmax: the proportion of small deletions (<1 kbp) was low, while that of large deletions ranging from several to several tens of kbp, and rearrangements was high. Many genes in the genome (> 10%) are composed of tandem duplicated genes that share functions. For knockout of the tandem duplicated genes, large deletions are required, and the appropriate deletion size is estimated to be around 5-10 kbp and 10-20 kbp based on the gene density in *Arabidpsis* and rice, respectively. No method is currently available to efficiently generate deletion mutants of this size. As such, higher LET irradiation is promising as a new mutagen suitable for the functional analysis of tandem duplicated genes.

(3) Innovative application of heavy-ion beams

We have formed a consortium for ion-beam breeding. It consisted of 24 groups in 1999, in 2016, it consisted of 173 groups from Japan and 10 from overseas. Breeding was performed previously using mainly flowers and ornamental plants. We have recently put a new Japanese barnyard millet cultivar with low amylose content and short culm, 'Nebarikko No. 2' on the market. Beneficial variants have been grown for various plant species, such as high yield rice, semi-dwarf early rice, semi-dwarf buckwheat, semi-dwarf barley, hypoallergenic peanut, spineless oranges, non-flowering Eucalyptus and lipids-hyperaccumulating unicellular alga. We collaborate with Miyagi prefecture and Tohoku University to breed salt-resistant lines in the more delicious commercial rice varieties, 'Hitomebore' and 'Manamusume'. Imbibed seeds were irradiated with the LETmax (C-ions) on 16 April, 2011. We isolated 73 candidate lines of salt-resistant mutants from 719 M_2 progenies grown in the saline paddy field in Tohoku University in 2012. From these, we selected 12 salt-resistant M_3 lines in 2013, 4 M_4 lines in 2014 and one M_5 line in 2015. The target of heavy-ion breeding is extended from flowers to crops like grains so that it will contribute to solve the global problems of food and environment.

Members

Team Leader
Tomoko ABE (concurrent: Group Director, Accelerator Applications Research Gr.)

Research & Technical Scientist
Kazuhide TSUNEIZUMI (Senior Research Scientist)
Masako IZUMI (Senior Research Scientist)
Teruyo TSUKADA (Senior Research Scientist)
Tokihiro IKEDA (concurrent)
Katsunori ICHINOSE (Senior Technical Scientist)
Hiroshi ABE (Senior Technical Scientist)
Ryouhei MORITA (Technical Scientist)

Contract Researchers
Hiroyuki ICHIDA
Yusuke KAZAMA

Postdoctoral Researcher
Kotaro ISHII

Technical Staff I
Yoriko HAYASHI
Yuki SHIRAKAWA

Technical Staff II
Sumie OHBU

Research Consultants
Masahiro MII

Part-time Workers
Hideo TOKAIRIN
Sachiko KOGURE
Taeko WAKANA
Mieko YAMADA
Haruka WATANABE (Aug.15 – Sep. 12, 2016)
Hitomi TAMURA (Aug.15 – Sep. 12, 2016)

Visiting Scientist
Makoto FUJIWARA (Univ. of Tokyo)
Masao WATANABE (Tohoku Univ.)
Hisashi TSUJIMOTO (Tottori Univ.)
Yutaka MIYAZAWA (Tohoku Univ.)
Toshinari GODO (Flower & Garden Bank)
Masanori TOMITA (CRIEPI)
Toshikazu MORISHITA (Nat'l. Inst. Agric. Res.)
Koji MURAI (Fukui Pref. Univ.)
Hinako TAKEHISA (Nat'l. Inst. Agric. Sci.)
Akiko HOKURA (Tokyo Denki Univ.)
Norihiro OHTSUBO (Kyoto Pref. Univ.)
Eitaro FUKATSU (Forestry and Forest Products Res. Inst.)
Tomonari HIRANO (Univ. of Miyazaki)
Yoichi SATO (Riken Food Co., Ltd.)
Ali FERJANI (Tokyo Gakugei Univ.)
Katsutomo SASAKI (Nat'l Agric. and Food Res. Org.)
Kunio SUZUKI (Technoflora, Co., Ltd.)
Kazumitsu MIYOSHI (Chiba. Univ.)
Makoto UBUKATA (Hokkaido Univ.)
Tadashi SATO (Tohoku Univ.)
Takeshi YAMAKI (Riken Vitamin Co., Ltd.)

Visiting Technicians
Takuji YOSHIDA (Takii Seed Co., Ltd.)
Daisuke SAITO (Riken Food Co., Ltd.)
Keiji IKEDA (KK SeaAct)

Research Fellows
Naoji WAKITA (Wadomari Cho Agr. Exp. Station)
Tadahito OOTUBO (Wadomari Cho Agr. Exp. Station)
Shunsuke IMANISHI (Natl. Inst.Veg. and Tea Sci.)
Tomihiro TAKESHITA (Wadomari Cho)
Yoshiharu TAKE (Wadomari Cho)
Hiroshi ASATO (Wadomari Cho)
Kenji OOYOSHI (Wadomari Cho)
Hironari UCHIDA (Saitama Pref. Res. Inst.)

Student Trainees
Yu IMAMURA (Tokyo Denki Univ.)
Kazuki TAKANASHI (Tokyo Denki Univ.)
Yoshihiro TAKAHASHI (Kitazato Univ.)
Takuya NISHINOBO (Tokyo Denki Univ.)
Koichi NAMBU (Tokyo Denki Univ.)
Naoko HIROSE (Tokyo Denki Univ.)

List of Publications & Presentations

Publications

[Journal]

(Original Papers) *Subject to Peer Review

遠藤幸子, 齋藤裕太郎, 阿部篤智, 野口協一, 新野清, 西村幸一, 酒井友幸, 高橋由信, 阿部知子: “ショクヨウギク新品種 ‘山園 K4 号’ の育成”, 山形県農業研究報告 **8**, 93-102 (2016). *

Kato M., Masamura N., Shono J., Okamoto D., Abe T., Imai S.: “Production and characterization of tearless and non-pungent onion”, SCIENTIFIC REPORTS **6**, Article No. 23779 (2016). *

Yamada K., Kazama Y., Mitra S., Marukawa Y., Arashida R., Abe T., Ishikawa T., Suzuki K.: “Production of a thermal stress resistant mutant Euglena gracilis strain using Fe-ion beam irradiation”, Bioscience, Biotechnology, and Biochemistry **80**, 1650-1656 (2016). *

Sato Y., Hirano T., Niwa K., Suzuki T., Fukunishi N., Abe T., Kawano S.: “Phenotypic differentiation in the morphology and nutrient uptake kinetics among Undaria pinnatifida cultivated at six sites in Japan”, Journal of Applied Phycology **28**, 3447-3458 (2016). *

Yamada K., Suzuki H., Takeuchi T., Kazama Y., Mitra S., Abe T., Goda K., Suzuki K., Iwata O.: “Efficient selective breeding of live oil-rich Euglena gracilis with fliorescence-actived cell sorting”, SCINTIFIC REPORTS **6**, Article No. 26327 (2016). *

Ishii K., Kazama Y., Hirano T., Hamada M., Ono Y., Yamada M., Abe T.: “AMAP: A pipeline for whole-genome mutation detection in *Arabidopsis thaliana*”, Genes & Genetics Systems **91**, 229-233(2016).*

Ishii K., Kazama Y., Morita R., Hirano T., Ikeda T., Usuda S., Hayashi Y., Ohbu S., Ikeda R., Nakamura Y., Abe T.: “Linear Energy Transfer-Dependent Change in Rice Gene Expression Profile after Heavy-Ion Beam Irradiation”, PLOS ONE **11**, e0160061 (2016). *

Ikeda T., Kojima T., Natsume Y., Kimura J., Abe T.: “Stable transmission of slow highly charged ions through tapered glass capillary with active discharging method for sub-micron sized beams”, Applied Physics Letters **109**, Article No. 133501 (2016). *

Morita R., Nakagawa M., Takehisa H., Hayashi Y., Ichida H., Usuda S., Ichinose K., Abe H., Shirakawa Y., Sato T., Fujiwara T. M., Itoh D.R., Abe T.: “Heavy-ion beam mutagenesis identified an essential gene for chloroplast development under cold stress conditions during both early growth and tillering stages in rice”, Bioscience, Biotechnology, and Biochemistry **81**, .271-282 (2016). *

Grasso R., Abe T., Cirrone A.P. G., Cuttone G., Gulino M., Musumeci F., Romeno F., Ryuto H., Scordino A.: “Effects of Ion Irradiation on Seedings Growth Monitored by Ultraweak Delayed Luminescence”, PLOS ONE **11**, Article No. e0167998 (2016). *

澤田倫平, 平野智也, 飯牟禮和彦, 阿部知子, 尾崎行生: “レタス(*Luctuca sativa L.*)プロトプラストへのイオンビーム照射によって出現した低ポリフェノールオキシターゼ活性を示す突然変異体”, 園芸学研究 **15**, 347-353 (2016). *

Ueno Y., Aikawa S., Niwa K., Abe T., Murakami A., Kondo A., Akimoto S.: “Variety in excitation energy transfer processes from phycobilisomes to photosystems I and II”, Photosynthesis Research, doi: 10. 1007/s11120-017-0345-3 (2017). *

(Review)

阿部知子, 林依子: “重イオンビームを用いた品種改良技術の開発とサクラ新品種の育成”, FB News **469**, 2-6(2016).

阿部知子: “古典園芸植物の復活を目指して”, エネルギーレビュー **36**, 25 (2016).

風間裕介, 石井公太郎, 阿部知子: “植物巨大 Y 染色体の遺伝子地図作成に成功―Y 染色体は進化の過程で大きな逆位を起こしていた”, 生物の科学 遺伝 **70**, 394-397 (2016)

風間裕介, 平野智也, 大田修平, 佐藤陽一, 村井耕二, 河野重行, 小野克徳, 阿部知子: “重イオンビーム育種によるグリーンイノベーションの創出”, 作物研究 **61**, 73-79 (2016)

阿部知子: “植物に出されたパズルに挑戦し、新たな花を創る”, NL だより **469**, 1(2017).

佐藤陽一, 阿部知子, 福西暢尚: “三陸ワカメ養殖における品種改良と複数回養殖に関する技術開発”, 水産学シリーズ **184** 新技術開発による東日本大震災からの復興・再生, 53-66 (2017).

[Others]

福西暢尚, 佐藤陽一, 市田裕之, 阿部知子, 平野智也: “三陸における特産海藻類の品種改良技術開発と新品種育成に関する拠点形成”, 日本水産学会誌, **82**, 160 (2016). *

Oral Presentations

(Domestic Conference)

久村麻子, 峯大樹, 阿部知子, 林依子, 平野智也: “奇形花の発生が少ない夏秋輪ギク「白涼」の育成”, イオンビーム育種研究会第 11 回大会, 福井, 5 月 (2016).

阿部知子: “未来をつくる七つ道具 イオンビームってなあに?”, イオンビーム育種研究会第 11 回大会, 福井, 5 月 (2016).

高城啓一, 畑下昌範, 平野智也, 風間裕介, 林依子, 塚田晃代, 阿部知子: “植物組織におけるイオンビーム照射後のγ-H2AX の分布と消長”, イオンビーム育種研究会第 11 回大会, 福井, 5 月 (2016).

石井公太郎, 平野智也, 風間裕介, 浜田道昭, 小野幸輝, 白川侑希, 大部澄江, 阿部知子: “重イオンビーム照射由来シロイヌナズナ変異体の全変異解析”, イオンビーム育種研究会第 11 回大会, 福井, 5 月 (2016).

佐藤陽一, 小野克徳, 平野智也, 市田裕之, 林依子, 福西暢尚, 阿部知子: “三陸産ワカメの品種改良と実用化”, イオンビーム育種研究会第 11 回大会, 福井, 5 月 (2016).

二羽恭介, 阿部知子: “養殖ノリの突然変異育種における効率的な選抜手法と高水温耐性株作出の試み”, 平成 28 年度日本水産学会秋季大会, 奈良, 9 月 (2016).

市田裕之, 森田竜平, 白川侑希, 林依子, 阿部知子: “イネゲノム/エキソーム解析による変異遺伝子の迅速同定と重イオンビーム誘発変異の解析”, 日本育種学会第 130 回講演会, 鳥取, 9 月 (2016).

阿部知子, 風間裕介, 市田裕之: “重イオンビーム品種改良技術の開発と変異体を用いた原因遺伝子解析”, 日本放射線影響学会 第 59 回大会, 広島, 10 月 (2016).

阿部知子, 市田裕之, 福西暢尚, 佐藤陽一, 平野智也: “重イオンビーム照射による三陸ワカメの品種改良”, DNA 鑑定学会第 9 回大会, 東京, 11 月 (2016).

池田時浩, 小島隆夫, 夏目好夫, 木村純, 阿部知子: “電極付きガラスキャピラリー光学系による低速マイクロイオンビーム安定供給のためのアクティブ放電法”, ビーム物理研究会 2016, 兵庫, 11 月 (2016).

Ikeda T., Kojima T., Natsume Y., Kimura J., Abe T.: “Active discharging method for stable transmission of ion beams through tapered glass capillary optics”, 第 17 回「イオンビームによる表面・界面解析」特別研究会, 京都, 12 月 (2016).

阿部知子: “加速器を利用した放射線育種による地域農業への貢献の展望”, 文部科学省主催アジア原子力協力フォーラム(FNCA)「持続可能な

農業のための放射線技術・放射線育種の応用に関する公開セミナー」, 福井, 12 月 (2016).
池田時浩, 小島隆夫, 夏目好夫, 木村純, 阿部知子: “高機能ガラスキャピラリー光学系による低速多価イオンマイクロビームの安定供給”, 日本物理学会第 72 回年次大会, 豊中, 3 月 (2017).
石川浩樹, 佐々木駿, 平野智也, 風間裕介, 阿部知子, 伊藤竜一, 藤原誠: “シロイヌナズナ葉緑体分裂異常変異体を用いた花粉発生過程における色素体増殖の解析”, 日本農芸化学会 2017 年度(平成 29 年度)大会, 京都, 3 月 (2017).
田中朋之, Rehenuma T., 阿部知子: “イネ突然変異系統 13-45 における白未熟粒発生機構の解析　第 3 報 : 温度応答性の定量的比較”, 第 243 回日本作物学会講演会, 東京, 3 月 (2017).
李鋒, 丹羽紗也佳, 西村宣之, 市田裕之, 森田竜平, 阿部知子, 加藤浩: “イネエキソーム解析によるガンマ線誘発突然変異の探索および原因遺伝子の迅速同定”, 日本育種学会第 131 回講演会, 名古屋, 3 月 (2017).
山谷浩史, 上妻馨梨, 中野道治, 林依子, 高見常明, 門田有希, 奥本裕, 坂本亘, 阿部知子, 草場信: “イネ stay-green 遺伝子 DCD1 の単離と機能解析”, 日本育種学会第 131 回講演会, 名古屋, 3 月 (2017).

Posters Presentations

(Domestic Conference)

石井公太郎, 風間裕介, 平野智也, 白川侑希, 大部澄江, 山田美恵子, 若菜妙子, 阿部知子: “重イオンビーム照射で作出したシロイヌナズナ巨大欠失変異体集団の形態と欠失領域の同定”, 日本植物形態学会第 28 回総会・大会, 沖縄, 9 月 (2016).
浅野円花, 大田修平, 山崎誠和, 石井公太郎, 風間裕介, 阿部知子, 河野重行: “微細藻類の核型解析 : クロレラゲノムの倍数化と重イオンビーム照射による染色体分断”, 日本植物形態学会第 28 回総会・大会, 沖縄, 9 月 (2016).
鈴木絢子, 清河ひかる, 郡司玄, 高橋和希, 浅岡真理子, 平野智也, 風間裕介, 阿部知子, 塚谷裕一, Ferjani A.: “det3-1 の矮小化は過剰なリグニン蓄積に起因するのか?”, 日本植物形態学会第 28 回総会・大会, 沖縄, 9 月 (2016).
風間裕介, 池田啓二, 彼谷邦光, 坂倉良男, 阿部知子: “放射線照射によるボトリオコッカスの浮揚現象”, 日本植物形態学会第 28 回総会・大会, 沖縄, 9 月 (2016).
風間裕介, 平野智也, 石井公太郎, 白川侑希, 大部澄江, 山田美恵子, 若菜妙子, 阿部知子: “シロイヌナズナの重イオンビーム欠失変異体集団を用いた必須染色体領域のマッピング”, 日本植物学会第 80 回大会, 沖縄, 9 月 (2016).
平野智也, 風間裕介, 石井公太郎, Vuong N. Q., 大部澄江, 國武久登, 阿部知子: “重イオンビーム照射由来シロイヌナズナ大輪変異体の全ゲノム変異解析”, 日本植物学会第 80 回大会, 沖縄, 9 月 (2016).
Suzuki J., Kiyokawa H., Gunji S., Takahashi K., Asaoka M., Hirano T., Kazama Y., Abe T., Tsukaya H., Ferjani A.: “The Whys and the Hows of flowering stem cracking: Evidenced by histological and genetic approaches”, 日本植物学会第 80 回大会, 沖縄, 9 月 (2016).
石井公太郎, 風間裕介, 平野智也, 山田美恵子, 大部澄江, 浜田道昭, 小野幸輝, 阿部知子: “変異検出パイプライン AMAP の開発と重イオンビームの全ゲノム変異スペクトラム解析”, 日本植物学会第 80 回大会, 沖縄, 9 月 (2016).
浅野円花, 大田修平, 山崎誠和, 石井公太郎, 風間裕介, 阿部知子, 河野重行: “クロレラゲノムの倍数化と重イオンビーム照射による染色体分断化と再構成”, 日本植物学会第 80 回大会, 沖縄, 9 月 (2016).
山谷浩史, 上妻馨梨, 中野道治, 林依子, 高見常明, 加藤裕介, 門田有希, 熊丸敏博, 奥本裕, 坂本亘, 阿部知子, 草場信: “イネ stay-green 突然変異体 dcd1 の分子遺伝学的解析”, 日本育種学会第 130 回講演会, 鳥取, 9 月 (2016).
林依子, 森田竜平, 一瀬勝紀, 臼田祥子, 白川侑希, 東海林英夫, 佐藤雅志, 阿部知子: “イネの種子含水率による重イオンビーム変異誘発の最適化”, 日本育種学会第 130 回講演会, 鳥取, 9 月 (2016).
森田竜平, 市田裕之, 白川侑希, 林依子, 臼田祥子, 一瀬勝紀, 東海林英夫, 佐藤雅志, 阿部知子: “イネ変異解析パイプラインによる重イオンビーム誘発突然変異の同定”, 日本育種学会第 130 回講演会, 鳥取, 9 月 (2016).
池田時浩, 小島隆夫, 夏目好夫, 木村純, 阿部知子: “ガラスキャピラリーによる低速多価イオンビームのサブミクロン化と安定供給のためのアクティブガイディング”, 原子衝突学会第 41 回年会, 富山, 12 月 (2016).
東條宏史, 中村あき, フェルジャニ アリ, 風間裕介, 阿部知子, 飯田秀利: “根の貫入が不可能な硬さの培地の表面で生き残れるシロイヌナズナ突然変異株のスクリーニング”, 第 58 回日本植物生理学会年会, 鹿児島, 3 月 (2017).
石井公太郎, 風間裕介, 森田竜平, 平野智也, 池田時浩, 臼田祥子, 林依子, 大部澄江, 本山立子, 長村吉晃, 阿部知子: “LET 依存的に変動するイネの遺伝子発現プロファイル”, 日本育種学会第 131 回講演会, 名古屋, 3 月 (2017).
森田竜平, 中川繭, 竹久妃奈子, 林依子, 市田裕之, 臼田祥子, 一瀬勝紀, 安部弘, 白川侑希, 東海林英夫, 佐藤雅志, 藤原誠, 伊藤竜一, 阿部知子: “重イオンビームで誘発したイネ温度感受性 virescent 変異体 csv1 の原因遺伝子同定と特性解析”, 日本育種学会第 131 回講演会, 名古屋, 3 月 (2017).

RIBF Research Division
Accelerator Applications Research Group
RI Applications Team

1. Abstract

The RI Applications Team develops production technologies of radioisotopes (RIs) at RIKEN RI Beam Factory (RIBF) for application studies in the fields of physics, chemistry, biology, engineering, medicine, pharmaceutical and environmental sciences. We use the RIs mainly for nuclear and radiochemical studies such as RI production and superheavy element chemistry. The purified RIs such as ^{65}Zn and ^{109}Cd are delivered to universities and institutes through Japan Radioisotope Association. We also develop new technologies of mass spectrometry for the trace-element analyses using accelerator technology and apply them to the research fields such as cosmochemistry, environmental science, archaeology and so on. We also develop chemical materials for ECR ion sources of heavy-ion accelerators in RIBF.

2. Major Research Subjects

(1) Research and development of RI production technology at RIBF
(2) RI application researches
(3) Development of trace element and isotope analyses and their applications to geoscience and environmental science
(4) Development of chemical materials for ECR ion sources of heavy-ion accelerators in RIBF

3. Summary of Research Activity

(1) Research and development of RI production technology at RIBF and RI application studies

Due to its high sensitivity, the radioactive tracer technique has been successfully applied for investigations of the behavior of elements in the fields of chemistry, biology, engineering, medicine, pharmaceutical and environmental sciences. We have been developing production technologies of useful radiotracers at RIBF and conducting their application studies in collaboration with many researchers in various fields. With 14-MeV proton, 24-MeV deuteron, and 50-MeV alpha beams from the AVF cyclotron, we presently produce about 40 radiotracers from ^{7}Be to ^{211}At. Among them, ^{65}Zn, ^{85}Sr, ^{88}Y, and ^{109}Cd are delivered to Japan Radioisotope Association for fee-based distribution to the general public in Japan. Our RIs are also distributed to researchers under the Supply Platform of Short-lived Radioisotopes for Fundamental Research, supported by the Ministry of Education, Culture, Sports, Science and Technology, Grant-in-Aid for Scientific Research on Innovative Areas. On the other hand, radionuclides of a large number of elements are simultaneously produced from metallic targets such as ^{nat}Ti, ^{nat}Ag, ^{nat}Hf, and ^{197}Au irradiated with a 135-MeV nucl.$^{-1}$ ^{14}N beam from the RIKEN Ring Cyclotron. These multitracers are also supplied to universities and institutes as collaborative researches.

In 2016, we developed production technologies of radioisotopes such as ^{28}Mg, ^{44m}Sc, ^{44}Ti, ^{48}Cr, ^{67}Cu, ^{75}Se, ^{88}Y, ^{121m}Te, ^{135m}Ba, and ^{211}At which were strongly demanded but lack supply sources in Japan. We also investigated the excitation functions for the ^{nat}Ti(α,x), ^{nat}Zn(d,x), ^{nat}Zn(α,x), ^{nat}Pd(d,x), ^{169}Tm(d,x), ^{nat}Lu(p,x), ^{nat}Lu(d,x), ^{nat}Ta(p,x), and ^{nat}Ta(d,x) reactions to quantitatively produce useful RIs. We used radiotracers of ^{61}Cu, ^{66}Ga, ^{69m}Zn, ^{88}Y, ^{99}Rh, and ^{139}Ce for application studies in chemistry, ^{67}Cu and ^{211}At in nuclear medicine, ^{88,89}Zr, ^{175}Hf, and ^{177}Ta in geochemistry, and ^{88}Zr and ^{121m}Te in environmental science. We also produced ^{65}Zn, ^{85}Sr, ^{88}Y, and ^{109}Cd for our scientific researches on a regular schedule and supplied the surpluses through Japan Radioisotope Association to the general public. In 2016, we accepted 5 orders of ^{65}Zn with a total activity of 24 MBq, 1 order of ^{85}Sr with 1 MBq, 2 orders of ^{88}Y with 2 MBq, and 2 orders of ^{109}Cd with 12 MBq. We also distributed ^{44m}Sc (3 MBq × 1), ^{67}Cu (10 MBq × 1), ^{88}Zr (2 MBq × 3), ^{95}Nb (2 MBq × 1), ^{121m}Te (2 MBq × 1), ^{175}Hf (2 MBq × 2), ^{179}Ta (2 MBq × 1), and ^{211}At (20 MBq × 1) under the the Supply Platform of Short-lived Radioisotopes for Fundamental Research.

(2) Superheavy element chemistry

Chemical characterization of newly-discovered superheavy elements (SHEs, atomic numbers $Z \geq 104$) is an extremely interesting and challenging subject in modern nuclear and radiochemistry. We are developing SHE production systems as well as rapid single-atom chemistry apparatuses at RIBF. Using heavy-ion beams from RILAC and AVF, ^{261}Rf ($Z = 104$), ^{262}Db ($Z = 105$), and ^{265}Sg ($Z = 106$) are produced in the ^{248}Cm(^{18}O,5n)^{261}Rf, ^{248}Cm(^{19}F,5n)^{262}Db, and ^{248}Cm(^{22}Ne,5n)^{265}Sg reactions, respectively, and their chemical properties are investigated.

We installed a gas-jet transport system to the focal plane of the gas-filled recoil ion separator GARIS at RILAC. This system is a promising approach for exploring new frontiers in SHE chemistry: the background radiation from unwanted products are strongly suppressed, the intense primary heavy-ion beam is absent in the gas-jet chamber, and hence the high gas-jet extraction yield is attained. Furthermore, the beam-free conditions make it possible to investigate new chemical systems. In 2016, the isotope of element 107 ^{266}Bh was produced in the ^{248}Cm(^{23}Na,5n)^{266}Bh reaction, and its decay properties were investigated with the rotating wheel apparatus MANON for α/SF spectrometry. Using ^{265}Sg atoms pre-separated by GARIS, the stability of the metal carbon bond in $Sg(CO)_6$ was investigated with a thermal decomposition setup under a large international collaboration led by Paul Scherrer Institute. To realize aqueous chemistry studies of Sg and Bh, we have been developing a continuous and rapid solvent extraction apparatus which consists of a continuous dissolution apparatus Membrane DeGasser (MDG), a Flow Solvent Extractor (FSE), and a liquid scintillation detector for α/SF-spectrometry. The performance of MDG and FSE were investigated using ^{170,174}Re and ^{176}Re produced in the ^{nat}Gd(^{23}Na,xn) and ^{152}Gd(^{23}Na,5n) reactions, respectively at GARIS.

At AVF, the distribution ratios (D) of ^{261}Rf in the Aliquat 336/HCl system were measured with the flow-type liquid-liquid extraction apparatus called as “flow Injection Solvent Extraction apparatus (ISE)” in collaboration with Osaka Univ. The reversed-phase extraction chromatography of ^{262}Db in the Aliquat 336/HF system were also conducted with Automated Rapid Chemistry Apparatus of JAEA in

collaboration with Niigata Univ. and JAEA. We also used radiotracers of ^{88}Zr, ^{90,95}Nb, ^{93m}Mo, ^{95m}Tc, ^{175}Hf, ^{178a,179}Ta, ^{177,179m,181}W, and ^{183,184m,184g}Re for model experiments of SHEs.

(3) Development of trace element and isotope analyses and their applications to geoscience and environmental science

We have been developing the ECR Ion Source Mass Spectrometer (ECRIS-MS) for trace element analyses. In 2016, we renovated the detection system of ECRIS-MS and evaluated sensitivity and mass resolution power. We equipped a laser-ablation system with an ion source and a pre-concentration system to achieve high-resolution analyses for noble gases such as Kr and Xe. This technique is expected to monitor the atmosphere around nuclear power plants.

Using the conventional ICP-MS, TIMS, IRMS and so on, we analyzed sediments such as a ferro-manganese nodule in the Pacific ocean to elucidate its growth history concerning the environmental changes in the ocean. We also studied lead and sulfur isotope ratios on cinnabar and asphalt samples from ancient ruins in Japan to elucidate the distribution of goods in the archaic society and to reveal the establishment of the Yamato dynasty in the period from Jomon to Tumulus. We also studied a feasibility to improve the sensitivity for the sulfur isotope ratios with the “trapping and focusing” techniques using a cryo-system.

(4) Development of chemical materials for ECR ion sources of RIBF

In 2016, we prepared metallic ^{238}U rods and $^{238}UO_2$ on a regular schedule for ^{238}U-ion accelerations with the 28-GHz ECR of RILAC II.

Members

Team Leader

Hiromitsu HABA

Research & Technical Scientist

Kazuya TAKAHASHI (Senior Research Scientist)

Postdoctoral Researcher

Yukiko KOMORI

Technical Staff I

Shinya YANOU

Research Consultant

Seiichi SHIBATA

Part-time Workers

Michiko KITAGAWA
Yu Vin SAHOO
Nozomi SATO
Keiko WATANABE

Visiting Scientists

Masayuki AIKAWA (Hokkaido Univ.)
Mayeen Uddin KHANDAKER (Univ. Malaya)
Takumi KUBOTA (Kyoto Univ.)
Aya SAKAGUCHI (Univ. of Tsukuba)
Miho TAKAHASHI (Tokyo Univ. Marine Sci. and Tech.)
Atsushi TOYOSHIMA (JAEA)
Takahiro YAMADA (Japan Rad. Assoc.)
Kazuhiko AKIYAMA (Tokyo Met. Univ.)
Hidetoshi KIKUNAGA (Tohoku Univ.)
Kazuhiro OOE (Niigata Univ.)
Hiroshi SHIMIZU (Rissho Univ.)
Masayoshi TODA (Tokyo Univ. Marine Sci. and Tech.)
Naoyuki UKON (Hokkaido Univ.)
Akihiko YOKOYAMA (Kanazawa Univ.)

Visiting Technicians

Yuichiro WAKITANI (Japan Rad. Assoc.)

Student Trainees

Ryuji AONO (Niigata Univ.)
Yuki HATTORI (Tokyo Univ. Marine Sci. and Tech.)
Junichi HIRATA (Tokyo Univ. Marine Sci. and Tech.)
Junpei INAGAKI (Univ. of Tsukuba)
Narumi KONDO (Osaka Univ.)
Takuya MORIYAMA (Niigata Univ.)
Tetuya NAGAOKA (Niigata Univ.)
Yu NAMBA (Niigata Univ.)
Kouki OUCHI (Osaka Univ.)
Yoshiki FUKUDA (Kanazawa Univ.)
Kazunori HAYASHI (Kanazawa Univ.)
Takumi IKEDA (Osaka Univ.)
Akimitsu KANDA (Osaka Univ.)
Kouki MORIYA (Kanazawa Univ.)
Risa MOTOYAMA (Niigata Univ.)
Masahiro NAGASE (Osaka Univ.)
Shuta OE (Kanazawa Univ.)
Moemi SAITOH (Hokkaido Univ.)
Daisuke SATO (Niigata Univ.)
Kaori SHIRAI (Niigata Univ.)
Shota TSUCHIYA (Niigata Univ.)
Ryohei YAMADA (Niigata Univ.)
Yukari YATSU (Kanazawa Univ.)
Yudai SHIGEKAWA (Osaka Univ.)
Tomohiro TOMITSUKA (Niigata Univ.)
Rufai Ahmed USMAN (Univ. Malaya)
Yuki YASUDA (Osaka Univ.)

List of Publications & Presentations

Publications

[Journal]

(Original Papers) *Subject to Peer Review

A. R. Usman, M. U. Khandaker, H. Haba, M. Murakami, and N. Otuka, "Measurements of deuteron-induced reaction cross-sections on natural nickel up to 24 MeV", Nuclear Instruments and Methods in Physics Research Section B **368**, 112–119 (2016).*

D. Kaji, K. Morimoto, H. Haba, E. Ideguchi, H. Koura, and K. Morita, "Decay properties of new isotopes ^{234}Bk and ^{230}Am, and even–even Nuclides ^{234}Cm and ^{230}Pu", Journal of the Physical Society of Japan **85**, 015002-1–2 (2016).*

S. Cao, Y. Wang, Z. Qin, F. Fan, H. Haba, Y. Komori, X. Wu, C. Tan, and X. Zhang, "Gas-phase chemistry of ruthenium and rhodium carbonyl complexes", Physical Chemistry Chemical Physics **18**, 119–125 (2016).*

S. Takács, M. P. Takács, F. Ditrói, M. Aikawa, H. Haba, and Y. Komori, "Activation cross sections of longer-lived radionuclides produced in germanium by alpha particle irradiation", Nuclear Instruments and Methods in Physics Research Section B **383**, 213–226 (2016).*

F. Ditrói, S. Takács, H. Haba, Y. Komori, M. Aikawa, Z. Szücs, and M. Saito, "Excitation function of the alpha particle induced nuclear reactions on enriched ^{116}Cd, production of the theranostic isotope ^{117m}Sn", Nuclear Instruments and Methods in Physics Research Section B **385**, 1–8 (2016).*

A. R. Usman, M. U. Khandaker, H. Haba, N. Otuka, M. Murakami, and Y. Komori, "Production cross-sections of radionuclides from α-induced reactions on natural copper up to 50 MeV", Applied Radiation and Isotopes **114**, 104–113 (2016).*

Y. Kasamatsu, T. Yokokita, K. Toyomura, Y. Shigekawa, H. Haba, J. Kanaya, M. Huang, Y. Ezaki, T. Yoshimura, K. Morita, and A. Shinohara, "Coprecipitation experiment with Sm hydroxide using a multitracer produced by nuclear spallation reaction: A tool for chemical studies with superheavy elements", Applied Radiation and Isotopes **118**, 105–116 (2016).*

T. Yokokita, Y. Kasamatsu, A. Kino, H. Haba, Y. Shigekawa, Y. Yasuda, K. Nakamura, K. Toyomura, Y. Komori, M. Murakami, T. Yoshimura, N. Takahashi, K. Morita, and A. Shinohara, "Observation of the chemical reaction equilibria of element 104, rutherfordium: Solid-liquid extraction of Rf, Zr, Hf and Th with Aliquat 336 resin from HCl", Dalton Transactions **45**, 18827–18831 (2016).*

J. Hirata, K. Takahashi, Yu Vin Sahoo, and M. Tanaka, "Laser ablation inductively coupled plasma mass spectrometry for quantitative imaging of elements in ferromanganese nodule", Chemical Geology **427**, 65–72 (2016).*

S. Sekimoto, T. Kobayashi, K. Takamiya, M. Ebihara, and S. Shibata, "Origin of spherule samples recovered from Antarctic ice sheet – Terrestrial or extraterrestrial?", Nuclear Engineering and Technology **48**, 293–298 (2016).*

S. Fujita, K. Goto-Azuma, M. Hirabayashi, A. Hori, Y. Iizuka, Y. Motizuki, H. Motoyama, and K. Takahashi, "Densification of layered firn in the ice sheet at Dome Fuji, Antarctica", Journal of Glaciology **62**, 103–123 (2016).*

[Proceeding]

(Original Paper) *Subject to Peer Review

H. Haba, "Superheavy element chemistry at GARIS", EPJ Web of Conferences **131**, 07006-1–6 (2016).*

[Book]

(Original Paper)

K. Takahashi, "Frequently used evaluations for aerial and solid pollution" in *Corrosion control and surface finishing* edited by H. Kanematsu and D. M. Barry, pp. 141–151, Springer (2016).

羽場宏光, "理科年表 国立天文台編 平成 29 年 第 90 冊", p. 582, 丸善出版, 2016 年 11 月 30 日.

Oral Presentations

[International Conference etc.]

H. Haba, "Superheavy element chemistry behind GARIS at RIKEN", Nobel Symposia, NS160: Chemistry and Physics of Heavy and Superheavy Elements, Scania, Sweden, May–June (2016).

H. Haba, "SHE nuclear chemistry at RIKEN", Seminar für Kern- und Radiochemie, Institut für Kernchemie, Johannes Gutenberg-Universität, Mainz, Germany, June (2016).

K. Takahashi, Y. Obi, and M. Tanaka, "The lead isotopes of aeolian dust observed at Saitama area (Japan) and their genetic implications", International Conference Series on Environmental and Food Monitoring (ISEAC-39), Hamburg, Germany, July (2016).

R. Eichler, M. Asai, H. Brand, N. M. Chiera, A. Di Nitto, R. Dressler, Ch. E. Düllmann, J. Even, R. Eichler, F. Fangli, M. Goetz, H. Haba, W. Hartmann, E. Jäger, D. Kaji, J. Kanaya, Y. Kaneya, J. Khuyagbaatar, B. Kindler, Y. Komori, B. Kraus, J. V. Kratz, J. Krier, Y. Kudou, N. Kurz, S. Miyashita, K. Morimoto, K. Morita, M. Murakami, Y. Nagame, K. Ooe, D. Piguet, N. Sato, T. K. Sato, J. Steiner, P. Steinegger, T. Sumita, M. Takeyama, K. Tanaka, T. Tomitsuka, A. Toyoshima, K. Tsukada, A. Türler, I. Usoltsev, Y. Wakabayashi, Y. Wang, N. Wiehl, A. Yakushev, S. Yamaki, S. Yano, S. Yamaki, and Z. Qin, "Experimentally assessing the metal-carbon bond stability in $Sg(CO)_6$", 9th International Conference on Nuclear and Radiochemistry (NRC9), Helsinki, Finland, Aug.–Sep. (2016).

T. Fukuchi, H. Haba, S. Yamamoto, Y. Watanabe, and S. Enomoto, "Dual isotope imaging of small animal by a positron emission tomography with additional γ-ray detectors", World Molecular Imaging Congress 2016, New York, USA, Sept. (2016).

A. R. Usman, M. U. Khandaker, H. Haba, and N. Karpuz, "Experimental and calculated excitation functions of ^{56}Mn from deuteron-induced nuclear reactions on nickel", 3rd International Conference on Computational and Experimental Science and Engineering (ICCESEN-2016), Antalya, Turkey, Oct. (2016).

T. Fukuchi, H. Haba, S. Yamamoto, Y. Watanabe, and S. Enomoto, "Positron emission tomography with additional γ-ray detectors for multiple probe imaging", 2016 IEEE NSS/MIC, Strasbourg, France, Oct.–Nov. (2016).

M. Aikawa, M. Saito, Y. Komori, H. Haba, S. Takács, F. Ditrói, and Z. Szűcs, "Activation cross sections of alpha-induced reactions on natural palladium for ^{103}Ag production", The 7th Asian Nuclear Reaction Database Development Workshop (AASPP 2016), Beijing, China, Nov. (2016).

H. Haba, "Forefront of superheavy element researches at RIKEN", Symposium for exploring prospective research –Pioneering new fields:

Forefront of RIKEN's science and beyond–, Wako, Japan, Nov. (2016).

[Domestic Conference]

羽場宏光, "理研 RI ビームファクトリーにおける RI 製造応用", 日本放射性医薬品協会賀詞交歓会,千代田区, 1 月 (2016).

羽場宏光, "理研における RI 製造", 東北大学電子光理学研究センター研究会 「放射性同位元素（RI）製造計画と多分野における RI 利用の現状」, 仙台市, 2 月 (2016).

羽場宏光, "理研 RI ビームファクトリーにおけるアルファ放射体利用", 第 7 回アルファ放射体実験室利用研究会, 仙台市, 2 月 (2016).

田中泰貴, 成清義博, 森田浩介, 藤田訓裕, 加治大哉, 森本幸司, 山木さやか, 若林泰生, 田中謙伍, 武山美麗, 米田晃, 羽場宏光, 小森有希子, 矢納慎也, B. J. P. Gall, Z. Asfari, H. Faure, 長谷部裕雄, M. Huang, 金谷淳平, 村上昌史, 吉田敦, 山口貴之, 門叶冬樹, 吉田友美, Z. Gan, L. Ma, H. Geissel, S. Hofmann, Y. Maurer, 山本翔也, 山野裕貴, 渡辺健友, 石澤倫, 浅井雅人, 青野竜士, 後藤真一, 鹿取謙二, "RIKEN-GARIS を用いた, 超重元素領域での融合障壁分布の研究", 日本物理学会第 71 回年次大会, 仙台市, 3 月 (2016).

羽場宏光, "加速器を用いた応用研究用ラジオアイソトープの製造", 日本物理学会第 71 回年次大会, 仙台市, 3 月 (2016).

羽場宏光, "理研 RI ビームファクトリーにおける RI 製造応用", 第 11 回 Eichrom Technologies 社製品ユーザーズセミナー, 千代田区, 4 月 (2016).

佐藤望, 矢納慎也, 羽場宏光, 小森有希子, 柴田誠一, 渡邉慶子, 加治大哉, 豊嶋厚史, 松本幹雄, "理研における At-211 製造", 第 53 回アイソトープ・放射線研究発表会, 文京区, 7 月 (2016).

矢納慎也, 羽場宏光, 柴田誠一, 小森有希子, 高橋和也, 佐藤望, 渡邉慶子, 脇谷雄一郎, 山田崇裕, 松本幹雄, "理研における頒布用精製 ^{67}Cu の製造開発", 第 53 回アイソトープ・放射線研究発表会, 文京区, 7 月 (2016).

羽場宏光, "短寿命 RI 供給プラットフォームについて", 2016 核化学夏の学校, 徳島市, 8 月 (2016).

齋藤萌美, 合川正幸, 羽場宏光, 小森有希子, サンドールタカーチ, "^{169}Tm への重陽子入射における ^{169}Yb の生成断面積について", 日本原子力学会 2016 年秋の大会, 久留米市, 9 月 (2016).

菊永英寿, 高宮幸一, 大槻勤, 羽場宏光, "^{48}Cr の半減期精密測定", 2016 日本放射化学会年会・第 60 回放射化学討論会, 新潟市, 9 月 (2016).

矢納慎也, 羽場宏光, 柴田誠一, 小森有希子, 高橋和也, 渡邉慶子, 脇谷雄一郎, 山田崇裕, 松本幹雄, "^{70}Zn(d,αn)^{67}Cu 反応による頒布用精製 ^{67}Cu の製造", 2016 日本放射化学会年会・第 60 回放射化学討論会, 新潟市, 9 月 (2016).

加治大哉, 森本幸司, 羽場宏光, 若林泰生, 武山美麗, 山木さやか, 小森有希子, 矢納慎也, 後藤真一, "GARIS-II を用いたホットフュージョン反応 ^{48}Ca+^{238}U→^{286}Cn*に関する研究", 2016 日本放射化学会年会・第 60 回放射化学討論会, 新潟市, 9 月 (2016).

海老原充, 大浦泰嗣, 白井直樹, 鶴田治雄, 森口祐一, 永川栄泰, 櫻井昇, 羽場宏光, 松崎浩之, 山形武靖, 永井尚生, 関本俊, "東電福島原発事故直後に採取された大気浮遊塵試料中の ^{129}I/^{131}I 比", 2016 日本放射化学会年会・第 60 回放射化学討論会, 新潟市, 9 月 (2016).

大浦泰嗣, 海老原充, 白井直樹, 鶴田治雄, 中島映至, 森口祐一, 大原利眞, 永川栄泰, 櫻井昇, 羽場宏光, 松崎浩之, "東電福島原発事故直後に採取された大気浮遊塵試料のオートラジオグラフと ^{129}I/^{137}Cs 比", 2016 日本放射化学会年会・第 60 回放射化学討論会, 新潟市, 9 月 (2016).

小森有希子, 羽場宏光, 大江一弘, 豊嶋厚史, 水飼秋菜, 佐藤大輔, 本山李沙, 矢納慎也, 渡邉慶子, 佐藤望, 山下さやか, 田中泰貴, 加治大哉, 森本幸司, 坂口綾, 稲垣純平, 菊永英寿, 重河優大, 笠松良崇, Jon Petter Omtvedt, "107 番元素ボーリウムの溶液化学研究に向けた GARIS ガスジェット装置による Re 同位体の製造とフロー溶媒抽出器を用いた Re のオンライン抽出", 2016 日本放射化学会年会・第 60 回放射化学討論会, 新潟市, 9 月 (2016).

田中康介, 秋山和彦, 羽場宏光, "化学的還元反応を用いた金属内包フラーレン分離の条件検討", 2016 日本放射化学会年会・第 60 回放射化学討論会, 新潟市, 9 月 (2016).

佐藤望, 矢納慎也, 羽場宏光, 小森有希子, 柴田誠一, 渡邉慶子, 加治大哉, 豊嶋厚史, 高橋和也, 松本幹雄, "理研における At-211 製造", 2016 日本放射化学会年会・第 60 回放射化学討論会, 新潟市, 9 月 (2016).

森田浩介, 森本幸司, 加治大哉, 羽場宏光, "GARIS を用いた超重元素研究の最前線－新元素認定までの道のり、周期表の拡張を目指した挑戦－", 2016 日本放射化学会年会・第 60 回放射化学討論会, 新潟市, 9 月 (2016).

羽場宏光, "理研 GARIS を用いた Sg カルボニル錯体の揮発性研究", 2016「超重元素の科学」研究会, 新潟市, 9 月 (2016).

小森有希子, "GARIS を用いた Sg と Bh の溶液化学研究", 2016「超重元素の科学」研究会, 新潟市, 9 月 (2016).

羽場宏光, "超重元素合成に関する理研の将来計画", 2016「超重元素の科学」研究会, 新潟市, 9 月 (2016).

高橋和也, 南武志, 上條信彦, 北川路子, Yu-Vin Sahoo, "硫黄同位体比分析による、北日本に産出する原油/アスファルトの識別の試み", 日本分析化学会年会・第 65 年会, 札幌市, 9 月 (2016).

岡部駿也, 田中美穂, 有我洋香, 高梨翠, 高橋和也, "シリカスケールの生成機構の鍵", 日本分析化学会年会・第 65 年会, 札幌市, 9 月 (2016).

羽場宏光, "理研 RIBF における応用研究用 RI の製造", 東京大学大学院工学系研究科原子力国際専攻高橋研究室セミナー, 文京区, 10 月 (2016).

羽場宏光, "理研 RIBF における医療用 RI 製造の現状と展望", 第 56 回日本核医学会学術総会・第 36 回日本核医学技術学会総会学術大会, 名古屋市, 11 月 (2016).

M. Aikawa, M. Saito, S. Ebata, Y. Komori, and H. Haba, "Activation cross sections of alpha-induced reactions on natural zinc for ^{68}Ge production", 2016 年度核データ研究会, つくば市, 11 月 (2016).

宗兼将之, 本村信治, 神野伸一郎, 上田真史, 羽場宏光, 吉川豊, 安井裕之, 榎本秀一, "抗糖尿病作用を有する亜鉛錯体の体内動態と化学形態の同時解析", 第 55 回日本薬学会・日本薬剤師会・日本病院薬剤師会中国四国支部学術大会, 岡山市, 11 月 (2016).

羽場宏光, "いかにして人工元素は合成されたか", 2016 年度（第 62 回）仁科記念講演会, 文京区, 12 月 (2016).

Posters Presentations

[International Conference etc.]

J. Inagaki, A. Sakaguchi, M. Inoue, A. Usui, H. Haba, T. Kashiwabara, S. Yamasaki, K. Sueki, and Y. Takahashi, "Fractionation of zirconium-hafnium in ferromanganese crusts", 26th Goldschmidt Conference, Yokohama, Japan, June (2016).

F. Ditrói, S. Takács, H. Haba, Y. Komori, M. Aikawa, Z. Szucs, and M. Saito, "Measurements of alpha particle induced reaction cross sections on ^{nat}Cd and ^{116}Cd for practical applications up to 50 MeV", 12th European Conference on Accelerators in Applied Research and Technology, Jyväskylä, Finland, July (2016).

H. Haba, F. Fan, D. Kaji, Y. Kasamatsu, H. Kikunaga, Y. Komori, N. Kondo, H. Kudo, K. Morimoto, K. Morita, M. Murakami, K. Nishio, K. Ooe, Z. Qin, N. Sato, A. Shinohara, M. Takeyama, T. Tanaka, A. Toyoshima, K. Tsukada, Y. Wakabayashi, Y. Wang, S. Yamaki, S. Yano, Y. Yasuda, T. Yokokita, and A. Yoneda, "Production and decay studies of ^{261}Rf, ^{262}Db, ^{265}Sg, and ^{266}Bh for superheavy element chemistry", 9th International Conference on Nuclear and Radiochemistry (NRC9), Helsinki, Finland, Aug.–Sep. (2016).

Y. Komori, H. Haba, K. Ooe, A. Toyoshima, A. Mitsukai, M. Murakami, D. Sato, R. Motoyama, S. Yano, K. Watanabe, A. Sakaguchi, J. Inagaki, H. Kikunaga, S. Wulff, and J. P. Omtvedt, "Development of a rapid solvent extraction apparatus for aqueous chemistry of the heaviest elements", 9th International Conference on Nuclear and Radiochemistry (NRC9), Helsinki, Finland, Aug.–Sep. (2016).

L. Lens, A. Yakushev, Ch. E. Düllmann, M. Asai, M. Block, H. M. David, J. Despotopulos, A. Di Nitto, K. Eberhardt, M. Götz, S. Götz, H. Haba, L. Harkness-Brennan, F. P. Heßberger, R.-D. Herzberg, D. Hinde, J. Hoffmann, A. Hübner, E. Jäger, D. Judson, J. Khuyagbaatar, B. Kindler, Y. Komori, J. Konki, J. V. Kratz, J. Krier, N. Kurz, M. Laatiaoui, S. Lahiri, B. Lommel, M. Maiti, A. K. Mistry, C. Mokry, K. Moody, Y. Nagame, J. P. Omtvedt, P. Papadakis, V. Pershina, D. Rudolph, J. Runke, M. Schädel, P. Scharrer, T. Sato, D. Shaughnessy, B. Schausten, J. Steiner, P. Thörle-Pospiech, N. Trautmann, K. Tsukada, J. Uusitalo, A. Ward, M. Wegrzecki, E. Williams, N. Wiehl, and V. Yakusheva, "Single-atom flerovium chemistry at TASCA", 9th International Conference on Nuclear and Radiochemistry (NRC9), Helsinki, Finland, Aug.–Sep. (2016).

A. Yokoyama, Y. Kitayama, Y. Fukuda, H. Kikunaga, M. Murakami, Y. Komori, S. Yano, H. Haba, K. Tsukada, and A. Toyoshima, "Extraction behavior of rutherfordium as a cationic fluoride complex with a TTA chelate extractant from HF/HNO_3 acidic solutions", 9th International Conference on Nuclear and Radiochemistry (NRC9), Helsinki, Finland, Aug.–Sep. (2016).

Y. Komori, M. Murakami, and H. Haba, "Measurement of production cross sections of Tc isotopes in deuteron-induced reactions on ^{nat}Mo up to 24 MeV", 9th International Conference on Nuclear and Radiochemistry (NRC9), Helsinki, Finland, Aug.–Sep. (2016).

[Domestic Conference]

山田亮平, 大江一弘, 後藤真一, 工藤久昭, 羽場宏光, 小森有希子, "フローインジェクション分析法を利用した 4 族元素 Zr、Hf のキレート抽出", 2016 日本放射化学会年会・第 60 回放射化学討論会, 新潟市, 9 月 (2016).

大江一弘, 山田亮平, 後藤真一, 工藤久昭, 羽場宏光, 小森有希子, "Rf の同族元素 Zr、Hf の 4-イソプロピルトロポロンを用いた溶媒抽出挙動", 2016 日本放射化学会年会・第 60 回放射化学討論会, 新潟市, 9 月 (2016).

佐藤大輔, 村上昌史, 大江一弘, 本山李沙, 羽場宏光, 小森有希子, 豊嶋厚史, 水飼秋菜, 菊永英寿, 後藤真一, 工藤久昭, "5 族元素 Nb, Ta のフッ化水素酸からの Aliquat 336 樹脂への抽出：分配係数の抽出剤濃度依存性の検討", 2016 日本放射化学会年会・第 60 回放射化学討論会, 新潟市, 9 月 (2016).

本山李沙, 大江一弘, 村上昌史, 羽場宏光, 後藤真一, 工藤久昭, "5 族元素 Nb, Ta の塩酸溶液からのトリイソオクチルアミンによる溶媒抽出－Ta トレーサー調製法の影響－", 2016 日本放射化学会年会・第 60 回放射化学討論会, 新潟市, 9 月 (2016).

水飼秋菜, 豊嶋厚史, 小森有希子, 羽場宏光, 浅井雅人, 塚田和明, 佐藤哲也, 永目諭一郎, "フロー抽出装置を用いたフッ化水素酸－Aliquat336 系におけるタングステンの溶媒抽出", 2016 日本放射化学会年会・第 60 回放射化学討論会, 新潟市, 9 月 (2016).

豊嶋厚史, 神田晃充, 池田卓海, 吉村崇, 篠原厚, 矢納慎也, 小森有希子, 羽場宏光, "アスタチンの酸化還元と溶媒抽出挙動", 2016 日本放射化学会年会・第 60 回放射化学討論会, 新潟市, 9 月 (2016).

神原正, 吉田敦, 羽場宏光, "陽電子放出核種による回転体検査法の開発", 2016 日本放射化学会年会・第 60 回放射化学討論会, 新潟市, 9 月 (2016).

RIBF Research Division
User Liaison and Industrial Cooperation Group

1. Abstract

The essential mission of the “User Liaison and Industrial Cooperation (ULIC) Group” is to maximize the research activities of RIBF by attracting users in various fields with a wide scope.

The ULIC Group consists of two teams.

The RIBF User Liaison Team provides various supports to visiting RIBF users through the User’s Office. The Industrial Cooperation Team supports potential users in industries who use the beams for application purposes or for accelerator related technologies other than basic research. Production of various radioisotopes by the AVF cyclotron is also one of the important mission. The produced radioisotopes are distributed to researchers in Japan for a charge through the Japan Radioisotope Association.

In addition the ULIC Group takes care of laboratory tours for RIBF visitors from public. The numbers of visitors amounts to 2,300 per year.

Members

Group Director
Hideyuki SAKAI

Special Temporary Employee
Tadashi KAMBARA

Senior Visiting Scientists
Ikuko HAMAMOTO (Lund Univ.)
Munetake ICHIMURA (Univ. of Tokyo)

Assistants
Katsura IWAI
Tomoko IWANAMI
Noriko KIYAMA
Tomomi OKAYASU
Yoko FUJITA
Yu NAYA

RIBF Research Division
User Liaison and Industrial Cooperation Group
RIBF User Liaison Team (User Support Office)

1. Abstract

To enhance synergetic common use of the world-class accelerator facility, the Radioisotope Beam Factory (RIBF), it is necessary to promote a broad range of applications and to maximize the facility's importance. The facilitation and promotion of the RIBF are important missions charged to the team. Important operational activities of the team include: i) the organization of international Program Advisory Committee (PAC) meetings to review experimental proposals submitted by RIBF users, ii) RIBF beam-time operation management, and iii) promotion of facility use by hosting outside users through the RIBF Independent Users program, which is a new-user registration program begun in FY2010 at the RIKEN Nishina Center (RNC) to enhance the synergetic common use of the RIBF. The team opened the RIBF Users Office in the RIBF building in 2010, which is the main point of contact for Independent Users and provides a wide range of services and information.

2. Major Research Subjects

(1) Facilitation of the use of the RIBF
(2) Promotion of the RIBF to interested researchers

3. Summary of Research Activity

(1) Facilitation of the use of the RIBF

The RIBF Users Office, formed by the team in 2010, is a point of contact for user registration through the RIBF Independent User program. This activity includes:

- registration of users as RIBF Independent Users,
- registration of radiation workers at the RIKEN Wako Institute,
- provision of an RIBF User Card (a regular entry permit) and an optically stimulated luminescence dosimeter for each RIBF Independent User, and
- provision of safety training for new registrants regarding working around radiation, accelerator use at the RIBF facility, and information security, which must be completed before they begin RIBF research.

The RIBF Users Office is also a point of contact for users regarding RIBF beam-time-related paperwork, which includes:

- contact for beam-time scheduling and safety review of experiments by the In-House Safety Committee,
- preparation of annual Accelerator Progress Reports, and
- maintaining the above information in a beam-time record database.

In addition, the RIBF Users Office assists RIBF Independent Users with matters related to their visit, such as invitation procedures, visa applications, and the reservation of on-campus accommodation.

(2) Promotion of the RIBF to interested researchers

- The team has organized an international PAC for RIBF experiments; it consists of leading scientists worldwide and reviews proposals in the field of nuclear physics (NP) purely on the basis of their scientific merit and feasibility. The team also assists another PAC meeting for material and life sciences (ML) organized by the RNC Advanced Meson Laboratory. The NP and ML PAC meetings are organized twice a year.
- The team coordinates beam times for PAC-approved experiments and other development activities. It manages the operating schedule of the RIBF accelerator complex according to the decisions arrived at by the RIBF Machine Time Committee.
- To promote research activities at RIBF, proposals for User Liaison and Industrial Cooperation Group symposia/mini-workshops are solicited broadly both inside and outside of the RNC. The RIBF Users Office assists in the related paperwork.
- The team is the point of contact for the RIBF users' association. It arranges meetings at RNC headquarters for the RIBF User Executive Committee of the users' association.
- The Team conducts publicity activities, such as arranging for RIBF tours, development and improvement of the RNC official web site, and delivery of RNC news via email and the web.

Members

Team Leader
Ken-ichiro YONEDA

Deputy Team Leader
Yasushi WATANABE (concurrent: Senior Research Scientist, Radiation Lab.)

Technical Staff I
Narumasa MIYAUCHI

RIBF Research Division
User Liaison and Industrial Cooperation Group
Industrial Cooperation Team

1. Abstract

Industrial cooperation team handles non-academic activities at RIBF corresponding to industries and to general public.

2. Major Research Subjects

(1) Fee-based distribution of radioisotopes produced at RIKEN AVF Cyclotron
(2) Support of industrial application using the RIBF accelerator beam and its related technologies including novel industrial applications.
(3) Development of real-time wear diagnostics of industrial material using RI beams

3. Summary of Research Activity

(1) Fee-based distribution of radioisotopes

This team has been handling fee-based distribution of radioisotopes since 2007. Radionuclides of Zn-65, Sr-85, Y-88 and Cd-109, which are produced by the RI application team at the AVF cyclotron, are distributed to nonaffiliated users under a Material Transfer Agreement (MTA) between Japan Radioisotope Association and RIKEN. In 2016, we delivered 2 shipments of Cd-109 with a total activity of 12 MBq, 5 shipments of Zn-65 with a total activity of 24 MBq, 2 shipments of Y-88 with an activity of 2 MBq and one shipment of Sr-85 with an activity of 1 MBq. The final recipients of the RIs were seven universities and one hospital.

(2) Support of Industrial application using RIBF

RNC promotes facility-sharing program “Promotion of applications of high-energy heavy ions and RI beams”. In this program, RNC opens the old part of the RIBF facility, which includes the AVF cyclotron, RILAC, RIKEN Ring Cyclotron and experimental instruments, to non-academic proposals from users including private companies. The proposals are reviewed by a program advisory committee, industrial PAC (InPAC). The proposals which have been approved by the InPAC are allocated with beam times and the users pay RIKEN the beam time fee. The intellectual properties obtained by the use of RIBF belong to the users. In order to encourage the use of RIBF by those who are not familiar with utilization of ion beams, the first two beam times of each proposal can be assigned to trial uses which are free of beam time fee.

The sixth InPAC meeting held in January 2017 reviewed two fee-based proposals from private companies and approved them. Until now, five proposals of fee-based utilization from three private companies have been performed. Private companies used heavy-ion beams of Ar-40 (95 MeV/A) and Kr-84 (70 MeV/A) at the E5A beamline for an irradiation test of space-use semi-conductors in the atmosphere. For future users, we have developed higher LET beams of Xe-136 (39 MeV/A) and Au-197 (18.4 MeV/A) at the same beamline.

(3) Development of real-time wear diagnostics using RI beams

We are developing a method to determine the spatial distribution of gamma-ray emitting RIs on periodically-moving objects, named “GIRO” (Gamma-ray Inspection of Rotating Object), that is based on the same principle as the medical PET imaging but is simpler and less expensive. This method can be used for real-time inspection of a closed system in a running machine. In 2016, the scintillation detectors were replaced by new ones and the gamma-ray collimators were modified on the test bench. We also tried single-photon emission computer tomography (SPECT) mode measurement.

Members

Team Leader
Atsushi YOSHIDA

Contract Researcher
Tadashi KAMBARA

Technical Staff I
Shinya YANOU (concurrent: RI Application Team)

List of Publications & Presentations

Publications

[Journal]

(Original Papers) *Subject to Peer Review

A.Yoshida, T.Kambara, A.Nakao, R.Uemoto, H.Uno, A.Nagano, H.Yamaguchi, T.Nakao, D.Kahl, Y.Yanagisawa, D.Kameda, T.Ohnishi , N.Fukuda, T.Kubo, “Wear diagnostics of industrial material using RI beams of 7Be and 22Na”, Nuclear Instruments and Methods in Physics Research Section B 317, 785-788 (2013) *

T. Kambara, A. Yoshida, H. Takeichi, "Gamma-ray inspection of rotating object", Nuclear Instruments and Methods in Physics Research A 797, 1-7 (2015) *.

T. Kambara, “Gamma-Ray Inspection of Rotating Object (GIRO)”, Nuclear Physics News Vol. 26, No.4, 26-29 (2016).

[Proceedings]
(Original Papers) *Subject to Peer Review
T. Kambara, A. Yoshida, Y. Yanagisawa, D. Kameda, N. Fukuda, T. Ohnishi, T. Kubo, R. Uemoto, A. Nagano, and H. Uno, ”Industrial Application of Radioactive Ion Beams at the RIKEN RI Beam Factory”, AIP Conference Proceedings 1412 (2011), American Institute of Physics *
[Book]
(Original Papers) *Subject to Peer Review
A. Yoshida, T. Kambara, R. Uemoto, “RI ビーム打込み法を用いた摩耗検査法の開発“, 月刊トライボロジー2014-08 No324 pg.16-18,新樹社(2014)
A. Yoshida, T. Kambara, “研究室紹介 No.43 理化学研究所仁科加速器研究センター産業連携チーム“, 月刊トライボロジー2015-02 No330 pg.66,新樹社(2014)
T. Kambara, "RI ビーム照射を用いた摩耗試験", 加速器 Vol. 12, No. 4(2015)

Oral Presentations
[International Conference etc.]
T. Kambara, et al., “Industrial Application of Radioactive Ion Beams at the RIKEN RI Beam Factory”, 11th International Conference on Applications of Nuclear Techniques, Crete, Greece, Jun (2011)
A.Yoshida, et al., “Wear diagnostics of industrial material using RI beams of 7Be and 22Na”, 16th International Conference on Electromagnetic Iso-tope Separators and Techniques Related to their Applications (EMIS2012), Matsue, Dec.(2012)
[Domestic Conference]
A.Yoshida, “RI ビームの工業応用－ 表面摩耗量検査法開発“, 理研シンポジウム第 16 回「トライボコーティングの現状と将来」, (トライボコーティング技術研究会主催), 和光, 2 月 (2014).
A.Yoshida, “理研 RI ビームバラエティ（産業利用まで）“, 第 54 回放射線科学研究会(エキゾチックビームシリーズ<12>), 大阪ニュークリアサイエンス協会, 大阪, 7 月(2014).
T. Kambara, "イオン照射による材料改質と摩耗試験", 日本物理学会 年次大会, 東北学院大学 仙台, 03/19-22 (2016)

Posters Presentations
[Domestic Conference]
A. Yoshida, T. Kambara, “ＲＩビームでオンライン精密摩耗量測定～摩耗のイメージング～“, nano tech 2016 第 15 回国際ナノテクノロジー総合展・技術会議, 01/27-29, 東京ビッグサイト, (2016)
T. Kambara, A. Yoshida, H. Haba, “陽電子放出核種による回転体検査法の開発”, 2016 日本放射化学会年会・第 60 回放射化学討論会, 新潟大学, 09/10-12,(2016)

RIBF Research Division
Safety Management Group

1. Abstract

The RIKEN Nishina Center for Accelerator-Based Science possesses one of the largest accelerator facilities in the world, which consists of two heavy-ion linear accelerators and five cyclotrons. This is the only site in Japan where uranium ions are accelerated. The center also has electron accelerators of microtron and synchrotron storage ring. Our function is to keep the radiation level in and around the facility below the allowable limit and to keep the exposure of workers as low as reasonably achievable. We are also involved in the safety management of the Radioisotope Center, where many types of experiments are performed with sealed and unsealed radioisotopes.

2. Major Research Subjects

(1) Safety management at radiation facilities of Nishina Center for Accelerator-Based Science
(2) Safety management at Radioisotope Center
(3) Radiation shielding design and development of accelerator safety systems

3. Summary of Research Activity

Our most important task is to keep the personnel exposure as low as reasonably achievable, and to prevent an accident. Therefore, we daily patrol the facility, measure the ambient dose rates, maintain the survey meters, shield doors and facilities of exhaust air and wastewater, replenish the protective supplies, and manage the radioactive waste. Advice, supervision and assistance at major accelerator maintenance works are also our task.

The radioactive argon gas in the RIBF experimental rooms was reduced by a partition. The argon gas was generated at around the target and beam dump, and it diffuse to experimental rooms slightly by air circulation. We installed an air partition tentatively. The air flow and the radioactive gas was successfully restricted.

We measured the radiation level and shielding power in the RILAC irradiation room. The RILAC accelerator will be upgraded and additional shield be required. The amount of the shield was estimated by this evaluation.

Minor improvements of the radiation safety systems were also done, for example, part of the radiation control system at RIBF building was renewed because it was developed by old programming language. The radiation monitors at the Nishina building has been replaced annually from 2015 because they get older, which were installed in 1986.

Members

Group Director
Yoshitomo UWAMINO

Deputy Group Director
Kanenobu TANAKA

Nishina Center Technical Scientists
Rieko HIGURASHI
Hisao SAKAMOTO
Takeshi MAIE (concurrent; Cryogenic Technology Team)

Technical Staff I
Atsuko AKASHIO
Tomoyuki DANTSUKA (concurrent; Cryogenic Technology Team)

Research Consultant
Masaharu OKANO (Japan Radiation Res. Soc.)

Visiting Scientists
Hee Seock LEE (POSTECH)
Joo-Hee OH (POSTECH))
Nam-Suk JUNG (POSTECH)
Takashi NAKAMURA (Shimizu Corp.)
Noriaki NAKAO (Shimizu Corp.)
Koji OHISHI (Shimizu Corp.)
Arim LEE (Pohang Accelerator Laboratory POSTECH)
Nobuhiro SHIGYO (Kyushu Univ.)

Student Trainees
Kentaro SUGIHARA

Assigned Employee
Hiroki MUKAI

Temporary Staffing
Ryuji SUZUKI

Part-time Workers

Hiroshi KATO
Satomi IIZUKA
Kimie IGARASHI
Hiroko AISO
Naoko USUDATE
Shin FUJITA
Yukiko SHIODA

Assistant

Tomomi OKAYASU (concurrent: User Liaison and Industrial Cooperation Group)

List of Publications & Presentations

Oral Presentations

[International Conference etc.]

Akashio, A., Tanaka, K., Imao, H., and Uwamino Y.: “Activation measurement by ^{238}U beam irradiation around 11A MeV on He gas”, 13th International Conference on Radiation Shielding & 19th Topical Meeting of the Radiation Protection & Shielding Division of the Ameriacn Nuclear Society 2016 (ICRS13-RPSD2016), Paris, France, October (2016).

Oh, J., Jung, N., Lee, H., Oranj, L., Nakao, N., Uwamino, Y. and Ko S.: “Neutron Production from thin Be target irradiated by 50 MeV/u ^{238}U beam.”, 13th International Conference on Radiation Shielding & 19th Topical Meeting of the Radiation Protection & Shielding Division of the Ameriacn Nuclear Society 2016 (ICRS13-RPSD2016), Paris, France, October (2016).

[Domestic Conference]

田中鐘信: "理化学研究所 RI ビームファクトリー加速器施設の緊急時対応”, 第４回加速器施設安全シンポジウム, 東海村, 1 月,(2017).

赤塩敦子, 田中鐘信, 今尾 浩士: “RIBF 加速器におけるヘリウムガスへのウランビーム 11MeV/u 照射による放射化評価”, 日本原子力学会 2017 年春の年会, 湘南, 3 月 (2016).

田中鐘信: “PHITS を用いた RI ビームファクトリー重イオン加速器施設の放射線影響評価”, PHITS 研究会, 熱海, 9 月 (2016).

Partner Institutions

The Nishina Center established the “Research Partnership System” in 2008. This system permits an external institute to develop its own projects at the RIKEN Wako campus in equal partnership with the Nishina Center. At present, three institutes, Center for Nuclear Study, the University of Tokyo (CNS); Institute of Particle and Nuclear Studies, KEK (KEK); and the Institute of Science and Technology, Niigata University (Niigata) are conducting research activities under the Research Partnership System.

CNS and the Nishina Center signed the partnership agreement in 2008. Until then, CNS had collaborated in joint programs with RIKEN under the “Research Collaboration Agreement on Heavy Ion Physics” (collaboration agreement) signed in 1998. The partnership agreement redefines procedures related to the joint programs while keeping the spirit of the collaboration agreement. The joint programs include experimental nuclear physics activities using CRIB, SHARAQ, and GRAPE at RIBF, theoretical nuclear physics activities with ALPHLEET, accelerator development, and activities at RHIC PHENIX.

The partnership agreement with the Niigata University was signed in 2010. The activity includes theoretical and experimental nuclear physics, and nuclear chemistry.

KEK started low-energy nuclear physics activity at RIBF in 2011 under the Research Partnership System. The joint experimental programs are based on KISS (KEK Isotope Separator). After the R&D studies on KISS, it became available for users from 2015. In this year, a new KEK branch, Wako Nuclear Science Center (WNSC) has been launched at the Wako campus to enhance the scientific activities of KISS.

The experimental proposals that request the use of the above-noted devices of CNS and KEK together with the other RIBF key devices are screened by the Program Advisory Committee (PAC). The PAC meetings are co-hosted by CNS and KEK.

The activities of CNS, Niigata, and KEK are reported in the following pages.

Partner Institution
Center for Nuclear Study, Graduate School of Science
The University of Tokyo

1. Abstract

The Center for Nuclear Study (CNS) aims to elucidate the nature of nuclear system by producing the characteristic states where the Isospin, Spin and Quark degrees of freedom play central roles. These researches in CNS lead to the understanding of the matter based on common natures of many-body systems in various phases. We also aim at elucidating the explosion phenomena and the evolution of the universe by the direct measurements simulating nuclear reactions in the universe. In order to advance the nuclear science with heavy-ion reactions, we develop AVF upgrade, CRIB and SHARAQ facilities in the large-scale accelerators laboratories RIBF. We started a new project OEDO for a new energy-degrading scheme, where a RF deflector system is introduced to obtain a good quality of low-energy beam. In 2016, a new group for fundamental symmetry has been added. We promote collaboration programs at RIBF as well as RHIC-PHENIX and ALICE-LHC with scientists in the world, and host international meetings and conferences. We also provide educational opportunities to young scientists in the heavy-ion science through the graduate course as a member of the department of physics in the University of Tokyo and through hosting the international summer school.

2. Major Research Subjects

(1) Accelerator Physics
(2) Nuclear Astrophysics
(3) Nuclear spectroscopy of exotic nuclei
(4) Quark physics
(5) Nuclear Theory
(6) OEDO/SHARAQ project
(7) Exotic Nuclear Reaction
(8) Low Energy Nuclear Reaction Group
(9) Active Target Development
(10) Fundamental Physics

3. Summary of Research Activity

(1) Accelerator Physics

One of the major tasks of the accelerator group is the AVF upgrade project that includes development of ion sources, upgrading the AVF cyclotron of RIKEN and the beam line to CRIB. Development of ECR heavy ion source is to provide new HI beams, higher and stable beams of metallic ions, and to improve the control system. The Hyper ECR and the Super ECR sources provide all the beams for the AVF cyclotron and support not only CRIB experiments but also a large number of RIBF experiments. Injection beam monitoring and control are being developed and studied in order to measure four-dimensional emittance. Detailed studies of the optics from the ion sources in consideration of the space charge effect are expected to improve transmission and qualities of beams for the RIBF facility. In 2016, The beam intensities of some light ions accelerated by AVF cyclotron have been doubled by improving the extraction system of the Hyper ECR.

(2) Nuclear Astrophysics

The nuclear astrophysics group in CNS is working for experimental studies with the low-energy RI beam separator CRIB. In FY2016, experiments on the alpha-cluster structure in the ^{22}Mg nucleus, ^{7}Be(n, α)/(n, p) astrophysical reactions using the Trojan Horse method, production of ^{7}Be-implanted target, and the proton resonant scattering experiment with ^{26}Al isomeric beam were performed at CRIB under international collaborations including Korean, Italian, UK, and Chinese groups. The isomeric ^{26}Al beam production at CRIB was for the first time, and a high isomeric purity of over 30% was achieved. A strong indication of an exotic linear-chain cluster structure in ^{14}C nucleus was presented based on the ^{10}Be+α resonant scattering experiment previously performed at CRIB.

(3) Nuclear structure of exotic nuclei

The NUSPEQ (NUclear SPectroscopy for Extreme Quantum system) group studies exotic structures in high-isospin and/or high-spin states in nuclei. The CNS GRAPE (Gamma-Ray detector Array with Position and Energy sensitivity) is a major apparatus for high-resolution in-beam gamma-ray spectroscopy. Missing mass spectroscopy using the SHARAQ is used for another approach on exotic nuclei. In 2016, the following progress has been made.

Experimental data taken in 2013 under the EURICA collaboration has been analyzed for studying octupole deformation in neutron-rich Ba isotopes and preparing publication. Exothemic charge exchange reaction (^{8}He,^{8}Li*(1+)) on ^{4}He has been analyzed for studying spin-dipole response of few-body system on the photon line. A new experiment measuring the ^{4}He(^{8}He,^{8}Be)4n reaction was performed for better statistics and better accuracy in order to verify a candidate of the ground state of the tetra neutrons just above the 4n threshold, which is under analysis.

A DAQ system for the CNS GRAPE was upgraded, where event building system is included for several digitizing modules based on sampling ADCs and FPGAs on boards.

(4) Quark Physics

Main goal of the quark physics group is to understand the properties of hot and dense nuclear matter created by colliding heavy nuclei at relativistic energies. The group has been involved in the PHENIX experiment at Relativistic Heavy Ion Collider (RHIC) at Brookhaven National Laboratory, and the ALICE experiment at Large Hadron Collider (LHC) at CERN. As for ALICE, the group has involved in the data analyses, which include the measurement of low-mass lepton pairs in Pb-Pb and p-Pb collisions, heavy flavor baryon measurements in pp and p-Pb collisions, particle correlations with large rapidity gap in p-Pb collisions, and searches for dibaryons in Pb-Pb collisions. The group has involved in the ALICE-TPC upgrade using a Gas Electron Multiplier (GEM). New readout chip of the TPC upgrade, called as SAMPA, was tested and development of the new data readout system for the TPC upgrade, which aims online data processing by utilizing FPGA and GPU, has begun in 2016.

(5) Nuclear Theory

The nuclear theory group participate a project, "Priority Issue 9 to be tackled by using the Post-K Computer" and promotes computational nuclear physics utilizing supercomputers. In 2016, we revealed the quantum phase transition of nuclear shape in neutron-rich Zr isotopes by the Monte Carlo shell model. In parallel, we have been promoting the CNS-RIKEN collaboration project on large-scale nuclear structure calculations and performed shell-model calculations under various collaborations with many experimentalists for investing the exotic structure of neutron-rich nuclei, such as ^{38,40}P, ^{48}Ca, ^{55}Ca, ^{128}Cd, and ^{132}Sn.

(6) OEDO/SHARAQ project

The OEDO/SHARAQ group pursues experimental studies of RI beams by using the high-resolution beamline and the SHARAQ spectrometer. A mass measurement by TOF-Brho technique for very neutron-rich calcium isotopes around N=34 was successfully performed. The parity-tansfer charge exchange (^{16}O, ^{16}F) was studied, since the reaction is expected to probe the 0^- strength in nuclei. The result of the study was recently published. The OEDO project, which is a major upgrade of the high-resolution beamline for RI beams with energies lower than 100 MeV/u, is ongoing. The beam line has been constructed in March 2017. The commissioning of the energy degrading scheme is scheduled in June 2017.

(7) Exotic Nuclear Reaction

The Exotic Nuclear Reaction group studies various exotic reactions induced by beams of unstable nuclei. One subject is inverse-kinematics (p,n) reaction. In 2016 a set of neutron counters PANDORA was developed and an in-beam test was performed. Candidate nuclei to study is high spin isomers such as ^{52}Fe(12^+). Development of isomer beam was carried out at HIMAC.

(8) Low Energy Nuclear Reaction Group

A new measurement of the isobaric analog resonances of RRC31 was analyzed. Due to the low production yield of ^{34}Si beam from ^{48}Ca at 64 MeV/nucleon which was 1 orders magnitudes smaller than the estimation of EPAX-2.15, we couldn't improve the excitation function though the experimental result was observed to be consistent with the previous measurement.

For the development of the exotic targets, the feasibility study of Ti-^{3}H was carried out by making a thin Ti-^{2}H target. The ^{2}H in the Ti-^{2}H target will desorb when the target is heated upto above 300 degrees in Celsius. As far as the target temperature is kept below 100 degrees, erosion of ^{3}H from Ti-^{3}H will be 0. Activity measurement after ^{20}Ne beam of 8.2 MeV/nucleon on the Ti-^{2}H target, any strong activity was not measured, meaning that Toyama Univ can decommission the target after the campaign of the experiments. A thin and higher concentration ratio of the target have been also under testing.

Single-crystal (sc) diamond detector is considered as a next-generation semiconductor detector. We found that the pulse height defect for fission fragments of ^{252}Cf was almost saturated with the electric field of 2 V/μm.

(9) Active Target Development

Two types of gaseous active target TPCs called GEM-MSTPC and CATs are developed and used for the missing mass spectroscopy. A new resonance in ^{30}S has been observed via the study of alpha inelastic scattering using GEM-MSTPC. The data analysis of astrophysical reaction (α, p) on ^{18}Ne and ^{22}Mg and the β-decay of ^{16}Ne followed by α emmision. The study of Equation of State of nuclear matter using CATs is ongoing. The data analysis of deuteron inelastic scattering on ^{15,16}O and ^{132}Xe measured at HIMAC by using CAT-S is in progress. The measurement of giant monopole resonance in ^{132}Sn by using CAT-S has been done at RIBF in April, 2016. Larger volume active target CAT-M is being developed aiming at 10-times larger yield.

(10) Fundamental Physics

To investigate the matter-antimatter asymmetry (CP violation) in the universe, and to understand the CP violating components in the fundamental interactions, the experimental project to search for the electric dipole moment (EDM) of the ^{210}Fr is going on. The thermal ionizer to produce the ^{210}Fr with fusion reaction, an optical lattice to accumulate the cooled atoms, and an atomic interferometer to measure the frequency of the spin precession of ^{210}Fr are ready now. The yield of the Fr ions with 10^6 Fr^+/s has been achieved, and the improvement of the trapping efficiency to get the high intensity cooled Fr atoms will be done by upgrading the laser optics.

Members

Director

Susumu SHIMOURA

Scientific Staff

Susumu SHIMOURA (Professor)
Yasuhiro SAKEMI (Professor)
Kentaro YAKO (Associate Professor)
Nobuaki IMAI (Associate Professor)
Noritaka SHIMIZU (Project Associate Professor)
Hidetoshi YAMAGUCHI (Lecturer)
Shin'ichiro MICHIMASA (Assistant Professor)
Taku GUNJI (Assistant Professor)
Shinsuke OTA (Assistant Professor)

Guest Scientists

Yutaka UTSUNO (Guest Associate Professor)
Yutaka MIZOI (Guest Associate Professor)

Technical Staff

Yasuteru KOTAKA

Techinical Assistants

Yukimitsu OHSHIRO
Mamoru KATAYANAGI
Reiko KOJIMA
Kazuyuki YOSHIMURA
Hiroshi KUREI

Project Research Associates

Tooru YOSHIDA
Olga BELIUSKINA

Post Doctoral Associates

Yosuke WATANABE
Philipp SCHROCK
Laszlo STUHL
Masanori DOZONO
Seiya HAYAKAWA
Chihiro IWAMOTO
Lei YANG
Rin YOKOYAMA

Graduate Students

Hiroshi TOKIEDA
Yuko SEKIGUCHI
Yuki YAMAGUCHI
Ryo NAKAJIMA
Keita KAWATA
Noritaka KITAMURA
Hideki SHIMIZU
Motonobu TAKAKI
Motoki KOBAYASHI
Soichiro MASUOKA
Shinichi HAYASHI
Kohei TERASAKI
Keijiro ABE

Administration Staff

Mikio OKI
Takako ENDO
Yuko SOMA
Ikuko YAMAMOTO
Yukino KISHI

List of Publications & Presentations

Publications

[Journal]

(Original Papers) *Subject to Peer Review

S. Hayakawa, S. Kubono, D. Kahl, H. Yamaguchi, D.N. Binh, T. Hashimoto, Y. Wakabayashi, J.J. He, N. Iwasa, S. Kato, T. Komatsubara, Y.K. Kwon, T. Teranishi, ``First direct measurement of the ^{11}C(alpha, p)^{14}N stellar reaction by an extended thick-target method", Physical. Review. C 93, 065802 (2016). *

H. Yamaguchi, D. Kahl, S. Hayakawa, Y. Sakaguchi, K. Abe, T. Nakao, T. Suhara, N. Iwasa, A. Kim, D.H. Kim, S.M. Cha, M.S. Kwag, J.H. Lee, E.J. Lee, K.Y. Chae, Y. Wakabayashi, N. Imai, N. Kitamura, P. Lee, J.Y. Moon, K.B. Lee, C. Akers, H.S. Jung, N.N. Duy, L.H. Khiem, and C.S. Lee, ``Experimental investigation of linear-chain structured nucleus in ^{14}C", Physics Letters B 766,11 (2017). *

L. Yang, C.J. Lin, H.M. Jia, D.X. Wang, L.J. Sun, N.R. Ma, F. Yang, Z.D. Wu, X.X. Xu, H.Q. Zhang, Z.H. Liu, and P.F. Bao, ``Optical model potentials for ^{6}He+^{64}Zn from ^{63}Cu(^{7}Li,^{6}He)^{64}Zn reactions", Physical Review C 95, 034616 (2017). *

R. G. Pizzone, G. D'Agata, M. La Cognata, I. Indelicato, C. Spitaleri, S. Blagus, S. Cherubini, P. Figuera, L. Grassi, G. L. Guardo, M. Gulino, S. Hayakawa, R. Kshetri, L. Lamia,M. Lattuada, T. Mijatovic, M. Milin, D.H. Miljanic D., L. Prepolec, G. G. Rapisarda, S. Romano, M. L. Sergi, N. Skukan, N. Soic, V. Tokic, A. Tumino, and M. Uroic, ``First Measurement of the ^{19}F(alpha,p)^{22}Ne Reaction at Energies of Astrophysical Relevance", Astrophysical Journal, 836, 57 (2017). *

O. Beliuskina, A.O. Strekalovsky, A.A. Aleksandrov, I.A. Aleksandrova, H.M. Devaraja, C. Heinz, S. Heinz, S. Hofmann, S. Ilich, N. Imai, D.V. Kamanin, M. Kis, G.N. Knyazheva, C. Kozhuharov, E.A. Kuznetsova, J. Maurer, G.V. Mishinsky, M. Pomorski, Yu.V. Pyatkov, O.V. Strekalovsky, M. Tr¨ager and V.E. Zhuchko, "Pulse-height defect in single-crystal CVD diamond detectors", Eur. Phys. J. A 53, 32 (2017)*.

M. Klintefjord, K. Hadynska-Klek, A. Gorgen, C. Bauer, F.L. Bello Garrote, S. Bonig, B. Bounthong, A. Damyanova, J.P. Delaroche, V.

Fedosseev, D.A. Fink, F. Giacoppo, M. Girod, P. Hoff, N. Imai, W. Korten, A.C. Larsen, J. Libert, R. Lutter, B.A. Marsh, P.L. Molkanov, H. Naidja, P. Napiorkowski, F. Nowacki, J. Pakarinen, E. Rapisarda, P. Reiter, T. Renstrom, S. Rothe, M.D. Seliverstov, B. Siebeck, S. Siem, J. Srebrny, T. Stora, P. Thole, T.G. Tornyi, G.M. Tveten, P. Van Duppen, M.J. Vermeulen, D. Voulot, N. Warr, F. Wenander, H.De Witte, M. Zielinska:"Structure of low-lying states in 140Sm studied by Coulomb excitation", Phys.Rev. C 93, 054303 (2016)*.

J. Lee, H. Liu, P. Doornenbal, M. Kimura, K. Minomo, K. Ogata, Y. Utsuno, N. Aoi, K. Li, M. Matsushita, H. Scheit, D. Steppenbeck, S. Takeuchi, H. Wang, H. Baba, E. Ideguchi, N. Kobayashi, Y. Kondo, S. Michimasa, T. Motobayashi, H. Sakurai, M. Takechi, and Y. Togano, “Asymmetry dependence of reduction factors from single-nucleon knockout of ^{30}Ne at ~230 MeV/nucleon”, Progress of Theoretical and Experimental Physics 2016, 083D01 (2016)*

C. Babcock, H. Heylen, M. L. Bissell, K. Blaum, P. Campbell, B. Cheal, D. Fedorov, R. F. Garcia Ruiz, W. Geithner, W. Gins, T. Day Goodacre, L.K. Grob, M. Kowalska, S. M. Lenzi, B. Maass, S. Malbrunot-Ettenauer, B. Marsh, R. Neugart, G. Neyens, W. Nörtershäuser, T. Otsuka, R. Rossel, S. Rothe, R. Sánchez, Y. Tsunoda, C. Wraith, L. Xie, and X. F. Yang, “Quadrupole moments of odd-A $^{53-63}$Mn: Onset of collectivity towards N=40”, Physics Letters B 760, 387 (2016)*

H. Heylen, M. De Rydt, G. Neyens, M. L. Bissell, L. Caceres, R. Chevrier, J. M. Daugas, Y. Ichikawa, Y. Ishibashi, O. Kamalou, T. J. Mertzimekis, P. Morel, J. Papuga, A. Poves, M. M. Rajabali, C. Stödel, J. C. Thomas, H. Ueno, Y. Utsuno, N. Yoshida, and A. Yoshimi, “High-precision quadrupole moment reveals significant intruder component in $^{33}_{13}Al_{20}$ ground state”, Physical Review C 94, 034312 (2016)*

T. Togashi, Y. Tsunoda, T. Otsuka, and N. Shimizu, “Quantum Phase Transition in the Shape of Zr isotopes”, Physical Review Letters 117, 172502 (2016)*

C. Kremer, S. Aslanidou, S. Bassauer, M. Hilcker, A. Krugmann, P. von Neumann-Cosel, T. Otsuka, N. Pietralla, V. Yu. Ponomarev, N. Shimizu, M. Singer, G. Steinhilber, T. Togashi, Y. Tsunoda, V. Werner, and M. Zweidinger, “First Measurement of Collectivity of Coexisting Shapes Based on Type II Shell Evolution: The Case of ^{96}Zr”, Physical Review Letters 117, 172503 (2016)*

H. Heylen, C. Babcock, R. Beerwerth, J. Billowes, M. L. Bissell, K. Blaum, J. Bonnard, P. Campbell, B. Cheal, T. Day Goodacre, D. Fedorov, S. Fritzsche, R. F. Garcia Ruiz, W. Geithner, Ch. Geppert, W. Gins, L. K. Grob, M. Kowalska, K. Kreim, S. M. Lenzi, I. D. Moore, B. Maass, S. Malbrunot-Ettenauer, B. Marsh, R. Neugart, G. Neyens, W. Nörtershäuser, T. Otsuka, J. Papuga, R. Rossel, S. Rothe, R. Sánchez, Y. Tsunoda, C. Wraith, L. Xie, X. F. Yang, and D. T. Yordanov, “Changes in nuclear structure along the Mn isotopic chain studied via charge radii”, Physical Review C 94, 054321 (2016)*

A. I. Morales, G. Benzoni, H. Watanabe, Y. Tsunoda, T. Otsuka, S. Nishimura, F. Browne, R. Daido, P. Doornenbal, Y. Fang, G. Lorusso, Z. Patel, S. Rice, L. Sinclair, P.-A. Söderström, T. Sumikama, J. Wu, Z. Y. Xu, A. Yagi, R. Yokoyama, H. Baba, R. Avigo, F. L. Bello Garrote, N. Blasi, A. Bracco, F. Camera, S. Ceruti, F. C. L. Crespi, G. de Angelis, M.-C. Delattre, Zs. Dombradi, A. Gottardo, T. Isobe, I. Kojouharov, N. Kurz, I. Kuti, K. Matsui, B. Melon, D. Mengoni, T. Miyazaki, V. Modamio-Hoybjor, S. Momiyama, D.R. Napoli, M. Niikura, R. Orlandi, H. Sakurai, E. Sahin, D. Sohler, H. Schaffner, R. Taniuchi, J. Taprogge, Zs. Vajta, J. J. Valiente-Dobón, O. Wieland, and M. Yalcinkaya, “Type II shell evolution in A=70 isobars from the N≥40 island of inversion”, Physics Letters B 765, 328 (2017)*

N. Paul, A. Corsi, A. Obertelli, P. Doornenbal, G. Authelet, H. Baba, B. Bally, M. Bender, D. Calvet, F. Château, S. Chen, J.-P. Delaroche, A. Delbart, J.-M. Gheller, A. Giganon, A. Gillibert, M. Girod, P.-H. Heenen, V. Lapoux, J. Libert, T. Motobayashi, M. Niikura, T. Otsuka, T. R. Rodríguez, J.-Y. Roussé, H. Sakurai, C. Santamaria, N. Shimizu, D. Steppenbeck, R. Taniuchi, T. Togashi, Y. Tsunoda, T. Uesaka, T. Ando, T. Arici, A. Blazhev, F. Browne, A. M. Bruce, R. Caroll, L. X. Chung, M.L. Cortés, M. Dewald, B. Ding, F. Flavigny, S. Franchoo, M. Górska, A. Gottardo, A. Jungclaus, J. Lee, M. Lettmann, B. D. Linh, J. Liu, Z. Liu, C. Lizarazo, S. Momiyama, K. Moschner, S. Nagamine, N. Nakatsuka, C. Nita, C. R. Nobs, L. Olivier, Z. Patel, Z. Podolyák, M. Rudigier, T. Saito, C. Shand, P.-A. Söderström, I. Stefan, R. Orlandi, V. Vaquero, V. Werner, K. Wimmer, and Z. Xu, “Are There Signatures of Harmonic Oscillator Shells Far from Stability? First Spectroscopy of ^{110}Zr”, Physical Review Letters 118, 032501 (2017)*

N. Tsunoda, T. Otsuka, N. Shimizu, M. Hjorth-Jensen, K. Takayanagi, and T. Suzuki, “Exotic neutron-rich medium-mass nuclei with realistic nuclear forces”, Physical Review C 95, 021304(R) (2017)*

V. Tripathi, R. S. Lubna, B. Abromeit, H. L. Crawford, S. N. Liddick, Y. Utsuno, P. C. Bender, B. P. Crider, R. Dungan, P. Fallon, K. Kravvaris, N. Larson, A. O. Macchiavelli, T. Otsuka, C. J. Prokop, A. L. Richard, N. Shimizu, S. L. Tabor, A. Volya, and S. Yoshida, “β decay of ^{38,40}Si (T_z=+5,+6) to low-lying core excited states in odd-odd ^{38,40}P isotopes”, Physical Review C 95, 024308 (2017)*

H.N. Liu, J. Lee, P. Doornenbal, H. Scheit, S. Takeuchi, N. Aoi, K.A. Li, M. Matsushita, D. Steppenbeck, H. Wang, H. Baba, E. Ideguchi, N. Kobayashi, Y. Kondo, G. Lee, S. Michimasa, T. Motobayashi, A. Poves, H. Sakurai, M. Takechi, Y. Togano, J.A. Tostevin, and Y. Utsuno, “Intruder configurations in the ground state of ^{30}Ne”, Physics Letters B 767, 58 (2017)*

He Wang, Hideaki Otsu, Hiroyoshi Sakurai, DeukSoon Ahn, Masayuki Aikawa, Takashi Ando, Shouhei Araki, Sidong Chen, Nobuyuki Chiga, Pieter Doornenbal, Naoki Fukuda , Tadaaki Isobe, Shunsuke Kawakami, Shoichiro Kawase, Tadahiro Kin, Yosuke Kondo, Shunpei Koyama, Shigeru Kubono, Yukie Maeda, Ayano Makinaga, Masafumi Matsushita, Teiichiro Matsuzaki, Shin’ichiro Michimasa, Satoru Momiyama, Shunsuke Nagamine, Takashi Nakamura, Keita Nakano, Megumi Niikura,Tomoyuki Ozaki, Atsumi Saito, Takeshi Saito, Yoshiaki Shiga, Mizuki Shikata, Yohei Shimizu, Susumu Shimoura, Toshiyuki Sumikama, Par-Anders Soderstrom, Hiroshi Suzuki, Hiroyuki Takeda, Satoshi Takeuchi, Ryo Taniuchi, Yasuhiro Togano, Junichi Tsubota, Meiko Uesaka, Yasushi Watanabe, Yukinobu Watanabe, Kathrin Wimmer, Tatsuya Yamamoto, Koichi Yoshida: ``Spallation reaction study for the long-lived fission product ^{107}Pd", Prog. Theor. Exp. Phys. 2017, 021D01 (2017) *

P. Doornenbal, H. Scheit, S. Takeuchi, N. Aoi, K. Li, M. Matsushita, D. Steppenbeck, H. Wang, H. Baba, E. Ideguchi, N. Kobayashi, Y. Kondo, J. Lee, S. Michimasa, T. Motobayashi, A. Poves,H. Sakurai, M. Takechi, Y. Togano, K. Yoneda: ``Mapping the deformation in the island of inversion: Inelastic scattering of ^{30}Ne and ^{36}Mg at intermediate energies",Phys. Rev. C 93, 044306 (2016) *

D.Q. Fang, Y.G. Ma, X.Y. Sun, P. Zhou, Y. Togano, N. Aoi, H. Baba, X.Z. Cai, X.G. Cao, J.G. Chen, Y. Fu, W. Guo, Y. Hara, T. Honda, Z.G. Hu, K. Ieki, Y. Ishibashi, Y. Ito, N. Iwasa, S. Kanno, T. Kawabata, H. Kimura, Y. Kondo, K. Kurita, M. Kurokawa, T. Moriguchi, H. Murakami, H. Ooishi, K. Okada, S. Ota, A. Ozawa, H. Sakurai, S. Shimoura, R. Shioda, E. Takeshita, S.Takeuchi, W.D. Tian, H.W. Wang, J.S. Wang, M. Wang, K. Yamada, Y. Yamada, Y. Yasuda, K. Yoneda, G.Q. Zhang, T. Motobayashi: ``Proton-proton correlations in distinguishing the two-proton emission mechanism of ^{23}Al and ^{22}Mg'', Phys. Rev. C94, 044621 (2016) *

H. Wang, N. Aoi, S. Takeuchi, M. Matsushita, T. Motobayashi, D. Steppenbeck, K. Yoneda, H. Baba, Zs. Dombradi, K. Kobayashi, Y. Kondo, J. Lee, H. Liu, R. Minakata, D. Nishimura, H. Otsu, H. Sakurai, D. Sohler, Y. Sun, Z. Tian, R. Tanaka, Zs. Vajta, Z. Yang, T. Yamamoto, Y. Ye, R. Yokoyama: ``First spectroscopic information from even-even nuclei in the region "southeast" of ^{132}Sn: Neutron-excitation dominance of the 2^{+1} state in ^{132}Cd", Phys. Rev. C 94, 051301 (2016) *

E. Ideguchi, G.S. Simpson, R. Yokoyama, Mn. Tanaka, S. Nishimura, P. Doornenbal, G. Lorusso, P. Aoderstrom, T. Sumikama, J. Wu, Z. Y.

Xu, N. Aoi, H. Baba, F. L. Bello Garrote, G. Benzoni, F. Browne, R. Daido, Y. Fang, N. Fukuda, A. Gottardo, G. Gey, S. Go, N. Inabe, T. Isobe, D. Kameda, K. Kobayashi, M. Kobayashi, I. Kojouharov, T. Komatsubara, T. Kubo, N. Kurz, I. Kuti, Z. Li, M. Matsushita, S. Michimasa, C.B. Moon, H. Nishibata, I. Nishizuka, A. Odahara, Z. Patel, S. Rice, E. Sahin, H. Sakurai, H. Schaffner, L. Sinclair, H. Suzuki, H. Takeda, J. Taprogge, Zs. Vajta, H. Watanabe, A. Yagi: ``μ s isomers of ^{158,160}Nd'', Phys. Rev. C94, 064322 (2016) *

M. Dozono, T. Uesaka, S. Michimasa, M. Takaki, M. Kobayashi, M. Matsushita, S. Ota, H. Tokieda, S. Shimoura:"Separated flow operation of the SHARAQ spectrometer for in-flight proton-decay experiments", Nucl. Instr. Meth. Phys. Res. A 830, 233--242 (2016) *

R. Yokoyama, S. Go, D. Kameda, T. Kubo, N. Inabe, N. Fukuda, H. Takeda, H. Suzuki, K. Yoshida, K. Kusaka, K. Tanaka, Y. Yanagisawa, M. Ohtake, H. Sato, Y. Shimizu, H. Baba, M. Kurokawa, D. Nishimura, T. Ohnishi, N. Iwasa, A. Chiba, T. Yamada, E. Ideguchi, T. Fujii, H. Nishibata, K. Ieki, D. Murai, S. Momota, Y. Sato, J.W. Hwang, S. Kim, O.B. Tarasov, D.J. Morrissey, B.M. Sherrill, G. Simpson, C.R. Praharaj: ``New K isomers in the neutron-rich N=100 isotones ^{162}Sm, ^{163}Eu, and ^{164}Gd'', Phys. Rev. C95, 034313 (2017) *

J. Wu, S. Nishimura, G. Lorusso, P. Moller, E. Ideguchi, P.H. Regan, G.S. Simpson, P. A. Soderstrom, P.M. Walker, H. Watanabe, Z.Y. Xu, H. Baba, F. Browne, R. Daido, P. Doornenbal, Y.F. Fang, G. Gey, T. Isobe, P.S. Lee, J.J. Liu, Z. Li, Z. Korkulu, Z. Patel, V. Phong, S. Rice, H. Sakurai, L. Sinclair, T. Sumikama, M. Tanaka, A. Yagi, Y.L. Ye, R. Yokoyama, G.X. Zhang, T. Alharbi, N. Aoi, F.L. Bello Garrote, G. Benzoni, A.M. Bruce, R.J. Carroll, K.Y. Chae, Z. Dombradi, A. Estrade, A. Gottardo, C.J. Griffin, H. Kanaoka, I. Kojouharov, F.G. Kondev, S. Kubono, N. Kurz, I. Kuti, S. Lalkovski, G.J. Lane, E.J. Lee, T. Lokotko, G. Lotay, C. B. Moon, H. Nishibata, I. Nishizuka, C.R. Nita, A. Odahara, Zs. Podolyak, O.J. Roberts, H. Schaffner, C. Shand, J. Taprogge, S. Terashima, Z. Vajta, S. Yoshida: ``94 β-Decay Half-Lives of Neutron-Rich $_{55}$Cs to $_{67}$Ho: Experimental Feedback and Evaluation of the r-Process Rare-Earth Peak Formation'', Phys. Rev. Lett. 118, 0722701 (2017) *

A.I. Morales, G. Benzoni, H. Watanabe, Y. Tsunoda, T. Otsuka, S. Nishimura, F. Browne, R. Daido, P. Doornenbal, Y. Fang, G. Lorusso, Z. Patel, S. Rice, L. Sinclair, P.A. Soderstrom, T. Sumikama, J. Wu, Z.Y. Xu, A. Yagi, R. Yokoyama, H. Baba, R. Avigo, F.L. Bello Garrote, N. Blasi, A. Bracco, F. Camera, S. Ceruti, F.C.L. Crespi, G. de Angelis, M.C. Delattre, Zs. Dombradi, A. Gottardo, T. Isobe, I. Kojouharov, N. Kurz, I. Kuti, K. Matsui, B. Melon, D. Mengoni, T. Miyazaki, V. Modamio-Hoybjor, S. Momiyama, D.R. Napoli, M. Niikura, R.Orlandi, H.Sakurai, E.Sahin, D.Sohler, H.Schaffner, R.Taniuchi, J.Taprogge, Zs. Vajta, J.J. Valiente-Dobon, O. Wieland, M. Yalcinkaya: ``Type II shell evolution in A=70 isobars from the N> 40 island of inversion'',Phys.~Lett.~B 765, 328 (2017) *

A. Adare et al. [PHENIX Collaboration], ``Angular decay coefficients of J/ψ mesons at forward rapidity from p+p collisions at $\sqrt{s}$ =510 GeV,'' Phys. Rev. D **95**, 092003 (2017) *

J. Adam et al. [ALICE Collaboration], ``W and Z boson production in p-Pb collisions at $\sqrt{s_{NN}}$ = 5.02 TeV,'' JHEP **1702**, 077 (2017) *

J. Adam et al. [ALICE Collaboration], ``Determination of the event collision time with the ALICE detector at the LHC,'' Eur. Phys. J. Plus **132**, no. 2, 99 (2017) *

A. Adare et al. [PHENIX Collaboration], ``Measurement of the relative yields of ψ(2S) to ψ(1S) mesons produced at forward and backward rapidity in pp, p+Al, p+Au, and ^{3}He+Au collisions at $\sqrt{s_{NN}}$=200 GeV,'' Phys. Rev. C **95**, no. 3, 034904 (2017) *

A. Adare et al. [PHENIX Collaboration], ``Nonperturbative-transverse-momentum effects and evolution in dihadron and direct photon-hadron angular correlations in pp collisions at $\sqrt{s}$ =510 GeV,'' Phys. Rev. D **95**, no. 7, 072002 (2017) *

J. Adam et al. [ALICE Collaboration], ``Jet-like correlations with neutral pion triggers in pp and central Pb–Pb collisions at 2.76 TeV,'' Phys. Lett. B **763**, 238 (2016) *

J. Adam et al. [ALICE Collaboration], ``J/ψ suppression at forward rapidity in Pb-Pb collisions at $\sqrt{s_{NN}}$ = 5.02 TeV", Phys. Lett. B **766**, 212 (2017) *

J. Adam et al. [ALICE Collaboration],``Enhanced production of multi-strange hadrons in high-multiplicity proton-proton collisions,'' Nature Phys. **13**, 535 (2017) *

J. Adam et al. [ALICE Collaboration], ``Higher harmonic flow coefficients of identified hadrons in Pb-Pb collisions at $\sqrt{s_{NN}}$ = 2.76 TeV,'' JHEP **1609**, 164 (2016) *

A. Adare et al. [PHENIX Collaboration], ``Measurements of double-helicity asymmetries in inclusive J/ψ production in longitudinally polarized p+p collisions at $\sqrt{s}$=510$ GeV,'' Phys. Rev. D **94**, no. 11, 112008 (2016) *

J. Adam et al. [ALICE Collaboration], ``Elliptic flow of electrons from heavy-flavour hadron decays at mid-rapidity in Pb-Pb collisions at $\sqrt{s_{NN}}$ =2.76 $ TeV,'' JHEP **1609**, 028 (2016) *

J. Adam et al. [ALICE Collaboration], ``D-meson production in p-Pb collisions at $\sqrt{s_{NN}}$=5.02 TeV and in pp collisions at $\sqrt{s}$=7 TeV,'' Phys. Rev. C **94**, no. 5, 054908 (2016) *

J. Adam et al. [ALICE Collaboration],``Measurement of azimuthal correlations of D mesons and charged particles in pp collisions at $\sqrt{s}$=7$ TeV and p-Pb collisions at $\sqrt{s_{NN}}$=5.02$ TeV,'' Eur. Phys. J. C **77**, no. 4, 245 (2017) *

J. Adam et al. [ALICE Collaboration],``Pseudorapidity dependence of the anisotropic flow of charged particles in Pb-Pb collisions at $\sqrt{s_{NN}}$=2.76$ TeV,'' Phys. Lett. B **762**, 376 (2016) *

J. Adam et al. [ALICE Collaboration],``Correlated event-by-event fluctuations of flow harmonics in Pb-Pb collisions at $\sqrt{s_{NN}}$=2.76$ TeV,'' Phys. Rev. Lett. **117**, 182301 (2016) *

J. Adam et al. [ALICE Collaboration],``Measurement of transverse energy at midrapidity in Pb-Pb collisions at $\sqrt{s_{NN}}$ = 2.76$ TeV,'' Phys. Rev. C **94**, no. 3, 034903 (2016) *

J. Adam et al. [ALICE Collaboration],``Centrality dependence of charged jet production in p–Pb collisions at$\sqrt{s_{NN}}$ = 5.02 TeV,'' Eur. Phys. J. C **76**, no. 5, 271 (2016) *

J. Adam et al. [ALICE Collaboration],``Centrality dependence of ψ(2S) suppression in p-Pb collisions at $\sqrt{s_{NN}}$ = 5.02 TeV,'' JHEP **1606**, 050 (2016) *

J. Adam et al. [ALICE Collaboration],``Measurement of D-meson production versus multiplicity in p-Pb collisions at $\sqrt{s_{NN}}$=5.02 TeV,'' JHEP **1608**, 078 (2016) *

J. Adam et al. [ALICE Collaboration], ``Particle identification in ALICE: a Bayesian approach,'' Eur. Phys. J. Plus **131**, no. 5, 168 (2016) *

J. Adam et al. [ALICE Collaboration], ``Anisotropic flow of charged particles in Pb-Pb collisions at $\sqrt{s_{NN}}$=5.02 TeV,'' Phys. Rev. Lett. **116**, no. 13, 132302 (2016) *

J. Adam et al. [ALICE Collaboration], ``Production of $K^*(892)^0$ and ϕ(1020) in p–Pb collisions at $\sqrt{s_{NN}}$ = 5.02 TeV,'' Eur. Phys. J. C **76**, no. 5, 245 (2016) *

J. Adam et al. [ALICE Collaboration], ``Multiplicity dependence of charged pion, kaon, and (anti)proton production at large transverse momentum in p-Pb collisions at $\sqrt{s_{NN}}$ = 5.02 TeV,'' Phys. Lett. B **760**, 720 (2016) *

J. Adam et al. [ALICE Collaboration], ``Multipion Bose-Einstein correlations in pp,p -Pb, and Pb-Pb collisions at energies available at the CERN Large Hadron Collider,'' Phys. Rev. C **93**, no. 5, 054908 (2016) *
J. Adam et al. [ALICE Collaboration], ``Multi-strange baryon production in p-Pb collisions at $\sqrt{s_{NN}}$ = 5.02$ TeV,'' Phys. Lett. B **758**, 389 (2016) *
J. Adam et al. [ALICE Collaboration], ``Centrality dependence of the charged-particle multiplicity density at midrapidity in Pb-Pb collisions at $\sqrt{s_{NN}}$ = 5.02 TeV,'' Phys. Rev. Lett. **116**, no. 22, 222302 (2016) *
J. Adam et al. [ALICE Collaboration], ``Measurement of an excess in the yield of J/ψ at very low p_T in Pb-Pb collisions at $\sqrt{s_{NN}}$ = 2.76 TeV,'' Phys. Rev. Lett. **116**, no. 22, 222301 (2016) *
J. Adam et al. [ALICE Collaboration], ``Pseudorapidity and transverse-momentum distributions of charged particles in proton–proton collisions at $\sqrt{s}$= 13 TeV,'' Phys. Lett. B **753**, 319 (2016) *
J. Adam et al. [ALICE Collaboration], ``Inclusive quarkonium production at forward rapidity in pp collisions at $\sqrt{s}$=8 TeV,'' Eur. Phys. J. C **76**, no. 4, 184 (2016) *
A. Adare et al. [PHENIX Collaboration], ``Measurements of directed, elliptic, and triangular flow in Cu+Au collisions at $\sqrt{s_{NN}}$=200$ GeV,'' Phys. Rev. C **94**, no. 5, 054910 (2016) *
A. Adare et al. [PHENIX Collaboration], ``Azimuthally anisotropic emission of low-momentum direct photons in Au+Au collisions at $\sqrt{s_{NN}}$=200$ GeV,'' Phys. Rev. C **94**, no. 6, 064901 (2016) *
J. Adam et al. [ALICE Collaboration], ``Measurement of electrons from heavy-flavour hadron decays in p-Pb collisions at $\sqrt{s_{NN}}$ = 5.02 TeV,'' Phys. Lett. B **754**, 81 (2016) *
J. Adam et al [ALICE Collaboration], ``Azimuthal anisotropy of charged jet production in $\sqrt{s_{NN}}$ = 2.76 TeV Pb-Pb collisions,'' Phys. Lett. B **753**, 511 (2016) *
J. Adam et al. [ALICE Collaboration], ``Direct photon production in Pb-Pb collisions at $\sqrt{s_{NN}}$ =$ 2.76 TeV,'' Phys. Lett. B **754**, 235 (2016) *
J. Adam et al. [ALICE Collaboration], ``Centrality evolution of the charged-particle pseudorapidity density over a broad pseudorapidity range in Pb-Pb collisions at $\sqrt{s_{NN}}$= 2.76 TeV,'' Phys. Lett. B **754**, 373 (2016) *
J. Adam et al. [ALICE Collaboration], ``Measurement of D_s^+ production and nuclear modification factor in Pb-Pb collisions at $\sqrt{s_{NN}}$ = 2.76 TeV,'' JHEP **1603**, 082 (2016) *
J. Adam et al. [ALICE Collaboration],``Multiplicity and transverse momentum evolution of charge-dependent correlations in pp, p–Pb, and Pb–Pb collisions at the LHC,'' Eur. Phys. J. C **76**, no. 2, 86 (2016) *
J. Adam et al. [ALICE Collaboration], ``Transverse momentum dependence of D-meson production in Pb-Pb collisions at $\sqrt{s_{NN}}$=$ 2.76 TeV,'' JHEP **1603**, 081 (2016) *
A. Adare et al. [PHENIX Collaboration], ``Scaling properties of fractional momentum loss of high-p_T hadrons in nucleus-nucleus collisions at $\sqrt{s_{NN}}$ from 62.4 GeV to 2.76 TeV,'' Phys. Rev. C **93**, no. 2, 024911 (2016) *
A. Adare et al. [PHENIX Collaboration], ``Transverse energy production and charged-particle multiplicity at midrapidity in various systems from $\sqrt{s_{NN}}$=7.7$ to 200 GeV,'' Phys. Rev. C **93**, no. 2, 024901 (2016) *
A. Adare et al. [PHENIX Collaboration], ``ϕ meson production in the forward/backward rapidity region in Cu+Au collisions at $\sqrt{s_{NN}}$=200 GeV,'' Phys. Rev. C **93**, no. 2, 024904 (2016) *
A. Adare et al. [PHENIX Collaboration], ``Forward J/ψ production in U+U collisions at $\sqrt{s_{NN}}$=193 GeV,'' Phys. Rev. C **93**, no. 3, 034903 (2016) *
A. Adare et al. [PHENIX Collaboration], ``Dielectron production in Au+Au collisions at $\sqrt{s_{NN}}$=200 GeV,'' Phys. Rev. C **93**, no. 1, 014904 (2016) *
A. Adare et al. [PHENIX Collaboration], ``Single electron yields from semileptonic charm and bottom hadron decays in Au+Au collisions at $\sqrt{s_{NN}}$=200 GeV,'' Phys. Rev. C **93**, no. 3, 034904 (2016) *
A. Adare et al. [PHENIX Collaboration], ``Centrality-dependent modification of jet-production rates in deuteron-gold collisions at $\sqrt{s_{NN}}$ =200 GeV,'' Phys. Rev. Lett. **116**, no. 12, 122301 (2016) *
J. Adam et al. [ALICE Collaboration], ``Study of cosmic ray events with high muon multiplicity using the ALICE detector at the CERN Large Hadron Collider,'' JCAP **1601**, no. 01, 032 (2016) *
J. Adam et al. [ALICE Collaboration], ``Centrality dependence of pion freeze-out radii in Pb-Pb collisions at $\sqrt{s_{NN}}$= 2.76 TeV,'' Phys. Rev. C **93**, no. 2, 024905 (2016) *
J. Adam et al. [ALICE Collaboration], ``Event shape engineering for inclusive spectra and elliptic flow in Pb-Pb collisions at $\sqrt{s_{NN}}$=2.76 TeV,'' Phys. Rev. C **93**, no. 3, 034916 (2016) *
J. Adam et al. [ALICE Collaboration], ``Elliptic flow of muons from heavy-flavour hadron decays at forward rapidity in Pb–Pb collisions at $\sqrt{s_{NN}}$= 2.76$ TeV,'' Phys. Lett. B **753**, 41 (2016) *
J. Adam et al. [ALICE Collaboration], ``Production of light nuclei and anti-nuclei in pp and Pb-Pb collisions at energies available at the CERN Large Hadron Collider,'' Phys. Rev. C **93**, no. 2, 024917 (2016) *
J. Adam et al. [ALICE Collaboration], ``Differential studies of inclusive J/ψ and ψ(2S) production at forward rapidity in Pb-Pb collisions at $\sqrt{s_{NN}}$=2.76 $ TeV,'' JHEP {¥bf **1605**}, 179 (2016) *
J. Adam et al. [ALICE Collaboration], ``Forward-central two-particle correlations in p-Pb collisions at $\sqrt{s_{NN}}$ = 5.02 TeV,'' Phys. Lett. B **753**, 126 (2016) *
A. Adare et al. [PHENIX Collaboration], ``Measurement of higher cumulants of net-charge multiplicity distributions in Au+Au collisions at $\sqrt{s_{NN}}$=7.7-200$ GeV,'' Phys. Rev. C **93**, no. 1, 011901 (2016) *
J. Adam et al. [ALICE Collaboration], ``Centrality dependence of the nuclear modification factor of charged pions, kaons, and protons in Pb-Pb collisions at $\sqrt{s_{NN}}$=2.76 TeV,'' Phys. Rev. C **93**, no. 3, 034913 (2016) *
A. Adare et al. [PHENIX Collaboration], ``Measurement of parity-violating spin asymmetries in W^{+-} production at midrapidity in longitudinally polarized p+p collisions,'' Phys. Rev. D **93**, no. 5, 051103 (2016) *
A. Adare et al. [PHENIX Collaboration],``Measurement of the higher-order anisotropic flow coefficients for identified hadrons in Au+Au collisions at $\sqrt{s_{NN}}$ = 200 GeV,'' Phys. Rev. C **93**, no. 5, 051902 (2016) *
B. Abelev et al. [ALICE Collaboration], ``Measurement of electrons from beauty hadron decays in pp collisions at $\sqrt{s}$=7$ TeV,'' Phys. Lett. B **721**, 13 (2013) Erratum: [Phys. Lett. B **763**, 507 (2016)] *
J. Yasuda et al.: ``Inverse kinematics (p,n) reactions studies using the WINDS slow neutron detector and the SAMURAI spectrometer'', Nucl.

Instr. and Meth. In Phys. Res. B 376, 393 (2016)*
A. Krasznahorkay et al.: ``Observation of anomalous internal pair creation in ^{8}Be: A possible indication of a light, neutral boson'', Phys. Rev. Lett. 042501 (2016)*
J.C. Zamora et al.: ``First measurement of isoscalar giant resonances in a stored-beam experiment'', Phys. Lett. B 763, 16 (2016)*
P. Russotto et al.: ``Results of the ASY-EOS experiment at GSI: The symmetry energy at supra-saturation density'', Phys. Rev. C 94 034608 (2016)*

[Proceedings]
(Original Papers) *Subject to Peer Review
D. Kahl, A. A. Chen, S. Kubono, H. Yamaguchi, D. N. Binh, J. Chen, S. Cherubini, N.N. Duy, T. Hashimoto, S. Hayakawa, N. Iwasa, H.S. Jung, S. Kato, Y.K. Kwon, S. Nishimura, S. Ota, K. Setoodehnia, T. Teranishi, H. Tokieda, T. Yamada, C.C. Yun and L.Y. Zhang: ``Experimental investigation of the ^{30}S(alpha, p) thermonuclear reaction in x-ray bursts'', EPJ Web of Conferences **109,** 04005 (2016).
Y.B. Wang, S.J. Jin, L. Jing, Z.Y. Han, X.X. Bai, B. Guo, Y.J. Li, Z.H. Li, G. Lian, J. Su, L.J. Sun, S.Q. Yan, S. Zeng, W.P. Liu, H. Yamaguchi, S. Kubono, J. Hu, D. Kahl, J.J He, J.S. Wang, X.D. Tang, S.W. Xu, P. Ma, N.T. Zhang, Z. Bai, M.R. Huang, B.L. Jia, S.L. Jin, J.B. Ma, S.B. Ma, W.H. Ma, Y.Y. Yang, L.Y. Zhang, H.S. Jung, J.Y. Moon, C.S. Lee. T. Teranishi, H.W. Wang, H. Ishiyama, N. Iwasa, T. Komatsubara and B.A. Brown: ``Two measurements of the ^{22}Na+p resonant scattering via thick-target inverse-kinematics method'', EPJ Web of Conferences **109,** 04010 (2016).
S. Kubono, H. Yamaguchi, S. Hayakawa, S.Q. Hou and J.J. He, ``Explosive Nuclear Burning in the pp-Chain Region and the Breakout Processes'', EPJ Web of Conferences **109** 01001 (2016).
S. Hayakawa, C. Spitaleri, N. Burtebayev, A. Aimaganbetov, P. Figuera, M. Fisichella, G.L. Guardo, S. Igamov, I. Indelicato, G. Kiss, S. Kliczewski, M. La Cognata, L. Lamia, M. Lattuada, E. Piasecki, G. G. Rapisarda, S. Romano, S. B. Sakuta, R. Siudak, A. Trzcinska, A. Tumino and A. Urkinbayev: ``Indirect Study of the ^{16}O + ^{16}O Fusion Reaction Toward Stellar Energies by the Trojan Horse Method'', Nucleus Nucleus 2015 (NN2015), Catania, Italy, EPJ Web of Conferences **109**, 09013 (2016).
H. Yamaguchi, D. Kahl, S. Hayakawa, Y. Sakaguchi, Y. Wakabayashi, T. Hashimoto, S. Cherubini, M. Gulino, C. Spitaleri, G.G. Rapisarda, M. La Cognata, L. Lamia, S. Romano, S. Kubono, N. Iwasa, T. Teranishi, T. Kawabata, Y.K. Kwon, D.N. Binh, L.H. Khiem, N.N. Duy, S. Kato, T. Komatsubara, A.Coc, N. de Sereville, F.Hammache, G. Kiss and S. Bishop: ``Studying astrophysical reactions with low-energy RI beams at CRIB'', EPJ Web of Conferences **117,** 09005 (2016).
G. D'Agata, C. Spitaleri, R.G. Pizzone, S. Blagus, P. Figuera, L. Grassi, G.L. Guardo, M. Gulino, S. Hayakawa, I. Indelicato, R. Kshetri, M. La Cognata, L. Lamia, M. Lattuada, T. Mijatović, M. Milin, D. Miljanic, L. Prepolec, M.L. Sergi, N. Skukan, N. Soic, V. Tokic, A. Tumino and M. Uroic: ``First evidences for ^{19}F(alpha,p)^{22}Ne at astrophysical energies'', 8th European Summer School on Experimental Nuclear Astrophysics, S. Tecla, Italy, J. of Phys.: Conf. Series, **703**, 012016 (2016).
M. Mazzocco, A. Boiano, C. Boiano, M. La Commara, C. Manea, C. Parascandolo, D. Pierroutsakou, C. Signorini, E. Strano, D. Torresi, H. Yamaguchi, D. Kahl, L. Acosta, P. Di Meo, J.P. Fernandez-Garcia, T. Glodariu, J. Grebosz, A. Guglielmetti, N. Imai, Y. Hirayama, H. Ishiyama, N. Iwasa, S.C. Jeong, H.M. Jia, N. Keeley, Y.H. Kim, S. Kimura, S. Kubono, J.A. Lay, C.J. Lin, G. Marquinez-Duran, I. Martel, H. Miyatake, M. Mukai, T. Nakao, M. Nicoletto, A. Pakou, K. Rusek, Y. Sakaguchi, A.M. Sanchez-Benitez, T. Sava, O. Sgouros, C. Stefanini, F. Soramel, V. Soukeras, E. Stiliaris, L. Stroe, T. Teranishi, N. Toniolo, Y. Wakabayashi, Y.X. Watanabe, L. Yang and Y.Y. Yang, ``^{7}Be- and ^{8}B-reaction dynamics at Coulomb barrier energies'', EPJ Web of Conferences **117,** 060006 (2016).
H. Yamaguchi, D. Kahl, S. Hayakawa, L. Yang, Y. Sakaguchi, K. Abe, H. Shimizu, and CRIB Collaboration, ``Overview of the activities at the low-energy beam separator CRIB'', Il Nuovo Cimento **39**C, 358 (2016).
D. Kahl, H. Yamaguchi, H. Shimizu, K. Abe, O. Beliuskina, S. M. Cha, K.Y. Chae, Z. Ge, S. Hayakawa, M.S. Kwag, D. H. Kim, J. Y. Moon, S.Y. Park, L. Yang: ”Explosive destruction of ^{26}Al'', Il Nuovo Cimento **39**C, 362 (2016).
S. Hayakawa: ``Trials for the cosmological ^{7}Li problem with 7Be beams at CRIB and collaborating studies'', Il Nuovo Cimento **39**C 370 (2016).
S.M. Cha, K.Y. Chae, K. Abe, S.H. Bae, S.H. Choi, D.N. Binh, N.N. Duy, K.I. Hahn, S. Hayakawa, B. Hong, H.S. Jung, D. Kahl, L.H. Khiem, A. Kim, D.H. Kim, E.J. Kim, G.W. Kim, M.J. Kim, K.J. Kwag, M.S. Kwag, Y.K. Kwon, C.S. Lee, E.J. Lee, S.I. Lim, B. Moon, J.Y. Moon, T. Nakao, S.Y. Park, H. Shimizu, H. Yamaguchi, L. Yang, and G. Zhuang, ``Study of alpha cluster structure in ^{22}Mg'', Il Nuovo Cimento **39**C, 371 (2016).
S. Hayakawa, C. Spitaleri, N. Burtebayev, A. Aimaganbetov, S.V. Artemov, P. Figuera, M. Fisichella, G.L. Guardo, S. Igamov, I. Indelicato, G.G. Kiss, S. Kubono, M. La Cognata, L. Lamia, M. Lattuada, M. Nassurlla, E. Piasecki, G.G. Rapisarda, S. Romano, S.B. Sakuta, A. Trzcinska, A. Tumino, A. Urkinbayev, and T. Zholdybayev, ``Trojan Horse Method for the Oxygen-Burning Process Reactions'', JPS Conf. Proc. **14,** 020406 (2017).
H. Yamaguchi, D. Kahl, S. Hayakawa, Y. Sakaguchi, K. Abe, H. Shimuzu, Y. Wakabayashi, T. Hashimoto, S. Cherubini, M. Gulino, C. Spitaleri, G. G. Rapisarda, M. La Cognata, L. Lamia, S. Romano, S. Kubono, N. Iwasa, T. Teranishi, T. Kawabata, Y. K. Kwon, D. N. Binh, L. H. Khiem, N. N. Duy, S. Kato, T. Komatsubara, A. Coc, N. de Sereville, F. Hammache, G. Kiss, and S. Bishop, ``Experimental Studies of Light-Ion Nuclear Reactions Using Low-Energy RI Beams'', JPS Conf. Proc. **14,** 010503 (2017).
D. Kahl, A. A. Chen, S. Kubono, H. Yamaguchi, D. N. Binh, J. Chen, S. Cherubini, N. N. Duy, T. Hashimoto, S. Hayakawa, N. Iwasa, H. S. Jung, S. Kato, Y. K. Kwon, S. Nishimura, S. Ota, K. Setoodehnia, T. Teranishi, H. Tokieda, T. Yamada, C. C. Yun, and L. Y. Zhang, ``30S(alpha, p) Thermonuclear Reaction Rate from Experimental Level Structure of 34Ar'', JPS Conf. Proc. **14,** 020510 (2017).
K. Abe, S. Hayakawa, H. Yamaguchi, and L. Lamia, ``Feasibility Study for the 7Be+n Reaction Measurements by Trojan Horse Method at CRIB'', JPS Conf. Proc. **14,** 020507 (2017).
Marisa Gulino, Silvio Cherubini, Claudio Spitaleri, Giuseppe Gabriele Rapisarda, Marco La Cognata, Livio Lamia, Rosario Gianluca Pizzone, Stefano Romano, Shigeru Kubono, Hidetoshi Yamaguchi, Seya Hayakawa, Yasuo Wakabayashi, Naohito Iwasa, Seigo Kato, Tetsuro Komatsubara, Takashi Teranishi, Alain Coc, Nicolas de Sereville, Fairouz Hammache, Gabor Kiss, Shawn Bishop, and Dam Nguyen Binh: ``The ^{18}F(n, alpha) Reaction: First Study of n-Induced Reaction on a Radioactive Nucleus Using the Trojan Horse Method'', JPS Conf. Proc. **14,** 021104 (2017).
N. Shimizu, Y. Utsuno, Y. Futamura, T. Sakurai, T. Mizusaki, T. Otsuka, “Stochastic estimation of level density in nuclear shell-model calculations”, EPJ Web of Conferences 122, 02003 (2016)*

T. Sumikama, D.S. Ahn, N. Fukuda, N. Inabe, T. Kubo, Y. Shimizu, H. Suzuki, H. Takeda, N. Aoi, D. Beaumel, K. Hasegawa, E. Ideguchi, N. Imai, T. Kobayashi, M. Matsushita, S. Michimasa, H. Otsu, S. Shimoura, T. Teranishi: ``First test experiment to produce the slowed-down RI beam with the momentum-compression mode at RIBF'', Proceedings of 17th International Conference on Electromagnetic Isotope Separators and Related Topics (EMIS2015), Nucl. Instr. Meth. Phys. Res. B 376, 180--184 (2016)

J. Yasuda, M. Sasano, R.G.T. Zegers, H. Baba, W. Chao, M. Dozono, N. Fukuda, N. Inabe, T. Isobe, G. Jhang, D. Kameda, T. Kubo, M. Kurata-Nishimura, E. Milman, T. Motobayashi, H. Otsu, V. Panin, W. Powell, H. Sakai, M. Sako, H. Sato, Y. Shimizu, L. Stuhl, H. Suzuki, S. Tangwancharoen, H. Takeda, T. Uesaka, K. Yoneda, J. Zenihiro, T. Kobayashi, T. Sumikama, T. Tako, T. Nakamura, Y. Kondo, Y. Togano, M. Shikata, J. Tsubota, K. Yako, S. Shimoura, S. Ota, S. Kawase, Y. Kubota, M. Takaki, S. Michimasa, K. Kisamori, C.S. Lee, H. Tokieda, M. Kobayashi, S. Koyama, N. Kobayashi, T. Wakasa, S. Sakaguchi, A. Krasznahorkay, T. Murakami, N. Nakatsuka, M. Kaneko, Y. Matsuda, D. Mucher, S. Reichert, D. Bazin, J.W. Lee: ``Inverse kinematics (p,n) reactions studies using the WINDS slow neutron detector and the SAMURAI spectrometer'', Proceedings of 17th International Conference on Electromagnetic Isotope Separators and Related Topics (EMIS2015), Nucl. Instr. Meth. Phys. Res. B 376, 393--396 (2016).

H. Sako et al. [J-PARC Heavy-Ion Collaboration], ``Studies of high density baryon matter with high intensity heavy-ion beams at J-PARC,'' Nucl. Phys. A **956**, 850 (2016).

T. Gunji [ALICE Collaboration], ``Overview of recent ALICE results,'' Nucl. Phys. A **956**, 11 (2016)

C. Zhao, T. Gunji et al., ``First performance results of the ALICE TPC Readout Control Unit 2,'' JINST **11**, no. 01, C01024 (2016).

K. Itahashi et al., ``Precision spectroscopy of pionic atoms and chiral symmetry in nuclei'', MESON 2016 14th International Workshop on meson production, properties and interaction, EPJ Web Conf. 130 (2016) 01017

M.L. Cortes et al., ``Inelastic scattering of ^{72}Ni, ^{74}Ni off a proton target'', XXI INTERNATIONAL SCHOOL ON NUCLEAR PHYSICS, NEUTRON PHYSICS AND APPLICATIONS & INTERNATIONAL SYMPOSIUM ON EXOTIC NUCLEI (ISEN-2015), J. of Phys. Conf. 724, (2016) 012008

L. Stuhl et al.: ``A newly developed wrapping method for scintillator detectors'', J. of Phys. Conf. Ser. 665, 012050 (2016).

T. Kröll et al.: ``Nuclear reactions in the storage ring ESR with EXL'', J. of Phys. Conf. Ser. 724, 012026 (2016).

M. Sasano et al.: ``Study of Gamow-Teller transitions from ^{132}Sn via the (p,n) reaction at 220 MeV/u in inverse kinematics'', Eur. Phys. J. Conf. 107, 06003 (2016).

R. Reifarth et al.: ``Nuclear astrophysics with radioactive ions at FAIR'', J. of Phys. Conf. Ser. 665, 012044 (2016).

[Book]

(Original Papers) *Subject to Peer Review

[Others]

下浦　享: ``テトラ中性子の探査'', ISOTOPE NEWS, 749, 7--9 (2017)

下浦　享: ``RIビームを用いたテトラ中性子研究'', 原子核研究, 61, 70--77 (2017)

Oral Presentations

[International Conference etc.]

H. Yamaguchi (oral): ``Study on alpha-cluster levels in non-4n nuclei using low-energy RI beams'', 11th International Conference on Clustering Aspects of Nuclear Structure and Dynamics, May 23-27, 2016, Conference Center of the Universita di Napoli Federico II, Napoli, Italy.

H. Shimizu (oral): ``Searching for the origin of galactic Al-26 with an experiment using isomeric Al-26 beam”, NIC-XIV School, June 13--16, 2016, Niigata University, Niigata, Japan.

H. Yamaguchi (oral, invited): ``Experimental studies of light-ion nuclear reactions using low-energy RI beams'', the 14th International Symposium on Nuclei in the Cosmos (NIC-XIV), June 19--24, 2016, Toki Messe, Niigata, Japan.

H. Yamaguchi (oral): ``Overview of CRIB projects'', the Second Sicily-East Asia Workshop on Low Energy Nuclear Physics (SEA2016), June 26--28, 2016, CNS, the University of Tokyo, Wako, Saitama, Japan.

S. Hayakawa (oral): ``Trials for the cosmological ^{7}Li problem with ^{7}Be beams at CRIB and collaborating studies'', the Second Sicily-East Asia Workshop on Low-energy Nuclear Physics (SEA2016), June 26-28, 2016, CNS, the University of Tokyo, Wako, Saitama, Japan.

H. Yamaguchi (oral): ``Recent activities at the low-energy RI beam separator CRIB'', RIBF users meeting 2016, Sep. 8-9, 2016, RIKEN, Wako, Saitama, Japan.

H. Yamaguchi (oral): ``Overview of recent experiments at CRIB'', SKKU mini workshop, Oct. 11, 2016, Sungkyunkwan University, Suwon, Korea.

S. Hayakawa (oral): ``Upcoming CRIB experiment: ^{7}Be + n reaction measurements by the Trojan horse method'', SKKU mini Workshop, Oct. 11, 2016, Suwon, Korea.

H. Yamaguchi (oral): ``Introduction of the low-energy RI beam facility CRIB and recent research activities at CRIB'', Nuclear Physics Seminar, Oct. 25, 2016, Beihang University, Beijing, China.

N. Imai, "OEDO and proton resonance elastic scattering" (invited) HIAS2016 2016/9/18-20, Canberra, Australia

N. Imai, "Physics program with low-energy RI beams" (invited) 2016/11/16-18 Daejeong, Korea, RNC-RISP RIB physics workshop

N. Shimizu, “Shape phase transition and shell evolution in large-scale shell-model calculations”, 8th Workshop on Quantum Phase Transitions in Nuclei and Many-Body Systems, Jun. 6-9, 2016, Prague, Czech Republic.

Y. Utsuno (invited), N. Shimizu, T. Otsuka, “Shell-model applications to gamma-ray strength function and level density”, NUSPIN 2016 Workshop of the Nuclear Spectroscopy Instrumentation Network and AGATA Physics Workshop, Jun. 27-Jul. 1, 2016, Venice, Italy.

N. Tsunoda, “Island of Inversion by microscopically derived shell-model Hamiltonian”, Direct Reactions with Exotic Beams (DREB) 2016, Jul. 11-15, 2016, Halifax, Canada.

Y. Tsunoda, “Monte Carlo shell model calculations for structure of nuclei around Z=28”, The 15th CNS International Summer School, Aug. 24-30, 2016, Wako, Japan.
N. Shimizu, “Large-scale shell-model studies for exotic nuclei and nuclear level densities”, International Conference Nuclear Theory in the Supercomputing Era - 2016, Sep. 19-23, 2016, Khabarovsk, Russia.
N. Shimizu, “Clustering structure in no-core Monte Carlo shell model”, Workshop on Nuclear Cluster Physics (WNCP2016), Nov. 14-17, 2016, Yokohama, Japan.
J. Menéndez, “Towards double-beta decay matrix elements with theoretical uncertainties”, First Tsukuba-CCS-RIKEN joint workshop on microscopic theories of nuclear structure and dynamics, Dec. 12-16, 2016, Tsukuba, Japan.
N. Shimizu, “Nuclear shell-model calculations in HPC”, First Tsukuba-CCS-RIKEN joint workshop on microscopic theories of nuclear structure and dynamics, Dec. 12-16, 2016, Tsukuba, Japan.
Y. Utsuno, S. Yoshida, N. Shimizu, T. Otsuka, T. Togashi, T. Suzuki, M. Honma, “Shell-model study of Gamow-Teller and first-forbidden β decay in the N=28 region”, 6th Workshop on Nuclear Fission and Spectroscopy of Neutron-Rich Nuclei, Mar. 20-24, 2017, Chamrousse, France.
S. Shimoura (invited): ``Tetraneutron states populated via ^{4}He(^{8}He, ^{8}Be) reaction'', The 11th International Conference on Clustering Aspects of Nuclear Structure and Dynamics (Cluster16), May. 23--27, 2016, Naples, Italy.
S. Shimoura (Oral): ``Tetra-neutron states populated by ^{4}He(^{8}He,^{8}Be) reaction'',The 9th International Conference on Direct Reactions with Exotic Beams (DREB2016), July 11--15, 2016,Halifax, Canada.
S. Shimoura (invited):``Interplay between reaction and structure in nuclear physics'', International Symposium on Modern Technique and its Outlook in Heavy ion Science (MOTO16), June 26--27, 2016, Rikkyo University, Tokyo, Japan.
M. Dozono (Oral): ``Separated flow operation of the SHARAQ spectrometer for in-flight proton-decay experiments'',International Symposium on Modern Technique and its Outlook in Heavy ion Science (MOTO16), June 26--27, 2016, Rikkyo University, Tokyo, Japan.
S. Michimasa (Invited): ``New Beamline with Optimized Energy-degrading Optics of RI beams'', The Second Sicily-East Asia Workshop on Low Energy Nuclear Physics (SEA2), June 26--28, 2016, Nishina Hall, RIKEN, Wako, Saitama, Japan.
S. Shimoura: ``Experimental studies of the tetra-neutron system by using RI-beam'', RIBF Discussion on the tetra-neutron system, August 3, 2016, Tohoku University, Sendai, Japan
S. Shimoura (invited):``Experimental studies of the tetra-neutron system by using RI-beam'', The 23rd European Conference on Few-Body Problems in Physics, Aug. 8--12, 2016, Aarhus, Denmark.
S. Michimasa (Invited):`` Recent Achievement of OEDO/SHARAQ system'', RIBF Users Meeting 2016, September 8--9, 2016, RIBF Conference Hall, RIKEN, Wako, Saitama, Japan.
S. Shimoura (invited): ``Charge Exchange Reaction of RI Beam to Populate Exotic States'', International Nuclear Physics Conference (INPC2016), Sep. 11--16, 2016, Adelaide, Australia.
S. Michimasa (Oral): ``Sharaq Spectrometer: High-resolution Spectroscopy Using Exotic Beams And Reactions'', International Nuclear Physics Conference (INPC2016), Sep. 11--16, 2016, Adelaide, Australia.
S. Michimasa (Oral): ``OEDO Beamline: New Energy-degrading Ion Optics of RI Beams'', International Nuclear Physics Conference (INPC2016), Sep. 11--16, 2016, Adelaide, Australia.
R. Yokoyama (Oral): ``Role Of Hexadecupole Deformation In The Shape Evolution Of Neutron-rich Nd Isotopes'', International Nuclear Physics Conference (INPC2016), Sep. 11--16, 2016, Adelaide, Australia.
M. Kobayashi (Oral): ``Time-of-flight Mass Measurements Of Neutron-rich Calcium Isotopes Beyond N=34”, International Nuclear Physics Conference (INPC2016), Sep. 11--16, 2016, Adelaide, Australia.
M. Takaki (Oral): ``Search for Double Gamow-Teller Resonance via Heavy-ion Double Charge Exchange Reaction'', International Nuclear Physics Conference (INPC2016), Sep. 11--16, 2016, Adelaide, Australia.
S. Shimoura (invited):{``Tetra-neutron system populated by exothermic double-charge exchange reaction ^{4}He(^{8}He,^{8}Be) at 190 MeV/u''},The 22nd International Spin Symposium, Sep. 25--30, 2016,Champaign, IL, USA.
S. Shimoura (invited): ``Tetra-neutron system studied by ^{4}He(^{8}He, ^{8}Be)'', ECT* Workshop on Physics beyond the limits of stability: exploring the continuum, Oct. 17--21, 2016, Trento, Italy
S. Michimasa (Invited): ``New energy-degraded beam project at RIBF -- OEDO project --'',KPS 2016 Fall Meeting, October 19--21, 2016, Kimdaejung Convention Center, Gwangju, Korea.
S. Shimoura (invited):``Tetra-neutron system studied by ^{4}He(^{8}He,^{8}Be)'', Workshop on Nuclear Cluster Physics (WNCP2016), Oct. 17--21, 2016, Kanto-Gakuin University, Yokohama, Japan
S. Shimoura (invited): ``Tetra-neutron system studied by using RI beam'',International Symposium on Neutron Star Matter (NSMAT2016), Recent Progress in Observations, Experiments and Theories, Oct. 21--24, 2016, Tohoku University, Sendai, Japan
S. Shimoura (invited):``Tetra-neutron system populated by reaction of exotic beam'',ESNT Workshop on Dynamics of highly unstable exotic light nuclei and few-body systems, January 30--February 3, 2017, Saclay, France
T. Gunji (Oral) for the ALICE Collaboration: “Low mass dielectron measurements in pp, p-Pb, and Pb-Pb collisions with ALICE at the LHC”, The 8th International Conference on Hard and Electromagnetic Probes of High-energy Nuclear Collisions (Hard Probes 2016), 9/23-27, 2016, Wuhan, China
T. Gunji (Oral) for the ALICE Collaboration: “Physics with heavy-ions and Dark Photon Searches at the LHC-ALICE experiment”, Apsen workshop on Particle Physics in 2017 : From the LHC to Dark Matter and Beyond, 3/20-25, 2017, Aspen, Colorado, USA, 3/20-3/25
Y. Watanabe (Oral) ; “Experimental overview on hadronic resonance production in high-energy nuclear collisions”, The 16th International Conference on Strangeness in Quark Matter (Strangeness in Quark Matter 2016), 6/26-7/1, 2016, Berkeley, USA
Y. Watanabe (Oral) for the ALICE Collaboration, “ALICE Overview”, 33rd Winter Workshop on Nuclear Dynamics, 1/8-14, 2017, Salt Lake City, USA
S. Ota (invited), ``CNS Active Target (CAT) for high-intensity beam experiment and the first experiment at RIBF'', Workshop on Software for Time Projection Chamber for Nuclear Physics Experiments, Aug. 8-10, 2016, MSU, US
H. Tokieda (invited), ``Event Search Algorithm for CAT'', Workshop on Software for Time Projection Chamber for Nuclear Physics Experiments, Aug. 8-10, 2016, MSU, US
C. Iwamoto (invited), ``Simulation for high-intensity heavy-ion beam injection in CAT'', Workshop on Software for Time Projection Chamber for Nuclear Physics Experiments, Aug. 8-10, 2016, MSU, US

L. Stuhl et al. (oral): ``A new low-energy plastic scintillation neutron detector for real time pulse shape discrimination'': The 26th International Nuclear Physics Conference (INPC2016), Sep 11—16, 2016, Adelaide, Australia.

[Domestic Conference]

早川勢也 (oral) : “トロイの木馬法による ^{7}Be+n ビッグバン元素合成反応の測定 (Measurement of the ^{7}Be+n Big-Bang nucleosynthesis reactions by the Trojan horse method) ”, 日本物理学会　第 72 回年次大会, 3 月 17 日～20 日, 大阪大学

清水英樹 (oral) : “CRIB における ^{26}Al 異性核反応の宇宙γ線観測量への寄与の研究（Study on e contribution of isomeric aluminum-26 reaction to cosmic gamma-ray observation with CRIB）”, 日本物理学会　第 72 回年次大会, 3 月 17 日～20 日, 大阪大学

N. Kitamura et al., “Shell structure of ^{35}Si studied by proton resonance scattering”, JPS 2016 fall meeting

O. Beliuskina et al., “Pulse height defect in CVD Diamond Detectors”, JPS 2016 fall meeting

N. Imai, “Single particle structure studies with the transfer reaction and the resonance elastic reaction” (invited) JPS meeting 2017, symposium for New aspects of direct reactions in probing exotic nuclei

角田佑介、大塚孝治、清水則孝、本間道雄、宇都野穣、“大規模殻模型計算による Z=28 近傍の核構造の研究”、日本物理学会 2016 年秋季大会、Sep. 21-24, 2016、宮崎大学木花キャンパス、宮崎

富樫智章、角田佑介、大塚孝治、清水則孝、“Zr 同位体における形の量子相転移のモンテカルロ殻模型による研究”、日本物理学会 2016 年秋季大会、Sep. 21-24, 2016、宮崎大学木花キャンパス、宮崎

吉田亨、清水則孝、阿部喬、大塚孝治、“Be, C 同位体の intrinsic 状態のモンテカルロ殻模型による研究”、日本物理学会 2016 年秋季大会、Sep. 21-24, 2016、宮崎大学木花キャンパス、宮崎

富樫智章、角田佑介、大塚孝治、清水則孝、“Zr 同位体における形の量子相転移のモンテカルロ殻模型による研究”、研究会「クラスター・平均場の両側面から見る原子核構造の多様性とそのダイナミクス」、Jan. 19-20, 2017、大阪市立大学、大阪

市川隆敏、清水則孝、宇都野穣、大塚孝治、“大規模殻模型計算による質量数 A=40 領域における 4p-4h 変形状態の系統的探索”、日本物理学会第 72 回年次大会、Mar. 17-20, 2017、大阪大学豊中キャンパス、大阪

宇都野穣、藤田佳孝、“二核子配位のガモフテラー遷移と陽子中性子対相関”、日本物理学会第 72 回年次大会、Mar. 17-20, 2017、大阪大学豊中キャンパス、大阪

清水則孝、富樫智章、大塚孝治、宇都野穣、吉田聡太、“ベイズ統計による殻模型計算解析”、日本物理学会第 72 回年次大会、Mar. 17-20, 2017、大阪大学豊中キャンパス、大阪

角田直文、大塚孝治、鈴木俊夫、高柳和雄、清水則孝、Morten Hjorth-Jensen、“核力に依拠した有効相互作用による殻模型計算でみる「逆転の島」の新しい様相”、日本物理学会第 72 回年次大会、Mar. 17-20, 2017、大阪大学豊中キャンパス、大阪

角田佑介 (受賞講演)、“Ni 同位体における新奇な変形共存現象と核子配位に依存した殻進化の研究”、日本物理学会第 72 回年次大会、Mar. 17-20, 2017、大阪大学豊中キャンパス、大阪

富樫智章、角田佑介、大塚孝治、清水則孝、“Zr 同位体とその近傍核における形の量子相転移のモンテカルロ殻模型による研究”、日本物理学会第 72 回年次大会、Mar. 17-20, 2017、大阪大学豊中キャンパス、大阪

角田直文、“Medium-mass nuclei from nuclear force”、基研研究会「核力に基づく核構造、核反応物理の展開」、Mar. 27-29, 2017、京都大学基礎物理学研究所、京都

下浦　享 (invited): ``イオンビームを用いた原子核研究と 放射線計測技術の現状と課題'', 放射線科学とその応用第１８６委員会　第１９回研究会, 2016年5月19日, 東京大学山上会館, 東京

下浦　享 (invited): ``RIビームを用いた原子核物理学研究と放射線測定技術'', 第62回放射線計測研究会, 2016年10月15日, 三菱総合研究所, 東京

S. Shimoura (invited):”Tetra-neutron system populated by exothermic double-charge exchange reaction'', 基研研究会「核力に基づく核構造、核反応物理の展開」, 2017年3月27--29日, 京都大学, 京都.

S. Masuoka 他: ``複数中性子識別のための反跳陽子飛跡検出器の開発II'', JPS Fall meeting, September 21--24, 2016, Miyazaki University, Miyazaki, Japan

Y. Yamaguchi, 他: ``DSPを用いた多重ガンマ線検出用Ge検出器アレイの為のデータ収集系の開発2'', JPS Fall meeting, September 21--24, 2016, Miyazaki University, Miyazaki, Japan

M. Kobayashi 他: ``飛行時間法を用いた中性子数34近傍Ca同位体の質量測定'', JPS Fall meeting, September 21--24, 2016, Miyazaki University, Miyazaki, Japan

R. Yokoyama, 他: ``中性子過剰Nd同位体の変形進化における十六重極変形の効果'', JPS Fall meeting, September 21--24, 2016, Miyazaki University, Miyazaki, Japan

S. Shimoura (invited): ``New energy degraded beam line at RIBF -- OEDO'',「超重元素の新展開」シンポジウム, JPS Spring meeting, March 17--20, 2017, Osaka University, Osaka, Japan

小高康照(oral):「4 次元エミッタンスデータによる AVF 入射軌道解析」, 第 13 回 AVF 合同打合せ, 2016 年 10 月 27-28 日, 東北大学 CYRI

大城幸光(oral):「CNS イオン源の現状」, 第 13 回 AVF 合同打合せ, 2016 年 10 月 27-28 日, 東北大学 CYRIC

S. Hayashi for the ALICE Collaboration, "Dielectron production from Heavy Quarks in p-Pb collisions at $\sqrt{s_{NN}}$ = 5.02 TeV with the ALICE detector ", JPS 2016 Autumn Meeting, Sep. 21-24, University of Miyazaki, Miyazaki, Japan

K. Terasaki for the ALICE Collabroation, “Search for exotic dibaryons and study of baryon-baryon correlations at LHC-ALICE”, JPS 2016 Autumn Meeting, Sep. 21-24, University of Miyazaki, Miyazaki, Japan

Y. Sekiguchi for the ALICE Collaboration, “”Study of two particle correlations in p-Pb collisions at $\sqrt{s_{NN}}$ = 5.02 TeVwith ALICE”, JPS 2016 Autumn Meeting, Sep. 21-24, University of Miyazaki, Miyazaki, Japan

大田晋輔、``重水素アクティブ標的を用いた錫領域不安定核の巨大共鳴の測定''日本物理学会第 72 回年次大会、2017 年 3 月 17 日～2017 年 3 月 20 日、大阪大学

大田晋輔(invited)、``CNS Active Target''、新学術領域『中性子星核物質』第二回検出器ワークショップ

Posters Presentations

[International Conference etc.]

S. Hayakawa, C. Spitaleri, N. Burtebayev, A. Aimaganbetov, S.V. Artemov, P. Figuera, M. Fisichella, G.L. Guardo, S. Igamov, I. Indelicato, G.G. Kiss, S. Kubono, M. La Cognata, L. Lamia, M. Lattuada, M. Nassurlla, E. Piasecki, G.G. Rapisarda, S. Romano, S.B. Sakuta, A. Trzcinska, A. Tumino, A. Urkinbayev, and T. Zholdybayev (poster): ``Trojan Horse Method for the Oxygen-Burning Process Reactions'', The 14th International Symposium on Nuclei in the Cosmos (NIC2016), Jun. 19-24, Niigata, Japan

K. Abe, S. Hayakawa, H. Yamaguchi, and L. Lamia (poster) : ``Feasibility Study for the ^{7}Be+n Reaction Measurements by Trojan Horse Method at CRIB'', The 14th International Symposium on Nuclei in the Cosmos (NIC2016), Jun. 19-24, Niigata, Japan

T. Togashi, “E1 strength function in Monte Carlo shell model”, The 15th CNS International Summer School, Aug. 24-30, 2016, Wako, Japan.

T. Yoshida, “Structure of Be and C isotopes with large-scale shell model calculations”, The 15th CNS International Summer School, Aug. 24-30, 2016, Wako, Japan

H. Murakami for the ALICE Collaboration, "Measurements of neutral mesons in pp collisions at $\sqrt{s}$ = 5.02TeV via conversion method with ALICE", Quark Matter 2017, Feb. 5-11, 2017, Chicago, USA

[Domestic Conference]

小高康照 :「ペッパーポット型エミッタンス測定器を用いた理研 AVF サイクロトロン入射系の解析」, 第 13 回日本加速器学会年会, 2016 年 8 月 8-10 日, 幕張メッセ国際会議場

Partner Institution
Center for Radioactive Ion Beam Sciences
Institute of Natural Science and Technology, Niigata University

1. Abstract

The Center for Radioactive Ion Beam Sciences, Niigata University, aims at uncovering the properties of atomic nuclei and heavy elements and their roles in the synthesis of elements, with use of the advanced techniques of heavy ion and radioactive ion beam experiments as well as the theoretical methods. Main research subjects include the measurements of various reaction cross sections and moments of neutron- or proton-rich nuclei, synthesis of super-heavy elements and radio-chemical studies of heavy nuclei, and theoretical studies of exotic nuclei based on quantum many-body methods and various nuclear models. In addition, we promote interdisciplinary researches related to the radioactive ion beam sciences, such as applications of radioactive isotopes and radiation techniques to material sciences, nuclear engineering and medicine. Many of them are performed in collaboration with RIKEN Nishina Center and with use of the RIBF facilities. The center emphasizes also its function of graduate education in corporation with the Graduate School of Science and Technology, Niigata University, which invites three researchers in RIKEN Nishina Center as visiting professors.

2. Major Research Subjects

(1) Reaction cross section and radii of neutron-rich nuclei
(2) Production of superheavy nuclei and radiochemistry of heavy elements
(3) Nuclear theory

3. Summary of Research Activity

(1) Measurements of matter and charge radii of exotic nuclei

The experimental nuclear physics group has studied the nuclear structures of exotic nuclei through the measurements of nuclear matter radii. The nuclear matter radii can be determined from interaction cross sections with the use of nuclear reaction model. At RIBF, RIKEN, we have performed experiments to measure interaction cross sections of F, Ne, Na, Mg, and Al isotopes and clarified the halo structure of ^{31}Ne, and also the development of strong deformation in those isotopes, $^{28\text{-}32}$Ne, $^{32\text{-}38}$Mg, which are located around and beyond the “island of inversion” region. Recently our new project to explore the equation of state (EOS) of nuclear matter has been started. For the understanding of the EOS of asymmetric nuclear matter, either highly proton deficient or neutron deficient, the investigation of the development of neutron skin thickness in the exotic nuclei give the crucial information. We have measured interaction cross sections and charge changing cross sections for $^{58\text{-}78}$Ni using BigRIPS fragments separator at RIBF in FY2016. While nuclear matter radii can be determined from interaction cross sections, the proton distribution radii will be determined from charge-changing cross sections, thus neutron skin thickness will be obtained. The data analysis are in progress.

(2) Production of superheavy nuclei and radiochemistry of heavy elements

The nuclear chemistry group has been investigating decay properties of super-heavy nuclei, measured the excitation functions of rutherfordium isotopes, and clarified the ambiguity of the assignment of a few-second spontaneously fissioning isotope of ^{261}Rf. The new equipment designed for measurement of short-lived alpha emitters is under development.
For the chemistry research of super-heavy elements, preparatory experiments, such as solvent extraction for the group 4, 5, and 6th elements and gaseous phase chemistry for group-4 elements, have been performed using radioisotopes of corresponding homolog elements.

(4) Nuclear theory

One of the main activities of the nuclear theory group concerns with developments of the nuclear density functional theory and exploration of novel correlations and excitations in exotic nuclei. A fully selfconsistent scheme of the quasiparticle random phase approximation (QRPA) on top of the Skyrme-Hartree-Fock-Bogoliubov mean-field for deformed nuclei has been developed in the group. The versatility of this method to describe the deformation splitting of the giant resonances associated with the onset of deformation has been demonstrated for the first time by the intensive numerical calculation performed for the light nuclei such as ^{28}Si and the comparison with the recent experimental data. For the medium-heavy nuclei, softening of the gamma vibration in the neutron-rich Dy isotopes observed by the EURICA experiment was successfully described, and the microscopic mechanism was made clear. The QRPA in the density functional framework has been developed in various directions. The continuum QRPA, which describes not only collective correlations but also coupling to unbound continuum states of nucleons, has been applied to describe the direct neutron capture reaction in the r-process nucleosynthesis. The QRPA is recently applied to describe collective excitation in inner crust of neutron stars. The continuum quasiparticle states are also analyzed to study possible pairing effects on low-lying p-wave resonances and s-wave scattering states in unbound odd-N nuclei. Cluster structure and the ab initio studies of light nuclei are also important research subjects of the theory group.

Members

Director
Masayuki MATSUO (Professor)

Scientific Staff

Hisaaki KUDO (Professor)
Takashi OHTSUBO (Associate Professor)
Shin-ichi GOTO (Associate Professor)
Shigeyoshi AOYAMA (Associate Professor)
Takuji IZUMIKAWA (Associate Professor)
Kenichi YOSHIDA (Assistant Professor)
Kazuhiro OOE (Assistant Professor)
Jun GOTO (Assistant Professor)
Maya TAKECHI (Assistant Professor)

Post Doctoral Associates

Tsunenori INAKURA

Graduate Students

Yoshihiko KOBAYASHI

List of Publications & Presentations

Publications

[Journal]

(Original Papers) *Subject to Peer Review

T. Peach, U. Garg, Y. K. Gupta, J. Hoffman, J. T. Matta, D. Patel, P. V. Madhusudhana Rao, K. Yoshida, M. Itoh, M. Fujiwara, K. Hara, H. Hashimoto, K. Nakanishi, M. Yosoi, H. Sakaguchi, S. Terashima, S. Kishi, T. Murakami, M. Uchida, Y. Yasuda, H. Akimune, T. Kawabata, M. N. Harakeh, and G. Colò, "Effect of ground-state deformation on isoscalar giant resonances in ^{28}Si", Physical Review C **93**, 064325 (2016).*

H. Watanabe, G. X. Zhang, K. Yoshida, P. M. Walker, J. J. Liu, J. Wu, P. H. Regan, P.-A. Soderstrom, H. Kanaoka, Z. Korkulu, P. S. Lee, S. Nishimura, A. Yagi, D. S. Ahn, T. Alharbi, H. Baba, F. Browne, A. M. Bruce, R. J. Carroll, K. Y. Chae, Zs. Dombradi, P. Doornenbal, A. Estrade, N. Fukuda, C. Griffin, E. Ideguchi, N. Inabe, T. Isobe, S. Kanaya, I. Kojouharov, F. G. Kondev, T. Kubo, S. Kubono, N. Kurz, I. Kuti, S. Lalkovski, G. J. Lane, C. S. Lee, E. J. Lee, G. Lorusso, G. Lotay, C.-B. Moon, I. Nishizuka, C. R. Nita, A. Odahara, Z. Patel, V. H. Phong, Zs. Podolyak, O. J .Roberts, H. Sakurai, H. Schaffner, "Long-lived *K* isomer and enhanced γ vibration in the neutron-rich nucleus ^{172}Dy: Collectivity beyond double midshell", Physics Letters B**760**, 641 (2016).*

K. Yoshida and H. Watanabe, "Enhanced collectivity of γ vibration in neutron-rich Dy isotopes with *N*=108-110", Progress of Theoretical and Experimental Physics **2016**, 123D02 (2016).*

Y. Kobayashi, M. Matsuo, "Effects of pairing correlation on the low-lyng quasiparticle resonance in neutron drip-line nuclei", Progress of Theoretical and Experimental Physics, **2016**, 013D01 (1-14) (2016).*

N. Nakatsuka, H. Baba, T. Aumann, R. Avigo, S.R. Banerjee, A. Bracco, C. Caesar, F. Camera, S. Ceruti, S. Chen, V. Derya, P. Doornenbal, A. Giaz, A. Horvat, K. Ieki, T. Inakura, N. Imai, T. Kawabata, N. Kobayashi, Y. Kondo, S. Koyama, M. Kurata-Nishimura, S. Masuoka, M. Matsushita, S. Michimasa, B. Million, T. Motobayashi, T. Murakami, T. Nakamura, T. Ohnishi, H.J. Ong, S. Ota, H. Otsu, T. Ozaki, A. Saito, H. Sakurai, H. Scheit, F. Schindler, P. Schrock, Y. Shiga, M. Shikata, S. Shimoura, D. Steppenbeck, T. Sumikama, I. Syndikus, H. Takeda, S. Takeuchi, A. Tamii, R. Taniuchi, Y. Togano, J. Tscheuschner, J. Tsubota, H. Wang, O. Wieland, K. Wimmer, Y. Yamaguchi, K. Yoneda, J. Zenihiro, "Observation of isoscalar and isovector dipole excitations in neutron-rich ^{20}O", Physical Letter B **768** (2017) 387-392*

D. T. Tran *et al*., "Charge-changing cross-section measurements of $^{12-16}$C at around 45*A* MeV and development of a Glauber model for incident energies 10*A*–2100*A* MeV", Phys. Rev. C 94, (2016) 064604

Y. K. Tanaka *et al*., "Measurement of Excitation Spectra in the ^{12}C(*p*, *d*) Reaction near the *η*′ Emission Threshold", Phys. Rev. Lett. 117, (2016) 202501

R. Kanungo *et al*., "Proton Distribution Radii of $^{12-19}$C Illuminate Features of Neutron Halos", Phys. Rev. Lett. 117, (2016) 102501

J. Lee *et al*., "First Measurement of Several β-Delayed Neutron Emitting Isotopes Beyond N = 126", Prog Theor Exp Phys (2016) 2016 (8)

R. Caballero-Folch *et al*., "Asymmetry dependence of reduction factors from single-nucleon knockout of ^{30}Ne at ~230 MeV/nucleon", Phys. Rev. Lett. 117, (2016) 012501

P. Doornenbal *et al*., "Mapping the deformation in the "island of inversion": Inelastic scattering of 30Ne and 36Mg at intermediate energies", Phys. Rev. C 93, (2016) 044306

I. Tanihata *et al*., "Observation of large enhancements of charge exchange cross sections with neutron-rich carbon isotopes", Prog Theor Exp Phys (2016) 2016 (4)

M. P. Reiter *et al*., "Rate capability of a cryogenic stopping cell for uranium projectile fragments produced at 1000 MeV/u", NIM B 376 (2016) 240

Y. Kawano, A. Munaim, J. Goto, Y. Shobugawa and M. Naito, "Sensing Space: Augmenting Scientific Data with Spatial Ethnography", GeoHumanities **2**, 485 (2016).*(Review)

吉田賢市，伊藤正俊，"変形原子核の巨大単極共鳴"，日本物理学会誌 **72**, 45 (2017).

[Proceedings]

(Original Papers) *Subject to Peer Review

A. Homma *et al*., "Measurements of Interaction Cross Sections for $^{19-27}$F Isotopes", JPS Conf. Proc. 14, 021010 (2017)

K. Nishizuka *et al*., "Measurements of Reaction Cross Sections for $^{9-11}$C", JPS Conf. Proc. 14, 021015 (2017)

E. Miyata *et al*., "Development of High Resolution TOF Detector for RI Beams Using Cherenkov Radiation", J Acta Phys.Polon. B48 (2017) 409

M. Tanaka *et al*., "Reaction Cross Sections for $^{13-15}$B and One-neutron Halo in 14B", J Acta Phys.Polon. B48 (2017) 461

J. Goto, Y. Shobugawa, Y. Kawano, Y. Amaya, T. Izumikawa, Y. Katsuragi, T. Shiiya, T. Suzuki, TA. Takahashi, TO Takahashi, H. Yoshida, and M. Naito, "Development of a Portable Gamma-ray Survey System for the Measurement of Air Dose Rates", JPS Conference Proceedings **11**, 070007 (2016).*

[Book]
(Original Papers) *Subject to Peer Review
内藤眞, 青木萩子, 野中昌法, 後藤淳, 菖蒲川由郷, 高橋俊博, 吉田秀義, 天谷吉宏, Y. Kawano, 岩佐有華, 齋藤智子, 西方真弓, 吉川夏樹, 原田直樹, 山城秀昭, 高橋剛, "BISHAMON の軌跡-Ⅱ ～福島支援 5 年間の記録～", 新潟日報事業社(2016)

[Others]
吉田賢市, 伊藤正俊, "変形原子核の巨大単極共鳴", 日本物理学会誌 **72**, 45 (2017).

Oral Presentations
[International Conference etc.]
K. Yoshida and H. Watanabe, "Enhanced Collectivity of Gamma Vibration in Neutron-rich Dy Isotopes with *N*=108-110", The Nuclear Structure 2016 Conference, Knoxville, USA, July 24-29, 2016.
K. Yoshida, "Spin-isospin Responses of Deformed Neutron-rich Nuclei", The 26th International Nuclear Physics Conference, Adelaide, Australia, September 11-16, 2016.
K. Yoshida, "Low-lying excitations in neutron-rich nuclei: Effects of deformation and pairing", The first Tsukuba-CCS-RIKEN joint workshop on Microscopic Theories of nuclear structure and dynamics, RIKEN, Wako, Saitama, December 12-16, 2016.
K. Yoshida, "Roles of neutron excess and deformation on charge-exchange collective modes of excitation", Recent Progresses in Nuclear Structure Physics 2016", YITP, Kyoto, December 19-23, 2016.
Y. Kobayashi, M. Matsuo, "Effects of pairing correlation on low-energy p- and s-wave scattering in neutron-rich nuclei" ECT* Workshop "Physics beyond the limits of stability: exploring the continuum", European Center for Theoretical Studies in Nuclear Physics and Related Areas, Trento, October 20, 2016.
Y. Kobayashi, M. Matsuo, "Effects of pairing correlation on the low-lying quasiparticle resonance in neutron drip-line nuclei", International Nuclear Physics Conference 2016, Adelaide Convention Center, Adelaide, September 13, 2016.
Y. Kobayashi, M. Matsuo, "Single-neutron resonance and pairing correlation in neutron-rich nuclei", Resonance and non-Hermitian Quantum Mechanics 2016, 2016 年 08 月 04 日,Research Center for Nuclear Physics, August 4, 2016.
T. Inakura, H. Nakada, "Constraining the slope parameter of symmetry energy from nuclear structure", International symposium on Neutron Star Matter, Tohoku University, Sendai, Miyagi, November 21-24, 2016.
T. Inakura, M. Matsuo, "Calculation of collective excitation of inner crust using density functional theory", The first Tsukuba-CCS-RIKEN joint workshop on Microscopic Theories of nuclear structure and dynamics, Center for Computational Science, University of Tsukuba, Tsukuba, Ibaraki, December 19-23, 2016.
M. Takechi, E. Miyata, *et al*. "Development of High Resolution *TOF* detector for RI Beams using Cherenkov Radiation", ZAKOPANE Conference on Nuclear Physics, Zakopane, Poland, 28, August - 4, September, 2016.
A. Homma *et al*., "Measurements of Reaction Cross Section for $^{19-27}$F Isotopes", ZAKOPANE Conference on Nuclear Physics, Zakopane, Poland, 28, August - 4, September, 2016.
M. Tanaka *et al*., "Reaction Cross Sections for $^{13-15}$B and One-neutron Halo in 14B", ZAKOPANE Conference on Nuclear Physics, Zakopane, Poland, 28, August - 4, September, 2016.

[Domestic Conference]
吉田賢市, "Deformation effect on giant resonances in ^{24}Mg and ^{28}Si", 日本物理学会 2016 年秋季大会, 宮崎大学, 9 月(2016).
吉田賢市, "Variety of excitation modes associated with nuclear deformation and superfluidity", クラスター・平均場の両側面から見る原子核構造の多様性とそのダイナミクス, 大阪市立大学, 1 月(2017).
吉田賢市, "Charge-exchange dipole excitations in deformed nuclei", 日本物理学会第 72 回年次大会, 大阪大学豊中キャンパス, 3 月(2017).
小林良彦, 松尾正之, "低エネルギーＳ波散乱が受ける対相関効果のＳ行列による分析", 日本物理学会第７２回年次大会,大阪大学豊中キャンパス, 2017 年 3 月
小林良彦、松尾正之, "中性子過剰核におけるＳ波散乱が受ける対相関効果", 日本物理学会 2016 年秋季大会,宮崎大学, 2016 年 9 月
稲倉恒法, 松尾正之, "中性子星内殻における超流動中性子・原子核系の集団運動", 日本物理学会 2016 年秋季大会,宮崎大学, 2016 年 9 月
稲倉恒法, 松尾正之, "中性子星内殻における超流動中性子・原子核系の集団運動", クラスター・平均場の両側面から見る原子核構造の多様性とそのダイナミクス, 大阪市立大学, 2017 年 1 月
稲倉恒法, "中性子星内殻における超流動中性子と原子核の集団運動", 実験と観測で解き明かす中性子星の核物質 第５回ウィンタースクール・研究会, 飯坂温泉, 福島 2017 年 2 月
稲倉恒法, 松尾正之, "密度汎関数理論による中性子内殻の集団励起モード", 日本物理学会第 72 回年次大会, 大阪大学豊中キャンパス, 2017 年 3 月
福田光順, 田中悠太郎, 田中聖臣, 西村太樹, 武智麻耶 ほか 29 名 "^{6,8}He の中性子剥離断面積と荷電変化断面積", 日本物理学会 2016 年秋季大会 宮崎大学 2016 年 9 月 21 - 24 日
田中悠太郎, 福田光順, 西村太樹, 武智麻耶, 田中聖臣, ほか 33 名 "反応断面積測定による ^{6,8}He の核構造" 日本物理学会 2016 年秋季大会 宮崎大学 2016 年 9 月 21 - 24 日
杜航, 福田光順, 西村太樹, 武智麻耶, 安部敬治郎 ほか 36 名 "^{15,16}C の反応断面積と核構造", 日本物理学会 2016 年秋季大会 宮崎大学 2016 年 9 月 21 - 24 日
大西康介, 福田光順, 西村太樹, 武智麻耶, 青木一矢 ほか 34 名, "中間エネルギー領域における ^{12}N の反応断面積と核構造" 日本物理学会 2016 年秋季大会 宮崎大学 2016 年 9 月 21 - 24 日
本間彰 ほか 67 名 "中性子過剰側 Ni 同位体の相互作用断面積測定", 日本物理学会 2017 年年次大会 大阪大学 2017 年 3 月 17 - 20 日
中村翔健, 武智麻耶 ほか 67 名 "Ni 領域中重核の陽子標的相互作用断面積測定", 日本物理学会 2017 年年次大会 大阪大学 2017 年 3 月 17 - 20 日

中村翔健, 武智麻耶 ほか 67 名 "Ni 領域中重核の陽子標的相互作用断面積測定", 日本物理学会 2017 年年次大会 大阪大学 2017 年 3 月 17 - 20 日
田中聖臣, ほか 67 名 "Ca, Ni 同位体の荷電変化断面積測定", 日本物理学会 2017 年年次大会 大阪大学 2017 年 3 月 17 - 20 日
八木翔一, ほか 25 名 "中間エネルギー領域における ^{10}Be の 反応断面積と核構造", 日本物理学会 2017 年年次大会 大阪大学 2017 年 3 月 17 - 20 日
田中悠太郎, ほか 67 名 "Ca 同位体の相互作用断面積と核構造", 日本物理学会 2017 年年次大会 大阪大学 2017 年 3 月 17 - 20 日
大西康介, ほか 33 名 "中間エネルギー領域における ^{12}N の 1 陽子剥離断面積", 日本物理学会 2017 年年次大会 大阪大学 2017 年 3 月 17 - 20 日
西塚賢治, ほか 49 名 "陽子過剰側 C 同位体の陽子、中性子密度分布", 日本物理学会 2017 年年次大会 大阪大学 2017 年 3 月 17 - 20 日
柳原陸斗, ほか 67 名 "Ni 領域中性子過剰核における核子剥離反応の系統的研究", 日本物理学会 2017 年年次大会 大阪大学 2017 年 3 月 17 - 20 日
宮田恵理, ほか 43 名 "チェレンコフ放射を利用した不安定核ビーム時間分解能検出器の研究 III", 日本物理学会 2017 年年次大会 大阪大学 2017 年 3 月 17 - 20 日
町田聖寛 ほか 31 名 "重イオン用 Ring-Imaging Cherenkov Counter の開発と性能評価", 日本物理学会 2017 年年次大会 大阪大学 2017 年 3 月 17 - 20 日
J. Goto, T. Takahashi, R. Endo, Y. Amaya, Y. Shobugawa, H. Yoshida, and M. Naito, "自動車走行サーベイシステム ASURA を用いた道路上の放射性セシウム沈着量調査", 日本原子力学会 2017 年春の年会, 東海大学湘南キャンパス, 3 月 (2017).
J. Goto, T. Takahashi, R. Endo, Y. Amaya, Y. Shobugawa, H. Yoshida, and M. Naito, "ASURA を用いた放射性セシウム沈着量調査", 第 4 回「原発事故被災地域における放射線量マッピングシステムの技術開発・運用とデータ解析に関する研究会」, 京都大学原子炉実験所, 1 月 (2017).
R. Endo, T. Takahashi, T. Kanbayashi, J. Goto, and M. Naito, "自動車走行サーベイシステム ASURA によるホットスポットの位置推定", 第 4 回「原発事故被災地域における放射線量マッピングシステムの技術開発・運用とデータ解析に関する研究会」, 京都大学原子炉実験所, 1 月 (2017).
K. Shirai, Y. Oshimi, S. Goto, K. Ooe and H. Kudo, "Rf 同族元素 Zr, Hf の塩化物に対する等温ガスクロマトグラフィ", 第 60 回放射化学討論会, 新潟大学五十嵐キャンパス, 9 月 (2016).
S. Goto, "新潟大における Zr,Hf および Rf 塩化物の気相化学研究および今後の計画", 2016「超重元素の科学」研究会, 新潟大学駅南キャンパス 「ときめいと」, 9 月 (2016).
K. Ooe, "固液、液液抽出法による Db のフッ化物錯形成と Rf のキレート錯形成の研究", 2016「超重元素の科学」研究会, 新潟大学駅南キャンパス 「ときめいと」, 9 月 (2016).
D. Sato, "105 番元素 Db の aliquat 336 樹脂を用いたフッ化水素酸からの抽出", 2017 超重元素の科学研究会, 日本原子力研究開発機構先端基礎研究センター, 3 月 (2017).

Posters Presentations

[International Conference etc.]

Y. Kobayashi, M. Matsuo, "Effects of pairing correlation on p-wave resonance and s-wave scattering in neutron-rich nuclei", RIBF Users Meeting 2016, RIKEN Nishina Center, September 8, 2016.
Y. Kobayashi, M. Matsuo,"Pairing correlation effects on width of quasiparticle resonance in neutron dripline nuclei", NIC-XIV School, Niigata University, June 15, 2016.
T. Inakura, M. Matsuo, "Systematic calculation of collective excitation of inner crust using density functional theory", International symposium on Neutron Star Matter, Tohoku University, Sendai, Miyagi, November 21-24, 2016.
K. Nishizuka, M. Takechi, T. Ohtsubo et al., "Measurement of reaction cross sections for $^{9-12}$C isotopes", ZAKOPANE Conference on Nuclear Physics, Zakopane, Poland 28, August - 4, September, 2016.
A. Homma, M. Takechi, T. Ohtsubo et al., "Measurements of reaction cross sections for $^{19-27}$F isotopes", Nuclei in the Cosmos XIV, Niigata, Japan 22-28, May, 2016.
K. Nishizuka, M. Takechi, T. Ohtsubo et al., "Measurement of Reaction Cross Sections for $^{9-12}$C Isotopes", Nuclei in the Cosmos XIV, Niigata, Japan 22-28, May, 2016.

[Domestic Conference]

R. Yamada, K. Ooe, S. Goto and H. Kudo, H. Haba, Y. Komori, "フローインジェクション分析法を利用した 4 族元素 Zr、Hf のキレート抽出", 第 60 回放射化学討論会, 新潟大学五十嵐キャンパス, 9 月 (2016).
K. Ooe, R. Yamada, S. Goto and H. Kudo, H. Haba, Y. Komori, "Rf の同族元素 Zr、Hf の 4-イソプロピルトロポロンを用いた溶媒抽出挙動", 第 60 回放射化学討論会, 新潟大学五十嵐キャンパス, 9 月 (2016).
D. Sato, M. Murakami, K. Ooe, R. Motoyama, H. Haba, Y. Komori, A. Toyoshima, A. Mitsukai, H. Kikunaga, S. Goto and H. Kudo, "5 族元素 Nb, Ta のフッ化水素酸からの Aliquat 336 樹脂への抽出：分配係数の抽出剤濃度依存性の検討", 第 60 回放射化学討論会, 新潟大学五十嵐キャンパス, 9 月 (2016).
R. Motoyama, K. Ooe, M. Murakami, H. Haba, S. Goto and H. Kudo, "5 族元素 Nb, Ta の塩酸溶液からのトリイソオクチルアミンによる溶媒抽出―Ta トレーサー調製法の影響―", 第 60 回放射化学討論会, 新潟大学五十嵐キャンパス, 9 月 (2016).

Partner Institution
Wako Nuclear Science Center, IPNS (Institute for Particle and Nuclear Studies)
KEK (High Energy Accelerator Research Organization)

1. Abstract

The KEK Isotope Separation System (KISS) has been constructed to experimentally study the β-decay properties of unknown neutron-rich nuclei near neutron magic number N = 126, which are of astrophysical interest. A new rotating target system was introduced and higher yields and more stable operational conditions were achieved. Resonance ionization spectroscopy for the hyperfine structure of ^{199}Pt was performed at KISS. An international collaboration with IBS (Institute of Basic Science), Korea, has been organized. As part of this collaboration, an array of super-clover germanium detectors was installed. A new project for comprehensive mass measurements with MRTOF mass spectrograph at KISS and other devices has started in collaboration with the RIKEN SLOWRI team.

2. Major Research Subjects

(1) Radioactive isotope beam production and manipulation for nuclear experiments.
(2) Explosive nucleosyhnthesis (r- and rp-process).
(3) Heavy ion reaction mechanism for producing heavy neutron-rich nuclei.
(4) Development of MRTOF mass spectrograph for short-lived heavy nuclei.
(5) Development of RNB probes for materials science applications.

3. Summary of Research Activity

KISS is an element-selective isotope separator, combining use of a magnetic mass separator with in-gas-cell resonant laser ionization. The gas cell, filled with argon gas of 75 kPa, a central component of KISS, from which only the element of interest are extracted as an ion beam for subsequent mass separation. In the cell, nuclei primarily produced by low-energy heavy-ion reactions are stopped (thermalization and neutralization), transported by buffer gas (gas-flow of ~75 kPa argon in the present case), and then re-ionized by laser irradiation just before the exit. The gas cell was fabricated to efficiently collect the reaction products produced by multi-nucleon transfer (MNT) reactions in the ^{136}Xe +^{198}Pt system. For the first extraction of the reaction products, the ^{136}Xe beam energy and ^{198}Pt target thickness were set at 10.8 MeV/u and 6 mg/cm^2, respectively. In FY2014, the half-life of ^{199}Pt was measured with β-ray telescopes and a tape transport system located at the focal point of KISS. The β-ray telescopes were composed of three double-layered thin plastic scintillators; thickness of the first and second layers was 0.5 mm and 1 mm, respectively. In order to reduce the background, low-activity lead blocks and a veto counter system consisting of plastic scintillator bars surrounded the telescopes. The background rate of these β-ray telescopes was measured to be 0.7 counts per second. For further reduction of the background rate, as low as 0.1 counts per hour, a gas counter based beta-ray telescope system was installed in FY2016. An array of germanium detectors consisting of four super-clover germanium crystals was also brought into operation in FY2016.

For higher primary beam intensities and higher extraction efficiency, a doughnut-shaped gas cell with a rotating target wheel setup has been developed for KISS. Using this setup, resonance ionization spectroscopy of the ground state hyperfine structure of Pt and Ir were performed. The nuclear g-factor and charge radius of the ground state and an isomeric state of ^{199}Pt were deduced from the experimental results.

Cross-section measurements were performed at GANIL in 2012 to investigate the feasibility of using MNT in the reaction system of ^{136}Xe on ^{198}Pt to produce heavy neutron-rich isotopes around mass number of 200 with the neutron magic number of 126; the analysis of the data has been completed. The cross sections of target-like fragments around N =126 were comparable to those estimated using the GRAZING code, and they appear to be mainly contributed by the reactions with low total energy loss with weak N/Z equilibration and particle evaporation. This suggests use of the MNT reactions with a heavy projectile at energies above the Coulomb barrier could be a promising means for production of neutron-rich isotopes around N = 126.

The multi-reflection time-of-flight mass spectrograph (MRTOF-MS) has been developed for direct mass measurements of short-lived heavy nuclei at KISS and other facilities. In FY2016, mass measurements of more than 80 nuclides, including short-lived ($T_{1/2}$ =10 ms) isotopes of Ra and several isotopes of the trans-uranium elements Es and Md were performed at GARIS-II in collaboration with the SLOWRI team and the Super Heavy Element Synthesis team of RIKEN. The highest precisions, achieved for Ga isotopes, reached a level of 0.03 ppm. For most of the well-known nuclides, agreement with the literature mass values was found. However, discrepancies were found in some literature values derived from pre-1980 indirect measurements. This suggests that such indirect measurements must be revised with comprehensive direct mass measurements. The masses of four isotopes of Es and Md were measured for the first time, allowing for confirmation of the N = 152 shell closure in Md. Using these new mass data as anchor-points, the masses of seven isotopes of super-heavy elements up to Mt were indirectly determined and comparisons with various nuclear mass models were performed.

The diffusion coefficient of lithium in solid materials used in secondary Li-ion batteries is one of the key parameters that determine how fast a battery can be charged. The reported Li diffusion coefficients in solid battery materials scatter over several order of magnitude. An in-situ nanoscale diffusion measurement method, using α-emitting radioactive ^{8}Li as a tracer, has been developed. In this method, while implanting a pulsed 8 keV beam of ^{8}Li, the α-particles emitted at small angles ($\theta = 10 \pm 1^\circ$) relative to the sample surface were detected as a function of time. The Li diffusion coefficient could then be determined from the time dependent yields of the α-particles, whose energy loss can be converted to nanometer-scale position information of diffused ^{8}Li. The method has been successfully applied to measure the lithium diffusion coefficients for an amorphous Li_4SiO_4 - Li_3VO_4 (LVSO) which was used as a solid electrolyte in a solid-state Li thin film battery, well-demonstrating that the present method has a sensitivity to the diffusion coefficients down to the level of 10^{-12} cm^2/s, corresponding with nanoscale Li diffusion. In FY2016, this method was used to determine Li diffusion coefficients in a spinel type Li compound of $LiMn_2O_4$ (LMO), which is used as the anode of a Li battery in an electric vehicle. A significant change in the time dependent yields of the α particles was

observed at the sample temperature of around 623 K and the measurements will be continued in order to obtain the temperature dependence of Li diffusion coefficients in LMO.

Members

Group Leader
Hiroari MIYATAKE

Researchers
Michiharu WADA
Yutaka WATANABE
Yoshikazu HIRAYAMA
Peter SCHURY

Technical Staff
Yutaka KAKIGUCHI
Michihiro OYAIZU

Visiting Researchers
Jun-young Moon (IBS)
Jin-hyung Park (IBS)

Student Trainees
Momo MUKAI (PhD. Student, Tsukuba Univ.)
Sota KIMURA (PhD. Student, Tsukuba Univ.)
Murad AHMED MD (PhD. Student, Tsukuba Univ.)

Assistant
Machiko IZAWA

List of Publications & Presentations

Publications

[Journal]

(Original Papers) *Subject to Peer Review

H. Kawamura, T. Akiyama, M. Hata, Y. Hirayama, M. Ikeda, Y. Ikeda, T. Ishii, D. Kameda, S. Mitsuoka, H. Miyatake, D. Nagae, Y. Nakaya, K. Ninomiya, M. Niita, N. Ogawa, J. Onishi, E. Seitaibashi, S. Tanaka, R. Tanuma, Y. Totsuka, T. Toyoda, Y.X. Watanabe, J. Murata, « A new measurement of electron transverse polarization in polarized nuclear beta-decay », Modern Physics Letter A 32, 1750058 (2017).*

E. Strano, D. Torresi, M. Mazzocco, N. Keeley, A. Boiano, C. Boiano, P. Di Meo, A. Guglielmetti, M. La Commara, P. Molini C. Manea, C. Parascandolo, D. Pierroutsakou, C. Signorini, F. Soramel, D. Filipescu, A. Gheorghe, T. Glodariu, J. Grebosz, S. Jeong, Y.H. Kim, J.A. Lay, H. Miyatake, M. Nicoletto, A. Pakou, K. Rusek, O. Sgouros, V. Soukeras, L. Stroe, N. Toniolo, A. Vitturi, Y. Watanabe, K. Zerva, « Discrimination of processes and optical model analysis in the 17O+58Ni collision around the coulomb barrier", Acta Physics Polon. B48 (2017) 615 *.

S.K. Das, T. Fukuda, Y. Mizoi, H. Ishiyama, H. Miyatake, Y.X. Watanabe, Y. Hirayama, S.C. Jeong, H. Ikezoe, M. Matsuda, K. Nishio, T. Hashimoto, « New measurement of the 8Li(α,n)11B reaction in a lower-energy region below the Coulomb barrier", Physical Review C 95, 055805 (2017) *

P. Schury, M. Wada, Y. Ito, D. Kaji, F. Arai, M. MacCormick, I. Murray, H. Haba, S. Jeong, S. Kimura, H. Koura, H. Miyatake, K. Morimoto, K. Morita, A. Ozawa, M. Rosenbusch, M. Reponen, P.-A. Söderström, A. Takamine, T. Tanaka, H. Wollnik, "First online multireflection time-of-flight mass measurements of isomer chains produced by fusion-evaporation reactions: Toward identification of superheavy elements via mass spectroscopy", Physical Review C 95, 011305(R) (2017) *

E. Strano, D. Torresi, M. Mazzocco, N. Keeley, A. Boiano, C. Boiano, P. Di Meo, A. Guglielmetti, M. La Commara, P. Molini, C. Manea, C. Parascandolo, D. Pierroutsakou, C. Signorini, F. Soramel, D. Filipescu, A. Gheorghe, T. Glodariu, J. Grebosz, S. Jeong, Y. H. Kim, J. A. Lay, H. Miyatake, M. Nicoletto, A. Pakou, K. Rusek, O. Sgouros, V. Soukeras, L. Stroe, N. Toniolo, A. Vitturi, Y. Watanabe, K. Zerva, « 17O+58Ni scattering and reaction dynamics around the Coulomb barrier», Physical Review C 94, 024622 (2016) *

T. Sonoda, T.Tsubota, M. Wada, I. Katayama, T.M. Kojima, M. Reponen, « A gas circulation and purification system for gas-cell-based low-energy RI-beam production », Review of Scientific Instruments, 87 (2016) 065104. *

A Hamaker, M. Brodeur, J.M. Kelly, J. Long, C. Nicoloff, S. Syan, B.E. Schult, P. Schury, M. Wada, «Experimental investigation of the repelling force from RF carpets », International Journal Mass Spectrometry, 404 (2016) 14-19. *

[Proceedings]

(Original Papers) *Subject to Peer Review

Torresi, E. Strano, M. Mazzocco, A. Boiano, C. Boiano, P. Di Meo, M. La Commara, C. Manea, M. Nicoletto, J. Grebosz, A. Guglielmetti, P. Molini, C. Parascandolo, D. Pierroutsakou, C. Signorini, F. Soramel, N. Toniolo, D. Filipescu, A. Gheorghe, T. Glodariu, S. Jeong, Y.H. Kim, J.A. Lay, H. Miyatake, A. Pakou, O. Sgouros, V. Soukeras, L. Stroe, A. Vitturi, Y. Watanabe, K. Zerva,«Elastic scattering of 17O+208Pb at energies near the Coulomb barrier »,EPJ Web of Conferences 117, 08027 (2016) *

P.Schury, M. Wada, Y.Ito, F. Arai, D. Kaji, S. Kimura, K. Morimoto, H. Haba, S. Jeong, H. Miyatake, H. Koura, K. Morita, M. Reponen, A. Ozawa, T. Sonoda, A. Takamine, H. Wollnik, «Status of the low-energy super-heavy element facility at RIKEN », Nucl. Inst. Meth. B376 (2016) 52-56 *

Y. Hirayama, Y.X. Watanabe, N. Imai, H. Ishiyama, S.C. Jeong, H.S. Jung, H. Miyatake, M. Oyaizu, S. Kimura, M. Mukai, Y.H. Kim, T. Sonoda, M. Wada, M. Huyse, Yu. Kudryavtsev,P. van Duppen, « On-line experimental results of an argon gas cell-based laser ion source (KEK Isotope Separation System) », Nucl. Inst. Meth. B376 (2016) 52-56.*

M. Mukai, Y. Hirayama, H. Ishiyama, H.S. Jung, H. Miyatake, M. Oyaizu, Y.X. Watanabe, S. Kimura, A. Ozawa, S.C. Jeong, T. Sonoda, « Search for efficient laser resonance ionization schemes of tantalum using a newly developed time-of-flight mass spectrometer in KISS », Nucl. Inst. Meth B376 (2016) 73-76.*

S. Kimura, H. Ishiyama, H. Miyatake, Y. Hirayama, Y.X. Watanabe, H.S. Jung, M. Oyaizu, M. Mukai, S.C. Jeong, A. Ozawa, « Development of the detector system for image-decay spectroscopy at the KEK Isotope Sepaator System », Nucl. Inst. Meth. B376 (2016) 338-340.*

H. Ishiyama, S.C. Jeong, Y.X. Watanabe, Y. Hirayama, N. Imai, H.S. Jung, H. Miyatake, M. Oyaizu, A. Osa, Y. Otokawa, M. Matsuda, K. Nishio, H. Makii, T.K. Sato, N. Kuwata, J. Kawamura, H. Ueno, Y.H. Kim, S. Kimura, M. Mukai, « Direct measurement of nanoscale lithium diffusion in solid battery materials using radioactive tracer of 8Li », Nucl. Instrum. Meth. B 376 (2016) 379-381. *

Y. Hirayama, Y. X. Watanabe, H. Miyatake, P. Schury, M. Wada, M. Oyaizu, Y. Kakiguchi, M. Mukai, S. Kimura, M. Ahmed, S. C. Jeong, J. Y. Moon, J. H. Park, “Nuclear spectroscopy of r-process nuclei around N = 126 using KISS”, NUOVO CIMENTO, 39 C (2016) 359 *

M. Mazzocco, A. Boiano, C. Boiano, M. La Commara, C. Manea, C. Parascandolo, D. Pierroutsakou, C. Signorini, E. Strano, D. Torresi, H. Yamaguchi, D. Kahl, L. Acosta, P. Di Meo, J.P. Fernandez-Garcia, T. Glodariu, J. Grebosz, A. Guglielmetti, N. Imai, Y. Hirayama, H. Ishiyama, N. Iwasa, S.C. Jeong, H.M. Jia, N. Keeley, Y.H. Kim, S. Kimura, S. Kubono, J.A. Lay, C.J Lin, G. Marquinez-Duran, I. Martel, H. Miyatake, M. Mukai, T. Nakao, M. Nicoletto, A. Pakou, K. Rusek, Y. Sakaguchi, A.M. Sánchez-Benítez, T. Sava, O. Sgouros, C, Stefanini, F. Soramel, V. Soukeras, E. Stiliaris, L. Stroe, T. Teranishi, N. Toniolo, Y. Wakabayashi, Y.X. Watanabe, L. Yang, Y.Y. Yang, “7Be- and 8B-reaction dynamics at Coulomb barrier energies”, EPJ Web of Conferences, 117, 06006 (2016) *

Y. Hirayama, H. Miyatake, Y.X. Watanabe, N. Imai, H. Ishiyama, S.C. Jeong, H.S. Jung, M. Oyaizu, M. Mukai, S. Kimura, T. Sonoda, M. Wada, Y.H. Kim, M. Huyse, Yu Kudryavtsev, P. van Duppen, “Beta-decay spectroscopy of r-process nuclei around N=126”, EPJ Web Conf. 109 08001, 1-6 (2016)

Oral Presentations

[International Conference etc.]

P. Schury, « Technical Issues in Achieving Long-Term Stability of MRTOF”, RISP Workshop on MRTOF, Nov. 18, 2016, Daejeon, Korea.

P. Schury, « Mass measurements with MRTOF”, RNC-RIPS Meeting, Nov. 17-19, 2016, Daejon, Korea.

Y.X. Watanabe, « Production of N=126 nuclei and beyond using deep inelastic transfer products at KISS », the 6th international conference on Fission and Properties of Neutron-rich Nuclei, Nov. 6-12, 2016, Florida, USA.

Y. Hirayama, « Recent spectroscopic activities using multi-nucleaon transfer reaction products at KISS », LA3NET Laser Ion Source Workshop, Oct. 24-25, 2016, Paris, France.

P. Schury, « Nuclear Physics with Slow and Stopped Beam at RIBF », KPS meeting, Oct. 19-21, 2016, Gwangju, Korea.

P. Schury, « Gas Catcher Systems Status: SLOWRI/PALIS, SlowSHE, and KISS”, Fragment Separator Expert Meeting, Aug. 30 – Sept. 2, 2016, Grand Rapids, Michigan, USA.

P. Schury, “Mass Measurements of r-process Nuclei at KISS and SLOWRI”, The 14th International Symposium on Nuclei in the Cosmos (NIC), June 19-24, 2016, Niigata, Japan.

Y.X. Watanabe, “Production of radioactive nuclei relevant to r-process by multinucleon transfer reaction for KISS”, The 14th International Symposium on Nuclei in the Cosmos (NIC), June 19-24, 2016, Niigata, Japan.

H. Soon, “Beta-decay half-lives of neutron rich nuclei and its impact on production of r-process elements”, The 14th International Symposium on Nuclei in the Cosmos (NIC), June 19-24, 2016, Niigata, Japan.

Y. Hirayama, “Spectroscopy of multi-nucleon transfer reaction products using KISS”, Stopping and Manipulation of Ions and related topics (SMI-2016), June 8-10, 2016, IMP, Lanzhou, China.

[Domestic Conference]

M. Wada, « Possibility of comprehensive mass measurements of heavy elements », Symposium on Perspective of super heavy element science, Mar. 17-20, Osaka, Japan.

Y.X. Watanabe, « Production of radioactive nuclei relevant to r-process by multinucleon transfer reactions for KISS », SSRI Workshop, Mar. 5-6, JAEA, Tokai, Japan.

Y. Hirayama, « Present status of KISS », SSRI Workshop, Mar. 5-6, JAEA, Tokai, Japan.

M. Mukai, « Development of low-background gas-counter for the beta spectroscopy at KISS », SSRI Workshop, Mar. 5-6, 2016, JAEA, Tokai, Japan.

P. Schury, « Observation of doubly-charged ions of Pb through Pu extracted from cryogenic gas cell and mass anayzed by MRTOF-MS », SSRI Workshop, Mar. 5-6 ,2016, JAEA, Tokai, Japan.

S. Kimura, « Precision mass measurements of proton-rich nuclei in A≈60-80 region with the multireflection time-of-flight mass spectrometer », SSRI Workshop, Mar. 5-6, 2016, JAEA, Tokai, Japan.

H. Miyatake, « KISS, SLOWRI 施設での低エネルギー核分光研究", KUR 専門研究会, Dec. 20-21, 2016, 京大原子炉、京都

H. Miyatake, “Recent Progress of the KISS project at KEK-WNSC”, 40th ASRC Int. Workshop on Experimental and Theoretical Advances in Fission and Heavy Nuclei, Dec. 12-13, 2016, JAEA 東海, Japan.,

M. Wada, “High precision nuclear spectroscopy with trapped radioactive ions”, The 2nd Cicily East Asia Workshop on Low-energy Nuclear Physics”, June 26-28, RIKEN, Japan.

Y. Hirayama, “Nuclear spectroscopy of r-process nuclei around N=126 using KISS”, The 2nd Cicily East Asia Workshop on Low-energy Nuclear Physics”, June 26-28, RIKEN, Japan.

Events (April 2016 — March 2017)

RNC

Apr. 6–8	RBRC Scientific Review Committee (SRC)
Apr. 23	Wako Open campus
May 30–31	The 5th International Advisory Committee for the RIKEN-RAL Muon Facility (RAL-IAC)
July 21–23	The 4th Nishina Center Advisory Council (NCAC)
June 3	The 22nd RBRC Management Steering Committee (MSC)
Aug. 1–12	Nishina School
Dec. 1–3	The 17th Program Advisory Committee for Nuclear Physics Experiments at RI Beam Factory (NP-PAC)
Dec. 5	Final Report of the former Associate Chief Scientist, Takashi Nakatsukasa
Dec. 14–16	The 10th RIKEN Advisory Council (RAC)
Jan. 13	The 6th Industrial Program Advisory Committee (In-PAC)
Jan. 19–20	The 13th Program Advisory Committee for Materials and Life Science Researches at RIKEN Nishina Center (ML-PAC)
Jan. 30	Research Review of the Chief Scientist, Tetsuo Hatsuda

CNS

Jul. 25	坂井光夫先生追悼講演会 http://indico.cns.s.u-tokyo.ac.jp/conferenceDisplay.py?confId=302
Aug. 24–30	The 15th CNS International Summer School(CNSSS16) http://indico.cns.s.u-tokyo.ac.jp/conferenceDisplay.py?confId=288

Niigata Univ.

	not held in FY2016

KEK

Aug, 18–26	KEK Summer Challenge 2016 http://www2.kek.jp/ksc/10th_2016/index.html
Sept, 2–3	SSRI-pns Collaboration Meeting 2016 http://research.kek.jp/group/wnsc/ssri-pns-jp/
Sept. 4	KEK Open Campus 2016 https://www2.kek.jp/openhouse/

Press Releases (April 2016 - March 2017)

RNC

Sep. 27	Stable transmission of slow highly charged ions through tapered glass capillary with active discharging method for sub-micron sized beams	Tomoko Abe and Tokihiro Ikeda; Ion Beam Breeding Team, Takao Kojima; SLOWRI team
Sep. 30	First Vertical Test of Superconducting QWR Prototype at RIKEN	Naruhiko Sakamoto, Kazunari Yamada, Yutaka Watanabe, Kenji Suda, Kazutaka Ozeki; High Gradient Cavity R&D Team, Osamu Kamigaito; High-Intensity Accelerator R&D Group
Dec. 14	Fate of the Tetraquark Candidate $Z_c(3900)$ from Lattice QCD	Yoichi Ikeda, Takumi Doi, Tetsuo Hatsuda; Quantum Hadron Physics Laboratory
Feb. 13	Spallation reaction study for the long-lived fission product ^{107}Pd	He Wang; Radioactive Isotope Physics Laboratory, Hiroyoshi Sakurai; Nuclear Transmutation Data Research Group, Hideaki Otsu; Fast RI Data Team
Feb.17	94 β-Decay Half-Lives of Neutron-Rich ^{55}Cs to ^{67}Ho: Experimental Feedback and Evaluation of the r-Process Rare-Earth Peak Formation	Jin Wu, Shunji Nishimura, Hiroyoshi Sakurai; Radioactive Isotope Physics Laboratory
Feb. 21	Are There Signatures of Harmonic Oscillator Shells Far from Stability? First Spectroscopy of ^{110}Zr	Pieter Doornenbal, Hiroyoshi Sakurai; Radioactive Isotope Physics Laboratory, Alexandre Obertelli, Tomohiro Uesaka; Spin Isospin Laboratory
Mar. 1	Study of the Reaction ^{48}Ca + ^{248}Cm → ^{296}Lv at RIKEN-GARIS	Daiya Kaji, Kouji Morimoto; Superheavy Element Device Development Team, Kosuke Morita; Research Group for Superheavy Element, Hiromitsu Haba; RI Applications Team
Mar. 6	Overview of the chemical composition and characteristics of Na^+ and Cl^- distributions in shallow samples from Antarctic ice core DF01 (Dome Fuji) drilled in 2001	Kazuya Takahashi, Yuko Motizuki, Yoichi Nakai; Astro-Glaciology Research Unit

CNS

Oct. 18	Quantum phase transition in the shape of nuclei and simulations using K computer	T. Otsuka, T. Togashi, Y. Tsunoda, N. Shimizu

VII. LIST OF PREPRINTS

List of Preprints (April 2016 — March 2017)

RIKEN NC-NP

164	Quantal rotation and its coupling to intrinsic motion in nuclei	T. Nakatsukasa, K. Matsuyanagi et al.
165	Giant dipole resonance in hot rotating nuclei	D.R. Chakrabarty, N. Dinh Dang et al.
166	Microscopic derivation of the Bohr-Mottelson collective Hamiltonian and its application to quadrupole shape dynamics	K. Matsuyanagi, M. Matsuo et al.
167	Improved treatment of blocking effect at finite temperature	N. Quang Hung, N. Dinh Dang et al.
168	Time-dependent density-functional description of nuclear dynamics	T. Nakatsukasa, K. Matsuyanagi et al.
169	Self-consistent collective coordinate for reaction path and inertial mass	K. Wen, T. Nakatsukasa
170	Determination of a dineutron correlation in Borromean nuclei via a quasi-free knockout (p,pn) reaction	Y. Kikuchi, K. Ogata et al.
171	Effective restoration of dipole sum rules within the renormalized random-phase approximation	N. Quang Hung, N. Dinh Dang et al.
172	Sum rule study for Double Gamow-Teller states	H. Sagawa, T. Uesaka
173	Angular momentum gated thermodynamic properties in T_c isotopes	B. Dey, D. Pandit et al.
174	Giant dipole resonance and shape transitions in hot and rotating ^{88}Mo	A. K. Rhine Kumar, P. Arumugam et al.
175	Simultaneous microscopic description of nuclear level density and radiative strength function	N. Quang Hung, N. Dinh Dang et al.
176	Time-dependent density-functional calculation of nuclear response functions	T. Nakatsukasa
177	Examining possible neutron-halo nuclei heavier than ^{37}Mg	I. Hamamoto

RIKEN NC- AC

3	SLOWRI 後段加速器の概念設計(v2)	S. Arai
4	IH 空洞の概略設計	S. Arai
5	GENRFQ-PREBUNCHER の入力データ	S. Arai
6	SLOWRI 後段加速器での異なる電荷質量比を持つイオンの同時加速	S. Arai

RIKEN MP

	Not Applicable	

RIKEN QHP

219	Nonperturbative RG analysis of five-dimensional O(*N*) models with cubic interactions	K. Kamikado, T. Kanazawa
220	Mobile impurity in a Fermi sea from the functional renormalization group analytically continued to real time	K. Kamikado, T. Kanazawa, S. Uchino
221	Fixed point structure of the Abelian Higgs model	G. Fejos, T. Hatsuda
222	Magnetic Shift of the Chemical Freezeout and Electric Charge Fluctuations	K. Fukushima, Y. Hidaka
223	Probing Multi-Strange Dibaryon with Proton-Omega Correlation in High-energy Heavy Ion Collisions	K. Morita, A. Ohnishi et al.
224	Relativistic Brueckner-Hartree-Fock theory for finite nuclei	S. Shen, J. Hu et al.
225	Scattering of universal fermionic clusters in the resonating group method	P. Naidon, S. Endo et al.
226	Universal clusters as building blocks of stable quantum matter	S. Endo, A. M. Garc et al.
227	Efimov physics: a review	P. Naidon, S. Endo
228	A non-boost-invariant solution of relativistic hydrodynamics in 1+3 dimensions	Y. Hatta, B. Xiao, D. Yang
229	Transverse flow induced by inhomogeneous magnetic fields in the Bjorken expansion	S. Pu, D. Yang
230	A Fast Algorithm for Lattice Hyperonic Potentials	H. Nemura, S. Aoki et al.
231	First results of baryon interactions from lattice QCD with physical masses (2) — S = −3 and S = −4 sectors $(\Xi\Xi, \Xi\Sigma, \Xi\Lambda - \Xi\Sigma)$ channels) —	N. Ishii, S. Aoki et al.
232	Revision of the brick wall method for calculating the black hole thermodynamic quantities	F. Lenz, K. Ohta, K. Yazaki
233	Hyperon puzzle, hadron-quark crossover and massive neutron stars	K. Masuda , T. Hatsuda, T. Takatsuka
234	Hadron–quark crossover and hot neutron stars at birth	K. Masuda, T. Hatsuda, T. Takatsuka
235	Effects of hadronic rescattering on multistrange hadrons in high-energy nuclear collisions	S. Takeuchi, K. Murase et al.
236	Equation of State for SU(3) Gauge Theory via the Energy-Momentum Tensor under Gradient Flow	M. Kitazawa, T. Iritani et al.
237	Lattice Quantum Chromodynamics (Chap. 3 in "An advanced course in computational nuclear physics − bridging the scales from quarks to neutron stars −"	T. Hatsuda
238	Pseudospin symmetry in nuclear structure and its supersymmetric representation	H. Liang
239	Self-consistent relativistic quasiparticle random-phase approximation and its applications to charge-exchange excitations	Z. M. Niu, Y. F. Niu et al.
240	Probing Resonances of the Dirac Equation with Complex Momentum Representation	Niu Li, Min Shi et al.
241	Tetraquark and Pentaquark Systems in Lattice QCD	F. Okiharu, T. Doi et al.
242	Overscreened Kondo effect, (color) superconductivity, and Shiba states in Dirac metals and quark matter	T. Kanazawa, S. Uchino
243	Improved radial basis function approach with the odd-even corrections	Z. M. Niu, B. H. Sun et al.
244	Mirage in Temporal Correlation functions for Baryon-Baryon Interactions in Lattice QCD	T. Iritani, T. Doi et al.
245	Measurement of the CKM angle ϕ_1 in $B\bar{B}^0 \to \bar{D}^{*0}h^0, \bar{D}^0 \to K_S^0\pi^+\pi^-$ decay with time-dependent binned Dalitz plot analysis	V. Vorobyev et al.
246	Study of Excited Ξ_c States Decaying into Ξ_c^0 and Ξ_c^+ Baryons	J. Yelton et al.
247	Measurement of the branching ration of to $\bar{B}^0 \to D^{*+}\tau^-\bar{\nu}_\tau$ relative to $\bar{B}^0 \to D^{*+}\ell^-\bar{\nu}_\ell$ decays with a semileptonic tagging method	Y. Sato et al.
248	Dynamical Pattern Selection of Growing Cellular Mosaic in Fish Retina	N. Ogawa, T. Hatsuda et al.
249	The hidden charm pentaquarks are the hidden color-octet *uud* baryons?	S. Takeuchi, M. Takizawa

250	Kinetic derivation of generalized phase space Chern-Simons theory	T. Hayata, Y. Hidaka
251	Virtual photon polarization in ultrarelativistic heavy-ion collisions	G. Baym, T. Hatsuda, M. Strickland
252	Hot Neutron Stars with Hadron-Quark Crossover	K. Masada, T. Hatsuda, T. Takaysuka
253	Luescher's finite volume test for two-baryon systems with attractive interactions	S. Aoki, T. Doi et al.
254	Baryon interactions in lattice QCD: the direct method vs. the HAL QCD potential method	T. Iritani et al.
255	Interacting fermions in rotation: chiral symmetry restoration, moment of inertia and thermodynamics	M. Chernodub, S. Gongyo
256	Phases of circle-compactified QCD with adjoint fermions at finite density	T. Kanazawa et al.
257	Relativistic Chiral Kinetic Theory from Quantum Field Theories	Y. Hidaka, S. Pu et al.
258	Probing the resonance in the Dirac equation with quadruple-deformed potentials by complex momentum representation method	Z. Fang, M. Shi et al.
259	Holographic Photon Production in Heavy Ion Collisions	I. Iatrakis, E. Kiritsis et al.
260	Relativistic Chiral Kinetic Theory from Quantum Field Theories	Y. Hidaka, S. Pu et al.
261	Transverse flow induced by inhomogeneous magnetic fields in the Bjorken expansion	S. Pu, D. Yang
262	Two impurities in a Bose-Einstein condensate: from Yukawa to Efimov attracted polarons	P. Naidon
263	Electric Field Screening with Backflow at Pulsar Polar Cap	S. Kisaka, K. Asano et al.
264	CALET Upper Limits on X-Ray and Gamma-Ray Counterparts of GW151226	O. Adriani, Y. Akaike et al.
265	Wide-band Spectra of Giant Radio Pulses from the Crab Pulsar	R. Mikami, K. Asano et al.
266	Black hole-neutron star binary merger: Dependence on black hole spin orientation and equation of state	K. Kawaguchi, K. Kyutoku et al.
267	High-resolution magnetohydrodynamics simulation of black hole-neutron star merger: Mass ejection and short gamma-ray burst	K. Kiuchi, Y. Sekiguchi et al.
268	Aligned spin neutron star-black hole mergers: a gravitational waveform amplitude model	F. Pannarale, E. Berti et al.
269	Gravitational-wave cutoff frequencies of tidally disruptive neutron star-black hole binary mergers	F. Pannarale, E. Berti et al.
270	Efficient magnetic-field amplification due to the Kelvin-Helmholtz instability in binary neutron star mergers	K. Kiuchi, P. Cerd et al.
271	Models of Kilonova/macronova emission from black hole-neutron star mergers	K. Kawaguchi, K. Kyutoku et al.
272	Effects of neutron-star dynamic tides on gravitational waveforms within the effective-one-body approach	T. Hinderer, A. Taracchini et al.
273	The unreasonable weakness of r-process cosmic rays in the neutron-star-merger nucleosynthesis scenario	K. Kyutoku, K. Ioka
274	Measurability of the tidal deformability by gravitational waves from coalescing binary neutron stars	K. Hotokezaka, K. Kyutoku et al.
275	Dynamical mass ejection from the merger of asymmetric binary neutron stars: Radiation-hydrodynamics study in general relativity	Y. Sekiguchi, K. Kiuchi et al.
276	Concise estimate of the expected number of detections for stellar-mass binary black holes by eLISA	K. Kyutoku, N. Seto
277	Gravitational-wave cosmography with eLISA and the Hubble tension	K. Kyutoku, N. Seto
278	Forecasting Tidal Disruption Events by Binary Black Hole Roulettes	N. Seto, K. Kyutoku
279	First results of baryon interactions from lattice QCD with physical masses (3) — Strangeness $S = -2$ two-baryon system	K. Sasaki, S. Aoki et al.
280	Kinetic Theory and Anomalous Transports in the Presence of the Phase-Space Non-abelian Berry Curvatures	T. Hayata, Y. Hidaka
281	QCD phase transition at real chemical potential with canonical approach	A. Nakamura, S. Oka, Y. Taniguchi

282	Canonical approach to finite density QCD with multiple precision computation	R. Fukuda, A. Nakamura, S. Oka
283	Sign problem in finite density lattice QCD	V. A. Goy, V. Bornyakov et al.
284	Entanglement in four-dimensional SU(3) gauge theory	E. Itou, K. Nagata1 et al.
285	Stable Yang-Lee zeros in a truncated fugacity series from the net baryon number multiplicity distribution	K. Morita, A. Nakamura
286	Doubly magic nuclei from Lattice QCD forces at MPS = 469 MeV	C. McIlroy C. Barbieri et al.
287	Search for a dark vector gauge boson decaying to $\pi+\pi-$ using $\eta\to\pi+\pi-\gamma$ decays	E. Won et al.
288	Observation of D0$\to\rho\,0\,\gamma$ and search for CP violation in radiative charm decays	T. Nanut et al.
289	Search for the 0^- glueball in Y(1S) and Y(2S) decays	S. Jia et al.
290	Search for D^0 decays to invisible final states at Belle	Y.-T. Lai et al.
291	Measurement of the τ lepton polarization and $R(D^*)$ in the decay $\bar{B}\to D^*\tau^-\bar{\nu}_\tau$	S. Hirose et al.
292	Lepton-Flavor-Dependent Angular Analysis of $B\to K^*\ell^+\ell^-$	S. Wehle et al.
293	Electric dipole moment of the deuteron in the standard model with $NN-\Lambda N-\Sigma N-\Sigma N$ coupling	N. Yamanaka
294	Review of the electric dipole moment of light nuclei	N. Yamanaka
295	A new matrix model	T. Kanazawa, M. Kieburg
296	Baryon interactions from lattice QCD with physical masses — Overview and S = 0, –4 sectors —	T. Doi, S. Aoki et al.
297	Baryon interactions from lattice QCD with physical masses — S = –3 sector: $\Xi\Sigma$ and $\Xi\Lambda-\Xi\Sigma$ —	N. Ishii, S. Aoki et al.
298	Baryon interactions from lattice QCD with physical masses — S = –2 sector —	K. Sasaki, S. Aoki et al.
299	Lambda-Nucleon and Sigma-Nucleon interactions from lattice QCD with physical masses	H. Nemura, S. Aoki et al.
300	Effects of rotation and boundaries on chiral symmetry breaking of relativistic fermions	M. Chernodub, S. Gongyo
301	Are two nucleons bound in lattice QCD for heavy quark masses? — Sanity check with Luscher's finite volume formula —	T. Iritani, S. Aoki et al.
302	Microscopic studies on nuclear spin-isospin properties — a personal perspective on covariant density functional theory	H. Liang
303	Search for $B\to h\bar{\nu}\nu$ decays with semileptonic tagging at Belle	J. Grygier et al.
304	Measurement of the Decays $B\to\eta\ell\nu_\ell$ and $B\to\eta'\ell\nu_\ell$ in Fully Reconstructed Events at Belle	C. Beleno et al.
305	First measurement of *T*-odd moments in $D^0\to K^0_S\pi^+\pi^-\pi^0$ decays	K. Prasanth et al.

CNS-REP

95	CNS Annual Report 2015	T. Gunji, Y. Kishi

Nishina Center Preprint server (not including Partner Institution) can be found at
http://nishina-preprints.riken.jp/

VIII. LIST OF SYMPOSIA, WORKSHOPS & SEMINARS

List of Symposia & Workshops (April 2016 — March 2017)

RNC

1	RIKEN BNL Research Center Workshop — High pT Physics in the RHIC-LHC Era — https://www.bnl.gov/pt2016/	BNL	Apr. 12–15
2	Experimental and Theoretical Applications of Spin-Resonance Techniques to Advanced Material Sciences http://library.riken.jp/secure/5567/20160525-	Hokkaido U.	May. 25
3	NIC-XIV School 2016 https://indico2.riken.jp/indico/conferenceDisplay.py?confId=—2103	Niigata U.	Jun. 13–17
4	Nuclei in the Cosmos XIV http://nic2016.jp/	Niigata U.	Jun. 19–24
5	International Symposium on Modern Technique and its Outlook in Heavy Ion Science (MOTO16) https://indico2.riken.jp/indico/conferenceDisplay.py?confId=2276	Rikkyo U.	Jun. 26–27
6	The 14th International Conference on Meson-Nucleon Physics and the Structure of the Nucleon (MENU2016) http://menu2016.riken.jp/	Kyoto U.	Jul. 25–30
7	Meson in Nucleus 2016 http://www2.yukawa.kyoto-u.ac.jp/~min2016/	Kyoto U.	Jul. 31 –Aug. 2
8	熱場の量子論とその応用 http://library.riken.jp/secure/5567/20160822-24--hatudaryousihadoronbuturigaku.docx	Suzuki Umetaro Hall	Aug. 22–24
9	Towards theoretical understanding of production reactions of superheavy elements http://indico2.riken.jp/indico/conferenceDisplay.py?confId=2354	RIBF Conference Room	Aug. 31
10	EURICA Celebration and Collaboration Meeting https://indico2.riken.jp/indico/conferenceDisplay.py?confId=2341	RIBF Conference Room	Sep. 6–7
11	RIBF Users Meeting 2016 https://indico2.riken.jp/indico/conferenceDisplay.py?confId=2340	RIBF Conference Room	Sep. 8–9
12	仁科記念講演会「ニホニウム発見」 http://www.nishina-mf.or.jp/kouen.html	U. Tokyo	Dec. 5
13	Chiral Matter: from quarks to Dirac semimetals http://tkynt2.phys.s.u-tokyo.ac.jp/cm2016/	Okochi Hall	Dec. 5–8
14	First Tsukuba-CCS-RIKEN joint workshop on microscopic theories of nuclear structure and dynamics https://www.ccs.tsukuba.ac.jp/ccs-riken-workshop2016/	RIBF Conference Room & U. Tsukuba	Dec. 12–16
15	The 7th Workshop on Muon Science and Accelerator Technologies https://indico2.riken.jp/indico/conferenceDisplay.py?confId=2432	RIBF Conference Room	Jan. 5–7
16	RIKEN BNL Research Center Workshop — QCD in Finite Temperature and Heavy-Ion Collisions — https://www.bnl.gov/qcdfinite17/	BNL	Feb.13–15
17	Second CORE-U Conference — Cosmic Polarimetry from Micro to Macro Scales — http://conf2nd.core-u.hiroshima-u.ac.jp/	Hiroshima U.	Feb.17–18
18	International Workshop on Strangeness Nuclear Physics 2017 https://indico2.riken.jp/indico/conferenceDisplay.py?confId=2389	Osaka Electro-Communication U.	Mar. 12–14

CNS

1	The second SEA workshop on Low Energy Nuclear Physics (SEA2016)	CNS	Jun. 26–28
2	Mini workshop in the framework of JSPS-FWO collaboration	U. Tokyo	Nov. 29
3	仁科記念講演会「ニホニウム発見」 http://www.nishina-mf.or.jp/kouen.html	U. Tokyo	Dec. 5

Niigata Univ.

1	NIC-XIV School 2016 https://indico2.riken.jp/indico/conferenceDisplay.py?confId=2103	Niigata U.	Jun. 13–17
2	2016 日本放射化学会年会・第 60 回放射化学討論会	Niigata U.	Sep. 10–12

List of Seminars (April 2016 — March 2017)

Nuclear Physics Monthly Colloquium

1	Rikutaro Yoshida (JLab EIC physics)	Status of the Electron-Ion Collider https://indico2.riken.jp/indico/conferenceDisplay.py?confId=2302	Aug. 4
2	Masahito Ueda (U. Tokyo)	Quantum many-body dynamics under continuous observation https://indico2.riken.jp/indico/conferenceDisplay.py?confId=2385	Nov. 30
3	Gottfried Munzenberg (GSI, University of Mainz)	Nihonium, Super heavy nuclei -some historical remarks- https://indico2.riken.jp/indico/conferenceDisplay.py?confId=2469	Mar. 13
4	Yuri Tsolakovich Oganessian (Flerov Laboratory of Nuclear Reactions JINR)	Discovery of Super heavy Nuclei https://indico2.riken.jp/indico/conferenceDisplay.py?confId=2469	Mar. 13
5	Kenji Fukushima (U. Tokyo)	Chirality and vorticity in heavy-ion collisions https://indico2.riken.jp/indico/conferenceDisplay.py?confId=2451	Mar. 31

RIBF Nuclear Physics Seminar

1	Yosuke Kondo (Tokyo Tech.)	Recent experimental studies for unbound oxygen isotopes http://indico2.riken.jp/indico/conferenceDisplay.py?confId=2218	Apr. 19
2	He Wang (RNC)	Spallation reaction study for long-lived fission products in nuclear waste: Cross section measurement for ^{137}Cs and ^{90}Sr on proton and deuteron https://indico2.riken.jp/indico/conferenceDisplay.py?confId=2223	May. 10
3	Hiroki Nishibata (RNC)	Newcomers' Seminar http://indico2.riken.jp/indico/conferenceDisplay.py?confId=2260	May. 24
4	Clementine Santamaria (NSCL)	Extension of the N = 40 Island of Inversion towards N = 50 below ^{78}Ni with MINOS at the RIBF http://indico2.riken.jp/indico/conferenceDisplay.py?confId=2293	Jun. 10
5	Makoto Fujiwara (TRIUMF)	Casting Light on Antimatter: Fundamental Physics with Trapped Antihydrogen https://indico2.riken.jp/indico/conferenceDisplay.py?confId=2312	Jul. 14
6	Yoritaka Iwata (Tokyo Tech. / Shibaura Inst. of Tech.)	Large scale shell model calculations for double beta decay of ^{48}Ca https://indico2.riken.jp/indico/conferenceDisplay.py?confId=2333	Jul. 26
7	N. Sandulescu (National Institute of Physics and Nuclear Engineering)	Proton-neutron pairing and quartet correlations in nuclei https://indico2.riken.jp/indico/conferenceDisplay.py?confId=2344	Jul. 29
8	Yong-Zhong Qian (U. of Minnesota)	The r-process: status & challenges https://indico2.riken.jp/indico/conferenceDisplay.py?confId=2358	Sep. 1
9	Yuki Yokokura (iTHES-CS)	Thermodynamic entropy as a Noether invariant https://indico2.riken.jp/indico/conferenceDisplay.py?confId=2366	Oct. 4
10	Takashi Hachiya (RBRC)	Measurement of single electrons from semileptonic charm and bottom hadron decays in Au + Au collisions at RHIC-PHENIX https://indico2.riken.jp/indico/conferenceDisplay.py?confId=2378	Oct. 11
11	Yuji Goto (RNC)	Precision measurement of the gluon polarization inside the proton https://indico2.riken.jp/indico/conferenceDisplay.py?confId=2379	Oct. 28
12	Gianluca COLO (U. of Milano, INFN)	Microscopic particle-vibration coupling calculations with applications to single-particle, collective and charge-exchange nuclear transitions https://indico2.riken.jp/indico/conferenceDisplay.py?confId=2407	Nov. 25
13	Shin Watanabe (RNC)	Reaction cross sections as a probe of deformation and shell structures https://indico2.riken.jp/indico/conferenceDisplay.py?confId=2396	Dec. 6
14	Xiaofei Yang (KU Leuven)	Nuclear structure studies by the measurement of nuclear spins, moments and charge radii via laser spectroscopy techniques https://indico2.riken.jp/indico/conferenceDisplay.py?confId=2408	Dec. 8

15	Costel Petrache (CNRS, Universite de Paris-Saclay)	Transverse wobbling and new chiral modes in lanthanide nuclei https://indico2.riken.jp/indico/conferenceDisplay.py?confId=2417	Dec. 22
16	Takahiro Nishi (RNC)	Precision spectroscopy of pionic atoms to study pion-nucleus interaction in medium https://indico2.riken.jp/indico/conferenceDisplay.py?confId=2434	Jan. 24
17	Takeshi Yamamoto (JAEA)	Study of charge symmetry breaking in A = 4 hypernuclear system via the gamma-ray spectroscopy experiment at J-PARC https://indico2.riken.jp/indico/conferenceDisplay.py?confId=2439	Feb. 7
18	Shinji Okada (RIKEN)	High-resolution Exotic Atom x-ray spectroscopy with TES microcalorimeters https://indico2.riken.jp/indico/conferenceDisplay.py?confId=2440	Feb. 14
19	Atsushi Tamii (Osaka U.)	np spin-correlation in the ground state studied by the sum-rules of the spin-M1 transition matrix elements and implications to the IS np pairing correlation https://indico2.riken.jp/indico/conferenceDisplay.py?confId=2470	Mar. 28
20	Stefano Gandolfi (Los Alamos National Laboratory)	Inhomogeneous neutron matter: what we can learn by trapping neutrons? https://indico2.riken.jp/indico/conferenceDisplay.py?confId=2488	Mar. 30

Lecture Series on Nuclear Physics

	not held in FY2016		

Special Seminar

1	Noriko Shiomitsu (Nishina Center Planning Office)	Successful approach to gaining a Kakenhi-grant	Sep. 27

Seminar by Each Laboratory

Theoretical Research Division

1	Hiromichi Nishimura (RBRC)	QHP Seminar: Complex spectrum of finite-density QCD	Apr. 19
2	Nguyen Dinh Dang (RNC)	QHP Seminar: Three decades of conquering giant dipole resonance in highly excited nuclei	Apr. 26
3	Ryutaro Fukuda (RIKEN)	QHP Seminar: Canonical approach to finite density QCD	May. 10
4	Hiroyuki Fujita (ISSP, U. Tokyo)	QHP Seminar: Chiral magnetic effect in Weyl semimetals: the role of electromagnetic field analysis	May. 17
5	Tingting Sun (Zhengzhou U. / Peking U.)	SNP Seminar: Relativistic mean field approaches for Ξ^- hypernuclei and current experimental data	May. 20
6	Shin Watanabe (RNC)	SNP Seminar: Dynamic properties of ^{6}Li elastic scattering	May. 20
7	Pablo A/ Morales (U. Tokyo)	QHP Seminar: Field theory of the perfect fluid	May. 31
8	Elena Caceres (Colima U. & U. Texas at Austin)	QHP Seminar: On holographic entanglement entropy and boundary causality in Gauss Bonnet gravity	Jun. 7
9	Yoshitaka Hatta (YITP, Kyoto U.)	QHP Seminar: Nucleon tomography at small-x	Jun. 7

10	Koichi Hamaguchi (U. Tokyo)	QHP Seminar: Some implications of the 750 GeV diphoton excess	Jun. 14
11	Jirina Stone (U. Tennessee)	SNP Seminar: Low energy nuclear structure modeling; Can it be improved?	Jun. 15
12	Takashi Mori (U. Tokyo)	QHP Seminar: Relaxation process of periodically driven quantum systems in the high-frequency regime	Jun. 21
13	Tamiaki Yoneya (U. Tokyo)	QHP Seminar: Covariantized M(atrix) theory for D-particles	Jun. 28
14	Keiichi Tamai (U. Tokyo)	QHP Seminar: Directed percolation universality in transition to turbulence	Jul. 5
15	Chung-Wen Kao (Chung-Yuan Christian U.)	QHP Seminar: Modeling the Fragmentation functions	Jul. 19
16	Qiang Zhao(Chinese Academy of Sciences)	SNP Seminar: Understanding the shortened lifetime of hypertriton	Aug. 1
17	Hideaki Iida (Far Eastern Federal U. / iTHES, RIKEN)	QHP Seminar: Field theoretical description of multi-layered Josephson junction and dynamics of Josephson vortices	Sep. 27
18	Roman Skibinski (Jagiellonian U.)	SNP Seminar: Recently developed two-nucleon interactions applied to three-nucleon systems	Oct. 3
19	Chihiro Matsui (U. Tokyo)	QHP Seminar: Multi-state extension of the asymmetric simple exclusion process	Oct. 11
20	Kazuhi Kanoda (U. Tokyo)	QHP Seminar: Spin liquids in molecular materials with quasi-triangular lattices	Oct. 18
21	Masashi Sugiyama (RIKEN AIP)	QHP Seminar: Machine Learning from Weak Supervision	Oct. 25
22	Emiko Hiyama (RNC)	SNP Seminar: Structure of the four-body tetra neutron	Nov. 7
23	Francisco Miguel MARQU, S MORENO (LPC (ENSICAEN))	SNP Seminar: The neutron as a building block of nuclei	Nov. 11
24	Yasunori Fujii (Advanced Research Institute for Science and Waseda U.)	QHP Seminar: A new estimate of the mass of the gravitational scalar field for Dark Energy	Nov. 15
25	Noriyuki Sogabe (Keio U.)	QHP Seminar: New dynamic critical phenomena in nuclear and quark superfluids	Nov. 22
26	Shi Pu (U. Tokyo)	QHP Seminar: Chiral magnetic effect and chiral kinetic theory	Nov. 29
27	Yuta Kikuchi (Kyoto U.)	QHP Seminar: Chiral magnetic effect without chirality source in asymmetric Weyl semimetals	Dec. 13
28	Yuya Tanizaki (RBRC)	QHP Seminar: Cheshire Cat Resurgence and Quasi-Exact Solvability	Dec. 20
29	Wolfram Weise (TU Munich)	QHP Seminar: In-medium phi meson sum rule and strangeness content of the nucleon	Jan. 16
30	Tomi Ohtsuki (Sophia U.)	QHP Seminar: Deep learning the quantum phase transitions in random electron systems	Jan. 17
31	Wolfram Weise (TU Munich)	QHP Seminar: Hyperon-nucleon interactions from SU(3) Chiral EFT and hyperon puzzle in neutron stars	Jan. 17
32	Yasuki Tachibana (MOE / Central China Normal U.)	QHP Seminar: Full jet with hydrodynamic response in QGP	Jan. 18

33	Taro Kimura (Keio U.)	QHP Seminar: Boundary Conditions of Topological Insulators and Weyl Semimetals	Jan. 24
34	Kazuo Takayanagi (Sophia U.)	QHP Seminar: Inverse scattering problem and generalized optical theorem	Jan. 31
35	Ade Irma Suriajaya (Nagoya U.)	QHP Seminar: Zeros of zeta and L-functions	Feb. 14
36	Rimantas Lazauskas (Université de Strasbourg)	SNP Seminar: Some developments in few-particle scattering problem based on complex-scaling method	Mar. 27
37	Rimantas Lazauskas (Université de Strasbourg)	SNP Seminar: On the possible existence of 4n resonances	Mar. 28

QHP Seminar -> http://ribf.riken.jp/QHP/seminar.html
SNP Seminar -> http://snp.riken.jp/seminar.html

Sub Nuclear System Research Division

1	Song Shu (Stonybrook U.)	Nuclear Theory & RIKEN seminar: Studying Nucleons in Soliton Models	Apr. 1
2	Xin-Nian Wang (LBNL/CCNU)	Nuclear Theory & RIKEN seminar: Vorticular fluid and Lambda Polarization in High-energy Heavy-ion Collisions	Apr. 15
3	Mark Strikman (Penn State U.)	RIKEN/BNL Lunch Time Talk: Color fluctuation phenomena in high energy hadron & photon-A collisions	Apr. 21
4	Dam T. Son (U. of Chicago)	Nuclear Theory & RIKEN seminar: A higher spin theory of neutral excitations of fractional quantum Hall fluids	Apr. 22
5	Sunghoon Jung (SLAC)	HET & RIKEN Seminar: Heavy Higgs Resonance Dip	Apr. 27
6	Alexei Tsvelik (BNL)	RIKEN/BNL Lunch Time Talk: Solving QCD2	Apr. 28
7	Gokce Basar (U. of Maryland)	Nuclear Theory & RIKEN seminar: Going with the flow: sign problem, Lefschetz thimbles and beyond	Apr. 29
8	Andreas Schaefer (U. of Regensburg)	HET & RIKEN Seminar: Calculating TMDs and DPDs on the lattice	May. 4
9	Xu-Guang Huang (Fudan U.)	RIKEN/BNL Lunch Time Talk: Vorticity in heavy-ion collisions and cold atoms	May. 5
10	Dennis Bazow (The Ohio State U.)	Nuclear Theory & RIKEN seminar: Fluid dynamics for the anisotropically expanding quark-gluon plasma	May. 6
11	Simon Mages (Forschungszentrum Juelich)	HET & RIKEN Seminar: Axions and Topology	May. 11
12	Stefan Rechenberger (U. of Darmstadt)	RIKEN/BNL Lunch Time Talk: The Functional Renormalization Group Method and Delayed Magnetic Catalysis	May. 12
13	Andrei Sadofyev (MIT)	Nuclear Theory & RIKEN seminar: Evolution of the jet opening angle distribution in holographic plasma	May. 13
14	Ramona Groeber (Roma Tre)	HET & RIKEN Seminar: Higgs Pair Production in Extensions of the Standard Model	May. 18
15	Gaoqing Cao (Fudan U.)	RIKEN/BNL Lunch Time Talk: Kosterlitz-Thouless transition and chiral rotation in external electromagnetic field	May. 19

16	Abhijit Majumdar (Wayne State U.)	Nuclear Theory & RIKEN seminar: The jet quenching parameter q-hat, and its relation to the TMDPDF	May. 20
17	Yuya Tanizaki (RBRC)	RIKEN/BNL Lunch Time Talk: Lefschetz-thimble path integral for studying the sign problem and Silver Blaze phenomenon	May.26
18	Xiaojun Yao (Duke U.)	RIKEN/BNL Lunch Time Talk: Static and dynamic screening effect on the resonant α-α scattering in a QED plasma	Jun. 16
19	Bin Wu (Ohio State U.)	RIKEN/BNL Lunch Time Talk: Leading log resummation in high-energy parton production in QCD matter	Jun. 23
20	Bin Wu (Ohio State U.)	Nuclear Theory & RIKEN seminar: On Pressure Isotropization in Heavy-Ion Collisions	Jun. 24
21	Sho Ozaki (Keio U.)	RIKEN/BNL Lunch Time Talk: Kondo effect in QCD	Jun. 30
22	Shuzhe Shi (Indiana U.)	RIKEN/BNL Lunch Time Talk: CME in Chiral Viscous Hydrodynamics	Jul. 14
23	Amir Rezaeian (The Federico Santa Maria Technical U.)	RIKEN/BNL Lunch Time Talk: Photon-jet Ridge at RHIC and the LHC	Aug. 4
24	Stefano Di Vita (DESY)	HET & RIKEN Seminar: Standard Model Vacuum Stability with a 125 GeV Higgs Boson	Aug. 12
25	Matt Sievert (BNL)	RIKEN/BNL Lunch Time Talk: Quark Polarization at Small x	Sep. 15
26	Hiromichi Nishimura (RBRC)	RIKEN/BNL Lunch Time Talk: Complex spectrum of QCD at finite density	Oct. 6
27	Marco Farina (Rutgers U.)	HET & RIKEN Seminar: Cannibal Dark Matter	Oct. 12
28	Raju Venugopalan (BNL)	RIKEN/BNL Lunch Time Talk: Kibble-Zurek dynamics and universal off-equilibrium scaling of critical cumulants in the QCD phase diagram	Oct. 13
29	Niklas Mueller (Heidelberg U.)	RIKEN/BNL Lunch Time Talk: Chiral magnetic effect and anomalous transport from real-time lattice simulations	Oct. 20
30	Chihi Nonaka (Nagoya U.)	Special Nuclear Theory & RIKEN seminar: A new relativistic viscous hydrodynamics code for high-energy heavy-ion collisions	Oct. 26
31	Stefania Gori (U. of Cincinnati)	HET & RIKEN Seminar: Collider signatures of flavorful Higgs bosons	Oct. 26
32	Chun Shen (BNL)	RIKEN/BNL Lunch Time Talk: Hybrid approach to relativistic heavy-ion collisions at the RHIC BES energies	Oct. 27
33	Genya Levin (Tel Aviv U.)	Nuclear Theory & RIKEN seminar: Perturbative QCD and beyond: Bose-Einstein correlation and ν_n at any n	Oct. 28
34	Amy Nicholson (UC Berkeley)	HET & RIKEN Seminar: Neutrinoless double beta decay from lattice QCD	Nov. 2
35	Yachao Qian (Stony Brook U.)	RIKEN/BNL Lunch Time Talk: Form Invariance, Topological Fluctuations and Mass Gap of Yang-Mills Theory	Nov. 3
36	Yi-Bo Yang (U. of Kentucky)	Nuclear Theory & RIKEN seminar: Glue spin from lattice QCD	Nov. 4
37	Chung Kao (U. of Oklahoma)	HET & RIKEN Seminar: When the Higgs meets the Top	Nov. 9
38	Enrico Rinaldi (RBRC)	RIKEN/BNL Lunch Time Talk: An overview of lattice field theory applications to dark matter searches	Nov.10

39	Alina Czajka (McGill U.)	Nuclear Theory & RIKEN seminar: Quantum-field-theoretical approach to shear and bulk relaxation times	Nov. 17
40	Armen Sedrakian (Frankfurt U.)	Nuclear Theory & RIKEN seminar: Phase structure and dynamics of dense QCD	Nov. 18
41	Luka Leskovec (U. of Arizona)	HET & RIKEN Seminar: Heavy meson decays to light resonances	Nov. 30
42	Stefan Flörchinger (Heidelberg U.)	Nuclear Theory & RIKEN seminar: Renormalization-group flow of the effective action of cosmological large-scale structures	Dec. 2
43	Ron Longacre (BNL)	Nuclear Theory & RIKEN seminar: Squeeze Out	Dec. 7
44	Rainer Fries (Texas A&M U.)	RIKEN/BNL Lunch Time Talk: Analytic Results for Color Glass In Space-Time Coordinates	Dec. 8
45	Michal Heller (Perimeter Institute)	Nuclear Theory & RIKEN seminar: Hydrodynamics, the gradient expansion and transient modes	Dec. 9
46	Hong Zhang (Ohio State U.)	HET & RIKEN Seminar: The Fate of Axion Stars	Dec. 14
47	Kevin Dusling (PRL)	Nuclear Theory & RIKEN seminar: Proton fluctuations and multi-particle rapidity correlations	Dec. 16
48	Jarkko Peuron (U. of Jyvaskyla)	RIKEN/BNL Lunch Time Talk: Plasmon mass scale and linearized gauge field fluctuations in classical Yang-Mills theory	Jan. 12
49	Paulo Bedaque (U. of Maryland)	Nuclear Theory & RIKEN seminar: Going with the flow: solving sign problems in complex space	Jan. 13
50	Fabian Rennecke (Heidelberg U.)	RIKEN/BNL Lunch Time Talk: Vector mesons and chiral symmetry restoration	Jan. 19
51	Andrey Tarasov (BNL)	RIKEN/BNL Lunch Time Talk: From small to moderate-x: beyond the eikonal approximation	Jan. 26
52	Naoto Tanji (U. of Heidelberg)	Nuclear Theory & RIKEN seminar: What shines brighter, Glasma or Quark-Gluon Plasma?	Jan. 27
53	Maxwell T. Hansen (Helmholtz Institute Mainz)	HET & RIKEN Seminar: Extracting scattering observables and resonance properties from lattice QCD	Feb. 15
54	Bowen Xiao (Central China Normal U.)	RIKEN/BNL Lunch Time Talk: The search for gluon saturation in pA collisions and at the EIC	Feb. 16
55	Michael Lublinsky (Ben-Gurion U.)	Nuclear Theory & RIKEN seminar: High energy QCD at NLO	Feb. 17
56	Raul A. Briceno (JLab)	HET & RIKEN Seminar: Few-body systems in QCD	Feb. 22
57	Masaru Hongo (RIKEN)	RIKEN/BNL Lunch Time Talk: Path-integral formula for local thermal equilibrium	Feb. 23
58	Akio Tomiya (Central China Normal U.)	RIKEN/BNL Lunch Time Talk: The Kibble-Zurek scaling for the Entanglement Entropy on the scalar field in 1+1 dimension	Feb. 27
59	Yoshimasa Hidaka (RNC)	RIKEN/BNL Lunch Time Talk: Generalized Nambu-Goldstone theorem	Mar. 2
60	Thorben Graf (U. of Frankfurt)	RIKEN/BNL Lunch Time Talk: Finite-Temperature Perturbative QCD confronts Lattice	Mar. 9
61	Duff Neill (LANL)	Nuclear Theory & RIKEN seminar: Universal Transverse Momentum Dependent Fragmentation	Mar. 17

62	Carlos Naya (Durham U.)	Nuclear Theory & RIKEN seminar: A solitonic approach to neutron stars: The (BPS) Skyrme model	Mar. 24
63	Luchang Jin (BNL)	RIKEN/BNL Lunch Time Talk: The hadronic light-by-light contribution to muon $g-2$ from lattice QCD	Mar. 30

RIKEN/BNL Lunch Time Talk -> https://sites.google.com/site/rikenlunch/talks

RIBF Research Division

1	Margherita Giustina (SRON)	High Energy Astrophysics Lab. Seminar Direct Probe of the Inner Accretion Flow around the Supermassive Black Hole in NGC 2617	Apr. 14
2	Kyoichiro Ozawa (KEK)	ハドロン物理学の展望 http://indico2.riken.jp/indico/conferenceDisplay.py?confId=2258	Apr. 27
3	Kouichi Hagino (Tohoku U.)	RIBF/post-RIBF and theory-experiment coupling http://indico2.riken.jp/indico/conferenceDisplay.py?confId=2269	May. 12
4	Kenta Itahashi (RNC)	物質の創成と真空の構造の解明をめざして http://indico2.riken.jp/indico/conferenceDisplay.py?confId=2270	May. 12
5	Kunihiko Odera (Nagoya U.)	年平均気温に見る太陽活動の影響 http://ribf.riken.jp/ag/ag.html	May. 18
6	Akihiro Yatabe (Wasada U.)	High Energy Astrophysics Lab. Seminar 強い磁場を伴う中性子星の放射に対する QED 効果	May. 24
7	Taku Gunji (CNS)	RHIC-LHC でのクォーク物質の物理と将来展望 http://indico2.riken.jp/indico/conferenceDisplay.py?confId=2274	May. 26
8	Takao Sakaguchi (BNL)	クオーク物質研究の動向と今後の展望 http://indico2.riken.jp/indico/conferenceDisplay.py?confId=2275	May. 26
9	Hiroaki Ohnishi (RNC)	ハドロン物理の現状と将来計画 http://indico2.riken.jp/indico/conferenceDisplay.py?confId=2306	Jun. 16
10	Peter Moroshkin (RIKEN CEMS)	Laser spectroscopy of Ba+ ions in superfluid He and in cold He gas https://indico2.riken.jp/indico/conferenceDisplay.py?confId=2350	Jul. 27
11	Masanori Hatashita （WERC）	イオンビーム照射によるコルジセピンを高生産する冬虫夏草菌の開発 None	Oct. 6
12	Takeshi Toyama (KEK)	J-PARC 加速器の非破壊ビームモニター https://indico2.riken.jp/indico/conferenceDisplay.py?confId=2413	Dec. 20
13	Atsushi Tatami (Kaneka Corporation)	Preparation of multi-layer graphene sheets and their applications for particle accelerators https://indico2.riken.jp/indico/conferenceDisplay.py?confId=2414	Dec. 22
14	Joele Mira (RNC)	Current status of the Cyclotron Facility at iThemba LABS https://indico2.riken.jp/indico/conferenceDisplay.py?confId=2464	Feb. 27
15	Teruaki Enoto (Kyoto U.)	High Energy Astrophysics Lab. Seminar 雷雲電場による電子加速の観測的研究の進展	Mar. 8
16	Yuuki Wada (U. Tokyo)	High Energy Astrophysics Lab. Seminar 雷雲ガンマ線の多地点検出を目指した可搬型検出器の開発と初期の観測成果	Mar. 8

High Energy Astrophysics Lab. Seminar -> http://astro.riken.jp/wordpress/?page_id=65

Niigata Univ.

1	Hiroya Suno (RIKEN AICS)	低温におけるトリプルアルファ反応	Jul. 14
2	Tatsuaki Kanai (Gunma U.)	重粒子線の生物効果と microdosimetry	Aug. 4
3	Toshio Suzuki (Nihon U.)	天体条件下での原子核の電子捕獲率・ベータ崩壊率と星の冷却過程，R 過程元素合成への応用	Nov. 4
4	Takumi Doi (RNC)	格子 QCD によるバリオン間相互作用	Dec. 6

理化学研究所
埼玉県　和光市　広沢
RIKEN 2017-041